Host and Viral Determinants of Antibody-Mediated Immunity Following SARS-CoV-2 Infection and Vaccination

Yannick Galipeau

This thesis is submitted to the Faculty of Medicine in partial fulfilment of the requirements for the degree of Doctorate in Philosophy with specialization in Microbiology and Immunology.

Department of Biochemistry, Microbiology and Immunology, Faculty of Medicine,
University of Ottawa

© Yannick Galipeau, Ottawa, Canada, 2025

ABSTRACT

Human respiratory viral pathogens have led to numerous pandemics over the course of history, each causing significant mortality, morbidity, and economic losses. The emergence of SARS-CoV-2 in late 2019, a human beta-coronavirus, stands as one of the latest examples. A critical component in responding to the spread of SARS-CoV-2 was the development of serological assays to measure antibody responses to both infection and vaccination. This thesis focuses on the comprehensive characterization of antibody-mediated responses to coronaviruses at the population level and in defined cohorts, enabled by a newly developed high-throughput, robust, and flexible serological platform. This approach supported large-scale investigations into the influence of demographics on viral seroepidemiology and vaccine-induced immunity. Our data provided critical insights to guide and monitor public health measures and informed how various antibody responses differ between certain demographic groups. We also investigated how pre-existing immunity to other human coronaviruses can functionally influence antibody responses to SARS-CoV-2. Additionally, we explored the roles of autoantibodies in the context of SARS-CoV-2 infection. Lastly, we investigated viral genomic evolution of highly pathogenic human coronaviruses (SARS-CoV, SARS-CoV-2, and MERS-CoV) and their associated host transcriptomic responses. Collectively, this work advances our understanding of the factors shaping antibody responses to respiratory pathogens and vaccines, highlighting the influence of demographic variables, pre-existing immunity, autoantibodies, and viral genomic evolution.

ACKNOWLEDGEMENTS

I am one of those who firmly believe that nobody is truly self-made, just as new science is incrementally built upon the work of previous scientists and prior discoveries. This thesis was built on a strong foundation of the people around me. They have all, in their own way, contributed to making this thesis a reality—a possibility. As such, I share this PhD thesis with them in mind.

To my parents, Camille and François Galipeau, I owe you more than I can put into words. Your sacrifices, love, and commitment to raising three strong, hardworking, and responsible children is a gift. You've always encouraged me to pursue my goals and to surpass them.

To my siblings, Chloé and Nicholas, my grandparents, and my family, thank you for always being there for me. Your presence in my life has been a source of unconditional support. Thank you for reminding me what truly matters.

To my friends, you've been at my side through it all. While not always able to relate or understand, you have all shown interest in and support for everything I wanted to accomplish. The laughs and moments we've shared have fueled me. I cherish the countless memories we've made. While I may not name each of you individually, I hope you recognize yourselves in these words and accept my deepest, most sincere gratitude.

To my scientific peers, mentees, and collaborators it has been a privilege to share this journey with you all. You've directly contributed to the success of this work, from near or far. A special thank you to Mariam who has shared this PhD journey with me through long hours in the lab, at conferences, and in our personal lives. I'd also like to acknowledge the contributions of the numerous study participants. Thank you.

To my scientific mentors, Dr. Martin Pelchat, Dr. Tommy Alain, Dr. Angela Crawley, and Dr. Curtis Cooper: I want to thank each of you personally for your support, commitment, wisdom, and time. You've supported me through all my endeavours and challenged me to become a better researcher and scientist.

Lastly, to my thesis supervisor, Dr. Marc-André Langlois: your work ethic, intelligence, passion, and commitment have been an example for me. Through a pandemic, you have taught me how to be a serious, critical, and confident scientist. You trusted me enough to give me the independence I needed to carry on this work and encouraged me to be curious. I am deeply grateful for your continued support and insight. It has been an honour to carry out this PhD under your mentorship.

REMERCIEMENTS

Je fais partie de ceux qui croient fermement que personne ne se construit entièrement seul, tout comme la science progresse par étapes, en s'appuyant sur les travaux et les découvertes de ceux qui nous ont précédés. Cette thèse repose sur des bases solides façonnées par les personnes qui m'entourent. Chacune d'elles, à sa manière, a contribué à rendre cette thèse possible. C'est donc avec eux à l'esprit que je partage ce doctorat.

À mes parents, Camille et François Galipeau, je vous dois bien plus que ce que les mots peuvent exprimer. Vos sacrifices, votre amour et votre dévouement à élever trois enfants forts, travailleurs et responsables sont un véritable cadeau. Vous m'avez toujours encouragé à poursuivre mes objectifs, et à les dépasser.

À mes frères et sœurs, Chloé et Nicholas, à mes grands-parents et à ma famille, merci d'avoir toujours été là pour moi. Votre présence dans ma vie a été une source de soutien inconditionnel. Merci de me rappeler ce qui compte vraiment.

À mes amis, vous avez été à mes côtés à chaque étape. Même si vous ne pouviez pas toujours comprendre ou vous identifier à mon parcours, vous avez tous manifesté de l'intérêt et m'avez soutenu dans tout ce que je voulais accomplir. Vos rires et les moments partagés m'ont porté. Je chéris les innombrables souvenirs que nous avons créés ensemble. Même si je ne vous nomme pas tous individuellement, j'espère que vous vous reconnaîtrez dans ces mots et que vous accepterez ma plus profonde et sincère gratitude.

À mes collègues scientifiques, mentorés et collaborateurs, ce fut un privilège de partager ce parcours avec vous. Vous avez directement contribué au succès de ce travail, de près ou de loin. Un merci tout particulier à Mariam, qui a partagé cette aventure doctorale à mes côtés, dans les longues heures passées au laboratoire, lors des conférences, et dans notre vie personnelle. Je tiens également à souligner la contribution des nombreux participants aux études. Merci.

À mes mentors scientifiques, Dr Martin Pelchat, Dr Tommy Alain, Dr Angela Crawley et Dr Curtis Cooper : je tiens à vous remercier personnellement pour votre soutien, votre engagement, votre sagesse et le temps que vous m'avez consacré. Vous m'avez accompagné dans toutes mes démarches et m'avez poussé à devenir un meilleur chercheur et scientifique.

Enfin, à mon directeur de thèse, Dr Marc-André Langlois : votre éthique de travail, votre intelligence, votre passion et votre engagement ont été pour moi un exemple. À travers une pandémie, vous m'avez appris à devenir un scientifique sérieux, critique et confiant. Vous m'avez fait confiance en m'accordant l'indépendance nécessaire pour mener à bien ce projet, tout en m'encourageant à rester curieux. Je vous suis profondément reconnaissant pour votre soutien et vos conseils constants. Ce fut un honneur de réaliser ce doctorat sous votre mentorat.

DECLARATION OF ACADEMIC ACHIEVEMENTS

Chapter 2 – Development and benchmarking of serological assays

2.1 A scalable serology solution for profiling humoral immune responses to SARS-CoV-2 infection and vaccination

Contribution:

This study presents the validation and development of serological approaches and high-throughput platforms in both Toronto and Ottawa. In Ottawa, YG led the development of serological and neutralization assays, including manual 96-well format assays and high-throughput 384-well format assays. YG also developed and validated the automated approaches. The study also details the data analysis pipeline used to address inter-plate variability and the methods employed to report titers, to which YG also contributed. The sections of the manuscript pertaining to the Ottawa platform were initially drafted by YG and subsequently revised by co-authors. Figures related to the Ottawa work were generated by YG or created in collaboration with YG, depending on the specific analysis. The peer-review process was co-led by YG.

2.2 Comparative performance of serum or plasma samples in sars-cov-2 serology and neutralization assays

Contribution:

This study comparing the performance of serum and plasma in serological assays was co-designed by YG and MAL. The assays used in this study were developed and validated by YG. The data was collected with YG and HAC and analyzed jointly following data analysis methods previously co-developed by YG. All of the figures were generated by YG. The initial draft was also written by YG and reviewed by all co-authors. YG led the peer-review process.

Chapter 3 – Harnessing serological assays in populational-based studies of sars-cov-2 immune responses

3.1 Cross-sectional Characterization of SARS-CoV-2 Antibody Levels and Decay Rates Following Infection of Unvaccinated Elderly Individuals

Contribution:

In this population-based study of unvaccinated elderly individuals following SARS-CoV-2 infection, the methods used to measure antibodies were developed by YG, including the

development of the high-throughput SARS-CoV-2 serology platform. The data analysis pipeline was co-developed by YG. The neutralization assays were developed by YG, and the neutralization measurements were performed by YG. The data analysis and generation of figures were performed jointly with MW and YG. The initial draft of the manuscript was written by YG and then reviewed by the other authors. YG led the peer-review process.

3.2 SARS-CoV-2 Seroprevalence in Indigenous Communities of the Northwest Territories in Canada: Insights from a Comparative Cohort Study

Contribution:

In this study, looking at the seroprevalence and levels of antibodies from SARS-CoV-2 infection and vaccination of Indigenous communities in NWT and urban samples in Ontario, YG developed the assays and high-throughput serological methods. YG led the initial exploratory data analysis and identified the key findings from the data. Subsequent data analysis and figure generation were performed jointly by YG and MW. The initial draft of the study was written by YG and then reviewed by other co-authors. YG is currently leading the peer-review process.

3.3Continuous false positive results by SARS-CoV-2 rapid antigen testing: a case report

Contribution:

This case study was co-designed by YG and MAL. YG co-coordinated sample collection and led the laboratory investigations. The data analysis and generation of figures was performed by YG. The first draft of the manuscript was written by YG as well as leading the peer-review process.

Chapter 4 – Impact of previous seasonal coronaviruses infection

---

4.1 Relative ratios of human seasonal coronavirus antibodies predict the efficiency of cross-neutralization of SARS-CoV-2 spike binding to ACE2

Contribution:
This study was co-designed by MAL and YG. YG developed the serological assays and performed the experiments (alongside VS). YG analyzed the experimental data and generated the dataset used for machine learning. YG generated the figures alongside MCC and SB. YG wrote the first draft of the manuscript and led the peer review process.

Chapter 5 – Autoantibodies in the context of SARS-CoV-2 infection

---

5.1 Autoantibodies targeting angiotensin-converting enzyme 2 are prevalent and not induced by SARS-CoV-2 infection

Contribution:

YG co-designed this study alongside MAL. YG developed all of the experimental approaches and collected the data alongside PM and NC (except for the ACE2 enzymatic activity experiments). YG performed the data analysis, including the statistical methods. The initial draft was written by YG and then reviewed by the co-authors. YG led the peer-review process.

Chapter 6 – Genomic evolution of pathogenic coronaviruses

6.1 Longitudinal transcriptomic analysis of MERS-CoV, SARS-CoV, and SARS-CoV-2 adaptation to a Vero-E6 cell system

In this study, YG conducted the data analysis in collaboration with MP. Specifically, YG processed the sequencing files, performed reference genome indexation, mapped the reads, and generated gene counts using Compute Canada servers. YG also carried out the statistical analyses of gene expression, as well as the protein-protein interaction and enrichment analyses. Figures were generated by YG and MP. The initial draft of the manuscript was written by YG.

TABLE OF CONTENTS

ABSTRACT ..... **II**

ACKNOWLEDGEMENTS ..... **III**

REMERCIEMENTS ..... **V**

DECLARATION OF ACADEMIC ACHIEVEMENTS ..... **VII**

LIST OF ABBREVIATIONS XIII
LIST OF FIGURES XV
LIST OF TABLES XXI

CHAPTER 1– INTRODUCTION **1**

1.1 RESPIRATORY VIRUSES AND THEIR PANDEMIC POTENTIAL 2
1.2 HUMAN CORONAVIRUSES 5
1.3 SARS-COV-2 10
1.4 VIRAL IMMUNE RESPONSES 15
1.5 SEROLOGY 22

RATIONALE, HYPOTHESIS AND OBJECTIVES **27**

RATIONALE 27
HYPOTHESIS 28
OBJECTIVES 28

CHAPTER 2 – DEVELOPMENT OF SEROLOGICAL ASSAYS **30**

RATIONALE 31
2.1 A SCALABLE SEROLOGY SOLUTION FOR PROFILING HUMORAL IMMUNE RESPONSES TO SARS-COV-2 INFECTION AND VACCINATION 32
2.2 COMPARATIVE PERFORMANCE OF SERUM AND PLASMA SAMPLES IN SARS-COV-2 SEROLOGY AND NEUTRALIZATION ASSAYS 91

CHAPTER 3 – HARNESSING SEROLOGICAL ASSAYS IN POPULATIONAL-BASED STUDIES OF SARS-COV-2 IMMUNE RESPONSES **112**

RATIONALE 113
3.1 CROSS-SECTIONAL CHARACTERIZATION OF SARS-COV-2 ANTIBODY LEVELS AND DECAY RATES FOLLOWING INFECTION OF UNVACCINATED ELDERLY INDIVIDUALS 114
3.2 SARS-COV-2 SEROPREVALENCE IN INDIGENOUS COMMUNITIES OF THE NORTHWEST TERRITORIES IN CANADA: INSIGHTS FROM A COMPARATIVE COHORT STUDY 151
3.3 CONTINUOUS FALSE POSITIVE RESULTS BY SARS-COV-2 RAPID ANTIGEN TESTING: A CASE REPORT 184

CHAPTER 4 –IMPACT OF PREVIOUS SEASONAL CORONAVIRUSES INFECTION **198**

RATIONALE 199
4.1 RELATIVE RATIOS OF HUMAN SEASONAL CORONAVIRUS ANTIBODIES PREDICT THE EFFICIENCY OF CROSS-NEUTRALIZATION OF SARS-COV-2 SPIKE BINDING TO ACE2 200

CHAPTER 5 – AUTOANTIBODIES IN THE CONTEXT OF SARS-COV-2 INFECTION 247

RATIONALE....248
5.1 AUTOANTIBODIES TARGETING ANGIOTENSIN-CONVERTING ENZYME 2 ARE PREVALENT AND NOT INDUCED BY SARS-COV-2 INFECTION....249

CHAPTER 6 – GENOMIC EVOLUTION OF PATHOGENIC CORONAVIRUSES 285

RATIONALE....286
6.1 LONGITUDINAL TRANSCRIPTOMIC ANALYSIS OF MERS-COV, SARS-COV, AND SARS-COV-2 ADAPTATION TO A VERO-E6 CELL SYSTEM....287

CONCLUSION....327

REFERENCES....340

APPENDIX I – ADDITIONAL WORK....353

A-1.1 CLINICAL AND SEROLOGICAL PREDICTORS OF POST COVID-19 CONDITION–FINDINGS FROM A CANADIAN PROSPECTIVE COHORT STUDY....354
A-1.2 HOMOGENEOUS SURROGATE VIRUS NEUTRALIZATION ASSAY TO RAPIDLY ASSESS NEUTRALIZATION ACTIVITY OF ANTI-SARS-COV-2 ANTIBODIES....384
A-1.3 SCALABLE AGROINFILTRATION-BASED PRODUCTION OF SARS-COV-2 ANTIGENS FOR USE IN DIAGNOSTIC ASSAYS AND SUBUNIT VACCINES....407
A-1.4 SEASONAL RESPIRATORY VIRUS CIRCULATION WAS DIMINISHED DURING THE COVID-19 PANDEMIC....432
A-1.5 COVID-19 VACCINE IMMUNOGENICITY IN PEOPLE WITH HIV....447
A-1.6 ANTIBODY NEUTRALIZATION CAPACITY AFTER CORONAVIRUS DISEASE 2019 VACCINATION IN PEOPLE WITH HIV IN CANADA....464
A-1.7 CORRELATES OF BREAKTHROUGH SARS-COV-2 INFECTIONS IN PEOPLE WITH HIV: RESULTS FROM THE CIHR CTN 328 STUDY....482
A-1.8 THE EFFECT OF DOSE-INTERVAL ON ANTIBODY RESPONSE TO MRNA COVID-19 VACCINES: A PROSPECTIVE COHORT STUDY....508
A-1.9 HOUSEHOLD TRANSMISSION OF SARS-COV-2 FROM UNVACCINATED ASYMPTOMATIC AND SYMPTOMATIC HOUSEHOLD MEMBERS WITH CONFIRMED SARS-COV-2 INFECTION: AN ANTIBODY-SURVEILLANCE STUDY....532
A-1.10 PREVALENCE OF SARS-COV-2 INFECTION AMONG OBSTETRIC PATIENTS IN OTTAWA, CANADA: A DESCRIPTIVE STUDY....552
A-1.11ANTIBODY SERONEGATIVITY IN COVID-19 RT-PCR–POSITIVE CHILDREN....571
A-1.12 LONGITUDINAL PROFILES OF PLASMA GELSOLIN, CYTOKINES AND ANTIBODY EXPRESSION PREDICT COVID-19 SEVERITY AND HOSPITALIZATION OUTCOMES....578
A-1.13 MULTIVARIATE ANALYSES AND MACHINE LEARNING LINK SEX AND AGE WITH ANTIBODY RESPONSES TO SARS-COV-2 AND VACCINATION....601
A-1.14 SEASONAL HUMAN CORONAVIRUSES OC43, 229E, AND NL63 INDUCE CELL SURFACE MODULATION OF ENTRY RECEPTORS AND DISPLAY HOST CELL-SPECIFIC VIRAL REPLICATION KINETICS....632
A-1.15 PLATELET ACTIVATION BY SARS-COV-2 IMPLICATES THE RELEASE OF ACTIVE TISSUE FACTOR BY INFECTED CELLS....662

A-1.16 SARS-CoV-2 Seroprevalence in Those Utilizing Public Transportation or Working in the Transportation Industry: A Rapid Review 687
A-1.17 Reduced seasonal coronavirus incidence in high risk population groups during the COVID 19 pandemic 713
A-1.18 Alcohol consumption does not influence SARS-CoV-2 vaccine immunogenicity: A stop the spread Ottawa cohort analysis 734
A-1.19 Systemic and Mucosal Antibody Responses to SARS-CoV-2 Variant-Specific Prime-and-Boost and Prime-and-Spike Vaccination: A Comparison of Intramuscular and Intranasal Bivalent Vaccine Administration in a Murine Model.....751
A-1.20 Characterization of Systemic and Mucosal Humoral Immune Responses to an Adjuvanted Intranasal SARS-CoV-2 Protein Subunit Vaccine Candidate in Mice.786
A-1.21 Differential Adaptive Immune Responses Following SARS-CoV-2 Infection in Children Compared to Adults 811
A-1.22 Humoral responses and serological assays in SARS-CoV-2 infections 832
A-1.23 Autoantibodies in COVID-19: implications for disease severity and clinical outcomes 874
A-1.24 Dried blood spot specimens for SARS-CoV-2 antibody testing: a multi-site multi-assay comparison 909
A-1.25 Comparative performance data for multiplex SARS-CoV-2 serological assays from a large panel of dried blood spot specimens 935
A-1.26 Cohort profile: Stop the Spread Ottawa (SSO)—a community-based prospective cohort study on antibody responses, antibody neutralization efficiency and cellular immunity to sars-cov-2 infection and vaccination.....967
A-1.27 Results of the Stop the Spread Ottawa (SSO) cohort study: a Canadian urban-based prospective evaluation of antibody responses and neutralization efficiency to SARS-CoV-2 infection and vaccination.....994

LIST OF ABBREVIATIONS

COVID-19 ; Coronavirus disease 2019
HIV; Human immunodeficiency virus
RSV; Respiratory syncytial virus
IAV; Influenza A virus
RNA; Ribonucleic acid
vRNA; Viral RNA
mRNA; Messenger RNA
RDRP; RNA-dependent RNA polymerase
S; Spike protein
M; Membrane protein
E; Envelope protein
N; Nucleocapsid protein
HE; Hemagglutinin-esterase
ACE2; Angiotensin-converting enzyme 2
CFR; Case fatality rate
DPP4; Dipeptidyl Peptidase 4
ARDS; Acute respiratory distress syndrome
VOC; Variant of concern
HI; Haemagglutination inhibition
mRNA-LNP; Messenger RNA-Lipid nanoparticle
VITT; Vaccine-induced thrombotic thrombocytopenia
IM; intra-muscular
PASC; Post-Acute Sequelae of SARS-CoV-2 Infection
EBV; Epstein-Barr virus
PAMPs; Pathogen-associated molecular patterns
DAMPs; damage-associated molecular patterns
RLRs; RIG-I-like receptors
NLRs; NOD-like receptors
TLRs; Toll-like receptors
IFN; interferon
GSDMD; gasdermin D
NK; Natural killer
IL; Interleukin
TNF; Tumour necrosis factor
APCs; Antigen-presenting cells
TCRs; T cell receptors
BCRs; B cell receptors
MHC; Major Histocompatibility Complex
ADCC; Antibody-dependent cellular cytotoxicity
ADCP; Antibody-dependent cellular phagocytosis
FcRs; Fc receptors
IgG; Immunoglobulin G
IgA; Immunoglobulin A
IgM; Immunoglobulin M

ELISA; Enzyme-linked immunosorbent assays
LFAs; Lateral flow assays
PRNTs; Plaque reduction neutralization tests
SCoVs; Seasonal coronaviruses
CoV; Coronavirus
SARS-CoV-2; Severe acute respiratory syndrome coronavirus 2
HRP; Horseradish peroxidase
DBS; Dried blood spot
RBD; Receptor binding domain
WHO; World Health Organization
CHO; Chinese Hamster Ovary
VHHs; single-domain antibodies
ROC; Receiver Operating Characteristic
BAU; Binding antibody unit
IU; International unit
SDS-PAGE; Sodium dodecyl sulfate-polyacrylamide gel electrophoresis
SEC-UPLC; Size-exclusion ultra-high performance liquid chromatography
SSTs; Serum separator tubes
PBMCs; Peripheral blood mononuclear cells
LTC; Long term care
PCR; Polymerase chain reaction
RLU; Relative light units
ED_{50}; Median effective dose
CT; Cycle threshold
NWT; Northwest Territories
HLA; Human Leukocyte Antigen
RAT; Rapid Antigen Tests
GPR; Gaussian process regression
SD: Standard deviation
FCM; Fuzzy c-means
HCV; Hepatitis C virus
MS; multiple sclerosis
GO; Gene Ontology
PPIs; Potential protein-protein interactions
VST; Variance stabilizing transformation
DEGs; Differentially expressed genes
Nsp; Non-structural protein
TCV; Turnip crinkle virus
RNA-seq; RNA sequencing
AI; Artificial intelligence

LIST OF FIGURES

Chapter 1: Introduction

Figure 1: SARS-CoV-2 representation of structural proteins of interest for serology……7
Figure 2: A phylogenetic tree of the seven common human coronaviruses……9
Figure 3: Global phylogenetic evolution of SARS-CoV-2……12
Figure 4: Overview of antibody isotype characteristics and dynamic following SARS-CoV-2 infection…….19
Figure 5: Overview of autoantibodies associated with SARS-CoV-2……...21
Figure 6: Overview of serological assays approach and characteristics……23
Figure 7: Graphical Abstract……..29

Chapter 2: Development of serological assays

2.1

Figure 1 - High-quality reagents for SARS-CoV-2 serology……35
Figure 2- Development of high-throughput ELISAs for plasma or serum……41
Figure 3- Conversion of Ottawa and Toronto ELISA data to WHO BAUs and comparison to the WHO Reference Panel 20/268……...44
Figure 4- Dose response curves or single-point snELISA and conversion to International Units using the WHO International Standard……..48
Figure 5- Visualisation of data from three antigen testing. The results are from known negative and positive samples……..50
Supplementary figure 1. Chromatogram traces for the purified ELISA antigens and detection reagents……..……74
Supplementary figure 2. Purification of recombinant anti-spike antibodies Supplementary figure 2. Purification of recombinant anti-spike antibodies……75
Supplementary figure 3. Titration curves of 32 serum samples from CBS using automated ELISAs to detect……76
Supplementary figure 4. Performance of the IgG chemiluminescent ELISAs with plasma and serum……..77

Supplementary figure 5. Comparison between o-Phenylenediamine dihydrochloride (OPD) and 3,3′,5,5′-tetramethylbenzidine (TMB) as colorimetric substrates for the manual 96-well plate ELISA……78

Supplementary figure 6. Comparison of IgG-HRP secondary antibody performance……..79

Supplementary figure 7. Elution and secondary antibody optimizations for IgG ELISAs using DBSs……..80

Supplementary figure 8. IgA and IgM ELISAs…….81

Supplementary figure 9. Conversion of serology data to WHO BAUs and validation of SARS-CoV-2 IgG profiling performed on the uOttawa automated serology platform……82

Supplementary figure 10. DBS Optimization……83

Supplementary figure 11. Processing and validation of the Ottawa automated serology platform……..84

Supplementary figure 12. ROC curve for NML panel 4 DBS IgG analysis……..85

Supplementary figure 13. Optimization and testing of NRC reagents for snELISA…….86

Supplementary figure 14. Optimization of the snELISA for the automated platform……...87

Supplementary figure 15. Optimized snELISA for the automated platform…….88

Supplementary figure 16. Optimization of the NRC reagents……...89

Supplementary figure 17. Optimization of IgG#5-HRP and recombinant antibodies for chemiluminescent assays……...90

2.2

Figure 1. Manual ELISA quantification of SARS-CoV-2 antibody titers in serum and plasma……...106

Figure 2. Automated platform quantification of SARS-CoV-2 antibody titers in serum and plasma…...107

Figure 3. Antibody neutralization efficiency between paired serum and plasma samples……108

Figure 4. Relative volume recovery rate in plasma and serum……..109

Supplementary Figure 1. Linear correlation between plasma and serum titer measurements in the pilot cohort…….110

Supplementary Figure 2. Linear correlation between plasma and serum titer measurements in the automated cohort……111

Supplementary Figure 3. Area under the curve (AUC) quantification of antibody levels in the pilot cohort…….112

Chapter 3: Harnessing serological assays in population-based studies of SARS-CoV-2 immune responses

3.1

Figure 1. Antibody levels and neutralization efficiency relative to age groups……..125

Figure 2.Antibody levels and neutralization efficiency relative to the time of serum/plasma collection…….…..…126

Figure 3.Age group–specific variation of antibody levels relative to the time of serum/plasma collection……..…128

Supplemental Figure 1. Cohort demographics……138

Supplemental Figure 2. Correlation between antibody levels and PCR results……..139

Supplemental Figure 3. No correlation observed between antibody levels and Ct values from PCR tests…….…….140

Supplemental Figure 4. Antibody levels relative to sex……..141

Supplemental Figure 4. Antibody levels relative to sex……..142

Supplemental Figure 5. IgA and IgM levels and correlation with neutralization efficiency…...143

Supplemental Figure 6. Variation of antibody levels relative to the time from serum/plasma collection and age group……..144

Supplemental Figure 7. Variation of antibody levels relative to time from serum/plasma collection and age group overlayed on scatter plot……..145

Supplemental Figure 8. Histogram and density distribution of samples by sex based on days between symptom onset and collection date……146

Supplemental Figure 9. Histogram and density distribution of samples by age groups based on days between symptom onset and collection date. Supplemental……...147

Supplemental Figure 10. Antibody levels of individuals within 30 days post symptom onset by age groups……148

3.2

Figure 1. Side-by-side comparison of the NWT Indigenous community cohort and urban cohorts……..170

Figure 2. Seroprevalence of previous SARS-CoV-2 infection in all three cohorts…….171

Figure 3. SARS-CoV-2 IgG antibody levels against the Spike, RBD and Nucleocapsid……..172

Figure 4 – Trajectories of antibody levels over time in relation to last vaccination, infection or both in the urban and Indigenous cohort…….173

Supplemental Figure 1. Cohorts anti-nucleocapsid levels in relation to collection time……176

Supplemental Figure 2. Antibody levels in relation to vaccine and infection status……...177

3.3

Figure 1. Timeline overview of positive RATs and specimen collection……189

Figure 2. Weekly results of RAT by swabbing technique and location……..190

Figure 3. Serology results of serum sample provided prior to week 1……190

Chapter 4: Impact of previous Seasonal coronaviruses infections

Figure 1 Seroprevalence of human CoVs. ELISA was used to detect spike (S-trimer) specific IgG antibody responses of four sCoVs……208

Figure 2 Concordance in sCoV seroprevalence using alternative antigens…….218

Figure 3 Evaluation of cross-reactive antibodies to three SARS-CoV-2 antigens in pre-pandemic serum samples……..220

Figure 4 Patterns of multi-antigen cross-reactivity against SARS-CoV-2 Spike-ACE2 interactions……...221

Figure 5 Neutralizing activity against SARS-CoV-2 Spike-ACE2 interactions…….222

Figure 6 Association of sCoV seroprevalence with SARS-CoV-2 antigen cross-reactivity and neutralization of SARS-CoV-2 Spike-ACE2 interactions……..224

Supplementary Figure 1. Comparison between pediatric samples under 2 years old to the complete cohort for each seasonal spike coronavirus…….236

Supplementary Figure 2. IgG-subclass antibody responses to SARS-CoV-2 antigens……..237

Supplementary Figure 3. Discordance of serological false positive per isotype and antigen…….238

Supplementary Figure 4. Global sensitivity analysis (GSA) results for the Gaussian process regression (GPR) model……..239

Chapter 5: Autoantibodies in the context of SARS-CoV-2 infection

Figure 1 - Overview of ACE2 serology results and establishment of seropositivity thresholds……259

Figure 2 - Influence of clinical features and demographic characteristics on ACE2 autoantibodies prevalence……261

Figure 3 - Persistence of autoantibodies in serum over time and association with previous SARS-CoV-2 infection……...262

Figure 4 - Effect of ACE2 autoantibodies on ACE2 enzymatic activity and SARS-CoV-2 spike-ACE2 binding……..265

Supplemental Figure 1. Cohort demographics……275

Supplemental Figure 2. Cohort demographics by sex…….276

Supplemental Figure 3. ACE2 autoantibodies levels according to serological evidence of SARS-CoV-2 infection……...277

Supplemental Figure 4. ACE2 autoantibodies levels by sex and by isotype……..278

Supplemental Figure 5. ACE2 autoantibodies levels by age groups and by isotype……..279

Supplemental Figure 6. Principal component analysis of ACE2 autoantibodies and classified by prior SARS-CoV-2 infection status……280

Supplemental Figure 7. Correlation between ACE2 autoantibodies and SARS-CoV-2 nucleocapsid IgG antibodies……...281

Supplemental Figure 8. ACE2 autoantibodies levels by vaccination status……...282

Chapter 6: Genomic evolution of pathogenic coronaviruses

Figure 1. Description of viral mutations acquired over time and viral titers…….303

Figure 2. Overview of the viral mutations on MERS-CoV, SARS-CoV and SARS-CoV-2….305

Figure 3. Differential gene expression between uninfected and infected VERO-E6 cells at baseline……...306

Figure 4. Clustering analysis of DEGs modulated over time for each virus……..307

Figure 5. Enrichment analysis of overrepresented gene ontology biological process terms within each cluster of DEGs modulated over time…….……308

Supplementary figure 1. Relative percentage substitution and deletion over time from supernatants and cells infected with MERS-CoV……...313

Supplementary figure 2. Relative percentage substitution and deletion over time from supernatants and cells infected with SARS-CoV……314

Supplementary figure 3. Relative percentage substitution and deletion over time from supernatants and cells infected with SARS-CoV-2…….315

Supplementary figure 4. Sequencing depth and coverage for MERS-CoV cellular extract samples…….316

Supplementary figure 5. Sequencing depth and coverage for MERS-CoV supernatant samples…….317

Supplementary figure 6. Sequencing depth and coverage for SARS-CoV cellular extract samples…….318

Supplementary figure 7. Sequencing depth and coverage for SARS-CoV supernatant samples…….319

Supplementary figure 8. Sequencing depth and coverage for SARS-CoV-2 cellular extract samples…….320

Supplementary figure 9. Sequencing depth and coverage for SARS-CoV-2 supernatant samples……321

Supplementary figure 10. Proportion of cellular mRNA or Viral RNA in the cell extract or supernatant……...322

Supplementary figure 11. Enrichment analysis of biological processes GO terms in shared upregulated genes atbaseline……323

Supplementary figure 12. Weekly mutation rate data for supernatant and cellular extract samples……324

Supplementary figure 13. Enrichment analysis of biological processes GO terms in each cluster of gene whose expression was modulated over time……...325

LIST OF TABLES

Chapter 2: Development of serological assays

2.1

Table 1. ELISA performance statistics for plasma or serum IgG (Toronto)……39

Table 2. ROC statistics for the DBS IgG ELISA (Ottawa)……..46

Table 3. ROC statistics for the DBS IgG ELISA (Toronto)…….46

2.2

Table 1. Cohort demographic analysis……105

Chapter 3: Harnessing serological assays in population-based studies of SARS-CoV-2 immune responses

3.1

Table 1. Cohort demographics and collected information based on molecular and IgG seroconversion……123

Table 2. Seroprevalence by cohorts……130

3.2

Table 1. General demographics and epidemiological characteristics of participants by cohort…….……..169

Supplementary Table 1. Supplementary demographic information……178

Supplementary Table 2. Vaccine characteristics by age groups and cohorts……..179

Supplementary Table 3. General demographic and characteristics of individuals included in the antibody trajectories analysis……...180

Supplementary Table 4. General demographic and characteristics of individuals included in the antibody trajectories analysis since their last vaccine……..181

Supplementary Table 5. General demographic and characteristics of convalescent individuals included in the antibody trajectories analysis……..……182

Supplementary Table 6. General demographic and characteristics of individuals included in the antibody trajectories analysis since last antigenic exposure…….…...183

Chapter 4: Impact of previous Seasonal coronaviruses infections

Table 1 Demographic information of each pre-pandemic cohort……207

Table 2 Seroprevalence of seasonal coronavirus (OC43, HKU1, 229E and NL63) IgG antibodies and IgG cross reactivity to SARS-CoV-2 antigens by cohorts……216

Table 3 Descriptive statistics of the protein-based neutralization assay by cohorts……223

Table S1. Demographic information of post-pandemic controls…….240

Table S2. Determination of SARS-CoV-2 assay cut-off values of the four cohorts combined and false discovery rate (FDR) per antigen, isotype & subtypes……...241

Table S3. Determination of SARS-CoV-2 assay cut-off values of pre-COVID-19 HCV and HIV patients and corresponding false discovery rate per antigen, isotype & subtypes…….……..242

Table S4. Determination of SARS-CoV-2 assay cut-off values of pre-COVID-19 > 70 years of age and corresponding false discovery rate per antigen, isotype & subtypes…….…….243

Table S5. Determination of SARS-CoV-2 assay cut-off values of pre-COVID-19 21 - 70 years of age and corresponding false discovery rate per antigen, isotype & subtypes……..244

Table S6. Determination of SARS-CoV-2 assay cut-off values of pre-COVID 19 < 21 years of age and corresponding false discovery rate per antigen, isotype & subtypes……..245

Table S7 Multi-antigen FDR calculation…….246

Table S8. Demographics of fuzzy mean clusters of patients segregated by serum antibody cross-reactivity……..247

Chapter 5: Autoantibodies in the context of SARS-CoV-2 infection

Table 1. Participant demographics and health characteristics based on SARS-CoV-2 infection history……..258

Supplemental Table 1. ACE2 autoantibody seroprevalence odd ratios and 95% confidence interval by isotype……283

Supplemental Table 2. Participant demographic information for enzymatic assay cohort…….284

Supplemental Table 3. Participant demographic for the ACE2 and Spike attachment……...285

Chapter 6: Genomic evolution of pathogenic coronaviruses

Supplementary Table 1: Number and Frequency of mutations found in the spike protein by domain……..326
Supplementary Table 2: Number and Frequency of mutations found in each protein of ORF1ab……327

CHAPTER 1– INTRODUCTION

1.1 Respiratory viruses and their pandemic potential

A Brief Account of Modern Pandemics

Recent events have highlighted the far-reaching and long-lasting impacts of respiratory viruses on both public health and economic well-being. For many, the emergence of SARS-CoV-2 and the subsequent COVID-19 pandemic were perceived as an isolated incident—a once-in-a-lifetime event. However, society's tendency to revert to the status quo in the post-pandemic period has contributed to a failure to recognize how frequent epidemics and pandemics caused by respiratory viruses can be.

The 1918 Spanish flu pandemic (1918–1919) is often referenced due to its documented impact and global spread. It is estimated that approximately 500 million individuals, one-third of the world's population at the time, were infected with death counts reaching an estimated 50 million (1). This pandemic was caused by the H1N1 influenza virus, a segmented, negative-sense, single-stranded RNA virus (2). Notably, almost all human influenza A cases today originate from drifted or reassorted viruses descending from the 1918 Spanish flu (3). Examples include the H2N2 pandemic (1957–1958), which resulted in an estimated 1.1 million deaths (4), and the H3N2 pandemic (1968–1969), which caused an estimated 0.5–2 million deaths (5). More recently, the H1N1pdm09 pandemic (2009) led to an estimated 151,700–575,600 deaths in its first year of circulation (6). Two strains of influenza A (H1N1 and H3N2) continue to circulate annually, causing mortality and morbidity in vulnerable populations while placing a significant burden on healthcare systems (7).

In addition to pandemics caused by influenza viruses, coronaviruses have triggered two outbreaks and one pandemic since the beginning of the 21st century. The first was the emergence of SARS-CoV (2002–2003), which spread to over 29 countries and resulted in approximately 8,422 probable cases, with a fatality rate of around 11% (8). Notably, this virus no longer circulates in the human population. Another coronavirus, MERS-CoV, emerged in 2012. While case numbers remain relatively low, with about 2,562 reported between 2012 and 2020, MERS-CoV has a high case fatality rate of approximately 33% (9). The most recent member of the coronavirus family to emerge is SARS-CoV-2, first detected in late 2019. This virus led to the COVID-19 pandemic,

which, as of February 2025, has caused over 777 million cases and more than 7.1 million deaths (10).

Spread and Evolution

Numerous pathogens have the potential to cause outbreaks, some of which can escalate into pandemics, regardless of whether they are respiratory viruses. For example, the human immunodeficiency virus (HIV) pandemic, with nearly 40 million individuals living with HIV worldwide, represents a non-respiratory viral pandemic (11). However, RNA respiratory viruses are particularly prone to rapid global spread due to their efficient mode of transmission and fast-paced evolution.

Respiratory viruses such as influenza, SARS-CoV-2, and respiratory syncytial virus (RSV), among others, are classified as respiratory viruses based on their cellular tropism for the respiratory tract, the respiratory nature of their clinical symptoms, and their transmission through respiratory secretions (12). Human-to-human transmission occurs through four primary routes: direct contact, indirect contact, droplets, and aerosols (13, 14). Aerosols are particles with a size < 5 μm, smaller than droplets. These particles can remain airborne for an extended period of time and travel relatively long distances, be carried and dispersed by air turbulence, diffusion or air currents (15). The role of aerosols in airborne transmission is increasingly recognized, as they enable long-distance spread and contribute to superspreader events, particularly in confined or high-traffic spaces (16). The COVID-19 pandemic has highlighted both the challenges and the effectiveness of public health interventions aimed at reducing transmission, such as masking and social distancing (17, 18).

Beyond transmission routes, intrinsic viral characteristics and host immune responses also influence transmissibility. Host immune defenses can, for instance, regulate the shedding of viral particles. SARS-CoV-2 vaccination has been shown to effectively reduce viral replication and shedding, thereby lowering transmission (19). The interplay between viral evolution and host immunity is a continuous process. Both influenza and SARS-CoV-2 have necessitated frequent vaccine updates due to their ability to rapidly acquire immune escape mutations, which significantly reduce vaccine effectiveness in preventing infection and transmission (20, 21). The rapid evolution of certain respiratory viruses, such as SARS-CoV-2, is an intrinsic characteristic that enables them to evade host immune pressure while also affecting viral replication within the respiratory tract, independently of immune factors. For example, the Omicron variant, which emerged in late 2021, demonstrated increased fitness in the upper respiratory tract compared to the ancestral strain (22).

Overall, respiratory viruses pose a particularly high risk of developing into pandemics, emphasizing the need for a deeper understanding of the factors that influence their transmission.

A Globalized World

Human pathogens, particularly viruses, circulate within populations and across countries' borders. This bidirectional relationship not only shapes public health responses but also influences the emergence and re-emergence of viruses. Additionally, the integration of economic and political activities in globalized nations affects both decision-making and the implementation of public health strategies (23).

Most human pathogens are believed to have zoonotic origins (24, 25), and respiratory viruses are no exception. A brief examination of the three most recent emerging coronaviruses; SARS-CoV, MERS-CoV, and SARS-CoV-2, reveals that all originated from spillover events involving non-human species. Understanding how certain pathogens cross the species barrier and subsequently transmit from human to human is a complex question. However, it is crucial to recognize that human behaviours and activities are intrinsically linked to the risk of spillover events. Factors such

as urbanization, deforestation, and climate change, largely driven by human activity, contribute to an increased risk of zoonotic transmission (26-29).

Beyond the role of human activities in pathogen emergence, the globalization of political and economic systems also impacts responses to outbreaks, which can quickly escalate into pandemics. For example, globalization has facilitated increased air travel and human movement between regions, heightening the risk of viral spread and complicating containment efforts (30). Furthermore, public health policies are often shaped by political climate; for instance, protectionist countries may impose travel restrictions more rapidly than highly globalized nations (23).

Ultimately, in an interconnected world, effective pandemic preparedness and response require coordinated global efforts.

1.2 HUMAN CORONAVIRUSES

Coronaviruses (CoVs) are enveloped, positive-sense, single-stranded RNA viruses belonging to the *Coronaviridae* family and *Coronavirinae* subfamily. They are further classified into four genera: *Alpha*, *Beta*, *Gamma*, and *Delta* coronaviruses, with only *Alpha* and *Beta* coronaviruses known to infect humans (31). Coronaviruses are spherical viral particles ranging from 118 to 140 nm in diameter, with spike proteins decorating their surface. These viral receptors give coronaviruses their classic appearance, reminiscent of a solar corona, from where they derive their name (32).

CoVs genome organization

Coronaviruses possess a relatively large, non-segmented genome of approximately 30 kb, encoding both structural and non-structural proteins (33, 34). While variations exist among human coronaviruses (hCoVs), their genomic organization follows a conserved pattern. Nearly two-thirds of the genome encodes non-structural proteins essential for viral replication and transcription. Within this region, two long polyproteins (pp1a and pp1ab) are translated, separated by a -1 ribosomal frameshift site. These polyproteins are subsequently cleaved into multiple non-structural

proteins, some of which form the RNA-dependent RNA polymerase and the replication-transcription complex. Downstream of these regions, additional open reading frames encode several subgenomic mRNAs, primarily responsible for structural and accessory proteins (35, 36). The CoV genome also features a 5′ cap and a 3′ poly-A tail, along with cis-acting regulatory elements at both ends (31, 37).

Structure of CoVs

Human coronaviruses share several key structural components, including spike (S), membrane (M), envelope (E), and nucleocapsid (N) proteins. Among these, S, M, and E are embedded in the viral membrane, while the N protein is located within the virion (38). The N protein, which is highly conserved among CoVs, contains an N-terminal RNA-binding domain that interacts with viral RNA, while its C-terminal dimerization domain facilitates oligomerization and interaction with the M protein (39, 40). The M protein, located in the viral membrane, plays a crucial role in virion assembly and membrane curvature (41). The E protein, although one of the least abundant structural proteins, forms ion channels in the viral membrane and contributes to spike protein maturation (31, 42). The S protein, a homotrimeric class I fusion protein, is highly glycosylated and undergoes proteolytic cleavage at different stages of infection. While the S1 domain contains the receptor-binding domain (RBD), which determines host specificity, the highly conserved S2 domain anchors the spike protein to the virion surface (43). Some coronaviruses, such as HCoV-HKU1 and HCoV-OC43, also encode an additional hemagglutinin-esterase (HE) protein (44).

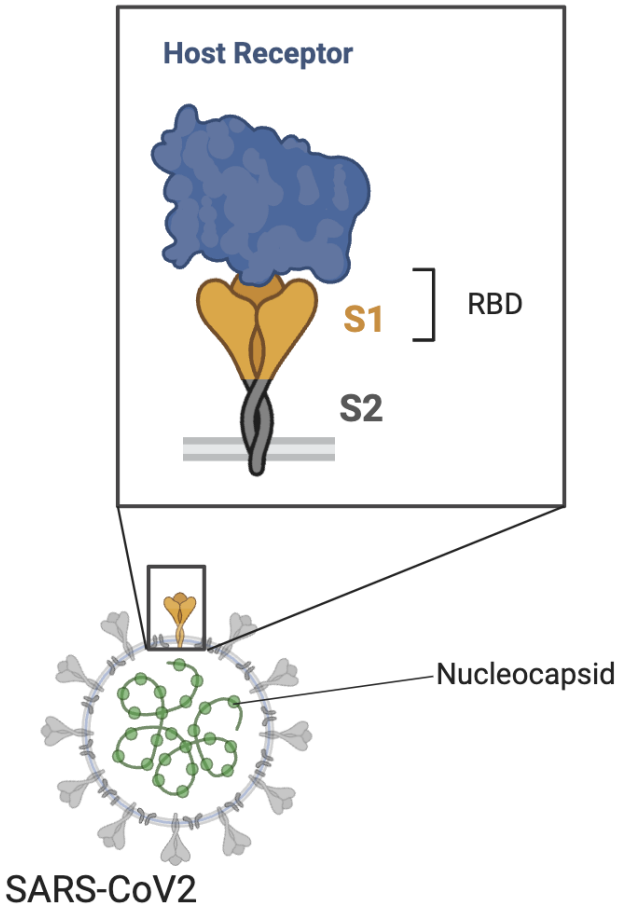


Figure 1: SARS-CoV-2 representation of structural protein of interest for serology. The nucleocapsid is highlighted in green and is located within the virion. The spike protein and its associated domain S1 and S2 are indicated. The receptor binding domain (RBD) is located within the S1 domain.

Replication cycle

The replication cycle of CoVs begins with the attachment of viral particles to host cell receptors via the spike protein. Most human coronaviruses bind to specific protein receptors, except for OC43, which binds to sialic acids on glycoproteins (45). After attachment, a conformational change in the spike protein facilitates membrane fusion, which occurs either at the plasma membrane or within endosomes following spike cleavage and/or endosomal acidification (46, 47). Following entry, the viral RNA is released into the cytoplasm, where it serves as a template for

translating pp1a and pp1ab polyproteins that drive viral replication and transcription (48). The replication of full-length viral genomic RNA and transcription of subgenomic mRNAs encoding structural proteins take place within specialized viral replication organelles (49). Structural proteins are processed through the secretory pathway in the endoplasmic reticulum-Golgi intermediate compartment, with the nucleocapsid protein associating with viral RNA for packaging into new virions, while the M protein facilitates membrane curvature and virion assembly (32, 50, 51). The E protein is thought to modify secretory pathways, promoting viral egress via exocytosis (31, 32).

Seasonal coronaviruses

Four human coronaviruses, OC43, NL63, 229E, and HKU1, are classified as seasonal coronaviruses (sCoVs). OC43 and 229E were first identified in the 1960s, while NL63 and HKU1 were discovered more recently in 2004 and 2005 (52-54). NL63 and 229E are Alpha coronaviruses, with NL63 using ACE2 as an entry receptor and 229E binding aminopeptidase N. OC43 and HKU1 are Beta coronaviruses that both bind 9-O-acetylated sialic acid. It is widely believed that human coronaviruses originated from bat CoVs, with NL63 likely spilling over directly from bats, while OC43, 229E, and HKU1 may have had intermediate hosts such as bovines, camelids, or rodents (55-59). These seasonal coronaviruses generally cause mild, self-limiting respiratory illness, but severe disease can occur in pediatric, elderly, and immunocompromised individuals (60-62). They exhibit seasonal infection patterns, with frequent reinfections occurring annually (63). A retrospective serological study by Edridge et al. found that individuals are commonly reinfected with seasonal coronaviruses approximately every 12 months (64). Currently, no vaccines are available for these viruses.

Pathogenic coronaviruses

In contrast to seasonal coronaviruses, three human coronaviruses—SARS-CoV, MERS-CoV, and SARS-CoV-2—are associated with severe disease and high mortality. SARS-CoV, which emerged in 2002-2003, uses ACE2 as its entry receptor and has an estimated case fatality rate (CFR) of

11% (65). It originated from bats, likely through an intermediate host, but no longer circulates in humans (66, 67). MERS-CoV, identified in 2012, uses DPP4 as its entry receptor and has a CFR of approximately 35% (68). It also originated from bats, with camels serving as an intermediate host (69, 70), and while it does not transmit efficiently between humans, it remains in circulation. SARS-CoV-2, which emerged in 2019, shares high sequence homology with SARS-CoV. Although it has a lower CFR than both SARS-CoV and MERS-CoV, it has resulted in widespread global transmission (71). Its origin likely involves a bat reservoir, though uncertainties remain regarding an intermediate host (72). These examples highlight the potential for novel pathogenic coronaviruses to emerge, emphasizing the importance of continued surveillance and pandemic preparedness.

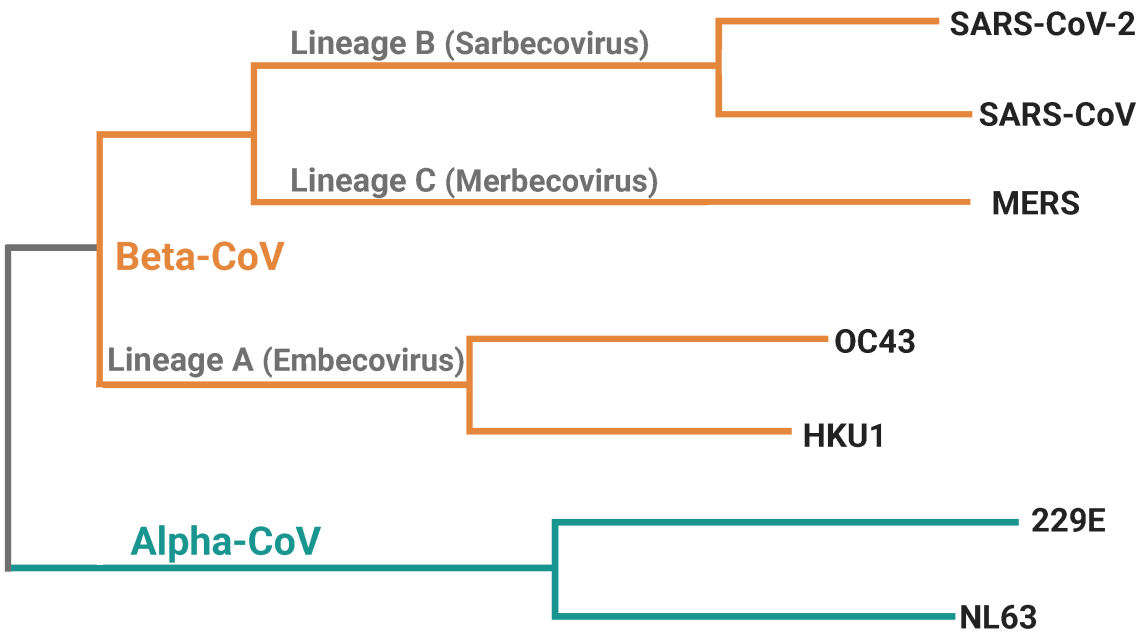


Figure 2: A phylogenetic tree of the seven common human coronaviruses. This was constructed using complete genome sequences aligned with Clustal Omega, based on reference genomes from NCBI. This figure was adapted from Galipeau, Greig, Liu, Driedger, and Langlois (2020), under the terms of the Creative Commons Attribution License (CC BY 4.0). © 2020 Galipeau et al. Published in *Frontiers in Immunology*. https://doi.org/10.3389/fimmu.2020.610688.

1.3 SARS-CoV-2

A Pandemic

In just a few years since its emergence, SARS-CoV-2 is estimated to have infected well over 777 million individuals, though this number is likely an underestimation due to the scaling down or cessation of testing and reporting in many jurisdictions (10). In addition, Reinfection does happen, with current estimates of the reinfection incidence rate being around 4.0 per 100 person-years (73). In most individuals, the virus causes symptoms resembling influenza, including fever, cough, myalgia, fatigue, headache, and loss of taste and smell (74). Some individuals have also reported gastrointestinal symptoms during SARS-CoV-2 infection (75). However, in certain cases, COVID-19 can lead to severe pneumonia and acute respiratory distress syndrome (ARDS), which can result in mortality. Risk factors for severe disease include older age and comorbidities such as diabetes and obesity, among others (76-78). Interestingly, asymptomatic infections have also been reported in some individuals (79). The wide spectrum of disease severity across the population remains a complex and unresolved question.

The rapid spread of the virus across every continent prompted public health agencies to implement measures aimed at monitoring and controlling its transmission. These measures varied between jurisdictions and evolved over time but included social distancing, masking, lockdowns, capacity limits in public spaces, travel restrictions, and testing requirements, among others (80, 81). While these interventions were largely effective, they were met with varying degrees of compliance worldwide. Beyond its direct impact on health, SARS-CoV-2 also had profound societal and economic repercussions. In the United States alone, the economic losses associated with the pandemic are estimated at $16 trillion (82).

Origins of SARS-CoV-2

The current scientific consensus indicates that SARS-CoV-2 most likely originated via a zoonotic spillover event, consistent with the emergence patterns of other coronaviruses. Genomic analyses

revealed that SARS-CoV-2 shares approximately 96% sequence identity with BatCoV RaTG13, a coronavirus isolated from Rhinolophus affinis bats in Yunnan, China (83). Additionally, related coronaviruses have been detected in illegally trafficked pangolins in Asia (84-86). These findings support the hypothesis that bats constitute the primary reservoir host, while other animal species may have acted as intermediate hosts or contributed to viral transmission pathways. Epidemiological data from the initial outbreak phase identified a cluster of early cases linked to a seafood and live animal market in Wuhan, China. Environmental sampling from the market detected SARS-CoV-2 along with DNA from civets, bamboo rats, and raccoon dogs, species previously implicated as potential intermediate hosts (87). Furthermore, phylogenetic analysis of viral genomes collected prior to February 2020 identified two distinct SARS-CoV-2 lineages, suggesting at least two independent zoonotic transmission events into the human population during mid to late November 2019 (88). While the definitive identification of the original reservoir species and any intermediary host(s) remains unclear, the available genomic and epidemiological evidence strongly supports the emergence of SARS-CoV-2 through multiple cross-species transmission events followed by human adaptation.

Emergence of Variants of SARS-CoV-2 Concern

The extensive scale of genomic surveillance of SARS-CoV-2 has allowed researchers to monitor the virus's evolution and the emergence of variants in real-time. Several factors drive the genetic evolution of SARS-CoV-2. First, the mutation rate is an intrinsic characteristic of the replication fidelity of its RNA-dependent RNA polymerase, estimated at 1×10^{-6} to 2×10^{-6} mutations per nucleotide per replication cycle (89, 90). This mutation rate is slightly lower than that of other RNA viruses due to the presence of a 3′ exonuclease proofreading mechanism in the coronavirus replication machinery (91, 92). Additionally, host-mediated viral genome editing can introduce further mutations, contributing to the overall mutation rate (93, 94). Recombination between different SARS-CoV-2 variants has also been documented, further increasing viral sequence diversity (95). The accumulation of sequence diversity through mutations, insertions, deletions, or recombination occurs within a broader context in which population transmission rates, immunity profiles, the number of infected individuals, and human mobility all influence SARS-CoV-2 evolution.

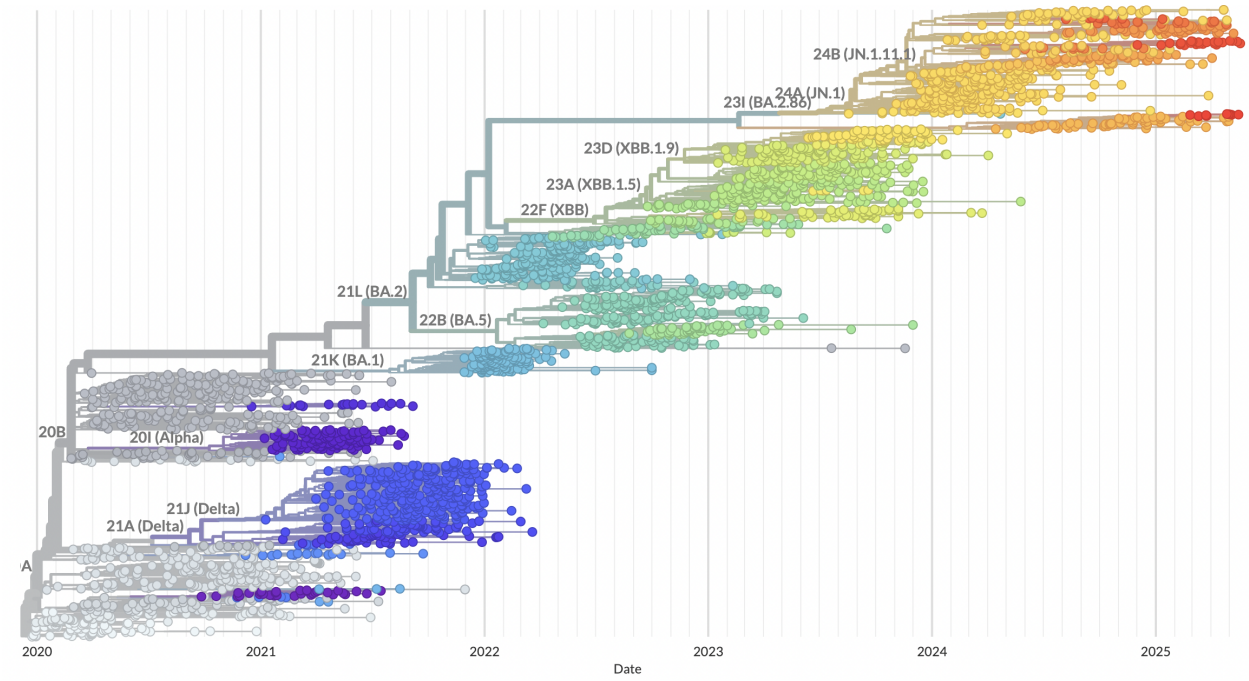


Figure 3: Global phylogenetic evolution of SARS-CoV-2. The data was accessed on June 17th 2025 and reproduced from Nextstrain (https://nextstrain.org), under the terms of the Creative Commons Attribution 4.0 International License (CC BY 4.0).

The first mutation that became dominant during the early days of the pandemic was D614G (96). Within a year of the virus's emergence, several lineages classified as variants of concern (VOCs) such as Alpha, Beta, and Gamma, appeared (97). Variants of concerns are defined as SARS-CoV-2 variants with modified phenotypic properties regarding their virulence, transmissibility, and their ability to evade an immune response (from vaccination, infection, or monoclonal antibodies) (98). By the fall of 2021, the Omicron lineage had emerged, becoming the dominant VOC (99). Extensive evolution within this lineage has resulted in Omicron sub-lineages that remain the predominant SARS-CoV-2 variants (100). Some of these mutations exhibit extensive immune evasion properties, reducing protection from both vaccine-induced and infection-acquired immunity (101, 102). The antigenic escape capabilities of certain mutations have challenged the efficacy of existing vaccines, prompting the reformulation of vaccines and the introduction of bivalent mRNA vaccinations. Increased viral fitness associated with some mutations has been linked to enhanced binding efficiency to ACE2, replication within specific regions of the respiratory tract, and susceptibility to neutralizing antibodies, among other factors (103).

Vaccination against SARS-CoV-2

The development of vaccines for SARS-CoV-2 has been identified as a priority to mitigate disease severity and mortality from infection and to reduce the transmission of SARS-CoV-2. Within a year, the first vaccines were approved and started being administered. This impressive achievement by the scientific community was made possible by the previous work on vaccine technologies and knowledge generated from studies on SARS-CoV. First, through previous studies on SARS-CoV, the Spike protein was identified as the main immunogenic target for vaccines given its immunogenicity and the fact that it is the only viral protein that can elicit neutralizing antibodies for coronaviruses. Early work had shown that neutralizing antibodies against the spike protein of SARS-CoV were protective in mice and non-human primates (104, 105). While neutralizing antibodies are not always predictive of protection for all pathogens, they often are associated with lower disease severity for respiratory viruses. For example, haemagglutination inhibition (HI) titers have been shown to be correlated with clinical protection against influenza A infection (106). Similarly, neutralizing antibodies to the spike protein of SARS-CoV-2 were associated with protection from infection (107-110).

Other than the selection of antigen for vaccine candidates, the vaccine platform can influence the resulting immunity. Three main vaccine platform technologies resulted in approved vaccines for SARS-CoV-2. These include the messenger RNA-Lipid nanoparticle (mRNA-LNP) based vaccines (Pfizer-BioNTech, Moderna), adenoviral vector vaccines (AstraZeneca, Johnson & Johnson), and protein subunit vaccines (Novavax, Medicago). The mRNA-LNP was vastly prioritized in North America with initial trials of the Moderna vaccine showing >90% efficacy at preventing COVID-19 illness (111, 112). The adenoviral vectors were also used in early vaccination campaigns in North America, with the efficacy of the AstraZeneca vaccine estimated at around 74% (113). These adenoviral vector vaccines were phased out in subsequent vaccine campaigns in Canada due to concerns of vaccine-induced thrombotic thrombocytopenia (VITT), a rare but serious side effect observed with this vaccine technology (114). While the evolution of SARS-CoV-2 has challenged the effectiveness of vaccines to prevent infection, they have and remain highly effective against severe disease and hospitalization (115, 116).

The challenges of currently available vaccines to mitigate transmission of SARS-CoV-2 highlight the difficulty of maintaining protective levels of immunity at the respiratory mucosa. This has prompted researchers to explore alternative routes of administration, such as intra-nasal administration (117, 118). These mucosal vaccine candidates are designed to elicit stronger mucosal immunity, where SARS-CoV-2 first establishes infection. While some have shown that vaccines administered intra-muscularly (IM) can elicit antibodies within the respiratory tract, it remains lower than what is elicited by infection within the respiratory compartment (119). Mucosal vaccines could also use pre-existing immunity against SARS-CoV-2 in a prime-boost strategy, which has shown promise in animal models (120). No mucosal vaccines for SARS-CoV-2 are currently approved for use in humans.

Morbidity & Long-COVID

Early in the pandemic, anecdotal reports emerged describing patients experiencing persistent and prolonged symptoms following SARS-CoV-2 infection (121, 122). Initially, this condition was referred to as "long COVID," and affected individuals "long haulers". More recently, the medical and scientific communities have formally recognized Post-Acute Sequelae of SARS-CoV-2 Infection (PASC)—also known as Chronic COVID Syndrome, post-COVID-19 Syndrome, or long-COVID as a diagnosis (123, 124). Large-scale epidemiological studies have revealed considerable variability in symptom presentation. The most reported symptoms include fatigue, muscle weakness, headache, shortness of breath, difficulty concentrating (brain fog), cough, loss of taste or smell, diarrhea, depression, anxiety, and chest pain (122). Less frequent but widely documented symptoms include intermittent fever, blurred vision, memory issues, sleep disturbances, skin conditions, and tinnitus (125, 126). Notably, multiple studies have observed a higher prevalence of PASC in women (125, 127, 128).

Although PASC presents significant clinical concerns, the phenomenon of post-viral syndromes is not new. Many well-studied pathogens are known to cause chronic symptoms in a subset of infected individuals (129-132). Similar reports of prolonged illness followed infections with MERS-CoV and SARS-CoV, despite viral clearance (133, 134). The underlying mechanisms

driving PASC remains undefined. Several areas of investigations are being pursued, including immune dysregulations (135, 136); reactivation of latent viruses such as Epstein-Barr virus (EBV) among others (137, 138); microbiota modification (139, 140); autoimmunity (141, 142); pro-coagulant state induced by infection (143) and among other hypotheses. Nonetheless, PASC represents a significant source of morbidity in some individuals following COVID-19.

1.4 Viral Immune Responses

Viruses constantly evolve to increase their replicative fitness, including acquiring mutations to evade immune responses (144). In response, the immune system has developed multiple layers and strategies to detect and control viral infections. These intricate defense mechanisms play crucial roles in determining the severity and outcome of an infection. The immune response to SARS-CoV-2 involves a complex interplay between innate and adaptive immunity. While the immune system is essential for clearing viral infections, in some cases, these same immune responses can be detrimental (e.g., hyperinflammation, cytokine storm), highlighting the importance of their regulation (145, 146). Furthermore, several environmental factors, such as demographic characteristics, comorbidities, and exposure to other pathogens, influence the effectiveness and breadth of these immune responses (147-149). A deeper understanding of host immune responses in the context of SARS-CoV-2 remains critical for developing more effective therapeutic strategies and vaccines against SARS-CoV-2 and future emerging coronaviruses.

Innate Immunity

The innate immune system serves as the first line of defense when a virus establishes infection. Broadly, various components of this immune arm can limit viral genome replication, restrict viral gene translation, eliminate infected cells, and accelerate adaptive immune responses. To initiate these innate responses, the cell must first recognize the virus. This process is mediated by cellular receptors that detect pathogen-associated molecular patterns (PAMPs) and damage-associated molecular patterns (DAMPs) (150, 151). Several classes of receptors, such as RIG-I-like receptors

(RLRs), nucleotide-binding oligomerization domain (NOD)-like receptors (NLRs), and Toll-like receptors (TLRs), accomplish this (152).

In the context of SARS-CoV-2, viral RNA can be detected by TLR3, TLR7, and RLRs such as MDA5 and LGP2 (153-155). This recognition activates downstream signaling pathways, ultimately leading to the production of type I and III interferons (IFNs) (156). These signaling molecules play crucial roles in antiviral responses, including recruiting innate immune cell populations. Additionally, innate immune sensors can trigger cell death pathways, such as the activation of the NLRP3 inflammasome, leading to the release of bioactive IL-1β and IL-18 and the cleavage of gasdermin D (GSDMD), resulting in a form of cell death called pyroptosis (157). Other sensors, including AIM2, IFI16, and cGAS, have also been identified as critical for detecting viral signatures during infection (158).

Beyond the responses of non-immune cells in restricting viral infections and releasing cytokines, innate immune cells play a significant role in controlling infection directly or by coordinating with the adaptive immune system. For example, macrophages are crucial for phagocytosing infected cells and releasing inflammatory cytokines such as IL-6, TNF-α, and IL-1β (159, 160). Natural killer (NK) cells are essential for eliminating infected cells, thereby promoting viral clearance (161). Dendritic cells, another key type of innate immune cell, act as a bridge between innate and adaptive immunity by functioning as antigen-presenting cells (APCs) (162).

Notably, innate immune cells contribute significantly to the release of pro-inflammatory cytokines. The production of these cytokines by both immune and non-immune cells in response to viral detection, infection-induced cell death, or immune-mediated mechanisms can lead to an uncontrolled inflammatory cascade, commonly referred to as a cytokine storm—one of the hallmarks of severe COVID-19 (146, 163). Therefore, the regulation of innate immune responses over time is critical for maintaining host health.

Adaptive Immunity

Following the initiation of the immune response by the innate immune system, the adaptive immune system plays a crucial role in further clearing the virus, establishing memory, and providing long-term protection. Adaptive immunity is divided into cellular immunity, mediated by T cells, and humoral immunity mediated by B cells and antibodies. Both T and B lymphocytes undergo a complex maturation process to generate highly specific T cell receptors (TCRs) and B cell receptors (BCRs) that recognize epitopes on the virus or infected cells (or antigens expressed on cells following immunization) with high specificity (164, 165).

T cells are classified into two major groups: CD4+ and CD8+ T cells. CD8+ cytotoxic T cells play a critical role in cellular immunity by recognizing viral peptides presented on MHC class I molecules and killing infected cells (166, 167). Because T cells recognize a wide variety of viral peptides, independent of native viral protein folding, CD8+ T cells are generally less susceptible to viral escape mutations (168). In contrast, CD4+ T cells do not have cytotoxic functions but are essential for B cell activation and CD8+ cytotoxic T cell proliferation (169). CD4+ helper T cells recognize viral peptides presented on MHC class II molecules of B cells via their TCRs, leading to cytokine production and signaling that support B cell activation and promote antibody production (169, 170). Other subpopulations of CD8+ and CD4+ T cells contribute to establishing immunity, immunological memory, and coordination of adaptive responses (171).

Humoral immunity is primarily mediated by B cells, which are responsible for generating antibodies with high affinity and specificity for viral proteins. B cells originate in the bone marrow, where naïve B cells eventually enter circulation (164). Upon infection, naïve B cells interact with CD4+ helper T cells in germinal centers, triggering their proliferation, class-switch recombination at the immunoglobulin locus, and affinity maturation of secreted antibodies (170). These processes result in the formation of a large population of B cells expressing high affinity immunoglobulins. Some of these B cells differentiate into plasma cells that actively secrete antibodies, while others become part of the memory B cell population or develop into long-lived plasma cells, both of which are essential for protection against future reinfection (170).

Antibody-Mediated Immunity

Antibody-mediated immunity plays an integral role in clearing SARS-CoV-2 infection and providing subsequent protection. Antibodies contribute to immunity through several mechanisms. First, neutralization refers to the ability of certain antibodies to prevent viral attachment and or entry into host cells. In the case of SARS-CoV-2, neutralizing antibodies bind to the spike protein, blocking its interaction with the ACE2 receptor (172). Most neutralizing epitopes on the spike protein are located in the receptor-binding domain, though some neutralizing antibodies target other regions of the spike (173).

Second, antibodies mediate effector functions through their Fc domain. These Fc-dependent effector mechanisms include antibody-dependent cellular cytotoxicity (ADCC), antibody-dependent cellular phagocytosis (ADCP), and complement activation, which occur through interactions with Fc receptors (FcRs) on innate immune cells (174). The function of antibodies is further shaped by their isotype, influencing both neutralization capacity and Fc effector activity. Immunoglobulin G (IgG) is the predominant antibody isotype in circulation in blood and plays a key role in long-term immunity. Immunoglobulin A (IgA), particularly dimeric secretory IgA, is crucial for mucosal immunity and neutralization at the respiratory tract, where SARS-CoV-2 infection occurs (175). Immunoglobulin M (IgM) is especially prevalent early in the immune response and contributes to viral neutralization, although with a lesser efficacy than IgGs (176). Each of these antibody isotypes have their own intrinsic properties, such as stability and half-life in circulation, which influence the duration of protection.

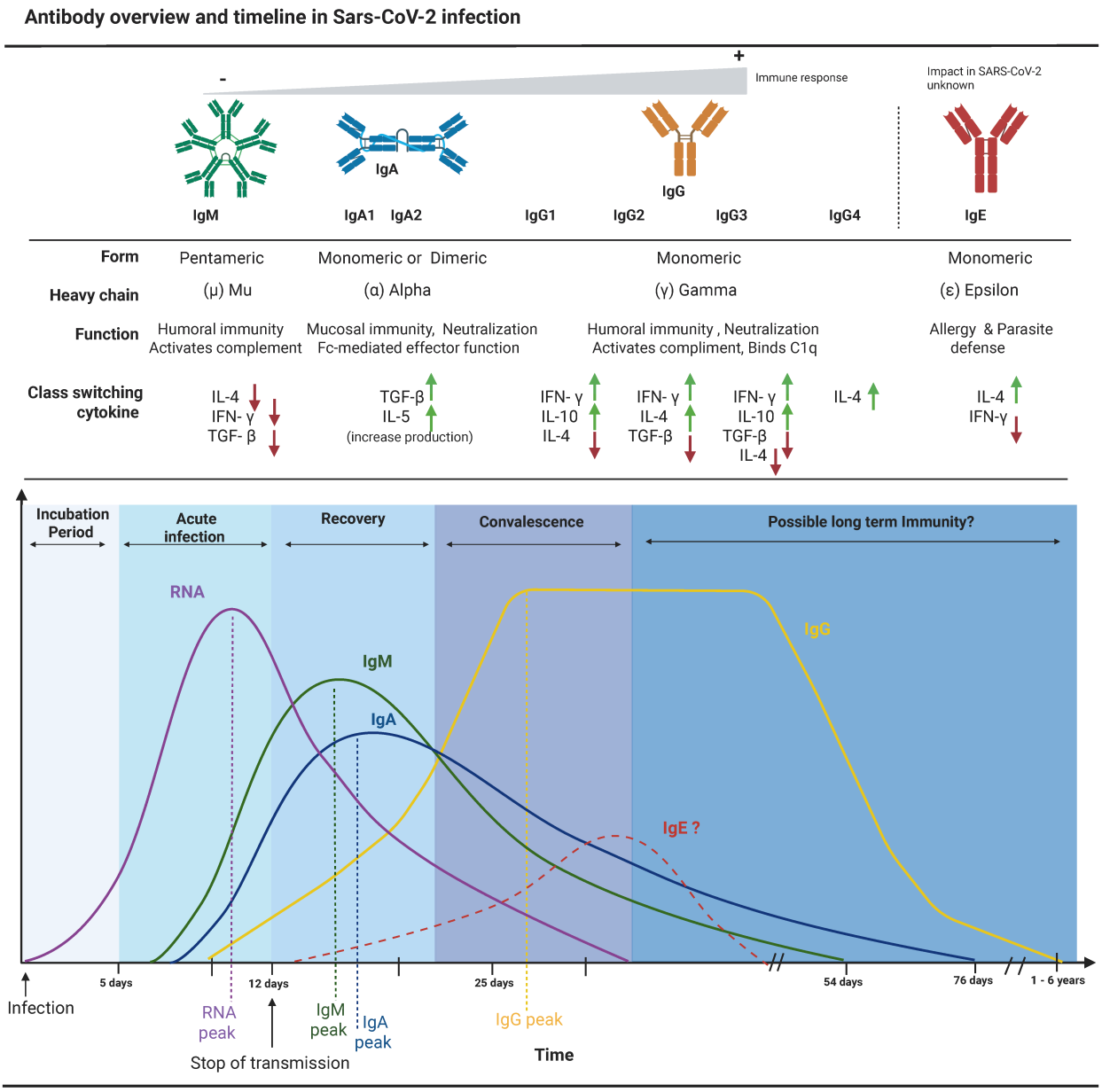


Figure 4: Overview of antibody isotype characteristics and dynamic following SARS-CoV-2 infection. This figure presents an overview of antibody isotype characteristics and their temporal dynamics following SARS-CoV-2 infection. It depicts the structure, associated heavy chain, and primary function of each isotype, along with cytokines involved in class switching. The timeline illustrates the typical appearance and decline of each isotype relative to viral RNA levels, based on current serological studies. Reproduced from Galipeau, Greig, Liu, Driedger, and Langlois (2020), under the terms of the Creative Commons Attribution License (CC BY 4.0). © 2020 Galipeau et al. Published in *Frontiers in Immunology*. https://doi.org/10.3389/fimmu.2020.610688.

Autoantibodies in SARS-CoV-2 infections

In the context of COVID-19, most patients experience mild to moderate symptoms, but a proportion of individuals develop severe or critical illness characterized by hyperinflammation, coagulopathy, and multi-organ dysfunction (177). These divergent clinical outcomes have spurred intensive research into the immunopathological mechanisms underlying COVID-19, including the role of autoimmunity. Accumulating evidence has demonstrated that SARS-CoV-2 infection can lead to the development of autoantibodies (178, 179). Autoantibodies are antibodies that recognize and bind self-proteins in individuals (180).

Several classes of autoantibodies have been reported in SARS-CoV-2 infections. Among the most studied are antinuclear antibodies (ANA), which target nuclear components such as DNA, histones, and RNA-binding proteins(181). ANA seroprevalence in COVID-19 patients varies widely, with elevated levels often associated with disease severity although low specificity limits their diagnostic value (182, 183). Anti-cytokine antibodies (ACAs), particularly those targeting type I interferons, have been implicated in severe COVID-19 (184). These autoantibodies can neutralize key cytokines, thereby impairing antiviral immunity. Their presence has been linked to adult-onset immunodeficiency and increased susceptibility to opportunistic infections (185, 186). Anti-phospholipid antibodies (APLAs), known for their role in thrombotic syndromes, have been observed in COVID-19-associated coagulopathy (187). While some studies link APLAs to thrombosis, others suggest they may be non-specific markers of severe illness (188, 189). Rheumatoid factors (RFs) have also been detected in SARS-CoV-2-infected individuals, with some evidence suggesting an association with increased disease severity (190, 191). Other autoantibody classes, including anti-citrullinated protein antibodies (ACPAs) and anti-neutrophil cytoplasmic antibodies (ANCAs), have been sporadically reported in COVID-19, though larger studies are needed to validate these findings (192, 193).

The presence of such autoantibodies raises important questions about the mechanisms through which SARS-CoV-2 may trigger a breakdown of immunological self-tolerance. Potential pathways include molecular mimicry, bystander activation, and epitope spreading processes that have been implicated in classical autoimmune diseases(142).

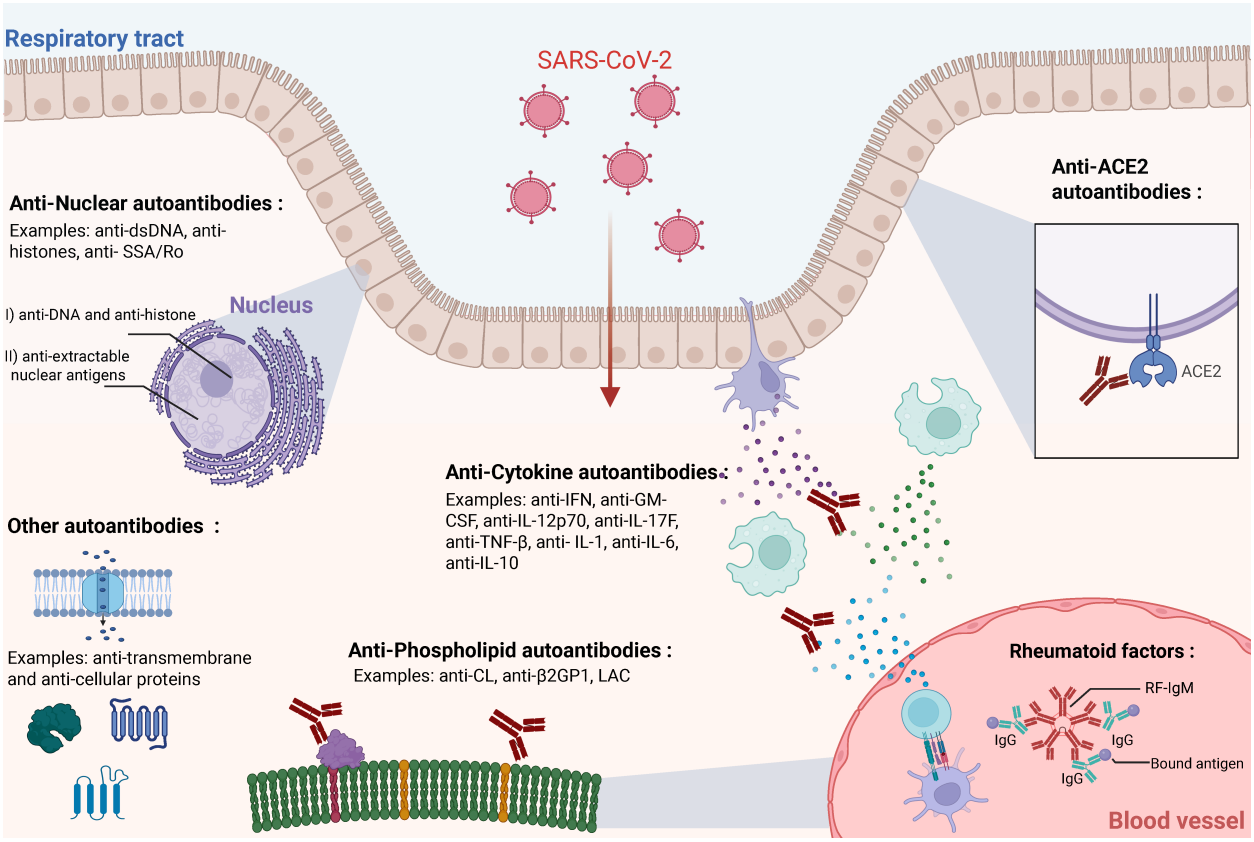


Figure 5. Overview of autoantibodies associated with SARS-CoV-2. Various types of autoantibodies have been associated with SARS-CoV-2 infection, including anti-ACE2, anti-cytokine antibodies (ACAs), antinuclear antibodies (ANAs), anti-phospholipid antibodies (APLAs), anti-ACE2 and rheumatoid factors (RFs). These autoantibodies can be detected in circulation and may act locally, such as at the respiratory epithelium the a primary site of viral infection. While IgG is the predominant isotype shown, IgM and IgA may also be involved. Reproduced from Galipeau, Cooper, and Langlois (2025), under the terms of the Creative Commons Attribution License (CC BY 4.0). © 2025 Galipeau, Cooper, and Langlois. This is an open-access article published in Frontiers in Immunology, https://doi.org/10.3389/fimmu.2024.1509289.

Understanding the origin, diversity, and pathogenic potential of autoantibodies in COVID-19 has implications in disease severity but also potentially for long-COVID also referred to as sequelae of COVID-19 (PASC). In this context, the study of autoantibody responses to SARS-CoV-2 provides a critical window into the intersection of infection and autoimmunity. Elucidating these

mechanisms is essential not only for improving the management of COVID-19 but also for advancing our broader understanding of virus-induced autoimmune phenomena.

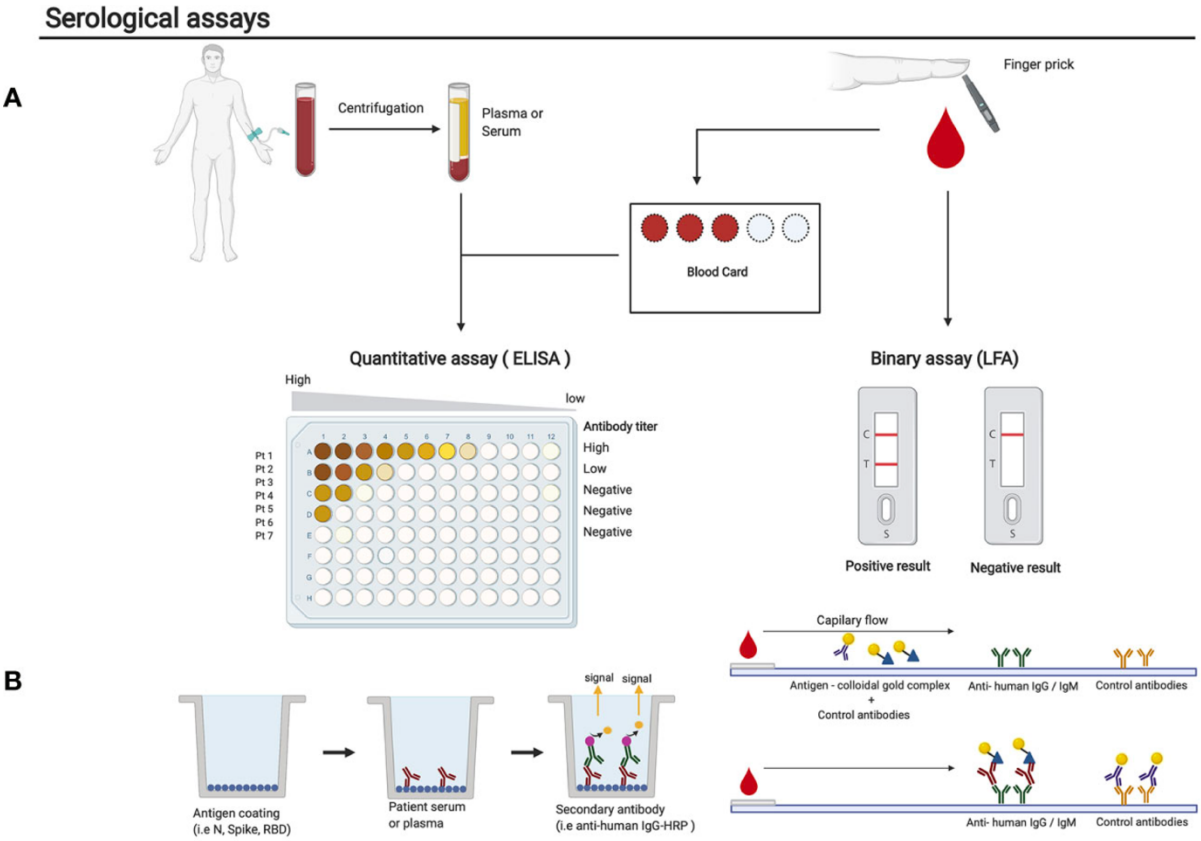
1.5 SEROLOGY

Serology is the study of antibodies in blood and other bodily fluids, primarily used to assess immune responses to infections, vaccinations, and autoimmune conditions. Serological assays detect and quantify antibodies, providing insights into prior viral exposure, immune protection, and population-level immunity (194). Several technologies have been developed, each with distinct applications.

Serological assays fall into two main categories. Enzyme-linked immunosorbent assays (ELISA) are widely used for their sensitivity, scalability and relative low cost. They can be easily automated and integrated with robotic equipment, making them ideal for high-throughput applications (195). Lateral flow assays (LFAs) are commonly used for rapid diagnostic testing, providing qualitative or semi-quantitative results, which make them well-suited for point-of-care applications (196).

While serology primarily quantifies antibodies, viral neutralization assays functionally measure the ability of antibodies to block viral entry and or attachment. Various laboratory strategies exist to assess neutralization efficiency, differing in speed and scalability (197). Plaque reduction neutralization tests (PRNTs) involve incubating a replicative virus with serial dilutions of a serum sample before applying it to a monolayer of susceptible cells (198). PRNTs are often regarded as the gold standard for neutralization studies due to their accuracy and specificity. However, they are labour intensive, and have significant limitations in speed and throughput. Additionally, depending on the pathogen, PRNTs may require high-level biocontainment laboratories, which are a limited resource. Pseudotyped virus neutralization assays offer a solution to the biocontainment challenges of PRNTs by using engineered viral particles that express the surface glycoproteins of the target virus but lack the ability to replicate (199). While these assays eliminate the need for high-level biosafety containment, they still require lengthy laboratory engineering and procedures and are not easily scalable. Protein-based neutralization assays use recombinant host and viral

receptors to measure the inhibition of binding in the presence of antibodies (200). These assays offer the greatest scalability and minimize biocontainment requirements and cost. However, their success depends on the proper identification and the successful production of recombinant host and viral receptors, which may not always be feasible.



C

	Quantitative assay (ELISA)	Binary assay (LFA)
Readout	Quantitative titer	Positive or negative
Usage	Laboratory assay	At home, clinic testing , POC
High throughput	Yes	No
Reliability	High / Moderate	Low
Cost	Low / Moderate	High

Figure 6 : Overview of serological assays approach and characteristics. LFAs and quantitative assays are compared for detecting antibodies. It outlines sample collection methods (venous blood for serum/plasma vs. finger prick for dried blood spots or direct use in LFAs), illustrates the basic procedures for ELISA (quantitative) and LFA (binary), and highlights the strengths and limitations of each approach. Reproduced from Galipeau, Greig, Liu, Driedger, and Langlois (2020), under the terms of the Creative Commons Attribution License (CC BY 4.0). © 2020 Galipeau et al. Published in *Frontiers in Immunology*. https://doi.org/10.3389/fimmu.2020.610688.

Serology and pandemic response

Sero-surveillance is a key component of an effective pandemic response due to their critical role in monitoring antibody responses following infection and vaccination. Throughout the COVID-19 pandemic, these assays had to be continuously adapted to reflect the evolving epidemiological landscape. Initially, serological assays were designed solely to detect antibodies resulting from SARS-CoV-2 infection, making the identification of prior infections relatively straightforward (201). However, the widespread rollout of SARS-CoV-2 vaccines, which primarily elicit antibodies targeting the spike (S) protein, necessitated adjustments in serological surveillance. Specifically, traditional serosurveys had to be refined to distinguish between vaccine-induced and infection-induced immunity. This was achieved by incorporating measurements of antibodies targeting the viral nucleocapsid (N) protein alongside those targeting the spike protein (195). Such differentiation is crucial for informing public health strategies, accurately evaluating the burden of infection in immunized populations and identifying breakthrough infections.

By employing assays that detect antibodies against both the spike and nucleocapsid proteins, and by collecting detailed vaccination histories, serosurveys can yield critical public health insights (202). These include estimates of the population-level burden of prior infection, the extent of vaccine-induced immunity, and the frequency of breakthrough infections. Such data inform decisions about where to target public health interventions and how to allocate limited resources, such as vaccines more effectively, which is particularly important in the context of a pandemic (202).

Moreover, as SARS-CoV-2 antigens continue to evolve, serological assays and serosurveys must be updated accordingly across diverse populations. For instance, the emergence of various variants of concern (VOCs) led to a decline in the protection afforded by initial vaccination series (20). Ongoing serological monitoring enables public health agencies, vaccine manufacturers, and the broader scientific community to design updated vaccines and adjust immunization strategies, ultimately ensuring that protective immunity is maintained across the population.

High-throughput considerations for serology

The rapid global spread of the virus posed unique challenges to the development and deployment of reliable, scalable serological assays. One of the primary challenges in SARS-CoV-2 serology has been the need to distinguish between different classes of antibodies (IgG, IgM, IgA), and to determine their specificity to key viral antigens such as the spike (S), receptor-binding domain (RBD), and nucleocapsid (N) proteins. Early in the pandemic, many assays varied in performance, with issues related to sensitivity, specificity, and cross-reactivity with other human coronaviruses. These inconsistencies complicated data interpretation, especially when used for public health decisions or estimates of population seroprevalence. As such, reliable serological assays can measure several classes of isotype antibodies over several SARS-CoV-2 specific antigens while accounting for cross-reactivity from seasonal coronaviruses.

Another major limitation was the scale at which testing needed to occur. Traditional serological platforms such as ELISA are robust and well-validated but can be labour-intensive and less amenable to high-throughput processing without significant automation. In the context of large-scale epidemiological studies, often involving thousands to hundreds of thousands of participants and samples there was a significant need for assays that were not only accurate but also scalable, reproducible, and cost-effective.

High-throughput serological platforms emerged as a critical solution to this challenge. Some approaches include multiplex bead-based immunoassays, protein microarrays, and automated ELISAs. These platforms allowed simultaneous testing of multiple antibody targets using small sample volumes. Their scalability enabled broad surveillance efforts to assess seroprevalence, vaccine response, and waning immunity over time across diverse populations. Importantly, they also supported longitudinal studies, helping to monitor immune dynamics at the population level and to inform vaccine strategy and policy.

While automated ELISA platforms offer significant advantages in scalability and throughput, their implementation presents several technical challenges. One key limitation is the small reaction volume required in high-density formats such as 384-well plates, which can increase variability

and reduce signal-to-noise ratios, particularly for low-abundance analytes. Additionally, well-to-well bleedthrough or edge effects can compromise assay fidelity, especially when high-signal samples are adjacent to negative or low-signal wells. The integration of robotic liquid handlers, plate washers and plate readers requires careful optimization and calibration to ensure consistent pipetting accuracy and reproducibility across large runs. Initial setup of automated workflows often involves extensive troubleshooting, including adapting existing protocols to smaller volumes and ensuring compatibility with robotic hardware. These technical hurdles must be carefully managed to maintain assay sensitivity, precision, and data quality in high-throughput applications. Further, this needs to be accompanied by a data analysis and management pipeline that can account for inter-plate variability and longitudinal variability.

Addressing the need for reliable, high-throughput testing platforms was essential to support large-scale studies and generate meaningful epidemiological insights during the COVID-19 pandemic. These innovations have not only informed our understanding of COVID-19 but also laid the groundwork for improved serological surveillance in future outbreaks.

.

RATIONALE, HYPOTHESIS AND OBJECTIVES

RATIONALE

The development of reliable serological assays is a priority for pandemic responses. Identifying antibody responses to a novel pathogen provides critical information for containing a pandemic and developing successful vaccines. Unlike molecular testing methods (e.g., RT-PCR), serological methods do not require sampling within the acute infection window. This enables retrospective measurements of SARS-CoV-2 prevalence across various communities. These data on SARS-CoV-2 burden help inform and assess the impact and effectiveness of public health measures.

Furthermore, serological assays provide a direct means to investigate humoral responses to SARS-CoV-2, guide vaccine development, and evaluate vaccine effectiveness in populations. For example, neutralizing antibodies are, at the moment, the best predictor of protection. As such, serological and neutralization assays can estimate immunity within certain high-risk groups, such as the elderly and individuals with a high burden of comorbidities. Data on immunogenicity can also inform vaccine schedules and the immune-evasive properties of viral variants.

A proper understanding of humoral responses, combined with a flexible serological platform, can also aid in the development of next-generation vaccines, such as intranasal/ mucosal vaccines, and can be repurposed to study related viruses (e.g., seasonal coronaviruses, influenza, and RSV). These assays also offer opportunities to investigate autoimmunity, particularly autoantibodies, which have long been linked to viral infections.

Overall, humoral responses are intricately influenced by both population-level and host-specific factors, as well as by viral characteristics such as mutation rate, pathogenicity, and host-pathogen interactions. Thus, a better understanding of how SARS-CoV-2 and other coronaviruses evolve is critical for advancing our knowledge of antibody-mediated immunity.

HYPOTHESIS

We hypothesize that measuring antibody responses and neutralization efficiency to SARS-CoV-2 by developing reliable and high-throughput serological assays will enable a better understanding of host factors and viral factors that influence humoral responses.

OBJECTIVES

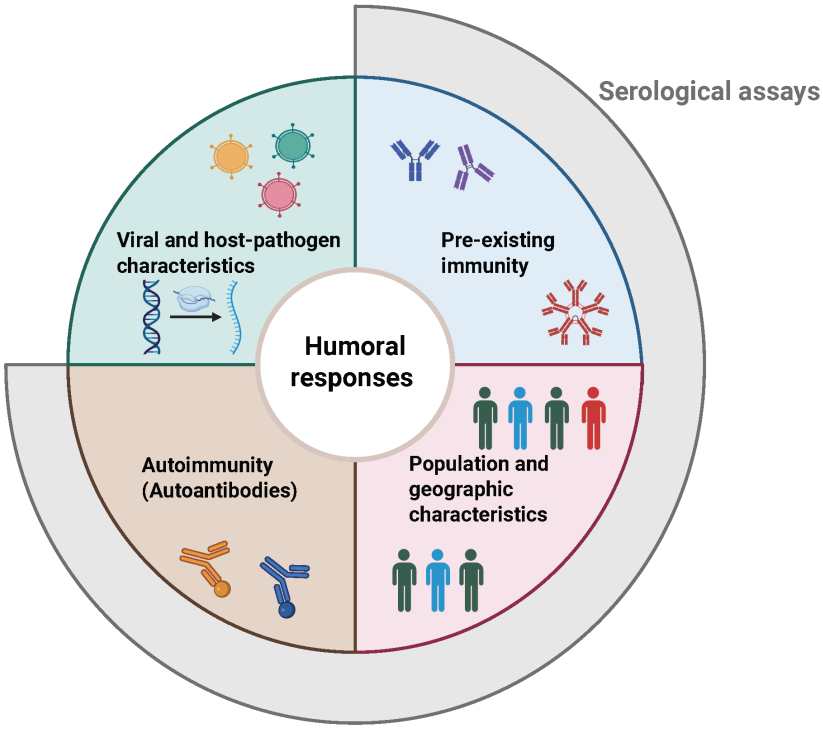
1. Development of high-throughput serological assays that are highly specific and sensitive to SARS-CoV-2. Further, these assays need to accommodate both serum, plasma and dried-blood spots. (Chapter 2)

2. Implementation of serological assays in large sero-epidemiological studies to understand how demographic and population characteristics impact SARS-CoV-2 humoral responses. (Chapter 3)

3. Investigate how pre-existing immunity to seasonal coronaviruses influence the neutralization efficiency of SARS-CoV-2. (Chapter 4)

4. Investigate the role and prevalence of ACE2 autoantibodies in the context of SARS-CoV-2. (Chapter 5)

5. Study the evolution of SARS-CoV, SARS-CoV-2 and MERS-CoV in an *in vitro* system, and better understand how viral evolution impacts the host-transcriptomic response. (Chapter 6)



Graphical abstract : : This PhD thesis investigates factors that influence and shape humoral responses in the context of SARS-CoV-2. This includes the development of serological assays to study how populational and demographic characteristics, pre-existing immunity, and autoantibodies shape humoral responses. In addition, viral and host-pathogen characteristics were also studied.

CHAPTER 2 – DEVELOPMENT OF SEROLOGICAL ASSAYS

RATIONALE

The development of robust serological assays for SARS-CoV-2 was a priority upon the emergence and spread of SARS-CoV-2 globally. In early 2020, large efforts were deployed to sequence the virus and identify its human receptor. This set the stage to produce several viral proteins recombinantly, enabling their use in the development of serological assays and protein-based neutralization assays.

While simple serological assays are of value, assays that are scalable and high-throughput were needed. Indeed, to support a large number of studies and to investigate large populations during the pandemic, a high-throughput automated SARS-CoV-2 serological platform was developed, along with an analysis pipeline to manage data and perform the normalization and quality control assessments required for large-scale serological studies. Furthermore, the assays needed to accommodate not only serum and plasma (the gold standard), but also dried blood spot samples, which can be collected without phlebotomy or direct contact with healthcare professionals. As such, significant research and development efforts were required to establish production systems for antigens, develop the serological assays, and build the necessary data management and analysis pipelines.

The following studies presented in this chapter describe the development of the serological assays used in subsequent studies presented in this thesis (section 2.1) and the performance of serum and plasma in serological assays and their implications for study design (section 2.2). Further, the evaluation of these assays against various commercial and in-house platforms across Canada are presented in Appendix A-1.24 and A-1.25.

2.1 A SCALABLE SEROLOGY SOLUTION FOR PROFILING HUMORAL IMMUNE RESPONSES TO SARS-COV-2 INFECTION AND VACCINATION

Preface

(This work has been previously published as a research article)

Colwill, K., **Galipeau, Y**., Stuible, M., Gervais, C., Arnold, C., Rathod, B., Abe, K.T., Wang, J.H., Pasculescu, A., Maltseva, M., Rocheleau, L., Pelchat, M., Fazel-Zarandi, M., Iskilova, M., Barrios-Rodiles, M., Bennett, L., Yau, K., Cholette, F., Mesa, C., Li, A.X., Paterson, A., Hladunewich, M.A., Goodwin, P.J., Wrana, J.L., Drews, S.J., Mubareka, S., McGeer, A.J., Kim, J., Langlois, M.-A., Gingras, A.-C. and Durocher, Y. (2022), **A scalable serology solution for profiling humoral immune responses to SARS-CoV-2 infection and vaccination**. Clin Transl Immunol, 11: e1380. https://doi.org/10.1002/cti2.1380

© 2022 The Authors. *Clinical & Translational Immunology* published by John Wiley & Sons Australia, Ltd on behalf of Australian and New Zealand Society for Immunology Inc.

This is an open access article under the terms of the Creative Commons Attribution-NonCommercial License, which permits use, distribution and reproduction in any medium, provided the original work is properly cited and is not used commercially.

Abstract

Objectives
Antibody testing against severe acute respiratory syndrome coronavirus 2 (SARS-CoV-2) has been instrumental in detecting previous exposures and analyzing vaccine-elicited immune responses. Here, we describe a scalable solution to detect and quantify SARS-CoV-2 antibodies, discriminate between natural infection- and vaccination-induced responses, and assess antibody-mediated inhibition of the spike-angiotensin converting enzyme 2 (ACE2) interaction.

Methods
We developed methods and reagents to detect SARS-CoV-2 antibodies by enzyme-linked immunosorbent assay (ELISA). The main assays focus on the parallel detection of immunoglobulin (Ig)Gs against the spike trimer, its receptor binding domain (RBD) and nucleocapsid (N). We automated a surrogate neutralisation (sn)ELISA that measures inhibition of ACE2-spike or -RBD interactions by antibodies. The assays were calibrated to a World Health Organization reference standard.

Results
Our single-point IgG-based ELISAs accurately distinguished non-infected and infected individuals. For seroprevalence assessment (in a non-vaccinated cohort), classifying a sample as positive if antibodies were detected for ≥ 2 of the 3 antigens provided the highest specificity. In vaccinated cohorts, increases in anti-spike and -RBD (but not -N) antibodies are observed. We present detailed protocols for serum/plasma or dried blood spots analysis performed manually and on automated platforms. The snELISA can be performed automatically at single points, increasing its scalability.

Conclusions
Measuring antibodies to three viral antigens and identify neutralising antibodies capable of disrupting spike-ACE2 interactions in high-throughput enables large-scale analyses of humoral immune responses to SARS-CoV-2 infection and vaccination. The reagents are available to enable scaling up of standardised serological assays, permitting inter-laboratory data comparison and aggregation.

Introduction

The severe acute respiratory syndrome coronavirus 2 (SARS-CoV-2) pandemic has already induced four major waves of infection in Canada, resulting in > 3.2M confirmed infections and > 36K deaths (as of 25 February 2022).[1] Overall seroprevalence estimates from natural infection during the pre-Omicron waves were relatively low compared to other countries,[2, 3] and protecting the population from coronavirus disease of 2019 (COVID-19) has therefore heavily relied on vaccination. Fortunately, the dramatic acceleration of vaccination in Canada over the past 8 months has decreased symptomatic infections, severe disease, and deaths;[4] as of 18 February 2022, 84% of the population 5 years and older were fully vaccinated.[5]

However, several important questions remain regarding both infection- and vaccination-induced humoral immunity, including the duration and decay of the immune response, the generation of functional neutralising antibodies, and the overall differences in humoral responses across groups of individuals with different co-morbidities or following vaccination with different brands and regimens. This information can help guide and prioritise public health programs, such as vaccine booster schedules.[6]

Plate-based enzyme-linked immunosorbent assays (ELISAs) are widely used scalable methods to quantitatively assess antibody responses to pathogens, including SARS-CoV-2. Microwells are coated with recombinant SARS-CoV-2 protein antigens, and biofluid samples (e.g. serum, plasma, main

eluate, or saliva) are added (Figure 1a). If antibodies that recognise the antigen are present, they are detected with a secondary antibody, typically linked to an enzyme (such as horseradish peroxidase (HRP)) that elicits a measurable change upon addition of a colorimetric or chemiluminescent substrate.

Because of their potent immunogenicity, antigens derived from the SARS-CoV-2 spike and nucleocapsid (N) proteins have been most frequently used in serological assays, including those developed by commercial vendors. Full proteins, protein segments, and even peptides have been used in these assays which, combined with their different formats and readouts, yield distinct sensitivity and specificity profiles. This can lead to confusion in interpreting results. For example,

conclusions about the persistence of antibodies to the nucleocapsid (N) protein differ depending on the platform used, and commercial vendors often do not disclose the exact amino acid sequence of their antigens.[7]

We have previously used ELISAs to show that immunoglobulin (Ig)G (but not IgM or IgA) against SARS-CoV-2 spike, receptor binding domain (RBD), and N can persist for at least 3–4 months in the serum and saliva of individuals with COVID-19,[8] an observation now corroborated and extended by several other studies describing the persistence of circulating IgGs up to 13 months (although with gradual declines; e.g. Sherina *et al.*,[9] Dan *et al.*,[10] Gallais *et al.*,[11] Feng *et al.*[12]). We also showed that the production of neutralising antibodies capable of preventing interactions between spike (or its RBD) and its target angiotensin converting enzyme 2 (ACE2) could be monitored using a plate-based surrogate neutralisation (sn)ELISA.[13] We demonstrated good correlations between this assay and both spike-pseudotyped lentiviral and authentic SARS-CoV-2 plaque neutralisation assays, suggesting that this could provide a scalable and suitable alternative to costly and labour-intensive classical antibody neutralisation assessment.

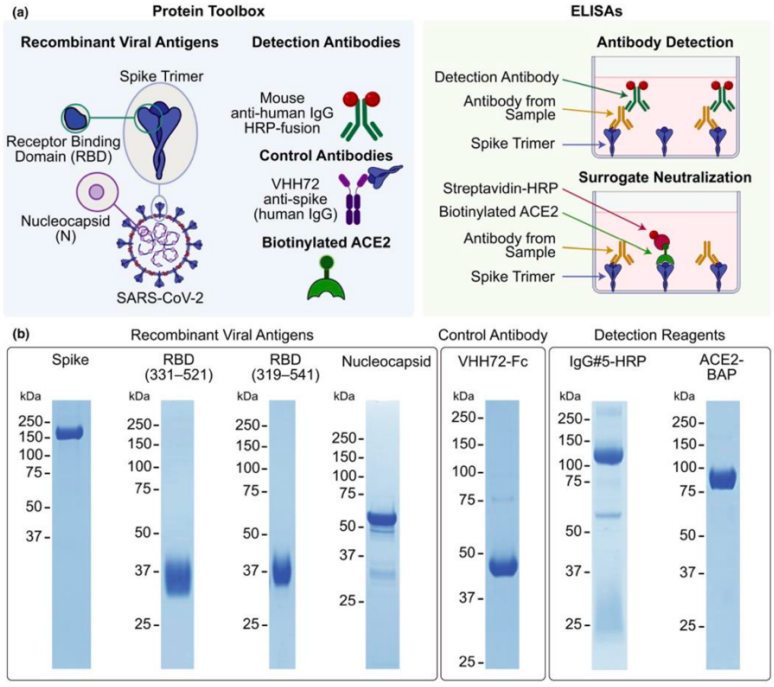


Figure 1 - High-quality reagents for SARS-CoV-2 serology. (a) Reagents comprising the protein toolbox (left panel) are used in high-throughput plate-based ELISAs for antibody detection and surrogate neutralisation (right

panel). **(b)** The reagents were analyzed on Coomassie-stained polyacrylamide gels under reducing conditions to assess their purity. Molecular weight markers (kDa) are shown to the left of the gels.

While laboratory-based ELISAs like ours have been developed around the world, the various sources of antigens and antibodies used by different groups (in addition to batch-to-batch variation within groups) impede national and international comparisons of seroprevalence and vaccine effectiveness. This is further challenged by the lack of agreed-upon reference standards, with the exception of pools of convalescent plasma distributed through the World Health Organization (WHO) to calibrate assays to standardised units.[14] Furthermore, assay performance variability over time remains incompletely examined. To address this, we have developed a reproducible and scalable SARS-CoV-2 serology solution using standardised protein reagents and protocols (Figure 1) and independent automated platforms in two Canadian laboratories in Toronto and Ottawa. This system has now been used to profile > 150K unique samples, demonstrating its scalability and robustness. Importantly, these reagents and protocols are available to the research community to enable implementation of these assays across laboratories.

Results

Reagent production

To facilitate comparison of SARS-CoV-2 serology results across Canada, we sought to develop and validate a scalable ELISA-based assay that leverages the mammalian protein expression expertise of the National Research Council of Canada (NRC) Human Health Therapeutics Research Centre. We optimised the production and purification of SARS-CoV-2 proteins (spike trimer, spike RBD, and N from the original Wuhan-Hu-1 strain) to generate large-scale high-purity batches of antigens (Figure 1b, Supplementary figures 1 and 2, Supplementary table 1). These were fused with purification tags ($(His)_6$ and FLAG, with or without a Twin Strep-tag) and were expressed in Chinese Hamster Ovary (CHO) cells either as stably transfected pools (spike) or through transient transfection (RBD, N).[8, 15] Antigens were purified by immobilised metal affinity chromatography (IMAC), with one or two additional purification steps performed for RBD and N (StrepTrap XT columns and/or preparative size exclusion chromatography, SEC). The spike and RBD proteins were highly pure when analyzed by SDS-PAGE (Figure 1b). By analytical SEC,

spike eluted as a major (> 95% integrated area) symmetrical peak of 490 kDa (consistent with its trimeric structure) with < 3% hexamers/aggregates, and both versions of RBD (encoding amino acids 319–541 and 331–521, respectively) eluted as single peaks with > 95% integrated area. For purified N, some truncated forms were visible by SDS-PAGE/Coomassie staining; however, by SEC, it eluted as a major (> 99% integrated area) peak with no apparent larger aggregates. Estimation of molecular weight of N was not possible by multiangle light scattering (MALS), but based on the SEC elution volume, it appears to be ~300 kDa. This is consistent with the formation of tetramers or hexamers by recombinant coronavirus N, as reported by others.[16] For recombinant protein production in CHO cells, post-purification yields ranged from 25 mg L^{-1} for RBD 331–521 to 370 mg L^{-1} for spike (Supplementary table 1).

The antigen toolbox was supplemented with a detection reagent, namely, an anti-human IgG monoclonal antibody (IgG#5) expressed as a HRP fusion in-frame to the heavy chain (HC) C-terminus. This reagent was developed to address an issue common to HRP-based detection reagents from commercial sources, which are usually polyclonal anti-IgG antibodies conjugated to HRP post-purification. These commercial reagents display variability due to the nature of the polyclonal serum used by each supplier, as well as the ratio of conjugated HRP molecules per antibody. IgG#5 was produced by co-transfecting HC and light chain (LC) expression vectors in CHO cells. As shown in Figure 1, the purified antibody consists of a predominant band at ~110 kDa, which represents the full-length HC-HRP fusion peptide. A minor band at ~55 kDa is likely a form of the HC lacking HRP (confirmed by western blotting with an anti-mouse-Fc antibody (data not shown)), while the LC presents as a smear between 25 and 37 kDa. Because of this heterogeneity, purified IgG#5-HRP gave a convoluted profile by analytical SEC (Supplementary figure 1).

To have a common reference that enables intra- and inter-lab comparisons of SARS-CoV-2 antibody responses, we also generated recombinant anti-spike antibodies. Compared to pools of serum or plasma from convalescent patients, these offer the advantage of being renewable, scalable and defined in sequence. Three recombinant single-domain antibodies (VHHs) were selected: VHH72 is a SARS-CoV and SARS-CoV-2 cross-reactive antibody described in Wrapp *et al.*,[17] and NRCoV2-04 and -20 are SARS-CoV-2 spike-binding VHHs developed in-house at the NRC. All antibodies were produced in CHO cells and purified on a MabSelect SuRe

column. VHH sequences were fused at the C-terminus to Fc1X7 (an antibody-dependent cellular cytotoxicity (ADCC)-attenuated variant of human Fc) to produce dimeric proteins upon secretion from CHO cells. VHH72-Fc eluted as a single symmetrical peak of 102 kDa with < 2% aggregates, NRCoV2-04-Fc eluted with a major peak of 67% integrated area and a peak of 90 kDa, and NRCoV2-20-Fc as a single peak of 100 kDa with < 2% aggregates (Supplementary figures 1 and 2; Supplementary table 1). The toolbox was further supplemented with a biotinylated ACE2 protein (used for snELISA), which was purified on both IMAC and Strep-Tactin XT Superflow columns and elutes from SEC as a single peak of 90 kDa (Supplementary figure 1).

While the goal is to ultimately have a fully NRC-sourced protein toolbox, the current set of reagents is complemented by a commercial anti-N antibody to quantify the anti-N response (see Methods). As described below, the assays can also be repurposed for IgA/M monitoring with commercial secondary antibodies and matching reference antibodies for calibration.

Direct detection ELISA

We previously developed ELISAs in 96-well colorimetric or 384-wellchemiluminescent formats to assess the persistence of antibody responses.[8] This first version relied on small-batch research-grade or commercial reagents that are not readily scalable for nationwide surveillance studies. Here, we have first benchmarked the NRC reagents described above, and defined the optimal antigen and secondary antibody amounts in a 384-well automated format (see Methods). The NRC protein toolkit was independently optimised on automated platforms in Toronto (a Thermo Fisher Scientific F7 platform) and Ottawa (a Hamilton system), leading to minor variations in the optimal amounts of antigens and detection reagents, in part due to differences in the detectors on each system (Supplementary table 2). While the platforms can be used to generate full titration curves from serum samples, single-point measurements more readily enable scaling up to thousands of samples and have been used in most large-scale studies to date.

Toronto platform

The optimal dilution for single-point ELISAs was established using a 10-point four-fold titration series starting with 0.25 µL positive control serum per well (a 1:40 dilution, which is the amount used previously[8]; Supplementary figure 3). A prozone (hook) effect was noted at the 1:40 dilution for samples with higher antibody levels, suggesting that a lower concentration was desirable. We

performed receiver operating characteristic (ROC) analysis on a set of 300 negative pre-COVID19 samples (collected prior to November 2019) and 211 PCR-confirmed convalescent patients (> 14 days post-symptom onset) at three different concentrations (Supplementary figure 4), optimising for an amount of serum that would work with all three antigens. The 0.0625 µL per well serum condition was selected for single-point ELISA based on a reduced hook effect on spike (compared to the highest amount) and better specificity and sensitivity characteristics on its RBD (compared to the lowest amount). A final ROC analysis combining data from a second replicate at 0.0625 µL per well at a false positive rate of < 1% revealed sensitivities of 94%, 92%, and 81% for spike trimer, RBD, and N respectively (Table 1, Supplementary figure 4b). Importantly, replicates from experiments conducted 8 weeks apart were highly correlated ($\rho > 0.87$ for all three antigens, Figure 2a), similar to our previous observations,[8] giving us confidence in conducting large-scale cohort studies.

Table 1. ELISA performance statistics for plasma or serum IgG (Toronto)

	spike	**RBD**	**N**	**≥ 2 positive antigens**
ROC analysis				
AUC	0.978	0.974	0.964	n/a
Threshold (Cut Point)	0.195	0.073	0.349	n/a
FPR	0.009	0.009	0.009	0.000
TPR	0.944	0.921	0.811	0.931
3 SDs from the mean of the negative controls				
Threshold	0.190	0.186	0.396	n/a
FPR	0.011	0.000	0.007	0.000
TPR	0.944	0.890	0.786	0.912
Samples used to assess performance †				
Sample cohort	**Replicates**	**Number**	**Total**	
Patients with COVID-19	1	211	392	
	2	181		
Pre-COVID-19 (negative)	1	300 for N and spike, 296 for RBD	560	
	2	260 for N and RBD, 258 for spike		

†Negative samples were excluded from the analysis for spike and RBD if one replicate was positive.

Ottawa platform

Early optimisations of the serological assay to identify the serum dilution within a linear range with the lowest non-specific reactivity to the negative serum were performed using the manual colorimetric ELISA (Supplementary figure 5). The colorimetric assay was used to test the performance of the HRP-conjugated antibodies, including six different anti-human IgG conjugate antibodies provided by the NRC (Supplementary figure 6a) with different characteristics and enzyme conjugation strategies (e.g. HRP fusion vs conjugation). While all candidates offered good detection, IgG#5—a direct HRP fusion—was selected for further assays, based on its superior quantitative capacity and extremely low non-specific reactivity within a standard reaction time (Supplementary figure 6b). This reagent was also compared to commercial polyclonal and monoclonal secondary antibodies for the detection of anti-spike, -RBD and -N IgG in DBS samples (see below and Supplementary figure 7c). While all antibodies correctly identified negative and positive DBS samples, IgG-#5-HRP offered the greatest distinction between the negative and positive distributions. To maintain a high level of specificity, the secondary antibody concentration and the nature of substrate were modified between the manual and automated ELISAs (see Supplementary table 2 for the final concentrations).

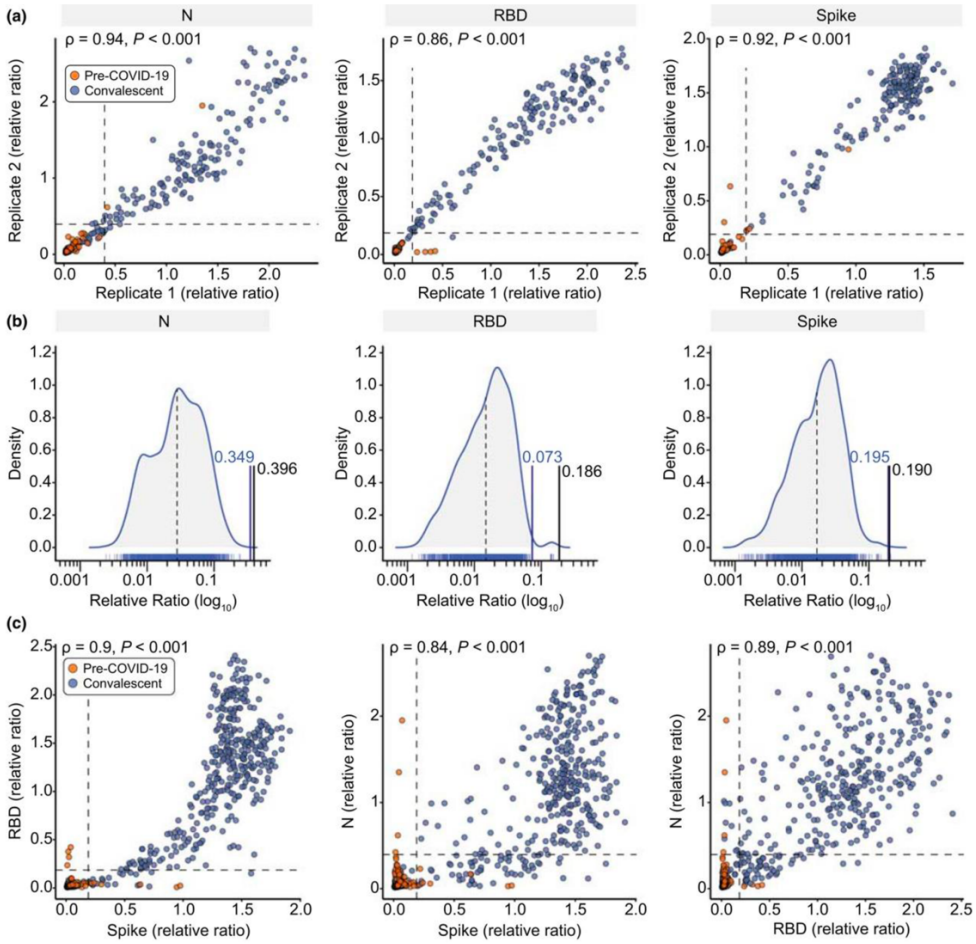


Figure 2- Development of high-throughput ELISAs for plasma or serum. (a) Known negative (pre-COVID-19) and positive (confirmed convalescent) samples (0.0625 µL/well) were tested in an automated antibody detection ELISA in two separate replicates 7 weeks apart. Spearman correlations are noted. **(b)** Density distributions of negative samples were plotted for each antigen. The black lines represent the mean of the negative distribution (dotted) and three SDs from the mean (solid; the relative ratio is indicated). The blue line represents the thresholds established by ROC analysis. **(c)** Comparison of the antigens with a set of known negative and positive samples at 0.0625 µL/well. Spearman correlations are shown. For both **a** and **c**, dashed lines represent the thresholds as defined by the 3-SD negative distribution shown in **b** and listed in Table **1**.

Setting positivity thresholds in seroprevalence studies

One concern with establishing thresholds based on a single sample set is that over time and with variations in sample type (e.g. venipuncture vs. capillary blood collection, different collection tubes and handling conditions), the background of the assay may change, affecting the threshold for reporting positives. In Toronto, we monitored the negative controls (blanks, pre-COVID-19 negative sera, commercially purified IgG, $n = 1320$ for spike and 1248 for N and RBD) used in 23 experiments conducted over 4 months. We calculated a threshold of 3 SDs from the mean of the log distribution of these controls and compared it to the thresholds established by ROC analysis (Figure 2b). The thresholds were very similar for N and spike, but the 3 SD range was more stringent for the RBD, decreasing the likelihood of false positive calls. We therefore adopted a threshold of 3 SDs from the mean of these controls for each antigen and recalculated our performance characteristics (Table 1). At this threshold, the specificity for RBD increases to 100% with a slight decrease in sensitivity to 89%, spike retained the same sensitivity and specificity (99% and 94%, respectively), whereas N's sensitivity decreased from 81% to 79% with 99% specificity. The same strategy was applied to IgM and IgA to define stringent thresholds (Supplementary figure 8, Supplementary table 3, see Methods for Ottawa).

Even with these conservative thresholds, an unacceptable number of false calls may be made in low seroprevalence situations (as in Canada, particularly during the first waves of infection). This is shown by the negative samples (red dots in Figure 2a) that passed the thresholds in individual assays. Importantly, these pre-COVID negatives were only ever positive in one test, in contrast to true positives, which tended to pass the positivity thresholds of ≥ 2 tests, consistent with the high correlation between the assays ($\rho > 0.84$ for all three combinations, with the highest correlation between spike and its RBD; Figure 2c). Our final determination of sample positivity in seroprevalence settings therefore requires that it exceeds the thresholds of at least 2 out of 3 antigens. As can be seen in Figure 2c, this strategy eliminates the false positive calls for the individual antigens (red dots) while retaining similar sensitivity (combined specificity of 100% and sensitivity of 91%).

Harmonisation between platforms and testing the WHO standards

To compare our ELISA-based assays with others, we tested them using WHOinternational reference panel 20/268, composed of five samples (Negative, Low, Mid, High, and Low S/High

N; Figure 3, Supplementary figure 9) and expressed the results in BAU mL^{-1} by comparing signals to the WHO International Standard (20/136). For this, we used single-point measurements from dilutions that were within the linear range of the international standard curve (Toronto) or the median of three dilutions (Ottawa). For all five samples, the median results from both labs were highly correlated ($\rho = 1$ for spike and N, 0.9 for RBD) and were between 0.5–2 fold of the geometric mean (red line with half arrows) reported in a multi-lab comparison by WHO.[14] Importantly, by applying a conversion formula to our relative ratios for expression in BAU mL^{-1} (Figure 3d, Supplementary table 4), our results can be readily compared to other national or international efforts. Using this formula, plasma or serum seropositivity thresholds for IgG are 34, 31 and 11 BAU mL^{-1} for nucleocapsid, RBD, and spike respectively (Toronto). When samples are diluted 1:2560, the assays can detect values up to 5344, 4454 and 1501 BAU mL^{-1} for N, RBD and spike respectively.

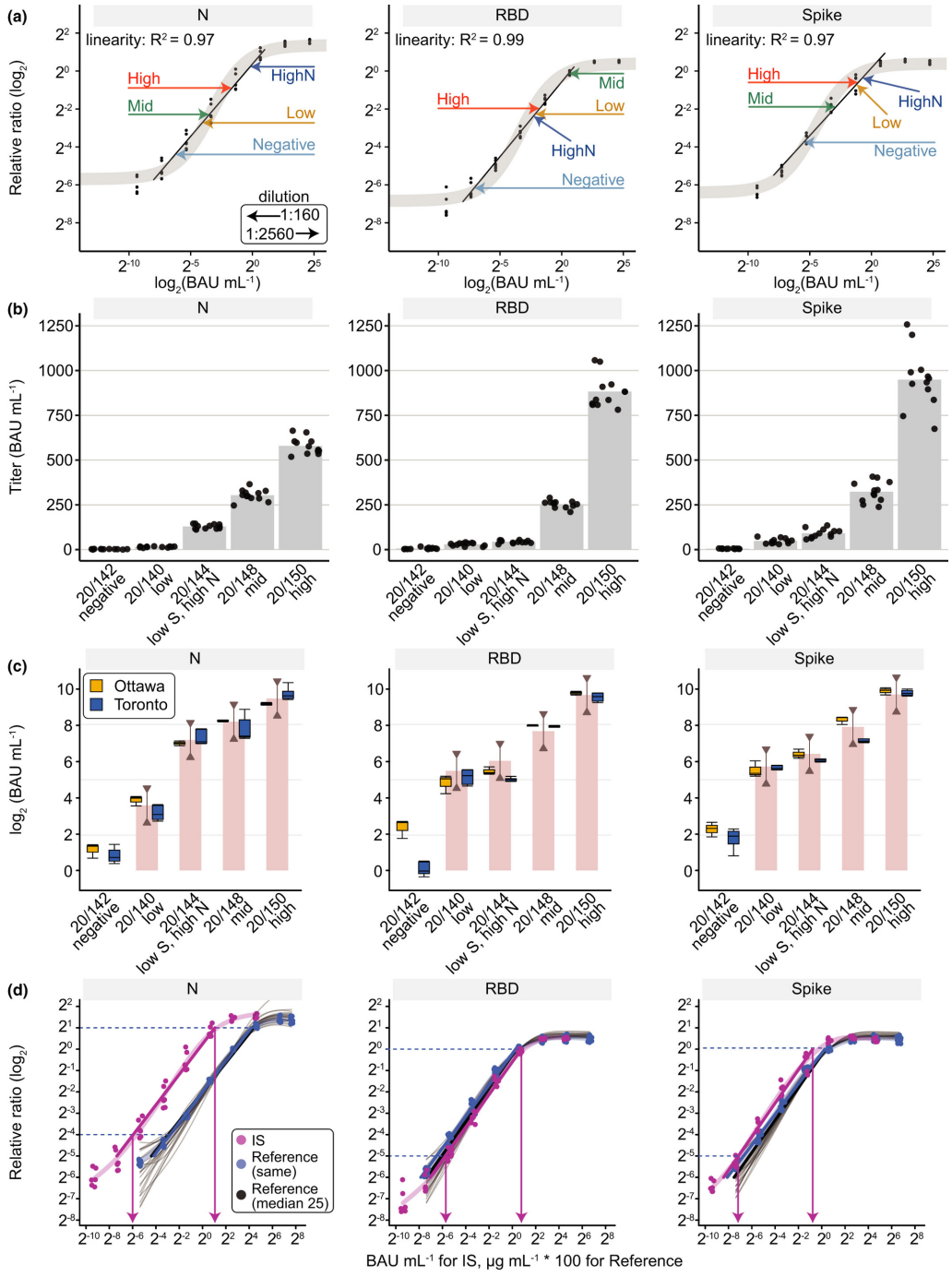


Figure 3- Conversion of Ottawa and Toronto ELISA data to WHO BAUs and comparison to the WHO Reference Panel 20/268. (a) The 20/268 reference panel at the indicated dilutions (arrows) was fitted onto a dose-response curve of the IS with the measured values expressed as relative ratios (Toronto). A 1:160 dilution (0.0625 µL/well) of sample was used except when it was out of the linear range of the fitted line in which case the 1:2560 dilution (0.0039 µL/well) was used. **(b)** IgG levels in the five samples in the 20/268 reference panel are represented for spike, its RBD, and N (n = 12, 4 replicates at 1:500, 1:1000, 1:2500 dilutions). **(c)** Box plots for Ottawa (orange) show the median of the 12 samples from B. Box plots for Toronto (blue) show the median of individual measurements (n = 4) for the selected dilution (1:2560 (0.0039 µL/well) for Mid and High for spike and N, High for RBD, the rest were at 1:160 (0.0625 µL/well)). The WHO bar graph shows the geometric mean from the WHO study and the lines with half arrows represent a 0.5–2-fold range from the geometric mean. **(d)** Reference curves (VHH72-Fc

for spike/RBD, anti-N for N) were plotted for each antigen either from the same tests in which the IS was analyzed or from 25 different tests over 3 months (shown as faded black lines with a thicker median line in black). The blue dashed lines represent the limits of the linear intervals for the curves and the pink arrows represent the BAU mL^{-1} at those points. As the reference curves are parallel to the IS within the linear interval, a conversion factor can be applied to convert relative ratios to international BAU mL^{-1} units (Supplementary table **4**). For illustrations purposes to show IS and reference curves in the same panel, the *x*-axis is BAU mL^{-1} for IS and μg mL^{-1} * 100 for the reference curves.

DBS testing

For serosurveillance, it is important to capture broad swaths of the Canadian population, and at-home sample collection is ideal for this, especially during times of lockdown or restricted movement. DBSs are easier to collect, more stable at room temperature, and considered non-hazardous when dried.[18, 19] We optimised the elution concentrations for both the colorimetric and automated assays (see Methods), and then compared the results of DBS samples and matching plasma samples using reference samples created by the National Microbiology Laboratory (NML; panel 1, with a total of 26 different DBSs and matching plasma samples; Supplementary figure 10a). Using NML panel 3, we also found a high correlation in signal between different punch sizes at a constant ratio of punch area to elution volume (Supplementary figure 10b).

However, despite this high correlation between the two sample types, the higher relative ratios of DBS samples compared to plasma or serum samples shifted the positive and negative density distributions, making direct application of the plasma/serum thresholds inappropriate for scoring seropositivity using DBSs (Supplementary figure 10c). ROC analysis was therefore performed in Toronto and in Ottawa on panel 4, also supplied by the NML (Tables 2 and 3, Supplementary figures 11 and 12), yielding sensitivities of 98% for spike and its RBD and 92% for N at a 1% false positive rate threshold in Toronto. By requiring 2 out of 3 calls to be positive, the specificity increased to 100% and the sensitivity was 98%. In Ottawa, at a 3% FDR, the assays achieved 100% sensitivity for each antigen with false positive rates of 2% for spike, 1% for its RBD, and 6% for N. When requiring 2 out of 3 calls to be positive, specificity and sensitivity were both 98%. In the final protocol, we opted to use two 3 mm punches, as this enables more flexibility and reproducibility when collections are not ideal (which would be typical of self-collection). The minimal sample requirement means the analysis can still be performed even when full DBSs are not provided.

Table 2. ROC statistics for the DBS IgG ELISA (Ottawa)

Antigen	**spike**	**RBD**	**N**	**≥ 2 positive antigens**
AUC	0.991	0.996	0.992	N/A
Threshold (Cut Point)	1.410	0.868	1.171	N/A
FPR	0.02	0.01	0.06	0.02
TPR	1.00	1.00	1.00	0.98
Number of samples used to generate ROC curves†				
Antigen	**spike**	**RBD**	**N**	**≥ 2 positive antigens**
Patients with COVID-19	97	97	97	97
Number excluded	2	2	2	2
Total analyzed	95	95	95	95
Pre-COVID-19 (negative)	90	90	90	90
Number excluded	0	0	0	0
Total analyzed	90	90	90	90

†NML panel 4. Each sample was analyzed once, and thresholds were defined at 3% FDR as described in Supplementary Figure 13. Two positive samples were excluded as they were early on in infection.

Table 3. ROC statistics for the DBS IgG ELISA (Toronto)

Antigen	**spike**	**RBD**	**N**	**≥ 2 positive antigens**
AUC	0.99	0.99	0.99	N/A
Threshold (Cut point)	0.482	0.324	0.642	N/A
FPR	0.01	0.01	0.01	0.00
TPR	0.98	0.98	0.92	0.98
Number of samples used to generate ROC curves†				
Antigen	**spike**	**RBD**	**N**	**≥ 2 positive antigens**
Patients with COVID-19	97	97	97	97
Number excluded	0	0	0	0
Total analyzed	97	97	97	97
Pre-COVID-19 (negative)	90	90	90	90
Number excluded	3	1	2	4
Total analyzed	87	89	88	86

†NML panel 4. Each sample was analyzed in duplicate (the unique numbers of samples are shown). Replicates were treated as separate samples in the ROC analysis. Negative samples were excluded from the analysis if the replicates were > 4 SDs from the mean.

snELISA

We previously reported an ELISA-based test that functions as a surrogate to more complex neutralisation assays employing live viruses, at least with regards to assessing antibodies that prevent the interaction of spike with the ACE2 receptor.[13] In this snELISA, a sample is added to a plate coated with RBD or spike antigens (Figure 1a). Instead of a secondary antibody, biotinylated ACE2 is added followed by streptavidin-HRP. If antibodies from the sample recognise the antigen, they will block biotinylated ACE2 from binding, leading to decreased signal when HRP substrate is added. The biotinylated ACE2 was first tested in a manual colorimetric assay using recombinant antibody and known negative and positive samples (Supplementary figure 13). Both the full-length spike trimer and the RBD domain (319–541 construct) were comparable to prior reagents produced at smaller scale. The assay was then transferred to an automated 384-well chemiluminescent format. Using a panel of samples from the Canadian Blood Services and from two donors after one or two doses of the BNT162b2 (aka Comirnaty; Pfizer-BioNTech) mRNA vaccine, the dose response curves between spike and its RBD were significantly correlated ($\rho = 0.90$; Figure 4a, Supplementary figure 13).

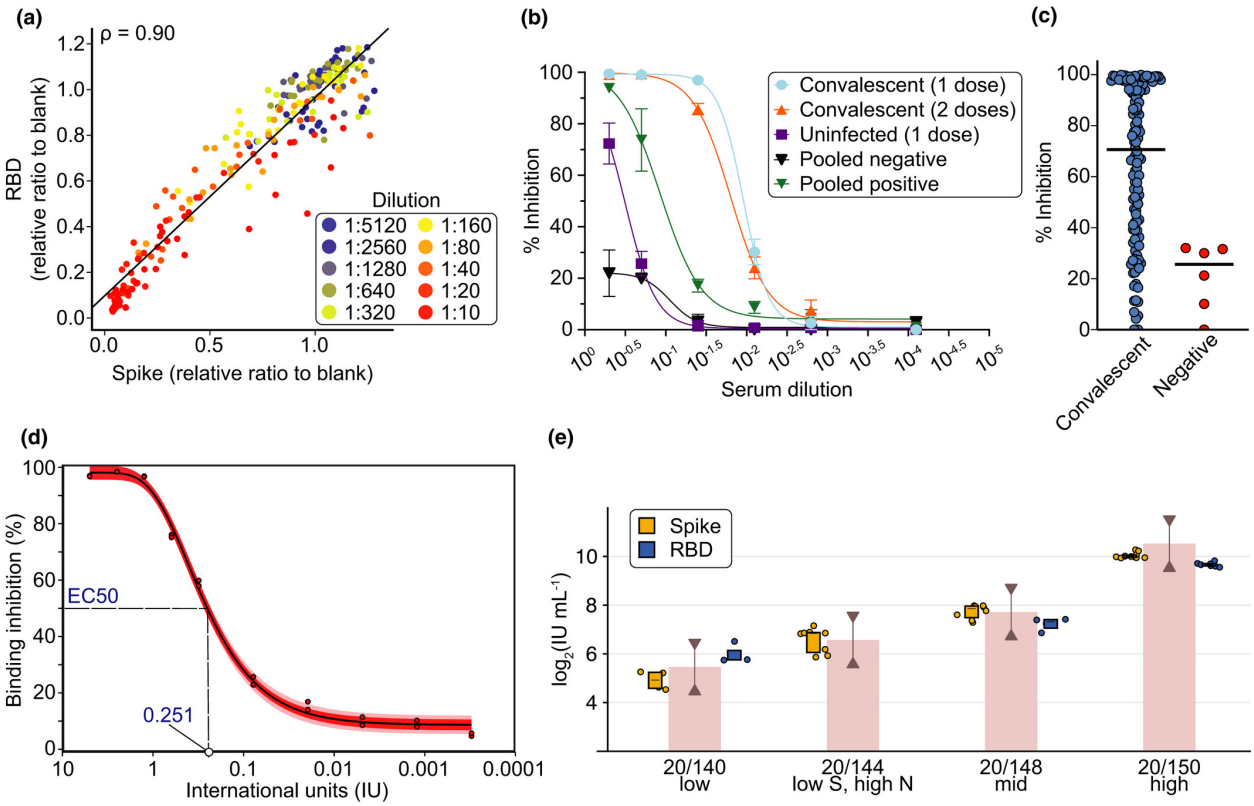


Figure 4- Dose response curves or single-point snELISA and conversion to International Units using the WHO International Standard. (a) Correlation of spike to RBD as snELISA antigens is shown for 11 samples in a 10-point dilution series (individual curves are shown in Supplementary figure **13**). **(b)** Dose response curves ($n = 4$) for the spike snELISA. Samples were from convalescent SARS-CoV-2 individuals 3 weeks after 1 or 2 doses of Comirnaty vaccine (Pfizer) or an uninfected individual (from a surveillance study) 3 weeks post-first dose of Comirnaty. Pooled sera were from 100 individuals with or without prior SARS-CoV-2 infection. **(c)** Single-point measurements (at 1:5 dilution) using the spike snELISA. **(d)** Titration of the neutralising activity of the WHO IS using snELISA. Raw luminescence values were converted to inhibition of ACE2-Spike binding; maximal signal (i.e. 0% inhibition) was measured in absence of convalescent plasma (PBS only). The normalised data was fitted with a four-parameter logistic function and the 95% confidence interval (in red) and two standard deviations (in pink) is shown. **(e)** Box plots for the WHO reference panel 20/268 using RBD (blue, Toronto, ACE2 source: Rini) or spike (orange, Ottawa) as antigens. For RBD, $n = 3$ at 1:10 dilution for Low, $n = 4$ at 1:10 dilution for Mid, $n = 7$ at 1:40 and 1:160 for High. For spike, $n = 12$ for High (4 replicates at 3 dilutions), $n = 8$ for LowS HighN and Mid (4 replicates at 2 dilutions) and $n = 4$ for Low (2 replicates at 2 dilutions). The WHO bar graph shows the geometric mean from the WHO study and the lines with half arrows represent a 0.5–2-fold range from the geometric mean. No inhibition was seen for the LowS HighN sample for RBD.

The snELISA was also implemented on the Ottawa automated platform. Titration of the coating antigen, streptavidin-HRP polymer, and luminescent substrate were performed with varying amounts of biotinylated ACE2 to establish the concentrations with optimal sensitivity, appropriate dynamic range, and a minimised hook effect at high ACE2 concentrations (Supplementary figure 14). The final concentration of ACE2 per well was established at 6.5 ng, using 100 ng/well of coated antigen and the substrate diluted 1:2. Using these conditions, we were able to generate consistent neutralisation efficiency measurements with serum and plasma (Figure 4b,

Supplementary figure 15), enabling us to calculate effective concentration for 50% inhibition (EC50) values for convalescent sera and in sera from doubly vaccinated individuals. We also tested a panel of 121 positive and six negative samples from the *Stop the Spread Ottawa* study as single-point measurements at a 1:5 dilution using spike as the antigen (Figure 4c). Convalescent samples ranged from 0% to 100% inhibition, with a median value of 70%. The six negative samples ranged from 0% to 32% inhibition with a median of 26%, consistent with our previous observation that pre-pandemic samples can achieve partial inhibition of the spike-ACE2 interaction due to cross-reactivity of antibodies targeting seasonal coronaviruses.[20] For DBS samples, four 3 mm punches eluted in 100 µL of PBS from a double-vaccinated individual showed measurable neutralisation activity (Supplementary figure 15); however, we were unable to measure neutralisation in DBS samples from convalescent or singly vaccinated individuals (in contrast to serum). Therefore, while it is possible to detect neutralisation activity from DBSs, this is limited to samples with high neutralising activity. Additionally, DBS samples might not be ideal for quantitative neutralisation measurements, as sample quality, paper saturation and disc punching consistency can interfere with the reproducibility and reliability of the results.

The final development performed with the snELISA was to correlate binding inhibition to international units (IUs) of the WHO International Standard (Figure 4d). By titrating the standard, we established the correlation between binding inhibition and IUs within the linear range of the curve, with 0.251 IUs being required to inhibit ACE2-spike interaction by 50% (EC50). We then tested the WHO reference panel 20/268 by snELISA using spike (Ottawa) or RBD (Toronto) as antigens (Figure 3e). For the low, mid and high samples, results from Toronto and Ottawa were between 0.5 and 2 fold of the geometric mean (red line with half arrows) reported in a multi-lab comparison by the WHO.[14] For the low S, high N sample, there was no inhibition of ACE2 binding in the snELISA using RBD as the antigen, in contrast to the snELISA using full-length spike, which detected inhibition levels similar to the WHO study. Given the numerous different protocols and strategies that are being used to measure neutralising antibodies such as spike-pseudotyped lentiviral assays, plaque reduction neutralisation tests (PRNT) and the snELISA, transforming the data to IUs will enable more robust cross-laboratory and cross-assay correlations to be performed.

Visualisation of the results of seroprevalence and vaccination studies

As defined above, the assays optimally use the IgG responses to three antigens (spike, RBD, N) to report seropositivity resulting from SARS-CoV-2 infection. To illustrate how vaccination cohorts differ from infected cohorts, we re-plotted a subset of the data from our training set (positives and negatives) as pairwise comparisons of spike and N on scatterplots, with the color intensity mapping to that of RBD (Figure 5a). We also replotted data from a cohort of vaccinated patients on dialysis[21] prior to vaccination and 6 weeks afterward (Figure 5b). As expected, the infected cohort contained samples largely positive for all three antigens tested, while the vaccinated cohort largely consisted of samples positive for spike and its RBD, but negative for N, which is not targeted by vaccines used in Canada. This type of visualisation helps define individuals with evidence of infection from those with antibodies resulting from vaccination.

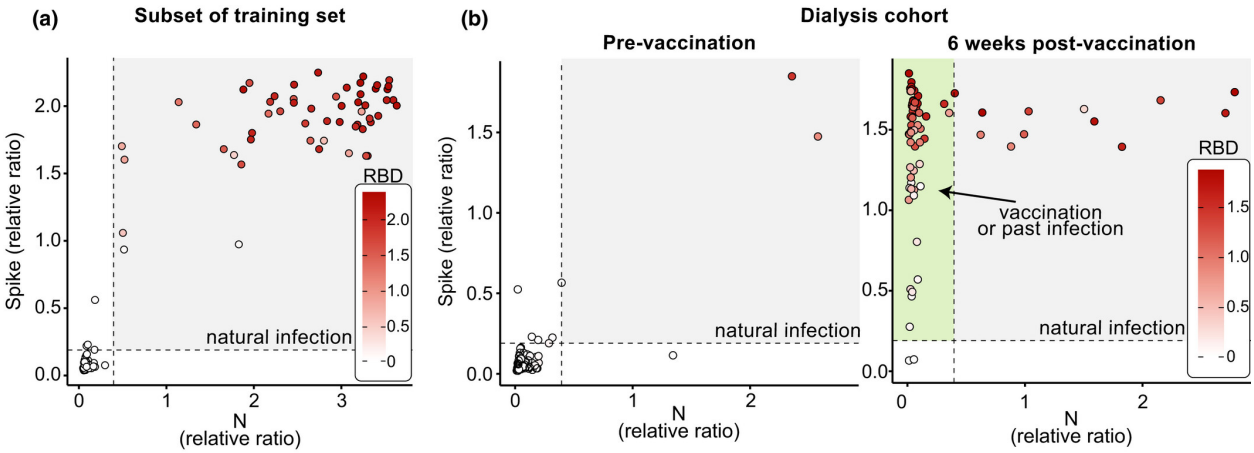


Figure 5- Visualisation of data from three antigen testing. The results are from known negative and positive samples (a) and samples from a longitudinal study of patients on dialysis at baseline and after their first vaccine dose **(b)**. The dashed lines represent the thresholds for spike and N. The area with positives for both spike and N (colored in gray) is indicative of natural infection and the area showing samples that are N-negative but spike-positive (and RBD-positive if colored) is highlighted in green on the right panel and is indicative of vaccination.

Discussion

In this paper, we describe a toolkit and protocols for both SARS-CoV-2 serosurveillance and vaccination response profiling that we applied to population studies in Canada. We have validated these reagents, produced and made available by the NRC, in two separate laboratories. The results can be expressed as relative ratios or can be converted into international units (BAU mL^{-1} for antibody detection, IU mL^{-1} for antibody neutralisation) to facilitate comparisons between labs

and with studies proposing correlates of protections based on these units.[22] We validated antibody detection and surrogate neutralisation assays in 96-well format (manual colorimetric assays) and on two different 384-well automated chemiluminescent platforms, enabling these reagents to be used at small-scale in laboratories with basic equipment and in dedicated high-throughput facilities equipped with different automation equipment.

All vaccines approved for use in Canada (also in USA and Europe) use spike as the immunogen.[23-25] For those who have been vaccinated, responses to spike (and its RBD) are expected, whereas a response to N is only expected after infection. Thus, it is of value to focus on these two orthogonal readouts when detecting and characterising immune responses.[26] Adding the spike RBD as a third antigen increases specificity (of the three antigens, it is the least conserved in coronaviruses[27-29]) and provides insight into possible protection, as it is also the antigen most correlated with neutralisation potential.[13, 30, 31]

By definition, single-point assays must make compromises in defining antigen/antibody/detection antibody amounts to ensure that a large fraction of measurements are within the linear range of quantification. Here, we have optimised the concentrations of the serum/plasma/DBS eluates used to capture the most positives (i.e. convalescent individuals) possible without inducing a hook effect. Still, in samples with very high antibody levels (including those from healthy individuals following two doses of vaccine), the measured antibody levels will saturate the assay, thereby preventing their accurate measurement. When the relative amounts of antibodies detected across samples is important to measure, expanded dilutions should be performed (note that this drastically decreases assay throughput and increases costs). As a compromise, in vaccinated cohorts, we routinely perform two-point dilution (16-fold difference) assays that expand the range of concentrations that can be measured in the linear range of quantification, from 1 to 1501 BAU mL^{-1} for spike, and from 3 to 4454 BAU mL^{-1} for RBD.

We also optimised our seropositivity thresholds to limit false positives, both by providing a stringent definition of positivity in each assay and by requiring that this positivity threshold be met in two separate assays to establish overall positivity in seroprevalence studies. While we felt this was essential to avoid inflating the positive calls in low prevalence settings, it may affect the overall sensitivity of the assays, especially following recent infection/vaccination (where

seroconversion for anti-spike often precedes that of RBD and N[8]) or as antibody levels decay. Other limitations stem from the selection of antigens, as those used in these assays are from the original Wuhan-Hu-1 strain, and it is possible that decreased sensitivity occurs when testing patients infected with variants, especially Omicron, which has 30 amino acid substitutions (15 within the RBD), three small deletions and one small insertion in the spike coding sequence[32] (although our initial results with non-vaccinated Omicron-infected convalescents indicate detection of anti-RBD IgG on this assay; optimisation of assays based on Omicron sequences is ongoing). Lastly, as assays using N generally have poorer specificity and sensitivity (at our defined thresholds) than RBD- and spike-based assays, they may not be ideal as a stand-alone method to define vaccine breakthrough infections, unless serial blood samples are available (in which case an increase in anti-N levels would indicate that an infection has occurred). Further assay development will include additional viral antigens not contained in the vaccines to increase the detection sensitivity for antibodies produced in breakthrough infections. The control over reagent production and quality, and the flexibility of the ELISA platforms to accommodate new antigens also provide a rapid route to testing immune responses to variants. All reagents and protocols are publicly available to enable the rapid deployment of these assays.

The validated automated ELISA assays described here are currently being used in multiple Canadian studies (with > 150 000 unique samples profiled to date). These include large serosurveys that monitor the global (and regional) humoral response (from both infection and vaccination) in the Canadian population, including the Canadian COVID-19 Antibody and Health Survey from Statistics Canada,[2] seroprevalence studies with Canadian Blood Services,[33, 34] the Action to Beat Coronavirus study,[35] and the Canadian Partnership for Tomorrow's Health study.[36] Additionally, these assays are used in > 30 studies focused on infection and/or vaccine responses across different cohorts, e.g. in persons predicted to have a weaker immune response (based, for example, on age[37] or health conditions[38]), or who are likely to be exposed to infection from the workplace. The results of the assays have critically helped informed public health decisions. Based on, e.g. a weak response to vaccine in older adults or patients on dialysis,[21, 39] or the decline in antibody levels post-dose 2 in residents of long-term care homes,[40, 41] prioritisations were made for second doses, vaccine type was recommended, or additional doses were accelerated in the populations studied. Combined with other studies coordinated by the COVID-19 Immunity

Task Force (CITF),[42] our serology studies help guide Canada's response to the COVID-19 pandemic.

Methods

Protein production

Spike trimer

The SARS-CoV-2 spike ectodomain construct (SmT1) from the Wuhan-Hu-1 strain with S1/S2 furin site mutations, K986P/V987P prefusion-stabilising mutations, and human resistin as a trimerisation partner[15] was produced using stably transfected Chinese Hamster Ovary (CHO) pools ($CHO^{BRI/2353™}$ cells) and purified as described.[8] To prepare reference material aliquots for distribution by the National Research Council of Canada (NRC) Metrology Research Centre, the bulk purified protein was formulated in PBS supplemented with 10 mM HEPES sodium salt. After aliquoting and one freeze-thaw cycle, protein integrity and purity were assessed by sodium dodecyl sulfate-polyacrylamide gel electrophoresis (SDS-PAGE; Figure 1b) and analytical size-exclusion ultra-high performance liquid chromatography (SEC-UPLC; Supplementary figure 1, Supplementary table 1). SEC-UPLC was run on an Acquity H-Class Bio UPLC system (Wyatt Technology, Santa Barbara, CA, USA) in phosphate buffered saline (PBS) + 0.02% Tween-20 on a 4.6 × 300 mm Acquity BEH450 column (2.5 µm bead size; Waters Limited, Mississauga, ON, Canada) coupled to a miniDAWN Multi-Angle Light Scattering (MALS) detector and Optilab T-rEX refractometer (Wyatt).

Nucleocapsid

N cDNA (corresponding to amino acids 1–419 of YP_009724397, Wuhan-Hu-1 strain) was synthesised by GenScript (Piscataway, NJ, USA; using *Cricetulus griseus* codon bias) with a C-terminal FLAG-Twin-Strep-tag-$(His)_6$ tag and cloned into the pTT5® expression plasmid (NRC) to create NCAP.[43] Expression by transient transfection of $CHO^{BRI/55E1™}$ cells was performed using a previously described high cell density method.[15] Since a significant proportion of N was released from transfected cells despite high viability, it was purified from the culture supernatant. Following centrifugation and filtration, supernatant harvested 7 days post-transfection was purified by immobilised metal affinity chromatography (IMAC) on a Ni Sepharose Excel column (Cytiva,

Vancouver, BC, Canada). The column was washed with 50 mM sodium phosphate buffer (pH 7.0) containing 25 mM imidazole and 300 mM NaCl, and N was eluted with 50 mM sodium phosphate buffer (pH 7.5) containing 300 mM imidazole and 300 mM NaCl. N was further purified by affinity chromatography on a StrepTrap XT Chromatography Column (Cytiva) equilibrated in Buffer W (100 mM Tris pH 8.0, 150 mM NaCl). The column was washed with Buffer W and bound protein was eluted with Elution Buffer (Buffer W supplemented with 50 mM biotin and 1 mM ethylenediaminetetraacetic acid (EDTA)). Purified N was buffer exchanged into Dulbecco's PBS (PBS) using a CentriPure P100 Gel Filtration Column (Apex Scientific, Maynooth, Ireland), sterile-filtered through a 0.2 μm membrane, and stored at −80°C. For preparation of reference material aliquots (NCAP-1) for distribution by National Research Council of Canada (NRC) Metrology, the bulk purified protein was processed through an additional buffer exchange in 50 mM Tris-HCl pH 8.0 supplemented with 150 mM sodium chloride. N integrity and purity was analyzed by SDS-PAGE and analytical SEC-HPLC, which was run in PBS supplemented with 200 mM arginine on a 5 × 150 mm Superdex 200 HR column (Cytiva).

Receptor binding domain

Amino acids 331–521of the SARS-CoV-2 spike protein (YP_009724390.1, Wuhan-Hu-1 strain) were cloned into the pTT5® vector using EcoRI and BamHI. The construct encodes an N-terminal human interleukin 10 signal peptide (MHSSALLCCLVLLTGVRA) followed by a Twin-Strep-tag II-$(His)_6$-FLAG tag fused to the RBD N-terminus. The construct was expressed by transient gene expression in $CHO^{BRI/55E1™}$ cells as described above.[15] Clarified culture supernatant harvested 8 d post-transfection was purified by IMAC on Ni Sepharose Excel columns as above. The IMAC eluate was buffer-exchanged using NAP-25 columns (Cytiva) into PBS before a second affinity purification step using Strep-Tactin XT Superflow (IBA Lifesciences, Göttingen, Germany), following the manufacturer's instructions. The pooled eluate (de-salted into PBS and concentrated) was applied to a Superdex-75 gel filtration column (Cytiva). SEC fractions containing RBD with low levels of high-molecular-weight contaminants were pooled. The second RBD construct ($RBD^{319–541}$) consists of amino acids 319–541 with a C-terminal $(His)_6$-FLAG tag. The protein was expressed and purified as described for $RBD^{331–521}$, except the Strep-Tactin XT purification step was omitted.

RBD and N antigens were compared against previously validated antigens produced by the Rini and Sicheri laboratories, respectively, and described in Isho *et al*.[8] and Abe *et al*.[13]

Recombinant antibody production

VHH and mAb sequences were synthesized by GenScript using *C. griseus* codon bias and cloned into the pTT5® plasmid. The llama single domain antibody (VHH) VHH72 was described previously (PDB entry 6WAQ_1).[17] Additional VHHs (NRCoV2-04 and NRCoV2-20) were isolated in-house from llamas immunised with recombinant SARS-CoV-2 trimeric spike ectodomain SmT1 (Supplementary figure 2). VHH sequences were fused to an antibody-dependent cell-mediated cytotoxicity (ADCC)-attenuated human IgG1 Fc domain (hFc1X7, from patent US 2019 352 383A1) to generate VHH72-Fc, NRCoV2-04-Fc and NRCoV2-20-Fc. The anti-human-IgG monoclonal antibodies (mAbs) IgG#5 and IgG#6 were derived from mice immunised with human IgG; heavy chain (HC) and light chain (LC) variable domain sequences (VH and VL) were fused to mouse IgG2a and mouse kappa LC constant domain sequences, respectively, to express full-length mAbs. The HC was fused in-frame at its C-terminus with ferric HRP (PDB: 1W4W_A) to create IgG#5-HRP and IgG#6-HRP. These mAbs were also tested as HRP conjugates (rather than HRP fusions) as described in Supplementary figure 6. For protein production, VHH or mAb HC/LC (50:50 w/w) plasmids were transfected into CHO$^{BRI/55E1™}$ cells using PEI-Max transfection reagent (Polysciences, Warrington, PA, USA) as described previously.[13, 15] Clarified 0.2 µm-filtered supernatants were loaded on 5 mL HiTrap MabSelect SuRe columns (Cytiva) equilibrated in PBS, and the columns were washed with PBS prior to antibody elution with 100 mM citrate buffer, pH 3.6. The eluted antibodies were formulated in PBS by buffer exchange using NAP-25 columns. Purified proteins were quantified based on their absorbance at 280 nm and analyzed by analytical size-exclusion on an Acquity BEH200 column (Waters) by UPLC-MALS system (as described above for the spike trimer) or on a 5 × 150 mm Superdex 200 HR column (Cytiva) coupled to a high-performance liquid chromatography (SEC-HPLC) system (Waters).

Biotinylated ACE2 production

The human ACE2 (UniProtKB-Q9BYF1) cDNA was synthesised by GenScript and optimised for expression in CHO cells. The construct encodes a human interleukin 10 signal peptide (MHSSALLCCLVLLTGVRA) followed by a Twin-Strep-tag II-$(His)_6$-FLAG tag on the

N-terminus of the mature ACE2 receptor ectodomain (amino acids 20–613). A biotin acceptor peptide (BAP) sequence (GLNDIFEAQKIEWHE) was added in-frame at the ACE2 C-terminus. The cDNA was cloned into pTT5® using EcoRI and BamHI. The ACE2-BAP cDNA was expressed by transient gene expression in CHO$^{BRI/55E1™}$ cells as described[15] with the addition of 5% (w/w) pTT5®-BirA (an *Escherichia coli* biotin ligase) expression plasmid as described previously.[44] Clarified culture supernatant harvested 8 days post-transfection was purified by IMAC on Ni Sepharose Excel columns as described for N above. The IMAC eluate was buffer-exchanged using NAP-25 columns into PBS before a second affinity purification step using Strep-Tactin XT Superflow. The pooled eluate (buffer-exchanged into PBS as above) was stored at −80°C. Biotinylated ACE2 from the NRC was compared against biotinylated ACE2 produced in the Rini lab and previously described in Abe *et al*.[13]

Participant recruitment and study approval

All research was performed in accordance with Canada's Tri-Council Policy Statement: Ethical Conduct for Research Involving Humans. External samples and data were transferred via material and data transfer agreements as appropriate. Samples were de-identified prior to transfer to the assay laboratory.

For Toronto cohorts

Negative control serum samples were from patients enrolled in cancer studies pre-COVID-19 (prior to November 2019; Mount Sinai Hospital (MSH) Research Ethics Board (REB) studies #01-0138-U and #01-0347-U), which were archived and frozen in the Lunenfeld-Tanenbaum Research Institute (LTRI) Biobank. Convalescent serum samples were obtained from in- and out-patients with polymerase chain reaction (PCR)-confirmed COVID-19 by the Toronto Invasive Bacterial Diseases Network in Toronto and the regional municipality of Peel, Ontario (REB studies #20-044 Unity Health Network, #02-0118-U/05-0016-C, MSH). Specimen-only Canadian Blood Services (CBS) serum donations were collected from individuals who met one or more of the following criteria: (1) an indication that they had a SARS-CoV-2-positive PCR test, (2) a declaration of having been a close contact of a COVID-19 case, (3) a travel history and clinical presentation compatible with COVID-19, and (4) signs and symptoms compatible with COVID-19. ELISAs

were conducted at the LTRI with MSH Research Ethics Board (REB) approval (study number: 20-0078-E). Samples from vaccinated individuals were obtained from Sunnybrook Health Sciences Centre (REB study #4814, Sunnybrook, #21-0049-E, MSH) and from MSH (REB study #20-0144-A).

For Ottawa cohorts

Pre-pandemic serum and plasma samples were collected between April 2015 and December 2019 from diverse sources, including the Eastern Ontario Regional Laboratory Association (EORLA) and the Ottawa Hospital (TOH). Pediatric samples were acquired from the BC Children's Hospital Biobank (BCCHB) in Vancouver, BC, Canada (REB#: H-07-20-6009). Pandemic samples were collected from longitudinal studies of severe and mild hospitalised cases of COVID-19 (REB # H-04-20-5727 and # H-11-20-6172), and from a surveillance study of at-risk and convalescent individuals called *Stop the Spread Ottawa* (REB # H-09-20-6135) at the Ottawa Hospital Research Institute and the University of Ottawa.

Sample collection, handling, and viral inactivation

Serum and plasma collection

Samples were collected using standard phlebotomy procedures at collection sites or self-collected by individuals after capillary puncture. In Toronto, inactivation of potential infectious viruses in plasma or serum was performed by incubation with Triton X-100 to a final concentration of 1% for 1 h prior to use.[8, 45] Serum and plasma samples collected and processed in Ottawa did not require viral inactivation, as they were handled and tested within the University of Ottawa CL2+ biocontainment facility.

DBS preparation

Samples were prepared at the National Microbiology Laboratory of Canada (NML) as in.[46] For panels 1–3, plasma from SARS-CoV-2 antibody-positive COVID-19 convalescent donors (MSH, Toronto) and SARS-CoV-2-negative donors (NML, Winnipeg) were used to generate matched

plasma and contrived DBS samples. For contrived DBS samples, fresh SARS-CoV-2 antibody-negative blood was centrifuged, the plasma was removed, and the red blood cells were resuspended 1:1 in antibody-positive plasma and spotted (5 × 75 µL) onto Whatman 903 Protein Saver Cards (GE Healthcare, Boston, MA, USA), which were dried at room temperature overnight, then stored with desiccant in gas-impermeable bags at −80°C until testing. SARS-CoV-2 antibody-negative blood was spotted directly from EDTA Vacutainer tubes onto DBS cards. For panel 4, both positive and negative blood samples were spotted directly from EDTA tubes. All matched plasma and contrived DBS samples were tested using the anti-SARS-CoV-2 ELISA IgG kit (EUROIMMUN, Lübeck, Germany), according to the manufacturer's instructions, to verify that donors were either positive or negative for SARS-CoV-2 antibodies prior to shipping to Toronto and Ottawa.

DBS handling: Toronto

Samples from DBS cards were punched manually using a 6 mm punch or in a semi-automated manner using a BSD600 Ascent puncher (BSD Robotics, Brisbane, QLD, Australia) with the indicated punch size. We first compared 6 mm circle punches from contrived DBSs and matching plasma samples (Supplementary figure 10) by eluting the punches in 250 µL PBST plus 1% Triton X-100 (0.226 mm^2 μL^{-1} eluate). After this initial test, to ensure sufficient eluate to test all three antigens from 1 or 2 3-mm punches, we selected a final elution ratio of 0.176 mm^2 μL^{-1} elution buffer (i.e. 80 µL for 2 × 3 mm punches). Eluted samples were centrifuged at 1000 × *g* for 30 s before transfer to 96-well plates. Eluates were diluted 1:4 in 1.3% Blocker BLOTTO (Thermo Fisher Scientific, Waltham, MA, USA) to a final concentration of 1% in PBST, unless otherwise specified.

DBS handling: Ottawa

Samples from DBS cards were punched manually or in a semi-automated manner using a DBS puncher (PerkinElmer, Woodbridge, ON, Canada; 3.2 mm discs) or a BSD600 Ascent puncher (BSD Robotics; 3 mm discs) and eluted in 100 µL per disc PBS + 1% Triton X-100 for up to 16 h (minimum 4 h) in 96-well U-bottom plates on a shaker at room temperature. Elution optimisation data are presented in Supplementary figure 7. Eluates were centrifuged at 216 × *g* for 2 min and diluted 1:2 in 2% milk + PBST for a final concentration of 1% milk in PBST.

Colorimetric direct ELISAs: Toronto protocol

Manual colorimetric ELISAs were adapted from assays described in Isho *et al*.[8] and Abe *et al*.[13] Antigens (spike trimer, RBD 331–521 and N) at the indicated amounts (in ng, see Supplementary table 2 for optimised amounts) were diluted in 50 µL PBS and adsorbed onto a 96-well high-binding polystyrene Greiner Bio-One plate (Thermo Fisher Scientific, #655061) overnight at 4°C. Wells were washed three times with 200 µL PBST and then blocked with 200 µL 3% w/v milk powder (BioShop Canada Inc., Burlington, ON, Canada, #ALB005.250) in PBST for 1–2 h at room temperature. Samples were diluted as indicated in 50 µL of 1% w/v (final) milk powder in PBST and added to each plate. A standard curve of recombinant antibody was added to each plate in 50 µL 1% w/v milk powder in PBST at the indicated concentrations. For spike and its RBD, the recombinant antibodies used were VHH72-Fc (NRC; see above), human anti-spike S1 IgG (clone HC2001, GenScript, #A02038), human anti-Spike S1 IgM (clone hIgM2001, GenScript, #A02046), and human anti-spike IgA (clone CR3022, Absolute Antibody, Oxford, UK, #Ab01680-16.0). For N, the antibodies used were human anti-nucleocapsid IgG (clone HC2003, GenScript, #A02039), anti-nucleoprotein IgM (CR3018 (03-018), Absolute Antibody, #Ab01690 -15.0), and anti-nucleoprotein IgA (CR3018 (03-018), Absolute Antibody, #Ab01690 -16.0). Negative control antibodies purified from human serum (final 1 µg mL^{-1}; human IgG, Sigma-Aldrich, Oakville, ON, Canada, #I4506; human IgM, Sigma-Aldrich #I8260, human IgA, Sigma-Aldrich, #I4036) and pools of positive and negative sera from 3 or 4 patients were added to each plate in 50 µL 1% w/v milk powder in PBST for quality control and to enable cross-plate comparisons. Samples were incubated for 2 h at room temperature, and wells were washed three times with 200 µL PBST. Anti-human secondary antibodies (recombinant anti-human IgG#5-HRP), goat anti-human IgG Fcy-HRP (Jackson ImmunoResearch Labs, West Grove, PA, USA, #109-035-098), goat anti-human IgM fc5u-HRP (Jackson ImmunoResearch Labs, #109-035-129), and goat anti-human IgA α chain-HRP (Jackson ImmunoResearch Labs, #109-035-127) were added to the plate at the indicated dilutions in 50 µL 1% w/v milk powder in PBST and incubated for 1 h at room temperature. Wells were washed three times with 200 µL PBST, then 50 µL of 1-Step Ultra TMB-ELISA Substrate Solution (Thermo Fisher Scientific, #34029) was added for 15 min at room temperature. The reaction was quenched with 50 µL Stop Solution for TMB Substrates (Thermo Fisher Scientific, #N600). The plates were read at 450 nm in a Cytation 3 Cell

Imaging Multi-Mode Reader (BioTek Instruments Inc., Winooski, VT, USA). Blank values (the mean of the blanks in each 96-well plate) were subtracted from all raw reads prior to data analysis.

Colorimetric direct ELISA: Ottawa protocol

Manual colorimetric ELISAs were modified from the assay described in Amanat *et al*.[47] High protein-binding Immulon 4 HBX clear 96-well plates (VWR International, Mississauga, ON, Canada, #62402-959, note these plates have also been tested and validated in Toronto) were coated with 50 µL of 2 µg mL^{-1} antigen (spike, RBD 319–541, and N diluted in sterile PBS (WISENT Inc, St-Bruno, QC, Canada, #311-010-CL)) were incubated at 4°C on a shaker overnight. The next day, coated plates were washed three times with 200 µL of PBST and blocked with 200 µL of 3% w/v skim milk powder in PBST for 1 h at room temperature on a shaker at 700 rpm. The blocking buffer was removed, and plates were washed three times with 200 µL PBST. Serum and plasma samples were diluted in 1% w/v skim milk powder in PBST. An isotype-specific standard curve was included on each plate to enable cross-plate comparison: anti-SARS-CoV-2 S CR3022 Human IgG1 (Absolute Antibody, Ab01680-10.0), anti-SARS-CoV-2 S CR3022 Human IgA (Absolute Antibody, Ab01680-16.0), or anti-SARS-CoV-2 S CR3022 Human IgM (Absolute Antibody, Ab01680-15.0). Serum/plasma samples, standard curve, positive and negative controls, and blanks (100 µL/well in 1% w/v skim milk in PBST) were added and incubated for 2 h at room temperature on a plate shaker at 700 rpm. The plates were washed four times with 200 µL PBST, HRP-linked secondary antibody diluted in 1% milk in PBST (50 µL) was added, and the plate was incubated for 1 h at room temperature on a shaker at 700 rpm. The final isotype-specific secondary antibodies used were anti-human IgG#5-HRP (Supplementary figure 6), anti-human IgA-HRP (Jackson ImmunoResearch Labs, 109-035-011), and anti-human IgM-HRP (Jackson ImmunoResearch Labs, 109-035-129). Plates were washed four times with 200 µL PBST and developed using 100 µL of SIGMAFAST OPD Tablets (Sigma-Aldrich, P9187) dissolved in 20 mL Gibco Water for Injection for Cell Culture (Thermo Fisher Scientific, A1287301, final concentration of 0.4 mg mL^{-1} OPD, 0.4 mg mL^{-1} urea hydrogen peroxide, and 0.05 M phosphate-citrate, pH 5.0). After 10 min of incubation in the dark, the reaction was stopped with 50 µL of 3 M HCl and the absorbance was measured at 490 nm using a PowerWave XS2 Plate Reader (BioTek Instruments). Wells filled with dilution buffer were used as background controls and their reads were subtracted

from serum values. Colorimetric assay optimisation data are presented in Supplementary figures 5 and 6.

Chemiluminescent direct ELISA: Toronto protocol and optimisation

Automated chemiluminescent ELISAs were adapted from assays first described in Isho *et al*.,[8] and performed using liquid dispensers (Biomek NXp (Beckman, Indianapolis, IN, USA), Multidrop Combi (Thermo Fisher Scientific)) and a washer (405 TS/LS LHC2 (Biotek Instruments)); all wash steps included four washes with 100 µL PBST) on a Thermo Fisher Scientific F7 Robot System at the Network Biology Collaborative Centre (nbcc.lunenfeld.ca). All incubations were performed at room temperature. Antigen (spike trimer, RBD 331–521, or N) at the indicated amounts (ng) were diluted in 10 µL PBS and dispensed into the wells of a 384-well LUMITRAC 600 high-binding polystyrene Greiner plate (Thermo Fisher Scientific, #781074). The plate was centrifuged at 233 × *g* for 1 min to ensure even coating, incubated overnight at 4°C, and washed. Wells were blocked with 80 µL of 5% Blocker BLOTTO for 1 h and then washed. Samples and controls (as in the colorimetric assay) were diluted as indicated in a final concentration of 1% Blocker BLOTTO in PBST, and 10 µL was added to each well from 96- or 384-well source plates. Plates were incubated for 2 h, and wells were washed with PBST. Secondary antibodies (as in the colorimetric assay) were diluted as indicated in 1% Blocker BLOTTO in PBST and 10 µL was added to each well. After incubation for 1–2 h, the wells were washed and 10 µL of ELISA Pico Chemiluminescent Substrate (Thermo Fisher Scientific, #37069, diluted 1:4 in ddH_2O) was dispensed into each well and mixed at 900 rpm for 10 s. After a 5–20-min incubation, plates were read on an EnVision 2105 Multimode Plate Reader (PerkinElmer) at 100 ms/well using an ultra-sensitive luminescence detector.

Protein reagents from the NRC (described above) were first optimised in the 96-well colorimetric manual assay using recombinant antibodies and serum samples from CBS (Supplementary figure 16). The final amount of antigen per well was then scaled down by 3.5–4-fold to migrate to 384-well format for the automated assay. Two concentrations of secondary antibody IgG#5-HRP (0.09 and 0.18 µg mL^{-1}) were assessed using dilution curves of the VHH72-Fc antibody (to detect spike and its RBD) or an anti-N antibody (to detect N; Supplementary figure 17), and the best concentration (0.18 µg mL^{-1}) was further tested on a dilution series of 32 serum samples provided

by CBS (Supplementary figure 3). We also tested anti-RBD NRCoV2-04-Fc and NRCoV2-20-Fc recombinant calibration antibodies, which were comparable to VHH72-Fc as reference curves (Supplementary figure 17). For IgA and IgM detection, reagents were first tested in the colorimetric assay (Supplementary figure 8). For chemiluminescent assays, 10 µL of goat anti-human IgA-HRP (1:10 000; 0.80 ng/well) or goat anti-human IgM-HRP (1:12 000, 0.66 ng/well) were used as secondary antibodies.

Chemiluminescent direct ELISAs: Ottawa protocol and optimization

Automated chemiluminescent ELISAs were based upon and optimised from assays first described in Amanat *et al*.,[47] and performed using MicroLab Star robotic liquid handlers (Hamilton, Reno, NV, USA) and a 405 TS/LS LHC2 plate washer (Biotek Instruments; all wash steps included four washes with 100 µL PBST) at the University of Ottawa, Faculty of Medicine (Roger Guindon Hall). All incubations were done at room temperature with shaking at 500–700 rpm. Antigens (spike, RBD 319–541, and N) were diluted in PBS and dispensed into the wells of a 384-well high-binding polystyrene Nunc plate (Thermo Fisher Scientific, #460372) at a final amount of 50 ng/well. The plates were centrifuged at 216 × *g* for 1 min to ensure even coating, incubated overnight rocking at 4°C, and washed. Wells were blocked with 80 µL of 3% w/v skim milk powder dissolved in PBST for 1 h and then washed. Samples and controls were diluted as indicated to a final concentration of 1% w/v skim milk powder in PBST and 10 µL was added to each well from a 96-well source plate. Plates were incubated for 2 h and wells were washed. Secondary antibodies (as in the colorimetric assay) were diluted as indicated in 1% w/v skim milk powder in PBST and 10 µL was added to each well. After incubation for 1 h, the wells were washed and 10 µL of ELISA Pico Chemiluminescent Substrate (diluted 1:2 in MilliQ H_2O) was dispensed into each well. After a 5 min incubation with shaking, plates were read on an Neo2 plate reader (BioTek Instruments) at 20 ms/well and a read height of 1.0 mm.

Colorimetric snELISAs: Toronto protocol and optimisation

The snELISA assay was performed as described[13] with the indicated antigens and ACE2. All wash steps included four washes in 200 µL PBST. RBD 319–541 or spike was adsorbed onto 96-well high-binding polystyrene Greiner Bio-One plates (Thermo Fisher Scientific, #655061) at 100 or 200 ng/well, respectively, in 50 µL PBS and incubated overnight at 4°C. Plates were washed, then blocked for 1–1.5 h at room temperature with 200 µL 3% bovine serum albumin (BSA; BioShop

Canada Inc., SKI400.1). After washing, serum or plasma was added to the plate at the indicated concentrations in 50 µL 1% BSA in PBST (final concentration) and incubated for 1 h. Wells were washed and incubated with 50 µL of biotinylated recombinant ACE2 as indicated for 1 h. After washing, wells were incubated with 44 ng Streptavidin-Peroxidase Polymer, Ultrasensitive (Sigma-Aldrich, S2438) for 1 h. The resultant signal was developed and quantified with TMB-ELISA in an identical manner to the colorimetric direct ELISAs. Due to day-to-day variations in signal, all optical density at 450 nm (OD_{450}) values were normalised to the OD_{450} of the well without serum or antibody for each sample. All values are expressed as ratios.

Chemiluminescent snELISAs: Toronto protocol

The automated snELISA assay was performed on the same F7 platform as the direct detection ELISA with the same washing protocol and incubation temperature. Greiner 384-well Lumitrac 600 plates were coated with RBD 319–541 (34 ng/well) or spike (50 ng/well) following the same protocol as for direct detection. Before each of the next four steps, the plates were washed four times with PBST: (1) the wells were blocked with 80 µL 3% BSA in PBST for 1 h; (2) Plasma or serum sample was dispensed at the indicated dilutions in 10 or 20 µL and incubated for 2 h; (3) 10 µL of ACE2-BAP (2.08 ng/well in 1% BSA in PBST) or ACE2-Rini (17 ng/well in 1% BSA in PBST) was added to each well and the plates were incubated for 1 h; (4) 10 µL of Streptavidin-Peroxidase Polymer, Ultrasensitive (15 ng/well in 1% BSA in PBST) was added to each well and the plates were incubated for 1 h. Addition of ELISA Pico Chemiluminescent Substrate and reading on the EnVision 2105 Multimode Plate Reader (PerkinElmer) were performed as for direct detection. All values were normalised to blanks (with no samples added) on the same 384 well plate.

Chemiluminescent snELISAs: Ottawa protocol

The surrogate neutralization ELISA first described in Abe *et al*.[13] was adapted and optimised for compatibility with the Hamilton MicroLab STAR robotic liquid handler. The methods for plate washing steps, incubations, and data acquisition were as described for the automated chemiluminescent ELISA. 384-well high-binding polystyrene Nunc plates (Thermo Fisher Scientific, #460372) were coated with 100 ng/well of spike or RBD 319–541, centrifuged in a plate spinner to ensure even coating, and incubated overnight with rocking at 4°C. Plates were washed,

80 µL of blocking solution (3% w/v skim milk powder in PBST) was added to each well, and the plates were incubated for 1 h at room temperature on a shaker at 700 rpm. During the blocking step, serum/plasma samples or DBS eluates were diluted in skim milk powder in PBST to a final milk concentration of 1% w/v. For single-point neutralisations, samples were diluted 1:5, or to calculate the half maximal effective concentration (EC50), the samples were titrated using a 5-point curve (1:5, 1:25, 1:125, 1:625, 1:6250). To facilitate quality control, downstream analysis, and cross-plate comparisons, standard curves of NRCoV2-20-Fc and three dilutions (1:5, 1:125, and 1:6250) of pooled positive and negative serum samples were included in quadruplicate on each plate. Serum-free/ACE2-free and serum-free wells were also included on each plate to establish the minimum and maximum signals, respectively. Plates were washed, and samples and controls (20 µL) were added to the wells and incubated for 2 h. Plates were then washed, and 6.5 ng of ACE2-BAP diluted in 1% w/v skim milk powder in PBST was added to each well and incubated for 1 h. Plates were again washed, and Streptavidin-Peroxidase Polymer (Sigma #S2438), diluted in 1% w/v skim milk powder in PBST at a concentration of 1.25 ng μL^{-1} (25 ng/well) was added to each well and incubated for 1 h. Plates were washed a final time and 20 µL of ELISA Pico Chemiluminescent Substrate (diluted 1:2 in MilliQ H_2O) was dispensed into each well. After a 5-min incubation, plates were read on an Neo2 plate reader (BioTek Instruments) at 20 ms/well and a read height of 1.0 mm. Assay optimisation data are presented in Supplementary figure 14.

Data analysis: Toronto

Quality control and determination of relative ratios

Raw values for each sample (luminescence counts per second) were normalised to a blank-subtracted reference point from the reference curve (0.0156 µg mL^{-1} for VHH72-Fc (for spike/RBD) or 0.0625 µg mL^{-1} for anti-N (for N)) to create relative ratios. For each automated test, the raw values and relative ratios of each control were compared to those of prior tests to confirm their similarity. The distributions of the raw values of the reference points and positive controls compared to the blanks and the reference points for each antigen compared to each other should be within the 90% confidence ellipse of the distributions of previous tests. In addition, the reference points should be within 15% coefficient of variation (CV) of prior runs. The $\log_{10}$ sample density distributions of the raw values and relative ratios were compared to prior runs to confirm

that they were within range. For points outside of these ranges, the individual control was either removed (e.g. if it was a single outlier out of the four on the plate) or the plate or test was repeated.

Receiver-operating characteristic (ROC) analysis

Samples acquired prior to November 2019 (pre-COVID) were considered true negatives and samples from convalescent patients with PCR-confirmed COVID-19 were considered true positives (for IgM and IgA analyses, we selected positives that were collected 20–40 days post-symptom onset). ROC analysis using relative ratios was performed with the pROC package in R[48] with default parameters. For IgG (serum/plasma and DBS), the analysis was performed in duplicate, with individual replicates considered individual samples. To avoid having samples with technical errors skew the threshold determination, negative plasma samples that were positive in only one replicate and negative DBS samples whose values were more than four standard deviations (SDs) from the mean of the log distribution of negative samples were removed from the analysis.

Thresholding based on the control mean

For plasma and serum IgG, negative controls (blanks, IgG pools, 0.25 and 0.0625 µL/well of a negative master mix (including equal volumes of four pre-COVID-19 samples (N2, N11, N39, N41), $n = 1320$ for spike, 1248 each for RBD and N) from 23 experiments over 4 months were included in the analysis. We used three SDs from the mean of the $\log_{10}$ distribution of the relative ratios of these negative controls as the threshold for each antigen. The same strategy was employed for IgA (72 negative controls from two experiments 1 month apart) and IgM (80 negative controls from three experiments over 2 months).

Scoring positives

Positive and negative results were first defined for each antigen, based on the defined thresholds. For projects where an overall assessment of the confidence of antibody detection in a sample is required, we imposed a sample-level rule: the sample must have passed positivity in at least 2 out of 3 antigen tests

Other data analyses

Plots were generated in R using the ggplot2, lattice, latticeExtra, grid, and gridExtra packages. Correlations between samples were calculated using the cor() function in the R stats package, using the Spearman method. The density distributions of the log of the signals scaled to the reference were separated using the normalmixEM mixtool function in the R mixtools package, based on an expected minimisation of only two subpopulations assumed to have a Gaussian distribution. normalmixEM initialisation, mean, and SD parameters were based on visual estimation of the density distribution of the log of the signal scaled to the reference. The initially assumed proportion between the two subpopulations was set to 50%. Density distributions were plotted using default R parameters (bandwidth: bw.nrd0, which implements a rule-of-thumb for choosing the bandwidth of a Gaussian kernel density estimator).

Calibration to the WHO standard for antibody detection

For each antigen, the relative ratio from the WHO International Standard (IS, National Institute for Biological Standards and Control (NIBSC, South Mimms, UK), Code 20/136, pooled convalescent plasma) at different sample dilutions (in binding antibody units (BAU) mL^{-1}) was represented in log-log scale. The response curve was modelled by an S-shaped sigmoid curve ($y = a \times x/(1 + b \times x) + c$, expressed in $\log_y$, $\log_x$ coordinates). The nls function (non-linear least squares) from the R stats package was used to best match the response to the measured data. The interval where the log response was considered linear to the log of the BAU mL^{-1} was selected visually. The lm (linear model) function from the R stats package was used to obtain the parameters of the linear approximation of the curve (Figure 3a). The WHO International Reference panel (NIBSC code 20/268), which contains pooled plasma samples that are Negative (code 20/142), Low (code 20/140), Low S High N (code 20/144), Mid (code 20/148), and High (code 20/150), was measured at different concentrations. Estimated BAU mL^{-1} values were obtained from the above linear approximation using only sample dilutions that were within this linear range, and further adjusted by accounting for the dilution factor. To convert from relative ratios (RRs) to BAU mL^{-1} for plasma or serum samples where only the reference curve was included in the same test, (Figure 3d), a conversion formula can be applied:

$$\log_2(\text{sample BAU/mL at dilution fold d}) = (\log_2(\text{sample RR}) - a)/b + \log_2(1/d)$$

where *a* and *b* represent the *y*-intercept and slope of the linear interval of the IS curve (Supplementary table 4).

Calibration to the WHO standard for snELISA

The WHO IS and the WHO International Reference Panel were analyzed by snELISA at the indicated dilutions to convert values to International Units (IU mL^{-1}). The same approach was applied as for the antibody detection ELISA except we used the sample relative ratio (RR) instead of the $\log_2$ of the sample RR because the linear range was larger. We then applied this formula:

$$\log_2(\text{sample IU/mL at dilution fold d}) = (\text{sample RR} - a)/b + \log_2(1/d)$$

where *a* and *b* represent the *y*-intercept and slope of the linear interval of the IS curve, respectively, and *d* is the dilution factor of the sample. For RBD as antigen, $a = 1.58$ and $b = -0.16$.

Data analysis: Ottawa

For consistency in data processing, a constant plate layout was established, containing all controls and standard curves in quadruplicate (Supplementary figure 11a). Luminescence values obtained from the isotype- and antigen-specific standard curve were modeled using a four-parameter log-logistic function to identify the inflection point (Supplementary figure 11b). Blank-subtracted luminescence values were scaled in relation to the curve to allow data normalisation for subsequent processing. Using a 3% false discovery rate (FDR) calculated using a density distribution from a screen of adult and pediatric pre-pandemic samples, a threshold was established for each isotype-antigen combination. Signal to threshold (also known as signal-to-cutoff, S/CO) ratios specific to each isotype-antigen combination were then calculated and sample positivity was determined (Supplementary figure 11c and d). For example, for IgG, both spike and N antigens were considered. If respective antigens were detected over the established threshold (S/CO ≥ 1), a positive call was made. All analyses were performed in R. Density distributions were determined using the default density function with default parameters. Standard curve processing was performed using the LL.4 four-parameter log-logistic self-starter function from the drc package in R,[49] also with default parameters. Plots were generated using the ggplot2 and reshape2 packages.

Using NML panel 4, containing known positive and negative DBS samples, the optimal FDR threshold value for SARS-CoV-2 IgG-positive calls was determined by testing FDRs of 1–100% and calculating the number of true positive (TP), false positive (FP), true negative (TN) and false negative (FN) samples. Maximum accuracy occurred at an FDR of 3% (Supplementary figure 11e). ROC curves and associated area under the curve measurements were generated in R using the pROC package with default parameters (Table 2, Supplementary figure 11f–h).

To convert luminescence values into BAU mL^{-1}, the WHO IS was titrated for spike, RBD and N (Supplementary figure 9). Scaled luminescence was calculated, as above, and response curves were modelled using the LL.4 four-parameter log-logistic self-starter function from the drc package with default parameters. The interval where the scaled luminescence response curves were considered linear to BAU was selected visually. Calibration of the three antigens was performed using the NIBSC 20/268 reference panel. The following formula was used to convert scaled luminescence values to BAU mL^{-1}:

$$BAUmL^{-1} = e^{((\ln(((Upper - Lower)/(ScaledLuminescence - Lower)) - 1)) / Slope + \ln(EC50))} \times dilutionfactor / assayvolum$$

For snELISA, the WHO IS was titrated and ACE2-spike binding inhibition was reported as a function of IUs. Blank adjusted luminescence values were converted to inhibition of ACE2-spike binding; maximal signal (i.e. 0% inhibition) was measured in absence of convalescent plasma (1% w/v skim milk powder in PBST). The normalised data was fitted using the LL.4 four-parameter log-logistic self-starter function from the drc package with default parameters in R to correlate binding inhibition to IUs. The following formula was used to convert binding inhibition % to IU mL^{-1}:

$$IUmL^{-1} = e^{((\ln(((Upper - Lower)/(\%\ inhibition - Lower)) - 1)) / Slope + \ln(EC50))} \times dilutionfactor / assayvolume$$

Reagent access

The reagents produced by the NRC and qualified as reference materials (spike [SMT1-1], N [NCAP-1] and hACE2-BAP) are available through the Metrology Research Centre Virtual Store (Virtual Store—National Research Council Canada: Products in Category Proteins (nrc-cnrc.gc.ca)). A limited panel of matched plasma and DBS is available upon request.

Acknowledgments

We thank Alex Pelletier, Denis L'Abbé, Mélanie Duchesne, Simon Lord-Dufour, Manon Ouimet, Brian Cass, Louis Bisson, Alina Burlacu, Jean-Sébastien Maltais, Sergio Alpuche-Lazcano and other members of the NRC-HHT Mammalian Cell Expression Section for their contribution to the cloning, expression and purification of the various recombinant proteins used in this study. The contribution of Joline Cormier to recombinant protein sample management is greatly appreciated. We are grateful to Joe Schrag, Roger Maurice, and Mathieu Coutu from NRC-HHT (Montreal) for SEC-UPLC and SEC-HPLC analyses. We thank Jamshid Tanha and Martin Rossotti from NRC-HHT (Ottawa) for providing NRCoV2-04-hFc1X7 and NRCoV2-20-hFc1X7 antibodies. We thank Frank Sicheri and Derek Ceccarelli (LTRI) for contributing bacterially expressed N and James Rini (University of Toronto) for contributing RBD and biotinylated ACE2 protein to compare with the reagents described here. We also thank Lauren Caldwell for preprocessing some of the data generated from automated ELISAs. We thank Bruce Mazer, Mel Krajden and members of the COVID-19 Immunity Task Force (CITF) for coordinating immune response studies across the country and for supporting assay development and implementation. This is NRC's publication #NRC-HHT_53561A. We acknowledge support from Ontario Together and funding from the Canadian Institutes of Health Research (CIHR; #VR1-172711, GA1-177703 and #439999) and the COVID-19 Immunity Task Force (CITF). We also acknowledge financial support from the NRC's Pandemic Response Challenge Program. Funding for initial assay development in the Gingras lab was provided through generous donations from the Royal Bank of Canada and the Krembil Foundation to the Sinai Health System Foundation. The robotics equipment used is housed in the Network Biology Collaborative Centre at the LTRI, a facility supported by the Canada Foundation for Innovation, the Ontario Government, and Genome Canada and Ontario Genomics (OGI-139). Assay development in the Langlois lab and the purchase of robotic equipment was supported by a grant from the CIHR (#VR2-172722 and VS2-175569) and supplemental funding from the CITF. KTA was a recipient of an Ontario Graduate Scholarship and is supported by a CIHR CGS-D studentship. YG is supported by a CIHR CGS-M studentship. MM holds a Queen Elizabeth II Graduate Scholarship in Science and Technology (QEII-GSST). A-CG is the Canada Research Chair in Functional Proteomics, and M-AL, A-CG, JLW, and SM are members of CoVaRR-Net, the CIHR Coronavirus Variants Rapid Response Network.

Conflict of interest

The authors declare no conflict of interest.

Author contributions

Karen Colwill: Conceptualization; Data curation; Investigation; Methodology; Project administration; Validation; Visualization; Writing – original draft; Writing – review & editing. **Yannick Galipeau:** Investigation; Methodology; Validation; Visualization; Writing – original draft; Writing – review & editing. **Matthew Stuible:** Investigation; Methodology; Resources; Visualization; Writing – original draft; Writing – review & editing. **Christian Gervais:** Investigation; Methodology; Resources; Validation; Writing – original draft. **Corey Arnold:** Data curation; Formal analysis; Investigation; Methodology; Validation; Visualization; Writing – original draft; Writing – review & editing. **Bhavisha Rathod:** Investigation; Methodology. **Kento T Abe:** Investigation; Visualization. **Jenny H Wang:** Investigation; Methodology. **Adrian Pasculescu:** Data curation; Formal analysis; Investigation; Methodology; Software; Validation; Visualization. **Mariam Maltseva:** Investigation; Methodology; Visualization. **Lynda Rocheleau:** Formal analysis; Investigation; Software; Visualization. **Martin Pelchat:** Data curation; Formal analysis; Investigation; Software; Visualization. **Mahya Fazel-Zarandi:** Investigation. **Mariam Iskilova:** Investigation; Methodology. **Miriam Barrios-Rodiles:** Investigation; Methodology; Supervision; Validation. **Linda Bennett:** Resources. **Kevin Yau:** Resources. **François Cholette:** Investigation; Methodology. **Christine Mesa:** Investigation; Methodology. **Angel Xinliu Li:** Resources. **Aimee Paterson:** Resources. **Michelle A Hladunewich:** Resources. **Pamela J Goodwin:** Resources. **Jeffrey L Wrana:** Supervision. **Steven J Drews:** Resources. **Samira Mubareka:** Resources. **Allison J McGeer:** Resources. **John Kim:** Investigation; Methodology; Resources; Supervision. **Marc-André Langlois:** Conceptualization; Funding acquisition; Project administration; Resources; Supervision; Writing – original draft; Writing – review & editing. **Anne-Claude Gingras:** Conceptualization; Funding acquisition; Project administration; Resources; Supervision; Writing – original draft; Writing – review & editing. **Yves Durocher:** Conceptualization; Funding acquisition; Investigation; Methodology; Project administration; Resources; Supervision; Writing – original draft; Writing – review & editing.

Code availability

Code is available upon request.

Data availability statement

Raw and normalised values from the automated assays are provided in Supplementary table 5. R scripts used to analyze the data are available upon request.

References

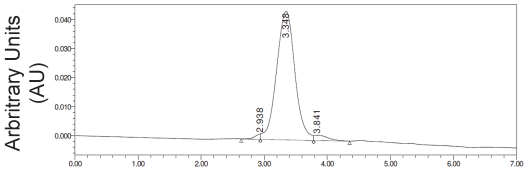
1. Johns Hopkins University COVID-19 Dashboard [December 9 2021]. Available from: https://coronavirus.jhu.edu/map.html.
2. Few Canadians had antibodies against SARS-CoV-2 in early 2021 - Statistics Canada [July 6 2021]. Available from: https://www150.statcan.gc.ca/n1/daily-quotidien/210706/dq210706a-eng.htm. 3. Serotracker [updated October 14 2021. Available from: https://serotracker.com/en/Explore.
4. Chung H, He S, Nasreen S, Sundaram ME, Buchan SA, Wilson SE, et al. Effectiveness of BNT162b2 and mRNA-1273 covid-19 vaccines against symptomatic SARS-CoV-2 infection and severe covid-19 outcomes in Ontario, Canada: test negative design study. BMJ. 2021;374:n1943.
5. Health Infobase Canada -COVID-19 Vaccination Coverage [updated November 27 2021. Available from: https://health-infobase.canada.ca/covid-19/vaccination-coverage/.
6. Van Caeseele P, Canadian Public Health Laboratory N, Bailey D, Canadian Society of Clinical C, Forgie SE, Association of Medical M, et al. SARS-CoV-2 (COVID-19) serology: implications for clinical practice, laboratory medicine and public health. Cmaj. 2020;192(34):E973-E9.
7. Favresse J, Eucher C, Elsen M, Gillot C, Van Eeckhoudt S, Dogne JM, et al. Persistence of Anti-SARS-CoV-2 Antibodies Depends on the Analytical Kit: A Report for Up to 10 Months after Infection. Microorganisms. 2021;9(3).
8. Isho B, Abe KT, Zuo M, Jamal AJ, Rathod B, Wang JH, et al. Persistence of serum and saliva antibody responses to SARS-CoV-2 spike antigens in COVID-19 patients. Science immunology. 2020;5(52).
9. Sherina N, Piralla A, Du L, Wan H, Kumagai-Braesch M, Andrell J, et al. Persistence of SARS-CoV-2-specific B and T cell responses in convalescent COVID-19 patients 6-8 months after the infection. Med (N Y). 2021;2(3):281-95 e4.
10. Dan JM, Mateus J, Kato Y, Hastie KM, Yu ED, Faliti CE, et al. Immunological memory to SARS-CoV-2 assessed for up to 8 months after infection. Science (New York, NY. 2021;371(6529).
11. Gallais F, Gantner P, Bruel T, Velay A, Planas D, Wendling MJ, et al. Evolution of antibody responses up to 13 months after SARS-CoV-2 infection and risk of reinfection. EBioMedicine. 2021;71:103561.
12. Feng C, Shi J, Fan Q, Wang Y, Huang H, Chen F, et al. Protective humoral and cellular immune responses to SARS-CoV-2 persist up to 1 year after recovery. Nat Commun. 2021;12(1):4984.
13. Abe KT, Li Z, Samson R, Samavarchi-Tehrani P, Valcourt EJ, Wood H, et al. A simple protein-based surrogate neutralization assay for SARS-CoV-2. JCI Insight. 2020;5(19).
14. Mattiuzo G, Bentley E, Hassall M, Routley S, Richardson S, Bernasconi V, et al. Establishment of the WHO International Standard and Reference Panel for anti-SARS-CoV-2 antibody. WHO Expert Committe on Biological Standardization. WHO/BS/2020.2403. 2020.
15. Stuible M, Gervais C, Lord-Dufour S, Perret S, L'Abbe D, Schrag J, et al. Rapid, high-yield production of full-length SARS-CoV-2 spike ectodomain by transient gene expression in CHO cells. J Biotechnol. 2021;326:21-7.
16. Shi C, Shin YO, Hanson J, Cass B, Loewen MC, Durocher Y. Purification and characterization of a recombinant G-protein-coupled receptor, Saccharomyces cerevisiae Ste2p, transiently expressed in HEK293 EBNA1 cells. Biochemistry. 2005;44(48):15705-14.
17. Wrapp D, De Vlieger D, Corbett KS, Torres GM, Wang N, Van Breedam W, et al. Structural Basis for Potent Neutralization of Betacoronaviruses by Single-Domain Camelid Antibodies. Cell. 2020;181(6):1436-41.
18. Dorion-Thibaudeau J, St-Laurent G, Raymond C, De Crescenzo G, Durocher Y. Biotinylation of the Fcgamma receptor ectodomains by mammalian cell co-transfection: application to the development of a surface plasmon resonance-based assay. J Mol Recognit. 2016;29(2):60-9.
19. Darnell ME, Taylor DR. Evaluation of inactivation methods for severe acute respiratory syndrome coronavirus in noncellular blood products. Transfusion. 2006;46(10):1770-7.

20. Cholette F, Mesa C, Harris A, Ellis H, Cachero K, Lecap P, et al. Dried blood spot specimens for SARS-CoV-2 antibody testing: A multi-site, multi-assay comparison. PREPRINT (Version 1) available at Research Square. 2021;DOI: 10.21203/rs.3.rs-366992/v1.
21. Amanat F, Stadlbauer D, Strohmeier S, Nguyen THO, Chromikova V, McMahon M, et al. A serological assay to detect SARS-CoV-2 seroconversion in humans. Nature medicine. 2020;26(7):1033-6.
22. Amanat F, Stadlbauer D, Strohmeier S, Nguyen THO, Chromikova V, McMahon M, et al. A serological assay to detect SARS-CoV-2 seroconversion in humans. Nature medicine. 2020.
23. Robin X, Turck N, Hainard A, Tiberti N, Lisacek F, Sanchez JC, et al. pROC: an open-source package for R and S+ to analyze and compare ROC curves. BMC bioinformatics. 2011;12:77.
24. Ritz C, Baty F, Streibig JC, Gerhard D. Dose-Response Analysis Using R. PloS one. 2015;10(12):e0146021.
25. Ye Q, West AMV, Silletti S, Corbett KD. Architecture and self-assembly of the SARS-CoV-2 nucleocapsid protein. Protein Sci. 2020;29(9):1890-901.
26. Morley GL, Taylor S, Jossi S, Perez-Toledo M, Faustini SE, Marcial-Juarez E, et al. Sensitive Detection of SARS-CoV-2-Specific Antibodies in Dried Blood Spot Samples. Emerg Infect Dis. 2020;26(12):2970-3.
27. Biosafety advisory: SARS-CoV-2 (Severe acute respiratory syndrome-related coronavirus 2) - Government of Canada [updated November 26 2020. Available from: https://www.canada.ca/en/public-health/services/laboratory-biosafety-biosecurity/biosafety-directives-advisories-notifications/novel-coronavirus-january-27.html.
28. Galipeau Y, Siragam V, Laroche G, Marion E, Greig M, McGuinty M, et al. Relative Ratios of Human Seasonal Coronavirus Antibodies Predict the Efficiency of Cross-Neutralization of SARS-CoV-2 Spike Binding to ACE2. medRxiv Preprint. 2021:2021.07.16.21260079.
29. Yau K, Abe KT, Naimark D, Oliver MJ, Perl J, Leis JA, et al. Evaluation of the SARS-CoV-2 Antibody Response to the BNT162b2 Vaccine in Patients Undergoing Hemodialysis. JAMA Netw Open. 2021;4(9):e2123622.
30. Feng S, Phillips DJ, White T, Sayal H, Aley PK, Bibi S, et al. Correlates of protection against symptomatic and asymptomatic SARS-CoV-2 infection. Nature medicine. 2021.
31. Approved COVID-19 Vaccines - Goverment of Canada [updated September 24 2021. Available from: https://www.canada.ca/en/health-canada/services/drugs-health-products/covid19-industry/drugs-vaccines-treatments/vaccines.html.
32. Approved COVID-19 Vaccines - US Food and Drug Administration [December 9 2021]. Available from: https://www.fda.gov/emergency-preparedness-and-response/coronavirus-disease-2019-covid-19/covid-19-vaccines.
33. COVID-19 approved vaccines - European Medicines Agency [December 9 2021]. Available from: https://www.ema.europa.eu/en/human-regulatory/overview/public-health-threats/coronavirus-disease-covid-19/treatments-vaccines/covid-19-vaccines.
34. Lv H, Wu NC, Tsang OT, Yuan M, Perera R, Leung WS, et al. Cross-reactive Antibody Response between SARS-CoV-2 and SARS-CoV Infections. Cell Rep. 2020;31(9):107725.
35. Ou X, Liu Y, Lei X, Li P, Mi D, Ren L, et al. Characterization of spike glycoprotein of SARS-CoV-2 on virus entry and its immune cross-reactivity with SARS-CoV. Nat Commun. 2020;11(1):1620.
36. Dobano C, Santano R, Jimenez A, Vidal M, Chi J, Rodrigo Melero N, et al. Immunogenicity and crossreactivity of antibodies to the nucleocapsid protein of SARS-CoV-2: utility and limitations in seroprevalence and immunity studies. Transl Res. 2021;232:60-74.
37. Rogers TF, Zhao F, Huang D, Beutler N, Burns A, He WT, et al. Isolation of potent SARS-CoV-2 neutralizing antibodies and protection from disease in a small animal model. Science (New York, NY. 2020;369(6506):956-63.
38. Premkumar L, Segovia-Chumbez B, Jadi R, Martinez DR, Raut R, Markmann A, et al. The receptor binding domain of the viral spike protein is an immunodominant and highly specific target of antibodies in SARS-CoV-2 patients. Science immunology. 2020;5(48).

39. Science Brief: Omicron (B.1.1.529) Variant [December 9 2021]. Available from: https://www.cdc.gov/coronavirus/2019-ncov/science/science-briefs/scientific-brief-omicron-variant.html.
40. Saeed S, O'Brien SF, Abe K, Yi QL, Rathod B, Wang J, et al. Severe acute respiratory syndrome coronavirus 2 (SARS-CoV-2) seroprevalence: Navigating the absence of a gold standard. PloS one. 2021;16(9):e0257743.
41. Tang X, Sharma A, Pasic M, Patrick B, Colwill K, Gelband H, et al. SARS-CoV-2 Seroprevalence During the First and Second Pandemic Waves in Canada. Lancet Preprint. 2021;Available from http://dx.doi.org/10.2139/ssrn.3903944. 42. CanPath National Study [June 23 2021]. Available from: https://canpath.ca/2021/06/early-results-from-canpaths-national-study-confirm-antibody-levels-are-stronger-after-receiving-two-doses-of-covid-19-vaccine.
43. Abe KT, Hu Q, Mozafarihashjin M, Samson R, Manguiat K, Robinson A, et al. Neutralizing antibody responses to SARS-CoV-2 variants in vaccinated Ontario long-term care home residents and workers. medRxiv Preprint. 2021:2021.08.06.21261721.
44. Vinh DC, Gouin J-P, Cruz-Santiago D, Canac-Marquis M, Bernier S, Bobeuf F, et al. Real-world serologic responses to Extended-interval and Heterologous COVID-19 mRNA vaccination in Frail Elderly - Interim report from a prospective observational cohort study. medRxiv Preprint. 2021:2021.09.16.21263704.

Supplementary Files

Spike (SMT1)

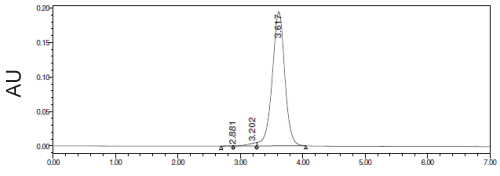


Sample Conc. (mg mL^{-1}): 0.80

UPLC-SEC, BEH450

	RT	% Area	Area	Height
1	2.938	1.17	10935	1914
2	3.348	95.76	894783	44280
3	3.841	3.07	28719	1839

RBD (331–521)

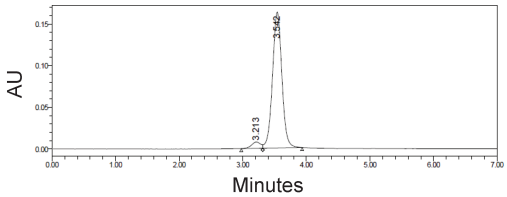


Sample Conc. (mg mL^{-1}): 1.07

UPLC-SEC, BEH200

	RT	% Area	Area	Height
1	2.881	0.05	1376	269
2	3.202	1.63	44817	3980
3	3.617	98.32	2709774	193790

RBD (319–541)

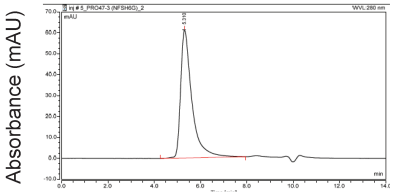


Sample Conc. (mg mL^{-1}): 0.98

UPLC-SEC, BEH200

	RT	% Area	Area	Height
1	3.213	4.25	74411	7654
2	3.542	95.75	1675802	163023

Nucleocapsid (NCAP)

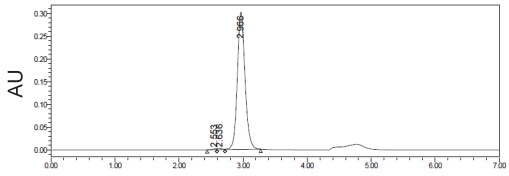


Sample Conc. (mg mL^{-1}): 1.4

HPLC-SEC, Superdex

	RT	% Area	Area	Height
1	5.31	100	2070500	61109

ACE2-BAP

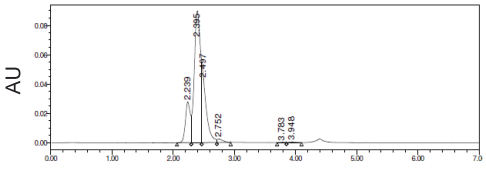


Sample Conc. (mg mL^{-1}): 0.80

UPLC-SEC, BEH200

	RT	% Area	Area	Height
1	2.553	0.34	8581	1746
2	2.636	0.52	13284	2203
3	2.966	99.14	2521768	301927

IgG#5-HRP

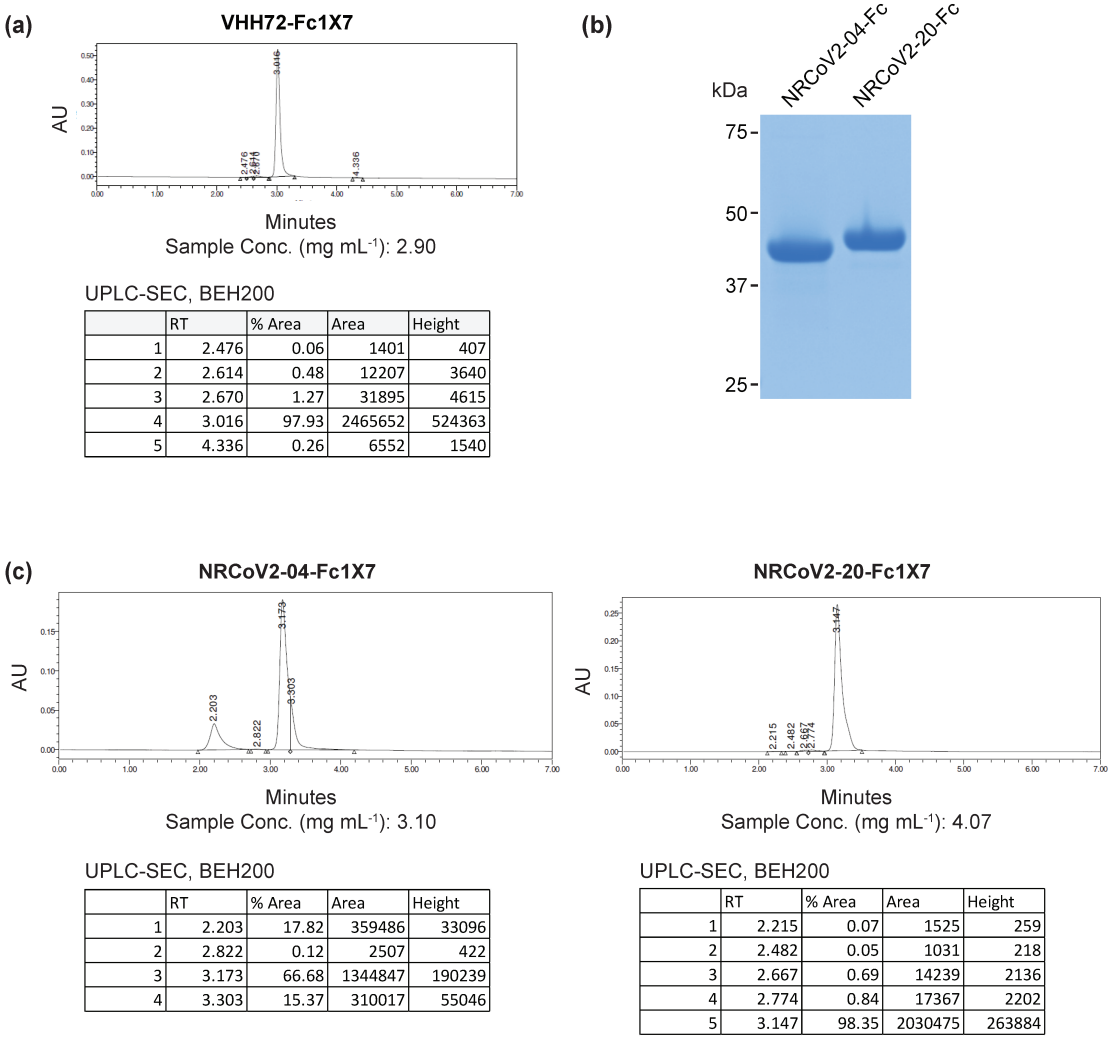


Sample Conc. (mg mL^{-1}): 0.60

UPLC-SEC, BEH200

	RT	% Area	Area	Height
1	2.239	14.43	151481	27895
2	2.395	59.64	625983	89609
3	2.497	24.12	253149	43384
4	2.752	1.44	15156	2291
5	3.783	0.1	999	206
6	3.948	0.27	2835	369

Supplementary figure 1. Chromatogram traces for the purified ELISA antigens and detection reagents.



UPLC-SEC, BEH200

	RT	% Area	Area	Height
1	2.476	0.06	1401	407
2	2.614	0.48	12207	3640
3	2.670	1.27	31895	4615
4	3.016	97.93	2465652	524363
5	4.336	0.26	6552	1540

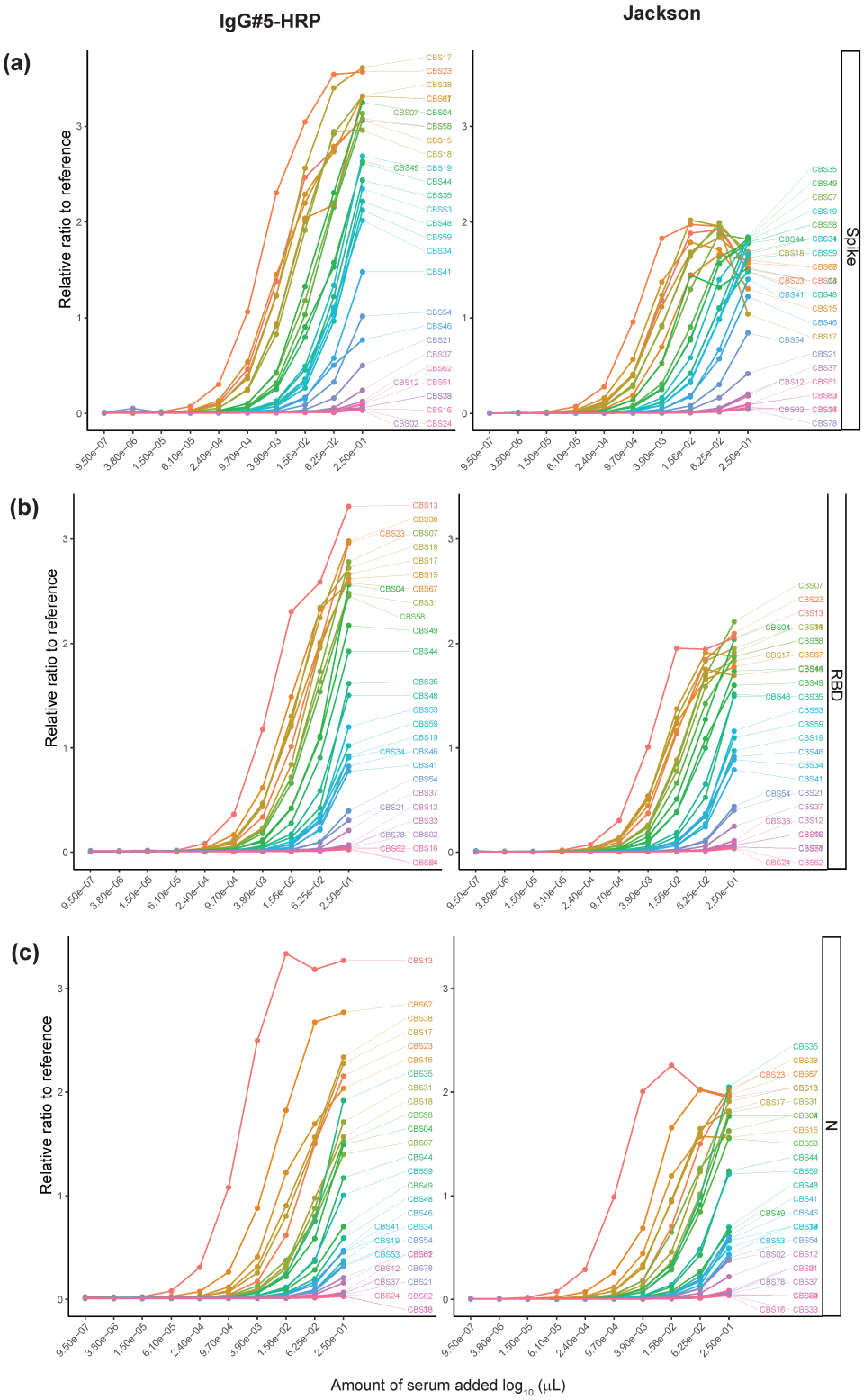
UPLC-SEC, BEH200

	RT	% Area	Area	Height
1	2.203	17.82	359486	33096
2	2.822	0.12	2507	422
3	3.173	66.68	1344847	190239
4	3.303	15.37	310017	55046

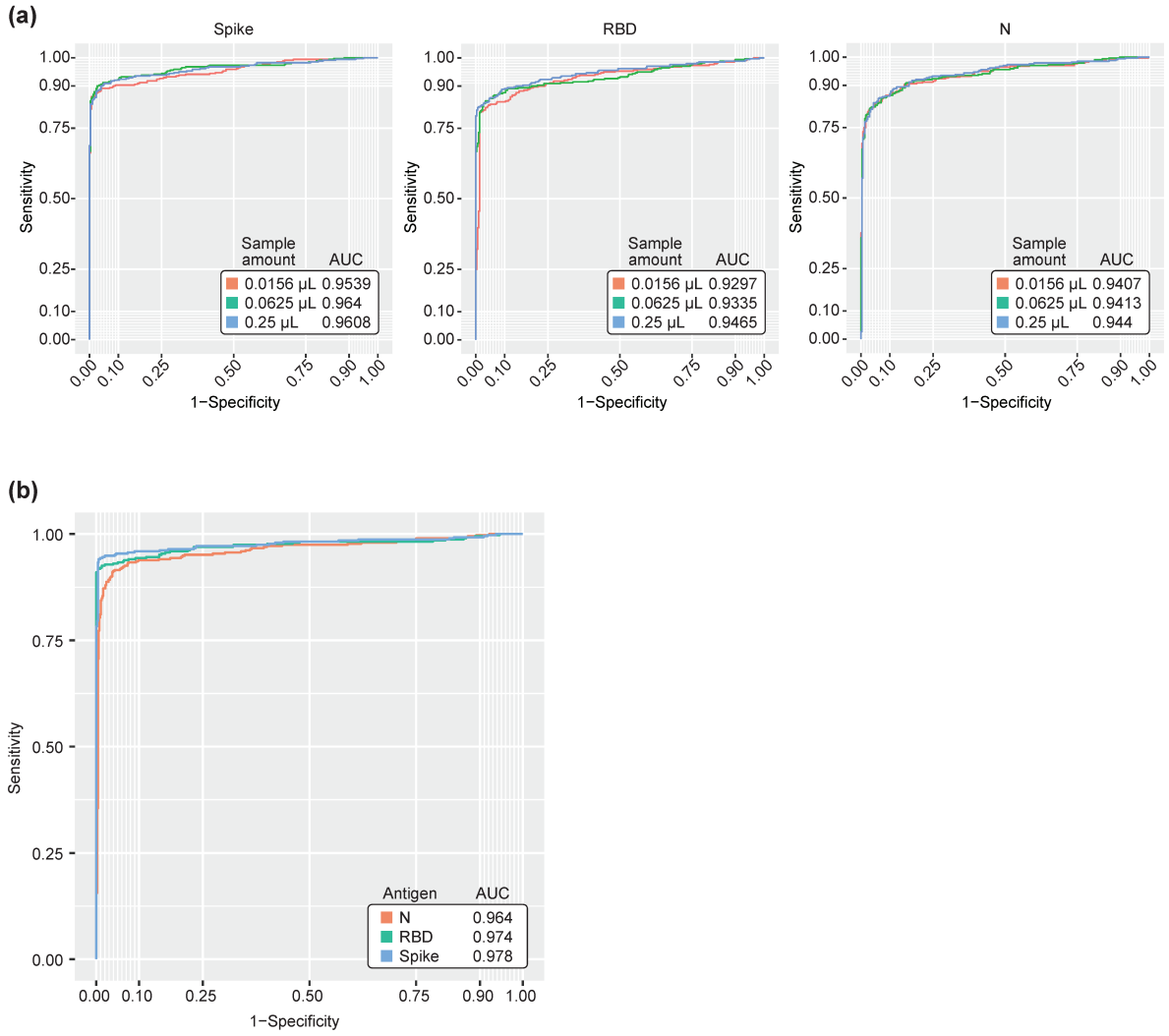
UPLC-SEC, BEH200

	RT	% Area	Area	Height
1	2.215	0.07	1525	259
2	2.482	0.05	1031	218
3	2.667	0.69	14239	2136
4	2.774	0.84	17367	2202
5	3.147	98.35	2030475	263884

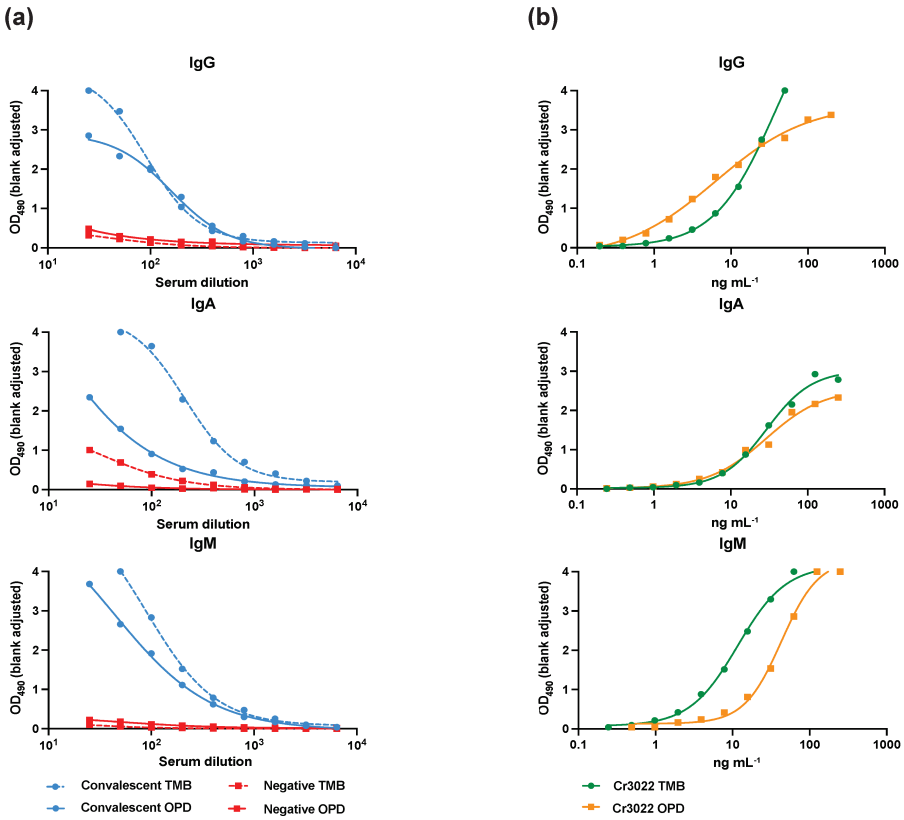
Supplementary figure 2. Purification of recombinant anti-spike antibodies. **(a)** Chromatogram trace for VHH72-Fc. **(b)** Two additional recombinant anti-spike antibodies were analyzed on Coomassie-stained polyacrylamide gels under reducing conditions to assess their purity. Molecular weight markers (kDa) are shown to the left of the gel. **(c)** Chromatogram traces for the two additional anti-spike antibodies.



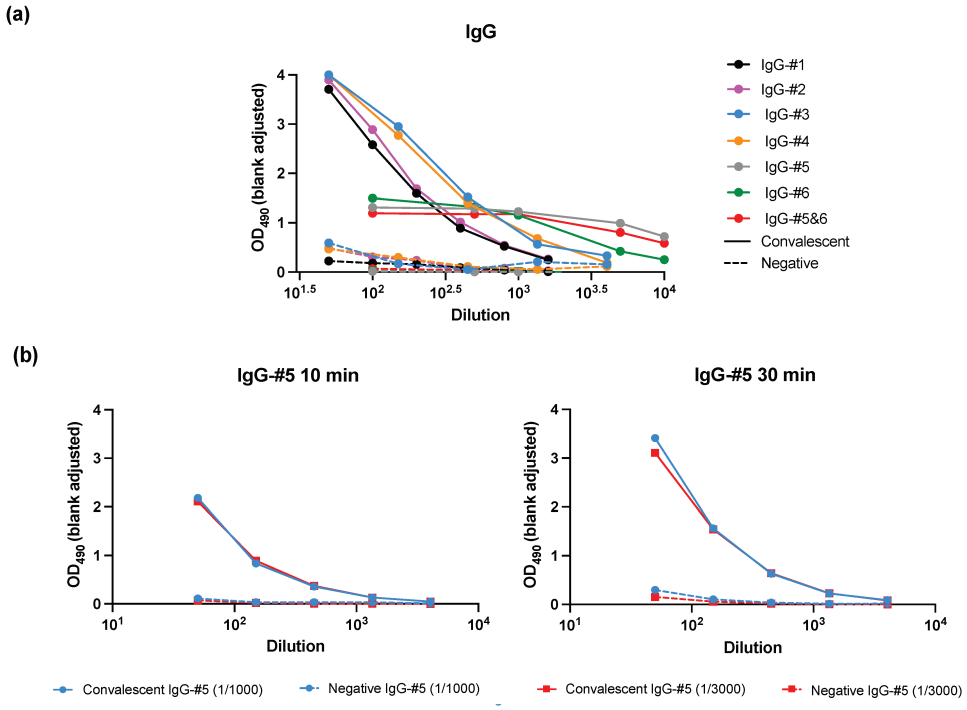
Supplementary figure 3. Titration curves of 32 serum samples from CBS using automated ELISAs to detect **(a)** spike, **(b)** RBD 331–521, and **(c)** N antibodies. IgG#5-HRP was used at 0.09 µg mL-1 and Jackson IgG-HRP was used at 0.02 µg mL-1.



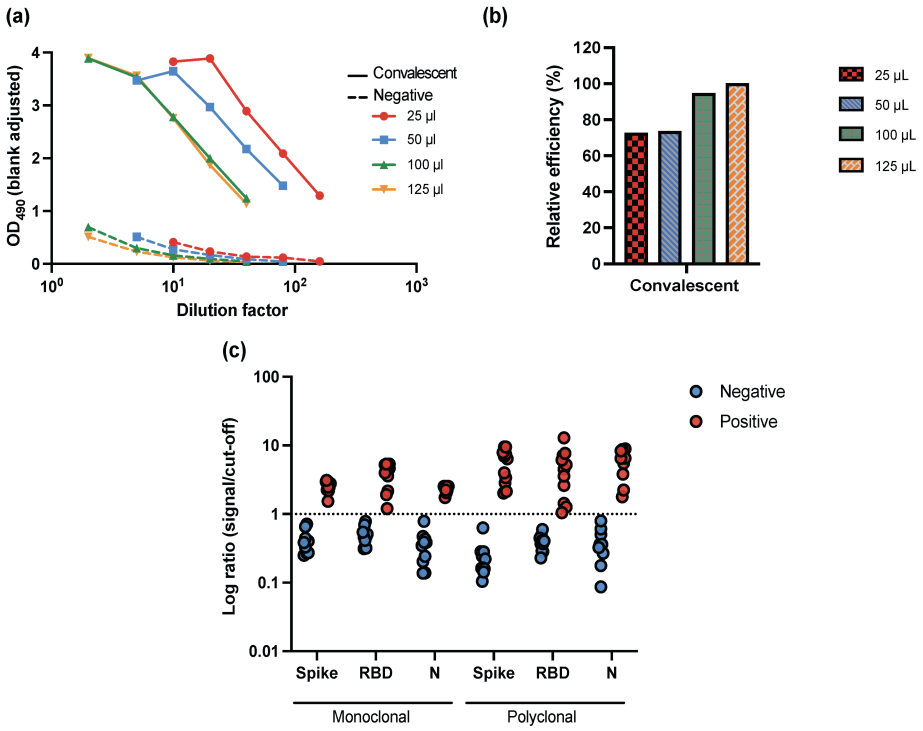
Supplementary figure 4. Performance of the IgG chemiluminescent ELISAs with plasma and serum. **(a)** ROC analyses of three different dilutions of negative (pre-COVID-19, *n* = 300) and positive (convalescent, *n* = 211) plasma and serum samples. The dilution is the amount of sample added per well. **(b)** ROC analysis at 0.0625 µL/well. A subset of samples from (a) (181 positive, 260 negative) were repeated and all samples from the 0.0625 µL dilution were treated as independent samples. Raw values were normalized to the 0.0156 µg mL-1 point in the reference curve for spike and RBD and to the 0.0625 µg mL-1 point for N. Performance statistics are shown in Table 1.



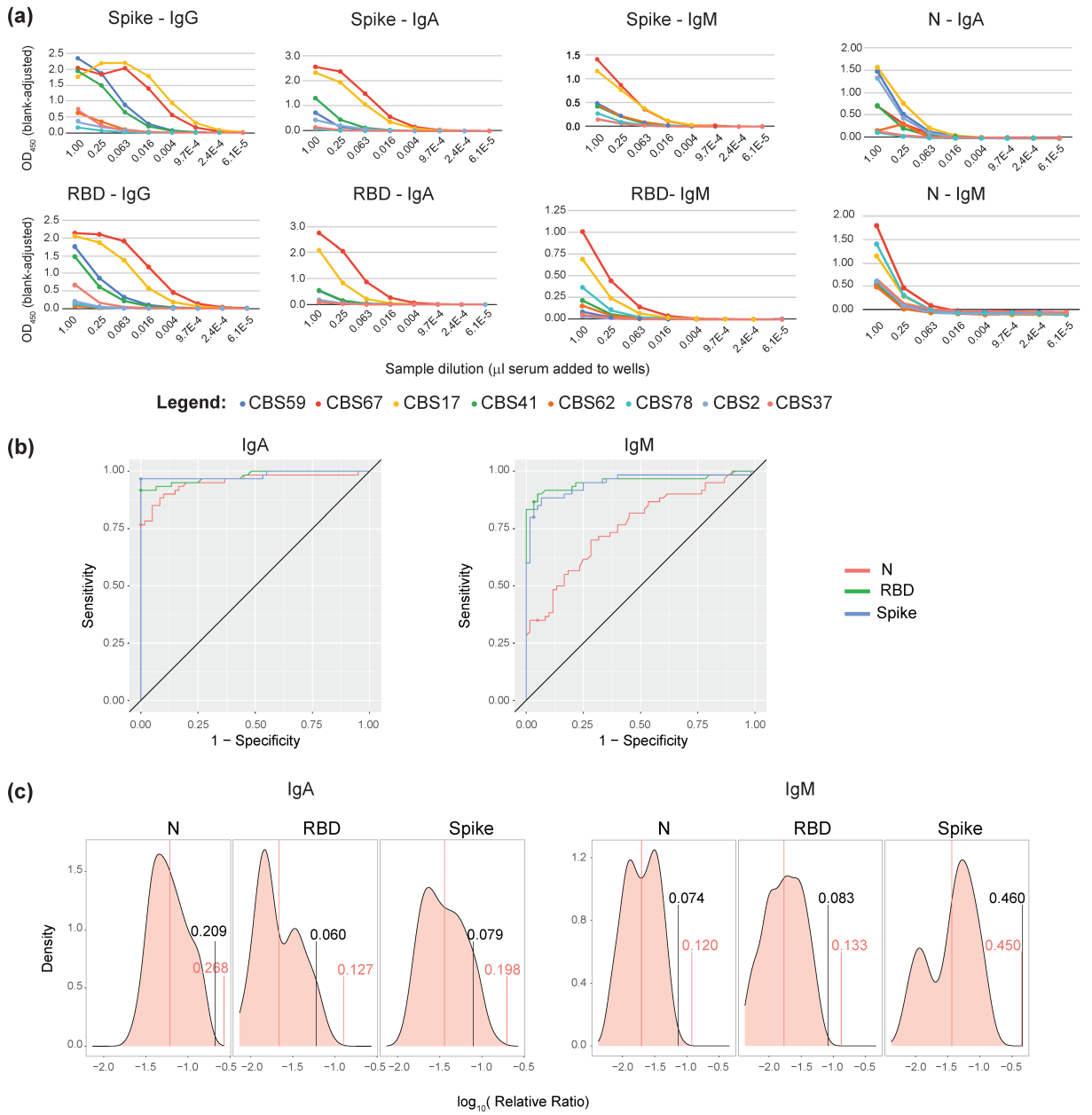
Supplementary figure 5. Comparison between o-Phenylenediamine dihydrochloride (OPD) and 3,3′,5,5′-tetramethylbenzidine (TMB) as colorimetric substrates for the manual 96-well plate ELISA. A final volume of 100 µL of substrate was added and incubated in the dark with shaking for 10 min before reactions were stopped by the addition of 50 µL of 3 M HCl. **(a)** A SARS-CoV-2 convalescent serum and a known negative serum were titrated to compare the relative performance of the substrates. Antibodies against the RBD (319–541, 100 ng/well) were measured using monoclonal IgG (Millipore A0170), IgA (The Jackson Laboratory 109-035-129), and IgM (The Jackson Laboratory 109-035-011) at 1:3,000. Absorbance at 490 nm was measured and blank-adjusted. **(b)** Titration of the commercial isotype-specific CR3022 clone (Absolute Antibody) against the RBD for all three main isotypes using TMB or OPD. CR3022 isotype-specific curves were generated on the same plates as the serum titration shown in (a) and were used as standard/calibration curves. TMB was more sensitive but did not substantially increase the dynamic range between the known negative and positive samples.



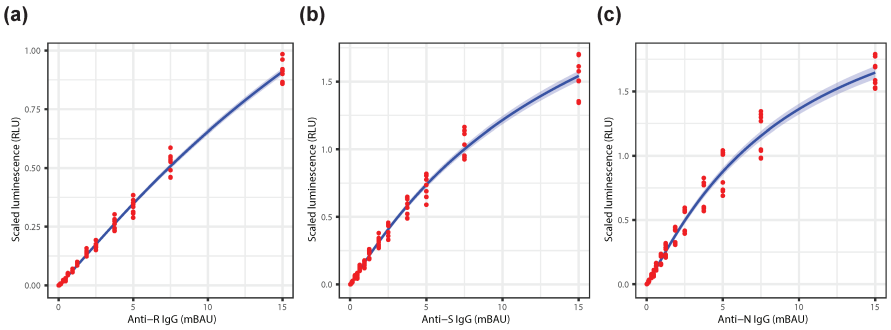
Supplementary figure 6. Comparison of IgG-HRP secondary antibody performance **(a)** Analysis of NRC IgG-HRP secondary (detection) antibodies. A convalescent SARS-CoV-2 serum and a known negative serum were titrated, and RBD-specific IgG antibodies were measured using different secondary antibodies at 1:3,000. Coated RBD (319–541) antigen was constant at 100 ng/well and OPD was used as the colorimetric substrate. IgG #5 and #6 are HRP fusions, while IgG-#1 to #4 are HRP conjugates that gave the highest signals. IgGs-#5 and #6 had the lowest cross-reactivity to the negative serum. Combining IgG #5 and #6 had no impact on the signal. IgG#5-HRP was chosen as the default IgG secondary for our serological assay. **(b)** Optimization of OPD development time and IgG#5-HRP concentration. Convalescent SARS-CoV-2 serum and known negative serum were titrated and RBD-specific IgG antibodies were measured using the IgG-#5-HRP at 1:1,000 and 1:3,000. Two reaction times were tested, and reactions were stopped by adding 3 M HCL. Increasing the reaction time resulted in a higher signal and increased dynamic range between the positive and negative sera. The higher concentration of IgG#5-HRP had no significant impact on the signal



Supplementary figure 7. Elution and secondary antibody optimizations for IgG ELISAs using DBSs. **(a)** To determine the optimal elution volume, a DBS sample from a convalescent SARS-CoV-2 individual (CoV-19) and a known negative DBS sample (CoV-20) were eluted in four different volumes of PBS from 3 mm DBS discs at room temperature overnight with shaking in a 96-well u-bottom plate. IgG antibodies against spike (100 ng/well) were measured using polyclonal IgG-HRP (Abcam, #ab97165; at 1:3,000) as a secondary antibody and developed with OPD. **(b)** The elution efficiency was calculated from the results shown in (a). To account for the different dilutions, the IgG-CR3022 standard curve was used to calculate the titers of anti-spike IgG in each elution volume. The 125 µL elution volume had the highest titers and was set at 100%, with other conditions calculated in relation to that value. Volumes of 100 or 125 µL enabled optimal elution, and elution efficiency was significantly impacted at lower volumes. Therefore, we used 100 µL/3 mm DBS disc in our downstream serology ELISAs, mitigating the need for highly concentrated eluates while maintaining good elution efficiency. **(c)** Signal to cutoff (S/CO) ratios were calculated for a panel of 20 contrived DBS specimens of known positive and negative samples produced by the NML. The samples were tested for IgG antibodies using monoclonal (IgG-#5-HRP) and polyclonal (ab97165) secondary antibodies for spike, RBD (319–541), and N. All DBS punches were eluted in 100 µL PBS overnight at room temperature. For the monoclonal secondary the eluate was used undiluted, while for the polyclonal antibody it was diluted 1:10. The cutoff was set at two SDs of the negative distribution.



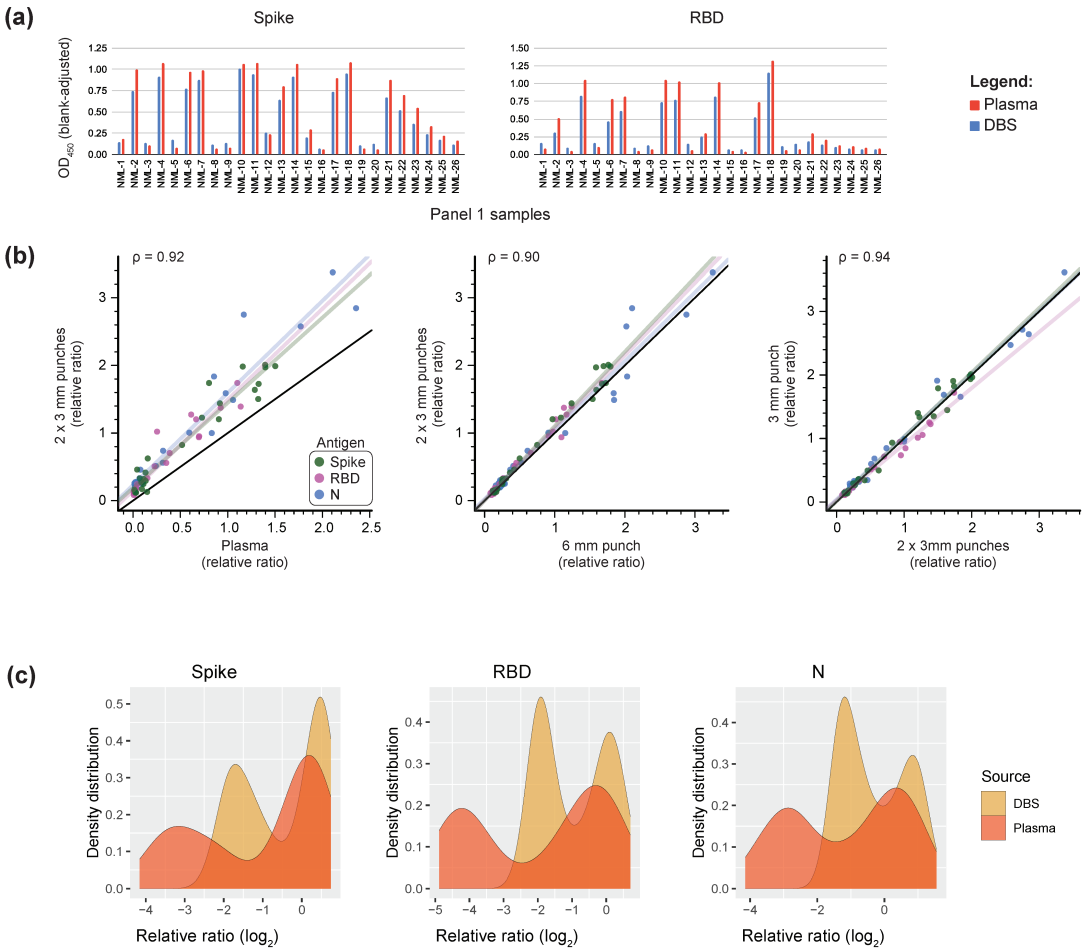
Supplementary figure 8. IgA and IgM ELISAs. **(a)** Titration curves of CBS samples were used to test the Jackson anti-IgA (1:10,000) and anti-IgM (1:60,000) HRP secondary antibodies using the manual assay on spike (200 ng/well), RBD (331–521, 75 ng/well), and N (25 ng/well), and to compare them against IgG curves generated using anti-IgG#5-HRP (1:10,000) for spike and RBD (see Supplementary Figure 13 for N). Due to precipitate formation in the IgA experiment at high sample concentrations, a 1:20,000 dilution was selected for subsequent experiments. **(b)** ROC analysis for IgM and IgA was performed using the automated assay on a sample set of PCR-confirmed COVID-19 cases 20–40 days post-symptom onset and negative (pre-COVID-19) samples (see Supplementary Table 4 for statistics). **(c)** Similar to IgG, we compared these thresholds to those determined by calculating three SDs from the mean of the negative control log distribution (two tests for IgA 1 month apart, n = 72; three tests for IgM over 2 months, n = 120). For IgA, this analysis suggested that the thresholds for spike and RBD based on the ROC were not sufficiently stringent. Similarly, for IgM, the thresholds for RBD and NP appeared lenient. The final thresholds selected for IgA and IgM were therefore based on three SDs from the mean of the negative controls (see Supplementary Table 3 for statistics).



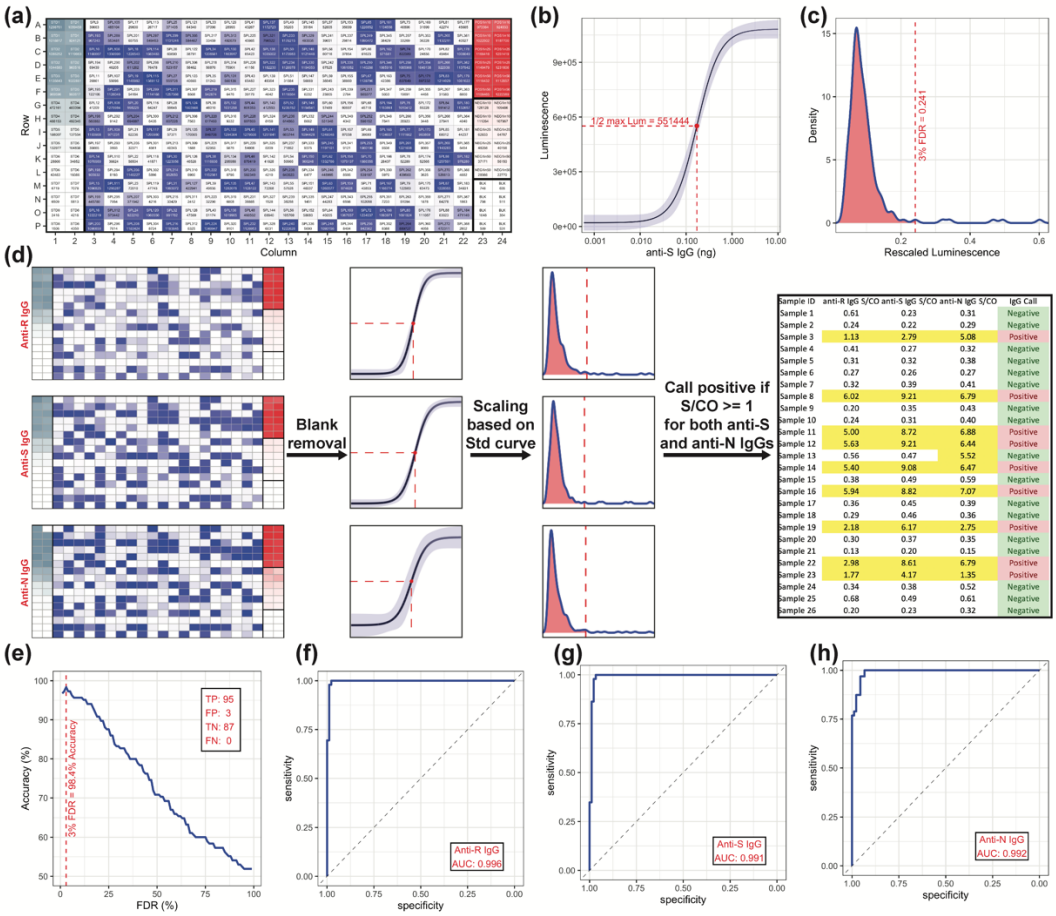
(d)

Sample ID	Anti-R IgG	Anti-S IgG	Anti-N IgG	IgG Call
Sample 1	0.592	0.065	0.114	Negative
Sample 2	0.237	0.063	0.108	Negative
Sample 3	1.103	0.891	4.021	Positive
Sample 4	0.405	0.078	0.117	Negative
Sample 5	0.306	0.091	0.136	Negative
Sample 6	0.269	0.075	0.099	Negative
Sample 7	0.313	0.111	0.150	Negative
Sample 8	12.247	7.179	23.931	Positive
Sample 9	0.198	0.099	0.154	Negative
Sample 10	0.236	0.089	0.145	Negative
Sample 11	8.017	6.075	30.774	Positive
Sample 12	10.387	7.173	12.667	Positive
Sample 13	0.547	0.134	5.360	Negative
Sample 14	9.428	6.854	13.167	Positive
Sample 15	0.369	0.137	0.210	Negative
Sample 16	11.869	6.277	79.842	Positive
Sample 17	0.354	0.127	0.142	Negative
Sample 18	0.292	0.129	0.131	Negative
Sample 19	2.320	2.819	1.185	Positive
Sample 20	0.294	0.104	0.129	Negative
Sample 21	0.137	0.058	0.060	Negative
Sample 22	3.462	5.861	23.680	Positive
Sample 23	1.815	1.512	0.493	Positive
Sample 24	0.337	0.108	0.184	Negative
Sample 25	0.657	0.137	0.215	Negative
Sample 26	0.205	0.067	0.118	Negative

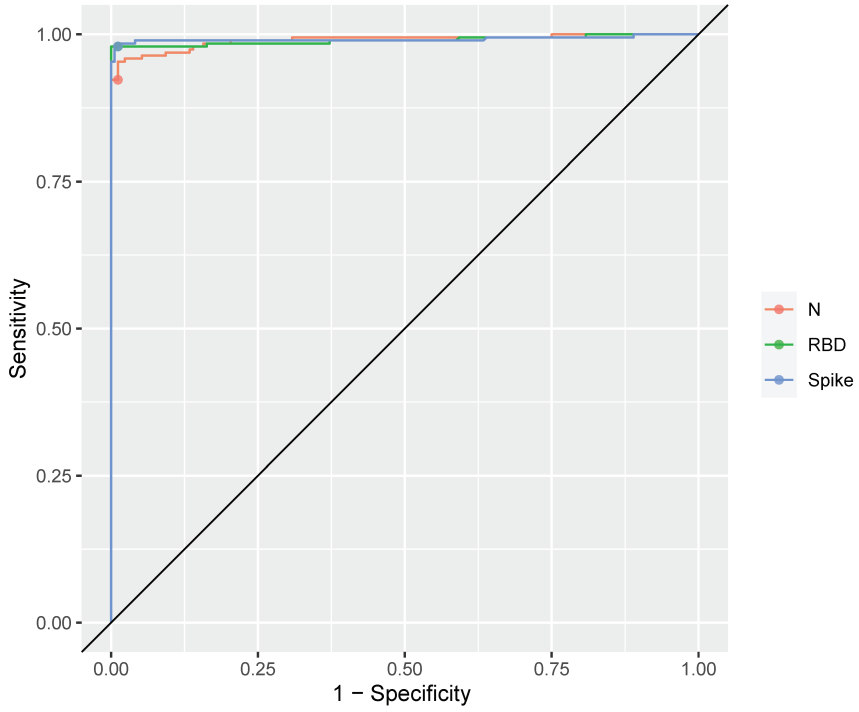
Supplementary figure 9. Conversion of serology data to WHO BAUs and validation of SARS-CoV-2 IgG profiling performed on the uOttawa automated serology platform. Calibrants used were the National Institute for Biological Standards and Control (NIBSC) reference panel (code: 20/268) and the First WHO International Standard (20/136). **(a)–(c)** Titration of the NIBSC 20/136 pooled convalescent serum for IgG using spike, RBD, and N. Linear regression using scaled luminescence values (as detailed in Supplementary Figure 11) and the viral titre in BAU µL-1 is shown. **(d)** Titers (BAU mL-1) and calls for the set of representative samples analyzed in Supplementary figure 11. Yellow, green, and red indicate samples above the 3% FDR threshold, overall negative samples, and overall positive samples, respectively. Samples were considered positive for SARS-CoV-2 IgG when both anti-S and anti-N IgG were detected above their thresholds.



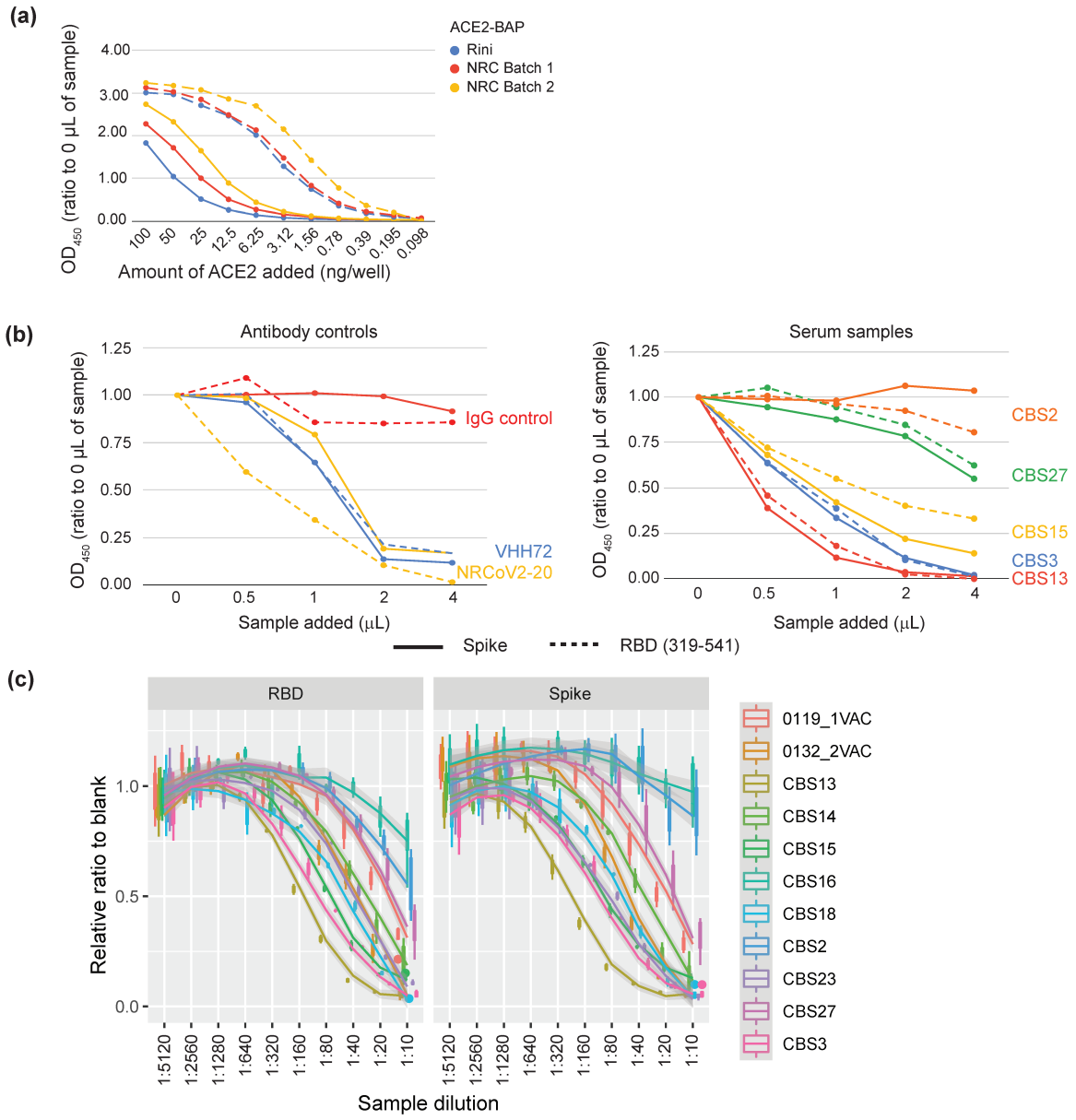
Supplementary figure 10. DBS Optimization. **(a)** 6 mm punches were taken from DBSs and eluted in 250 µL PBST plus 1% Triton X-100 (a 500 µL elution volume was initially tested but was too dilute). 50 µL of eluate or 1 µL of plasma diluted in 50 µL 1% w/v milk power in PBST were added to wells coated with 200 ng spike or 75 ng RBD (Rini) for colorimetric ELISA using 1:60,000 Jackson anti-IgG HRP as the secondary antibody. Blank-subtracted samples were normalized to positive serum pools analyzed on the same plate. **(b)** Correlation of DBSs to plasma (left panel) and different size DBS punches to each other (middle and right panels) for the indicated antigen (n = 26, NML panel 3, 1:4 dilution of DBS eluate). **(c)** Density distributions of DBS and matching plasma samples from NML panels 1–3 (n = 96). The shift in the DBS density distribution means that thresholds established for plasma cannot be used directly to call positives using DBSs.



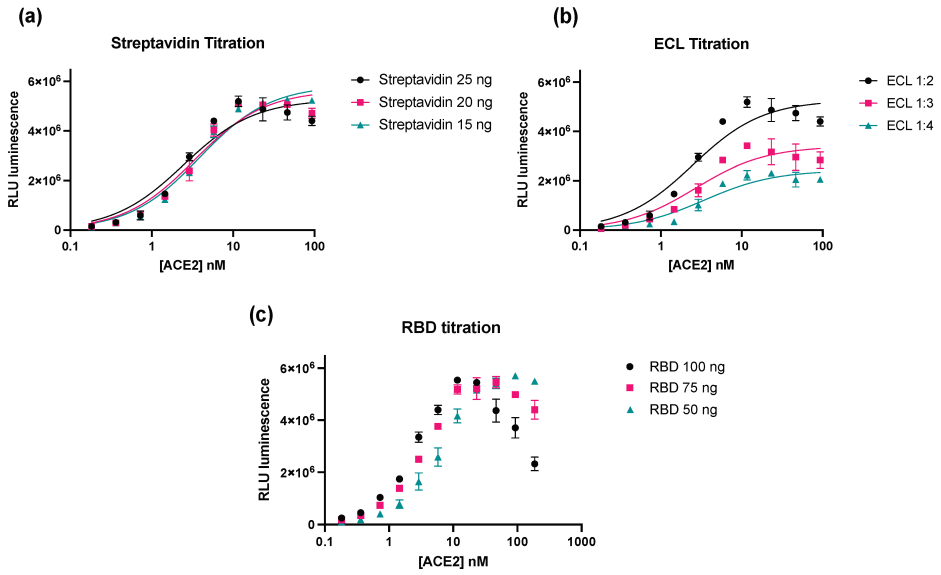
Supplementary figure 11. Processing and validation of the Ottawa automated serology platform. **(a)** Raw luminescence values generated by the automated platform, shown on the established plate map. Color intensities are relative to luminescence values from a prototypical run. Standards, test samples, and controls are colored gray, blue, and red respectively. For each well, sample identifications and luminescence values are also indicated. **(b)** The IC50 luminescence value of the standard curve is used to scale sample values. The curve is derived from the standard samples shown in (a) and modelled using a four-parameter log-logistic function. The shaded blue area indicates the 95% confidence interval, and both the red point and dashed lines specify the inflection point of the curve. The luminescence value at the inflection point is used to scale all the values for a given antigen on the plate for further processing. **(c)** FDR determination using pre-pandemic samples. Anti-S IgG luminescence values from DBSs were rescaled as in (b), and a density distribution was used to determine a threshold corresponding to a 3% FDR (dashed line). The red area includes 97% of the scaled luminescence values. **(d)** Pipeline used to call SARS-CoV-2 IgG positive samples. For each plate, blank values were subtracted, the luminescence was rescaled based on luminescence values at the inflection points of the respective standard curves, and signal to cutoff (S/CO) values were calculated. Samples were considered overall positive for SARS-CoV-2 IgG when both anti-S and anti-N IgG were detected with S/CO ≥ 1. Yellow, green, and red backgrounds in the table on the right indicate S/CO ≥ 1, negative, and positive samples, respectively. **(e)** Determination of the optimal FDR threshold for SARS-CoV-2 IgG positive calls. FDRs of 1–100% were plotted as in C for anti-RBD, -spike, and -N IgG. For each FDR value, the number of true positive (TP), false positive (FP), true negative (TN), and false negative (FN) samples were calculated based on DBS samples provided by the NML (Panel 4) to determine the calling accuracy (i.e. the percentage of TP+TN samples). A maximum accuracy of 98.4% was obtained with a 3% FDR. The inset shows the sample distributions for the four specificity statistics at a 3% FDR. **(f–h)** ROC analyses of the three IgGs used in the analysis. S/CO values and true sample identifications from the NML were used as parameters for each analysis. Calculated AUC values are indicated.



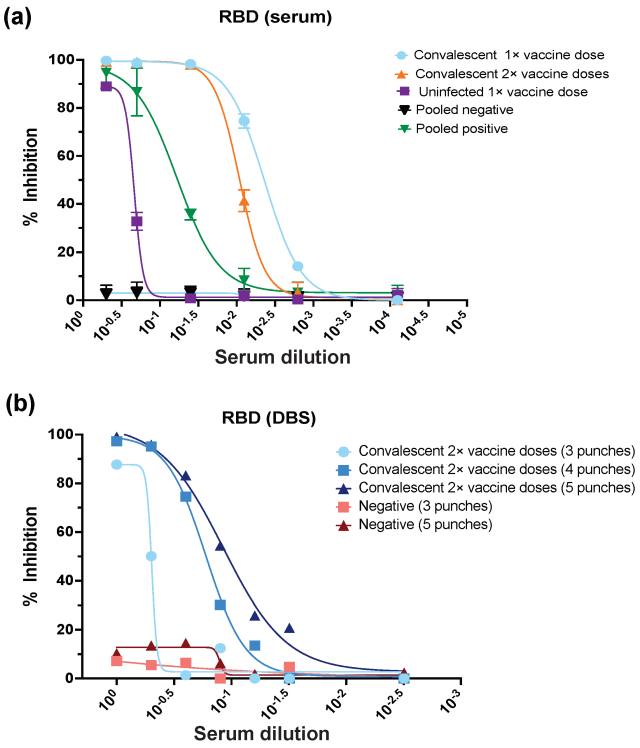
Supplementary figure 12. ROC curve for NML panel 4 DBS IgG analysis. DBS eluates were analyzed for antibodies against the three antigens as indicated. Samples were diluted 1:4 and analyzed on the F7 platform in Toronto in 384-well chemiluminescent format. Statistics and sample numbers are provided in Table 3.



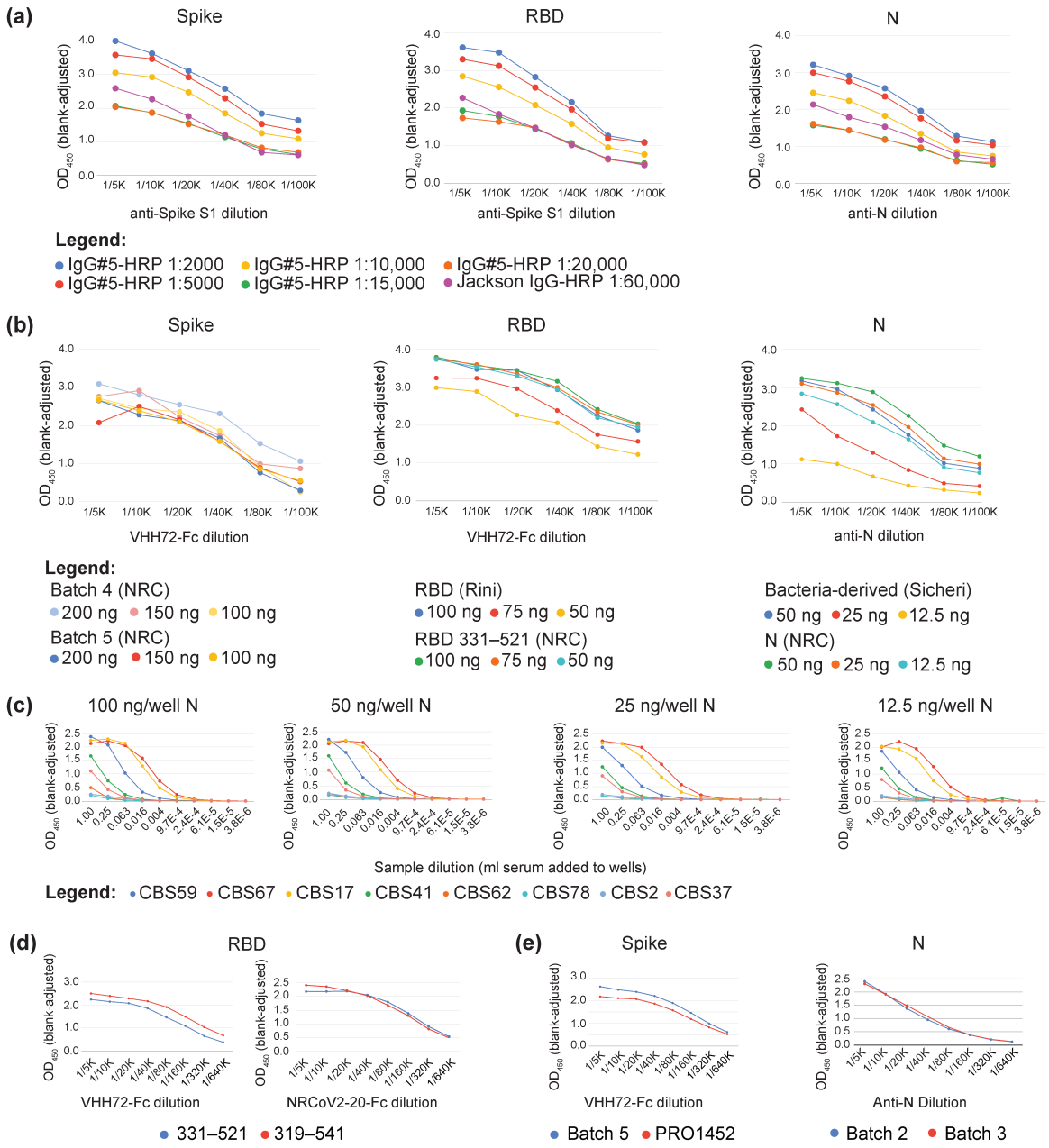
Supplementary figure 13. Optimization and testing of NRC reagents for snELISA. **(a)** To determine the amount of ACE2-BAP to add to the manual snELISA, 500 ng of VHH72-Fc (positive control, solid line) or IgG (negative control, dashed line) was added to a plate coated with 200 ng/well of spike. The indicated amount of ACE2 from the NRC was compared to the validated ACE2 reagent from the Rini lab. Batch 2 ACE2 was enriched for biotinylation using a Monomeric Avidin Ultralink column (Pierce). For the colorimetric assay, 6.25 ng/well was selected as the optimal concentration for ACE2-BAP as it was most comparable to biotinylated ACE2 from the Rini lab, showed good separation between the controls, and maintained a high signal for the IgG control. **(b)** Using the optimized amount of ACE2-BAP Batch 1 (6.25 ng/well for spike, 1.56 ng/well for RBD), titration curves were generated for spike and its RBD using antibody controls (left panel) and CBS samples (right panel). Spike and RBD had similar profiles, with clear separation between controls and samples. **(c)** Dose-response curves for spike and RBD, linked to Figure 4A. Values are normalized to the blank (no sample added).



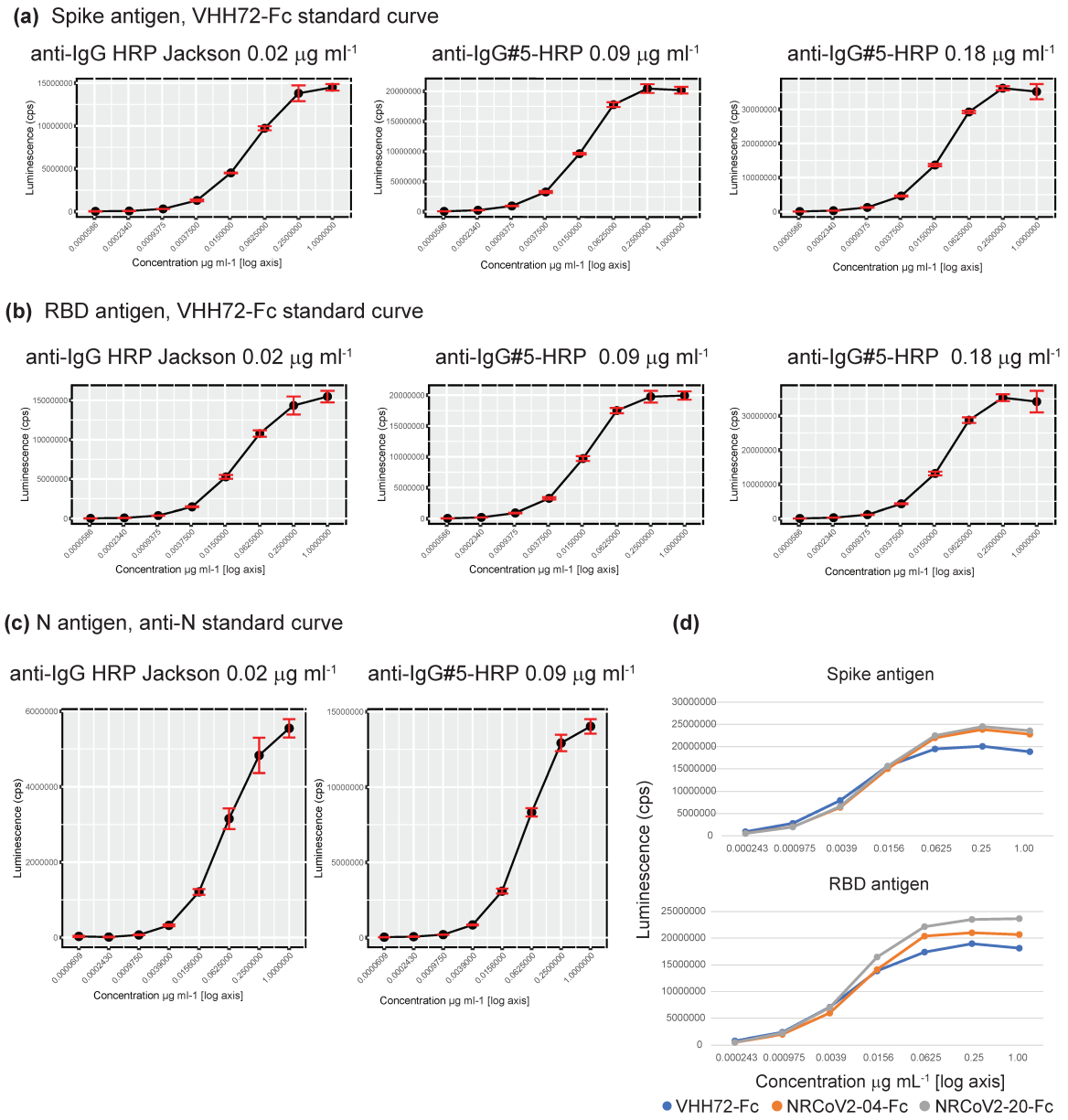
Supplementary figure 14. Optimization of the snELISA for the automated platform. **(a)** The streptavidin-HRP polymer (Sigma #S2438) was titrated (25, 20, and 15 ng/well) in 100 ng/well RBD and a substrate to sample ratio of 1:2 while varying the ACE2 concentration from 0.25 to 128 ng/well. Adjusting the streptavidin-HRP concentration had limited impact, highlighting its saturation. **(b)** The luminescence substrate (Thermo Fisher Scientific, #37069) was titrated by dilution in MilliQ H_2O (1:2, 1:3, and 1:4) while maintaining the RBD at 100 ng/well and the streptavidin-HRP at 25 ng/well and varying the ACE2 concentration as in (a). **(c)** The coated RBD concentration was titrated (100, 75, and 50 ng/well) while maintaining streptavidin-HRP at 25 ng/well and the luminescence substrate at 1:2 and varying the ACE2 concentration from 0.25 to 256 ng per well. A profound hook-effect was noticed at high ACE2 concentrations.



Supplementary figure 15. Optimized snELISA for the automated platform. **(a)** Inhibition of ACE2 binding to RBD (319–541) in the presence of different sources of serum. A 6-point titration of the serum enables the calculation of EC50 values. Serum samples were from a convalescent SARS-CoV-2 individual 3 weeks-post first vaccination (Comirnaty) and 3 weeks post-second vaccination (Comirnaty), an individual with no prior SARS-CoV-2 infection (Surveillance) 3 weeks post-first vaccination (Comirnaty), and pooled sera from individuals (n = 100) with or without prior SARS-CoV-2 infection. The assay was performed with 100 ng/well of RBD (319–541), challenged with 6.5 ng/well of ACE2, and detected with 25 ng/well of streptavidin-HRP polymer. **(b)** For DBS neutralization, a comparison between three, four, and five (3 mm) punches eluted in 100 µL was performed on DBS samples from the twice-vaccinated convalescent individual in (a) and a known negative sample. Four and five punches had similar performance, which was significantly lower with three. To calculate the percent inhibition, luminescence values were scaled to assays without serum (max signal). Serum samples were analyzed in quadruplicate while DBS samples were analyzed once.



Supplementary figure 16. Optimization of the NRC reagents. **(a)** Different dilutions of IgG#5-HRP were compared to Jackson IgG-HRP by colorimetric ELISA. Antigen amounts: spike (200 ng/well, NRC), RBD (75 ng/well, Rini), and N (25 ng/well, Sicheri). Anti-spike S1 IgG (GenScript, 1 mg mL-1 stock) or anti-N IgG (GenScript, 1 mg mL-1 stock) were diluted as indicated. Based on the similarity of its curve with that of the Jackson antibody, the 1:10,000 dilution of IgG#5-HRP was selected. **(b)** Different dilutions of NRC antigens were compared to previously used antigens 8. VHH72-Fc and anti-N IgG antibodies were diluted as indicated. Based on the similarity of the curves to those of prior antigens, the same were selected for spike (200 ng/well) and its RBD (75 ng/well). **(c)** Due to the difference in signal between N produced in bacteria vs. in mammalian cells, we performed an extended titration analysis of CBS samples to determine the amount of antigen. Based on the shape of the curves and to conserve reagents, 25 ng/well of N was chosen for manual colorimetric assays. **(d)** Comparison of two different RBD proteins (75 ng/well). **(e)** Comparison of two different batches of spike SmT1 (200 ng/well) and N (25 ng/well). For B to E, IgG#5-HRP was used at 1:10,000.



Supplementary figure 17. Optimization of IgG#5-HRP and recombinant antibodies for chemiluminescent assays. **(a)** and **(b)** Two different concentrations of IgG#5-HRP (selected based on the colorimetric assay) were compared to the Jackson IgG secondary antibody. Note that the scales differ between graphs to illustrate their similar binding curves. For spike and its RBD, 0.09 and 0.18 µg mL-1 produced similar curve profiles to the Jackson secondary, with all curves beginning to plateau at 0.25 µg mL-1. Increased secondary antibody did result in higher luminescence signal, suggesting that the antigen is the limiting factor at higher primary antibody levels. For subsequent experiments, 0.09 µg mL-1 was selected. **(c)** For N, 0.09 µg mL-1 of IgG#5-HRP was compared to the Jackson secondary. **(d)** Two alternative recombinant antibodies against the RBD were tested by ELISA for use in standard curves with the spike and RBD antigens. Both alternates had similar binding profiles to VHH72. Antigens for all tests: spike (batch 5, 50 ng/well), RBD (331–521, 20 ng/well), N (7 ng/well). Antigen concentrations for automated chemiluminescent assays were decreased 3.5–4-fold from the optimal concentrations for the manual colorimetric assay.

2.2 Comparative Performance of Serum and Plasma Samples in SARS-CoV-2 Serology and Neutralization Assays

Preface

(This work has been previously published as a research article)

Chentoufi, H. A.*, **Galipeau, Y**.*, Arnold, C., Dewar-Darch, D., Dyks, A., Cooper, C., & Langlois, M. A. (2025). **Comparative performance of serum and plasma samples in SARS-CoV-2 serology and neutralization assays**. *Journal of virological methods*, *337*, 115186. https://doi.org/10.1016/j.jviromet.2025.115186

© 2025 The Author(s). Published by Elsevier B.V. This is an open access article under the CC BY-NC license (http://creativecommons.org/licenses/by- nc/4.0/)

Abstract

The SARS-CoV-2 pandemic catalyzed the rapid development and deployment of serological assays, which have been pivotal for monitoring antibody responses to infection and vaccination, guiding vaccine design, and shaping public health strategies. Historically, serum and plasma samples have been considered largely interchangeable in serological testing. However, the precise extent of their similarity or potential differences in antibody detection and quantification remains poorly characterized. This distinction is critical as the choice of sample type carries practical and economic implications, particularly in large-scale seroprevalence studies. To address this, we evaluated IgG, IgM, and IgA antibodies targeting key SARS-CoV-2 antigens (spike, RBD, and N) and assessed neutralization efficiency in 124 paired serum and plasma samples collected simultaneously. Using both manual and automated serological and neutralization assays, we demonstrated that while serum and plasma differ in recovered volume, this difference does not affect antibody concentration or functional neutralization. Our findings confirm that serum and plasma are effectively interchangeable for SARS-CoV-2 serological studies, providing robust evidence to support streamlined, flexible, and cost-effective study designs without compromising data accuracy.

Introduction

Through global COVID-19 research efforts, large-scale serological sampling has been widely utilized in Canada (1, 2). SARS-CoV-2 serological testing has been instrumental in understanding immune responses, assessing seroprevalence, guiding vaccine development, and evaluating vaccine efficacy across diverse populations (3, 4). Additionally, these assays have enabled the detection of prior or asymptomatic infections by identifying antibodies against non-vaccine antigens (5). The pivotal role of serological assays in the pandemic response has driven the development of hundreds of different types of assays varying in automation, throughput, sensitivity, and specificity (6).

SARS-CoV-2 serological assays now commonly utilize various sample types, including serum, plasma, dried blood spots (DBS), and sometimes alternative matrices like saliva and breastmilk (7, 8). Venipuncture blood draws remain the clinical standard, with most assays using serum or plasma. Serum, derived from blood after coagulation, is typically collected in micro-ionized silica clot-activator vacutainer tubes, more commonly known as serum separator tubes (SSTs) and processed by centrifugation to remove cellular components, fibrin clots, and clotting factors. Plasma, by contrast, is collected with anticoagulants such as EDTA, citrate, or heparin to prevent clot formation and preserve coagulation factors, making it the cell-free supernatant of centrifuged blood (9, 10).

Beyond biochemical differences, serum and plasma also differ in processing time and downstream applications. Plasma, for instance, can be processed immediately and used for simultaneous peripheral blood mononuclear cells (PBMCs) isolation (11, 12). Plasma is also usually prioritized for multiplexed cytokines analysis (13). Additionally, plasma yields 5–20% more volume than serum (9, 14). Despite these variations, the impact of sample type on SARS-CoV-2 serological assay performance and antibody quantification remains poorly understood.

While serum and plasma have been interchangeably used in various biochemical and clinical assays, their equivalence is not universal. WHO guidelines recommend serum for certain infectious disease diagnostics, such as complement fixation or bacterial agglutination tests, but allow serum or plasma interchangeably for others, including ELISAs, hemagglutination tests, and

immunoblots (9). Studies have demonstrated variability in analyte concentrations depending on sample type. For example, ELISAs detecting beta-2-microglobulin and Plasmodium falciparum histidine-rich protein 2 showed significantly lower concentrations in plasma compared to serum (15). One study which compared three qualitative commercial platforms highlighted small discordances between serum and plasma in a small cohort (16). However, IgG antibodies against herpes simplex virus type 2, dengue, and rubella generally show negligible differences across sample types (17-19). Similarly, mycobacterial antigens often yield comparable antibody titers between sample types (20). Contrastingly, metabolomic and lipidomic studies reveal significant differences based on collection tubes, underscoring the need for careful consideration in sample type selection depending on the assay and analyte (21). Here, we aimed to evaluate the interchangeability of serum and plasma in quantitative SARS-CoV-2 serological and neutralization assays.

Methods

Ethics statement

This research complies with all relevant ethical regulations. The Ottawa Health Science Network Research Ethics Board approval was obtained (Certificates: H-09-20-6135 and H-07-20-6009).

Serum and plasma sample collection

An initial pilot cohort was selected using blood samples from 10 randomly selected participants. Inclusion criteria included individuals ≥18 years of age with a self-reported history of SARS-CoV-2 infection or vaccination. Informed consent was obtained from all participants prior to blood collection. Venipuncture was performed using standard procedures, with one 5 mL tube containing a separator gel and clot activator (Gold-capped, Serum Separator Tube - SST BD Vacutainer #367986) used for serum collection and one 5 mL tube with EDTA (Purple-capped, EDTA-coated BD vacutainer #367863) for plasma collection. Serum samples were incubated at room temperature for 30 minutes to facilitate clot formation before centrifugation at 1000xg for 10 minutes. Plasma samples were obtained by centrifuging whole blood at 1000xg for 10 minutes immediately after collection. These samples were stored at 4°C prior to serological measurements. Moreover, 79 paired serum and plasma samples and an additional independent 32 paired serum and plasma samples from the Stop the Spread Ottawa study (SSO) from the CoVaRR-Net biobank

were selected at random for the measurement of antibodies and neutralization efficiency, respectively (22). These samples were stored at -80°C prior to serological measurements. Eligibility for the SSO study included individuals ≥18 years of age in the Ottawa region at risk of SARS-CoV-2 exposure/infection due to occupation or health conditions or with any history of COVID-19 natural infection confirmed by positive PCR test and or RAT (22).

SARS-CoV-2 antibody quantification

Antibodies against the spike protein (ancestral strain), receptor binding domain (RBD) and nucleocapsid (N) of SARS-CoV-2 were measured using previously described serological assays (5). First, in the pilot cohort, antibody quantification was carried out via manual assays. This enabled the quantification in technical quadruplicate and to titrate (10-point dilution (1:25, 1:50, 1:100, 1:200, 1:400, 1:800, 1:3200, 1:12800, 1:51200, and 1: 204800)) the participant sample. An automated version of the same serological assays used manually was then carried out on a Microlab STAR robotic liquid handler (Hamilton) fitted with an integrated 405 TS/LS LHC2 plate washer (Biotek). To assess variations in signal between plates, the same controls were included in each assay. These controls included pooled serum and a titration of an isotype and antigen-specific recombinant monoclonal antibody: anti-SARS-CoV-2 S CR3022 Human IgG1 (Absolute Antibody, Ab01680-10.0), anti-SARS-CoV-2 S CR3022 Human IgA (Absolute Antibody, Ab01680-16.0), or anti-SARS-CoV-2 S CR3022 Human IgM (Absolute Antibody, Ab01680-15.0). The luminescence signal of this standard curve was then modelled using a four-parameter log-logistic regression, and the inflection point was established. Blank subtracted values were then scaled in relation to this inflection point and presented as scaled luminescence. These values were then converted to Laboratory Units (LU/mL) or Binding Antibody Units (BAU/mL) from the WHO international standard (NIBSC, 20/136), enabling inter-study comparisons. In the pilot cohort, all points within the linear range were converted to titers and their average was used subsequently. In the automated cohort, the first dilution (1:100) was used to convert IgA and IgM measurements to a titer measurement. In the case of IgG, the dilution (1:100 or 1:10 000) within the linear range was selected to be converted to a titer measurement.

Measurement of Antibody Neutralization Efficiency

A protein-based surrogate neutralizing ELISA (snELISA) was used to measure the neutralization efficiency of the antibodies in serum and plasma. The complete methods are described here (5). Briefly, serum and plasma samples were serially diluted to plot a 5-point curve (1:5, 1:25, 1:125, 1:625, 1:6250). Pooled positive and negative sera were included as controls along with a titration of the NRCoV2-20-Fc (NRC) recombinant monoclonal antibody, to create a standard curve. Luminescence values were adjusted to the blank wells (serum-free, no ACE2), and the average maximal signal of the plate was established on on serum-free wells (unimpeded ACE2-spike interaction). The percentage inhibition was then calculated by measuring the relative reduction in spike / ACE2 interaction (0% inhibition = maximal ACE2-spike binding). The titrated serum or plasma samples were modelled using a four-parameter log-logistic regression, and reciprocal half-maximal inhibitory dilution (ID50) was calculated.

Volume recovery measurement

To measure the plasma or serum volume recovery, the mass of the whole blood tube was recorded prior to centrifugation and after the plasma or serum was collected. The volume of recovered plasma and serum was also measured.

Results

Cohort design

To evaluate differences in antibody quantification between serum and plasma samples, we first conducted a pilot study with a small cohort (n=10) recruited between February 21 and March 6, 2023. This cohort had a mean age of 24.5 years (range: 21–41 years) and was predominantly female (70%), all reported either a previous SARS-CoV-2 infection or vaccination (Table 1). The small size of this cohort enabled high-resolution serological measurements by performing assays in technical quadruplicates across a 10-point titration series for each antigen and antibody isotype. To explore variability across a broader population, we conducted a confirmatory study using a larger cohort from the Stop the Spread Ottawa study, a previously described ongoing longitudinal study (2). Paired serum and plasma samples stored in a biobank were randomly selected, yielding 79 samples for serological analysis (ages: 23–75 years; 56.9% female) and another additional 32 samples from the biobank were randomly selected for neutralization assays (ages: 24–71 years; 93.8% female) (Table 1). This two-step approach allowed for both detailed technical analysis and validation across a diverse population.

Serum or plasma does not impact antibody titer measurements

There is currently limited understanding of how serum versus plasma impacts antibody quantification for SARS-CoV-2. To address this, we first measured IgG, IgM, and IgA against the trimeric spike protein of SARS-CoV-2 and IgG against the nucleocapsid with high resolution in a small pilot cohort (Figure 1). Each sample underwent a 10-point titration to ensure quantification within the linear range, and scaled luminescence signals were converted into antibody titers (lab units or international units). No significant differences in antibody titers between serum and plasma were detected in the pilot cohort (Figure 1, Supp. Figure 1).

To validate these findings, we analyzed a larger cohort using a benchmark high-throughput automated serology platform. IgG, IgM, and IgA antibodies were quantified against SARS-CoV-2 spike protein, receptor binding domain (RBD), and nucleocapsid in 79 individuals with paired serum and plasma samples (Figure 2, Supp. Figure 2). Across all parameters, serum and plasma measurements showed no significant differences, except for spike IgG ($p=0.0279$) and RBD IgA ($p=0.0249$). However, the observed effect sizes were minimal, with mean differences between

both serum and plasma groups of 0.045 LU/mL for RBD IgA and 7.86 BAU for spike IgG. Further, knowing that some samples in this cohort had titers of over 3 400 BAU/mL for Spike IgG, these differences are likely attributable to experimental variation, indicating no meaningful biological differences between the sample types.

Serum or plasma does not impact neutralization efficiency

To determine whether functional antibody measurements, such as neutralization, are comparable between serum and plasma, we conducted a surrogate protein-based neutralization assay routinely used in large-scale population studies (5). Initially, this assay was performed on the pilot cohort using both EDTA plasma and SST serum samples, with each sample titrated to calculate reciprocal half-maximal inhibitory dilutions. No significant differences in neutralization efficiency beyond experimental variation were observed between the two sample types (Figure 3A).

To validate these results, the assay was performed on an automated platform using samples from 32 SSO participants, again showing no detectable differences in neutralization efficiency between serum and plasma. To confirm these findings were not limited to the ancestral SARS-CoV-2 strain, neutralization assays were also conducted using the XBB1.5 spike protein. Once more, plasma and serum demonstrated equivalent performance (Figure 3B–C). These results suggest that serum and plasma are interchangeable for functional neutralization measurements across SARS-CoV-2 variants.

Volume recovery rate is higher in plasma than in serum

While no differences in performance were observed in serological and neutralization measurements, plasma collection is well-documented to yield a higher volume recovered compared to an equivalent blood draw for serum (14). To quantify this variation, we randomly selected 10 additional SSO serum and plasma samples. The tubes were weighed immediately after blood collection and again after serum or plasma was harvested. Our analysis revealed that EDTA plasma collection resulted in a significantly higher recovered volume compared to serum ($p=0.0002$) (Figure 4), with serum volumes averaging 4% less than their plasma counterparts. This finding highlights a practical advantage of plasma collection in maximizing sample volume for downstream applications.

Discussion

The choice of sample type during the design of large-scale seroprevalence and humoral response studies carries significant implications. Despite its importance, there is limited guidance on whether serum or plasma should be prioritized and whether both can be used interchangeably in SARS-CoV-2 serological studies. In this study, we addressed this gap by performing high-resolution serological measurements in a pilot cohort of 10 individuals and validating these findings in an independent confirmatory cohort of 79 individuals using an automated benchmark assay. Across both cohorts, no biologically significant differences in antibody quantification were observed between serum and plasma, irrespective of antibody isotype (IgG, IgA, IgM) or antigen (spike, RBD, N).

Furthermore, neutralization efficiency, assessed both manually and using an automated platform, remained consistent between serum collected in SST tubes and plasma collected with EDTA. These results strongly suggest that serum and plasma are interchangeable in serological studies, with no need to account for sample type during data analysis.

Although biochemical differences between serum and plasma are well-documented (21), our findings indicate that antibody concentrations remain unaffected. Notably, as in previous studies, we observed significantly lower volume recovery from serum compared to plasma (9, 14). However, this lower serum volume did not translate into differences in antibody quantification, suggesting that any loss of antibodies is proportional to the reduced volume, thereby maintaining consistent relative antibody concentrations in serum. It is also possible that the concentration changes are below the sensitivity of our serological assays.

The decision to use serum or plasma in large-scale serological surveys should therefore consider logistical factors such as sample storage, downstream applications, and cost. For studies targeting rare or low-abundance antibodies that may require sample concentration, plasma may offer an advantage due to its higher recovered volume. Nonetheless, this study robustly demonstrates that both plasma and serum samples perform equivalently in SARS-CoV-2 serological assessments.

It is important to note that this study focused solely on antibodies specific to SARS-CoV-2 and did not measure any other human analyte. Given the consistent performance of serum and plasma across different isotypes and antigens, it is likely that these findings can be extrapolated to other viral antigens or serological targets. However, it remains essential for end users to validate these conclusions within their specific assay platforms and systems to ensure accuracy and reliability.

Funding:
This work was supported in part by a COVID-19 Rapid Response grant Canadian Institute of Health Research (CIHR) grant (VR2-172722) and from a grant supplement by the COVID-19 Immunity Task Force (CITF) to M-AL. Additionally, YG is supported by a Charles Best and Frederick Banting (CGS-Doctoral award) from CIHR (476885).

Contributors:
HA and CA performed the data collection. HA and YG performed the data analysis. YG, CA and M-A.L developed the high throughput serology platform. HA, YG and M-A L designed this study. CC and AD collected and coordinated blood samples. HA, YG, and M-A.L wrote and formatted the manuscript. All authors have edited and approved the manuscript.

Data sharing:
The data used in this study can be obtained by request from M-A.L (langlois@uottawa.ca)

Declaration of interest:
The authors declare no conflict of interest relevant to the present manuscript.

Role of the Funder/Sponsor:
The funding sources played no role in the study design, data collection, analysis, writing of the manuscript, and decision to publish.

Generative AI: During the preparation of this work the authors used ChatGPT for limited English editing purposes only. After using this tool, the authors reviewed and edited the content as needed and take full responsibility for the content of the publication.

Acknowledgments:
We would like to acknowledge past and current members of the high-throughput SARS-CoV-2 Serology and Diagnostic facility at the University of Ottawa. We would also want to acknowledge the CoVaRR-Net biobank for providing serum and plasma samples from the Stop the Spread Ottawa study.

References

1. Statistic Canada. Canadian COVID-19 Antibody and Health Survey (CCAHS) – Cycle 2 2024 [Available from: https://www.statcan.gc.ca/en/survey/household/5339.
2. Keeshan A, Galipeau Y, Heiskanen A, Collins E, McCluskie PS, Arnold C, et al. Results of the Stop the Spread Ottawa (SSO) cohort study: a Canadian urban-based prospective evaluation of antibody responses and neutralisation efficiency to SARS-CoV-2 infection and vaccination. BMJ Open. 2023;13(10):e077714.
3. Duarte N, Yanes-Lane M, Arora RK, Bobrovitz N, Liu M, Bego MG, et al. Adapting Serosurveys for the SARS-CoV-2 Vaccine Era. Open Forum Infectious Diseases. 2021;9(2).
4. Krammer F, Simon V. Serology assays to manage COVID-19. Science. 2020;368(6495):1060-1.
5. Colwill K, Galipeau Y, Stuible M, Gervais C, Arnold C, Rathod B, et al. A scalable serology solution for profiling humoral immune responses to SARS-CoV-2 infection and vaccination. Clinical & Translational Immunology. 2022;11(3):e1380.
6. Galipeau Y, Greig M, Liu G, Driedger M, Langlois M-A. Humoral Responses and Serological Assays in SARS-CoV-2 Infections. Frontiers in Immunology. 2020;11(3382).
7. Isho B, Abe KT, Zuo M, Jamal AJ, Rathod B, Wang JH, et al. Persistence of serum and saliva antibody responses to SARS-CoV-2 spike antigens in COVID-19 patients. Science Immunology. 2020;5(52):eabe5511.
8. Cholette F, Mesa C, Harris A, Ellis H, Cachero K, Lacap P, et al. Dried blood spot specimens for SARS-CoV-2 antibody testing: A multi-site, multi-assay comparison. PLOS ONE. 2021;16(12):e0261003.
9. World Health Organization. Use of anticoagulants in diagnostic laboratory investigations 2002 [Available from: https://iris.who.int/handle/10665/65957.
10. Mathew J, Sankar P, Varacallo M. Physiology, Blood Plasma. StatPearls. Treasure Island (FL) ineligible companies. Disclosure: Parvathy Sankar declares no relevant financial relationships with ineligible companies. Disclosure: Matthew Varacallo declares no relevant financial relationships with ineligible companies.: StatPearls Publishing
Copyright © 2024, StatPearls Publishing LLC.; 2024.
11. Riedhammer C, Halbritter D, Weissert R. Peripheral Blood Mononuclear Cells: Isolation, Freezing, Thawing, and Culture. In: Weissert R, editor. Multiple Sclerosis: Methods and Protocols. New York, NY: Springer New York; 2016. p. 53-61.
12. Wei Y-h, Zhang C-b, Yang X-w, Ji M-d. The Feasibility of Using Lithium-Heparin Plasma From a Gel Separator Tube as a Substitute for Serum in Clinical Biochemical Tests. Laboratory Medicine. 2010;41(4):215-9.
13. Rosenberg-Hasson Y, Hansmann L, Liedtke M, Herschmann I, Maecker HT. Effects of serum and plasma matrices on multiplex immunoassays. Immunol Res. 2014;58(2-3):224-33.
14. Plebani M, Banfi G, Bernardini S, Bondanini F, Conti L, Dorizzi R, et al. Serum or plasma? An old question looking for new answers. Clinical Chemistry and Laboratory Medicine (CCLM). 2020;58(2):178-87.
15. Bjerrum OW, Birgens HS. Measurement of beta-2-microglobulin in serum and plasma by an enzyme-linked immunosorbent assay (ELISA). Clin Chim Acta. 1986;155(1):69-76.
16. Haselmann V, Kittel M, Gerhards C, Thiaucourt M, Eichner R, Costina V, et al. Comparison of test performance of commercial anti-SARS-CoV-2 immunoassays in serum and plasma samples. Clin Chim Acta. 2020;510:73-8.

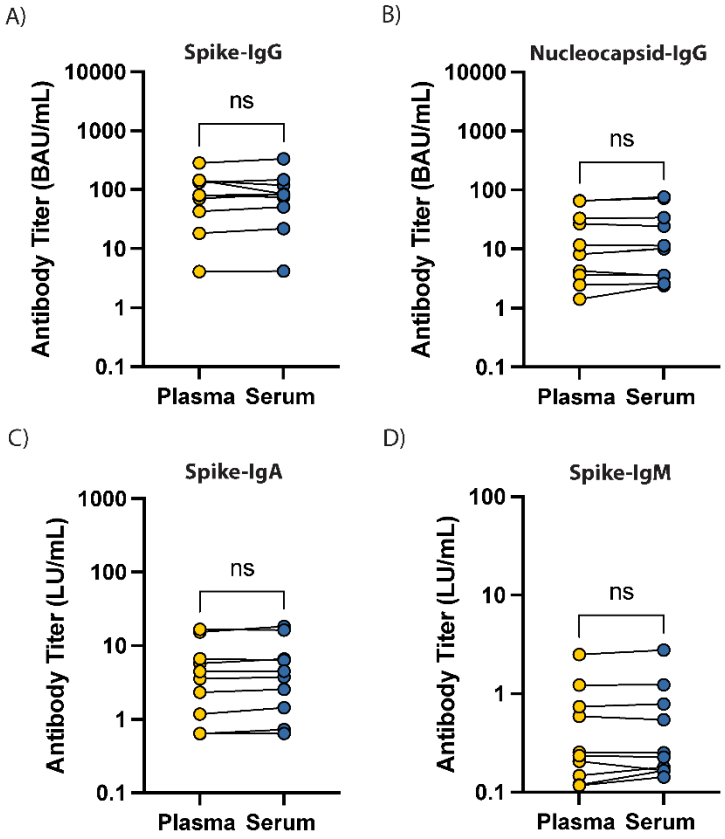
17. Cherpes TL, Meyn LA, Hillier SL. Plasma versus serum for detection of herpes simplex virus type 2-specific immunoglobulin G antibodies with a glycoprotein G2-based enzyme immunoassay. J Clin Microbiol. 2003;41(6):2758-9.
18. Oliveira LC, Kawasato KH, Otta MS, Lima LP, Okay TS. Collection tubes with or without gel separator did not interfere with detection of rubella virus antibodies IgM and IgG. J Clin Lab Anal. 2007;21(5):330-4.
19. Deza-Cruz I, Mill A, Rushton S, Kelly P. Comparison of the Use of Serum and Plasma as Matrix Specimens in a Widely Used Noncommercial Dengue IgG ELISA. Am J Trop Med Hyg. 2019;101(2):456-8.
20. Siev M, Yu X, Prados-Rosales R, Martiniuk FT, Casadevall A, Achkar JM. Correlation between serum and plasma antibody titers to mycobacterial antigens. Clin Vaccine Immunol. 2011;18(1):173-5.
21. Vignoli A, Tenori L, Morsiani C, Turano P, Capri M, Luchinat C. Serum or Plasma (and Which Plasma), That Is the Question. J Proteome Res. 2022;21(4):1061-72.
22. Collins E, Galipeau Y, Arnold C, Bosveld C, Heiskanen A, Keeshan A, et al. Cohort profile: Stop the Spread Ottawa (SSO)—a community-based prospective cohort study on antibody responses, antibody neutralisation efficiency and cellular immunity to SARS-CoV-2 infection and vaccination. BMJ Open. 2022;12(9):e062187.

Table 1. Cohort demographic analysis. Demographic data across cohorts was compiled and presented based on their inclusion in either the serology, neutralization, or the pilot cohort[1].

		Automated Cohort		Pilot Cohort (n=10)
		Serology Cohort (n=79)	**Neutralization Cohort (n=32)**	
Age	**Mean (SD)**	48.9 (14.5)	46.9(10.8)	24.5(5.94)
	Median	50	49	22
	Min-Max	23-75	24-71	21-41
Sex	**Female (%)**	34 (56.9%)	30 (93.8%)	7 (70.0%)
	Male (%)	45 (43.1%)	2 (6.2%)	3 (30.0%)

[1] The pilot cohort consisted of 10 individuals recruited between February 21st, 2023, and March 6th, 2023. Two independent larger confirmatory cohorts (serology cohort (n= 79) and neutralization cohort (n=32)) were established from samples selected from the Stop the Spread Ottawa (SSO) study biobank. The samples were selected at random from plasma and serum drawn between September 14th 2020 to September 28th 2021.

Figures



.

Figure 1. Manual ELISA quantification of SARS-CoV-2 antibody titers in serum and plasma. Manual serology ELISA was conducted to determine IgG, IgA, and IgM antibody titers against the spike and IgG antibody titers against the nucleocapsid in the pilot cohort (n=10). All steps were performed manually, with 10-point serial dilution, in quadruplicate. Antibody titer of anti-spike and anti-N IgG was calculated based on relative ratios to binding antibody units (BAU)/mL based on the WHO international reference standard. Anti-spike IgA and IgM antibodies were converted to lab units (LU/mL). Paired two-tailed t-test was used to establish statistical significance $p \leq 0.05$ (*), $p \leq 0.01$ (**), $p \leq 0.001$ (***), $p \leq 0.0001$ (****).

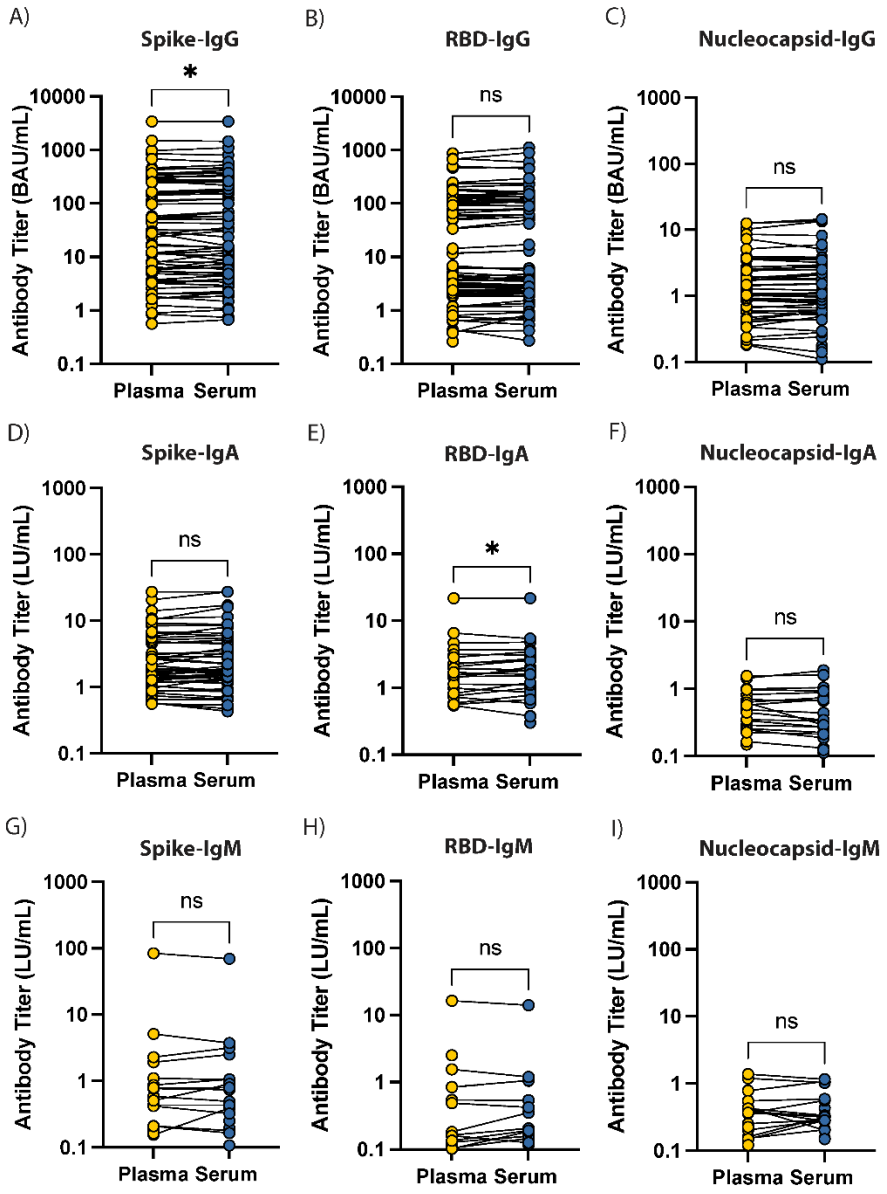


Figure 2. Automated platform quantification of SARS-CoV-2 antibody titers in serum and plasma. Automated serology ELISAs was conducted to determine IgG, IgA, and IgM antibody titers against the spike, RBD, and N antigens in the serology cohort (n= 79). Samples were diluted by a factor of 100 and 10000 and run in duplicate. The dilution within the linear range was selected. The mean of the technical duplicate is shown here. A-C) Antibody titer of IgG spike, RBD, and N was calculated based on the WHO International Reference Standard (BAU)/mL. One sample was excluded due to assay failure for the IgG isotype, and two additional samples were excluded for spike-IgG given they exceeded our accepted experimental variability. D-F) IgA and G-I) IgM antibody titers were converted to lab units (LU/mL). Wilcoxon matched-pairs signed rank test was used to establish statistical significance, $p \leq 0.05$ (*), $p \leq 0.01$ (**), $p \leq 0.001$ (***), $p \leq 0.0001$ (****).

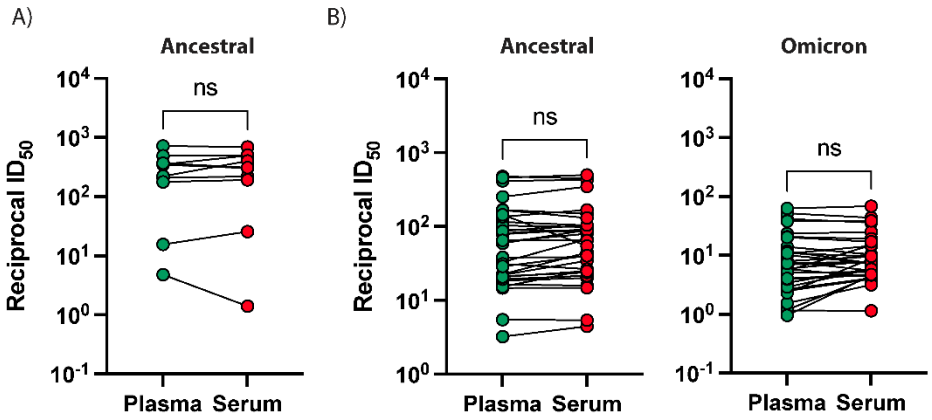


Figure 3. Antibody neutralization efficiency between paired serum and plasma samples. Reciprocal half maximal inhibitory dilution (ID50) of neutralizing antibodies measured from the inhibition of ACE2-spike interaction A) performed manually or B) performed on the automated platform. A 5-point surrogate neutralization assay (snELISA) was conducted against both ancestral (Whu-1) and omicron (XBB.1.5) spikes. The Y-axis is shown on a log10 scale. Wilcoxon matched-pairs signed rank test was used to establish statistical significance, $p \leq 0.05$ (*), $p \leq 0.01$ (**), $p \leq 0.001$ (***), $p \leq 0.0001$ (****).

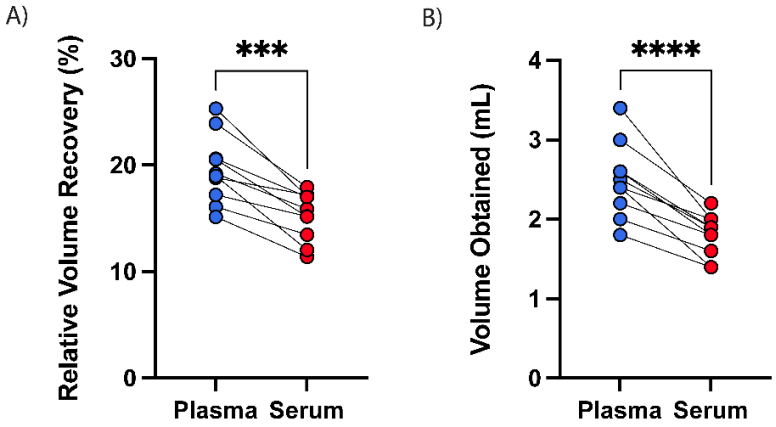
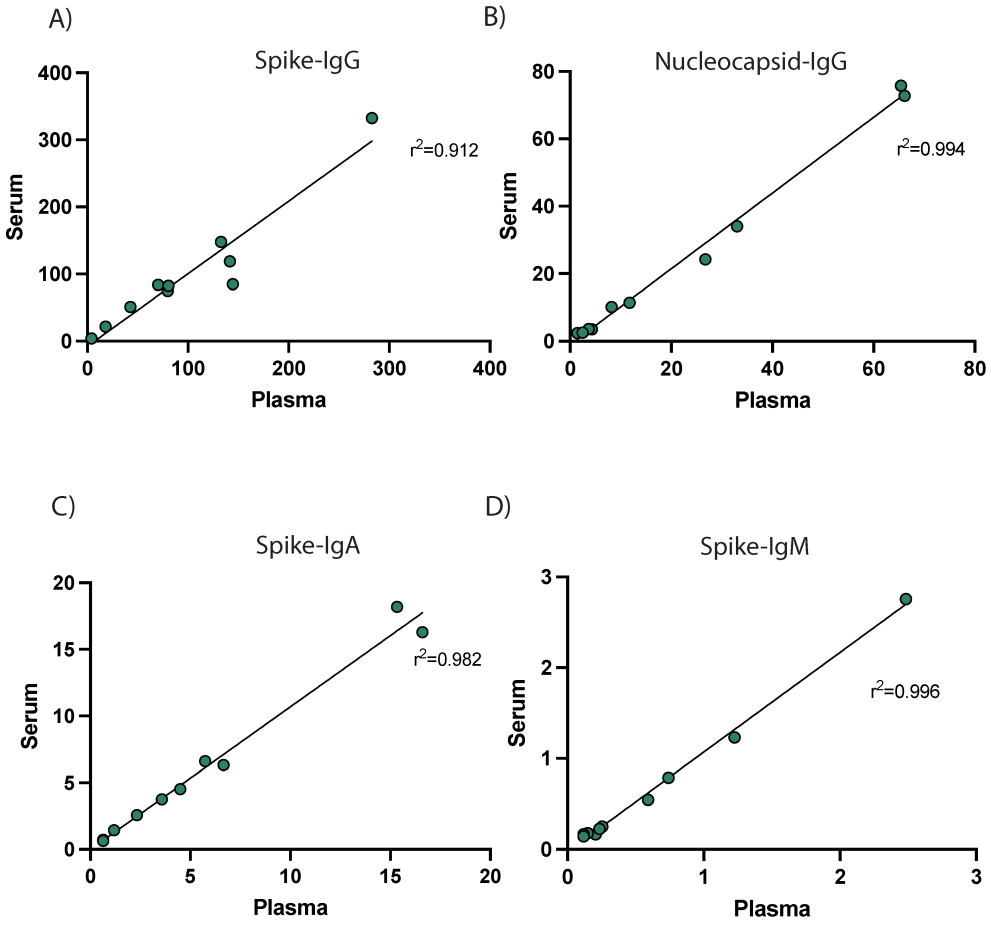
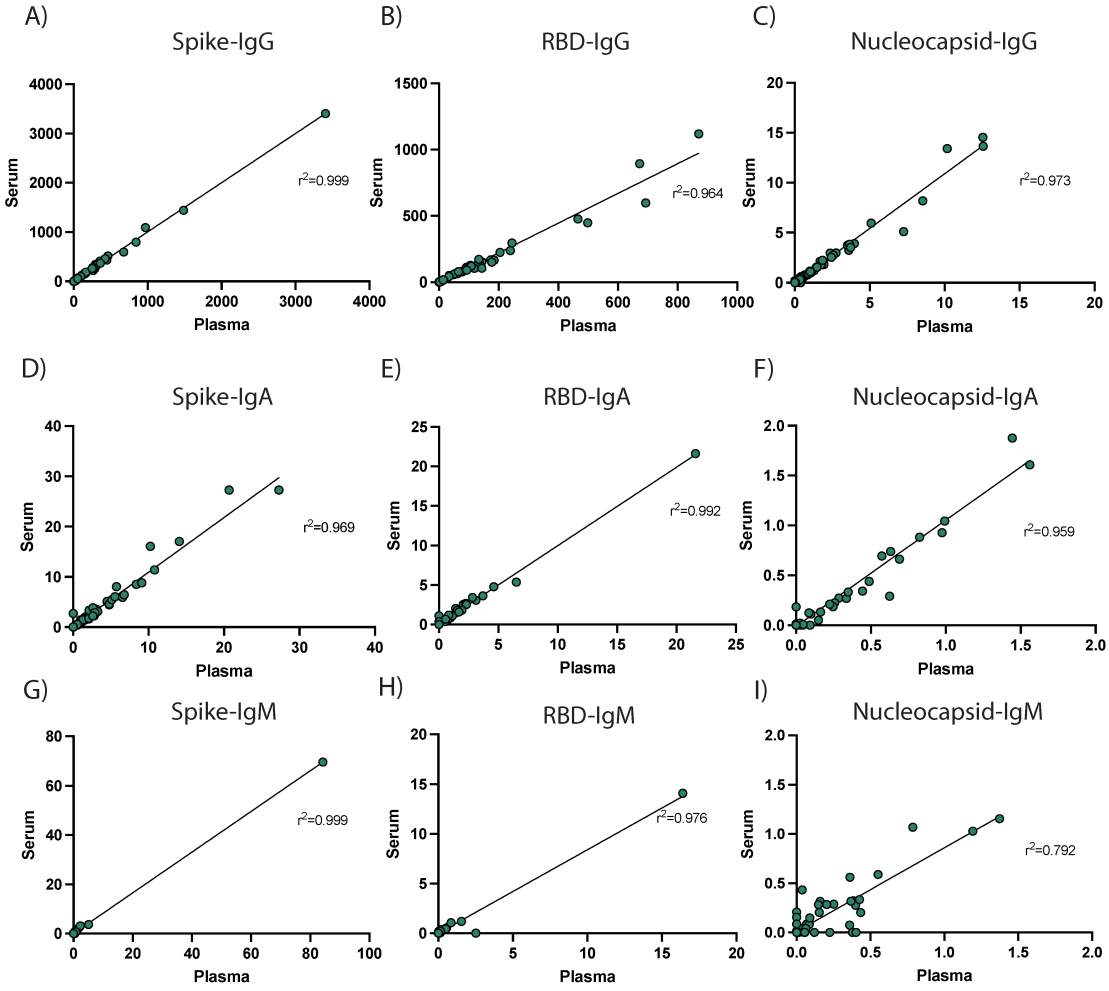


Figure 4. Relative volume recovery rate in plasma and serum. Ten additional individuals were recruited and provided serum and plasma samples. The mass of the vacutainer after the blood draw and after serum/plasma extraction was measured, along with the volume of serum and plasma extracted from each sample. Paired two-tailed t-test was used to establish statistical significance, $p \leq 0.05$ (*), $p \leq 0.01$ (**), $p \leq 0.001$ (***), $p \leq 0.0001$ (****).

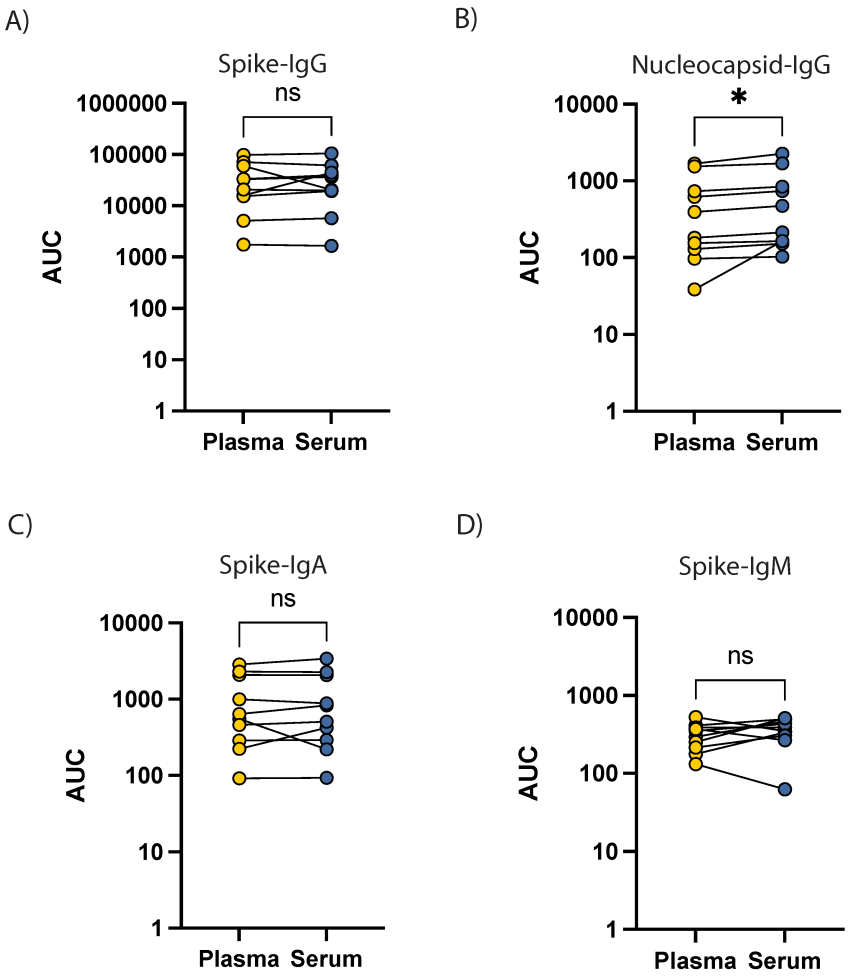
Supplementary Files



Supplementary Figure 1. Linear correlation between plasma and serum titer measurements in the pilot cohort. Manual serology ELISA was conducted to determine IgG, IgA, and IgM antibody titers against the spike and IgG antibody titers against the nucleocapsid in the pilot cohort (n=10). All steps were performed manually, with 10-point serial dilution, in quadruplicate. Antibody titer of anti-spike and anti-N IgG was calculated based on relative ratios to binding antibody units (BAU)/mL based on the WHO international reference standard. Anti-spike IgA and IgM antibodies were converted to lab units (LU/mL).



Supplementary Figure 2. Linear correlation between plasma and serum titer measurements in the automated cohort. Automated serology ELISAs was conducted to determine IgG, IgA, and IgM antibody titers against the spike, RBD, and N antigens in the serology cohort (n= 79). Samples were diluted by a factor of 100 and 10000 and run in duplicate. A-C) Antibody titer of IgG spike, RBD, and N was calculated based on the WHO International Reference Standard (BAU)/mL. One sample was excluded due to assay failure for the IgG isotype, and two additional samples were excluded for spike-IgG given they exceeded our accepted experimental variability. D-F) IgA and G-I) IgM antibody titers were converted to lab units (LU/mL).



Supplementary Figure 3. Area under the curve (AUC) quantification of antibody levels in the pilot cohort. Manual serology ELISA was conducted to determine IgG, IgA, and IgM antibody titers against the spike and IgG antibody titers against the nucleocapsid in the pilot cohort (n=10). All steps were performed manually, with 10-point serial dilution, in quadruplicate. Antibody titer of anti-spike and anti-N IgG was calculated based on relative ratios to binding antibody units (BAU)/mL based on the WHO international reference standard. Anti-spike IgA and IgM antibodies were converted to lab units (LU/mL). Paired two-tailed t-test was used to establish statistical significance $p \leq 0.05$ (*), $p \leq 0.01$ (**), $p \leq 0.001$ (***), $p \leq 0.0001$ (****).

CHAPTER 3 – HARNESSING SEROLOGICAL ASSAYS IN POPULATIONAL-BASED STUDIES OF SARS-COV-2 IMMUNE RESPONSES

RATIONALE

Serological assays directly provide primarily two types of data: seroprevalence information (whether antibodies from infection or vaccination are present or not) and antibody quantification measurements, which can evaluate antibody titers. Furthermore, it was known early in the pandemic that patient characteristics such as age and the presence of comorbidities (e.g., diabetes, obesity) were correlated with greater disease severity and poorer outcomes. This highlighted the importance of population-based studies.

In fact, several unknowns during the SARS-CoV-2 pandemic had real-world ramifications. For example, questions regarding the durability of humoral immunity, SARS-CoV-2 transmission, the effectiveness of public health measures, vaccine efficacy against variants of concern, and the impact of demographics on immunity remained unanswered. Serological assays provided a powerful tool to generate data aimed at addressing these questions.

By harnessing the high-throughput capacity of the serological assay developed in Chapter 2, it became possible to establish and support numerous population-based studies. A study examining the decay rates and levels of antibodies in unvaccinated elderly individuals was carried out (Section 3.1). Another study investigated immunity levels and exposure to SARS-CoV-2 in Indigenous populations in the Canadian Arctic (Section 3.2). Finally, serological data were able to demonstrate that rapid antigen tests (RATs) could, in some cases, cause prolonged and sustained false positives in SARS-CoV-2-naïve individuals (Section 3.3).

3.1 Cross-sectional Characterization of SARS-CoV-2 Antibody Levels and Decay Rates Following Infection of Unvaccinated Elderly Individuals

Preface

(This work has been previously published as a research article)

Whelan M.*, **Galipeau Y.***, White-Al Habeeb N.*, Konforte D., Abou El Hassan M., Booth RA., Arnold C., Langlois MA., Pelchat M. **Cross-sectional Characterization of SARS-CoV-2 Antibody Levels and Decay Rates Following Infection of Unvaccinated Elderly Individuals**. Open Forum Infect Dis. 2023 Jul 20;10(8):ofad384. doi: 10.1093/ofid/ofad384.

© The Author(s) 2023. Published by Oxford University Press on behalf of Infectious Diseases Society of America.

This is an Open Access article distributed under the terms of the Creative Commons Attribution-NonCommercial-NoDerivs licence (https://creativecommons.org/licenses/by-nc-nd/4.0/), which permits non-commercial reproduction and distribution of the work, in any medium, provided the original work is not altered or transformed in any way, and that the work is properly cited.

Abstract

Background
SARS-CoV-2 infections have disproportionally burdened elderly populations with excessive mortality. While several contributing factors exists, questions remain about the quality and duration of humoral antibody–mediated responses resulting from infections in unvaccinated elderly individuals.

Methods
Residual serum/plasma samples were collected from individuals undergoing routine SARS-CoV-2 polymerase chain reaction testing in a community laboratory in Canada. The samples were collected in 2020, before vaccines became available. IgG, IgA, and IgM antibodies against SARS-CoV-2 nucleocapsid, trimeric spike, and its receptor-binding domain were quantified via a high-throughput chemiluminescent enzyme-linked immunosorbent assay. Neutralization efficiency was also quantified through a surrogate high-throughput protein–based neutralization assay.

Results
This study analyzed SARS-CoV-2 antibody levels in a large cross-sectional cohort (N = 739), enriched for elderly individuals (median age, 82 years; 75% >65 years old), where 72% of samples tested positive for SARS-CoV-2 by polymerase chain reaction. The age group ≥90 years had higher levels of antibodies than that <65 years. Neutralization efficiency showed an age-dependent trend, where older persons had higher levels of neutralizing antibodies. Antibodies targeting the nucleocapsid had the fastest decline. IgG antibodies targeting the receptor-binding domain remained stable over time, potentially explaining the lack of neutralization decay observed in this cohort.

Conclusions
Despite older individuals having the highest levels of antibodies postinfection, they are the cohort in which antibody decay was the fastest. Until a better understanding of correlates of protection is acquired, along with the protective role of nonneutralizing antibodies, booster vaccinations remain important in this demographic.

Introduction

Since its emergence, SARS-CoV-2 has disproportionally affected elderly populations through increased COVID-19 disease severity, poor clinical outcomes, and excess mortality [1–3]. In fact, by April 2020, half of COVID-19–related deaths in Canada were individuals aged ≥69 years who were living in long-term care (LTC) [1]. By May 2021, seniors aged ≥65 years in Canada accounted for 93% of COVID-19–related deaths [4].

Factors influencing this disproportionate effect on the elderly remain unclear but are likely mediated by epidemiologic and biological factors. The link between LTC and infectious disease outbreak susceptibility has been studied and established [5, 6]. This link is thought to be explained in part by various attributes of the LTC setting. For example, seniors residing in LTC settings are frequently exposed to numerous other residents through shared rooms and common areas and indirectly through contact with LTC personnel [5, 7]. In addition, maintaining physical distancing was complicated by residents requiring high levels of care, resulting in prolonged close contact with LTC personnel and a decreased ability to follow infection control measures [8].

In addition, elderly individuals present distinct comorbidity profiles that inherently make them more at risk of poor outcomes following COVID-19 infection [2, 9]. In Canada, an estimated 37% of seniors aged ≥65 years and close to 50% of seniors >85 years reported living with ≥2 chronic conditions, including cancer, cardiovascular disease, diabetes, hypertension, respiratory disease, and others [10].

In contrast to younger populations, elderly individuals display distinct differences in innate and adaptive immune responses. Two phenomena act synergistically and are believed to affect immune responses in older people: immunosenescence and inflammaging [11]. Inflammaging refers to the low but chronic presence of proinflammatory mediators, which increases with age [12, 13], while immunosenescence refers to the reduced effectiveness of the immune system as we age, such as the hyporesponsive nature of some immune cells [11, 14]. For example, macrophages/monocytes and dendritic cells can have reduced expression and function of various Toll-like receptors with age [15]. In the case of neutrophils, impaired formation of neutrophil extracellular traps was

reported in aging [16] as well as diminished chemotaxis [17]. Reduced infiltration was noted in macrophages and a dendritic cell population, as was a reduction in phagocytosis [15, 18]. Impairment in innate cell functions, such as defects in antigen presentation, in combination with an inflammaging environment can affect adaptive response initiation [19]. In fact, CD4+ and CD8+ T cells display significant reduction in T-cell receptor repertoire with age, a process most likely linked with thymic involution [20]. In addition to the contracted repertoire, a reduction in naive T cells is documented with age [21], and the ones that remain display reduced expansion and T effector functions [14, 22]. B cells in older persons have impairments in undergoing somatic hypermutation, which can lead to lower-affinity antibodies [11]. Like T cells, it appears that naive B cells are reduced in numbers and the overall repertoire is affected with age [23]. In addition to intrinsic age-related defects in B-cell development and function, it is believed that the lower quality of T- and B-cell interaction caused by aging T cells extrinsically affects B-cell differentiation, expansion, and antibody production [14].

The impact of the aging immune system has been highlighted in immunization response studies against various pathogens. For example, a reduction in vaccine responsiveness has been documented for influenza A [24], hepatitis B [25], pneumococcal disease [26], and more recently SARS-CoV-2 [27, 28] in older individuals.

Given the rapid development and implementation of vaccine programs in most countries, vaccine-induced humoral responses have been described. However, few groups have focused on humoral responses in elderly cohorts who are vaccine naive. Tut et al showed in a cohort of 152 individuals that the elderly generate high levels of antibodies following infection [29]. Others have characterized elderly humoral responses in various study designs [30–36] and highlighted the fact that elderly people generate higher levels of antibodies following infection than those who are younger [33–36]. Despite these studies, the complete evaluation of all antibody isotypes (IgG, IgM, and IgA) and neutralization efficiency has not been done in large elderly cohorts. Furthermore, a significant proportion of the elderly in some countries is not yet protected and remains unvaccinated. While the decline rate of vaccine-induced antibodies has been extensively characterized, antibody decay rates from natural infection have not been described, to our knowledge, in an elderly-enriched vaccine-naive cohort.

Methods

This research complies with all relevant ethical regulations. Ethical approval was obtained from the University of Ottawa REB (H-11-20-6172). Serum/plasma samples provided to University of Ottawa researchers by LifeLabs were deidentified at the source.

Sample Collection

Residual serum and plasma samples from routine clinical testing in a community laboratory were collected. Samples were selected if the individual had a SARS-CoV-2 PCR test completed within 180 days prior to serum/plasma collection. Serum samples were incubated at room temperature for 30 minutes prior to centrifugation at 3000 rpm for 10 minutes. For individuals that did not have serum available, plasma samples were isolated after centrifuging whole blood at ≤1300 RCF for 10 minutes. Specimens were collected from April to September 2020 and stored at -80°C after routine testing was complete. Patient data including time since PCR, cycle threshold value from PCR, time since symptom onset, age, and sex were collected. Given that samples were collected from residual serum/plasma from routine clinical testing in a community laboratory, participants medical charts was not available and as such information on disease severity was not captured. The study protocol and material transfer agreement was approved by the Privacy Officer at LifeLabs.

Measurements of antibody levels in sera

Antibodies were measured using a high-throughput direct chemiluminescent ELISA (full methods described previously). SARS-CoV-2 antigens (spike ectodomain (Wuhan) with S1/S2 furin site mutations, prefusion stabilising mutations and human resistin as a trimerization partner; receptor binding domain (amino acids 331-521 of YP_009724390.1); nucleocapsid (amino acids 1–419 of YP_009724397)) were generously provided by Dr. Yves Durocher, National Research Council of Canada (NRC), Montréal (2). The assays were performed using a Microlab STAR robotic liquid handler (Hamilton) fitted with a 405 TS/LS LHC2 plate washer (Biotek). Initially, 50ng /well of the antigen of interest diluted in PBS was coated in a 384 well high-binding polystyrene Nunc plate (Thermo Fisher Scientific, #460372) in a final volume of 10uL. The plates were then centrifuged

at 216xg and incubated overnight at 4°C. The plates were then washed four times with 100uL of PBS-T and blocked with 80uL of 3% w/v skim milk powder dissolved in PBST for 1 h and then washed (as described before). Samples or controls were diluted by a factor of 100 and 10000 in 1% w/v skim milk powder dissolved in PBST and 10uL was added to the respective wells. After a 2h incubation, the plates were washed once more and 10uL of the secondary antibody was added to each well and incubated for another hour. Secondary antibodies used were anti-Human IgG#5-HRP (Dr. Yves Durocher, NRC) diluted 1 in 5400, anti-human IgA-HRP (Jackson ImmunoResearch Labs, 109-035-011) diluted 1 in 8000, and anti-human IgM-HRP (Jackson ImmunoResearch Labs, 109-035-129) diluted 1 in 9600. After the incubation, plates were washed one last time and 10uL of ELISA Pico Chemiluminescent Substrate (Thermo Fisher Scientific #37069) diluted 1:2 in ddH_2O was added to each well and incubated for 5 minutes. Luminescent signal was measured on a Neo2 plate reader (Biotek) at 20ms/well at a read height of 1.0mm.

Serology data analysis

To assess variations in signal between plates and ensure quality control, a series of controls was added in quadruplicate on each plate. These controls included pooled serum from convalescent individuals, vaccinated individuals and unvaccinated, unexposed individuals. Furthermore, a titration of an isotype and antigen specific recombinant monoclonal antibody: anti-SARS-CoV-2 S CR3022 Human IgG1 (Absolute Antibody, Ab01680-10.0), anti-SARS-CoV-2 S CR3022 Human IgA (Absolute Antibody, Ab01680-16.0), or anti-SARS-CoV-2 S CR3022 Human IgM (Absolute Antibody, Ab01680-15.0) was also added in quadruplicate. As described in Colwill *et al.* (1), luminescence signal of this standard curve was then modeled using a four-parameters log-logistic regression and inflexion point established. Blank subtracted values were then scaled in relation to this inflexion point and presented as scaled luminescence hereby allowing data normalization between assay plates and used in subsequent analyses. Individuals were identified as positive (convalescent) if they had antibodies (IgG or combination of IgA/IgM) higher than the established thresholds (see Colwill *et al.*(1)) for at least the nucleocapsid and an additional target (spike and/or RBD). Briefly, the seropositivity threshold were established at a false discovery rate (FDR) of 3% of the density distribution of a large set of pre-pandemic sera. A specific threshold was calculated for each combination of antigen and antibody isotype.

Measurement of neutralization efficiency

A protein based surrogate neutralization (snELISA) was used to measure neutralization efficiency of the antibodies in sera. The complete methods are described here. First, 384-well high-binding polystyrene Nunc plates (Thermo Fisher Scientific, #460372) were coated with 100 ng/well of recombinant spike protein (NRC) in a final volume of 10uL, centrifuged at 216xg and incubated overnight at 4°C. The plates were then blocked with 80uL of 3% w/v skim milk powder dissolved in PBST for 1 h with rocking and then washed (as described above). Serum/plasma samples were then diluted 1 in 20 in 1% w/v skim milk powder dissolved in PBST and 20uL was added to each well. Furthermore, a set of pooled positive and negative sera was also added in as controls along with a titration NRCoV2-20-Fc (NRC), a recombinant monoclonal antibody, to create a standard curve. After a 2-hour incubation, plates were washed and 6.5ng of biotinylated recombinant ACE2 (NRC) was added to each well in a final volume of 20uL and incubated for 1 hour with shaking. Plates were then washed and bound ACE2 was detected with the addition of Streptavidin-Peroxidase Polymer (Sigma #S2438), diluted in 1% w/v skim milk powder in PBST, 25 ng/well was added to each well in a final volume of 20uL and incubated for 1 h. The plates were then washed and developed with the addition of 20uL of ELISA Pico Chemiluminescent Substrate (diluted 1:2 in MilliQ H_2O). After a 5-min incubation, plates were read on an Neo2 plate reader (BioTek Instruments) at 20 ms/well and a read height of 1.0 mm.

Luminescence values were adjusted to the blank (serum free, no ACE2 condition) and average maximal signal of the plate established using the serum free with ACE2 condition. Percentage inhibition was then established by measuring the reduction in spike / ACE2 interaction (0% inhibition; maximal ACE2-Spike binding).

Statistical analysis and data modeling

Statistical analyses were performed in R version 4.2.1. Individuals with missing data or samples that did not meet the quality standards for the neutralization assay were excluded from the study. Differences and clustering of serological results and PCR results were assessed using a confusion table and a principal component analysis (PCA), the latter using the scaled luminescence values from the ELISAs and the calls from the PCR tests as variables. The correlation between antibody

levels and PCR Ct values was assessed using only the samples that were positive for SARS-CoV-2-specific antibodies. Scatter plots of antibody levels depending on PCR Ct values for these samples revealed no correlation between the two variables so no further analysis was performed. The effect of sex and age on antibody level and neutralization was assessed by calculating the median and interquartile range (IQR) of the different groups and the distribution of each group was displayed as violin plots with the IQR and the median. Mann-Whitney U tests were used to compare the groups as their distributions were not normal. The Bonferroni correction was applied to adjust for multiplicity.

The correlation between antibody levels and number of days between symptom onset and sample collection was studied using a generalized linear model with a regression of the gamma family as this type of regression provided the model with the best fit to the data. SARS-CoV-2-positive samples that had been collected between 10 and 100 days after symptom onset were used in this analysis (n=185). The effect of age on the antibody levels over time was assessed by adding age as an interacting variable to the generalized linear model used to study the interaction between antibody level and time of collection. Four-parameters log-logistic regression using the drm package in R were used to study the relationship between antibody level and neutralization efficiency. The correlation between neutralization efficiency and the number of days between symptom onset and sample collection was assessed using a linear model.

Results

Establishment of an Elderly Unvaccinated Cohort

Between 28 April 2020 and 21 September 2020, residual serum and plasma samples from a community laboratory in Canada were collected from 766 individuals who had undergone polymerase chain reaction (PCR) testing for SARS-CoV-2 within the previous 180 days. Nine samples were excluded due to low sample volume. In addition, 18 were removed due to a lack of metadata or errors within that could not be corrected. The final cohort was composed of 739 participants, among which the median age was 82 years (SD = 18.9; Table 1, Supplementary Figure 1*A*); 252 (34.1%) were male; and 533 (72.1%) had received a positive diagnosis for SARS-CoV-2 through PCR testing. After PCR testing, a serum/plasma sample was collected when

contributors provided serum or plasma at the request of their health care providers, resulting in various time points after the onset of COVID-19 symptoms, ranging from 1 to 162 days with a median of 40 (SD = 33.3; Supplementary Figure 1*B*).

Table 1. Cohort demographics and collected information based on molecular and IgG seroconversion. Demographic data on individuals and sample information used in subsequent analyses were compiled and presented based on seroconversion to IgG (Sero+/-) and results of molecular (PCR) testing for SARS-CoV-2 (PCR+/-).

	Total	**PCR+ / Sero+**	**PCR- / Sero-**	**PCR+ / Sero-**	**PCR- / Sero+**
	n= 739	n=454	n=194	n=79	n=12
Age					
Mean (SD)	75.2 (18.9)	76.3 (18.6)	73.2 (18.8)	71.1 (20.5)	83.0 (10.5)
Median	82.0	83.0	78.0	79.5	85.0
Min - Max	21-105	21-105	23-100	22-98	60-97
Sex n(%)					
Male	252 (34.1)	147 (32.4)	74 (38.1)	25 (31.7)	6 (50.0)
Female	486 (65.76)	307 (67.6)	119 (61.3)	54 (68.4)	6 (50.0)
Indeterminate	1 (0.14)	0 (0.00)	1 (0.52)	0 (0.00)	0 (0.00)
Days between symptom onset & collection date					
Mean (SD)	45.5 (33.3)	49.8 (34.8)	33.6 (20.9)	40.5 (37.2)	25 (13.9)
Median	40.0	43.0	38.0	33.0	33.0
Min - Max	1-162	4-162	1-72	1-153	9-33
Number of patients with information on date of collection	233	199	22	12	0
Collection site n(%)					
Long term care	442 (59.8)	262 (57.7)	121 (62.4)	48 (60.8)	11 (91.7)
Hospital-ICU	1 (0.14)	1 (0.22)	0 (0.00)	0 (0.00)	0 (0.00)
Not reported	296 (40.1)	191 (42.1)	73 (37.6)	31 (39.2)	1 (8.30)

Comparison between results from PCR testing and serologic analyses showed the following: 454 (61.4%) participants had received a positive diagnosis for SARS-CoV-2 through PCR and had detectable levels of antibodies; 194 (26.5%) had received a negative diagnosis for SARS-CoV-2 through PCR and had no detectable levels of antibodies; 79 (10.7%) had received a positive diagnosis for SARS-CoV-2 through PCR but had no detectable levels of antibodies; and 12 (1.6%) had received a negative diagnosis for SARS-CoV-2 through PCR but had detectable levels of antibodies (Table 1).

Elderly Individuals Generate Higher Levels of Antibodies Against SARS-CoV-2

The effect of age on the antibody response following SARS-CoV-2 infection was investigated. To do so, the cohort of 513 participants who were SARS-CoV-2 positive with data on age was divided into 3 age groups—hereafter, <65 (n = 126), 65–89 (n = 252), and ≥90 (n = 135) years—given the overall age distribution of our cohort (Supplementary Figure 1*A*). The <65 group had significantly lower anti-RBD (anti–receptor-binding domain), anti-S, and anti-N IgGs than the 65–89 and ≥90 groups (Figure 1, Supplementary Table 2). Significance was tested with a Mann-Whitney *U* test instead of an analysis of variance due to the nonnormal distribution. The same trend was observed for IgA levels, with the <65 group having the lowest overall levels for anti-RBD ($P < .05$), anti-S ($P < .01$), and anti-N ($P < .01$) IgA of all 3 age groups (Figure 1*B*). The difference in IgM levels between the <65 group and the 65–89 and ≥90 groups was not as pronounced as the one for IgG and IgA, although the level of anti-N IgM of the <65 group was significantly lower than that from 65–89 ($P = .0025$) and ≥90 ($P = .027$; Figure 1*C*). Neutralization efficiency also varied across age groups. Indeed, the <65 group had a significantly lower median neutralization efficiency than the 65–89 group ($P = .000005$) and the ≥90 group ($P = .00019$; Figure 1*D*), which correlated with its lower overall antibody levels as compared with the 65–89 and ≥90 groups.

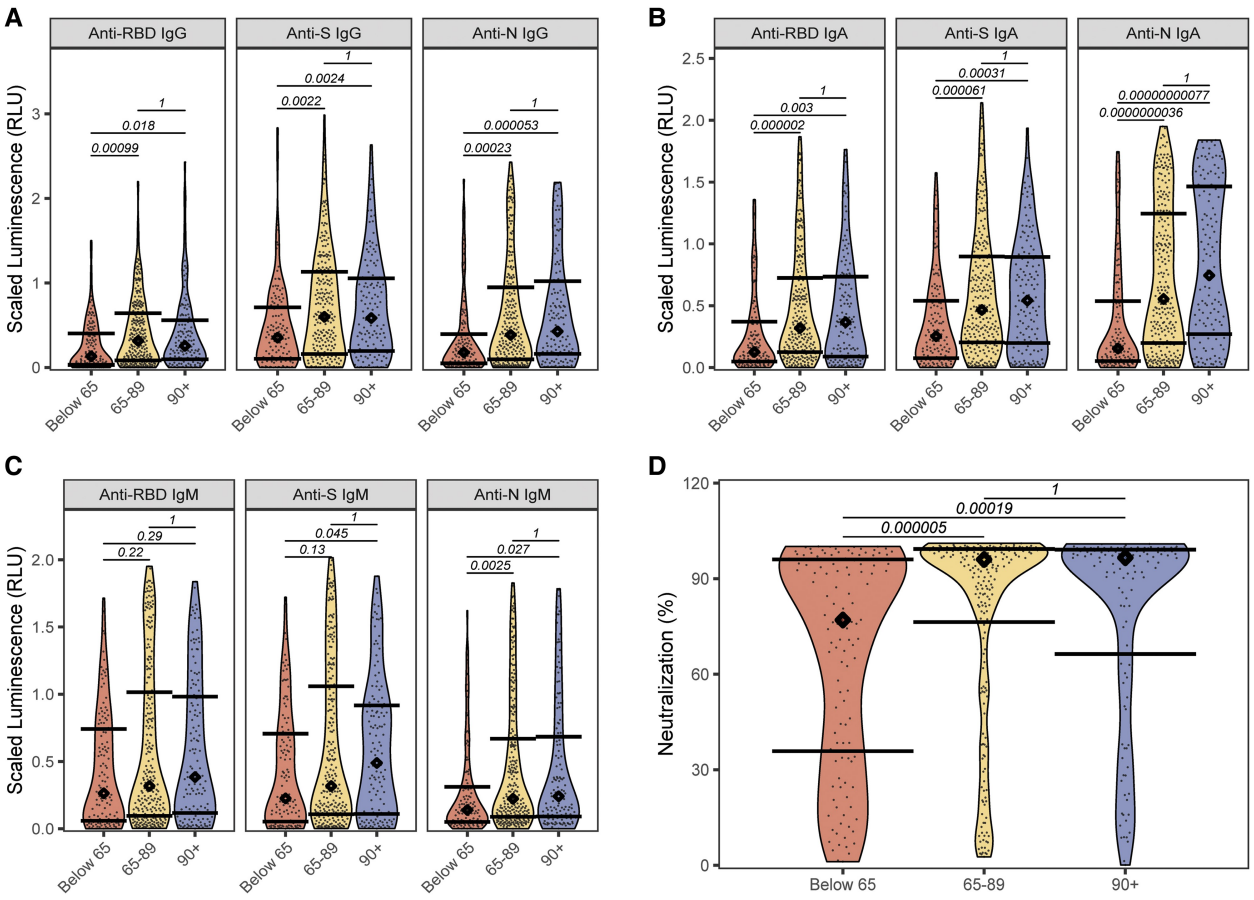


Figure 1. Antibody levels and neutralization efficiency relative to age groups. *A–C*, Levels of anti-RBD, anti-S, and anti-N IgG, IgA, and IgM relative to their corresponding age groups (<65, 65–89, and ≥90 years). *D*, Neutralization efficiency relative to the age group. For all panels, medians are indicated by diamonds and IQRs by horizontal segments. Serum/plasma was diluted by a factor of 100 for IgA and IgM and 10 000 for IgG. *P* values presented above the violin plots were calculated with a Mann-Whitney *U* test (n = 513). RBD, receptor-binding domain; RLU, relative light units.

Relationship Between IgG Level and Neutralization Over Time

The relationship between the time of serum/plasma collection, calculated as the number of days between symptom onset and sample collection, and antibody levels was characterized through generalized linear models with a gamma regression. This analysis used only the 216 SARS-CoV-2–positive samples containing information about the time of symptom onset and serum/plasma collection. The data set was further trimmed to contain the 185 samples that were collected between 10 and 100 days after symptom onset, as antibody production is limited during the first

days following symptom onset and the few samples that were collected before 10 days (n = 10) and after 100 days (n = 21) were not sufficient for analysis over that period. The specificity of the antigen was added as an interacting variable in the model so that the slope would vary depending on the antigen target, meaning that anti-S, anti-RBD, and anti-N antibodies were allowed to vary differently from one another across time. Interestingly, anti-RBD IgG levels did not show a decrease in samples up to 100 days after onset of symptoms and remained relatively constant over the time observed (slope = 0.00066 relative light units [RLU]/d). Levels of anti-S IgG (slope = −0.00456 RLU/d) and anti-N IgG (slope = −0.00682 RLU/d) displayed higher decay with anti-N IgG having a faster decay rate than anti-S IgG (Figure 2*A*, Supplementary Table 4). IgA and IgM decay rates were overall faster than the ones for IgG, as expected (Supplementary Figure 5*A*–*C*). This suggests an antigen/isotype-specific decay rate after infection.

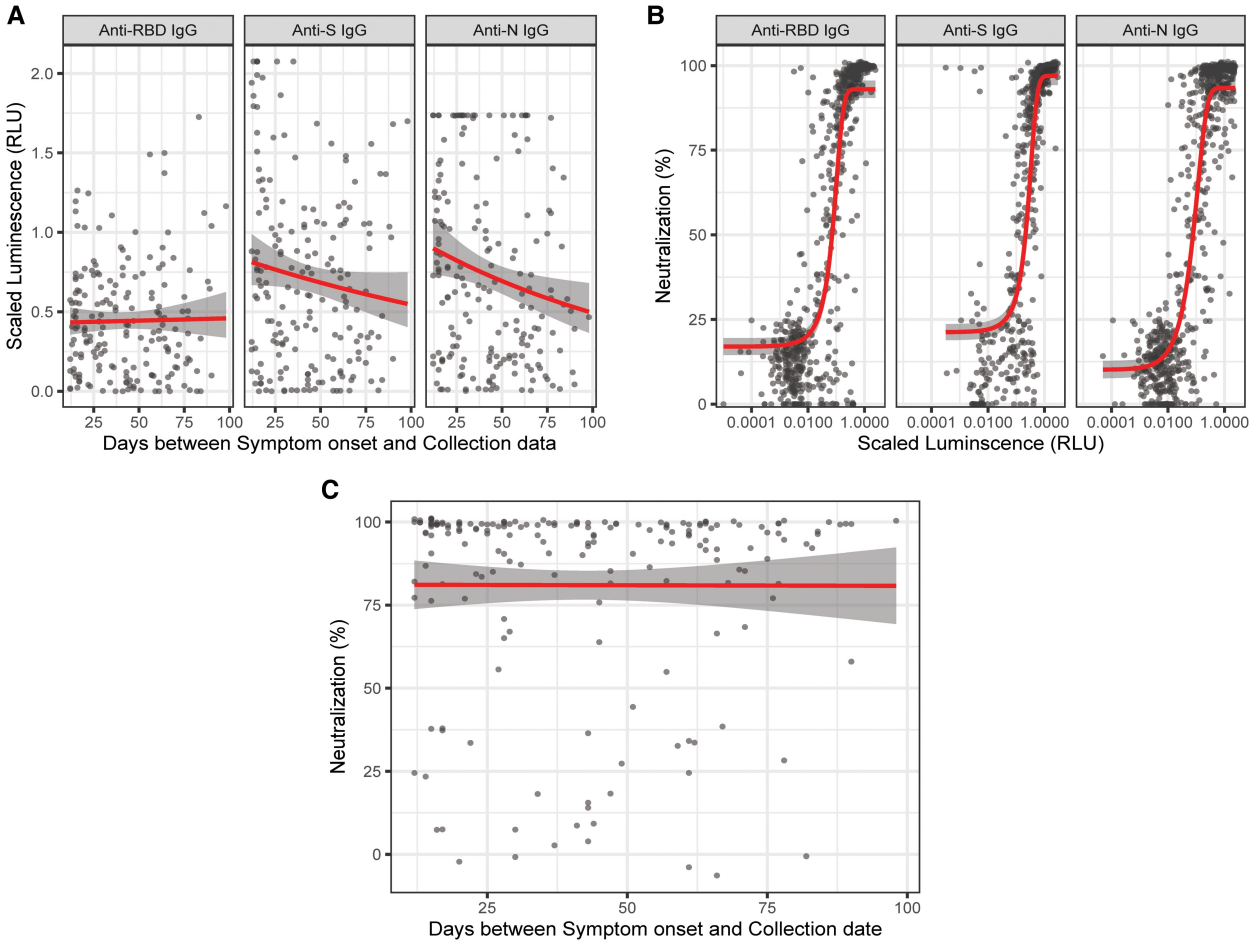


Figure 2. Antibody levels and neutralization efficiency relative to the time of serum/plasma collection. *A*, Levels of IgG raised against RBD, S, and N relative to the number of days between the onset of symptoms and serum/plasma collection. A generalized linear model of the gamma family was generated to model IgG-level variations as a function

of time per the following formula: scaled luminescence number of days × IgG antigen (line). The SE of the model is displayed (shaded area) (n = 185). *B*, The relationship between neutralization efficiency and IgG levels was modeled via a 4-parameter log-logistic regression per the following formula: neutralization scaled luminescence for each IgG antigen (line). The SE of the model is displayed (shaded area) (n = 739). *C*, Neutralization efficiency was based on the number of days between symptom onset and serum/plasma collection. The relationship was modeled with a linear model per the following formula: neutralization number of days (line). The SE of the model is displayed (shaded area) (n = 185). Serum/plasma was diluted by a factor of 100 for IgA and IgM and 10 000 for IgG. RBD, receptor-binding domain; RLU, relative light units.

To determine if this decrease in antibody levels affects the neutralization efficiency, the relationship between the neutralization efficiency and antibody levels was modeled on the whole cohort via a 4-parameter log-logistic regression (Figure 2*B*). The levels of anti-RBD IgG (median effective dose [ED_{50}] = 1.18), anti-S IgG (ED_{50} = 1.7) and anti-N IgG (ED_{50} = 1.01) all positively correlated with neutralization. Similar trends were observed for IgA and IgM (Supplementary Figure 5*C* and *D*, Supplementary Table 3). The relationship between neutralization efficiency and time of serum/plasma collection was then modeled through a linear model. Although antibody levels were lower in samples collected later after symptom onset and the neutralization efficiency positively correlated with antibody levels, neutralization efficiency varied very little with the time of serum/plasma collection (slope = −0.0036; Figure 2*C*).

Modeling of Antibody Decline Reveals That Decline Rate Is Increased With Age

The effect of age on the decrease of antibody levels was investigated. The relationship among antibody levels, time of serum/plasma collection, and age was modeled with a generalized linear model with a gamma regression on the 216 SARS-CoV-2–positive samples with data for the time of serum/plasma collection after symptom onset. The data set was further trimmed to the 185 samples that were collected between 10 and 100 days after symptom onset. Interestingly, the ≥90 group had faster decrease rates for anti-S IgG and anti-N IgG than the <65 and 65–89 groups (Figure 3*A*, Supplementary Figure 6*A* and *B*, Supplementary Table 4). This suggests that although the ≥90 group had overall higher anti-S IgG and anti-N IgG levels when compared with the <65 and 65–89 groups, they appeared to decay at a faster rate to reach similar or even lower levels than the ones in the younger groups by day 100 after symptom onset. This faster decay rate for the ≥90 group was also observed for all IgAs and IgMs, although the rate of decrease was faster than IgGs. Interestingly, the IgG, IgA, and IgM levels for the <65 group did not vary much with time, with the exception of anti-N IgG, anti-S IgA, and anti-N IgA, which decreased with time (Figure

3, Supplementary Figures 6 and 7). These results suggest that although younger populations mounted a less potent immune response following SARS-CoV-2 infection, their antibody levels were more stable than those of older individuals during the 100-day period that was studied.

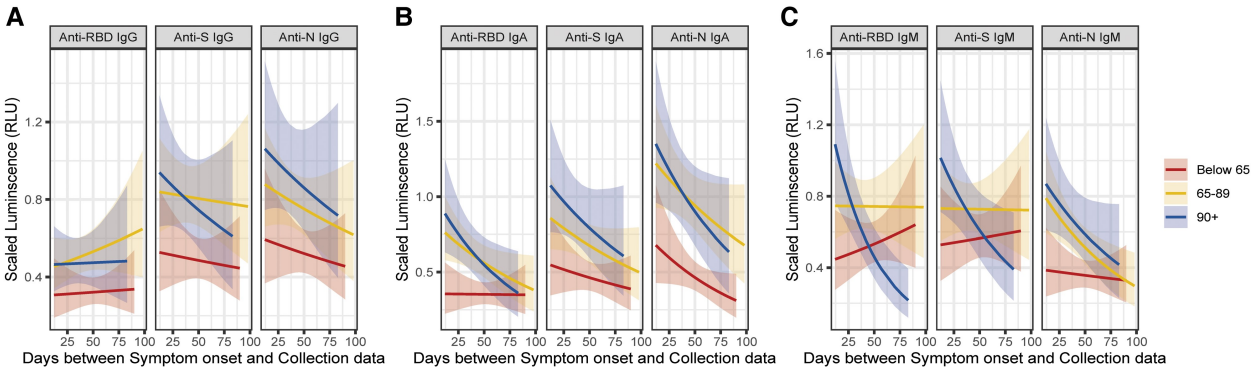


Figure 3. Age group–specific variation of antibody levels relative to the time of serum/plasma collection. *A–C*, Levels of anti-RBD, anti-S, and anti-N IgG, IgA, and IgM based on the number of days between onset of symptoms and serum/plasma collection per age group (<65, 65–89, and ≥90 years). The relationship was modelized with a generalized linear model of the gamma family per the following formula: scaled luminescence number of days × IgG antigen × age group (colored line). The SE of the models is displayed in the lighter section around the regression (n = 185). RBD, receptor-binding domain; RLU, relative light units.

Discussion

Disease-related comorbidities, aging immune system, and changing living circumstances (home care, LTC, hospital stay) are a few important factors that can render elderly people more susceptible to poor clinical outcomes. During the COVID-19 pandemic, questions were raised regarding how the humoral immune system responds following SARS-CoV-2 infection in the elderly. Considerable research efforts have been dedicated to elucidate characteristics of antibody responses to SARS-CoV-2, as these represent the best known correlate of protection [37].

In this study, we collected serum/plasma from 739 individuals, 75% of whom were >65 years old, between April and September 2020, prior to vaccine availability in Canada (Table 1, Supplementary Figure 1). A retrospective study that examined mortality during our recruitment period reported that elderly populations aged ≥65 years accounted for 93% of deaths attributed to

COVID-19 [4]. Molecular testing was initially performed and identified 533 people with active SARS-CoV-2 infection. From these, 79 (10.7%) did not seroconvert to IgG or IgA/IgM despite being positive by PCR. Upon further analysis of the 79 who had cycle threshold (Ct) data available, a large proportion had Ct values >36 for the N gene, which suggests a low viral load at the time of testing or a false-positive PCR result. Low levels of viral RNA, which could be associated with a very mild infection, may not be sufficient in certain persons to elicit a detectable antibody response. In addition, cross-reactive seasonal coronavirus T cells have been reported to abrogate SARS-CoV-2 infection, resulting in a lack of seroconversion [38]. A few groups have noted an increased lack of seroconversion in those with asymptomatic and mild infection, in patients with a body mass index >30, and in children [39, 40]. In addition, the decreased prevalence of naive B cells and weaker interactions with T cells, for example, are likely contributors to higher frequencies of nonseroconversion in older people [14, 22].

The majority (85.2%) of individuals with positive PCR tests seroconverted (Tables 1 and 2). Serology profiling identified an additional 12 who tested negative by PCR but had detectable levels of antibodies, likely indicating an infection prior to molecular testing. Seroprevalence thresholds were previously established by our group by setting these at a 3% false discovery rate from the density distribution of a large panel of serum and plasma collected prior to 2019 [41]. In addition, to limit false positives from cross-reactivity with seasonal coronaviruses [42], participants were classified as convalescent seropositive if they had IgG antibodies to the nucleocapsid and another antigen (RBD and/or spike). To track early seroconversion events, patients were also identified as positive if they had IgA and IgM antibodies.

Table 2. Seroprevalence by cohorts. Individuals were segregated in three distinct cohorts based on the age distribution of the cohort. Demographic information, as well as isotype and antigen-specific seroprevalence is reported. Samples were considered positive for distinct antibodies based on a threshold set at 3% false discovery rate of the density distribution from pre-pandemic serum/plasma samples.

	Combined n= 688	**Below 65 yrs** n= 174	**65-89 yrs** n= 342	**90 yrs and over** n= 172
Age				
Mean (SD)	75.15 (18.8)	47.6 (12.4)	80 (7.3)	93.4 (3.1)
Median	82	50	82	93
Min - Max	21-105	21-64	65-89	90-105
Sex n(%)				
Female	461 (67)	122 (70.1)	202 (59.1)	137 (79.7)
Male	227 (33)	52 (29.9)	140 (40.9)	35 (20.3)
Days between symptom onset & collection date				
Mean (SD)	48.60 (35.09)	60.36 (35.60)	46.77 (35.06)	35.82 (29.46)
Median	43	57	37	25
Min - Max	1-162	1-161	1-162	3-127
Number of patients with information on date of collection	228	75	98	55
IgG n(%)				
RBD	451 (65.6)	105 (60.3)	223 (65.2)	123 (71.5)
Spike	521 (75.7)	128 (73.6)	253 (74)	140 (81.4)
Nucleocapsid	460 (66.9)	105 (60.3)	230 (67.3)	125 (72.7)
IgA n(%)				
RBD	369 (53.6)	69 (39.7)	202 (59.1)	98 (53.5)
Spike	389 (56.5)	79 (45.4)	204 (59.7)	106 (61.6)
Nucleocapsid	379 (55.1)	65 (37.4)	202 (59.1)	112 (65.1)
IgM n(%)				
RBD	363 (52.8)	80 (46)	185 (54.1)	98 (57)
Spike	348 (50.6)	77 (44.5)	176 (51.5)	95 (55.2)
Nucleocapsid	197 (28.6)	32 (18.4)	107 (31.3)	58 (33.7)
Neutralization				
Mean (SD)	58.6 (40)	50.6 (37.9)	60.6 (40.6)	62.8 (40.1)
Median	76.7	44.3	85	90.1

Principal component analysis on the serology and PCR results showed a good clustering of the population in populations that were SARS-CoV-2 positive and negative (PC1 and PC2 explained 72.4% and 11.4% of the variance, respectively), particularly when only IgG levels were taken into consideration (PC1 and PC2 explained 93.8% and 3.6% of the variance; Supplementary Figure 2). This suggests that samples classified as positive by PCR had detectable levels of IgG and that the serologic data could be used to distinguish SARS-CoV-2–positive samples from SARS-CoV-2–negative ones. Although the principal component analysis showed a correlation between IgG levels and PCR results, no correlation was observed between IgG levels and PCR Ct values (Supplementary Figure 3). This suggests that although a positive PCR diagnosis for SARS-CoV-2 correlated with detectable SARS-CoV-2–specific IgG, the PCR Ct was independent to the levels of antibody detected following infection in this data set. Decentralized community PCR testing that was performed over various sites, including LTC homes and collection centers, may confound the data. In addition, samples were collected at various time points during acute infection, further complicating any attempt to using Ct values as a proxy for the amount of viral RNA measured during infection.

When antibody levels from the 533 SARS-CoV-2–positive samples with data on sex were compared, no significant differences in serologic results for IgG were found between females and males (Supplementary Figure 4*A*). In the case of IgA, females had significantly lower levels of anti-RBD ($P = .045$) and anti-S ($P = .047$; Supplementary Figure 4*B*, Supplementary Table 1). Females also had significantly lower levels of anti-RBD IgM ($P = .001$) and anti-S IgM ($P = .004$; Supplementary Figure 4*C*). Days between collection time and symptom onset were similar between males and females (Supplementary Figure 8). Differences in antibody by sex could be explained by characteristics of SARS-CoV-2 infections (disease severity, viral load, etc) and immune responses in both groups. Whether these differences seen in IgA and IgM levels are biologically relevant remains unclear.

When categorizing antibody levels by age groups (Table 2, Figure 1), we observed an age-dependent correlation with antibody levels. In fact, the ≥90 group consistently had significantly higher levels of antibodies than the <65 group, regardless of antibody isotype or viral antigen target. Other groups have reported similar trends [32, 33, 35]. This is somewhat in opposition to

what is observed following SARS-CoV-2 immunizations, where age is negatively correlated with vaccine responses [28, 43]. Given that sera were collected for up to 180 days following symptom onset, a later collection time for some of the age groups is a possible cofounding factor. Unfortunately, days between sample collection and symptom onset was available for only 33.1% of the cohort with detectable levels of antibodies. A density distribution by age group, for which this information was available, highlighted some differences, with a higher proportion of sera collected earlier in the ≥90 group (Supplementary Figure 9). However, considering samples collected within 30 days after symptom onset (Supplementary Figure 10), the same trend was observed, with older individuals having higher levels of antibodies. This observation may be due to the positive correlation between SARS-CoV-2 antibody responses and disease severity in previous studies [44, 45]. Given that older age is itself a risk factor for severe infections, higher levels of antibodies are likely an indirect result of high and persisting levels of viral antigens associated with infection severity. Presumably, a higher level of proinflammatory markers associated with increased disease severity could also contribute to an increased production of antibodies. Unfortunately, disease severity scores were not collected as part of this study, and because most patients remained in LTC or unspecified locations, hospitalization status was not an appropriate estimate of disease severity in our data set. It is possible that immunologic recall from previous coronavirus infection contributed to some of the differences in antibody levels in this cohort.

Given the importance of neutralizing antibodies in viral clearance and subsequent protection, we used a high-throughput protein–based surrogate neutralization assay to measure ACE2-spike interactions, considering that the number of samples in this cohort was prohibitive for PRNT50. Our assay has been shown to correlate with PRNT50 and has been validated with the World Health Organization's international reference panel [41, 46], and it is now used to validate new methods [47]. In this cohort, we showed that neutralization followed similar trends as antibody levels, whereas neutralization efficiency was positively correlated with age, with those aged >65 years having a significant higher level of neutralization activity overall (Table 2, Figure 1). Although B cells in the elderly have been shown to exhibit impairments in somatic hypermutation and affinity maturation processes [11, 13], we demonstrated that elderly persons generated high levels of antibody capable of efficiently neutralizing spike interactions with its receptor ACE2. In fact,

because neutralization stems from infection-acquired immunity, all antibodies measured in this work correlated with neutralization (Figure 2, Supplementary Figure 5). Cross-sectional analysis of neutralization in relation to time since symptom onset revealed that neutralizing antibodies remained stable for at least 100 days in this cohort.

As expected, IgM and IgA antibodies against all 3 antigens (S, N, RBD) showed the fastest decay (Supplementary Table 4, Figure 3*B* and *C*, Supplementary Figure 6). It is worth noting that while all age groups showed a rapid decline for IgA, the group aged <65 years displayed more stable IgM levels over time, most likely due to the influence of outliers, which skewed an already slower decline in contrast to the other age groups. Interestingly, in the case of IgG, antibodies targeting the nucleocapsid and the spike protein decayed at various rates, but antibodies targeting the RBD remained stable and even demonstrated an increase over time (Figure 3*A*). Since RBD is the principal target of neutralizing antibodies, this relative stability over time could explain the absence of a neutralization decline in our cohort [48]. In addition, antibodies targeting the nucleocapsid, regardless of isotype, showed the fastest decay, which is in line with previous knowledge [49, 50]. While decay rates are highly dependent on the target antigen and antibody isotype, age appears to influence the decline rate. In all cases, individuals aged ≥90 years showed the fastest decay despite the initial higher levels of antibodies.

Given that serum/plasma samples were collected up to 180 days following PCR testing, it is reasonable to assume that most patients survived SARS-CoV-2 infection, although information on outcome or disease severity was unavailable. In addition, recruitment occurred in early spring to fall of 2020, suggesting that most infections were caused by the ancestral SARS-CoV-2 strain, prior to variants in Canada. Nonetheless, this characterization of antibody responses in the elderly highlights that despite age, most individuals developed robust levels of antibodies with an associated high neutralization potential that remained stable over 100 days. We also showed that antibody decay rates increased with age and were dependent on the isotype and antigen. These data, in combination with studies examining vaccine-induced immune responses, Fc-mediated function, and cellular immunity, will contribute to our knowledge of natural and hybrid immunity, particularly in the elderly population.

Acknowledgments. We acknowledge past and current members of the high-throughput SARS-CoV-2 serology and diagnostic facility at the University of Ottawa: Danielle Dewar-Darch, Justino Hernandez Soto, Yuchu Dou, Abishek Xavier, Erika Marion (past), Jian-Jun Jia (past), and Smita Upamaka (past). We also acknowledge Kim Blais and Parvinder Sohal at LifeLabs for managing the collection of samples and sample database.

Author Contributors. Y. G. and C. A. developed and optimized the experimental approach and performed the data collection. Y. G., C. A., and M.-A. L. developed the high-throughput serology platform alongside R. A. B. M. W. and M. P. performed the data analysis. N. W.-A. H., D. K., and M. A. E. H. coordinated sample collection and collected related data. Y. G., M. W., M. P., and M.-A. L. wrote and formatted the manuscript. All authors edited and approved the manuscript.

Patient consent statement. Patients' written consent was obtained for secondary use of deidentified samples by LifeLabs Medical Laboratory Services. The design of the work was approved by the uOttawa ethical review board.

Data sharing. The data used in this study can be obtained by request from M.-A. L. (langlois@uottawa.ca) or M. P. (mpelchat@uottawa.ca).

Financial support. This work was supported in part by a COVID-19 Rapid Response Grant from the Canadian Institute of Health Research (VR2-172722) and from a grant supplement by the COVID-19 Immunity Task Force to M.-A. L. Production of COVID-19 reagents was financially supported by the National Research Council of Canada's Pandemic Response Challenge Program. Additionally, Y. G. and M. W. are supported by a Charles Best and Frederick Banting CGS-Doctoral Award from the Canadian Institute of Health Research (476885 and 476877).

Role of the funder/sponsor. The funding sources played no role in the study design, data collection, analysis, writing of the manuscript, and decision to publish.

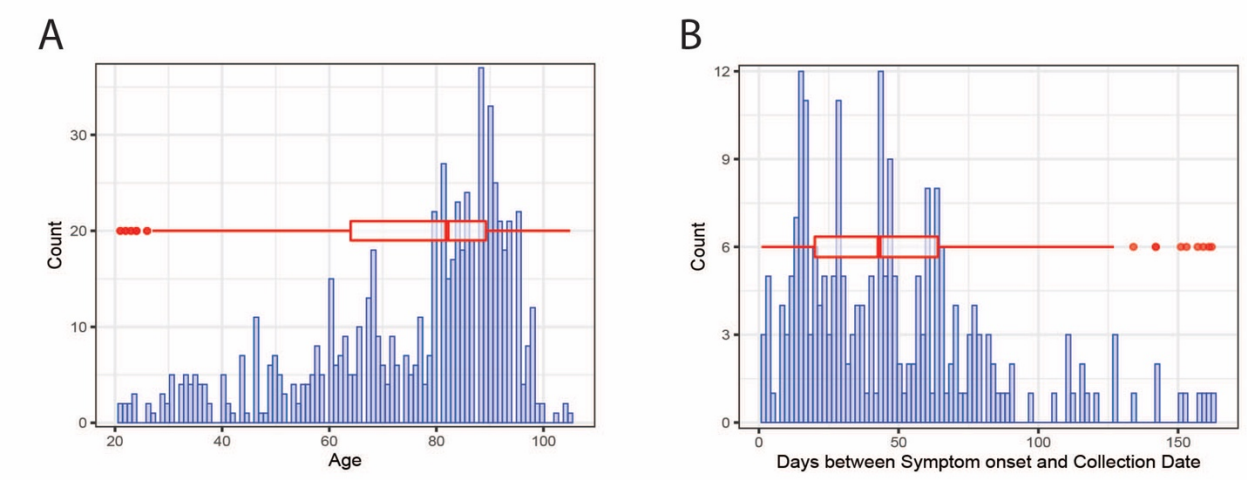
References

1. Fisman DN, Bogoch I, Lapointe-Shaw L, McCready J, Tuite AR. Risk Factors Associated With Mortality Among Residents With Coronavirus Disease 2019 (COVID-19) in Long-term Care Facilities in Ontario, Canada. JAMA Network Open **2020**; 3:e2015957-e.
2. Onder G, Rezza G, Brusaferro S. Case-Fatality Rate and Characteristics of Patients Dying in Relation to COVID-19 in Italy. JAMA **2020**; 323:1775-6.
3. Santesmasses D, Castro JP, Zenin AA, et al. COVID-19 is an emergent disease of aging. Aging Cell **2020**; 19:e13230.
4. Statistic Canada. Insights on Canadian Society: Impact of the COVID-19 pandemic on Canadian seniors. Available at: https://www150.statcan.gc.ca/n1/pub/75-006-x/2021001/article/00008-eng.htm. 2022.
5. Strausbaugh LJ, Sukumar SR, Joseph CL. Infectious disease outbreaks in nursing homes: an unappreciated hazard for frail elderly persons. Clin Infect Dis **2003**; 36:870-6.
6. Lum HD, Mody L, Levy CR, Ginde AA. Pandemic Influenza Plans in Residential Care Facilities. Journal of the American Geriatrics Society **2014**; 62:1310-6.
7. Li J, Birkhead GS, Strogatz DS, Coles FB. Impact of Institution Size, Staffing Patterns, and Infection Control Practices on Communicable Disease Outbreaks in New York State Nursing Homes. American Journal of Epidemiology **1996**; 143:1042-9.
8. Thompson DC, Barbu MG, Beiu C, et al. The Impact of COVID-19 Pandemic on Long-Term Care Facilities Worldwide: An Overview on International Issues. Biomed Res Int **2020**; 2020:8870249.
9. Mason KE, Maudsley G, McHale P, Pennington A, Day J, Barr B. Age-Adjusted Associations Between Comorbidity and Outcomes of COVID-19: A Review of the Evidence From the Early Stages of the Pandemic. Frontiers in Public Health **2021**; 9.
10. Public Health Agency of Canada. Aging and chronic diseases: A profile of Canadian seniors. Available at: https://www.canada.ca/en/public-health/services/publications/diseases-conditions/aging-chronic-diseases-profile-canadian-seniors-report.html. 2023.
11. Bartleson JM, Radenkovic D, Covarrubias AJ, Furman D, Winer DA, Verdin E. SARS-CoV-2, COVID-19 and the aging immune system. Nature Aging **2021**; 1:769-82.
12. Franceschi C, Campisi J. Chronic inflammation (inflammaging) and its potential contribution to age-associated diseases. J Gerontol A Biol Sci Med Sci **2014**; 69 Suppl 1:S4-9.
13. Fulop T, Larbi A, Dupuis G, et al. Immunosenescence and Inflamm-Aging As Two Sides of the Same Coin: Friends or Foes? Frontiers in Immunology **2018**; 8.
14. Weiskopf D, Weinberger B, Grubeck-Loebenstein B. The aging of the immune system. Transpl Int **2009**; 22:1041-50.
15. Montgomery RR, Shaw AC. Paradoxical changes in innate immunity in aging: recent progress and new directions. J Leukoc Biol **2015**; 98:937-43.
16. Hazeldine J, Harris P, Chapple IL, et al. Impaired neutrophil extracellular trap formation: a novel defect in the innate immune system of aged individuals. Aging Cell **2014**; 13:690-8.
17. Brubaker AL, Rendon JL, Ramirez L, Choudhry MA, Kovacs EJ. Reduced neutrophil chemotaxis and infiltration contributes to delayed resolution of cutaneous wound infection with advanced age. J Immunol **2013**; 190:1746-57.
18. Wong CK, Smith CA, Sakamoto K, Kaminski N, Koff JL, Goldstein DR. Aging Impairs Alveolar Macrophage Phagocytosis and Increases Influenza-Induced Mortality in Mice. The Journal of Immunology **2017**; 199:1060-8.
19. Zhao J, Zhao J, Legge K, Perlman S. Age-related increases in PGD(2) expression impair respiratory DC migration, resulting in diminished T cell responses upon respiratory virus infection in mice. J Clin Invest **2011**; 121:4921-30.
20. Britanova OV, Putintseva EV, Shugay M, et al. Age-related decrease in TCR repertoire diversity measured with deep and normalized sequence profiling. J Immunol **2014**; 192:2689-98.

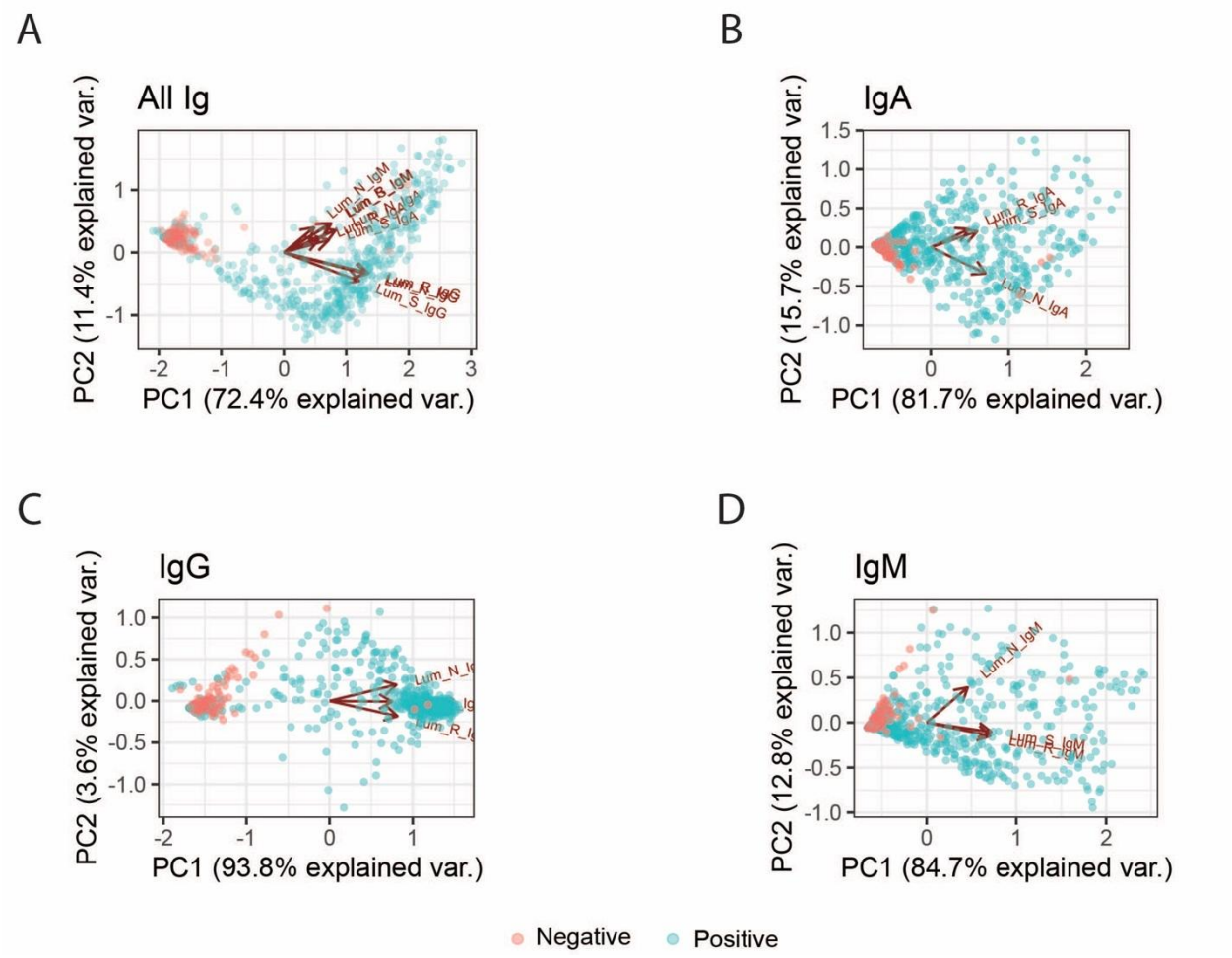
21. Fagnoni FF, Vescovini R, Passeri G, et al. Shortage of circulating naive CD8(+) T cells provides new insights on immunodeficiency in aging. Blood **2000**; 95:2860-8.
22. Gruver AL, Hudson LL, Sempowski GD. Immunosenescence of ageing. J Pathol **2007**; 211:144-56.
23. Weksler ME, Szabo P. The Effect of Age on the B-Cell Repertoire. Journal of Clinical Immunology **2000**; 20:240-9.
24. Seidman JC, Richard SA, Viboud C, Miller MA. Quantitative review of antibody response to inactivated seasonal influenza vaccines. Influenza Other Respir Viruses **2012**; 6:52-62.
25. Vermeiren AP, Hoebe CJ, Dukers-Muijrers NH. High non-responsiveness of males and the elderly to standard hepatitis B vaccination among a large cohort of healthy employees. J Clin Virol **2013**; 58:262-4.
26. van Werkhoven CH, Huijts SM, Bolkenbaas M, Grobbee DE, Bonten MJ. The Impact of Age on the Efficacy of 13-valent Pneumococcal Conjugate Vaccine in Elderly. Clin Infect Dis **2015**; 61:1835-8.
27. Naaber P, Tserel L, Kangro K, et al. Dynamics of antibody response to BNT162b2 vaccine after six months: a longitudinal prospective study. The Lancet Regional Health - Europe **2021**; 10:100208.
28. Wei J, Stoesser N, Matthews PC, et al. Antibody responses to SARS-CoV-2 vaccines in 45,965 adults from the general population of the United Kingdom. Nature Microbiology **2021**; 6:1140-9.
29. Tut G, Lancaster T, Butler MS, et al. Robust SARS-CoV-2-specific and heterologous immune responses in vaccine-naïve residents of long-term care facilities who survive natural infection. Nature Aging **2022**; 2:536-47.
30. Pichler D, Baumgartner M, Kimpel J, et al. Marked Increase in Avidity of SARS-CoV-2 Antibodies 7-8 Months After Infection Is Not Diminished in Old Age. J Infect Dis **2021**; 224:764-70.
31. Epstude J, Skiba M, Harsch IA. Antibody titers and rapid antigen testing in elderly patients with SARS-CoV-2 pneumonia vs. staff of ICU and "Covid-19" wards. GMS Hyg Infect Control **2021**; 16:Doc11.
32. Selva KJ, van de Sandt CE, Lemke MM, et al. Systems serology detects functionally distinct coronavirus antibody features in children and elderly. Nature Communications **2021**; 12:2037.
33. Wong NS, Lee SS, Chan DPC, et al. Trajectory patterns of SARS-CoV-2 neutralising antibody response in convalescent COVID-19 patients. Communications Medicine **2022**; 2:53.
34. Wang X, Guo X, Xin Q, et al. Neutralizing Antibody Responses to Severe Acute Respiratory Syndrome Coronavirus 2 in Coronavirus Disease 2019 Inpatients and Convalescent Patients. Clin Infect Dis **2020**; 71:2688-94.
35. Vilibic-Cavlek T, Stevanovic V, Ilic M, et al. SARS-CoV-2 Seroprevalence and Neutralizing Antibody Response after the First and Second COVID-19 Pandemic Wave in Croatia. Pathogens **2021**; 10:774.
36. Wu F, Wang A, Liu M, et al. Neutralizing antibody responses to SARS-CoV-2 in a COVID-19 recovered patient cohort and their implications. medRxiv **2020**:2020.03.30.20047365.
37. Khoury DS, Cromer D, Reynaldi A, et al. Neutralizing antibody levels are highly predictive of immune protection from symptomatic SARS-CoV-2 infection. Nature Medicine **2021**; 27:1205-11.
38. Swadling L, Diniz MO, Schmidt NM, et al. Pre-existing polymerase-specific T cells expand in abortive seronegative SARS-CoV-2. Nature **2022**; 601:110-7.
39. Bhatt M, Zemek RL, Tang K, et al. Antibody Seronegativity in COVID-19 RT-PCR–Positive Children. The Pediatric Infectious Disease Journal **2022**; 41:e318-e20.
40. Johannesen CK, Rezahosseini O, Gybel-Brask M, et al. Risk Factors for Being Seronegative following SARS-CoV-2 Infection in a Large Cohort of Health Care Workers in Denmark. Microbiology Spectrum **2021**; 9:e00904-21.
41. Colwill K, Galipeau Y, Stuible M, et al. A scalable serology solution for profiling humoral immune responses to SARS-CoV-2 infection and vaccination. Clinical & Translational Immunology **2022**; 11:e1380.
42. Galipeau Y, Siragam V, Laroche G, et al. Relative Ratios of Human Seasonal Coronavirus Antibodies Predict the Efficiency of Cross-Neutralization of SARS-CoV-2 Spike Binding to ACE2. eBioMedicine **2021**; 74.

43. Mwimanzi F, Lapointe HR, Cheung PK, et al. Older Adults Mount Less Durable Humoral Responses to Two Doses of COVID-19 mRNA Vaccine but Strong Initial Responses to a Third Dose The Journal of Infectious Diseases **2022**; 226:983-94.
44. Peluso MJ, Takahashi S, Hakim J, et al. SARS-CoV-2 antibody magnitude and detectability are driven by disease severity, timing, and assay. Science Advances **2021**; 7:eabh3409.
45. Chen X, Pan Z, Yue S, et al. Disease severity dictates SARS-CoV-2-specific neutralizing antibody responses in COVID-19. Signal Transduction and Targeted Therapy **2020**; 5:180.
46. Abe KT, Li Z, Samson R, et al. A simple protein-based surrogate neutralization assay for SARS-CoV-2. JCI Insight **2020**; 5.
47. Kim SJ, Yao Z, Marsh MC, et al. Homogeneous surrogate virus neutralization assay to rapidly assess neutralization activity of anti-SARS-CoV-2 antibodies. Nature Communications **2022**; 13:3716.
48. Du L, Yang Y, Zhang X. Neutralizing antibodies for the prevention and treatment of COVID-19. Cellular & Molecular Immunology **2021**; 18:2293-306.
49. Grandjean L, Saso A, Torres Ortiz A, et al. Long-Term Persistence of Spike Protein Antibody and Predictive Modeling of Antibody Dynamics After Infection With Severe Acute Respiratory Syndrome Coronavirus 2. Clin Infect Dis **2022**; 74:1220-9.
50. Van Elslande J, Oyaert M, Lorent N, et al. Lower persistence of anti-nucleocapsid compared to anti-spike antibodies up to one year after SARS-CoV-2 infection. Diagnostic Microbiology and Infectious Disease **2022**; 103:115659.

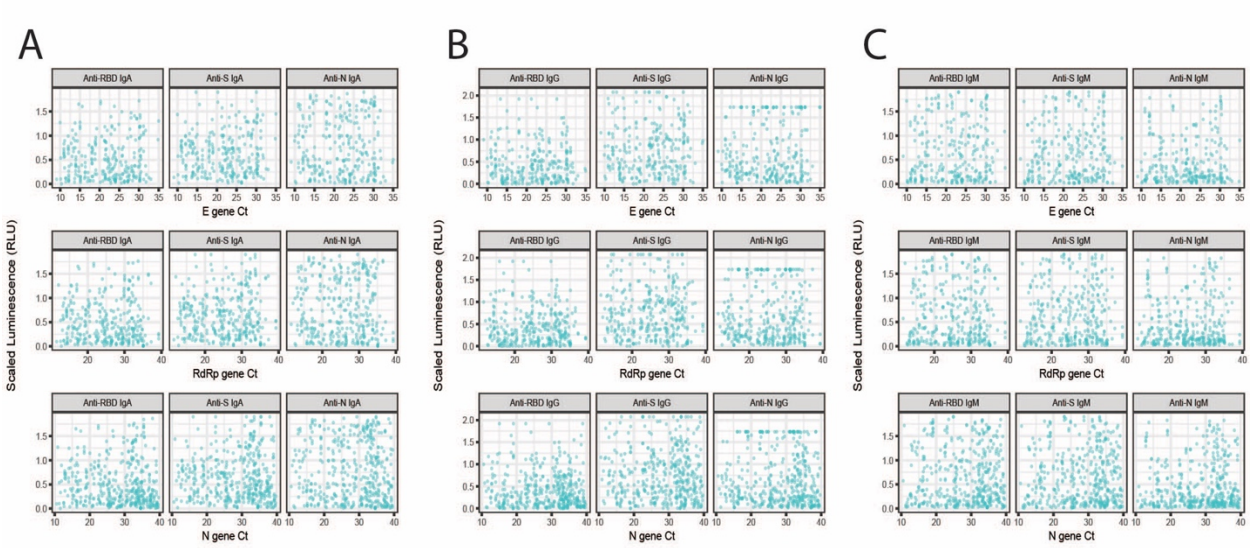
Supplementary Files



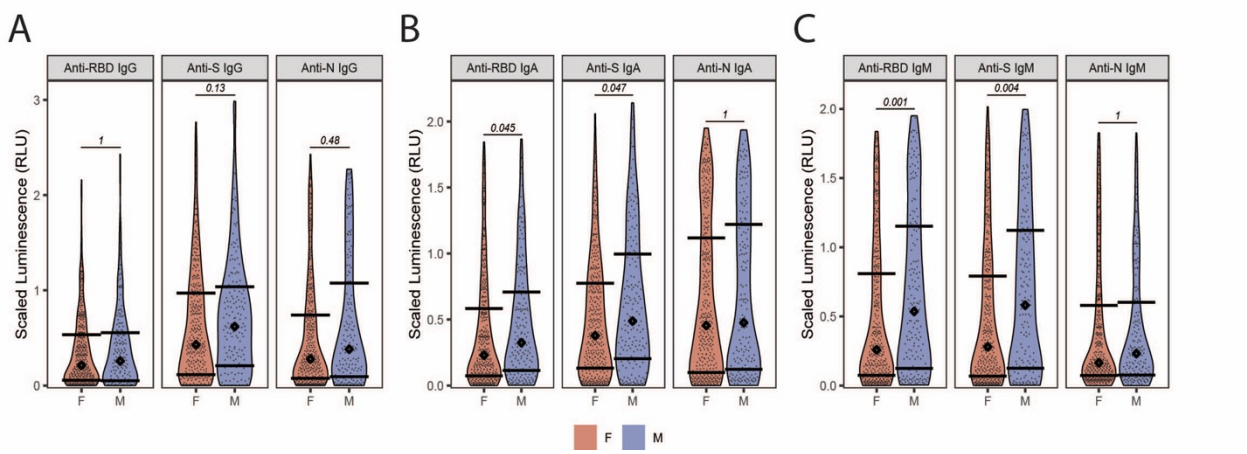
Supplemental Figure 1. Cohort demographics. (A) Age (years) distribution in the whole cohort. (B) Distribution of the number of days between symptom onset and serum/plasma collection date (n=739) (A-B) The number of individuals is represented as count on the y axis of the graphs. The red boxplots overlayed on the histogram represent the distribution of the cohort, with the median, different quantiles and the outliers.



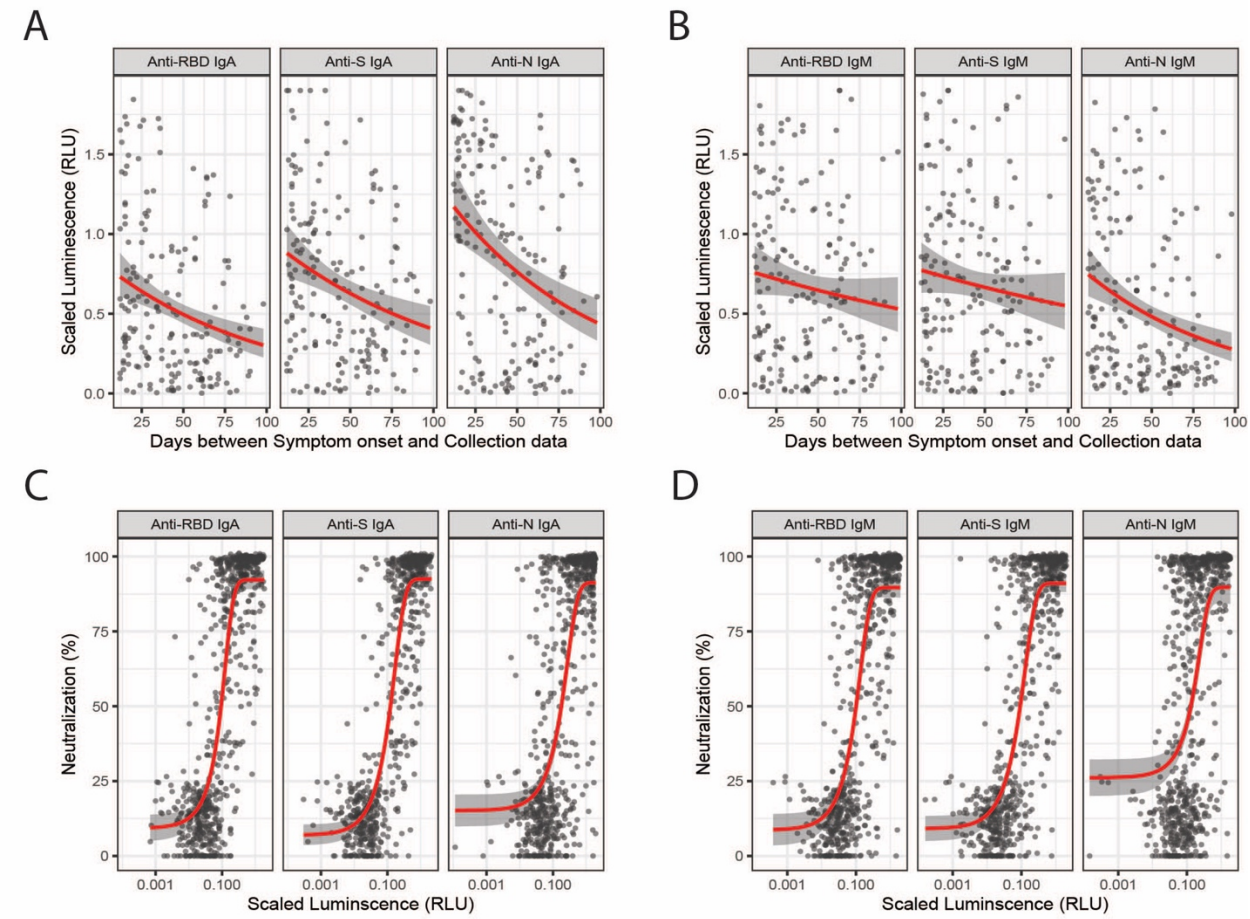
Supplemental Figure 2. Correlation between antibody levels and PCR results. Principal component analysis (PCA) showing the clustering between the results from the PCR tests and all antibodies. PCA showing the clustering between the results from the PCR tests and IgA (B), IgG (C) and IgM (D) (A-D: n=739).



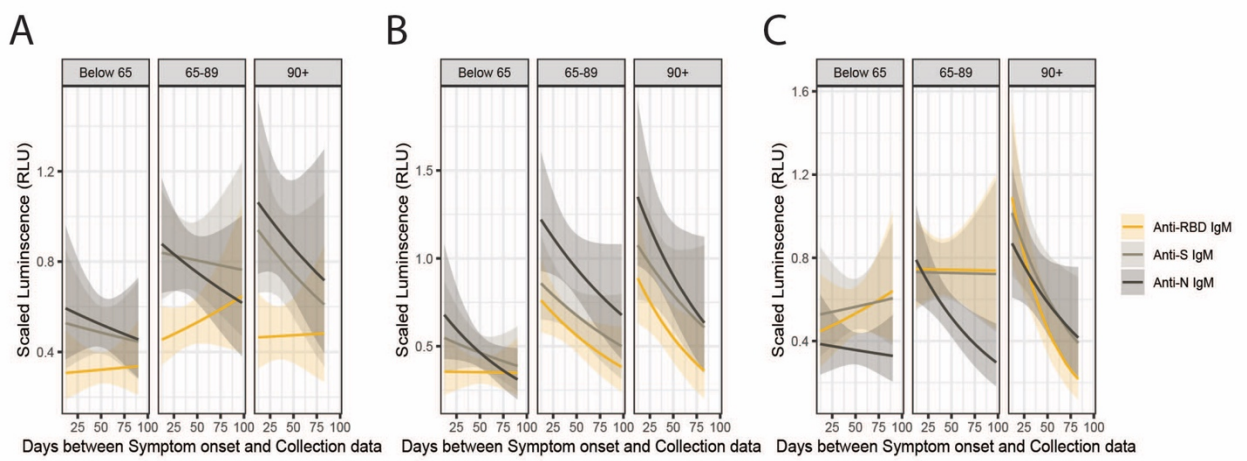
Supplemental Figure 3. No correlation observed between antibody levels and Ct values from PCR tests. Levels of IgA (A), IgG (B) and IgM (C) based on the Ct values from the three PCR that were performed on the samples. Serum/plasma was diluted by a factor of 100 for IgA and IgM and further diluted to a factor of 10,000 for IgG (E gene: n=271, RdRp gene: n=335, N gene: n=440).



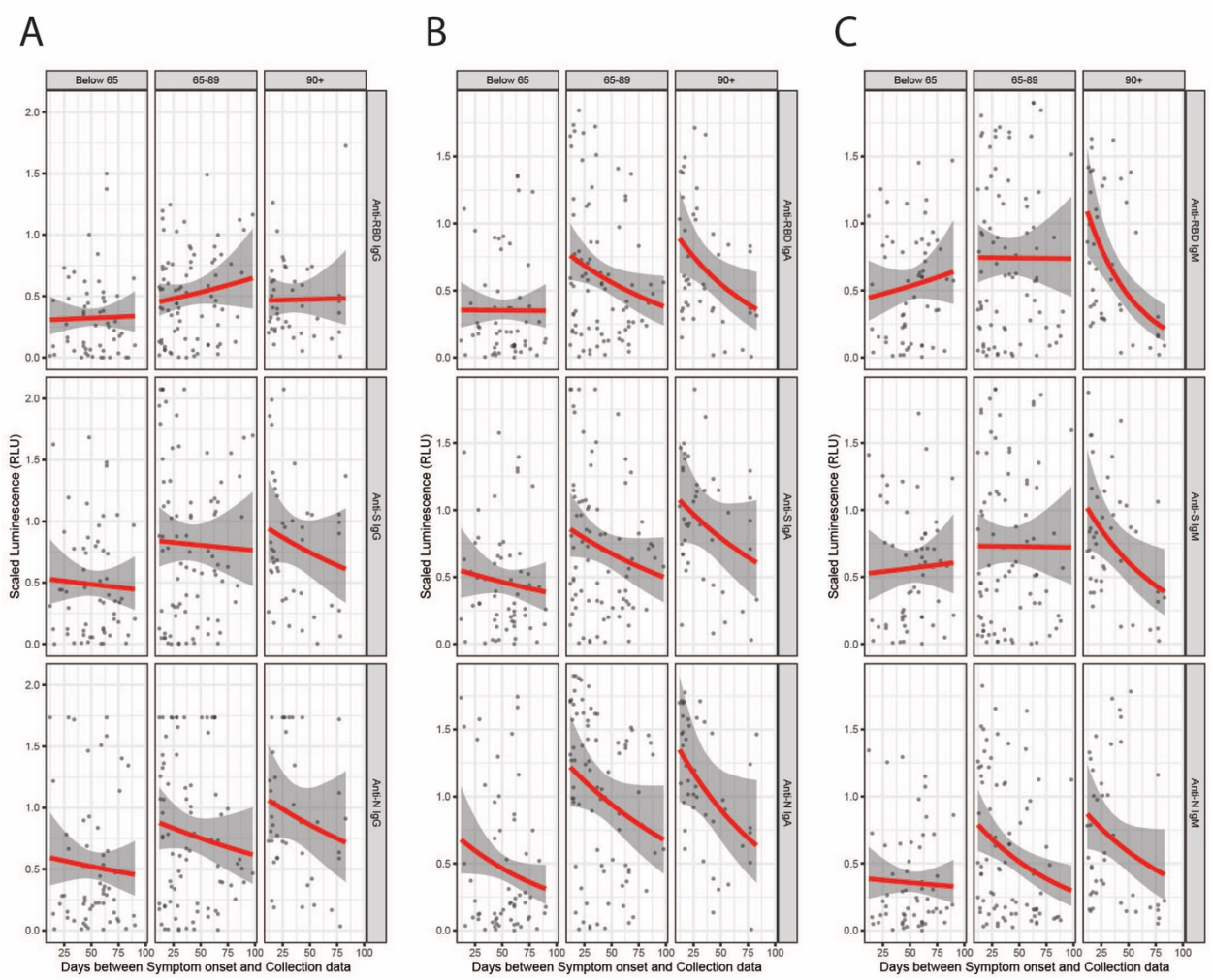
Supplemental Figure 4. Antibody levels relative to sex. Levels of IgG (A), IgA (B) and IgM (C) raised against the receptor binding domain (RBD) of the spike protein, spike (S) and the nucleocapsid (N) based on sex. (A-C) Medians are indicated by diamonds, the first and third quantiles are represented by the lower and upper horizontal segments, respectively. The p-values indicated above the violins were calculated using a Mann-Whitney U test. Serum/plasma was diluted by a factor of 100 for IgA and IgM and further diluted to a factor of 10,000 for IgG (n=533).



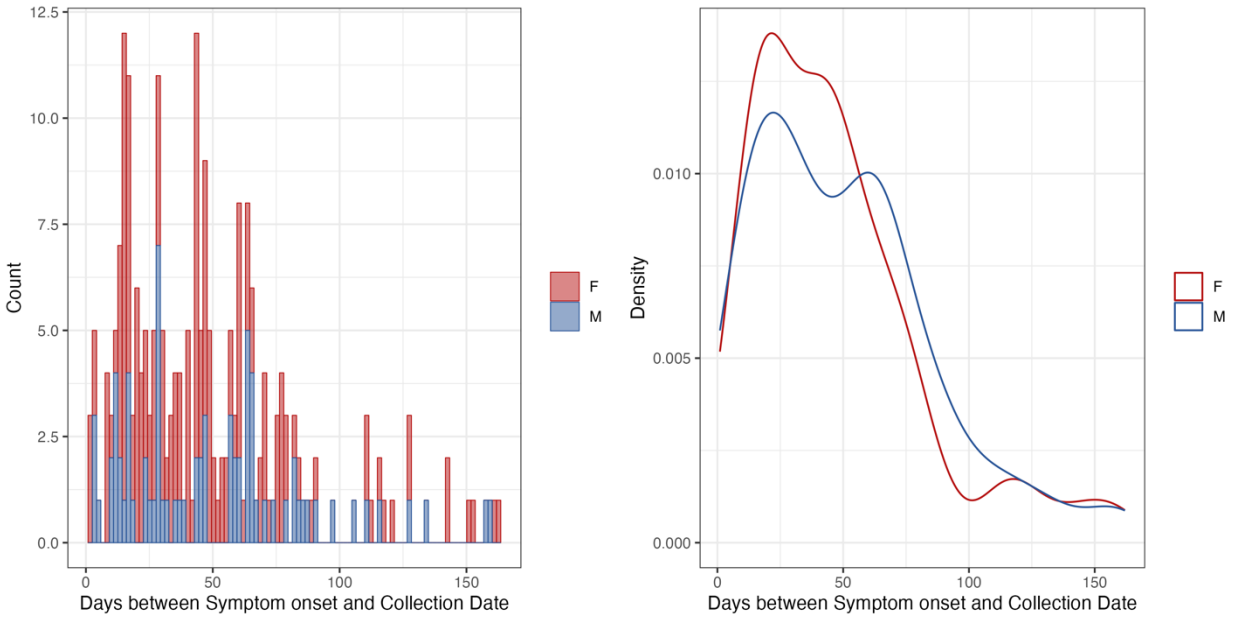
Supplemental Figure 5. IgA and IgM levels and correlation with neutralization efficiency. Levels of anti-RBD, anti-S and anti-N IgA (A) and IgM (B) based on the number of days between the symptom onset and serum/plasma collection. (A-B) A generalized linear model with of the gamma family was generated to modelized the variation of IgA levels with time using the following formula: Scaled Luminescence ~ Number of days * IgA antigen (red line). The standard error of the model is displayed in grey. Serum/plasma was diluted by a factor of 100 (n=185). (C) The neutralization potency of the sample based on the IgA (C) and IgM (D) levels. (C-D) The relationship was modeled using a four-parameters log-logistic regression using the following formula: Neutralization ~ Scaled Luminescence for each of the IgA antigens (red line). The standard error of the model is displayed in grey (n=739).



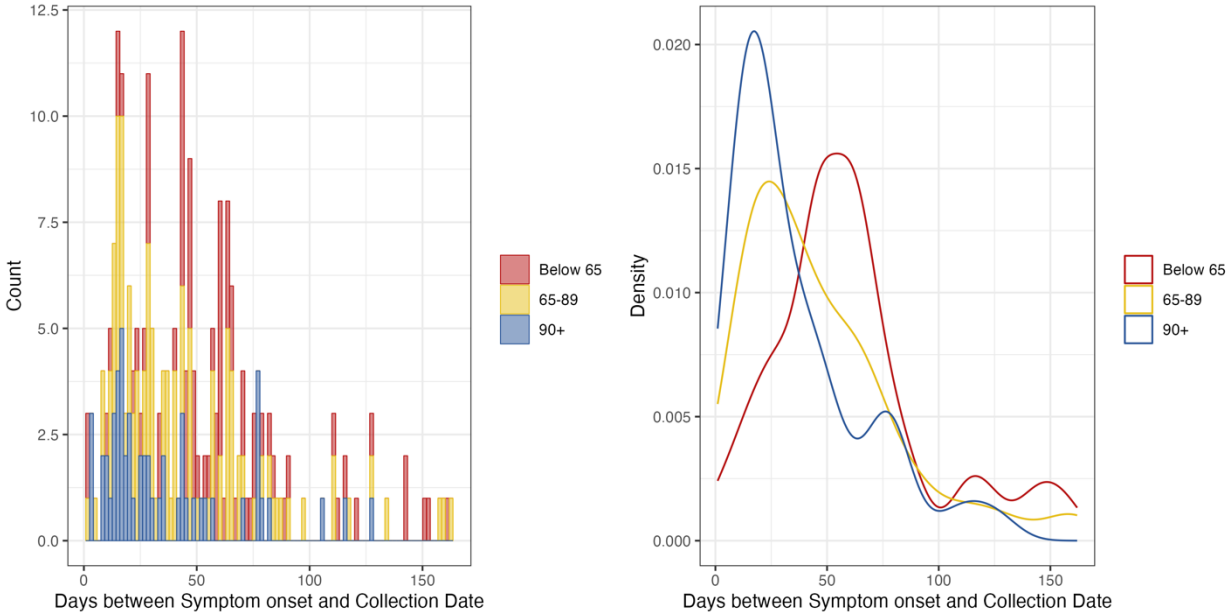
Supplemental Figure 6. Variation of antibody levels relative to the time from serum/plasma collection and age group. Levels of anti-RBD, anti-S and anti-N IgG (A), IgA (B) and IgM (C) based on the number of days between the symptom onset and serum/plasma collection and age groups (Below 65, 65-89 and 90+). (A-C) The relationship was modeled using a generalized linear model of the gamma family using the following formula: Scaled Luminescence ~ Number of days * IgG antigen * Age group, displayed as colored lines, with the standard error of the model displayed in the lighter section around the regression. Serum/plasma was diluted by a factor of 100 for IgA and IgM and further diluted to a factor of 10,000 for IgG (n=185).



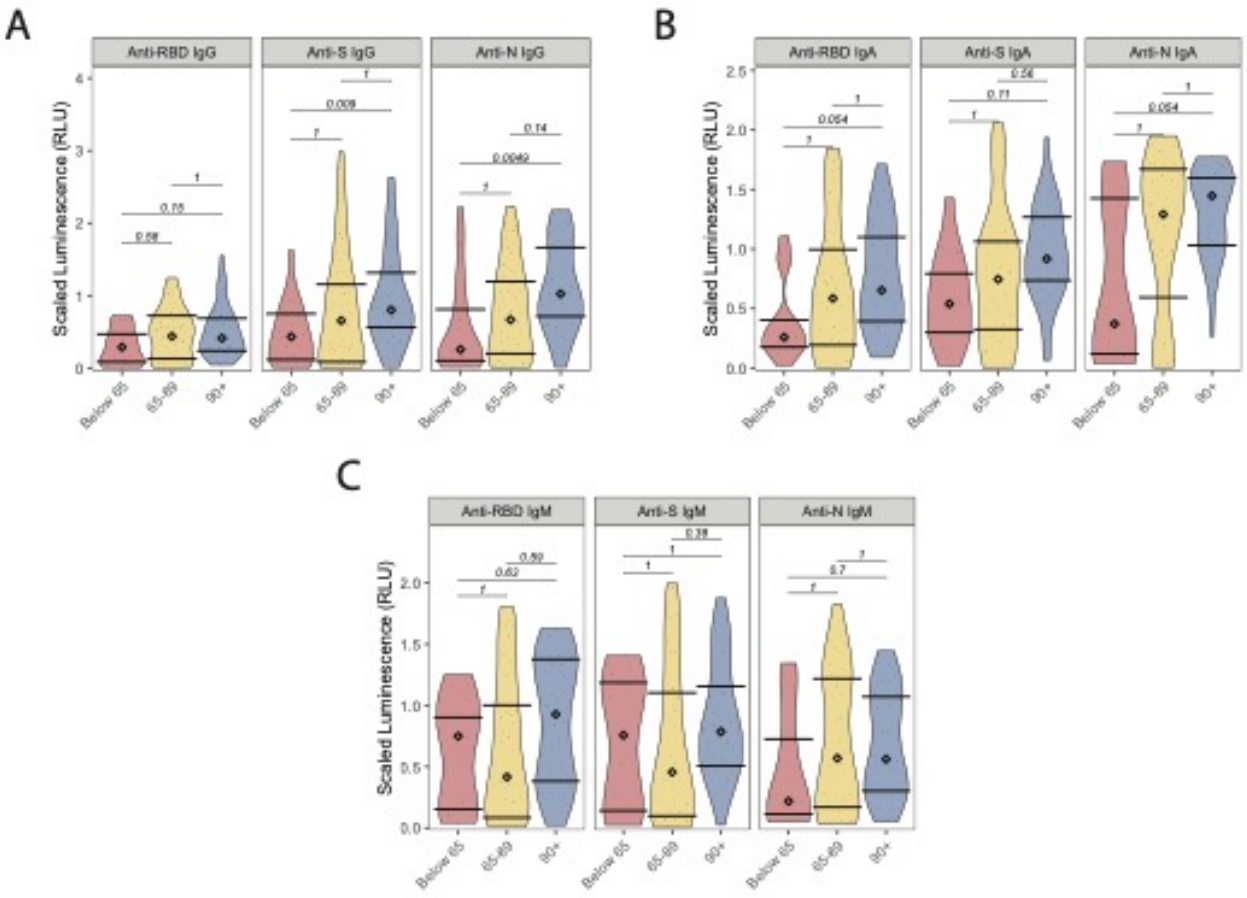
Supplemental Figure 7. Variation of antibody levels relative to time from serum/plasma collection and age group overlayed on scatter plot. Levels of anti-RBD, anti-S and anti-N IgG (A), IgA (B) and IgM (C) based on the age group (Below 65, 65-89 and 90+), displayed as a gamma regression model overlayed above a scatter plot. The relationship was modeled using a generalized linear model of the gamma family using the following formula: Scaled Luminescence ~ Number of days * IgG antigen * Age group, displayed as a red line, with the standard error of the model displayed in grey. Serum/plasma was diluted by a factor of 100 for IgA and IgM and further diluted to a factor of 10,000 for IgG (n=185).



Supplemental Figure 8. Histogram and density distribution of samples by sex based on days between symptom onset and collection date. Samples with information on days between symptom onset and collection date (n=228) were segregated between female (red) and male (blue). The distribution of the days between symptom onset and when the samples were collected are similar between both groups.



Supplemental Figure 9. Histogram and density distribution of samples by age groups based on days between symptom onset and collection date. Samples with information on days between symptom onset and collection date (n=228) were segregated between individuals aged under 65yrs. old (red), 65-89 yrs. old (yellow) and 90 yrs. old and over (blue) .



Supplemental Figure 10. Antibody levels of individuals within 30 days post symptom onset by age groups. Levels of IgG (A), IgA (B) and IgM (C) raised against the receptor binding domain (RBD) of the spike protein, spike (S) and the nucleocapsid (N) for individuals that had a sample collected within 30 days post symptom onset. Only individuals that had information collected on days between symptom onset and collection date were included. (A-C) Medians are indicated by diamonds, the first and third quantiles are represented by the lower and upper horizontal segments, respectively. The p-values indicated above the violins were calculated using a Mann-Whitney U test. Serum/plasma was diluted by a factor of 100 for IgA and IgM and further diluted to a factor of 10,000 for IgG (Total n=85, Below 65 n=13, 65-89 n=42, 90+ n=30).

Supplemental Table 1. Antibody levels relative to sex. Statistical information on the levels of the different antibody isotypes, depending on their antigen specificity and the sex of the individuals in the study.

			Female	Male
RBD				
	IgG	Mean (SD)	0.35 (0.38)	0.39 (0.43)
		Median	0.21	0.26
		Min - Max	0 – 2.16	0 – 2.43
	IgA	Mean (SD)	0.4 (0.43)	0.48 (0.44)
		Median	0.23	0.32
		Min - Max	0 – 1.84	0.002 – 1.87
	IgM	Mean (SD)	0.48 (0.51)	0.68 (0.59)
		Median	0.26	0.54
		Min - Max	0 – 1.83	0.004 – 1.95
Trimeric Spike				
	IgG	Mean (SD)	0.61 (0.59)	0.73 (0.64)
		Median	0.43	0.62
		Min - Max	0 – 2.76	0 – 2.98
	IgA	Mean (SD)	0.5 (0.45)	0.63 (0.53)
		Median	0.38	0.49
		Min - Max	0 – 2.06	0.002 – 2.14
	IgM	Mean (SD)	0.49 (0.51)	0.68 (0.59)
		Median	0.28	0.58
		Min - Max	0 – 2.01	0 – 1.83
Nucleocapsid				
	IgG	Mean (SD)	0.52 (0.58)	0.64 (0.68)
		Median	0.28	0.38
		Min - Max	0 – 2.43	0 – 2.27
	IgA	Mean (SD)	0.65 (0.59)	0.69 (0.61)
		Median	0.45	0.48
		Min - Max	0 – 1.95	0.001 – 1.94
	IgM	Mean (SD)	0.4 (0.47)	0.4 (0.43)
		Median	0.16	0.23
		Min - Max	0 – 1.82	0 – 1.83

Supplemental Table 2. Antibody levels relative to age. Individuals were segregated in three distinct cohorts based on the age distribution of the cohort. Statistical information on the levels of the different antibody isotypes, depending on their antigen specificity and the age of the individuals is reported.

			Below 65 yrs	65-89 yrs	90 yrs and over
RBD					
	IgG	Mean (SD)	0.25 (0.29)	0.41 (0.41)	0.41 (0.45)
		Median	0.13	0.31	0.25
		Min - Max	0 – 1.5	0 – 2.2	0 – 2.43
	IgA	Mean (SD)	0.28 (0.33)	0.49 (0.46)	0.46 (0.44)
		Median	0.12	0.32	0.37
		Min - Max	0.001 – 1.36	0.001 – 1.87	0.002 – 1.76
	IgM	Mean (SD)	0.43 (0.43)	0.6 (0.6)	0.58 (0.53)
		Median	0.26	0.32	0.38
		Min - Max	0 – 1.7	0.002 – 1.95	0.001 – 1.84
Trimeric Spike					
	IgG	Mean (SD)	0.46 (0.48)	0.72 (0.64)	0.72 (0.6)
		Median	0.35	0.6	0.58
		Min - Max	0 – 2.83	0 – 2.98	0 – 2.63
	IgA	Mean (SD)	0.37 (0.37)	0.61 (0.51)	0.59 (0.45)
		Median	0.25	0.47	0.54
		Min - Max	0.001 – 1.57	0.001 – 2.14	0.003 – 1.94
	IgM	Mean (SD)	0.43 (0.43)	0.6 (0.59)	0.6 (0.51)
		Median	0.23	0.32	0.49
		Min - Max	0.001 – 1.72	0.002 – 2.01	0.001 – 1.88
Nucleocapsid					
	IgG	Mean (SD)	0.35 (0.46)	0.61 (0.64)	0.66 (0.64)
		Median	0.18	0.38	0.43
		Min - Max	0 – 2.22	0.001 – 2.43	0.002 – 2.19
	IgA	Mean (SD)	0.37 (0.45)	0.73 (0.58)	0.84 (0.62)
		Median	0.15	0.55	0.75
		Min - Max	0.001 – 1.74	0.001 – 1.95	0.002 – 1.84
	IgM	Mean (SD)	0.28 (0.34)	0.46 (0.49)	0.45 (0.49)
		Median	0.14	0.22	0.24
		Min - Max	0 – 1.62	0 – 1.83	0 – 1.78
Neutralization		Mean (SD)	65.4 (34.19)	77.46 (32.81)	76.58 (33.55)
		Median	76.66	95.58	96.55
		Min - Max	1.15 – 100.14	2.66 – 101.12	0.1 – 100.93

Supplementary Table 3. Neutralization efficiency relative to antibody levels. The relationship between neutralization efficiency and antibody levels was modeled using a four-parameter log-logistic regression. The level of antibody required to reach a neutralization efficiency of 50% (ie. ED50), the slope intercept, lower and upper limits were calculated and reported in relation to the antibody isotype and antigen specificity.

		Slope intercept (Std Error)	Lower limit (Std Error)	Upper Limit (Std Error)	ED50 (Std Error)
RBD					
	IgG	-10.18 (1.29)	0.41 (5.9)	92.99 (1.31)	1.18 (0.02)
	IgA	-7.81 (1.7)	-14.25 (15.77)	92.22 (1.57)	1.18 (0.05)
	IgM	-6.04 (1.42)	-33.45 (30.01)	89.63 (1.7)	1.11 (0.09)
Trimeric Spike					
	IgG	-3.53 (0.27)	9.68 (1.69)	96.95 (1.37)	1.7 (0.05)
	IgA	-4.38 (0.76)	-52.72 (34.09)	92.49 (1.35)	1.09 (0.12)
	IgM	-5.57 (1.08)	-55.9 (40.97)	91.07 (1.49)	1.04 (0.1)
Nucleocapsid					
	IgG	-5.95 (0.66)	-70.05 (26.57)	93.37 (1.17)	1.01 (0.05)
	IgA	-2.73 (0.61)	-36.41 (41.41)	91.27 (1.89)	1.15 (0.28)
	IgM	-3.72 (0.81)	-0.04 (17.97)	89.72 (2.81)	1.27 (0.15)

Supplemental Table 4. Cohort-specific antibodies decline rate and half-life. Antibody levels in relation to time since symptom onset were modeled using a generalized linear model of the gamma family. Antibodies decay rates (ie, slope in RLU/day) were calculated and reported in relation to the various established age dependant cohorts.

		Combined	**Below 65 yrs**	**65-89 yrs**	**90 yrs and over**
		n= 185	n= 59	n= 82	n= 44
RBD					
Slope (Std Error)					
	IgG	0.00066 (0.0026)	0.00118 (0.0067)	0.00412 (0.0034)	0.00052 (0.0048)
	IgA	-0.01027 (0.0027)	-0.00022 (0.0073)	-0.00803 (0.0037)	-0.01268 (0.0045)
	IgM	-0.00413 (0.0025)	0.00461 (0.0051)	-0.00011 (0.0038)	-0.02271 (0.0051)
Trimeric Spike					
Slope (Std Error)					
	IgG	-0.00456 (0.0026)	-0.00216 0.0062)	-0.0011 (0.0038)	-0.00608 (0.0044)
	IgA	-0.00891 (0.0023)	-0.00441 (0.0059)	-0.00628 (0.0033)	-0.00804 (0.0034)
	IgM	-0.00393 (0.0024)	0.00176 (0.0051)	-0.00015 (0.0039)	-0.01345 (0.0041)
Nucleocapsid					
Slope (Std Error)					
	IgG	-0.00682 (0.0026)	-0.00339 (0.0069)	-0.00409 (0.0036)	-0.00552 (0.0039)
	IgA	-0.01128 (0.0023)	-0.00999 (0.0074)	-0.00683 (0.0027)	-0.01064 (0.003)
	IgM	-0.01150 (0.003)	-0.00205 (0.0068)	-0.01135 (0.0042)	-0.01035 (0.0057)

3.2 SARS-CoV-2 Seroprevalence in Indigenous Communities of the Northwest Territories in Canada: Insights from a Comparative Cohort Study

Preface

(This manuscript is under review)

Yannick Galipeau*, Marilyn Whelan*, Fariba Kolahdooz, Corey Arnold, André Corriveau, Jesse Papenburg, Karen Doucette, Carolyn Gotay, Kami Kandola, Martin Pelchat, Marc-André Langlois, and Sangita Sharma. **SARS-CoV-2 Seroprevalence in Indigenous Communities of the Northwest Territories in Canada: Insights from a Comparative Cohort Study**. (2025)

Research in context

Evidence before this study
Indigenous communities worldwide experience disproportionate health burdens from respiratory infections, including higher mortality rates during pandemics. In Canada, Indigenous populations were prioritized for early COVID-19 vaccination due to elevated risks linked to socioeconomic disparities, healthcare access limitations, and comorbidities. However, data on SARS-CoV-2 seroprevalence, immune response durability, and underreporting of infection in these remote communities remain scarce. Prior studies have reported increased infection rates in Indigenous populations but have not comprehensively assessed infection-acquired versus vaccine-induced immunity, nor compared these findings to non-Indigenous populations to examine disparities in immune responses and public health interventions.

Added value of this study
This study is the most comprehensive examination of SARS-CoV-2 exposure in remote Indigenous communities of the Northwest Territories (NWT), Canada. By analyzing blood samples, we measured antibody levels from both infection and vaccination and compared them to those of a similar urban population.The findings provide key insights into differences in infection rates, unreported cases, and immune responsesin a population that has historically faced barriers to healthcare. Conducted in full partnership with Indigenous leaders and community members, this research prioritized cultural safety and ethical collaboration, ensuring that the study reflects the needs and experiences of the communities involved.

Implications of all the available evidence
Findings reveal a markedly higher burden of SARS-CoV-2 infection in Indigenous communities compared to urban populations, with a significant proportion of infections going unreported. This highlights critical gaps in diagnostic access and pandemic surveillance in geographically isolated regions. Despite these disparities, antibody levels and decay rates were similar between Indigenous and non-Indigenous individuals, emphasizing the effectiveness of COVID-19 vaccination programs. However, the study raises pressing concerns about future pandemic preparedness, equitable access to testing, and healthcare infrastructure in remote Indigenous communities. Strengthening community-led surveillance, targeted vaccination strategies, and healthcare accessibility will be essential to mitigating infectious disease risks and ensuring equitable health outcomes in underserved populations.

Abstract

Background
Indigenous communities in Arctic Canada experience disproportionate health disparities and higher mortality from respiratory infections, exacerbated by geographic isolation and limited healthcare access. While these communities were prioritized for early COVID-19 vaccination, the extent of prior SARS-CoV-2 infection, immune response durability, and potential gaps in pandemic preparedness remain unclear.

Methods
In partnership with a regional Indigenous government, we conducted a seroprevalence study in four Indigenouscommunities in the Northwest Territories (NWT), collecting demographic and health data alongside dried blood spot (DBS) samples from March to April 2023. IgG antibodies against SARS-CoV-2 nucleocapsid, spike, and receptor-binding domain (RBD) were quantified using a high-throughput chemiluminescent ELISA platform. These data were compared to an age- and vaccine-matched urban cohort in Ottawa, Ontario.

Findings
Seroprevalence of SARS-CoV-2 infection was significantly higher in NWT Indigenous communities (78%) compared to the urban cohort (46%). Nearly half (45%) of Indigenous participants with serological evidence of infection were unaware of prior SARS-CoV-2 exposure, indicating substantial underreporting. Despite higher infection rates, antibody levels and decay trajectories were comparable between Indigenous and non-Indigenous cohorts, suggesting similar immune responses to vaccination and infection. Hybrid immunity (infection plus vaccination) was the primary driver of antibody levels in Indigenous communities.

Interpretation
These findings reveal a disproportionately high burden of SARS-CoV-2 infection in remote Indigenous communities, with significant underreporting that may impede effective public health responses. The comparable antibody-mediated immunity across cohorts highlights the efficacy of vaccination programs but also showcases critical gaps in diagnostic access and pandemic surveillance in Indigenous regions. Strengthening community-based testing, vaccine booster strategies, and healthcare resource allocation is essential to mitigating future infectious disease threats in underserved populations.

Funding
Supported by the Canadian Institutes of Health Research (CIHR) and the COVID-19 Immunity Task Force (CITF).

Introduction

The COVID-19 pandemic has profoundly impacted lives across the globe. Extensive SARS-CoV-2 immunization campaigns were carried out in many countries that effectively reduced the severity of COVID-19 infection and associated mortality. By 2023, seroprevalence studies indicated that most people in Canada had acquired antibodies against SARS-CoV-2 through natural infection and vaccination (1). Although mRNA-based vaccines have been regularly updated to better reflect the evolution and emergence of SARS-CoV-2 variants, breakthrough infections and post-COVID conditions still occur (2). These cases remain challenging to manage and continue to impose significant costs and pressure on the healthcare system (3, 4). Moreover, some populations remain at higher risk of adverse infection outcomes due to pre-existing health conditions, limited health care, demographic characteristics, and geographical location, among other factors.

There have been various lines of evidence suggesting heterogeneity in the severity and burden of SARS-CoV-2 infection. Demographic characteristics such as age, sex, and ethnicity are known factors that can impact immune responses to vaccines and infection in general. For example, older adults are disproportionately at higher risk of severe disease and excess mortality following SARS-CoV-2 infection (5-8). Antibody-mediated immune responses following infection or vaccination have also been shown to be impacted by age (9, 10). In addition, some studies have highlighted differences in immune responses and outcomes between males and females (11, 12). It is interesting to note that post-COVID condition prevalence is significantly higher in women (13-15). The effect of ethnicity on COVID-19 outcomes remains unclear. Genetic factors such as Human Leukocyte Antigen (HLA) polymorphisms could underlie differences in adaptive immune responses and can be influenced by ethnicity (16).

The disproportionate burden of severe disease and mortality from respiratory viruses in Indigenous communities has been widely reported. It is estimated that during the 1918 influenza pandemic, Māori mortality was 7-fold higher than European (17), and mortality of First Nations community members in Canada was 8-fold higher (18). More recently, during the H1N1 influenza pandemic of 2009, Native Americans and Alaska Natives had a 4-fold higher mortality when compared to

the non-Indigenous population (19). In Canada, the hospitalization rate for First Nations people was 3-fold higher than the non-Indigenous Canadian population (20).

Medical history, living conditions, and access to healthcare facilities and social inequities are intersecting factors that contribute to increased risk of SARS-CoV-2 infection and of severe COVID-19 (21, 22). Inequity in COVID-19 outcomes among Indigenous communities worldwide has been documented (23). During pandemics, Indigenous communities may experience higher infection and mortality rates due to socioeconomic conditions such as crowded housing, limited healthcare access, and the presence of comorbidities (23, 24). Furthermore, the seroprevalence of infection-acquired SARS-CoV-2 antibodies is reported to be higher within Indigenous communities when compared to Caucasians (25). Canada's National Advisory Committee on Immunization recognized that racialized, marginalized and other underserved populations in Canada were disproportionately affected by COVID-19 and prioritized Indigenous communities for early COVID-19 vaccination and for booster doses (26, 27). Indigenous peoples comprise 5% of the total Canadian population, with 1.1% of Indigenous community members residing in Northwest Territories (NWT) (28, 29). Within NWT, 78.6% of the population had received at least one dose of COVID-19 vaccine by March 2023(30).

The immune response of Indigenous communities following COVID-19 vaccination or infection remains underexplored, particularly regarding antibody-mediated responses in Arctic Canada. Data on the burden of COVID-19, vaccine coverage, and antibody waning dynamics in Indigenous communities are limited. Improved understanding of infection-acquired, vaccine-acquired, and hybrid immunity in Indigenous communities will inform the development of tailored health interventions and vaccine policies for remote and isolated communities in NWT and across Canada.

Methods

Context

The project involved a partnership with a regional Indigenous Government covering four communities in NWT. A community advisory board, composed of Elders, local healthcare professionals, community members, and policymakers offered guidance throughout the project. The regional population is approximately 3000 people, 93% of whom are Indigenous (31). The communities vary in remoteness, health status, and transportation infrastructure (32). At the time the project was developed, SARS-CoV-2-vaccination rates in the communities ranged from 50-75%.

Ethics

The project received ethical approval from the University of Alberta's Research Ethics Board and a research license from the Department of Education, Culture and Employment, Government of Northwest Territories in Inuvik, NWT. A formal research agreement was signed with the Indigenous Government. Participants provided written informed consent prior to participating.

Recruitment and data collection

Self-identifying Indigenous community members aged 19 years or older who had lived in the community for the past two months were eligible to participate. The Indigenous Community Project Lead, with local research assistants and community partners, carried out recruitment via telephone, radio, social media (Facebook, Instagram), posters, pamphlets, and in-person at the local Band Office and during community events. Recruitment materials were distributed in English and the local Indigenous language. Participants were given a gift card to the local food store as a thank you. Participants were invited to a designated place in the community where a trained research assistant collected informed consent and demographics, health status, and COVID-19 infection and vaccine information through a questionnaire. The local Indigenous language was utilized when necessary. Data were entered in real-time into a secure system (REDCap). The sessions were audio recorded with participant permission to ensure data accuracy. The dried blood spot (DBS) procedure was adapted from the Northern Inter-Tribal Health Authority's Procedure for Collection and Shipment of Blood by DBS Testing and followed laboratory protocol (33). A single-use pip lancet was used to collect the blood spot samples onto absorbent filter paper. DBS samples were couriered to the Langlois Laboratory at the University of Ottawa for COVID-19 antibody analysis.

Full methods for serology measurements and statistical methods are available in supplementary materials.

Results:

Establishment of an Indigenous Northwest Territories cohort and matched urban cohorts

In total, 433 participants provided a DBS sample between March 6th to April 24th, 2023, of which 383 were of sufficient quality and accompanied by a completed study questionnaire and included in this study. The age of participants ranged from 19-86 years old with a mean age of 46.2 years. In this cohort, 46.0% (n=176) identified as female with all reporting First Nations ancestry (Table 1). In terms of health status, 24.3% (n=93) of participants reported excellent health, 52.2% (n=200) reported good health, 20.4% (n=78) reported fair health, and 3.1% (n=12) reported poor or very poor health, and 54.1% (n=207) reported current tobacco use. To contextualize the result, two urban cohorts from the Ottawa region were selected. The urban samples and data were obtained from the Stop the Spread Ottawa (SSO) study, a four-year longitudinal study which collected serum/plasma and DBS samples as well as various demographic and epidemiological data. The initial cohort and study design characteristics were reported previously (34, 35). To address questions regarding seroprevalence in Indigenous communities, two urban cohorts were established using samples collected during the same timeframe as the Indigenous NWT cohort (Figure 1A). The first urban cohort (serum) comprised 157 individuals, with 66.9% (n=105) identifying as women and the second urban cohort (DBS) comprised 119 individuals, with 41.2% (n=49) identifying as women. Both cohorts were matched to the demographic and vaccination characteristics of the Indigenous NWT cohort (Figure 1), providing comparative insights into vaccine responses and antibody levels. Importantly, these cohorts comprised DBS samples similar to the Indigenous NWT cohort, allowing for direct comparison between identical sample collection types without conversion. Urban cohorts were selected to closely match the age and sex distribution of the NWT Indigenous population as accurately as possible (Figure 1, Table 1).

Indigenous Northwest Territories communities have a higher seroprevalence of SARS-CoV-2 infection

Serology allows for the monitoring of past exposure to the virus without the need for molecular testing, which requires sampling during an active infection. IgG antibodies against the nucleocapsid protein, the spike protein and the receptor binding domain (RBD) of SARS-CoV-2 were measured as described previously (36). A seropositivity threshold corresponding to a 3% false discovery rate was established using a density distribution of previously measured pre-pandemic samples. In addition, samples had to be positive for nucleocapsid (N) antibodies, and spike (S) or RBD to be classified as a previous SARS-CoV-2 infection, thereby reducing cross-reactivity from seasonal coronaviruses (37). 74.4% (n=285) of NWT Indigenous participants had anti-S antibodies against SARS-CoV-2. Of participants with these antibodies, 68.1% (n=261) also had anti-N antibodies, indicating a history of SARS-CoV-2 infection. Overall, slightly over 72% of individuals in the Indigenous NWT cohort had serological markers indicating previous infection. Comparing the Indigenous NWT cohort, collected from March 6 to April 24, 2023, with an urban cohort collected from February 6 to April 28, 2023 (Figure 1), only 46% of individuals in the urban cohort had serological markers of previous infection. If the NWT Indigenous cohort had the same seroprevalence of previous infection as the urban cohort during the same period, there would have been 109 fewer infected individuals, representing 28.5% of the NWT Indigenous cohort.

Indigenous Northwest Territories communities underreported SARS-CoV-2 infection

In the NWT Indigenous cohort, 41.51% reported contracting COVID-19 at least once during the pandemic. Of participants who reported this, 70.44% reported having the disease once, 21.38% twice, and 6.29% three times. In comparison, 55.4 % of the urban cohort reported contracting COVID-19 during that same period (Figure 2). The proportions can be compared to the total number of previous infections identified by serology to assess the concordance between self-reported and laboratory-confirmed infections. For instance, in the urban cohort matched in time with the NWT Indigenous cohort, only 16% of individuals did not report a previous infection despite having serological markers of infection. This is comparable to the urban cohort collected earlier in the pandemic, where only 4.8% had antibodies indicating a previous infection without self-reporting a COVID-19 infection. This is in striking contrast to the NWT Indigenous cohort in which 46% had serological markers of COVID-19 infection but did not self-report being infected (Figure 2). Overall, the concordance between self-reported infection and serology was the lowest

in the NWT Indigenous cohort at 44.6%, compared to 58.6% and 78.2% in the urban cohorts. Notably, the proportion of individuals who reported COVID-19 infection but lacked serological markers of previous infection was lowest in the NWT Indigenous cohort at 9.4%, compared to 17% and 25.5% in the urban cohorts (Figure 2). The discordant self-reports may indicate infections that occurred long ago, with waning nucleocapsid antibodies. Alternatively, the reports may be due to false-positive PCR or rapid antigen test results, which have been documented previously (38, 39).

Indigenous and non-Indigenous individuals mount similar antibody levels

A large majority of the NWT Indigenous cohort (90.6%, n=347) reported receiving at least one COVID-19 vaccination, with most participants having received two (50.1%) or three (31.6%) doses (Table 1) at the time of study. This was comparable to the urban DBS cohort, where 29.4% and 47.06% had received two or three doses, respectively (Figure 1). Combining vaccination status with seroprevalence data, it is estimated that 77.5% of the Indigenous cohort have hybrid immunity (antibodies from both vaccination and infection), compared to 19.2% in the urban DBS cohort. Only about 21.7% of the NWT Indigenous cohort had immunity from vaccination alone in contrast to 75.3% of the urban DBS cohort. When comparing antibody levels between the NWT Indigenous cohort and the urban DBS cohort (matched by age, sex and vaccine status; Figure 1), no biologically significant differences were observed for RBD and spike antibody levels. However, the NWT Indigenous cohort exhibited significantly higher levels of antibodies against the nucleocapsid protein, indicating not only a higher seropositivity for nucleocapsid antibodies but also elevated antibody levels (Figure 3). When comparing vaccine-acquired immunity to hybrid immunity in the NWT Indigenous cohort, higher levels of antibodies against the spike and RBD were observed (Figure 3). As expected, hybrid immunity also resulted in higher levels of antibodies in the urban DBS cohort. Given that age is a risk factor for severe SARS-CoV-2 infection and can adversely affect humoral responses, antibody levels were compared across age groups within the cohorts. For the nucleocapsid antibodies, no clear trend was observed between age groups. Interestingly, the 50-65 years old group in the NWT Indigenous cohort had the highest levels of anti-N antibodies while the same group in the urban cohort was the lowest. The trend of higher anti-spike and anti-RBD antibody levels in older age groups within the NWT Indigenous cohort may be explained by differences in vaccination profiles across age groups. For instance, the

proportions of individuals who received three or more vaccines were 16.4% in the 19-29 age group and 26.7% in the 30-49 age group, compared to 49.6% and 71.1% in the 50-65 and 65+ age groups, respectively (Supp. Table 2). Overall, there are minimal differences between the urban-matched cohort and the NWT Indigenous cohort, indicating that Indigenous and non-Indigenous individuals can achieve similar levels of antibody-mediated immunity following vaccination and infection.

Northwest Territories Indigenous communities and the urban cohort have similar antibody trajectories

To investigate decline over time, individuals with a reported date of vaccination or infection were selected from the overall Indigenous cohort and urban cohort (Supp. Table 3). A generalized linear model, using either a gamma or Gaussian distribution based on the best fit for the data, was employed to assess the decline of antibody levels over time since the last vaccination, infection, or antigenic exposure (vaccine or infection) to position the sample in time (Figure 4). In the urban cohort, Spike and RBD antibody levels decayed over time as expected post-vaccination. However, in the NWT Indigenous cohort, antibody levels unexpectedly increased between 300-800 days post-vaccination, likely due to SARS-CoV-2 infections, as a similar increase was observed in nucleocapsid antibodies. When comparing days since the last infection, the urban and Indigenous cohorts exhibited nearly identical trends, further suggesting that Indigenous and non-indigenous individuals mount similar antibody responses. When individuals are classified based on the most recent antigenic exposure whether an infection or a vaccination, the model between the two cohorts overlaps, with a slightly higher rate of decay in the urban cohort. Overall, the antibody levels over time were very similar between the both cohorts.

Discussion:

There are currently limited data on SARS-CoV-2 vaccines and COVID-19 infection-acquired immunity in Indigenous communities in the Canadian Arctic. Given the historically higher risk of adverse outcomes and increased mortality from respiratory viral infections in Indigenous communities, it is essential to improve our understanding of antibody-mediated immunity in the communities (18, 20, 40). This study collected 383 DBS samples from four Indigenous communities in NWT, and SARS-CoV-2 spike-IgG, RBD-IgG, and nucleocapsid-IgG were

measured against the ancestral strain. To our knowledge, this represents one of the largest Indigenous cohorts studied for SARS-CoV-2 antibody-mediated immunity which presents a unique opportunity to gain valuable insights into SARS-CoV-2 exposure and quantify infection- and vaccine-induced immunity (Table 1, Supp. Table 1). Additionally, two non-Indigenous cohorts were selected for comparison. One urban cohort from the Ottawa region was chosen to match the collection window of the NWT Indigenous cohort, and a second urban cohort was selected to match the vaccination status and sample collection method (i.e., DBS).

The vaccination rate in the NWT Indigenous cohort was high, with approximately 91% of participants having received at least one SARS-CoV-2 vaccine dose, nearly 10% higher than the Canadian average at the time of the study(30). By using serological data, nearly three out of four participants in the Indigenous cohort had serological markers indicative of a previous SARS-CoV-2 infection. In contrast, less than one in two individuals in the urban cohort had serological markers of SARS-CoV-2 infection during the same period (Table 1, Figure 2). This finding underscores that Indigenous communities in NWT experienced significantly higher rates of SARS-CoV-2 infection compared to a non-Indigenous urban cohort, aligning with previous observations of higher seroprevalence among Indigenous populations across Canada (25, 41).

Several factors may have contributed to the higher seroprevalence of SARS-CoV-2 infection in Indigenous communities. Firstly, the failure to identify active COVID-19 cases may have resulted in sustained chains of transmission. In addition, high household densities, and limited access to testing and to PPE are all factors that may have contributed to a higher number of SARS-CoV-2 infections. Urban communities, on the other hand, had access to timely data on SARS-CoV-2 prevalence through molecular testing reports and wastewater surveillance, enabling individuals to make informed decisions to mitigate personal COVID-19 exposure risk. Such programs were not available in small rural and remote Indigenous communities in NWT. Beyond surveillance, adequate access to resources and infrastructure remains key to efficiently use surveillance data in these communities in managing future outbreaks.

Serological data also indicated that COVID-19 infections were substantially underreported in the NWT Indigenous communities. This discrepancy between COVID-19, the actual burden of

COVID-19, and self-reported cases in Indigenous communities may be attributed to several factors. For example, a significant proportion of cases may have been asymptomatic or presented with mild symptoms that did not prompt individuals to seek confirmatory testing. Additionally, the overlap in symptoms between COVID-19 and other common illnesses, such as the cold or flu, may have led some individuals to mistakenly attribute a SARS-CoV-2 infection to another illness, particularly when symptoms were mild (42-44). The asymptomatic cases may have been overlooked and the infections may only be noticeable after close contacts, such as family members, relatives, friends, or coworkers, develop symptoms and were diagnosed with COVID-19. It is also possible that individuals in the community may not had timely access to testing methods (i.e., PCR, rapid antigen tests (RAT)). Overall, the significant underreporting of SARS-CoV-2 infection emphasizes the critical role of systematic widespread testing (i.e. PCR, RAT, serology), resources, and infrastructure to isolate infectious individuals, and contact tracing efforts in effectively controlling the spread of the virus in Indigenous communities in NWT (45, 46).

The antibodies developed in response to both vaccination and infection wane over time, a normal physiological process (47, 48). Currently, no data exist on SARS-CoV-2 antibody decay in Indigenous communities in Canada, which is critical for the booster vaccine schedule. Antibody modelling over time following vaccination levels showed stable antibody levels, and even increasing with time in the NWT Indigenous cohort, likely due to SARS-CoV-2 infections (Figure 4A-B). In participants with a SARS-CoV-2 infection date, a faster Spike and RBD antibody decay for the Indigenous cohort was observed, which may be explained by differences in vaccine uptake (Figure 4C-D). Knowing that most of the participants had acquired antibodies from both vaccination and infection, thereby mounting a hybrid immunity, we also looked at the trends over time using the last antigenic exposure whether this was a vaccine or an infection (Figure 4E-F). This revealed nearly identical trends between Indigenous and non-Indigenous cohorts. More importantly, the decay observed does not suggest that Indigenous individuals in NWT have distinct profiles over time and confirm appropriate levels of antibodies in the population. However, future studies with longitudinal sampling from the same individuals further in time will better address these questions.

While the presence of antibodies indicates previous exposure to the virus or vaccination, it does not fully reflect an individual's level of immunity or protection against SARS-CoV-2 infection or COVID-19 (49, 50). Additionally, we did not assess neutralization efficiency, Fc-mediated functions, or other immune components, such as T-cell responses and memory B cells, that contribute to protection against COVID-19 (47, 51, 52). Our analysis was limited to antibodies against the ancestral SARS-CoV-2 antigen, which may not fully represent current antibody levels against circulating variants. Potential biases in participant recruitment, including recall bias, may also be present in this study.

This study provides critical insights into antibody-mediated immunity within Indigenous communities in the Canadian Arctic, revealing a significantly higher burden of SARS-CoV-2 infection compared to urban non-Indigenous populations. Notably, a substantial proportion of individuals were unaware of personal infection status, underscoring the crucial need for accessible and systematic SARS-CoV-2 testing and adequate resources to identify and effectively manage active cases. It may also provide insight into how COVID-19 burden was perceived by community members. Our findings demonstrate that Indigenous individuals mount comparable antibody responses to non-Indigenous individuals following infection and vaccination, addressing concerns about potential disparities in immune response. However, the study also emphasizes the importance of continued public health measures, including timely testing, vaccine boosters, access to PPE, and dissemination of relevant health information, to protect the communities. Ongoing longitudinal study will be vital for monitoring antibody decay and guiding future health interventions.

The high burden of SARS-CoV-2 infection and under-self-reporting in NWT Indigenous communities highlight the risk that respiratory viral outbreak poses in the communities. Beyond COVID-19, respiratory viruses with higher case fatality rates are a significant concern for the communities. The apparent unreliability of self-reporting and higher seroprevalence suggests vulnerabilities for future pandemic preparedness, highlighting the need for stringent safeguards and resources in NWT Indigenous communities. These findings represent an important step toward tailored public health strategies that address the unique needs of Indigenous communities in NWT and across other remote areas of the country.

Funding :

This work was supported in part by a COVID-19 Rapid Response grant through the Canadian Institutes of Health Research (CIHR) grant (VR2-172722) and from a grant supplement by the COVID-19 Immunity Task Force (CITF) to M-AL, as well as by a CIHR grant (FRN 179417) to SS. Production of COVID-19 ELISA reagents was financially supported by the NRC's Pandemic Response Challenge Program. Additionally, YG and MW are supported by a Charles Best and Frederick Banting (CGS-Doctoral award) from CIHR (476885 and 476877).

Contributors :
SS and FK wrote the original grants with JP, MYL, and KD providing valuable expertise in immunology in the grant and throughout the project, with AC, CG, and KK providing input into the communities, cultural safety, as well as extensive logistics in the grant as well as undertaking this massive project in NWT communities. FK, and SS oversaw all research activities in all communities NWT. YG, CA and M-A.L developed the high throughput serology platform. MW, YG and MP performed the data analysis. YG, MW, MP, FK and M-A.L wrote, edited and formatted the manuscript. All authors have edited and approved the final manuscript.

Declaration of interest :
JP reports grants from Merck, and personal fees from Enanta, outside the submitted work The other authors declare no conflict of interest relevant to the present manuscript.

Role of the Funder/Sponsor:
The funding sources played no role in the study design, data collection, analysis, writing of the manuscript, and decision to publish.

Acknowledgments:
We would like to acknowledge past and current members of the high-throughput SARS-CoV-2 Serology and Diagnostic Facility at the University of Ottawa as well as the CoVaRR-Net biobank for providing serum and plasma samples from the Stop the Spread Ottawa study. We also would like to acknowledge Mercedes Yanes-Lane for her contributions.We are very grateful for the partnership of the Indigenous Government and four communities in Northwest Territories and would like to thank all community members for sharing and participating, as well as past and current members of the Indigenous and Global Health Research Group who facilitated this project.

References:

1. Murphy TJ, Swail H, Jain J, Anderson M, Awadalla P, Behl L, et al. The evolution of SARS-CoV-2 seroprevalence in Canada: a time-series study, 2020-2023. Cmaj. 2023;195(31):E1030-e7.
2. O'Mahoney LL, Routen A, Gillies C, Ekezie W, Welford A, Zhang A, et al. The prevalence and long-term health effects of Long Covid among hospitalised and non-hospitalised populations: A systematic review and meta-analysis. EClinicalMedicine. 2023;55:101762.
3. Kapinos KA, Peters RM, Jr, Murphy RE, Hohmann SF, Podichetty A, Greenberg RS. Inpatient Costs of Treating Patients With COVID-19. JAMA Network Open. 2024;7(1):e2350145-e.
4. McNaughton CD, Austin PC, Sivaswamy A, Fang J, Abdel-Qadir H, Daneman N, et al. Post-acute health care burden after SARS-CoV-2 infection: a retrospective cohort study. Canadian Medical Association Journal. 2022;194(40):E1368-E76.
5. Fisman DN, Bogoch I, Lapointe-Shaw L, McCready J, Tuite AR. Risk Factors Associated With Mortality Among Residents With Coronavirus Disease 2019 (COVID-19) in Long-term Care Facilities in Ontario, Canada. JAMA Network Open. 2020;3(7):e2015957-e.
6. Santesmasses D, Castro JP, Zenin AA, Shindyapina AV, Gerashchenko MV, Zhang B, et al. COVID 19 is an emergent disease of aging. Aging cell. 2020;19(10):e13230.
7. Onder G, Rezza G, Brusaferro S. Case-Fatality Rate and Characteristics of Patients Dying in Relation to COVID-19 in Italy. JAMA. 2020;323(18):1775-6.
8. Skowronski DM, Kaweski SE, Irvine MA, Chuang ESY, Kim S, Sabaiduc S, et al. Risk of hospital admission and death from first-ever SARS-CoV-2 infection by age group during the Delta and Omicron periods in British Columbia, Canada. Canadian Medical Association Journal. 2023;195(42):E1427-E39.
9. Whelan M, Galipeau Y, White-Al Habeeb N, Konforte D, Abou El Hassan M, Booth RA, et al. Cross-sectional Characterization of SARS-CoV-2 Antibody Levels and Decay Rates Following Infection of Unvaccinated Elderly Individuals. Open Forum Infectious Diseases. 2023;10(8).
10. Naaber P, Tserel L, Kangro K, Sepp E, Jürjenson V, Adamson A, et al. Dynamics of antibody response to BNT162b2 vaccine after six months: a longitudinal prospective study. The Lancet Regional Health - Europe. 2021;10:100208.
11. Takahashi T, Ellingson MK, Wong P, Israelow B, Lucas C, Klein J, et al. Sex differences in immune responses that underlie COVID-19 disease outcomes. Nature. 2020;588(7837):315-20.
12. Scully EP, Haverfield J, Ursin RL, Tannenbaum C, Klein SL. Considering how biological sex impacts immune responses and COVID-19 outcomes. Nature Reviews Immunology. 2020;20(7):442-7.
13. Kopel J, Perisetti A, Roghani A, Aziz M, Gajendran M, Goyal H. Racial and Gender-Based Differences in COVID-19. Frontiers in Public Health. 2020;8.
14. Silva J, Takahashi T, Wood J, Lu P, Tabachnikova A, Gehlhausen JR, et al. Sex differences in symptomatology and immune profiles of Long COVID. medRxiv. 2024:2024.02.29.24303568.
15. Sylvester SV, Rusu R, Chan B, Bellows M, O'Keefe C, Nicholson S. Sex differences in sequelae from COVID-19 infection and in long COVID syndrome: a review. Current Medical Research and Opinion. 2022;38(8):1391-9.
16. Bose T, Pant N, Pinna NK, Bhar S, Dutta A, Mande SS. Does immune recognition of SARS-CoV2 epitopes vary between different ethnic groups? Virus Res. 2021;305:198579.
17. Summers JA, Baker M, Wilson N. New Zealand's experience of the 1918-19 influenza pandemic: a systematic review after 100 years. N Z Med J. 2018;131(1487):54-69.
18. Kelm M-E. British Columbia First Nations and the influenza pandemic of 1918-19. BC Studies: The British Columbian Quarterly. 1999(122):23-48.
19. CDC. Deaths related to 2009 pandemic influenza A (H1N1) among American Indian/Alaska Natives - 12 states, 2009. MMWR Morb Mortal Wkly Rep. 2009;58(48):1341-4.
20. Boggild AK, Yuan L, Low DE, McGeer AJ. The impact of influenza on the Canadian First Nations. Can J Public Health. 2011;102(5):345-8.

21. Kopel J, Perisetti A, Roghani A, Aziz M, Gajendran M, Goyal H. Racial and gender-based differences in COVID-19. Frontiers in public health. 2020;8:418.
22. Xia Y, Ma H, Moloney G, Velásquez García HA, Sirski M, Janjua NZ, et al. Geographic concentration of SARS-CoV-2 cases by social determinants of health in metropolitan areas in Canada: a cross-sectional study. Canadian Medical Association Journal. 2022;194(6):E195-E204.
23. Power T, Wilson D, Best O, Brockie T, Bourque Bearskin L, Millender E, et al. COVID-19 and Indigenous Peoples: An imperative for action. J Clin Nurs. 2020;29(15-16):2737-41.
24. Petrov AN, Welford M, Golosov N, DeGroote J, Devlin M, Degai T, et al. Lessons on COVID-19 from Indigenous and remote communities of the Arctic. Nature Medicine. 2021;27(9):1491-2.
25. Bobrovitz N, Arora RK, Cao C, Boucher E, Liu M, Donnici C, et al. Global seroprevalence of SARS-CoV-2 antibodies: a systematic review and meta-analysis. PloS one. 2021;16(6):e0252617.
26. Ng JJ, Choong A. Thromboembolic events in patients with SARS-CoV-2. J Vasc Surg. 2020.
27. Guidance on the prioritization of key populations for COVID-19 immunization 2021 [Available from: https://www.canada.ca/en/public-health/services/immunization/national-advisory-committee-on-immunization-naci/guidance-key-populations-early-covid-19-immunization.html#a6.
28. Statistics Canada. Table 17-10-0009-01 Population estimates, quarterly [Available from: https://www150.statcan.gc.ca/t1/tbl1/en/cv.action?pid=1710000901.
29. Lapland ACUo. Arctic Indigenous Peoples [Available from: https://www.arcticcentre.org/EN/arcticregion/Arctic-Indigenous-Peoples.
30. Government of Canada. COVID-19 vaccination: Vaccination coverage [Available from: https://health-infobase.canada.ca/covid-19/vaccination-coverage/.
31. NWT Bureau of Statistics. Population Estimates By Community: Government of Northwest Territories; [cited 2023 April 20]. Available from: https://www.statsnwt.ca/population/population-estimates/bycommunity.php.
32. GNWT Infrastructure. Highways, Ferries, and Winter Roads: Government of the Northwest Territories; [cited 2023 April 20]. Available from: https://www.inf.gov.nt.ca/en/transportation.
33. Adebayo T. Procedure for Collection and Shipment of Blood by Dried Blood Spot Testing. In: Authority NI-TH, editor. 2019.
34. Collins E, Galipeau Y, Arnold C, Bosveld C, Heiskanen A, Keeshan A, et al. Cohort profile: Stop the Spread Ottawa (SSO)—a community-based prospective cohort study on antibody responses, antibody neutralisation efficiency and cellular immunity to SARS-CoV-2 infection and vaccination. BMJ Open. 2022;12(9):e062187.
35. Keeshan A, Galipeau Y, Heiskanen A, Collins E, McCluskie PS, Arnold C, et al. Results of the Stop the Spread Ottawa (SSO) cohort study: a Canadian urban-based prospective evaluation of antibody responses and neutralisation efficiency to SARS-CoV-2 infection and vaccination. BMJ Open. 2023;13(10):e077714.
36. Colwill K, Galipeau Y, Stuible M, Gervais C, Arnold C, Rathod B, et al. A scalable serology solution for profiling humoral immune responses to SARS-CoV-2 infection and vaccination. Clinical & Translational Immunology. 2022;11(3):e1380.
37. Galipeau Y, Siragam V, Laroche G, Marion E, Greig M, McGuinty M, et al. Relative Ratios of Human Seasonal Coronavirus Antibodies Predict the Efficiency of Cross-Neutralization of SARS-CoV-2 Spike Binding to ACE2. eBioMedicine. 2021;74.
38. Egbelowo OF, Fox SJ, Gibson GC, Meyers LA. Model for Interpreting Discordant SARS-CoV-2 Diagnostic Test Results. Emerg Infect Dis. 2024;30(2):388-91.
39. Galipeau Y, Xavier A, Dyks A, Cooper C, Langlois M-A. Continuous false positive results by SARS-CoV-2 rapid antigen testing: a case report. Frontiers in Public Health. 2023;11.
40. Betts JM, Weinman AL, Oliver J, Braddick M, Huang S, Nguyen M, et al. Influenza-associated hospitalisation and mortality rates among global Indigenous populations; a systematic review and meta-analysis. PLOS Glob Public Health. 2023;3(4):e0001294.

41. O'Brien SF, Deeks SL, Hatchette T, Pambrun C, Drews SJ. SARS-CoV-2 seroprevalence in Nova Scotia blood donors. Journal of the Association of Medical Microbiology and Infectious Disease Canada. 2024;9(1):32-45.
42. Pooley N, Abdool Karim SS, Combadiere B, Ooi EE, Harris RC, El Guerche Seblain C, et al. Durability of Vaccine-Induced and Natural Immunity Against COVID-19: A Narrative Review. Infect Dis Ther. 2023;12(2):367-87.
43. Li M, Zhang Y, Lu J, Li L, Gao H, Ma C, et al. Asymptomatic COVID-19 Individuals Tend to Establish Relatively Balanced Innate and Adaptive Immune Responses. Pathogens. 2021;10(9).
44. Boyton RJ, Altmann DM. The immunology of asymptomatic SARS-CoV-2 infection: what are the key questions? Nat Rev Immunol. 2021;21(12):762-8.
45. Pan X, Chen D, Xia Y, Wu X, Li T, Ou X, et al. Asymptomatic cases in a family cluster with SARS-CoV-2 infection. Lancet Infect Dis. 2020;20(4):410-1.
46. Chan JF, Yuan S, Kok KH, To KK, Chu H, Yang J, et al. A familial cluster of pneumonia associated with the 2019 novel coronavirus indicating person-to-person transmission: a study of a family cluster. Lancet. 2020;395(10223):514-23.
47. Chivese T, Matizanadzo JT, Musa OAH, Hindy G, Furuya-Kanamori L, Islam N, et al. The prevalence of adaptive immunity to COVID-19 and reinfection after recovery - a comprehensive systematic review and meta-analysis. Pathog Glob Health. 2022;116(5):269-81.
48. Goldblatt D, Alter G, Crotty S, Plotkin SA. Correlates of protection against SARS-CoV-2 infection and COVID-19 disease. Immunol Rev. 2022;310(1):6-26.
49. Spellberg B, Nielsen TB, Casadevall A. Antibodies, Immunity, and COVID-19. JAMA Intern Med. 2021;181(4):460-2.
50. Sadarangani M, Marchant A, Kollmann TR. Immunological mechanisms of vaccine-induced protection against COVID-19 in humans. Nat Rev Immunol. 2021;21(8):475-84.
51. Moss P. The T cell immune response against SARS-CoV-2. Nat Immunol. 2022;23(2):186-93.
52. Zuo J, Dowell AC, Pearce H, Verma K, Long HM, Begum J, et al. Robust SARS-CoV-2-specific T cell immunity is maintained at 6 months following primary infection. Nat Immunol. 2021;22(5):620-6.

Table 1. General demographics and epidemiological characteristics of participants by cohort. Self-reported demographics and epidemiological information were collected as part of each study. Serological markers of previous infection were determined by dual seropositivity to the nucleocapsid and the spike or RBD antigen.

	Northwest Territories cohort n (%)	**Seroprevalence Urban cohort (Serum)** n (%)	**Antibody levels Urban cohort (DBS)** n (%)
Number of individuals	383	157	119
Number of individuals with follow up samples	0 (0%)	0 (0%)	64 (23.62%)
Age (years), mean ±SD	46.24 ±15.5	52.11 ±13.48	49.89 ±12.79
Age groups (years)			
19-29	67 (17.49%)	5 (3.18%)	4 (3.36%)
30-49	150 (39.16%)	59 (37.58%)	59 (49.58%)
50-65	127 (33.16%)	64 (40.76%)	38 (31.93%)
>65	38 (9.92%)	29 (18.47%)	18 (15.13%)
Unknown	1 (0.26%)	0 (0%)	0 (0%)
Gender			
Woman	176 (45.95%)	105 (66.88%)	49 (41.18%)
Man	207 (54.05%)	52 (33.12%)	70 (58.82%)
Ethnicity			
First Nations	383 (100%)	0 (0%)	0 (0%)
Inuit/Metis	0 (0%)	1 (0.64%)	0 (0%)
Other**	0 (0%)	156 (99.36%)	119 (100%)
Education			
Elementary school	31 (8.09%)	0 (0%)	1 (0.84%)
Middle school	171 (44.65%)	0 (0%)	0 (0%)
High school	75 (19.58%)	2 (1.27%)	4 (3.36%)
Post-secondary	25 (6.53%)	150 (95.54%)	111 (93.28%)
Other***	2 (0.52%)	0 (0%)	0 (0%)
None	79 (20.63%)	0 (0%)	0 (0%)
Unsure/skipped	0 (0%)	5 (3.18%)	3 (2.52%)
Diagnosed with health conditions			
Yes	85 (22.19%)	91 (57.96%)	72 (60.50%)
No	298 (77.81%)	66 (42.04%)	47 (39.50%)
Currently use tobacco			
Yes	207 (54.05%)	6 (3.82%)	5 (4.20%)
No	176 (45.95%)	151 (96.18%)	114 (95.80%)
Received C19 vaccination			
Yes	347 (90.60%)	155 (98.73%)	91 (76.47%)
No	36 (9.40%)	2 (1.27%)	28 (23.53%)
Number of C19 vaccinations received			
1	13 (3.39%)	0 (0%)	0 (0%)
2	192 (50.13%)	9 (5.73%)	35 (29.41%)
3	121 (31.59%)	32 (20.38%)	56 (47.06%)
4	20 (5.22%)	60 (38.22%)	0 (0%)
5 +	1 (0.26%)	54 (34.39%)	0 (0%)
Self-reported having C19			
Yes	159 (41.51%)	87 (55.41%)	44 (36.97%)
No	224 (58.49%)	70 (44.59%)	75 (63.03%)
Serological markers of previous infection			
Yes	279 (72.85%)	72 (45.86%)	23 (19.33%)
No	104 (27.15%)	85 (54.14%)	96 (80.67%)

******Caucasian (2), non-indigenous (2)

***Day school (1), Edmonton school (1)

Figure Legends

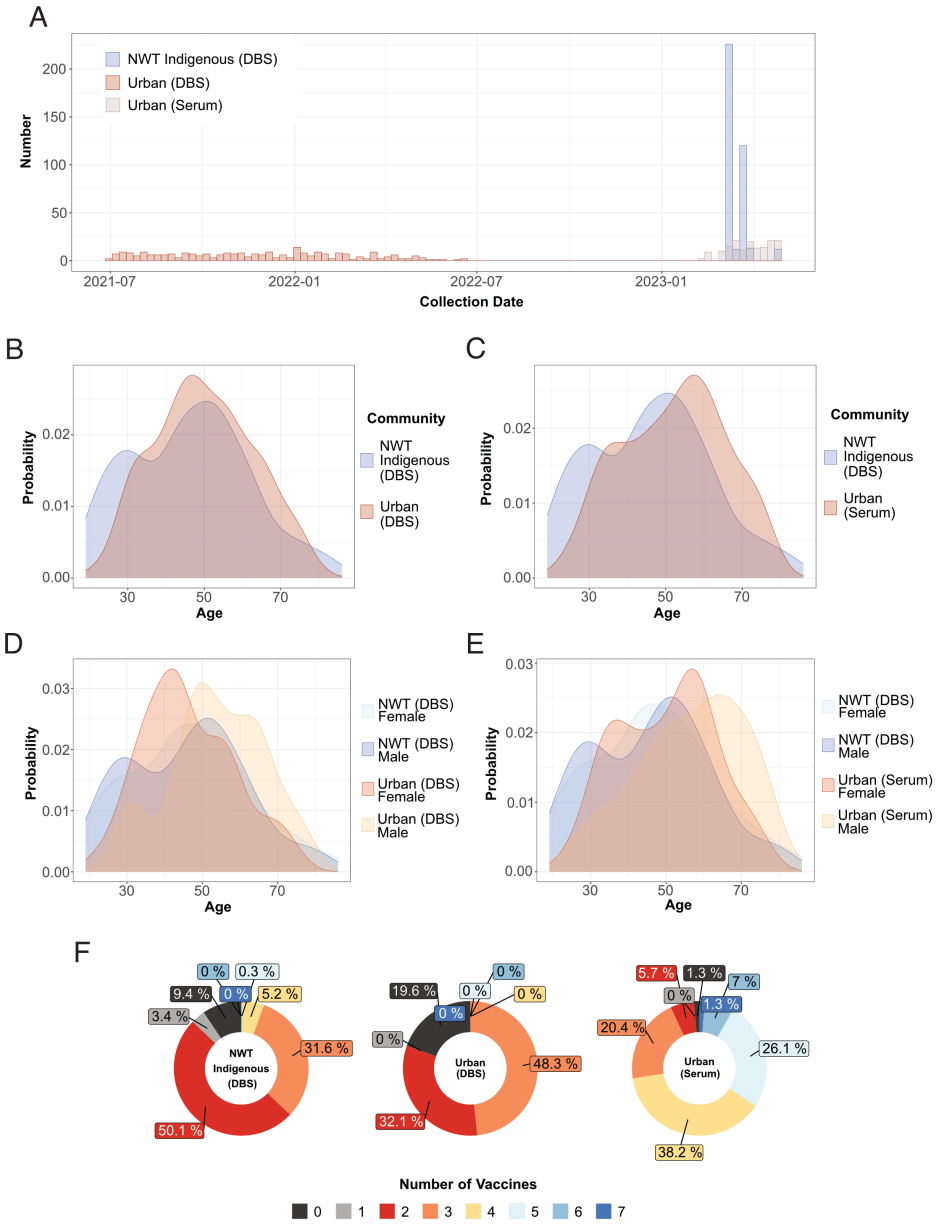


Figure 1. Side-by-side comparison of the NWT Indigenous community cohort and urban cohorts. Two urban cohorts were selected to provide context for the NWT Indigenous community cohort: one cohort matched the collection period, and the other matched the collection method (i.e., dried blood spots). A) Number of samples from each cohort by date. B) Age distribution of the NWT Indigenous community cohort and the DBS urban cohort (matched vaccine profile). C) Age distribution of the NWT Indigenous community cohort and the serum urban cohort (matched collection window). D) Age distribution by sex of the NWT Indigenous community cohort and the DBS urban cohort. E) Age distribution by sex of the NWT Indigenous community cohort and the serum urban cohort. F) Proportion of individuals in each cohort by number of vaccines at collection time.

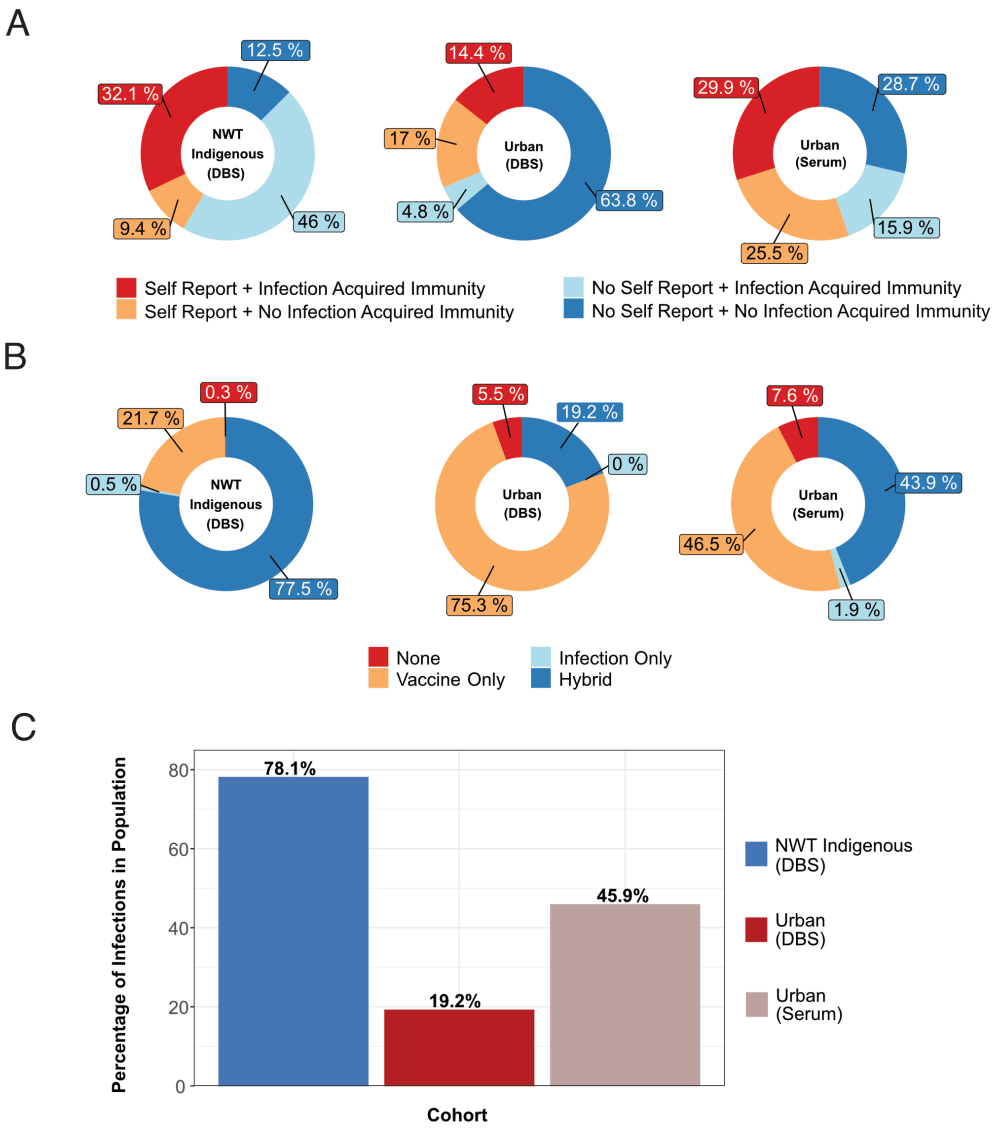


Figure 2. Seroprevalence of previous SARS-CoV-2 infection in all three cohorts. A) Proportions of individuals in each cohort with serological markers of previous infection compared to individuals without, along with the proportion of individuals who self-reported or did not report a history of SARS-CoV-2 infection. B) Predicted sources of SARS-CoV-2 immunity (vaccine-acquired, infection-acquired, or hybrid) based on serological markers of previous infection and vaccination status in each cohort. C) Comparative levels of previous SARS-CoV-2 infection in each cohort as determined by serology results.

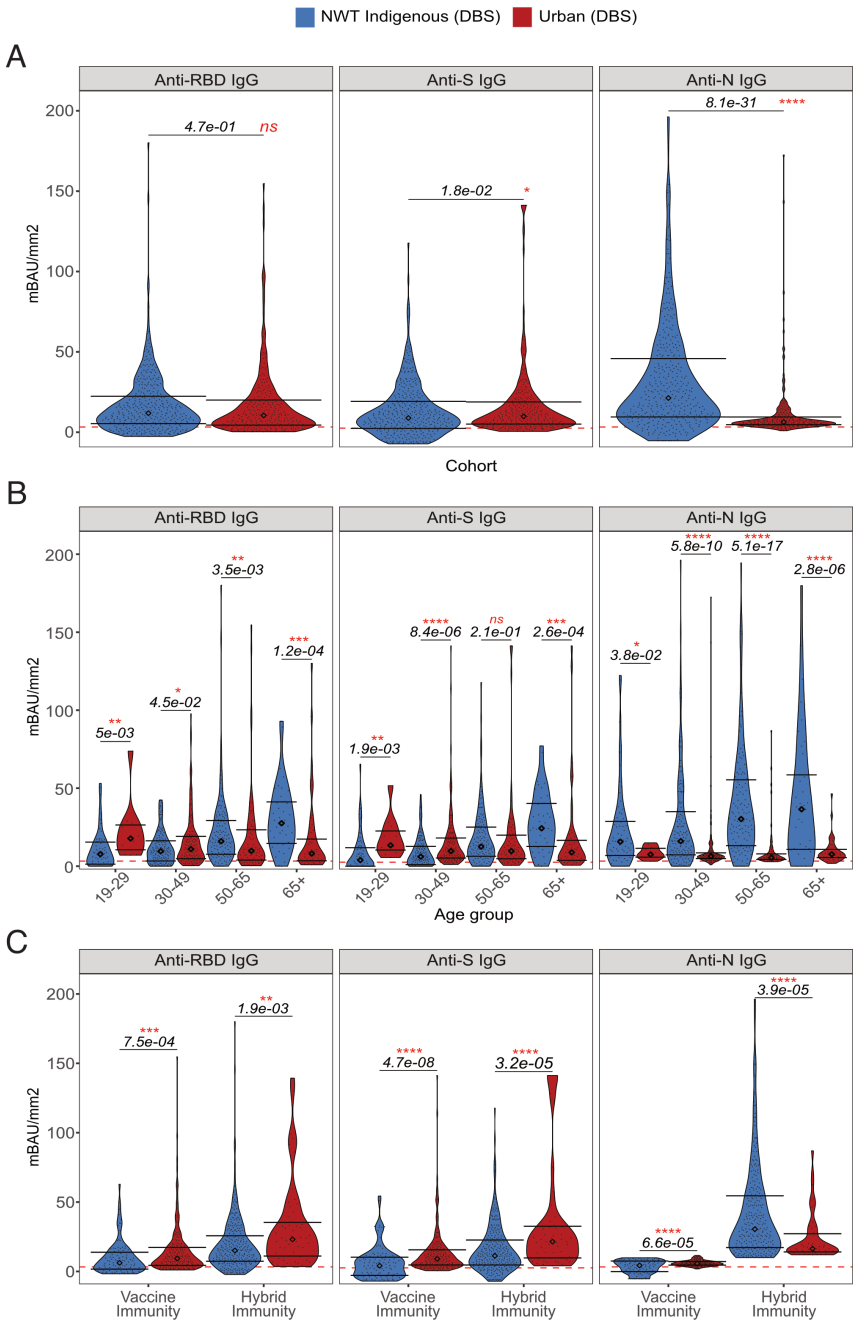


Figure 3. SARS-CoV-2 IgG antibody levels against the Spike, RBD and Nucleocapsid. A) Overall antibody levels by cohort (NWT Indigenous community cohort and urban (DBS) cohort). B) Antibody levels stratified by cohort and age group. C) Antibody levels categorized by source of immunity (vaccine-acquired or hybrid immunity). In all panels, medians are represented by diamonds, and interquartile ranges (IQR) are indicated by horizontal lines. Statistical significance and P values were determined using the Mann-Whitney U test.

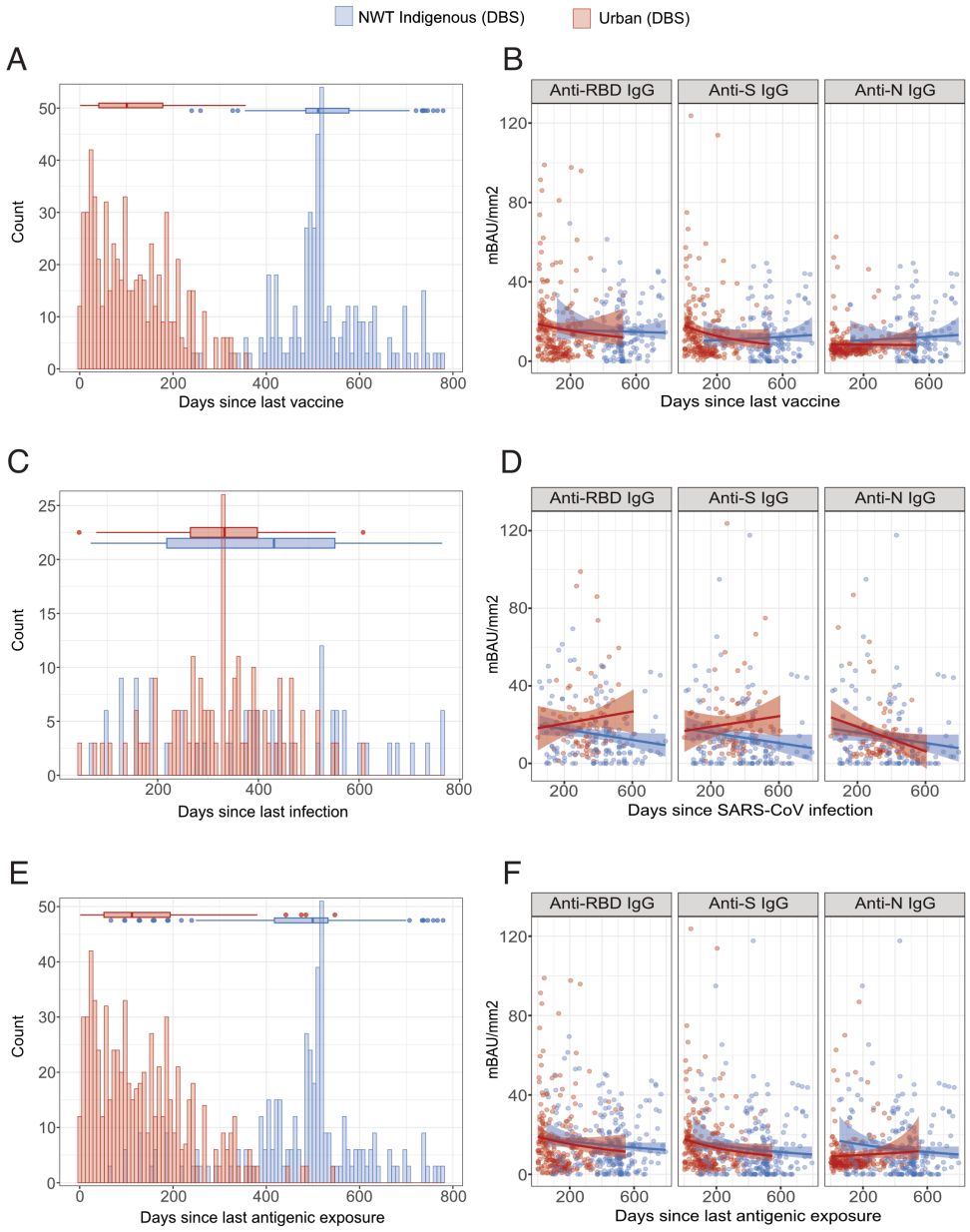


Figure 4 – Trajectories of antibody levels over time in relation to last vaccination, infection or both in the urban and Indigenous cohort. Overall distribution of each cohort and the levels of anti-RBD, anti-S and anti-N IgG based on the number of days between sample collection and the last vaccine received (A-B), the last infection (C-D) and the last antigenic exposure (vaccine or infection; E-F). The boxplots overlayed on the histograms (A, C and E) represent the distribution of the cohort, with the median, different quantiles and the outliers for each cohort. The relationship between the number of days since antigenic exposure and levels of antibodies (B, D and F) was modelized and represented as colored lines with the standard error displayed as the lighter area around the model using a generalized linear model of the gamma (B and F) or Gaussian (D) family using the following formula: mBAU/mm2 ~ Number of days * IgG antigen * Cohort.

Supplementary material

Serological analysis

Dried blood spots were punched as 3mm diameter discs and eluted in PBS solution +1% Triton. Automated chemiluminescent ELISAs were performed on a Hamilton Microlab STAR Liquid Handling System(1). COVID-19 antigens (spike/S, receptor-binding domain/R, or nucleocapsid/N) were coated on a 384-well protein-binding assay plate. Prior to blood spot application, wells were blocked with a skim milk solution to eliminate non-specific signals. Diluted dried blood spot eluates, standard curves, and controls were then added to the assay plates. Plates were incubated for two hours at room temperature, then HRP-conjugated secondary antibodies were added to each well and incubated for one hour at room temperature, followed by the addition of a luminescent substrate. COVID-19 antibodies in blood spots were detected as a relative level of HRP-generated chemiluminescent signal, as read by a BioTek NeO2 plate reader. Collected dried blood spot samples were destroyed immediately upon completion of laboratory analysis. Dried blood spot results were categorized into one of four possible outcomes: 1. anti-N positive and anti-S positive: suggestive of immunity from infection alone or infection and vaccination; 2. anti-S positive only: suggestive of immunity from prior vaccination only; 3. anti-N positive only: indeterminate immune status; and 4. anti-N negative and anti-S negative: non-immune.

Data analysis

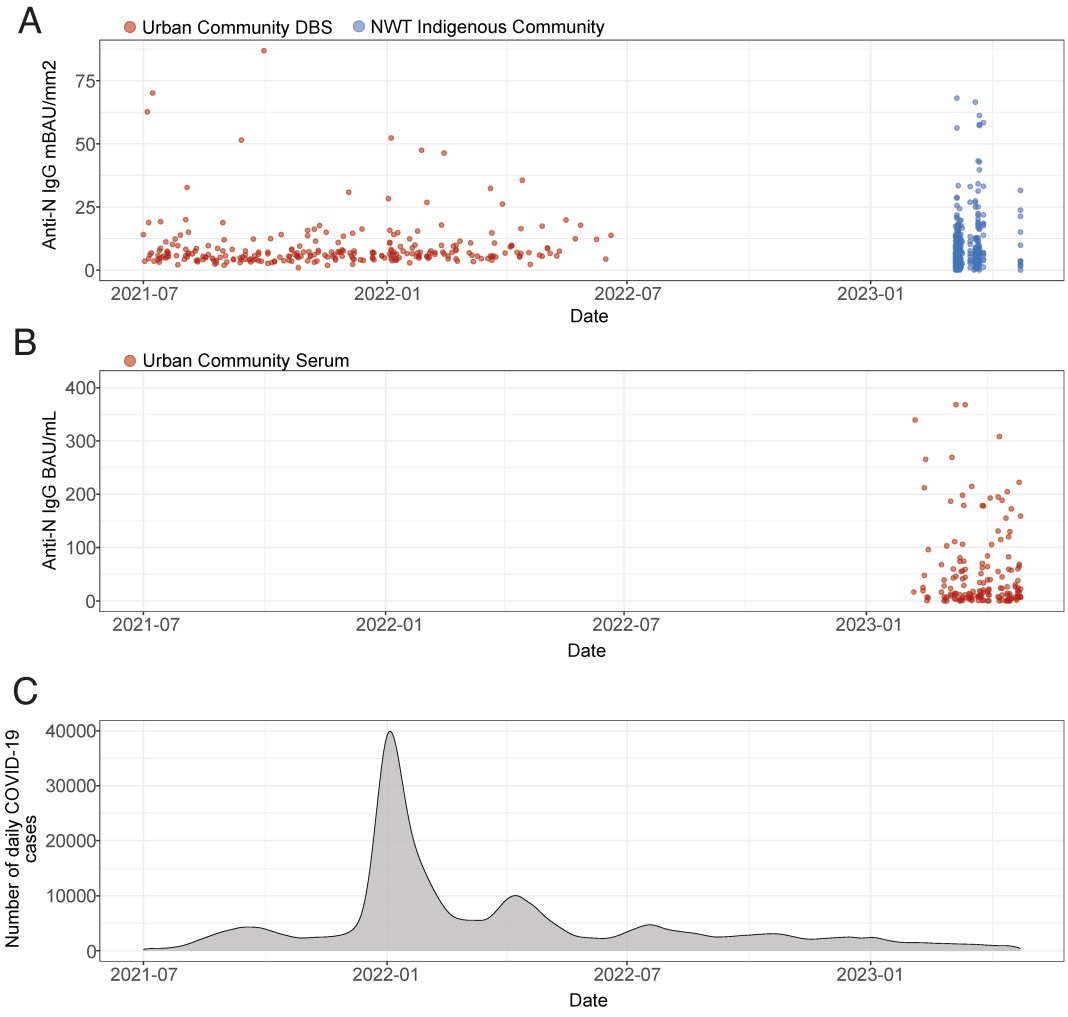
Statistical analyses were performed in R version 4.2.1. Individuals in all three cohorts with missing metadata with variables used in this analysis were removed from the study. The urban cohorts were further randomly trimmed down to obtain cohorts with similar sex and age distribution. The self-report discrepancy was assessed by comparing the reported infection from individuals and the serological markers detected by our platform. Samples were deemed positive for SARS-CoV-2 infection markers if their mBAU/mm2 or BAU/mL value for N-IgG and R-IgG or S-IgG were above our cutoffs (N-IgG: 3.25097 mBAU/mm2 and 17.8 BAU/mL, R-IgG: 6.76249 mBAU/mm2 and 45.13749 BAU/mL, S-IgG: 2.55172 mBAU/mm2 and 30.44072 BAU/mL). Samples were deemed positive for vaccine-induced immunity if their mBAU/mm2 or BAU/mL for R-IgG and

S-IgG were above our cutoffs. The types of immunity were determined using the serological markers detected by our platform. Individuals with an immunity derived only from vaccines were only positive for anti-R-IgG and anti-S-IgG, but not for anti-N-IgG whereas individuals with an immunity only derived from SARS-CoV-2 infection were only positive for anti-N-IgG.

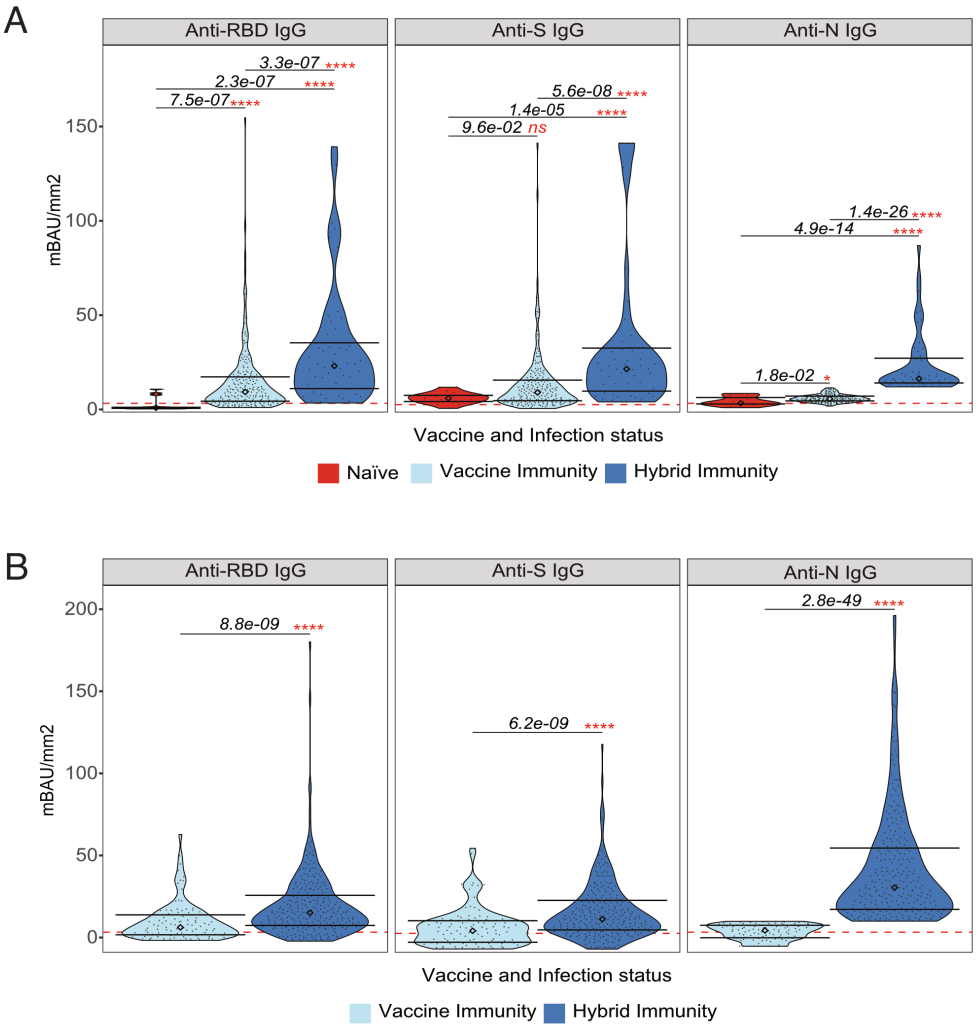
The difference in antibody content between cohorts was assessed by calculating their median and interquartile range (IQR) and displaying the distribution of each cohort using violin plots with the IQR and median. Because the distribution was not normal, Mann-Whitney U tests were used to compare the groups. The Bonferroni correction was applied to adjust for multiplicity. The effect of age and SARS-CoV-2 infection on antibody content for each cohort was assessed in the same manner. Prior to statistical analysis, the distribution was assessed, and outliers were removed. No samples were removed for the overall distribution of antibody content for the cohorts, 1 sample from the Northwest Territories Indigenous cohort was removed from the age group analysis and 2 samples from the Northwest Territories Indigenous cohort and 15 from the urban cohort DBS were removed from the immunity type analysis.

The correlation between antibody levels and the number of days since the last vaccination and the sample collection date was assessed using a generalized linear model with a gamma regression, as was the correlation between antibody levels and the number of days since the last exposure to SARS-CoV-2 antigens (vaccination or infection) and the sample collection date. For the correlation between antibody levels and the number of days since the last SARS-CoV-2 infection, a linear model was used as it provided the best fit for the data. The analysis was restricted to 800 days for all models, as samples beyond this time frame negatively impacted the model fit. In all three correlation studies, individuals without recorded vaccine or infection dates were excluded. Specifically, 227 samples from the Northwest Territories Indigenous cohort and 60 samples from the urban DBS cohort were excluded from the correlation between days since the last vaccine and sample collection date. For the correlation between days since the last SARS-CoV-2 infection and sample collection date, 334 samples from the Northwest Territories Indigenous cohort and 187 samples from the urban DBS cohort were excluded. Finally, 227 samples from the Northwest Territories Indigenous cohort and 5 samples from the urban DBS cohort were excluded from the

correlation between days since the last exposure to SARS-CoV-2 antigens and sample collection date.



Supplemental Figure 1. Cohorts anti-nucleocapsid levels in relation to collection time. A) Dried blood spot samples collected for the urban community cohort (DBS) and the NWT Indigenous community cohort. B) Serum samples selected to match the time of collection of the NWT Indigenous community cohort. C) Reported SARS-CoV-2 infection cases in Canada over the same period. The data was obtained from Berry *et al.* (2)



Supplemental Figure 2. Antibody levels in relation to vaccine and infection status. A) Dried blood spot samples collected from the urban community cohort (DBS) grouped by infection and vaccination status as well as SARS-CoV-2 antigen (Spike, RBD and Nucleocapsid) B) Dried blood spot samples collected from the NWT Indigenous community cohort antibody levels grouped by infection and vaccination status as well as SARS-CoV-2 antigen (Spike, RBD and Nucleocapsid). No individual in this cohort was unvaccinated and had no history of SARS-CoV-2 infection.

Supplementary Table 1. **Supplementary demographic information.** Individuals from the NWT Indigenous community cohort were asked to answer questions regarding their health and other personal characteristics.

	Northwest Territory Indigenous community cohort n (%)
Community	
Community A	276 (72.06%)
Community B	22 (5.74%)
Community C	71 (18.54%)
Community D	14 (3.66%)
Cultural or on the land education	
Yes	331 (86.42%)
No	52 (13.58%)
Self-reported health status	
Excellent	93 (24.28%)
Good	200 (52.22%)
Fair	78 (20.37%)
Poor/very poor	12 (3.13%)
Diagnosed with health conditions	
Yes	85 (22.19%)
No	298 (77.81%)
Reason for suspecting C19 infection (most recent time)* **	
Rapid test	65 (16.97%)
PCR test	62 (16.19%)
Symptom profile	24 (6.27%)
Confirmed by healthcare providers	6 (1.57%)
Other	2 (0.52%)

Supplementary Table 2. Vaccine characteristics by age groups and cohorts.

Supplementary Table 2. Vaccine characteristics by age groups and cohorts. The proportion of total vaccines received by individuals across cohorts and age groups was compiled, including those who had not received any vaccines.

	Northwest Territory cohort n (%)	**Seroprevalence Urban cohort (Serum)** n (%)	**Antibody levels Urban cohort (DBS)** n (%)
19-29 (years)			
None	6 (8.96%)	0 (0%)	2 (50.00%)
1 Vaccine	4 (5.97%)	0 (0%)	0 (0%)
2 Vaccines	46 (68.66%)	1 (20.00%)	1 (25.00%)
3 Vaccines	11 (16.42%)	4 (80.00%)	1 (25.00%)
4 Vaccines	0 (0%)	0 (0%)	0 (0%)
5+ Vaccines	0 (0%)	0 (0%)	0 (0%)
30-49 (years)			
None	19 (12.67%)	0 (0%)	11 (18.64%)
1 Vaccine	8 (5.33%)	0 (0%)	0 (0%)
2 Vaccines	83 (55.33%)	5 (8.47%)	20 (33.90%)
3 Vaccines	39 (26.00%)	14 (23.73%)	28 (47.46%)
4 Vaccines	1 (0.67%)	26 (44.07%)	0 (0%)
5+ Vaccines	0 (0%)	14 (23.73%)	0 (0%)
50-65 (years)			
None	7 (5.51%)	2 (3.13%)	10 (26.32%)
1 Vaccine	1 (0.79%)	0 (0%)	0 (0%)
2 Vaccines	56 (44.09%)	4 (6.25%)	10 (26.32%)
3 Vaccines	52 (40.94%)	13 (20.31%)	18 (47.37%)
4 Vaccines	10 (7.87%)	23 (35.94%)	0 (0%)
5+ Vaccines	1 (0.79%)	22 (34.38%)	0 (0%)
65+ (years)			
None	4 (10.53%)	0 (0%)	5 (27.78%)
1 Vaccine	0 (0%)	0 (0%)	0 (0%)
2 Vaccines	7 (18.42%)	0 (0%)	4 (22.22%)
3 Vaccines	18 (47.37%)	4 (13.79%)	9 (50.00%)
4 Vaccines	9 (23.68%)	7 (24.14%)	0 (0%)
5+ Vaccines	0 (0%)	18 (62.07%)	0 (0%)

Supplementary Table 3. General demographic and characteristics of individuals included in the antibody trajectories analysis. Individuals with a date of infection or a date of vaccination were included for the analysis of antibody levels over time (Figure 4).

	Northwest Territory cohort n (%)	**Antibody levels Urban cohort** n (%)
Number of individuals	156 (40.73%)	118 (99.16%)
Number of samples	156 (40.73%)	266 (98.16%)
Age (years), mean ±SD	45.94 ±14.65	49.81 ±12.81
Age range	19-81	21-80
Gender		
Woman	65 (41.67%)	69 (58.47%)
Man	91 (58.33%)	49 (41.53%)
Received C19 vaccination		
Yes	156 (100%)	90 (76.27%)
No	0 (0%)	28 (23.73%)
Number of C19 vaccinations received		
1	5 (3.21%)	0 (0%)
2	97 (62.18%)	35 (29.66%)
3	51 (32.69%)	55 (46.61%)
4	3 (1.92%)	0 (0%)
5 +	0 (0%)	0 (0%)
Serological markers of previous infection		
Yes	126 (80.23%)	22 (18.64%)
No	30 (19.23%)	96 (81.36%)

Supplementary Table 4. General demographic and characteristics of individuals included in the antibody trajectories analysis since their last vaccine. Individuals who received a vaccine and provided a reported date of vaccination were included in the analysis of antibody levels over time.

	Northwest Territory cohort n (%)	**Antibody levels Urban cohort** n (%)
Number of individuals	156 (40.73%)	92 (77.31%)
Number of samples	156 (40.73%)	211 (77.86%)
Age (years), mean ±SD	45.94 ± 14.65	49.01 ± 12.61
Age range	19-81	25-80
Gender		
Woman	65 (41.67%)	57 (61.96%)
Man	91 (58.33%)	35 (38.04%)
Received C19 vaccination		
Yes	156 (100%)	92 (100%)
No	0 (0%)	0 (0%)
Number of C19 vaccinations received		
1	5 (3.21%)	0 (0%)
2	97 (62.18%)	35 (38.04%)
3	51 (32.69%)	57 (61.96%)
4	3 (1.92%)	0 (0%)
5 +	0 (0%)	0 (0%)
Serological markers of previous infection		
Yes	126 (80.77%)	17 (18.48%)
No	30 (19.23%)	75 (81.52%)

Supplementary Table 5. General demographic and characteristics of convalescent individuals included in the antibody trajectories analysis. Individuals who had a previous SARS-CoV-2 infection and reported a date of infection were included in the analysis of antibody levels over time.

	Northwest Territory cohort n (%)	**Antibody levels Urban cohort** n (%)
Number of individuals	49 (12.79%)	43 (36.13%)
Number of samples	49 (12.79%)	84 (31.00%)
Age (years), mean ±SD	41.33 ± 13.78	48.17 ± 12.95
Age range	19-75	25-73
Gender		
Woman	22 (44.90%)	24 (55.81%)
Man	27 (55.10%)	19 (44.19%)
Received C19 vaccination		
Yes	49 (100%)	32 (74.42%)
No	0 (0%)	11 (25.58%)
Number of C19 vaccinations received		
1	1 (2.04%)	0 (0%)
2	35 (71.43%)	12 (27.91%)
3	12 (24.49%)	20 (46.51%)
4	1 (2.04%)	0 (0%)
5 +	0 (0%)	0 (0%)
Serological markers of previous infection		
Yes	39 (79.59%)	18 (41.86%)
No	10 (20.41%)	25 (58.14%)

Supplementary Table 6. General demographic and characteristics of individuals included in the antibody trajectories analysis since last antigenic exposure. Individuals who were previously infected by SARS-CoV-2 and/or received a vaccination and who reported a date of infection and/or vaccination were included for the analysis of antibody levels over time.

	Northwest Territory cohort n (%)	**Antibody levels Urban cohort** n (%)
Number of individuals	156 (40.73%)	101 (84.87%)
Number of samples	156 (40.73%)	239 (88.19%)
Age (years), mean ±SD	45.94 ± 14.65	49.21 ± 12.78
Age range	19-81	25-80
Gender		
Woman	65 (41.67%)	60 (59.41%)
Man	91 (58.33%)	41 (40.59%)
Received C19 vaccination		
Yes	156 (100%)	90 (89.11%)
No	0 (0%)	11 (10.89%)
Number of C19 vaccinations received		
1	5 (3.21%)	0 (0%)
2	97 (62.18%)	35 (34.65%)
3	51 (32.69%)	55 (54.46%)
4	3 (1.92%)	0 (0%)
5 +	0 (0%)	0 (0%)
Serological markers of previous infection		
Yes	126 (80.77%)	22 (21.78%)
No	30 (19.23%)	79 (78.22%)

References

1. Colwill K, Galipeau Y, Stuible M, Gervais C, Arnold C, Rathod B, et al. A scalable serology solution for profiling humoral immune responses to SARS-CoV-2 infection and vaccination. Clinical & Translational Immunology. 2022;11(3):e1380.
2. Berry I, O'Neill M, Sturrock SL, Wright JE, Acharya K, Brankston G, et al. A sub-national real-time epidemiological and vaccination database for the COVID-19 pandemic in Canada. Scientific Data. 2021;8(1):173.

3.3 CONTINUOUS FALSE POSITIVE RESULTS BY SARS-COV-2 RAPID ANTIGEN TESTING: A CASE REPORT

Preface

(This work has been previously published as a research article)

Galipeau Y., Xavier A., Dyks A., Cooper C., Langlois MA. **Continuous false positive results by SARS-CoV-2 rapid antigen testing: a case report**. Front Public Health. 2023 Nov 3;11:1240308. doi: 10.3389/fpubh.2023.1240308.

© 2023 Galipeau, Xavier, Dyks, Cooper and Langlois. This is an open-access article distributed under the terms of the Creative Commons Attribution License (CC BY). The use, distribution or reproduction in other forums is permitted, provided the original author(s) and the copyright owner(s) are credited and that the original publication in this journal is cited, in accordance with accepted academic practice. No use, distribution or reproduction is permitted which does not comply with these terms.

Abstract

Efficient and rapid identification of active SARS-CoV-2 infections has been key to monitoring and mitigating the spread of the virus. The implementation of nucleic acid testing (e.g., RT-PCR) was broadly adopted by most public health organizations at the national and community levels across the globe, which was followed by more accessible means of home testing including lateral flow immunochromatographic assay (LFA), also known as a rapid antigen test. Here we report the case of an adult female who repeatedly and consecutively tested positive by RAT (BTNX inc). This sustained false positive was not linked with an active SARS-CoV-2 infection, which was ruled out by RT-PCR and serological analyses. SARS-CoV-2 serology revealed no detectable levels of antibodies against the nucleocapsid suggesting no recent prior infection by SARS-CoV-2. This continuous false positive was limited to BTNX testing devices. This case report aims to describe that such continuous false positives can occur and describes alternative testing approaches that can be performed to confirm RAT results. In addition, broader awareness of such occurrences is warranted in the healthcare and public health community to avoid unnecessary negative impacts on individual's day to day life.

Introduction

The ability to rapidly identify SARS-CoV-2 infected individuals has been central to most public health measures across the globe and is a major component to contact tracing initiatives. Population-level testing requirements prompted the establishment of testing centers that conducted viral nucleic acid detection (i.e., RT-PCR) (1, 2). Despite being the gold standard detection method of SARS-CoV-2 in clinical samples, and its broad use early in the pandemic, RT-PCR testing has some important limitations (i.e., expensive laboratory equipment, reliance on highly qualified laboratory and medical workers, non-point-of-care testing, etc.). In light of these limitations, countries like Canada have endorsed the usage of at-home Rapid Antigen Tests (RAT) (3–5).

Several studies have investigated RAT performances in real life settings. In a cohort of 72,382 paired RT-PCR and RAT, Eyre et al. reported an overall sensitivity of 63.2% (6). This estimate is in line with other studies (7, 8). While sensitivity is increased in symptomatic individuals, RATs overall have a lower sensitivity compared to RT-PCR. In addition, despite concerns that SARS-CoV-2 RAT could cross-react with other pathogens such as seasonal coronaviruses (OC43, 229E, NL63, HKU-1), RATs are regarded as highly specific. In fact, several studies reported specificities that ranged from 99.71% (6), 99.95% (9) 100% (10).

Given that a vast array of RATs have been authorized by the federal regulatory bodies, their relative real-world performance, technology used, and their usage vary (10, 11). In this case report, we will focus primarily on the RAT from BTNX inc (COV-19C25). This lateral immunochromatographic at-home test kit is designed to detect SARS-CoV-2 nucleocapsid in nasopharyngeal secretions (12). Here we report the case of a 47 year old female who consistently and consecutively tested positive by RAT despite any laboratory or clinical evidence of SARS-CoV-2 infection.

Case description

A 47-year-old Caucasian female first tested positive by rapid antigen test (RAT) on December 28th 2021. At that time, she remained positive for over 2 weeks until she stopped self-testing. Following Canadian public health recommendations, she tested herself regularly by RAT after a high-risk contact, or when experiencing COVID-19 associated symptoms. Repeated self-testing with RAT yielded a constant positive result. After each positive RAT result, she followed recommendations from public health to self-isolate. She was careful about masking and wore N95 in public spaces. Given that RATs were repeatedly positive, she contacted public health authorities for guidance and they recommended she stop testing. On the other hand, her family physician told her to keep testing, thereby suggesting that she was still contagious. These conflicting recommendations have led to confusion, distress and uncertainty for the subject. The numerous isolation periods have impacted her day-to-day life, impacted her family, and prevented her from visiting friends and relatives.

We were contacted in early fall 2022 to offer guidance on the continuous SARS-CoV-2 positive results on RAT given the mixed recommendations from her physician and local public health. Her medical history included an allergy to dust mites and mild asthma that did not require medication. Her SARS-CoV-2 vaccination history included a first dose of (Pfizer) on May 1st 2021, a second dose of (Moderna) on June 19th 2021, a third dose of (Moderna) on November 19th 2021, and a fourth dose of (Pfizer) on August 9th 2022.

We collected a blood sample to investigate SARS-CoV-2 associated antibodies in serum. We also requested that she provide a saliva sample every week for a month for molecular testing. At the time of providing the saliva sample, we also asked that she perform a set of RAT tests, which included 3 BTNX tests. One test was performed following the manufacturer's instructions (swabbing of the nasal cavity), the other was a swab of the oral cavity, and the third comprised of combination swabbing techniques of both sites. For the first week, a RAT from another supplier was also performed simultaneously (Figure 1).

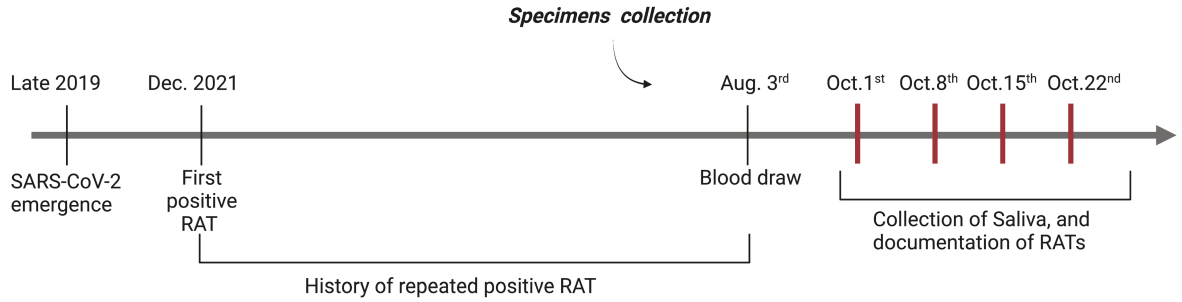


Figure 1. Timeline overview of positive RATs and specimen collection. A visual representation of both the subject testimony in regards to the history of positive RATs and sample collection (Blood, RATs) as part of this case report. Red vertical bars represent the four weeks where we documented positive RAT for this case report, and where the subject provided saliva samples.

All four weekly RATs that were performed following manufacturer recommended swabbing techniques or the combination of oral and nasal swabbing techniques yielded unambiguous positive results. All four weekly RATs performed by oral swabbing were negative (Figure 2). Interestingly, a RAT from another supplier (FlowFlex) was performed in the first week and was negative, suggesting that the positivity might be limited to BTNX kits only. Nucleic acid testing from the saliva samples provided for each week was negative for SARS-CoV-2 E and N gene, thus suggesting the absence of an active or persistent infection. SARS-CoV-2 IgG antibody measurements against the N and S proteins were performed. Only antibodies against the Spike protein were detected beyond our positivity threshold (Figure 3). Given the lack of antibodies against the N protein, a recent SARS-CoV-2 infection was deemed unlikely.

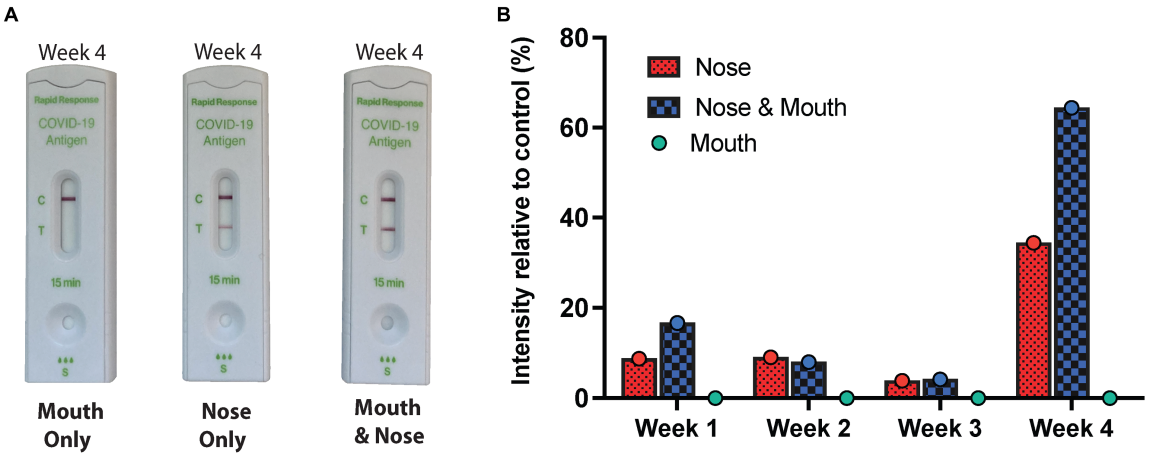


Figure 2. Weekly results of RAT by swabbing technique and location. **(A)** An overview of the RATs by swabbing technique for week 4 from photographed RAT performed at home. As described, the nasal cavity was swabbed (deep and anterior nasal swab), the oral cavity (throat and cheeks) as well as the combination of both swabbing techniques. The RATs were performed sequentially in the same session and photographed. **(B)** An overview of the RAT's band intensity in relation to the control band for every week and for the three swabbing techniques.

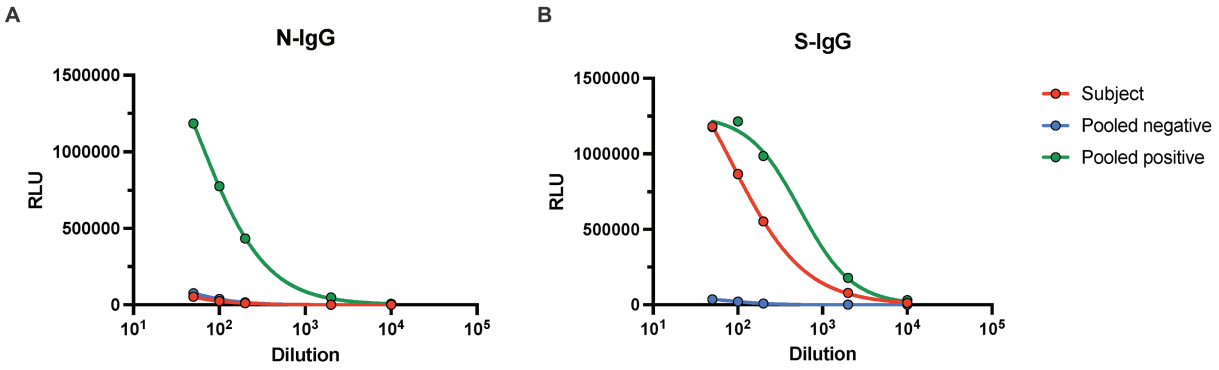


Figure 3. Serology results of serum sample provided prior to week 1. A blood sample was provided prior to performing the RATs, and serum was isolated. Antibodies against the SARS-CoV-2 **(A)** nucleocapsid and **(B)** Spike protein was performed using a previously established chemiluminescent ELISA serological assay. IgG antibodies were measured by titrating the subject's serum sample (red). In addition, a titration of a negative (blue) and positive (green) pooled serum from residual blood was included as positive and negative controls. Here the blank adjusted relative luminescence units (RLU) intensity is shown. IgG antibody titer against the nucleocapsid was below conversion threshold, IgG titer against the spike protein was estimated to be 130.41 BAU/mL.

Discussion

While false positives occur with any diagnostic tests, including RATs, here we report the case of a continuous false positive. To document the events related to the positive RAT and to investigate potential sources of cross-reactivity, a series of RATs were performed. One weekly RAT was performed for four weeks by anterior and deep nasal swabbing as per manufacturer's instructions. Each of these RATs were positive, confirming the subject's testimony (Figure 2B). Given that Canadian public health authorities were also recommending individuals to swab the oral cavity (throat and cheeks) in combination with anterior and deep nasal swabbing to increase sensitivity (13, 14), we also asked that a RAT with both swabbing techniques (oral and nasal swabbing) and oral swabbing alone be performed sequentially in one session. Interestingly, all of the oral cavity RATs were negative (Figure 2). The RATs performed with the combinatorial swabbing technique echoed the results seen with the nasal cavity swabbing technique and were all positive. Notably, the signal intensity of the RATs on week four was higher than previous three weeks. Given that RATs are non-quantitative tests it is difficult to comment if this is caused by a better swabbing technique resulting in a greater amount of biological material applied to the RAT or a true increase in signal. In addition, a RAT from another supplier was performed in parallel on week one and resulted in a negative result. This echoes previous documented RATs from the participant outside of this study's timeframe where RAT from FlowFlex and Abbott remained negative despite a concurrent positive on BTNX RAT.

While the subject did not display any COVID-19 related symptoms at the time of taking the RATs, we still collected saliva samples to perform nucleic acid testing given that subclinical asymptomatic SARS-CoV-2 infections have been documented (15–18). The multiplex qPCR showed no detectable levels of SARS-CoV-2 N and E genes. An internal control (Human RPP30 gene) was also included to validate RNA extraction efficiency from the saliva. These data also align with the fact that no close contacts to the subject tested positive or developed COVID-19 related symptoms. In light of this, the possibility of an active SARS-CoV-2 infection was ruled out.

SARS-CoV-2 antigen deposition in various tissue following infection have been documented previously (19, 20). As such, we next investigated whether the positive RAT could be from deposited nucleocapsid protein from a prior infection. We measured IgG antibodies against the spike protein and the nucleocapsid of SARS-CoV-2 (Wuhan). We calculated an overall titer of 130.41 BAU/mL of anti-spike IgG antibodies, while antibodies against the N protein were below the seroprevalence threshold. Given the lack of antibodies recognizing the nucleocapsid, we can conclude that the spike antibodies are vaccine-elicited and that prior to performing the RAT, this subject had no serological markers suggesting a prior infection. While it is true that antibodies decay with time, it is unlikely that a RAT would detect true nucleocapsid protein without an associated detectable antibody response and/or a positive RT-PCR result.

The source driving the false positive signal on BTNX devices remains unclear. In principle, endogenous peptides could cross-react with BTNX RAT antibodies within the devices. It is also possible that cross-reactivity be driven by exogenous peptides from the microbiome. Given the proprietary nature of the antibodies used in each RATs by the various manufacturers, further investigation on how the antibody selection contributes to false positives is difficult. Anecdotally, the subject's children and family direct members did not generate a false positive result on RATs.

Conclusion

Continuous false positives can occur with RATs despite their overall high positive predictive value. A confirmatory RAT from another supplier could be used as confirmation. Molecular testing remains the gold standard to confirm active infections. Serological testing can rule out chronic or previous SARS-CoV-2 infections in the vast majority of cases. Increased awareness by the medical and public health community of the existence of individuals that continuously test positive is warranted to avoid unnecessary isolation periods and subsequent impact on an individual's mental health, family, professional activities, social and day-to-day life.

Data availability statement
The raw data supporting the conclusions of this article will be made available by the authors, without undue reservation.

Ethics statement
Ethical approval was obtained from the University of Ottawa REB (H-11-20-6172) for the studies involving humans. The studies were conducted in accordance with the local legislation and institutional requirements. The participants provided their written informed consent to participate in this study. Written informed consent was obtained from the individual(s) for the publication of any potentially identifiable images or data included in this article.

Author contributions
YG and M-AL wrote the manuscript. YG performed the serology experiments and created the figures. AX performed the qPCR experiments. AD provided participant coordination and sample collection. CC offered clinical perspective and insights. All authors contributed to the article and approved the submitted version.

Funding
M-AL holds a Faculty of Medicine Chair of Excellence in Pandemic Viruses and Preparedness Research. YG holds a Canadian Institute of Health Research (CIHR) Frederick Banting and Charles Best graduate scholarship (CGS-Doctoral, 476885). This study was supported in part by a COVID-19 Rapid Response grant by the Canadian Institute of Health Research (CIHR, VR2-172722) and by a grant supplement by the Canadian Immunity Task Force (CITF) to M-AL. The funding sources played no role in the study design, data collection, analysis, writing of the manuscript, and the decision to publish.

Conflict of interest
The authors declare that the research was conducted in the absence of any commercial or financial relationships that could be construed as a potential conflict of interest.

Publisher's note
All claims expressed in this article are solely those of the authors and do not necessarily represent those of their affiliated organizations, or those of the publisher, the editors and the reviewers. Any product that may be evaluated in this article, or claim that may be made by its manufacturer, is not guaranteed or endorsed by the publisher.

References

1. Honein MA, Christie A, Rose DA, Brooks JT, Meaney-Delman D, Cohn A, et al. Summary of Guidance for Public Health Strategies to Address High Levels of Community Transmission of SARS-CoV-2 and Related Deaths, December 2020. MMWR Morb Mortal Wkly Rep. 2020;69(49):1860-7.
2. Chen YT, Yen YF, Yu SH, Su EC. An Examination on the Transmission of COVID-19 and the Effect of Response Strategies: A Comparative Analysis. Int J Environ Res Public Health. 2020;17(16).
3. Blanchard AC, Desforges M, Labbé A-C, Nguyen CT, Petit Y, Besner D, et al. Evaluation of Real-life Use of Point-of-care Rapid Antigen Testing for SARS-CoV-2 in Schools (EPOCRATES): a cohort study. CMAJ Open. 2022;10(4):E1027-E33.
4. Schwartz KL, Bogoch, II, MacInTosh D, Barrow J, Sindrey D, Jha P, et al. SARS-CoV-2 rapid antigen screening of asymptomatic employees: a pilot project. Can J Public Health. 2022;113(6):898-903.
5. Government of Canada. Interim guidance on the use of rapid antigen detection tests for the identification of SARS-CoV-2 infection 2022 [Available from: https://www.canada.ca/en/public-health/services/diseases/2019-novel-coronavirus-infection/guidance-documents/use-rapid-antigen-detection-tests.html.
6. Eyre DW, Futschik M, Tunkel S, Wei J, Cole-Hamilton J, Saquib R, et al. Performance of antigen lateral flow devices in the UK during the alpha, delta, and omicron waves of the SARS-CoV-2 pandemic: a diagnostic and observational study. The Lancet Infectious Diseases. 2023.
7. Chu VT, Schwartz NG, Donnelly MAP, Chuey MR, Soto R, Yousaf AR, et al. Comparison of Home Antigen Testing With RT-PCR and Viral Culture During the Course of SARS-CoV-2 Infection. JAMA Internal Medicine. 2022;182(7):701-9.
8. Wölfl-Duchek M, Bergmann F, Jorda A, Weber M, Müller M, Seitz T, et al. Sensitivity and Specificity of SARS-CoV-2 Rapid Antigen Detection Tests Using Oral, Anterior Nasal, and Nasopharyngeal Swabs: a Diagnostic Accuracy Study. Microbiology Spectrum. 2022;10(1):e02029-21.
9. Gans JS, Goldfarb A, Agrawal AK, Sennik S, Stein J, Rosella L. False-Positive Results in Rapid Antigen Tests for SARS-CoV-2. JAMA. 2022;327(5):485-6.
10. Navero-Castillejos J, Casals-Pascual C, Narváez S, Cuesta G, Hurtado JC, Fernandez M, et al. Diagnostic Performance of Six Rapid Antigen Tests for SARS-CoV-2. Microbiology Spectrum. 2022;10(2):e02351-21.
11. Pickering S, Batra R, Merrick B, Snell LB, Nebbia G, Douthwaite S, et al. Comparative performance of SARS-CoV-2 lateral flow antigen tests and association with detection of infectious virus in clinical specimens: a single-centre laboratory evaluation study. The Lancet Microbe. 2021;2(9):e461-e71.
12. BTNX INC. COVID-19 Antigen Rapid Test Device [Available from: https://www.btnx.com/Product?id=2010.
13. Jüni P BS, Corbeil A, et al. Use of Rapid Antigen Tests during the omicron wave. Science Briefs of the Ontario COVID-19 Science Advisory Table. . 2022;3(56).
14. Ontario Government. Rapid testing for at-home use [Available from: https://www.ontario.ca/page/rapid-testing-home-use#section-2.
15. Jonczyk R, Stanislawski N, Seiler LK, Blume H, Heiden S, Lucas H, et al. Combined Prospective Seroconversion and PCR Data of Selected Cohorts Indicate a High Rate of Subclinical SARS-CoV-2 Infections—an Open Observational Study in Lower Saxony, Germany. Microbiology Spectrum. 2022;10(1):e01512-21.
16. Chen Y, Tong X, Wang J, Huang W, Yin S, Huang R, et al. High SARS-CoV-2 antibody prevalence among healthcare workers exposed to COVID-19 patients. Journal of Infection. 2020;81(3):420-6.
17. Suzuki T, Aizawa K, Shibuya K, Yamanaka S, Anzai Y, Kurokawa K, et al. Prevalence of Asymptomatic SARS-CoV-2 Infection in Japan. JAMA Network Open. 2022;5(12):e2247704-e.

18. Avanzato VA, Matson MJ, Seifert SN, Pryce R, Williamson BN, Anzick SL, et al. Case Study: Prolonged Infectious SARS-CoV-2 Shedding from an Asymptomatic Immunocompromised Individual with Cancer. Cell. 2020;183(7):1901-12.e9.
19. Gaebler C, Wang Z, Lorenzi JCC, Muecksch F, Finkin S, Tokuyama M, et al. Evolution of antibody immunity to SARS-CoV-2. Nature. 2021;591(7851):639-44.
20. Cheung CCL, Goh D, Lim X, Tien TZ, Lim JCT, Lee JN, et al. Residual SARS-CoV-2 viral antigens detected in GI and hepatic tissues from five recovered patients with COVID-19. Gut. 2022;71(1):226-9.

Supplementary Files

Methods

Sample Collection

Blood was collected using an SST vacutainer and serum was isolated after a 1300xg spin at 4°C for 5 minutes. The specimen was subsequently stored at 4°C until antibody levels were measured.

Measurements of antibody levels in sera

Antibodies were measured using a high-throughput direct chemiluminescent ELISA (full methods described previously). Briefly, SARS-CoV-2 antigens (spike ectodomain (Wuhan) with S1/S2 furin site mutations, prefusion stabilizing mutations and human resistin as a trimerization partner and nucleocapsid (amino acids 1–419 of YP_009724397)) were generously provided by Dr. Yves Durocher, National Research Council of Canada (NRC), Montréal. The assays were performed manually, in a 384 well format. Initially, 50ng /well of the antigen of interest diluted in PBS was coated in a high-binding polystyrene Nunc plate (Thermo Fisher Scientific, #460372) in a final volume of 10uL. The plates were then centrifuged at 216xg and incubated overnight at 4°C and then washed four times with 100uL of PBS-T. The plates were then blocked with 80uL of 3% w/v skim milk powder dissolved in PBST for 1 h and then washed (as described before). Samples or controls were diluted to the indicated dilution in 1% w/v skim milk powder dissolved in PBST and 10uL was added to the respective wells. Controls included a calibration curve anti-SARS-CoV-2 S CR3022 Human IgG1 (Absolute Antibody, Ab01680-10.0), Human anti-Nucleocapsid IgG (Genscript -HC2003 A02039)pooled human sera, and non-specific Ig control. After a 2h incubation, the plates were washed once more and 10uL of the secondary antibody was added to each well and incubated for another hour. Secondary antibodies used were anti-Human IgG#5-HRP (Dr. Yves Durocher, NRC) diluted 1 in 5400. After the incubation, plates were washed one last time and 10uL of ELISA Pico Chemiluminescent Substrate (Thermo Fisher Scientific #37069) diluted 1:2 in ddH_2O was added to each well and incubated for 5 minutes. Luminescent signal was measured on a Neo2 plate reader (Biotek) at 20ms/well at a read height of 1.0mm.

An antibody titer in international units (BAU/mL) was calculated as previously described. Briefly, the WHO international standard (20/136) was titrated and modelled using a four-parameter log-logistic regression with the DRC package in R. Blank adjusted luminescence values of the samples were scaled by dividing the values by the inflection point of the isotype-antigen specific calibration curve present in quadruplicate on each plate. Scaled luminescence values in the linear range were then converted to BAU/mL.

Measurement of Viral RNA in saliva

Saliva was collected using a saliva collection tube (DNA Genotek: OMNIgene·ORAL OM- 505) in the morning, prior to food or liquid intake. Tubes were kept at room temperature until they were processed for vRNA extraction using the QIA amp Viral RNA Mini Kit (Qiagen, Cat#52906) following the manufacturer's instructions with minor modifications. Prior to RNA extraction, all samples were incubated in a water bath at 50°C for 30 min prior to RNA extraction. 140µL of each sample was used for extraction in duplicate and the RNA was eluted with 60µL of AVE buffer. qPCR was performed using Reliance One-Step RT-qPCR Kit (Bio-Rad #12010176). Reactions were set up with 10 µL of RNA, 5 µL 4X Reliance RT-qPCR supermix, 1µL 20x primer/probe), and 4 µL of nuclease free water to a final reaction volume of 20 µL. A list of primers and probes used can be found below. A CFX96 Touch™ Real-Time PCR (Bio-Rad) instrument was used with the following conditions initial RT at 50°C, 60 minutes, followed by polymerase activation at 95°C for 10 minutes, and 40 cycles of denaturation, annealing/extension at 95°C/10 s, then 55°C/60 s, respectively.

N gene :

Probe : 5FAM/ACCCCGCAT/ZEN/TACGTTTGGTGGACC/3IABkFQ

Primer FWD : GACCCCAAAATCAGCGAAAT

Primer REV : TCTGGTTACTGCCAGTTGAATCTG

E gene :

Probe : 5TexRd-XN/ACACTAGCCATCCTTACTGCGCTTCG/3IAbRQSp

Primer FWD : ACAGGTACGTTAATAGTTAATAGCGT

Primer REV : ATATTGCAGCAGTACGCACACA

Human RPP30 :

Probe : 5HEX/TTCTGACCT/ZEN/GAAGGCTCTGCGCG/3IABkFQ

Primer FWD : AGATTTGGACCTGCGAGCG

Primer REV : GAGCGGCTGTCTCCACAAGT

Rapid antigen tests

A series of RATs was performed in parallel for 4 weeks. These included one RAT from BTNX (COV-19C25) performed in accordance with the manufacturer's instructions (anterior and deep nasal swabbing), one RAT from BTNX (COV-19C25) performed by swabbing the oral cavity (throat and cheeks), and one RAT from BTNX (COV-19C25) performed with a combination or nasal and oral swabbing. BTNX RATs used in the timeframe of this study had the following lot numbers: I2203054, I2202101, I2202287, I2201363. In addition, for the first week, an additional RAT from FlowFlex (L631-118B5) was performed following the manufacturer's recommendations. ImageJ was used to quantify band intensity from the RATs photos : (band intensity / Control band intensity) x100%

CHAPTER 4 –IMPACT OF PREVIOUS SEASONAL CORONAVIRUSES INFECTION

RATIONALE

Human seasonal coronaviruses, notably 229E, HKU-1, NL63, and OC43, are viruses that commonly infect human populations. These viruses typically cause mild, cold-like upper respiratory infections and are endemic to the human population, with most individuals first exposed during early childhood (203, 204). Interestingly, a longitudinal study by Edridge et al., which followed individuals from 1985 to 2020, demonstrated that reinfection is frequent, occurring approximately every 12 months, with some cases of reinfection observed as early as six months after the previous exposure (64). Consequently, nearly everyone possesses some degree of pre-existing immunity to seasonal coronaviruses.

Although SARS-CoV-2 shares relatively low overall homology with seasonal coronaviruses, certain antigens exhibit a higher degree of sequence similarity. For example, the S2 domain of the spike protein in HKU-1 shares 41.2% amino acid sequence homology with that of SARS-CoV-2. Beyond the S2 domain, the nucleoprotein is also relatively conserved across coronaviruses. These similarities raise important questions about the extent of cross-reactivity between antibodies generated in response to seasonal coronaviruses and those targeting SARS-CoV-2. This cross-reactivity has implications not only for the specificity and performance of SARS-CoV-2 serological assays but also for understanding whether pre-existing, cross-reactive immunity may offer some level of protection.

The present study was conducted on a large number of pre-2019 serum samples (from individuals unexposed to SARS-CoV-2) to quantify the extent of cross-reactivity with seasonal coronaviruses and to assess their neutralizing potential against SARS-CoV-2.

4.1 Relative ratios of human seasonal coronavirus antibodies predict the efficiency of cross-neutralization of SARS-CoV-2 spike binding to ACE2

Preface

(This work has been previously published as a research article)

Galipeau Y, Siragam V, Laroche G, Marion E, Greig M, McGuinty M, Booth RA, Durocher Y, Cuperlovic-Culf M, Bennett SAL, Crawley AM, Giguère PM, Cooper C, Langlois MA. **Relative Ratios of Human Seasonal Coronavirus Antibodies Predict the Efficiency of Cross-Neutralization of SARS-CoV-2 Spike Binding to ACE2**. EBioMedicine. 2021 Dec;74:103700. doi: 10.1016/j.ebiom.2021.103700.

© 2021 The Authors. Published by Elsevier B.V. This is an open access article under the CC BY-NC-ND license (http://creativecommons.org/licenses/by-nc-nd/4.0/)

Abstract

Background
Antibodies raised against human seasonal coronaviruses (sCoVs), which are responsible for the common cold, are known to cross-react with SARS-CoV-2 antigens. This prompts questions about their protective role against SARS-CoV-2 infections and COVID-19 severity. However, the relationship between sCoVs exposure and SARS-CoV-2 correlates of protection are not clearly identified.

Methods
We performed a cross-sectional analysis of cross-reactivity and cross-neutralization to SARS-CoV-2 antigens (S-RBD, S-trimer, N) using pre-pandemic sera from four different groups: pediatrics and adolescents, individuals 21 to 70 years of age, older than 70 years of age, and individuals living with HCV or HIV. Data was then further analysed using machine learning to identify predictive patterns of neutralization based on sCoVs serology.

Findings
Antibody cross-reactivity to SARS-CoV-2 antigens varied between 1.6% and 15.3% depending on the cohort and the isotype-antigen pair analyzed. We also show a range of neutralizing activity (0-45%) with median inhibition ranging from 17.6 % to 23.3 % in serum that interferes with SARS-CoV-2 spike attachment to ACE2 independently of age group. While the abundance of sCoV antibodies did not directly correlate with neutralization, we show that neutralizing activity is rather dependent on relative ratios of IgGs in sera directed to all four sCoV spike proteins. More specifically, we identified antibodies to NL63 and OC43 as being the most important predictors of neutralization.

Interpretation
Our data support the concept that exposure to sCoVs triggers antibody responses that influence the efficiency of SARS-CoV-2 spike binding to ACE2, which may potentially impact COVID-19 disease severity through other latent variables.

Funding
This study was supported by a grant by the CIHR (VR2 -172722) and by a grant supplement by the CITF, and by a NRC Collaborative R&D Initiative Grant (PR031-1).

Research in Context

Evidence before this study

There is a growing body of evidence showing that within the population there are varying levels of pre-existing immunity to SARS-CoV-2 infection and possibly COVID-19 disease severity. This immunity is believed to be attributable in part to prior infection by four prevalent seasonal coronaviruses (sCoVs) responsible for the common cold. Pre-existing immunity can be assessed by measuring antibodies directed to sCoVs that also cross-react to SARS-CoV-2 antigens. The SARS-CoV-2 spike and, more specifically, the receptor binding domain are the primary targets for neutralizing antibodies. It is unclear to what extent cross-reactive antibodies to SARS-CoV-2 have neutralizing potential and whether they contribute to COVID-19 disease severity.

Added value of this study

Here we carried out a detailed analysis of sCoVs seroprevalence in samples acquired before the pandemic from individuals of various age groups and in people living with HIV and HCV. We then analyzed the frequency of all the different types of antibodies that cross-react to three SARS-CoV-2 antigens. We found a high number of people with cross-reactive antibodies, surprisingly we also observed that some people have antibodies that block the SARS-CoV-2 spike from binding to its human receptor, ACE2. By using *in vitro* and *in silico* methods such as machine learning, we were able to accurately predict which individuals can neutralize SARS-CoV-2 spike-ACE2 interactions based on their relative ratios of antibodies against the four sCoVs.

Implications of all the available evidence

We demonstrate that it is not absolute levels of sCoVs antibodies that are predictive of neutralization but the relative ratios to all four sCoVs, with NL63 being the most weighted for this prediction. Machine learning also highlighted the existence of latent variables that contribute to the neutralization and that may be related to cellular immune responses triggered by the infection of certain sCoVs. This study is one of the first to identify a functional relationship between prior-exposure to sCoVs and the establishment of a certain degree of neutralization to SARS-CoV-2 spike-ACE2 interactions by way of cross-reactive antibodies.

Introduction

Four endemic human sCoVs (229E, OC43, NL63, and HKU1) are highly prevalent worldwide and cause common and recurrent respiratory infections [1–3]. A retrospective prevalence study of acute respiratory infections in France found that OC43 is the most prevalent sCoV followed by NL63, HKU1, and finally 229E [4]. While nearly every adult has been exposed and demonstrates humoral responses to one or several of these sCoV [5–7], immunity to each specific sCoV wanes over time. A 35-year longitudinal study revealed that reinfections by a same sCoV were regularly observed at 6 and 9 months post-infection, but most were most frequently observed after 12 months [3]. These findings highlight that sterilizing immunity to these viruses is short-lived and that the relative ratios of antibodies against any one of the four sCoVs is highly variable and dependent on the most recent exposure. This study also indicates that exposure to one sCoV does not offer complete protection against infection by the other viruses, but it is unclear how prior immunity affects disease severity.

Seasonal CoVs generally share an overall low degree of sequence similarities with SARS-CoV-2 proteins and only the alphacoronavirus NL63 also utilizes ACE2 as an entry receptor [8,9]. Nevertheless, conserved epitopes on the spike S2 domain are believed to be responsible for antibody and T-cell cross reactivity between sCoVs and other human betacoronaviruses such as SARS-CoV-1, SARS-CoV-2 and MERS-CoV [10–14]. Furthermore, the nucleocapsid (N) is one of the most conserved antigens across all human CoVs [15]. In fact, antibodies against sCoV antigens impede the specificity of serological tests against SARS-CoV-2 when full length S-trimer and N antigens are used in the assay (reviewed here: [16]). While neutralizing activity directed against the SARS-CoV-2 S protein, more specifically the receptor binding domain (S-RBD), have been extensively described, non-RBD neutralizing epitopes have also been identified on both the S1 and S2 subunits [17–20]. Furthermore, antibodies can exhibit non-neutralizing effector functions such as ADCC and complement-fixing that restrict SARS-CoV-2 infection by binding to viral protein epitopes expressed on the surface of infected cells, including S and N antigens [21–24].

While antibody and T-cell responses of SARS-CoV-2 convalescent individuals have been well characterized [24–26], the influence of pre-existing immunity, both humoral and cellular, from exposure to sCoVs is not yet clearly established. Several recent studies have investigated the impact of prior immunity to sCoVs on SARS-CoV-2 infection, neutralization, and disease severity [1,6,10,12,27-31], discordance in the findings remains. Some studies have shown weak or no cross-protective antibodies in pre-pandemic blood of donors *in vitro* [1,6,31], while several other studies have demonstrated various lines of evidence for antibody and T cell cross-neutralization, and even protection against COVID-19 disease severity [10,14,25,29,32-34].

Here, we assessed the seroprevalence of sCoVs, along with the neutralization activity and cross-reactivity to the S-trimer, S-RBD and N of SARS-CoV-2, in pre-COVID-19 pandemic sera across four study groups. Our results provide insight into population subgroup variations in the seroprevalence of the four sCoVs, antibody isotype-specific cross-reactivity to SARS-CoV-2 spike (S-trimer), nucleocapsid (N), the receptor binding domain (S-RBD). We also assessed the neutralizing potential of antibodies in pre-pandemic serum that interfere with S binding to the ACE2 receptor. While neutralization of S-trimer binding to ACE2 was detected to various degrees, this activity remained low compared to the neutralizing potential resulting from SARS-CoV-2 infection. However, using several machine learning approaches, we were able to identify a functional dependence on prior sCoV exposure that includes both directly measured and latent variables. These enabled us to model neutralization via Gaussian process regression (GPR) using sCoV seroprevalence data. In agreement to previous studies, we do not find a direct correlation between sCoV antibody levels and the intensity of the neutralization [1,32,35]. However, we do identify a strong predictive correlation between neutralization of S binding and relative ratios of antibodies directed against the different sCoVs. These data support the concept that latent variables associated with sCoV exposure have a predictive and protective role against SARS-CoV-2 infection and possibly disease severity.

2 Materials and Methods

2.1 Ethics statement

Use of human samples for this study was approved by the University of Ottawa Ethics Review Board: Certificates H-04-20-5727, H-04-21-6643 and H-07-20-6009. Informed consent was provided by all participants

.

2.2 Pre-pandemic cohort

The current study collected pre-pandemic serum or plasma samples separated into four cohorts for a total of 580 enrolled patients. The cohorts selected for inclusion in this study are described in (Table 1), any serum or plasma samples collected prior to SARS-CoV-2 spread in Ottawa with corresponding demographic information was eligible for inclusion. Specimens with insufficient volume (<100µL) were excluded. Serum and plasma samples were sourced from multiple locations including the Eastern Ontario Regional Laboratory Association (EORLA), the Ottawa Hospital (TOH), and the Icahn School of Medicine at Mount Sinai. Specimens were collected between April 1 2015 and March 4 2020. All the pre-pandemic patient samples were obtained prior to the COVID-19 pandemic in Ottawa. Pediatric samples were acquired from the BC Children's Hospital Biobank (BCCHB) in Vancouver, BC, Canada (REB#: H-07-20-6009). Due to potential impact of immunosuppression and chronic viral infection on seroprevalence of sCoV antibodies and cross-reactivity, sera from individuals living with HIV and HCV was obtained from The Ottawa Hospital (TOH) and Ottawa Hospital Research Institute (OHRI). The patient's demographic information and clinical outcomes were obtained from hospital records.

2.3 Pandemic samples

As a reference group for the neutralization and seasonal CoVs serology experiments, serum samples from individuals post-2019 were used. Samples were acquired within several different research studies and separated by their provenance. The control group for the neutralization (Fig. 5) were individuals hospitalized for SARS-CoV-2 infection (mild and severe) and were further separated by day post positive PCR test. The individuals for reference group in Figure 1 were convalescent individuals with a PCR-confirmed history of SARS-CoV-2 infection. The antibody levels of this group were monitored using the same protocol and platform

used to assess the seroprevalence of sCoVs but probed using SARS-CoV-2 S-trimer. The negative reference group was comprised of individuals with no history of SARS-CoV-2 infection who are currently enrolled in an ongoing SARS-CoV-2 surveillance study. Basic demographic information was collected and combined in Table S1. Any serum samples acquired within the mentioned studies with corresponding informed consent and demographic information were eligible. Vaccinated individuals and samples with no clear identification or low volume were excluded.

Table 1 Demographic information of each pre-pandemic cohort. Serum and plasma samples collected pre-2019 were organized in four distinct cohorts. Basic demographic information was collected and compiled from patient files.

Cohorts	# of Subjects	Age range (yrs)	Female % (Mean Age ±SD)	Male % (Mean Age ± SD)
< 21 yrs	193	1-20 yrs	40% (9 ±6 yrs)	60% (8 ± 5 yrs)
21-70 yrs	273	21-70 yrs	55% (51 ±14 yrs)	45% (53 yrs ±12yrs)
> 70 yrs	64	71-97 yrs	56% (80 ±7 yrs)	44% (79 ±7 yrs)
HCV & HIV	50	18-80 yrs	41% (51 ± 18 yrs)	59% (57±13 yrs)

Abbreviations: SD, standard deviation.

2.4 Detection of anti-SARS-CoV-2 Responses in Serum Samples by ELISA

A detailed account of the ELISA assay and methods used in this study is available here [36]. Antibody responses in pre-pandemic serum samples of all four cohorts were tested for the presence of cross-reactive antibodies of the main isotypes (IgA, IgM, IgG, and IgE) and IgG subtypes (IgG1, IgG2, IgG3, and IgG4). SARS-CoV-2 antigens S-trimer, S-RBD, and N were diluted in sterile 1X PBS (Multicell #311-010-CL) to 2 µg/mL and used to coat a 96-well plates (VWR #62402-959) using a volume of 50µL and incubated on a 4°C shaker overnight. The next day, the plates were washed three times with PBS-T and were subsequently blocked with buffer (PBS-T + 3% non-fat milk powder) for one hour. The patient serum samples were diluted 1/50 in dilution buffer [1X PBS + 0.1% Tween (Fisher #BP337-500) (PBS-T), + 1% non-fat milk] in a final volume of 100µL

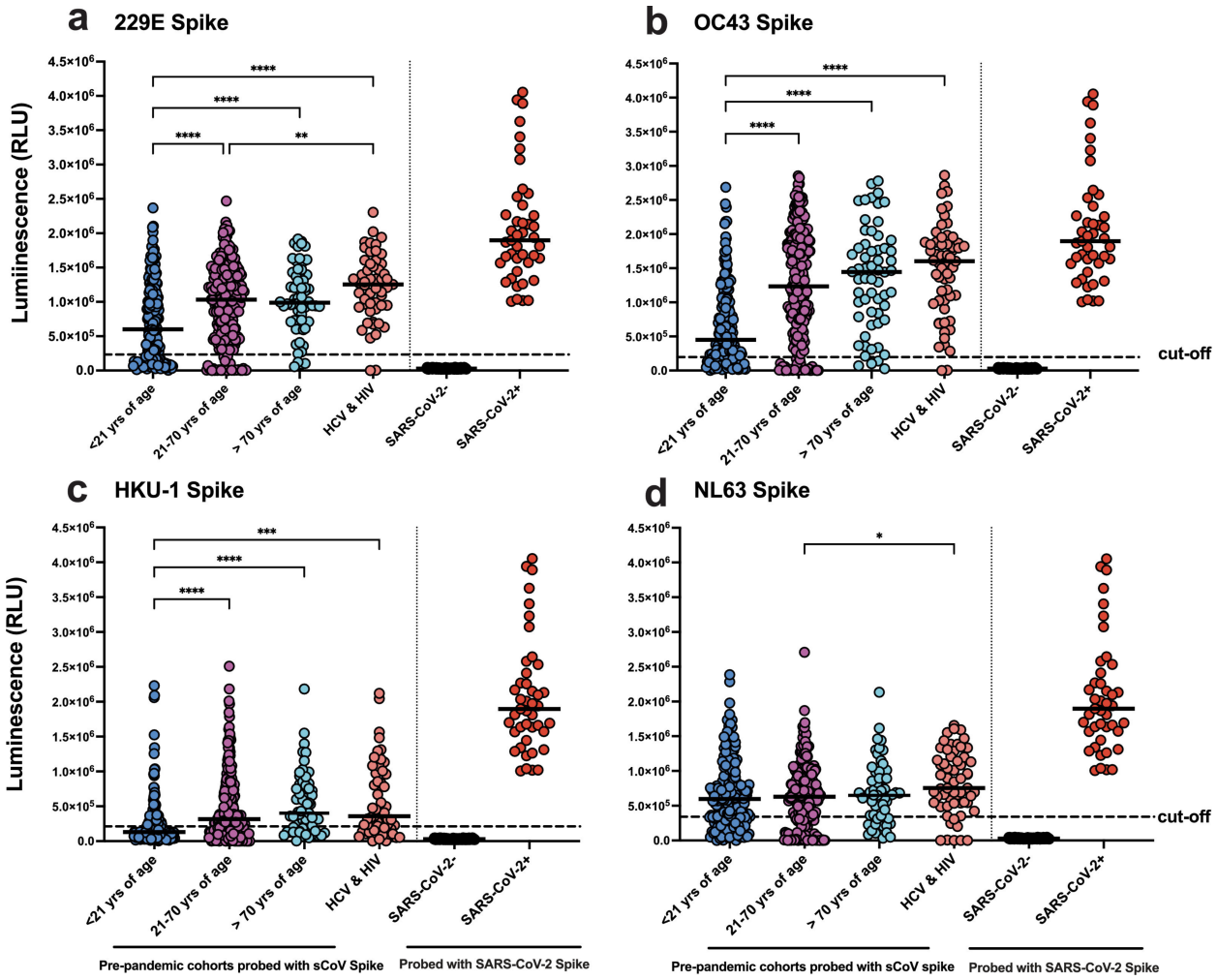


Figure 1 Seroprevalence of human CoVs. ELISA was used to detect spike (S-trimer) specific IgG antibody responses of four sCoVs: 229E (a), OC43 (b), HKU1 (c) and NL63 (d). Four different cohorts of Pre-COVID-19 pandemic serum and plasma samples were analyzed: < 21 yrs of age [n=193], 21-70 yrs of age [n=251, serum was insufficient to perform all tests on 22 of the entire 273 person cohort], > 70 yrs of age [n=60, serum volume was insufficient to perform all tests on 4 of the entire 64 person cohort], and persons with HCV or HIV [n=50 of which 9 patients were sampled twice at 6 or 12 months intervals for n=59 samples]. Demographics are in Table S1. Note in each panel the same control groups are presented as a range comparison. Controls were SARS-CoV-2 negative individuals from a surveillance study [n=115] and SARS-CoV-2 PCR-confirmed individuals [n=43] challenged against the SARS-CoV-2 S-trimer protein. Demographics of the pandemic cohorts are in Table S1. Dotted lines represent the cut-off values calculated from seronegative pediatric samples (Fig. S1). Statistics were one-way ANOVA with Welch correction and Games Howell *post hoc* multiple comparisons test for pairwise differences. *p<0.05, **p<0.01, ***p<0.001, ****p<0.0001.

Accordingly, the control calibration antibodies were prepared with appropriate dilutions to generate the calibration curve (anti-COVID Ig). The dilutions for each curve were as follows: total IgG and IgG1 1/5000 followed by 1:2 serial dilutions; IgM, IgA, and IgG2 1/4000 followed by 1:2 serial dilutions; and IgG3 and IgG4 1/10,000 followed by 1:2 serial dilutions. Blocking solution on ELISA plates was removed after one hour followed by the addition of 100µL of the diluted serum samples and control antibodies to the appropriate wells. The plates were incubated with samples for two hours at room temperature (RT) on a shaker (700rpm). After two hours, the plates were washed three times with 200µL PBS-T followed by the addition of secondary-HRP antibodies (1:3000) diluted in dilution buffer. 50µL of the appropriate diluted secondary antibody-HRP was added to each well and the plates were incubated at RT with shaking (700rpm). After one hour of incubation, the plates were washed four times and developed using OPD tablets (Sigma, P9187) dissolved in 20mL of water for infection (WFI) (Thermo Fisher A1287301). After ten minutes incubating in the dark, 50µl of 3M HCl (Fisher #7647-01) was added to each well to stop the reaction and the optical density (OD) at 490nm was measured using a BIO-TEK Power Wave XS2 Plate Reader. Wells filled with dilution buffer in place of serum represented background controls and were subtracted from the patient serum values.

2.5 Calculation of Cut-Off Values

To establish consistent and unbiased cut-offs, a systematic approach for each combination of antigen and isotype was used. Using the blank subtracted values from the serological assays a preliminary cut off was established at 2 standard deviations (2SD) of the mean of all values. Values over that threshold were then excluded from further calculation of the final cut-off. To establish the final cut-off, the mean and standard deviation were recalculated using exclusively values under the preliminary cut-off. A final cut-off was then established at 2SD of the mean of the distribution under the preliminary cut-off. Values over that final cut-off value were considered positive (ratio to cut-off higher than 1) and values under the final cut-off were considered negative.

To establish the seasonal coronavirus cut-offs, a set of pediatric samples aged between 1-2 years old was used as the reference population due to the high prevalence of seropositivity in adults. The same two pass exclusion strategy at 2SD of the mean was used on that reference group as described above.

2.6 Surrogate Neutralization ELISA (snELISA) assay

To evaluate neutralization activity against the SARS-CoV-2 S protein, we carried out a surrogate neutralization ELISA (snELISA) [25]. Detailed methods for the snELISA are available here [36]. This neutralization assay was performed using 384-well Immuno plates (Thermofisher, 460372) coated with full length SARS-CoV-2 S-trimer protein diluted in PBS (30µL/well of 2µg/mL), followed by an overnight rotating incubation at 4°C. The next day, plates were washed two times with 50µl of PBS-T and further incubated with 40µL blocking buffer for one hour on a plate shaker at a speed of 400 rpm. After incubation the plates were washed with PBS-T followed by the addition of pre-COVID-19 serum patient samples diluted 1:4 in dilution buffer (20 µL/well). The plates were further incubated for one hour and washed three times with PBS-T. Biotinylated ACE2 was diluted in dilution buffer to 0.05ng/µL, followed by 20 µL being added to each well (1 ng/well) and a one-hour incubation (400 rpm). After incubation the plates were washed three more times with PBS-T followed by incubation with 20µL of 5ng/µL Streptavidin-Peroxidase polymer diluted in dilution buffer (Sigma#S2438) for 1 hr at 400 rpm. After incubation the plates were washed three times with 60µL of PBS-T. 20µL of SuperSignal ELISA Pico Chemiluminescent substrate diluted 1:2 in PBS was added to each well to measure the luminescence (RLU) signal. Neutralizing activity was determined by calculating the % inhibition against SARS-CoV-2 S proteins using the following equation:

*% Inhibition = 100 – [(average mean of the serum sample/control median)*100].*

2.7 Statistical and Machine learning analyses

Data analysis was conducted using GraphPad Prism v9, R and Matlab 2021a (Matworks Inc.). Univariate analysis was performed using one-way or two-way ANOVA where appropriate. Welch corrections were applied to all analyses. *Post* hoc tests were Games-Howell's multiple comparisons when group sizes were greater than 50 or Dunnett T3 when less than 50. Sample clustering was performed using fuzzy c-means (FCM) clustering method (fcm function running under Matlab). FCM allows each feature to belong to more than one group by providing a degree of membership, "belonging", to each cluster through maximizing proximity between similar features and distance between dissimilar features. FCM is based on the minimization of the objective function: $J_m = \sum_{i=1}^{N}\sum_{j=1}^{C} u_{ij}^{m} \| x_i - c_j \|^2$ where $m \in (1, \infty)$ is the "fuzzyfication" factor (with m=1 equating FCM to crisp K-means clustering), u_{ij}^{m} is the membership degree for feature x_i to the

cluster *j* with c_j defining the cluster center. Higher membership value indicates stronger belonging to the cluster with membership value of 1 indicating that feature is only associated with the single cluster. Sample clustering was based on serum antibody cross-reactivity to SARS-CoV-2 antigens (N, S-RBD, S-trimer) for IgA, IgM and IgG and capacity of these antibodies to inhibit Spike-ACE2 binding measured for 507 samples. FCM clustering fuzzyfication factor *m* was 1.3 with FCM optimization running until minimum improvement in objective function is $1e^{-5}$.

Correlation analysis was performed using Pearson and Signed distance correlation metrics calculated on z-score normalized features within each group divided into Responders and combined set of Non-responders and Partial responders. Signed distance correlation was performed using an in-house Matlab routine based on the distance correlation method presented by Szekely and Rizzo (35) with correlation signs derived from Pearson correlation analysis. Distance correlation *p*-values were calculated using Student's *t* cumulative distribution function (tcdf function in Matlab). Correlation was determined for 507 samples. Out of this set 12 samples were missing measurements for sCoV. Therefore, correlation calculations were performed both for only 495 samples excluding samples with missing data and for KNN imputed dataset (with N=10 using Euclidean distance). Two approaches obtained the same result. Both Pearson and Distance correlations with $p<0.05$ and absolute value above 0.2 were shown in the Figure 5. Correlation was performed separately for Responder group (Neutralization value ≥ 26%) and remaining subjects (Neutralization value <26%). Shown are correlation values for the responder group. Group of Nonresponders and Partial responders had no correlation for the represented groups at shown threshold levels.

Feature selection was performed using machine learning method Relieff (36). Relieff predicts classification rank, i.e. within the group significance, for each feature in the training set classification, of serum antibody cross-reactivity to 4 different SARS-CoV-2 antigens (N, S-RBD, S-trimer) for IgA, IgM and IgG and separately for antibodies for seasonal viruses (OC43, HKU-1, 229E, NL63). Relieff provides feature selection for classification, i.e. regression, to a continual variable in this case the % inhibition of ACE2-Spike protein interaction. Relieff ranks predictor features by weight for regression to response vector. Negative predictor weight indicates that this is not a good predictor feature and large positive weights are assigned to important predictors.

Feature weight decreases if it differs from that of features in nearby instances of the same class more than nearby instances of the other class.

Gaussian process regression (GPR) method was used for the development of a model of percent inhibition of ACE2-Spike protein interaction from the antibody levels for seasonal viruses. GPR is a nonparametric, probabilistic model that introduces latent variables as a function of measured features (here viral vectors) where the new feature function, $f(x)$, has joint Gaussian distribution (for all features) with optimized kernel that is used to ensure feature distance dependent correlation. Optimized model is: $y = h(x)^T\beta + f(x)$ - where y is the fitted function (target), x are the variables in this case measurement of seasonal virus antibodies, $h(x)$ are a set of basis functions that transform the original feature vector x and β is the vector of basis function coefficients, weights, for contribution of $h(x)$ to the model. Kernel function used in the model was rational quadratic following optimization. Both feature selection and GPR were performed for 507 samples. GPR provides the regression model with confidence interval as well as predictor weights for the model.

Sample classification was performed using two-layer neural network analysis with 10 hidden neurons and trained with Levenberg-Marquardt backpropagation algorithm with cross-validation with 70% training, 15% test and 15% validation sample division. Classification was performed with sample labels as responsive and non-responsive and using seasonal virus measurements only

2.8 SARS-CoV-2 ELISA Antigens and Antibodies

To evaluate the functional antibody responses of sCoV antibodies against different SARS-CoV-2 proteins, SARS-CoV-2 S-trimer, S-RBD, and N proteins were used as coating antigen (see antigen production). The following secondary and control antibodies were used during ELISA experiments. Secondary antibodies: Anti-human IgG-HRP (NRC anti-hIgG#5-HRP fusion), anti-human IgA-HRP RRID:AB_2337580 (Jackson ImmunoResearch, 109-035-011), anti-human IgM-HRP RRID:AB_2337588 (Jackson ImmunoResearch 109-035-129), anti-human IgE-HRP RRID:AB_258466 (Sigma A9667-2ML), anti-human IgG1-HRP RRID:AB_2796627 (Southern Biotek 9054-05), anti-human IgG2-HRP RRID:AB_2796633 (Southern Biotek 9060-05), anti-human IgG3-HRP RRID:AB_2796699 (Southern Biotek, 9210-05), and anti-human IgG4-HRP

RRID:AB_2796691 (Southern Biotek, 9200-05). Control antibodies: Anti-SARS-CoV-2 S CR3022 Human IgG1 (Absolute Antibody, Ab01680-10.0), Anti-SARS-CoV-2 S CR3022 Human IgA (Absolute Antibody, Ab01680-16.0), Anti-SARS-CoV-2 S CR3022 Human IgM (Absolute Antibody, Ab01680-15.0), Anti-SARS-CoV-2 S CR3022 Human IgE (Absolute Antibody, Ab01680-14.0), Anti-SARS-CoV-2 S CR3022 Human IgG1 (Absolute Antibody Ab01680-10.0), Anti-SARS-CoV-2 S CR3022 Human IgG2 (Absolute Antibody Ab01680-11.0), Anti-SARS-CoV-2 S CR3022 Human IgG3 (Absolute Antibody Ab01680-12.1), and Anti-SARS-CoV-2 S CR3022 Human Ig4 (Absolute Antibody Ab01680-13.12).

2.9 Presence of Reactive IgGs to sCoVs

To determine if the pre-COVID-19-pandemic sera contained IgGs against the four sCoVs, the S-trimer proteins of 229E and NL63 were purchased from creative diagnostics (DAGC134-HCoV-229E; DAGC133-NL63), while OC43 and HKU1 S-trimer proteins were produced for the study (see Antigen Production below). Using our High Throughput Serological Platform (Hamilton Microlab Star, Biotek 405Ls) we automated the Elisa protocol described in this paper with slight modifications. The serological assay was performed in 384 high binding plates (Thermo Fisher, 460372) using a volume of 12.5 µL to coat each well. Plates were blocked using 80µL of blocking buffer per well. The concentration of antigen, antibodies, and sample diluents were kept as above, although the volume was reduced to 10µL per well. To develop the plates a luminescent substrate (Thermo Fisher, 37069) was used and RLU measured by a Biotek Neo2 plate reader.

2.10 Antigen Production

To produce the S-RBD of SARS-CoV-2 a plasmid encoding the S-RBD (MN908947) containing amino acid 319-541 with an N-terminal secretory protein sequence was generously given to us by Dr Florian Krammer (Mount Sinai, NYC). The 229E S-RBD (P15423) was cloned in pCAGGs plasmid with a hexa-his Tag (C-term) with secretory signal (N-term) and transfected into 293F cells RRID:CVCL_D603 maintained in Freestyle 293 expression media (Thermo Fisher, 12338018) at 37°C, 7% CO2, with shaking (125rpm). A total of 600 millions cells in 200mL of media were transfected with 200µg of the respective plasmid using ExpiFectamine (Thermo Fisher, 14525). Three days post-transfection the cells were spun down at 4000g for 20min at 4°C and supernatants filtered through a 0.22µm stericup vacuum filter (Millipore Sigma,

S2GPU10RE). The filtered supernatant was purified using a Ni-NTA resin (Qiagen, 30210), and washed four times with a washing buffer containing 20nM imidazole. The protein of interest was then eluted with three column volumes of the elution buffer containing 234mM of imidazole. The eluted volume was concentrated and the buffer exchanged for PBS using a 10kDa Amicon filter (Millipore Sigma, UFC901008). The concentration was measured and integrity verified by SDS-Page.

The spike ectodomain (SARS2: MN908947; OC43: AAT84362.1; HKU1: Q0ZME7.1) cDNA constructs with furin site mutated, two stabilizing prefusion proline mutations, the human resistin as trimerization partner and a C-terminal FLAG-(His)6 (SARS2) or FLAG-Twin Strep Tag-(His)6 (OC43 and HKU1) tag were cloned into pTT241 vector and transfected in CHO2353 to generate stable pools. SARS-CoV-2 spike was purified by IMAC as described previously while OC43and HKU1 spikes were purified by IMAC followed by StrepTrap HP (Cytiva) affinity chromatography according to the manufacturer's instructions. All purification steps were performed at room temperature. Integrity and purity of the purified spikes was analyzed by SDS-PAGE and analytical size-exclusion ultra-high performance liquid chromatography (SEC-UPLC).
The nucleocapsid (SARS2: YP_009724397; OC43: AY391777; HKU1: HM034837) cDNAs with a C-terminal FLAG-Twin Strep Tag-(HisG)6 tag were synthesized by Genscript (*Cricetulus griseus* codon bias) and cloned in the cDNA into pTT5™ expression plasmid. Expression was achieved by transient gene expression in CHO55E1 cells [39] using polyethylenimine as a transfection reagent. The protein was purified from the clarified cell culture supernatant harvested at day 7 post-transfection. Following centrifugation and filtration, clarified supernatant was loaded on a Nickel Sepharose Excel column (Cytiva Life Sciences). The column was washed with 50 mM sodium phosphate buffer pH 7.0 containing 25 mM imidazole and 300 mM NaCl and protein was eluted with 50 mM sodium phosphate buffer pH 7.5 containing 300 mM imidazole and 300 mM NaCl. Nucleocapsid protein was further purified by affinity chromatography on a StrepTrap™ XT column (Cytiva Life Sciences) equilibrated in 100 mM Tris pH 8.0, 150 mM NaCl (Buffer W). Following washing with 5 column volumes of Buffer W, bound proteins were eluted with Buffer W containing 50 mM biotin and 1 mM EDTA. Purified nucleocapsid protein was buffer exchanged in DPBS using a Centripure P100 column, sterile-filtered through 0.2 µm membrane, aliquoted and stored at -80°C. All purification steps were performed at room temperature. Integrity and

purity of the purified nucleocapsid was analyzed by SDS-PAGE and analytical size-exclusion high performance liquid chromatography (SEC-HPLC).

The human ACE2 (Q9BYF1: aa 20-613: TIEE…WSPY) cDNA with an N-terminal human interleukin-10 signal peptide (MHSSALLCCLVLLTGVRA) followed by a Twin-StreptagII – (His)6 – FLAG tag was synthesized by Genscript with codon-optimization for expression in CHO cells. A biotin acceptor peptide sequence (BAP: GLNDIFEAQKIEWHE) was added in-frame at the C-terminus of ACE2. The cDNA was cloned into pTT5 and ACE2-BAP cDNA was expressed by transient gene expression in CHO55E1 cells as described above with the addition of 5% (w:w) of pTT5-BirA (*E. coli* biotin ligase) expression plasmid. Clarified culture supernatant harvested at 8 days post-transfection was purified by IMAC on nickel Sepharose excel as described above. IMAC eluate was loaded on a Strep-Tactin XT Superflow (IBA, Gottingen, Germany), following manufacturer's instructions. Pooled Strep-Tactin eluate (buffer-exchanged into DPBS) was stored at -80°C.

2.11 Role of funding source

The funding sources played no role in the study design, data collection, data analysis, interpretation, writing of the report, and the decision of paper submission.

3 Results

3.1 Exposure to all four sCoVs is endemic throughout the population

We acquired human serum and plasma samples, drawn prior to 2019, thus ensuring no previous exposure to SARS-CoV-2. We performed a cross-sectional profiling where a total of 580 patients were grouped into four cohorts based on age and viral infection. Cohorts were: pediatric samples of children and young adults less than 21 years of age (n=193), adults 21-70 yrs of age (n=273), adults greater than 70 years of age (n=64), and individuals living with HCV or HIV (n= 50) of whom nine were followed longitudinally (Table 1). Nine patients received two longitudinal blood draws and sCoV seroprevalence was assessed at both time points (separated by 6-12 months) for

a total of 589 samples. Each cohort was sex-balanced with mean age equivalence across sexes (Table 1).

We first investigated the prevalence of pre-exposure to the endemic sCoVs in the pre-COVID-19-pandemic cohorts (Fig. 1). Although the four sCoVs (HCoV-OC43, HCoV-229E, HCoV-HKU1, and HCoV-NL63) are prevalent worldwide [40], there seems to be a pattern of reinfections by sCoVs that cycles every 12 months [3]. We screened pre-COVID-19 serum samples for sCoV anti-S IgG (229E, OC-43, HKU1, and NL63) using our high-throughput ELISA platform [41,42]. As a reference to frame the dynamic range of our assays, SARS-CoV-2 anti-S data of confirmed negative (pandemic) (n=115) and SARS-CoV-2 PCR-confirmed positive samples (n=43) is presented (Table S1). Our results show that a majority of pre-pandemic samples were seropositive for IgG antibodies against OC43, NL63, and 229E S proteins (Fig. 1 and Table 2).

Table 2 Seroprevalence of seasonal coronavirus (OC43, HKU1, 229E and NL63) IgG antibodies and IgG cross reactivity to SARS-CoV-2 antigens by cohorts. False discovery rate (FDR) was used to describe the percentage of cross reactivity by single and a combination of antigen (S-RBD, N, S-trimer). Combined weighted cross reactivity and seroprevalence is also shown.

Cohorts	**sCoV Prevalence (%)**				**SARS-CoV-2 IgG FDR (%)**						
					Single antigen			**Two antigens**			**Three antigens**
	OC43	**HKU-1**	**NL63**	**229E**	**RBD**	**S**	**N**	**RBD + S**	**RBD +N**	**S +N**	**RBD + S + N**
HCV & HIV	96.6	72.9	86.4	96.6	8.47	6.78	15.3	1.69	3.39	1.69	0.00
> 70 Yrs	93.3	71.7	73.3	93.3	1.56	1.56	14.1	0.00	0.00	0.00	0.00
21-70 Yrs	85.3	75.3	74.3	86.1	3.67	4.40	12.5	1.10	0.73	0.73	0.36
< 21 Yrs	72.5	34.7	70.5	68.9	5.70	6.22	6.74	2.59	2.59	1.04	1.04
Weighted Total (all)	82.9	60.7	74.6	82.1	4.58	4.92	11.0	1.53	1.58	0.85	0.51

3.2 Children and adolescents display lower prevalence to sCoVs

One major hurdle in estimating the seroprevalence of IgGs against the four sCoVs is the lack of a true negative reference population. To overcome this challenge, we used a small subset of pediatric

samples aged from 1 to 2 years old and established the cut-off at two standard deviations of their mean (Fig. S1). The advantage of using these samples is that it limits the probability that these individuals were exposed to the virus due to their young age, although there is still the possibility of vertically-transferred IgG from the mother through breastmilk [43–45]. From these cut-offs, we were able to estimate a relative seroprevalence of sCoVs in the four cohorts. We found that children and adolescents and young adults less than 21 years of age had significantly lower 229E, OC43, and HKU1 sCoV seroprevalence than all other cohorts (Fig. 1 and Table 2). For example, seroprevalence of HKU1 in persons < 21 yrs of age was about 34.7%, which agrees with Dijkman et al. who found HKU1 seroconversion in pediatric individuals to be around 36% [46]. Additionally, the total cohort weighted HKU1 average seroprevalence of 60.7% is in agreement with Severance et al. which calculated the seroprevalence of HKU1 at 59.2% [47]. Furthermore, this lower seroprevalence in pediatric samples corroborates previous observations where seroconversion from 229E and NL63 exposure occurs on average 3.5 years following birth [7,48] (Fig. S1). Across all cohorts, we found an overall size-weighted seroprevalence of 82.9% for OC43, 82.1% for 229E, and 74.6% for NL63 (Table 2). Our calculated seroprevalence for OC43 and 229E is in line with previous studies [5,47,49].

3.3 sCoV antibodies are cross-reactive

To ensure the specificity of sCoV detection, we tested co-reactivity between the S-trimer proteins of each of the sCoV along with an additional antigen (S-RBD or N) on a subset of samples (Fig. 2A). It is expected that upon virus exposure and seroconversion, antibodies are detected against both S-trimer and N, and S-trimer and S-RBD antigens of the same virus. Antigen discordance in single-positive samples is likely the result of S-trimer cross-reactivity to other sCoV. We then compared the proportion of samples that were dual-positive for S-trimer and N of OC43 and HKU1, and S and S-RBD of 229E (Fig. 2b). Positive concordance between the spikes and alternative antigens (i.e., N or S-RBD) for the four cohorts ranged between 67 – 76% (Fig. 2b). These results highlight that there is a relatively high level of cross-reactivity between the S-trimer proteins of sCoVs which compromises assay specificity. Therefore, this data indicate that an accurate determination of sCoVs seroprevalence should measure antibody levels against more than one antigen to minimize the potential of S-trimer protein cross-reactivity.

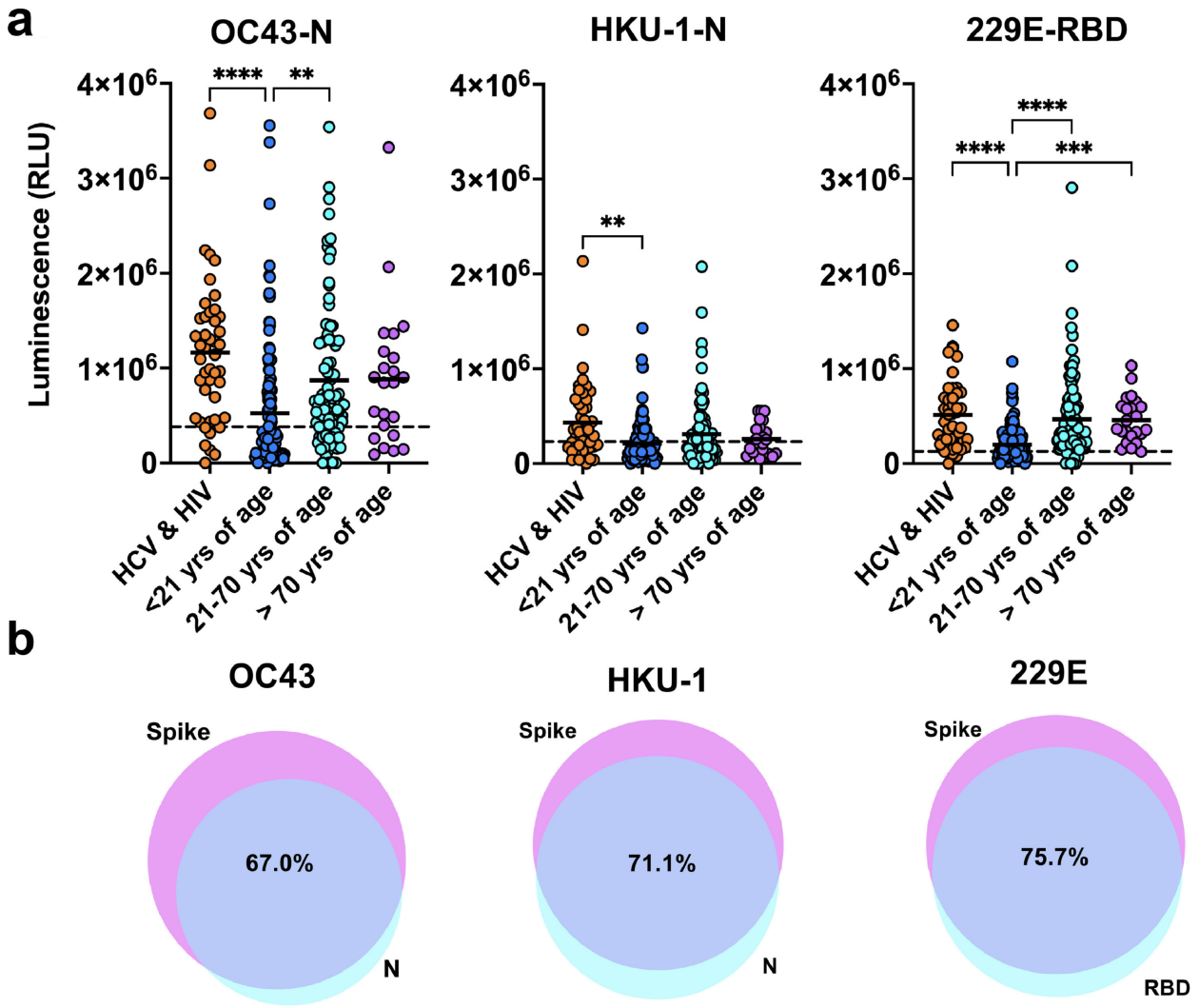


Figure 2 Concordance in sCoV seroprevalence using alternative antigens. (a) Seroprevalence of each cohort < 21 yrs of age [n=129], 21-70 yrs of age [n=111], > 70 yrs of age [n=23], and persons with HCV or HIV [n=45] using alternative antigens is represented (nucleocapsid for OC43 and HKU1, and S-RBD for 229E). The cut-off was calculated at 2 standard deviation using pediatric samples aged 1-2 years as a negative group. Statistics were one-way ANOVA with Welch correction, *post-hoc* tests were Games-Howell's multiple comparison tests *p<0.05, **p<001, ***p<0.001, ****p<0.0001. (b) Concordance between using the respective sCoV spike and alternative antigen to evaluate seroprevalence. Percentages of positive concordance between S-trimer and alternative antigens are indicated in each Venn diagram. Venn diagram have been generated using BioVenn online.

3.4 Antibodies to sCoVs cross-react to SARS-CoV-2 antigens

We next assessed the seroprevalence of IgA, IgM, IgG and IgE binding to SARS-CoV-2 antigens S-trimer, S-RBD, and N in pre-pandemic serum samples (Fig. 3 and Tables 2 and S2-S7) using our high throughput serological assay [31]. Cut-offs were set at 2 standard deviations (2 SD) above the mean values of the presumed negative sample population. Among pre-pandemic cohorts, 4.6% and 4.9% of samples displayed IgG reactivity against the SARS-CoV-2 S-RBD and S-trimer antigens, respectively (Fig. 3g and 3h, and Table 2). In contrast, the N antigen appeared to be more cross-reactive, showing a higher number of samples that were positive for IgG cross-reactive antibodies (6.7% - 15.3%) (Fig. 3i and Table 2). Given the importance of N as a common target for serological assays [50–52], efforts to accurately measure cross-reactivity to this antigen are critical to account for false positive results. This is especially important when considering that the N antigen of the four sCoVs has on average the highest level of sequence homology to the N of SARS-CoV-2, and that a recent infection by a sCoV could exacerbate such cross-reactivity through immunological imprinting [1,16]. Regardless of their levels, anti-N antibodies are unlikely to offer protection against SARS-CoV-2 entry given that they do not neutralize the virus. Finally, the role of IgE antibodies in mediating immune responses against SARS-CoV-2 infection is currently unknown although IgE antibodies can play a major role in allergic reactions and inflammation [53]. Our results show that cross-reactive sCoV IgE antibodies are rare and are unlikely to have a detectable role in influencing SARS-CoV-2 infections (Fig. 3j - 3l, and Table S7) Fig. 4.

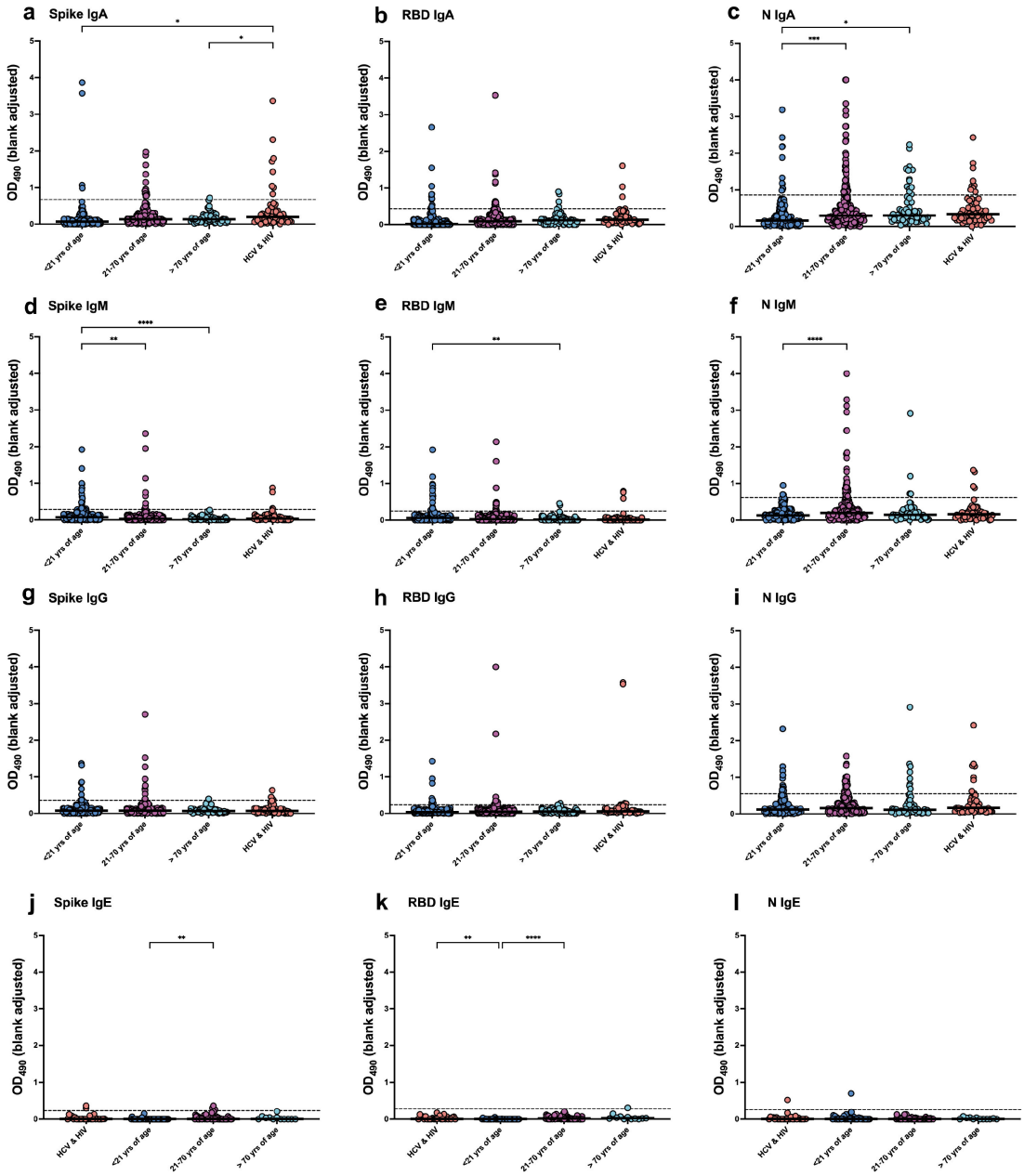


Figure 3 Evaluation of cross-reactive antibodies to three SARS-CoV-2 antigens in pre-pandemic serum samples. We probed for IgA, IgM, IgG and IgE cross-reactive antibodies to the following SARS-CoV-2 antigens: S-trimer, S-RBD and N antigens by ELISA. The levels of IgA (a, b, and c), IgM (d, e, and f), IgG (g, h, and i) and IgE (j, k, and l) are shown as OD490 values calculated after adjusting the blank from each serum sample. Dotted lines represent the cut-off values established at 2 SD from the mean value of presumed-negative samples (see Materials and Methods). The false discovery rate (FDR) for each condition are presented in Supplementary Tables S3 to S7. Statistics were one-way ANOVA with Welch correction and Games Howell *post hoc* multiple comparisons test for pairwise differences in A-I where n=193 (<21 yrs of age), n=273 (21-70 yrs of age), n=64 (>70 yrs of age), n=59 (HCV & HIV cohort (50 persons of which 9 were sampled twice 6 or 12 months apart). In panels J-L, serum volumes were sufficient to analyze n=53 (<21 yrs of age), n=68 (21-70 yrs of age), n=12 (>70 yrs of age), n=28 (HCV & HIV cohort). Given sample sizes, statistics were one-way ANOVA with Welch correction and post-hoc tests were Dunnett T3 multiple comparison tests, *p<0.05, **p<001, ***p<0.001, ****p<0.0001.

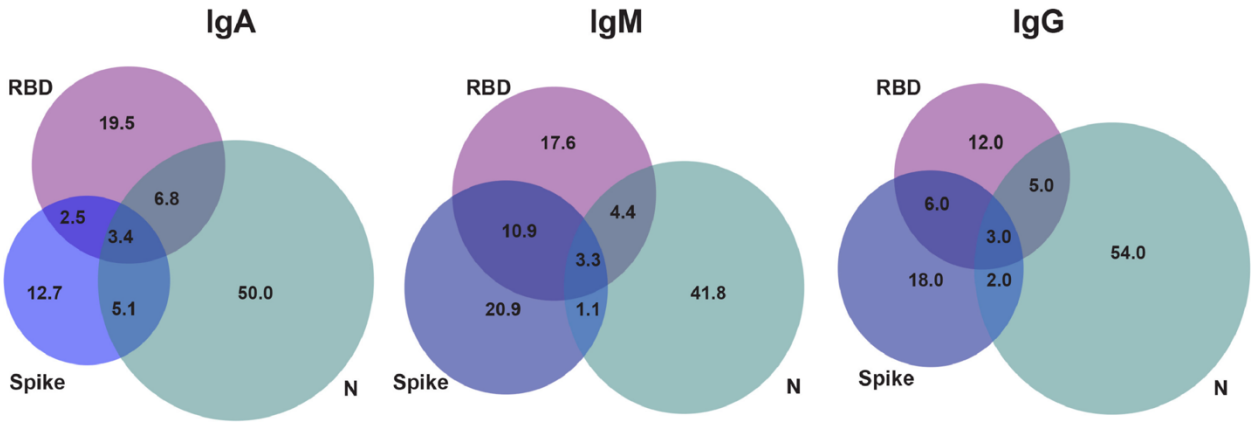


Figure 4 Patterns of multi-antigen cross-reactivity against SARS-CoV-2 Spike-ACE2 interactions. Venn Diagram showing the cross-reactivity patterns across all three antigens probed for IgA, IgM and IgG. Most cross-reactive events are for a single antigen. BioVenn online was used to generate the quantitative Venn diagram [49].

We further investigated cross-reactivity of the IgG1, IgG2, IgG3, and IgG4 isotype subclasses against the three SARS-CoV-2 antigens (Figs. S2, S3, and Tables S2-S7). Our analysis revealed that most of the IgG subclass antibodies in pre-pandemic sera only exhibited low levels of cross-reactivity with SARS-CoV-2 antigens. Detection of cross-reactive IgG3 antibodies is interesting, as it has been shown that SARS-CoV-2 S-specific IgG3 subclass levels increase with COVID-19 disease severity [54]. We further wanted to assess the false discovery rate (FDR) when two or three antigens are used for the analysis. For this, we performed a comparison of all the serology results across three antibody isotypes and three antigens to determine if a positive sample is positive for only one or multiple antigens and/or isotypes (Figs. 5, S3 and Tables 2 and S7). We found that in most cases, a positive sample is restricted to only one isotype and/or one viral antigen. This highlights the importance and value of considering simultaneously more than one antigen for SARS-CoV-2 serological testing. We calculated the FDR for each specific cohort disaggregated by individual antigen-isotype/subtype (Tables S2-S6), and we also calculated the FDR for each combination of antigen and isotype/subtype (Tables 1 and S7). While the IgG FDR for our complete pre-pandemic cohort ranged from 5% to 11% when probing individual antigens, these values dropped to between 0.9% to 1.6% when probing two antigens, and 0.5% when all three antigens are used to determine seropositivity (Table 2).

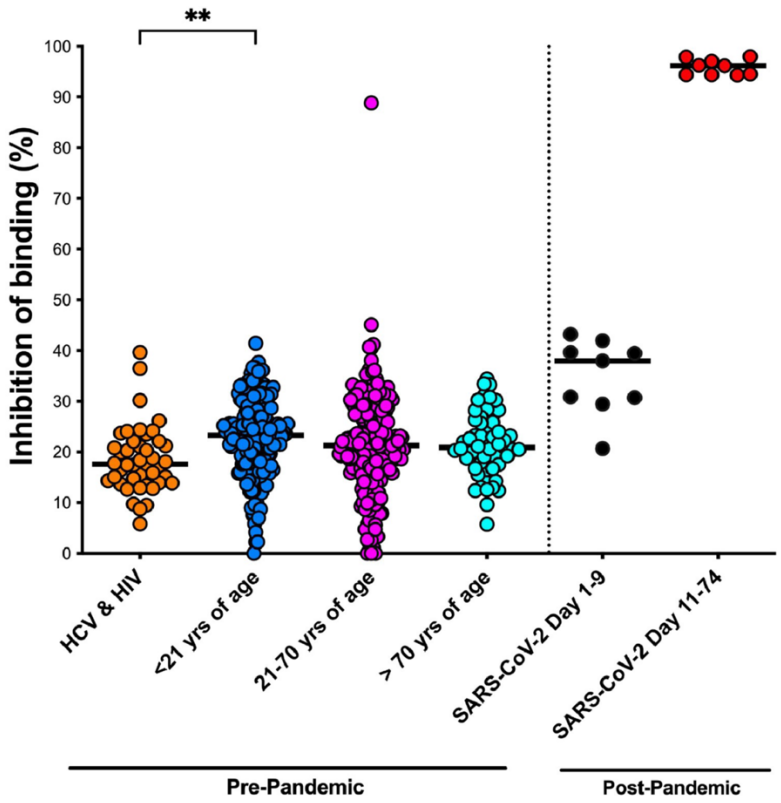


Figure 5 Neutralizing activity against SARS-CoV-2 Spike-ACE2 interactions. Neutralizing activity of 507 serum samples across the four cohorts were tested for the ability to inhibit Spike-ACE2 interactions. The snELISA assay involves coating plates with the SARS-CoV-2 S-trimer protein and applying serum, washing and challenging with biotinylated ACE2 [21]. The plot shows the percentage of inhibition relative to the no serum control. Each point is the mean of quadruplicate values. Control samples are constituted of the serum of SARS-CoV-2 infected individuals collected 1 to 9 days after testing positive by PCR (black), or 11 to 74 days post-PCR (red). Statistics were one-way ANOVA with Welch correction, *post-hoc* tests were Games-Howell's multiple comparison tests *p<0.05, **p<001, ***p<0.001, ****p<0.0001.

3.5 sCoV antibodies partially cross-neutralize SARS-CoV2 antigens

Previous studies have reported the presence of cross-reactive antibodies to SARS-CoV-2 S-trimer protein in pre-pandemic blood samples [1,12,28,55,56]. However, while generally limited information is available pertaining to levels of cross-neutralization of SARS-CoV-2, some information has been published with regards to the neutralization of S-pseudotyped viruses [1,31]. Given the importance of neutralizing antibodies that target the SARS-CoV-2 S-trimer [28,57-59], we evaluated the relative efficacy of sCoV antibodies to inhibit SARS-CoV-2 Spike-ACE2 interactions using a protein-based surrogate neutralization ELISA (snELISA) assay [55,36]. Inhibition of Spike-ACE2 interaction varied from 0-45%, with a single patient showing an inhibition level of 89% (21 yr old, male; epilepsy), with median levels ranging between 18-23%

(Fig. 5, Table 3). Very weak neutralizing activity was previously observed by others in a different experimental system that measured infection by S-pseudotyped viruses [1,31]. By contrast, we identified a moderate yet distinct pattern of neutralization between cohorts of pre-pandemic samples.

Table 3 Descriptive statistics of the protein-based neutralization assay by cohorts. Median values and range (minimum and maximum values) of the percentages of the inhibition of SARS-CoV-2 spike-ACE2 was calculated by cohorts from the protein based surrogate neutralization assay (snELISA).

	ACE2 Binding Inhibitions (%)		
Cohort	**Median**	**Min value**	**Max value**
HCV & HIV	17.6	5.83	39.7
< 21 yrs	23.3	0.00	41.4
21 - 70 yrs	21.3	0.00	45.1*
> 70 yrs	21.9	5.77	34.4
SARS-CoV-2 Day 1-9	37.9	20.7	43.2
SARS-CoV-2 Day 11-74	96.2	94.3	98.0

Patient P1-G5 was excluded from this analysis (89% inhibition).

3.6 Abundance of sCoV antibodies does not predict SARS-CoV-2 neutralization

Next, we asked if there was an association between sCoV antibody levels with the levels of neutralization observed. Using fuzzy c-means unsupervised clustering, we clustered samples into 10 distinct groups of human sera from 507 of our 580 patients from which we had sufficient material to monitor the degree of inhibition of SARS-CoV-2 Spike-ACE2 interaction and cross-reactivity with SARS-CoV-2 S-RBD, S-trimer, and N proteins (Fig 6a). Subjects stratified independently of age and sex or other prior viral infection (HIV & HCV) (Fig. 6a, Table S8). We found that these clusters defined a continuum of SARS-CoV-2 neutralization in patients ranging from 0% inhibition to 45% (Fig. 6b). Interestingly, one pre-pandemic sample displayed high level of neutralization (89%), this serum sample also displayed high IgG cross-reactivity against S-RBD (O.D.= 2.172) and S-trimer (O.D.=2.707) along with high IgA cross-reactivity against S-RBD (O.D.=0.275) and S-trimer (O.D.=0.233). Additionally, the presence of autoantibodies against ACE2 that block spike binding could also theoretically contribute to the neutralization given that autoantibodies are detected in epilepsy [42–44]. Additional neutralization assays using S-pseudotyped viruses are on-going to confirm this observation.

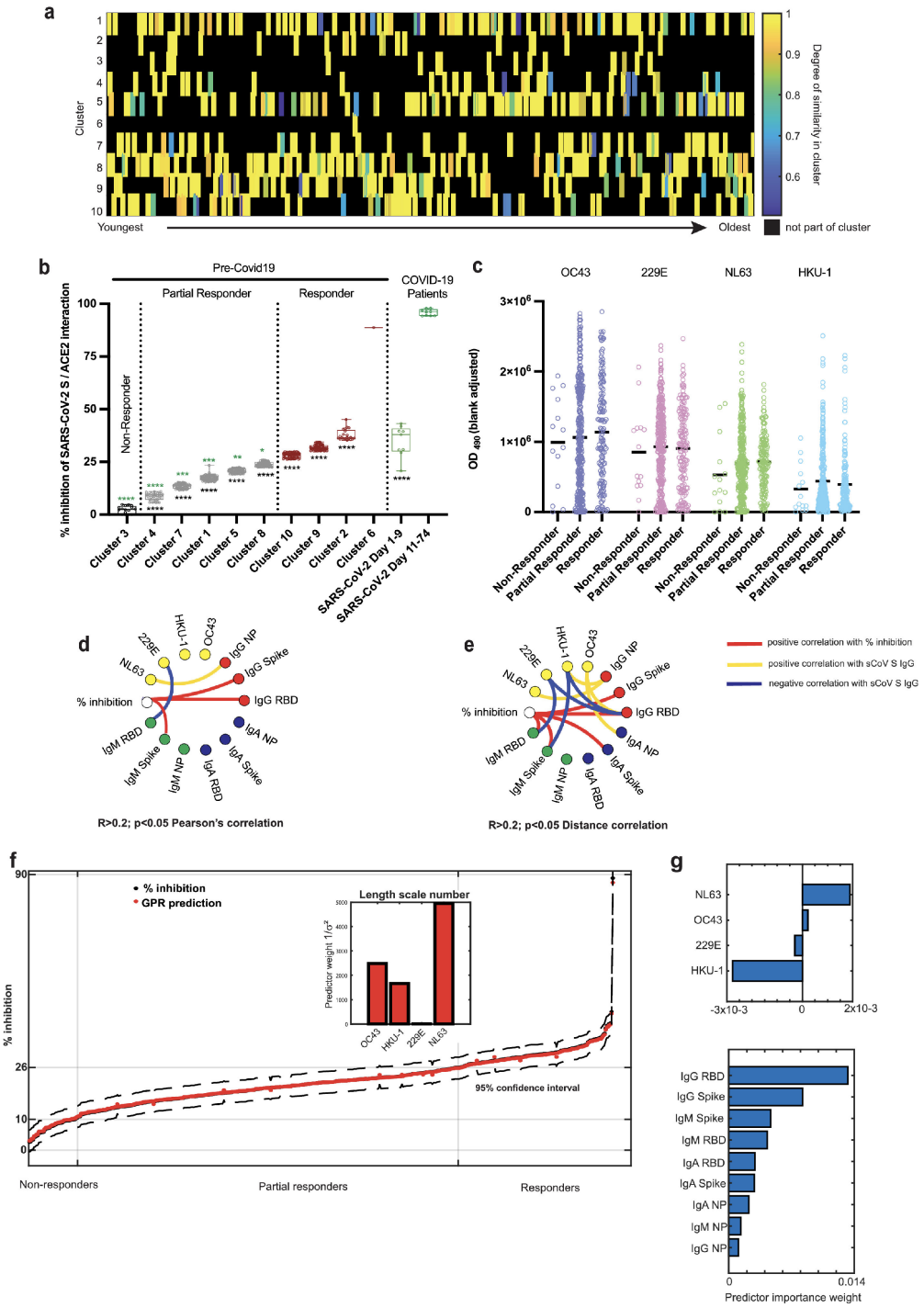


Figure 6 Association of sCoV seroprevalence with SARS-CoV-2 antigen cross-reactivity and neutralization of SARS-CoV-2 Spike-ACE2 interactions. (a) Fuzzy c-means clustering segregated 507 patients into 10 clusters across all 4 cohorts (with fuzzyfication factor m=1.3) based on serum antibody cross-reactivity and capacity of these antibodies to inhibit SARS CoV-2 Spike binding to ACE2. Patient stratification was independent of age or sex (Table S8). Data represent degree of cluster identification as a measure of similarity of all features per patient. Colours indicate membership values over 0.5 - 1.0 with highest values indicating the strongest cluster confidence assignment. (b) Clusters stratified patients with increasing capacity to inhibit interaction between the SARS-CoV-2 spike protein and ACE2. Data represent percentage of inhibition relative to the no serum control. Boxes extend from 25th to 75th

percentile. Whiskers delineate minimum and maximum points. Each patient point is the mean of quadruplicate values. Each cluster (with the exception of cluster 6 composed of a single patient with robust neutralizing activity) was compared to control samples constituting of serum of infected individuals collected 1 to 9 days after testing positive by PCR for SARS-CoV-2 (green asterisks) or to Non-Responders (cluster 8, black asterisks). Statistics were one-way ANOVA with Welch correction for unequal standard deviation, post-hoc Dunnett's T3 *p<0.05, **p<0.01, ***p<0.001, ****p<0.0001 green vs SARS-CoV-2, black vs cluster 3. Subjects that failed to inhibit SARS-CoV-2 Spike-ACE2 interactions were dubbed Non-Responders (black, Cluster 3). Subjects that exhibited significantly higher neutralizing activity than Non-Responders yet significantly lower neutralizing activity than COVID-19 patients (green) were dubbed Partial Responders (grey). Patients that exhibited significantly higher neutralizing activity than Non-Responders yet comparable activity to COVID-19 patients were dubbed Responders (red). (c) Abundance of sCOVs does not discriminate capacity to neutralize SARS-CoV-2 Spike-ACE-2 interaction. There is no statistical difference between sCOV abundances between groups. Statistics were one-way ANOVA with Welch correction for unequal standard deviation, post-hoc Dunnett's T3. (d) Using Pearson's correlation level over 0.2 and p<0.05, % inhibition of SARS-CoV-2 spike-ACE2 interaction associated strongly with cross-reactivity with SARS-CoV-2 IgG S-RBD and IgG S-trimer while the abundance of antibodies to NL63 S-trimer correlated with IgG N. The 229-E abundance of antibodies showed negative correlation with IgM S-RBD. (e) Signed distance correlation for Responder group (shown for correlation greater then 0.2, p<0.05) reveal that % inhibition of SARS-CoV-2 spike- ACE2 interaction associates strongly with SARS-CoV-2 S-trimer IgM S-RBD, IgM S-trimer, IgA S-trimer, IgG S-RBD, and IgG S-trimer. Abundance of antibodies to NL63 spike and HKU1 correlate positively with IgG N, OC43 spike with IgG S-RBD and IgA N. 229E shows negative correlation with IgM S-RBD, IgM S-trimer while HKU1 shows negative correlation with IgM S-trimer and IgG S-RBD. (f) Gaussian process regression (GPR) model for % inhibition of ACE2-Spike protein interaction predicted from sCoVs antibody abundance showing predictive model with model 95% confidence intervals (dashed lines) as well as predictor weight, i.e., relevance of each feature for the model performance, shown as an inset. In the figure, the importance of the feature increases with the predictor weight shown with NL63 being the most important predictor of latent variables providing GPR model and 229E the least relevant in the model building (g) Relieff feature selection for % inhibition of ACE2-Spike protein interaction determined for sCoVs antibody abundance and SARS-CoV-2 cross-reactivity measures separately. Shown are features' weight values with negative weight indicating no significance in regression and significance in the model increasing with the predictor importance weight.

We then further sub-divided these patient clusters into three groups: Non-Responders, Partial Responders, and Responders based on their similarity to newly infected SARS CoV-2 patients (Day 1-9 from testing positive) with respect to SARS-CoV-2 neutralization (Table S1). Sera from 3% of all subjects (N=16, Cluster 3) did not neutralize binding of SARS CoV-2 S to ACE2 (Non-Responders, Fig. 6b). Sixty eight percent of all subjects were Partial Responders, exhibiting significantly higher neutralizing activity than Non-responders, yet significantly lower neutralizing activity than newly infected COVID-19 patients (Fig. 6b). Twenty-nine percent of subjects were Responders, exhibiting significantly higher neutralizing activity than Non-responders and comparable activity to that of newly infected COVID-19 patients (Fig. 6b). We asked what pattern of sCoV reactivity against their respective S-trimer proteins discriminated these groups. We found no statistical difference in the levels of antibodies against OC43-S, 229E-S, HKU1-S, or NL63-S (Fig. 6c). Moreover, the vast majority of cross-reactive SARS-CoV-2 antibodies were directed

against the N antigen (Tables 2 and S7). These data suggested that absolute abundance of sCoV anti-S IgG antibodies did not dictate neutralization.

3.7 Relative ratios of sCoV antibodies predict neutralization

To identify critical features underlying neutralization response, we used Pearson's correlation analysis to determine major linear correlations as well as signed distance correlation to obtain information about linear, non-linear and indirect, and more distant associations. Through these analyses, we were able to discern a pattern of seroprevalence to sCoVs that closely associated with the capacity to neutralize Spike-ACE2 interactions. First, the percent inhibition of Spike-ACE2 binding in the Responder group positively associated with higher levels of SARS-CoV-2 cross-reactive IgG S-trimer and IgG S-RBD antibodies (at a Pearson's correlation above 0.2 and $p<0.05$), as expected (Fig. 6d), and additionally with abundances of IgM S-RBD, IgM S-trimer and IgA S-trimer antibodies (at a distance correlation level above 0.2 and $p<0.05$) (Fig. 6e). Of these five neutralization correlates, abundances of OC43 S-trimer IgG associated with higher levels of SARS-CoV-2 cross-reactive IgG S-RBD and IgA N. Additionally, levels of NL63 S-trimer and HKU1 S-trimer IgG positively associated with levels of cross-reactive IgG N (Fig. 6e). At lower distance correlation level of 0.17 there was also direct correlation between NL63 and the percent inhibition (not shown). Conversely, abundances of anti-229E S-trimer IgG negatively correlated with both SARS-CoV-2 IgM S-RBD (Pearson's correlation, distance correlation, Fig. 6d) and IgG S-RBD (distance correlation, Fig. 6e). Finally, HKU1 S-trimer IgG levels negatively correlated (via distance correlation) with IgM S-trimer and IgG S-RBD (Fig. 6e).

Taken together, these data suggest that NL63 S and, to a lesser extent, OC43 S antibody levels positively associate with correlates of percent inhibition while 229E and HKU-1 negatively associate with correlates of percent inhibition. These data are consistent with Selva *et al.* who have shown that elderly individuals with higher sCoV exposure show increased levels of cross-reactive SARS-CoV-2 IgA and IgG responses, while children show elevated SARS-CoV-2 IgM and is associated with less frequent exposures [60]. Here, we show that these responses link to OC43 S-trimer Ab abundance. In our analysis, cross-reactive SARS-CoV-2 IgM levels negatively correlated with 229E and HKU1 anti-S antibodies. Thus, a higher abundance of these antibodies

is associated with a decreased neutralizing probability following exposure to these two sCoVs according to our model. Percent inhibition is in turn correlated with anti-SARS-CoV-2 IgM (IgM S-RBD and IgM Spike), IgA Spike and IgG (IgG S-trimer and IgG S-RBD), possibly indicating a different source of protection in our responder group members belonging to different age groups. These results are in excellent agreement with further statistical analysis of the feature significance for classification, regression to percent neutralization determined using Relieff. Although there was no statistically significant difference in the levels of antibodies against sCoVs between the three groups (Fig. 6c), Relieff selection of the most significantly different features related to the continual value of percent neutralization demonstrated that levels of NL63 and OC43 have the positive, i.e., significant, classification weight to percent neutralization (Fig. 6g). This result is supported by their positive correlation with IgG N, IgG S-RBD and IgA N. Finally, IgG S-RBD, IgG S-trimer, IgM S-trimer and IgM S-RBD have the highest classification weight according to Relieff analysis, in agreement with the correlation analysis in Figures 6d and 6e providing additional confirmation that the pattern of sCoV S antibodies in Responders underlies neutralization capacity.

3.8 Cross-reactive antibodies and latent variables impact neutralization

To test this hypothesis computationally, we asked whether we could use only sCoV S reactivity to predict neutralization of the SARS-CoV-2 Spike-ACE2 interaction (Fig. 6f). We used a Gaussian process regression (GPR) method to explore the functional relationship between sCoV S antibody levels and the percent inhibition of ACE2. The GPR model, using sCoV antibody levels as predictors, provided excellent agreement with percent inhibition of ACE2 for all three patient groups (Non-responders, Partial Responders and Responders, Fig. 6g). Because GPR optimizes variable projection, weights, as well as covariance as a function of the latent variables, these results indicate that sCoV antibody measurements, when combined with latent variables, (i.e., variables that are not measured but can be determined as functions of measured values), dramatically improve prediction of percent inhibition of ACE2 interaction. GPR analysis also provides a confidence interval of this prediction, i.e., error level of the prediction (indicated in dashed lines in Fig. 6f). The significance of a variable in the developed GPR model, measured as the weight of the predictor indicates major significance of NL63 in modeling followed by OC43 and HKU1. In

this analysis predictor weight of 229E is significantly lower. This is once again in agreement with the correlation analyses demonstrating 229E is indirectly negatively correlated with percent inhibition (Fig. 6e). Global sensitivity analysis (GSA) apportioning the outputs uncertainty to the uncertainty of each input factor over their entire range and with input factors varied simultaneously is calculated using Sobol method and quasi-random Monte Carlo sampling. GSA shows once again major significance of NL63 in the variance of the output and second highest uncertainly contribution of 229E, showing in correlation analysis major negative correlation with the % neutralization. GSA results for the GPR model presented in Figure 6 are shown in Supplementary Figure 4. Taken together, these data link the capacity of pre-pandemic sera to neutralize SARS CoV-2 Spike-ACE2 binding to both specific patterns of elevated antibody levels against NL63 S-trimer and OC43 S-trimer as well as additional unknown factors, yet to be identified, conferred by this specific pattern of cross-reactive antibodies to SARS-CoV-2 S (Fig. 6e).

4 Discussion

Seroprevalence of sCoVs antibodies measured using our high-throughput ELISA platform has highlighted that there is a very large range in antibody levels against sCoVs. Interestingly, measuring seroprevalence of sCoVs using a single antigen is prone to specificity challenges due to cross-reactivity between sCoV antigens. We show that only 67% to 76% of spike-positive samples were also positive when probed with a second antigen from the same virus (Fig. 2b). This indicates that we are over-reporting seroprevalence of individual sCoVs. Additionally, while there is no statistical difference in seroprevalence between adults and elderly individuals, there appears to be a modest decrease in prevalence in younger individuals for 229E, OC43 and HKU1. A recent paper by Selva et al. also observed that children have fewer exposures to sCoVs than older adults [60]. Exactly how high levels of antibodies against sCoVs or recency of infection by sCoVs may influence COVID-19 disease severity remains unclear. However, our data highlights relatively high levels of cross-reactivity against certain SARS-CoV-2 antigens, with N being the most frequently detected at 11% overall prevalence, while S-trimer displayed about 5% prevalence (Table 2). These values are comparable to another study that showed 16.2% cross reactivity to N and 4.2% for S-trimer [1]. Small differences between our two studies can be accounted for by

cohort composition that affects certain antigen/isotype pairs disproportionately (Figs. 3, S2 and tables S2-S6). Also, differences in S-RBD and S-trimer FDR (Table 2), and thereby assay specificity, can be caused by the methods used for antigen production. Glycosylation patterns can vary depending on the cell expression system and also the smaller S-RBD antigen can potentially expose new epitopes that might be hidden when it is part of the full size S-trimer.

Although some studies have indicated that no detectable SARS-CoV-2 neutralization activity was detected in pre-pandemic blood samples using various types of assays [1,31,60], the snELISA that we used was able to discern small variations from 0% to 45% in Spike-ACE2 binding inhibition. Although snELISAs are not capable of providing the same complete assessment of whole virus entry neutralization as measured when using live replicative virus, this methodology does enable an isolated and focused assessment of one parameter of the neutralization which is the binding of the viral spike to its host receptor. Small variations at this level can have profound implications during an actual infection in a human host that could perhaps be missed using cell lines to assess neutralization with live virus, the current gold standard. Spike-pseudotyped lentiviruses are also useful surrogates to study neutralization and viral entry, but lentiviruses bud from the cell surface and likely harbor a different lipid and host molecule compositions in their envelope than SARS-CoV-2 that mostly egress through exocytosis and possibly also through the lysosomal pathways [61,62]. Given these differences in the biochemical and immunological composition of the envelopes of lentiviruses and betacoronaviruses, neutralization data obtained with pseudotyped lentiviruses should not be considered as definitive.

Nevertheless, in agreement with previous studies, we also did not identify a direct link between the abundance of sCoV S-trimer antibodies and neutralization of Spike-ACE2 interactions (Fig. 6c). However, our data do indicate that cross-reactive IgG against S-trimer and S-RBD of SARS-CoV-2 have a positive correlation with neutralization efficiency, and also to a lesser degree, IgM against S-trimer and S-RBD, and IgA against S-trimer (Fig. 6d and 6e). An even more interesting observation is how NL63 correlates with cross-reactive N IgGs (Fig. 6d), a similar observation was also made by another group [32]. While N antibodies are unlikely to be neutralizing, antibody Fc effector functions such as antibody-dependant cell mediated cytotoxicity

(ADCC) and complement activation may have an indirect influence on other antiviral pathways in a live infected host.

Despite a small number of studies reporting undetectable cross-neutralization or unlikely protection by sCoVs antibodies [1,31,60], there is a large body of evidence that supports a role for prior exposure to sCoVs with milder COVID-19 disease severity and/or detectable immunity to SARS-CoV-2 [6,7,10,13,29,33,34,63,64]. Using machine learning approaches, we present here data that reconcile these differences by providing evidence that it is the relative pattern of prior sCoV antibody levels in sera, and not total levels, that predict neutralization intensity levels. Additionally, GPR analysis shows that latent variables, that have not been identified in this work but that can be inferred from the measures of sCoVs, provide a model that accurately predicts the percent inhibition of Spike-ACE2 binding.

In light of the ongoing COVID-19 pandemic, public health measures are geared towards reducing exposure to the virus, reducing mortality and hospitalization. The predictive value of our model offers an alternative way to evaluate neutralization by using serological assays against sCoVs which are easier, more accessible and use less resources than traditional virus-based neutralization assays. Furthermore, our predictive model contributes to the growing body of evidence in support of the protective outcome of prior exposure to sCoVs, NL63 in particular. It is well understood that humoral responses are only one arm of the immune system, evidence that cross-reactive T cells play a role in protection is also gaining momentum [33]. With latent factors being here identified to exert an influence over Spike - ACE2 binding, an understanding of how sCoV may diminish the severity of COVID-19 will require a broader investigation. The current study design does not allow for the analysis of causal relationships *in vivo* nor causal relationship between sCoV and any latent factors. Additionally, further molecular and omics measurements in these patient samples such as characterizing T cell responses, measuring antibody responses against other sCoVs antigens, measuring other isotypes against sCoVs would likely contribute to a better understanding of the observed effects. In future work, it will be critical to evaluate if our GPR analysis can predict COVID-19 severity by way of the functional relationship of sCoV antibodies that inhibit Spike - ACE2 interactions.

Contributors
YG, VS, EM, GL carried out the experiments. MG and PMG supported assay development. M-AL & YG designed the study. YG, VS, SALB, MCC and M-AL wrote the manuscript. YD contributed to the design of spike, N, ACE2 constructs, expression and purification procedures. RAB sourced specimens, co-designed high-throughput analysis. MM and CC provided samples and AMC facilitated serum sample processing. SALB and MCC contributed to sample collection, data verification/processing and performed all of the sCoV analyses with YG and M-AL. All of the authors have edited and contributed to the review of the manuscript.

Data sharing statement
The data used in this study can be obtained by request to M.A.L (langlois@uottawa.ca)

Declaration of Competing Interest
The authors declare no conflict of interest relevant to the present manuscript.

Acknowledgments
The authors would like to thank Anne-Claude Gingras for helpful comments on the manuscript and members of the Mammalian Cell Expression Section at HHT-NRC for their valuable contribution at producing several of the recombinant proteins used in this study. This study was supported in part by a COVID-19 Rapid Response grant by the Canadian Institutes of Health Research (CIHR; #VR2 - 172722) and by a grant supplement by the COVID-19 Immunity Task Force (CITF) to M-A Langlois and by the National Research Council of Canada Collaborative R&D Initiative Pandemic Response Challenge Program Grant to SAL Bennett and M Cuperlovic-Culf (PR031-1). Production of COVID-19 reagents was financially supported by the NRC's Pandemic Response Challenge Program. M.-A.L. holds a Canada Research Chair in Molecular Virology and Intrinsic Immunity. S.A.L.B holds a University Research Chair in Neurolipidomics. Y.G. holds a CIHR Frederick Banting and Charles Best graduate scholarship (CGS-M).

References

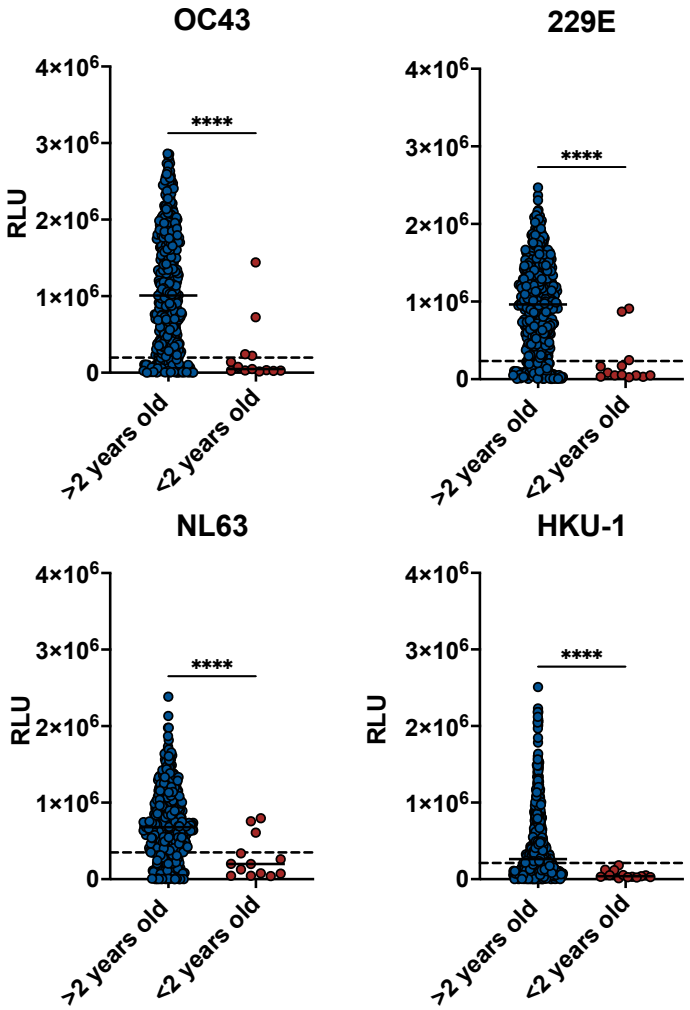
1. Anderson EM, Goodwin EC, Verma A, Arevalo CP, Bolton MJ, Weirick ME, et al. Seasonal human coronavirus antibodies are boosted upon SARS-CoV-2 infection but not associated with protection. Cell. 2021;184(7):1858-64.e10.
2. Gaunt ER, Hardie A, Claas EC, Simmonds P, Templeton KE. Epidemiology and clinical presentations of the four human coronaviruses 229E, HKU1, NL63, and OC43 detected over 3 years using a novel multiplex real-time PCR method. J Clin Microbiol. 2010;48(8):2940-7.
3. Edridge AWD, Kaczorowska J, Hoste ACR, Bakker M, Klein M, Loens K, et al. Seasonal coronavirus protective immunity is short-lasting. Nat Med. 2020;26(11):1691-3.
4. Masse S, Capai L, Villechenaud N, Blanchon T, Charrel R, Falchi A. Epidemiology and Clinical Symptoms Related to Seasonal Coronavirus Identified in Patients with Acute Respiratory Infections Consulting in Primary Care over Six Influenza Seasons (2014-2020) in France. Viruses. 2020;12(6).
5. Gorse GJ, Patel GB, Vitale JN, O'Connor TZ. Prevalence of Antibodies to Four Human Coronaviruses Is Lower in Nasal Secretions than in Serum. Clinical and Vaccine Immunology. 2010;17(12):1875-80.
6. Song G, He WT, Callaghan S, Anzanello F, Huang D, Ricketts J, et al. Cross-reactive serum and memory B-cell responses to spike protein in SARS-CoV-2 and endemic coronavirus infection. Nat Commun. 2021;12(1):2938.
7. Majdoubi A, Michalski C, O'Connell SE, Dada S, Narpala S, Gelinas J, et al. A majority of uninfected adults show preexisting antibody reactivity against SARS-CoV-2. JCI Insight. 2021;6(8).
8. V'kovski P, Kratzel A, Steiner S, Stalder H, Thiel V. Coronavirus biology and replication: implications for SARS-CoV-2. Nature Reviews Microbiology. 2021;19(3):155-70.
9. Hicks J, Klumpp-Thomas C, Kalish H, Shunmugavel A, Mehalko J, Denson JP, et al. Serologic Cross-Reactivity of SARS-CoV-2 with Endemic and Seasonal Betacoronaviruses. J Clin Immunol. 2021;41(5):906-13.
10. Grzelak L, Temmam S, Planchais C, Demeret C, Tondeur L, Huon C, et al. A comparison of four serological assays for detecting anti-SARS-CoV-2 antibodies in human serum samples from different populations. Sci Transl Med. 2020;12(559).
11. Okba NMA, Muller MA, Li W, Wang C, GeurtsvanKessel CH, Corman VM, et al. Severe Acute Respiratory Syndrome Coronavirus 2-Specific Antibody Responses in Coronavirus Disease Patients. Emerg Infect Dis. 2020;26(7):1478-88.
12. Lv H, Wu NC, Tsang OT, Yuan M, Perera R, Leung WS, et al. Cross-reactive Antibody Response between SARS-CoV-2 and SARS-CoV Infections. Cell Rep. 2020;31(9):107725.
13. Ladner JT, Henson SN, Boyle AS, Engelbrektson AL, Fink ZW, Rahee F, et al. Epitope-resolved profiling of the SARS-CoV-2 antibody response identifies cross-reactivity with endemic human coronaviruses. Cell Rep Med. 2021;2(1):100189.
14. Trivedi SU, Miao C, Sanchez JE, Caidi H, Tamin A, Haynes L, et al. Development and Evaluation of a Multiplexed Immunoassay for Simultaneous Detection of Serum IgG Antibodies to Six Human Coronaviruses. Scientific Reports. 2019;9(1):1390.
15. Galipeau Y, Greig M, Liu G, Driedger M, Langlois M-A. Humoral Responses and Serological Assays in SARS-CoV-2 Infections. Frontiers in Immunology. 2020;11(3382).
16. Piccoli L, Park YJ, Tortorici MA, Czudnochowski N, Walls AC, Beltramello M, et al. Mapping Neutralizing and Immunodominant Sites on the SARS-CoV-2 Spike Receptor-Binding Domain by Structure-Guided High-Resolution Serology. Cell. 2020;183(4):1024-42.e21.
17. McCallum M, De Marco A, Lempp FA, Tortorici MA, Pinto D, Walls AC, et al. N-terminal domain antigenic mapping reveals a site of vulnerability for SARS-CoV-2. Cell. 2021;184(9):2332-47.e16.
18. Andreano E, Nicastri E, Paciello I, Pileri P, Manganaro N, Piccini G, et al. Extremely potent human monoclonal antibodies from COVID-19 convalescent patients. Cell. 2021;184(7):1821-35.e16.

19. Graham C, Seow J, Huettner I, Khan H, Kouphou N, Acors S, et al. Neutralization potency of monoclonal antibodies recognizing dominant and subdominant epitopes on SARS-CoV-2 Spike is impacted by the B.1.1.7 variant. Immunity. 2021;54(6):1276-89.e6.
20. McMahan K, Yu J, Mercado NB, Loos C, Tostanoski LH, Chandrashekar A, et al. Correlates of protection against SARS-CoV-2 in rhesus macaques. Nature. 2021;590(7847):630-4.
21. Anand SP, Prevost J, Nayrac M, Beaudoin-Bussieres G, Benlarbi M, Gasser R, et al. Longitudinal analysis of humoral immunity against SARS-CoV-2 Spike in convalescent individuals up to 8 months post-symptom onset. Cell Rep Med. 2021;2(6):100290.
22. McAndrews KM, Dowlatshahi DP, Dai J, Becker LM, Hensel J, Snowden LM, et al. Heterogeneous antibodies against SARS-CoV-2 spike receptor binding domain and nucleocapsid with implications for COVID-19 immunity. JCI Insight. 2020;5(18).
23. Grifoni A, Weiskopf D, Ramirez SI, Mateus J, Dan JM, Moderbacher CR, et al. Targets of T Cell Responses to SARS-CoV-2 Coronavirus in Humans with COVID-19 Disease and Unexposed Individuals. Cell. 2020;181(7):1489-501.e15.
24. Braun J, Loyal L, Frentsch M, Wendisch D, Georg P, Kurth F, et al. SARS-CoV-2-reactive T cells in healthy donors and patients with COVID-19. Nature. 2020;587(7833):270-4.
25. Le Bert N, Tan AT, Kunasegaran K, Tham CYL, Hafezi M, Chia A, et al. SARS-CoV-2-specific T cell immunity in cases of COVID-19 and SARS, and uninfected controls. Nature. 2020;584(7821):457-62.
26. Anderson DE, Tan CW, Chia WN, Young BE, Linster M, Low JH, et al. Lack of cross-neutralization by SARS patient sera towards SARS-CoV-2. Emerging Microbes & Infections. 2020;9(1):900-2.
27. Prévost J, Gasser R, Beaudoin-Bussières G, Richard J, Duerr R, Laumaea A, et al. Cross-Sectional Evaluation of Humoral Responses against SARS-CoV-2 Spike. Cell Reports Medicine. 2020;1(7).
28. Sagar M, Reifler K, Rossi M, Miller NS, Sinha P, White LF, et al. Recent endemic coronavirus infection is associated with less-severe COVID-19. The Journal of Clinical Investigation. 2021;131(1).
29. Huang AT, Garcia-Carreras B, Hitchings MDT, Yang B, Katzelnick LC, Rattigan SM, et al. A systematic review of antibody mediated immunity to coronaviruses: kinetics, correlates of protection, and association with severity. Nature Communications. 2020;11(1):4704.
30. Poston D, Weisblum Y, Wise H, Templeton K, Jenks S, Hatziioannou T, et al. Absence of Severe Acute Respiratory Syndrome Coronavirus 2 Neutralizing Activity in Prepandemic Sera From Individuals With Recent Seasonal Coronavirus Infection. Clinical Infectious Diseases. 2020.
31. Morgenlander WR, Henson SN, Monaco DR, Chen A, Littlefield K, Bloch EM, et al. Antibody responses to endemic coronaviruses modulate COVID-19 convalescent plasma functionality. J Clin Invest. 2021;131(7).
32. Schulien I, Kemming J, Oberhardt V, Wild K, Seidel LM, Killmer S, et al. Characterization of pre-existing and induced SARS-CoV-2-specific CD8(+) T cells. Nat Med. 2021;27(1):78-85.
33. Mateus J, Grifoni A, Tarke A, Sidney J, Ramirez SI, Dan JM, et al. Selective and cross-reactive SARS-CoV-2 T cell epitopes in unexposed humans. Science. 2020;370(6512):89-94.
34. Khan T, Rahman M, Ali FA, Huang SSY, Ata M, Zhang Q, et al. Distinct antibody repertoires against endemic human coronaviruses in children and adults. JCI Insight. 2021;6(4).
35. Székely GJ, Rizzo ML, Bakirov NK. Measuring and testing dependence by correlation of distances. The Annals of Statistics. 2007;35(6):2769-94, 26.
36. Robnik-Šikonja M, Kononenko I. Theoretical and Empirical Analysis of ReliefF and RReliefF. Machine Learning. 2003;53(1):23-69.
37. Poulain A, Perret S, Malenfant F, Mullick A, Massie B, Durocher Y. Rapid protein production from stable CHO cell pools using plasmid vector and the cumate gene-switch. J Biotechnol. 2017;255:16-27.
38. Wevers BA, van der Hoek L. Recently discovered human coronaviruses. Clin Lab Med. 2009;29(4):715-24.
39. Stadlbauer D, Amanat F, Chromikova V, Jiang K, Strohmeier S, Arunkumar GA, et al. SARS-CoV-2 Seroconversion in Humans: A Detailed Protocol for a Serological Assay, Antigen Production, and Test Setup. Current Protocols in Microbiology. 2020;57(1):e100.

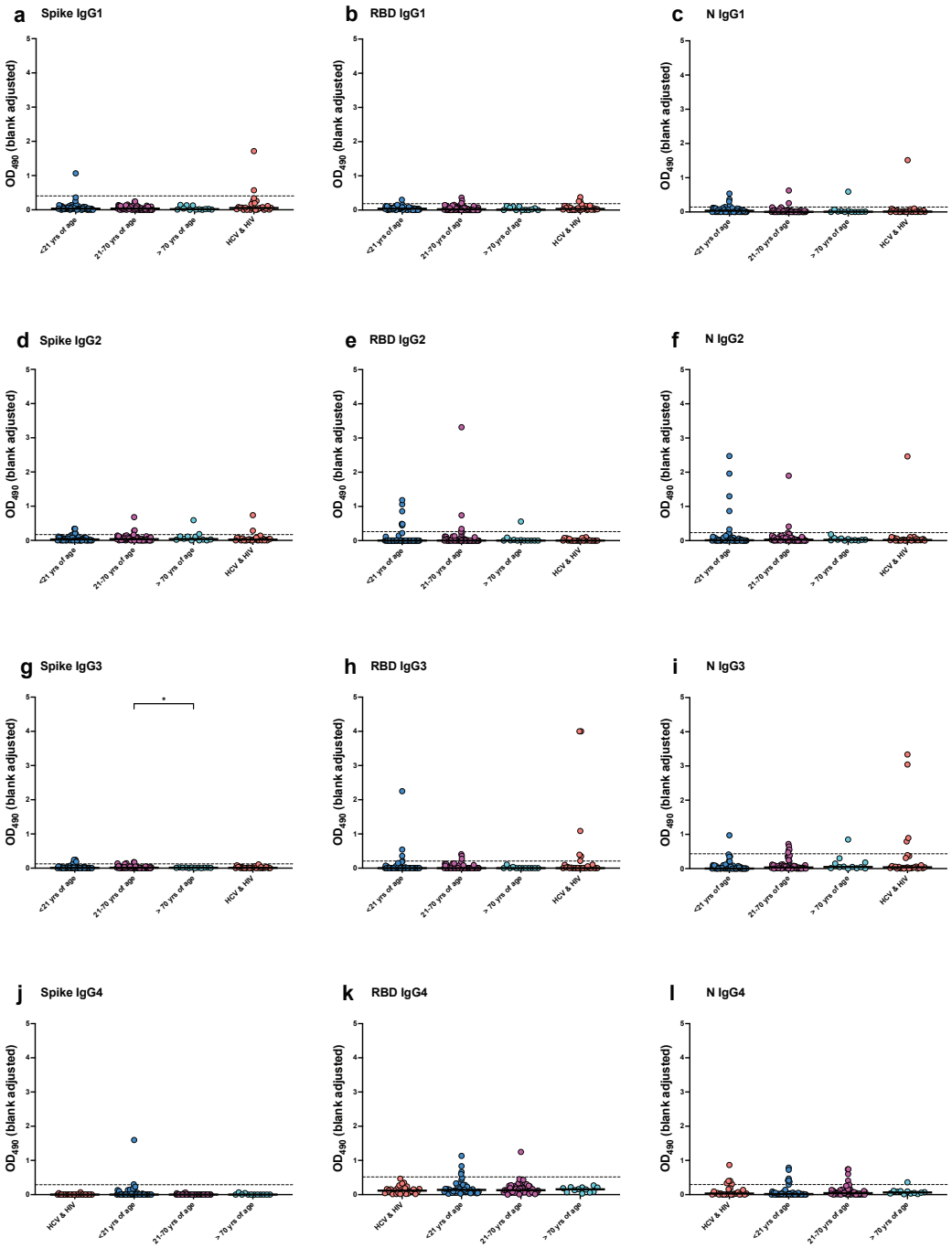
40. Isho B, Abe KT, Zuo M, Jamal AJ, Rathod B, Wang JH, et al. Persistence of serum and saliva antibody responses to SARS-CoV-2 spike antigens in COVID-19 patients. Science Immunology. 2020;5(52):eabe5511.
41. Leuridan E, Hens N, Hutse V, Aerts M, Van Damme P. Kinetics of maternal antibodies against rubella and varicella in infants. Vaccine. 2011;29(11):2222-6.
42. Leuridan E, Van Damme P. Passive transmission and persistence of naturally acquired or vaccine-induced maternal antibodies against measles in newborns. Vaccine. 2007;25(34):6296-304.
43. Niewiesk S. Maternal antibodies: clinical significance, mechanism of interference with immune responses, and possible vaccination strategies. Front Immunol. 2014;5:446.
44. Dijkman R, Jebbink MF, Gaunt E, Rossen JW, Templeton KE, Kuijpers TW, et al. The dominance of human coronavirus OC43 and NL63 infections in infants. J Clin Virol. 2012;53(2):135-9.
45. Severance EG, Bossis I, Dickerson FB, Stallings CR, Origoni AE, Sullens A, et al. Development of a Nucleocapsid-Based Human Coronavirus Immunoassay and Estimates of Individuals Exposed to Coronavirus in a U.S. Metropolitan Population. Clinical and Vaccine Immunology. 2008;15(12):1805-10.
46. Dijkman R, Jebbink MF, El Idrissi NB, Pyrc K, Müller MA, Kuijpers TW, et al. Human Coronavirus NL63 and 229E Seroconversion in Children. Journal of Clinical Microbiology. 2008;46(7):2368-73.
47. van Tol S, Mögling R, Li W, Godeke G-J, Swart A, Bergmans B, et al. Accurate serology for SARS-CoV-2 and common human coronaviruses using a multiplex approach. Emerging Microbes & Infections. 2020;9(1):1965-73.
48. Ahmed SF, Quadeer AA, McKay MR. Preliminary Identification of Potential Vaccine Targets for the COVID-19 Coronavirus (SARS-CoV-2) Based on SARS-CoV Immunological Studies. Viruses. 2020;12(3).
49. Algaissi A, Alfaleh MA, Hala S, Abujamel TS, Alamri SS, Almahboub SA, et al. SARS-CoV-2 S1 and N-based serological assays reveal rapid seroconversion and induction of specific antibody response in COVID-19 patients. Scientific Reports. 2020;10(1):16561.
50. Grzelak L, Temmam S, Planchais C, Demeret C, Tondeur L, Huon C, et al. A comparison of four serological assays for detecting anti–SARS-CoV-2 antibodies in human serum samples from different populations. Science Translational Medicine. 2020;12(559):eabc3103.
51. Amarasekera M. Immunoglobulin E in health and disease. Asia Pac Allergy. 2011;1(1):12-5.
52. Goh YS, Chavatte J-M, Lim Jieling A, Lee B, Hor PX, Amrun SN, et al. Sensitive detection of total anti-Spike antibodies and isotype switching in asymptomatic and symptomatic individuals with COVID-19. Cell Reports Medicine.
53. Abe KT, Li Z, Samson R, Samavarchi-Tehrani P, Valcourt EJ, Wood H, et al. A simple protein-based surrogate neutralization assay for SARS-CoV-2. JCI Insight. 2020;5(19).
54. Wang Y, Zhang L, Sang L, Ye F, Ruan S, Zhong B, et al. Kinetics of viral load and antibody response in relation to COVID-19 severity. The Journal of Clinical Investigation. 2020;130(10).
55. Liu L, Wang P, Nair MS, Yu J, Rapp M, Wang Q, et al. Potent neutralizing antibodies against multiple epitopes on SARS-CoV-2 spike. Nature. 2020;584(7821):450-6.
56. Brouwer PJM, Caniels TG, van der Straten K, Snitselaar JL, Aldon Y, Bangaru S, et al. Potent neutralizing antibodies from COVID-19 patients define multiple targets of vulnerability. Science. 2020;369(6504):643-50.
57. Zost SJ, Gilchuk P, Chen RE, Case JB, Reidy JX, Trivette A, et al. Rapid isolation and profiling of a diverse panel of human monoclonal antibodies targeting the SARS-CoV-2 spike protein. Nature Medicine. 2020;26(9):1422-7.
58. Selva KJ, van de Sandt CE, Lemke MM, Lee CY, Shoffner SK, Chua BY, et al. Systems serology detects functionally distinct coronavirus antibody features in children and elderly. Nature Communications. 2021;12(1):2037.
59. Ghosh S, Dellibovi-Ragheb TA, Kerviel A, Pak E, Qiu Q, Fisher M, et al. beta-Coronaviruses Use Lysosomes for Egress Instead of the Biosynthetic Secretory Pathway. Cell. 2020;183(6):1520-35 e14.
60. V'Kovski P, Kratzel A, Steiner S, Stalder H, Thiel V. Coronavirus biology and replication: implications for SARS-CoV-2. Nat Rev Microbiol. 2021;19(3):155-70.

61. Dugas M, Grote-Westrick T, Vollenberg R, Lorentzen E, Brix T, Schmidt H, et al. Less severe course of COVID-19 is associated with elevated levels of antibodies against seasonal human coronaviruses OC43 and HKU1 (HCoV OC43, HCoV HKU1). Int J Infect Dis. 2021;105:304-6.
62. Shrock E, Fujimura E, Kula T, Timms RT, Lee I-H, Leng Y, et al. Viral epitope profiling of COVID-19 patients reveals cross-reactivity and correlates of severity. Science. 2020;370(6520):eabd4250.

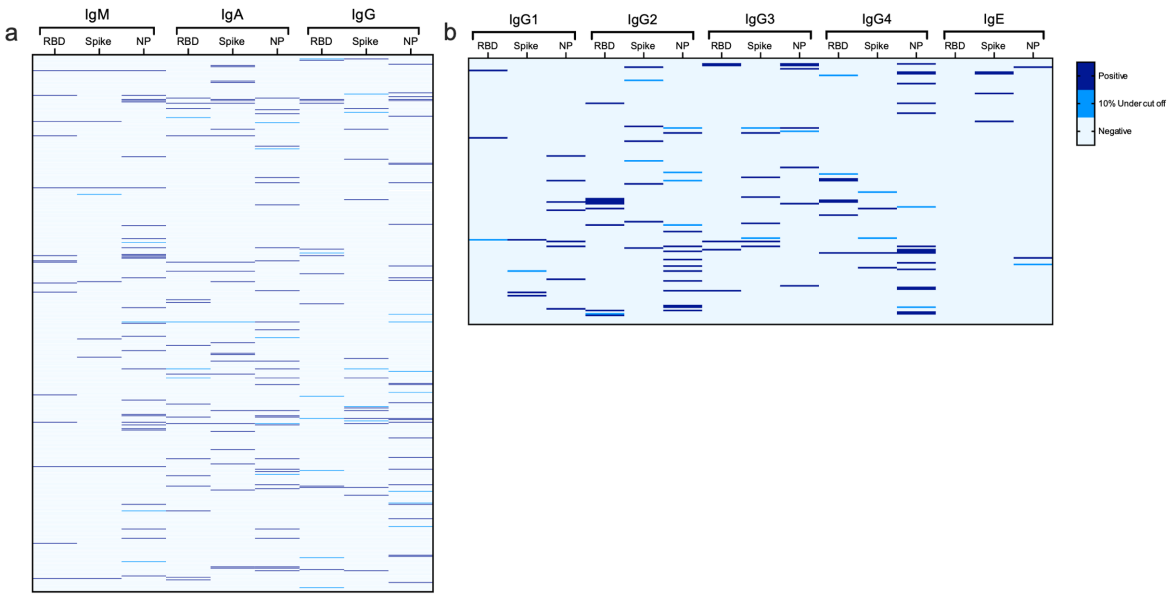
Supplementary material



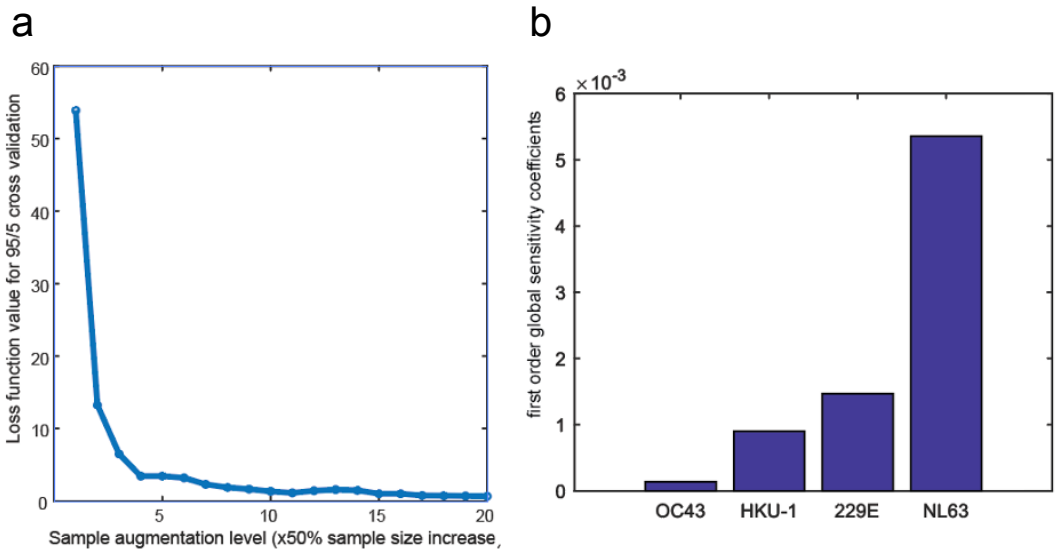
Supplementary Figure 1. Comparison between pediatric samples under 2 years old to the complete cohort for each seasonal spike coronavirus. Pediatric individuals under two years old that were used to establish the cut-offs are indicated (red) in contrast to the seroprevalence of the combination of the four cohorts (Blue). <2 yrs of age [n=13], >2 yrs of age [n=550]. Welch's unpaired T test was performed to establish statistical significance *p<0.05, **p<0.01, ***p<0.001, ****p<0.0001.



Supplementary Figure 2. IgG-subclass antibody responses to SARS-CoV-2 antigens. The pre-COVID-19 patient cohort samples (x-axis) of HCV & HIV [n=28]; **< 21 yrs,** n=[53]; **21 - 70 yrs** [n=68]; **> 70 yrs** [n=12]; were tested for the reactivity of IgG1 IgG2 IgG3 and IgG4 to the SARS-CoV-2 S-trimer protein **(a, d, g, j)** S-RBD **(b, e, h, k)** and nucleocapsid **(c, f, i ,l)**. The ELISA OD_{490} values indicates the raw OD subtracted from the background. Cut-off values calculated by two rounds of exclusion at 2 Standard deviation from the negative distribution was indicated on each graph. Statistics were one-way ANOVA with Welch correction, *post-hoc* tests were Games-Howell's multiple comparison tests *p<0.05, **p<001, ***p<0.001, ****p<0.0001.



Supplementary Figure 3. Discordance of serological false positive per isotype and antigen. (a) An alignment of the signal to cut-off ratio for each sample was performed by isotype (IgG, IgM, IgA) and antigens (S-RBD, S-Trimer, N) on 589 samples from which 9 were longitudinal. Values over cut-offs (dark blue) and 10% under cut offs (light blue) are indicated. **(b)** An alignment of the signal to cut-off ratio for was performed by subtypes (IgG1, IgG2, IgG3, IgG4) and IgE and antigens (RBD, Spike, N) on 161 randomly selected samples.



Supplementary Figure 4. Global sensitivity analysis (GSA) results for the Gaussian process regression (GPR) model. **(a)** The effect of sample size increase was determined using up-sampling with SMOTE algorithm on the loss function in the cross-validation study of our GPR model showing major increase in cross validation accuracy (reduced Loss function) with sample size increase. Loss function is calculated as: $L = \sum_{j=1}^{n} w_j I\{y_j^{model} \neq y_j\}$ where w_j is the weight for observation j normalized so that they sum to the corresponding prior class probability. **(b)** GSA showing the contribution of the uncertainty of each input factor on the uncertainty of the output. (Calculations were performed using library FLAX running under Matlab (2021). Global Sensitivity Analysis Toolbox ; MATLAB Central File Exchange. Retrieved September 25, 2021). Shown are first order global sensitivity coefficients calculated for 30,000 samples for the quasi-random Monte Carlo sampling calculated using Fourier amplitude sensitivity test (FAST) (Saltelli, A., and Bolado, R. (1998). An alternative way to compute Fourier amplitude sensitivity test (FAST). *Comput. Stat. Data Anal.* 26, 445–460. doi: 10.1016/S0167-9473(97)00043-1).

Table S1. Demographic information of post-pandemic controls. Serum samples collected in various longitudinal studies of SARS-CoV-2 infected and non-infected individuals were used as reference groups. Demographic information was collected from the respective study or patient file and compiled.

Cohorts	SARS-CoV-2 status	# of Subjects	Age range (yrs)	Female % (Mean Age ± SD)	Male % (Mean Age ± SD)
SARS-CoV-2 convalescent	Positive	45	23-72	73 (49 ±13 yrs)	27 (45 ±13 yrs)
SARS-CoV-2 negative	Negative	115	22-73	68 (42 ±12 yrs)	32 (44 ±12yrs)
SARS-CoV-2 11-74 days post PCR	Positive	9	24-90	33 (62 ± 15yrs)	67 (60 ± 25 yrs)
SARS-CoV-2 1-9 days post PCR	Positive	9	46-88	44 (72 ± 18yrs)	56 (68 ± 13yrs)

SD: standard deviation

Table S2. Determination of SARS-CoV-2 assay cut-off values of the four cohorts combined and false discovery rate (FDR) per antigen, isotype & subtypes. Cut-off values were calculated from two exclusion cycles at 2 standard deviations from the negative distributions. Any sample above that designated cut-off was included to determine the FDR

SARS-CoV-2 antigen	Anti-human antibodies	Cut-off	False discovery rate (%)
RBD	IgA	0.428	6.45
	IgM	0.243	5.60
	IgG	0.240	4.58
	IgG1	0.186	4.35
	IgG2	0.262	6.83
	IgG3	0.207	7.45
	IgG4	0.517	3.11
	IgE	0.278	0.59
S	IgA	0.670	4.92
	IgM	0.290	5.60
	IgG	0.357	4.92
	IgG1	0.405	1.86
	IgG2	0.169	8.07
	IgG3	0.125	5.59
	IgG4	0.289	1.86
	IgE	0.230	3.11
N	IgA	0.857	13.24
	IgM	0.617	7.98
	IgG	0.551	11.0
	IgG1	0.143	5.59
	IgG2	0.232	5.59
	IgG3	0.432	6.83
	IgG4	0.294	9.94
	IgE	0.260	1.24

Table S3. Determination of SARS-CoV-2 assay cut-off values of pre-COVID-19 HCV and HIV patients and corresponding false discovery rate per antigen, isotype & subtypes. Cut-off values were calculated from two exclusion cycles at 2 standard deviations from the negative distributions. Any sample above that designated cut-off was included to determine the FDR.

SARS-CoV-2 antigen	Anti-human antibodies	Cut-off	False discovery rate (%)
RBD	IgA	0.428	6.78
	IgM	0.243	5.08
	IgG	0.240	8.47
	IgG1	0.186	10.7
	IgG2	0.262	0.00
	IgG3	0.207	21.4
	IgG4	0.517	0.00
	IgE	0.278	0.00
S	IgA	0.670	13.6
	IgM	0.290	6.78
	IgG	0.357	6.78
	IgG1	0.405	7.14
	IgG2	0.169	7.14
	IgG3	0.125	0.00
	IgG4	0.289	0.00
	IgE	0.230	7.14
N	IgA	0.857	15.3
	IgM	0.617	6.78
	IgG	0.551	15.3
	IgG1	0.143	3.57
	IgG2	0.232	3.57
	IgG3	0.432	14.3
	IgG4	0.294	17.9
	IgE	0.260	3.57

Table S4. Determination of SARS-CoV-2 assay cut-off values of pre-COVID-19 > 70 years of age and corresponding false discovery rate per antigen, isotype & subtypes.
Cut-off values were calculated from two exclusion cycles at 2 standard deviations from the negative distributions. Any sample above that designated cut-off was included to determine the FDR.

SARS-CoV-2 antigen	Anti-human antibodies	Cut-off	False discovery rate (%)
RBD	IgA	0.428	6.25
	IgM	0.243	3.13
	IgG	0.240	1.56
	IgG1	0.186	0.00
	IgG2	0.262	8.33
	IgG3	0.207	0.00
	IgG4	0.517	0.00
	IgE	0.278	8.33
S	IgA	0.670	1.56
	IgM	0.290	0.00
	IgG	0.357	1.56
	IgG1	0.405	0.00
	IgG2	0.169	16.7
	IgG3	0.125	0.00
	IgG4	0.289	0.00
	IgE	0.230	0.00
N	IgA	0.857	21.9
	IgM	0.617	6.25
	IgG	0.551	14.1
	IgG1	0.143	8.33
	IgG2	0.232	0.00
	IgG3	0.432	8.33
	IgG4	0.294	8.33
	IgE	0.260	0.00

Table S5. Determination of SARS-CoV-2 assay cut-off values of pre-COVID-19 21 - 70 years of age and corresponding false discovery rate per antigen, isotype & subtypes. Cut-off values were calculated from two exclusion cycles at 2 standard deviations from the negative distributions. Any sample above that designated cut-off was included to determine the FDR.

SARS-CoV-2 antigen	Anti-human antibodies	Cut-off	False discovery rate (%)
RBD	IgA	0.428	5.86
	IgM	0.243	4.40
	IgG	0.240	3.66
	IgG1	0.186	4.41
	IgG2	0.262	5.88
	IgG3	0.207	4.41
	IgG4	0.517	1.47
	IgE	0.278	0.00
S	IgA	0.670	5.86
	IgM	0.290	3.30
	IgG	0.357	4.40
	IgG1	0.405	0.00
	IgG2	0.169	4.41
	IgG3	0.125	5.88
	IgG4	0.289	0.00
	IgE	0.230	4.41
N	IgA	0.857	15.8
	IgM	0.617	12.8
	IgG	0.551	12.5
	IgG1	0.143	2.94
	IgG2	0.232	4.41
	IgG3	0.432	7.35
	IgG4	0.294	5.88
	IgE	0.260	0.00

Table S6. Determination of SARS-CoV-2 assay cut-off values of pre-COVID 19 < 21 years of age and corresponding false discovery rate per antigen, isotype & subtypes. Cut-off values were calculated from two exclusion cycles at 2 standard deviations from the negative distributions. Any sample above that designated cut-off was included to determine the FDR.

SARS-CoV-2 antigen	Anti-human antibodies	Cut-off	False discovery rate (%)
RBD	IgA	0.428	7.25
	IgM	0.243	8.29
	IgG	0.240	5.70
	IgG1	0.186	1.89
	IgG2	0.262	11.3
	IgG3	0.207	5.66
	IgG4	0.517	7.55
	IgE	0.278	0.00
S	IgA	0.670	2.07
	IgM	0.290	10.4
	IgG	0.357	6.22
	IgG1	0.405	1.89
	IgG2	0.169	11.3
	IgG3	0.125	9.43
	IgG4	0.289	3.77
	IgE	0.230	0.00
N	IgA	0.857	6.22
	IgM	0.617	2.07
	IgG	0.551	6.74
	IgG1	0.143	9.43
	IgG2	0.232	9.43
	IgG3	0.432	1.89
	IgG4	0.294	11.3
	IgE	0.260	1.89

Table S7 Multi-antigen FDR calculation.

Table S7 Multi-antigen FDR calculation. False discovery rate of all four cohorts combined using a single antigen, combinations of two antigens and three antigens were compared by each isotype and subtype.

Antibody Isotype	Single antigen FDR (%)			Two antigen FDR (%)			Three antigen FDR (%)
	RBD	Spike	N	RBD + S	RBD + N	S + N	RBD + S+N
IgA	6.45	4.92	13.2	1.19	1.87	1.70	0.68
IgM	5.60	5.60	7.98	2.21	1.19	0.68	0.51
IgG	4.58	4.92	11.0	1.53	1.53	0.85	0.51
IgG1	4.35	1.86	5.59	0.62	0.62	0.00	0.00
IgG2	6.83	8.07	5.59	0.62	0.62	0.00	0.00
IgG3	7.45	5.59	6.83	0.62	1.86	0.62	0.00
IgG4	3.11	1.86	9.94	0.62	0.62	0.62	0.62
IgE	0.62	3.11	1.24	0.00	0.00	0.00	0.00

Table S8. Demographics of fuzzy mean clusters of patients segregated by serum antibody cross-reactivity. Cross-reactivity against 3 different SARS-CoV-2 antigens (N, RBD, Spike) for IgA, IgM and IgG were included with capacity of these antibodies to inhibit Spike-ACE2 binding.

Cluster # (n)	Age Mean ± SD (Range)	Sex (% Female)
1 (79)	41±26 (1-90 yrs)	58
2 (21)	32±23 (3-69 yrs)	42
3 (16)	45±24 (4-68 yrs)	38
4 (36)	45±26 (1-79 yrs)	44
5 (86)	45±26 (1-90 yrs)	47
6 (1)	21 yrs	0
7 (53)	41±28 (2-80 yrs)	42
8 (89)	35±28 (1-90 yrs)	47
9 (65)	35±28 (2-96 yrs)	57
10 (60)	36±28 (1-97 yrs)	50

Total n = 507*; *Subject 137-48 (56 yrs old, Female from HCV&HIV cohort) was weakly clustered in multiple clusters and was not associated with a single group. This sample was excluded from the analysis.

CHAPTER 5 – AUTOANTIBODIES IN THE CONTEXT OF SARS-COV-2 INFECTION

RATIONALE

The factors and mechanisms underlying the development of autoimmune conditions remain poorly understood. It is generally believed that both predisposing genetic factors and environmental exposures contribute to the onset of autoimmunity. Among environmental triggers, viral infections have long been implicated as potential contributors to autoimmune disease in certain individuals. In fact, multiple lines of evidence support a link between viral infections and the development of autoimmunity. For example, Epstein–Barr virus (EBV) infection has been associated with a 32-fold increased risk of developing multiple sclerosis (205). In addition, viral infections frequently lead to the production of autoantibodies—antibodies that recognize self-antigens such as cytokines, cell surface receptors, and nuclear components, among others.

Given the broad spectrum of disease severity and outcomes associated with SARS-CoV-2 infection—including the observation that some individuals do not fully return to baseline health following infection (e.g., Long-COVID)—it has been hypothesized that SARS-CoV-2 may contribute to the development of autoimmune pathologies in certain individuals.

Early in the pandemic, studies revealed that the presence of autoantibodies against type I interferons (IFNs) was associated with more severe SARS-CoV-2 infection outcomes (184). This finding highlighted the potential role of autoantibodies in SARS-CoV-2 pathogenesis. Subsequent preliminary reports suggested that ACE2, the receptor used by SARS-CoV-2 for cell entry, might also be targeted by autoantibodies. However, these studies were limited by small cohort sizes, insufficient negative control groups, and a lack of mechanistic insights into the potential biological consequences of such autoantibodies.

This chapter addresses these gaps by investigating the prevalence and functional role of ACE2 autoantibodies (Section 5.1). A review of the broader evidence linking autoantibody induction to SARS-CoV-2 infection outcomes is shown in Appendix A-1.23.

5.1 Autoantibodies targeting angiotensin-converting enzyme 2 are prevalent and not induced by SARS-CoV-2 infection

Preface

(This work has been previously published as a research article)

Galipeau Y, Castonguay N, McCluskie PS, Sonoda MT, Keeshan A, Collins E, Arnold C, Pelchat M, Burns K, Cooper C, Langlois MA. **Autoantibodies targeting angiotensin-converting enzyme 2 are prevalent and not induced by SARS-CoV-2 infection**. FASEB J. 2025 Feb 28;39(4):e70390. doi: 10.1096/fj.202402694R.

© 2025 The Author(s). The FASEB Journal published by Wiley Periodicals LLC on behalf of Federation of American Societies for Experimental Biology.

This is an open access article under the terms of the Creative Commons Attribution-NonCommercial License, which permits use, distribution and reproduction in any medium, provided the original work is properly cited and is not used for commercial purposes.

Abstract

Clinical outcomes resulting from SARS-CoV-2 infection vary widely, ranging from asymptomatic cases to the development of mild to severe respiratory illness, and in some instances, chronic lingering disease and mortality. The underlying biological mechanisms driving this wide spectrum of pathogenicity among certain individuals and demographics remain elusive. Autoantibodies have emerged as potential contributors to the severity of COVID-19. Although preliminary reports have suggested the induction of antibodies targeting Angiotensin-Converting Enzyme II (ACE2) post-infection, this assertion lacks confirmation in large-scale studies. In this study, our objective is to comprehensively characterize and quantify the prevalence and expression levels of autoantibodies directed against ACE2 in a sizable cohort ($n = 464$). Our findings reveal that ACE2-reactive IgM antibodies are the most prevalent, with an overall seroprevalence of 18.8%, followed by IgG at 10.3% and IgA at 6.3%. Longitudinal analysis of individuals with multiple blood draws showed stable ACE2 IgG and IgA levels over time. Upon stratifying individuals based on molecular testing for SARS-CoV-2 or serological evidence of past infection, no significant differences were observed between groups. Functional assessment of ACE2 autoantibodies demonstrated that they are non-neutralizing and failed to inhibit spike-ACE2 interaction or affect the enzymatic activity of ACE2. Our results highlight that ACE2 autoantibodies are prevalent in the general population and were not induced by SARS-CoV-2 infection in our cohort. Notably, we found no substantiated evidence supporting a direct role for ACE2 autoantibodies in SARS-CoV-2 pathogenesis.

Introduction

SARS-CoV-2 has profoundly impacted our day-to-day lives, in part not only through socio-economic impacts and excess mortality but also through morbidity associated with post-COVID-19 conditions (i.e., Long-COVID, PASC, PCC).[1] Although the scientific and medical communities have been intensely focusing on understanding SARS-CoV-2 pathogenesis, biological factors and mechanisms driving the heterogeneity of disease severity remain unclear. Several studies have highlighted that autoimmunity could be a factor impacting SARS-CoV-2 infection severity and recovery.[2-4]

Links between viral infection and autoimmunity have been extensively documented. For example, Epstein–Barr virus (EBV) infection was recently linked with a 32-fold increased risk of developing multiple sclerosis (MS). While no causal or mechanistic evidence exists, as of today, EBV is thought to be a leading driver of MS.[5] While evidence of autoimmune disease development following SARS-CoV-2 infections is currently anecdotal, several studies have reported the high prevalence of autoantibodies in COVID-19 patients. These autoantibodies include antinuclear antibodies, anti-cytokine antibodies, and anti-phospholipid autoantibodies.[6-12] While some autoantibodies may have an important role in homeostasis and are not associated with specific diseases (i.e., natural autoantibodies),[13] most autoantibodies have been studied in the context of autoimmune pathologies. Interestingly, one group has shown that anti-IFN antibodies are detected in individuals with severe COVID-19, whereas none of the mild or asymptomatic individuals had anti-IFN autoantibodies in circulation in their cohort. These autoantibodies were able to neutralize type 1 IFNs, preventing their antiviral functions,[8] thereby suggesting a role for autoantibodies in SARS-CoV-2 pathogenesis. These autoantibodies may represent a physiologically significant mechanism for regulating aberrant or excessive cytokine responses.[14-16]

ACE2's role in the renin-angiotensin system pathway has been extensively described. Briefly, ACE catalyzes the formation of angiotensin-II from the removal of two amino acids from the precursor angiotensin-I. ACE2 further enzymatically removes the carboxy-terminal phenylalanine from angiotensin-II, yielding angiotensin-(1-7), with both having downstream effects that are important for maintaining blood pressure, electrolyte balance, and fluid homeostasis. Of note, ACE2 can also generate angiotensin-(1-9).[17, 18] ACE2 is expressed across several organ systems from the

intestinal tract, kidneys, heart, lungs, and others.[19] In addition, ACE2 has also been identified as the cognate receptor for three coronaviruses, SARS-CoV, SARS-CoV-2, and NL63.[20-22] Given the relevance of ACE2 in the viral entry of SARS-CoV-2, some have suggested that autoantibodies targeting ACE2 could impact COVID-19 severity.[3] In a small cohort, Arthur et al. reported that 81% of previously SARS-CoV-2-infected individuals expressed antibodies targeting ACE2. These autoantibodies were found in 93% of hospitalized individuals with SARS-CoV-2 but were undetected in the control cohort.[23] In another cohort, Casciola et al. found an association between anti-ACE2 IgM autoantibodies and severe COVID-19, with the ability to activate the complement and impact the vascular endothelial environment.[24]

While studies found corroborating evidence of ACE2 autoantibodies in individuals with COVID-19,[25, 26] others did not. For example, in a screen by Chang et al., ACE2 autoantibodies were detected in only one individual of the study cohort despite the identification of numerous other autoantibodies in several individuals.[9] The implication of ACE2 autoantibodies in SARS-CoV-2 pathogenesis remains unclear as ACE2 autoantibodies have been detected and associated with other medical conditions (i.e., Parkinson's disease, vasculopathy, and rheumatoid arthritis,) independently of prior SARS-CoV-2 infection.[27-31] In addition, the limited size of the control cohorts in studies involving SARS-CoV-2-infected individuals impedes proper statistical interpretation of the results.

Here, we performed an in-depth characterization of ACE2 autoantibodies (IgG, IgA, and IgM) in the sera of 464 individuals, including 131 individuals with a history of prior SARS-CoV-2 infection. In addition, we functionally characterized anti-ACE2 autoantibodies, notably whether they could inhibit ACE2 enzymatic activity or block ACE2 and SARS-CoV-2 spike interactions.

2 Materials and Methods

2.1 Participant recruitment and sample processing

Individuals for this study were recruited from the ongoing Stop the Spread Ottawa (SSO) study.[32] Individuals 18 years and older with a history of SARS-CoV-2 infection or at risk of infection were recruited. Individuals having at least one blood draw by December 2021 with a

corresponding participant questionnaire were included in this study. Clinical and demographic information (including sex information) of the participants were captured. Serum collection was performed according to current standard phlebectomy procedures and samples were de-identified before reception at the SARS-CoV-2 High Throughput Serology and Diagnostics Facility located at the University of Ottawa, Faculty of Medicine. Sera was stored short-term at 4°C or frozen long-term at −80°C. Approval was granted by The Ottawa Health Science Network Research Ethics Board (Certificates: H-09-20-6135 and H-07-20-6009). Informed consent was obtained from all participants.

2.2 SARS-CoV-2 and ACE2 antibody measurements

Antibodies against SARS-CoV-2 were measured using a high-throughput direct chemiluminescent ELISA (full methods described previously).[33] ACE2 autoantibodies were measured using a similar method on the same platform used for SARS-CoV-2 antibodies with minor modifications. Briefly, recombinant ACE2 protein (generously provided by Dr. Yves Durocher, National Research Council of Canada (NRC), Montréal) was diluted in PBS (5 μg/mL working concentration) and was coated in a 384 well high-binding polystyrene Nunc plate (Thermo Fisher Scientific, #460372) to a final amount of 50 ng of protein per well. Coated plates were briefly centrifuged to evenly distribute ACE2 solution and incubated overnight at 4°C. Plates were then blocked for 1 h to remove nonspecific binding using 80 μL of 3% w/v skim milk powder dissolved in 100 μL of PBS + 1% Tween (PSB-T). Samples were diluted 1 in 80 in 1% w/v skim milk powder dissolved in PBS-T, and 10 μL was added to respective wells and incubated for 2 h.10 μL of HRP-labeled secondary antibody was added to each well and incubated for 1 h. Secondary antibodies used were anti-Human IgG#5-HRP (fusion-HRP construct) (Dr. Yves Durocher, NRC) diluted 1 in 5400; Anti-human IgA-HRP (Jackson ImmunoResearch Labs, 109-035-011) diluted 1 in 8000; and anti-human IgM-HRP (Jackson ImmunoResearch Labs, 109-035-129) diluted 1 in 9600. To detect bound secondary antibodies, 10 μL of ELISA Pico Chemiluminescent Substrate (Thermo Fisher Scientific #37069) diluted 1:2 in ddH2O was added to each well and incubated for 5 min. Luminescence was measured on a Synergy NEO2 plate reader (Agilent) at 20 ms/well at a read height of 1.0 mm. Relative luminescence units (RLU) were blank-subtracted and used for subsequent analysis. Plate wells were washed 4× following each incubation (except the final 5 min incubation) with 100 μL of PBS + 1% Tween (PSB-T) using a 405 TS/LS LHC2 plate washer (Biotek Instruments).

2.3 ACE2 enzymatic activity

To investigate whether endogenous ACE2 antibodies were able to inhibit ACE2 activity, a neutralization reaction was performed. 2 µL of serum samples (negative control, surveillance, convalescent) was added to 0.1 µg/mL of recombinant human ACE2 (rhACE2, R&D systems, Minnesota, MN, USA, cat. 933-ZN) for 30 min at room temperature under agitation. 10 µL of neutralized samples was transferred to 96-well black plates containing 15 µM of fluorogenic ACE2 substrate Mca-APK(Dnp) (Anaspec, Fremont, CA, USA, cat. AS-60757), to a final concentration of 11.25 µM.[34] Samples were assayed in duplicates without ACE2 inhibitor and in singles with 10−5 M ACE2 inhibitor MLN-4760 (Calbiochem, San Diego, CA, cat. 530616). Following a 30-min incubation at room temperature, fluorescence was measured in a FLUOstar Galaxy fluorometer (BMG Labtech, Ortenberg, Germany), detecting emission at 405 nm and excitation at 320 nm. Data are presented as Relative Fluorescence Units (RFU) baseline-subtracted using samples with MLN-4760 and normalized by volume of input serum (RFU/µL).

2.4 Depletion of SARS-CoV-2 spike antibodies in sera

To measure ACE2 autoantibody impact on ACE2 and SARS-CoV-2 spike interaction, serum samples were first depleted of spike-reactive antibodies. One hundred nanograms per well of spike protein (NRC) was coated in a high-binding polystyrene Nunc plate (Thermo Fisher Scientific, #460372) in a final volume of 10 µL in PBS. Plates were briefly centrifuged to ensure even coating and incubated at 4°C overnight. The next day, plates were washed as described previously and blocked using 80 µL of 3% w/v skim milk powder dissolved in PBST for 1 h. Plates were washed, and selected serum samples were mixed with 1:1 with 1% w/v skim milk powder dissolved in PBST (final of 50 µL) and applied to the wells. The diluted samples were incubated for 2 h with shaking, transferred to a new blocked plate coated with SARS-CoV-2 spike and incubated for another 2 h. Samples were transferred once again and incubated overnight at 4°C to be used in the spike binding assay the next day.

2.5 Spike and ACE2 binding assay

This protein-based assay was modified from a previously published surrogate neutralization assay.[33] First, recombinant SARS-CoV-2 spike protein (generously provided by Dr. Yves Durocher, National Research Council of Canada (NRC), Montréal) was diluted in PBS and was coated in a 384 well high-binding polystyrene Nunc plate (Thermo Fisher Scientific, #460372) at 50 ng/well with a final volume of 10 µL/well. The plates were then centrifuged at 216 *g* and incubated overnight at 4°C. The plates were then washed four times with 100 µL of PBS-T using a 405 TS/LS LHC2 plate washer (Biotek Instruments). The wells were then blocked with 80 µL of 3% w/v skim milk powder dissolved in PBST for 1 h and then washed (as described before). Samples that were not depleted were diluted 1 in 2 in 1% w/v skim milk powder dissolved in PBST. Previously depleted samples were already diluted 1 in 2. 20 µL of each sample was added to the plate along with 6.5 ng /well of recombinant biotinylated ACE2 (provided by the NRC) and incubated for 2 h with shaking. The plates were washed once again and bound ACE2 was detected by adding 5.2 ng/well in a final volume of 20 µL/well of streptavidin-peroxidase polymer (Thermo Fisher #N200), diluted in 1% w/v skim milk powder dissolved in PBST. After a 1-h incubation, the plates were then washed and developed with the addition of 20 µL of ELISA Pico Chemiluminescent Substrate (Thermo Fisher Scientific #37069), diluted 1:2 in MilliQ H2O. After a 5-min incubation, plates were read on a Neo2 plate reader (BioTek Instruments) at 20 ms/well and a read height of 1.0 mm. Luminescence values were adjusted to the blank (serum-free, no ACE2 condition) and the average maximal signal of the plate was established using the serum-free with ACE2 condition. Percentage inhibition was then established by measuring the reduction in spike/ACE2 interaction (0% inhibition; maximal ACE2-Spike binding).

2.6 Data analysis

Data, statistical analyses, and figures were processed in R (4.2.3). BioVenn was used to generate quantitative Venn diagrams.

3 Result

3.1 Identification of previous SARS-CoV-2 infections in a cross-sectional cohort

To study ACE2 autoantibodies following SARS-CoV-2 infection, serum samples of individuals enrolled in Stop the Spread Ottawa study were used.[32, 35] This community-based prospective cohort study on immune responses to SARS-CoV-2 infection and vaccination recruited individuals with a previous history of, or were at risk for, SARS-CoV-2 infection. Individuals with at least one blood draw by December 2021 with corresponding consent and demographic information were included in this study. In total, 464 individuals between ages 18 and 74 were included in this study with an average age of 43.5 years (SD = 13.5 years) among which 67.2% were female and the majority were Caucasian (89.7%). Within the cohort, 131 individuals were identified as having been infected by SARS-CoV-2 previously (Table 1, Figures S1 and S2). SARS-CoV-2 infections were self-reported to the study coordinators following a positive PCR test, diagnosed by a physician, or identified by a positive result by rapid antigen testing. Additionally, any individuals with IgG antibodies against the nucleocapsid (N) and Spike (S) above seroprevalence positivity thresholds were also identified as having been infected by SARS-CoV-2. This allowed the inclusion of asymptomatic and unreported infections. Our seropositivity threshold based on N and S dual positivity, reported and used previously,[33, 35, 36] was set at a 3% false discovery rate of the density distribution of a large set of prepandemic sera. A sensitivity analysis was also performed utilizing a more stringent definition of SARS-CoV-2 infection, only considering 88 individuals with serological evidence of previous SARS-CoV-2 infection (Figure S3).

3.2 Measurement and seroprevalence of ACE2 autoantibodies

IgG, IgA, and IgM antibodies able to bind recombinant ACE2 were measured using a chemiluminescent direct ELISA platform that has been used and validated extensively for populational-based serological studies.[33, 35, 37-40] Sera dilution used to measure ACE2 antibodies was validated and optimized to minimize background signal. For setting a seropositivity threshold, a systematic approach as described before was used.[41] To establish cut-offs for IgG and IgA, values over 2 standard deviations of the mean were excluded, the new mean was recalculated, and a final threshold was set at 2 standard deviations. IgM seropositivity threshold was similarly established by excluding any values over 2 standard deviations of the mean and by recalculating the new mean, but the final threshold was set at 1 standard deviation given the spread of IgM values. The cut-off thresholds were inspected for robustness (Figure 1). Any samples with a signal-to-threshold ratio of 1 or under were presumed negative. This allowed an evaluation of the relative seroprevalence

of all main isotypes of antibodies able to recognize ACE2 in sera of a large adult cohort (Table 1). ACE2-IgM antibodies were the most common with a seroprevalence of 18.8%. IgA seroprevalence in the overall cohort was the lowest at around 6.3% followed by IgG at 10.3%. Only a small fraction of the individuals with ACE2 autoantibodies simultaneously had all three isotypes present. The most common combination was IgG and IgM being detected together in 7.8% of the individuals with ACE2 antibodies. Less than 3% of individuals with ACE2 autoantibodies had either IgG/IgA or IgA/IgM detected simultaneously (Figure 1).

Table 1. Participant demographics and health characteristics based on SARS-CoV-2 infection history. Individuals who reported SARS-CoV-2 infection whether following a positive PCR test or confirmation by a medical professional, and individuals who had serological markers of prior infection (anti-N & anti-S IgG) were classified as individuals with a previous history of SARS-CoV-2 infection.

	Combined (n= 464)	**Previous history of SARS-CoV-2 infection** (n=131)	**No history of SARS-CoV-2 infection** (n=333)
Age (y.)			
Mean (SD)	43.5(13.5)	46.5(15.4)	42.3(12.5)
Median	42.5	45.0	42.0
Range	18-74	21-74	18-74
Sex			
Female Nb.(%)	312(67.2)	75(57.3)	237(71.2)
Ethnicity Nb (%)			
White	416(89.7)	116(88.5)	300(90.0)
Aboriginal	8(1.7)	1(0.8)	7(2.1)
Arab	9(1.9)	2(1.5)	7(2.1)
Black	5(1.1)	3(2.3)	2(0.6)
South Asian	5(1.1)	3(2.3)	2(0.6)
Other	21(4.5)	6(4.6)	15(4.5)
BMI			
Nb. with BMI Info	222	58	164
Mean (SD)	27.8	28.5	27.6
Median	26.7	27.5	26.4
Range	17.6 - 53.2	21.8 - 41.5	17.6 - 53.2
SARS-CoV-2 diagnosis Nb (%)			
Self-reported	121(26.1)	121(92.4)	-
Serology	87(18.8)	87(66.4)	-
Vaccinated Nb (%)	19(4.1)	4(3.1)	15(4.5)
ACE2 seroprevalence (%)			
IgG	10.3	6.1	12.0
IgA	6.3	7.6	5.7
IgM	18.8	12.2	21.3
IgG and/or IgA and/or IgM	30.4	22.9	33.3

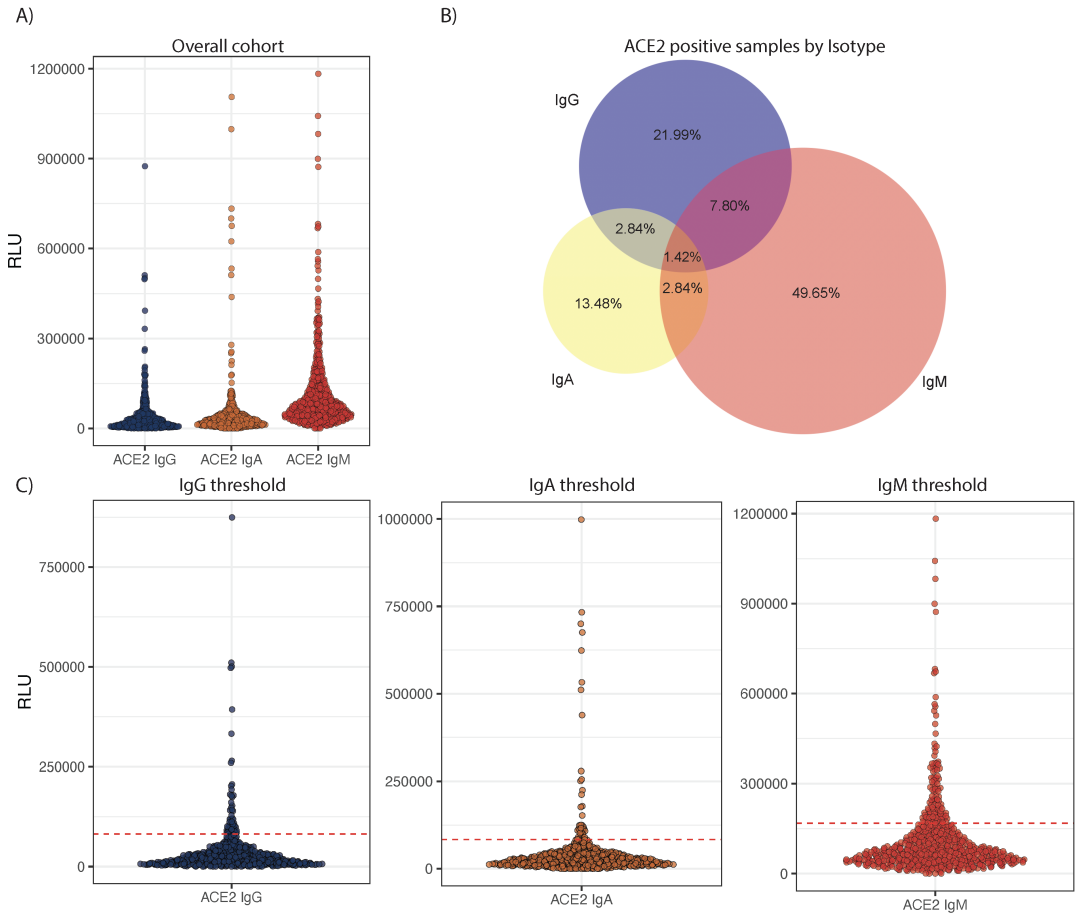


Figure 1 - Overview of ACE2 serology results and establishment of seropositivity thresholds. (A) Overall view of anti-ACE2 IgG, IgA, and IgM antibodies of the full cohort, including longitudinal sampling. (B) Quantitative Venn diagram representation of the distribution between IgM, IgA, and IgG ACE2 autoantibodies in the overall cohort of ACE2-positive individuals. (C) IgG, IgA, and IgM anti-ACE2 antibodies and associated threshold. IgG and IgA threshold was set at two cycles of 2 standard deviations (SD) from the mean of the presumed negative distribution. IgM threshold was set by a first cycle at 2SD and a second at 1SD from the mean of the presumed negative distribution.

3.3 Clinical association and kinetics of ACE2 autoantibodies

Demographic and clinical data were available and matched to samples included in this study. The impact of several variables such as age, sex, comorbidities, and diagnosed conditions on ACE2 autoantibody seroprevalence and levels was explored. No differences were seen between the sexes for anti-ACE2 IgG and IgA, whereas levels of ACE2-IgM were elevated in the females in our cohort ($p = .00041$) (Figure S4). For comparison of age, individuals were stratified into groups: ages 18–30, 31–40, 41–50, 51–60, and 60–74. No differences in the levels of anti-ACE2 IgG and IgA were observed between age groups. For anti-ACE2 IgM, individuals in the 18–30 group had elevated levels compared to the 41–50, 51–60, and 60–74 groups. Individuals in the 31–40 group also had higher levels when compared to the 60–74 group (Figure S5). While some age-related differences are statistically significant, the biological differences between groups are small. The association between seroprevalence of ACE2 autoantibodies seroprevalence and sex was assessed. Anti-ACE2 IgM seroprevalence was positively associated with the female sex (OR 1.95 (1.12–3.38)), whereas males were associated with a lower seroprevalence of anti-ACE2 IgM (OR 0.51 (0.30–0.89)) (Figure 2, Table S1). A higher seroprevalence of anti-ACE2 IgG was observed for individuals with neurological conditions (OR 5.48 (1.27–23.69)). This association was not seen with anti-ACE2 IgA or IgM. No other comorbidity or medical condition correlated with a higher or lower seroprevalence of ACE2 autoantibodies across all isotypes. During the study period, a subset of individuals provided one or two follow-up serum samples enabling us to investigate the kinetics of the various anti-ACE2 isotypes across time (Figure 3). Levels of IgG antibodies remained relatively stable over time (one individual displayed a strong increase in both subsequent sample collections). Interestingly, IgA levels remained relatively stable, with a few individuals showing a slight decay over time. As expected, anti-ACE2 IgM levels display a high degree of variability over time, likely due to the intrinsic half-life of IgM antibodies.

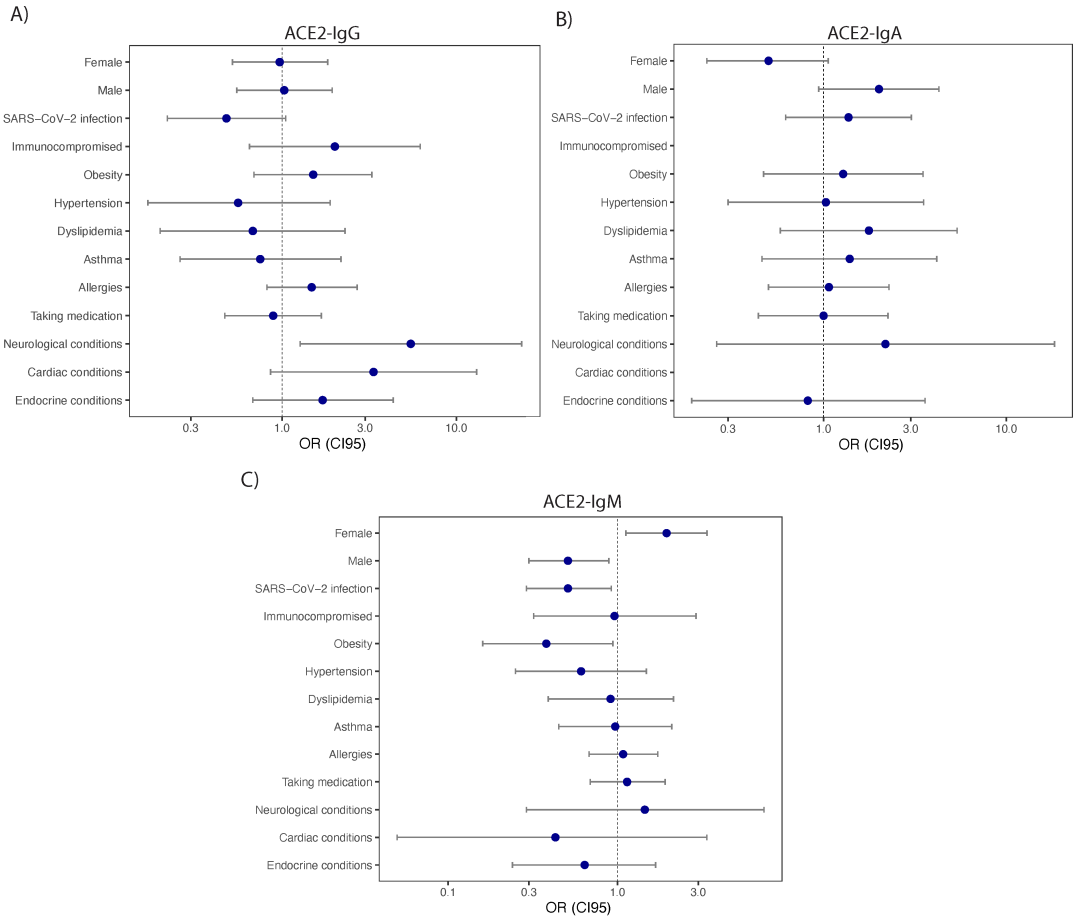


Figure 2 - Influence of clinical features and demographic characteristics on ACE2 autoantibodies prevalence. Odd ratios (OR) and 95% confidence interval (CI) were calculated for demographic characteristics and clinical features for individuals in relation to (A) IgG, (B) IgA and (C) IgM ACE2 autoantibodies. A table with a complete list of OR and 95% CI is available in the Table S1. The OR (CI95) are shown here on a log10 formatted axis.

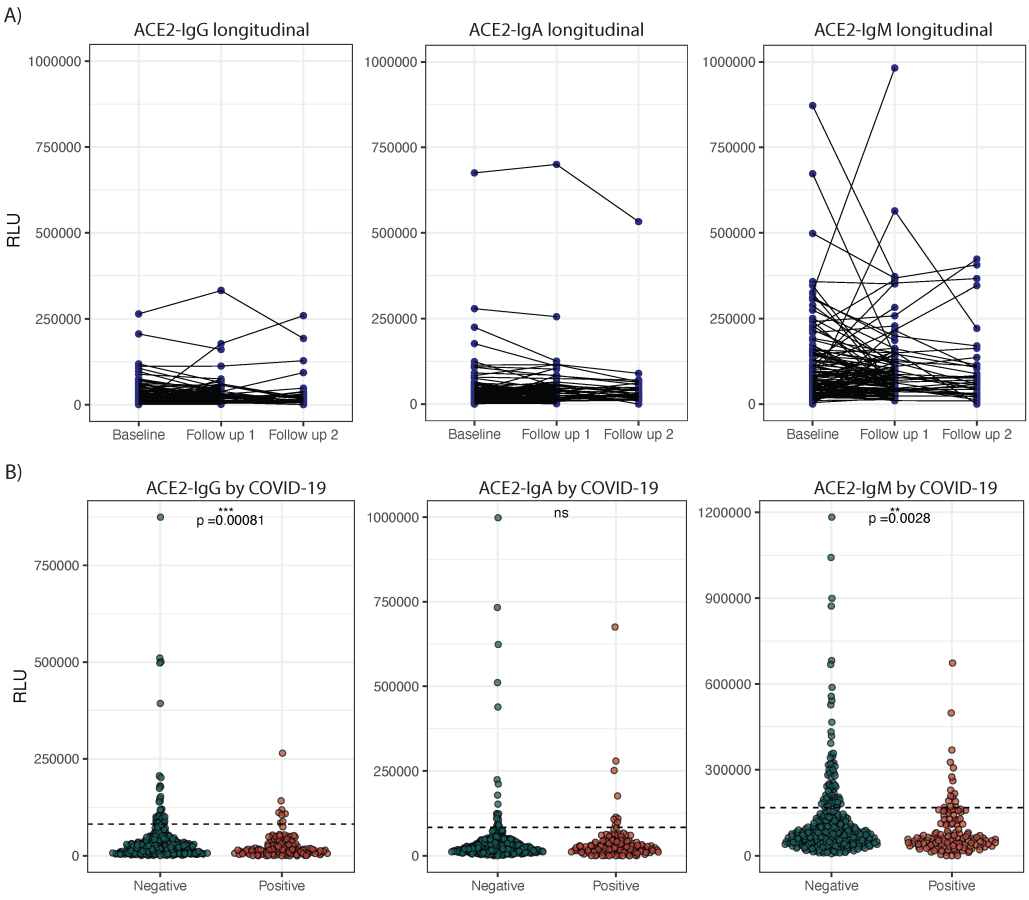


Figure 3 - Persistence of autoantibodies in serum over time and association with previous SARS-CoV-2 infection. (A) Some individuals had one or two follow-up samples. ACE2 IgG, IgA, IgM is shown longitudinally (Follow up 1 (n = 120), median time between draws (SD) = 35 days (10), Follow up 2 (n = 35), median time between draws (SD) = 37 days (6)). (B) IgG, IgA, and IgM ACE2 autoantibodies levels are shown for individuals who never had SARS-CoV-2 and for individuals who had serological markers of SARS-CoV-2 infection and/or self-reported a SARS-CoV-2 infection. Unpaired two-sided Wilcoxon test was used to establish statistical significance (n = 464), $p \leq 0.05$ (*), $p \leq 0.01$ (**), $p \leq 0.001$ (***), $p \leq 0.0001$ (****).

3.4 Absence of association between previous SARS-CoV-2 infection and levels of ACE2 autoantibodies

Individuals in the overall cohort, who were previously affected by SARS-CoV-2 infections, were identified to investigate whether ACE2 autoantibodies are induced by COVID-19. To identify SARS-CoV-2 convalescent individuals, we employed (1) an inclusive definition of participants who self-reported a SARS-CoV-2 infection as well as participants with serological markers of previous SARS-CoV-2 infection and (2) a stringent definition of participants that only had serological markers of previous infection. The levels of anti-ACE2 antibodies for each isotype were compared between individuals with no history of SARS-CoV-2 infection and individuals identified with previous SARS-CoV-2 infection using the inclusive definition (Figure 3) and individuals who only displayed serological markers of previous infection (Figure S3). In both groups, no differences in anti-ACE2 IgG or IgA levels were detected. In both analysis groups, anti-ACE2 IgM antibodies were elevated in individuals with no history of previous infection in contrast to either convalescent group (p = .006 & .0028). Likewise, a prior history of SARS-CoV-2 was not associated with a higher or lower seroprevalence of IgA and IgG ACE2 autoantibodies. IgM ACE2 autoantibodies were associated with a lower seroprevalence in individuals with prior SARS-CoV-2 infections (OR 0.51 (0.29–0.92)) (Figure 2). Global analysis of ACE2 autoantibodies by PCA failed to identify convalescent individuals based on their levels of ACE2 autoantibodies (Figure S6). To investigate whether ACE2 autoantibody levels were associated with the intensity of humoral responses to recent SARS-CoV-2 infections, we explored the association of IgG, IgA, and IgM ACE2 autoantibodies to the levels of IgG antibodies against SARS-CoV-2 nucleocapsid (Figure S7). There was no association between ACE2 autoantibodies levels and nucleocapsid IgG intensity ($R2 < 0.005$). In this cohort, there is no evidence that prior SARS-CoV-2 infection results in a higher seroprevalence or levels of ACE2 autoantibodies in sera.

3.5 ACE2 autoantibodies fail to inhibit ACE2 enzymatic activity or ACE2-spike interaction

While ACE2 autoantibodies are not elevated in levels or prevalence following SARS-CoV-2 infection in this cohort, their capacity to impact ACE2 either enzymatically or as a viral entry receptor was further investigated. A first subset of individuals (n = 103) displaying variable levels of ACE2 autoantibodies were selected to investigate the ability of serum ACE2 autoantibodies to inhibit ACE2 enzymatic activity (Figure 4, Table S3). No differences in enzymatic activity were

detected between sera positive for ACE2 autoantibodies ($p = .52$) (Figure 4B). Interestingly, individuals who had a previous history of SARS-CoV-2 infection showed an elevated ACE2 enzymatic activity ($p = .00043$) (Figure 4C). We next explored the potential of ACE2 autoantibodies to block SARS-CoV-2 spike and ACE2 interactions, as previous research has demonstrated the potential of using anti-ACE2 antibodies to block SARS-CoV-2 viral entry in vitro.[42, 43] By modifying a previously developed protein-based surrogate neutralization assay,[33] we measured the ability of sera from individuals with varying levels of ACE2 antibodies to inhibit ACE2/spike interaction (Figure 4D). Given that 65.5% of the samples were convalescent sera which contained antibodies against the spike protein (Table S3), these antibodies would confound our ability to measure the neutralizing contribution of ACE2 autoantibodies. As such, a series of depletion steps were performed by incubating sera in wells with recombinant SARS-CoV-2 spike protein to remove spike-reactive antibodies with potential ACE2-spike neutralizing capacity (Figure 4E). While this approach significantly reduced the levels of anti-spike antibodies, some samples retained relatively high levels of antibodies post-depletion, likely due to a high initial titer of anti-spike. The percent of inhibition of the interaction between SARS-CoV-2 spike and ACE2 was measured pre- and postdepletion (Figure 4F). A reduction in the ability of sera to inhibit ACE2/spike interactions was measured postdepletion confirming that antispike antibodies were a key source of neutralization. However, a few individuals displayed inhibition levels above 50% postdepletion. To understand if this was due to anti-ACE2 antibodies as opposed to antispike antibodies in samples where levels of anti-spike antibodies postdepletion remained elevated, postdepletion ACE2/spike inhibition levels were classified by ACE2 autoantibody seroprevalence (Figure 4G). No differences in inhibition were detected, regardless of whether or not samples had detectable levels of ACE2 autoantibodies. Rather, the inhibition capacity of serum correlated with the levels of antispike antibodies postdepletion (Figure 4H). In addition, given that over 65% of the samples were from convalescent individuals, there is nothing to suggest that ACE2 autoantibodies from convalescent individuals differ (Table S3). The sera used in this assay was minimally diluted (1:1) with the assay buffer, with no neutralization detected. This contrasts SARS-CoV-2 antibodies, which in our experience, on average, can completely inhibit ACE2 and spike interaction at 1:25 to 1:125 in those same assay conditions. Overall, these results suggest that ACE2 autoantibodies at biological concentrations found in serum are unable to inhibit ACE2 and SARS-CoV-2 spike interaction.

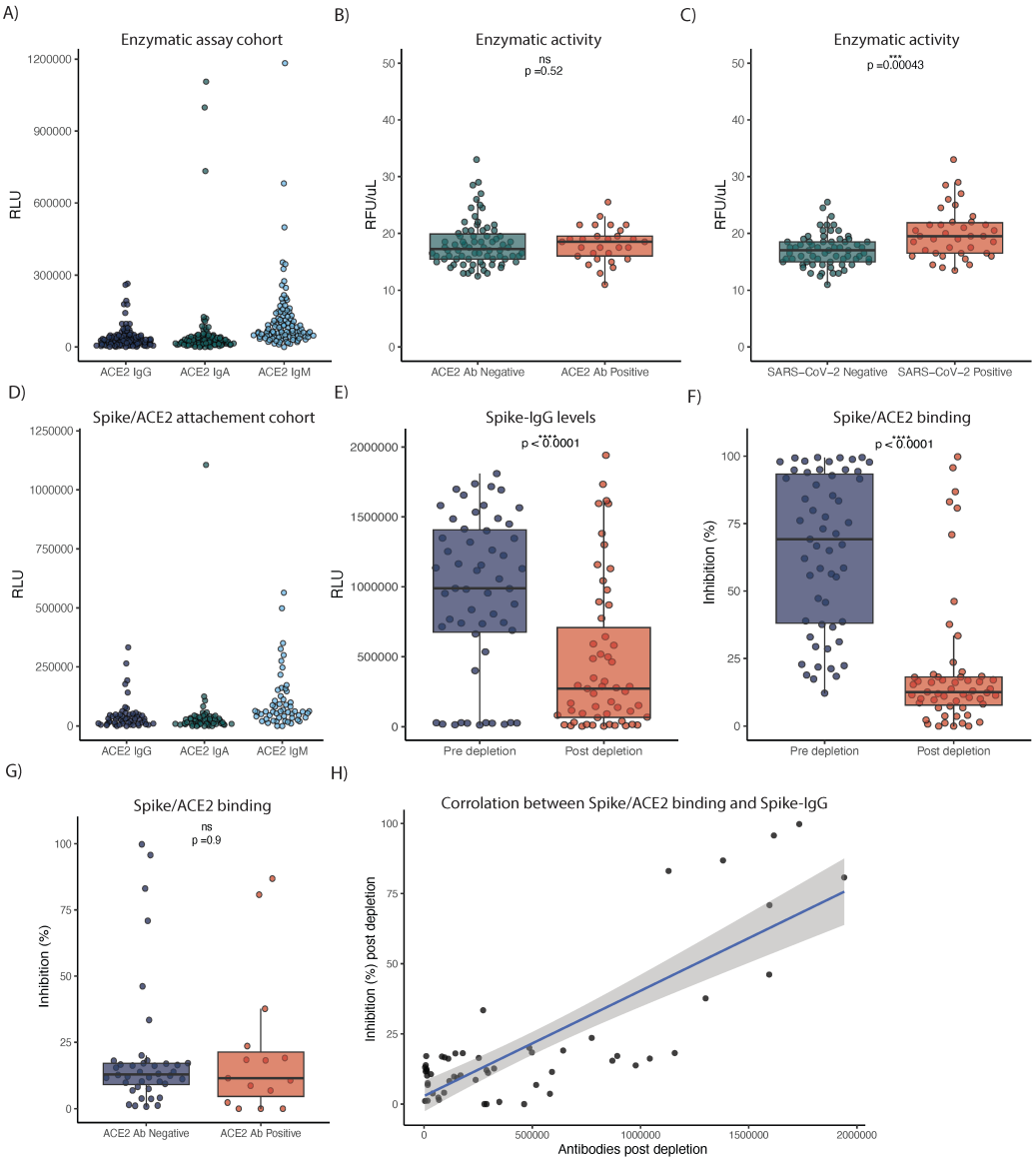


Figure 4 - Effect of ACE2 autoantibodies on ACE2 enzymatic activity and SARS-CoV-2 spike-ACE2 binding. (A) ACE2 autoantibodies levels (IgG, IgA, IgM) in a subset of samples for which ACE2 enzymatic activity was assessed. (B) Levels of ACE2 enzymatic activity in individuals who had IgG and/or IgA and/or IgM ACE2 autoantibodies in contrast to the individuals who had no detectable ACE2 autoantibodies. (C) Levels of ACE2 enzymatic activity in individuals who self-reported a SARS-CoV-2 infection and/or had serological markers of previous infection. (D) ACE2 autoantibodies levels in a subset of samples in which ACE2 and spike interaction was assessed. (E) Anti-Spike IgG antibodies levels pre- and post-depletion in sera. (F) % inhibition representing the ability of the sera to inhibit spike and ACE2 interaction pre- and post-depletion. (G) % inhibition representing the ability of the sera to inhibit spike and ACE2 interaction in individuals who had IgG and/or IgA and/or IgM ACE2 autoantibodies above threshold in contrast to the individuals who had no detectable ACE2 autoantibodies. (H) Linear correlation between the ability of sera to inhibit Spike and ACE2 binding and the levels of Spike IgG antibodies in depleted sera. Unpaired two-sided Wilcoxon test was used to establish statistical significance where applicable, $p \leq 0.05$ (*), $p \leq 0.01$ (**), $p \leq 0.001$ (***), $p \leq 0.0001$ (****).

4 Discussion

ACE2 autoantibodies have been described in numerous studies before SARS-CoV-2 emergence.[29] Previously, ACE2 autoantibodies have been linked with various health conditions such as Parkinson's disease, systemic sclerosis, and rheumatoid arthritis.[27, 28, 30] Given the role of ACE2 as the cognate receptor of SARS-CoV-2, scientific interest in ACE2 autoantibodies has resurfaced. Several studies have recently investigated ACE2 autoantibodies in small control and SARS-CoV-2 convalescent cohorts. These cohorts describing ACE2 autoantibodies have not simultaneously described the seroprevalence of all three main isotypes of antibodies (IgG, IgM, IgA) and the study sample sizes were small. By using the serum of individuals enrolled in the *Stop the Spread Ottawa Study*,[32] we were able to generate a cross-sectional cohort of 333 healthy control individuals and 131 individuals with a laboratory-confirmed and self-reported history of previous SARS-CoV-2 infection thereby addressing sample size concerns (Table 1, Figures S1 and S2).

There are currently no recognized or standardized negative controls to establish seroprevalence to ACE2, and as such, the thresholds for this study were established by excluding high responders and setting the threshold from the presumed negative distribution of samples (Figure 1). We found that overall, nearly 1 in 5 individuals had detectable levels of ACE2-IgM. This echoes observations in a Japanese cohort that reported an ACE-IgM seroprevalence of 15%.31 For anti-ACE2 IgG antibodies, we estimated a seroprevalence of 10.3%. A previous report of ACE2 IgG seroprevalence in a cohort of 20 control individuals was estimated at around 8.7%.[30] Simultaneous IgM and IgG reactivity to ACE2 in individuals with detectable levels of ACE2 autoantibodies was estimated at 7.8% in our cohort, and a previous study had estimated this parameter at 6%.[31] To our knowledge, we are the first group to measure IgA antibodies targeting ACE2. In our cohort, the seroprevalence of ACE2-IgA was 6.3%, with <3% of individuals simultaneously positive for ACE2 IgG, IgA, and IgM autoantibodies. Overall, the percentage of individuals who had ACE2 autoantibodies of any isotype in our cohort was 30.4%.

Demographic information and comorbidity data were collected alongside serum samples, which we leveraged to investigate the various factors that may influence ACE2 autoantibody seroprevalence or their abundance intensity. Females had a higher seroprevalence and higher levels

of ACE2-IgM. Stratifying by age, only significant differences in autoantibody levels were seen for ACE2-IgM, with older individuals displaying lower levels. Several types of autoantibodies including antinuclear antibodies and anti-cardiolipin antibodies have been shown to increase with age.[44-46] Perhaps surprisingly, individuals aged between 60 and 74 years had significantly lower ACE2-IgM than younger individuals (Figure S5). The impact of co-morbidities on anti-ACE2 antibody prevalence and levels was assessed. Conditions including hypertension, dyslipidemia, allergies, immunocompromised status, asthma, medication, cardiac conditions, and endocrine conditions were not associated with higher or lower seroprevalence of ACE2 autoantibodies (Figure 2 and Table S1). Obesity was marginally associated with a lower seroprevalence of ACE2-IgM, but this was limited to the IgM isotype. Interestingly, a higher seroprevalence of ACE2-IgG antibodies was associated with neurological conditions, but the low numbers of individuals with neurological conditions in our cohort impede further conclusions. While ACE2 has been linked with other health conditions, our cohort was sampled from the general population that limits our ability to measure associations with rare pathologies. When looking at the longitudinal trend of ACE2 autoantibodies for individuals with one or two follow-up serum collections, IgA and IgG antibodies remained relatively stable over time, whereas IgM fluctuated (Figure 3). While it is unclear whether what triggers the production of ACE2 autoantibodies, the increased rate of decay of IgM compared to IgG and IgA is most likely due to its intrinsic shorter half-life and the inability to bind FcRn (key receptor for IgG recycling).[47-49]

Several groups have previously reported that ACE2 autoantibodies could be induced by SARS-CoV-2 infection. For example, a small cohort study found that 81% of convalescent individuals ($n = 32$) and 93% of hospitalized acute SARS-CoV-2 infection ($n = 15$) had detectable ACE2 autoantibodies that were undetectable in their control group ($n = 13$). Other groups have found similar observations.[24, 25] To explore whether SARS-CoV-2 induced or correlated with ACE2 autoantibodies in our cohort, we identified two cohorts of convalescent individuals. The first cohort included individuals who had substantial levels of IgG against the N and S protein (i.e., the serological marker of a previous infection) of SARS-CoV-2 and/or declared having been infected by SARS-CoV-2 to our study coordinators. The inclusion of self-reported infection addresses concerns of misidentifying convalescent individuals in which anti-N or anti-S decayed beyond our seropositivity threshold over time. The second cohort of convalescent individuals included only

individuals who had serological and/or laboratory evidence of prior infection, hereby constituting a stringent cohort eliminating subjective assessment of SARS-CoV-2 infection and patient bias. Principal component analysis failed to find clusters of convalescent individuals based on ACE2 autoantibody levels (Figure S6). In line with this, levels of IgG, IgA, and IgM ACE2 autoantibodies were not more elevated in the convalescent group (Figure 3). In fact, it appears that ACE2 IgM was elevated in nonconvalescent individuals. These data demonstrate that ACE2 antibodies are not more prevalent or present at a higher titer in SARS-CoV-2 convalescent sera. Furthermore, we asked if antibody titers against the N protein correlate with ACE2 autoantibodies. This could suggest a disease severity-dependent relationship. We found no association or association clusters between either ACE2 autoantibody isotype or SARS-CoV-2 N antibody levels (Figure S7). This further suggests that while we may not detect ACE2 autoantibody induction shortly after an infection, as shown by some groups, we show that ACE2 antibodies are decoupled with SARS-CoV-2 antibodies, and if induced in some cases, short-lived.

Our observations are in contrast with several previous studies. It is possible that high disease severity could impact ACE2 autoantibodies levels. Indeed, most studies have been focused on hospitalized or severe COVID-19 infections.[23, 25] For example, a recent study found higher median ACE2 IgG intensity in moderate/severe cases of COVID-19 in contrast to mild convalescent individuals.[50] However, it is important to mention that the overall seroprevalence was similar between convalescent individuals and pre-COVID-19 sera. Other studies also found that ACE2 autoantibodies were increased in those with severe COVID-19 infection.[51, 52] While severity scores for most convalescent individuals were not measured for all the serum samples, to our knowledge, none had to be admitted to the ICU, suggesting mostly asymptomatic and mild–moderate COVID-19 infections. However, we cannot completely rule out severe infections in some individuals, given the self-reported nature of the cohort. The link with disease severity is not obvious. In fact, in a large protein array screen of severe COVID-19 infections, ACE2 autoantibodies were only detected in one individual while several individuals had autoantibodies to numerous other proteins such as cytokines.[9] Moreover, in a recent study that screened 1139 convalescent individuals for ACE2-IgG, the authors found that the majority of individuals who had ACE2-IgG did not require hospitalization following SARS-CoV-2 infection.[53] It remains possible that severe infection can induce ACE2 autoantibodies. It was reported that severe SARS-CoV-2 infection can induce low

selection pressure of B cells, which was associated with de novo autoreactivity.[54] In this study, we show that ACE2 autoantibodies are not exclusive to SARS-CoV-2 convalescent individuals but are common in the general population concordant with observations of these antibodies with other pathologies and in healthy populations.[29, 31] These ACE2 autoantibodies may have an important regulatory role; however, no data currently exist to support this hypothesis. Some studies have also suggested that ACE2 autoantibodies could arise from molecular mimicry or from spike/ACE2 aggregates making their way to germinal centers. One study noticed an increase in ACE2-IgG following vaccination.[50] In the small subset of individuals vaccinated against SARS-CoV-2 in our cohort, we did not observe this effect (Figure S8). Others have proposed anti-idiotype antibodies as a possible explanation. However, given that the seroprevalence did not differ in vaccinated or in convalescent individuals in relation to our control cohort, the data do not currently support this hypothesis. It is also possible that ACE2 autoantibodies occur as the result of molecular mimicry of another pathogen. However, there is no evidence in support.

The function, if any, of autoantibodies targeting ACE2 remains unclear. Some groups have shown data that ACE2 enzymatic activity could be inhibited by these antibodies,[23] while others showed the contrary.[52] We used a subset of our cohort to investigate if ACE2 enzymatic activity is impacted by the presence of plasma containing various levels of ACE2 autoantibody (Figure 4). We found that ACE2 antibodies did not impact enzymatic activity. We found the ACE2 enzymatic activity to be higher in individuals with a previous history of SARS-CoV-2 infection. This could be explained by a higher amount of soluble ACE2 previously reported in convalescent individuals resulting in higher baseline enzymatic activity in our assay.55 We also explored the possibility that ACE2 autoantibodies may be protective by neutralizing SARS-CoV-2 by preventing ACE2/spike interactions. This effect is difficult to measure in convalescent individuals given that antibodies against the spike protein would overwhelmingly contribute to the neutralization of SARS-CoV-2. As such, we depleted serum samples of antibodies that could bind to the spike protein. In some cases, the depletion process was incomplete, likely due to the initially very high titer of anti-spike antibodies. The depleted sera were then used in a protein-based neutralization assay to measure the interaction between the spike and the ACE2. While some individuals still had neutralization ability, these were linked with samples with incomplete antispike depletion (Figure 4). In samples with no residual spike antibodies, the neutralization ability of the sera was lost, suggesting that

ACE2 autoantibodies cannot block these interactions. This suggests that either these anti-ACE2 antibodies recognize epitopes on ACE2 that do not interfere with the ACE2/spike binding or the concentration and affinity of ACE2 antibodies in sera are not able to outcompete the affinity of the spike protein for ACE2.

This study is focused on the detection of ACE2 autoantibodies in individuals who did not require hospitalization for SARS-CoV-2 infection. In addition, we were not able to longitudinally monitor ACE2 levels continuously prior to and post-SARS-CoV-2 infection as the prevalence of SARS-CoV-2 infection in the Ottawa region in late 2020 was low. Furthermore, we did not investigate the presence of ACE2 autoantibodies at mucosal surfaces, such as the upper respiratory tract. We focused our understanding of ACE2 autoantibodies in their role in SARS-CoV-2 pathogenesis; however, ACE2 autoantibodies may play a role in other physiological processes independently of infection, which were beyond the scope of this work.

5 Conclusion

This is the first large cohort study to report the simultaneous seroprevalence of IgG, IgA, and IgM antibodies in sera able to bind ACE2. We found no evidence that ACE2 autoantibodies were induced by SARS-CoV-2 infection and were rather common in SARS-CoV-2 naïve individuals. We also demonstrate that these autoantibodies are not able to inhibit SARS-CoV-2 spike and ACE2 interactions, or able to block ACE2 enzymatic activity. The relevance of ACE2 autoantibodies in homeostasis, health, or disease remains unclear.

Author contributions
Y.G. and M.-A.L. designed the study. Y.G. developed the assays and performed the experiments together with N.C. and P.S.M., C.C., E.C., A.K., recruited participants, coordinated sample collection, and collected participant data. M.T.S. and K.B. performed and analyzed the ACE2 enzymatic activity assay. M.P. and C.A. analyzed COVID-19 serology. Y.G. performed the data analysis. Y.G. and M.-A.L. wrote and formatted the manuscript. All authors have read, edited and approved the manuscript.

Acknowledgments
We acknowledge the involvement of previous and current members of the University of Ottawa Serology and Diagnostics High Throughput Facility including: Danielle Dewar-Darch, Justino Hernandez Soto, Abishek Xavier, Nicholas Bradette, Klaudia Baumann, Gwendoline Ward, Yuchu Dou, and Lynda Rocheleau. We also acknowledge everyone involved in the Stop the Spread Ottawa study including participants. Production of COVID-19 reagents was financially supported by NRC's Pandemic Response Challenge Program. The graphical abstract was created in https://BioRender.com.

Funding information
This work was supported by a Canadian Institute of Health Research (CIHR) grant (VR2-172722) and from a supplement by the COVID-19 Immunity Task Force (CITF) to M-A.L. Additionally, Y.G. is supported by a Charles Best and Frederick Banting CGS-D from CIHR (476885). M.-A.L. holds a Faculty of Medicine Chair of Excellence in Pandemic Viruses and Preparedness Research. The funding sources played no role in the study design, data collection, analysis, writing of the manuscript, and decision to publish.

Disclosures
The authors declare no conflict of interest relevant to the present manuscript.

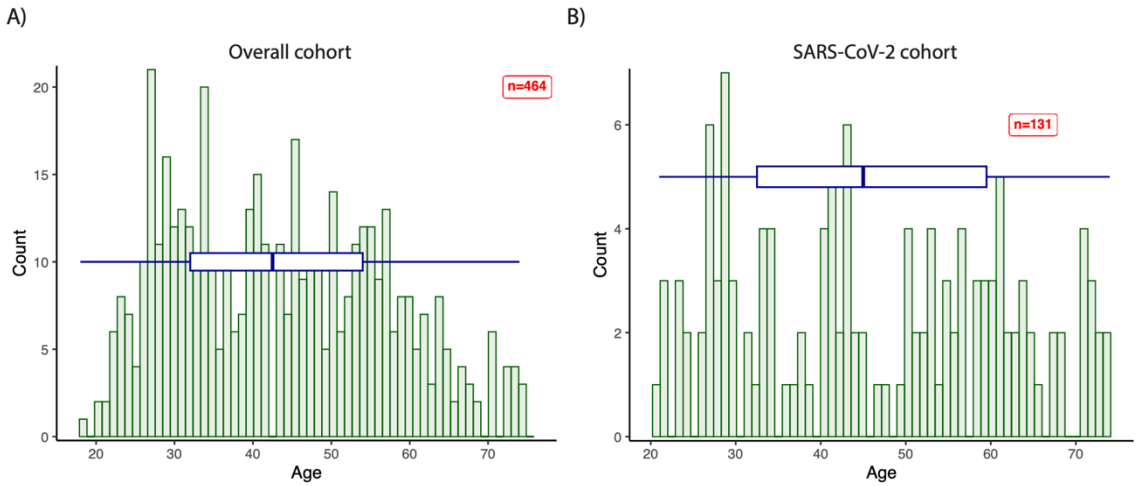
References

1. Wang H, Paulson KR, Pease SA, Watson S, Comfort H, Zheng P, et al. Estimating excess mortality due to the COVID-19 pandemic: a systematic analysis of COVID-19-related mortality, . *The Lancet.* 2022;399(10334):1513-36.
2. Anaya J-M, Herrán M, Beltrán S, and Rojas M. Is post-COVID syndrome an autoimmune disease? *Expert Review of Clinical Immunology*. 2022;18(7):653-66.
3. McMillan P, Dexhiemer T, Neubig RR, and Uhal BD. COVID-19—A Theory of Autoimmunity Against ACE-2 Explained. *Frontiers in Immunology*. 2021;12.
4. Mobasheri L, Nasirpour MH, Masoumi E, Azarnaminy AF, Jafari M, and Esmaeili S-A. SARS-CoV-2 triggering autoimmune diseases. *Cytokine.* 2022;154:155873.
5. Bjornevik K, Cortese M, Healy BC, Kuhle J, Mina MJ, Leng Y, et al. Longitudinal analysis reveals high prevalence of Epstein-Barr virus associated with multiple sclerosis. *Science.* 2022;375(6578):296-301.
6. Gazzaruso C, Carlo Stella N, Mariani G, Nai C, Coppola A, Naldani D, et al. High prevalence of antinuclear antibodies and lupus anticoagulant in patients hospitalized for SARS-CoV2 pneumonia. *Clin Rheumatol.* 2020;39(7):2095-7.
7. Lerma LA, Chaudhary A, Bryan A, Morishima C, Wener MH, and Fink SL. Prevalence of autoantibody responses in acute coronavirus disease 2019 (COVID-19). *J Transl Autoimmun.* 2020;3:100073.
8. Bastard P, Rosen LB, Zhang Q, Michailidis E, Hoffmann H-H, Zhang Y, et al. Autoantibodies against type I IFNs in patients with life-threatening COVID-19. *Science.* 2020;370(6515):eabd4585.
9. Chang SE, Feng A, Meng W, Apostolidis SA, Mack E, Artandi M, et al. New-onset IgG autoantibodies in hospitalized patients with COVID-19. *Nature Communications.* 2021;12(1):5417.
10. Helms J, Tacquard C, Severac F, Leonard-Lorant I, Ohana M, Delabranche X, et al. High risk of thrombosis in patients with severe SARS-CoV-2 infection: a multicenter prospective cohort study. *Intensive Care Med.* 2020;46(6):1089-98.
11. Xiao M, Zhang Y, Zhang S, Qin X, Xia P, Cao W, et al. Antiphospholipid Antibodies in Critically Ill Patients With COVID-19. *Arthritis Rheumatol.* 2020;72(12):1998-2004.
12. Galipeau Y, Cooper C, and Langlois M-A. Autoantibodies in COVID-19: implications for disease severity and clinical outcomes. *Frontiers in Immunology.* 2025;15.
13. Siloşi I, Siloşi CA, Boldeanu MV, Cojocaru M, Biciuşcă V, Avrămescu CS, et al. The role of autoantibodies in health and disease. *Rom J Morphol Embryol.* 2016;57(2 Suppl):633-8.
14. Bergman R, Ramon M, Wildbaum G, Avitan-Hersh E, Mayer E, Shemer A, et al. Psoriasis patients generate increased serum levels of autoantibodies to tumor necrosis factor-alpha and interferon-alpha. *J Dermatol Sci.* 2009;56(3):163-7.
15. Sjöwall C, Ernerudh J, Bengtsson AA, Sturfelt G, and Skogh T. Reduced anti-TNFalpha autoantibody levels coincide with flare in systemic lupus erythematosus. *J Autoimmun.* 2004;22(4):315-23.
16. Morimoto AM, Flesher DT, Yang J, Wolslegel K, Wang X, Brady A, et al. Association of endogenous anti-interferon-α autoantibodies with decreased interferon-pathway and disease activity in patients with systemic lupus erythematosus. *Arthritis Rheum.* 2011;63(8):2407-15.
17. Ni W, Yang X, Yang D, Bao J, Li R, Xiao Y, et al. Role of angiotensin-converting enzyme 2 (ACE2) in COVID-19. *Critical Care.* 2020;24(1):422.
18. Donoghue M, Hsieh F, Baronas E, Godbout K, Gosselin M, Stagliano N, et al. A novel angiotensin-converting enzyme-related carboxypeptidase (ACE2) converts angiotensin I to angiotensin 1-9. *Circ Res.* 2000;87(5):E1-9.
19. Hikmet F, Méar L, Edvinsson Å, Micke P, Uhlén M, and Lindskog C. The protein expression profile of ACE2 in human tissues. *Mol Syst Biol.* 2020;16(7):e9610.
20. Li W, Moore MJ, Vasilieva N, Sui J, Wong SK, Berne MA, et al. Angiotensin-converting enzyme 2 is a functional receptor for the SARS coronavirus. *Nature.* 2003;426(6965):450-4.

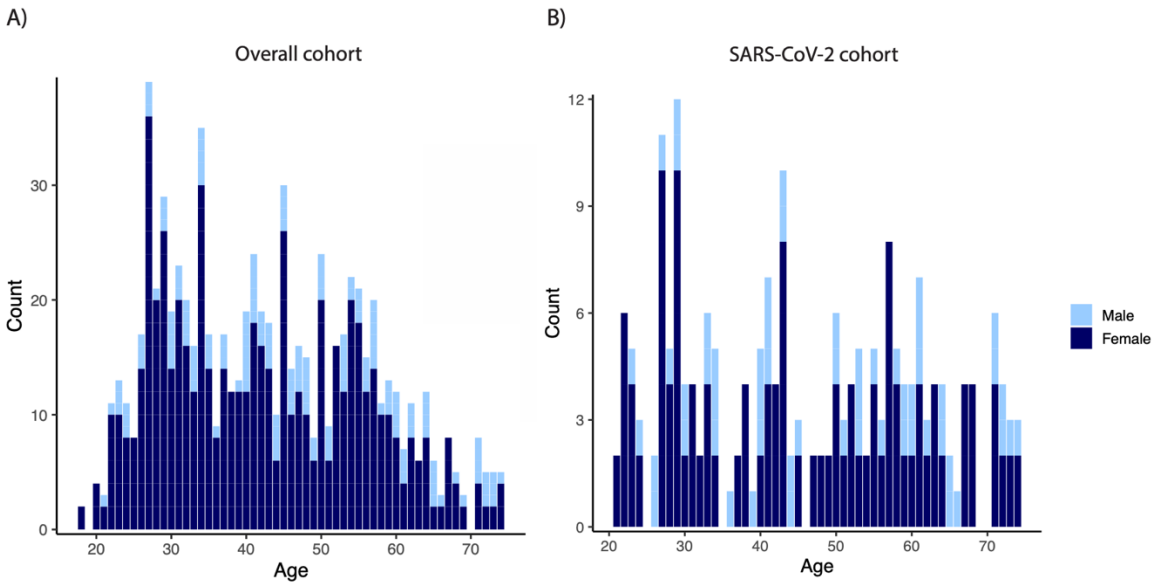
21. Shang J, Ye G, Shi K, Wan Y, Luo C, Aihara H, et al. Structural basis of receptor recognition by SARS-CoV-2. *Nature.* 2020;581(7807):221-4.
22. Hofmann H, Pyrc K, van der Hoek L, Geier M, Berkhout B, and Pöhlmann S. Human coronavirus NL63 employs the severe acute respiratory syndrome coronavirus receptor for cellular entry. *Proc Natl Acad Sci U S A.* 2005;102(22):7988-93.
23. Arthur JM, Forrest JC, Boehme KW, Kennedy JL, Owens S, Herzog C, et al. Development of ACE2 autoantibodies after SARS-CoV-2 infection. *PLOS ONE.* 2021;16(9):e0257016.
24. Casciola-Rosen L, Thiemann DR, Andrade F, Trejo-Zambrano MI, Leonard EK, Spangler JB, et al. IgM anti-ACE2 autoantibodies in severe COVID-19 activate complement and perturb vascular endothelial function. *JCI Insight.* 2022;7(9).
25. Rodriguez-Perez AI, Labandeira CM, Pedrosa MA, Valenzuela R, Suarez-Quintanilla JA, Cortes-Ayaso M, et al. Autoantibodies against ACE2 and angiotensin type-1 receptors increase severity of COVID-19. *J Autoimmun.* 2021;122:102683.
26. Lai Y-C, Cheng Y-W, Chao C-H, Chang Y-Y, Chen C-D, Tsai W-J, et al. Antigenic Cross-Reactivity Between SARS-CoV-2 S1-RBD and Its Receptor ACE2. *Frontiers in Immunology.* 2022;13.
27. Khajeh Pour S, Scoville C, Tavernier SS, and Aghazadeh-Habashi A. Plasma angiotensin peptides as biomarkers of rheumatoid arthritis are correlated with anti-ACE2 auto-antibodies level and disease intensity. *Inflammopharmacology.* 2022;30(4):1295-302.
28. Labandeira CM, Pedrosa MA, Quijano A, Valenzuela R, Garrido-Gil P, Sanchez-Andrade M, et al. Angiotensin type-1 receptor and ACE2 autoantibodies in Parkinson´s disease. *npj Parkinson's Disease.* 2022;8(1):76.
29. Takahashi Y, Haga S, Ishizaka Y, and Mimori A. Autoantibodies to angiotensin-converting enzyme 2 in patients with connective tissue diseases. *Arthritis Research & Therapy.* 2010;12(3):R85.
30. Miziołek B, Sieńczyk M, Grzywa R, Łupicka-Słowik A, Kucharz E, Kotyla P, et al. The prevalence and role of functional autoantibodies to angiotensin-converting-enzyme-2 in patients with systemic sclerosis. *Autoimmunity.* 2021;54(4):181-6.
31. Mecoli CA, Yoshida A, Paik JJ, Lin CT, Danoff S, Hanaoka H, et al. Presence and Implications of Anti-Angiotensin Converting Enzyme-2 Immunoglobulin M Antibodies in Anti-Melanoma-Differentiation-Associated 5 Dermatomyositis. *ACR Open Rheumatol.* 2022;4(5):457-63.
32. Collins E, Galipeau Y, Arnold C, Bosveld C, Heiskanen A, Keeshan A, et al. Cohort profile: Stop the Spread Ottawa (SSO)—a community-based prospective cohort study on antibody responses, antibody neutralisation efficiency and cellular immunity to SARS-CoV-2 infection and vaccination. *BMJ Open.* 2022;12(9):e062187.
33. Keeshan A, Galipeau Y, Heiskanen A, Collins E, McCluskie PS, Arnold C, et al. Results of the Stop the Spread Ottawa (SSO) cohort study: a Canadian urban-based prospective evaluation of antibody responses and neutralisation efficiency to SARS-CoV-2 infection and vaccination. *BMJ Open.* 2023;13(10):e077714.
34. Colwill K, Galipeau Y, Stuible M, Gervais C, Arnold C, Rathod B, et al. A scalable serology solution for profiling humoral immune responses to SARS-CoV-2 infection and vaccination. *Clinical & Translational Immunology.* 2022;11(3):e1380.
35. Collins E, Galipeau Y, Arnold C, Bhéreur A, Booth R, Buchan AC, et al. CLINICAL AND SEROLOGICAL PREDICTORS OF POST COVID-19 CONDITION – FINDINGS FROM A CANADIAN PROSPECTIVE COHORT STUDY. *medRxiv.* 2023:2023.07.29.23293334.
36. Costiniuk CT, Singer J, Lee T, Langlois MA, Arnold C, Galipeau Y, et al. COVID-19 vaccine immunogenicity in people with HIV. *Aids.* 2023;37(1):F1-f10.
37. Bhatt M, Plint AC, Tang K, Malley R, Huy AP, McGahern C, et al. Household transmission of SARS-CoV-2 from unvaccinated asymptomatic and symptomatic household members with confirmed SARS-CoV-2 infection: an antibody-surveillance study. *CMAJ Open.* 2022;10(2):E357-E66.
38. Cholette F, Fabia R, Harris A, Ellis H, Cachero K, Schroeder L, et al. Comparative performance data for multiplex SARS-CoV-2 serological assays from a large panel of dried blood spot specimens. *Heliyon.* 2022;8(9):e10270.

39. Whelan M, Galipeau Y, White-Al Habeeb N, Konforte D, Abou El Hassan M, Booth RA, et al. Cross-sectional Characterization of SARS-CoV-2 Antibody Levels and Decay Rates Following Infection of Unvaccinated Elderly Individuals. *Open Forum Infectious Diseases.* 2023;10(8).
40. Galipeau Y, Siragam V, Laroche G, Marion E, Greig M, McGuinty M, et al. Relative Ratios of Human Seasonal Coronavirus Antibodies Predict the Efficiency of Cross-Neutralization of SARS-CoV-2 Spike Binding to ACE2. *eBioMedicine.* 2021;74.
41. Chaouat AE, Brizic I, Kucan Brlic P, Atari N, Kliker L, Alfi O, et al. Anti-human ACE2 antibody neutralizes and inhibits virus production of SARS-CoV-2 variants of concern. *iScience.* 2022;25(9):104935.
42. Chen Y, Zhang Y-N, Yan R, Wang G, Zhang Y, Zhang Z-R, et al. ACE2-targeting monoclonal antibody as potent and broad-spectrum coronavirus blocker. *Signal Transduction and Targeted Therapy.* 2021;6(1):315.
43. Vadasz Z, Haj T, Kessel A, and Toubi E. Age-related autoimmunity. *BMC Medicine.* 2013;11(1):94.
44. Manoussakis MN, Tzioufas AG, Silis MP, Pange PJ, Goudevenos J, and Moutsopoulos HM. High prevalence of anti-cardiolipin and other autoantibodies in a healthy elderly population. *Clin Exp Immunol.* 1987;69(3):557-65.
45. Andersen-Ranberg K, HØier-Madsen M, Wiik A, Jeune B, and Hegedus L. High prevalence of autoantibodies among Danish centenarians. *Clin Exp Immunol.* 2004;138(1):158-63.
46. Schroeder HW, Jr., and Cavacini L. Structure and function of immunoglobulins. *J Allergy Clin Immunol.* 2010;125(2 Suppl 2):S41-52.
47. Barth WF, Wochner RD, Waldmann TA, and Fahey JL. Metabolism of human gamma macroglobulins. *The Journal of Clinical Investigation.* 1964;43(6):1036-48.
48. Pyzik M, Rath T, Lencer WI, Baker K, and Blumberg RS. FcRn: The Architect Behind the Immune and Nonimmune Functions of IgG and Albumin. *J Immunol.* 2015;194(10):4595-603.
49. Tsoi JYH, Cai J, Situ J, Lam WJ, Shun EHK, Leung JKY, et al. Autoantibodies against angiotensin-converting enzyme 2 (ACE2) after COVID-19 infection or vaccination. *Journal of Medical Virology.* 2023;95(12):e29313.
50. Geanes ES, McLennan R, LeMaster C, and Bradley T. Autoantibodies to ACE2 and immune molecules are associated with COVID-19 disease severity. *Commun Med (Lond).* 2024;4(1):47.
51. Lebedin M, García CV, Spatt L, Ratswohl C, Thibeault C, Ostendorf L, et al. Discriminating promiscuous from target-specific autoantibodies in COVID-19. *Eur J Immunol.* 2023;53(5):e2250210.
52. Hallmann E, Sikora D, Poniedziałek B, Szymański K, Kondratiuk K, Żurawski J, et al. IgG autoantibodies against ACE2 in SARS-CoV-2 infected patients. *Journal of Medical Virology.* 2023;95(1):e28273.
53. Woodruff MC, Ramonell RP, Haddad NS, Anam FA, Rudolph ME, Walker TA, et al. Dysregulated naive B cells and de novo autoreactivity in severe COVID-19. *Nature.* 2022;611(7934):139-47.
54. Lundström A, Ziegler L, Havervall S, Rudberg AS, von Meijenfeldt F, Lisman T, et al. Soluble angiotensin-converting enzyme 2 is transiently elevated in COVID-19 and correlates with specific inflammatory and endothelial markers. *J Med Virol.* 2021;93(10):5908-16.
55. Xiao F, and Burns KD. Measurement of Angiotensin Converting Enzyme 2 Activity in Biological Fluid (ACE2). *Methods Mol Biol.* 2017;1527:101-15.

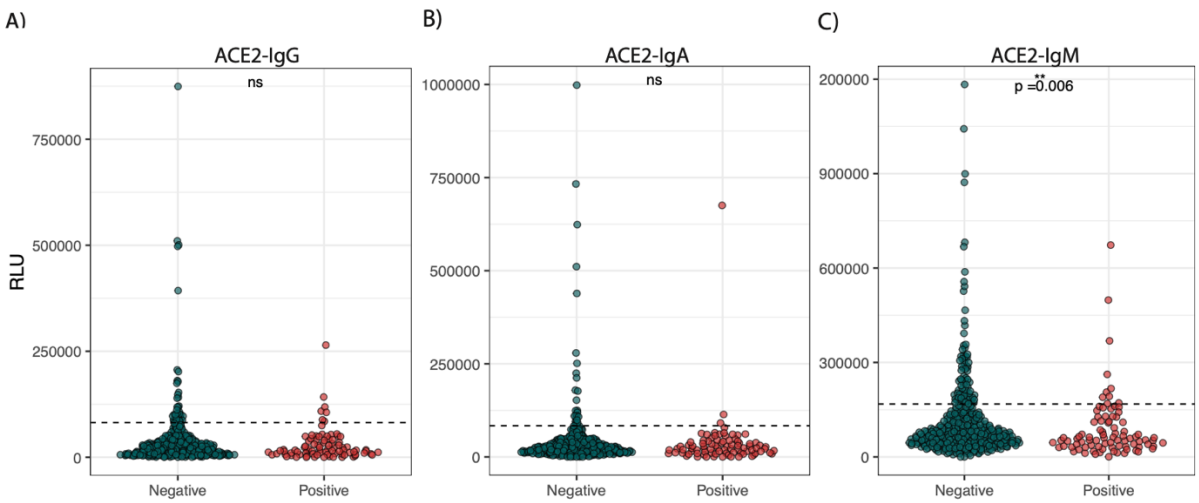
Supplementary Materials



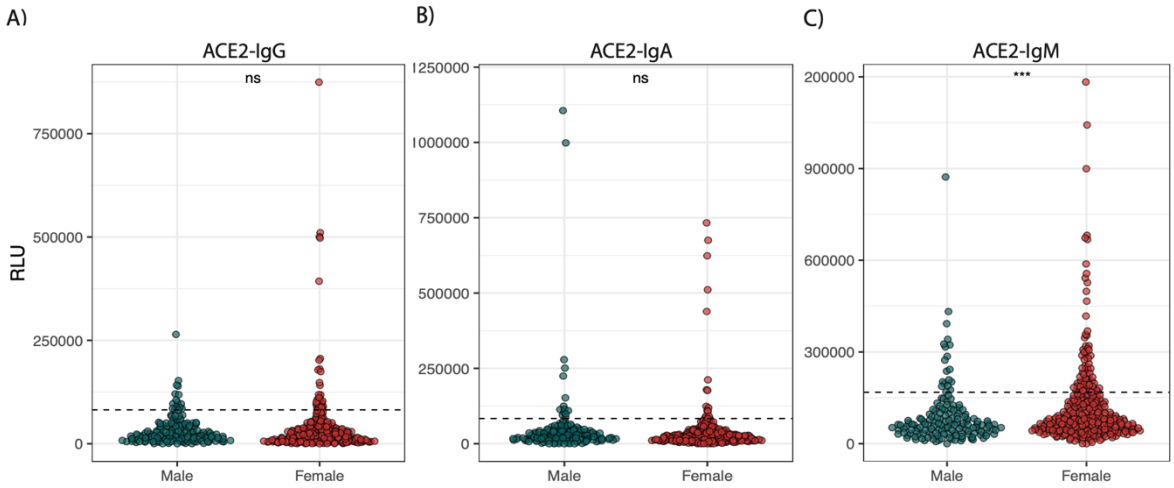
Supplemental Figure 1. Cohort demographics. A) Age (years) distribution in the whole cross-sectional cohort (n=464). B) Age (years) distribution of individuals with serological evidence of prior SARS-CoV-2 infection and or self-reported a prior infection (n=131). The number of individuals is represented as count on the y axis of the graphs. The boxplots overlayed on the histogram represent the distribution of the cohort, with the median, and different quantiles.



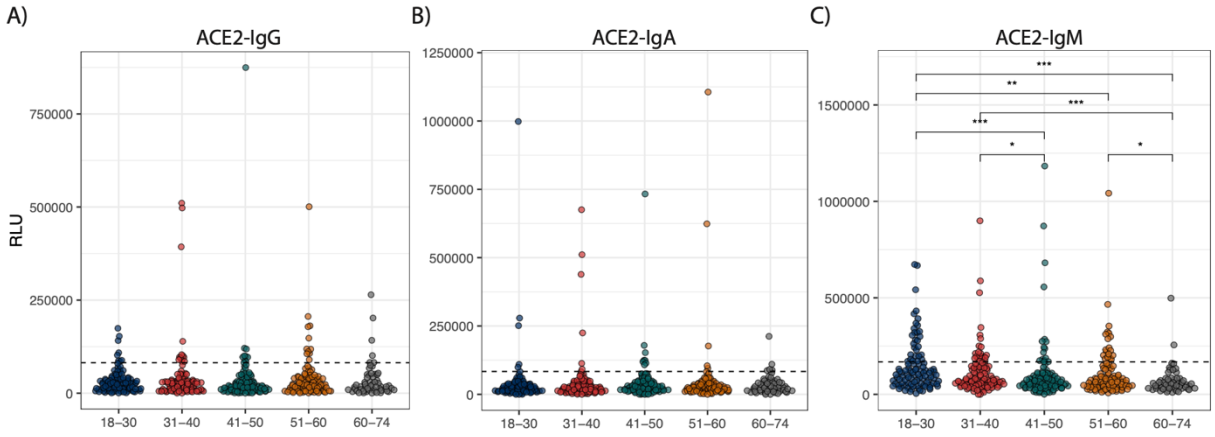
Supplemental Figure 2. Cohort demographics by sex. A) Age (years) and sex distribution in the whole cross-sectional cohort (n=464). B) Age (years) and sex distribution of individuals with serological evidence of prior SARS-CoV-2 infection and or self-reported a prior infection (n=131). The number of individuals is represented as count on the y axis of the graphs.



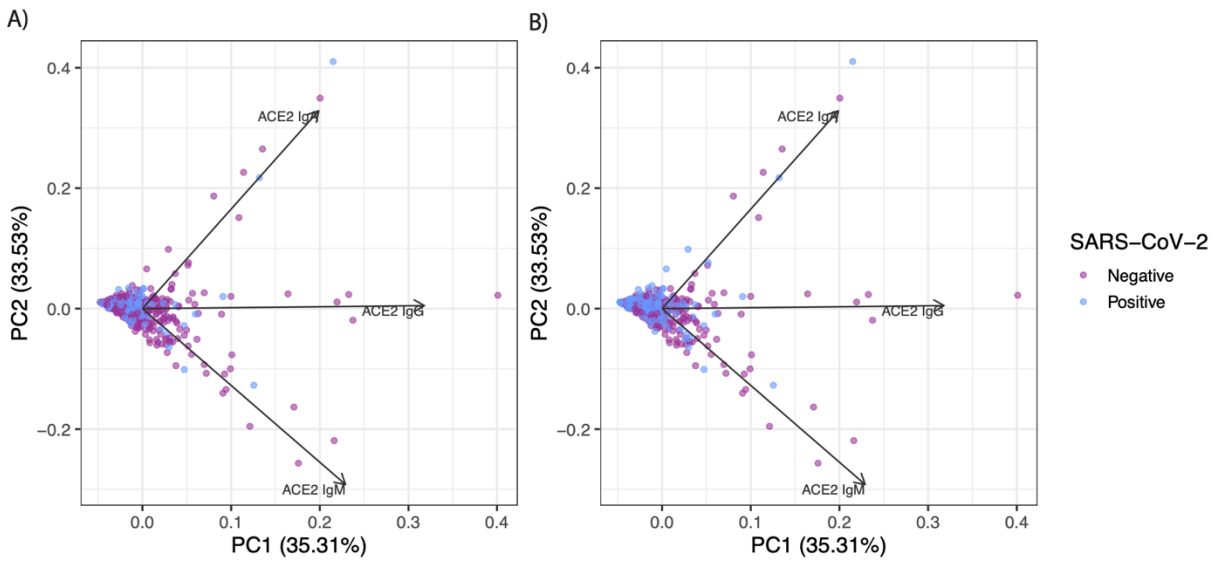
Supplemental Figure 3. ACE2 autoantibodies levels according to serological evidence of SARS-CoV-2 infection. A-C) IgG, IgA, IgM ACE2 autoantibodies levels are shown for individuals who never had SARS-CoV-2 and for individuals who had serological markers of previous infection (anti-SARS-CoV-2 N and S IgG positive). Unpaired two-sided Wilcoxon test was used to establish statistical significance (n=464), , $p \leq 0.05$ (*), $p \leq 0.01$ (**), $p \leq 0.001$ (***), $p \leq 0.0001$ (****).



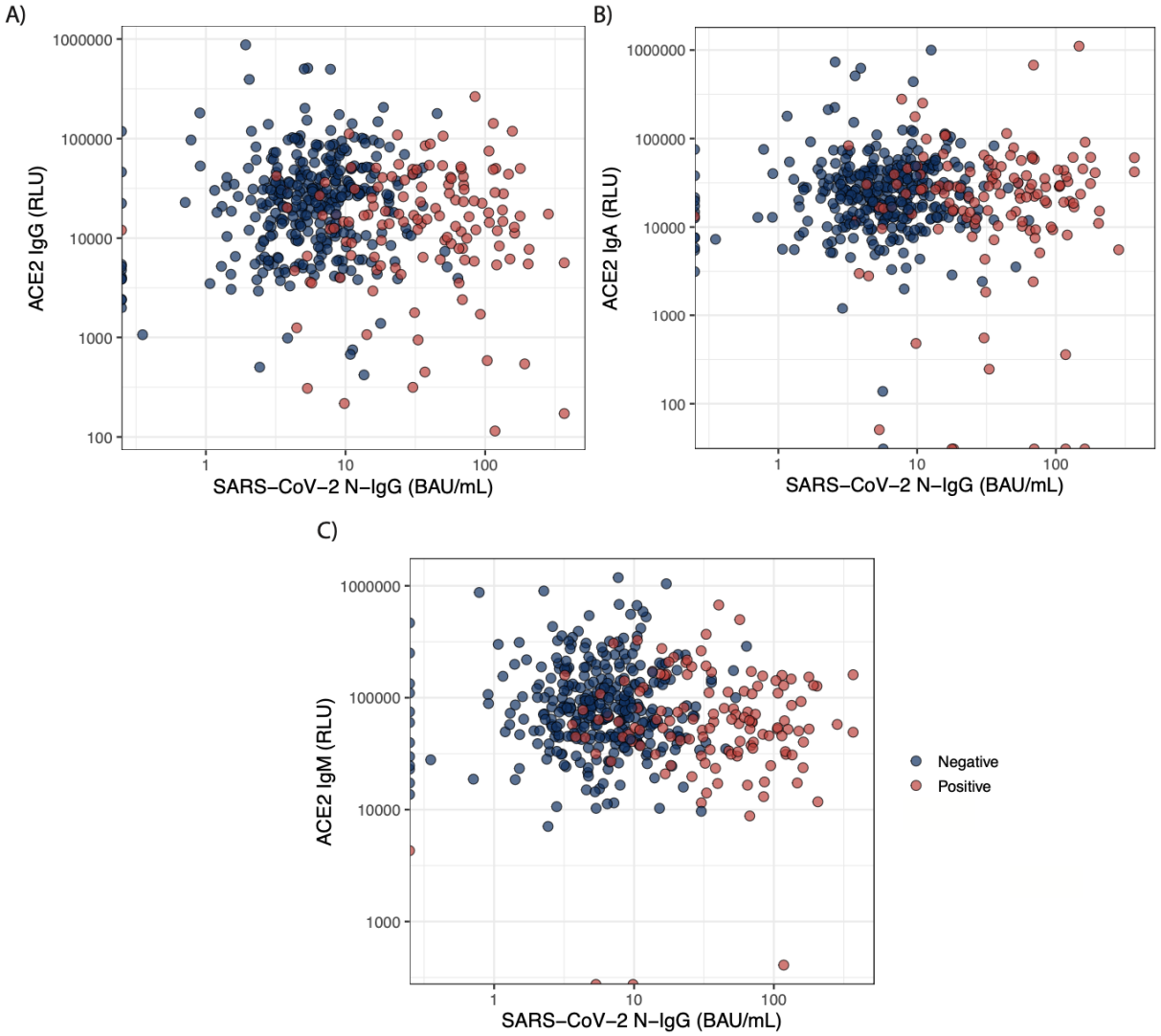
Supplemental Figure 4. ACE2 autoantibodies levels by sex and by isotype. A-C) IgG, IgA, IgM ACE2 autoantibodies levels are shown for all individuals in the cross-sectional cohort. Unpaired two-sided Wilcoxon test was used to establish statistical significance (n=464), , $p \leq 0.05$ (*), $p \leq 0.01$ (**), $p \leq 0.001$ (***), $p \leq 0.0001$ (****).



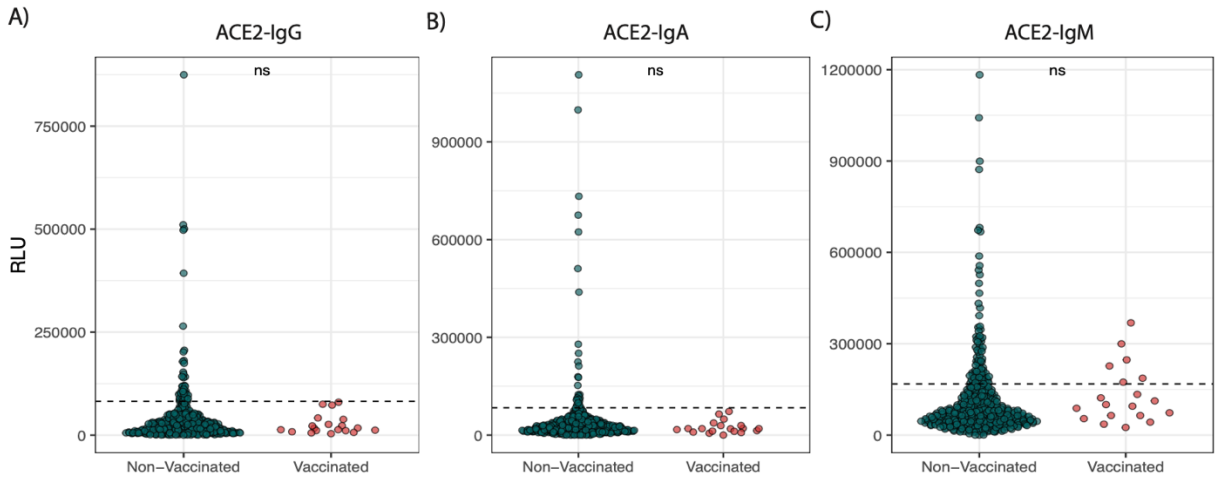
Supplemental Figure 5. ACE2 autoantibodies levels by age groups and by isotype. A-C) IgG, IgA, IgM ACE2 autoantibodies levels are shown for all individuals in the cross-sectional cohort. Kruskal-Wallis test was used for global statistical significance and Wilcoxon test was used for multiple comparisons for pairwise differences (n=464), , $p \leq 0.05$ (*), $p \leq 0.01$ (**), $p \leq 0.001$ (***), $p \leq 0.0001$ (****).



Supplemental Figure 6. Principal component analysis of ACE2 autoantibodies and classified by prior SARS-CoV-2 infection status. Principal component analysis (PCA) showing the clustering between SARS-CoV-2 prior infection and ACE2 autoantibody (IgG, IgA, IgM) levels. A) Individuals who have serological markers of SARS-CoV-2 infection. B) Individuals having serological markers of prior SARS-CoV-2 infection and/or self-reported a prior infection.



Supplemental Figure 7. Correlation between ACE2 autoantibodies and SARS-CoV-2 nucleocapsid IgG antibodies. Individuals were further classified on their SARS-CoV-2 infection status (identified by serology or self-reported). Correlation between A) ACE2-IgG B) ACE2-IgA C) ACE2-IgM antibodies and N-IgG. X and Y axis were formatted in Log10 scales.



Supplemental Figure 8. ACE2 autoantibodies levels by vaccination status. A-C) IgG, IgA, IgM ACE2 autoantibodies levels are shown for all individuals in the cross-sectional cohort. Unpaired two-sided Wilcoxon test was used to establish statistical significance (n=464), , $p \leq 0.05$ (*), $p \leq 0.01$ (**), $p \leq 0.001$ (***), $p \leq 0.0001$ (****).

Supplemental Table 1. ACE2 autoantibody seroprevalence odd ratios and 95% confidence interval by isotype. Demographic and clinical information collected as part of the study were evaluated on their influenced on ACE2 autoantibody seroprevalence (IgG, IgA, IgM).

	ACE2 IgG (OR, (95%CI)	ACE2 IgA (OR, (95%CI)	ACE2 IgM (OR, (95%CI)
Female	0.97 (0.52 - 1.83)	0.50 (0.23 - 1.06)	1.95 (1.12 - 3.38)
Male	1.03 (0.55 - 1.94)	2.01 (0.94 - 4.28)	0.51 (0.30 - 0.89)
SARS-CoV-2 infection	0.48 (0.22 - 1.05)	1.37 (0.62 - 3.02)	0.51 (0.29 - 0.92)
Immunocompromised	2.01 (0.65 - 6.21)	- *	0.96 (0.32 - 2.91)
Obesity	1.51 (0.69 - 3.28)	1.28 (0.47 - 3.50)	0.38 (0.16 - 0.94)
Hypertension	0.56 (0.17 - 1.89)	1.03 (0.30 - 3.53)	0.61 (0.25 - 1.48)
Dyslipidemia	0.68 (0.20 - 2.30)	1.77 (0.58 - 5.38)	0.91 (0.39 - 2.14)
Asthma	0.75 (0.26 - 2.18)	1.39 (0.46 - 4.16)	0.97 (0.45 - 2.09)
Allergies	1.48 (0.82 - 2.70)	1.07 (0.50 - 2.28)	1.08 (0.68 - 1.73)
Taking medication	0.89 (0.47 - 1.68)	1.00 (0.44 - 2.25)	1.14 (0.69 - 1.91)
Neurological conditions	5.48 (1.27 - 23.69)	2.18 (0.26 - 18.37)	1.45 (0.29 - 7.33)
Cardiac conditions	3.35 (0.86 - 13.08)	- *	0.43 (0.05 - 3.37)
Endocrine conditions	1.71 (0.68 - 4.34)	0.82 (0.19 - 3.59)	0.64 (0.24 - 1.68)

*Odd ratios and confidence intervals could not be measured given the low seroprevalence of IgA anti-ACE2 in these groups

Supplemental Table 2. Participant demographic information for enzymatic assay cohort

Supplemental Table 2. Participant demographic information for enzymatic assay cohort. The enzymatic activity of ACE2 was measured in the presence of serum from a subset of individuals of the initial cohort.

	Enzymatic Assay cohort (n=103)
Age (y.)	
Mean (SD)	45.73(14.0)
Median	45.0
Range	24-73
Sex	
Female Nb. (%)	65(63.1)
Previous SARS-CoV-2 infection Nb. (%) (Serology and/or self-reported)	38(36.9)
ACE2 seroprevalence	
IgG (%)	9.71
IgA (%)	7.77
IgM (%)	15.5

Supplemental Table 3. Participant demographic for the ACE2 and Spike attachment. The ability of ACE2 to bind the spike protein of SARS-CoV-2 was measured in the presence of serum from a subset of individuals of the initial cohort.

	Combined (n=55)
Age (y.)	
Mean (SD)	46.4(15.7)
Median	45.0
Range	25-73
Sex	
Female Nb. (%)	27(49.1)
Previous SARS-CoV-2 infection Nb. (%) (Serology and/or self-reported)	36(65.5)
ACE2 seroprevalence	
IgG (%)	9.09
IgA (%)	5.45
IgM (%)	16.4

CHAPTER 6 – GENOMIC EVOLUTION OF PATHOGENIC CORONAVIRUSES

RATIONALE

Humoral immune responses are intrinsically shaped by pathogen characteristics. Factors such as tissue tropism, the site of infection, immune evasion strategies, and antigenic properties all influence how pathogens modulate the adaptive immune response. Furthermore, viruses exist under constant evolutionary pressure, making host–pathogen interactions inherently dynamic over time. For example, the emergence of SARS-CoV-2 variants of concern during the pandemic not only altered viral fitness but also affected the effectiveness of both vaccine-induced and infection-acquired immunity. Therefore, it is critical to improve our understanding of SARS-CoV-2 evolution and its bidirectional interactions with the host.

To gain insight into host–pathogen interactions and viral evolution, a longitudinal in vitro experiment was conducted using Vero E6 cells infected with SARS-CoV-2, SARS-CoV, and MERS-CoV. While SARS-CoV and MERS-CoV are closely related to SARS-CoV-2, they differ in disease severity, transmissibility, and case fatality rates. In this study, all three beta coronaviruses were serially passaged weekly for six months. RNA sequencing was performed on both supernatant and cellular extracts, enabling simultaneous analysis of viral genome evolution and host transcriptomic responses. This approach allowed for the identification of both shared characteristics and virus-specific signatures in evolution, as well as the transcriptional changes induced in host cells.

Overall, this chapter investigates the evolution of highly pathogenic coronaviruses and examines how long-term in vitro viral evolution influences host gene transcription over a six-month period.

6.1 Longitudinal transcriptomic analysis of MERS-CoV, SARS-CoV, and SARS-CoV-2 adaptation to a Vero-E6 cell system

Preface

(This work is presented as a manuscript in preparation)

Galipeau Y, Castonguay N, Duque D ,Tran, A, Pelchat M, Langlois MA. **Longitudinal transcriptomic analysis of MERS-CoV, SARS-CoV, and SARS-CoV-2 adaptation to a Vero-E6 cell system.** 2025.

Abstract

The pathogenic coronaviruses family has been known to produce pandemic-like viruses through spillover events from their primary animal reservoirs to humans. The emergence and spread of SARS-CoV, MERS-CoV and recently SARS-CoV-2 are of particular concern for human health. The RNA-dependant RNA polymerase of these viruses is error-prone allowing the acquisition of new mutations during their replication cycle, which is a critical driving force for viral evolution, immune evasion and host adaptation. Despite their shared similarities, significant differences in disease severity, transmissibility and fatality rate exist between them. To better understand their evolution and associated host-transcriptomic responses, all three viruses were passaged weekly in Vero-E6 cells for a total of 24 weeks. Supernatants and cellular extract were collected, and RNA sequencing was performed. We demonstrate ascending viral titers and the acquisition of numerous mutations and deletions spanning the viral genomes with most being in the S or ORF1ab coding region. These mutations had various trajectories over time, some being transient and others persisting, highlighting the complex nature of viral evolution. Differentially expressed host genes were monitored, we identified 462 shared upregulated and 44 downregulated genes at baseline between all three viruses. We also identified genes whose expression was modulated over time, revealing how each virus evolution strategy impacted host-transcriptomic responses. Very few modulated genes were shared between coronaviruses, demonstrating different evolutionary strategies over time. The adaptation of these three coronaviruses suggests complex virus-host interactions that favour viral virulence and increased infectivity.

Introduction

Several coronaviruses (CoVs) can establish infections in human populations with various impacts on health. For example, some cause mild, cold-like symptoms and are referred to as seasonal coronaviruses, as reinfection is common (HKU-1, OC43, NL63, and 229E) (1, 2). However, three other coronaviruses—SARS-CoV, SARS-CoV-2, and MERS-CoV—are significantly more pathogenic in humans. The emergence of SARS-CoV in 2002 resulted in fewer than 10,000 cases, with an overall case fatality rate of 10% (3-5). Notably, SARS-CoV is no longer circulating in humans. In the case of MERS-CoV, first detected in 2012, fewer than 3,000 cases have been reported globally, but with a high case fatality rate of 36% (6, 7). SARS-CoV-2, the most recent coronavirus to emerge in late 2019, was responsible for the COVID-19 pandemic, which has resulted in well over 7 million deaths (8).

Coronaviruses are positive-sense, single-stranded RNA viruses, with approximately two-thirds of their genome translated into two long polyproteins (pp1a and pp1ab) separated by a -1 ribosomal frameshift site. These polyproteins are proteolytically cleaved into numerous non-structural proteins, some of which form the RNA-dependent RNA polymerase (RdRp) and the replication-transcription complex (9, 10). Downstream of this region, the remainder of the viral genome is transcribed into a nested set of subgenomic mRNAs, encoding structural and accessory proteins (7, 11).

The RdRp of coronaviruses is error-prone, leading to the accumulation of mutations during replication (12). Contrary to other RNA viruses, the intrinsic mutation rate of CoVs is lower as coronaviruses possess a 3′ exonuclease proofreading mechanism, which increases RdRp fidelity (13). In addition, viral mutations can arise via host-mediated viral genome editing. For example, some data suggest that ADARs and APOBECs may edit SARS-CoV-2 genomes (14-16). Recombination and genomic deletions have also been reported, contributing to viral sequence diversity (17, 18). Furthermore, these drivers of viral evolution operate within a broader ecological context, in which factors such as population transmission rates, immune profiles, the number of infected individuals, and human mobility all influence coronavirus evolution.

As obligate intracellular pathogens, viruses rely on host interactions to complete their replication cycle and as such have evolved strategies to manipulate cellular resources and evade immune detection. In response, host cells have developed mechanisms to sense viral infections and limit their spread. For example, in the context of SARS-CoV-2, viral RNA can be detected by TLR3, TLR7, and RLRs such as MDA5 and LGP2, leading to the modulation of interferon-inducible genes and the release of inflammatory cytokines (19-21). Other non-immune pathways have also been implicated, including the response to ER stress, unfolded protein response, and apoptotic signaling (22).

While several gene expression datasets exist for coronavirus infections, very few directly compare all three pathogenic coronaviruses. Further, studies performing experimental evolution of viruses are rare. None thus far directly monitor viral adaptation alongside host-transcriptomic responses. Here SARS-CoV-2, SARS-CoV and MERS-CoV were experimentally evolved for 24 weeks and host transcriptomic responses were monitored, revealing the complex nature of coronavirus evolution and host interactions. This dataset sheds light on how these viruses modulate host gene expression during their evolution, ultimately enhancing viral fitness in a Vero cellular system.

Methods

Virus and Cells

The following virus isolates were used in this study: hCOV-19/Canada/ON-VIDO-01/2020 (B, Ancestral SARS-CoV-2), SARS-CoV/Tor2 and (MERS-CoV)/EMC/2012. SARS-CoV and SARS-CoV-2 were both obtained from the National Microbiology Laboratory, Winnipeg, Canada. MERS-CoV was obtained from Bart Haagmans, Erasmus University. Viruses were propagated in Vero E6 cells and quantified in Vero cells by plaque assay.

Viral passaging

MERS-CoV, SARS-CoV, or SARS-CoV-2 were passaged in Vero E6 cells for 24 weeks. On the first passage (week 1), cells were infected at an MOI of 0.01. Samples were subsequently blind passage from weeks 2 to 24 by infecting new cells with 1 ml of previous passage collected at 7 dpi (days post-infection). Samples were diluted in 100 ml infection media (1X DMEM, high glucose media supplemented with 1X non-essential amino acid, 100 U/mL penicillin-streptomycin, 1 mM

sodium pyruvate, and 0.1% bovine serum albumin) and adsorbed on Vero E6 cells for 1 h at 37°C. Inoculum was removed and 2 mL fresh infection media was added, and cells were incubated at 37°C/5% CO_2. Infected cell monolayer was pelleted by centrifugation at 48 hpi and resuspended directly into 1 mL 1X DNA/RNA Shield (Zymo Research, Irvine, California). Supernatants were collected at 7 dpi, centrifuge-clarified and transferred directly to 1mL 2X DNA/RNA Shield (Zymo Research, Irvine, California). Samples were stored at -80°C.

Plaque Assay

This assay was performed exclusively within the NRC CL-3 facility. Briefly, the supernatants were subjected to 1 in 10 serial dilutions in infection media (1X DMEM, high glucose media supplemented with 1X non-essential amino acid, 100 U/mL penicillin-streptomycin, 1 mM sodium pyruvate, and 0.1% bovine serum albumin). Diluted virus inoculum was adsorbed on Vero cells for 1 h at 37°C before the inoculum was removed and cell monolayer was overlaid with 1X infection media with 0.6% ultrapure, low-melting point agarose. The assay was incubated at 37oC/5% CO2 for 72 h. After incubation, cells were fixed with 10% formaldehyde and stained with crystal violet. Plaques were enumerated and plaque forming unit (PFU) per mL was determined.

RNA extraction and Sequencing.

RNA was extracted using the QIAGEN viral RNA minikit and Total RNA Kit (Zymo Research, Irvine, California) for the supernatant and cell lysates, respectively. Library preparation of the RNA samples with NEBnext rRNA depletion kit. Samples were sequenced using Genome Quebec Illumina NovaSeq6000 platform with 100 bp with ~25 million reads per samples.

Sequencing alignment to both VERO and viral genomes

Reads were aligned to a merged genome of Chlorocebus sabaeus (ChlSab1.1, GCA_000409795.2) and respective virus (SARS-CoV-1 (AY278741.1), SARS-CoV-2 (NC_045512.2), or MERS-CoV (NC_019843.3)) with HISAT2 (v2.2.1), using default parameters. The BAM files were then sorted and indexed with Samtools (v1.16.1). Variant calling was performed with bcftools (v1.11), using default parameters, and only variations with depth higher than 1000 were considered as significant. Large deletions were quantified by determining the ratio of the average read depths within the

deletions to the average read depths at 20 positions upstream and downstream. All result were analyzed in R (v4.4.2).

Differential gene expression

Transcript counts were determined using HTSeq-count (v2.0.2) with the annotated *Chlorocebus sabaeus* GTF file (ChlSab1.113). Gene counts were then imported into R (v4.4.2), and genes with fewer than 10 counts over the time period were filtered out. RNA-seq normalization and differential expression analysis were performed using DESeq2 (v1.46.0) , which accounts for sequencing depth and overdispersion using the median of ratios method (23). Identification of differentially expressed genes (DEGs) at baseline was performed by comparing infected cells at weeks 2–8 to a biological triplicate of uninfected VERO-E6 cells, and gene-wise statistical testing was conducted using the Wald test with default parameters. Genes were considered significantly differentially expressed if they had a p-adjusted value below 0.001 and a log$_2$fold change above 2. Identification of genes modulated over time was performed by applying a natural spline with three degrees of freedom to model time as a non-linear variable, allowing for flexibility in expression over time. Statistical testing was performed using the likelihood ratio test (LRT) to identify genes whose expression significantly differed from the null model. To gain insight into the biological role of DEGs, Gene Ontology (GO) and pathway enrichment analysis were carried out using gprofiler2 (v.0.2.3) (24). Quantitative Venn diagrams were graphed with BioVenn (v1.1.3). Potential protein-protein interactions (PPIs) among differentially expressed genes were identified using the STRING database (25). Clusters of DEGs modulated over time were identified by applying variance stabilizing transformation (VST) to gene expression data prior to z-score normalization. k-means clustering was performed, with the optimal number of clusters determined using Calinski-Harabasz scores. Semantic clustering of enriched GO terms was performed using REVIGO with default parameters (26).

Results

MERS-CoV, SARS-CoV, and SARS-CoV-2 acquired mutations spanning their genome

Several mutations were identified through next-generation RNA sequencing of supernatant samples collected biweekly over the 24-week period during which SARS-CoV, MERS-CoV, and

SARS-CoV-2 were experimentally replicated in Vero E6 cells. Differences in the frequency of nucleotide substitutions were observed between the viruses (Figure 1A). For instance, the frequency of transition mutations in SARS-CoV-2 was 16.8% lower than in SARS-CoV and 7.5% lower than in MERS-CoV. Interestingly, C-to-U mutations were most frequent in all viruses accounting for 55.6%, 29.4% and 33.3 of all mutations in SARS-CoV, SARS-CoV-2 and MERS-CoV, respectively. When examining the distribution of these mutations over time across the viral genomes, the majority were in the S gene and ORF1ab region for each virus (Figure 1B). Mutations were also detected, though to a lesser extent, in genes encoding structural proteins such as N, M, and E, as well as in accessory genes, which differ between viruses. Only one significant mutation was identified in the 3′ UTR, occurring in MERS-CoV (Figure 2). Only two deletions were detected: a deactivating deletion (ΔV16-R129) in the MERS-CoV ORF5 gene and a deletion (ΔA684-Q690) in the spike protein of SARS-CoV-2.

When examining the location of these mutations within the spike protein, most were found in the S2 domain for MERS-CoV and SARS-CoV, whereas 70% of the spike mutations in SARS-CoV-2 were in the S1 (non-RBD) region (Supplementary Table 1). The deletion ΔA684-Q690 in the spike protein was positioned at the S1/S2 boundary, potentially inactivating the polybasic cleavage site PRRA684R↓. Within the ORF1ab region, 23–43% of all mutations identified were in NSP3, and 50% in NSP16 of the SARS-CoV-2.

These mutations exhibited different trajectories over time (Figure 1D, Supplementary Figures 1–3). In MERS-CoV, only a small number of mutations were transient, whereas 27–29% of mutations in SARS-CoV-2 and SARS-CoV followed a transient pattern. Some mutations became dominant early (by week 2) and remained present throughout the experiment, with a similar proportion observed across all three viruses. Mutations detected in supernatant samples mirrored those found in cellular extracts (Supplementary Figures 1–3). Additionally, some mutations followed an upward trajectory, differing from fixed mutations as they were absent in the early weeks of evolution. Mutations within each viral gene were distributed among these three trajectories (Figure 1D). ORF1ab and S mutations were the most frequently fixed, accounting for 57–80% of all fixed mutations suggesting significant pressure for adaptation of for viral entry and replication were

Serial passaging resulted in increased pathogenicity in Vero-E6 cells.

Viral titers were measured using plaque-forming units (PFU) at each passage. Due to the increasing pathogenicity of the virus to VERO-E6 cells, the supernatants used to infect were diluted 100-fold at weeks 9 and 18. All three viruses exhibited an increase in relative PFU/mL, indicating that they adapted over the 24-weeks period to become increasingly pathogenic in VERO cells (Figure 1C). When comparing baseline to endpoint and accounting for dilutions, viral titers increased $10^{4.2}$-fold for MERS-CoV, 10^{4}-fold for SARS-CoV, and $10^{4.6}$-fold for SARS-CoV-2. This significant pathogenic effect in VERO-E6 cells was further reflected in the RNA sequencing data. A higher proportion of cell-derived RNA was detected in the supernatant compared to viral RNA, likely due to the extensive cytopathic effects observed (Supplementary Figure 10). Conversely, in cellular extracts, most of the sequenced RNA was of viral origin Supplementary Figure 10)., emphasizing the extent to which each of these coronaviruses hijacks cellular transcription.

MERS-CoV, SARS-CoV, and SARS-CoV-2 share common differentially expressed host genes upon infection

To gain insight into the transcriptional host response in infected cells at baseline, RNA sequencing data from cellular extracts at weeks 2–8 were treated as pseudo-replicates for statistical purposes and compared to a triplicate of uninfected cells. Using as thresholds a p-adjusted value of 0.001 and a log2fold change of +/- 2, we identified 506 differentially expressed genes (DEGs) common to all three viruses (Figure 3A-B). SARS-CoV infection resulted in the highest number of DEGs, with over 3,200 genes impacted. In contrast, SARS-CoV-2 and MERS-CoV induced differential expression in 1,116 and 1,740 genes, respectively. Among these DEGs, most were upregulated in SARS-CoV and SARS-CoV-2**.** In contrast, MERS-CoV displayed a distinct profile, with 33% of DEGs downregulated (Figure 3B-C).

Interestingly, 462 upregulated DEGs were shared by all three viruses upon infection. Enrichment analysis of overrepresented molecular function terms of those shared upregulated genes, the vast majority were genes encoding DNA binding proteins (Figure 3D). Kinase activity, protein binding and genes associated with the TNF pathway were to a lesser extent also enriched. No significant enrichment was detected within the shared 44 downregulated DEGs between all three viruses.

However, protein-protein interaction (PPI) analysis revealed two clusters of proteins. Several proteins of the 20S proteasome complex were downregulated, including PSMA7 and PSMA2 which are part of the alpha subunit and PSMB3 which is part of the beta subunit and PSMG2 a proteasome assembly chaperone. Other proteins involved in proteostasis such as DESI1 a SUMO protease and SEC61G involved in protein translocation into the ER were also downregulated (Figure 3E). A second cluster of proteins involved in nucleotide metabolism was also identified. These involved proteins such as NUDT16 (Nudix hydrolase 16), NT5C2 (Cytosolic 5'-nucleotidase II), ENTPD4 (Ectonucleoside triphosphate diphosphohydrolase 4) as well as proteins such as RRM1 (Ribonucleotide reductase M1 subunit) and NME1 (Nucleoside Diphosphate Kinase 1) (Figure 3E).

MERS-CoV, SARS-CoV, and SARS-CoV-2 modulated several key genes over time which clustered differently

To gain insight into the impact of viral acquired mutations on gene expression over the 24-weeks period, genes whose expression significantly fluctuated over time were identified. MERS-CoV, SARS-CoV and SARS-CoV-2 modulated over time 1050, 1783 and 393 genes, respectively (Figure 4A, C, E). Clustering analysis was performed to investigate potential trajectories. Optimal cluster numbers were determined by Calinski-Harabasz scores prior to k-means clustering. For each virus, two clusters were identified out of their respective total modulated genes. In the case of MERS-CoV, one cluster represented genes whose expression trajectory was increasing while the other cluster represented genes whose expression was decreasing over the weeks. Similarly, SARS-CoV-2 also had a cluster of genes that had an increasing trajectory; however, the second cluster was comprised of genes that initially had an upward trajectory but then declined. In the case of SARS-CoV, one cluster was comprised of genes that initially had an upward trajectory but then reverted to their initial expression and one cluster of genes that had a reverse U-shape trajectory (Figure 4B, D, F). Interestingly, very few modulated genes (n=9) were shared between VERO cells infected by each virus. This contrasts with DEGs observed early after infection where over 500 genes were common between infected cells regardless of the coronavirus. This suggests that each virus evolved to modulate different genes over time.

Enrichment analysis of gene ontology biological processes terms was performed on each cluster to gain insight into their biological functions. No significant enrichment was found in cluster 2 of SARS-CoV and SARS-CoV-2 infected cells. The top 80 significantly enriched biological process terms were visualized using Revigo which clusters semantically similar terms (26). For MERS-CoV, transcripts for proteins associated with apoptotic processes, protein folding and metabolic processes were upregulated (cluster 1; upward trajectory). Amongst downregulated genes (cluster 2; downward trajectory), transcripts for proteins associated with protein transport and localization, signalling regulation and transduction were identified. In the case of SARS-CoV (cluster ; reversed U-shape trajectory), transcripts for proteins related to cell-cell adhesion were enriched along with one large cluster associated with ion transport. Another cluster was associated with general cell metabolism processes such as cell differentiation. In the case of SARS-CoV-2 (cluster 1; initially upward, then downward trajectory), one large cluster was enriched in terms related to RNA metabolic processes and regulation of transcription. Another cluster was associated with the negative regulation of processes such as signal transduction, signalling, and metabolism. Interestingly, one small cluster of terms associated with innate responses and responses to viruses was enriched. Overall, each virus had unique enriched biological processes compared to each other.

Discussion

We report the longitudinal transcriptomic analysis of SARS-CoV, SARS-CoV-2, and MERS-CoV in VERO-E6 cells over a total duration of 24 weeks. During this period, the titers of each virus increased by 10^4-fold. This significant increase in titers was concordant with the acquisition of mutations in each viral genome. In this experimental system, viral adaptation occurred as a result of sequence diversity mediated by RdRp errors and the possible contribution of host-mediated viral genome editing (e.g., APOBEC, ADAR) (15, 27). Presumably, advantageous mutations that positively increase viral fitness were selected. However, bottleneck events imposed at transmission —or in this case, at each passage or dilution event—can limit variation, and some mutations may be passed on by chance (28). The impact of dilution events in our data was noticeable, particularly

at week 8 for MERS-CoV, where this coincided with the emergence of several mutations (Supplementary Fig. 1). Overall, despite differences in mutation rates among the viruses, which ranged from 1.02 × 10š⁵ to 1.29 × 10š⁵ mutations/nt/week in supernatant samples, each virus showed a similar increase in pathogenicity (Supplementary Fig. 12).

Viral populations can differ between those replicating within a host cell and those that are transmitted, due to selective pressures associated with egress and transmission. This phenomenon, linked with the concept of quasispecies, was investigated here (29, 30). However, limited differences were observed between viral mutations found in the cell extract versus the supernatant (Supplementary Fig. 1–3), which is mostly explained by the cytopathic effect of these viruses on VERO cells in culture, as suggested by the large amount of cellular RNA observed in supernatant samples (Supplementary Fig. 10).

Most spike mutations occurred in the S2 domain, a stark contrast to mutations observed for SARS-CoV-2 in the human population. This is most likely the result of the absence of evolutionary pressure from immunity, such as neutralizing antibodies, in our system (31). When adjusting for viral gene lengths, the spike protein was a mutation hotspot for all three viruses. This suggests that a significant advantage can presumably be gained through more efficient binding, rapid entry, and fusion. The deletion that inactivated the polybasic cleavage site in SARS-CoV-2 became dominant by week two and was maintained. The loss of the furin cleavage site has been reported previously in VERO-E6 cells, suggesting that it provides a VERO-specific fitness advantage (32, 33).

In addition, another deletion that inactivated ORF5 in MERS-CoV became dominant by week 2 and was retained over the 6-month period. ORF5 in MERS-CoV is a non-structural accessory protein unique to MERS-CoV. While not well characterized, some data support a role in the modulation of NF-κB and suppression of inflammation (34, 35). As Vero cells are known to have impaired type I IFN responses, it is possible that ORF5 does not confer a fitness advantage in this culture system (36). There are observations that ORF5 is not required for MERS-CoV replication in cell culture (34, 37), suggesting that the role of ORF5 may provide an advantage only in vivo. A nucleotide substitution in ORF3 of MERS-CoV introduced a stop codon at the beginning of this

accessory protein. This inactivating mutation was present in 99.8% of supernatant sequences at week 2 and was maintained throughout the evolution experiment. One study showed that ORF3 deletion did not impact MERS-CoV viral titers in Vero cells suggesting that like ORF5 it may not be essential for replication processes in Vero (34). Within the ORF1ab region, no mutations were detected in nsp9–nsp12, while all three viruses had mutations in nsp3 (Supplementary Table 2).

Given that each passage resulted in only one cellular extract and one supernatant sample, the cellular extracts from weeks 2–8 were pooled and treated as a pseudo-replicate. This enabled the identification of differentially expressed genes resulting from the infection, by reducing the impact of viral evolution on host transcriptomic responses. By considering only upregulated and downregulated DEGs shared between all three viruses, we identified conserved transcriptomic markers among highly pathogenic coronaviruses. Interestingly, a minority (8.7%) of shared DEGs were downregulated. Protein–protein interaction analysis revealed several genes associated with the 20S proteasome. Three proteasome-related genes directly encoded subunits (PSMA7, PSMA2, PSMB3), and one was a proteasome assembly chaperone. One can conceptualize that controlling proteostasis could be a viral strategy aimed at limiting viral protein degradation and increasing assembly efficiency.

The constitutive 20S proteasome is the basis of the 20S immunoproteasome, which is induced by IFN-γ and TNF signaling and is more efficient at generating peptides for presentation on MHC-I molecules (38, 39). While antigen-presenting immune cells have higher expression of the immunoproteasome, the constitutive 20S proteasome can also generate peptides for MHC-I presentation (40, 41). Downregulation of the 20S proteasome could be a strategy employed by MERS-CoV, SARS-CoV, and SARS-CoV-2 to limit MHC-I presentation. One proteomic study of nasopharyngeal samples from SARS-CoV-2-infected individuals reported the downregulation of several proteasomal subunits, such as PSMC1, PSMD2, and PSMD7 (42). Here, we show that this may be a conserved strategy among highly pathogenic coronaviruses. However, we cannot rule out that this downregulation occurs as a host-mediated response.

Another network of proteins downregulated by all coronaviruses included those associated with nucleotide metabolism. One protein, NUDT16 (Nudix hydrolase 16), a non-canonical RNA

decapping enzyme, was previously shown to be differentially expressed in SARS-CoV and SARS-CoV-2 in in vitro infections (43). Here, we report that MERS-CoV infection in vitro also downregulated its expression. This may be a strategy used by these viruses to protect their transcripts from degradation. Some viruses are known to modulate RNA decapping enzymes—for example, the capsid protein of the turnip crinkle virus (TCV) modulates DCP1 (an mRNA decapping enzyme) via the ubiquitination degradation pathway, thereby limiting antiviral RNA decay (44). Other enzymes, such as NT5C2 (cytosolic 5'-nucleotidase II), ENTPD4 (ectonucleoside triphosphate diphosphohydrolase 4), as well as proteins such as RRM1 (ribonucleotide reductase M1 subunit) and NME1 (nucleoside diphosphate kinase 1), were also downregulated. While limited experimental data exist regarding their roles in coronavirus infection, alterations in their respective activity could influence nucleotide availability, potentially impacting viral replication efficiency.

Next, we identified several genes whose expression was modulated over time for each viral adaptation (Figure 4). Since all experimental conditions were conserved, it is reasonable to presume that the modulation of these genes was the result of changes in the viral genomes over time. We found that different trajectories existed in the expression of these modulated genes. Less than 0.3% of modulated genes were shared between all three viruses, with the vast majority being host genes uniquely modulated by one virus. Overall, this suggests distinct and unique viral adaptation strategies (Figure 5). Enrichment analysis revealed interesting clusters of related biological processes. For example, MERS-CoV upregulates over time several genes associated with apoptosis and its regulation, suggesting that its adaptation could modulated cell death pathways. In contrast, MERS-CoV downregulates over time biological processes related to protein transport and localization were enriched, as well as several clusters related to signaling, including responses to cytokines. For SARS-CoV, transcripts for proteins associated with ion transport were enriched. These biological processes were not present in any cluster for the other viruses, which may indicate a unique strategy use by SARS-CoV during its adaptation to Vero cells. In the case of SARS-CoV-2, several terms related to the regulation of RNA metabolism and transcription were enriched. In addition, transcripts for genes associated with innate immune responses were identified. Overall, correlating the effects of specific viral mutations on these cellular proceeses

will require further experimental work. However, we highlight here the unique strategies employed by each virus over the course of the 24-weeks adaptation period.

Several limitations exist in this study. First, Vero cells were used to perform the evolution experiment since they support the infection of all three coronaviruses and do not pose a risk of generating human-adapted coronaviruses. However, limitations arise from the fact that Vero cells have impaired antiviral signaling and are not of human origin. Additionally, this evolution experiment was performed entirely in vitro, without the influence of the immune system on viral evolution. To identify DEGs and determine statistical significance at baseline, a pseudo-replicate of samples from weeks 2–8 was used, which may introduce additional variability or noise into our analysis. For genes modulated over time, a spline model with three degrees of freedom was used to introduce flexibility; however, it is possible that more complex gene expression patterns were missed.

Overall, this study is the first to report the longitudinal adaptation of three coronaviruses SARS-CoV, SARS-CoV-2, and MERS-CoV in Vero cells over a 24-week period. During this time, viral mutations, and PFU were monitored. This experiment provided insight into the distinct adaptation strategies employed by each virus. Furthermore, the identification of shared differentially expressed genes (DEGs) among these coronaviruses revealed important findings about their biology.

Funding:

This work was supported in part by a COVID-19 Rapid Response grant through the Canadian Institutes of Health Research (CIHR) grant (VR2-172722) and from a grant supplement by the COVID-19 Immunity Task Force (CITF) to M-AL. Additionally, YG is supported by a Charles Best and Frederick Banting (CGS-Doctoral award) from CIHR (476885).

Contributors:

The study was designed by MP, M-A.L. and AT. The viral passaging and titter measurements were performed by DD and AT. NC performed the RNA extraction. MP and YG carried out the RNA-Seq analysis and generated the figures. YG, MP and M-A.L wrote, edited and formatted the manuscript. All authors have edited and approved the final manuscript.

Declaration of interest:

The authors declare no conflict of interest relevant to the present manuscript.

Role of the Funder/Sponsor:

The funding sources played no role in the study design, data collection, analysis, writing of the manuscript, and decision to publish.

Data availability:

Sequencing data files can be found here:

Scripts used for the analysis is available upon request to langlois@uottawa.ca or mpelchat@uottawa.ca

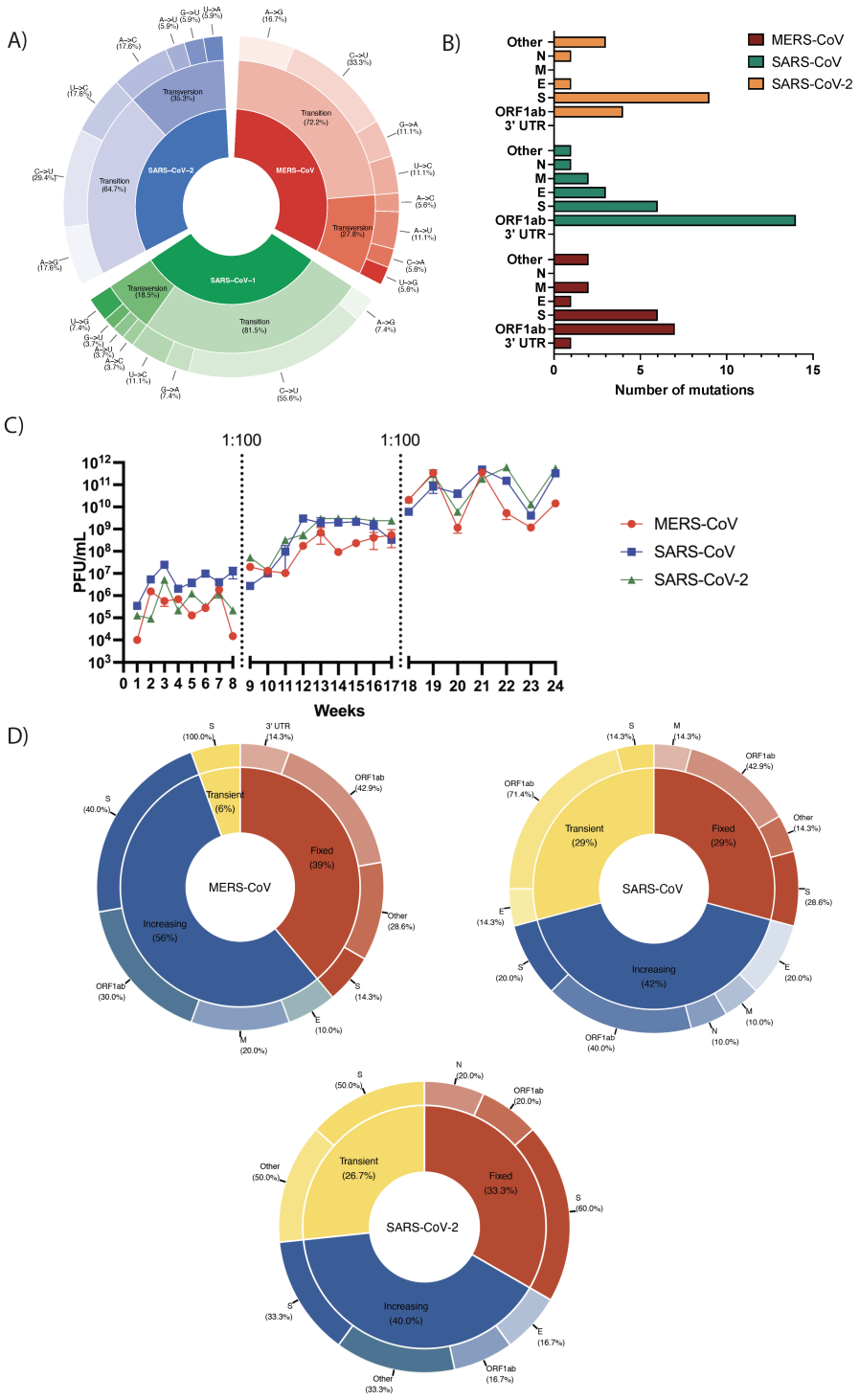


Figure 1. Description of viral mutations acquired over time and viral titers. A) Summary of the relative percentage of transversion and transition point mutations in supernatant samples for MERS-CoV, SARS-CoV-2 and SARS-CoV. B) Number of mutations (including deletions) per viral gene for each virus, only genes with at least one mutation for at least one virus are shown. Other refers to mutations found outside of structural genes, ORF1ab region or 3' UTR. C) Infectious viral titer of MERS-CoV, SARS-CoV, SARS-CoV-2 over time. Plaque-forming assays were performed in a technical triplicate for each weekly

supernatant sample for all three viruses. The dilution of transferred supernatant for passaging at week 9 and week 18 is also indicated. D) Frequency of mutation trajectory per virus. Mutations were considered fixed if their frequency was over 99% by the second time point.

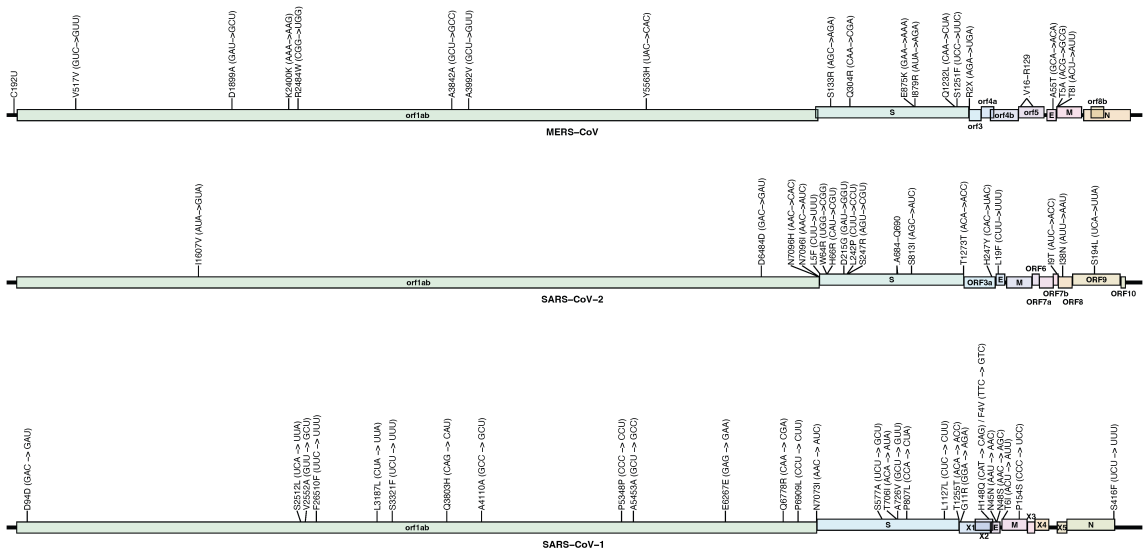


Figure 2. Overview of the viral mutations on MERS-CoV, SARS-CoV and SARS-CoV-2.
Figure 2. Overview of the viral mutations on MERS-CoV, SARS-CoV and SARS-CoV-2. Summary of all mutations and deletions over the 24-week time were mapped at their location within each virus genome. Nucleotide change was indicated as well as the amino acid substitution if applicable.

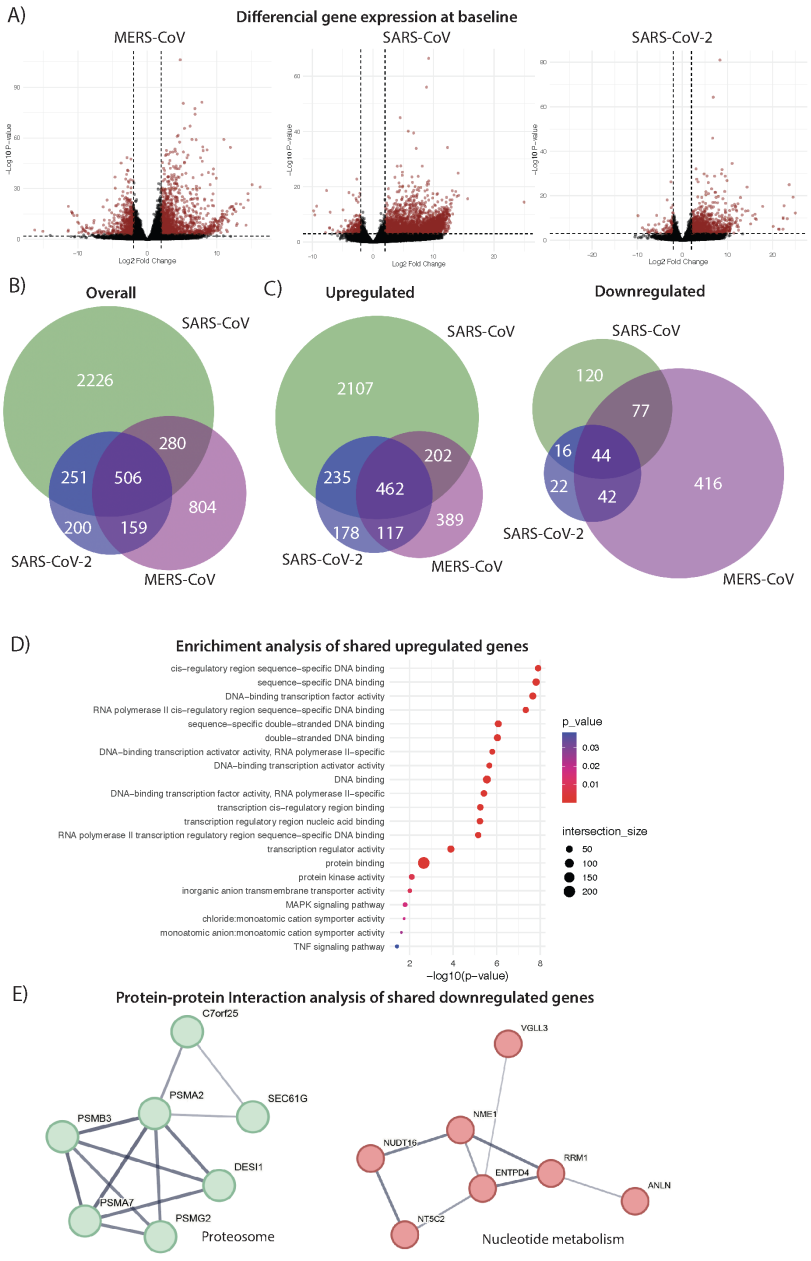


Figure 3. Differential gene expression between uninfected and infected VERO-E6 cells at baseline. A) Gene expression counts from infected cells at weeks 2-8 were compared to gene expression of a triplicate of uninfected VERO-E6 cells. Genes were considered significant if their p-adjusted value was smaller than 0.001 and had an absolute log2 fold change of +/- 2. B) Venn diagram of DEGs were compiled and compared between viruses. C) Venn diagram of upregulated and downregulated DEGs compared between viruses. D) Enrichment analysis of overrepresented gene ontology molecular function terms within shared upregulated DEGs for all three viruses. The number of genes associated with each term and p-value is also shown C) Potential protein-protein interactions (PPIs) network analysis among shared downregulated DEGs for all three viruses identified using the STRING database. Line width corresponds to the confidence of the predicted interaction, with thicker lines indicating stronger evidence-based scores.

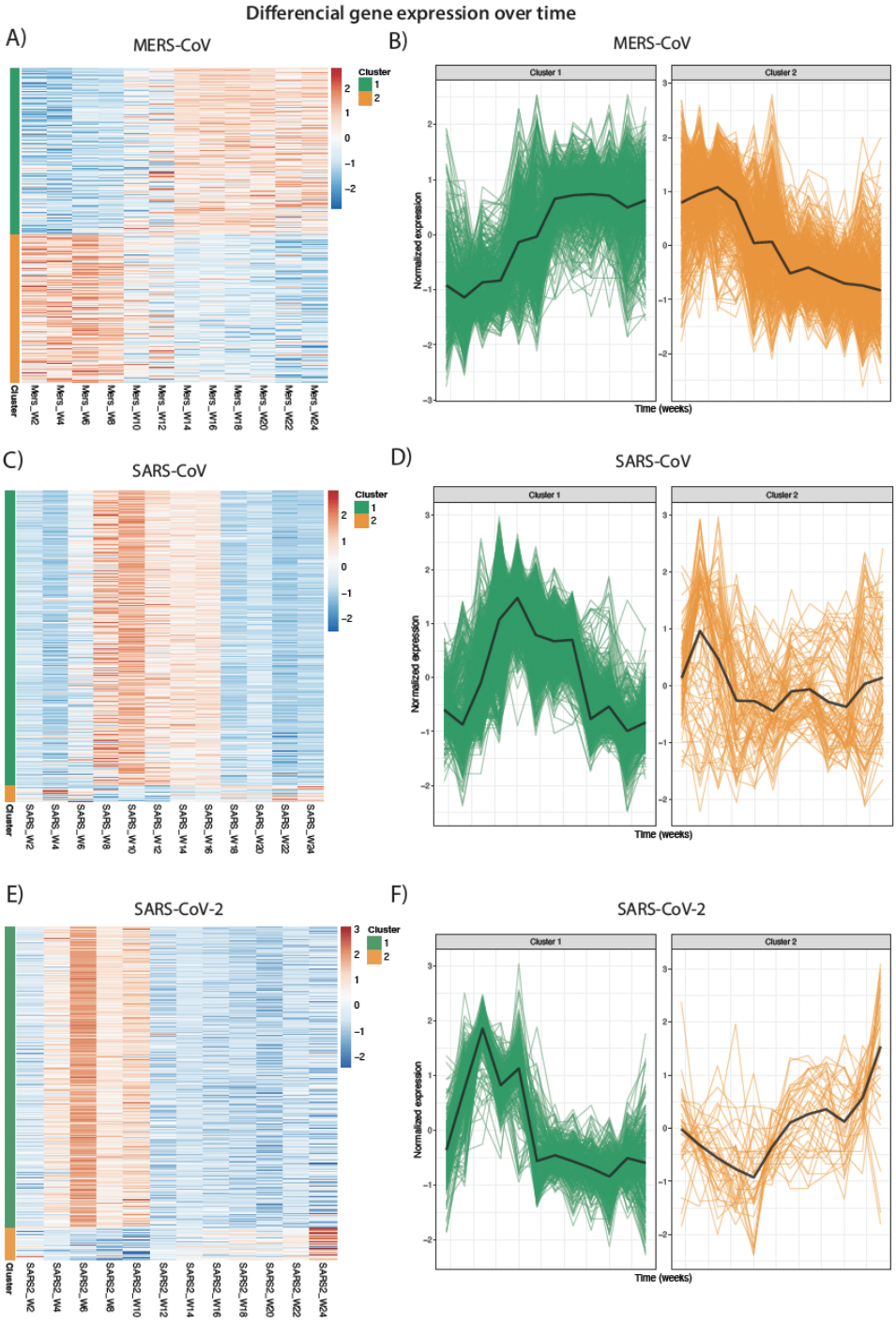


Figure 4. Clustering analysis of DEGs modulated over time for each virus. Genes modulated over time were considered significant if their p-adjusted value was smaller than 0.05. A, C, E) Z-Score heatmap of DEGs expression over time for each week sent for RNA-seq. Cluster membership is also shown on the y-axis. B, D, F) Trajectories of DEGs expression modulated over time by cluster membership for each virus. The mean expression trajectory for the cluster is shown as a black line.

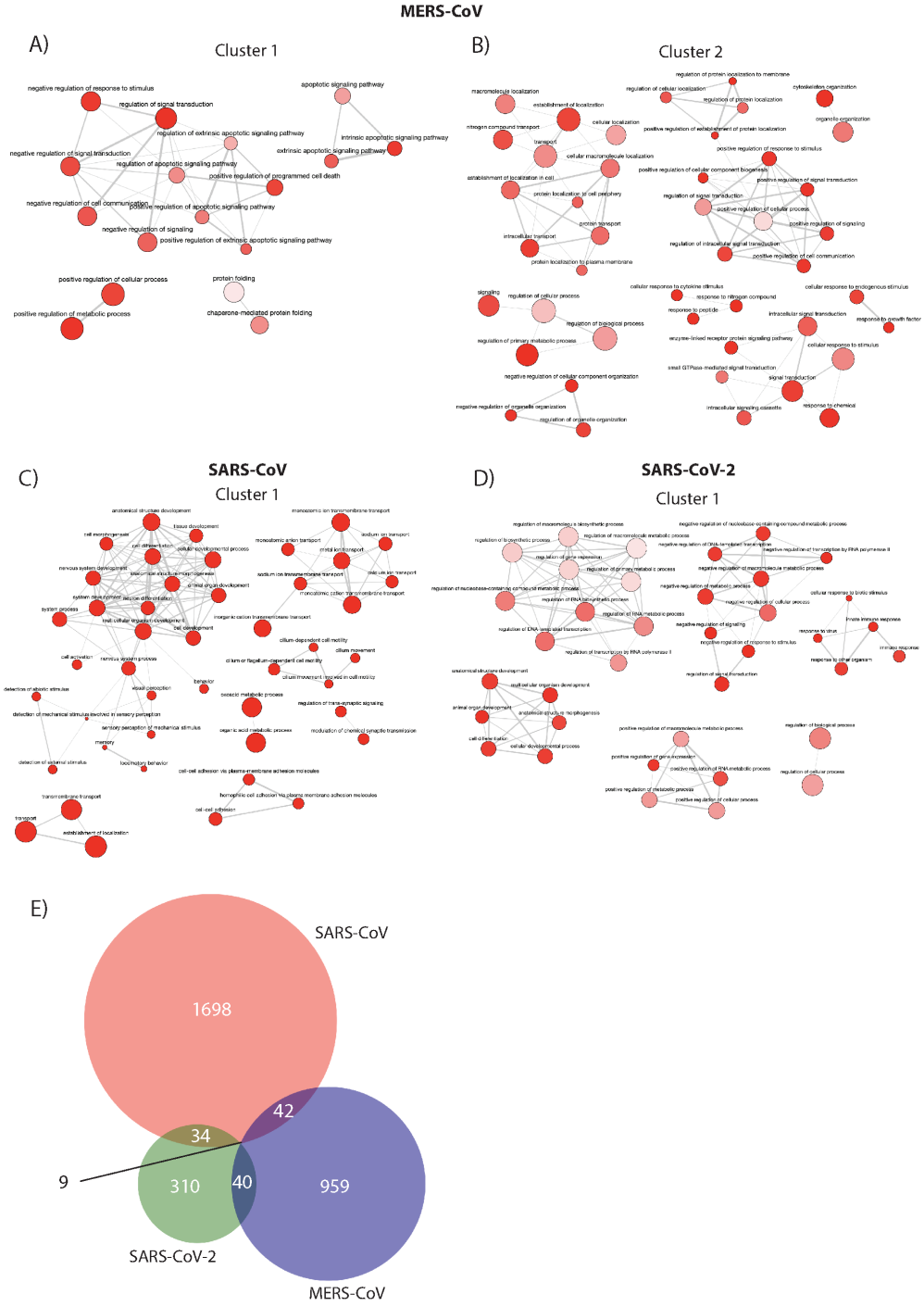


Figure 5. Enrichment analysis of overrepresented gene ontology biological process terms within each cluster of DEGs modulated over time. A-D) Semantic similarity network of GO terms for each cluster identified in the k-means analysis was performed using Revigo (26). The top 80 GO terms were considered for visualization. Node size represents the frequency of the GO term in the database, edges indicate semantic similarity, and colours represent p-value intensity (darker indicates a higher p-value). Cluster 2 for

SARS-CoV and SARS-CoV-2 were excluded given the lack of significant enrichment of GO terms. E) Venn diagram of significant DEGs modulated over time among the three viruses.

References

1. Edridge AWD, Kaczorowska J, Hoste ACR, Bakker M, Klein M, Loens K, et al. Seasonal coronavirus protective immunity is short-lasting. Nat Med. 2020;26(11):1691-3.
2. Galipeau Y, Siragam V, Laroche G, Marion E, Greig M, McGuinty M, et al. Relative Ratios of Human Seasonal Coronavirus Antibodies Predict the Efficiency of Cross-Neutralization of SARS-CoV-2 Spike Binding to ACE2. eBioMedicine. 2021;74.
3. Hui DS, Chan MC, Wu AK, Ng PC. Severe acute respiratory syndrome (SARS): epidemiology and clinical features. Postgrad Med J. 2004;80(945):373-81.
4. Pormohammad A, Ghorbani S, Khatami A, Farzi R, Baradaran B, Turner DL, et al. Comparison of confirmed COVID-19 with SARS and MERS cases - Clinical characteristics, laboratory findings, radiographic signs and outcomes: A systematic review and meta-analysis. Rev Med Virol. 2020;30(4):e2112.
5. WHO. Summary of probable SARS cases with onset of illness from 1 November 2002 to 31 July 2003 2004 [Available from: https://www.who.int/csr/sars/country/table2004_04_21/en/.
6. WHO. Middle East respiratory syndrome coronavirus – Saudi Arabia 2025 [Available from: https://www.who.int/emergencies/disease-outbreak-news/item/2022-DON422.
7. de Wit E, van Doremalen N, Falzarano D, Munster VJ. SARS and MERS: recent insights into emerging coronaviruses. Nature Reviews Microbiology. 2016;14(8):523-34.
8. WHO. WHO COVID-19 dashboard 2025 [Available from: https://data.who.int/dashboards/covid19/deaths?n=o.
9. Brian DA, Baric RS. Coronavirus genome structure and replication. Curr Top Microbiol Immunol. 2005;287:1-30.
10. Fehr AR, Perlman S. Coronaviruses: an overview of their replication and pathogenesis. Methods Mol Biol. 2015;1282:1-23.
11. Masters PS. The molecular biology of coronaviruses. Adv Virus Res. 2006;66:193-292.
12. Amicone M, Borges V, Alves MJ, Isidro J, Zé-Zé L, Duarte S, et al. Mutation rate of SARS-CoV-2 and emergence of mutators during experimental evolution. Evol Med Public Health. 2022;10(1):142-55.
13. Minskaia E, Hertzig T, Gorbalenya AE, Campanacci V, Cambillau C, Canard B, et al. Discovery of an RNA virus 3'->5' exoribonuclease that is critically involved in coronavirus RNA synthesis. Proc Natl Acad Sci U S A. 2006;103(13):5108-13.
14. Di Giorgio S, Martignano F, Torcia MG, Mattiuz G, Conticello SG. Evidence for host-dependent RNA editing in the transcriptome of SARS-CoV-2. Sci Adv. 2020;6(25):eabb5813.
15. Kim K, Calabrese P, Wang S, Qin C, Rao Y, Feng P, et al. The roles of APOBEC-mediated RNA editing in SARS-CoV-2 mutations, replication and fitness. Sci Rep. 2022;12(1):14972.
16. Ringlander J, Fingal J, Kann H, Prakash K, Rydell G, Andersson M, et al. Impact of ADAR-induced editing of minor viral RNA populations on replication and transmission of SARS-CoV-2. Proc Natl Acad Sci U S A. 2022;119(6).
17. Meng B, Kemp SA, Papa G, Datir R, Ferreira I, Marelli S, et al. Recurrent emergence of SARS-CoV-2 spike deletion H69/V70 and its role in the Alpha variant B.1.1.7. Cell Rep. 2021;35(13):109292.

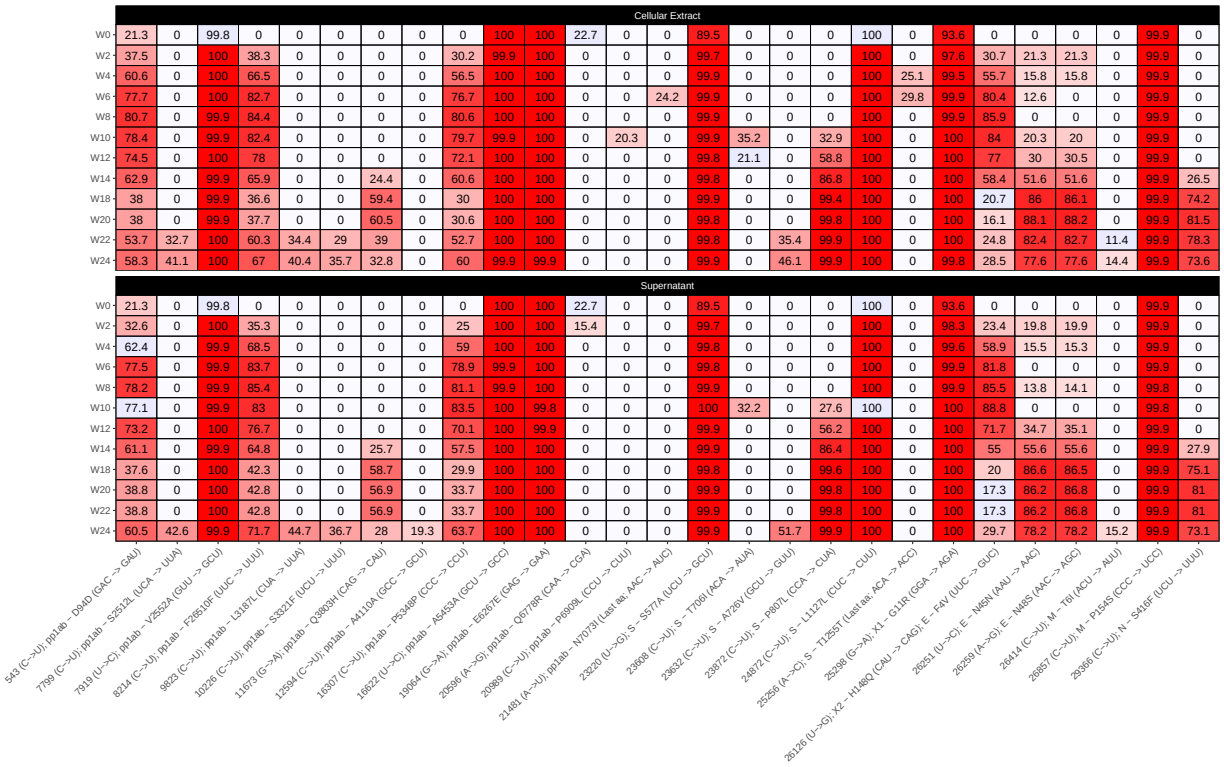
18. Li J-Y, Wang H-Y, Cheng Y-X, Ji C, Weng S, Han N, et al. Comprehensive detection and dissection of interlineage recombination events in the SARS-CoV-2 pandemic. Virus Evolution. 2024;10(1).
19. Liu G, Gack MU. Distinct and Orchestrated Functions of RNA Sensors in Innate Immunity. Immunity. 2020;53(1):26-42.
20. Totura AL, Whitmore A, Agnihothram S, Schäfer A, Katze MG, Heise MT, et al. Toll-Like Receptor 3 Signaling via TRIF Contributes to a Protective Innate Immune Response to Severe Acute Respiratory Syndrome Coronavirus Infection. mBio. 2015;6(3):e00638-15.
21. Yamada T, Takaoka A. Innate immune recognition against SARS-CoV-2. Inflammation and Regeneration. 2023;43(1):7.
22. Sun G, Cui Q, Garcia G, Wang C, Zhang M, Arumugaswami V, et al. Comparative transcriptomic analysis of SARS-CoV-2 infected cell model systems reveals differential innate immune responses. Scientific Reports. 2021;11(1):17146.
23. Love MI, Huber W, Anders S. Moderated estimation of fold change and dispersion for RNA-seq data with DESeq2. Genome Biology. 2014;15(12):550.
24. Kolberg L, Raudvere U, Kuzmin I, Vilo J, Peterson H. gprofiler2 -- an R package for gene list functional enrichment analysis and namespace conversion toolset g:Profiler. F1000Res. 2020;9.
25. Szklarczyk D, Kirsch R, Koutrouli M, Nastou K, Mehryary F, Hachilif R, et al. The STRING database in 2023: protein-protein association networks and functional enrichment analyses for any sequenced genome of interest. Nucleic Acids Res. 2023;51(D1):D638-d46.
26. Supek F, Bošnjak M, Škunca N, Šmuc T. REVIGO summarizes and visualizes long lists of gene ontology terms. PLoS One. 2011;6(7):e21800.
27. Eskier D, Karakülah G, Suner A, Oktay Y. RdRp mutations are associated with SARS-CoV-2 genome evolution. PeerJ. 2020;8:e9587.
28. Clarke DK, Duarte EA, Moya A, Elena SF, Domingo E, Holland J. Genetic bottlenecks and population passages cause profound fitness differences in RNA viruses. J Virol. 1993;67(1):222-8.
29. Dudouet P, Colson P, Aherfi S, Levasseur A, Beye M, Delerce J, et al. SARS-CoV-2 quasi-species analysis from patients with persistent nasopharyngeal shedding. Scientific Reports. 2022;12(1):18721.
30. Rocheleau L, Laroche G, Fu K, Stewart CM, Mohamud AO, Côté M, et al. Identification of a High-Frequency Intrahost SARS-CoV-2 Spike Variant with Enhanced Cytopathic and Fusogenic Effects. mBio. 2021;12(3):10.1128/mbio.00788-21.
31. Raharinirina NA, Gubela N, Börnigen D, Smith MR, Oh D-Y, Budt M, et al. SARS-CoV-2 evolution on a dynamic immune landscape. Nature. 2025;639(8053):196-204.
32. Johnson BA, Xie X, Bailey AL, Kalveram B, Lokugamage KG, Muruato A, et al. Loss of furin cleavage site attenuates SARS-CoV-2 pathogenesis. Nature. 2021;591(7849):293-9.
33. Peacock TP, Goldhill DH, Zhou J, Baillon L, Frise R, Swann OC, et al. The furin cleavage site in the SARS-CoV-2 spike protein is required for transmission in ferrets. Nature Microbiology. 2021;6(7):899-909.
34. Menachery VD, Mitchell HD, Cockrell AS, Gralinski LE, Yount BL, Graham RL, et al. MERS-CoV Accessory ORFs Play Key Role for Infection and Pathogenesis. mBio. 2017;8(4):10.1128/mbio.00665-17.

35. Yang Y, Zhang L, Geng H, Deng Y, Huang B, Guo Y, et al. The structural and accessory proteins M, ORF 4a, ORF 4b, and ORF 5 of Middle East respiratory syndrome coronavirus (MERS-CoV) are potent interferon antagonists. Protein Cell. 2013;4(12):951-61.
36. Sène M-A, Xia Y, Kamen AA. Overview of recent advances in Vero cells genomic characterization and engineering for high-throughput vaccine manufacturing. Clinical and Translational Discovery. 2022;2(2):e40.
37. Scobey T, Yount BL, Sims AC, Donaldson EF, Agnihothram SS, Menachery VD, et al. Reverse genetics with a full-length infectious cDNA of the Middle East respiratory syndrome coronavirus. Proc Natl Acad Sci U S A. 2013;110(40):16157-62.
38. McCarthy MK, Weinberg JB. The immunoproteasome and viral infection: a complex regulator of inflammation. Frontiers in Microbiology. 2015;6.
39. Ferrington DA, Gregerson DS. Immunoproteasomes: structure, function, and antigen presentation. Prog Mol Biol Transl Sci. 2012;109:75-112.
40. Tenzer S, Stoltze L, Schönfisch B, Dengjel Jr, Müller M, Stevanović S, et al. Quantitative Analysis of Prion-Protein Degradation by Constitutive and Immuno-20S Proteasomes Indicates Differences Correlated with Disease Susceptibility1. The Journal of Immunology. 2004;172(2):1083-91.
41. Schmidtke G, Schregle R, Alvarez G, Huber EM, Groettrup M. The 20S immunoproteasome and constitutive proteasome bind with the same affinity to PA28αβ and equally degrade FAT10. Molecular Immunology. 2019;113:22-30.
42. Vanderboom PM, Mun DG, Madugundu AK, Mangalaparthi KK, Saraswat M, Garapati K, et al. Proteomic Signature of Host Response to SARS-CoV-2 Infection in the Nasopharynx. Mol Cell Proteomics. 2021;20:100134.
43. Nobel FA, Kamruzzaman M, Jebin RA, Uddin MN, Ruhee NN, Babu G, et al. Revealing biomarkers and major pathways between SARS-CoV-2 and SARS-like viruses using transcriptomics analysis. Human Gene. 2024;40:201292.
44. Wu K, Xie Q, Liu X, Fu Y, Li S, Yu X, et al. Capsid protein of turnip crinkle virus suppresses antiviral RNA decay by degrading Arabidopsis Dcp1 via ubiquitination pathway. The Plant Journal. 2025;121(5):e70075.

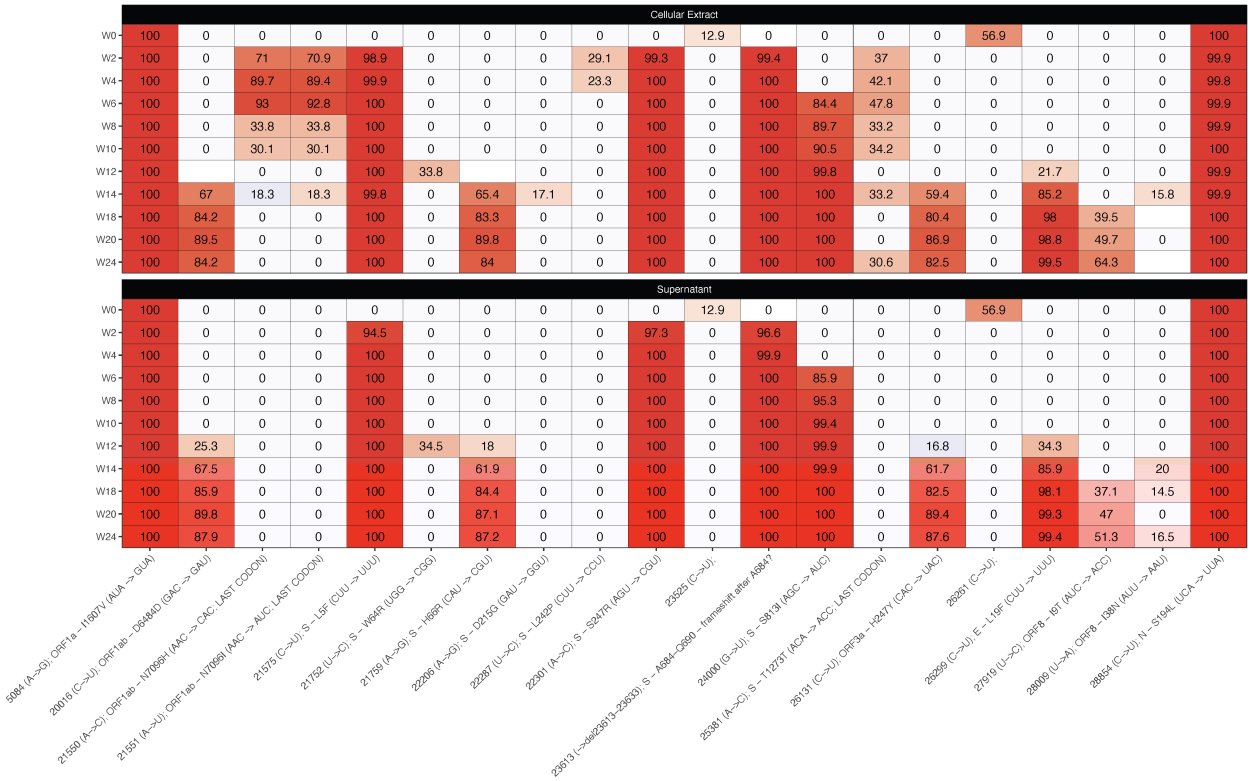
Supplementary material



Supplementary figure 1. Relative percentage substitution and deletion over time from supernatants and cells infected with MERS-CoV. The relative % substitution mutations or deletion (X-axis) over the 24 weeks. Amino-acid change is also identified if applicable. Blue squares represent mutations that were common but not statistically significant.

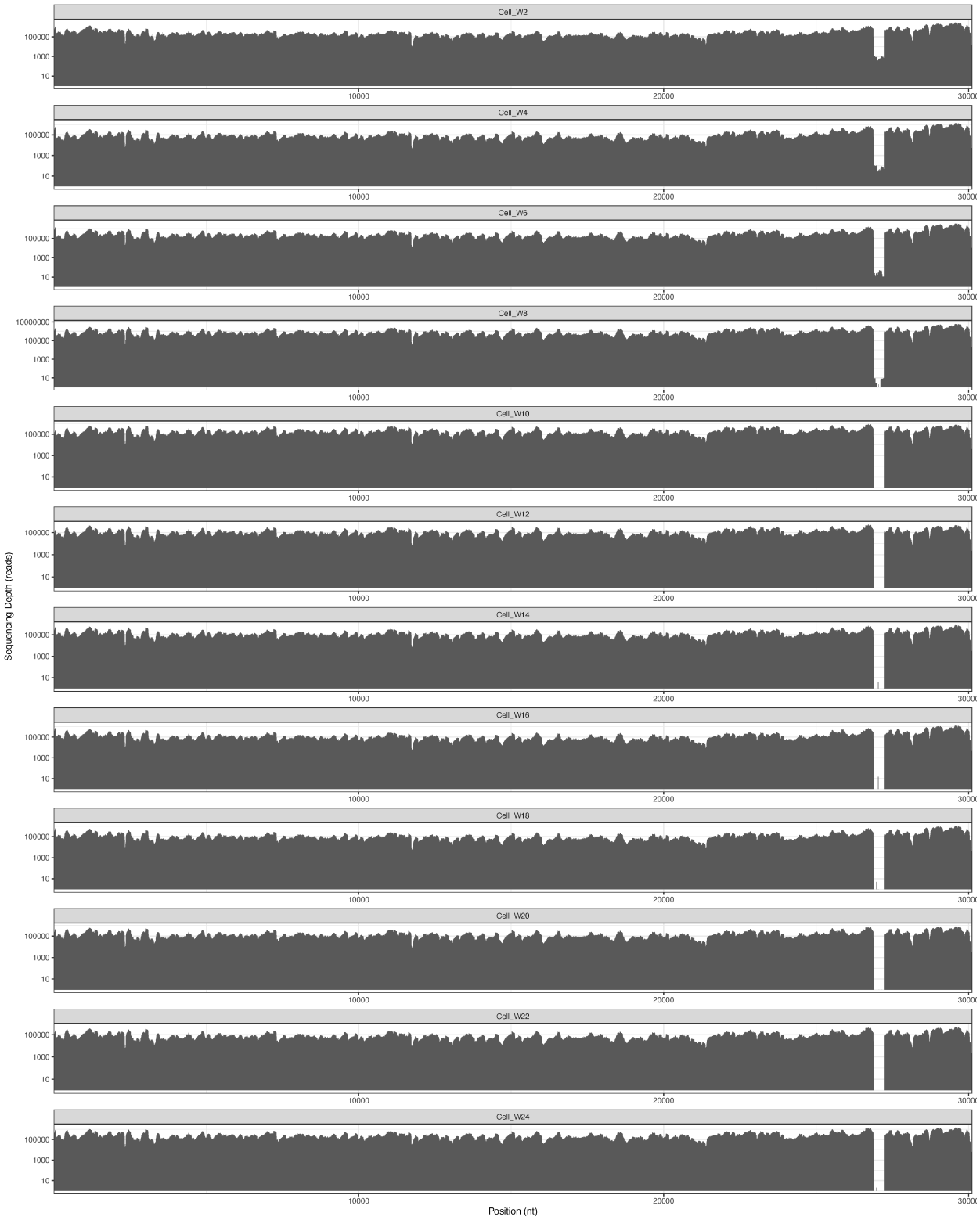


Supplementary figure 2. Relative percentage substitution and deletion over time from supernatants and cells infected with SARS-CoV. The relative % substitution mutations or deletion (X-axis) over the 24 weeks. Amino-acid change is also identified if applicable. Blue squares represent mutations that were common but not statistically significant. Week 16 was excluded as the supernatant sequencing result did not meet quality control.

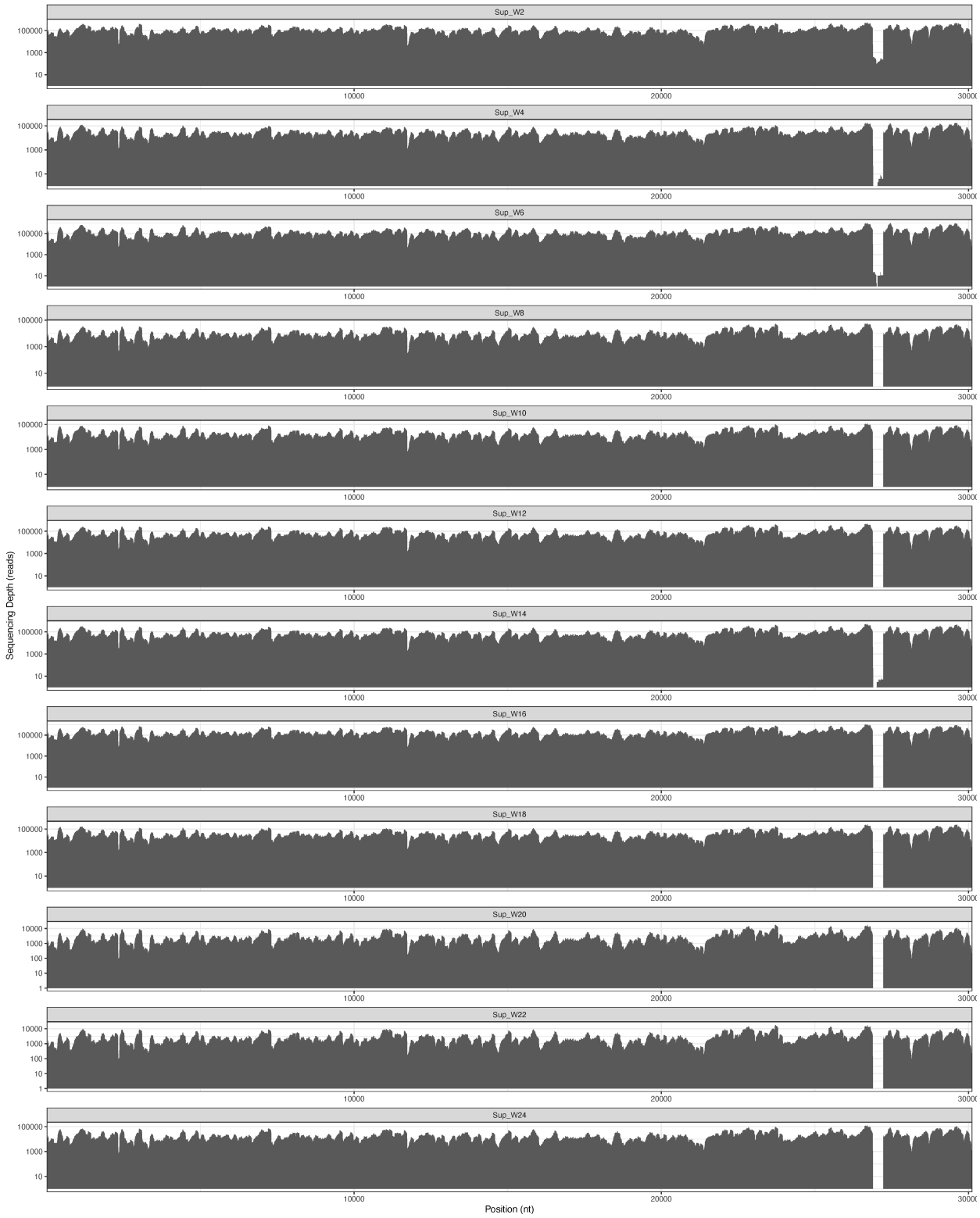


Supplementary figure 3. Relative percentage substitution and deletion over time from supernatants and cells infected with SARS-CoV-2.

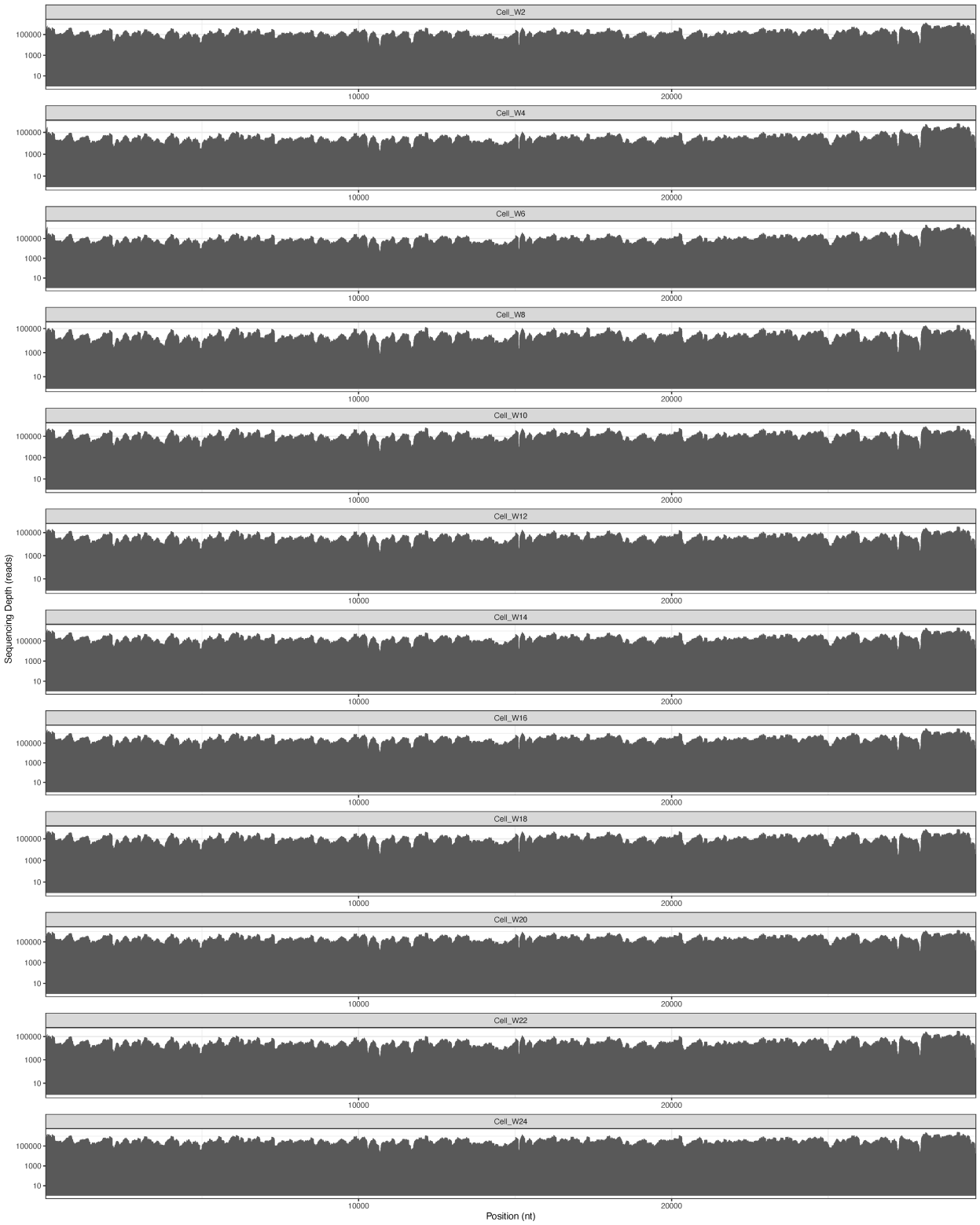
The relative % substitution mutations or deletion (X-axis) over the 24 weeks. Amino-acid change is also identified if applicable. Blue squares represent mutations that were common but not statistically significant. Week 16 was excluded as the supernatant sequencing result did not meet quality control.



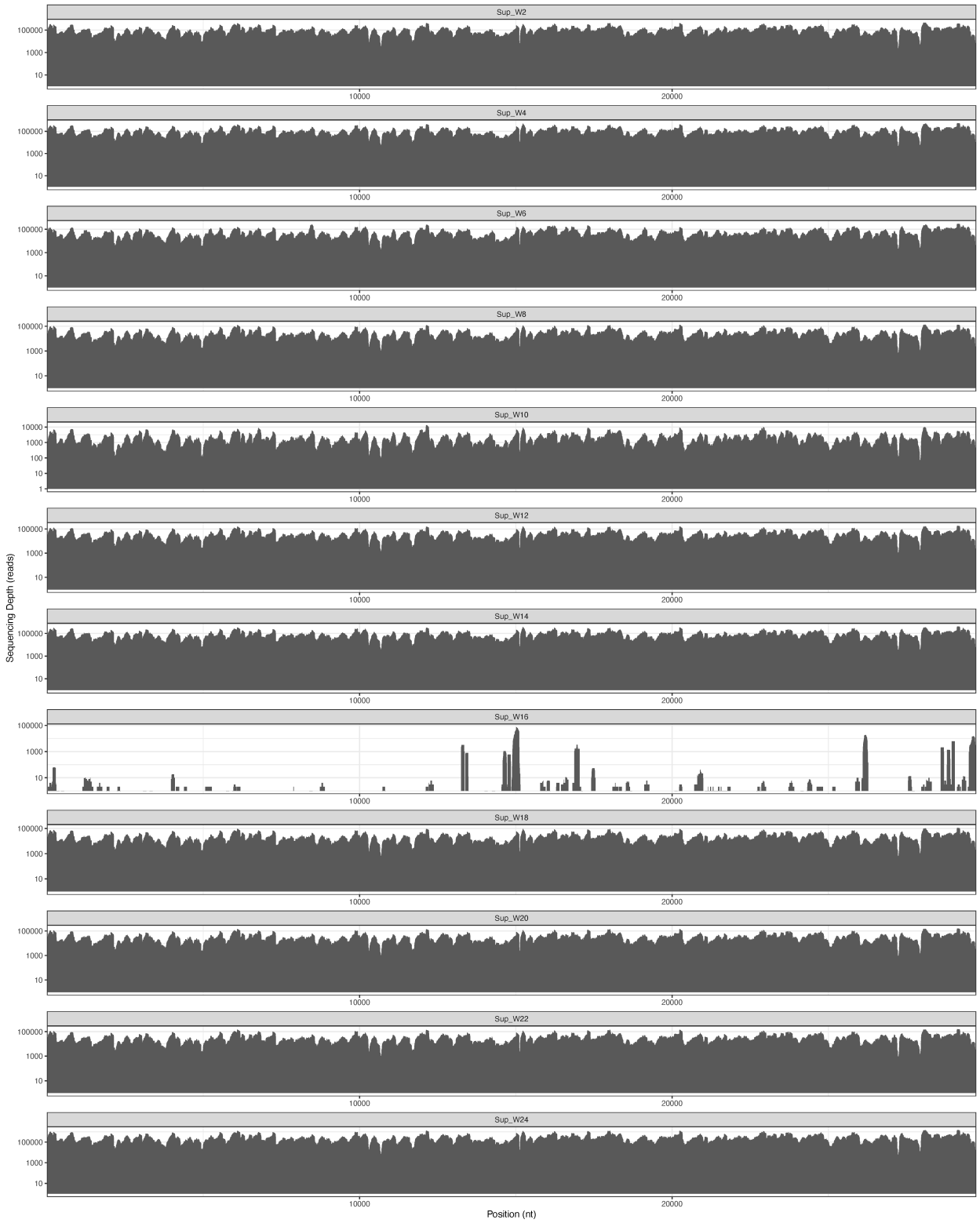
Supplementary figure 4. Sequencing depth and coverage for MERS-CoV cellular extract samples. The number of reads is formatted on a log10 scale (y-axis). A deactivating deletion in the ORF5 region appeared at week 2.



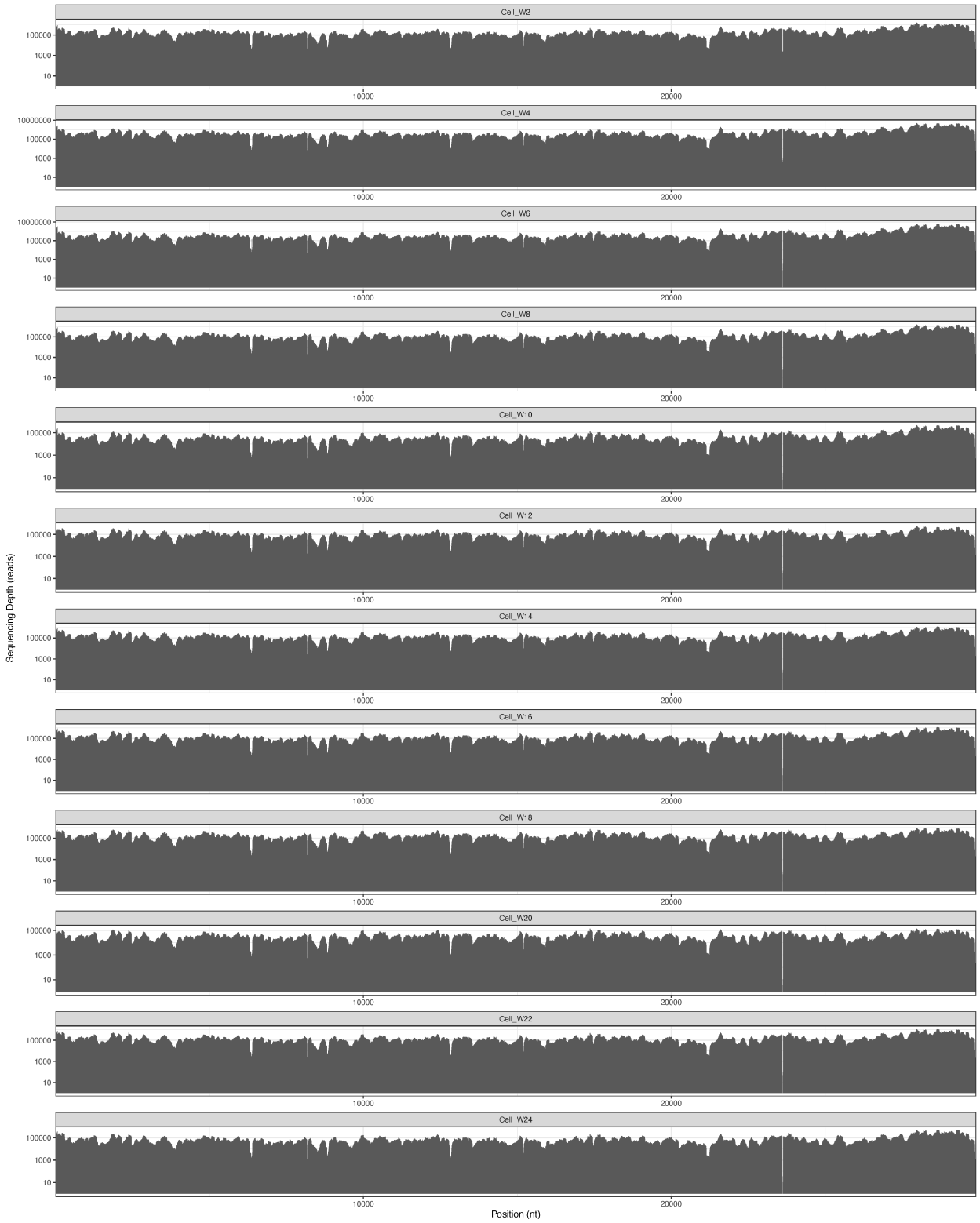
Supplementary figure 5. Sequencing depth and coverage for MERS-CoV supernatant samples. The number of reads is formatted on a log10 scale (y-axis). A deactivating deletion in the ORF5 region appeared at week 2.



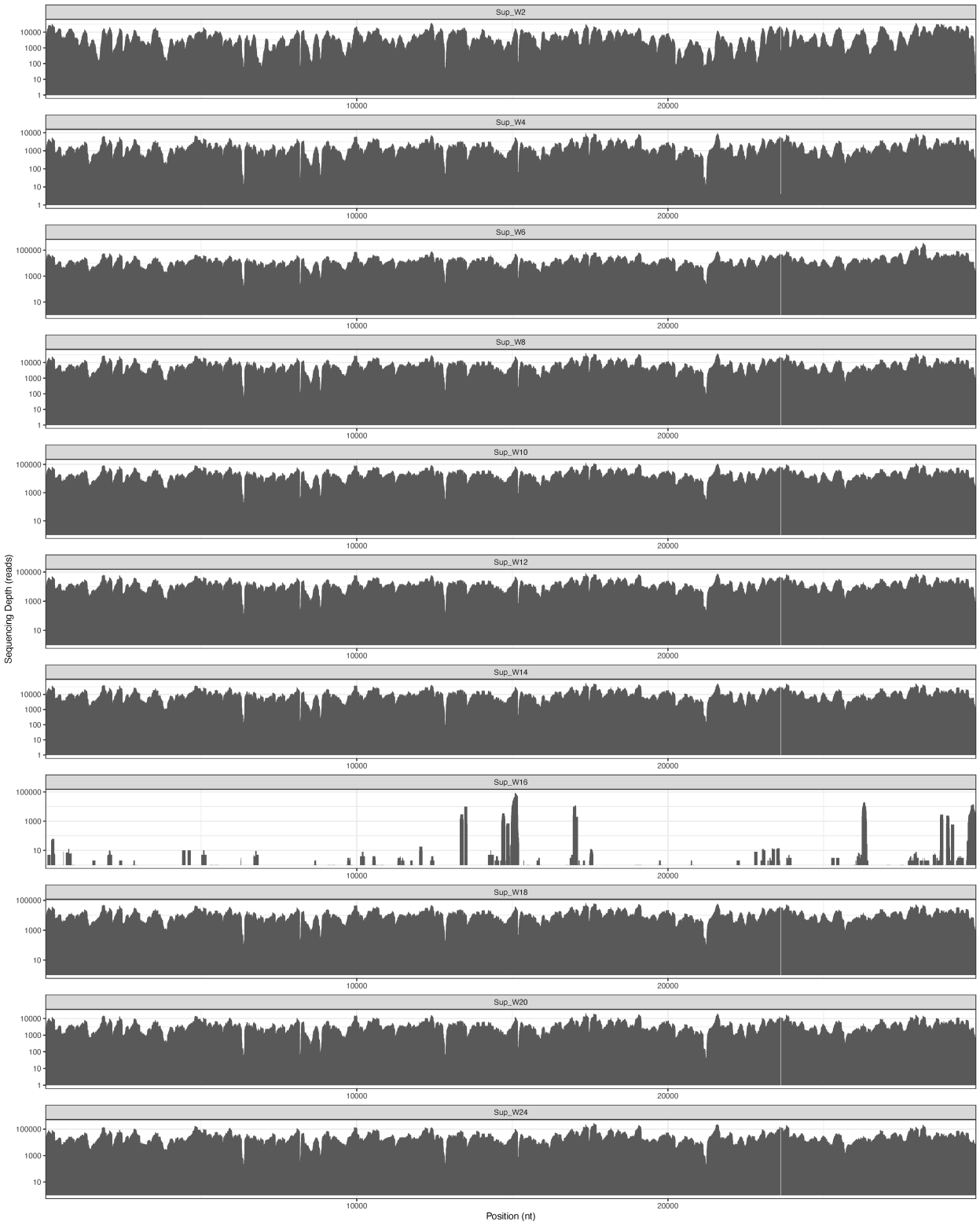
Supplementary figure 6. Sequencing depth and coverage for SARS-CoV cellular extract samples. The number of reads is formatted on a log10 scale (y-axis).



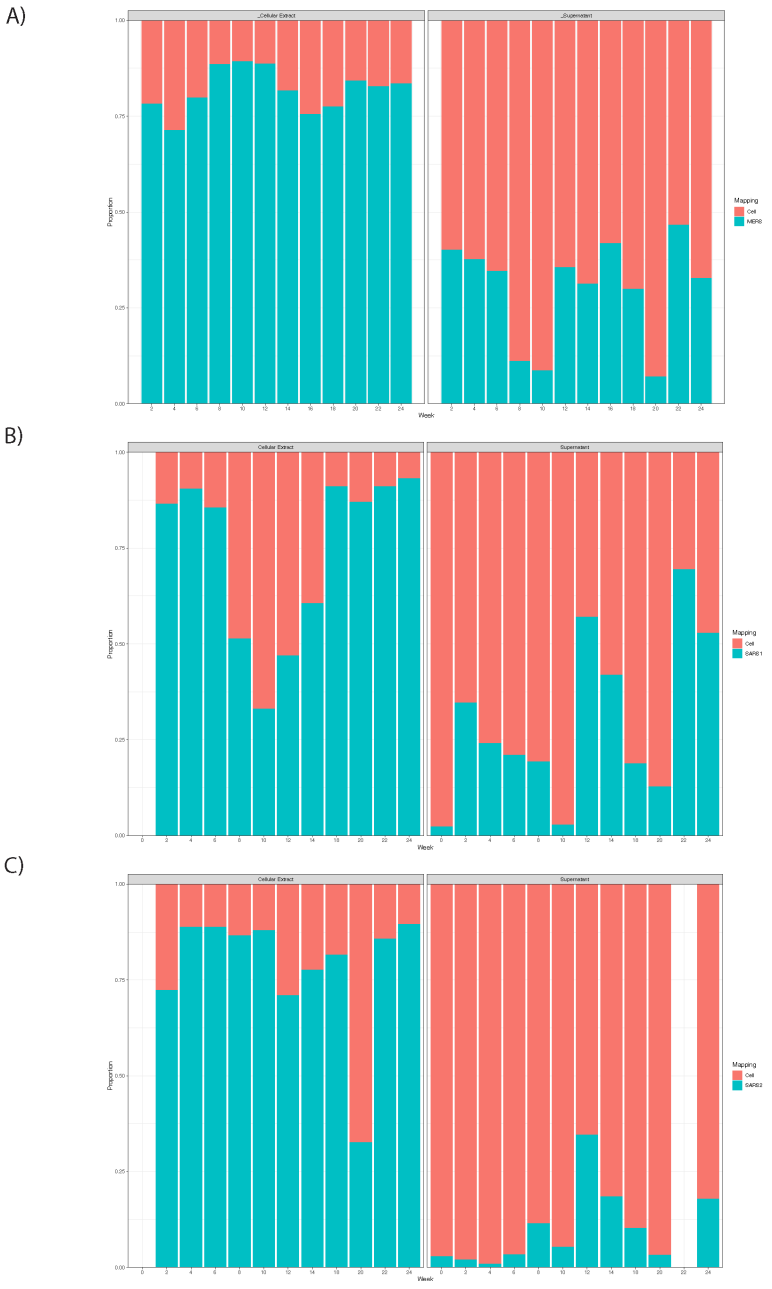
Supplementary figure 7. Sequencing depth and coverage for SARS-CoV supernatant samples. The number of reads is formatted on a log10 scale (y-axis).



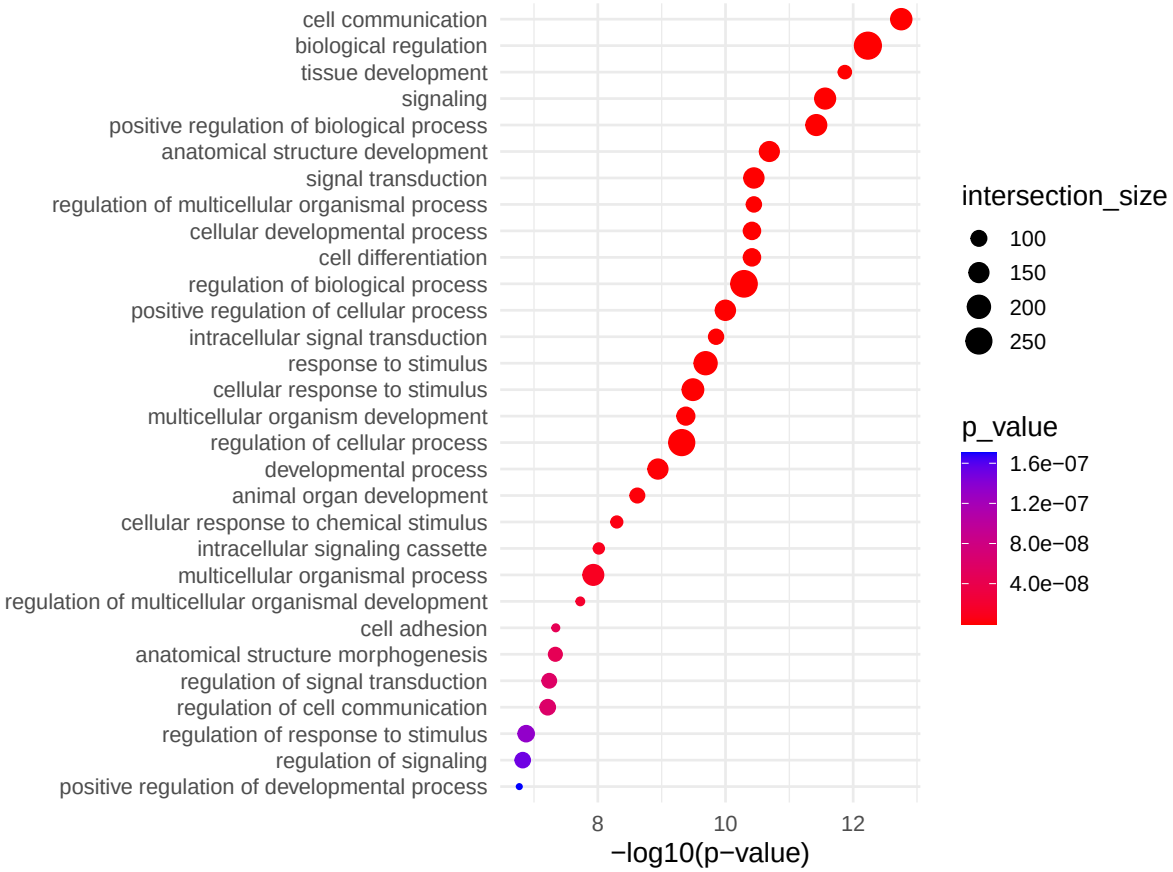
Supplementary figure 8. Sequencing depth and coverage for SARS-CoV-2 cellular extract samples. The number of reads is formatted on a log10 scale (y-axis).



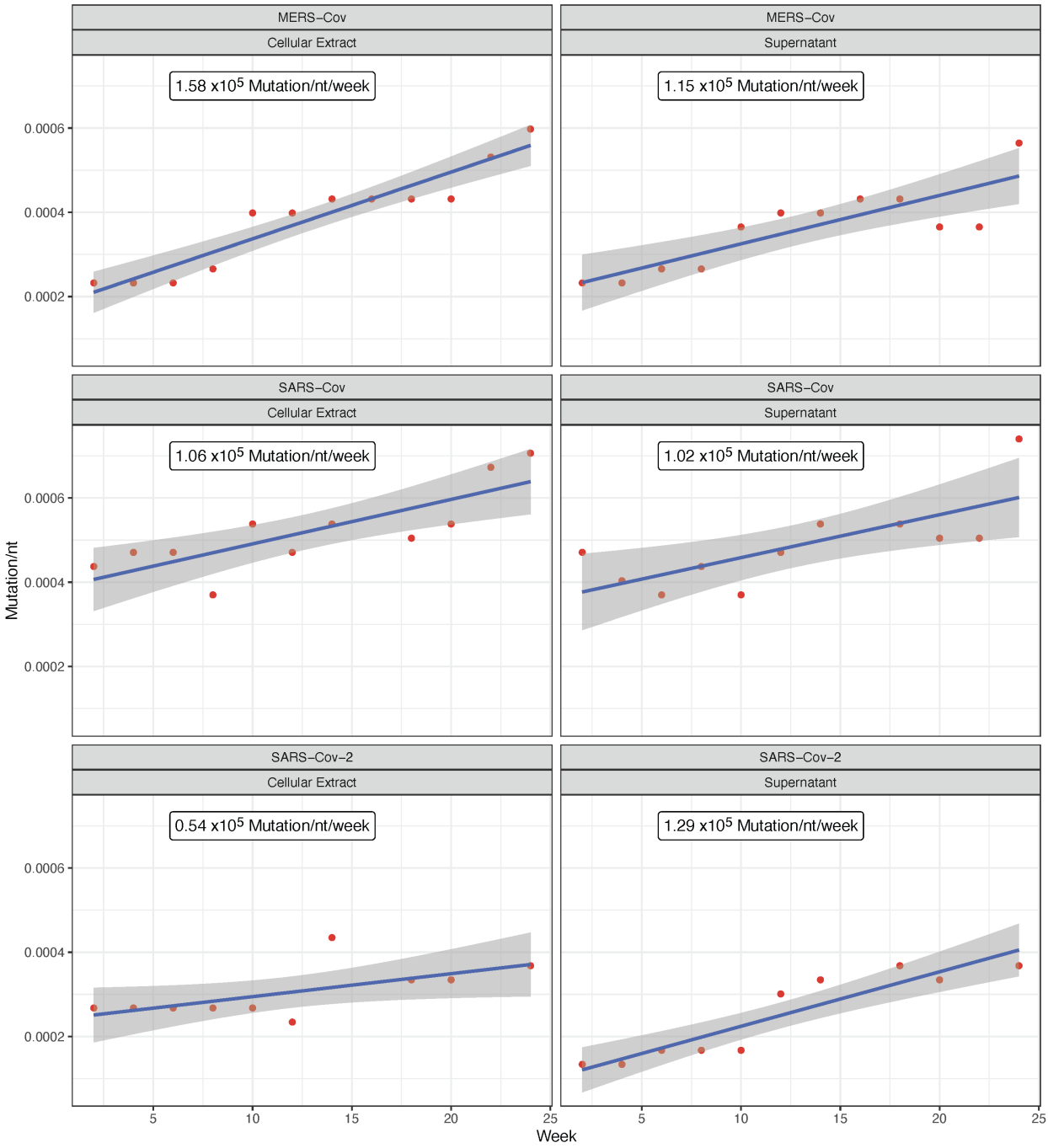
Supplementary figure 9. Sequencing depth and coverage for SARS-CoV-2 supernatant samples. The number of reads is formatted on a log10 scale (y-axis). No supernatant was sequenced at week 22.



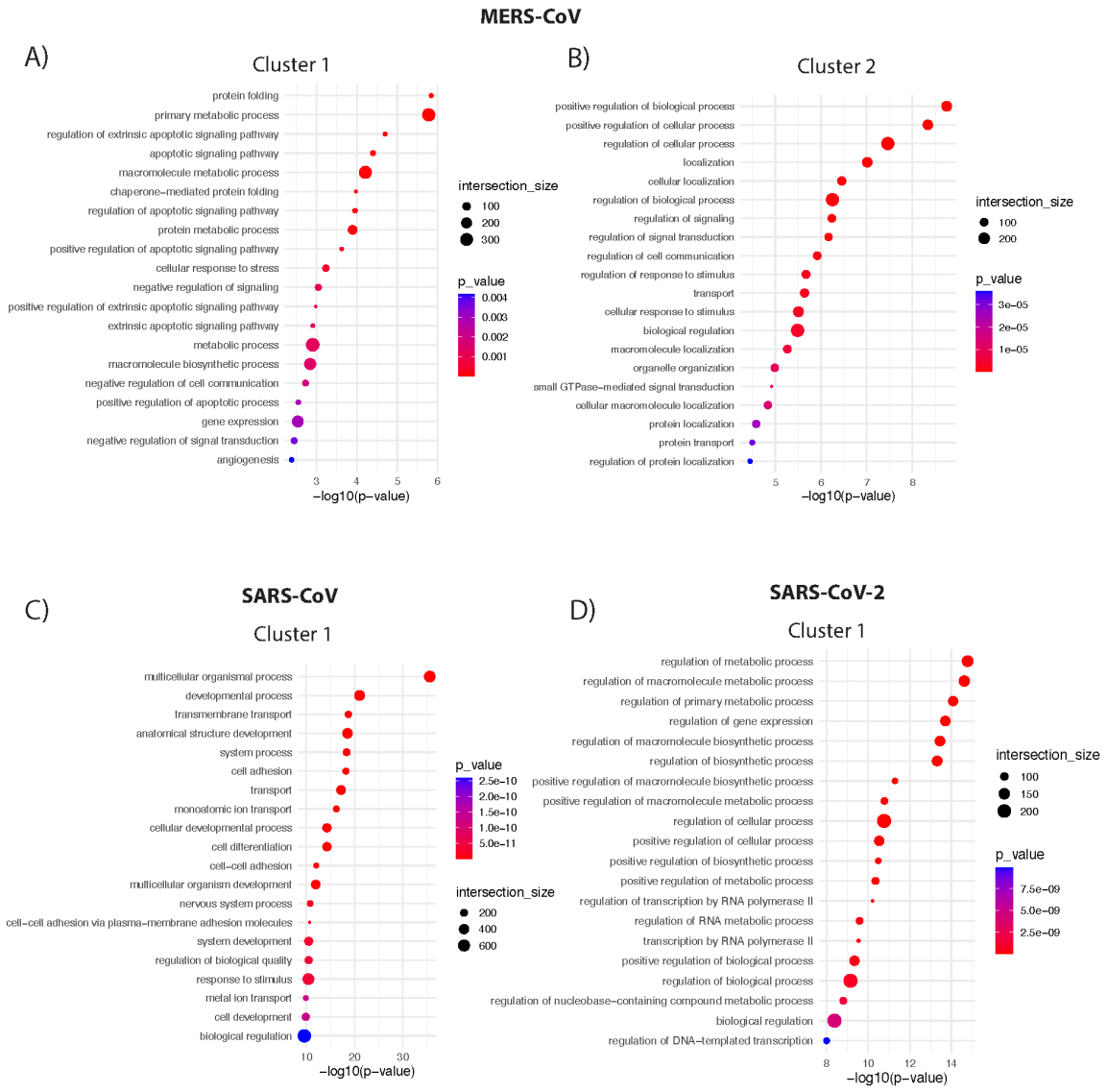
Supplementary figure 10. Proportion of cellular mRNA or Viral RNA in the cell extract or supernatant. A) MERS-CoV B) SARS-CoV C) SARS-CoV-2.



Supplementary figure 11. Enrichment analysis of biological processes GO terms in shared upregulated genes at baseline.



Supplementary figure 12. Weekly mutation rate data for supernatant and cellular extract samples. Linear regression is shown for each sample type for SARS-CoV, SARS-CoV-2 and MERS-CoV.



Supplementary figure 13. Enrichment analysis of biological processes GO terms in each cluster of gene whose expression was modulated over time. The top 20 most significant terms are shown here with the intersection size representing the number of genes associated with the BP: GO term.

Supplementary Table 1: Number and Frequency of mutations found in the spike protein by domain.

Domain	**MERS-CoV** (Nb (%))	**SARS-CoV** (Nb (%))	**SARS-CoV-2** (Nb (%))
S2	4 (66)	4 (80)	3 (30)
S1	2 (33	1 (20)	7 (70)
RBD	-	-	-

Supplementary Table 2: Number and Frequency of mutations found in each protein of ORF1ab. Functions differences exist between viruses. The frequency is calculated based on total number of ORF1ab mutations for each virus.

Protein (nsp)	SARS-CoV (Nb (%))	SARS-CoV-2 (Nb (%))	MERS-CoV (Nb (%))	General function
nsp1	1(7.1)	-		Host translation inhibition, immune evasion
nsp2	-	-	1(14)	Unknown, possible role in host interactions
nsp3	3(21)	1(25)	3(43)	Papain-like protease (PLpro), deubiquitination
nsp4	1(7.1)	-	-	Membrane rearrangement for replication
nsp5 (3CLpro)	1(7.1)	-	-	Main protease, cleaves polyproteins
nsp6	1(7.1)	-	1(14)	Restricts autophagosome expansion
nsp7	-	-	-	Cofactor for RNA polymerase
nsp8	1(7.1)	-	1(14)	Primase activity, enhances polymerase function
nsp9	-	-	-	RNA binding protein
nsp10	-	-	-	Cofactor for nsp14/nsp16
nsp11	-	-	-	Unknown
nsp12 (RdRp)	-	-	-	RNA-dependent RNA polymerase (RdRp)
nsp13 (Helicase)	2 (14)	-	1(14)	Helicase, unwinds RNA
nsp14 (ExoN)	1(7.1)	-	-	Exoribonuclease, methyltransferase
nsp15 (EndoU)	1(7.1)	1(25)	-	Endoribonuclease (NendoU), evades immune response
nsp16 (2'-O-MTase)	2(14)	2(50)	-	2'-O-methyltransferase, RNA cap modification

CONCLUSION

The COVID-19 pandemic has resulted in significant mortality and morbidity, alongside profound economic and societal disruptions. The extent of the pandemic has resulted in unprecedented research efforts in understanding the biology of the virus, the immune response associated with infection as well as intense efforts in the development and evaluation of immunization approaches. This thesis describes the development of serological methods for SARS-CoV-2 and examines various factors that impact antibody-mediated immunity. As shown by this body of work, serological tools are a key component of a well-coordinated pandemic response. In addition, data from serological studies provide valuable information to answer scientific questions relating to factors that impact antibody-mediated responses. Here, this thesis investigates primarily how population and demographic features, pre-exposure to other coronaviruses shape antibody immunity. Further, autoantibodies in the context of SARS-CoV-2 were also investigated. Finally, immune responses are intrinsically linked to virus biology hence, host-transcriptomic responses were investigated in the context of a SARS-CoV-2, SARS-CoV and MERS-CoV longitudinal adaptation experiment.

Serological assays for SARS-CoV-2

The ability to measure antibodies from infection or vaccination is central to both the development of vaccines but also to properly monitor and understand viral spread within various populations. First, given that antibodies remain in circulation for several weeks to months they enables the identification of previous infection without requiring sampling within the infectious window. This allows capture of individuals who did not report COVID-19 infection, did not undergo molecular testing during acute infection, or asymptomatic infections which can easily be undetected without serological measurements. Further, serological measurements of antibodies following vaccination enable the monitoring of efficacy in individuals with comorbidities, immune-compromising conditions or other. It also enables the monitoring of vaccine induced and infection induced immunity against emerging variants of concern.

In **Chapter 2**, this thesis focuses on developing high-throughput serological methods for SARS-CoV-2. Section 2.1 describes the design, protocols, and data analysis pipelines established to measure antibodies targeting the nucleocapsid, receptor-binding domain (RBD), and spike proteins, as well as the development of a protein-based surrogate neutralization assay. Considerable effort was invested in designing assays that meet four key criteria: (1) acceptable sensitivity and specificity; (2) compatibility with automated laboratory equipment; (3) capacity to report normalized antibody titers, including in international units; and (4) flexibility to accommodate various biological samples, including dried blood spots, plasma, serum, milk, and other antibody-containing fluids. In addition, a protein-based neutralization assay was implemented, which demonstrated correlation with PRNT50 and was calibrated against a standardized reference panel. Particular emphasis was placed on ensuring that both the neutralization and serological assays were amenable to high-throughput processing. This was achieved by minimizing reaction volumes (10 µL) and integrating automated equipment, including liquid handlers and plate washers, enabling the processing of large cohorts in serological studies that would otherwise have been unfeasible. Overall, the developed serological platform supports the execution of several thousand assays per week and is readily scalable.

In Appendix A-1.24 and A-1.25, we report the comparative performance of our serological assays on blinded samples coordinated by the National Microbiology Laboratory, in comparison with other academic and commercial platforms. The study presented in A-1.24 highlighted that several existing platforms demonstrated suboptimal specificity and sensitivity. In contrast, our assay correctly identified 100% of the samples in this set, while also maintaining an excellent dynamic range between positive and negative results. These findings also highlights the utility and robustness of dried blood spot (DBS) samples in the design of seroprevalence studies. The ability to mail DBS cards to the laboratory without requiring trained healthcare personnel for sampling, cold-chain storage, or in-person visits presents a significant advantage in terms of cost-effectiveness and accessibility for large-scale surveillance efforts.

Furthermore, we developed an automated pipeline to perform protein-based neutralization assays using DBS samples, an approach that is not commonly implemented. Although technically challenging, we demonstrated that functional assessment of antibody responses from DBS is feasible and reliable. Our neutralization assay was also employed as a benchmark to evaluate the

performance of other novel assays, as presented in Section A-1.2. Finally, in Section A-1.22, we review the literature on serological and antibody-mediated immune responses to SARS-CoV-2 during the first year of the pandemic.

Population characteristics influence antibody-mediated immunity

In **Chapter 3**, this thesis presents work carried out in various population- and community-based studies. These studies involved large cohorts of participants, in which serological parameters and neutralization efficiency were measured using serological methods developed and validated in Chapter 2. By applying these methods, it was possible to quantify several classes of antibodies (i.e., IgG, IgM, and IgA) against various antigens (i.e., nucleocapsid, spike, and RBD). The high-throughput nature of our assays enabled antibody titer measurements in both longitudinal study designs and studies with large sample sizes, ranging from several hundred to thousands of participants.

In Sections A-1.26 and A-1.27, this thesis focuses on the establishment of *Stop the Spread Ottawa*, a longitudinal study of approximately 1,000 participants who provided DBS and serum/plasma samples monthly, alongside clinical and demographic information. This cohort served as a control group in several studies included in this thesis and provided opportunities to study both infection-acquired and vaccine-acquired immunity in healthy individuals. In Section 3.1, the impact of age was investigated in a cross-sectional study of unvaccinated elderly individuals following COVID-19. We found that the longevity of antibody-mediated immunity was reduced, with older age associated with higher decay rates. Additional studies found in the appendix explored antibody-mediated responses in various populations with specific conditions, comorbidities, or demographic factors (A-1.1, A-1.5, A-1.6, A-1.7, A-1.8, A-1.9, A-1.10, A-1.11, A-1.12, A-1.13, A-1.18, A-1.21).

Serological approaches were also used in Section 3.2 to investigate antibody-mediated immunity and the seroprevalence of previous SARS-CoV-2 infections in Indigenous communities in the Northwest Territories (NWT). When compared to a control cohort sampled during the same time period, we found that Indigenous communities in the NWT were disproportionately impacted by SARS-CoV-2 infection. Additionally, nearly two-thirds of participants were unaware of their

convalescent status. Overall, this study highlights critical gaps in diagnostic access and pandemic surveillance in geographically isolated regions and raises concerns about future pandemic preparedness, equitable access to testing, and healthcare infrastructure in remote Indigenous communities.

Pre-existing immunity to SARS-CoV-2

Whether exposure to seasonal coronaviruses such as NL63, HKU-1, OC43, or 229E has any influence on antibody-mediated responses to SARS-CoV-2 was a significant question in the field early in the pandemic. First, cross-reactivity from SCoVs antigens can impede the specificity of SARS-CoV-2 serological assays, and second, these cross-reactive antibodies could be protective. In **Chapter 4**, we show that most individuals have high levels of SCoV antibodies, and a proportion of samples are cross-reactive in varying proportions depending on the SARS-CoV-2 antigen and antibody isotype. Interestingly, we show that only a minority of these samples are pan cross-reactive, so by considering more than one antigen, it is possible to achieve very high specificity for SARS-CoV-2 seropositivity calls.

To investigate the function of cross-reactive antibodies in unexposed individuals, we show that these antibodies can inhibit the attachment of the SARS-CoV-2 spike to ACE2, suggesting a possible protective role of SCoVs against SARS-CoV-2. In these samples, SCoV antibody titers were used in machine learning approaches to predict their impact on SARS-CoV-2 spike and ACE2 attachment. We show that by using seasonal coronavirus spike antibody titers, we can accurately predict their experimental inhibition of SARS-CoV-2 and ACE2 attachment. Overall, this work highlights that pre-exposure to closely related viruses has ramifications for SARS-CoV-2 serological assay design and analysis, but we also show a possible functional role for these cross-reactive antibodies. Other aspects of SCoV biology and seroprevalence were also investigated in this thesis (A-1.4, A-1.14, A-1.17).

Autoimmunity to ACE2

In **Chapter 5**, this thesis investigates the prevalence and association of autoantibodies in the context of SARS-CoV-2. Autoimmunity and autoantibodies have long been associated with viral

infections, and a significant quantity of literature investigating their association with COVID-19 has been published throughout the pandemic. In section A-1.23, we review the current evidence linking various classes of autoantibodies to COVID-19. We find that only a minority of these autoantibodies have functional links to SARS-CoV-2 pathogenicity (e.g., anti-IFN and SARS-CoV-2 severity), with several studies investigating the seroprevalence in small cohorts. This limits the interpretation of their role in SARS-CoV-2 pathogenicity. We also discuss possible molecular mechanisms that may lead to the development of such antibodies over the course of a viral infection.

In section 5.1, we focus on autoantibodies that recognize and bind to the ACE2 protein. This study investigates the seroprevalence and levels of ACE2 autoantibodies in individuals with or without previous SARS-CoV-2 infection. The cohorts included in this study represent the largest cohort in which ACE2 autoantibodies have been investigated thus far. We show that regardless of infection status, nearly 1 in 5 individuals have ACE2 antibodies in circulation. Contrary to other reports, we found no correlation with SARS-CoV-2 infection. While we initially hypothesized that these antibodies could block the ACE2 receptor and prevent SARS-CoV-2 spike attachment, we found that these antibodies were unable to do so. They also did not impact the enzymatic activity of ACE2. Questions remain about how such antibodies are generated and what role, if any, they may have in physiology.

Several questions remain regarding the role of autoantibodies during and after viral infection, with some hypothesizing that they may play a role in post-COVID-19 conditions. Over the course of the review, a bias towards studying autoantibodies during high-severity infections, or simply in the context of autoimmune pathologies, has resulted in limited understanding of the possible regulatory role of such antibodies.

SARS-CoV-2, SARS-CoV and MERS-CoV

From the early 2000s until now, three highly pathogenic coronaviruses have emerged and established infection within human populations. In **Chapter 6**, this thesis examines the evolution of SARS-CoV, SARS-CoV-2, and MERS-CoV over the span of 24 weeks in an in vitro cell

system. This study is one of the few to directly compare all three highly pathogenic coronaviruses in parallel in an experimental evolution experiment. By performing RNA sequencing on supernatants and cellular extracts, the bi-directional relationship between host responses and viral evolution can be investigated. Further, since all three viruses were treated in the same way, it is possible to investigate shared and unique features of viral evolution and host transcriptomic responses between them. Over this time period, the viral titers increased, and each virus acquired numerous mutations and deletions spanning the viral genomes. In addition to investigating the evolution of each virus, the associated modulation of host genes was explored, revealing a distinct evolutionary strategy. We also report various shared differentially expressed genes (DEGs) that these coronaviruses share between them, shedding light on important conserved pathways. For example, in this work, we show that all three coronaviruses downregulate important proteins of the 20S proteasome, among others.

Overall, the biology of these human coronaviruses has important ramifications for antibody responses. For example, the evolution of each viral gene directly impacts the binding of antibodies to the various antigens. However, other features of the biology of these viruses can and do impact antibody responses, such as replication speed, the number of released viral particles, how each virus evades innate sensing, and how they modulate the release of inflammatory cytokines, among other features. To better understand adaptive immune responses, it is critical to understand host and viral interactions.

Related work

The serological assays developed in this thesis have also been applied to other areas of investigation. Notably, they have been adapted to work for samples from mice, which has enabled work in studying protein-based vaccine strategies from plant and mammal recombinant systems (A-1.3), as well as the investigation of mucosal delivery and mucosal immunity (A-1.19, A-1.20). These important areas of investigation highlight that flexible serological assays can be easily adapted to investigate immunity in pre-clinical analysis studies or other pathogens of concern. Flexibility in the design of data analysis and automated infrastructures are key components of Canada's future response to pandemics.

Future avenues for serological assays

The COVID-19 pandemic has catalyzed unprecedented growth in the development and implementation of high-throughput serological assays. While early efforts relied heavily on manual or semi-automated ELISA platforms, recent advances have emphasized automation and multiplexing as essential features for large-scale immunological surveillance. In the context of pandemic responses, multiplexing refers not only to the ability to process large numbers of samples but also to the capacity to detect antibodies against a broad range of antigens. This type of multiplexing is essential for sampling diverse populations that vary in geography, health status, comorbidities, and demographics. Moreover, serological surveys of large cohorts must also account for viral evolution. The need to test large sample sizes against a wide range of antigens that reflect the ongoing evolution of the pathogen poses a significant challenge for many current methods.

Here in this thesis, we showed that the automation of ELISA-based serological assays in a 384-well plate format could address some of these challenges. However, there is still progress to be made regarding throughput, integration with AI and ML data analysis, robotic automation, standardization and sustainability.

Some multiplexing strategies could enable current platforms to address some of the throughput concerns regarding cohort sizes and antigen scope. For example, Luminex-based immunoassays and VirScan represent two powerful yet distinct approaches to high-throughput serological analysis (206-208). The Luminex platform relies on bead-based multiplexing, where each microsphere can be conjugated to a specific antigen, such as spike (S), receptor-binding domain (RBD), or nucleocapsid (N) for example and is identified by a unique bead signature (209). This format allows simultaneous quantification of antibodies against dozens of antigens from a small volume of serum, making it ideal for evaluating responses to multiple variants of concern (VOCs) or for comparing immune responses across large populations. In contrast, VirScan is based on phage display technology, using a library of bacteriophages that collectively encode short peptides from nearly all known human viruses. Following immunoprecipitation and sequencing, VirScan provides an unbiased view of an individual's viral exposure history. While Luminex assays offer quantitative and functional insights into antibody responses against structurally intact or

conformationally sensitive antigens, VirScan excels in mapping linear epitope recognition. Together, these technologies can offer complementary windows into humoral immunity (210).

Another avenue to adapt current platforms consists of conjugating isotype-specific secondary antibodies to fluorophores instead of enzymes like horseradish peroxidase (HRP). This approach enables the simultaneous measurement of multiple antibody isotypes, and potentially subtypes, from a single 384-well plate format. By labelling each secondary antibody with spectrally distinct fluorophores, different excitation and emission wavelengths can be used to distinguish and quantify each isotype within the same well.

Next, the improvement and optimization of automation processes represent another avenue for increasing the throughput of serological assays. This includes refining current workflows using liquid handling systems, such as staggering steps or increasing the speed and efficiency of the automated equipment itself. Additionally, integrating advanced robotic components such as robotic arms that transfer plates between dispensers, incubators, sealers, and readers can further reduce cycle times and improve overall assay efficiency.

Integrating artificial intelligence (AI) into serological analyses offers substantial benefits in data interpretation, assay optimization, and predictive modelling. AI algorithms, particularly those based on machine learning and deep learning, can efficiently process large, complex datasets generated by high-throughput platforms, identifying subtle patterns and correlations that may be missed by traditional analyses (211, 212). By better incorporating clinical metadata, AI could also uncover links between serological signatures and disease severity, vaccine responsiveness, or protection, making it a powerful tool for public health surveillance and individualized risk assessment. Furthermore, AI approaches may be valuable in managing raw serological data by accounting for variability in temperature, humidity, lot and batch effects, as well as well-to-well signal bleed-through, thereby ensuring higher data quality and more reliable downstream analyses.

The proliferation of serological platforms risks increasing data fragmentation. Therefore, standardization across platforms remains a critical priority. For example, in the case of SARS-CoV-2, the adoption of WHO international standards for Binding Antibody Units (BAU mLš¹)

and IU-calibrated neutralization was essential for enabling cross-platform calibration and consistent reporting (213). As multi-laboratory studies are an effective way to increase throughput and validate findings, it is vital that such international standards be made available early during a pandemic and remain accessible for benchmarking emerging approaches.

Finally, high-throughput serological approaches face significant sustainability challenges. Large-scale serosurveys and routine operations on automated platforms often involve the consumption of millions of plastic consumables, including 96- or 384-well plates, pipette tips, reservoirs, and sealing films. This generates substantial biomedical plastic waste and contributes to the environmental footprint of laboratory research. To address these concerns, there is a growing need for research and development focused on optimizing consumable use and minimizing waste. One promising avenue is the adoption of reusable or recyclable components. For instance, some protocols for the washing and re-use of robotic pipette tips, which can significantly reduce both plastic waste and operating costs, could be implemented (214, 215). However, significant research and development will be required to ensure that recycled tips perform as well as brand-new ones. Advances in tip-washing technologies, combined with sterilization protocols and tracking systems, now make such practices increasingly feasible in high-throughput settings.

Serosurveys and pandemic preparedness

Serological surveys are critical tools in pandemic preparedness and response, providing insight into population-level exposure, immunity, and vulnerability to infectious diseases. By measuring the presence of antibodies against a pathogen in a representative sample of a population, serosurveys help to reveal the true burden of infection, including asymptomatic or undiagnosed cases that are often missed by case-based surveillance. In the context of emerging infectious diseases like COVID-19, serological data can guide public health interventions, inform vaccine policy, and refine epidemiological models. Moreover, when conducted systematically and over time, serosurveys offer a longitudinal view of immunity trends that is essential for anticipating future waves of infection and allocating resources accordingly.

One of the primary roles of serosurveys in pandemic preparedness is their ability to estimate the cumulative incidence of infection. Early in an outbreak, diagnostic testing is typically limited, and many infections, especially mild or asymptomatic cases, can go undetected. Serological assays, which detect antibodies produced in response to infection or vaccination, provide a retrospective measure of exposure. This allows public health authorities to determine the true spread of a pathogen, assess the proportion of the population that remains susceptible, and estimate key epidemiological parameters such as the infection fatality rate (IFR). These estimates are crucial for tailoring mitigation strategies and evaluating the effectiveness of public health interventions, such as lockdowns, school closures, or mask mandates among others.

Serosurveys also offer critical insight into population-level immunity, particularly in the context of vaccination campaigns. Antibody prevalence studies can help assess vaccine coverage and identify gaps in immunization among different demographic or geographic subgroups. This is essential for achieving and sustaining herd immunity thresholds. Additionally, by distinguishing between antibodies induced by infection and those induced by vaccination, using antigen-specific assays that target, for instance, nucleocapsid versus spike proteins, serosurveys can estimate the proportion of the population with hybrid immunity, an important factor in predicting protection against severe disease.

Serosurveys become even more powerful when integrated with biobanking infrastructures that support the long-term storage of biological specimens under standardized conditions. Biobanked serum, plasma, and DBS samples allow researchers to return to previously collected material as new technologies, assays, or questions emerge. For example, stored samples from early phases of a pandemic can later be analyzed for antibodies to newly identified variants, cross-reactive pathogens, or emerging zoonotic threats. This retrospective capacity is essential for understanding immune cross-reactivity, validating diagnostic assays, or even identifying early transmission. For this reason, pandemic preparedness frameworks should include the development of national and international biobank networks that are linked to surveillance activities, subject to ethical oversight, and accessible to both public health authorities and researchers under fair use policies (216, 217).

Access to relevant and representative samples is another crucial element of successful serosurveillance. Sampling strategies must be inclusive and statistically robust, with deliberate efforts to cover a wide range of demographics, geographic areas, socioeconomic contexts, and clinical backgrounds. This includes ensuring adequate representation from vulnerable populations such as the elderly, immunocompromised individuals, healthcare workers, and those living in densely populated or underserved regions. Ethical and logistical considerations such as informed consent, anonymization, and secure data sharing must also be addressed proactively to enable broad participation and facilitate global data integration. Cross-border sample sharing and harmonization of protocols are particularly important in the context of a global health emergency, where comparing immune landscapes across countries can help coordinate responses and avoid duplication of efforts.

From a global health governance perspective, the importance of serosurveys is reflected in the World Health Organization's Pandemic Accord and related frameworks (218, 219). These documents emphasize the need for timely, transparent, and standardized serological surveillance as a core capacity for pandemic preparedness. The goal is to enable countries to rapidly deploy validated serosurveys which can strengthen collective situational awareness during a pandemic or an outbreak.

In the context of variant emergence, serosurveys are instrumental in tracking antigenic drift and immune escape. Repeated surveys using multiplexed or variant-specific assays can help determine whether antibodies generated against earlier strains retain efficacy against newly circulating variants. These data are essential not only for risk assessment but also for guiding vaccine updates and formulating boosting strategies. Furthermore, serosurveys can be used to detect changes in antibody titres over time, helping to understand the durability of natural and vaccine-induced immunity.

Despite their utility, serosurveys face several challenges that must be addressed to maximize their impact. These include technical issues such as assay sensitivity, specificity, and platform standardization; logistical challenges in sampling and data collection; and the need for timely data analysis and dissemination. For example, without standardized reference materials such as

WHO-calibrated binding antibody units (BAU/mL), cross-study comparisons may be unreliable. Additionally, the establishment of accessible biobanks and clear governance around sample use is critical to ensuring that specimens collected during pandemics can continue to contribute to scientific understanding after the acute phase has passed.

Serosurveys are indispensable tools in pandemic preparedness, response, and recovery. They provide a unique lens into past infection and immunity trends that complements real-time case surveillance. When implemented strategically and supported by biobanking, inclusive sampling strategies, and international standardization, serosurveys can guide resource allocation, shape vaccination strategies, monitor variant impact, and support equitable public health interventions. Embedding serological capacity into national and global preparedness infrastructure, as recommended by the WHO will be key to improving our ability to detect, monitor, and respond to future pandemics with agility and precision.

Conclusion

In conclusion, this work highlights the critical role of serological assays in advancing our understanding of antibody-mediated immunity during infectious disease outbreaks. Throughout the COVID-19 pandemic, these tools proved essential not only for tracking population-level exposure but also for guiding vaccine development, evaluating immune responses, and informing public health strategies. As the threat of emerging and re-emerging pathogens continues to grow, the ability to rapidly develop, validate, and deploy robust serological assays will remain a cornerstone of effective pandemic response and preparedness. Continued investment in serological research infrastructure is vital to ensure that we can monitor possible outbreaks and remain equipped to meet the challenges of future global health emergencies.

REFERENCES

1. Taubenberger JK, Morens DM. 1918 Influenza: the mother of all pandemics. Emerg Infect Dis. 2006;12(1):15-22.
2. Dou D, Revol R, Östbye H, Wang H, Daniels R. Influenza A Virus Cell Entry, Replication, Virion Assembly and Movement. Front Immunol. 2018;9:1581.
3. Morens DM, Taubenberger JK, Fauci AS. Predominant role of bacterial pneumonia as a cause of death in pandemic influenza: implications for pandemic influenza preparedness. J Infect Dis. 2008;198(7):962-70.
4. Viboud C, Simonsen L, Fuentes R, Flores J, Miller MA, Chowell G. Global Mortality Impact of the 1957-1959 Influenza Pandemic. J Infect Dis. 2016;213(5):738-45.
5. Saunders-Hastings PR, Krewski D. Reviewing the History of Pandemic Influenza: Understanding Patterns of Emergence and Transmission. Pathogens. 2016;5(4).
6. Dawood FS, Iuliano AD, Reed C, Meltzer MI, Shay DK, Cheng PY, et al. Estimated global mortality associated with the first 12 months of 2009 pandemic influenza A H1N1 virus circulation: a modelling study. Lancet Infect Dis. 2012;12(9):687-95.
7. Iuliano AD, Roguski KM, Chang HH, Muscatello DJ, Palekar R, Tempia S, et al. Estimates of global seasonal influenza-associated respiratory mortality: a modelling study. Lancet. 2018;391(10127):1285-300.
8. Chan-Yeung M, Xu RH. SARS: epidemiology. Respirology. 2003;8 Suppl(Suppl 1):S9-14.
9. Zhang AR, Shi WQ, Liu K, Li XL, Liu MJ, Zhang WH, et al. Epidemiology and evolution of Middle East respiratory syndrome coronavirus, 2012-2020. Infect Dis Poverty. 2021;10(1):66.
10. WHO. WHO COVID-19 dashboard 2025 [Available from: https://data.who.int/dashboards/covid19/deaths?n=o.
11. WHO. HIV data and statistics 2025 [Available from: https://www.who.int/teams/global-hiv-hepatitis-and-stis-programmes/hiv/strategic-information/hiv-data-and-statistics.
12. Leung NHL. Transmissibility and transmission of respiratory viruses. Nat Rev Microbiol. 2021;19(8):528-45.
13. Killingley B, Nguyen-Van-Tam J. Routes of influenza transmission. Influenza Other Respir Viruses. 2013;7 Suppl 2(Suppl 2):42-51.
14. Brankston G, Gitterman L, Hirji Z, Lemieux C, Gardam M. Transmission of influenza A in human beings. Lancet Infect Dis. 2007;7(4):257-65.
15. Ehsanifar M. Airborne aerosols particles and COVID-19 transition. Environ Res. 2021;200:111752.
16. Morawska L, Milton DK. It Is Time to Address Airborne Transmission of Coronavirus Disease 2019 (COVID-19). Clin Infect Dis. 2020;71(9):2311-3.
17. Murphy C, Lim WW, Mills C, Wong JY, Chen D, Xie Y, et al. Effectiveness of social distancing measures and lockdowns for reducing transmission of COVID-19 in non-healthcare, community-based settings. Philos Trans A Math Phys Eng Sci. 2023;381(2257):20230132.

18. Heiskanen A, Galipeau Y, Little J, Mortimer L, Ramotar K, Langlois MA, et al. Seasonal respiratory virus circulation was diminished during the COVID-19 pandemic. Influenza Other Respir Viruses. 2023;17(1):e13065.
19. Braeye T, Catteau L, Brondeel R, van Loenhout JAF, Proesmans K, Cornelissen L, et al. Vaccine effectiveness against transmission of alpha, delta and omicron SARS-COV-2-infection, Belgian contact tracing, 2021-2022. Vaccine. 2023;41(20):3292-300.
20. Chakraborty C, Sharma AR, Bhattacharya M, Lee SS. A Detailed Overview of Immune Escape, Antibody Escape, Partial Vaccine Escape of SARS-CoV-2 and Their Emerging Variants With Escape Mutations. Front Immunol. 2022;13:801522.
21. Wang Z, Schmidt F, Weisblum Y, Muecksch F, Barnes CO, Finkin S, et al. mRNA vaccine-elicited antibodies to SARS-CoV-2 and circulating variants. Nature. 2021;592(7855):616-22.
22. Wickenhagen A, Flagg M, Port JR, Yinda CK, Goldin K, Gallogly S, et al. Evolution of Omicron lineage towards increased fitness in the upper respiratory tract in the absence of severe lung pathology. Nat Commun. 2025;16(1):594.
23. Bickley SJ, Chan HF, Skali A, Stadelmann D, Torgler B. How does globalization affect COVID-19 responses? Global Health. 2021;17(1):57.
24. Jones KE, Patel NG, Levy MA, Storeygard A, Balk D, Gittleman JL, et al. Global trends in emerging infectious diseases. Nature. 2008;451(7181):990-3.
25. Woolhouse ME, Gowtage-Sequeria S. Host range and emerging and reemerging pathogens. Emerg Infect Dis. 2005;11(12):1842-7.
26. Ostfeld RS. Biodiversity loss and the rise of zoonotic pathogens. Clin Microbiol Infect. 2009;15 Suppl 1:40-3.
27. Morand S, Lajaunie C. Outbreaks of Vector-Borne and Zoonotic Diseases Are Associated With Changes in Forest Cover and Oil Palm Expansion at Global Scale. Front Vet Sci. 2021;8:661063.
28. Tian H, Zhou S, Dong L, Van Boeckel TP, Pei Y, Wu Q, et al. Climate change suggests a shift of H5N1 risk in migratory birds. Ecological Modelling. 2015;306:6-15.
29. Esposito MM, Turku S, Lehrfield L, Shoman A. The Impact of Human Activities on Zoonotic Infection Transmissions. Animals (Basel). 2023;13(10).
30. Recchi E, Ferrara A, Rodriguez Sanchez A, Deutschmann E, Gabrielli L, Iacus S, et al. The impact of air travel on the precocity and severity of COVID-19 deaths in sub-national areas across 45 countries. Scientific Reports. 2022;12(1):16522.
31. Payne S. Chapter 17 - Family Coronaviridae. In: Payne S, editor. Viruses: Academic Press; 2017. p. 149-58.
32. Fehr AR, Perlman S. Coronaviruses: an overview of their replication and pathogenesis. Methods Mol Biol. 2015;1282:1-23.
33. Brian DA, Baric RS. Coronavirus genome structure and replication. Curr Top Microbiol Immunol. 2005;287:1-30.
34. Lu R, Zhao X, Li J, Niu P, Yang B, Wu H, et al. Genomic characterisation and epidemiology of 2019 novel coronavirus: implications for virus origins and receptor binding. Lancet. 2020;395(10224):565-74.
35. Masters PS. The molecular biology of coronaviruses. Adv Virus Res. 2006;66:193-292.
36. Wu C-r, Yin W-c, Jiang Y, Xu HE. Structure genomics of SARS-CoV-2 and its Omicron variant: drug design templates for COVID-19. Acta Pharmacologica Sinica. 2022;43(12):3021-33.

37. Miao Z, Tidu A, Eriani G, Martin F. Secondary structure of the SARS-CoV-2 5'-UTR. RNA Biol. 2021;18(4):447-56.
38. Justo Arevalo S, Castillo-Chávez A, Uribe Calampa CS, Zapata Sifuentes D, Huallpa CJ, Landa Bianchi G, et al. What do we know about the function of SARS-CoV-2 proteins? Front Immunol. 2023;14:1249607.
39. Kang S, Yang M, Hong Z, Zhang L, Huang Z, Chen X, et al. Crystal structure of SARS-CoV-2 nucleocapsid protein RNA binding domain reveals potential unique drug targeting sites. Acta Pharm Sin B. 2020.
40. Zeng W, Liu G, Ma H, Zhao D, Yang Y, Liu M, et al. Biochemical characterization of SARS-CoV-2 nucleocapsid protein. Biochem Biophys Res Commun. 2020;527(3):618-23.
41. Zhang Z, Nomura N, Muramoto Y, Ekimoto T, Uemura T, Liu K, et al. Structure of SARS-CoV-2 membrane protein essential for virus assembly. Nature Communications. 2022;13(1):4399.
42. Boson B, Legros V, Zhou B, Siret E, Mathieu C, Cosset FL, et al. The SARS-CoV-2 envelope and membrane proteins modulate maturation and retention of the spike protein, allowing assembly of virus-like particles. J Biol Chem. 2021;296:100111.
43. Li F. Structure, Function, and Evolution of Coronavirus Spike Proteins. Annu Rev Virol. 2016;3(1):237-61.
44. Huang X, Dong W, Milewska A, Golda A, Qi Y, Zhu QK, et al. Human Coronavirus HKU1 Spike Protein Uses O-Acetylated Sialic Acid as an Attachment Receptor Determinant and Employs Hemagglutinin-Esterase Protein as a Receptor-Destroying Enzyme. J Virol. 2015;89(14):7202-13.
45. Krempl C, Schultze B, Herrler G. Analysis of cellular receptors for human coronavirus OC43. Adv Exp Med Biol. 1995;380:371-4.
46. Matsuyama S, Nagata N, Shirato K, Kawase M, Takeda M, Taguchi F. Efficient activation of the severe acute respiratory syndrome coronavirus spike protein by the transmembrane protease TMPRSS2. J Virol. 2010;84(24):12658-64.
47. Belouzard S, Chu VC, Whittaker GR. Activation of the SARS coronavirus spike protein via sequential proteolytic cleavage at two distinct sites. Proc Natl Acad Sci U S A. 2009;106(14):5871-6.
48. V'kovski P, Kratzel A, Steiner S, Stalder H, Thiel V. Coronavirus biology and replication: implications for SARS-CoV-2. Nature Reviews Microbiology. 2021;19(3):155-70.
49. Andronov L, Han M, Zhu Y, Balaji A, Roy AR, Barentine AES, et al. Nanoscale cellular organization of viral RNA and proteins in SARS-CoV-2 replication organelles. Nature Communications. 2024;15(1):4644.
50. Krijnse-Locker J, Ericsson M, Rottier PJ, Griffiths G. Characterization of the budding compartment of mouse hepatitis virus: evidence that transport from the RER to the Golgi complex requires only one vesicular transport step. J Cell Biol. 1994;124(1-2):55-70.
51. Siu YL, Teoh KT, Lo J, Chan CM, Kien F, Escriou N, et al. The M, E, and N structural proteins of the severe acute respiratory syndrome coronavirus are required for efficient assembly, trafficking, and release of virus-like particles. J Virol. 2008;82(22):11318-30.
52. van der Hoek L, Pyrc K, Jebbink MF, Vermeulen-Oost W, Berkhout RJ, Wolthers KC, et al. Identification of a new human coronavirus. Nat Med. 2004;10(4):368-73.
53. Woo PC, Lau SK, Chu CM, Chan KH, Tsoi HW, Huang Y, et al. Characterization and complete genome sequence of a novel coronavirus, coronavirus HKU1, from patients with pneumonia. J Virol. 2005;79(2):884-95.

54. Otieno JR, Cherry JL, Spiro DJ, Nelson MI, Trovão NS. Origins and Evolution of Seasonal Human Coronaviruses. Viruses. 2022;14(7).
55. Huynh J, Li S, Yount B, Smith A, Sturges L, Olsen John C, et al. Evidence Supporting a Zoonotic Origin of Human Coronavirus Strain NL63. Journal of Virology. 2012;86(23):12816-25.
56. Vijgen L, Keyaerts E, Moës E, Thoelen I, Wollants E, Lemey P, et al. Complete genomic sequence of human coronavirus OC43: molecular clock analysis suggests a relatively recent zoonotic coronavirus transmission event. J Virol. 2005;79(3):1595-604.
57. Vijgen L, Keyaerts E, Lemey P, Maes P, Van Reeth K, Nauwynck H, et al. Evolutionary history of the closely related group 2 coronaviruses: porcine hemagglutinating encephalomyelitis virus, bovine coronavirus, and human coronavirus OC43. J Virol. 2006;80(14):7270-4.
58. Corman VM, Eckerle I, Memish ZA, Liljander AM, Dijkman R, Jonsdottir H, et al. Link of a ubiquitous human coronavirus to dromedary camels. Proc Natl Acad Sci U S A. 2016;113(35):9864-9.
59. Lau SK, Woo PC, Li KS, Tsang AK, Fan RY, Luk HK, et al. Discovery of a novel coronavirus, China Rattus coronavirus HKU24, from Norway rats supports the murine origin of Betacoronavirus 1 and has implications for the ancestor of Betacoronavirus lineage A. J Virol. 2015;89(6):3076-92.
60. Kuypers J, Martin ET, Heugel J, Wright N, Morrow R, Englund JA. Clinical disease in children associated with newly described coronavirus subtypes. Pediatrics. 2007;119(1):e70-6.
61. Otieno GP, Murunga N, Agoti CN, Gallagher KE, Awori JO, Nokes DJ. Surveillance of endemic human coronaviruses (HCoV-NL63, OC43 and 229E) associated with childhood pneumonia in Kilifi, Kenya. Wellcome Open Res. 2020;5:150.
62. Falsey AR, Walsh EE, Hayden FG. Rhinovirus and coronavirus infection-associated hospitalizations among older adults. J Infect Dis. 2002;185(9):1338-41.
63. Killerby ME, Biggs HM, Haynes A, Dahl RM, Mustaquim D, Gerber SI, et al. Human coronavirus circulation in the United States 2014-2017. J Clin Virol. 2018;101:52-6.
64. Edridge AWD, Kaczorowska J, Hoste ACR, Bakker M, Klein M, Loens K, et al. Seasonal coronavirus protective immunity is short-lasting. Nat Med. 2020;26(11):1691-3.
65. Chan-Yeung M, Xu R-H. SARS: epidemiology. Respirology. 2003;8(s1):S9-S14.
66. Lau SK, Woo PC, Li KS, Huang Y, Tsoi HW, Wong BH, et al. Severe acute respiratory syndrome coronavirus-like virus in Chinese horseshoe bats. Proc Natl Acad Sci U S A. 2005;102(39):14040-5.
67. Li W, Shi Z, Yu M, Ren W, Smith C, Epstein JH, et al. Bats are natural reservoirs of SARS-like coronaviruses. Science. 2005;310(5748):676-9.
68. Hui DS, Azhar EI, Kim YJ, Memish ZA, Oh MD, Zumla A. Middle East respiratory syndrome coronavirus: risk factors and determinants of primary, household, and nosocomial transmission. Lancet Infect Dis. 2018;18(8):e217-e27.
69. Annan A, Baldwin HJ, Corman VM, Klose SM, Owusu M, Nkrumah EE, et al. Human betacoronavirus 2c EMC/2012-related viruses in bats, Ghana and Europe. Emerg Infect Dis. 2013;19(3):456-9.
70. Hemida MG, Elmoslemany A, Al-Hizab F, Alnaeem A, Almathen F, Faye B, et al. Dromedary Camels and the Transmission of Middle East Respiratory Syndrome Coronavirus (MERS-CoV). Transbound Emerg Dis. 2017;64(2):344-53.
71. Horita N, Fukumoto T. Global case fatality rate from COVID-19 has decreased by 96.8% during 2.5 years of the pandemic. J Med Virol. 2023;95(1):e28231.

72. Burki T. The origin of SARS-CoV-2. The Lancet Infectious Diseases. 2020;20(9):1018-9.
73. Racine É, Boivin G, Longtin Y, McCormack D, Decaluwe H, Savard P, et al. The REinfection in COVID-19 Estimation of Risk (RECOVER) study: Reinfection and serology dynamics in a cohort of Canadian healthcare workers. Influenza and Other Respiratory Viruses. 2022;16(5):916-25.
74. Cevik M, Kuppalli K, Kindrachuk J, Peiris M. Virology, transmission, and pathogenesis of SARS-CoV-2. Bmj. 2020;371:m3862.
75. Lin L, Jiang X, Zhang Z, Huang S, Zhang Z, Fang Z, et al. Gastrointestinal symptoms of 95 cases with SARS-CoV-2 infection. Gut. 2020;69(6):997-1001.
76. Rosenthal N, Cao Z, Gundrum J, Sianis J, Safo S. Risk Factors Associated With In-Hospital Mortality in a US National Sample of Patients With COVID-19. JAMA Network Open. 2020;3(12):e2029058-e.
77. Liu X-q, Xue S, Xu J-b, Ge H, Mao Q, Xu X-h, et al. Clinical characteristics and related risk factors of disease severity in 101 COVID-19 patients hospitalized in Wuhan, China. Acta Pharmacologica Sinica. 2022;43(1):64-75.
78. Kalligeros M, Shehadeh F, Mylona EK, Benitez G, Beckwith CG, Chan PA, et al. Association of Obesity with Disease Severity Among Patients with Coronavirus Disease 2019. Obesity. 2020;28(7):1200-4.
79. Ma Q, Liu J, Liu Q, Kang L, Liu R, Jing W, et al. Global Percentage of Asymptomatic SARS-CoV-2 Infections Among the Tested Population and Individuals With Confirmed COVID-19 Diagnosis: A Systematic Review and Meta-analysis. JAMA Network Open. 2021;4(12):e2137257-e.
80. Ayouni I, Maatoug J, Dhouib W, Zammit N, Fredj SB, Ghammam R, et al. Effective public health measures to mitigate the spread of COVID-19: a systematic review. BMC Public Health. 2021;21(1):1015.
81. Talic S, Shah S, Wild H, Gasevic D, Maharaj A, Ademi Z, et al. Effectiveness of public health measures in reducing the incidence of covid-19, SARS-CoV-2 transmission, and covid-19 mortality: systematic review and meta-analysis. Bmj. 2021;375:e068302.
82. Cutler DM, Summers LH. The COVID-19 Pandemic and the $16 Trillion Virus. JAMA. 2020;324(15):1495-6.
83. Zhou P, Yang XL, Wang XG, Hu B, Zhang L, Zhang W, et al. A pneumonia outbreak associated with a new coronavirus of probable bat origin. Nature. 2020;579(7798):270-3.
84. Lam TT-Y, Jia N, Zhang Y-W, Shum MH-H, Jiang J-F, Zhu H-C, et al. Identifying SARS-CoV-2-related coronaviruses in Malayan pangolins. Nature. 2020;583(7815):282-5.
85. Nga NTT, Latinne A, Thuy HB, Long NV, Ngoc PTB, Anh NTL, et al. Evidence of SARS-CoV-2 Related Coronaviruses Circulating in Sunda pangolins (Manis javanica) Confiscated From the Illegal Wildlife Trade in Viet Nam. Frontiers in Public Health. 2022;Volume 10 - 2022.
86. Xiao K, Zhai J, Feng Y, Zhou N, Zhang X, Zou J-J, et al. Isolation of SARS-CoV-2-related coronavirus from Malayan pangolins. Nature. 2020;583(7815):286-9.
87. Crits-Christoph A, Levy JI, Pekar JE, Goldstein SA, Singh R, Hensel Z, et al. Genetic tracing of market wildlife and viruses at the epicenter of the COVID-19 pandemic. Cell. 2024;187(19):5468-82.e11.
88. Pekar JE, Magee A, Parker E, Moshiri N, Izhikevich K, Havens JL, et al. The molecular epidemiology of multiple zoonotic origins of SARS-CoV-2. Science. 2022;377(6609):960-6.

89. Sanjuán R, Nebot MR, Chirico N, Mansky LM, Belshaw R. Viral mutation rates. J Virol. 2010;84(19):9733-48.
90. Amicone M, Borges V, Alves MJ, Isidro J, Zé-Zé L, Duarte S, et al. Mutation rate of SARS-CoV-2 and emergence of mutators during experimental evolution. Evol Med Public Health. 2022;10(1):142-55.
91. Robson F, Khan KS, Le TK, Paris C, Demirbag S, Barfuss P, et al. Coronavirus RNA Proofreading: Molecular Basis and Therapeutic Targeting. Mol Cell. 2020;79(5):710-27.
92. Markov PV, Ghafari M, Beer M, Lythgoe K, Simmonds P, Stilianakis NI, et al. The evolution of SARS-CoV-2. Nature Reviews Microbiology. 2023;21(6):361-79.
93. Di Giorgio S, Martignano F, Torcia MG, Mattiuz G, Conticello SG. Evidence for host-dependent RNA editing in the transcriptome of SARS-CoV-2. Sci Adv. 2020;6(25):eabb5813.
94. Ringlander J, Fingal J, Kann H, Prakash K, Rydell G, Andersson M, et al. Impact of ADAR-induced editing of minor viral RNA populations on replication and transmission of SARS-CoV-2. Proc Natl Acad Sci U S A. 2022;119(6).
95. Jackson B, Boni MF, Bull MJ, Colleran A, Colquhoun RM, Darby AC, et al. Generation and transmission of interlineage recombinants in the SARS-CoV-2 pandemic. Cell. 2021;184(20):5179-88.e8.
96. Plante JA, Liu Y, Liu J, Xia H, Johnson BA, Lokugamage KG, et al. Spike mutation D614G alters SARS-CoV-2 fitness. Nature. 2021;592(7852):116-21.
97. GISAID. Tracking of hCoV-19 Variants 2025 [Available from: https://gisaid.org/hcov19-variants/.
98. Salehi-Vaziri M, Fazlalipour M, Seyed Khorrami SM, Azadmanesh K, Pouriayevali MH, Jalali T, et al. The ins and outs of SARS-CoV-2 variants of concern (VOCs). Arch Virol. 2022;167(2):327-44.
99. Toovey OTR, Tang JW. The emergence of the Omicron variant. Clin Infect Pract. 2022;13:100134.
100. Kaku Y, Okumura K, Padilla-Blanco M, Kosugi Y, Uriu K, Hinay AA, Jr., et al. Virological characteristics of the SARS-CoV-2 JN.1 variant. The Lancet Infectious Diseases. 2024;24(2):e82.
101. Carabelli AM, Peacock TP, Thorne LG, Harvey WT, Hughes J, de Silva TI, et al. SARS-CoV-2 variant biology: immune escape, transmission and fitness. Nature Reviews Microbiology. 2023;21(3):162-77.
102. Thomson EC, Rosen LE, Shepherd JG, Spreafico R, da Silva Filipe A, Wojcechowskyj JA, et al. Circulating SARS-CoV-2 spike N439K variants maintain fitness while evading antibody-mediated immunity. Cell. 2021;184(5):1171-87.e20.
103. Meganck RM, Edwards CE, Mallory ML, Lee RE, Dang H, Bailey AB, et al. SARS-CoV-2 variant of concern fitness and adaptation in primary human airway epithelia. Cell Reports. 2024;43(4).
104. Bisht H, Roberts A, Vogel L, Bukreyev A, Collins PL, Murphy BR, et al. Severe acute respiratory syndrome coronavirus spike protein expressed by attenuated vaccinia virus protectively immunizes mice. Proc Natl Acad Sci U S A. 2004;101(17):6641-6.
105. Gao W, Tamin A, Soloff A, D'Aiuto L, Nwanegbo E, Robbins PD, et al. Effects of a SARS-associated coronavirus vaccine in monkeys. The Lancet. 2003;362(9399):1895-6.
106. Coudeville L, Bailleux F, Riche B, Megas F, Andre P, Ecochard R. Relationship between haemagglutination-inhibiting antibody titres and clinical protection against influenza:

development and application of a bayesian random-effects model. BMC Med Res Methodol. 2010;10:18.
107. Fong Y, Huang Y, Benkeser D, Carpp LN, Áñez G, Woo W, et al. Immune correlates analysis of the PREVENT-19 COVID-19 vaccine efficacy clinical trial. Nat Commun. 2023;14(1):331.
108. Fong Y, McDermott AB, Benkeser D, Roels S, Stieh DJ, Vandebosch A, et al. Immune correlates analysis of the ENSEMBLE single Ad26.COV2.S dose vaccine efficacy clinical trial. Nat Microbiol. 2022;7(12):1996-2010.
109. Khoury DS, Cromer D, Reynaldi A, Schlub TE, Wheatley AK, Juno JA, et al. Neutralizing antibody levels are highly predictive of immune protection from symptomatic SARS-CoV-2 infection. Nature Medicine. 2021;27(7):1205-11.
110. Atti A, Insalata F, Carr EJ, Otter AD, Foulkes S, Wu MY, et al. Antibody correlates of protection against Delta infection after vaccination: A nested case-control within the UK-based SIREN study. J Infect. 2023;87(5):420-7.
111. Baden LR, Sahly HME, Essink B, Kotloff K, Frey S, Novak R, et al. Efficacy and Safety of the mRNA-1273 SARS-CoV-2 Vaccine. New England Journal of Medicine. 2021;384(5):403-16.
112. Sahly HME, Baden LR, Essink B, Doblecki-Lewis S, Martin JM, Anderson EJ, et al. Efficacy of the mRNA-1273 SARS-CoV-2 Vaccine at Completion of Blinded Phase. New England Journal of Medicine. 2021;385(19):1774-85.
113. Falsey AR, Sobieszczyk ME, Hirsch I, Sproule S, Robb ML, Corey L, et al. Phase 3 Safety and Efficacy of AZD1222 (ChAdOx1 nCoV-19) Covid-19 Vaccine. N Engl J Med. 2021;385(25):2348-60.
114. Greinacher A, Langer F, Makris M, Pai M, Pavord S, Tran H, et al. Vaccine-induced immune thrombotic thrombocytopenia (VITT): Update on diagnosis and management considering different resources. J Thromb Haemost. 2022;20(1):149-56.
115. Tenforde MW, Patel MM, Ginde AA, Douin DJ, Talbot HK, Casey JD, et al. Effectiveness of Severe Acute Respiratory Syndrome Coronavirus 2 Messenger RNA Vaccines for Preventing Coronavirus Disease 2019 Hospitalizations in the United States. Clinical Infectious Diseases. 2021;74(9):1515-24.
116. Lu Y, Lindaas A, Matuska K, Izurieta HS, McEvoy R, Menis M, et al. Real-world Effectiveness of mRNA COVID-19 Vaccines Among US Nursing Home Residents Aged ≥65 Years in the Pre-Delta and High Delta Periods. Open Forum Infectious Diseases. 2024;11(3).
117. Dhama K, Dhawan M, Tiwari R, Emran TB, Mitra S, Rabaan AA, et al. COVID-19 intranasal vaccines: current progress, advantages, prospects, and challenges. Hum Vaccin Immunother. 2022;18(5):2045853.
118. Alu A, Chen L, Lei H, Wei Y, Tian X, Wei X. Intranasal COVID-19 vaccines: From bench to bed. EBioMedicine. 2022;76:103841.
119. Tang J, Zeng C, Cox TM, Li C, Son YM, Cheon IS, et al. Respiratory mucosal immunity against SARS-CoV-2 after mRNA vaccination. Sci Immunol. 2022;7(76):eadd4853.
120. Mao T, Israelow B, Peña-Hernández MA, Suberi A, Zhou L, Luyten S, et al. Unadjuvanted intranasal spike vaccine elicits protective mucosal immunity against sarbecoviruses. Science. 2022;378(6622):eabo2523.
121. Callard F, Perego E. How and why patients made Long Covid. Soc Sci Med. 2021;268:113426.

122. Kamal M, Abo Omirah M, Hussein A, Saeed H. Assessment and characterisation of post-COVID-19 manifestations. Int J Clin Pract. 2021;75(3):e13746.
123. Greenhalgh T, Knight M, A'Court C, Buxton M, Husain L. Management of post-acute covid-19 in primary care. Bmj. 2020;370:m3026.
124. Davis HE, McCorkell L, Vogel JM, Topol EJ. Long COVID: major findings, mechanisms and recommendations. Nature Reviews Microbiology. 2023.
125. Davis HE, Assaf GS, McCorkell L, Wei H, Low RJ, Re'em Y, et al. Characterizing long COVID in an international cohort: 7 months of symptoms and their impact. eClinicalMedicine. 2021;38.
126. Carfì A, Bernabei R, Landi F. Persistent Symptoms in Patients After Acute COVID-19. Jama. 2020;324(6):603-5.
127. Post-COVID-19 syndrome: in it for the long haul. EBioMedicine. 2021;67:103424.
128. Sudre CH, Murray B, Varsavsky T, Graham MS, Penfold RS, Bowyer RC, et al. Attributes and predictors of long COVID. Nature Medicine. 2021;27(4):626-31.
129. Bannister BA. Post-infectious disease syndrome. Postgrad Med J. 1988;64(753):559-67.
130. Rebman AW, Aucott JN. Post-treatment Lyme Disease as a Model for Persistent Symptoms in Lyme Disease. Front Med (Lausanne). 2020;7:57.
131. Seet RC, Quek AM, Lim EC. Post-infectious fatigue syndrome in dengue infection. J Clin Virol. 2007;38(1):1-6.
132. Epstein L, Wong KK, Kallen AJ, Uyeki TM. Post-Ebola Signs and Symptoms in U.S. Survivors. N Engl J Med. 2015;373(25):2484-6.
133. Ahmed H, Patel K, Greenwood DC, Halpin S, Lewthwaite P, Salawu A, et al. Long-term clinical outcomes in survivors of severe acute respiratory syndrome and Middle East respiratory syndrome coronavirus outbreaks after hospitalisation or ICU admission: A systematic review and meta-analysis. J Rehabil Med. 2020;52(5):jrm00063.
134. Hui DS, Joynt GM, Wong KT, Gomersall CD, Li TS, Antonio G, et al. Impact of severe acute respiratory syndrome (SARS) on pulmonary function, functional capacity and quality of life in a cohort of survivors. Thorax. 2005;60(5):401-9.
135. Klein J, Wood J, Jaycox JR, Dhodapkar RM, Lu P, Gehlhausen JR, et al. Distinguishing features of long COVID identified through immune profiling. Nature. 2023;623(7985):139-48.
136. Phetsouphanh C, Darley DR, Wilson DB, Howe A, Munier CML, Patel SK, et al. Immunological dysfunction persists for 8 months following initial mild-to-moderate SARS-CoV-2 infection. Nat Immunol. 2022;23(2):210-6.
137. Zubchenko S, Kril I, Nadizhko O, Matsyura O, Chopyak V. Herpesvirus infections and post-COVID-19 manifestations: a pilot observational study. Rheumatol Int. 2022;42(9):1523-30.
138. Durstenfeld MS, Peluso MJ, Peyser ND, Lin F, Knight SJ, Djibo A, et al. Factors Associated with Long Covid Symptoms in an Online Cohort Study. medRxiv. 2022.
139. Yeoh YK, Zuo T, Lui GC, Zhang F, Liu Q, Li AY, et al. Gut microbiota composition reflects disease severity and dysfunctional immune responses in patients with COVID-19. Gut. 2021;70(4):698-706.
140. Proal AD, VanElzakker MB. Long COVID or Post-acute Sequelae of COVID-19 (PASC): An Overview of Biological Factors That May Contribute to Persistent Symptoms. Frontiers in Microbiology. 2021;12.
141. Wallukat G, Hohberger B, Wenzel K, Fürst J, Schulze-Rothe S, Wallukat A, et al. Functional autoantibodies against G-protein coupled receptors in patients with persistent Long-COVID-19 symptoms. J Transl Autoimmun. 2021;4:100100.

142. Galipeau Y, Cooper C, Langlois M-A. Autoantibodies in COVID-19: implications for disease severity and clinical outcomes. Frontiers in Immunology. 2025;15.
143. Charfeddine S, Ibn Hadj Amor H, Jdidi J, Torjmen S, Kraiem S, Hammami R, et al. Long COVID 19 Syndrome: Is It Related to Microcirculation and Endothelial Dysfunction? Insights From TUN-EndCOV Study. Front Cardiovasc Med. 2021;8:745758.
144. Minkoff JM, tenOever B. Innate immune evasion strategies of SARS-CoV-2. Nature Reviews Microbiology. 2023;21(3):178-94.
145. Merad M, Martin JC. Pathological inflammation in patients with COVID-19: a key role for monocytes and macrophages. Nature Reviews Immunology. 2020;20(6):355-62.
146. Mehta P, McAuley DF, Brown M, Sanchez E, Tattersall RS, Manson JJ. COVID-19: consider cytokine storm syndromes and immunosuppression. The Lancet. 2020;395(10229):1033-4.
147. Brockman MA, Mwimanzi F, Lapointe HR, Sang Y, Agafitei O, Cheung PK, et al. Reduced Magnitude and Durability of Humoral Immune Responses to COVID-19 mRNA Vaccines Among Older Adults. The Journal of Infectious Diseases. 2021;225(7):1129-40.
148. Swadling L, Diniz MO, Schmidt NM, Amin OE, Chandran A, Shaw E, et al. Pre-existing polymerase-specific T cells expand in abortive seronegative SARS-CoV-2. Nature. 2022;601(7891):110-7.
149. Murray SM, Ansari AM, Frater J, Klenerman P, Dunachie S, Barnes E, et al. The impact of pre-existing cross-reactive immunity on SARS-CoV-2 infection and vaccine responses. Nature Reviews Immunology. 2023;23(5):304-16.
150. Land WG. Role of DAMPs in respiratory virus-induced acute respiratory distress syndrome—with a preliminary reference to SARS-CoV-2 pneumonia. Genes & Immunity. 2021;22(3):141-60.
151. Sievers BL, Cheng MTK, Csiba K, Meng B, Gupta RK. SARS-CoV-2 and innate immunity: the good, the bad, and the “goldilocks”. Cellular & Molecular Immunology. 2024;21(2):171-83.
152. Iwasaki A. A virological view of innate immune recognition. Annu Rev Microbiol. 2012;66:177-96.
153. Liu G, Gack MU. Distinct and Orchestrated Functions of RNA Sensors in Innate Immunity. Immunity. 2020;53(1):26-42.
154. Totura AL, Whitmore A, Agnihothram S, Schäfer A, Katze MG, Heise MT, et al. Toll-Like Receptor 3 Signaling via TRIF Contributes to a Protective Innate Immune Response to Severe Acute Respiratory Syndrome Coronavirus Infection. mBio. 2015;6(3):e00638-15.
155. Yamada T, Takaoka A. Innate immune recognition against SARS-CoV-2. Inflammation and Regeneration. 2023;43(1):7.
156. Kim Y-M, Shin E-C. Type I and III interferon responses in SARS-CoV-2 infection. Experimental & Molecular Medicine. 2021;53(5):750-60.
157. Ferreira AC, Soares VC, de Azevedo-Quintanilha IG, Dias SdSG, Fintelman-Rodrigues N, Sacramento CQ, et al. SARS-CoV-2 engages inflammasome and pyroptosis in human primary monocytes. Cell Death Discovery. 2021;7(1):43.
158. Zhou Z, Zhang X, Lei X, Xiao X, Jiao T, Ma R, et al. Sensing of cytoplasmic chromatin by cGAS activates innate immune response in SARS-CoV-2 infection. Signal Transduct Target Ther. 2021;6(1):382.

159. Lian Q, Zhang K, Zhang Z, Duan F, Guo L, Luo W, et al. Differential effects of macrophage subtypes on SARS-CoV-2 infection in a human pluripotent stem cell-derived model. Nat Commun. 2022;13(1):2028.
160. Knoll R, Schultze JL, Schulte-Schrepping J. Monocytes and Macrophages in COVID-19. Front Immunol. 2021;12:720109.
161. Lee MJ, Blish CA. Defining the role of natural killer cells in COVID-19. Nature Immunology. 2023;24(10):1628-38.
162. Wang X, Guan F, Miller H, Byazrova MG, Cndotti F, Benlagha K, et al. The role of dendritic cells in COVID-19 infection. Emerg Microbes Infect. 2023;12(1):2195019.
163. Coperchini F, Chiovato L, Croce L, Magri F, Rotondi M. The cytokine storm in COVID-19: An overview of the involvement of the chemokine/chemokine-receptor system. Cytokine Growth Factor Rev. 2020.
164. LeBien TW, Tedder TF. B lymphocytes: how they develop and function. Blood. 2008;112(5):1570-80.
165. Germain RN. T-cell development and the CD4–CD8 lineage decision. Nature Reviews Immunology. 2002;2(5):309-22.
166. Moss P. The T cell immune response against SARS-CoV-2. Nature Immunology. 2022;23(2):186-93.
167. Bergamaschi L, Mescia F, Turner L, Hanson AL, Kotagiri P, Dunmore BJ, et al. Longitudinal analysis reveals that delayed bystander CD8+ T cell activation and early immune pathology distinguish severe COVID-19 from mild disease. Immunity. 2021;54(6):1257-75.e8.
168. Woldemeskel BA, Garliss CC, Blankson JN. SARS-CoV-2 mRNA vaccines induce broad CD4+ T cell responses that recognize SARS-CoV-2 variants and HCoV-NL63. J Clin Invest. 2021;131(10).
169. Swain SL, McKinstry KK, Strutt TM. Expanding roles for CD4+ T cells in immunity to viruses. Nature Reviews Immunology. 2012;12(2):136-48.
170. Chen S, Guan F, Candotti F, Benlagha K, Camara NOS, Herrada AA, et al. The role of B cells in COVID-19 infection and vaccination. Front Immunol. 2022;13:988536.
171. Lam N, Lee Y, Farber DL. A guide to adaptive immune memory. Nature Reviews Immunology. 2024;24(11):810-29.
172. Pang NY-L, Pang AS-R, Chow VT, Wang D-Y. Understanding neutralising antibodies against SARS-CoV-2 and their implications in clinical practice. Military Medical Research. 2021;8(1):47.
173. Chen Y, Zhao X, Zhou H, Zhu H, Jiang S, Wang P. Broadly neutralizing antibodies to SARS-CoV-2 and other human coronaviruses. Nature Reviews Immunology. 2023;23(3):189-99.
174. Zhang A, Stacey HD, D'Agostino MR, Tugg Y, Marzok A, Miller MS. Beyond neutralization: Fc-dependent antibody effector functions in SARS-CoV-2 infection. Nature Reviews Immunology. 2023;23(6):381-96.
175. Alqahtani SAM. Mucosal immunity in COVID-19: a comprehensive review. Front Immunol. 2024;15:1433452.
176. Zhou W, Xu X, Chang Z, Wang H, Zhong X, Tong X, et al. The dynamic changes of serum IgM and IgG against SARS-CoV-2 in patients with COVID-19. J Med Virol. 2021;93(2):924-33.
177. Wiersinga WJ, Rhodes A, Cheng AC, Peacock SJ, Prescott HC. Pathophysiology, Transmission, Diagnosis, and Treatment of Coronavirus Disease 2019 (COVID-19): A Review. Jama. 2020;324(8):782-93.

178. McMillan P, Dexhiemer T, Neubig RR, Uhal BD. COVID-19—A Theory of Autoimmunity Against ACE-2 Explained. Frontiers in Immunology. 2021;12.
179. Mobasheri L, Nasirpour MH, Masoumi E, Azarnaminy AF, Jafari M, Esmaeili S-A. SARS-CoV-2 triggering autoimmune diseases. Cytokine. 2022;154:155873.
180. Elkon K, Casali P. Nature and functions of autoantibodies. Nat Clin Pract Rheumatol. 2008;4(9):491-8.
181. Li H, Zheng Y, Chen L, Lin S. High titers of antinuclear antibody and the presence of multiple autoantibodies are highly suggestive of systemic lupus erythematosus. Scientific Reports. 2022;12(1):1687.
182. Gagiannis D, Steinestel J, Hackenbroch C, Schreiner B, Hannemann M, Bloch W, et al. Clinical, Serological, and Histopathological Similarities Between Severe COVID-19 and Acute Exacerbation of Connective Tissue Disease-Associated Interstitial Lung Disease (CTD-ILD). Frontiers in Immunology. 2020;11.
183. Lerma LA, Chaudhary A, Bryan A, Morishima C, Wener MH, Fink SL. Prevalence of autoantibody responses in acute coronavirus disease 2019 (COVID-19). J Transl Autoimmun. 2020;3:100073.
184. Bastard P, Rosen LB, Zhang Q, Michailidis E, Hoffmann H-H, Zhang Y, et al. Autoantibodies against type I IFNs in patients with life-threatening COVID-19. Science. 2020;370(6515):eabd4585.
185. Höflich C, Sabat R, Rosseau S, Temmesfeld B, Slevogt H, Döcke WD, et al. Naturally occurring anti-IFN-gamma autoantibody and severe infections with Mycobacterium cheloneae and Burkholderia cocovenenans. Blood. 2004;103(2):673-5.
186. Döffinger R, Helbert MR, Barcenas-Morales G, Yang K, Dupuis S, Ceron-Gutierrez L, et al. Autoantibodies to interferon-gamma in a patient with selective susceptibility to mycobacterial infection and organ-specific autoimmunity. Clin Infect Dis. 2004;38(1):e10-4.
187. Helms J, Tacquard C, Severac F, Leonard-Lorant I, Ohana M, Delabranche X, et al. High risk of thrombosis in patients with severe SARS-CoV-2 infection: a multicenter prospective cohort study. Intensive Care Med. 2020;46(6):1089-98.
188. Gil-Etayo FJ, Garcinuño S, Lalueza A, Díaz-Simón R, García-Reyne A, Pleguezuelo DE, et al. Anti-Phospholipid Antibodies and COVID-19 Thrombosis: A Co-Star, Not a Supporting Actor. Biomedicines. 2021;9(8).
189. Serrano M, Espinosa G, Lalueza A, Bravo-Gallego LY, Diaz-Simón R, Garcinuño S, et al. Beta-2-Glycoprotein-I Deficiency Could Precipitate an Antiphospholipid Syndrome-like Prothrombotic Situation in Patients With Coronavirus Disease 2019. ACR Open Rheumatol. 2021;3(4):267-76.
190. Elghali M, Bannour I, Touil I, Changuel M, Brahem Y, Jaoued O, et al. Increased Rheumatoid Factor production in patients with severe COVID-19. Diagn Microbiol Infect Dis. 2024;109(3):116284.
191. Amjadi MF, Parker MH, Adyniec RR, Zheng Z, Robbins AM, Bashar SJ, et al. Novel and unique rheumatoid factors cross-react with viral epitopes in COVID-19. J Autoimmun. 2024;142:103132.
192. Uppal NN, Kello N, Shah HH, Khanin Y, De Oleo IR, Epstein E, et al. De Novo ANCA-Associated Vasculitis With Glomerulonephritis in COVID-19. Kidney Int Rep. 2020;5(11):2079-83.

193. Perrot L, Hemon M, Busnel JM, Muis-Pistor O, Picard C, Zandotti C, et al. First flare of ACPA-positive rheumatoid arthritis after SARS-CoV-2 infection. Lancet Rheumatol. 2021;3(1):e6-e8.
194. Galipeau Y, Greig M, Liu G, Driedger M, Langlois M-A. Humoral Responses and Serological Assays in SARS-CoV-2 Infections. Frontiers in Immunology. 2020;11(3382).
195. Colwill K, Galipeau Y, Stuible M, Gervais C, Arnold C, Rathod B, et al. A scalable serology solution for profiling humoral immune responses to SARS-CoV-2 infection and vaccination. Clinical & Translational Immunology. 2022;11(3):e1380.
196. Owen SI, Williams CT, Garrod G, Fraser AJ, Menzies S, Baldwin L, et al. Twelve lateral flow immunoassays (LFAs) to detect SARS-CoV-2 antibodies. J Infect. 2022;84(3):355-60.
197. Liu KT, Han YJ, Wu GH, Huang KA, Huang PN. Overview of Neutralization Assays and International Standard for Detecting SARS-CoV-2 Neutralizing Antibody. Viruses. 2022;14(7).
198. Bewley KR, Coombes NS, Gagnon L, McInroy L, Baker N, Shaik I, et al. Quantification of SARS-CoV-2 neutralizing antibody by wild-type plaque reduction neutralization, microneutralization and pseudotyped virus neutralization assays. Nature Protocols. 2021;16(6):3114-40.
199. Nie J, Li Q, Wu J, Zhao C, Hao H, Liu H, et al. Quantification of SARS-CoV-2 neutralizing antibody by a pseudotyped virus-based assay. Nature Protocols. 2020;15(11):3699-715.
200. Abe KT, Li Z, Samson R, Samavarchi-Tehrani P, Valcourt EJ, Wood H, et al. A simple protein-based surrogate neutralization assay for SARS-CoV-2. JCI Insight. 2020;5(19).
201. Krammer F, Simon V. Serology assays to manage COVID-19. Science. 2020;368(6495):1060-1.
202. Duarte N, Yanes-Lane M, Arora RK, Bobrovitz N, Liu M, Bego MG, et al. Adapting Serosurveys for the SARS-CoV-2 Vaccine Era. Open Forum Infect Dis. 2022;9(2):ofab632.
203. Majdoubi A, Michalski C, O'Connell SE, Dada S, Narpala S, Gelinas J, et al. A majority of uninfected adults show preexisting antibody reactivity against SARS-CoV-2. JCI Insight. 2021;6(8).
204. Dijkman R, Jebbink MF, El Idrissi NB, Pyrc K, Müller MA, Kuijpers TW, et al. Human Coronavirus NL63 and 229E Seroconversion in Children. Journal of Clinical Microbiology. 2008;46(7):2368-73.
205. Bjornevik K, Cortese M, Healy BC, Kuhle J, Mina MJ, Leng Y, et al. Longitudinal analysis reveals high prevalence of Epstein-Barr virus associated with multiple sclerosis. Science. 2022;375(6578):296-301.
206. Shrewsbury JV, Vitus ES, Koziol AL, Nenarokova A, Jess T, Elmahdi R. Comprehensive phage display viral antibody profiling using VirScan: potential applications in chronic immune-mediated disease. Journal of Virology. 2024;98(11):e01102-24.
207. Ruhs EC, Chia WN, Foo R, Peel AJ, Li Y, Larman HB, et al. Applications of VirScan to broad serological profiling of bat reservoirs for emerging zoonoses. Frontiers in Public Health. 2023;Volume 11 - 2023.
208. Roy DR, Kemp TJ, Haynesworth K, Loftus SA, Pinto LA. Development, Validation, and Utilization of a Luminex-Based SARS-CoV-2 Multiplex Serology Assay. Microbiol Spectr. 2023;11(2):e0389822.
209. Cox A, Stevens M, Kallon D, Gupta A, White E. Comparative evaluation of Luminex based assays for detection of SARS-CoV-2 antibodies in a transplantation laboratory. J Immunol Methods. 2023;517:113472.

210. Xu GJ, Kula T, Xu Q, Li MZ, Vernon SD, Ndung'u T, et al. Viral immunology. Comprehensive serological profiling of human populations using a synthetic human virome. Science. 2015;348(6239):aaa0698.
211. Klein S, Dhakal S, Yin A, Escarra-Senmarti M, Demko Z, Pisanic N, et al. Application of machine learning models to identify serological predictors of COVID-19 severity and outcomes. Res Sq. 2023.
212. Dhakal S, Yin A, Escarra-Senmarti M, Demko ZO, Pisanic N, Johnston TS, et al. Application of machine learning algorithms to identify serological predictors of COVID-19 severity and outcomes. Communications Medicine. 2024;4(1):249.
213. Hempel H, Page M, Kemp T, Semper A, Brooks T, Pinto LA. The importance of using WHO International Standards to harmonise SARS-CoV-2 serological assays. The Lancet Microbe. 2024;5(3):e301-e5.
214. Berger SS, Høgberg J, Kuntke F, Obari L, Larsen H. Automated wash and reuse of disposable pipette tips in a SARS-CoV-2 RT-qPCR diagnostic pipeline. Diagnostic Microbiology and Infectious Disease. 2024;109(1):116241.
215. Pedrazzi B, Treyer A, Cohen R, Bowman A, Acevedo-Skrip J, Kearns K, et al. Greening automation: Wash and Re-use of disposable 384-well liquid handling tips to enable sustainable high-throughput vaccine development. SLAS Technology. 2023;28(5):375-9.
216. Juozapaitė D, Minkauskas M, Laurinaitytė I, Simutytė M, Griškevičius L, Naumovas D. The COVID-19 pandemic reveals the wide-ranging role of biobanks. Front Public Health. 2023;11:1256601.
217. Peeling RW, Boeras D, Wilder-Smith A, Sall A, Nkengasong J. Need for sustainable biobanking networks for COVID-19 and other diseases of epidemic potential. The Lancet Infectious Diseases. 2020;20(10):e268-e73.
218. WHO. True extent of SARS-CoV-2 Infection through seroprevalence studies 2025 [Available from: https://www.who.int/news/item/03-02-2022-true-extent-of-sars-cov-2-infection-through-seroprevalence-studies?utm_source=chatgpt.com.
219. WHO. Pandemic prevention, preparedness and response agreement 2025 [Available from: https://www.who.int/news-room/questions-and-answers/item/pandemic-prevention--preparedness-and-response-accord.

APPENDIX I – ADDITIONAL WORK

A-1.1 Clinical and serological predictors of post COVID-19 condition–findings from a Canadian prospective cohort study

Preface

(This work has been previously published as a research article)

Collins E, **Galipeau Y**, Arnold C, Bhéreur A, Booth R, Buchan AC, Cooper C, Crawley AM, McCluskie PS, McGuinty M, Pelchat M, Rocheleau L, Saginur R, Gravel C, Hawken S, Langlois MA, Little J. **Clinical and serological predictors of post COVID-19 condition-findings from a Canadian prospective cohort study**. Front Public Health. 2024 May 9;12:1276391.

https://doi.org/10.3389/fpubh.2024.1276391

© 2024 Collins, Galipeau, Arnold, Bhéreur, Booth, Buchan, Cooper, Crawley, McCluskie, McGuinty, Pelchat, Rocheleau, Saginur, Gravel, Hawken, Langlois and Little.

This is an open-access article distributed under the terms of the Creative Commons Attribution License (CC BY). The use, distribution or reproduction in other forums is permitted, provided the original author(s) and the copyright owner(s) are credited and that the original publication in this journal is cited, in accordance with accepted academic practice. No use, distribution or reproduction is permitted which does not comply with these terms.

Abstract

Introduction
More than 3 years into the pandemic, there is persisting uncertainty as to the etiology, biomarkers, and risk factors of Post COVID-19 Condition (PCC). Serological research data remain a largely untapped resource. Few studies have investigated the potential relationships between post-acute serology and PCC, while accounting for clinical covariates.

Methods
We compared clinical and serological predictors among COVID-19 survivors with (n = 102 cases) and without (n = 122 controls) persistent symptoms ≥12 weeks post-infection. We selected four primary serological predictors (anti-nucleocapsid (N), anti-Spike, and anti-receptor binding domain (RBD) IgG titres, and neutralization efficiency), and specified clinical covariates *a priori*.

Results
Similar proportions of PCC-cases (66.7%, n = 68) and infected-controls (71.3%, n = 87) tested positive for anti-N IgG. More cases tested positive for anti-Spike (94.1%, n = 96) and anti-RBD (95.1%, n = 97) IgG, as compared with controls (anti-Spike: 89.3%, n = 109; anti-RBD: 84.4%, n = 103). Similar trends were observed among unvaccinated participants. Effects of IgG titres on PCC status were non-significant in univariate and multivariate analyses. Adjusting for age and sex, PCC-cases were more likely to be efficient neutralizers (OR 2.2, 95% CI 1.11–4.49), and odds was further increased among cases to report deterioration in quality of life (OR 3.4, 95% CI 1.64–7.31). Clinical covariates found to be significantly related to PCC included obesity (OR 2.3, p = 0.02), number of months post COVID-19 (OR 1.1, p < 0.01), allergies (OR 1.8, p = 0.04), and need for medical support (OR 4.1, p < 0.01).

Conclusion
Despite past COVID-19 infection, approximately one third of PCC-cases and infected-controls were seronegative for anti-N IgG. Findings suggest higher neutralization efficiency among cases as compared with controls, and that this relationship is stronger among cases with more severe PCC. Cases also required more medical support for COVID-19 symptoms, and described complex, ongoing health sequelae. More data from larger cohorts are needed to substantiate results, permit subgroup analyses of IgG titres, and explore for differences between clusters of PCC symptoms. Future assessment of IgG subtypes may also elucidate new findings.

Introduction

Post COVID-19 Condition (PCC), also known as Long COVID or Post-acute sequelae of COVID-19 (PASC), is a major public health concern with severe and pervasive impacts on physical and mental health (1–6). More than 3 years into the pandemic, continued disparities as to the definition, presumed etiology, and prevalence of PCC deter efforts to detect and manage this condition (6–8). Recent findings suggest that 10–20% of adults infected by COVID-19 will develop long-term symptoms (4, 6, 9). These estimates tend to be higher in studies on patients hospitalized in the acute phase of illness and/or preceding the Omicron era (4, 6, 9, 10). Also, knowledge of how COVID-19 vaccination and infection/reinfection by SARS-CoV-2 Variants of Concern (VOCs) impact PCC onset, manifestations, and longevity continues to evolve (1, 11–14). There is an enduring need for rigorous, interdisciplinary efforts to examine multi-domain risk and protective factors of PCC onset, severity, and longevity, and its impacts on the healthcare system and economy (3–5, 15).

Efforts to understand potential PCC predictors have largely relied on clinical records and self-reports of demographics, health history, and initial disease sequelae (16–18). These studies have highlighted a number of potential clinical predictors (including age; sex; ethnicities; comorbidities, namely asthma, obesity, immune deficiency, lung disease, heart disease, kidney disease, and diabetes; severity, type, number, and duration of acute symptoms; need for hospitalization; lower socioeconomic status; stress; allergies; and smoking) (5, 6, 8, 17–19), but are often bereft of variations in humoral response profile, which may be driven by severity and trajectory of COVID-19 infection and sequelae. There is a need to explore whether the inclusion of serological data can improve prediction of PCC, as compared with models based solely on clinical predictors. Also, if people with PCC are less likely to elicit a robust and sustained serological response post-infection, as compared to people without PCC, a blind reliance on serological evidence to diagnose COVID-19 infection may lead to underestimates of prevalence, and potentially exclude many people with PCC from participation in research studies, and qualifying for access to needed supports and services (3, 5, 16, 20, 21).

Studies on COVID-19 survivors comparing post-acute serological response between those with and without persistent symptoms have yielded highly mixed results (16, 20, 22–29). Some reports suggest that people with PCC are more likely to have lower titres post-infection, as compared with survivors of COVID-19 without persistent symptoms. Non-detectable levels of antibodies post-infection may indicate need for testing strategies other than serological analysis. For example, Krishna et al. found evidence of persistent SARS-CoV-2-specific T cell responses in seronegative (negative for both anti-Spike and anti-N SARS-CoV-2 IgG) patients with PCC (21). Conversely, other studies have found higher post-infection antibody titers to be associated with PCC, or no difference in humoral response in relation to persistent symptoms. Interpretation of these conflicting results is further complicated by differences in study populations, sample sizes, type of assay, number and type/subtype of target antigens, collection procedures, timing of sampling, and definition/assessment of PCC (5).

In this report, we summarize baseline findings for people found to have previous COVID-19 infection in a large Canadian prospective cohort study. We aimed to (1) describe clinical and serological characteristics among those with and without symptoms persisting ≥12 weeks post COVID-19, and (2) estimate associations between serological markers and PCC, accounting for clinical covariates. Among PCC-cases, we also described symptom characteristics, severity, and impact on quality of life.

Materials and methods

Study population

The present analysis relates to a subgroup of participants from the Stop the Spread Ottawa (SSO) cohort study. Briefly, the SSO study on COVID-19 immune response recruited over 1,000 adults in the Ottawa region from September 2020 to September 2021. All adults ≥18 years of age in the Ottawa region (1) at heightened risk of COVID-19 exposure/infection due to occupation or health condition, or (2) with any history of COVID-19 infection, confirmed by positive PCR test and/or serology, were eligible to participate. Starting in October 2020, participants provided monthly blood and saliva samples over a 10-month period. Enrolment closed September 2021. Conduct of

this study was reviewed and approved by The Ottawa Health Science Network Hospital Research Ethics Board (2020–0481). All participants provided informed and written consent.

Selection of PCC-cases and infected-controls

All SSO participants who reported a pre-baseline positive PCR test (external to study) and/or tested positive by serology at baseline (signal-to-cutoff ratio – S/CO ≥1.0 for anti-N IgG and S/CO ≥1.0 for either anti-S IgG or anti-RBD IgG) were considered for inclusion. Further inclusion criteria were that participants had contributed ≥1 blood specimen, and been assessed for persistent symptoms ≥12 weeks post initial positive PCR test (or, in the absence of positive test, due to which infection date could not be discerned, ≥12 weeks post baseline visit). Participants meeting these inclusion criteria were defined to be PCC-cases if they reported any persistent symptoms, or infected-controls if they reported no persistent symptoms ≥12 weeks post-positive COVID-19 test/baseline visit. Participants who reported the presence or absence of persistent symptoms <12 weeks post-infection and then left the study were excluded. Though we included participants regardless of vaccination status, less than a quarter of participants (23.2%, $n = 52$) received ≥1 COVID-19 vaccines ≥14 days prior to baseline visit, and few participants (2.2%, $n = 5$) received ≥1 vaccines ≥14 days prior to COVID-19 infection date.

Serological predictors

At baseline, one (5 mL) tube with a separator gel with clot activator for serum and two (10 mL × 2) tubes with EDTA for lymphocyte isolation were drawn. Serological testing included main isotypes IgA, IgM, IgG against COVID-19 N, RBD, and Spike antigens. Neutralizing efficiency against the SARS-CoV-2 Spike protein was also assessed. Full methods were published previously (30).

We examined the relationship between PCC and (1) anti-Spike, anti-N, and anti-RBD IgG titres (scaled luminescent units - SLU); and (2) % efficient neutralizers (≥85% inhibition against SARS-CoV-2 Spike protein). The cut-off for neutralization efficiency was determined by the study team to develop the in-house made surrogate neutralization enzyme-linked immunosorbent assay (snELISA) used for SSO serological analysis (31).

Collection of data on clinical covariates and PCC descriptors

Participants in the study responded to questions at baseline, and three- and 10- months post baseline via an electronic survey with the following categories: demographics and health history; severity of COVID-19 signs and symptoms; risks of exposure; and socioeconomic and psychosocial impacts of the pandemic. Responses in all categories were compared between PCC-cases and infected-controls. All participants were asked to complete the 10-item Kessler Psychological Distress Scale (K10), an internationally validated tool for the screening and assessment of psychological distress (32). Participants who reported a pre-baseline positive PCR test also completed the 15-item Impact of Event Scale (IES), used to assess for post-traumatic stress (PTS) symptoms (33).

Dates of COVID-19 positive tests and vaccines were self-reported by participants and verified where possible through use of medical and laboratory records, including Eastern Ontario Regional Laboratory Association (EORLA) reports and The Ottawa Hospital COVID-19 Registry to identify SARS-CoV-2. We reported the small numbers of PCC-cases and infected-controls without any lab-confirmed evidence of past infection (where self-reported PCR test could not be verified by laboratory record, and with negative serology at baseline).

Participants reporting persistent symptoms at time of survey completion were asked to self-rate severity of chronic symptoms, and impact of symptoms on quality of life (QoL). PCC descriptors (symptom type and severity of symptoms) and need for healthcare/medical supports were compared between cases who did and did not report worsening QoL due to PCC symptoms.

Statistical analysis

Descriptive analyses included frequency tables (categorical) and measures of center or spread (continuous). Bivariate analyses were conducted between each predictor and outcome, and among predictors using the chi-square/Fisher's exact test (categorical) and Wilcoxon-Rank Sum test (continuous) at alpha level 0.05. We constructed a series of logistic regression models to assess the relationship between each primary serological predictor (anti-Spike, anti-N, and anti-RBD IgG levels, and neutralizing efficiency) and PCC, respectively. All covariates considered for inclusion were identified *a priori*. We assessed each model for confounding, collinearity, and outliers. Given few missing data (<5% per variable), we decided to use complete case analysis. In each model, we tested for interactions between the primary predictor, and sex or time post-infection. Age, number

of months post COVID-19, and IgG titres were fit with restricted cubic splines (RCS, 3 knots at the 10th, 50th and 90th percentiles) to account for potential non-linearities (34), using the rms R package. For each primary predictor, we compared a minimally adjusted model (age and sex) with the best performing fully adjusted model. We used the Bayesian information criterion (BIC) to inform the selection of covariates for the fully adjusted model. We reported unadjusted and adjusted odds ratios with 95% confidence intervals (CIs) and goodness-of-fit using the C-statistic (34). We presented receiver operating characteristic (ROC) curves and plotted results for RCS-transformed predictors by sex. We used sensitivity analyses to assess effects from removing (1) outliers, (2) receipt of ≥1 pre-infection COVID-19 vaccines; (3) receipt of ≥2 pre-baseline COVID-19 vaccines, and (4) baseline serology collected <14 days or > 365 days post COVID-19 infection, or where days post COVID-19 could not be determined given no record of infection prior to study blood sampling. All analyses were conducted with SAS 9.4 and R, 4.2.1.

Results

Comparisons of serological and clinical predictors

Demographics and health history

We identified 102 PCC-cases and 122 infected-controls meeting study criteria. Figure 1 displays the selection procedures of study participants. Baseline characteristics are summarized in Table 1. Participants ranged in age from 21 to 75 years old. There were less males among PCC-cases (35.3%, $n = 36$), than infected-controls (42.6%, $n = 52$). Few participants were non-white (12.1%, $n = 27$). Over 75% of participants were employed at time of baseline visit ($n = 176$), and about 26% ($n = 58$) reported annual household income before taxes as $150,000 or more. PCC-cases had higher rates of pre COVID-19 obesity (25.5%, $n = 26$); asthma (13.7%, $n = 14$); and diabetes (8.8%, $n = 9$), as compared to infected-controls (obesity – 13.1%, $n = 16$; asthma – 6.6%, $n = 8$; diabetes – 4.1%, $n = 5$).

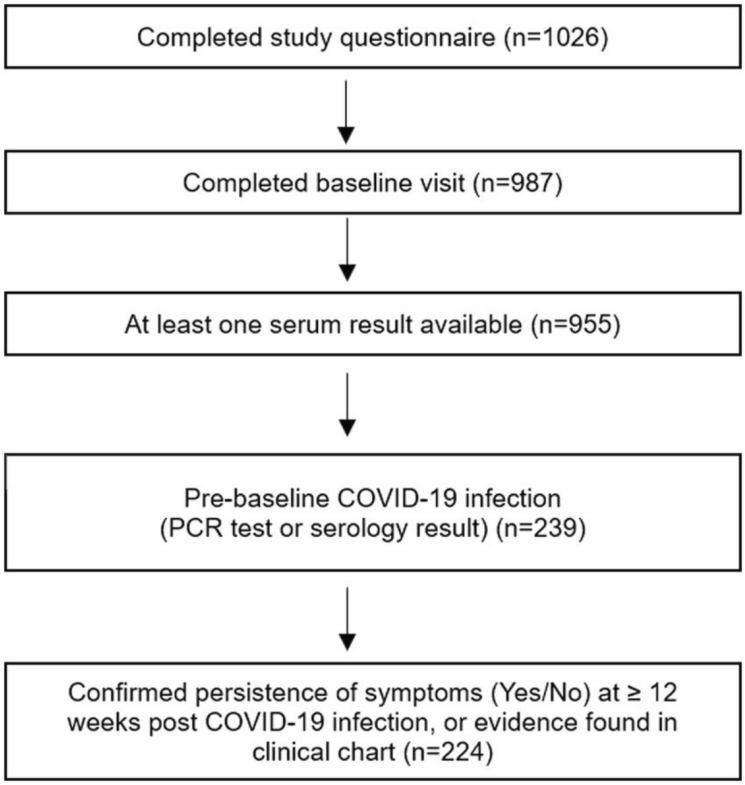


Figure 1. Selection of study participants from the Stop the Spread Ottawa study. Of 1,026 participants, 239 had a pre-baseline COVID-19 infection, attended baseline visit, and had ≥1 serology result available. Of these, 224 participants had evidence (documented in study questionnaires and/or clinical charts) confirming persistence (n = 102) or no persistence (n = 122) of symptoms ≥12 weeks post-infection.

TABLE 1: Baseline characteristics of PCC-cases with symptoms persisting ≥12 weeks and infected-controls without persistent symptoms

	Cases (n=102)[b]	Controls (n=122)[c]	*P* value[d]
Median age, years (IQR)	50 (21)	45 (25)	0.14
Sex, male (%)	36 (35.3)	52 (42.6)	0.28
Race, white (%)	92 (90.2)	105 (86.1)	0.34
Born in Canada (%)	91 (89.2)	104 (85.2)	0.31
Lives with ≥1 other person (%)	92 (90.2)	108 (88.5)	0.83
Allergies, any (%)	57 (55.9)	51 (41.8)	0.04
Smoker, former (%)	29 (28.4)	24 (19.7)	0.71
Smoker, current (%)	3 (2.9)	3 (2.5)	0.12
Employed at time of baseline visit (%)	79 (79.0)	97 (80.8)	0.93
Status of employment before the pandemic (%)	---	---	---
Permanent	67 (67.7)	76 (62.8)	REF
Contract/temporary	8 (8.1)	12 (9.9)	0.57
Self-employed	7 (7.1)	9 (7.4)	0.81
No paid employment but seeking work	2 (2.0)	1 (0.8)	0.51
No paid employment and not seeking paid work	13 (13.1)	22 (18.2)	0.30
Median hours of work per week before the pandemic (IQR)	37.5 (10.0)	37.5 (18.0)	0.57
Annual household income before taxes in past 12 months (%)	---	---	---
$0 - $29,999	6 (6.0)	3 (2.5)	0.23
$30,000 - $59,999	11 (11.0)	13 (10.7)	0.98
$60,000 to $89,999	14 (14.0)	16 (13.1)	0.57
$90,000 to $119,999	13 (13.0)	15 (12.3)	REF
$120,000 to $149,999	10 (10.0)	7 (5.7)	0.49
$150,000 or more	32 (32.0)	26 (21.3)	0.43
Prefer not to answer	12 (12.0)	9 (7.4)	0.37
Do not know	2 (2.0)	0 (0)	---
Median number of people supported by annual income (IQR)	2 (2.0)	2 (2.0)	0.46
Change in employment due to the COVID-19 pandemic (%)	---	---	---
	3 (3.0)	3 (2.5)	0.64
Lost job	16 (16.0)	12 (9.8)	0.10
Reduced income/hours	64 (64.0)	95 (77.9)	REF
No change	16 (16.0)	12 (9.8)	0.10
Increased income/hours			
Lost days of work due to infectious respiratory illness (%)	38 (37.3)	32 (26.2)	0.08
Median number of days work lost to respiratory illness (range)	--- 14 (2 – 120)	--- 10 (2 – 35)	--- 0.28
Impact of pandemic on ability to meet essential needs and financial commitments (%)	--- ---	--- ---	--- ---
Not at all	74 (74.0)	94 (77.7)	REF
Can still meet most of essential/financial needs	20 (20.0)	22 (18.2)	0.68
Can still meet some of essential/financial needs	5 (5.0)	5 (4.1)	0.71
Unable to meet most of essential/financial needs	2 (2.0)	0 (0.0)	1.00
Current level of education (%)	---	---	---

Elementary school	0 (0.0)	1 (0.8)	1.00
High school	5 (5.1)	11 (9.2)	0.44
Trade, technical or vocation school	4 (4.0)	5 (4.2)	0.88
Diploma from community college	29 (29.3)	17 (14.2)	0.02
University certificate before Bachelor's	3 (3.0)	4 (3.3)	0.96
Bachelor's degree	33 (33.3)	46 (38.3)	REF
Graduate degree	21 (21.2)	32 (26.7)	0.81
Prefer not to answer	5 (5.1)	3 (2.5)	0.27
Pre COVID-19 comorbidities (%)	---	---	---
Pregnancy	1 (1.0)	0 (0)	1.00
Cancer	4 (3.9)	2 (1.6)	0.42
Diabetes	9 (8.8)	5 (4.1)	0.17
HIV	1 (1.0)	3 (2.5)	0.63
Other immune condition	6 (5.9)	3 (2.5)	0.31
Obesity	26 (25.5)	16 (13.1)	0.02
Heart condition	8 (7.8)	6 (4.9)	0.42
Asthma	14 (13.7)	8 (6.6)	0.11
Lung disease	4 (3.9)	3 (2.5)	0.70
Liver disease	0 (0)	4 (3.3)	0.13
Kidney disease	1 (1.0)	2 (1.6)	1.00
Hematological condition	2 (2.0)	2 (1.6)	1.00
Neurological condition	7 (6.9)	4 (3.3)	0.23
Organ / bone marrow transplant	0 (0)	1 (0.8)	1.00
Other health condition	50 (49.0)	50 (41.7)	0.27
Receiving treatment that suppresses immune system	6 (5.9)	3 (2.5)	0.31
COVID-19 vaccination and infection history	---	---	---
Received ≥2 COVID-19 vaccines ≥14 days prior to baseline visit (%)	11 (10.9)	21 (17.2)	0.17
Received ≥1 COVID-19 vaccine ≥14 days prior to baseline visit (%)	24 (23.8)	28 (23.0)	0.92
Received ≥1 COVID-19 vaccine ≥14 days prior to infection (%)	0 (0.0)	5 (4.1)	<0.01
Days between first pre-baseline vaccine and baseline visit, median (IQR)[i]	65.0 (59.5)	102.0 (76.0)	0.12
Days between second pre-baseline vaccine and baseline visit, median (IQR)[j]	62.0 (42.0)	63.0 (29.0)	0.81
History of positive pre-baseline PCR test[a] (%)	99 (97.1)	102 (83.6)	<0.01
Date of initial infection, range (month/year)	Mar 2020 – Aug 2021	Mar 2020 – Aug 2021	---
Wave of initial infection[k] (%)	---	---	---
Wave 1, March 2020 – August 2020	50 (50.5)	35 (34.3)	0.07
Wave 2, September 2020 – February 2021	34 (34.3)	45 (44.1)	0.80
Wave 3, March 2021 – August 2021	15 (15.2)	22 (21.6)	REF
Sought medical attention for COVID-19 symptoms (%)	51 (50.0)	24 (19.7)	<0.01
Hospitalized for COVID-19 (%)	12 (11.8)	1 (0.8)	0.05

Days between baseline visit and pre-baseline PCR, median (IQR)	---	---	---
	186 (153)	115 (149)	<0.01
Days between baseline visit and pre-baseline PCR test, range	12 – 414	13 – 384	---
Days between pre-baseline PCR and first assessment of persistent symptoms (≥12 weeks post COVID-19), median (IQR)	---	---	---
	---	---	---
	255 (183)	153 (161)	<0.01
Days between baseline visit and first assessment of persistent symptoms (≥12 weeks post COVID-19), median (IQR)	---	---	---
	70.0 (95.0)	84.5 (74.0)	0.48
Asymptomatic (%)	0 (0.0)	13 (10.7)	<0.01
Severity of acute illness, self-rated, median (IQR)[g]	7.5 (3.5)	6.0 (3.0)	<0.01
Kessler Psychological Distress Scale (K10), mean (SD)	20.2 (7.6)	16.0 (6.3)	<0.01
	10 – 40	10 – 38	---
K10, range	51 (51.5)	94 (79.7)	REF
Likely to be well (10-19), (%)	25 (25.3)	10 (8.5)	<0.01
Likely to have mild mental disorder (20-24), (%)	8 (8.1)	7 (5.9)	0.17
	15 (15.2)	7 (5.9)	<0.01
Likely to have moderate mental disorder (25-29), (%)			
Likely to have severe mental disorder (30-50), (%)			
Impact of Event Scale (IES), mean (SD)	18.5 (17.7)	10.1 (13.7)	<0.01
IES, range	0 – 65	0 – 56	---
Subclinical range (0-8)	39 (40.6)	56 (48.7)	REF
Mild range (9-25)	21 (21.9)	26 (22.6)	0.68
Moderate range (26-43)	21 (21.9)	10 (8.7)	0.01
Severe range (44+)	12 (12.5)	3 (2.6)	<0.01
Baseline serology results[e]	---	---	---
Positive call for anti-Spike IgG, SCO[h] >1.0 (%)	96 (94.1)	109 (89.3)	0.24
Positive call for anti-RBD IgG, SCO[h] >1.0 (%)	97 (95.1)	103 (84.4)	0.02
Positive call for anti-N IgG, SCO[h] >1.0 (%)	68 (66.7)	87 (71.3)	0.47
Median anti-N IgG (IQR)	0.96 (1.25)	0.90 (1.04)	0.82
Anti-N IgG, range	0.03 – 2.04	0.06 – 2.01	---
Median anti-Spike IgG (IQR)	1.50 (0.61)	1.42 (0.73)	0.20
Anti-Spike IgG, range	0.01 – 2.57	0.01 – 2.58	---
Median anti-RBD IgG (IQR)	1.25 (1.17)	1.16 (1.35)	0.67
Anti-RBD IgG, range	0.00 – 3.20	0.00 – 2.80	---
Median %Neutralization (IQR)	11.3 (85.1)	11.6 (60.0)	0.22
Neutralizing efficiency (%)	---	---	---
Neutralization ≤ 30% (weak to negative response)	64 (62.7)	79 (64.8)	REF
	12 (11.8)	27 (22.1)	0.12
>30% Neutralization <85%	26 (25.5)	16 (13.1)	0.05
≥85% Neutralization (efficient neutralizers)			

[a]99 cases and 102 controls reported pre-baseline PCR test. Other cases (n=3) and controls (n=20) had laboratory-confirmed history of infection by serology at baseline visit only;
[b]Number missing for variables, Cases: Employed 2; Status 3; Hours before 4; Income 2; Number of people supported 3; Change due to pandemic 2; Education 3; Impacted 2; Severity of COVID 3; K10 3; IES 6; Vaccination dates 1;
[c]Number missing for variables, Controls: Other condition 2; Employment 2; Status 1; Hours before 7; Income 1; Number of people supported 3; Education 2; Impacted 1; Severity of COVID 7; K10 4; IES 7;
[d] *P* value <0.05: chi-squared and Fisher's exact tests used for categorical variables; Wilcoxon Rank Sum test used for continuous variables;
[e]All participants had baseline serology collected, % neutralization was not missing for any samples;
[g]Participants asked: "On a scale of 1 to 10, 10 being the worst you have ever felt, how would you rate your symptoms overall on this day?";
[h]Signal-to-cutoff ratio;
[i]Among participants to receive ≥1 pre-baseline COVID-19 vaccines (n=52) ≥14 days prior to baseline visit;
[j]Among participants to receive ≥2 pre-baseline COVID-19 vaccines (n=32) ≥14 days prior to baseline visit;
[k]From March 2020 – August 2021, the dominant SARS-CoV-2 strains in Ontario, Canada were Wild type (Waves 1 and 2) and Alpha variant /B1.1.17 (Wave 3)

COVID-19 infection and vaccination history

Most participants reported a pre-baseline PCR test (89.7%, *n* = 201), of which we were able to verify 92.5% (*n* = 186) by laboratory or clinical record. Of the 7.5% (*n* = 15) we were not able to verify, only two participants had negative serology at baseline. Participants who did not report a pre-baseline PCR test and had serological markers of infection at baseline (10.3%, *n* = 23) were also included so long as they were assessed for symptoms persisting ≥12 weeks. Approximately 23% of PCC-cases (*n* = 24) and infected-controls (*n* = 28) received ≥1 vaccines ≥14 days prior to baseline visit, while 10.9% of cases (*n* = 11) and 17.2% of controls (*n* = 21) received ≥2 vaccines ≥14 days before baseline visit (Table 1). Results for unvaccinated and vaccinated participants are presented in Supplementary Tables S1A,B, respectively. Among the 201 participants who reported a pre-baseline PCR test, (81.6%, *n* = 164) were infected in Waves 1 and 2 (March 2020 – February 2021) when the Wild type SARS-CoV-2 strain was dominant in Ontario, Canada, while 37 (18.4%) were infected during Wave 3 (March 2021 – August 2021), when the Alpha variant/B1.1.17 was dominant in Ontario, Canada [Table 1; (35, 36)]. No participants reported more than one infection prior to study assessment. Few PCC-cases (11.8%, *n* = 12) and infected-controls (0.8%, *n* = 1) were hospitalized for COVID-19. However, half of PCC-cases (*n* = 51) reported seeking medical attention for COVID-19 symptoms other than hospitalization, as compared to infected-controls (19.7%, *n* = 24). Among controls, 10.7% (*n* = 13) were asymptomatic while all cases had symptoms during acute illness. PCC-cases also self-rated the severity of overall symptoms higher (median of 7.5/10, IQR 3.5) on the worst day of acute illness, as compared to controls (median of 6.0/10 IQR 3.0). Participants to test positive by serology only, with no self-report of positive PCR test at baseline, were not asked to self-rate symptom severity and date of onset is often indeterminable. PCC-cases had a significantly longer follow-up time (median 186 days, IQR 183)

between pre-baseline PCR and baseline serological sampling, as compared with infected-controls (median 115 days, IQR 149, $p < 0.01$).

Anti-N, anti-spike, and anti-RBD IgG titres

Similar proportions of cases (66.7%, $n = 68$) and controls (71.3%, $n = 87$, $p = 0.47$) tested positive for anti-N IgG. Cases tended to have higher IgG titres (anti-N, anti-Spike, and anti-RBD), but differences were non-significant. Findings were similar upon restricting to unvaccinated participants (Supplementary Table S1A) and varying post-infection time intervals (Supplementary Tables S2A–C; 14–365 days; 14–180 days; and 14–90 days post COVID-19 infection). Unvaccinated PCC-cases had higher anti-Spike IgG levels (median 1.45, IQR 0.79) than unvaccinated infected-controls (median 1.29, IQR 0.86, $p = 0.14$). Among participants who attended baseline 14–365 days, 14–180, or 14–90 days post-infection, IgG titres remained consistently higher among cases, except for anti-RBD assessed 14–90 days post-infection (PCC-cases – median anti-RBD 0.92, IQR 1.17; infected-controls – 1.03, IQR 1.40, $p = 0.04$).

Neutralizing efficiency

More cases (25.5%, $n = 26$) than controls (13.1%, $n = 16$) were efficient neutralizers (≥85% neutralizing efficiency). As expected, most efficient neutralizers had received ≥1 COVID-19 vaccines prior to baseline serology sampling (Supplementary Table S1B). However, median neutralization efficiency was somewhat higher among non-vaccinated cases (7.17, IQR 20.35), as compared to non-vaccinated controls (3.62, IQR 17.40, $p = 0.45$), despite the former having a significantly longer median time interval (cases – 205, IQR 163 days; controls – 84, IQR 152, $p < 0.01$) between COVID-19 onset and baseline visit (Supplementary Table S1A). Among 52 (23.2%) participants to receive ≥1 vaccines ≥14 days prior to baseline visit (Supplementary Table S1B), cases had somewhat higher neutralizing efficiency (median 98.69, IQR 4.62), than controls (median 87.96, IQR 35.28, $p = 0.06$). Similar trends were observed when limiting to different post-infection time intervals (Supplementary Tables S2A–C).

Socioeconomic and psychosocial impacts of the pandemic and COVID-19 infection

The majority of participants reported no change in employment or ability to meet essential needs due to the COVID-19 pandemic (Table 1). Differences in annual household income were

TABLE 2: Persisting symptoms (≥12 weeks post COVID-19 onset) and baseline serology of PCC-cases who did (n=65) and did not (n=37) report worsened quality of life

	All (n=102)	Worsened quality of life post COVID-19 (n=65)	Quality of life not worsened post COVID-19 (n=37)
Median days post COVID-19 (IQR)[a]	255.0 (183.0)	246.0 (181.0)	255.5 (189.0)
Range, days post COVID-19[a]	75 – 451	79 – 451	75 – 343
Date of initial infection, range (month/year)	Mar 2020 – Aug 2021	Mar 2020 – June 2021	Mar 2020 – Aug 2021
Wave of initial infection[b] (%)	---	---	---

non-significant. Somewhat more PCC-cases (37.3%, $n = 38$) reported one or more lost days of work due to respiratory illness and a higher number of days lost (median 14, IQR 118), than infected-controls (median 10, IQR 33, $p = 0.28$). Cases had a higher mean K10 (Kessler Psychological Distress Scale) score (20.2, SD 7.6) as compared to controls (16.0, SD 6.3, $p < 0.01$), and more cases were likely to have mild (25.3%, $n = 25$), moderate (8.1%, $n = 8$), and severe (15.2%, n = 15) mental disorder, than controls (mild disorder – 8.5%, $n = 10$; moderate disorder – 5.9%, n = 7; and severe disorder – 5.9%, $n = 7$), using K10 cut-offs established previously (32). PCC-cases also had a higher mean IES (Impact of Event Scale) score (18.5, SD 17.7) than infected-controls without PCC (10.1, SD 13.7, $p < 0.01$). Applying previously applied IES cut-offs (33), more PCC-cases had moderate (21.9%, $n = 21$) and severe (12.5%, $n = 12$) distress than infected-controls (moderate distress – 8.7%, $n = 10$; severe distress – 2.6%, $n = 3$).

Descriptors of post COVID-19 condition

Table 2 delineates the number and type of persistent symptoms among all PCC-cases ($n = 102$), those cases who reported worsened QoL post COVID-19 ($n = 65$), and those who did not ($n = 37$). The three most frequent symptoms described by PCC-cases with worsened QoL were fatigue (73.8%, $n = 48$); shortness of breath (64.6%, $n = 42$); and difficulties with thinking/concentrating (60.0%, $n = 39$). Among PCC-cases who did not report worsened QoL (36.3%, $n = 37$), the most common symptoms were loss of smell ($n = 14$, 37.8%); loss of taste ($n = 9$, 24.3%); and fatigue ($n = 12$; 32.4%). The majority of cases (89.2%, $n = 91$) reported ongoing symptoms for a median of 255 days (IQR 183; range 75–451 days) at time of first assessment for PCC. Among these cases, those who reported worsened QoL self-rated severity of persisting symptoms higher (median 4.0, IQR 4.0) than the other cases (median 2.0, IQR 2.0) on a scale of 1–10 (Table 2). PCC-cases endorsing worsened QoL also reported a higher number of post COVID-19 symptoms (median 6.0, IQR 9.0), than cases not reporting worsened QoL (median 2.0, IQR 3.0).

Wave 1, March 2020 – Aug 2020	50 (50.5)	30 (47.6)	20 (55.6)
Wave 2, Sept 2020 – Feb 2021	34 (34.3)	24 (38.1)	10 (27.8)
Wave 3, March 2021 – Aug 2021	15 (15.2)	9 (14.3)	6 (16.7)
Symptoms ongoing at time of assessment (%)	91 (89.2)	63 (96.9)	28 (75.7)
If ongoing, median severity of symptoms on day of assessment[c] (IQR)	--- 4.0 (3.0)	--- 4.0 (4.0)	--- 2.0 (2.0)
Symptoms	---	---	---
Median number of persistent symptoms (IQR)	4.0 (6.0)	6.0 (9.0)	2.0 (3.0)
Fatigue (%)	60 (58.8)	48 (73.8)	12 (32.4)
Shortness of breath (%)	49 (48.0)	42 (64.6)	7 (18.9)
Cough (%)	24 (23.5)	19 (29.2)	5 (13.5)
Joint pain (%)	24 (23.5)	22 (33.8)	2 (5.4)
Muscle pain (%)	31 (30.4)	24 (36.9)	7 (18.9)
Chest pain (%)	27 (26.5)	22 (33.8)	5 (13.5)
Headache (%)	33 (32.4)	28 (43.1)	5 (13.5)
Dizziness (%)	24 (23.5)	22 (33.8)	2 (5.4)
Loss of smell (%)	37 (36.3)	23 (35.4)	14 (37.8)
Loss of taste (%)	33 (32.4)	24 (36.9)	9 (24.3)
Fast or pounding heartbeat (%)	28 (27.5)	23 (35.4)	5 (13.5)
Irritability (%)	22 (21.6)	21 (32.3)	1 (2.7)
Difficulties with thinking/concentrating (%)	44 (43.1)	39 (60.0)	5 (13.5)
Memory loss (%)	32 (31.4)	29 (44.6)	3 (8.1)
Confusion (%)	27 (26.5)	16 (24.6)	1 (2.7)
Difficulty sleeping (%)	31 (30.4)	26 (40.0)	5 (13.5)
Rash (%)	9 (8.8)	7 (10.8)	2 (5.4)
Hair loss (%)	20 (19.6)	14 (21.5)	6 (16.2)
Nausea (%)	9 (8.8)	9 (13.8)	0 (0)
Loss of appetite (%)	6 (5.9)	6 (9.2)	0 (0)
Diarrhea (%)	9 (8.8)	9 (13.8)	0 (0)
Other (%)	11 (10.8)	5 (7.7)	6 (16.2)
Worsened quality of life post COVID (%)[d]	--- 65 (63.7)	--- 65 (100.0)	--- ---
Yes	31 (30.4)	---	31 (83.8)
No	6 (5.9)	---	6 (16.2)
Other[e]			
Baseline serology results[e]	---	---	---
Positive call for anti-Spike IgG, SCO[f] >1.0 (%)	96 (94.1)	61 (93.8)	35 (94.6)
Positive call for anti-RBD IgG, SCO[f] >1.0 (%)	97 (95.1)	61 (93.8)	36 (97.3)
Positive call for anti-N IgG, SCO[f] >1.0 (%)	68 (66.7)	45 (69.2)	23 (62.2)
Median anti-N IgG, (IQR)	0.96 (1.25)	1.10 (1.24)	0.86 (1.25)
Anti-N IgG, range	0.03 – 2.04	0.03 – 2.04	0.06 – 1.93
Median anti-Spike IgG (IQR)	1.50 (0.61)	1.54 (0.51)	1.45 (0.66)
Anti-Spike IgG, range	0.01 – 2.57	0.01 – 2.57	0.02 – 2.19
Median anti-RBD IgG (IQR)	1.25 (1.17)	1.29 (1.28)	1.07 (1.10)
Anti-RBD IgG, range	0.00 – 3.20	0.00 – 3.20	0.08 – 2.85
Median %Neutralization (IQR)	11.3 (85.1)	17.2 (92.8)	8.0 (38.2)
Neutralizing efficiency (%)	---	---	---
Neutralization ≤ 30% (weak to negative	--- 64 (62.7)	--- 37 (56.9)	--- 27 (73.0)

response)	12 (11.8)	7 (10.8)	5 (13.5)
>30% Neutralization <85%	26 (25.5)	21 (32.3)	5 (13.5)
≥85% Neutralization (efficient neutralizers)			

[a]99 cases and 102 controls reported pre-baseline PCR test. Other cases (n=3) and controls (n=20) had laboratory-confirmed history of infection by serology at baseline visit only;
[b]From March 2020 – August 2021, the dominant SARS-CoV-2 strains in Ontario, Canada were Wild type (Waves 1 and 2) and Alpha variant /B1.1.17 (Wave 3);
[c]Participants asked "On a scale of 1 to 10, 10 being the worst you have ever felt, how would you rate your symptoms overall today?";
[d]Participants asked "Do you believe the quality of life you have now is worse than the quality of life you had before experiencing symptoms that were/may have been caused by COVID-19?"
[e]Responses to "Other": loss of smell but not impactful (n=2); palpitations but made lifestyle changes that improved symptoms (n=1); difficult to determine as broke wrist due to COVID vertigo (n=1); mild symptoms but not back to baseline (n=2);
[f]Signal-to-cutoff ratio

Univariate analyses–serological and clinical predictors of PCC

Table 3 presents crude odds ratios (ORs) with 95% CIs for all variables specified *a priori* and considered for model inclusion (age, sex, time post-infection (months), asthma requiring medication, conditions/treatments which may suppress the immune system (cancer, HIV, chronic kidney or liver disease, diabetes, organ or bone marrow recipient, other immune deficiency, or receiving treatment that weakens immune system), obesity, smoking, income, allergies, and hospitalization or need for medical attention for COVID-19 symptoms). Unadjusted odds of PCC were 2.3 (95% CI 0.91–5.64) given asthma; 2.3 (95% CI 0.73–6.99) given diabetes; 1.8 (95% CI 1.04–3.00) given any allergies; 1.6 (95% CI 0.88–2.98) given history of smoking; and 0.7 (95% CI 0.43–1.26) given male sex. Not accounting for covariates, participants to have been hospitalized/sought medical attention for COVID-19 symptoms were over four times more likely to have PCC (OR 4.1, 95% CI 2.26–7.38). Crude ORs for anti-Spike, anti-RBD, and anti-N titres were non-significant. Unadjusted odds of PCC for efficient neutralizers was 2.3 (95% CI 1.14–4.51), as compared to non-efficient neutralizers. Comparing only PCC-cases to report reduced QoL due to symptoms ($n = 65$) with infected-controls (n = 122), the crude odds of PCC given efficient neutralization further increased to 3.2 (95% CI 1.53–6.62), while negligible increases were observed for other serological predictors (anti-Spike – OR 1.5, 95% CI 0.88–2.56; anti-N – OR 1.2, 95% CI 0.69–1.92; anti-RBD – OR 1.1, 95% CI 0.74–1.58).

TABLE 3: Crude ORs (95%CIs) for Post COVID-19 symptoms: variables considered for analysis prior to modelling

Variable	Reference[a]	Estimate	Standard Error	*P* value	Odds Ratio	CI (95%)
Age	NA	0.01	0.01	0.24	1.0	0.99, 1.03
Sex	Female	-0.31	0.28	0.26	0.7	0.43, 1.26

Time post infection, months	NA	0.07	0.02	0.00	1.1	1.03, 1.11
History of asthma	No asthma	0.82	0.47	0.08	2.3	0.91, 5.64
Condition/treatment that may suppress immune system	None	0.11	0.42	0.79	1.1	0.49, 2.57
Diabetes	No diabetes	0.82	0.57	0.16	2.3	0.73, 6.99
Smoking	No smoking	0.48	0.31	0.12	1.6	0.88, 2.98
Obesity	No obesity	0.82	0.35	0.02	2.3	1.14, 4.51
Household income, $60,000 – $199,999	≥ $120,000	-0.27	0.31	0.38	0.8	0.41, 1.41
Household income, $0 – $59,999	≥ $120,000	-0.19	0.37	0.61	0.8	0.40, 1.72
Allergies, any	No allergies	0.57	0.27	0.04	1.8	1.04, 3.00
Sought medical help or hospitalized for COVID-19 symptoms	Did not seek help/ not hospitalized	1.41	0.30	<.01	4.1	2.26, 7.38
% Neutralization, efficient neutralizers	<85%	0.82	0.35	0.02	2.3	1.14, 4.51
Anti-IgG titres (Spike)	NA	0.35	0.24	0.14	1.4	0.89, 2.26
Anti-IgG titres (RBD[b])	NA	0.08	0.17	0.64	1.1	0.77, 1.52
Anti-IgG titres (N[c])	NA	0.07	0.23	0.77	1.1	0.69, 1.66

[a]Reference for categorical variables;
[b]Spike protein receptor binding domain;
[c]Nucleocapsid protein

Multivariate analyses–serological predictors of PCC accounting for clinical covariates

Figure 2 compares the effect of IgG titres transformed with restricted cubic splines ($k = 2$, percentiles =10, 50, 90) on odds of PCC in minimally adjusted (covariates – sex and age) and fully adjusted (covariates – sex, age, time since COVID-19 infection, sought medical help/required hospitalization for COVID-19 symptoms, and allergies) models. Using the 10th percentile as the referent and adjusting for age, females tended to have elevated odds of PCC, as compared with males (Figure 2). Inter-sex differences in adjusted odds of PCC were reduced in fully adjusted models. Upon testing for pre-specified interactions (each serological predictor and sex; each serological predictor and time post-infection), none were significant.

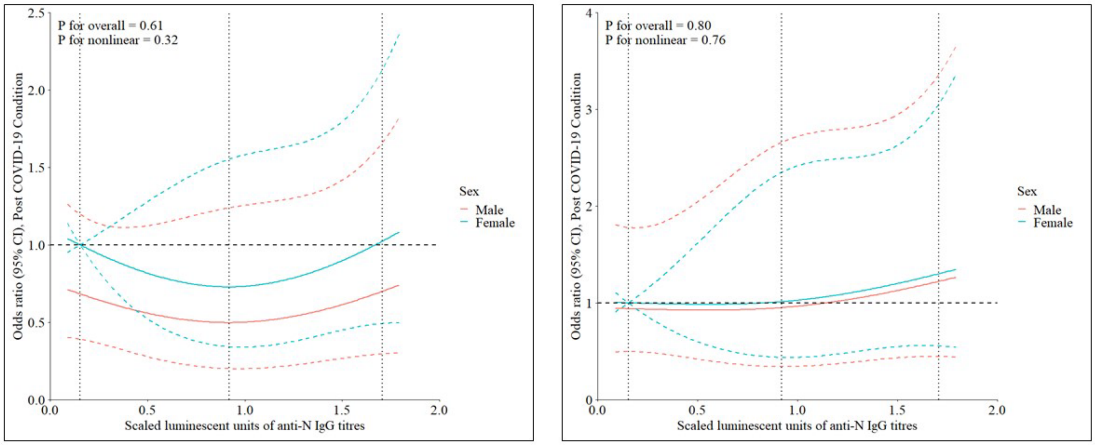


Figure 2. Effect of anti-N titers on odds of Post-COVID-19 Condition. Models on the left are minimally adjusted (adjusted for sex and age) and models on the right are fully adjusted (adjusted for age, sex, allergies, hospitalization or sought medical assistance for COVID-19 symptoms, and time (months) since infection). IgG titres were transformed with restricted cubic splines ($k = 3$, percentiles = 10, 50, 90).

Supplementary Tables S3A–D present the multivariable model output. Nonlinear relationships between PCC and RCS-transformed predictors were found to be non-significant, with the exception of time post-infection. Area under the curve (AUC) was 0.58–0.59 for minimally adjusted models and 0.73 for fully adjusted models (Supplementary Figure S1). Adjusted odds of PCC given changes in IgG titres remained non-significant. Efficient neutralization was a significant predictor of PCC, accounting for age and sex (OR 2.2, 95% CI 1.11–4.49), and odds was further increased upon restricting to cases to report reduced quality of life (OR 3.4, 95% CI 1.64–7.31). In the fully adjusted model, odds of PCC given neutralizing efficiency ≥85% was 2.0 (95% CI 0.89–4.54). Allergies (OR 1.9, 95% CI 1.00–3.54), time post-infection (OR 1.9, 95% CI 1.06–3.51), and need for hospitalization/medical help for COVID-19 symptoms (OR 3.2, 95% CI 1.61–6.24) were associated with PCC in the fully adjusted model (Supplementary Table S3D). Upon removing all cases (10.8%, $n = 11$) and controls (17.2%, $n = 21$) to receive ≥2 COVID-19 vaccines ≥14 days prior to baseline visit, efficient neutralizers had increased odds of PCC in minimally (OR 3.8, 95% CI 1.40–10.31) and fully adjusted (OR 2.8, 95% CI 0.91–8.31) models. However, these results should be interpreted with caution given the wide confidence intervals, and the result for the fully adjusted model is statistically non-significant. Odds of PCC given neutralization ≥85% also increased upon removal of participants (PCC-cases, $n = 0$; infected-controls, n = 5) to receive ≥1 COVID-19 vaccines ≥14 days prior to infection in minimally (OR

2.5, 95% CI 1.22–5.19) and fully adjusted (OR 2.2, 95% CI 0.94–5.09) models, though the latter remained non-significant.

Discussion

In our study of a largely non-hospitalized cohort infected with COVID-19 prior to baseline visit, we assessed for relationships between serological markers and PCC, accounting for clinical covariates. We also described the sequelae, quality of life, and health care needs of PCC-cases. Main findings from our study include:

1. Anti-N was a less reliable indicator of past COVID-19 infection than anti-Spike or anti-RBD, among unvaccinated PCC-cases and infected-controls.
2. Among PCC-cases, anti-N, anti-RBD, and anti-Spike IgG titres tended to be higher, as compared to infected-controls. However, associations between PCC and IgG titres remained non-significant in unadjusted and adjusted logistic regression analyses.
3. More PCC-cases were efficient neutralizers (≥85% neutralization) than infected controls. In both unvaccinated and vaccinated subgroups, median neutralization efficiency was somewhat higher among cases than controls.
4. PCC-cases to report worsened quality of life had higher IgG titres and median neutralization efficiency, and a larger proportion of efficient neutralizers, as compared to PCC-cases who did not so report.
5. Clinical covariates associated with PCC and used in multivariate analyses included allergies, time post-infection, and seeking medical help for COVID-19 symptoms.
6. PCC-cases, especially those to report worsened quality of life, were more likely than infected-controls to seek medical help for COVID-19 symptoms, and describe complex and enduring health needs long after initial infection.

Seropositivity to SARS-COV-2 nucleoprotein, as compared to response elicited by spike/RBD

Following vaccination for COVID-19, serological response to SARS-CoV-2 nucleoprotein can indicate past infection. However, only 69.2% (n = 155) of all participants tested positive for anti-N at baseline. Anti-N seropositivity did not improve upon limiting to participants to have blood drawn 14–90 days post-infection (Supplementary Table S2C). Restricting to non-vaccinated participants (Supplementary Table S1A), more tested positive for anti-Spike and/or anti-RBD than anti-N. Also, PCC-cases were more likely to be seropositive for anti-Spike and/or anti-RBD than infected-controls despite having a significantly higher number of days between infection and first blood draw. We suspect that the sensitivity of SARS-CoV-2 nucleoprotein would have improved given shorter time intervals between infection and serological sampling as anti-N IgG has been

found to decay more rapidly than anti-Spike IgG (37–40). Our findings suggest diminished reliability of anti-N as a marker of past disease as more time elapses between infection and serological testing. Unfortunately, the baseline serological assessment for cases and controls was conducted an average of 4–8 months post-infection and we cannot examine for decay at earlier timepoints.

Associations between post COVID-19 condition and IgG titres

Associations between IgG levels and PCC were non-significant in univariate and multivariate analyses. Other studies have found post-infection IgG titres between COVID-19 survivors with and without persistent symptoms to be comparable (41–43), though varying definitions of PCC, time intervals between infection and blood sampling, initial severity of the cohort (e.g., hospitalized vs. non-hospitalized), target antigen(s), and other sources of heterogeneity limit comparability of findings. In contrast, García-Abellán et al. found lower S1/S2 IgG titres measured at 12 months post-admission to be associated with persistent symptoms (defined as having a score above the third quartile in any items of a self-rated COVID-19 symptom questionnaire at six- and 12-months post-admission) (25). Blomberg et al. reported higher Spike IgG and microneutralizing antibody titres to be associated with both number of persisting symptoms and Chalder Fatigue Scale score assessed 6 months post-infection (24).

Neutralization efficiency and post COVID-19 condition

Efficient neutralization was significantly associated with PCC, controlling for age and sex. This relationship was further strengthened upon comparing only PCC-cases to report worsened QoL with infected-controls. Neutralizing antibody activity has been found to correlate with initial COVID-19 disease severity (44–46). Severe acute disease can cause organ damage, immune dysregulation, hypercoagulation, activation of mast cells, and other pathophysiological mechanisms suspected to contribute to PCC (7, 47). Though few in our cohort were hospitalized during acute illness, these results may signify a more robust post-infection response among PCC-cases, especially those with debilitating persisting symptoms. The association between SARS-CoV-2 antibody neutralization and persisting symptoms for 3 months or longer has been documented previously (48). However, upon comparing Omicron BA.5 variant and wildtype

neutralizing response, Buck et al. found only the former to be independently and significantly associated with PCC.

Clinical predictors and complex medical needs of cases

Clinical covariates found to be strongly associated with PCC included pre COVID-19 allergies and need for hospitalization/medical support. As per Table 1, 55.9% of PCC-cases had ≥1 allergy, as compared to 41.8% of infected-controls. The two most frequent allergies were reactions to medications (33.3% PCC-cases; 23.0% infected-controls) and pollen (26.5% PCC-cases; 19.9% infected-controls). Cases also reported a wider range of allergies than controls. These findings align with the theory that atypical response to initial infection due to dysfunctional mast cells may manifest as more severe and long-lasting sequelae (49, 50). Allergy status has previously been documented as a potential risk factor for persistent symptoms among adults and children (50–53). However, findings are especially limited among adult cohorts and more research on allergic phenotypes is required (52).

During analysis, we noted that need for medical attention may not exclusively refer to supports sought in the acute phase of illness. A few participants (Table 4) reported seeking medical attention for chronic symptoms post-infection (e.g., one case described seeking help at the Post COVID-19 care clinic). Unfortunately, it was often not possible to discern from our cohort when help was sought post disease onset. While this data issue limits the value of this variable as a proxy for acute illness severity, our findings that more PCC-cases required medical attention (50.0%), as well as different types of medical attention (2–5 types required by 23.0%), as compared with infected-controls, are important in the context of understanding the complex health needs of people with PCC. We also found that cases who reported worsened QoL post COVID-19 were more likely to require medical support (61.5%), as compared with cases who did not report worsened QoL. The most common sources of medical support sought by cases were (1) family doctor/primary care provider (29.4% for all cases; 43.1% for cases with worsened QoL); (2) public health testing center (20.6% for all cases; 24.6% for cases with worsened QoL); and (3) emergency department (20.6% for all cases; 27.7% for cases with worsened QoL), Table 4. Findings from K10 and IES surveys also suggest a higher burden of mental health needs among PCC-cases (Table 1), and Table 2 describes high diversity, severity, and longevity of PCC symptoms among cases. At time of first assessment, 89.2% of cases ($n = 91$) reported symptoms persisting long after initial disease

(median 255 days, IQR 183). Given ongoing labor shortages in the healthcare sector, many people with PCC may not gain timely access to care. Our findings support the need for ample staff and resources to respond to prolonged, recurrent, and diverse needs across multiple health domains. For example, more Post COVID-19 care clinics may improve the well-being, function, and quality of life of this population while reducing burden on the mainstream health system (54–60).

TABLE 4: Type of medical attention sought for COVID-19 symptoms

	Cases (n=102)[a]	Cases with worsened quality of life (n=65)	Controls (n=122)[b]
Type of medical attention sought, %	51 (50.0)	40 (61.5)	24 (19.7)
Family doctor/primary care provider	30 (29.4)	28 (43.1)	5 (4.1)
Occupational Health	7 (6.9)	6 (9.2)	2 (1.6)
Public Health Testing Centre	21 (20.6)	16 (24.6)	9 (7.4)
Walk-in or Urgent Care Clinic	3 (2.9)	3 (4.6)	1 (0.8)
Emergency Department	21 (20.6)	18 (27.7)	8 (6.6)
Telehealth	6 (5.9)	5 (7.7)	1 (0.8)
Other[a]	7 (6.9)	6 (9.2)	2 (1.6)
Number of types of medical attention sought, %	---	---	---
1	28 (27.5)	21 (32.3)	20 (16.4)
2	7 (6.9)	7 (10.8)	4 (3.3)
3	11 (10.8)	9 (13.8)	0 (0)
4	4 (3.9)	4 (6.2)	0 (0)
5	1 (1.0)	1 (1.5)	0 (0)

[a]"Other" for Cases includes Naturopath = 1; Naturopath and physiotherapist=2; Ottawa Public Health=1; Physiotherapist=1; Physiotherapist, massage therapist, and respiratory therapist=1; Post COVID care clinic=1;"Other" for Controls includes Oral Surgeon - bacteria on my tongue=1; Blood tests EKG performed related to chest pains after first dose of vaccine=1

Limitations

Several limitations may have influenced findings. First, most of our participants were not hospitalized for COVID-19. Given that people with more severe disease tend to elicit higher antibody titres (61, 62), results may have varied if more of our cohort required hospitalization during acute illness. Second, participants had limited diversity in terms of age, race, employment, pre COVID-19 comorbidities, and income status. Most reported high household income, were well-educated and employed pre COVID-19, and generally healthy. A study sample more representative of the total population at risk of PCC may have generated different findings. Third, as most clinical data was self-reported through electronic questionnaires, there Is risk of response

bias. Fourth, results from subgroup analyses of varying post-infection intervals (Supplementary Tables S2A–C) were limited by smaller sample sizes, and wave of infection Was a potentially confounding factor. For example, only One case and two controls infected March 2020–august 2020 had blood drawn 14–90 days post-infection (Supplementary Tables S2C). Fifth, study sample size also limited opportunity to assess for differences in serological response as a function of PCC subtypes. There is poor consensus on how subtypes of PCC character and severity should be defined (63). We used self-reported quality of life due to persistent symptoms as a proxy of PCC severity. Other studies have found that certain PCC symptoms/clusters correlate with stronger or weaker serological response post COVID-19. For example, Molnar et al. found serum levels of anti-spike IgG and anti-N IgG to be significantly lower in patients with severe fatigue post COVID-19, As compared to patients with non-severe fatigue (64), while Su et al. reported high anti-N IgG In cases of neurological PCC (65). Sixth, as only five controls and no cases received ≥1 COVID-19 vaccines ≥14 days prior infection, this study afforded limited opportunity to examine The protective capacity of hybrid immunity (66). Seventh, in lieu of established cut-offs for neutralization efficiency, these were derived by study team members to develop the in-house snELISA used in SSO. Lastly, the availability of IgG antibody subtypes would have permitted more detailed analyses. IgG subtypes exhibit distinct structural and functional properties. Notably, IgG1 and IgG3 antibodies, potent activators of effector mechanisms, play a critical role in early response to viral infections (67) and have been found to correlate with advanced COVID-19 severity, age, and comorbidities (68–70). Consequently, examining the distribution patterns of IgG subtypes holds promise for uncovering nuanced insights into SARS-CoV-2 immune response, and potentially elucidating connections between clinical risk factors, serological markers, and post-acute sequelae. However, as yet there are few reports on IgG subtypes in relation to PCC and this is a gap that warrants comprehensive investigation (16, 71, 72).

Next, steps

Given highly mixed results in the literature, we are undertaking a robust review on post-acute serological predictors of PCC. This strategy will allow us to examine trends in serological markers and associations with persistent sequelae among multiple studies with varying cohort characteristics and procedures to collect and analyze post-acute findings. We will investigate and report on different sources of heterogeneity which may influence trends. We will also attempt to

integrate review estimates in future analyses of SSO study data through use of Bayesian logistic regression. Given our limited sample size and distribution, encompassing prior information from the literature will facilitate more detailed and diverse analyses of serological predictors, accounting for clinical covariates. Finally, assessment of IgG subtypes will be pursued once available.

Conclusion

In summary, we found associations between Post COVID-19 Condition (PCC) and anti-N, anti-Spike, and anti-RBD IgG titres to be non-significant. However, as compared to infected-controls, PCC-cases had significantly higher neutralization efficiency, especially those to report deteriorated quality of life. Future investigations of IgG subtypes and PCC symptom clusters may elucidate new findings. Comparison with other studies is hampered by gross heterogeneity in cohort characteristics, definitions of PCC, and laboratory procedures. Standardized reporting of PCC and serological results would advance current efforts to collate and analyze inter-study findings. Finally, cases with PCC reported complex, ongoing sequelae a median of 255 days (183 IQR) post COVID-19, which underscores the potential need for health supports and services long after infection.

Funding
The author(s) declare financial support was received for the research, authorship, and/or publication of this article. EC is supported by the AI4PH Scholarship Program, funded by CIHR (Canadian Institutes of Health Research - Instituts de recherche en santé du Canada). YG is supported by a Charles Best and Frederick Banting (CGS-Doctoral award) from CIHR (476885). The Stop the Spread Ottawa study is funded by CIHR (424425), the COVID-19 Immunity Task Force (CITF), and the University of Ottawa. The study extension is funded by the Coronavirus Variants Rapid Response Network (CoVaRR-Net) (156941) (https://covarrnet.ca/investigating-long-term-variables-to-sars-cov-2-infection-and-vaccine-immunity/). CoVaRR-Net is funded by an operating grant from CIHR (FRN# 175622). We also acknowledge in-kind support from the NRC's Pandemic Response Challenge Program.

Acknowledgments
The authors acknowledge all investigators and partner organizations contributing to the project: CIs: Steffany Bennett, Pranesh Chakraborty, Miroslava Culf-Cuperlovic, Yves Durocher, Jennifer Quaid, Mary Simmerling. Partner organizations: National Research Council (NRC) of Canada, the Ottawa Hospital Research Institute, the University of Ottawa, and CoVaRR-Net (Coronavirus Variants Rapid Response Network). COVID-19 reagents (viral antigens, ACE2-biotin and anti-human IgG-HRP fusion) were generously provided by Yves Durocher at the NRC Montreal. UOttawa Serology and Diagnostics High Throughput Facility is supported by Danielle Dewar-Darch, Justino Hernandez Soto, and Abishek Xavier.

Conflict of interest
The authors declare that the research was conducted in the absence of any commercial or financial relationships that could be construed as a potential conflict of interest.

Publisher's note
All claims expressed in this article are solely those of the authors and do not necessarily represent those of their affiliated organizations, or those of the publisher, the editors and the reviewers. Any product that may be evaluated in this article, or claim that may be made by its manufacturer, is not guaranteed or endorsed by the publisher.

Supplementary material available here:
https://www.frontiersin.org/articles/10.3389/fpubh.2024.1276391/full#supplementary-material

References

1. CDC. COVID-19 and Your Health. Centers for Disease Control and Prevention. Published December 16, 2022. https://www.cdc.gov/coronavirus/2019-ncov/long-term-effects/index.html
2. Canada PHA of. Post-COVID-19 condition (long COVID). Published August 20, 2021. https://www.canada.ca/en/public-health/services/diseases/2019-novel-coronavirus-infection/symptoms/post-covid-19-condition.html
3. Long Covid Impact on Adult Americans: Early Indicators Estimating Prevalence and Cost. Solve Long COVID Initiative, April 5, 2022. https://solvecfs.org/wp-content/uploads/2022/04/Long_Covid_Impact_Paper.pdf
4. Government of Canada SC. Canadian COVID-19 Antibody and Health Survey (CCAHS). Published October 13, 2022. https://www23.statcan.gc.ca/imdb/p2SV.pl?Function=getSurvey&SDDS=5339
5. Davis HE, McCorkell L, Vogel JM, Topol EJ. Long COVID: major findings, mechanisms and recommendations. *Nat Rev Microbiol*. 2023;21(3):133-146. doi:10.1038/s41579-022-00846-2
6. Understanding the Post COVID-19 Condition (Long COVID) in Adults and the Expected Burden for Ontario. Ontario COVID-19 Science Advisory Table. doi:10.47326/ocsat.2022.03.65.1.0
7. Castanares-Zapatero D, Chalon P, Kohn L, et al. Pathophysiology and mechanism of long COVID: a comprehensive review. *Annals of medicine*. 2022;54(1). doi:10.1080/07853890.2022.2076901
8. Perlis RH, Santillana M, Ognyanova K, et al. Prevalence and Correlates of Long COVID Symptoms Among US Adults. *JAMA Netw Open*. 2022;5(10):e2238804-e2238804. doi:10.1001/jamanetworkopen.2022.38804
9. Post-COVID-19 Condition in Canada: What we know, what we don't know, and a framework for action. Published May 17, 2023. https://science.gc.ca/site/science/en/office-chief-science-advisor/initiatives-covid-19/post-covid-19-condition-canada-what-we-know-what-we-dont-know-and-framework-action
10. Chen C, Haupert SR, Zimmermann L, et al. Global Prevalence of Post COVID-19 Condition or Long COVID: A Meta-Analysis and Systematic Review. J Infect Dis. Published online April 16, 2022:jiac136. doi:10.1093/infdis/jiac136
11. Azzolini E, Levi R, Sarti R, et al. Association Between BNT162b2 Vaccination and Long COVID After Infections Not Requiring Hospitalization in Health Care Workers. *JAMA*. 2022;328(7):676-678. doi:10.1001/jama.2022.11691
12. Fernández-de-las-Peñas C, Notarte KI, Peligro PJ, et al. Long-COVID Symptoms in Individuals Infected with Different SARS-CoV-2 Variants of Concern: A Systematic Review of the Literature. *Viruses*. 2022;14(12). doi:10.3390/v14122629
13. Byambasuren O, Stehlik P, Clark J, et al. Effect of covid-19 vaccination on long covid: systematic review. *BMJ Medicine*. 2023;2(1). doi:10.1136/bmjmed-2022-000385
14. Notarte KI, Catahay JA, Velasco JV, et al. Impact of COVID-19 vaccination on the risk of developing long-COVID and on existing long-COVID symptoms: A systematic review. eClinicalMedicine. 2022;53. doi:10.1016/j.eclinm.2022.101624
15. Munblit D, Nicholson TR, Needham DM, et al. Studying the post-COVID-19 condition: research challenges, strategies, and importance of Core Outcome Set development. *BMC Med*. 2022;20(1):1-13. doi:10.1186/s12916-021-02222-y
16. Cervia C, Zurbuchen Y, Taeschler P, et al. Immunoglobulin signature predicts risk of post-acute COVID-19 syndrome. *Nat Commun*. 2022;13(1):1-12. doi:10.1038/s41467-021-27797-1
17. Knight DRT, Munipalli B, Logvinov II, et al. Perception, Prevalence, and Prediction of Severe Infection and Post-acute Sequelae of COVID-19. *The American Journal of the Medical Sciences*. 2022;363(4):295-304. doi:10.1016/j.amjms.2022.01.002
18. Fabbri A, Voza A, Riccardi A, Vanni S, De Iaco F. Unfavorable Outcome and Long-Term Sequelae in Cases with Severe COVID-19. *Viruses*. 2023;15(2):485. doi:10.3390/v15020485

19. Tsampasian V, Elghazaly H, Chattopadhyay R, et al. Risk Factors Associated With Post−COVID-19 Condition: A Systematic Review and Meta-analysis. *JAMA Intern Med*. Published online March 23, 2023. doi:10.1001/jamainternmed.2023.0750
20. Jia X, Cao S, Lee AS, et al. Anti-nucleocapsid antibody levels and pulmonary comorbid conditions are linked to post–COVID-19 syndrome. *JCI Insight*. 2022;7(13). doi:10.1172/jci.insight.156713
21. Krishna BA, Lim EY, Mactavous L, et al. Evidence of previous SARS-CoV-2 infection in seronegative patients with long COVID. eBioMedicine. 2022;81:104129. doi:10.1016/j.ebiom.2022.104129
22. García-Abellán J, Padilla S, Fernández-González M, et al. Antibody Response to SARS-CoV-2 is Associated with Long-term Clinical Outcome in Patients with COVID-19: a Longitudinal Study. J Clin Immunol. 2021;41(7):1490-1501. doi:10.1007/s10875-021-01083-7
23. Gaebler C, Wang Z, Lorenzi JCC, et al. Evolution of antibody immunity to SARS-CoV-2. *Nature*. 2021;591(7851):639-644. doi:10.1038/s41586-021-03207-w
24. Blomberg B, Mohn KGI, Brokstad KA, et al. Long COVID in a prospective cohort of home-isolated patients. *Nat Med*. 2021;27(9):1607-1613. doi:10.1038/s41591-021-01433-3
25. García-Abellán J, Fernández M, Padilla S, et al. Immunologic phenotype of patients with long-COVID syndrome of 1-year duration. *Front Immunol*. 2022;13. doi:10.3389/fimmu.2022.920627
26. Gerhards C, Thiaucourt M, Kittel M, et al. Longitudinal assessment of anti-SARS-CoV-2 antibody dynamics and clinical features following convalescence from a COVID-19 infection. *International Journal of Infectious Diseases*. 2021;107:221-227. doi:10.1016/j.ijid.2021.04.080
27. Lier J, Stoll K, Obrig H, et al. Neuropsychiatric phenotype of post COVID-19 syndrome in non-hospitalized patients. *Front Neurol*. 2022;13. doi:10.3389/fneur.2022.988359
28. Augustin M, Schommers P, Stecher M, et al. Post-COVID syndrome in non-hospitalised patients with COVID-19: a longitudinal prospective cohort study. *The Lancet Regional Health - Europe*. 2021;6:100122. doi:10.1016/j.lanepe.2021.100122
29. Durstenfeld MS, Peluso MJ, Kelly JD, et al. Role of antibodies, inflammatory markers, and echocardiographic findings in postacute cardiopulmonary symptoms after SARS-CoV-2 infection. *JCI Insight*. 2022;7(10). doi:10.1172/jci.insight.157053
30. Collins E, Galipeau Y, Arnold C, et al. Cohort profile: Stop the Spread Ottawa (SSO)—a community-based prospective cohort study on antibody responses, antibody neutralisation efficiency and cellular immunity to SARS-CoV-2 infection and vaccination. *BMJ Open*. 2022;12(9):e062187. doi:10.1136/bmjopen-2022-062187
31. Colwill K, Galipeau Y, Stuible M, et al. A scalable serology solution for profiling humoral immune responses to SARS-CoV-2 infection and vaccination. Clinical & Translational Immunology. 2022;11(3):e1380. doi:10.1002/cti2.1380
32. Kessler RC, Andrews G, Colpe LJ, et al. Short screening scales to monitor population prevalences and trends in non-specific psychological distress. Psychological Medicine. 2002;32(6):959-976. doi:10.1017/S0033291702006074
33. Horowitz M, Wilner N, Alvarez W, et al. Impact of Event Scale: a measure of subjective stress. Psychosomatic medicine. 1979;41(3). doi:10.1097/00006842-197905000-00004
34. Harrell, FE. Regression modeling strategies. Second edition, Springer, 2015.
35. Layton AT, Sadria M. Understanding the dynamics of SARS-CoV-2 variants of concern in Ontario, Canada: a modeling study. Sci Rep. 2022;12(1):1-16. doi:10.1038/s41598-022-06159-x
36. Ontario Dashboard. Ontario COVID-19 Science Advisory Table. Published September 8, 2022. https://covid19-sciencetable.ca/ontario-dashboard/
37. Elslande JV, Oyaert M, Lorent N, et al. Lower persistence of anti-nucleocapsid compared to anti-spike antibodies up to one year after SARS-CoV-2 infection. Diagnostic Microbiology and Infectious Disease. 2022;103(1):115659. doi:10.1016/j.diagmicrobio.2022.115659
38. Van den Hoogen LL, Smits G, van Hagen CCE, et al. Seropositivity to Nucleoprotein to detect mild and asymptomatic SARS-CoV-2 infections: A complementary tool to detect breakthrough infections after COVID-19 vaccination? Vaccine. 2022;40(15):2251-2257. doi:10.1016/j.vaccine.2022.03.009

39. Krutikov M, Palmer T, Tut G, et al. Prevalence and duration of detectable SARS-CoV-2 nucleocapsid antibodies in staff and residents of long-term care facilities over the first year of the pandemic (VIVALDI study): prospective cohort study in England. *The Lancet Healthy Longevity*. 2022;3(1):e13-e21. doi:10.1016/S2666-7568(21)00282-8
40. Whitaker HJ, Gower C, Otter AD, et al. Nucleocapsid antibody positivity as a marker of past SARS-CoV-2 infection in population serosurveillance studies: impact of variant, vaccination, and choice of assay cut-off. medRxiv. Published online October 26, 2021:2021.10.25.21264964. doi:10.1101/2021.10.25.21264964
41. Seeßle J, Waterboer T, Hippchen T, et al. Persistent Symptoms in Adult Patients 1 Year After Coronavirus Disease 2019 (COVID-19): A Prospective Cohort Study. *Clin Infect Dis*. 2022;74(7):1191-1198. doi:10.1093/cid/ciab611
42. Peluso MJ, Lu S, Tang AF, et al. Markers of Immune Activation and Inflammation in Individuals With Postacute Sequelae of Severe Acute Respiratory Syndrome Coronavirus 2 Infection. *J Infect Dis*. 2021;224(11):1839-1848. doi:10.1093/infdis/jiab490
43. Ozonoff A, Schaenman J, Jayavelu ND, et al. Phenotypes of disease severity in a cohort of hospitalized COVID-19 patients: Results from the IMPACC study. *eBioMedicine*. 2022;83. doi:10.1016/j.ebiom.2022.104208
44. García-Abellán J, Fernández M, Padilla S, et al. Immunologic phenotype of patients with long-COVID syndrome of 1-year duration. *Front Immunol*. 2022;13:920627. doi:10.3389/fimmu.2022.920627
45. Blomberg B, Mohn KGI, Brokstad KA, et al. Long COVID in a prospective cohort of home-isolated patients. *Nat Med*. 2021;27(9):1607-1613. doi:10.1038/s41591-021-01433-3
46. Sancilio A, Schrock JM, Demonbreun AR, et al. COVID-19 symptom severity predicts neutralizing antibody activity in a community-based serological study. *Sci Rep*. 2022;12(1):1-7. doi:10.1038/s41598-022-15791-6
47. Garcia-Beltran WF, Lam EC, Astudillo MG, et al. COVID-19-neutralizing antibodies predict disease severity and survival. *Cell*. 2021;184(2):476-488.e11. doi:10.1016/j.cell.2020.12.015
48. Liu L, To KKW, Chan KH, et al. High neutralizing antibody titer in intensive care unit patients with COVID-19. Emerging Microbes & Infections. Published online July 20, 2020. https://www.tandfonline.com/doi/abs/10.1080/22221751.2020.1791738
49. Castanares-Zapatero D, Chalon P, Kohn L, et al. Pathophysiology and mechanism of long COVID: a comprehensive review. *Annals of medicine*. 2022;54(1). doi:10.1080/07853890.2022.2076901
50. Batiha GES, Al-kuraishy HM, Al-Gareeb AI, Welson NN. Pathophysiology of Post-COVID syndromes: a new perspective. Virol J. 2022;19(1):1-20. doi:10.1186/s12985-022-01891-2
51. Buck AM, Deitchman AN, Takahashi S, et al. The Breadth of the Neutralizing Antibody Response to Original SARS-CoV-2 Infection is Linked to the Presence of Long COVID Symptoms. *medRxiv*. 2023:2023.03.30.23287923. doi:10.1101/2023.03.30.23287923
52. Afrin LB, Weinstock LB, Molderings GJ. Covid-19 hyperinflammation and post-Covid-19 illness may be rooted in mast cell activation syndrome. *International Journal of Infectious Diseases*. 2020;100:327-332. doi:10.1016/j.ijid.2020.09.016
53. Osmanov IM, Spiridonova E, Bobkova P, et al. Risk factors for post-COVID-19 condition in previously hospitalised children using the ISARIC Global follow-up protocol: a prospective cohort study. *European Respiratory Journal*. 2022;59(2). doi:10.1183/13993003.01341-2021
54. Kostev K, Smith L, Koyanagi A, Konrad M, Jacob L. Post-COVID-19 conditions in children and adolescents diagnosed with COVID-19. Pediatr Res. Published online May 14, 2022:1-6. doi:10.1038/s41390-022-02111-x
55. Jacobs ET, Catalfamo CJ, Columbo PM, et al. Pre-existing conditions associated with post-acute sequelae of COVID-19. Journal of Autoimmunity. 2023;135:102991. doi:10.1016/j.jaut.2022.102991
56. Bell ML, Catalfamo CJ, Farland LV, et al. Post-acute sequelae of COVID-19 in a non-hospitalized cohort: Results from the Arizona CoVHORT. *PLOS ONE*. 2021;16(8):e0254347. doi:10.1371/journal.pone.0254347

57. Santhosh L, Block B, Kim SY, et al. Rapid design and implementation of Post-COVID-19 Clinics. Chest. 2021;160(2):671. doi:10.1016/j.chest.2021.03.044
58. Ibrahim Mohamed HM, Atya M sayed, Ahmed GH, Abdelmohsen SA, Sobhy KM, Hussein AM. Telehealth program: Effect of Physiotherapy Intervention on Dyspnea, Fatigue and Functional Status of Post COVID-19 Syndrome patients. *Assiut Scientific Nursing Journal*. 2022;10(32):265-280. doi:10.21608/asnj.2022.167006.1437
59. Houben S, Bonnechère B. The Impact of COVID-19 Infection on Cognitive Function and the Implication for Rehabilitation: A Systematic Review and Meta-Analysis. *International Journal of Environmental Research and Public Health*. 2022;19(13):7748. doi:10.3390/ijerph19137748
60. Garg A, Subramain M, Barlow PB, et al. Patient Experiences with a Tertiary Care Post-COVID-19 Clinic. *Journal of Patient Experience*. Published online January 17, 2023. doi:10.1177/23743735231151539
61. Nowakowski S, Kokonda M, Sultana R, et al. Association between Sleep Quality and Mental Health among Patients at a Post-COVID-19 Recovery Clinic. *Brain Sciences*. 2022;12(5):586. doi:10.3390/brainsci12050586
62. Levan S, Mourad M, Block B, Shah R, Santhosh L. Impact of a Multidisciplinary Post-COVID-19 Clinic on Hospital Admissions and ED Visits. *Chest*. Published online January 2023:S0012369223000090. doi:10.1016/j.chest.2022.12.031
63. Kotb N, Barreto L, Janaudis-Ferreira T. Post-exertional malaise in pulmonary rehabilitation after COVID-19: Are we not giving enough attention? Canadian Journal of Respiratory, Critical Care, and Sleep Medicine. 2023;7(2):93-118. doi:10.1080/24745332.2022.2150722
64. Park JH, Cha MJ, Choi H, et al. Relationship between SARS-CoV-2 antibody titer and the severity of COVID-19. *Journal of Microbiology, Immunology and Infection*. 2022;55(6):1094-1100. doi:10.1016/j.jmii.2022.04.005
65. Yan X, Chen G, Jin Z, et al. Anti-SARS-CoV-2 IgG levels in relation to disease severity of COVID-19. Journal of Medical Virology. 2022;94(1):380-383. doi:10.1002/jmv.27274
66. Basharat S, Chao YS, McGill SC. Subtypes of Post–COVID-19 Condition: A Review of the Emerging Evidence. *cjht*. 2022;2(12). doi:10.51731/cjht.2022.516
67. Molnar T, Varnai R, Schranz D, et al. Severe fatigue and memory impairment are associated with lower serum level of anti-SARS-CoV-2 antibodies in patients with post-COVID symptoms. *Journal of Clinical Medicine*. 2021;10(19):4337. doi:10.3390/jcm10194337
68. Su Y, Yuan D, Chen DG, et al. Multiple early factors anticipate post-acute COVID-19 sequelae. *Cell*. 2022;185(5):881-895.e20. doi:10.1016/j.cell.2022.01.014
69. Bobrovitz N, Ware H, Ma X, et al. Protective effectiveness of previous SARS-CoV-2 infection and hybrid immunity against the omicron variant and severe disease: a systematic review and meta-regression. *The Lancet Infectious Diseases*. 2023;23(5):556-567. doi:10.1016/S1473-3099(22)00801-5
70. Vidarsson G, Dekkers G, Rispens T. IgG Subclasses and Allotypes: From Structure to Effector Functions. Frontiers in Immunology. 2014;5. doi:10.3389/fimmu.2014.00520
71. Yates JL, Ehrbar DJ, Hunt DT, et al. Serological analysis reveals an imbalanced IgG subclass composition associated with COVID-19 disease severity. Cell Reports Medicine. 2021;2(7):100329. doi:10.1016/j.xcrm.2021.100329
72. Korobova ZR, Zueva EV, Arsentieva NA, et al. Changes in Anti-SARS-CoV-2 IgG Subclasses over Time and in Association with Disease Severity. Viruses. 2022;14(5):941. doi:10.3390/v14050941
73. Luo H, Jia T, Chen J, Li X, Zhang R, Sun C. The Characterization of Disease Severity Associated IgG Subclasses Response in COVID-19 Patients. Front Immunol. 2021;12:632814. doi:10.3389/fimmu.2021.632814
74. Abel J, Walter AJ, Glück V, et al. IgG4 serum levels are not elevated in cases of Post-COVID syndrome. bioRxiv. Published online March 1, 2023:2023.03.01.530454. doi:10.1101/2023.03.01.530454
75. Cervia C, Zurbuchen Y, Taeschler P, Ballouz T, Menges D, Hasler S, et al. Immunoglobulin signature predicts risk of post-acute COVID-19 syndrome. Nat Commun (2022) 13:446. doi: 10.1038/s41467-021-27797-1

76. Collins E, Philippe E, Gravel CA, Hawken S, Langlois MA, Little J. Serological markers and long COVID—A rapid systematic review. European Journal of Clinical Investigation. Published online December 11, 2023:e14149. doi:10.1111/eci.14149

A-1.2 Homogeneous surrogate virus neutralization assay to rapidly assess neutralization activity of anti-SARS-CoV-2 antibodies

Preface

(This work has been previously published as a research article)

Kim SJ, Yao Z, Marsh MC, Eckert DM, Kay MS, Lyakisheva A, Pasic M, Bansal A, Birnboim C, Jha P, **Galipeau Y**, Langlois MA, Delgado JC, Elgort MG, Campbell RA, Middleton EA, Stagljar I, Owen SC. **Homogeneous surrogate virus neutralization assay to rapidly assess neutralization activity of anti-SARS-CoV-2 antibodies**. Nat Commun. 2022 Jul 1;13(1):3716.

https://doi.org/10.1038/s41467-022-31300-9

© The Author(s) 2022. This article is licensed under a Creative Commons Attribution 4.0 International License, which permits use, sharing, adaptation, distribution and reproduction in any medium or format, as long as you give appropriate credit to the original author(s) and the source, provide a link to the Creative Commons license, and indicate if changes were made. The images or other third party material in this article are included in the article's Creative Commons license, unless indicated otherwise in a credit line to the material. If material is not included in the article's Creative Commons license and your intended use is not permitted by statutory regulation or exceeds the permitted use, you will need to obtain permission directly from the copyright holder. To view a copy of this license, visit http://creativecommons.org/ licenses/by/4.0/.

Abstract

The COVID-19 pandemic triggered the development of numerous diagnostic tools to monitor infection and to determine immune response. Although assays to measure binding antibodies against SARS-CoV-2 are widely available, more specific tests measuring neutralization activities of antibodies are immediately needed to quantify the extent and duration of protection that results from infection or vaccination. We previously developed a 'Serological Assay based on a Tri-part split-NanoLuc® (SATiN)' to detect antibodies that bind to the spike (S) protein of SARS-CoV-2. Here, we expand on our previous work and describe a reconfigured version of the SATiN assay, called Neutralization SATiN (Neu-SATiN), which measures neutralization activity of antibodies directly from convalescent or vaccinated sera. The results obtained with our assay and other neutralization assays are comparable but with significantly shorter preparation and run time for Neu-SATiN. As the assay is modular, we further demonstrate that Neu-SATiN enables rapid assessment of the effectiveness of vaccines and level of protection against existing SARS-CoV-2 variants of concern and can therefore be readily adapted for emerging variants.

Introduction

SARS-CoV-2 continues to threaten the world's health as emerging variants of concern have the potential to circumvent deployed vaccines. Simple and rapid SARS-CoV-2 serological tests are needed to accurately measure the level and duration of neutralization activity of antibodies that arise from natural infection or vaccination. Currently, there are several FDA-approved serological tests under Emergency Use Authorizations (EUA), many of which can detect IgM or IgG against SARS-CoV-2, but do not measure their neutralization efficacy specifically[1,2,3]. Functional neutralizing antibody titers are often measured with pseudotyped viruses, however, long assay time and discrepancies in published assay protocols have limited their use[4,5,6]. Alternatively, surrogate virus neutralization assays have been developed to circumvent the use of pseudovirions[7,8,9,10]. Although some of these assays have shown successful measurement for serosurveillance of clinical samples, they often resemble ELISA, requiring multiple time-consuming binding and washing steps, while others have not yet reported successful measurement of clinical samples, likely due to the instability of recombinant proteins in serum and plasma. Here, we report the development of a homogeneous surrogate virus neutralization assay (hsVNA) called "Neu-SATiN" by reconfiguring our previously designed serological assay (Serological Assay based on split Tri-part Nanoluciferase; SATiN)[11] to quantify the degree of neutralization from antibodies directly from plasma or serum. SATiN is a serological assay based on a protein-protein interaction approach for detection of IgGs against the Spike protein of SARS-CoV-2[12].

In our previous report, we developed SATiN as a homogeneous serological assay platform that utilizes a tri-part NanoLuc®, which is split into two small peptide tags, β9 and β10 (each about 1 kDa), and one large fragment, Δ11S (18 kDa). The SATiN assay utilizes spike protein and Protein G tagged with either β9 or β10. Upon simultaneous binding of the tagged spike protein and Protein G to anti-SARS-CoV-2 antibody, β9 and β10 are brought into proximity which induces refolding of Δ11S into active luciferase, producing glow-type luminescence[11]. Using the same tri-part NanoLuc®, we now show the development of a homogeneous neutralization assay version of SATiN (Neu-SATiN). In Neu-SATiN, enzyme fragment peptides, β9 or β10, are fused to the ACE2 receptor, the target of infection, and to the SARS-CoV-2 spike (S) protein. We hypothesized that when the ACE2 and the S proteins interact, the fused split-NanoLuc® fragments are driven to within ~100 Å of each other, allowing Δ11S to reconstitute into fully functional NanoLuc®.

Importantly, when the interaction between the ACE2 and S proteins is blocked by neutralizing antibodies, the tags are prevented from interacting and subsequent complementation of NanoLuc® is blocked (Fig. 1a). Therefore, in Neu-SATiN, the level of neutralization correlates with the decrease of luminescence. As the assay is intentionally modular, full-length ectoderm of the S protein of SARS-CoV-2 variants of concern can be quickly produced and swapped with wild-type S protein to assess immunological protection. Moreover, as Neu-SATiN is designed to be a "mix-and-read" assay that is performed at the conventional lab bench, the actual hands-on time is <30 min, significantly improving turnaround time.

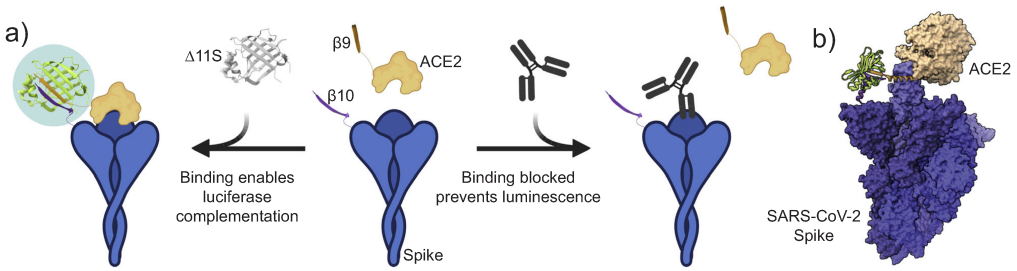


Fig. 1: General schematic of the Neu-SATiN COVID-19 neutralization assay and molecular modeling of spike (S) protein and ACE2 interaction. a Tri-part NanoLuc® peptide fragments are individually fused to recombinant S protein (purple) and ACE2 (tan). Interaction of S protein and ACE2 induces complementation of the split-luciferase and 'turns on' luminescence (left). In the presence of neutralizing antibodies, the interaction between S protein and ACE2 is blocked, preventing luminescence (right). Figure generated using BioRender. **b** Molecular model of the predicted refolding of NanoLuc® (PDB ID: 5IBO) is shown (green) after complementation of fragments β10 and β9 is driven by the interaction between full spike protein (trimer) and ACE2 (PDB ID: 7A97).

Results

Protein fusion design and testing

We considered three options for fusing the split-luciferase fragments to the SARS-CoV-2 spike (S) protein and its target, the human ACE2 receptor: (1) N-terminus, (2) C-terminus, or (3) both termini. Although surface loops are possible fusion points, modifying these domains may interfere with neutralizing antibody binding. Based on our previous experience, we know that reconstitution of split-NanoLuc® is most efficient when the fusion locations are within ~50–100 Å[13,14,15]. We

used molecular modeling to determine possible fusion points on S protein and ACE2 that place fragments within this proximity (Figs. 2a and 3a).

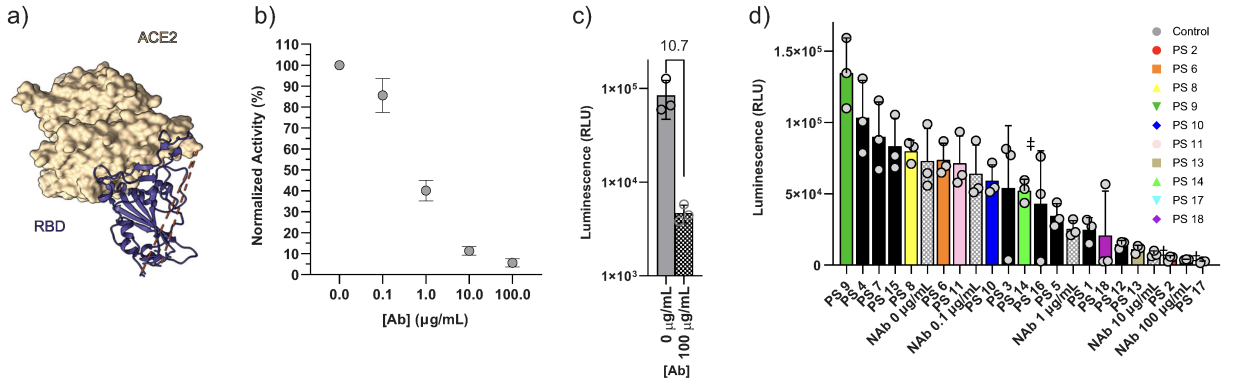


Fig. 2: Binder pair screening in human serum and patient samples (PS 1–18).a Molecular modeling of the distances between N-terminus of ACE2 to the N-terminus of RBD is ~60 Å and to the C-terminus is ~53 Å (PDB ID: 6M0J). As such, luciferase fragments can be fused at either terminus of RBD and N-terminus of ACE2. **b** (S)RBD-β9 and β10-ACE2 binder pair was screened with increasing concentrations of neutralizing Ab (NAb, Sino Biological 40592-MM57) in human serum. **c** Using (S)RBD-β9 and β10-ACE2 binder pair, the signal between 0 µg/mL of NAb (darker color) vs. 100 µg/mL of NAb (lighter color adjacent bar) shows a 10-fold decrease upon neutralization. **d** Testing 18 patient plasma samples: (S)RBD-β9 and β10-ACE2 were mixed directly with plasma samples, followed by the addition of the detection solution (Δ11S and substrate). Samples 16, 17, and 18 (indicated by ‡ above bar) are known to be convalescent whereas other samples are from ICU patients with unknown antibody presence/levels. Source data are provided as a Source data file.

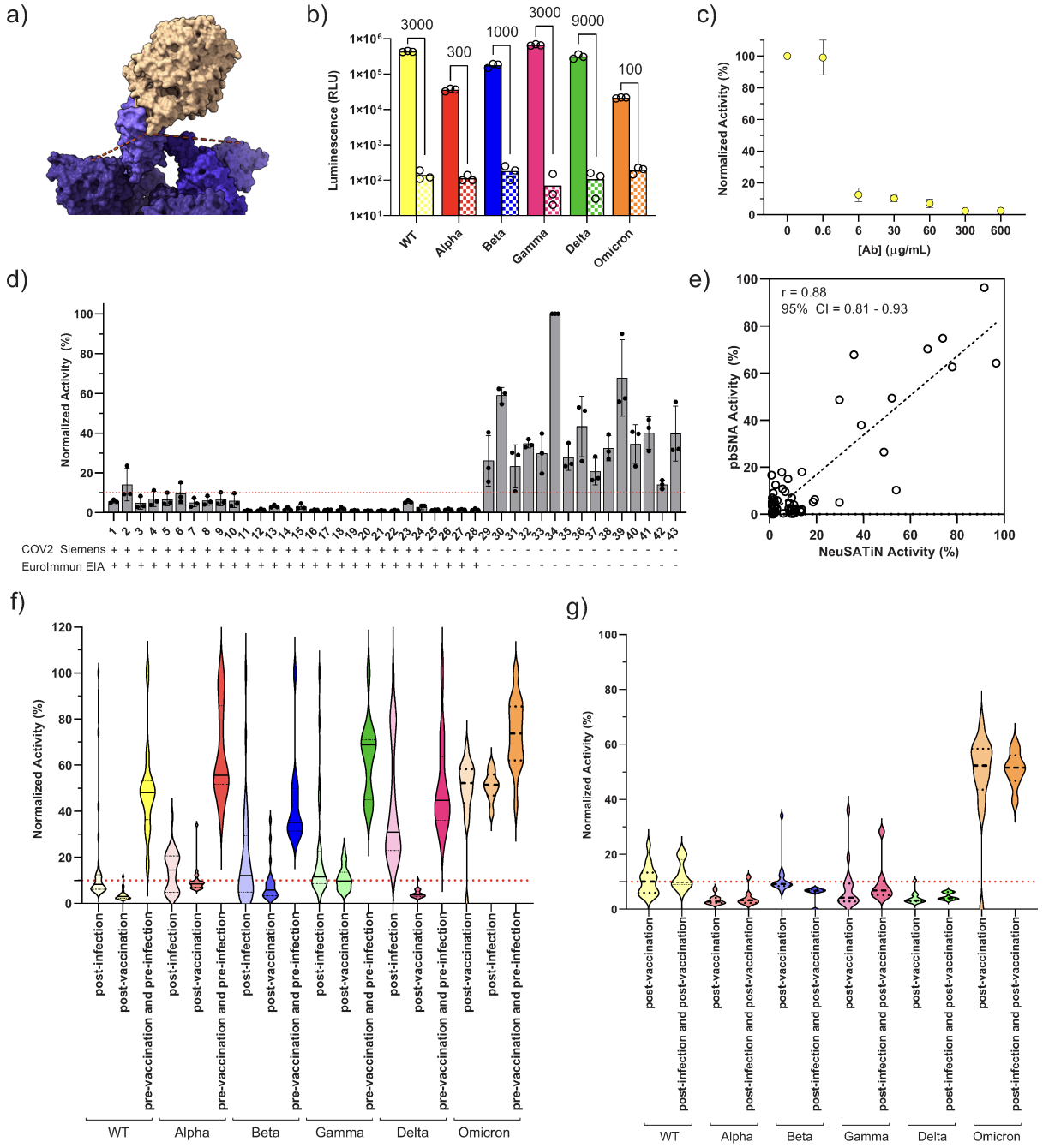


Fig. 3: Validation of full spike proteins (wild type and variants) and ACE2 binders in the serosurveillance of clinical samples. a Molecular modeling of the distances between N-terminus of ACE2 to the N-termini of nearest S protein is ~48 Å and ~88 Å, respectively (PDB ID: 7A97). **b** Comparison of signal and background for the full spike (wild type and variants) and ACE2 pairs. **c** Serial dilution of a commercially available NAb (Sino Biological, 40592-R001) in the presence of β10-(S)WT and β9-ACE2-Fc pair. **d** Serum samples that have been tested previously on two different COVID-19 detection assays were also tested using Neu-SATiN. Wild type full spike protein with β10 tag (β10-(S)WT) and ACE2 with β9 tag (β9-ACE2-Fc) was used as the binders. Signals from patient samples were normalized to the signal from normal human serum with the binders alone (no neutralizing antibodies). The red dotted line at 10% activity (i.e., 90% neutralization) indicates the cutoff line to distinguish neutralizing samples from the non-neutralizing samples; '+' and '−' signs below the sample number indicate the result from two prior tests detecting anti-SARS-CoV-2 antibodies (COV2G Siemens 1st Gen and EUROIMMUN EIA). **e** Activity measured in

protein-based surrogate neutralization assay (pbSNA) versus neu-SATiN for the wild-type (WT) variant shows high correlation with a Pearson's correlation test *r* value of 0.88. $N = 66$. **f** Neutralization efficacy of patient samples against WT and variant S proteins. Samples used in (**d**) ($n = 43$) were tested with an additional $n = 35$ patient samples that were positive for anti-SARS-CoV-2 antibodies. Luminescence signals from each patient serum were measured and normalized to human serum (no NAb). Known post-vaccination, post-infection, and negative (no known infection or vaccination) samples were plotted separately. Red dotted line at 10% indicates the cutoff between the negative samples and the positive samples for distinction of neutralization. **g** Comparison of serum data from patients that were vaccinated to patients that were vaccinated after a documented infection ($n = 40$). All patient samples were collected before November 2021, prior to any known Omicron infections. Source data are provided as a Source data file.

To test feasibility, we initially built the system using only the receptor-binding domain (RBD) of the SARS-CoV-2 spike protein and ACE2. Based on molecular modeling of RBD and ACE2 (Fig. 2a)[16], the distance from the N-terminus of ACE2 to the N-terminus of RBD is ~60 Å and to the C-terminus is ~53 Å (PDB ID: 6M0J). In contrast, the C-terminus of ACE2 is more than 100 Å away from either terminus of RBD and thus was excluded as a potential tag fusion site. The complete list of binders used in this study is listed in Supplementary Table 2. Using purified recombinant proteins, we confirmed that the engineered RBD and ACE2 binders with complementary tags produced detectable luminescent signal when combined with the large fragment of the split luciferase, Δ11S, in human serum. Each binder combination shows substantial luminescence; however, there are differences in signal-to-background ratios (Supplementary Fig. 1a). We also confirmed substantial decrease in the signal when the binders were incubated with neutralizing antibody (NAb) (Sino Biological, 40592-MM57), indicating inhibition of RBD binding to ACE2 to prevent complementation of the split-luciferase fragments. For any given pair, the fractional decrease in luminescent signal as a function of increasing concentration of NAb displays a typical dose–response curve for inhibition that is specific to the NAb (Supplementary Fig. 1b). This suggests that although the maximum signal intensity produced by each binder pair is different, the proportional decrease in the signal in the presence of NAb is similar. Therefore, the ability to measure NAb antiviral activity is feasible with several different pairs. We characterized binder pairs further by calculating IC50 of the NAb using each pair and stability of the complex in high concentrations of non-binding IgG (Supplementary Fig. 1c, d). We selected the pair (S)RBD-β9 and β10-ACE2 based on the lowest discrepancy in IC50 value compared to the manufacturer's report and in resolving concentration to response.

Evaluation of Neu-SATiN on convalescent samples

After validating Neu-SATiN's ability to detect NAb activity, we validated the assay with clinical plasma samples from actively infected (from ICU) and convalescent patients (n = 18). The plasma samples were tested and binned into 5 different groups in respect to their relative luminescence compared to the control NAb (Fig. 2d). Of the convalescent patient samples (PS 16, 17, 18), patient sample 17 (PS 17) showed inhibition similar to 100 µg/mL of the control NAb. PS 16 and PS 18 were not as effective as PS 17, but still showed significant decrease in luminescence intensity compared to 0 µg/mL of NAb. As the neutralization activity depends on the epitope, affinity and concentration of the antibodies, the comparison between the control antibody and the antibodies in patient plasma is only relative. Nevertheless, our data confirm that Neu-SATiN is able to distinguish the presence or absence of antiviral antibodies and quantify the relative level of neutralization directly in clinical samples.

We compared Neu-SATiN to a pseudovirus neutralization (PSV) assay based on a human immunodeficiency virus (HIV) system with luciferase gene reporter (Supplementary Fig. 1e, f). The results from Neu-SATiN and PSV assay show good correlation at highest antibody concentrations (Extended Fig. 1e, f) with a Pearson's r value of 0.86. Correlation is slightly lower across all IgG concentrations (Supplementary Fig. 1e) with a Pearson's r value of 0.81. Both PSV assay and Neu-SATiN showed that PS 17 had the highest inhibition activity, and this was similar to the positive control (human serum spiked with 100 µg/mL NAb).

Neu-SATiN full-length S protein evaluation of serum samples with differing levels of virus protection

Even though many of the antibodies produced by vaccines target the RBD of S protein[17,18], the more pressing concern is protection against variants of concern which often have mutations outside of the RBD[19,20]. In fact, all currently approved vaccines in US and Canada are based on full-length S protein sequences and have been generated before the onset of variants in 2021. As such, we expanded Neu-SATiN using ACE2 and the full ectodomain of S protein, trimerized through the foldon domain, including known amino acid substitutions to stabilize conformation[21]. We hypothesized that using the full, trimerized S protein should provide a more comprehensive measurement of the neutralization effect. Molecular modeling was used again to examine the distances between the termini of two proteins (Fig. 3a) using PDB ID: 7A9722. Based on this

analysis, we decided to fuse β10 to the N-terminus of S protein and β9 to the N-terminus of ACE2. The length of linker connecting the proteins to the tags was also doubled from 9 to 18 amino acids to increase the flexibility of the tags and to encompass a broader range of potential binding confirmations. Consistent with previous studies[23], we found the interaction between S ectodomain and ACE2 monomer is relatively low, likely due to ACE2 instability, and decided to use a dimerized ACE2 binder created by fusing the ACE2 N-terminal domain (a.a. 16–614) with the human IgG Fc fragment (Supplementary Table 1). These two binders, denoted as β10-(S)-WT and β9-ACE2-Fc, were validated for binding-induced luminescence (Fig. 3b). The full wild-type spike protein (WT) version of the binder pair shows average luminescence signal of 1.6×106 RLU indicating successful complementation of the split-NanoLuc® fragments and shows a robust 3000-fold signal-to-background ratio. We produced mutated S proteins for each of the major SARS-CoV-2 variants of concern: Alpha, Beta, Gamma, Delta, and Omicron[19,20] (mutation sequences in Supplementary Table 2). The mutations were made throughout the ectodomain of S protein and not just limited to the RBD. Additional mutations were made to the furin cleavage site to prevent unwanted degradation of the binders by cell culture proteases and to enable purification of recombinant proteins[24,25]. The orientation of the tags on each protein was kept the same: β10-(S)Variant and β9-ACE2-Fc. All five variants (Alpha, Beta, Gamma, Delta, and Omicron) produced distinct luminescence signals with high signal-to-background (Fig. 3b). The neutralization of the WT pair (WT S protein with ACE2) corresponds well with concentrations of a NAb (Sino Biological, 40592-R001) (Fig. 3c); however, there was limited neutralization of most of the variants using this NAb (Supplementary Fig. 2).

We obtained another set of serum samples ($n = 43$) that have been tested with two different Emergency Use Authorized COVID-19 S protein-binding antibody assays: (1) COV2G Siemens 1st Gen (target antigen: RBD, cutoff: ≥1.0), and (2) EUROIMMUN (target antigen: S1, cutoff: ≥1.1). The samples can be further categorized into three different groups: (1) SARS-CoV-2 exposed with no vaccination history (post-infection, Samples 1–18), (2) SARS-CoV-2 exposed with vaccination history (post-infection and post-vaccination, Samples 19–28), and (3) neither exposed nor vaccinated (no infection and no vaccination, Samples 29–43). All of the samples were screened with our full-length-WT S protein Neu-SATiN for the presence of neutralizing

antibodies. Commercial human serum spiked with NAb (Sino Biological, 40592-R001) was used as a positive control and to determine relative neutralization activity of the patient samples.

Samples with previous infection history (Samples 1–28, $n = 28$) showed normalized activity score <10% (Fig. 3d—indicated by red dotted line) in Neu-SATiN, with the exception of Sample 2 (frequency = 27/28, 96%). These were also the samples that scored >20.00 in Siemens 1st Gen and >8 in EUROIMMUN EIA, both indicating the presence of anti-SARS-CoV-2 antibodies against the WT S protein (Supplementary Table 3). Intriguingly, when the patients were previously infected and then vaccinated (Samples 19–28, $n = 10$), their sera showed normalized activity scores of 5% or below (frequency = 10/10, 100%). The various levels of neutralization shown in Samples 1–18 are possibly due to difference in sample collection day post-infection, as it is known that antibody levels are highest 4–5 weeks after symptom onset[26,27]. Conversely, all SARS-CoV-2 negative patients (Samples 29–43, $n = 15$), based on standard antibody test, showed signals above 10% (frequency = 15/15, 100%), indicating no neutralization activity. Further, the activity of Neu-SATiN was benchmarked against a protein-based neutralization assay (Supplementary Fig. 3) of the wild-type variant spike protein, showing good correlation with a Pearson's r value of 0.88 ($N = 66$) (Fig. 3e) and of the Omicron variant spike protein (Supplementary Fig. 4). The protein-based neutralization assay is performed by coating microwells with recombinant SARS-CoV-2 Spike trimer and then adding plasma from patient samples. An ACE2-HRP construct is used to assess the presence of neutralizing antibodies that prevent binding of ACE2 to Spike trimer.

Altogether, the data supports that our newly developed Neu-SATiN neutralization assay is a reliable surrogate test that shows congruent results compared to already established tests. As we recognize that immunities generated by vaccination versus infection are known to produce antibodies targeting different parts of S protein[28] and that the protection against variants based on vaccination and/or previous infection is variable, we tested the same patient samples used to validate β10-(S)WT/ β9-ACE2-Fc, along with an additional set of infected patients ($n = 35$), for the samples' neutralization efficacies towards different variants of concern. Since a universal NAb that can neutralize WT and all variants is not available, we were not able to determine relative degree of neutralization compared to a known concentration of NAb for each of the variants, but only for the WT. Instead, we compared fractional decrease in luminescence signal from the

positive samples to negative samples for each variant pair; the highest signal observed from the negative group was considered 100% activity (i.e., no decrease in signal) and subsequent decrease in signal was determined for the positive groups. As shown in Fig. 3f, the NAb negative samples (darkest color violin plots) tend to display a wide range of signal compared to the NAb positive groups. Overall, the mean fractional signal observed from the positive samples (post-infection or post-vaccination) tested either with WT or variant pairs were 10% or lower. In other words, the signal measured from the positive samples were <10% of the signal from the negative group. This suggests that most of the samples within the positive groups have some level of neutralization ability towards each of the variant SARS-CoV-2s. In particular, both WT and Gamma variant were neutralized almost fully by immunity generated by vaccination; however, there appears to be a subset of samples within the Delta, Alpha, and Beta variant groups with minimal neutralization even after infection and/or vaccination (Fig. 3g). It was also notable that natural immunity generated by infection with SARS-CoV-2 was not sufficient to neutralize the Gamma variant and that vaccination was required for stronger neutralization and that almost all samples were ineffective at neutralizing the Omicron variants. These observations are potentially due to antibodies produced by immunities targeting different parts of S proteins can cause differences in recognizing mutated sites[28,29]. Another potential explanation is that the infective strains are also unknown and could induce different responses. Without further information on which vaccines were received by these patients or the sample collection dates post onset of symptoms, we are not able to determine the exact correlation between vaccination and difference in protection against variants.

Potency of NAb determination by Neu-SATiN

To expand on our observations, we tested serial dilutions of FDA EUA-approved neutralizing antibodies Regn10933 (casirivimab), Regn10987 (imdevimab), and JS016 (etesevimab), as well as sera with known vaccination history ($n = 24$). Having such data is informative in detecting the lowest effective concentrations (titers) and therefore determining the potency of NAbs. Of the FDA EUA antibodies, imdevimab was the most effective against WT, Alpha, Beta, Gamma, and Delta variants of the S protein. The other two antibodies, casirivimab and etesevimab, were most potent against WT but showed variable potency against variant S proteins. There was no effective neutralization observed for the Beta strain with either antibody (Fig. 4a) and none of these

antibodies display any potency to inhibit the Omicron variant, suggesting their limitation in fighting the current pandemic of Omicron dominancy. For the serosurveillance of patient samples (Fig. 4b), no neutralizing activity was observed in patients that were not vaccinated, as expected. The patients with one dose showed negligible potency compared to the patients with two doses with samples collected <50 days after the last dose. For samples collected >50 days after receiving two doses, the potency of antibodies significantly reduced as indicated by shift in titration curve towards the right, consistent with recent reports of waning immunity for some vaccines[30]. In quantifying these patient samples in terms of the 50% neutralization titer (Fig. 4c), the majority show strong neutralization against WT and the least potency against Beta variant, with the other variants of concern intermediate.

Discussion

Since the outbreak of the COVID-19 pandemic, the importance of a virus neutralization assay has risen. Virus neutralization assays are the main tools for developing vaccine and therapeutic strategies[31,32,33]. Although the PSV assay is effective in measuring the degree of infection, maintaining cell cultures and making pseudovirus particles are labor intensive with potential safety concerns[34]. Moreover, batch-to-batch variability in virus production and cell transfection efficiency limit standardization and robust assay results[35]. Numerous immunoassays for rapid detection of anti-SARS-CoV-2 antibodies have been developed, however, these assays mainly focus on capturing and detecting antibodies binding to virus proteins (e.g., spike or nucleocapsid)[2]. Since it is well known that mere binding does not necessarily imply neutralization[36], a true neutralization assay for the better understanding of protective immunity against SARS-CoV-2 is needed. To circumvent the use of virus particles and cells, surrogate versions of neutralization assays have been developed[7,8,9]. These assays often use ELISA or similar platforms, with multiple time-consuming binding and washing steps, preventing high-throughput screening[37]. In need of an accurate yet more rapid virus neutralization assay, we developed Neu-SATiN as a homogeneous surrogate virus neutralization assay (hsVNA), using a split-luciferase system.

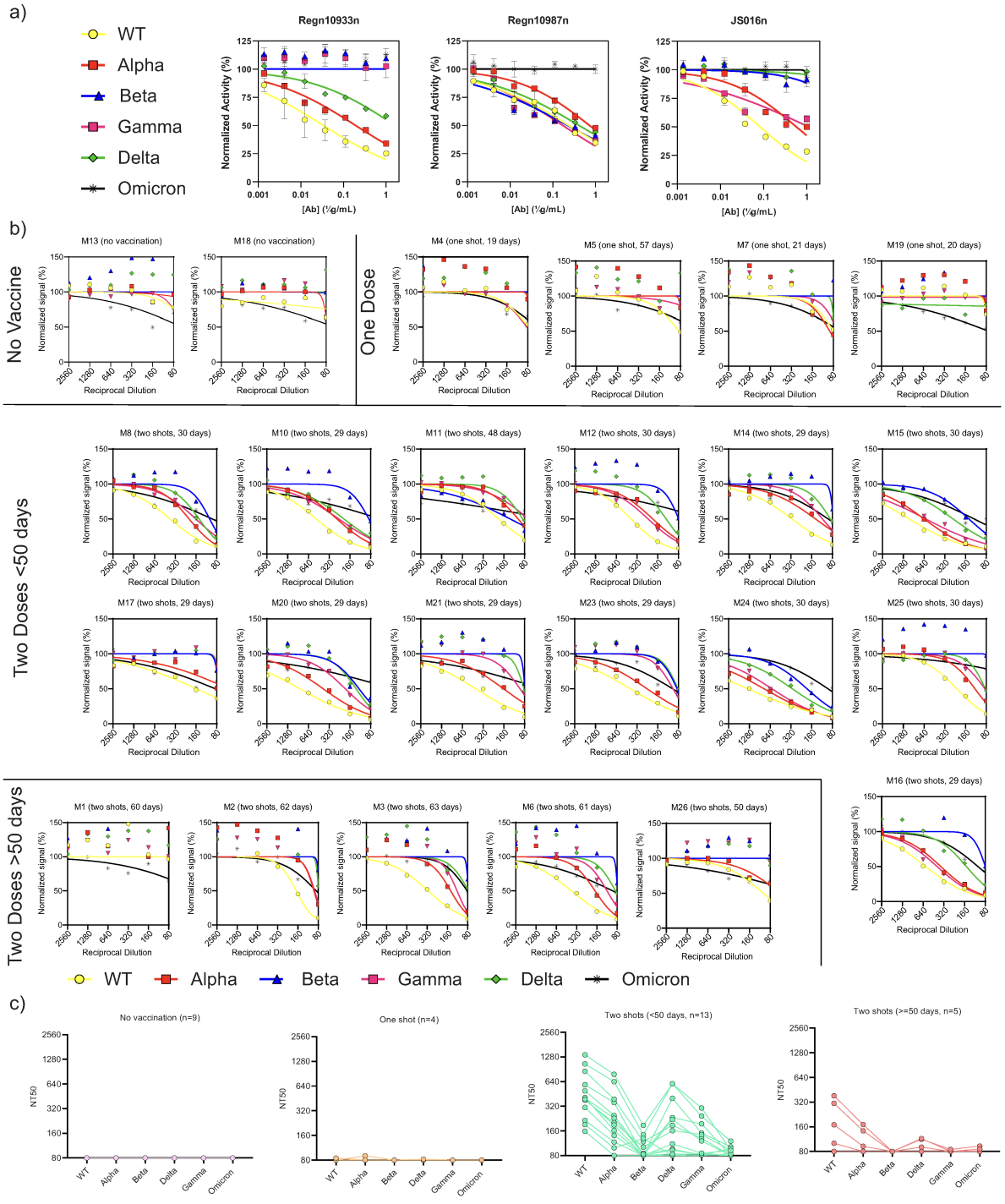


Fig. 4: Assessing the potency of neutralizing antibodies.a Neutralizing capabilities of FDA EUA-approved therapeutic antibodies Regn10933 (left, casirivimab), Regn10987 (center, imdevimab), and JS016 (right, etesevimab) were evaluated using Neu-SATiN against different S variants. **b** Evaluation of neutralizing antibodies in individuals with unvaccinated sera ($n = 2$), with one vaccination dose ($n = 4$), with two vaccination doses and collected within 50 days after the second shot ($n = 13$, intervals between shots were 21–37 days), and with two vaccination doses collected more than 50 days after the second shot ($n = 5$, intervals between shots were 21–36 days). **c** Aggregated data showing titers at 50% neutralization (NT50) for each group. Source data are provided as a Source data file.

There have been several reports describing efforts to develop surrogate virus neutralization (sVNA) assays for the detection of antibodies against SARS-CoV-2[38,39,40,41]. These reports show capabilities as surrogate assays; however, many of these platforms require chemical modification and conjugation of proteins to beads or other solid surfaces, requiring intermediate purification and/or washing steps to remove unbound reagents and analytes. In contrast, Huang et al. reported the development of an hsVNA using the binary version of split-NanoLuc®. Although the approach is similar to the platform we report here, the authors used a monomeric or dimeric form of S1 domain of spike protein tagged with β10 (SmBiT), paired with ACE2 (LgBiT, NanoLuc® beta strands 1 through 9)[38], which was shown to have limited detection of non-RBD targeting antibodies. The importance of conformational changes in spike protein-altering ACE2 binding has been emphasized in many studies[22,42]. Also, with new variants of concern emerging, many of the deployed vaccines and second-wave vaccines in development are targeting full spike protein[43,44,45]. We initially designed our assay by investigating the interactions between ACE2 and RBD[10]. The result is in agreement with reports that neutralization activities of NAb mostly come from anti-RBD immunoglobulins[36,46]; however, immunologic response can also produce antibodies against epitopes outside of the RBD and may require the trimeric structure of the full spike protein for binding. This compelled us to develop stabilized, trimeric, full-length spike (both WT and major variants of concern) versions of the binders and stable, dimerized ACE2 receptor. The data presented in Fig. 3 demonstrates that β10-(S)WT/β9-ACE2-Fc can differentiate the degree of neutralization directly from patient sera and that variant versions of the spike binders can distinguish anti-SARS-CoV-2 NAb positive serum samples from negative samples (Fig. 3e, f). In addition, Neu-SATiN can provide quantitative analysis of NT50 and thus enables the measurement of potency of anti-SARS-CoV-2 antibodies against different strains (Fig. 4). Combined, this provides a comprehensive screen of a patient's level of protection against the current variants of concern. As the assay is modular, emerging variants of interest can be quickly produced and incorporated as we have demonstrated with the inclusion of the Omicron variant that become prominent during the initial review of this manuscript. As all the patient samples were collected before November 2021, prior to any known wide-spread Omicron infections, our results also suggest that prior infection/vaccination does not provide significant neutralizing protection against the variant.

The results obtained with Neu-SATiN correlate with PSV assays and other antigen-based assays in detecting the neutralization potential of antibodies in clinical samples. It is important to note that natural immunity can produce antibodies that bind several antigens and function through alternate mechanisms, including antibody-dependent phagocytosis (ADP) or antibody-dependent cellular cytotoxicity (ADCC). Although the current format of Neu-SATiN cannot measure these types of antiviral activity, the majority of vaccines use Spike domains[17,18]; therefore, this assay can be used to assess protection developed from immunization. One advantage of Neu-SATiN is that it can be performed homogenously and directly using plasma or serum, which significantly reduces hands-on assay time to <30 min and can be run under standard lab conditions. Importantly, we have demonstrated that the split-NanoLuc® based Neu-SATiN can be applied to full-length spike proteins of the original strain and variants to test neutralization levels of convalescent patient sera. Having a modular technology as a surrogate assay that can be easily adopted as a point-of-care tool is important in tracing and adapting to the evolution of the current pandemic.

Methods

Ethical statement

Studies were approved by relevant ethical boards: ARUP/University of Utah Institutional Review Board (IRB-approved protocol 0007740) and Office of Environmental Health and Safety at the University of Toronto (REB-approved protocol REB 20-107). Informed consent was obtained for participants and no compensation was provided.

Cell lines, cell culture media and antibodies, and cloning reagents

The HEK293 cell line was provided by Prof. Jason Moffat at University of Toronto and was originally purchased from ATCC (CRL-1573). CaLu-3 cells were purchased from ATCC (HTB-55). HEK293 cell culture reagents were purchased from Thermo Fisher Scientific. Cloning reagents were purchased from NEB. Two neutralizing antibodies: 40592-MM57 (used for RBD pair screening) and 40592-R001 (used for WT pair screening) were purchased from Sino Biological. Regn10933 (CPC511A), Regn10987 (CPC512A), and JS016 (CPC516A) were purchased from Cell Sciences. Various antibody dilutions were used in this work, with final

concentrations in assays ranging from 0 to 600 μg/mL. Specific concentrations can be found within the Figures and corresponding Figure legends.

Clinical samples

Samples were obtained from either the University of Utah School of Medicine, ARUP Laboratories, or from Unity Health. University of Utah School of Medicine (total $n = 16$) were obtained from infected patients within 48 h of admission to ICU ($n = 13$) or within 3–5 weeks of positive PCR test for convalescent patients ($n = 3$). Samples for determining neutralization (total $n = 63$) in uninfected, infected, and/or vaccinated were generously provided by ARUP Laboratories (IRB-approved protocol 0007740). Samples for antibody titer and serosurveillance studies (total $n = 24$) were collected from Unity Health employees, enrolled through REB-approved protocol REB 20-107, Toronto. All samples were deidentified.

Vector construction and transient transfection in HEK293 cells

Vector cloning for the binder expression was performed as previously reported[11]. All cDNA were cloned into an in-house mammalian expression vector derived from pCMV5 with a signal peptide sequence appended at the N-termini and an octa-histidine stretch at the C-termini. For the constructs that had the tag at the N-termini, either β9 or β10 sequence was placed after the signal peptide, followed by the binder sequence. Likewise, the constructs with C-terminus tag had β9 or β10 sequence right before octa-histidine (Supplementary Table 1). The final products were transfected into HEK293 cells using polyethylenimine Max (Polysciences).

Production and purification of binders

HEK293 cells transfected with binder constructs were cultured in DMEM supplied with 10% FBS and 1X antimycotic-antibiotic mixture. Typically, cells were seeded at 50% confluency, and the media was collected every day until the cells became fully confluent. The collected media was filtered through 0.22 μm PES filter before purification. Purification was done on AKTA FPLC using HisPurTM Cobalt Resin. Tween-20 (0.01%), trehalose (0.1%), and glycerol (10%) were added to the final product and kept at −80 °C before use.

Reconstitution of split-NanoLuc® driven by (S)RBD and ACE2 interaction

For the screening of (S)RBD binders with ACE2 binders, 10 µL of commercial human serum (Sigma-Aldrich®, S1-100ML) spiked with titrating concentrations from 0 µg/mL to 100 µg/mL of the neutralizing antibody (Sino Biological, 40592-MM57) was combined with 5 µL of (S)RBD binders (10 pmol) and 5 µL of ACE2 binders (10 pmol), and incubated for 30 min. The incubation was done using white, round bottom 96-well plates at room temperature with vigorous shaking. Then, the "detection solution" which consists of coelentrazine (substrate) and Δ11S was premixed, and 80 µL of the detection solution was added to each well. The final concentrations of the substrate, coelentrazine, was 10 µM and the large enzyme fragment, Δ11S, was 500 nM per well in a total volume of 100 µL. Luminescent signal was measured using TECAN Infinite M1000Pro in a kinetic cycle. The results reported here are from the 30-min timepoint.

Split NanoLuc®-based virus neutralization assay: testing spiked samples and convalescent samples

Measuring neutralization activity of clinical samples was done in a similar fashion as described above: 10 µL of clinical samples were mixed with 10 pmol of spike protein (5 µL; full S or (S)variant) and 10 pmol of ACE2 fusion (5 µL). All three components were incubated together for 30 min with vigorous shaking. Then, 80 µL of the detection solution (defined above) was added (final total volume per well was 100 µL) and the kinetic cycle of luminescent was measured. For serial dilutions to quantify activity of low titer samples, the assays were performed in a buffer containing 20 mM Tris (pH 7.5), 0.1% Tween-20, 2 mM TCEP, 2 mM EDTA, 25 mM NaCl, and 0.05% BSA. Serum samples (12.5 µL) were first diluted in a volume of 50 µL of buffer, followed by additional one-half serial dilutions up to 6 times. An aliquot (5 µL) of the diluted sample was mixed with 5 µL of β10 modified S binder (20 nM; full S or (S)Variant) and incubated for 30 min. An aliquot (5 µL) of the reaction mixture was further mixed with 45 µL of substrate mixture containing 555.6 nM β9-ACE2-Fc, 100 nM Δ11S, 22.2 µM furimazine (substrate). After 1 h incubation, luminescence signals were measured using a microplate reader. The inhibition curve of a sample against S protein variant was obtained by fitting the readings at different dilutions into the normalized response model with variable slope in GraphPad. The titer of 50% neutralization was calculated according to each model.

Testing spiked samples and convalescent samples with pseudovirus neutralization (PSV) assay

The active sera (from patients in ICU) and convalescent sera were purified using protein G magnetic beads (Promega Corporation, G7471) as per manufacturer's instruction. The concentrations of purified IgG were measured using NanoDrop 2000. Pseudovirions were produced by co-transfecting 293T human embryonic kidney cells using PEI transfection reagent (Polysciences, Inc., Warrington, PA) with NL4-3 HIV-1 genome (pNL4-3.Luc.R-E-, including the firefly luciferase gene inserted into the nef coding sequence and frameshift mutations in Env and Vpr) and a plasmid encoding the desired virus fusion protein (pCAGGS-SARS2-S-cFlag D614G, kind gift of M. Farzan[47] for SARS-CoV-2 S or pMDG VSV-G for VSV as a specificity control). Forty hours post-transfection, pseudovirus-containing supernatant was filtered (0.45 µM) and concentrated by ultracentrifugation (26,000 × *g*, 2 h) through a 20% sucrose/TNE (10 mM Tris pH 7.6, 100 mM NaCl, 1 mM EDTA) cushion, and the pellet resuspended in TNE, aliquoted and stored at −80 °C. To measure inhibition of infectivity, 50 µL of 2 × IgG (purified from patient sera) diluted in media was added to CaLu-3 cells (ATCC HTB-55) in a 96-well format, each concentration in triplicate. Fifty microliters of pseudovirus diluted in media + 16 µg/mL DEAE-dextran was added and plates were spinoculated at 2100 × *g*, 30 min, 10 °C. At 20 h, virus and inhibitor were removed via aspiration, and fresh media was replenished. At 40 h, the cells were lysed, and the luciferase activity was measured (Bright-Glo luciferase assay system, Promega, Madison, WI). To determine the normalized luciferase value, average luciferase activity for no virus wells was first subtracted and then the luciferase signals were normalized to the average luciferase activity for no inhibitor wells.

Protein-based surrogate neutralization assay (pbSNA)

This assay was performed as previously reported[48]. A 384-well high-binding polystyrene Nunc plates (Thermo Fisher Scientific, #460372) were coated with 100 ng/well of full-length trimeric spike protein provided by the National Research Council Canada (NRC). The plates were centrifuge at 216 × *g* for 2 min to ensure even coating and incubated overnight with rocking at 4 °C. The serum samples were diluted using a Hamilton MicroLab STAR robotic liquid handler. All plate washing steps included four washes with 100 µL of PBST and were carried using a 405 TS/LS LHC2 plate washer (Biotek Instruments). After the coating step, the plates were washed

and blocked for 1 h at room temperature with 80 µL of 3% w/v skim milk powder in PBST. The plates were washed once more and the serum, diluted in 1% w/v skim milk powder in PBST, was added at a final volume of 20 µL per well and incubated with shaking for 2 h. A standard curve of purified neutralizing monoclonal antibody (NRCoV2-20-Fc, NRC) was added alongside a set of pooled negative/positive serum. The plates were then washed and 20 µL of recombinant biotinylated ACE2 (NRC) was added (6.5 ng/well) and incubated with shaking for 1 h. The plates were then washed to remove unbound ACE2 and 20 µL of Streptavidin-Peroxidase Polymer (Sigma #S2438) was added to each well (25 ng/well) and incubated for 1 h with shaking. Plates were washed one last time and developed by adding 20 µL of ELISA Pico Chemiluminescent Substrate (diluted 1:2 in MilliQ H2O) was dispensed into each well. After a 5-min incubation, plates were read on an Neo2 plate reader (BioTek Instruments) at 20 ms/well and a read height of 1.0 mm. Luminescence signal were blank adjusted, and percentage of ACE2-Spike interaction determined by dividing the luminescence values by the maximal signal (no serum control; maximal ACE2-spike binding; 0% inhibition).

Statistics and reproducibility

All data are presented as mean ± standard deviation (SD) and the number of biological repeats, as well as sample size, are reported. No statistical method was performed to predetermine sample size. Statistical analyses were performed using GraphPad Prism 9. Correlation between the Neu-SATiN assay and other assays (PSV or pbSNA) was analyzed using Pearson product–moment correlation.

Acknowledgements
We thank the members of Shawn Owen's and Igor Stagljar's lab for their suggestions. This work was supported by the Toronto COVID-19 Action Fund (Connaught Award # 0000313897) to Igor Stagljar and supported by intramural funding from the Office of the Vice President for Research and the 3i Initiative at the University of Utah to Shawn Owen.

Contributions
S.J.K. conceptualized the Neu-SATiN assay, was actively involved in experiments and data analysis, and wrote the bulk of the manuscript. Z.Y. was actively involved in designing and preparing probes, conducted experiments and data analysis, and assisted in manuscript editing. M.C.M. was actively involved in many experiments and data analysis and assisted in manuscript writing. D.M.E. and M.S.K. conceptualized and performed the pseudovirus assay and contributed to manuscript editing. A.L. was involved in probe preparation. M.P., A.B., C.B., and P.J. contributed to providing patient samples. Y.G. and M.L. coordinated the protein-based serum neutralization assay. J.C.D. and M.G. coordinated patient samples and performed ELISA neutralization assays. R.A.C. and E.A.M. contributed to providing patient samples. I.S. and S.C.O. guided and supervised the work, contributed to assay development and manuscript writing as well as coordinated the preparation of the manuscript. All authors approved its content.

Competing interests
A patent covering all the main aspects/key elements of the Neu-SATiN assay has been filed by the governing council of the University of Toronto with the US Patent Office. The application is currently pending. I.S., S.C.O., S.J.K., and Z.Y. are named as coinventor on the patent application. The remaining authors declare no competing interests.

Supplementary material:
https://static-content.springer.com/esm/art%3A10.1038%2Fs41467-022-31300-9/MediaObjects/41467_2022_31300_MOESM1_ESM.pdf

References

1. Ravi, N., Cortade, D. L., Ng, E. & Wang, S. X. Diagnostics for SARS-CoV-2 detection: a comprehensive review of the FDA-EUA COVID-19 testing landscape. Biosens. Bioelectron. 165, 112454 (2020).
2. Oh, H., Ahn, H. & Tripathi, A. A closer look into FDA-EUA approved diagnostic techniques of Covid-19. Acs Infect. Dis. 7, 2787–2800 (2021).
3. Carter, L. J. et al. Assay techniques and test development for COVID-19 diagnosis. ACS Cent. Sci. 6, 591–605 (2020).
4. Cantoni, D., Mayora-Neto, M. & Temperton, N. The role of pseudotype neutralization assays in understanding SARS CoV-2. Oxf. Open Immunol. 2, iqab005 (2021).
5. Ferrara, F. & Temperton, N. Pseudotype neutralization assays: from laboratory bench to data analysis. Methods Protoc. 1, 8 (2018).
6. Muruato, A. E. et al. A high-throughput neutralizing antibody assay for COVID-19 diagnosis and vaccine evaluation. Nat. Commun. 11, 1–6 (2020).
7. Abe, K.T. et al. A simple protein-based surrogate neutralization assay for SARS-CoV-2. JCI Insight 5, e142362 (2020).
8. Tan, C. W. et al. A SARS-CoV-2 surrogate virus neutralization test based on antibody-mediated blockage of ACE2–spike protein–protein interaction. Nat. Biotechnol. 38, 1073–1078 (2020).
9. Byrnes, J. R. et al. Competitive SARS-CoV-2 serology reveals most antibodies targeting the spike receptor-binding domain compete for ACE2 binding. MSphere 5, e00802–e00820 (2020).
10. Azad, T. et al. SARS-CoV-2 S1 NanoBiT: a nanoluciferase complementationbased biosensor to rapidly probe SARS-CoV-2 receptor recognition. Biosens. Bioelectron. 180, 113122 (2021).
11. Yao, Z. et al. A homogeneous split-luciferase assay for rapid and sensitive detection of anti-SARS CoV-2 antibodies. Nat. Commun. 12, 1–8 (2021).
12. Snider, J. et al. Fundamentals of protein interaction network mapping. Mol. Syst. Biol. 11, 848 (2015).
13. Dixon, A. S., Kim, S. J., Baumgartner, B. K., Krippner, S. & Owen, S. C. A tripart protein complementation system using antibody-small peptide fusions enables homogeneous immunoassays. Sci. Rep. 7, 8186 (2017). 14. Kim, S. J., Dixon, A. S., Adamovich, P. C., Robinson, P. D. & Owen, S. C. Homogeneous immunoassay using a tri-part split-luciferase for rapid quantification of anti-TNF therapeutic antibodies. ACS Sens. 6, 1807–1814 (2021).
15. Kim, S. J., Dixon, A. S. & Owen, S. C. Split-enzyme immunoassay to monitor EGFR-HER2 heterodimerization on cell surfaces. Acta Biomater. 135, 225–233 (2021).
16. Lan, J. et al. Structure of the SARS-CoV-2 spike receptor-binding domain bound to the ACE2 receptor. Nature 581, 215–220 (2020).
17. Sahin, U. et al. COVID-19 vaccine BNT162b1 elicits human antibody and TH 1 T cell responses. Nature 586, 594–599 (2020).
18. Min, L. & Sun, Q. Antibodies and vaccines target RBD of SARS-CoV-2. Front. Mol. Biosci. 8, 247 (2021).
19. Harvey, W. T. et al. SARS-CoV-2 variants, spike mutations and immune escape. Nat. Rev. Microbiol. 19, 409–424 (2021).
20. Khateeb, J., Li, Y. & Zhang, H. Emerging SARS-CoV-2 variants of concern and potential intervention approaches. Crit. Care 25, 1–8 (2021).
21. Hsieh, C.-L. et al. Structure-based design of prefusion-stabilized SARS-CoV-2 spikes. Science 369, 1501–1505 (2020).
22. Benton, D. J. et al. Receptor binding and priming of the spike protein of SARS-CoV-2 for membrane fusion. Nature 588, 327–330 (2020).
23. Xiao, T. et al. A trimeric human angiotensin-converting enzyme 2 as an antiSARS-CoV-2 agent. Nat. Struct. Mol. Biol. 28, 202–209 (2021).

24. Hoffmann, M., Kleine-Weber, H. & Pöhlmann, S. A multibasic cleavage site in the spike protein of SARS-CoV-2 is essential for infection of human lung cells. Mol. Cell 78, 779–784.e775 (2020).
25. Xia, S. et al. The role of furin cleavage site in SARS-CoV-2 spike proteinmediated membrane fusion in the presence or absence of trypsin. Signal Transduct. Target. Ther. 5, 1–3 (2020).
26. Dispinseri, S. et al. Neutralizing antibody responses to SARS-CoV-2 in symptomatic COVID-19 is persistent and critical for survival. Nat. Commun. 12, 1–12 (2021).
27. Tea, F. et al. SARS-CoV-2 neutralizing antibodies: Longevity, breadth, and evasion by emerging viral variants. PLoS Med. 18, e1003656 (2021).
28. Greaney, A. J. et al. Antibodies elicited by mRNA-1273 vaccination bind more broadly to the receptor binding domain than do those from SARS-CoV-2 infection. Sci. Trans. Med. 13, eabi9915 (2021).
29. Skelly, D. T. et al. Two doses of SARS-CoV-2 vaccination induce robust immune responses to emerging SARS-CoV-2 variants of concern. Nat. Commun. 12, 1–12 (2021).
30. Israel, A. et al. Large-scale study of antibody titer decay following BNT162b2 mRNA vaccine or SARS-CoV-2 infection. Vaccines. 10, 64 (2022).
31. Khoury, D.S. et al. Neutralizing antibody levels are highly predictive of immune protection from symptomatic SARS-CoV-2 infection. Nat. Med. 127, 1205–1211 (2021).
32. Lu, Y. et al. Advances in neutralization assays for SARS CoV 2. Scand. J. Immunol. 94, e13088 (2021).
33. Dashdorj, N. J. et al. Direct comparison of antibody responses to four SARSCoV-2 vaccines in Mongolia. Cell Host Microbe 29, 1738–1743.e1734 (2021).
34. Amanat, F. et al. An in vitro microneutralization assay for SARS CoV 2 serology and drug screening. Curr. Protoc. Microbiol. 58, e108 (2020).
35. Riepler, L. et al. Comparison of four SARS-CoV-2 neutralization assays. Vaccines 9, 13 (2021).
36. Nayak, K. et al. Characterization of neutralizing versus binding antibodies and memory B cells in COVID-19 recovered individuals from India. Virology 558, 13–21 (2021).
37. Lu, H., Stratton, C. W. & Tang, Y. W. An evolving approach to the laboratory assessment of COVID 19. J. Med. Virol. 92, 1812–1817 (2020).
38. Huang, D. et al. A rapid assay for SARS-CoV-2 neutralizing antibodies that is insensitive to antiretroviral drugs. J. Immunol. 207, 344–351 (2021).
39. Huang, L. et al. Novel nanostructure-coupled biosensor platform for one-step high-throughput quantification of serum neutralizing antibody after COVID19 vaccination. Biosens. Bioelectron. 199, 113868 (2022).
40. Gniffke, E. P. et al. Plasma from recovered COVID-19 patients inhibits spike protein binding to ACE2 in a microsphere-based inhibition assay. J. Infect. Dis. 222, 1965–1973 (2020).
41. Fiedler, S. et al. Antibody affinity governs the inhibition of SARS-CoV-2 spike/ ACE2 binding in patient serum. ACS Infect. Dis. 7, 2362–2369 (2021).
42. Yan, R. et al. Structural basis for the different states of the spike protein of SARS-CoV-2 in complex with ACE2. Cell Res. 31, 717–719 (2021).
43. Kyriakidis, N. C., López-Cortés, A., González, E. V., Grimaldos, A. B. & Prado, E. O. SARS-CoV-2 vaccines strategies: a comprehensive review of phase 3 candidates. npj Vaccines 6, 1–17 (2021).
44. Krammer, F. SARS-CoV-2 vaccines in development. Nature 586, 516–527 (2020).
45. Samrat, S. K., Tharappel, A. M., Li, Z. & Li, H. Prospect of SARS-CoV-2 spike protein: potential role in vaccine and therapeutic development. Virus Res. 288, 198141 (2020).
46. Niu, L., Wittrock, K. N., Clabaugh, G. C., Srivastava, V. & Cho, M. W. A structural landscape of neutralizing antibodies against SARS-CoV-2 receptor binding domain. Front. Immunol. 12, 647934 (2021).
47. Zhang, L. et al. SARS-CoV-2 spike-protein D614G mutation increases virion spike density and infectivity. Nat. Commun. 11, 1–9 (2020).
48. Colwill, K. et al. A scalable serology solution for profiling humoral immune responses to SARS-CoV-2 infection and vaccination. Clin. Transl. Immunol. 11, e1380 (2022).

A-1.3 Scalable agroinfiltration-based production of SARS-CoV-2 antigens for use in diagnostic assays and subunit vaccines

Preface

(This work has been previously published as a research article)

Demone J, Maltseva M, Nourimand M, Nasr-Sharif M, **Galipeau Y**, Alarcon EI, Langlois MA, MacLean AM. **Scalable agroinfiltration-based production of SARS-CoV-2 antigens for use in diagnostic assays and subunit vaccines**. PLoS One. 2022 Dec 14;17(12):e0277668.

https://doi.org/10.1371/journal.pone.0277668

© 2022 Demone et al. This is an open access article distributed under the terms of the Creative Commons Attribution License, which permits unrestricted use, distribution, and reproduction in any medium, provided the original author and source are credited.

Abstract
Agroinfiltration is a method used in biopharming to support plant-based biosynthesis of therapeutic proteins such as antibodies and viral antigens involved in vaccines. Major advantages of generating proteins in plants is the low cost, massive scalability and the rapid yield of the technology. Herein, we report the agroinfiltration-based production of glycosylated SARS-CoV-2 Spike receptor-binding domain (RBD) protein. We show that it exhibits high-affinity binding to the SARS-CoV-2 receptor angiotensin-converting enzyme 2 (ACE2) and displays folding similar to antigen produced in mammalian expression systems. Moreover, our plant-expressed RBD was readily detected by IgM, IgA, and IgG antibodies from the serum of SARS-CoV-2 infected and vaccinated individuals. We further demonstrate that binding of plant-expressed RBD to ACE2 is efficiently neutralized by these antibodies. Collectively, these findings demonstrate that recombinant RBD produced via agroinfiltration exhibits suitable biochemical and antigenic features for use in serological and neutralization assays, and in subunit vaccine platforms.

Introduction

Agroinfiltration is a well-established method used frequently in plant biology in which a strain of the Gram-negative alpha-Proteobacterial species *Agrobacterium tumefaciens* is 'injected' with a needleless syringe into plant leaves. This bacterial plant pathogen then employs a specialized secretion system to genetically transform plant host nuclei by transferring genes of interest into recipient host cells with a high degree of efficiency. The transient transformation of *Nicotiana benthamiana* via agroinfiltration is one of the most rapid methods to efficiently express recombinant proteins in any eukaryotic system [1]. Unlike traditional stably transformed transgenic plants that may require many months to generate, we can transiently transform the leaves of *N. benthamiana* to (co-)express one or multiple proteins simultaneously, observing high levels of protein expression in 3–4 days. This system is highly responsive and flexible. It is well-suited for supporting the rapid development of viral antigen-based diagnostic tests, such as serological assays to detect antibodies in blood, and vaccines against diseases such as COVID-19 in real time where the occurrence of viral variants represent an ever-evolving target.

In this work, we describe the development of a rapid and flexible agroinfiltration-based platform for the production of recombinant SARS-CoV-2 Spike Receptor-Binding Domain (RBD) in the plant *Nicotiana benthamiana*. This platform is simple, massively scalable, cost-effective and easily adaptable to reflect rapid changes in circulating viral sequences. The RBD of the viral spike is the region primarily involved in binding to the cell surface receptor of the virus, the angiotensin converting enzyme 2 (ACE2) receptor [2]. Most neutralizing antibodies against SARS-CoV-2 are directed to RBD [3–5]. A number of studies have already demonstrated the feasibility of plant-based RBD antigen development: histidine-tagged RBD has been expressed at levels as high as 8 ug/g leaf biomass [6], and similar RBD antigens exhibit effective neutralizing responses in mice [7] and non-human primates [8].

The system we describe here utilizes *Agrobacterium tumefaciens*-mediated transient transformation of *N. benthamiana* (Fig 1), to enable the biosynthesis of high-quality SARS-CoV-2 RBD antigen *in planta*. This accessible and cost-effective process requires approximately only six weeks, encompassing seed germination to delivery of the tandem-purified antigen. We demonstrate in this study that plant expressed RBD displays similar biochemical, structural and

antigenic properties as RBD produced in classical mammalian cell expression systems, thereby indicating its suitability for use in diagnostic tests.

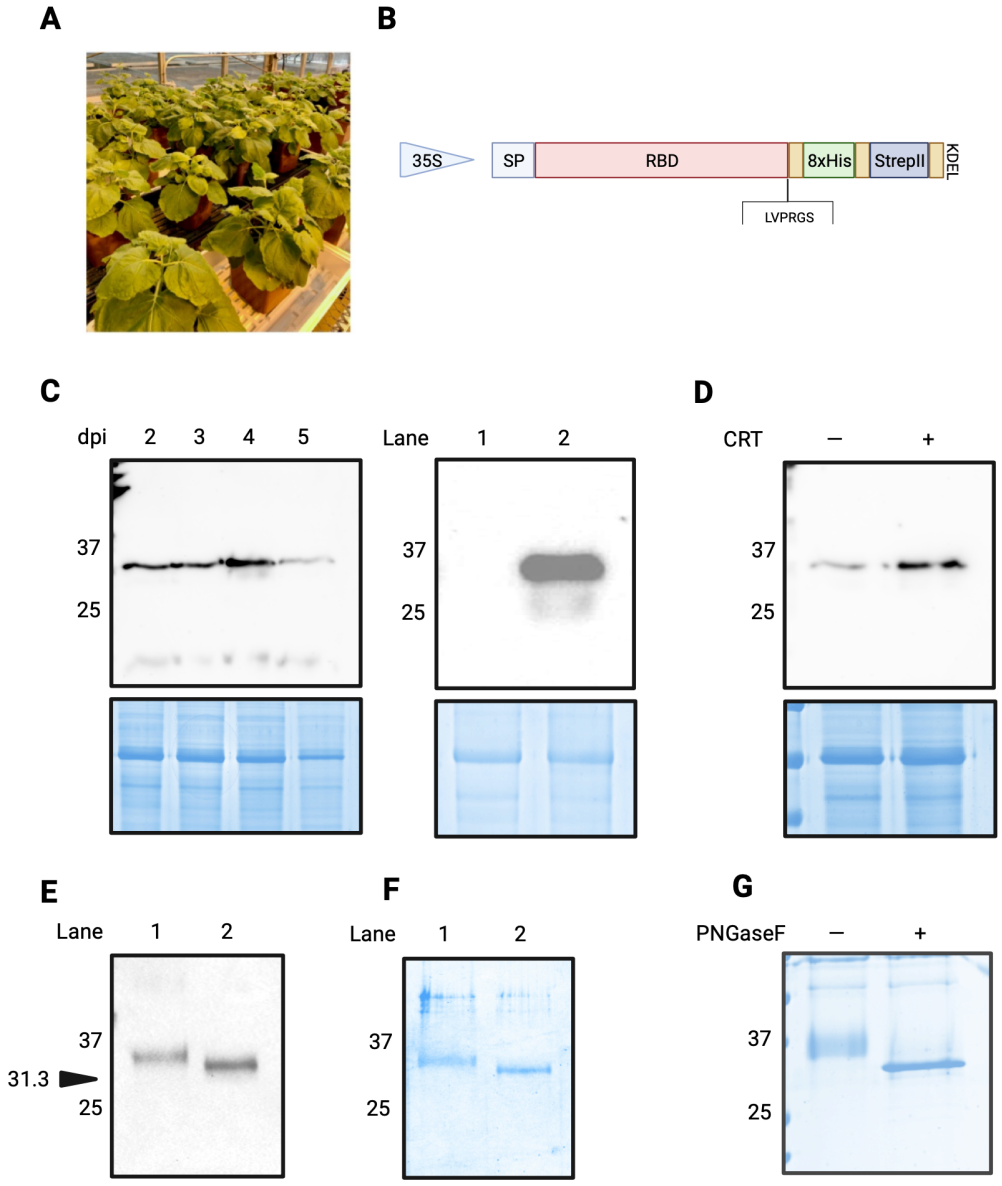


Fig 1. Expression and purification of SARS-CoV-2 RBD in *Nicotiana benthamiana*.(A) Agro-infiltrated *Nicotiana benthamiana* growing in greenhouse. (B) Schematic representation of genetic construct used to express SARS-CoV-2 RBD *in planta*. The SARS-CoV-2 sequence was expressed as a recombinant protein with a dual 8xHis and Twin-Strep II tag, interspersed with Gly-Ser linkers (gold boxes). An ER-retention KDEL sequence was positioned at the C-terminus, and a Thrombin cleavage site (LVPRGS) was included for tag removal. (C) Left panel: Anti-His IB of samples obtained from *N. benthamiana* 2 to 5 days post-infiltration (dpi) with RBD construct in B. Loading control at 5 dpi reproducibly demonstrates reduced abundance of protein due to initiation of tissue necrosis at this time. Right panel: NT control (lane 1) compared to RBD expressed in *N. benthamiana* with calreticulin (lane 2). Anti-his IB. (D) Co-infiltration of human calreticulin (CRT) increases expression levels of RBD in *N. benthamiana*. Samples collected 4dpi. Anti-his IB. (E) Anti-S1 IB of purified RBD expressed in *N. benthamiana* (lane 1) and control RBD expressed in mammalian 293F cells (lane 2). Arrow indicates expected

migration of a protein corresponding to 31.3 kDa. (F) CBB-stained SDS-PAGE of purified RBD expressed in *N. benthamiana* (lane 1) and control RBD expressed in mammalian 293F cells (lane 2). (G) CBB-stained SDS-PAGE of plant-derived RBD treated with (+) and without (-) the amidase Peptide-N-Glycosidase F (PNGaseF), an enzyme that cleaves *N*-linked glycan chains. SP, signal peptide. IB, immunoblot. CBB, Coomassie Brilliant Blue. NT, non-transformed.

Aside from diagnostics assays, SARS-CoV-2 antigens can also be utilized in adjuvanted subunit vaccines [9–11], as well as unadjuvanted vaccines when used as a booster shot [12]. While most SARS-CoV-2 vaccines focus on intramuscular delivery systems, development of a subunit nasal spray vaccine offers a complementary method to increase mucosal immunity to SARS-CoV-2 variants and provide vaccine-hesitant and needle-phobic individuals with alternative immunization options [13]. Protein subunit vaccine platforms have been extensively characterized and have an established safety and efficacy profile against multiple pathogens such as Shingles, Hepatitis B and Meningitis B [14]. The effectiveness of plant-expressed proteins in vaccines has been demonstrated in animal models where they induced potent mucosal immune responses and protection following intranasal immunization [15, 16]. Vaccines produced in plants offer several advantages over traditional manufacturing processes, including significantly lower production costs, increased scalability, and a negligible risk of contamination with human pathogens [17]. These advantages are critical parameters towards facilitating equitable vaccine access to the world's population.

Materials and methods

Plant materials and growth conditions

Wild-type *Nicotiana benthamiana* plants were grown in a greenhouse equipped with 400-Watt high pressure sodium (HPS) light bulbs set at a 20h light/4h dark photoperiod at 25°C for five weeks prior to infiltration. Plants were fertilized once per week using Miracle-Gro (24-8-16) at a concentration of 1.1 g/L. Seeds were germinated on a weekly basis and 56 two-week-old seedlings were transplanted to individual pots once a week.

Gene synthesis

The RBD sequence was obtained from the Wuhan strain (NC_045512) Spike sequence spanning amino acids 319 to 540. The sequence designed for expression in *N. benthamiana* had a C-terminal thrombin cleavage site, 8xhis tag, a Twin-Strep-tag®, and a KDEL sequence for ER-retention. An

endoplasmic reticulum targeting signal peptide derived from *Nicotiana tabacum* PR-1a signal peptide (amino acids 1 to 31) was added to the N-terminal side of the RBD sequence. The construct was codon-optimized for *N. benthamiana* expression and was synthesized by GenScript into the pHREAC vector [18] via BsaI sites. Lectin-binding human chaperone calreticulin (NP_004334.1) was codon-optimized for *N. benthamiana* and synthesized in the pHRE vector [18].

Transient expression in Nicotiana benthamiana

Prior to infiltration, pHREAC-RBD and pHRE-calreticulin were freshly transformed into *Agrobacterium tumefaciens* strains AGL1 and Gv2260, respectively, via electroporation. A single colony was used to inoculate each 5 mL starter culture, and each culture was sub-cultured once in two litres of LB broth containing 50 mg/L ampicillin and 50 mg/L kanamycin at 28°C. The final cultures were grown to an optical density at 600nm (OD600) of 0.6 and were centrifuged and resuspended in MMA buffer (10 mM MES, 10 mM $MgCl_2$, 200 μM acetosyringone, pH 5.6). Unless otherwise indicated, *Agrobacterium* containing the pHREAC-RBD and pHRE-calreticulin constructs were combined and incubated at room temperature for one hour prior to infiltration, to a final OD600 of 0.25 (pHREAC-RBD) and 0.1 (pHRE-CRT). Small-scale infiltration was performed by using 1 mL needleless syringes to inject *Agrobacterium* into the abaxial side of the leaves. Large-scale infiltration was performed via vacuum infiltration using three litres of infiltration solution. Leaves were gently scored, and individual plants were inverted and placed into the vacuum chamber for 2–3 minutes at a pressure of 5 bar. The vacuum was repeatedly applied until the plant was fully infiltrated. Infiltrated leaves were marked and plants were returned to the greenhouse until collection. Twenty-five plants were typically infiltrated per large-scale infiltration, equating to approximately 200 grams of fresh leaf biomass.

Total soluble protein extraction

Leaves co-infiltrated with pHREAC-RBD and pHRE-calreticulin were collected 4–5 dpi (days post-infiltration). Leaf spines were removed, and tissue was homogenized in liquid nitrogen with mortar and pestle. Protein extracts were prepared under native conditions. For each FPLC run: 60 grams of ground tissue were resuspended in 270 mL of ice-cold buffer (PBS (20 mM NaH_2PO_4, 280 mM NaCl, 6 mM KCl), 10 mM imidazole, pH 7.4) and vortexed for five minutes. Ten microlitres of Lysonase Bioprocessing Reagent (Sigma Aldrich Canada Ltd; Etobicoke, Ontario)

was added and the lysate was incubated at 4°C for 15 minutes while gently shaking. Lysate were vortexed again and sonicated three times for 1 minute using a Kontes micro ultrasonic cell disruptor set at 70 output. Lysate was centrifuged for 45 minutes at 20,442 x *g* at 4°C to pellet cell debris. Supernatants were filtered using several layers of cheesecloth and subsequently filtered using Corning one liter 0.22 µM polyethersulfone (PES) sterilizing low-binding filters (Corning, Incorporated; Corning, NY, USA).

Purification of RBD using HisPur™ Ni-NTA resin

Clarified total protein extract was passed through a HisPur Ni-NTA resin column (5 mL bed volume; Cytiva, Marlborough, US), pre-equilibrated with five volumes of imidazole binding buffer (PBS, 10 mM imidazole buffer, pH 7.4) using a fast protein liquid chromatography (FPLC) system (AKTA Pure; GE Healthcare systems). The column was washed with twenty bed volumes of binding buffer (PBS, 10 mM imidazole, pH 7.4) at a flow rate of 5 mL/minute. Protein was eluted using five bed volumes of elution buffer (PBS, 500 mM imidazole, pH 7.4) at a flow rate of 2 mL/minute. Samples were collected as 2 mL fractions. In initial experiments, aliquots of each fraction were visualized via immunoblotting (anti-His antibody; Cat: SAB2702218, Sigma Aldrich Canada, Oakville, Canada) to identify fractions enriched for RBD, which we found to consistently correspond to a visible peak eluting from the column in fractions 25 to 35.

Purification of RBD using Strep-Tactin resin

Fractions corresponding to the protein peak from the HisPur Ni-NTA resin were pooled and protein was further purified using a Strep-Tactin resin column (5 mL bed volume; Cytiva, Marlborough, US) using the AKTA Pure system. The Strep-Tactin column was pre-equilibrated with five bed volumes of binding buffer (PBS, pH 7.4) prior to sample loading, and the column was then washed with 10 bed volumes of binding buffer (PBS, pH 7.4). Protein was eluted using six bed volumes of StrepTrap elution buffer (PBS, 5 mM *d*-Desthiobiotin, pH 7.4) at a flow rate of 2 mL/minute. Samples were collected as 0.5 mL fractions. In initial experiments, aliquots of each fraction were immunoblotted (probed with anti-His antibody) and protein was also visualized via SDS-PAGE gels stained with Coomassie blue staining solution. We reproducibly detected RBD within fractions 22 to 33, which corresponded to the visible peak eluting from the column. Peak samples were collected, pooled, and concentrated to 500 µL using a Vivaspin 20 column (GE Healthcare;

Mississauga, Canada). Plant and mammalian RBD were run on an SDS-PAGE gel and Coomassie-stained for analysis. Both proteins were also immunoblotted with anti-S1 (1: 2000) antibody (Cat: PA5-81795, Invitrogen) and a goat anti-rabbit secondary antibody (1: 10 000).

Further processing of RBD protein

Thrombin cleavage was performed to remove the tag from purified RBD protein. Ten microlitres of thrombin (1U/μL) were added to the 500 μL sample of purified RBD protein and incubated at 22°C for 20 hours. To remove the cleaved 3 kDa tag from the final product, the reaction was passed through a Strep-Tactin resin column (5 mL bed volume) as described above. Flowthrough fractions corresponding to the peak were collected and concentrated to 500 μL using a Vivaspin 20 column (GE Healthcare, Mississauga, Canada). Protein concentration was quantified using the Bio-Rad Protein Assay and used BSA for standard curve preparation. Protein purity was analyzed using SDS-PAGE and protein was visualized using Coomassie blue staining solution.

PNGase F assay

PNGase F, an amidase, is an enzyme used to cleave *N*-linked glycans from glycoproteins and was used to assess the glycosylation status of plant-expressed RBD. Briefly, 20 μg of partially purified plant RBD protein (following elution from the StrepTrap column) was incubated with denaturation buffer at 100°C for 10 minutes. The sample was chilled to halt the denaturation process and GlycoBuffer 2 (New England Biolabs), NP-40, and PNGase F were added to the sample. The sample was incubated at 37°C for one hour and analyzed on an SDS-PAGE gel. Bands were visualized using a Coomassie blue staining solution.

Circular dichroism (CD) spectra and secondary structure calculations

CD spectra were recorded in a J-810 CD spectrophotometer from Jasco analytical instruments equipped with a temperature-controlled Peltier system at 37±0.2°C. Spectra were measured in 0.2 mm path length cuvettes (50 μL of sample) and recorded using a scan rate of 100 nm/min, in high sensitivity mode between 200–250 nm (1.0 nm intervals). Total number of accumulations per spectra was set as five. The equipment is routinely calibrated with camphorsulfonic acid. A mammalian RBD standard was used as a reference protein for the CD analysis and secondary

structure calculation (Cat: Pro1151-3, National Research Council, Ottawa, Canada). Secondary structural analyses were carried out using the BeStSel analysis server [19].

Indirect ELISA to assess ACE2 binding (Kd measurement)

To evaluate protein binding, an indirect ELISA was carried out. Plant or mammalian produced SARS-CoV-2 RBD protein were diluted in sterile 1X PBS (Multicell #311-010-CL) to 4 µg/mL and coated onto a 384-well Immuno plates (Thermofisher, #460372) (12.5 µL/well) overnight at 4°C. Plates were washed three times with 100 µL of PBS-T (PBS, 1% Tween-20) using a BIOTEK plate washer (model ELX405) and blocked for one hour with blocking buffer (PBS-T + 3% non-fat milk powder, w/v) while shaking (700rpm) at room temperature. Biotinylated ACE2 as produced in Abe et al., was diluted in dilution buffer (PBS-T + 1% non-fat milk powder, w/v) to 258 ng/µL and subsequently 1:2 serially diluted [20]. Plates were washed thrice with PBS-T, followed by addition of 20 µL per well of titrated soluble ACE2 and incubated for one hour while shaking at room temperature. Plates were again washed thrice with PBS-T followed by the addition of 20 µL per well of Streptavidin-Peroxidase polymer (Sigma #S2438) diluted in dilution buffer to 1.25 ng/µL. After a one hour incubation with shaking, plates were washed thrice with PBS-T and 20 µL of freshly prepared SuperSignal ELISA Pico Chemiluminescent Substrate (Thermo Scientific, #37069) (mixed 1:1 ratio and diluted in equal volume with dH_2O, (V:V)) was added to each well. Following 5 mins of incubation on a shaker, the luminescence signal (relative light units; RLU) was measured with BIO-TEK Synergy Neo2 plate reader at 20 ms/well at a read height of 1.0 mm. Wells filled with dilution buffer in place of ACE2 accounted for background luminescence and were subtracted from the titrated ACE2 values. Dissociation constant (K_D) was determined using 4-parameter curve fitting with GraphPad Prism 9.1.2 software.

Indirect ELISA to evaluate anti-SARS-CoV-2 immunoreactivity in serum samples (serology)

Plant or mammalian produced SARS-CoV-2 RBD protein were diluted in sterile 1X PBS to 2 µg/mL and coated onto a 96-well plates (VWR #62402–959) (50 µL/well) overnight at 4°C. Plates were washed three times with 200 µL of PBS-T and blocked for one hour with a blocking buffer (PBS-T + 3% non-fat milk powder, w/v) on a shaker at room temperature. Serum samples were diluted 1:50 in dilution buffer (PBS-T + 1% non-fat milk powder, w/v). In conjunction, titration curves of conformation-dependent monoclonal IgM (Absolute Antibody, Ab01680-15.0), IgA

(Absolute Antibody, Ab01680-16.0), and IgG (Absolute Antibody, Ab01680-10.0) CR3022 antibodies were used as reference material to assess protein folding. CR3022 antibodies were diluted 1:2000, followed by 1:2 serial dilution to establish a calibration curve. After blocking, plates were washed thrice with PBS-T, and followed by addition of 100 µL of the respective diluted serum samples and CR3022 antibodies. The plates were incubated for two hours on a shaker at room temperature, washed thrice with PBS-T followed by the addition of 50 µL of the respective secondary-HRP antibody at specified dilutions (1:4000 secondary anti-human IgG-HRP (NRC anti-hIgG#5-HRP fusion), anti- human 1:8000 IgA-HRP (Jackson ImmunoResearch, 109-035-011) or 1:9600 anti- human IgM-HRP (Jackson ImmunoResearch, 109-035-129)). Plates were incubated for one hour on a shaker, washed thrice with PBS-T followed by the addition with 100 µL of the diluted SuperSignal ELISA Pico Chemiluminescent Substrate. Luminescence intensity was measured with BIO-TEK Synergy Neo2 plate reader for 20ms/well at a read height of 1.0 mm. Wells filled with dilution buffer in place of serum accounted for background luminescence and were subtracted from the patient serum values.

Surrogate neutralization ELISA (snELISA) assay to evaluate neutralization activity in serum samples

The described methodology was adapted from the surrogate neutralization ELISA assay as shown in Abe *et al*. (2020) for the evaluation of the relative inhibition of neutralizing antibodies to RBD protein from binding to soluble ACE2 [20, 21]. Briefly, plant or mammalian produced SARS-CoV-2 RBD protein were diluted in sterile 1X PBS to 8 µg/mL and coated onto a 384-well Immuno plates (12.5 µL/well) overnight at 4°C. Plates were washed three times with PBS-T and blocked for one hour while shaking. Serum samples were 1:5 serially diluted in a dilution buffer, applied to wells (20 µL/well) and incubated for 2 hours while shaking at room temperature. Plates were washed thrice, followed by the addition of biotinylated ACE2 diluted to 0.35 ng/µL in a dilution buffer (20 µL/well). Plates were washed thrice with PBS-T followed by the addition of 20 µL per well of Streptavidin-Peroxidase polymer diluted in dilution buffer to 1.25 ng/µL. Following one hour incubation, plates were washed thrice with PBS-T and freshly prepared SuperSignal ELISA Pico Chemiluminescent Substrate was applied (20 µL/well). Following 5 mins of incubation while shaking, luminescence intensity was measured with BIO-TEK Synergy Neo2 plate reader for 20ms/well at a read height of 1.0 mm. Control wells were filled with a dilution buffer in place of

serum followed by the addition of ACE2 to assess maximum binding signal. Relative percent inhibition was calculated as follows:

% Inhibiton = (1- (Average mean of serum sample / Average mean of maximum signal)) X100

Serum dilution resulting in a 50% inhibition (half-maximal inhibitory dilution (ID_{50})) of RBD protein from binding ACE2 receptor was determined using 4-parameter fitting with GraphPad Prism 9.1.2 software.

RBD production in mammalian cells

For comparison, a mammalian RBD was produced in HEK 293F cells and purified. Briefly, a plasmid generously provided by Dr Florian Krammer (Mount Sinai, NYC) encoding the Whuhan-Hu-1 RBD (MN908947) sequence coding for the amino acid 319–541 and fused with the N-terminal SARS-CoV-2 spike secretory signal and a C-terminal hexa-histidine tag was transfected into 293F cells cultivated in Freestyle 293 expression media (Thermo Fisher, #12338018) at 37°C, 7% CO_2, while shaking (125rpm). A total of 600 million cells resuspended in 200 mL were transfected with 200 µg of plasmid using ExpiFectamine (Thermo Fisher, 14525). Three days post-transfection, cell supernatant was harvested by centrifugation (4000xg for 20 mins at 4°C) and filtered through a low binding 0.22 µm stericup vacuum filter (Millipore Sigma, S2GPU10RE). The filtered supernatant was incubated for 2 hours at room temperature with 6ml of Ni-NTA resin (Qiagen, 30210). The column containing the mix of supernatant and resin was washed four times with a washing buffer containing 20mM imidazole, 300mM NaCl and 57.5mM of $NaH_2PO_4 \cdot H_2O$. The RBD protein was then eluted with three column volumes of the elution buffer containing 234mM of imidazole, 300mM NaCl and 57.5mM of $NaH_2PO_4 \cdot H_2O$. The eluted solution was concentrated and the buffer was replaced with PBS using a 10kDa Amicon filter (Millipore Sigma, UFC901008). RBD protein integrity was verified by SDS-PAGE, aliquoted to minimize freeze-thaw cycles and stored at -80°C. RBD used for CD analysis was produced by the National Research Council of Canada and was a gift from Yves Durocher. RBD production details are published elsewhere [21].

Patient samples and collection

Use of human samples for this study was approved by the University of Ottawa Ethics Review Board: Certificates H-04-20-5727, H-04-21-6643 and H-07-20-6009. All participants gave informed written consent to participate in the study. The negative sample was taken from an individual with no history of SARS-CoV-2 infection and tested with PCR. Pooled negative samples were obtained from individuals negative for SARS-CoV-2 as tested by PCR and serology assay. Serum samples from convalescent or vaccinated patients enrolled in surveillance studies from different research studies post-2019. Samples were collected using standard phlebotomy procedures. Samples were de-identified and held at 4°C for short term handling and testing at University of Ottawa CL2+ biocontainment facility. All research was performed in accordance with current guidelines and regulations.

Results

A codon-optimized RBD sequence corresponding to the Wuhan-Hu-1 isolate of SARS-CoV-2 was cloned into the pHREAC vector backbone [18] a plant-specific expression platform that has been demonstrated to achieve among the highest levels of *in vivo* protein expression reported in *N. benthamiana* (Fig 1B). The RBD sequence was flanked on the N-terminal side by an endoplasmic reticulum targeting signal peptide derived from *Nicotiana tabacum* PR-1a signal peptide (amino acids 1–31), and on the C-terminal side by a tandem affinity tag consisting of an 8xHis (OctoHis) tag and a Twin-Strep-tag (Fig 1B). The dual affinity tags were separated by a glycine-serine linker, flanked by a thrombin cleavage site (LVPRGS) that was positioned directly upstream of the affinity tags, and an ER retention signal (KDEL) located downstream and adjacent to two tandem stop codons. For an initial assessment of expression, samples were flash frozen in liquid nitrogen, ground, and resuspended in SDS-PAGE loading buffer. These crude samples were next analyzed using immunoblot analysis (Fig 1C & 1D) prior to purification.

Initial screening of the sequence validated expression vector demonstrated that the greatest expression was achieved using *Agrobacterium tumefaciens* strain AGL1 when infiltrated into five-to-six-week-old *N. benthamiana* leaves that were collected four days post-infiltration (dpi) (Fig 1C, left panel), with lower levels of protein expression also observed at 2-, 3-, and 5 dpi. At 3dpi leaves began to develop chlorosis and subsequently reduced photosynthesis, becoming

increasingly necrotic 5dpi onward. We did not observe a signal in NT (non-transformed) plants when crude extracts were immunoblotted with anti-His (Fig 1C, right panel). Margolin et al. (2019) had previously demonstrated much enhanced expression of a trimeric Spike mimetic protein in *N. benthamiana* when co-expressed in the presence of human calreticulin [22] thus we assessed expression of RBD in the presence and absence of this chaperone. Co-infiltrating with calreticulin (CRT) produced a noticeable increase in RBD expression levels (Fig 1D) and we thus opted to co-express calreticulin with RBD in subsequent infiltrations, with the assumption that the human chaperone may promote proper RBD folding. All RBD samples revealed a band that migrated slightly above the expected molecular weight of 31.3 kDa. Plant-expressed RBD migrates slightly above the mammalian-expressed RBD control (Fig 1E & 1F), possibly due to differences in glycosylation profiles. Immunoblot analysis using an antibody raised against the SARS-CoV-2 S1 region of the Spike protein confirmed the identity of both plant and mammalian RBD. The S1 antibody also recognized a band at ~75 kDa for the plant RBD sample only, suggesting homodimer formation.

To scale up purification, we agroinfiltrated production batches of 25–30 five-to-six-week old plants (Fig 1A) equivalent to approximately 200 grams fresh biomass) under a vacuum. As described in the methods, protein was partially purified by passing lysate through a Ni-NTA column, corresponding to purification of the 8xHis moiety of the tag. Fractions corresponding to the peak detected at 280 nm were visualized using immunoblot analysis to confirm presence and integrity of protein and were then loaded onto a StrepTrap column. Peak fractions were visualized via immunoblot, pooled, concentrated, and digested overnight with thrombin to remove the 8xHis-Twin-Strep-tag. The digested sample was passed through the StrepTrap column a second time to remove the cleaved tag, and aliquots of the purified protein were analyzed on a Coomassie gel (Fig 1F). A band on the Coomassie gel was visualized migrating at approximately 35 kDa, corresponding to the band recognized on the RBD immunoblot by an anti-S1 antibody (Fig 1E). We next assessed the glycosylation status of the plant and mammalian RBD antigens: the Spike protein of SARS-CoV-2 has 22 *N*-linked glycosylation sites, two of which are located within RBD [23]. Peptide-*N*-glycosidase F (PNGase F) digestion of the plant-expressed RBD protein confirmed that it was glycosylated by a shift in band size (Fig 1G). We estimate the purification

yield of RBD at up to 10 ug per gram of fresh leaf mass, in line with other *in planta* production systems that also utilize a histidine-tag [6, 24].

We next performed a comprehensive functional assessment of the RBD produced in *N. benthamiana* in comparison to RBD produced in mammalian cells. Appropriate folding of the RBD antigen is critical for its interaction with the human ACE2 receptor and for the development of antibodies that will target and neutralize native virus and viral variants. We characterized the biochemical properties of the plant-expressed RBD by circular dichroism spectra (CD). More specifically we compared the folding of plant RBD to mammalian expressed RBD standard. We show that the spectral profile of plant-expressed RBD is largely similar to the mammalian expressed RBD, both displaying a single minimum at ~206 nm, consistent with previously reported profiles [25, 26] (Fig 2A). This is further reflected in the analysis of the secondary structure composition by BeStSel analysis server, which shows an overall similar distribution with small differences in α-helical content estimation, which could be due to different post-translational modifications between plant and mammalian cells (Fig 2B).

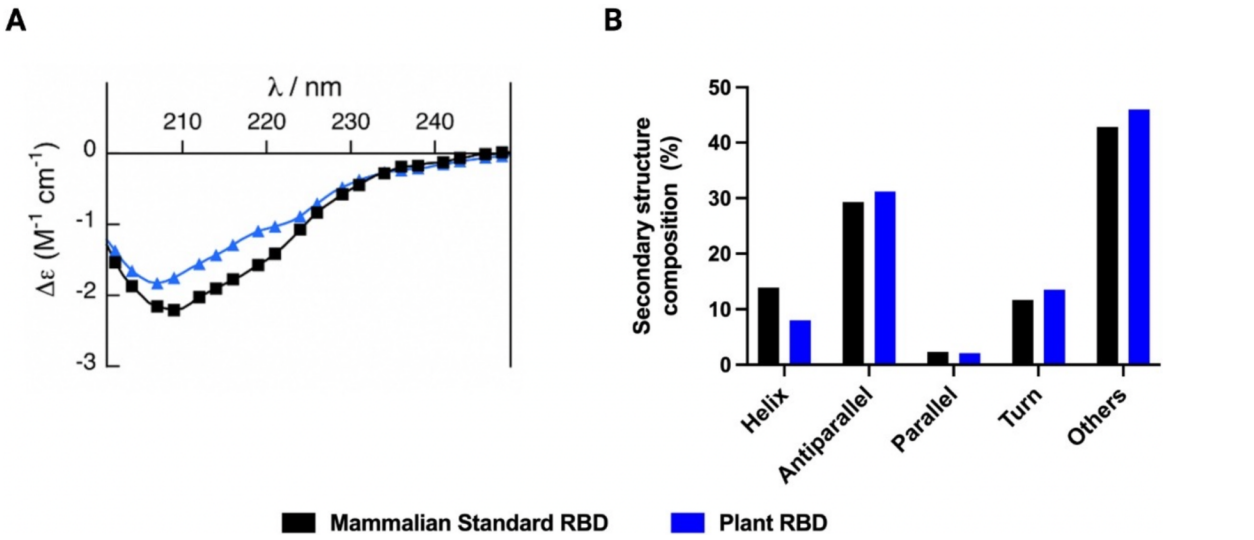


Fig 2. Biochemical evaluation of plant-expressed RBD by circular dichroism (CD). A) Spectral profiles of mammalian standard (black) and plant (blue) expressed RBD in PBS buffer pH 7.4 at 37°C (200–250 nm). Data expressed in molar circular dichroism (Δε) calculated from averaging 5 independent spectra of each sample. B) Secondary structure content in percentage calculated for mammalian and plant-derived RBD in PBS buffer pH 7.4 at 37°C (200–250 nm). Content was calculated using BeStSel analysis server by direct analysis of the raw data (mDeg) from the CD system. Molecular weights for both proteins were considered as 35 kDa.

To evaluate plant-expressed RBD receptor binding kinetics, we first examined its interaction with ACE2. Fig 3 summarizes the three types of ELISA-based assays that were conducted for the functional assessment of the RBD antigens. For this purpose, binding kinetics between soluble and serially titrated ACE2 protein and immobilized plant- and mammalian-RBD were evaluated by indirect enzyme-linked immunosorbent assay (ELISA) (Fig 3A). We found that plant-expressed RBD readily binds to ACE2 with high affinity (K_D = 8.21 nM, R^2 = 0.993), and at a comparable level to RBD expressed in mammalian 293F cells (K_D = 6.90 nM, R^2 = 0.981) (Fig 4A). Similar binding kinetics have been reported by other studies, however the slightly lower value of the plant derived equilibrium dissociation constant (K_D) could be attributed to minor differences in glycosylation and other post-translational modifications as a result of the different expression platforms [27–30].

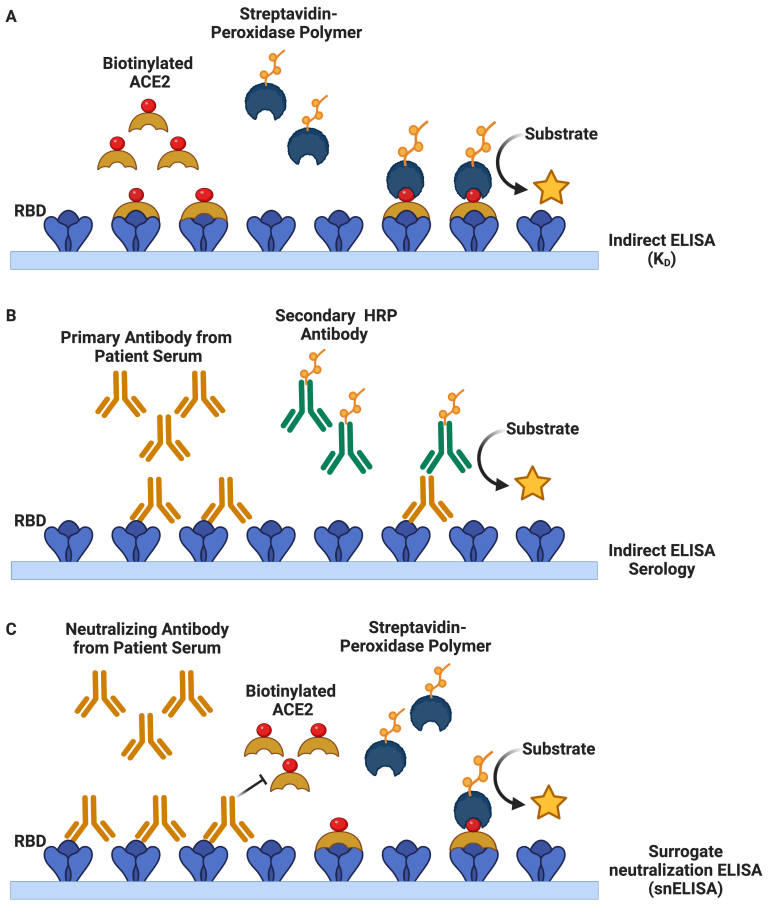


Fig 3. Schematic representations of the different types of ELISA used to characterize plant-expressed RBD.(A) Indirect ELISA (Kd) set up for the evaluation of binding kinetics of soluble human ACE2 to immobilized RBD. (B) Indirect ELISA (serology) set up for the evaluation of binding and recognition of commercial monoclonal and serum IgG, IgM and IgA antibodies to immobilized RBD. (C) Surrogate neutralization ELISA (snELISA) set up to evaluate relative inhibition of anti-SARS-CoV-2 neutralizing antibodies in blocking immobilized RBD from binding soluble ACE2.

Next, we examined whether plant-expressed RBD was recognized by sera from COVID-19 convalescent, partially and fully vaccinated individuals. To this effect, human sera was added to immobilized plant RBD and we probed for the binding of three classes of antibodies (IgG, IgM, and IgA) by ELISA (Figs 3B and 4B). Here, we show that plant RBD was readily detected by IgM, IgA, and IgG antibodies from naturally infected convalescent, vaccinated or convalescent and vaccinated individuals (Fig 4B). We reveal detection and high titers of IgG antibodies comparable to the mammalian-expressed RBD across all samples tested. We also report that IgM and IgA immunoreactivity to plant-expressed RBD was comparable but slightly less efficient in comparison to mammalian-derived RBD. Non-specific binding of antibodies to antigen-naïve individuals was minimal for both RBD antigens tested (Fig 4B). In contrast to previously published results [31, 32], our plant-expressed RBD was bound by conformation-dependent monoclonal

IgM, IgA, and IgG CR3022 antibodies (Fig 4C). This constitutes a further indirect indication that the plant RBD antigen is folded similarly to the mammalian counterpart and exposes the conformational epitope for this antibody. While we note comparable half-maximal inhibitory dilution (ID_{50}) values for IgG CR3022 (plant $ID_{50} = 1.8x10^{-5}$, mammalian $ID_{50} = 1.2x10^{-5}$), we did observe slightly reduced binding of the IgA CR3022 antibody to plant-derived RBD ($6.9x10^{-5}$) compared to mammalian-expressed RBD ($3.4x10^{-5}$), respectively (Fig 4C and 4D). Post-translational modifications such as glycosylation may also explain these small differences in IgA and IgM binding [27], although we also cannot exclude the possibility of minor unfavourable folding motifs that could contribute to these observations.

Lastly, we investigated the relative efficacy of human serum neutralizing antibodies in blocking the immobilized plant RBD's interaction with soluble ACE2 by surrogate neutralization ELISA (snELISA) (Fig 3C) [20, 33]. As mentioned previously, most neutralizing antibodies produced by natural infection or vaccine immunity are directed to the RBD of the spike protein [3–5]. Neutralization of plant RBD-ACE2 interactions by human serum antibodies is therefore an additional indicator of adequate and functional protein folding and of neutralizing epitope accessibility on plant RBD. Serum was added to immobilized plant-expressed RBD and then binding to soluble biotinylated ACE2 receptor was evaluated (Fig 4E). We then measured the inhibition of the binding as a function of the serum dilution. Our observations indicate that human antibodies were able to bind plant-expressed RBD and neutralize its binding to the ACE2 receptor with similar kinetics to the mammalian-expressed RBD (Fig 4F). In fact, we observed generally greater ID_{50} values for the plant-expressed RBD, thereby indicating that its interactions with the ACE2 receptor were more efficiently disrupted by neutralizing antibodies.

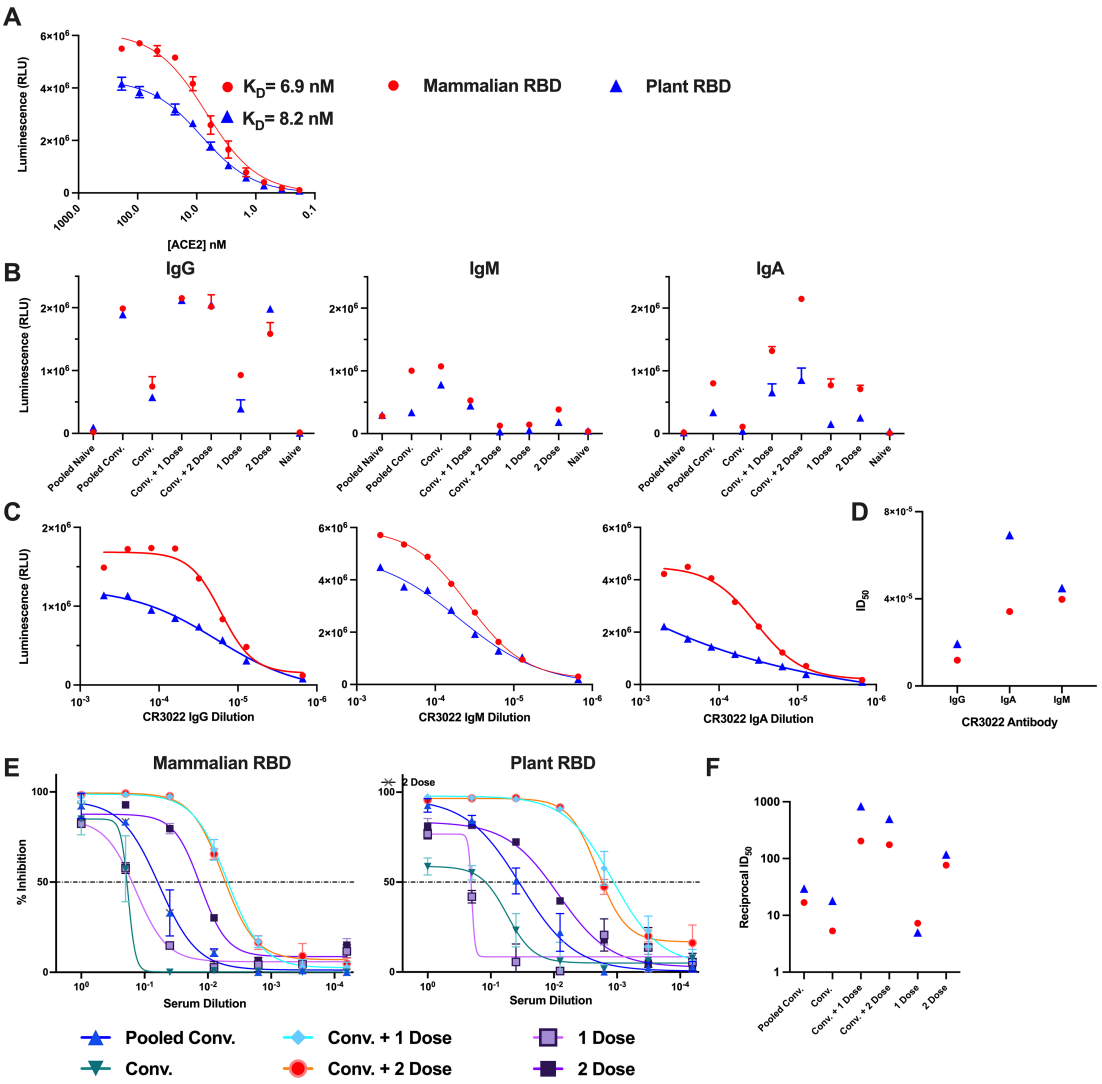


Fig 4. Evaluation of plant-expressed RBD protein functionality, folding and binding kinetics. A comprehensive assessment of protein function of the RBD produced in *N. benthamiana* as it pertains to protein folding and binding to ACE2 receptor, recognition and neutralization by antibodies in sera from SARS-CoV-2 exposed individuals. (A) Indirect ELISA demonstrating binding kinetics of soluble human ACE2 to immobilized mammalian RBD (red circle) and plant RBD (blue triangle). (B) Binding and recognition of immobilized mammalian and plant produced RBD by IgG, IgM and IgA polyclonal antibodies in sera of pooled naïve (unvaccinated, uninfected individuals; n>100), pooled convalescent (pooled Conv.) (n>100), convalescent and vaccinated with one dose (Conv. + 1 dose), convalescent and vaccinated with two doses (Conv. + 2 dose), vaccinated with one dose (1 dose), vaccinated with 2 doses (2 doses) of Pfizer (BNT162b2) and naïve (PCR negative confirmed). Pooled sera are samples pooled from a surveillance study of 100 individuals with (pooled convalescent) or without (pooled naïve) prior SARS-CoV-2 infection. While the rest of the samples were collected from single individuals from each category described above. (C) Binding and recognition of immobilized mammalian and plant produced RBD by conformation dependant monoclonal IgG, IgM, and IgA CR3022 antibodies and (D) their half-maximal inhibitory dilution (ID_{50}) values. (E) Relative inhibition percentage of anti-SARS-CoV-2 neutralizing antibodies in blocking immobilized mammalian and plant produced RBD from binding to soluble ACE2 by snELISA. This assay is representative of technical triplicates or quadruplicates and presented as mean ± standard deviation. (F) Reciprocal ID_{50} values from (E) for mammalian- and plant-expressed RBD.

Discussion

We have demonstrated that plant-expressed RBD retains folding and functionality comparable to mammalian produced RBD as evaluated by CD analysis, binding to host cell receptor ACE2, recognition by the conformation-dependant monoclonal CR3022 antibody directed to RBD, and binding of polyclonal antibodies from sera of SARS-CoV-2-infected and vaccinated individuals. Although we did note a reduced ability of human IgM and IgA antibodies to bind plant-expressed RBD as compared to mammalian-expressed RBD, similar binding of IgG, which have high affinity to the target antigen, was observed. Additionally, binding of plant-expressed RBD to the ACE2 receptor was efficiently neutralized by antibodies from sera of convalescent, partially and fully vaccinated individuals. Collectively, these findings demonstrate that recombinant RBD produced in *N. benthamiana* exhibits suitable biochemical, structural, and antigenic features for testing as antigen in a subunit vaccine platform.

There are many advantages in developing a plant-based platform for viral antigen production, one of which is its flexibility to rapidly pivot to express antigens for emerging SARS-CoV-2 variants of concern. In six weeks, it is possible to produce the purified RBD of a new variant from an expression plasmid. The amount produced is directly linked to the number of plants grown, which can be cost-effectively scaled up to meet any laboratory requirements; growing of *N. benthamiana* does not require sophisticated or costly installations, making this technology broadly accessible worldwide. SARS-CoV-2 antigens are required in serological assays to measure antibodies in blood raised against the virus from exposure or induced by vaccines. Viral RBD and Spike proteins are also an integral part of ELISA-based antibody neutralization assays, as the one used in this study [20]. These types of assays are critical for measuring the potential of new variants of concern to evade vaccine immunity. Furthermore, purification yields of this RBD antigen could conceivably be doubled simply by changing the tagging system, i.e. switching out of the standard 8xhistidine tag for a FLAG-tag, a phenomenon observed in a comparative study [24]. Such a modification may also negate the cost-effectiveness of the procedure proposed in our study, however, and so further analysis is required. The expression system used to drive recombinant protein production also has a dramatic effect on purification yield, as demonstrated by the use of

the potato virus X-based pEff vector [34]. Incorporating this vector into our protocol in the future could easily fast-track the scaling-up process.

As variants continue to emerge, the viral targets of vaccines and vaccination technology also need to evolve to match the pathogen's evolutionary pace. Vaccines targeting the Spike or RBD of several variants, called multivalent vaccines, will be important to help immune responses focus on specific mutations [35, 36]. Different vaccine technologies will also have a major role to play to diversify cellular and humoral immune responses to help combat disease severity and transmission. For instance, new vaccines based on different technologies to the original mRNA and adenovirus-based vaccines are now entering and emerging from clinical trials. Protein subunit, viral vector and virus-like particle (VLP) vaccines are but a few, including a new plant-based adjuvanted VLP vaccine by Medicago [37–39]. Delivery methods such as oral and intranasal vaccine technologies that stimulate mucosal immunity specialized in reducing transmissions will also become critical for moving out of the acute stage of this pandemic [40, 41]. As customizing vaccines to new variants will be critical in keeping SARS-CoV-2 infections and transmissions in check, so will be the rapid biomanufacturing of viral antigens that are critical components for some of these vaccine technologies.

The data presented in this study therefore sets the stage for further investigating the use of cost-effective and massively scalable plant-based viral antigen in protein subunit vaccines given its comparable properties to its animal cell-expressed counterpart. Such protein antigens have already shown great promise in various research studies and clinical trials [9, 10, 42].

Limitations of the study

The degree to which the native glycosylation profile of viral antigen is reconstituted is an important consideration to the selection of an expression system, and the expression of a heterologous (glyco)protein in a plant-based platform will yield a glycosylation profile that is distinct from that of mammalian systems [43]. Plants and animals differ in terms of both *N*- and *O*-linked glycosylation, with plants producing highly specific glycans that are absent in other eukaryotes (for example, β(1,2)-xylose and α(1,3)-fucose), and lacking others such as sialic acid [44]. Moreover, there is increasing evidence that heterologous glycoproteins may be under-glycosylated

(i.e., display reduced glycan occupancy) when expressed in plants [45]. Importantly, plant-manufactured VLP-based vaccines against both influenza and SARS-CoV-2 have been demonstrated to be safe and effective in humans, despite containing plant-specific glycan structures [39, 46, 47] and ongoing initiatives to humanize the glycosylation systems of plants offer great potential [48]. In this study, it is also worth noting that the RBD of the SARS-CoV-2 Spike protein is not subject to extensive post-translational modifications and glycosylation, particularly in comparison to other heavily decorated viral proteins that are more challenging to produce in plants. Ultimately, it is yet unknown whether different glycosylation patterns are a caveat to producing our plant-derived antigen for diagnostics and subunit vaccines. Currently ongoing studies in animals will reveal the potential and efficacy of plant-expressed antigen as a subunit vaccine for SARS-CoV-2.

Acknowledgments
We are grateful for helpful discussions and advice from Rima Menassa and colleagues at Agriculture and Agri-Food Canada, London Research and Development Centre, Canada, Emmanuel Margolin, Edward Rybicki and colleagues from Biopharming Research Unit, University of Cape Town, South Africa, and Dominique Michaud, Université Laval, Canada. We gratefully acknowledge the excellent support of Michelle Brazeau, University of Ottawa, in her management of our greenhouse.

Data Availability: All relevant data are within the paper and its Supporting information files.

Competing interests: The authors have declared that no competing interests exist.

Funding: This study was funded in part by a COVID-19 Rapid Response grant by the Canadian Institute of Health Research (CIHR, #VR2 – 172722) and by a grant supplement by the Canadian Immunity Task Force (CITF) to MAL. MM holds a Queen Elizabeth II Graduate Scholarship in Science and Technology (QEII-GSST) and YG holds a Canadian Institute of Health Research (CIHR) Frederick Banting and Charles Best graduate scholarship (CGS-M). Production of RBD was supported financially by the National Research Council Canada Pandemic Response Challenge program. Greenhouse management was supported by funding from the University of Ottawa Faculty of Science. The funders had no role in study design, data collection and analysis, decision to publish, or preparation of the manuscript.

Author Contributions
Conceptualization: Marc-Andre´ Langlois, Allyson M. MacLean. Funding acquisition: Marc-Andre´ Langlois, Allyson M. MacLean. Investigation: Jordan Demone, Mariam Maltseva, Maryam Nourimand, Mina Nasr-Sharif, Yannick Galipeau, Emilio I. Alarcon. Methodology: Allyson M. MacLean. Resources: Marc-Andre´ Langlois, Allyson M. MacLean. Supervision: Marc-Andre´ Langlois, Allyson M. MacLean. PLOS ONE Plant-based production of SARS-CoV-2 antigen PLOS ONE | https://doi.org/10.1371/journal.pone.0277668 December 14, 2022 14 / 17 Validation: Jordan Demone, Mariam Maltseva, Maryam Nourimand, Emilio I. Alarcon, Marc-Andre´ Langlois. Writing – original draft: Jordan Demone, Mariam Maltseva, Maryam Nourimand, MarcAndre´ Langlois, Allyson M. MacLean. Writing – review & editing: Mariam Maltseva, Emilio I. Alarcon, Marc-Andre´ Langlois, Allyson M. MacLean

References

1.Bally J, Jung H, Mortimer C, Naim F, Philips JG, Hellens R, et al. The rise and rise of Nicotiana benthamiana: A plant for all reasons. Annual Review of Phytopathology 2018. https://doi.org/10.1146/annurev-phyto-080417-050141 PMID: 30149789

2. Hoffmann M, Kleine-Weber H, Schroeder S, Kru¨ger N, Herrler T, Erichsen S, et al. SARS-CoV-2 Cell Entry Depends on ACE2 and TMPRSS2 and Is Blocked by a Clinically Proven Protease Inhibitor. Cell 2020; 181. https://doi.org/10.1016/j.cell.2020.02.052 PMID: 32142651

3. Piccoli L, Park YJ, Tortorici MA, Czudnochowski N, Walls AC, Beltramello M, et al. Mapping Neutralizing and Immunodominant Sites on the SARS-CoV-2 Spike Receptor-Binding Domain by Structure-Guided High-Resolution Serology. Cell 2020. https://doi.org/10.1016/j.cell.2020.09.037 PMID: 32991844

4. Yang J, Wang W, Chen Z, Lu S, Yang F, Bi Z, et al. A vaccine targeting the RBD of the S protein of SARS-CoV-2 induces protective immunity. Nature 2020. https://doi.org/10.1038/s41586-020-2599-8 PMID: 32726802

5. Garcia-Beltran WF, Lam EC, Astudillo MG, Yang D, Miller TE, Feldman J, et al. COVID-19-neutralizing antibodies predict disease severity and survival. Cell 2021. https://doi.org/10.1016/j.cell.2020.12.015 PMID: 33412089

6. Rattanapisit K, Shanmugaraj B, Manopwisedjaroen S, Purwono PB, Siriwattananon K, Khorattanakulchai N, et al. Rapid production of SARS-CoV-2 receptor binding domain (RBD) and spike specific monoclonal antibody CR3022 in Nicotiana benthamiana. Scientific Reports 2020. https://doi.org/10.1038/ s41598-020-74904-1 PMID: 33077899

7. Royal JM, Simpson CA, McCormick AA, Phillips A, Hume S, Morton J, et al. Development of a SARSCoV-2 vaccine candidate using plant-based manufacturing and a tobacco mosaic virus-like nano-particle. Vaccines (Basel) 2021; 9(11):1347. https://doi.org/10.3390/vaccines9111347 PMID: 34835278

8. Siriwattananon K, Manopwisedjaroen S, Shanmugaraj B, Rattanapisit K, Phumiamorn S, Sapsutthipas S, et al. Plant-produced receptor-binding domain of SARS-CoV-2 elicits potent neutralizing responses in mice and non-human primates. Frontiers in Plant Science 2021; 12. https://doi.org/10.3389/fpls.2021.682953 PMID: 34054909

9. Akache B, Renner TM, Tran A, Deschatelets L, Dudani R, Harrison BA, et al. Immunogenic and efficacious SARS-CoV-2 vaccine based on resistin-trimerized spike antigen SmT1 and SLA archaeosome adjuvant. Scientific Reports 2021; 11. https://doi.org/10.1038/s41598-021-01363-7 PMID: 34750472

10. Tabynov K, Turebekov N, Babayeva M, Fomin G, Yerubayev T, Yespolov T, et al. An adjuvanted subunit SARS-CoV-2 spike protein vaccine provides protection against Covid-19 infection and transmission. Npj Vaccines 2022; 7. https://doi.org/10.1038/s41541-022-00450-8 PMID: 35197485

11. Wu Y, Huang X, Yuan L, Wang S, Zhang Y, Xiong H, et al. A recombinant spike protein subunit vaccine confers protective immunity against SARS-CoV-2 infection and transmission in hamsters. Science Translational Medicine 2021; 13. https://doi.org/10.1126/scitranslmed.abg1143 PMID: 34285130

12.Mao T, Goldman-Israelow B, Suberi A, Zhou L, Reschke M, Pena-hernandez M, et al. Unadjuvanted intranasal spike vaccine booster elicits robust protective mucosal immunity against sarbecoviruses. BioRxiv 2022. https://doi.org/10.1101/2022.01.24.477597 PMID: 35118464

13. Alu A, Chen L, Lei H, Wei Y, Tian X, Wei X. Intranasal COVID-19 vaccines: From bench to bed. EBioMedicine 2022; 76. https://doi.org/10.1016/j.ebiom.2022.103841 PMID: 35085851

14. di Pasquale A, Preiss S, da Silva FT, Garc¸on N. Vaccine adjuvants: From 1920 to 2015 and beyond. Vaccines (Basel) 2015; 3. https://doi.org/10.3390/vaccines3020320 PMID: 26343190

15. Wang SH, Smith D, Cao Z, Chen J, Acosta H, Chichester JA, et al. Recombinant H5 hemagglutinin adjuvanted with nanoemulsion protects ferrets against pathogenic avian influenza virus challenge. Vaccine 2019; 37. https://doi.org/10.1016/j.vaccine.2019.02.002 PMID: 30795941

16. Smith D, Streatfield SJ, Acosta H, Ganesan S, Fattom A. A nanoemulsion-adjuvanted intranasal H5N1 influenza vaccine protects ferrets against homologous and heterologous H5N1 lethal challenge. Vaccine 2019; 37. https://doi.org/10.1016/j.vaccine.2019.08.071 PMID: 31495593
17.Yao J, Weng Y, Dickey A, Wang KY. Plants as factories for human pharmaceuticals: Applications and challenges. International Journal of Molecular Sciences 2015; 16. https://doi.org/10.3390/ ijms161226122 PMID: 26633378
18. Peyret H, Brown JKM, Lomonossoff GP. Improving plant transient expression through the rational design of synthetic 50 and 30 untranslated regions. Plant Methods 2019. https://doi.org/10.1186/s13007-019-0494-9 PMID: 31548848
19. Micsonai A, Wien F, Kernya L, Lee YH, Goto Y, Re´fre´giers M, et al. Accurate secondary structure prediction and fold recognition for circular dichroism spectroscopy. Proc Natl Acad Sci U S A 2015; 112. https://doi.org/10.1073/pnas.1500851112 PMID: 26038575
20. Abe KT, Li Z, Samson R, Samavarchi-Tehrani P, Valcourt EJ, Wood H, et al. A simple protein-based surrogate neutralization assay for SARS-CoV-2. JCI Insight 2020; 5. https://doi.org/10.1172/jci.insight.142362 PMID: 32870820
21. Colwill K, Galipeau Y, Stuible M, Gervais C, Arnold C, Rathod B, et al. A scalable serology solution for profiling humoral immune responses to SARS-CoV-2 infection and vaccination. Clinical and Translational Immunology 2022; 11. https://doi.org/10.1002/cti2.1380 PMID: 35356067
22. Margolin E.; Verbeek M.; Meyers A.; Chapman R.; Williamson A.L.; Rybicki EP. Calreticulin co-expression supports high level production of a recombinant SARS-CoV-2 spike mimetic in Nicotiana benthamiana. BioRxiv 2020. https://doi.org/10.1101/2020.06.14.150458
23. Zhou D, Tian X, Qi R, Peng C, Zhang W. Identification of 22 N-glycosites on spike glycoprotein of SARS-CoV-2 and accessible surface glycopeptide motifs: Implications for vaccination and antibody therapeutics. Glycobiology 2021; 31. https://doi.org/10.1093/glycob/cwaa052 PMID: 32518941
24. Mamedov T, Yuksel D, Ilgın M, Gu¨rbu¨zaslan I, Gulec B, Mammadova G, et al. Production and characterization of nucleocapsid and RBD cocktail antigens of SARS-CoV-2 in Nicotiana benthamiana plant as a vaccine candidate against COVID-19. Vaccines (Basel). 2021; 9(11). Epub 2021/11/28. https://doi. org/10.3390/vaccines9111337 PMID: 34835268
25. Maffei M, Montemiglio LC, Vitagliano G, Fedele L, Sellathurai S, Bucci F, et al. The nuts and bolts of SARS-CoV-2 spike receptor-binding domain heterologous expression. Biomolecules 2021; 11. https://doi.org/10.3390/biom11121812 PMID: 34944456
26. Consortium AA. Structural and functional comparison of SARS-CoV-2-spike receptor binding domain produced in Pichia pastoris and mammalian cells. Sci Rep 2020; 10. https://doi.org/10.1038/s41598- 020-78711-6 PMID: 33311634
27. Gong Y, Qin S, Dai L, Tian Z. The glycosylation in SARS-CoV-2 and its receptor ACE2. Signal Transduction and Targeted Therapy 2021; 6. https://doi.org/10.1038/s41392-021-00809-8 PMID: 34782609
28. Lan J, Ge J, Yu J, Shan S, Zhou H, Fan S, et al. Structure of the SARS-CoV-2 spike receptor-binding domain bound to the ACE2 receptor. Nature 2020; 581. https://doi.org/10.1038/s41586-020-2180-5 PMID: 32225176 29. Tian X, Li C, Huang A, Xia S, Lu S, Shi Z, et al. Potent binding of 2019 novel coronavirus spike protein by a SARS coronavirus-specific human monoclonal antibody. Emerging Microbes and Infections 2020; 9. https://doi.org/10.1080/22221751.2020.1729069 PMID: 32065055
30. Walls AC, Park YJ, Tortorici MA, Wall A, McGuire AT, Veesler D. Structure, Function, and Antigenicity of the SARS-CoV-2 Spike Glycoprotein. Cell 2020. https://doi.org/10.1016/j.cell.2020.02.058 PMID: 32155444
31.Shin Y-J, Ko¨nig-Beihammer J, Vavra U, Schwestka J, Kienzl NF, Klausberger M, et al. N-Glycosylation of the SARS-CoV-2 Receptor Binding Domain Is Important for Functional Expression in Plants. Frontiers in Plant Science 2021; 12. https://doi.org/10.3389/fpls.2021.689104 PMID: 34211491
32. Klausberger M, Duerkop M, Haslacher H, Wozniak-Knopp G, Cserjan-Puschmann M, Perkmann T, et al. A comprehensive antigen production and characterisation study for easy-to-implement, specific and

quantitative SARS-CoV-2 serotests. EBioMedicine 2021; 67. https://doi.org/10.1016/j.ebiom.2021.103348 PMID: 33906067
33. Anderson DE, Tan CW, Chia WN, Young BE, Linster M, Low JGH, et al. Lack of cross-neutralization by SARS patient sera towards SARS-CoV-2. Emerging Microbes and Infections 2020; 9. https://doi.org/ 10.1080/22221751.2020.1761267 PMID: 32380903
34. Mardanova ES, Kotlyarov RY, Ravin NV. High-yield production of receptor binding domain of SARSCoV-2 linked to bacterial flagellin in plants using self-replicating viral vector pEff. Plants (Basel) 2021; 10(12). Epub 2021/12/29. https://doi.org/10.3390/plants10122682 PMID: 34961153
35. Callaway E, Ledford H. How to redesign COVID vaccines so they protect against variants. Nature 2021; 590. https://doi.org/10.1038/d41586-021-00241-6 PMID: 33514888
36. Stokel-Walker C. How are vaccines being adapted to meet the changing face of SARS-CoV-2? BMJ 2022; 377:o1257. https://doi.org/10.1136/bmj.o1257 PMID: 35649582
37.Dunkle LM, Kotloff KL, Gay CL, A´ ñez G, Adelglass JM, Barrat Herna´ndez AQ, et al. Efficacy and Safety of NVX-CoV2373 in Adults in the United States and Mexico. New England Journal of Medicine 2022; 386. https://doi.org/10.1056/NEJMoa2116185 PMID: 34910859
38. Afkhami S, D'Agostino MR, Zhang A, Stacey HD, Marzok A, Kang A, et al. Respiratory mucosal delivery of next-generation COVID-19 vaccine provides robust protection against both ancestral and variant strains of SARS-CoV-2. Cell 2022; 185. https://doi.org/10.1016/j.cell.2022.02.005 PMID: 35180381
39. Hager KJ, et al. Efficacy and Safety of a Recombinant Plant-Based Adjuvanted Covid-19 Vaccine. The New England Journal of Medicine 2022; 386:2084–96. https://doi.org/10.1056/NEJMoa2201300 PMID: 35507508 40. Mouro V, Fischer A. Dealing with a mucosal viral pandemic: lessons from COVID-19 vaccines. Mucosal Immunology 2022; 15:584–94. https://doi.org/10.1038/s41385-022-00517-8 PMID: 35505121
41. Lavelle EC, Ward RW. Mucosal vaccines—fortifying the frontiers. Nature Reviews Immunology 2022; 22. https://doi.org/10.1038/s41577-021-00583-2 PMID: 34312520
42. Zhang R, Li D, Xu K, Yang C, Luo T, Zhao X, et al. A protein subunit vaccine booster following two doses of inactivated SARS-CoV-2 vaccine provides high neutralisation of SARS-CoV-2 and its variants in mice. The Lancet Microbe 2022; 3. https://doi.org/10.1016/S2666-5247(21)00331-1 PMID: 34977828
43. Margolin E, Crispin M, Meyers A, Chapman R, Rybicki EP. A roadmap for the molecular farming of viral glycoprotein vaccines: engineering glycosylation and glycosylation-directed folding. Frontiers in Plant Science 2020. https://doi.org/10.3389/fpls.2020.609207 PMID: 33343609
44. Margolin E, Chapman R, Williamson AL, Rybicki EP, Meyers AE. Production of complex viral glycoproteins in plants as vaccine immunogens. Plant Biotechnology Journal 2018. https://doi.org/10.1111/pbi. 12963 PMID: 29890031
45. Margolin E, Allen JD, Verbeek M, van Diepen M, Ximba P, Chapman R, et al. Site-Specific Glycosylation of Recombinant Viral Glycoproteins Produced in Nicotiana benthamiana. Frontiers in Plant Science 2021; 12. https://doi.org/10.3389/fpls.2021.709344 PMID: 34367227
46. Ward BJ, Makarkov A, Se´guin A, Pillet S, Tre´panier S, Dhaliwall J, et al. Efficacy, immunogenicity, and safety of a plant-derived, quadrivalent, virus-like particle influenza vaccine in adults (18–64 years) and older adults (ʎ 65 years): two multicentre, randomised phase 3 trials. The Lancet 2020. https://doi.org/ 10.1016/S0140-6736(20)32014-6
47. Ward BJ, Landry N, Tre´panier S, Mercier G, Dargis M, Couture M, et al. Human antibody response to N-glycans present on plant-made influenza virus-like particle (VLP) vaccines. Vaccine 2014; 32. https:// doi.org/10.1016/j.vaccine.2014.08.079 PMID: 25240757
48. Jansing J, Sack M, Augustine SM, Fischer R, Bortesi L. CRISPR/Cas9-mediated knockout of six glycosyltransferase genes in Nicotiana benthamiana for the production of recombinant proteins lacking β1,2-xylose and core α-1,3-fucose. Plant Biotechnology Journal 2019. https://doi.org/10.1111/pbi.12981 PMID: 29969180

A-1.4 SEASONAL RESPIRATORY VIRUS CIRCULATION WAS DIMINISHED DURING THE COVID-19 PANDEMIC

Preface

(This work has been previously published as a research article)

Heiskanen A, **Galipeau Y**, Little J, Mortimer L, Ramotar K, Langlois MA, Cooper CL. **Seasonal respiratory virus circulation was diminished during the COVID-19 pandemic**. Influenza Other Respir Viruses. 2023 Jan;17(1):e13065. Epub 2022 Nov 11.

https://doi.org/10.1111/irv.13065

© 2022 The Authors. *Influenza and Other Respiratory Viruses* published by John Wiley & Sons Ltd.

This is an open access article under the terms of the http://creativecommons.org/licenses/by/4.0/ License, which permits use, distribution and reproduction in any medium, provided the original work is properly cited.

Abstract

Background

Measures introduced during the COVID-19 pandemic intended to address the spread of SARS-CoV-2 may also influence the incidence of other common seasonal respiratory viruses (SRV). This evaluation reports laboratory-confirmed cases of common SRV in a well-defined region of central Canada to address this issue.

Methods

Surveillance data for common non-SARS-CoV-2 SRV in Ottawa, Canada, was provided by the Eastern Ontario Regional Laboratory Association (EORLA) reference virology lab. Weekly reports of the number of positive tests and the proportion that yielded positive results were analyzed from August 26, 2018, to January 2, 2022.

Results

A drastic reduction in influenza and other common SRV was observed during the 2020–2021 influenza season in the Ottawa region. Influenza was virtually undetected post-SARS-CoV-2 emergence. Rhinoviruses and enteroviruses were the only viruses that remained relatively unaffected during this period.

Conclusions

We speculated that the introduction of nonpharmaceutical measures including masking to prevent SARS-CoV-2 transmission contributed to the near absence of SRV in the Ottawa region. These measures should remain a key component in addressing spikes in SRV activity and future pandemics.

Introduction

Since emerging in late 2019, SARS-CoV-2 has caused unprecedented morbidity and mortality worldwide. Public health policymakers have implemented nonpharmaceutical public health measures to mitigate SARS-CoV-2 spread including the use of face coverings, targeted lockdowns and stay-at-home orders, physical distancing, school closures, restricted international travel, mandated quarantine, and reduced close contacts. In Ontario, most of these measures were put into place from March 12 to 30, 2020. Testing regulations and access to testing varied by stage of the pandemic and availability of tests.

Influenza, RSV, and other common respiratory viruses typically follow predictable seasonal patterns with high activity levels in the winter months. Australia and New Zealand saw a 98% decrease in influenza incidence during the 2020 peak influenza or "flu" season. Reduced activity was also reported for common respiratory illnesses such as the respiratory syncytial virus (RSV); seasonal human coronaviruses (HCoV); parainfluenza virus types 1, 2, 3, and 4 (PIVs); and human metapneumovirus (HMPV). Irregular seasonal behavior was observed in enteroviruses (EV), adenoviruses (AV), and rhinoviruses (RV) throughout the Southern Hemisphere.[1, 2] Similar patterns were observed throughout the winter influenza season in the Northern Hemisphere. Minimal influenza and RSV activity were reported during peak seasons in the UK and Europe, where most respiratory illness-related healthcare visits were accredited to COVID-19.[3] Surveillance data from the United States showed that influenza and RSV were circulating at historically low levels from March 2020 to May 2021. HCoV, PIV, and HMPV activity decreased in March 2020 and remained low through May 2021, after which HCoV and PIV rose to prepandemic levels. The increase in HCoV, RSV, and PIV in the spring of 2021 was inconsistent with historical seasonal peaks usually observed in the winter months. RV and EV activity decreased in March 2020 but returned to prepandemic levels in May 2020.[4] A study utilizing Canadian surveillance data reported an absence of most respiratory viruses including influenza A, influenza B, and RSV during 2020–2021. The exception was enteroviruses and rhinoviruses, which were continuously detected throughout the pandemic.[5]

This evaluation utilized surveillance data to evaluate the effect of SARS-CoV-2 pandemic countermeasures on seasonal respiratory virus circulation in the Ottawa region. Ottawa is a diverse city consisting of a broad spectrum of communities and socioeconomic conditions. Consequently, we believe that our results are broadly applicable to developed world settings.

2 Methods

2.1 Design and setting

This observational study was conducted using publicly available surveillance data from the Ottawa region. The catchment area included the 1.3 million people living in the Champlain region, Ontario's most eastern Local Health Integrated Network (LHIN). The Champlain region population is concentrated in the city of Ottawa and also spans east and west sharing a 465 km border with Quebec. This region is ethnically and linguistically diverse; 19.8% identify French as their first language, and at least 2.8% are recent immigrants.[6] The vast majority of samples were obtained from patients assessed at The Ottawa Hospital and Children's Hospital of Eastern Ontario (CHEO) thereby capturing both adult and pediatric population data.

2.2 Data sources

Specimens were collected from the Champlain region population and submitted to the Eastern Ontario Regional Laboratory Association (EORLA) regional reference virology lab based at CHEO. These data are in the public domain and circulated weekly to several sources including the Public Health Agency of Canada (PHAC) as part of the Respiratory Virus Detection Surveillance System and FluWatch report.[7] All data included in this analysis were obtained from publicly available de-identified datasets. As such, ethics board and laboratory approval were not required.

2.3 Measures/variables

Respiratory viruses of interest included: influenza A, influenza B, respiratory syncytial virus, parainfluenza viruses 1–4, human metapneumovirus, seasonal human coronaviruses (HCoV-229E, HCoV-OC42, HCoV-NL63, and HCoV-HKU1), adenovirus, enterovirus, rhinovirus, and SARS-CoV-2. Health Canada-approved assays were used for viral detection. Almost all tests were multiplex reverse transcriptase real-time PCR assays, except for one SARS-CoV-2 assay that was

a TMA-based nucleic acid amplification assay. A description of the tests used for each virus can be found in Table 1. Data from non-SARS-CoV-2 respiratory virus activities were reported weekly from August 26, 2018, to December 26, 2021. SARS-CoV-2 data were reported from August 26, 2020, to December 26, 2021. Influenza season was defined as from the beginning of November to the end of April. A case was defined as a laboratory-confirmed positive test for each respiratory virus. Percent positive values were calculated as the number of tests that yielded positive results divided by the total number of tests performed for a given week expressed as a percentage for each virus.

TABLE 1. Types of tests used to measure the seroprevalence of each respiratory virus. Location of where testing was performed within the catchment area and contextual factors and restrictions in place that may have impacted the measured seroprevalence of SARS-CoV-2 and common respiratory viruses in the Ottawa region.

Virus	Type of test used	Location	Testing restrictions
Influenza A Influenza B RSV	-Hologic FluA/B/RSV assay -Luminex Aries FluA/B/RSV assay	-Testing performed for some of the community hospitals (QCH, Montfort, Glengarry, Cornwall, Hawkesbury, Renfrew) in addition to TOH and CHEO	-Largely unrestricted. Testing was almost always performed if it is requested.
HMPV Endemic HCOVs Enterovirus Rhinovirus Adenovirus Parainfluenza viruses (1–4)	-Allplex respiratory virus panel 2 -Allplex respiratory virus panel 3	->99% of requests are from TOH and CHEO	-Mid 2020 onward, most hospitalized patients were not tested for respiratory viruses other than influenza A, influenza B, RSV, SARS-CoV-2 -Testing was restricted and must be approved by a microbiologist unless ordered by ID
SARS-CoV-2	-Allplex 2019-n CoV assay -Cobas SARS-CoV-2 assay -Aptima SARS-CoV-2 assay -Fusion SARS-CoV-2 assay	-Entire catchment area	-Subject to local and provincial guidelines

Abbreviations: CHEO, Children's Hospital of Eastern Ontario; HCoV, human coronavirus; HMPV, human metapneumovirus; QHC, Queensway Carleton Hospital; RSV, respiratory syncytial virus; SARS-CoV-2, severe acute respiratory syndrome coronavirus 2; TOH, The Ottawa Hospital.

2.4 Statistical methods

The number of positive laboratory results and the percent positive value of each virus were summarized using combination line and bar graphs. Enterovirus and rhinovirus data were reported as a single value. Data for parainfluenza virus types 1–4 were combined and presented in one chart due to the trivial number of reported cases.

3 Results

An overview of the number of non-SARS-CoV-2 specimens submitted to the EORLA laboratory for testing and the number of positive results for each virus from 2018 to 2021 is provided in

Figure 1. From the beginning of November to the end of April, approximately 7300 specimens were tested in the 2018–2019 season, 1800 in 2019–2020, and 9800 in 2020–2021. Viral peaks largely consisting of influenza and RSV occurred from November to February of the 2018–2019 and 2019–2020 winter season. An obvious absence of viral respiratory illness was reported from March 2020 onward including during the typical flu season of 2020–2021. Enterovirus and rhinovirus returned to endemic levels in August 2020, whereas viral activity for other respiratory illnesses remained low. RSV resumed prepandemic activity levels in September 2021.

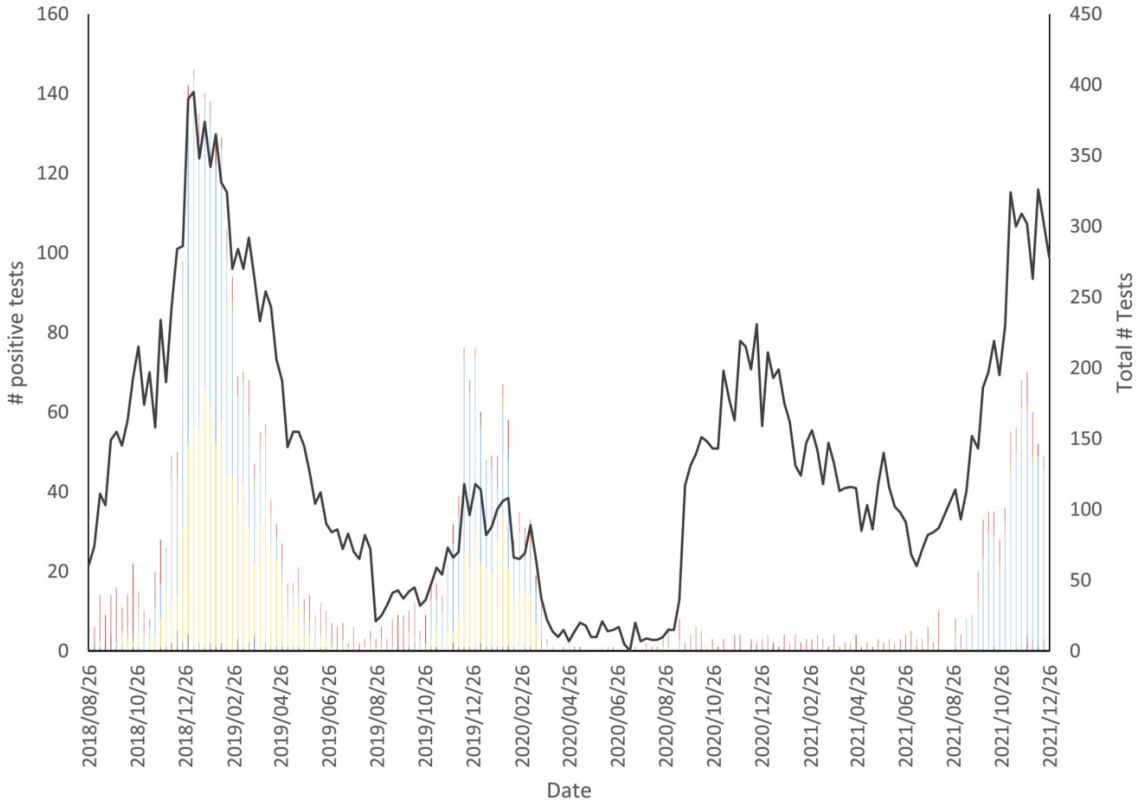


Figure 1- Total number of tests performed and number of positive common respiratory virus cases collected weekly in the Ottawa region.

The number of positive specimens and the percent of specimens that tested positive for each respiratory virus are described in Figure 2. Influenza A was dominant in the 2018–2019 winter season and both influenza A and B were prominent in the winter of 2019–2020. Influenza activity

was negligible following the onset of the COVID-19 pandemic in March 2020 (Figure 2a). The RSV season in Ontario and North America in general usually starts between November and January and generally lasts 3–4 months.[8] Besides an absence of activity in 2020–2021, standard RSV seasonality was observed throughout the study period (Figure 2b). HMPV was observed at consistently low levels from December 2018 to June 2019 and December 2019 to February 2020. No activity was observed in March 2020 and one spike in detection was recorded in February 2021 (Figure 2c). Typical endemic coronavirus seasonality consistent with pre-COVID-19 seasonal norms occurred in the 2018–2019 season with a peak from December to February and continued activity into early spring of 2019. Reduced incidence was detected the following winter with few positive cases and no activity identified over the 2020–2021 winter. Following several atypically early cases of HCoV in the spring of 2021, HCoV began to increase to prepandemic levels in the winter of 2021–2022 (Figure 2d). Enterovirus and rhinovirus activity remained largely unchanged by the COVID-19 pandemic aside from a brief period from March 2020 to July 2020, in which few cases were detected. A spike of positive specimens in August 2020 preceded a return to prepandemic levels of viral activity (Figure 2e). Two positive cases of adenovirus were detected from March 2020 to September 2020, after which approximately one case was found every few weeks, analogous to prepandemic incidence rates (Figure 2f). In 2018–2019, parainfluenza activity was highest from February to June. Reduced activity was seen in the 2019–2020 season, with no positive cases detected in the peak 2020–2021 winter season. Parainfluenza activity returned to prepandemic levels in June of 2021 (Figure 2g). The reduction in common respiratory virus activity coincided with an increase in SARS-CoV-2 activity that began in August 2020 (Figure 2h).

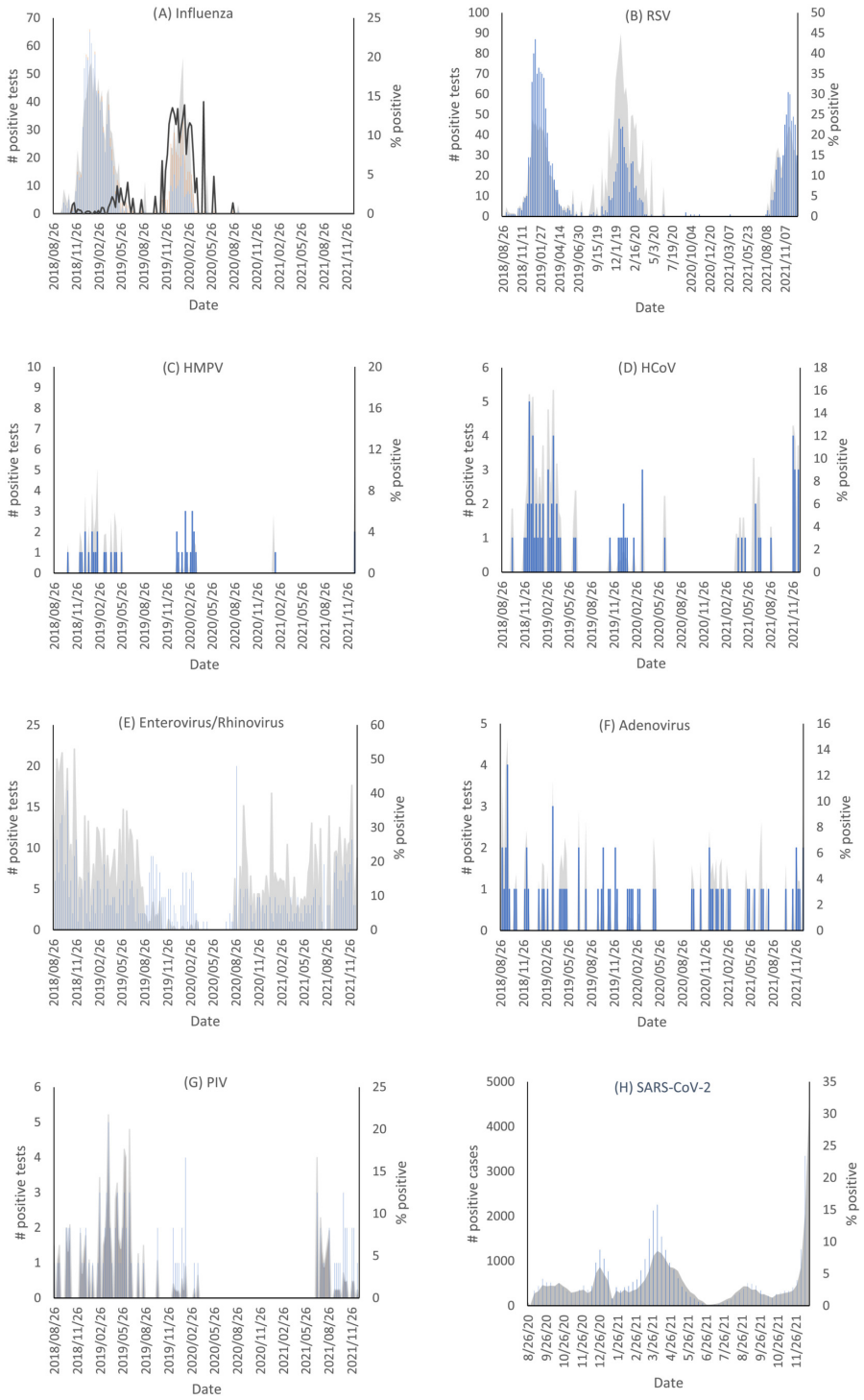


Figure 2- Number of positive tests and proportion of submitted tests that yielded positive results for influenza A and B, respiratory syncytial virus, human metapneumovirus, endemic human coronaviruses, entero/rhinoviruses, adenoviruses, parainfluenzas 1–4, and COVID-19 collected weekly from the Ottawa region. The shaded regions and line (2a) represent the test positivity as a percent. The bars represent the number of positive test results reported each week

4 Discussion

A clear absence of surveyed non-SARS-CoV-2 activity was observed beginning in March 2020, which lasted until August 2021. This timeline coincides with the introduction of public health measures in the Ottawa region and suggests that these measures implemented to mitigate SARS-CoV-2 transmission effectively reduced cases of seasonal respiratory viruses in the region. Consistent with trends observed worldwide,[2, 5, 9, 10] influenza and RSV saw the greatest decline in activity. Influenza has been practically undetected in the region since the onset of the COVID-19 pandemic. RSV was absent during the 2020–2021 season but returned to prepandemic levels the following season.

There are several reasons as to why COVID-19 mitigation measures have proven to be highly effective against common respiratory viruses such as influenza compared to SARS-CoV-2. Although influenza and SARS-CoV-2 are both spread through droplet transmission, influenza has lower transmissibility (R0 = 1.3) compared to the ancestral strain of SARS-CoV-2 (R0 = 2.0–4.0).[11] Consequently, measures including mask wearing and physical distancing may be more efficient at preventing influenza transmission.[4] Further, a degree of immunity to common respiratory viruses is already present in the population. A higher dose exposure and persistent viral load may be required for common respiratory infections to flourish compared to the novel SARS-CoV-2, which may have a competitive advantage in an immunologically naïve population.[3] In accordance with other jurisdictions, our evaluation also observed atypical HCoV and PIV activity. Children have been known to propagate respiratory illness to their households and communities, so it is possible that school closures may have blunted viral outbreaks that usually occur in the fall and winter.[4, 12] Reopening of schools is likely a key explanation for the reappearance of RSV to prepandemic levels in the fall of 2021. Rhinoviruses, adenoviruses, and enteroviruses remained relatively unaffected by the COVID-19 pandemic in this study and worldwide.[3-5, 9] This persistence may be attributed to varied modes of transmission compared to SARS-CoV-2, higher survival time on surfaces, or lack of envelope, which could provide protection against sanitizing and handwashing behaviors.

Although there is compelling evidence that public health measures have reduced seasonal respiratory virus activity alternative hypotheses should be considered. Additional theories include the vast immunologic naivety of the host population and the capabilities of SARS-CoV-2 as a pathogenic competitor. Interferon-stimulated immunity caused by a viral infection can provide nonspecific interference, deferring other viruses from establishing in a population.[13-15] Interference is thought to limit coinfection rates and contributes to the seasonality of common respiratory viruses including influenza.[8] It is possible that the presence of SARS-CoV-2 is outcompeting other viruses in the respiratory tract, delaying future outbreaks of respiratory viruses. Seasonal coronaviruses and SARS-CoV-2 share over 30% sequence homology in the S2 subunit, which may result in overlapping immune epitopes.[16] Some studies have indicated that previous infection by seasonal HCoVs reduces the risk of infection and severity of SARS-CoV-2.[16-18] Other studies have suggested that vaccination or natural infection by SARS-CoV-2 may boost antibodies and protect against endemic coronaviruses.[18-25] These views are not universal and conflicting findings argue that antibodies may be increased but do not provide protection from infection or hospitalization.[26] Frequent recombination[27, 28] and waning natural immunity[29] characteristic of the HCoV family suggest that any cross-immunity provided by infection or vaccination will not be strong enough to prevent future infections or inhibit seasonal HCoV circulation. Data from this study support the hypothesis that cocirculation of endemic coronaviruses and SARS-CoV-2 is possible, as seasonal HCoV activity returned to the Ottawa area in April 2021 despite ongoing waves of COVID-19 infection. However, atypical seasonality was observed, which may reflect the effects of cross-protection or viral interference. Further studies will hopefully fully elucidate the effect of SARS-CoV-2 on seasonal HCoV circulation and the complex immunological interactions between the two.

As measures are relaxed and vaccination is increasingly relied upon to control COVID-19, the resurgence of respiratory viruses is expected and already occurring in some locations.[1] Reduced transmission over the past 2 years has distorted the pool of susceptible individuals and may change the epidemiology of respiratory viruses for years to come. Early exposure and frequent stimulations early in life train the immune system to effectively respond to threats and have been linked to a fortified immune response in adulthood. Lack of immune stimulation caused by nonpharmaceutical public health measures over the past 2 years may result in immune deficits in

children with negative consequences when the pandemic resolves.[30] Opening international borders and increasing human mobility may also stimulate viral circulation as influenza transmission and seasonality have been partially attributed to international travel.[31] Although rare, co-infection by influenza and SARS-CoV-2 has been shown to result in an increased risk of severe illness and death (RR:5.92; 95%CI: 3.21–10.91) compared to patients with neither.[14] Testing for influenza and other respiratory viruses should remain a priority. The COVID-19 pandemic has demonstrated that nonpharmaceutical interventions are an important component in controlling viral transmission that should also be applied to seasonal respiratory virus outbreaks. Reinstating mask mandates or social distancing during influenza season or in high-risk environments such as schools is anticipated to reduce transmission or even prevent future outbreaks of common respiratory viruses. The pandemic has also illustrated that remote work or school is feasible in some industries and supports social distancing theories. Now that the infrastructure is available, employees and students may be encouraged to stay home if they are feeling ill, reducing the risk of viral outbreaks in schools or workplaces. Clinicians should also be aware of an increase in respiratory virus activity that does not follow recurrent norms and encourage influenza vaccination.

This analysis is subject to several limitations. Due to the ecological nature of this study causation cannot be inferred. However, these findings are substantiated by a growing body of evidence that has documented similar patterns and suggest that public health measures meant to prevent SARS-CoV-2 transmission have interfered with seasonal respiratory virus activity worldwide.[2-5, 9, 10] It is possible that reduced testing and redirected patient flow underestimated viral activity. Those experiencing viral respiratory illness may have been sent to COVID-19-specific test sites instead of usual care where surveillance occurs. There was a short period during the summer of 2020 when testing using the extended respiratory virus panel (extended respiratory panel of all viruses excluding SARS-CoV-2, influenza A, influenza B, and RSV) was suspended to cope with COVID-19. This may have resulted in an underestimation of the true number of cases. More detailed information on contextual factors that may have influenced the number of tests completed can be found in Table 1. Others may have been hesitant or incapable of accessing usual care or testing services amid lockdowns and COVID-19 precautions. CHEO received 34% more specimens in the 2020–2021 influenza season compared to the 2018–2019 influenza season, so it is unlikely that testing capacity largely underestimated viral activity for influenza A, influenza B, or RSV. No

seasonal spikes in influenza incidence, RSV hospital, and ICU admissions were observed, which also supports the proposal that findings truly represent reduced community circulation. Relatedly, Australia had more liberal testing criteria than Canada and still found only 33 positive influenza tests out of 60,031 tested specimens during peak season.[2] Another limitation was that the influenza vaccination rate was not measured in this evaluation. Findings from the 2020–2021 Canadian Seasonal Influenza Vaccination Coverage Survey indicated that influenza vaccination coverage in the 2020–2021 season (40%) was slightly reduced but comparable to the 2019–2020 season (42%) and 2018–2019 season (42%).[32] It is likely the rates were similar in this evaluation. However, as this variable was not measured, the exact proportion of the population vulnerable to infection is unknown and may have affected reported influenza infection rates. Finally, the surveillance data used in this analysis may not be fully representative of the Ottawa population at risk for RV infection as not all viral testing occurred at the CHEO virology laboratory. Individuals tested for SRVs through the Public Health Ontario Laboratory were not captured in these data.

5 Conclusion

This study describes a near absence of seasonal respiratory viruses in the Ottawa region for the 2020/2021 respiratory virus season. Findings from this study add to a growing body of evidence that suggests that public health measures introduced to prevent the spread of SARS-CoV-2 have also reduced laboratory-confirmed seasonal respiratory virus infections. These measures should continue to be strategically utilized to prevent, or at least diminish, the burden of future seasonal respiratory virus spikes and in response to further pandemics.

CONFLICTS OF INTEREST

The authors declare no conflicts of interest.

ETHICAL APPROVAL

All data included in this analysis were obtained from publicly available de-identified datasets; therefore, ethical approval or lab approval was not required.

AUTHOR CONTRIBUTIONS

Aliisa Heiskanen: Conceptualization; data curation; formal analysis; investigation; methodology; project administration; writing-original draft; writing-review and editing. Yannick Galipeau: Methodology; writing-review and editing. Julian Little: Writing-review and editing. Leanne Mortimer: Data curation; methodology; resources; writing-review and editing. Karamchand Ramotar: Data curation; methodology; resources; writing-review and editing. Marc-André Langlois: Writing-review and editing. Curtis L Cooper: Conceptualization; investigation; methodology; project administration; supervision; writing-review and editing.

References

1. Yeoh DK, Foley DA, Minney-Smith CA, et al. Impact of coronavirus disease 2019 public health measures on detections of influenza and respiratory syncytial virus in children during the 2020 Australian winter. Clin Infect Dis. 2021;72(12):2199-2202. doi:10.1093/cid/ciaa1475
2. Olsen SJ, Azziz-Baumgartner E, Budd AP, et al. Decreased influenza activity during the COVID-19 pandemic—United States, Australia, Chile, and South Africa, 2020. Am J Transplant. 2020;20(12): 3681-3685. doi:10.1111/ajt.16381
3. Tang JW, Bialasiewicz S, Dwyer DE, et al. Where have all the viruses gone? Disappearance of seasonal respiratory viruses during the COVID-19 pandemic. J Med Virol. 2021;93(7):4099-4101. doi:10.1002/jmv.26964 4. Olsen SJ, Winn AK, Budd AP, et al. Changes in influenza and other respiratory virus activity during the COVID-19 pandemic—United States, 2020–2021. Morb Mortal Wkly Rep. 2021;70(29):1013-1019. doi:10.15585/mmwr.mm7029a1
5. Groves HE, Piché-Renaud P-P, Peci A, et al. The impact of the COVID-19 pandemic on influenza, respiratory syncytial virus, and other seasonal respiratory virus circulation in Canada: a populationbased study. Lancet Reg Health-am. 2021;1:100015.
6. Statistics Canada. Census Profile, 2016 Census Champlain Health region Ontario. 2016. https://www12.statcan.gc.ca/censusrecensement/2016/dp-pd/prof/details/page.cfm?Lang=E&Geo1=HR&Code1=3511&Geo2=PR&Code2=35&SearchText=Champlain&SearchType=Begins&SearchPR=01&B1=All&GeoLevel=PR&GeoCode=3511&TABID=1&type=0
7. Respiratory Virus Detections in Canada. Available online: https:// www.canada.ca/en/public-health/services/surveillance/respiratoryvirus-detections-canada.html
8. Respiratory Syncytial Virus Prophylaxis for High-Risk Infants Program Reference Manual. Available online: https://www.health.gov. on.ca/en/pro/programs/drugs/funded_drug/pdf/rsv_season2021- 2022.pdf
9. Yum S, Hong K, Sohn S, Kim J, Chun BC. Trends in viral respiratory infections during COVID-19 pandemic, South Korea. Emerg Infect Dis. 2021;27(6):1685-1688. doi:10.3201/eid2706.210135
10. Huang QS, Wood T, Jelley L, et al. Impact of the COVID-19 nonpharmaceutical interventions on influenza and other respiratory viral infections in New Zealand. Nat Commun. 2021;12:1-7.
11. Wu Z, Harrich D, Li Z, Hu D, Li D. The unique features of SARSCoV-2 transmission: comparison with SARS-CoV, MERS-CoV and 2009 H1N1 pandemic influenza virus. Rev Med Virol. 2021;31:e2171.
12. Greenberg SB. Update on human rhinovirus and coronavirus infections. Thieme Medical Publishers. 2016;37(04):555-571. doi:10.1055/ s-0036-1584797
13. Stowe J, Tessier E, Zhao H, et al. Interactions between SARS-CoV-2 and influenza, and the impact of coinfection on disease severity: a test-negative design. Int J Epidemiol. 2021;50(4):1124-1133. doi:10.1093/ije/dyab081
14. Nickbakhsh S, Mair C, Matthews L, et al. Virus–virus interactions impact the population dynamics of influenza and the common cold. Proc Natl Acad Sci. 2019;116(52):27142-27150. doi:10.1073/pnas.1911083116 15. Tanner H, Boxall E, Osman H. Respiratory viral infections during the 2009–2010 winter season in Central England, UK: incidence and patterns of multiple virus co-infections. Eur J Clin Microbiol Infect Dis. 2012;31(11):3001-3006. doi:10.1007/s10096-012-1653-3
16. Ng KW, Faulkner N, Cornish GH, et al. Preexisting and de novo humoral immunity to SARS-CoV-2 in humans. Science. 2020; 370(6522):1339-1343. doi:10.1126/science.abe1107
17. Steinman JB, Lum FM, Ho PP, Kaminski N, Steinman L. Reduced development of COVID-19 in children reveals molecular checkpoints gating pathogenesis illuminating potential therapeutics. Proc Natl Acad Sci. 2020;117(40):24620-24626. doi:10.1073/pnas.2012358117
18. Yamaguchi T, Shinagawa T, Kobata H, Nakagawa H. Immunity against seasonal human coronavirus OC43 mitigates fatal deterioration of COVID-19. Int J Infect Dis. 2021;109:261-268. doi:10.1016/j.ijid.2021.07.015

19. Kellam P, Barclay W. The dynamics of humoral immune responses following SARS-CoV-2 infection and the potential for reinfection. J Gen Virol. 2020;101(8):791-797. doi:10.1099/jgv.0.001439
20. Song G, He W, Callaghan S, et al. Cross-reactive serum and memory B-cell responses to spike protein in SARS-CoV-2 and endemic coronavirus infection. Nat Commun. 2021;12(1):2938 doi:10.1038/s41467-021-23074-3
21. Aydillo T, Rombauts A, Stadlbauer D, et al. Immunological imprinting of the antibody response in COVID-19 patients. Nat Commun. 2021; 12(1):3781 doi:10.1038/s41467-021-23977-1
22. Woldemeskel BA, Garliss CC, Blankson JN. SARS-CoV-2 MRNA vaccines induce broad CD4+ T cell responses that recognize SARS-CoV-2 variants and HCoV-NL63. J Clin Invest. 2021;131(10): e149335 doi:10.1172/JCI149335
23. Nguyen-Contant P, Embong AK, Kanagaiah P, et al. S proteinreactive IgG and memory B cell production after human SARS-CoV-2 infection includes broad reactivity to the S2 subunit. MBio. 2020; 11(5):e01991-20 doi:10.1128/mBio.01991-20
24.Amanat F, Thapa M, Lei T, et al. SARS-CoV-2 MRNA vaccination induces functionally diverse antibodies to NTD, RBD, and S2. Cell. 2021;184(15):3936-3948. doi:10.1016/j.cell.2021.06.005
25. Lawrenz J, Xie Q, Zech F, et al. SARS-CoV-2 vaccination boosts neutralizing activity against seasonal human coronaviruses. Clin Infect Dis. 2022;75(1):e653-e661. doi:10.1093/cid/ciac057
26. Anderson EM, Goodwin EC, Verma A, et al. Seasonal human coronavirus antibodies are boosted upon SARS-CoV-2 infection but not associated with protection. Cell. 2021;184(7):1858-1864. doi:10.1016/j.cell.2021.02.010
27. Zhang Y, Li J, Xiao Y, et al. Genotype shift in human coronavirus OC43 and emergence of a novel genotype by natural recombination. J Infect. 2015;70(6):641-650. doi:10.1016/j.jinf.2014.12.005
28. Bobay LM, O'Donnell AC, Ochman H. Recombination events are concentrated in the spike protein region of Betacoronaviruses. PLoS Genet. 2020;16(12):e1009272 doi:10.1371/journal.pgen.1009272
29. Edridge AW, Kaczorowska J, Hoste AC, et al. Seasonal coronavirus protective immunity is short-lasting. Nat Med. 2020;26(11): 1691-1693. doi:10.1038/s41591-020-1083-1
30. Cohen R, Ashman M, Taha M-K, et al. Pediatric infectious disease group (GPIP) position paper on the immune debt of the COVID-19 pandemic in childhood, how can we fill the immunity gap? Infect Dis Now. 2021;51(5):418-423. doi:10.1016/j.idnow.2021.05.004
31. Lofgren E, Fefferman NH, Naumov YN, Gorski J, Naumova EN. Influenza seasonality: underlying causes and modeling theories. J Virol. 2007;81(11):5429-5436. doi:10.1128/JVI.01680-06
32. Vaccine uptake in Canadian adults 2021. Government of Canada. Available online: https://www.canada.ca/en/public-health/services/ immunization-vaccines/vaccination-coverage/highlights-2020-2021- seasonal-influenza-survey/full-report.html. DOI: 2022.06.1

A-1.5 COVID-19 VACCINE IMMUNOGENICITY IN PEOPLE WITH HIV

Preface

(This work has been previously published as a research article)

Costiniuk CT, Singer J, Lee T, Langlois MA, Arnold C, **Galipeau Y**, Needham J, Kulic I, Jenabian MA, Burchell AN, Shamji H, Chambers C, Walmsley S, Ostrowski M, Kovacs C, Tan DHS, Harris M, Hull M, Brumme ZL, Lapointe HR, Brockman MA, Margolese S, Mandarino E, Samarani S, Vulesevic B, Lebouché B, Angel JB, Routy JP, Cooper CL, Anis AH; COVAXHIV Study Group. **COVID-19 vaccine immunogenicity in people with HIV**. AIDS. 2023 Jan 1;37(1):F1-F10. doi: 10.1097/QAD.0000000000003429. Epub 2022 Nov 18. Erratum in: AIDS. 2023 Mar 01;37(3):559. doi: 10.1097/01.aids.0000919260.32406.0b.

http://dx.doi.org/10.1097/QAD.0000000000003429

Copyright © 2022 The Author(s). Published by Wolters Kluwer Health, Inc.

This is an open access article distributed under the terms of the Creative Commons Attribution-Non Commercial-No Derivatives License 4.0 (CCBY-NC-ND), where it is permissible to download and share the work provided it is properly cited. The work cannot be changed in any way or used commercially without permission from the journal. http://creativecommons.org/licenses/by-nc-nd/4.0

Abstract

Objectives:
Many vaccines require higher/additional doses or adjuvants to provide adequate protection for people with HIV (PWH). Our objective was to compare COVID-19 vaccine immunogenicity in PWH to HIV-negative individuals.

Design:
In a Canadian multi-center prospective, observational cohort of PWH receiving at least two COVID-19 vaccinations, we measured vaccine-induced immunity at 3 and 6 months post 2nd and 1-month post 3rd doses.

Methods:
The primary outcome was the percentage of PWH mounting vaccine-induced immunity [co-positivity for anti-IgG against SARS-CoV2 Spike(S) and receptor-binding domain proteins] 6 months post 2nd dose. Univariable and multivariable logistic regressions were used to compare COVID-19-specific immune responses between groups and within subgroups.

Results:
Data from 294 PWH and 267 controls were analyzed. Immunogenicity was achieved in over 90% at each time point in both groups. The proportions of participants achieving comparable anti-receptor-binding domain levels were similar between the group at each time point. Anti-S IgG levels were similar by group at month 3 post 2nd dose and 1-month post 3rd dose. A lower proportion of PWH vs. controls maintained vaccine-induced anti-S IgG immunity 6 months post 2nd dose [92% vs. 99%; odds ratio: 0.14 (95% confidence interval: 0.03, 0.80; $P = 0.027$)]. In multivariable analyses, neither age, immune non-response, multimorbidity, sex, vaccine type, or timing between doses were associated with reduced IgG response.

Conclusion:
Vaccine-induced IgG was elicited in the vast majority of PWH and was overall similar between groups. A slightly lower proportion of PWH vs. controls maintained vaccine-induced anti-S IgG immunity 6 months post 2nd dose demonstrating the importance of timely boosting in this population

Background and objectives

Vulnerability to acquisition and symptomatic/severe COVID-19 outcomes in people with HIV (PWH) is compounded by aging, multi-morbidity, and sociodemographic factors [1,2]. Although sub-optimal immunogenicity to common vaccines is well documented in PWH [3,4], initial studies on COVID-19 vaccines in PWH excluded those with advanced age or lower $CD4^+$ T-cell counts [5,6]. Subsequent studies yielded divergent findings regarding COVID-19 immune response in HIV immune-responders vs. non-responders [7,8]. Few studies compared responses with COVID-19 vaccine between PWH and HIV-negative participants over longer time periods, and little information is available on response to 3rd or booster vaccination in PWH. To address this knowledge gap, we established a pan-Canadian prospective cohort of PWH receiving COVID-19 vaccines to assess humoral immunogenicity in diverse PWH to compare immunogenicity responses in PWH vs. HIV-negative controls; and to describe the safety and tolerability of COVID-19 vaccines in PWH [9]. An exploratory objective was to determine if subpopulations of PWH respond differently to COVID-19 vaccination [9]. Our study is among few to date reporting on immune responses following 3rd COVID-19 vaccination dose in PWH [10–12].

Study design and methods

The current multi-center prospective observational cohort study (CTN 328) of PWH recruited from sites in Montreal, Toronto, Ottawa, and Vancouver, with the plan to compare the COVID-19 immune response produced by vaccination, with that of HIV-negative controls, who had data collected at the same time points, in a parallel cohort study (Stop the Spread Ottawa-SSO) [13]. The CTN328 protocol was previously published [9], and later amended to accommodate 3rd and 4th doses/boosters. Enrollment occurred from April to June 2021 in Vancouver and June 2021–January 2022 for remaining sites. The SSO study enrolled 1002 individuals from March to August 2021. Written informed consent was obtained from all participants and ethical approval was obtained from all Research Ethics Boards (Supplementary Information, https://links.lww.com/QAD/C715).

Participants

Inclusion criteria included age of at least 16 years; having received, or planning to receive, at least one dose of COVID-19 vaccine; HIV-seropositive. Exclusion criteria included receipt of any blood product or immunoglobulin preparation within 1 month of vaccination; signs or symptoms of active COVID-19 at enrollment. Sites were encouraged to enroll PWH previously excluded from initial COVID-19 vaccine studies (Supplementary Information, https://links.lww.com/QAD/C715) [9]. Participants who had received two COVID-19 vaccine doses prior to enrolment were eligible to participate if their 2nd vaccine dose had been administered at most 4 months post 1st dose.

A subset of immunocompetent SSO participants was used as HIV-negative controls and was included if they had undergone parallel blood collection in relation to vaccination time. A detailed description of this cohort was recently published [13].

Study visits

In the initial protocol, participants were to attend five visits over 12 months: pre-vaccination; 1 month following 1st dose; and at 3, 6, and 12 months following the 2nd dose. When the 3rd doses/boosters became available in Canada in the summer 2021 [14], we modified our protocol to include an additional visit at 1 month after this dose. Moderately–severely immunocompromised individuals in some provinces were given a 3rd dose [15] as part of the primary series. In accordance with Public Health Agency of Canada guidelines, 3rd doses of the mRNA-1273 vaccine were 50 μg (vs. 100 μg 1st and 2nd doses) for those under 65 years [16] whereas 3rd doses of the BNT162b2 vaccine were the same as for 1st and 2nd doses (30 μg). For the presented analysis, we evaluated samples collected at 3 and 6 months after 2nd dose and 1 month after the 3rd dose.

Data collection

Methods for medical and HIV history, COVID-19 Questionnaire administration, sample collection, and vaccine safety, as previously published [9] can be found in Supplementary Information, https://links.lww.com/QAD/C715.

Humoral immunity (SARS-CoV-2 binding antibodies):

For each time point, we evaluated levels of IgG targeting the SARS-CoV-2 Spike trimer (S) protein, receptor-binding domain (RBD) of spike, and nucleocapsid (N) protein using an automated high-throughput chemiluminescent ELISA [17,18]. We distinguished vaccine-induced immunity by co-positivity for S and RBD protein and infection-induced immunity by co-positivity of S and N protein (signal to cutoff ratio ≥1.0) [17]. IgG antibody titers [binding antibody units (BAU)/ml] were generated by a conversion model (4-parameter log-logistic curve based on measurements from the WHO International Standard) (NIBSC 20.136). Assay description was previously published [13,18] and it has been used in other Canadian studies [13,19,20], enabling future results comparison across cohorts.

Outcomes

The primary outcome was the percentage of PWH with COVID-19 vaccine-induced immunity, as assessed by COVID-19-specific IgG ELISA 6 months post 2nd dose. Given changes in vaccine policies advocating for a 3rd/booster dose, a secondary outcome was added to assess the percentage of individuals with COVID-19-specific IgG antibodies and 6 months post 2nd vs. 1-month post 3rd dose. Anti-S and Anti-RBD levels were also examined between groups. An exploratory objective was to determine the percentage of PWH with COVID-19-specific IgG at 6 months post 2nd dose, stratified by various sub-populations of PWH.

Statistical analyses

All analyses were performed using Statistical Analysis System (SAS) software version 9.4 (SAS Institute, Cary, NC, USA). Logistic regression analysis was used to compare the humoral immune response between the PWH and control groups. Confounder adjustment was not considered due to insufficient participants with unsatisfactory immune responses. Quantile regression adjusted for vaccine-related variables (vaccine type, time between doses) and participant characteristics (age, sex, race, 'stable'/'reference' population – $CD4^+$cell count >350 cells/μl, suppressed viral load and ≤ 1 comorbidity) and multi-morbidity, defined as at least two comorbidities (yes/no) [9] was used for IgG S, RBD and N levels as the data did not conform with normality assumption even after log transformation. We performed univariate analysis to determine whether there were factors associated with IgG S and RBD protein levels in PWH. Following univariate analysis, age, sex,

vaccine-related variables, and variables with *P* less than 0.1 in univariate analysis were further included in a multivariable model to further explore associations with participant characteristics.

Results

A total of 375 PWH were enrolled. Two hundred and sixty-seven of 1002 SSO participants were included as controls. PWH and controls with COVID-19 infection prior to vaccination and during follow-up, up until the time point of interest, were excluded from further analysis (Fig. 1) as they would be expected to have a more robust response following vaccine administration than those who were naïve to natural COVID infection [21,22]. Individuals were also excluded if they had received less than two vaccine doses or if samples were unavailable at the time points of interest.

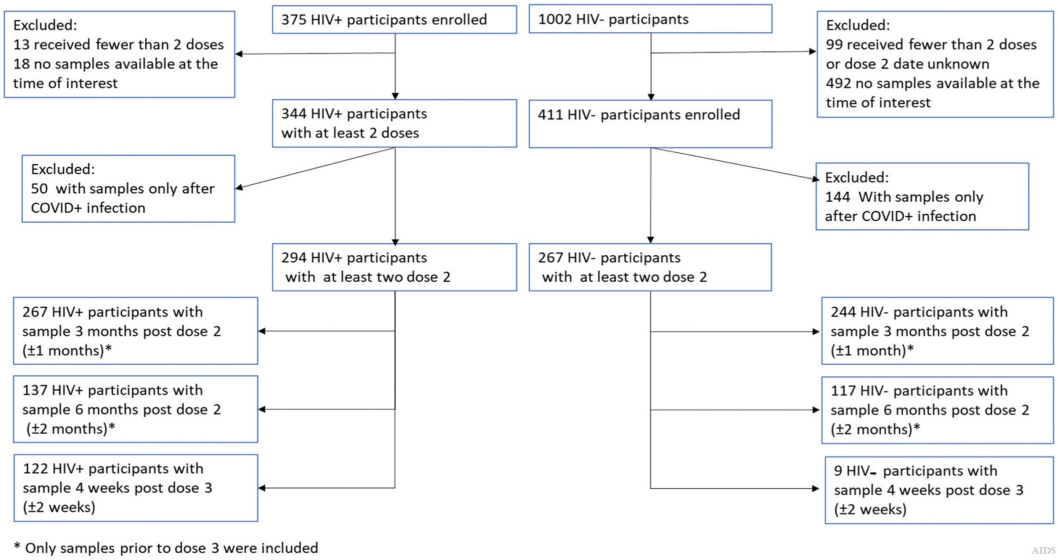


Fig. 1: *Study profile:* Total of 1377 participants (375 HIV+ and 1002 HIV−) from two observational cohorts were assessed for the study.

Baseline characteristics for 294 PWH and 267 HIV-negative controls included in the final analysis are presented in Table 1a and Supplement Table 1, https://links.lww.com/QAD/C717. Median ages were 54.4 [interquartile range (IQR) 42.3, 62.8] and 42.0 years (IQR 34.0, 54.0) for PWH and controls, respectively. PWH were 77% male vs. 26% of controls, while 47% PWH were aged at least 55 years vs. 23% of controls. Median duration of HIV infection was 17 (IQR 8, 25) years

(Table 1b). Median $CD4^+$ T-cell count was 650 (434, 855) cells/μl and $CD4^+$ T-cell nadir was 256 (IQR 120, 444) cells/μl. Approximately 20% had a history of an AIDS-defining illness. Eleven percent had a detectable HIV viral load within the last 6 months. Nearly all were on antiretroviral therapy (ART) (97.6%). Over 70% of participants were on integrase strand inhibitor-based regimens. Common comorbidities included obesity (21% vs. 14% in PWH and controls, respectively), dyslipidemia (15% vs. 8%), and hypertension (14% vs. 9%) (Supplement Tables 2a and b, https://links.lww.com/QAD/C717). At enrollment, 71 PWH had not yet received any COVID-19 vaccine doses, 106 had received a single dose, and 117 had received a second dose (Table 2). By the time of data analysis in June 2022, 54 individuals had received a 2nd, 214 had received a 3rd, and 26 had received a 4th dose (samples collected after the 4th dose were not included in the current analysis). BNT162b2 and mRNA-1273 were the most commonly administered vaccines (94% in PWH and 99% in controls).

Humoral immune response: anti-receptor-binding domain binding antibody response after 2nd and 3rd vaccine doses

Ninety-six percentage of PWH mounted detectable positive RBD and S levels 3 months after the 2nd dose and 92% of PWH maintained detectable RBD and S levels at 6 months post 2nd dose (Table 3). One month post 3rd/booster dose, 100% of PWH had detectable RBD and S levels. There was no difference in antibody levels between PWH and controls at 3 months after 2nd dose [odds ratio (OR): 0.67 (95% confidence interval (CI): 0.25, 1.81)]. There were less PWH than controls with detectable antibody responses at 6 months post 2nd dose [OR: 0.14 (95% CI: 0.03, 0.80); $P = 0.027$]. There was no difference between PWH and controls when stratified by sex. The same trend as the overall cohort was observed at the 6-month time point with fewer PWH having a positive response in both sexes. Of PWH in the ‘stable’/‘reference’ population, 96.2% achieved a response 3 months post 2nd dose, 95.2% maintained this response at 6 months post 2nd dose and 100% obtained a response 1-month post 3rd dose (Table 3). No difference in immunogenicity was detected between this group and the ‘nonstable’ PWH populations.

Table 1 - Characteristics of participants with samples prior to COVID infection, HIV+ participants, and controls.

(a) Characteristics of participants with samples prior to COVID infection, *n* (%)

Variable	HIV$^+$, $n=294$	HIV$^-$, $n=267$
Median (IQR)/Range	54.4 (42.3, 62.8)/(19.7, 83.5)	42.0 (34.0, 54.0)/(20.0, 79.0)
Age		
<35	36 (12.4)	68 (25.5)
35–44	46 (15.8)	78 (29.2)
45–54	70 (24.1)	60 (22.5)
55–64	85 (29.2)	40 (15.0)
65–74	43 (14.8)	19 (7.1)
≥75	11 (3.8)	2 (0.7)
Sex		
Male	227 (77.2)	70 (26.2)
Female	65 (22.1)	197 (73.8)
Prefer to self describe	2 (0.7)	0 (0.0)
Self-declared race or ethnicity		
White	186 (63.3)	241 (90.3)
Indigenous	5 (1.7)	3 (1.1)
Asian/Filipino	19 (6.5)	6 (3.24)
Black	54 (18.4)	0 (0.0)
Latin American	23 (7.8)	3 (1.1)
Arab/West Asian	5 (1.7)	5 (1.9)
Prefer to self-describe/Other	16 (5.4)	8 (3.0)
Subpopulation		
Age >55 years	139/291 (47.8)	61/267 (22.8)
Multi-morbidity (≥2 comorbidities)	84/288 (29.2)	46/265 (17.4)

(b) HIV-related characteristics of HIV$^+$ participants with samples prior to COVID infection, *n* (%)

Duration of HIV infection, years ($n=273$)	
Median (IQR)/Range	17.0 (8.0, 25.0)/(0.0, 39.0)
Duration of HIV infection, years ($n=273$)	
<10	76 (27.8)
10–19	92 (33.7)
20+	105 (38.5)
CD4$^+$ nadir (cells/μl) ($n=166$)	
Median (IQR)/Range	256 (120, 444)
<100	36 (21.7)
100–199	33 (19.9)
200–299	29 (17.5)
300–399	20 (12.0)
≥400	48 (28.9)
CD4$^+$ cell count (cells/μl) ($n=273$)	
Median (IQR)/Range	650 (434, 855)/(9, 1800)
CD4$^+$ cell count (cells/μl) ($n=273$)	
<250	18 (6.6)
250–349	17 (6.2)
350–499	57 (20.9)
500–999	149 (54.6)
≥1000	32 (11.7)
CD4$^+$/CD8$^+$ ratio ($n=261$)	
Median (IQR)/Range	0.85 (0.58, 1.24)/(0.00, 2.50)
CD4$^+$/CD8$^+$ ratio ≥0.75, *n* (%)	151/261 (57.9)
Detectable viral load for at least 6 months, *n* (%)	31/289 (10.7)
If detectable, highest viral load over past 6 months ($n=240$) (copies/ml)/Median (IQR)/Range	269 (62, 2479)/(20, 1.00E+07)
ART regimen	
None	7 (2.4)
NRTI-based regimen	3 (1.0)
NNRTI-based regimen	25 (8.5)
PI-based regimen	8 (2.7)
INSTI-based regimen	213 (72.4)
Other[a]	38 (12.9)
Subpopulation	
Immune non-responder[b]	23/276 (8.3)
HIV+ stable/reference (CD4$^+$ cell count ≥350, suppressed VL and ≤1 comorbidity)	145/271 (53.5)

ART, antiretroviral therapy; IQR, interquartile range; INSTI, integrase strand transfer inhibitor; NRTI, nucleoside reverse transcriptase inhibitor; NNRTI, non-nucleoside reverse transcriptase inhibitor; PI, protease inhibitor; VL, viral load.
[a]Regimens containing combinations of above and/or other drug classes (i.e., cell-entry inhibitor).
[b](CD4$^+$ cell count <350, CD4$^+$/CD8$^+$ cell count <0.75, suppressed VL).

Table 2 - COVID-19 vaccination of participants with samples prior to COVID infection.

Variable	HIV+, $n=294$	HIV−, $n=267$
Number of COVID-19 vaccine dose received at *study enrollment*		
None	71 (24.1)	
Received 1 dose of a 2-dose schedule	106 (36.1)	
Received 2 doses of a 2-dose schedule, or 1 dose of a 1-dose schedule	117 (39.8)	
Number of COVID-19 vaccine dose received at *time of data analysis*		
2	54 (18.4)	
3	214 (72.8)	
4	26 (8.8)	
Types of COVID-19 vaccines received, doses 1 and 2		
Unknown	0	1
mRNA–mRNA	252 (85.7)	230 (86.5)
ChAdOx1–mRNA	23 (7.8)	35 (13.2)
ChAdOx1–ChAdOx1	18 (6.1)	1 (0.4)
Ad26.COV2.S	1 (0.3)	0 (0.0)
Types of COVID-19 vaccines received, dose 3		
Unknown	6	
BNT162b2	95 (40.6)	
mRNA-1273	139 (59.4)	
Received same type of vaccine for all 3 doses		
Unknown	2	
Yes, BNT162b2	59 (24.8)	
Yes, mRNA-1273	47 (19.7)	
No	132 (55.5)	
Time between first and second doses in days		
Median (IQR)/Range	61 (52, 76)/(20, 135)	46 (31, 75) (19, 125)
No. of missing or N/A (Janssen)	1	1
Time between second and third doses in days		
Median (IQR)/Range	181 (162, 191)/(55, 285)	

IQR, interquartile range.

Table 3 - (a) Number of participants positive for vaccine Immunity (anti-S and receptor-binding domain) after COVID-19 vaccination, *n* (%).

Subgroup and time point	HIV+	HIV−	Odds ratio[a] HIV+ vs. HIV− (95% CI)	*P*
All participants				
3 months post dose 2 (±1 month)	257/267 (96.3)	238/244 (97.5)	0.67 (0.25, 1.81)	0.428
6 months post dose 2 (±2 months)	126/137 (92.0)	116/117 (99.1)	0.14 (0.03, 0.80)	0.027
4 weeks post dose 3 (±2 weeks)	122/122 (100.0)	9/9 (100.0)	–	
Among males				
3 months post dose 2 (±1 month)	200/208 (96.2)	62/64 (96.9)	0.94 (0.22, 4.01)	0.937
6 months post dose 2 (±2 months)	99/109 (90.8)	29/29 (100.0)	0.16 (0.01, 2.96)	0.219
4 weeks post dose 3 (±2 weeks)	107/107 (100.0)	3/3 (100.0)	–	
Among females				
3 months post dose 2 (±1 month)	55/57 (96.5)	176/180 (97.8)	0.57 (0.12, 2.76)	0.482
6 months post dose 2 (±2 months)	26/27 (96.3)	87/88 (98.9)	0.30 (0.03, 3.12)	0.316
4 weeks post dose 3 (±2 weeks)	14/14 (100.0)	6/6 (100.0)	–	

(b) Number of HIV+ stable/reference[b] and non-stable participants positive for vaccine Immunity (anti-S and receptor-binding domain) after COVID-19 vaccination, *n* (%)

	HIV+ stable/reference participants			
Time point	No	Yes	Odds ratio (95% CI)	*P*
3 months post dose 2 (±1 month)	107/112 (95.5)	127/132 (96.2)	1.19 (0.35, 4.00)	0.783
6 months post dose 2 (±2 months)	56/63 (88.9)	60/63 (95.2)	2.29 (0.61, 8.68)	0.221
4 weeks post dose 3 (±2 weeks)	47/47 (100.0)	61/61 (100.0)	–	

CI, confidence interval; VL, viral load.
[a]Unadjusted odds ratio was presented.
[b]$CD4^+$ cell count ≥350, suppressed VL and ≤1 comorbidity.

Antibody responses to SARS-CoV-2 full-length receptor-binding domain proteins – IgG RBD and spike protein in PWH and controls are presented in Supplemental Fig. 1, https://links.lww.com/QAD/C716 and Supplement Table 3, https://links.lww.com/QAD/C717. In both groups, IgG titers declined at 6 months after the 2nd dose relative to 3 months post 2nd dose, and were higher at 4 weeks post 3rd dose/booster (Supplemental Figs. 2 and 3, https://links.lww.com/QAD/C716). Median anti-S IgG was lower in PWH than the controls at 3 and 6 months post 2nd dose [adjusted difference in median: −0.15 log10 BAU/ml (95% CI: −0.24, −0.07) ($P < 0.001$) and −0.21 (95% CI: −0.35, −0.06) ($P = 0.005$), respectively]. Median anti-RBD levels were not statistically different between PWH and controls at 3 months post 2nd dose [adjusted difference in median: −0.13 log10 BAU/ml (95% CI: −0.26, 0.01) ($P = 0.062$) and 6 months post 2nd dose (adjusted difference in median: 0.01 log10 BAU/ml (95% CI: −0.30, 0.31) ($P = 0.960$)]. At 4 weeks post 3rd dose, median anti-S, and anti-RBD IgG were not statistically significantly different between groups [adjusted difference in median: −0.13 log10 BAU/ml (95% CI: −0.61, 0.35) ($P = 0.599$) and −0.06 log10 BAU/mL (95% CI: −0.80, 0.68) ($P = 0.875$), respectively] (Supplemental Fig. 2, https://links.lww.com/QAD/C716 and Supplement Table 3, https://links.lww.com/QAD/C717).

In univariate analysis, the presence of single or multiple comorbidities did not influence IgG response in PWH (Supplement Table 4, https://links.lww.com/QAD/C717). Examining differences in median IgG RBD and IgG S protein in relation to HIV-related characteristics by univariate quantile regression suggested that $CD4^+$ nadir and $CD4^+$ cell count predicted first time point immunogenicity. No other HIV-related variables (HIV infection status or being immune non-responder) showed this effect. Similarly, neither having a detectable vs. undetectable viral load in the past 6 months nor type of ART regimen was predictive of IgG response (Supplement Table 5, https://links.lww.com/QAD/C717). In multivariable comparisons within the PWH group, neither age nor sex was predictive of IgG levels. Higher $CD4^+$ cell count and having received an mRNA type of vaccine were positively associated with IgG RBD and S levels at both 3 and 6 months post 2nd dose but not at 4 weeks post 3rd dose/booster (Table 4).

Table 4 - Association between IgG spike (a) and receptor-binding domain response (b) and PWH characteristics by multivariable quantile regression.

(a) Association *between IgG spike* response and participant characteristics by multivariable quantile regression

Time point	3 months post dose 2 (±1 month)		6 months post dose 2 (±2 months)		4 weeks post dose 3 (±2 weeks)	
Comparison	Difference (95% CI)	*P*	Difference (95% CI)	*P*	Difference (95% CI)	*P*
Age (per 10 years increase)	−0.01 (−0.03, 0.02)	0.719	0.02 (−0.05, 0.10)	0.539	−0.02 (−0.11, 0.06)	0.618
Sex now						
Male	−0.02 (−0.15, 0.11)	0.752	−0.09 (−0.29, 0.11)	0.388	−0.27 (−0.60, 0.07)	0.119
Female	Referent		Referent		Referent	
$CD4^+$ cell count (per 100 cells/μl increase)	0.02 (0.00, 0.03)	0.043	0.03 (−0.01, 0.06)	0.122	−0.02 (−0.06, 0.02)	0.350
Types of COVID-19 vaccines received, doses 1 and 2						
mRNA–mRNA	0.69 (0.37, 1.00)	<0.001	1.32 (1.06, 1.58)	<0.001	0.07 (−0.46, 0.59)	0.804
ChAdOx1–mRNA	0.65 (0.28, 1.03)	<0.001	1.32 (0.96, 1.67)	<0.001	−0.14 (−0.88, 0.60)	0.713
ChAdOx1–ChAdOx1	Referent		Referent		Referent	
Time between 1st and 2nd doses (per 10 days increase)	−0.01 (−0.04, 0.02)	0.488	−0.05 (−0.13, 0.02)	0.174	−0.02 (−0.09, 0.06)	0.679
Received same type of vaccine for all 3 doses						
Yes, BNT162b2 ($n = 59$)					−0.44 (−0.75, −0.12)	0.007
Yes, mRNA-1273 ($n = 47$)					−0.10 (−0.37, 0.17)	0.465
No ($n = 132$)					Referent	
Time between 2nd and 3rd doses (per 10 days increase)					0.02 (−0.02, 0.06)	0.246

(b) Association *between IgG* receptor-binding domain response and participant characteristics by multivariable quantile regression

Time point	3 months post dose 2 (±1 month)		6 months post dose 2 (±2 months)		4 weeks post dose 3 (±2 weeks)	
Comparison	Difference (95% CI)	*P*	Difference (95% CI)	*P*	Difference (95% CI)	*P*
Age (per 10 years increase)	−0.03 (−0.07, 0.02)	0.223	0.00 (−0.10, 0.09)	0.939	0.02 (−0.09, 0.12)	0.750
Sex						
Male	0.09 (−0.10, 0.29)	0.348	−0.09 (−0.37, 0.19)	0.535	−0.19 (−0.62, 0.25)	0.403
Female	Referent		Referent		Referent	
Self-declared race or ethnicity						
Black	0.16 (−0.01, 0.34)	0.071	0.01 (−0.28, 0.30)	0.933	−0.06 (−0.56, 0.45)	0.820
Other	0.00 (−0.19, 0.19)	0.964	0.08 (−0.18, 0.34)	0.543	0.18 (−0.18, 0.54)	0.316
White	Referent		Referent		Referent	
$CD4^+$ cell count (per 100 cells/μl increase)	0.04 (0.02, 0.07)	0.001	0.03 (−0.02, 0.07)	0.279	−0.01 (−0.05, 0.03)	0.505
Types of COVID-19 vaccines received, doses 1 and 2						
mRNA–mRNA	0.65 (0.27, 1.02)	<0.001	0.87 (0.40, 1.33)	<0.001	−0.19 (−0.76, 0.37)	0.497
ChAdOx1–mRNA	0.46 (−0.01, 0.94)	0.055	0.67 (−0.04, 1.39)	0.066	−0.42 (−1.24, 0.41)	0.320
ChAdOx1–ChAdOx1	Referent		Referent		Referent	
Time between 1st and 2nd doses (per 10 days increase)	0.00 (−0.04, 0.04)	0.965	−0.05 (−0.15, 0.05)	0.310	−0.02 (−0.09, 0.05)	0.594
Received same type of vaccine for all 3 doses						
Yes, BNT162b2					−0.31 (−0.60, −0.01)	0.043
Yes, mRNA-1273					0.06 (−0.24, 0.36)	0.703
No					Referent	
Time between 2nd and 3rd doses (per 10 days increase)					0.03 (−0.01, 0.07)	0.173

CI, confidence interval.

Tolerability and safety

Overall, vaccines were very well tolerated in PWH. Most participants experienced pain at the injection site within the first 7 days after 2nd dose (65%) and 3rd dose/booster (66%) and fatigue after the booster. The severity of local and systemic reactions is outlined in Supplement Fig. 3, https://links.lww.com/QAD/C716.

Discussion

We present findings from a large and comprehensive study cohort of PWH receiving COVID-19 vaccination. Reassuringly, we found that the vast majority of PWH obtained a detectable antibody response at 3 and 6 months following 2nd dose and 1 month following a 3rd or booster dose. Importantly, PWH aged more than 55 years, immune non-responders (HIV-positive individuals in

whom the administration of ART, although successful in suppressing viral replication, cannot properly rebuild circulating $CD4^+$ cell numbers), and those with multimorbidity achieved similar antibody levels to COVID-19 vaccines compared with HIV-negative controls. In line with other studies, we also found that COVID-19 vaccines were safe and well tolerated in PWH [10–12].

The importance of advanced age on diminished vaccine immunogenicity is well documented [23]. Poor antibody production following influenza vaccination has been observed in older PWH [24,25]. In HIV-negative individuals, antibody levels to COVID-19 mRNA vaccines were lower in older adults after 1st and 2nd doses, in adjusted multivariable analyses, including sociodemographic and chronic health and vaccine-related variables [26]. Cossu *et al.* found reduced anti-S response to vaccination in PWH vs. HIV-negative controls, despite most PWH in their study having $CD4^+$ cell count of more than 500 cells/μl [27]. They attributed this discrepancy to multi-morbidity burden in older adults [27]. In our study, age did not influence COVID-19 vaccine response. Similar to findings of other reports [10,11,12], our data suggest that PWH may retain antibodies for a shorter duration of time following initial vaccination when compared with controls, with a 3rd vaccine dose resulting in improved levels of immune response. We believe that our data support timely, serial booster administration to PWH.

$CD4^+$ cell count and HIV viral load are used by clinicians to predict vaccine immunogenicity [3,4]. Although we only had 18 (6.6%) PWH with $CD4^+$ cell counts less than 250 cells/μl, neither low-level $CD4^+$ cell count nor detectable viral load, was a predictor of diminished antibody levels. In line with our findings, Vergori *et al.*[12] stratified PWH by $CD4^+$ cell count and found robust response 15 days after 3rd dose. Antinori *et al.*[10] also stratified participants by current $CD4^+$ cell count. Similarly to our study, a fewer proportion of individuals with lower $CD4^+$ cell counts mounted detectable antibody responses, but this proportion increased with increasing vaccine doses [10]. Furthermore, we did not find that ability to mount antibody responses was affected by sex, age, baseline $CD4^+$ cell count, a finding which is in keeping with other studies [11].

In the general older population, comorbidity burden contributes to poor COVID-19 vaccine response [28]. Multi-morbidity did not affect humoral immune response in our study. One possible explanation is that our study participants are closely followed in clinic and their comorbidities are

generally well-managed. To date, no other studies examining PWH have identified an association between obesity and vaccine immunogenicity. There is evidence for sex-based differences in humoral immune response with certain types of vaccinations in HIV-negative populations [29]. However, we and others have not observed any sex difference in the context of COVID-19 vaccination [10–12,19].

Several limitations are acknowledged. As recruitment began in May 2021, we missed obtaining baseline samples from many elderly and Indigenous participants who were considered priority vaccination groups in Canada and therefore received vaccination in early 2021 [14]. Provinces differed based on type of vaccine administered and vaccine dosing intervals [14]. Our results may not be generalizable to PWH who are not on ART [30,31]. The number of PWH participants with low $CD4^+$ cell counts and without full HIV RNA suppression, and those with data at the 1-month post 3rd dose time were low which limited the robustness of our analysis. As most participants received mRNA vaccine, we could not assess temporal differences of immunogenicity based on vaccine type. Furthermore, the assays used only assess binding antibody levels to wildtype or 'original' SARS-CoV-2. BAUs at 3 months post 2nd dose could suggest somewhat diminished COVID-19 vaccine immunogenicity in PWH compared with controls. Further studies, looking into the ratio between IgG-S BAU and protection against infection in PWH and aged individuals are warranted. Wei *et al.*[32] inferred that antibody to S protein of about 100 BAU/ml gave about 67% protection against the delta variant, although after a 2nd dose many individuals did not achieve this antibody level.

In summary, adult PWH with well-controlled HIV on ART mount antibody responses following 2nd and 3rd COVID-19 vaccine doses similar to HIV-negative individuals. Diminishing proportions of PWH with detectable antibody levels argue for timely serial booster dosing to maintain seroprotection. Additional information related to durability of humoral immune response, neutralization capacity, and the contribution of cell-mediated immunity will complement these current findings and inform COVID-19 vaccination clinical guidelines for PWH.

Acknowledgements
The authors thank the CTN staff who were involved in the planning and preparation of this study, in addition to the CTN Scientific Review Committee and the Community Advisory Board, for their expedited review and helpful comments. They also thank all of the participants for their time and commitment. In addition, the authors thank study coordinators and study nurses: Florian Bobeuf, Claude Vertzagias, Lina Del Balso, Nathalie Paisible, Guillaume Theriault, Hansi Peiris, Lianne Thai, Rosemarie Clarke, Erin Collins, Nadia Ohene-Adu, Aron Dyks, and Jill Jackson; data manager Elisa Lau; laboratory staff: Tara Mabanga, Yulia Alexandrova, Ralph-Sydney Mboumba Bouassa, Erik Pavey, Stephanie Burke-Schinkel, Danielle Dewar-Darch, Justino Hernandez Soto, Abishek Xavier, Yuchu Dou, Yuchu Dou, Sarah Speckmaier, Nadia Moran-Garcia, Hanwei Sudderuddin, Maggie Duncan and Evan Barad. The authors also thank physicians who assisted with recruitment.

Authors' contributions
Co-principal investigators of the study are C.T.C., C.L.C., and A.H.A. C.T.C. and C.L.C. conceived the study and led the proposal and protocol development. C.T.C. wrote the first draft of the article. J.S. is the biostatistician who provided methodological expertise and performed sample size calculations. All other authors contributed to protocol development, study design, and development of the proposal. C.T.C., M.A.L., C.A., Y.G., M.A.J., M.O., M.A.B., and Z.L.B. designed the laboratory evaluations. S.S. oversaw lab specimen processing and lab database development. M.A.L., C.A., and Y.G. were responsible for studies on humoral immunity. J.S. oversaw data analysis between groups and subgroup analyses. T.L. performed data analyses. All authors critically reviewed and approved the final article.

COVID-19 RBD antigen as well as the antihIgG#5-HRP fusion antibody were generously provided by Dr Yves Durocher, National Research Council of Canada (NRC), Montreal.

C.T.C. is supported by a Fonds de recherche du Québec-Santé (FRQS) Junior 2 career award. A.N.B. holds a Canada Research Chair Tier 2 Canada Research Chair (CRC) in sexually transmitted infection (STI) Prevention. MAL holds a CRC in Molecular Virology and Intrinsic Immunity. M.A.J. holds a CRC, Tier 2, in human immunovirology. S.W. is supported by a Research Chair in HIV Clinical Care and Aging from the Ontario HIV Treatment Network. D.T. is supported by a Tier 2 CRC in HIV Prevention and STI Research. M.A.B. holds a Canada Research Chair, Tier 2, in viral pathogenesis and immunity. Z.L.B. holds a Scholar Award from the Michael Smith Foundation for Health Research. B.L. is supported by two career awards: a Senior Salary Award from Fonds de recherche du Québec–Santé (FRQS) (#311200) and the LE 250, from the Quebec's Ministry of Health for researchers in Family Medicine. Also, B.L. holds a Canadian Institutes of Health Research (CIHR), Strategy for Patient-Oriented Research (SPOR) Mentorship Chair in Innovative Clinical Trials for HIV Care. J.P.R. holds a Lowenstein Chair in Hematology.

The current project was supported by funding from the Public Health Agency of Canada, through the Vaccine Surveillance Reference group and the COVID-19 Immunity Task Force (grant number: 2122-HQ-000075), and the CTN (grant number: N/A). Production of COVID-19 reagents

was financially supported by the National Research Council of Canada (NRC)'s Pandemic Response Challenge Program.
Trial registration: clinicaltrials.gov NCT04894448.

Conflicts of interest
The authors declare that they have no competing interests.

References

1. Tesoriero JM, Swain CE, Pierce JL, Zamboni L, Wu M, Holtgrave DR, et al. COVID-19 outcomes among persons living with or without diagnosed HIV infection in New York state. *JAMA Netw Open* 2021; 4:e2037069.
2. Weiser JK, Tie Y, Beer L, Neblett Fanfair R, Shouse RL. Racial/ethnic and income disparities in the prevalence of comorbidities that are associated with risk for severe COVID-19 among adults receiving HIV care, United States, 2014–2019. *J Acquir Immune Defic Syndr* 2021; 86:297–304.
3. Crum-Cianflone NF, Sullivan E. Vaccinations for the HIV-infected adult: a review of the current recommendations, Part I. *Infect Dis Ther* 2017; 6:303–331.
4. Crum-Cianflone NF, Sullivan E. Vaccinations for the HIV-infected adult: a review of the current recommendations, Part II. *Infect Dis Ther* 2017; 6:333–361.
5. Bergman P, Blennow O, Hansson L, Mielke S, Nowak P, Chen P, et al. Safety and efficacy of the mRNA BNT162b2 vaccine against SARS-CoV-2 in five groups of immunocompromised patients and healthy controls in a prospective open-label clinical trial. *EBioMedicine* 2021; 74:103705.
6. Levy I, Wieder-Finesod A, Litchevsky V, Biber A, Indenbaum V, Olmer L, et al. Immunogenicity and safety of the BNT162b2 mRNA COVID-19 vaccine in people living with HIV-1. *Clin Microbiol Infect* 2021; 27:1851–1855.
7. Frater J, Ewer KJ, Ogbe A, Pace M, Adele S, Adland E, et al. Safety and immunogenicity of the ChAdOx1 nCoV-19 (AZD1222) vaccine against SARS-CoV-2 in HIV infection: a single-arm substudy of a phase 2/3 clinical trial. *Lancet HIV* 2021; 8:e474–e485.
8. Sistere-Oro M, Andrade N, Wortmann DDJ, Du J, Garcia-Giralt N, Gonzalez-Cao M, et al. Anti-SARS-COV-2 specific immunity in HIV immunological nonresponders after mRNA-based COVID-19 vaccination. *Front Immunol* 2022; 13:994173.
9. Costiniuk CT, Singer J, Langlois MA, Kulic I, Needham J, Burchell A, et al. CTN 328: immunogenicity outcomes in people living with HIV in Canada following vaccination for COVID-19 (HIV-COV): protocol for an observational cohort study. *BMJ Open* 2021; 11:e054208.
10. Antinori A, Cicalini S, Meschi S, Bordoni V, Lorenzini P, Vergori A, et al. Humoral and cellular immune response elicited by mRNA vaccination against severe acute respiratory syndrome coronavirus 2 (SARS-CoV-2) in people living with human immunodeficiency virus receiving antiretroviral therapy based on current CD4 T-lymphocyte count. *Clin Infect Dis* 2022; 75:e552–e563.
11. Gianserra L, Dona MG, Giuliani E, Stingone C, Pontone M, Buonomini AR, et al. Immunogenicity and safety of BNT162b2 homologous booster vaccination in people living with HIV under effective cART. *Vaccines (Basel)* 2022; 10:1243.
12. Vergori A, Cozzi Lepri A, Cicalini S, Matusali G, Bordoni V, Lanini S, et al. Immunogenicity to COVID-19 mRNA vaccine third dose in people living with HIV. *Nat Commun* 2022; 13:4922.
13. Collins E, Galipeau Y, Arnold C, Bosveld C, Heiskanen A, Keeshan A, et al. Cohort profile: Stop the Spread Ottawa (SSO)—a community-based prospective cohort study on antibody responses, antibody neutralisation efficiency and cellular immunity to SARS-CoV-2 infection and vaccination. *BMJ Open* 2022; 22:e062187.
14. Ministry of Health. COVID-19 vaccine booster recommendation. Version 8.3 22 July 2022.
15. Canada Public Health Agency Canada 2022. Available at: https://www.canada.ca/en/public-health/services/publications/healthy-living/canadian-immunization-guide-part-4-active-vaccines/page-26-covid-19-vaccine.html [Accessed 31 May 2022]
16. Public Health Agency of Canada 2022. Available at: https://www.canada.ca/en/health-canada/news/2021/11/health-canada-authorizes-the-use-of-the-moderna-spikevax-covid-19-vaccine-as-a-booster-shot.html. [Accessed 12 November 2021]
17. Cholette F, Fabia R, Harris A, Ellis H, Cachero K, Schroeder L, et al. Comparative performance data for multiplex SARS-CoV-2 serological assays from a large panel of dried blood spot specimens. *Heliyon* 2022; 8:e10270.

18. Colwill K, Galipeau Y, Stuible M, Gervais C, Arnold C, Rathod B, et al. A scalable serology solution for profiling humoral immune responses to SARS-CoV-2 infection and vaccination. *Clin Transl Immunol* 2022; 11:e1380.
19. Vinh DC, Gouin JP, Cruz-Santiago D, Canac-Marquis M, Bernier S, Bobeuf F, et al. Real-world serological responses to extended-interval and heterologous COVID-19 mRNA vaccination in frail, older people (UNCoVER): an interim report from a prospective observational cohort study. *Lancet Healthy Longev* 2022; 3:e166–e175.
20. Fakhraei R, Erwin E, Alibhai KM, Murphy MSQ, Dingwall-Harvey ALJ, White RR, et al. Prevalence of SARS-CoV-2 infection among obstetric patients in Ottawa, Canada: a descriptive study. *CMAJ Open* 2022; 10:E643–E651.
21. Blain H, Tuaillon E, Gamon L, Pisoni A, Miot S, Picot MC, et al. Spike antibody levels of nursing home residents with or without prior COVID-19 3 weeks after a single BNT162b2 vaccine dose. *JAMA* 2021; 325:1898–1899.
22. Saadat S, Rikhtegaran Tehrani Z, Logue J, Newman M, Frieman MB, Harris AD, et al. Binding and neutralization antibody titers after a single vaccine dose in healthcare workers previously infected with SARS-CoV-2. *JAMA* 2021; 325:1467–1469.
23. Gustafson CE, Kim C, Weyand CM, Goronzy JJ. Influence of immune aging on vaccine responses. *J Allergy Clin Immunol* 2020; 145:1309–1321.
24. Pallikkuth S, De Armas LR, Pahwa R, Rinaldi S, George VK, Sanchez CM, et al. Impact of aging and HIV infection on serologic response to seasonal influenza vaccination. *AIDS* 2018; 32:1085–1094.
25. Parmigiani A, Alcaide ML, Freguja R, Pallikkuth S, Frasca D, Fischl MA, et al. Impaired antibody response to influenza vaccine in HIV-infected and uninfected aging women is associated with immune activation and inflammation. *PLoS One* 2013; 8:e79816.
26. Brockman MA, Mwimanzi F, Lapointe HR, Sang Y, Agafitei O, Cheung PK, et al. Reduced magnitude and durability of humoral immune responses to COVID-19 mRNA vaccines among older adults. *J Infect Dis* 2022; 225:1129–1140.
27. Cossu MV, Mileto D, Giacomelli A, Oreni L, Bracchitta F, Pellicciotta M, et al. Does the co-morbidity burden contribute to suboptimal immunological responses to COVID-19 vaccination in people living with HIV?. *J Infect Dis* 2022; jiac286doi: 10.1093/infdis/jiac286.
28. Sogaard OS, Reekie J, Johansen IS, Nielsen H, Benfield T, Wiese L, et al. Characteristics associated with serological COVID-19 vaccine response and durability in an older population with significant comorbidity: the Danish Nationwide ENFORCE Study. *Clin Microbiol Infect* 2022; 28:1126–1133.
29. Fink AL, Klein SL. The evolution of greater humoral immunity in females than males: implications for vaccine efficacy. *Curr Opin Physiol* 2018; 6:16–20.
30. Noe S, Ochana N, Wiese C, Schabaz F, Von Krosigk A, Heldwein S, et al. Humoral response to SARS-CoV-2 vaccines in people living with HIV. *Infection* 2022; 50:617–623.
31. Overton ET, Sungkanuparph S, Powderly WG, Seyfried W, Groger RK, Aberg JA. Undetectable plasma HIV RNA load predicts success after hepatitis B vaccination in HIV-infected persons. *Clin Infect Dis* 2005; 41:1045–1048
32. Wei J, Pouwels KB, Stoesser N, Matthews PC, Diamond I, Studley R, et al. Antibody responses and correlates of protection in the general population after two doses of the ChAdOx1 or BNT162b2 vaccines. *Nat Med* 2022; 28:1072–1082.

A-1.6 Antibody neutralization capacity after coronavirus disease 2019 vaccination in people with HIV in Canada

Preface

(This work has been previously published as a research article)

Costiniuk CT, Singer J, Lee T, **Galipeau Y**, McCluskie PS, Arnold C, Langlois MA, Needham J, Jenabian MA, Burchell AN, Samji H, Chambers C, Walmsley S, Ostrowski M, Kovacs C, Tan DHS, Harris M, Hull M, Brumme ZL, Lapointe HR, Brockman MA, Margolese S, Mandarino E, Samarani S, Vulesevic B, Lebouché B, Angel JB, Routy JP, Cooper CL, Anis AH; COVAXHIV Study Group. **Antibody neutralization capacity after coronavirus disease 2019 vaccination in people with HIV in Canada**. AIDS. 2023 Oct 1;37(12):F25-F35. doi: 10.1097/QAD.0000000000003680. Epub 2023 Aug 2.

https://doi.org/10.1097/qad.0000000000003680

Copyright © 2023 The Author(s). Published by Wolters Kluwer Health, Inc.

This is an open access article distributed under the terms of the Creative Commons Attribution-Non Commercial-No Derivatives License 4.0 (CCBY-NC-ND), where it is permissible to download and share the work provided it is properly cited. The work cannot be changed in any way or used commercially without permission from the journal. http://creativecommons.org/licenses/by-nc-nd/4.0

Abstract

Objectives:
Many vaccines require higher/additional doses or adjuvants to provide adequate protection for people with HIV (PWH). Here, we compare coronavirus disease 2019 (COVID-19) vaccine-induced antibody neutralization capacity in PWH vs. HIV-negative individuals following two vaccine doses.

Design:
In Canadian prospective observational cohorts, including a multicentre study of PWH receiving at least two COVID-19 vaccinations (mRNA or ChAdOx1-S), and a parallel study of HIV-negative controls (Stop the Spread Ottawa Cohort), we measured vaccine-induced neutralization capacity 3 months post dose 2 (±1 month).

Methods:
COVID-19 neutralization efficiency was measured by calculating the half maximal inhibitory dilution (ID50) using a high-throughput protein-based neutralization assay for Ancestral (Wuhan), Delta and Omicron (BA.1) spike variants. Univariable and multivariable quantile regression were used to compare COVID-19-specific antibody neutralization capacity by HIV status.

Results:
Neutralization assays were performed on 256 PWH and 256 controls based on specimen availability at the timepoint of interest, having received two vaccines and known date of vaccination. There was a significant interaction between HIV status and previous COVID-19 infection status in median ID50. There were no differences in median ID50 for HIV+ vs. HIV-negative persons without past COVID-19 infection. For participants with past COVID-19 infection, median ICD50 was significantly higher in controls than in PWH for ancestral SARS-CoV-2 and Omicron variants, with a trend for the Delta variant in the same direction.

Conclusion:
Vaccine-induced SARS-CoV-2 neutralization capacity was similar between PWH vs. HIV-negative persons without past COVID-19 infection, demonstrating favourable humoral-mediated immunogenicity. Both HIV+ and HIV-negative persons demonstrated hybrid immunity.

Trial registration:
clinicaltrials.gov NCT04894448.

Introduction

People with HIV (PWH) are vulnerable to acquisition and severe COVID-19 outcomes because of combined risk factors [1,2] and sub-optimal immunogenicity to routine vaccines [3,4]. Studies in PWH early in the pandemic frequently excluded those with risk factors for sub-optimal response to vaccination, including advanced age or lower $CD4^+$ T-cell counts [5,6]. Knowledge gaps fuelled the establishment of a pan-Canadian prospective cohort of PWH receiving COVID-19 vaccines to: assess humoral immunogenicity in diverse PWH; compare immunogenicity responses in PWH vs. HIV-negative controls, and describe safety and tolerability of COVID-19 vaccines in PWH [7,8].

Antibody neutralization capacity is highly predictive of immune protection and vaccine efficacy [9,10]. We previously demonstrated that COVID-19 vaccine-specific immunity, defined as co-positivity for anti-IgG against SARS-CoV-2 Spike (S) and receptor binding domain (RBD) proteins, was achieved in over 90% of PWH and HIV-negative controls at 3 and 6 months post second and 1 month post third doses [8]. Proportions of participants achieving comparable anti-RBD levels were similar by HIV status at each timepoint. We previously observed that anti-S IgG levels were lower in PWH than HIV-negative controls at 3 and 6 months post second vaccine dose [8]. As we had more specimens available at the 3 month rather than 6 month post second-vaccine dose timepoint, we chose to focus on the 3 month post second-dose timepoint for neutralization studies. We chose this timepoint as we had hypothesized that differences in neutralization capacity, if present between PWH vs. HIV-negative controls, may become more evident at this time point.

Methods

The CTN 328 study is a multicentre prospective observational cohort study of PWH recruited from four sites of Canadian cities, as described [8]. Written informed consent was obtained from all participants (Supplementary Information, https://links.lww.com/QAD/C948).

Participants

For PWH in the CTN 328 study, inclusion criteria included: age at least 16 years; having received, or planning to receive, at least one dose of COVID-19 vaccine; HIV-seropositive. Exclusion

criteria included: receipt of any blood product or immunoglobulin preparation within 1 month of vaccination; signs/symptoms of active COVID-19 at enrolment [8]. Subpopulations of PWH included at least 55 years, HIV immune nonresponders ($CD4^+$ T-cell count remains <350 cells/μl despite suppressed viral load on ART) and PWH with multimorbidity (≥2 comorbidities). We aimed to enrol a diversity of PWH including those who were relatively stable or unstable as evidenced by $CD4^+$ T-cell count less than 350, $CD4^+/CD8^+$ less than 0.75 and suppressed viral load [7,8]. For HIV-negative controls, a subset of immunocompetent Stop the Spread Ottawa (SSO) participants were selected and included if they had undergone parallel blood collection in relation to vaccination time [11]. Equal numbers of HIV+ and HIV− participants were randomly selected from individuals who had specimens available at the time point of interest on whose specimens neutralization assays were performed. Matching by participant characteristics was not performed.

Study visits

Participants were to attend up to six visits over 12 months: prevaccination; 1 month following first dose; at 3, 6 and 12 months following the second dose; and 1 month after the third dose. For the presented analysis, we performed neutralization assays on samples collected at 3 months post second dose.

Data collection

Methods related to medical and HIV history, COVID-19 questionnaire administration, sample collection and vaccine safety, in addition to levels of immunoglobulins G (IgG) were previously published [7,8]. Neutralization assays were performed using an automated protein-based surrogate neutralization (sn) ELISA measuring inhibition of ACE2-spike interactions by antibodies. As previously published [12,13], this ELISA-based test functions as a surrogate to live virus neutralization assays for evaluating antibodies that prevent spike and ACE2 receptor interaction. It can measure neutralization efficiency for Ancestral, Delta and Omicron (BA.1) variants. Levels of SARS-CoV-2 Spike trimer (S) protein, receptor-binding domain (RBD) of spike, and nucleocapsid (N) protein were measured using an automated high-throughput chemiluminescent ELISA [12,14]. Vaccine-induced immunity was defined as co-positivity for S and RBD protein and infection-induced immunity was defined as co-positivity of S and N protein (signal to cut-off ratio ≥1.0) [12,14]. This ELISA has been calibrated to the WHO reference standard. As data can be

transformed to international units cross-laboratory and cross-assay correlations is facilitated. IgG antibody titters (binding antibody units (BAU)/ml) were generated by a conversion model (four-parameter log-logistic curve based on measurements from the WHO International Standard) (NIBSC 20.136). Assay description was previously published [11,12]. History of previous COVID-19 infection was defined as having endorsed having a positive SARS-CoV-2 PCR test (based on participant or site report) or evidence of co-positivity of S and N protein.

Outcomes

The main outcome of interest was the difference in median COVID-19 neutralization efficiency, as measured by half maximal inhibitory dilution (ID50) for Ancestral (Wuhan), Delta and Omicron (BA.1) spike variants, in PWH vs. HIV-negative controls stratified by prior COVID-19 infection status. An exploratory objective was to determine COVID-19 vaccine-induced neutralization efficiency in PWH 3 months post second dose, stratified by various sub-populations of PWH and based on history of prior COVID-19 infection.

Statistical analyses

All analyses were performed using Statistical Analysis System (SAS) software version 9.4 (SAS Institute, Cary, North Carolina, USA). Quantile regression analysis was used to compare neutralization capacity for Ancestral, Delta and Omicron (BA.1) variant ID50 neutralization titters between PWH and control groups as the data did not conform with normality assumption even after log transformation. The analysis adjusted for vaccine-related variables (vaccine type, time between doses) and participant characteristics (age, sex, race and multimorbidity, defined as at least two comorbidities [yes/no)] [9]. An interaction term between participant groups (HIV+ vs. control) and past COVID infection (yes/no) was included in the regression model to allow for potentially different neutrialization capacity response by these factors. Within PWH, we further performed univariate quantile regression analysis to determine whether there were factors associated with weaker neutralization capacity. After univariate analysis, age, sex, vaccine-related variables and variables with $P < 0.1$ in univariate analysis were further included in a multivariable model to further explore associations with participant characteristics. Multivariate analysis was only performed within PWH-naive to natural COVID-19 infection, as there was not enough participants with past COVID-19 infection to perform a separate analysis.

Results

A total of 375 PWH and 1002 SSO participants were enrolled. Individuals were excluded if they had received less than two vaccine doses, if the date of the second vaccine was unknown, or if samples were unavailable at the time point of interest (Supplemental Figure 1, https://links.lww.com/QAD/C946). We then randomly selected 256 samples out of 311 available for PWH, and 256 samples out of 381 available for controls, at the 3-month post dose 2 (+/− 1 month) time point, to perform neutralization assays.

Baseline characteristics for 256 PWH and 256 HIV-negative controls included in the final analysis are presented in Table 1 and Supplement Table 1, https://links.lww.com/QAD/C949. Of 256 in each group, 45 (17.6%) PWH and 56 (21.9%) controls had a history of COVID-19 infection at some point prior to 3 months post dose 2 (+/−1 month). Median ages were 54.2 (IQR 43.4–62.8) and 45.5 years (IQR 35–57) for PWH and controls, respectively. PWH were 72% men vs. 35% of controls, whereas 48% PWH were aged at least 55 years vs. 31% of controls. Median duration of HIV was 17 (IQR 10–25) years (Table 2). Median $CD4^+$ T-cell count was 631 (430.5–838.5) cells/μl and 22% had a nadir $CD4^+$ T-cell count below 100 cells/μl.

Fourteen percent of PWH had a detectable HIV viral load within the last 6 months. Nearly all were on ART (96.9%) and 70% were on integrase strand inhibitors. Frequent comorbidities included obesity (24 vs. 16% in PWH and controls, respectively), dyslipidaemia (17 vs. 11%) and hypertension (16 vs. 13%) (Supplement Table 2a, https://links.lww.com/QAD/C949).

In the current analysis, performed on March 2023, 88% of PWH and 86% of controls included in the analysis had received at least two mRNA vaccines. BNT162b2 and mRNA-1273 were the most commonly administered vaccines. Time interval between vaccine doses is shown in Table 3.

Table 1 - Characteristics of participants.

Variable	All participants			Participants without past COVID-19 infection			Participants with past COVID-19 infection		
	HIV+ ($n=256$)	HIV− ($n=256$)	*P*	HIV+ ($n=211$)	HIV− ($n=200$)	*P*	HIV+ ($n=45$)	HIV− ($n=56$)	*P*
COVID infection prior to 3 months post dose 2 (±1 month) sample [*n* (%)]	45 (17.6)	56 (21.9)	–	0 (0%)	0 (0%)	–	45 (100.0)	56 (100.0)	–
Time since COVID infection, days prior to sample collection									0.244
Median (IQR)	–	–		–	–		263 (126, 338)	306 (168, 472)	
Range	–	–		–	–		(25–685)	(17–583)	
Missing	–	–		–	–		19	2	
Age			<0.001			<0.001			0.133
Median (IQR)	54.2 (43.4, 62.8)	45.5 (35.0, 57.0)		54.6 (44.0, 63.6)	45.0 (36.0, 56.0)		53.3 (42.8, 60.2)	49.0 (33.0, 58.5)	
Range	(19.7–83.5)	(22.0–79.0)		(19.7–83.5)	(22.0–79.0)		(25.9–73.9)	(23.0–75.0)	
			<0.001			<0.001			0.342
Number missing	1	0		1	0		0	0	
<35	30 (11.8)	59 (23.0)		24 (11.4)	42 (21.0)		6 (13.3)	17 (30.4)	
35–44	40 (15.7)	62 (24.2)		33 (15.7)	55 (27.5)		7 (15.6)	7 (12.5)	
45–54	64 (25.1)	56 (21.9)		50 (23.8)	44 (22.0)		14 (31.1)	12 (21.4)	
55–64	73 (28.6)	52 (20.3)		60 (28.6)	39 (19.5)		13 (28.9)	13 (23.2)	
65–74	38 (14.9)	24 (9.4)		33 (15.7)	18 (9.0)		5 (11.1)	6 (10.7)	
≥75	10 (3.9)	3 (1.2)		10 (4.8)	2 (1.0)		0 (0.0)	1 (1.8)	
Sex			<0.001			<0.001			0.04
Male	183 (71.5)	89 (34.8)		153 (72.5)	64 (32.0)		30 (66.7)	25 (44.6)	
Female	72 (28.1)	167 (65.2)		57 (27.0)	136 (68.0)		15 (33.3)	31 (55.4)	
Prefer to self describe	1 (0.4)	0 (0)		1 (0.5)	0 (0.0)		0 (0.0)	0 (0.0)	
Self-declared race or ethnicity[a]			<0.001			<0.001			<0.001
White	138 (54.5)	228 (89.1)		123 (58.9)	179 (89.5)		15 (34.1)	49 (87.5)	
Black	59 (23.3)	0 (0)		41 (19.6)	0 (0.0)		18 (40.9)	0 (0.0)	
Other	56 (22.1)	28 (10.9)		45 (21.5)	21 (10.5)		11 (25.0)	7 (12.5)	
Unknown	3	0		2	0		1	0	
Subpopulation									
Age >55 years	121/255 (47.5)	79/256 (30.9)	<0.001	103/210 (49.0)	59/200 (29.5)	<0.001	18/45 (40.0)	20/56 (35.7)	0.659
Multimorbidity (≥2 comorbidities)	90/252 (35.7)	56/253 (22.1)	<0.001	74/208 (35.6)	44/199 (22.1)	0.003	16/44 (36.4)	12/54 (22.2)	0.123

[a]Multiple could be selected.

Table 2 - HIV-related characteristics for HIV+ participants.

Variable	All HIV+ participants $N=256$	HIV + participants without past COVID-19 infection $N=211$	HIV+ participants without past COVID-19 infection $N=45$
Duration of HIV infection (years)			
Median (IQR)	17.0 (10.0–25.0)	17.0 (10.0–25.5)	18.0 (9.0–24.0)
Range	(0.0–38.0)	(0.0–38.0)	(0.0–34.0)
Missing/unknown	20	15	5
<10	58 (24.6)	47 (24.0)	11 (27.5)
10–19	84 (35.6)	73 (37.2)	11 (27.5)
20+	94 (39.8)	76 (38.8)	18 (45.0)
$CD4^+$ nadir (cells/μl)			
Median (IQR)/range			
Unknown	86	73	13
<100	38 (22.4)	26 (18.8)	12 (37.5)
100–199	32 (18.8)	26 (18.8)	6 (18.8)
200–299	36 (21.2)	32 (23.2)	4 (12.5)
300–399	21 (12.4)	19 (13.8)	2 (6.3)
≥400	43 (25.3)	35 (25.4)	8 (25.0)
$CD4^+$ cell count (cells/μl)			
Median (IQR)	631.0 (430.5–838.5)	630.0 (431.0–843.0)	660.0 (387.0–805.0)
Range	(9.0–1800.0)	(9.0–1800.0)	(48.0–1050.0)
Missing	16	14	2
$CD4^+$ cell count (cells/μl)			
Unknown	16	14	2
<250	22 (9.2)	14 (7.1)	8 (18.6)
250–349	15 (6.3)	14 (7.1)	1 (2.3)
350–499	43 (17.9)	40 (20.3)	3 (7.0)
500–999	136 (56.7)	107 (54.3)	29 (67.4)
≥1000	24 (10.0)	22 (11.2)	2 (4.7)
$CD4^+/CD8^+$ ratio			
Median (IQR)	0.82 (0.56–1.21)	0.84 (0.55–1.24)	0.80 (0.59–1.20)
Range	(0.00–3.30)	(0.00–2.50)	(0.09–3.30)
Missing	24	22	2
$CD4^+/CD8^+$ ratio ≥0.75 [*n* (%)]	129/232 (55.6)	107/189 (56.6)	22/43 (51.2)
Detectable viral load for at least 6 months [*n* (%)]	35/250 (14.0)	21/207 (10.1)	14/43 (32.6)
If detectable, highest viral load over past 6 months (copies/ml)			
Median (IQR)	116 (40–1940)	189 (62–1940)	42 (25–323)
Range	(20–817096)	(20–680000)	(20–817096)
ART regimen			
None	8 (3.1)	6 (2.8)	2 (4.4)
NRTI-based regimen	5 (2.0)	3 (1.4)	2 (4.4)
NNRTI-based regimen	21 (8.2)	17 (8.1)	4 (8.9)
PI-based regimen	8 (3.1)	7 (3.3)	1 (2.2)
INSTI-based regimen	175 (68.4)	149 (70.6)	26 (57.8)
Other[b]	39 (15.2)	29 (13.7)	10 (22.2)
Subpopulation			
Immune nonresponder[a]	24/243 (9.9)	21/200 (10.5)	3/43 (7.0)
HIV+ stable/reference ($CD4^+$ ≥350, suppressed viral load and ≤1 comorbidity)	110/241 (45.6)	94/198 (47.5)	16/43 (37.2)

[a]$CD4^+$ <350, $CD4^+/CD8^+$ <0.75, suppressed viral load.
[b]regimens containing combinations of above and/or other drug classes (i.e. cell-entry inhibitor).

Table 3 - Types of coronavirus disease 2019 vaccination of participants.

	All participants			HIV + participants without past COVID-19 infection			HIV+ participants without past COVID-19 infection		
Variable	HIV+	HIV−	*P*	HIV+	HIV−	*P*	HIV+	HIV−	*P*
Types of COVID-19 vaccines received, dose 1 and 2 (%)			0.004			0.002			0.341
mRNA–mRNA	225 (87.9)	220 (85.9)		181 (85.8)	169 (84.5)		44 (97.8)	51 (91.1)	
ChAdOx1–mRNA	17 (6.6)	22 (12.9)		17 (8.1)	30 (15.0)		0 (0.0)	3 (5.4)	
ChAdOx1–ChAdOx1	13 (5.1)	2 (0.8)		12 (5.7)	1 (0.5)		1 (2.2)	1 (1.8)	
Ad26.COV2.S or Other	1 (0.4)	1 (0.4)		1 (0.5)	0 (0.0)		0 (0.0)	1 (1.8)	
Time between first and second doses in days			<0.001			<0.001			0.566
Median (IQR)	61.0 (51.0–77.0)	57.0 (34.0–77.0)		62.0 (51.0–79.0)	56.0 (31.0–78.0)		57.0 (36.0–67.0)	62.0 (35.0–77.0)	
Range	(20.0–238)	(19.0–125.0)		(20.0–135.0)	(19.0–125.0)		(21.0–238.0)	(21.0–112.00	
Number missing or N/A (Ad26.COV2.S)	1	1		1	1		0	0	
Time between first and second doses in days			<0.001			<0.001			0.754
≤30	1	1		1	1		0	0	
31–60	24 (9.4)	56 (22.0)		18 (8.6)	49 (24.6)		6 (13.3)	7 (12.5)	
>60	94 (36.9)	84 (32.9)		75 (35.7)	64 (32.2)		19 (42.2)	20 (35.7)	
Number missing or N/A (Ad26.COV2.S)	137 (53.7)	115 (45.1)		117 (55.7)	86 (43.2)		20 (44.4)	29 (51.8)	

ID50 after coronavirus disease 2019 vaccination at 3 months post dose 2 (+/−1 month)

PWH and controls with COVID-19 infection prior to vaccination and during follow-up, up until the time point of interest, were analyzed separately from participants naive to natural COVID-19 infection as the former would be expected to have a more robust response following vaccine administration than the latter [21,22]. In participants naive to natural COVID-19 infection, median ID50 at 3 months post dose 2 (+/−1 month) did not differ between PWH vs. controls for Ancestral, Delta and Omicron variants using adjusted quantile regression (Table 4). In participants with past COVID-19 infection, median (IQR) ID50 was 89.3 (45.1, 185.7), 137.2 (81.3, 222.1) (adjusted difference (95% CI): −58.2 (−104.2, −12.1) (P = 0.013) for the Ancestral variant in PWH vs controls. Median (IQR) ID50 for the Delta variant was 61.0 (22.6, 133.0) in PWH vs controls (81.2 (47.7, 159.8) (adjusted difference (95% CI): −24.9 (−61.6, 11.9) (P = 0.184) and for the Omicron variant 11.5 (4.1, 37.1) *vs* 20.5 (10.1, 45.8) (adjusted difference (95% CI): −10.4 (−18.2, −2.6)) (P = 0.009). Comparison of ID50 between cohorts is depicted in Fig. 1.

Table 4 - Median (interquartile range) ID50 after COVID-19 vaccination at 3 months post dose 2 (±1 month).

	HIV + participants without past COVID-19 infection[a]				HIV+ participants with past COVID-19 infection[a]				
Antigen	HIV+	HIV−	Difference in median for HIV+ vs. HIV− (95% CI)[b]	*P*	HIV+	HIV−	Difference in median for HIV+ vs. HIV− (95% CI)~	*P*	P^{homo}
Wuhan	34.1 (14.4–67.3)	40.2 (19.9–66.1)	−2.4 (−13.5 to 8.8)	0.676	89.3 (45.1)	137.2 (81.3–222.1)	−58.2 (−104.2 to −12.1)	0.013	0.026
Delta	20.4 (7.6–37.8)	24.7 (13.2–44.3)	−2.9 (−10.8 to 5.0)	0.465	61.0 (22.6–133.0)	81.2 (47.7–159.8)	−24.9 (−61.6 to 11.9)	0.184	0.269
Omicron	4.4 (2.7–8.6)	4.9 (2.7–8.3)	−0.3 (−1.8 to 1.2)	0.716	11.5 (4.1–37.1)	20.5 (10.1–45.8)	−10.4 (−18.2 to −2.6)	0.009	0.017

P^{homo} is the *P* value from the test of homogeneity by COVID infection status.
[a]Based on site report, participant questionnaires and IgG assay.
[b]Based on quantile regression with an interaction term between HIV status and COVID infection status and adjusted for age, sex, race (white/black/other), multimorbidity (≥2 comorbidities), vaccine type and time between vaccine doses.

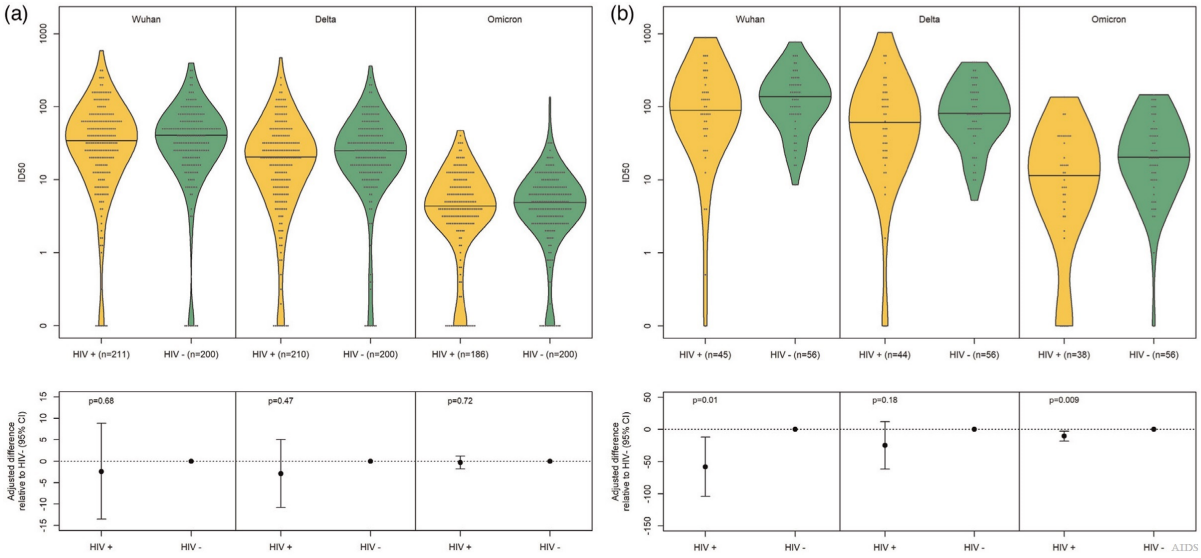


Fig. 1: Difference in ID50 between cohorts to Ancestral, Delta and Omicron variants in participants without past COVID-19 infection and (a) and with past COVID-19 infection (b) in HIV+ and HIV− participants at 3 months after dose 2 (+/−1 month).

Three months post second vaccine dose (+/−1 month), there was no difference in ID50 within subgroups of PWH in univariate analyses using quantile regression (Table 5). For example, there was no difference in PWH who were immune nonresponders with multimorbidity in univariate analyses (Table 5) or when stratified by sex (Table 6).

Table 5 - Difference in median interquartile range ID50 by participant characteristics within HIV+ participants using quantile regression.

	HIV + participants without past COVID-19 infection ($n=211$)						HIV+ participants with past COVID-19 infection ($n=45$)					
Comparison	Wuhan	*P*	Delta	*P*	Omicron	*P*	Wuhan	*P*	Delta	*P*	Omicron	*P*
Age >55 years	−10.5 (−23.3, 2.3)	0.108	−4.2 (−12.2, 3.8)	0.301	−1.1 (−2.2, 0.1)	0.074	−37.5 (−121.7, 46.7)	0.374	−52.4 (−130.0, 25.1)	0.180	3.3 (−15.8, 22.5),	0.728
Immune nonresponder ($CD4^+$ <350 cells/μl, $CD4^+/CD8^+$ <0.75, suppressed VL)	4.2 (−34.8, 43.1)	0.832	2.1 (−13.7, 17.9)	0.795	1.0 (−3.6, 5.7)	0.669	–		–	–	–	–
Multimorbidity (≥2 comorbidities)	−10.2 (−22.7, 2.3)	0.109	−1.3 (−9.1, 6.6)	0.754	−1.3 (−2.5, 0.0)	0.047	59.2 (−61.1, 179.5)	0.326	29.4 (−59.9, 118.6)	0.510	7.2 (−11.2, 25.6)	0.431
HIV+ stable/reference ($CD4^+$ ≥350 cells, suppressed VL and ≤1 comorbidity)	3.0 (−11.4, 17.4)	0.683	0.0 (−5.9, 6.0)	0.997	0.9 (−0.4, 2.1)	0.167	−66.0 (−146.7, 14.6)	0.106	−33.9 (−114.5, 46.8)	0.401	−7.5 (−24.5, 9.4)	0.372

VL, viral load.

Table 6 - Difference in median interquartile range ID50 by participant characteristics within HIV+ participants using quantile regression.

	HIV + participants without past COVID-19 infection ($n=211$)						HIV+ participants with past COVID-19 infection ($n=45$)					
Comparison	Wuhan difference (95% CI)	*P*	Delta difference (95% CI)	*P*	Omicron difference (95% CI)	*P*	Wuhan difference (95% CI)	*P*	Delta difference (95% CI)	*P*	Omicron difference (95% CI)	*P*
Age (per 10 years increase)	−3.6 (−8.2, 1.0)	0.122	−1.7 (−4.7, 1.2)	0.252	−0.6 (−1.1, −0.2)	0.003	12.0 (−26.6, 50.6)	0.533	3.3 (−31.3, 37.9)	0.847	2.3 (−2.9, 7.6)	0.375
<35	20.2 (1.7, 38.7)	0.033	16.5 (2.2, 30.7)	0.024	4.5 (2.0, 7.0)	<0.001	–		–		–	
35–44	−0.4 (−18.3, 17.5)	0.966	8.6 (−3.3, 20.6)	0.157	1.5 (−0.7, 3.8)	0.179	–		–		–	
45–54	1.6 (−22.9, 26.0)	0.900	10.8 (−0.4, 21.9)	0.059	0.7 (−0.8, 2.3)	0.358	–		–		–	
55–64	−2.7 (−20.6, 15.2)	0.768	9.3 (−3.0, 21.5)	0.139	0.8 (−0.7, 2.4)	0.273	–		–		–	
≥65	Referent		Referent		–		–		–			
Sex												
Male	−9.7 (−30.5, 11.1)	0.357	−5.8 (−12.1, 0.5)	0.073	−0.6 (−2.5, 1.4)	0.558	−46.4 (−130.7, 37.9)	0.273	−66.6 (−136.3, 3.0)	0.060	−2.5 (−18.8, 13.9)	0.760
Female	Referent		Referent				Referent		Referent			
Self-declared race or ethnicity												
Black	31.7 (15.6, 47.8)	<0.001	16.9 (0.5, 33.3)	0.043	3.6 (1.0, 6.2)	0.006	98.3 (3.9, 192.7)	0.042	76.5 (24.9, 128.1)	0.005	12.6 (−11.1, 36.3)	0.288
Other	4.1 (−7.1, 15.3)	0.469	6.4 (−0.6, 13.3)	0.074	0.3 (−1.0, 1.6)	0.666	21.1 (−57.5, 99.7)	0.591	43.7 (−30.2, 117.7)	0.239	9.9 (−9.7, 29.5)	0.310
White	Referent		Referent				Referent		Referent			
Medical conditions												
Hypertension	4.7 (−27.2, 36.5)	0.773	2.4 (−12.9, 17.7)	0.759	0.0 (−1.8, 1.8)	0.992	–		–		–	
Diabetes	6.0 (−27.9, 15.8)	0.588	1.6 (−11.3, 14.4)	0.809	−0.4 (−2.7, 2.0)	0.767	–		–		–	
Dyslipidaemia	4.5 (−17.6, 26.5)	0.689	6.0 (−6.8, 18.8)	0.355	−0.2 (−2.1, 1.6)	0.803	–		–		–	
Chronic lung disease	−6.0 (−38.0, 25.9)	0.711	−4.1 (18.4, 10.2)	0.576	0.0 (−2.3, 2.2)	0.998	–		–		–	
Obesity	1.4 (−22.8, 25.6)	0.910	0.0 (−10.0, 9.9)	0.994	−0.7 (−2.2, 0.9)	0.379	74.8 (−100.9, 250.5)	0.395	41.1 (−79.8, 161.9)	0.496	27.3 (2.4, 52.3)	0.033
BMI per 10-unit increase	−2.7 (−17.9, 12.5)	0.725	−0.7 (−6.7, 5.4)	0.829	−0.1 (−1.0, 0.7)	0.786	95.2 (−47.1, 237.5)	0.184	88.0 (−46.3, 222.3)	0.193	20.0 (−6.7, 46.7)	0.138

CI. confidence interval.

Association between ID50 and participant characteristics by multivariate quantile regression is shown in Table 7. Within PWH naive to natural COVID-19 infection, when adjusted for age, sex, $CD4^+$ cell count, vaccine type and time between vaccine doses, black African/black Caribbean participants had significantly higher neutralization capacity than white participants for Ancestral but not for Delta or Omicron variants. Correlation between ID50 and antibody level within PWH at month 3 postdose 2 (±1 month) (Supplemental Figure 2, https://links.lww.com/QAD/C947), illustrated high concordance between the two levels.

Table 7 - Association between ID50 and patient characteristics by multivariable quantile regression.[a]

Comparison	HIV + participants without past COVID-19 infection ($n = 195$)					
	Wuhan difference (95% CI)	*P*	Delta difference (95% CI)	*P*	Omicron difference (95% CI)	*P*
Age						
<35	11.9 (−3.9, 27.8)	0.140	6.1 (−10.1, 22.4)	0.458	1.8 (−1.4, 5.0)	0.258
35–44	0.5 (−15.4, 16.5)	0.937	−1.1 (−13.7, 11.5)	0.866	0.9 (−1.3, 3.1)	0.435
45–54	6.5 (−9.4, 22.3)	0.476	2.6 (−9.4, 14.6)	0.669	0.7 (−1.4, 2.9)	0.497
55–64	−4.1 (−17.5, 9.4)	0.551	3.7 (−7.9, 15.3)	0.532	0.9 (−0.8, 2.6)	0.286
≥65	Referent		Referent		Referent	
Sex						
Male	2.4 (−8.8, 13.5)	0.676	2.8 (−5.7, 11.3)	0.517	−0.3 (−1.9, 1.4)	0.747
Female	Referent		Referent			
Self-declared race or ethnicity						
Black	20.5 (5.5, 35.6)	0.008	15.6 (−0.7, 31.8)	0.060	1.7 (−1.1, 4.5)	0.232
Other	−5.1 (−18.6, 8.4)	0.458	7.2 (−2.6, 17.0)	0.148	−0.5 (−2.2, 1.1)	0.530
White	Referent		Referent		Referent	
$CD4^+$ cell count (cells/μl)						
$CD4^+$ cell count (per 100 cells/μl increase)	1.8 (0.1, 3.4)	0.038	0.8 (−0.6, 2.1)	0.271	0.2 (−0.0, 0.4)	0.127
Types of COVID-19 vaccines received, doses 1 and 2						
mRNA–mRNA	27.8 (16.1, 39.4)	<0.001	13.7 (4.2, 23.2)	0.005	2.6 (0.8, 4.5)	0.006
ChAdOx1–mRNA	12.8 (0.1, 25.4)	0.048	10.8 (−0.5, 22.0)	0.060	0.8 (−1.3, 2.9)	0.463
ChAdOx1–ChAdOx1	Referent		Referent		Referent	
Time between first and second doses						
Time between first and second doses (per 10 days increase)	−0.2 (−2.8, 2.4)	0.869	−1.1 (−3.0, 0.8)	0.252	0.2 (−0.2, 0.5)	0.395

CI, confidence interval.
[a]Age, sex, vaccine-related variables and variables with $P < 0.1$ in the univariate analysis were included in the multivariable model.

Discussion

We previously reported that the vast majority of PWH obtained a detectable antibody titre at 3 and 6 months following second dose, and 1 month following a third or booster dose [8]. We also reported that vaccine-induced antibody titres were overall similar between PWH vs. HIV-negative controls [8]. PWH aged older than 55 years, immune nonresponders and those with multimorbidity achieved similar antibody levels to COVID-19 vaccines compared with HIV-negative controls. In the current study examining neutralization capacity, we focused on the 3 months post second dose timepoint. Reassuringly, we did not find any difference in PWH vs. controls in persons without prior COVID-19 infection. Within PWH without past COVID-19 infection, younger age (<35), higher $CD4^+$ cell count or $CD4^+/CD8^+$ ratio, and vaccine type (mRNA) was associated with higher neutralization capacity. Shorter duration between doses was associated with higher neutralization capacity but only in univariate analyses. We had intended to evaluate PWH with past COVID-19 infection, however, our sample size was insufficient to assess all key variables.

In general, hybrid immunity acquired through combined vaccination and natural infection is associated with more robust immune response than either vaccination or natural infection alone [15–17]. Hybrid immunity is thought to specifically enhance Omicron variant neutralization. Verburgh *et al.* compared severe SARS-CoV-2 vaccine-induced and hybrid B-cell and T-cell responses in middle-aged PWH vs. HIV-negative controls who were highly comparable in terms of demographics and lifestyle [18]. PWH mounted equally robust immunity following vaccination and even more robust stronger immunity was observed in both groups following naturally acquired SARS-CoV-2 infection [18]. Meanwhile, Lu *et al.* examined humoral longitudinal observational study in PWH following primary inactivated SARS-CoV-2 vaccination. Neutralizing antibodies were detected 1 month following booster vaccine in all PWH and the titre increased six-fold compared with that associated with the primary vaccination, similar to what was observed in HIV-negative controls [19]. Neutralizing antibody titre declined over time after booster vaccine but remained higher at 6 months than following primary vaccine [19]. Neutralizing antibody response was elevated after booster vaccine in PWH with $CD4^+$ cell count less than 200 cells/μl, although this boosting effect was lower compared with higher $CD4^+$ cell count subgroups [19]. It is unclear why PWH with previous COVID-19 infection in our study exhibited higher neutralization capacity than PWH without past infection but weaker neutralization capacity for Ancestral and Omicron variants when compared with HIV-negative controls who also had past infection. As many SSO participants were healthcare workers and individuals working in public-facing environments, these individuals received vaccination, on average, earlier and with shorter intervals between doses than the general population. We speculate that timing of natural infection in relation to vaccination may have contributed to our observation. Therefore, it is possible that uncontrolled confounding may have accounted for this difference between groups. As time of infection was unknown for fewer than half of the HIV+ participants, it was not possible to control for time of infection as a variable.

Within PWH, black African/Caribbeans had higher neutralization capacity than for whites for all variants. In a cross-sectional analysis involving healthcare workers in the United Kingdom, SARS-CoV-2 spike-specific total antibody titre, neutralizing antibody titre and ELISpot count were compared by ethnic group [20]. This study found that humoral and cellular immune responses to SARS-CoV-2 vaccination were stronger in South Asian HCWs than white HCWs, and differences

were most pronounced early following vaccination [20]. The reasons for our findings are unclear, although we suspect it relates to uncontrolled confounding.

In the current study, we observed that older age was associated with weaker neutralization capacity for Ancestral, Delta and Omicron variants. Advanced age is associated with diminished vaccine immunogenicity [21], due in part to intrinsic defects in B cells leading to sub-optimal antibody function [22–24]. Furthermore, 'inflammaging', which refers to increased low-grade systemic inflammation as persons age, is known to impact PWH [25,26].

We previously did not observe differences in antibody titres in PWH with $CD4^+$ T-cell counts less than 350 cells/μl vs. higher counts. However, other groups have reported diminished anti-S vaccine response and neutralization capacity in PWH vs. HIV-uninfected controls [27,28]. Differences amongst findings in PWH may be because of discrepancies in multimorbidity burden in older adults, type and number of vaccines received and time interval between vaccinations [27–30]. Third dose vaccines elicited better neutralizing antibody responses in PWH with longer time intervals between vaccines [30]. Furthermore, although there is evidence for sex-based differences in humoral immune response with certain types of vaccinations in HIV-negative populations [30], we and others have not observed any sex difference in antibody level or neutralization capacity in the context of COVID-19 vaccination [10–12,19]. Moreover, in both PWH vs. HIV-negative controls, some participants had a high antibody titre but low ID50. However, given the small number of these individuals who had discordance between antibody titre and neutralization capacity, the importance of this finding, if any, is unclear.

We acknowledge several limitations. COVID-19 vaccinations became available in Canada in December 2020 but recruitment commenced in May 2021, resulting in missed opportunity to obtain baseline prevaccination blood in populations prioritized for vaccination (e.g. elderly, indigenous people) [31]. There were differences in vaccine type and dosing interval by province [31]. Numbers of PWH participants not receiving ART therapy and/or low $CD4^+$ cell counts were relatively small. Thus, results may not be generalizable to all PWH [32]. The number of PWH with past COVID-19 infection was also relatively low, precluding robust multivariable assessment.

In summary, adult PWH without past COVID-19 infection with well controlled HIV on ART achieved vaccine-induced SARS-CoV-2 neutralization capacity that is similar to HIV-negative persons. Increasing age is associated with diminished neutralization capacity, and which might be impacted by HIV in those with past COVID-19. This phenomenon requires further exploration. Study of humoral immune response durability, the contribution of cell-mediated immunity and low-grade chronic inflammation will complement our current findings.

Acknowledgements

The authors thank the CTN staff who were involved in the planning and preparation of this study, in addition to the CTN Scientific Review Committee and the Community Advisory Board, for their expedited review and helpful comments. They also thank all of the participants for their time and commitment. In addition, the authors thank study coordinators and study nurses: Florian Bobeuf, Claude Vertzagias, Lina Del Balso, Nathalie Paisible, Guillaume Theriault, Hansi Peiris, Lianne Thai, Rosemarie Clarke, Erin Collins, Nadia Ohene-Adu, Aron Dyks and Jill Jackson; data manager Elisa Lau; laboratory staff: Tara Mabanga, Yulia Alexandrova, Ralph-Sydney Mboumba Bouassa, Erik Pavey, Stephanie Burke-Schinkel, the University of Ottawa Serology and Diagnostics High Throughput Facility: Danielle Dewar-Darch, Justino Hernandez Soto, Abishek Xavier, Nicholas Bradette, Klaudia Baumann, Gwendoline Ward and Yuchu Dou. The authors also thank physicians who assisted with recruitment.

COVID-19 antigens as well as the antihIgG#5-HRP fusion antibody were generously provided by Dr Yves Durocher, National Research Council of Canada (NRC), Montreal.

C.T.C. is supported by a Fonds de recherche du Québec-Santé (FRQS) Junior 2 career award. A.B. holds a Canada Research Chair Tier 2 Canada Research Chair (CRC) in sexually transmitted infection (STI) Prevention. M.A.L. holds a CRC, Tier 2, in human immunovirology. M.A.J. holds a CRC, Tier 2, in human immunovirology. S.W. is supported by a Research Chair in HIV Clinical Care and Aging from the Ontario HIV Treatment Network. D.T. is supported by a Tier 2 CRC in HIV Prevention and STI Research. M.A.B. holds a Canada Research Chair, Tier 2, in viral pathogenesis and immunity. Z.L.B. holds a Scholar Award from the Michael Smith Foundation for Health Research. B.L. is supported by a career award LE 250 from the Quebec's Ministry of Health for researchers in Family Medicine, FRQS Junior 2 career award and holds a Canadian Institutes for Health Research Strategy for Patient Oriented Research (SPOR) Mentorship Chair in Innovative Clinical Trials. J.P.R. holds a Lowenstein Chair in Hematology. Y.G. is supported by a Charles Best and Frederick Bandting (CGS-Doctoral award) from CIHR (476885).

Funding This project was supported by funding from the Public Health Agency of Canada, through the Vaccine Surveillance Reference group and the COVID-19 Immunity Task Force (grant number: 2122-HQ-000075) and the CTN (grant number: N/A). Production of COVID-19 reagents was financially supported by NRC's Pandemic Response Challenge Program.

Authors' contributions: co-principal investigators of the study are C.T.C., C.L.C. and A.H.A. C.T.C. and C.L.C. conceived the study, led the proposal and protocol development. C.T.C. wrote the first draft of the manuscript. J.S. is the biostatistician who provided methodological expertise and performed sample size calculations. All other authors contributed to protocol development, study design and development of the proposal. C.T.C., M.A.L., Y.G., C.A., M.A.J., M.O., M.B. and Z.B. designed the laboratory evaluations. S.S. oversaw lab specimen processing and lab database development. Y.G., C.A., P.M. and M.A.L. were responsible for studies on humoral immunity. J.S. oversaw data analysis between groups and subgroup analyses. T.L. performed data analyses. All authors critically reviewed and approved the final manuscript.

Conflicts of interest There are no conflicts of interests.

References

1. Tesoriero JM, Swain CE, Pierce JL, Zamboni L, Wu M, Holtgrave DR, et al. COVID-19 outcomes among persons living with or without diagnosed HIV infection in New York state. *JAMA Netw Open* 2021; 4:e2037069.
2. Weiser JK, Tie Y, Beer L, Neblett Fanfair R, Shouse RL. Racial/ethnic and income disparities in the prevalence of comorbidities that are associated with risk for severe COVID-19 among adults receiving HIV Care, United States, 2014-2019. *J Acquir Immune Defic Syndr* 2021; 86:297–304.
3. Crum-Cianflone NF, Sullivan E. Vaccinations for the HIV-infected adult: a review of the current recommendations, part I. *Infect Dis Ther* 2017; 6:303–331.
4. Crum-Cianflone NF, Sullivan E. Vaccinations for the HIV-infected adult: a review of the current recommendations, part II. *Infect Dis Ther* 2017; 6:333–361.
5. Bergman P, Blennow O, Hansson L, Mielke S, Nowak P, Chen P, et al. COVAXID-collaborator group. Safety and efficacy of the mRNA BNT162b2 vaccine against SARS-CoV-2 in five groups of immunocompromised patients and healthy controls in a prospective open-label clinical trial. *EBioMedicine* 2021; 74:103705.
6. Levy I, Wieder-Finesod A, Litchevsky V, Biber A, Indenbaum V, Olmer L, et al. Immunogenicity and safety of the BNT162b2 mRNA COVID-19 vaccine in people living with HIV-1. *Clin Microbiol Infect* 2021; 27:1851–1855.
7. Costiniuk CT, Singer J, Langlois MA, Kulic I, Needham J, Burchell A, et al. CTN 328: immunogenicity outcomes in people living with HIV in Canada following vaccination for COVID-19 (HIV-COV): protocol for an observational cohort study. *BMJ Open* 2021; 11:e054208.
8. Costiniuk CT, Singer J, Lee T, Langlois MA, Arnold C, Galipeau Y, et al. COVAXHIV Study Group. COVID-19 vaccine immunogenicity in people with HIV. *AIDS* 2023; 37:F1–F10.
9. Gilbert PB, Montefiori DC, McDermott AB, Fong Y, Benkeser D, Deng W, et al. Immune Assays Team§, Moderna, Inc. Team§, Coronavirus Vaccine Prevention Network (CoVPN)/Coronavirus Efficacy (COVE) Team§, United States Government (USG)/CoVPN Biostatistics Team§. Immune correlates analysis of the mRNA-1273 COVID-19 vaccine efficacy clinical trial. *Science* 2022; 375:43–50.
10. Khoury DS, Cromer D, Reynaldi A, Schlub TE, Wheatley AK, Juno JA, et al. Neutralizing antibody levels are highly predictive of immune protection from symptomatic SARS-CoV-2 infection. *Nat Med* 2021; 27:1205–1211.
11. Collins E, Galipeau Y, Arnold C, Bosveld C, Heiskanen A, Keeshan A, et al. Cohort profile: Stop the Spread Ottawa (SSO)—a community-based prospective cohort study on antibody responses, antibody neutralisation efficiency and cellular immunity to SARS-CoV-2 infection and vaccination. *BMJ Open* 2022; 22:e062187.
12. Colwill K, Galipeau Y, Stuible M, Gervais C, Arnold C, Rathod B, et al. A scalable serology solution for profiling humoral immune responses to SARS-CoV-2 infection and vaccination. *Clin Transl Immunol* 2022; 11:e1380.
13. Abe KT, Li Z, Samson R, Samavarchi-Tehrani P, Valcourt EJ, Wood H, et al. A simple protein-based surrogate neutralization assay for SARS-CoV-2. *JCI Insight* 2020; 5:142362.
14. Cholette F, Fabia R, Harris A, Ellis H, Cachero K, Schroeder L, et al. COVID-19 Immunity Task Force (CITF) working group. Comparative performance data for multiplex SARS-CoV-2 serological assays from a large panel of dried blood spot specimens. *Heliyon* 2022; 8:e10270.
15. Hoffmann M, Behrens GMN, Arora P, Kempf A, Nehlmeier I, Cossmann A, et al. Effect of hybrid immunity and bivalent booster vaccination on omicron sublineage neutralisation. *Lancet Infect Dis* 2023; 23:25–28.
16. Wang Z, Muecksch F, Schaefer-Babajew D, Finkin S, Viant C, Gaebler C, et al. Naturally enhanced neutralizing breadth against SARS-CoV-2 one year after infection. *Nature* 2021; 595:426–431.
17. Zaballa ME, Perez-Saez J, de Mestral C, Pullen N, Lamour J, Turelli P, et al. Specchio-COVID19 study group. Seroprevalence of anti-SARS-CoV-2 antibodies and cross-variant neutralization capacity

after the Omicron BA.2 wave in Geneva, Switzerland: a population-based study. *Lancet Reg Health Eur* 2023; 24:100547.
18. Verburgh ML, van Pul L, Grobben M, Boyd A, Wit F, van Nuenen AC, et al. Robust vaccine-induced as well as hybrid B- and T-cell immunity across SARS-CoV-2 vaccine platforms in people with HIV. *Microbiol Spectr* 2023; 11:e0115523.
19. Lu T, Chen Z, Cao Y, Ao L, Li Z, Gu X, et al. Dynamic immunogenicity after primary and booster inactivated SARS-CoV-2 vaccination in people living with HIV: a longitudinal observational study. *J Med Virol* 2023; 95:e28730.
20. Martin CA, Nazareth J, Jarkhi A, Pan D, Das M, Logan N, et al. Ethnic differences in cellular and humoral immune responses to SARS-CoV-2 vaccination in UK healthcare workers: a cross-sectional analysis. *EClinicalMedicine* 2023; 58:101926.
21. Gustafson CE, Kim C, Weyand CM, Goronzy JJ. Influence of immune aging on vaccine responses. *J Allergy Clin Immunol* 2020; 145:1309–1321.
22. Frasca D, Blomberg BB. Aging induces B cell defects and decreased antibody responses to influenza infection and vaccination. *Immun Ageing* 2020; 17:37.
23. Pallikkuth S, De Armas LR, Pahwa R, Rinaldi S, George VK, Sanchez CM, et al. Impact of aging and HIV infection on serologic response to seasonal influenza vaccination. *AIDS* 2018; 32:1085–1094.
24. Parmigiani A, Alcaide ML, Freguja R, Pallikkuth S, Frasca D, Fischl MA, et al. Impaired antibody response to influenza vaccine in HIV-infected and uninfected aging women is associated with immune activation and inflammation. *PLoS One* 2013; 8:e79816.
25. Sieg SF, Shive CL, Panigrahi S, Freeman ML. Probing the Interface of HIV and inflammaging. *Curr HIV/AIDS Rep* 2021; 18:198–210.
26. Pereira B, Xu XN, Akbar AN. Targeting inflammation and immunosenescence to improve vaccine responses in the elderly. *Front Immunol* 2020; 11:583019.
27. Cossu MV, Mileto D, Giacomelli A, Oreni L, Bracchitta F, Pellicciotta M, et al. Does the co-morbidity burden contribute to suboptimal immunological responses to COVID-19 vaccination in people living with HIV?. *J Infect Dis* 2022; doi: 10.1093/infdis/jiac286. [Epub ahead of print].
28. Wu S, Zou S, Ming F, Wu M, Guo W, Xing Z, et al. Humoral immune response to inactivated COVID-19 vaccination at the 3rd month among people living with HIV. *BMC Infect Dis* 2023; 23:34.
29. Antinori A, Cicalini S, Meschi S, Bordoni V, Lorenzini P, Vergori A, et al. HIV-VAC Study Group. Humoral and cellular immune response elicited by mRNA vaccination against severe acute respiratory syndrome coronavirus 2 (SARS-CoV-2) in people living with human immunodeficiency virus receiving antiretroviral therapy based on current CD4 T-lymphocyte count. *Clin Infect Dis* 2022; 75:e552–e563.
30. Wang Y, Li J, Zhang W, Liu S, Miao L, Li Z, et al. Extending the dosing interval of COVID-19 vaccination leads to higher rates of seroconversion in people living with HIV. *Front Immunol* 2023; 14:1152695.
31. Ministry of Health. COVID-19 vaccine booster recommendation.Version 8.3. July 22.
32. Noe S, Ochana N, Wiese C, Schabaz F, Von Krosigk A, Heldwein S, et al. Humoral response to SARS-CoV-2 vaccines in people living with HIV. *Infection* 2022; 50:617–623.

A-1.7 Correlates of breakthrough SARS-CoV-2 infections in people with HIV: results from the CIHR CTN 328 Study

Preface

(This work has been previously published as a research article)

Costiniuk CT, Lee T, Singer J, **Galipeau Y**, Arnold C, Langlois MA, Needham J, Jenabian MA, Burchell AN, Samji H, Chambers C, Walmsley S, Ostrowski M, Kovacs C, Tan DHS, Harris M, Hull M, Brumme ZL, Lapointe HR, Brockman MA, Margolese S, Mandarino E, Samarani S, Lebouché B, Angel JB, Routy JP, Cooper CL, Anis AH; COVAXHIV Study Group. **Correlates of Breakthrough SARS-CoV-2 Infections in People with HIV: Results from the CIHR CTN 328 Study**. Vaccines (Basel). 2024 Apr 23;12(5):447.

https://doi.org/10.3390/vaccines12050447

© 2024 by the authors. Licensee MDPI, Basel, Switzerland. This article is an open access article distributed under the terms and conditions of the Creative Commons Attribution (CC BY) license (https://creativecommons.org/licenses/by/4.0/).

Abstract

COVID-19 breakthrough infection (BTI) can occur despite vaccination. Using a multi-centre, prospective, observational Canadian cohort of people with HIV (PWH) receiving ≥2 COVID-19 vaccines, we compared the SARS-CoV-2 spike (S) and receptor-binding domain (RBD)-specific IgG levels 3 and 6 months post second dose, as well as 1 month post third dose, in PWH with and without BTI. BTI was defined as positivity based on self-report measures (data up to last study visit) or IgG data (up to 1 month post dose 3). The self-report measures were based on their symptoms and either a positive PCR or rapid antigen test. The analysis was restricted to persons without previous COVID-19 infection. Persons without BTI remained COVID-19-naïve until ≥3 months following the third dose. Of 289 participants, 92 developed BTI (31.5 infections per 100 person-years). The median days between last vaccination and BTI was 128 (IQR 67, 176), with the most cases occurring between the third and fourth dose (n = 59), corresponding to the Omicron wave. In analyses adjusted for age, sex, race, multimorbidity, hypertension, chronic kidney disease, diabetes and obesity, a lower IgG S/RBD (log10 BAU/mL) at 1 month post dose 3 was significantly associated with BTI, suggesting that a lower IgG level at this time point may predict BTI in this cohort of PWH.

1. Introduction

HIV infection induces both humoral and cell-mediated immune defects, impacting the severity of respiratory infections, as well as vaccine-induced immune responses [1]. During the COVID-19 pandemic, people with HIV (PWH) had twice the risk of hospitalization compared to HIV-negative individuals [2], and large studies showed up to a threefold increased risk of COVID-19-related mortality in PWH [3,4,5,6,7]. The vulnerability of PWH to severe COVID-19 outcomes stems from a combination of risk factors including high rates of smoking, multimorbidity [8] and social determinants of health [9,10]. Importantly, the suboptimal immunogenicity to many common vaccines in PWH is well recognized and may be attributed, in part, to ongoing B cell dysfunction and ongoing immune activation, resulting in inappropriate responses to stimuli [11,12,13]. HIV infection, especially in the context of low CD4 T cell counts (<200 cells/mm3) and unsuppressed viral loads [14,15], may cause predisposition to poor immunogenicity to various vaccines such as influenza [16], pneumococcal [17,18], meningococcal [19] and hepatitis A [20,21,22] and B vaccines [23,24]. Additional vulnerabilities increase the risk of SARS-CoV-2 acquisition and symptomatic/severe COVID-19 in PWH, including multimorbidity and membership in socioeconomic or racialized groups disproportionately affected by COVID-19 [25]. As the majority of PWH enrolled in COVID-19 vaccine trials have had normal CD4 T cell counts (>500 cells/mm3) and few comorbidities [26,27], these immunogenicity results may not be generalizable to the wide spectrum of PWH who are followed in Canadian centres.

Despite advances in understanding the immunogenicity outcomes in PWH, there remains a paucity of data regarding COVID-19 breakthrough infection (BTI) in PWH. The objective of the current study was to compare the socioeconomic, clinical and vaccine immune response correlates of BTI following two and three doses of COVID-19 vaccines in a prospective Canadian cohort of PWH enrolled in a vaccine immunogenicity study (CTN 328). This knowledge could help to identify persons at risk for BTI and inform us on whether different vaccine strategies, such as additional vaccine boosters for certain individuals, may portend benefit.

2. Materials and Methods

The CTN 328 study was designed and implemented in 2020 to address the knowledge gaps regarding the COVID-19 vaccine responses in diverse PWH and HIV-negative participants over long time periods, when little information was available on the responses to third or booster vaccinations in PWH. It was also designed to describe the safety and tolerability of COVID-19 vaccines in PWH [28]. An exploratory objective was to determine whether subpopulations of PWH respond differently to COVID-19 vaccination [28]. The CTN 328 was a multi-centre, prospective, observational cohort study of PWH recruited from sites in Montreal, QC, Toronto, ON, Ottawa ON, and Vancouver, BC with the aim of comparing their COVID-19 vaccine-induced immune response with that of HIV-negative controls. The CTN 328 protocol was previously published [28] and later amended to accommodate third and fourth doses/boosters. Enrolment occurred from April to June 2021 in Vancouver and from June 2021 to January 2022 for the remaining sites [29,30]. The participants attended visits prior to and following the vaccine dosing for phlebotomy and questionnaire completion [29,30].

2.1. Ethics Statement

This study was conducted in accordance with the Declaration of Helsinki and approved by the McGill University Health Centre Research Ethics Board (REB) under protocol 2022-7857, the Ottawa Health Science Network REB under protocol 20210361-01H, the University Health Network REB under protocol 21-5504 and the University of British Columbia Providence Health Care and Simon Fraser University REBs under protocols #H21-01515 and #H21-00742. Written informed consent was obtained from all the participants.

2.2. Human Participants

The inclusion criteria for participation in the CTN 328 study were (must meet all criteria) (1) age ≥16 years; (2) living with HIV (for the PWH group); (3) planning on receiving a COVID-19 vaccine or has received no more than 2 doses at enrolment; (4) able to provide signed, informed consent; (5) able to attend study visits. The exclusion criteria included signs or symptoms of active COVID-19 at enrolment [28].

Subpopulations of PWH were prioritized for the study enrolment: (1) Older age (≥55 years) given its association with immunosenescence, comorbidities and reduced vaccine efficacy [31,32]; (2)

Immune non-responders (CD4 T cell count < 350 cells/mm3, CD4/CD8 < 0.75 with an undetectable viral load for at least 6 months). Immune non-responders may be at risk of more adverse COVID-19-related outcomes than HIV immune responders [7,33]; (3) Multimorbidity (defined as having ≥2 comorbidities) given the association with worse COVID-19 outcomes with COVID-19 [34]; (4) An HIV-positive 'stable' or 'reference' group (undetectable HIV viral load for at least 6 months, CD4 T cell counts ≥ 350 cells/mm3 and a maximum of one comorbidity). The sites were encouraged to enrol PWH at risk of worse outcomes due to COVID-19 infection, such as the subpopulations described above [28,29], because at-risk participants had been excluded from many of the vaccine trials that had been reported. The current analysis was restricted to persons who received 2 or more vaccine doses

2.3. Study Visits

For the present analysis, we evaluated samples collected between 11 August 2021 and 20 April 2022 at 3 and 6 months after the 2nd dose and 1 month after the 3rd dose. Moderately to severely immunocompromised individuals in some provinces were given a 3rd dose [35] as part of the primary series. Of note, in the 3 provinces enrolling participants, PWH were not included in this group. In accordance with the Public Health Agency of Canada guidelines, the 3rd doses of the mRNA-1273 vaccine were 50 µg (vs. 100 µg 1st and 2nd doses) for those under 65 years [36,37], whereas the 3rd doses of the BNT162b2 vaccine were the same as for the 1st and 2nd doses (30 µg).

2.4. Sociodemographic Health and Clinical History

Sociodemographic and general health information were captured via participant self-reporting. The data were gathered from interviews and clinic chart reviews following written informed consent and included comorbidities, medications, body mass index and history and date of COVID-19 infection. COVID-19 infection was based on a positive PCR test and/or self-report with a rapid antigen test (RAT). With regards to HIV history, we extracted year of HIV diagnosis, nadir and most recent CD4 T cell counts and ART regimen [28,29]. We also collected contextual information related to risk factors, including working in an environment in close proximity to others, working in a hospital or healthcare facility, the number of individuals living in the participant's household and the number of bedrooms and bathrooms in the household.

2.5. Definition of BTI and Clinical Evaluation for COVID-19 Infection

BTI was defined as positivity based on the self-reporting (data up to the last study visit) or IgG data (only available up to 1 month post dose 3). Thus, all the BTI after 1 month post dose 3 was based on self/site reporting. The self-reporting was based on symptoms and either a positive PCR or rapid antigen test. All participants who developed symptoms consistent with COVID-19 throughout the study were asked to go to their nearest testing centre for testing. Participants were asked to notify the study staff by telephone of the test result so that this could be recorded.

COVID-19-like symptoms were defined as a temperature >38.0 °C associated with any one or more of the following clinical symptoms: feverishness/chills; cough; tachypnea/dyspnea; wheezing/stridor; rhinorrhea; sore throat; myalgias; loss of smell or taste; diarrhea. Participants were asked to record the signs and symptoms of COVID-19-like illness daily until resolution. These signs and symptoms are outlined in Appendix A. Hospitalizations, as disclosed by the participant or clinic records, were recorded.

2.6. Sample Collection

At each visit, blood was collected to isolate serum and plasma [28,29].

2.7. Humoral Immunity (SARS-CoV-2 Binding Antibodies)

The levels of IgG targeting the SARS-CoV-2 spike trimer (S) protein, spike receptor-binding domain (RBD) and nucleocapsid (N) protein were measured using an automated high-throughput chemiluminescent ELISA [38,39]. Vaccine-induced immunity was distinguished by co-positivity with the S and RBD protein and infection-induced immunity by co-positivity with the S and N protein (signal-to-cutoff ratio ≥ 1.0) [38] This assay was selected since it has been used in other Canadian studies [40,41,42], enabling future comparison of the results across cohorts.

If someone was anti-N-seropositive but an infection was not self/site-reported, they were still included in the BTI group. However, the timing of infection was uncertain in this case, so the sample date for anti-N seropositivity was used as the infection date.

For those with anti-N seropositivity after dose 2 (without self-reported infection), they were only counted as having a BTI if they had a negative anti-N result after dose 2 prior to anti-N seropositivity. This way, we could be sure that the infection occurred after dose 2. We excluded cases that did not satisfy this criterion. The IgG antibody titres (binding antibody units (BAU)/mL) were generated using a conversion model (4-parameter log-logistic curve based on measurements from the WHO International Standard) [43].

2.8. Statistical Analysis

All the analyses were performed using Statistical Analysis System (SAS) software version 9.4 (SAS Institute, Cary, NC, USA). We examined the differences in the proportions of participants with BTI vs. without BTI between a stratified sub-population of interest (persons ≥ 55 years old, immune non-responders (CD4 < 350 cells/mm3, CD4/CD8 ratio < 0.75, UD VL) and the HIV reference population (CD4 ≥ 350 cells/mm3, UD VL and ≤1 comorbidity). We also examined the differences in the proportions of PWH developing BTI based on having received the ChAdOx1 vaccine as at least one of the first two vaccine doses and those who received mRNA vaccines for both doses. These comparisons were based on the Chi-square test or Fisher's exact test as appropriate. Other continuous variables, such as age and CD4 count, were compared between groups using the Wilcoxon rank sum test. Descriptive statistics were used to determine number of days between the last vaccine dose and BTI. We also examined the difference in the IgG spike/RBD (log10 BAU/mL) levels at 3 and 6 months post dose 2 (±2 months) and 1 month post dose 3 (±2 weeks) in participants with vs. without BTI after these time points using the Wilcoxon rank sum test. Only IgG data prior to breakthrough infection were included. We further conducted logistic regression adjusted for age, sex, multimorbidity, hypertension, chronic kidney disease, diabetes and obesity to examine the effect of IgG spike/RBD on the odds of BTI. We did not adjust for vaccine type since it was believed that vaccine type would be too highly collinear with IgG to be included as an adjustment variable. No adjustment for multiple comparisons was made given the exploratory nature of the study. p values < 0.05 were considered statistically significant.

2.9. Data Availability

The data presented in this study may be made available upon written request to the corresponding author.

3. Results

3.1. Participant Characteristics Stratified by BTI

A total of 375 PWH were enrolled in the CTN 328 study, of whom 289 (77.1%) individuals were included in the current analysis. Thus, all BTI 1 month post dose 3 was based on self/site reporting. The self-reporting was based on symptoms and either a positive PCR or rapid antigen test. Of 289 participants, 92 (31.8%) developed BTI, equating to 31.5 infections per 100 person-years. Individuals were excluded if they had COVID-19-like symptoms and PCR-confirmed COVID-19 infection prior to their second vaccine dose (n = 44/375, 11.7%); if the timing of COVID-19 infection was unconfirmed (n = 25/375, 6.7%); if these infections were identified only using IgG data and it could not be confirmed that the infection occurred after dose 2; if they did not receive dose 2 or if they were lost to follow-up following dose 2 (n = 17/375, 4.5%). The median number (IQR) of days between last vaccination and BTI was 128 (67, 176), with most of the cases occurring after the third dose and before the fourth dose (n = 59). The baseline characteristics for PWH with (n = 92) and without (n = 197) BTI are presented in Table 1 and Supplementary Table S1.

An undetectable HIV viral load 6 months preceding enrolment was observed in PWH without vs. with BTI (91% vs. 87%, $p = 0.279$), respectively. Of the individuals with BTI, 4 individuals (2%) were not on ART, whereas all the individuals without BTI were on ART. In both groups, greater than two-thirds of the PWH were on integrase strand inhibitor regimens (73.1 vs. 73.9%), and the ART regimen did not significantly differ between groups ($p = 0.052$).

The most frequent comorbidities included obesity (20.4% vs. 20.7% without vs. with BTI, respectively, $p = 0.961$), dyslipidemia (15.5% vs. 12% without vs. with BTI, respectively, $p = 0.420$) and hypertension (16.1% vs. 8.7% without vs. with BTI, respectively, $p = 0.091$), but these did not differ significantly between those without and those with BTI (**Supplementary Table S1**). The participants with vs. without BTI did not differ in terms of their age, sex, ethnicity, duration of HIV, CD4 or nadir CD4 count or comorbidities. There were no significant differences in the proportions of participants with BTI vs. without BTI who were persons ≥ 55 years old, immune non-responders (CD4 < 350 cells/mm3, CD4/CD8 ratio < 0.75, UD VL) or in the HIV reference population (CD4 ≥ 350 cells/mm3, UD VL and ≤1 comorbidity).

Table 1. Participant characteristics stratified based on COVID-19 BTI

Variable	Participants without COVID-19 BTI (n = 197)	Participants with COVID-19 BTI (n = 92)	*p*
Age			0.098
Median (IQR)	54.8 (45.1, 62.8)	53.6 (39.7, 61.7)	
Range	(19.7, 81.6)	(24.3, 83.5)	
# Missing	1 (0.5%)	0 (0%)	
Sex, n (%)			0.786
Male	150 (76.1)	73 (79.3)	
Female	45 (22.8)	19 (20.7)	
Prefer to self-describe	2 (1.0)	0 (0.0)	
Self-declared race or ethnicity [1], n (%)			0.125
White	118 (60.2)	60 (65.9)	
Black	38 (19.4)	9 (9.9)	
Other	40 (20.4)	22 (24.2)	
Unknown	1	1	
Sub-population, n (%)			
Age ≥ 55 years	97/196 (49.5)	39/92 (42.4)	0.261
Multimorbidity (≥2 comorbidities)	56/191 (29.3)	23/92 (25.0)	0.448
Immune non-responder [2]	18/187 (9.6)	7/85 (8.2)	0.713
HIV + stable/reference (CD4 ≥ 350, suppressed VL and ≤1 comorbidity)	96/183 (52.5)	48/85 (56.5)	0.54
Duration of HIV infection, years			0.778
Median (IQR)	17.0 (8.0, 25.0)	16.0 (7.0, 26.0)	
Range	(0.0, 38.0)	(0.0, 39.0)	
Missing/unknown	19 (9.6%)	3 (3.2%)	
Duration of HIV infection, years, n (%)			0.963
Unknown	19	3	
<10	50 (28.1)	26 (29.2)	
10–19	57 (32.0)	29 (32.6)	
20+	71 (39.9)	34 (38.2)	
CD4 nadir (cells/mm^3)			0.161
Median (IQR)	220.0 (120.0, 400.0)	293.0 (146.5, 427.0)	
Range	(1.0, 900.0)	(10.0, 900.0)	
Unknown	72 (36.5%)	32 (34.8%)	
CD4 nadir (cells/mm^3), n (%)			0.334
<100	27 (21.6)	7 (11.7)	
100–199	25 (20.0)	12 (20.0)	
200–299	27 (21.6)	12 (20.0)	
300–399	14 (11.2)	12 (20.0)	
≥400	32 (25.6)	17 (28.3)	
Unknown	72	32	
CD4 count (cells/mm^3)			0.409
Median	620.0 (422.0, 855.0)	667.0 (446.0, 865.0)	
Range	(9.0, 1800.0)	(84.0, 1180.0)	
Missing	11 (5.6%)	9 (9.8%)	
CD4 count (cells/mm^3), n (%)			0.763
<250	12 (6.5)	6 (7.2)	
250–349	15(8.1)	3 (3.6)	
350–499	38(20.4)	18 (21.7)	
500–999	100 (53.8)	46 (55.4)	
≥1000	21(11.3)	10 (12.0)	
Unknown	11	9	
CD4/CD8 ratio			0.048
Median (IQR)	0.80 (0.51, 1.15)	0.90 (0.60, 1.33)	
Range	(0.00, 2.50)	(0.15, 2.40)	
Missing	21 (10.7%)	12 (13.0%)	
CD4/CD8 ratio ≥ 0.75, n (%)	93/176 (52.8)	51/80 (63.8)	0.103
Undetectable viral load for at least 6 months, n (%)	177/195 (90.8)	77/89 (86.5)	0.279
ART regimen, n (%)			0.052
NRTI-based regimen	2 (1.0)	1 (1.1)	
NNRTI-based regimen	21 (10.7)	3 (3.3)	
PI-based regimen	6 (3.0)	2 (2.2)	
INSTI-based regimen	144 (73.1)	68 (73.9)	
Other [3]	20 (10.2)	18 (19.6)	
None	4 (2.0)	0 (0.0)	
Paid or unpaid work in an environment where you work in close proximity to other people, n (%)	59/193 (30.6)	32/90 (35.6)	0.403
Working in hospital or healthcare facility, n (%)	9/193 (4.7)	3/90 (3.3)	0.605
Number of individuals (including participant) living in household, n (%)			0.268
1	98 (51.9)	39 (43.3)	
2	68 (36.0)	36 (40.0)	
3	17 (9.0)	8 (8.9)	
4 or more	6 (3.2)	7 (7.8)	
Unknown	8	2	
Number of bedrooms in household per person, mean (SD)	1.3 (0.7)	1.1 (0.6)	0.124
Number of bathrooms in household per person, mean (SD)	1.0 (0.5)	1.0 (0.5)	0.788

[1] Multiple could be selected. [2] (CD4 < 350, CD4/CD8 < 0.75, suppressed VL). [3] Regimens containing combinations of the above and/or other drug classes (i.e., cell entry inhibitor). Comparisons were based on Chi-square test or Fisher's exact test as appropriate. Other continuous variables, such as age and CD4 count, were compared between groups using Wilcoxon rank sum test.

3.2. Numbers and Types of Vaccines Received Stratified by BTI

The vast majority of the participants had received mRNA vaccines. In the current analysis, performed in September 2023, 83% of PWH without BTI and 89% with BTI had received at least two mRNA vaccines (either BNT162b2 and/or mRNA-1273). The types of vaccines received and the time interval between vaccine doses are shown in Table 2. More individuals with BTI had received ChAdOx1 vaccines, as one or both of the first two doses, than individuals who had received mRNA vaccines for both doses ($p = 0.004$).

Table 2. Types of vaccines received and time interval between doses in PWH without vs. with BTI.

	Breakthrough Infection No	Breakthrough Infection Yes	*p*
Types of COVID-19 vaccines received, doses 1 and 2, n (%)			0.004
mRNA–mRNA	182 (89.7)	71 (76.3)	
ChAdOx1–mRNA	13 (6.4)	9 (9.7)	
ChAdOx1–ChAdOx1	7 (3.4)	12 (12.9)	
Janssen/Novavax	1 (0.5)	1 (1.1)	
Types of COVID-19 vaccines received, dose 3, n (%)			0.929
Unknown/received only 2 doses	34	13	
BNT162b2	67 (67/163, 41.1)	32 (32/79, 40.5)	
mRNA-1273	96 (96/163, 58.9)	47 (47/79, 59.5)	
Number of vaccine doses received at the time of BTI, n (%)			-
2	-	25 (26.9)	
3	-	59 (63.4)	
4	-	9 (9.7)	
Number of days since last vaccine dose (IQR)		127.5 (67, 176)	
Number of days since second dose (for persons who develop BTI between second and third doses) (n = 25)	-	168 (135, 182)	-
Number of days since third dose (for persons who develop BTI between third and fourth doses) (n = 59)		108 (55, 167)	
Follow-up time from dose 2 to study end or BTI, months (median, IQR)	14.0 (11.5, 17.3)	8.8 (6.1, 10.9)	<0.001
Follow-up time from third dose (for those who did not have BTI prior to third dose)	8.8 (6.1, 12.4)	3.9 (1.9, 5.7)	<0.001
Follow-up time from fourth dose (for those who did not have BTI prior to fourth dose)	1.6 (1.0, 3.3)	0.6 (0.3, 1.4)	0.017

Comparisons were based on Chi-square test or Fisher's exact test as appropriate. Other continuous variables, were compared between groups using Wilcoxon rank sum test.

3.3. SARS-CoV-2 Antibody Concentrations Stratified by BTI

The median titres of IgG spike/RBD (log10 BAU/mL) at 3 months post dose 2 (±1 month), months post dose 2 (±2 months) and 1 month post dose 3 (±2 weeks) are depicted in Figure 1 and Table 3. Only serology data prior to breakthrough infection were included. In the analyses adjusted for age, sex, race, multimorbidity, hypertension, chronic kidney disease, diabetes and obesity, a lower IgG spike/RBD value (log10 BAU/mL) at 1 month post dose 3 was significantly associated with BTI in PWH.

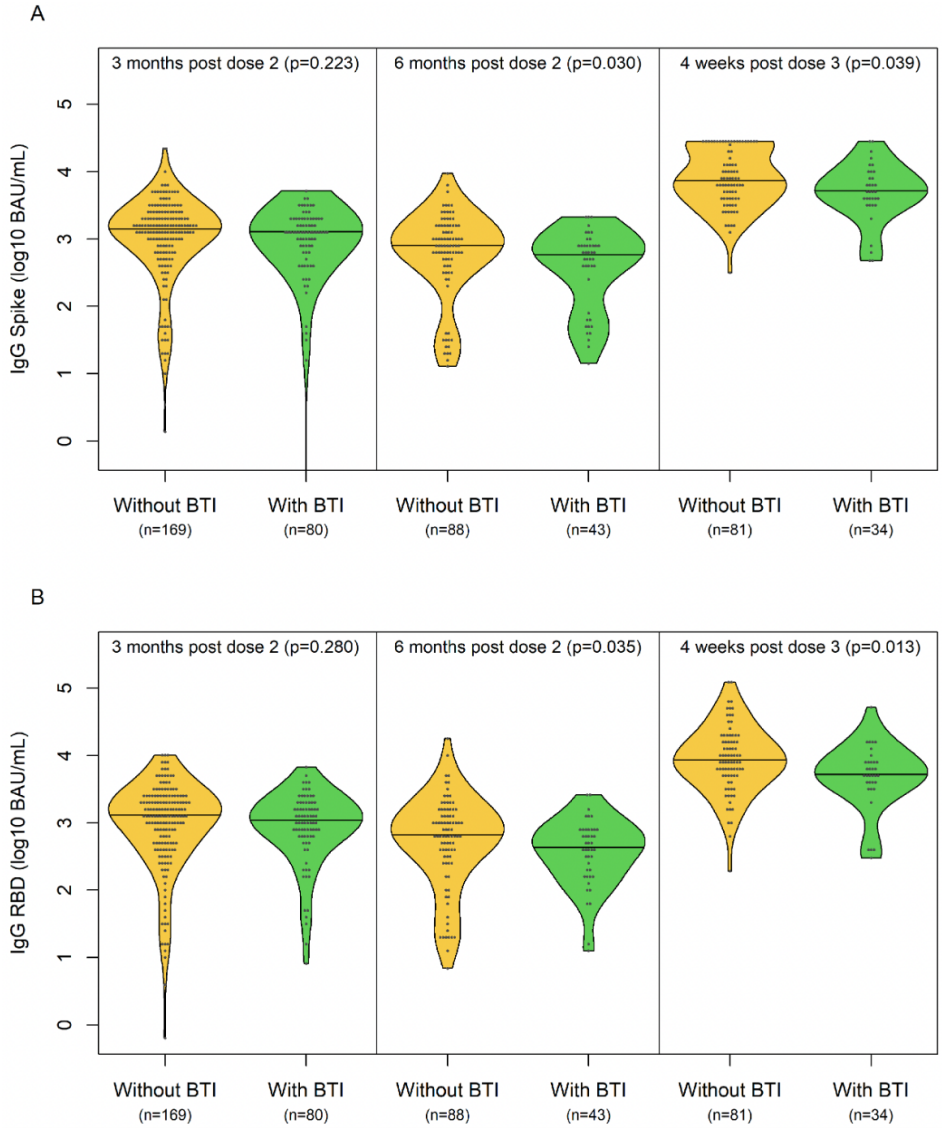


Figure 1. Median (IQR) IgG spike/RBD (log10 BAU/mL) at 3 months post dose 2 (±1 month), 6 months post dose 2 (±2 months) and 1 month post dose 3 (±2 weeks) in participants without (yellow) and with (green) breakthrough infection. (**A**) Median (IQR) IgG spike (log10 BAU/mL); (**B**) median (IQR) IgG RBD (log10 BAU/mL).

Table 3. Adjusted odds ratio of breakthrough infection per log10 BAU/mL decrease in IgG.

Time Point [1]		aOR (95% CI) [2]	P^{adj} [3]
3 months post dose 2 (±1 month)	IgG spike	1.21 (0.73, 1.99)	0.464
	IgG RBD	1.19 (0.74, 1.91)	0.381
6 months post dose 2 (±2 months)	IgG spike	1.74 (0.95, 3.16)	0.071
	IgG RBD	1.71 (0.92, 3.19)	0.092
1 month post dose 3 (±2 weeks)	IgG spike	2.83 (1.02, 7.87)	0.046
	IgG RBD	2.84 (1.13, 7.15)	0.027

1 Only data prior to breakthrough infection were included. Participants who developed BTI prior to any of these time points were excluded from these time points. 2 Adjusted odds ratio of breakthrough infection per log10 BAU/mL decrease in IgG. 3 Logistic regression adjusted for age, sex, multimorbidity, hypertension, chronic kidney disease, diabetes and obesity was used to examine the effect of IgG spike/RBD on the odds of BTI.

3.4. Clinical Presentation of Participants with BTI

Most of the participants with BTI had mild symptoms (Table S2), encompassing fever, cough, sore throat, malaise, headache, muscle pain, nausea, vomiting, diarrhea and/or loss of taste/smell [44]. Shortness of breath was seen in 12 individuals (17.4%) with BTI for whom their symptoms were captured, suggesting that a nearly a fifth of individuals had moderate infection [44]. We did not capture data on abnormal chest imaging, which is also suggestive of moderate infection. Three participants were hospitalized (Table S3). We did not capture information that enabled us to differentiate between severe illness (SpO2 < 94% on room air, ratio of arterial partial pressure of oxygen to fraction of inspired oxygen (PaO2/FiO2) < 300 mm Hg, a respiratory rate > 30 breaths/min or lung infiltrates > 50%) and critical illness (respiratory failure, septic shock and/or multiple organ dysfunction) [44]. None of the participants died.

4. Discussion

In this study, we examined BTI arising in a large cohort of PWH in Canada enrolled in a prospective observational study on COVID-19 vaccine immunogenicity. BTI occurred at a rate of 31.5 infections per 100 person-years in the PWH. Whereas other studies examining BTI in PWH have been conducted over the course of the pandemic, most of these studies have examined BTI based on HIV status (i.e., HIV-positive vs. HIV-negative). These studies yielded variable results. Furthermore, some studies have found that the severity of COVID-19 illness was similar between

PWH and HIV-negative individuals [45,46,47,48], whereas other studies have found increased severity amongst PWH compared to HIV-negative persons [49,50,51,52,53]. One study which examined the risk of COVID-19 hospitalization in the pre-Omicron era found that PWH had about a two times greater risk of COVID-19 hospitalization than HIV-negative individuals in crude analyses, which was attenuated in propensity-score-weighted models [2]. This study found the risk differential could be explained by sociodemographic factors and history of comorbidity, underscoring the need to address the social and comorbid vulnerabilities (e.g., injecting drugs) that are more prominent among PWH [2]. The discrepancies across studies have been attributed to small sample sizes, a lack of HIV-negative control groups, the confounding inherent in observational studies or them having been conducted prior to the COVID-19 vaccine rollout. Moreover, finding an ideal control group remains a challenge for HIV studies since this group would, in theory, be individuals identical to the HIV-seropositive group in all aspects except for HIV status [54].

A study conducted by Coburn et al. combined electronic-health-record-based cohort data from integrated health systems and academic centres to examine PWH fully vaccinated prior to 30 June 2021 and HIV-negative individuals matched by date of full vaccination, age, race and ethnicity and sex. Among 113,994 patients (33,029 PWH and 80,965 HIV-negative controls) followed until 31 December 2021 [55], the risk of severe illness (defined as hospitalization within 28 days following SARS-CoV-2 BTI, with a primary or secondary COVID-19 discharge diagnosis) was low for both groups (6.8% of 3649 vaccinated PWH and HIV-negative individuals) and did not differ by HIV status overall [55]. BTI was 28% higher in the PWH than the HIV-negative persons (adjusted hazard ratio, 1.28 [95% CI, 1.19–1.37]) [55]. Most of the people with BTI were aged 55 or older (60%) and male (89%) [55]. In another study by Sun et al., cohort study data from the National COVID Cohort Collaborative (N3C), using a centralized electronic-medical-record-based repository of COVID-19 clinical data from academic medical centres across the US, were analyzed [56]. Amongst persons with HIV who had received a full vaccination series between December 2020 and September 2021, the IR of breakthrough infection was 7.1 (95% CI, 7.1–7.2) per 1000 person-months for people without immune dysfunction vs. 9.1 (95% CI, 8.8–9.4) per 1000 person-months for person with HIV infection [56]. Furthermore, HIV infection was independently associated with an increased BTI rate compared to persons without HIV or another

form of immune compromise [56]. Importantly, the associations were independent of demographic characteristics, geographic region and comorbidity burden.

We found that the PWH who developed BTI were similar to the PWH who did not develop BTI with regards to age, sex, ethnicity, HIV duration, CD4 count and comorbidities. Although our study did not examine the severity of BTI, Coburn et al. found that severe breakthrough infection was 59% higher in the PWH with CD4 counts less than 350 cells/mm3 compared to the HIV-negative controls (aHR, 1.59; 95% CI, 0.99 to 2.46; $p = 0.049$) [55]. Furthermore, in multivariable analyses among PWH, Coburn et al. found that being female and older was associated with an increased risk of BTI. Other possible reasons for the differences between our study and the previously published study may relate to the types of individuals included in these studies and economic disparities. As regards vaccine type, we observed that the PWH who received ChAdOx1 vaccines as either one or two of their first two doses had significantly more BTIs than those who received mRNA vaccines for both doses. This finding has been observed in other studies [57]. mRNA vaccines are recognized for their ability to elicit strong immune responses compared to non-mRNA vaccines [58].

A very small number of participants in our study who developed BTI were hospitalized, and nobody died. These findings suggest that vaccination appeared to attenuate the disease severity in those acquiring infection. In the study by Coburn et al., mechanical ventilation and death were rare among PWH with BTI. When mechanical ventilation and death did occur, it was more likely in persons over 55 years of age with one or more comorbidity [55]. Although our study was not designed to assess the severity of COVID-19 infection amongst persons with BTI, these findings are nonetheless reassuring.

Interestingly, we found that PWH with BTI had a significantly lower median IgG spike/RBD level at 1 month post dose 3 than the participants without BTI. This observation suggests that lower IgG may predict BTI at this time point in this cohort. Although studies in both PWH and HIV-negative populations have tried to identify the protective antibody level against BTI, few have identified a specific cutoff [59].

In a systematic review of COVID-19 vaccine antibody responses in PWH which included studies from 1 January 2020 to 31 March 2022, Chun et al. reviewed 28 studies from 12 countries. Twenty-two (73%) studies reported high COVID-19 vaccine seroconversion rates in PWH, although PWH with lower baseline CD4 counts and CD4/CD8 ratios and higher baseline viral loads had lower seroconversion rates and antibody titres [60,61]. To date, there is still no consensus on what constitutes the best correlate of immune protection, and there are no disease-specific correlates of immune protection. In a large prospective longitudinal population-based study of COVID-19 in the general population, Vivaldi et al. observed correlations between vaccine-induced anti-spike antibody titres and protection against severe BTI [57]. Several studies have demonstrated that higher levels of neutralizing antibodies are associated with immune protection from symptomatic BTI infection following vaccination [62,63,64,65,66].

As IgG is involved in binding viruses, it makes intuitive sense there may be an association between lower IgG levels preceding BTI, although neutralizing antibody titres during the first months after vaccination may be better correlated with vaccine effectiveness [62,66] and have been predictive of the risk of BTI [62,65,67]. However, no specific antibody or neutralizing threshold titre has yet been identified that can predict the degree of protection, as it changes over time with waning or boosting. Moreover, it is worth underscoring that rates of BTI are a consequence of an individual's level of immunity at a particular moment in time, the variant to which a person is exposed and the severity of the illnesses [67] BTI is influenced by, including their timing, frequency, severity and degree of infectiousness. BTI is important, as it is informative regarding the duration of restrictions in order to limit transmission and the need for additional booster doses or changes to dosing intervals [67].

SARS-CoV-2 vaccines have been designed to elicit immune responses—including the formation of antibodies against the outer spike protein of the Ancestral strain. However, SARS-CoV-2 variants, including Omicron, harbour mutations in the spike protein. Omicron harbours greater than 30 mutations in its virus' spike protein, which attaches to cells, thereby increasing the chance of infection [68]. Moreover, Omicron and other variants are more transmissible than the Ancestral strain and are more able to evade antibody response, resulting in more BTIs [69]. Antibody waning, along with antigenic drift, limits the ability of long-term immunity to prevent reinfection.

Furthermore, while earlier variants had a few mutation amino acids in their RBDs, Omicron harbours 15 RBD mutations—many in key antibody sites—preventing antibody binding. In addition, while earlier variants required both ACE2 and TMPRSS2 proteins to inject their genomes into a cell, Omicron bound only to ACE2. As many cells do not have TMPRSS2 on their exterior, if the virus does not need the surface protein, it has a wider number of potential target cells. Furthermore, unlike Delta, which had a subdued interferon response, Omicron activated interferon signaling [70]. Omicron infections tended to be less severe, but they were also associated with rises in cases and significant increases in hospitalizations and deaths. Therefore, Omicron and its subvariants quickly became dominant starting in late 2021, as they were more transmissible and also evaded antibodies more than prior variants. Consequently, there was an increase in BTIs [70,71,72].

Although this is not included in the current manuscript, more research needs to be dedicated to understanding the role of cell-mediated immunity and mucosal immunity in the nasal, oropharyngeal and pulmonary tissues in relation to protection against SARS-CoV-2 and other emerging viral infections [**69**,**73**,**74**,**75**,**76**]. In vaccinated HIV-negative individuals infected with SARS-CoV-2 during the Omicron wave, there were increased spike-specific responses during the infection of vaccinated compared to unvaccinated individuals [**73**]. Spike-specific clusters of CD4 T cells and plasmablasts expanded, and CD8 T cells were potently activated during the first week. In contrast, memory B cell activation, neutralizing antibody production and the primary responses to non-spike antigens occurred during the second week.

Given the importance of different arms of the immune system working synergistically, it is likely that the best correlate of protection will be a combination of measures. HIV induces a wide spectrum of immune abnormalities and is characterized by chronic low-grade inflammation despite ART Cell-mediated immunity [**61**,**74**,**75**,**76**,**77**,**78**,**79**] and antibody-dependent cell cytotoxicity merit examination, especially given the underlying propensity of HIV to infect and target CD4 T cells, which play a role in establishing vaccine memory, and to induce dysfunction in cytotoxic CD8 T cell response [**80**].

Measures of mucosal immunity should also be given greater attention given that this is the first site of immune defense. In HIV-negative individuals, it has been demonstrated that a local secretory component-associated IgA response is induced by COVID-19 mRNA vaccination that persists in some, but not all, individuals. The serum and saliva IgA responses were modestly correlated at 2–4 weeks post dose 2. Interestingly, the levels of anti-spike serum IgA (but not IgG) at this time point were lower in the participants who subsequently become infected with SARS-CoV-2 [**81**].

Our study has several limitations. An important limitation is the risk of misclassification bias. During many time periods during the pandemic, PCR tests were reserved for healthcare workers, hospitalized persons and residents in long-term care facilities. During other time periods, rapid antigen tests were in short supply in some regions. Therefore, participants may have had symptoms, but diagnostic testing may not have been easily accessible. Ascertainment of BTI was based on patient-initiated healthcare seeking, as opposed to being systematic. Thus, there may have been cases of asymptomatic BTI that were not captured. We acknowledge that relying on self-report and IgG data may introduce bias, as BTI in those vaccinated or who have had a prior infection may result in mild symptoms or even a lack of symptoms. Self-reporting can also impact representativeness and accuracy due to self-selection and recall biases. Moreover, there was a considerable overlap in the antibody levels between both those with and without BTI such that one cannot identify a threshold level of antibody that predicts protection. We did not determine the duration of BTI, nor the duration of post COVID chronic symptomatology. Furthermore, we did not report on the neutralization efficiency, as neutralization assays are still in progress at this time. The relative lack of information on disease severity is another limitation. This study was conducted in Canada, which has a well-developed healthcare system, and therefore its findings may not be generalizable to PWH in other countries. Even within Canada, the recruitment sites were large urban tertiary care clinics, and the participants may not necessarily be representative of other PWH in rural regions who differ in their access to healthcare, adherence to preventative behaviours and social determinants of health. Furthermore, our findings may not be generalizable to all the SARS-CoV-2 variants in circulation given that our study was conducted when the Alpha, Delta and Omicron variants were circulating. Given the timing of most of the BTIs in our study (between the third and fourth vaccine doses), most of the BTIs occurred when Omicron was circulating.

5. Conclusions

In summary, BTIs were more common in participants who received ChAdOx1 vaccines as the primary series. BTI was not associated with age or HIV-related factors. PWH with BTI following COVID-19 vaccination had lower median IgG Spike/RBD antibody levels 1 month post dose 3 than those who did not develop BTI at this point, suggesting that antibody levels at this time point may be a predictor of BTI in this cohort. However, given the large overlap in the IgG spike/RBD antibody levels between groups, this statement requires some caution in its interpretation. Ongoing evaluation is needed to determine the optimal correlates of immune protection and the durability of immune response in order to further inform vaccine guidelines and policies.

Supplementary Materials
The following supporting information can be downloaded at**https://www.mdpi.com/article/10.3390/vaccines12050447/s1**, Table S1: Participant characteristics stratified based on COVID-19 BTI; Table S2: COVID-19 symptoms based on presence or absence of BTI for participants self-reporting BTI; Table S3: Characteristics of the three participants with BTI who were hospitalized due to COVID-19.

Author Contributions
Conceptualization, C.T.C., C.L.C. and A.H.A.; data curation: T.L., J.S., Y.G. and C.A.; formal analysis: T.L., J.S., Y.G., C.A. and M.-A.J.; funding acquisition: C.T.C., J.S., M.-A.L., J.N., A.N.B., H.S., C.C., S.W., M.O. and A.H.A.; investigation: C.T.C., T.L., J.S., Y.G., C.A., M.-A.J., J.N., M.-A.J., A.N.B., H.S., C.C., S.W., M.O., C.K., D.H.S.T. and C.L.C.; methodology: C.T.C., J.S., T.L., Y.G., C.A., M.-A.L., J.N., M.-A.J., M.A.B., H.S., C.C., S.W., M.O., C.K., D.H.S.T., M.H. (Marianne Harris), M.H. (Mark Hull), Z.L.B., H.R.L., M.A.B., S.M., E.M., S.S., B.L., J.B.A., J.-P.R., C.L.C. and A.H.A.; project administration: C.T.C., Y.G., C.A., J.N., M.-A.J., A.N.B., H.S., S.W., M.O., C.K., D.H.S.T., M.H. (Marianne Harris), M.H. (Mark Hull), Z.L.B., H.R.L., M.A.B., S.M., E.M., S.S., J.B.A., J.-P.R., C.L.C. and A.H.A.; resources: M.-A.L., M.-A.J., Z.L.B. and A.H.A.; software: T.L.; supervision: C.T.C., J.S., T.L., C.A., M.-A.L., J.N., M.-A.J., M.A.B., H.S., S.W., M.H. (Marianne Harris), M.H. (Mark Hull), Z.L.B., H.R.L., M.A.B.,S.S., J.B.A., C.L.C. and A.H.A.; validation: T.L., Y.G. and C.A.; visualization: C.T.C., T.L., J.S., Y.G., C.A., M.-A.L., J.N., A.N.B. and H.S.; writing—original: C.T.C. All authors have read and agreed to the published version of the manuscript.

Funding
This research was supported by funding from the Public Health Agency of Canada, through the Vaccine Surveillance Reference group and the COVID-19 Immunity Task Force (grant number: 2122-HQ-000075) and the CTN (grant number: N/A). The production of the COVID-19 reagents was financially supported by NRC's Pandemic Response Challenge Program.

Institutional Review Board Statement
This study was conducted in accordance with the Declaration of Helsinki and approved by the McGill University Health Centre Research Ethics Board (REB) (#2022-7857), Ottawa Health Science Network REB (#20210361-01H), University Health Network REB (#21-5504) and the University of British Columbia Providence Health Care and Simon Fraser University REB s(#H21-01515, #H21-00742)).

Informed Consent Statement
Informed consent was obtained from all the participants of the study.

Data Availability Statement
The data presented in this study may be made available upon written request to the corresponding author. Researchers wishing to access the CITF core data elements can submit an application to the CITF Data Access Committee.

Acknowledgments
The authors thank the CTN staff who were involved in the planning and preparation of this study, in addition to the CTN Scientific Review Committee and the Community Advisory Board for their expedited review and helpful comments. They also thank all of the participants for their time and commitment. In addition, the authors thank the study coordinators and study nurses Florian Bobeuf, Claude Vertzagias, Lina Del Balso, Nathalie Paisible, Guillaume Theriault, Hansi Peiris, Lianne Thai, Rosemarie Clarke, Erin Collins, Nadia Ohene-Adu, Aron Dyks and Jill Jackson; the data manager Elisa Lau; the laboratory staff Tara Mabanga, Yulia Alexandrova, Ralph-Sydney Mboumba Bouassa, Erik Pavey and Stephanie Burke-Schinkel and the members of the University of Ottawa Serology and Diagnostics High-Throughput Facility, including Danielle Dewar-Darch, Justino Hernandez Soto, Abishek Xavier, Nicholas Bradette, Klaudia Baumann, Gwendoline Ward and Yuchu Dou. The authors also thank the physicians who assisted with recruitment. The COVID-19 antigens as well as the anti-hIgG#5-HRP fusion antibody were generously provided by Yves Durocher, the National Research Council of Canada (NRC), Montreal. C.T.C. is supported by a Fonds de recherche du Québec-Santé (FRQS) Junior 2 career award. A.B. holds a Canada Research Chair Tier 2 Canada Research Chair (CRC) position in sexually transmitted infection (STI) prevention. MAL holds a CRC position, Tier 2, in human immunovirology. M.A.J. holds a CRC position, Tier 2, in human immunovirology. S.W. is supported by a Research Chair position in HIV Clinical Care and Aging with the Ontario HIV Treatment Network. D.T. is supported by a Tier 2 CRC position in HIV Prevention and STI Research. M.A.B. holds a Canada Research Chair position, Tier 2, in viral pathogenesis and immunity. Z.L.B. holds a Scholar Award from Michael Smith Health Research BC. BL is supported by a career award LE 250 from the Quebec Ministry of Health for researchers in family medicine and an FRQS Junior 2 career award and holds a Canadian Institutes of Health Research Strategy for Patient-Oriented Research (SPOR) Mentoring Chair position in Innovative Clinical Trials. J.P.R. holds a Lowenstein Chair role in Hematology. Y.G. is supported by a Charles Best and Frederick Banting (CGS Doctoral) award from the CIHR (476885).

Conflicts of Interest
The authors declare no conflicts of interest. The CITF had no role in the design of the study; in the collection, analyses or interpretation of the data; in the writing of the manuscript or in the decision to publish the results.

References

1. Beck, J.M.; Rosen, M.J.; Peavy, H.H. Pulmonary complications of HIV infection. Report of the Fourth NHLBI Workshop. Am. J. Respir. Crit. Care Med. 2001, 164, 2120–2126.
2. Puyat, J.H.; Fowokan, A.; Wilton, J.; Janjua, N.Z.; Wong, J.; Grennan, T.; Chambers, C.; Kroch, A.; Costiniuk, C.T.; Cooper, C.L.; et al. Risk of COVID-19 hospitalization in people living with HIV and HIV-negative individuals and the role of COVID-19 vaccination: A retrospective cohort study. Int. J. Infect. Dis. 2023, 135, 49–56.
3. Davies, M.A. HIV and risk of COVID-19 death: A population cohort study from the Western Cape Province, South Africa. medRxiv 2020.
4. Geretti, A.M.; Stockdale, A.J.; Kelly, S.H.; Cevik, M.; Collins, S.; Waters, L.; Villa, G.; Docherty, A.; Harrison, E.M.; Turtle, L.; et al. Outcomes of COVID-19 related hospitalization among people with HIV in the ISARIC WHO Clinical Characterization Protocol (UK): A prospective observational study. Clin. Infect. Dis. 2020, 73, e2095–e2106.
5. Williamson, E.J.; Walker, A.J.; Bhaskaran, K.; Bacon, S.; Bates, C.; Morton, C.E.; Curtis, H.J.; Mehrkar, A.; Evans, D.; Inglesby, P.; et al. Factors associated with COVID-19-related death using OpenSAFELY. Nature 2020, 584, 430–436.
6. Vizcarra, P.; Perez-Elias, M.J.; Quereda, C.; Moreno, A.; Vivancos, M.J.; Dronda, F.; Casado, J.L.; Team, C.-I. Description of COVID-19 in HIV-infected individuals: A single-centre, prospective cohort. Lancet HIV 2020, 7, e554–e564.
7. Augello, M.; Bono, V.; Rovito, R.; Tincati, C.; Marchetti, G. Immunologic Interplay Between HIV/AIDS and COVID-19: Adding Fuel to the Flames? Curr. HIV/AIDS Rep. 2023, 20, 51–75.
8. Wong, C.; Gange, S.J.; Moore, R.D.; Justice, A.C.; Buchacz, K.; Abraham, A.G.; Rebeiro, P.F.; Koethe, J.R.; Martin, J.N.; Horberg, M.A.; et al. Multimorbidity Among Persons Living with Human Immunodeficiency Virus in the United States. Clin. Infect. Dis. 2018, 66, 1230–1238.
9. Fehr, D.; Lebouche, B.; Ruppenthal, L.; Brownc, M.; Obasc, N.; Bourbonniere, E.; Girouard, J.; Massicotte, A.; Jenabian, M.A.; Almomen, A.A.; et al. Characterization of people living with HIV in a Montreal-based tertiary care center with COVID-19 during the first wave of the pandemic. AIDS Care 2022, 34, 663–669.
10. Almomen, A.; Cox, J.; Lebouche, B.; Cheng, M.P.; Frenette, C.; Routy, J.P.; Costiniuk, C.T. Short Communication: Ongoing Impact of the Social Determinants of Health During the Second and Third Waves of the COVID-19 Pandemic in People Living with HIV Receiving Care in a Montreal-Based Tertiary Care Center. AIDS Res. Hum. Retroviruses 2022, 38, 359–362.
11. Lane, H.C.; Masur, H.; Edgar, L.C.; Whalen, G.; Rook, A.H.; Fauci, A.S. Abnormalities of B-cell activation and immunoregulation in patients with the acquired immunodeficiency syndrome. N. Engl. J. Med. 1983, 309, 453–458.
12. Cobos Jimenez, V.; Wit, F.W.; Joerink, M.; Maurer, I.; Harskamp, A.M.; Schouten, J.; Prins, M.; van Leeuwen, E.M.; Booiman, T.; Deeks, S.G.; et al. T-Cell Activation Independently Associates with Immune Senescence in HIV-Infected Recipients of Long-term Antiretroviral Treatment. J. Infect. Dis. 2016, 214, 216–225.
13. Austin, J.W.; Buckner, C.M.; Kardava, L.; Wang, W.; Zhang, X.; Melson, V.A.; Swanson, R.G.; Martins, A.J.; Zhou, J.Q.; Hoehn, K.B.; et al. Overexpression of T-bet in HIV infection is associated with accumulation of B cells outside germinal centers and poor affinity maturation. Sci. Transl. Med. 2019, 11, eaax0904.
14. Amoah, S.; Mishina, M.; Praphasiri, P.; Cao, W.; Kim, J.H.; Liepkalns, J.S.; Guo, Z.; Carney, P.J.; Chang, J.C.; Fernandez, S.; et al. Standard-Dose Intradermal Influenza Vaccine Elicits Cellular Immune Responses Similar to Those of Intramuscular Vaccine in Men with and Those without HIV Infection. J. Infect. Dis. 2019, 220, 743–751.

15. Kroon, F.P.; van Dissel, J.T.; de Jong, J.C.; Zwinderman, K.; van Furth, R. Antibody response after influenza vaccination in HIV-infected individuals: A consecutive 3-year study. Vaccine 2000, 18, 3040–3049.
16. Klein, M.B.; Lu, Y.; DelBalso, L.; Cote, S.; Boivin, G. Influenzavirus infection is a primary cause of febrile respiratory illness in HIV-infected adults, despite vaccination. Clin. Infect. Dis. 2007, 45, 234–240.
17. French, N.; Gordon, S.B.; Mwalukomo, T.; White, S.A.; Mwafulirwa, G.; Longwe, H.; Mwaiponya, M.; Zijlstra, E.E.; Molyneux, M.E.; Gilks, C.F. A trial of a 7-valent pneumococcal conjugate vaccine in HIV-infected adults. N. Engl. J. Med. 2010, 362, 812–822.
18. Glaser, J.B.; Volpe, S.; Aguirre, A.; Simpkins, H.; Schiffman, G. Zidovudine improves response to pneumococcal vaccine among persons with AIDS and AIDS-related complex. J. Infect. Dis. 1991, 164, 761–764.
19. MacNeil, J.R.; Rubin, L.G.; Patton, M.; Ortega-Sanchez, I.R.; Martin, S.W. Recommendations for Use of Meningococcal Conjugate Vaccines in HIV-Infected Persons—Advisory Committee on Immunization Practices, 2016. MMWR Morb. Mortal. Wkly. Rep. 2016, 65, 1189–1194.
20. Wallace, M.R.; Brandt, C.J.; Earhart, K.C.; Kuter, B.J.; Grosso, A.D.; Lakkis, H.; Tasker, S.A. Safety and immunogenicity of an inactivated hepatitis A vaccine among HIV-infected subjects. Clin. Infect. Dis. 2004, 39, 1207–1213.
21. Crum-Cianflone, N.F.; Wilkins, K.; Lee, A.W.; Grosso, A.; Landrum, M.L.; Weintrob, A.; Ganesan, A.; Maguire, J.; Klopfer, S.; Brandt, C.; et al. Long-term durability of immune responses after hepatitis A vaccination among HIV-infected adults. J. Infect. Dis. 2011, 203, 1815–1823.
22. Kemper, C.A.; Haubrich, R.; Frank, I.; Dubin, G.; Buscarino, C.; McCutchan, J.A.; Deresinski, S.C.; California Collaborative Treatment, G. Safety and immunogenicity of hepatitis A vaccine in human immunodeficiency virus-infected patients: A doubleblind, randomized, placebo-controlled trial. J. Infect. Dis. 2003, 187, 1327–1331.
23. Overton, E.T.; Sungkanuparph, S.; Powderly, W.G.; Seyfried, W.; Groger, R.K.; Aberg, J.A. Undetectable plasma HIV RNA load predicts success after hepatitis B vaccination in HIV-infected persons. Clin. Infect. Dis. 2005, 41, 1045–1048.
24. El Chaer, F.; El Sahly, H.M. Vaccination in the Adult Patient Infected with HIV: A Review of Vaccine Efficacy and Immunogenicity. Am. J. Med. 2019, 132, 437–446.
25. Weiser, J.K.; Tie, Y.; Beer, L.; Neblett Fanfair, R.; Shouse, R.L. Racial/Ethnic and Income Disparities in the Prevalence of Comorbidities that Are Associated with Risk for Severe COVID-19 Among Adults Receiving HIV Care, United States, 2014-2019. J. Acquir. Immune Defic. Syndr. 2021, 86, 297–304.
26. Ramasamy, M.N.; Minassian, A.M.; Ewer, K.J.; Flaxman, A.L.; Folegatti, P.M.; Owens, D.R.; Voysey, M.; Aley, P.K.; Angus, B.; Babbage, G.; et al. Safety and immunogenicity of ChAdOx1 nCoV-19 vaccine administered in a prime-boost regimen in young and old adults (COV002): A single-blind, randomised, controlled, phase 2/3 trial. Lancet 2021, 396, 1979–1993.
27. COVID-19 Vaccine (ChAdOx1 nCoV-19) Trial in South African Adults with and without HIV-Infection. Available online: https://clinicaltrials.gov/ct2/show/NCT04444674?cond=HIV+and+COVID&draw=4 (accessed on 6 May 2021).
28. Costiniuk, C.T.; Singer, J.; Langlois, M.A.; Kulic, I.; Needham, J.; Burchell, A.; Jenabian, M.A.; Walmsley, S.; Ostrowski, M.; Kovacs, C.; et al. CTN 328: Immunogenicity outcomes in people living with HIV in Canada following vaccination for COVID-19 (HIV-COV): Protocol for an observational cohort study. BMJ Open 2021, 11, e054208.
29. Costiniuk, C.T.; Singer, J.; Lee, T.; Langlois, M.A.; Arnold, C.; Galipeau, Y.; Needham, J.; Kulic, I.; Jenabian, M.A.; Burchell, A.N.; et al. COVID-19 vaccine immunogenicity in people with HIV. AIDS 2023, 37, F1–F10.
30. Costiniuk, C.T.; Singer, J.; Lee, T.; Galipeau, Y.; McCluskie, P.S.; Arnold, C.; Langlois, M.A.; Needham, J.; Jenabian, M.A.; Burchell, A.N.; et al. Antibody neutralization capacity after coronavirus disease 2019 vaccination in people with HIV in Canada. AIDS 2023, 37, F25–F35.

31. Pereira, B.; Xu, X.N.; Akbar, A.N. Targeting Inflammation and Immunosenescence to Improve Vaccine Responses in the Elderly. Front. Immunol. 2020, 11, 583019.
32. Wagner, A.; Garner-Spitzer, E.; Jasinska, J.; Kollaritsch, H.; Stiasny, K.; Kundi, M.; Wiedermann, U. Age-related differences in humoral and cellular immune responses after primary immunisation: Indications for stratified vaccination schedules. Sci. Rep. 2018, 8, 9825.
33. Braunstein, S.L.; Wahnich, A.; Lazar, R. COVID-19 Outcomes Among People with HIV and COVID-19 in New York City. J. Infect. Dis. 2023, 228, 1571–1582.
34. Gallant, J.; Hsue, P.Y.; Shreay, S.; Meyer, N. Comorbidities Among US Patients with Prevalent HIV Infection-A Trend Analysis. J. Infect. Dis. 2017, 216, 1525–1533.
35. Public Health Agency of Canada 2022. Available online: https://www.canada.ca/en/public-health/services/publications/ healthy-living/canadian-immunization-guide-part-4-active-vaccines/page-26-covid-19-vaccine.html (accessed on 31 May 2022).
36. Public Health Agency of Canada. Available online: https://www.canada.ca/en/health-canada/news/2021/11/health-canadaauthorizes-the-use-of-the-moderna-spikevax-covid-19-vaccine-as-a-booster-shot.html (accessed on 15 February 2022).
37. Ministry of Health. COVID-19 Vaccine Booster Recommendation. Available online: https://www.ontario.ca/page/covid-19 -vaccines#:~:text=If%20you%20are%20at%20increased,available%20closer%20to%20fall%202024 (accessed on 22 July 2022).
38. Cholette, F.; Fabia, R.; Harris, A.; Ellis, H.; Cachero, K.; Schroeder, L.; Mesa, C.; Lacap, P.; Arnold, C.; Galipeau, Y.; et al. Comparative performance data for multiplex SARS-CoV-2 serological assays from a large panel of dried blood spot specimens. Heliyon 2022, 8, e10270.
39. Colwill, K.; Galipeau, Y.; Stuible, M.; Gervais, C.; Arnold, C.; Rathod, B.; Abe, K.T.; Wang, J.H.; Pasculescu, A.; Maltseva, M.; et al. A scalable serology solution for profiling humoral immune responses to SARS-CoV-2 infection and vaccination. Clin. Transl. Immunol. 2022, 11, e1380.
40. Collins, E.; Galipeau, Y.; Arnold, C.; Bosveld, C.; Heiskanen, A.; Keeshan, A.; Nakka, K.; Shir-Mohammadi, K.; St-DenisBissonnette, F.; Tamblyn, L.; et al. Cohort profile: Stop the Spread Ottawa (SSO) —A community-based prospective cohort study on antibody responses, antibody neutralisation efficiency and cellular immunity to SARS-CoV-2 infection and vaccination. BMJ Open 2022, 22, e062187.
41. Vinh, D.C.; Gouin, J.P.; Cruz-Santiago, D.; Canac-Marquis, M.; Bernier, S.; Bobeuf, F.; Sengupta, A.; Brassard, J.P.; Guerra, A.; Dziarmaga, R.; et al. Real-world serological responses to extended-interval and heterologous COVID-19 mRNA vaccination in frail, older people (UNCoVER): An interim report from a prospective observational cohort study. Lancet Healthy Longev. 2022, 3, e166–e175.
42. Fakhraei, R.; Erwin, E.; Alibhai, K.M.; Murphy, M.S.Q.; Dingwall-Harvey, A.L.J.; White, R.R.; Dimanlig-Cruz, S.; LaRose, R.; Grattan, K.; Jia, J.J.; et al. Prevalence of SARS-CoV-2 infection among obstetric patients in Ottawa, Canada: A descriptive study. CMAJ Open 2022, 10, E643–E651.
43. NIBSC 20.136; 4-Parameter Log-Logistic Curve Based on Measurements from the World Health Organization International Standard. WHO: Geneva, Switzerland, 2022.
44. National Institutes of Health. Clinical Spectrum of SARS-CoV-2 Infection NIH COVID-19 Treatment Guidelines. Available online: https://www.covid19treatmentguidelines.nih.gov/overview/clinical-spectrum/ (accessed on 6 March 2023).
45. Collins, L.F.; Moran, C.A.; Oliver, N.T.; Moanna, A.; Lahiri, C.D.; Colasanti, J.A.; Kelley, C.F.; Nguyen, M.L.; Marconi, V.C.; Armstrong, W.S.; et al. Clinical characteristics, comorbidities and outcomes among persons with HIV hospitalized with coronavirus disease 2019 in Atlanta, Georgia. AIDS 2020, 34, 1789–1794.
46. Shalev, N.; Scherer, M.; LaSota, E.D.; Antoniou, P.; Yin, M.T.; Zucker, J.; Sobieszczyk, M.E. Clinical Characteristics and Outcomes in People Living with Human Immunodeficiency Virus Hospitalized for Coronavirus Disease 2019. Clin. Infect. Dis. 2020, 71, 2294–2297.
47. Ceballos, M.E.; Ross, P.; Lasso, M.; Dominguez, I.; Puente, M.; Valenzuela, P.; Enberg, M.; Serri, M.; Munoz, R.; Pinos, Y.; et al. Clinical characteristics and outcomes of people living with HIV hospitalized with COVID-19: A nationwide experience. Int. J. STD AIDS 2021, 32, 435–443.

48. Durstenfeld, M.S.; Sun, K.; Ma, Y.; Rodriguez, F.; Secemsky, E.A.; Parikh, R.V.; Hsue, P.Y. Association of HIV infection with outcomes among adults hospitalized with COVID-19. AIDS 2022, 36, 391–398.
49. Bhaskaran, K.; Rentsch, C.T.; MacKenna, B.; Schultze, A.; Mehrkar, A.; Bates, C.J.; Eggo, R.M.; Morton, C.E.; Bacon, S.C.J.; Inglesby, P.; et al. HIV infection and COVID-19 death: A population-based cohort analysis of UK primary care data and linked national death registrations within the OpenSAFELY platform. Lancet HIV 2021, 8, e24–e32.
50. Tesoriero, J.M.; Swain, C.E.; Pierce, J.L.; Zamboni, L.; Wu, M.; Holtgrave, D.R.; Gonzalez, C.J.; Udo, T.; Morne, J.E.; Hart-Malloy, R.; et al. COVID-19 Outcomes Among Persons Living with or without Diagnosed HIV Infection in New York State. JAMA Netw. Open 2021, 4, e2037069.
51. Yang, X.; Sun, J.; Patel, R.C.; Zhang, J.; Guo, S.; Zheng, Q.; Olex, A.L.; Olatosi, B.; Weissman, S.B.; Islam, J.Y.; et al. Associations between HIV infection and clinical spectrum of COVID-19: A population level analysis based on US National COVID Cohort Collaborative (N3C) data. Lancet HIV 2021, 8, e690–e700.
52. Dong, Y.; Li, Z.; Ding, S.; Liu, S.; Tang, Z.; Jia, L.; Liu, J.; Liu, Y. HIV infection and risk of COVID-19 mortality: A meta-analysis. Medicine 2021, 100, e26573.
53. Dandachi, D.; Geiger, G.; Montgomery, M.W.; Karmen-Tuohy, S.; Golzy, M.; Antar, A.A.R.; Llibre, J.M.; Camazine, M.; Diaz-De Santiago, A.; Carlucci, P.M.; et al. Characteristics, Comorbidities, and Outcomes in a Multicenter Registry of Patients with Human Immunodeficiency Virus and Coronavirus Disease 2019. Clin. Infect. Dis. 2021, 73, e1964–e1972.
54. Wong, C.; Althoff, K.; Gange, S.J. Identifying the appropriate comparison group for HIV-infected individuals. Curr. Opin. HIV AIDS 2014, 9, 379–385.
55. Coburn, S.B.; Humes, E.; Lang, R.; Stewart, C.; Hogan, B.C.; Gebo, K.A.; Napravnik, S.; Edwards, J.K.; Browne, L.E.; Park, L.S.; et al. Analysis of Postvaccination Breakthrough COVID-19 Infections Among Adults with HIV in the United States. JAMA Netw. Open 2022, 5, e2215934.
56. Sun, J.; Zheng, Q.; Madhira, V.; Olex, A.L.; Anzalone, A.J.; Vinson, A.; Singh, J.A.; French, E.; Abraham, A.G.; Mathew, J.; et al. Association Between Immune Dysfunction and COVID-19 Breakthrough Infection After SARS-CoV-2 Vaccination in the US. JAMA Intern. Med. 2022, 182, 153–162.
57. Vivaldi, G.; Jolliffe, D.A.; Holt, H.; Tydeman, F.; Talaei, M.; Davies, G.A.; Lyons, R.A.; Griffiths, C.J.; Kee, F.; Sheikh, A.; et al. Risk factors for SARS-CoV-2 infection after primary vaccination with ChAdOx1 nCoV-19 or BNT162b2 and after booster vaccination with BNT162b2 or mRNA-1273: A population-based cohort study (COVIDENCE UK). Lancet Reg. Health Eur. 2022, 22, 100501.
58. Lee, J.; Woodruff, M.C.; Kim, E.H.; Nam, J.H. Knife's edge: Balancing immunogenicity and reactogenicity in mRNA vaccines. Exp. Mol. Med. 2023, 55, 1305–1313.
59. Walmsley, S.; Ravindran, R.; Clarke, R.; Wouters, B.; Silva, A.; Gingras, A.C.; Szadkowski, L. COVID-19 breakthrough infections in vaccinated participants of the Safety and Efficacy of Preventative COVID Vaccines sub-study. J. Assoc. Med. Microbiol. Infect. Dis. Can. 2022, 7, 333–342.
60. Chun, H.M.; Milligan, K.; Agyemang, E.; Ford, N.; Rangaraj, A.; Desai, S.; Wilder-Smith, A.; Vitoria, M.; Zulu, I. A Systematic Review of COVID-19 Vaccine Antibody Responses in People with HIV. Open Forum Infect. Dis. 2022, 9, ofac579.
61. Augello, M.; Bono, V.; Rovito, R.; Tincati, C.; Bianchi, S.; Taramasso, L.; Di Biagio, A.; Callegaro, A.; Maggiolo, F.; Borghi, E.; et al. Association between SARS-CoV-2 RNAemia, skewed T cell responses, inflammation, and severity in hospitalized COVID-19 people living with HIV. iScience 2024, 27, 108673.
62. Khoury, D.S.; Cromer, D.; Reynaldi, A.; Schlub, T.E.; Wheatley, A.K.; Juno, J.A.; Subbarao, K.; Kent, S.J.; Triccas, J.A.; Davenport, M.P. Neutralizing antibody levels are highly predictive of immune protection from symptomatic SARS-CoV-2 infection. Nat. Med. 2021, 27, 1205–1211.
63. Feng, S.; Phillips, D.J.; White, T.; Sayal, H.; Aley, P.K.; Bibi, S.; Dold, C.; Fuskova, M.; Gilbert, S.C.; Hirsch, I.; et al. Correlates of protection against symptomatic and asymptomatic SARS-CoV-2 infection. Nat. Med. 2021, 27, 2032–2040.

64. Gilbert, P.B.; Montefiori, D.C.; McDermott, A.B.; Fong, Y.; Benkeser, D.; Deng, W.; Zhou, H.; Houchens, C.R.; Martins, K.; Jayashankar, L.; et al. Immune correlates analysis of the mRNA-1273 COVID-19 vaccine efficacy clinical trial. Science 2022, 375, 43–50.
65. Bergwerk, M.; Gonen, T.; Lustig, Y.; Amit, S.; Lipsitch, M.; Cohen, C.; Mandelboim, M.; Levin, E.G.; Rubin, C.; Indenbaum, V.; et al. Covid-19 Breakthrough Infections in Vaccinated Health Care Workers. N. Engl. J. Med. 2021, 385, 1474–1484.
66. Earle, K.A.; Ambrosino, D.M.; Fiore-Gartland, A.; Goldblatt, D.; Gilbert, P.B.; Siber, G.R.; Dull, P.; Plotkin, S.A. Evidence for antibody as a protective correlate for COVID-19 vaccines. Vaccine 2021, 39, 4423–4428.
67. Lipsitch, M.; Krammer, F.; Regev-Yochay, G.; Lustig, Y.; Balicer, R.D. SARS-CoV-2 breakthrough infections in vaccinated individuals: Measurement, causes and impact. Nat. Rev. Immunol. 2022, 22, 57–65.
68. Martin, D.P.; Lytras, S.; Lucaci, A.G.; Maier, W.; Gruning, B.; Shank, S.D.; Weaver, S.; MacLean, O.A.; Orton, R.J.; Lemey, P.; et al. Selection Analysis Identifies Clusters of Unusual Mutational Changes in Omicron Lineage BA.1 That Likely Impact Spike Function. Mol. Biol. Evol. 2022, 39, msac061.
69. Hoffmann, M.; Kruger, N.; Schulz, S.; Cossmann, A.; Rocha, C.; Kempf, A.; Nehlmeier, I.; Graichen, L.; Moldenhauer, A.S.; Winkler, M.S.; et al. The Omicron variant is highly resistant against antibody-mediated neutralization: Implications for control of the COVID-19 pandemic. Cell 2022, 185, 447–456 e411.
70. Kumar, S.; Thambiraja, T.S.; Karuppanan, K.; Subramaniam, G. Omicron and Delta variant of SARS-CoV-2: A comparative computational study of spike protein. J. Med. Virol. 2022, 94, 1641–1649.
71. Chatterjee, S.; Bhattacharya, M.; Nag, S.; Dhama, K.; Chakraborty, C. A Detailed Overview of SARS-CoV-2 Omicron: Its SubVariants, Mutations and Pathophysiology, Clinical Characteristics, Immunological Landscape, Immune Escape, and Therapies. Viruses 2023, 15, 167.
72. Menni, C.; Valdes, A.M.; Polidori, L.; Antonelli, M.; Penamakuri, S.; Nogal, A.; Louca, P.; May, A.; Figueiredo, J.C.; Hu, C.; et al. Symptom prevalence, duration, and risk of hospital admission in individuals infected with SARS-CoV-2 during periods of omicron and delta variant dominance: A prospective observational study from the ZOE COVID Study. Lancet 2022, 399, 1618–1624.
73. Keeton, R.; Tincho, M.B.; Ngomti, A.; Baguma, R.; Benede, N.; Suzuki, A.; Khan, K.; Cele, S.; Bernstein, M.; Karim, F.; et al. T cell responses to SARS-CoV-2 spike cross-recognize Omicron. Nature 2022, 603, 488–492.
74. Grifoni, A.; Weiskopf, D.; Ramirez, S.I.; Mateus, J.; Dan, J.M.; Moderbacher, C.R.; Rawlings, S.A.; Sutherland, A.; Premkumar, L.; Jadi, R.S.; et al. Targets of T Cell Responses to SARS-CoV-2 Coronavirus in Humans with COVID-19 Disease and Unexposed Individuals. Cell 2020, 181, 1489–1501.e1415.
75. Braun, J.; Loyal, L.; Frentsch, M.; Wendisch, D.; Georg, P.; Kurth, F.; Hippenstiel, S.; Dingeldey, M.; Kruse, B.; Fauchere, F.; et al. SARS-CoV-2-reactive T cells in healthy donors and patients with COVID-19. Nature 2020, 587, 270–274.
76. Yang, Y.; Miller, H.; Byazrova, M.G.; Cndotti, F.; Benlagha, K.; Camara, N.O.S.; Shi, J.; Forsman, H.; Lee, P.; Yang, L.; et al. The characterization of CD8(+) T-cell responses in COVID-19. Emerg. Microbes Infect. 2024, 13, 2287118.
77. Deeks, S.G.; Tracy, R.; Douek, D.C. Systemic effects of inflammation on health during chronic HIV infection. Immunity 2013, 39, 633–645.
78. Hoffmann, C.; Casado, J.L.; Harter, G.; Vizcarra, P.; Moreno, A.; Cattaneo, D.; Meraviglia, P.; Spinner, C.D.; Schabaz, F.; Grunwald, S.; et al. Immune deficiency is a risk factor for severe COVID-19 in people living with HIV. HIV Med. 2021, 22, 372–378.
79. Marchitto, L.; Chatterjee, D.; Ding, S.; Gendron-Lepage, G.; Tauzin, A.; Boutin, M.; Benlarbi, M.; Medjahed, H.; Sylla, M.; Lanctot, H.; et al. Humoral Responses Elicited by SARS-CoV-2 mRNA Vaccine in People Living with HIV. Viruses 2023, 15, 2004.
80. Bhattacharyya, S.; Crain, C.R.; Goldberg, B.; Gaiha, G.D. Features of functional and dysfunctional CD8+ T cells to guide HIV vaccine development. Curr. Opin. HIV AIDS 2023, 18, 257–263.

81. Sheikh-Mohamed, S.; Isho, B.; Chao, G.Y.C.; Zuo, M.; Cohen, C.; Lustig, Y.; Nahass, G.R.; Salomon-Shulman, R.E.; Blacker, G.; Fazel-Zarandi, M.; et al. Systemic and mucosal IgA responses are variably induced in response to SARS-CoV-2 mRNA vaccination and are associated with protection against subsequent infection. Mucosal Immunol. 2022, 15, 799–808.

A-1.8 The effect of dose-interval on antibody response to mRNA covid-19 vaccines: a prospective cohort study

Preface

(This work has been previously published as a research article)

Almeida ND, Schiller I, Ke D, Sakr E, Plesa M, Vanamala S, Moneger AL, Bazan M, Lucchesi C, Wozniak N, Fritz JH, Piccirillo CA, Pelchat M, Arnold C, **Galipeau Y**, McCluskie PS, Langlois MA, Dasgupta K, Mazer BD. **The effect of dose-interval on antibody response to mRNA COVID-19 vaccines: a prospective cohort study**. Front Immunol. 2024 Feb 16;15:1330549.

https://doi.org/10.3389/fimmu.2024.1330549

Copyright © 2024 Almeida, Schiller, Ke, Sakr, Plesa, Vanamala, Moneger, Bazan, Lucchesi, Wozniak, Fritz, Piccirillo, Pelchat, Arnold, Galipeau, McCluskie, Langlois, Dasgupta and Mazer

This is an open-access article distributed under the terms of the Creative Commons Attribution License (CC BY). The use, distribution or reproduction in other forums is permitted, provided the original author(s) and the copyright owner(s) are credited and that the original publication in this journal is cited, in accordance with accepted academic practice. No use, distribution or reproduction is permitted which does not comply with these terms.

Abstract

Background
Vaccination against COVID-19 is highly effective in preventing severe disease and hospitalization, but primary COVID mRNA vaccination schedules often differed from those recommended by the manufacturers due to supply chain issues. We investigated the impact of delaying the second dose on antibody responses to COVID mRNA-vaccines in a prospective cohort of health-care workers in Quebec.

Methods
We recruited participants from the McGill University Health Centre who provided serum or participant-collected dried blood samples (DBS) at 28-days, 3 months, and 6 months post-second dose and at 28-days after a third dose. IgG antibodies to SARS-CoV2 spike (S), the receptor-binding domain (RBD), nucleocapsid (N) and neutralizing antibodies to the ancestral strain were assessed by enzyme-linked immunosorbent assay (ELISA). We examined associations between long (≤89 days) versus short (<89 days) between-dose intervals and antibody response through multivariable mixed-effects models adjusted for age, sex, prior covid infection status, time since vaccine dose, and assay batch.

Findings
The cohort included 328 participants who received up to three vaccine doses (>80% Pfizer-BioNTech). Weighted averages of the serum (n=744) and DBS (n=216) cohort results from the multivariable models showed that IgG anti-S was 31% higher (95% CI: 12% to 53%) and IgG anti-RBD was 37% higher (95% CI: 14% to 65%) in the long *vs*. short interval participants, across all time points.

Introduction
Our study indicates that extending the covid primary series between-dose interval beyond 89 days (approximately 3 months) provides stronger antibody responses than intervals less than 89 days. Our demonstration of a more robust antibody response with a longer between dose interval is reassuring as logistical and supply challenges are navigated in low-resource settings.

Introduction

The COVID-19 era began in December 2019, with the first reports of infection in Wuhan, China (1). Within one year, randomized controlled trial data demonstrated striking effectiveness of mRNA-based vaccines against the wild type of virus or ancestral strain, reducing rates of infection and hospitalization. Uptake of mRNA sequences coding for COVID-19 spike proteins induces vaccinated individuals to produce spike (S) proteins and form anti-S and anti-Receptor Binding Domain (RBD) antibodies. These antibodies can further be evaluated for their ability to neutralize the virus (2). Infection with SARS-CoV2 can be distinguished from the response to current mRNA vaccines by the presence of antibodies to the viral nucleocapsid (N) protein (3), induced only by infection.

Immunization schedules for vaccines frequently involve two or more injections as the primary series. In the original clinical trials of mRNA vaccines, the primary vaccine doses were spaced by 21 days for BNT162b2 from Pfizer and 28 days for mRNA-1273 from Moderna (4, 5). These relatively short intervals were likely designed to confer protection quickly, given the urgency of the pandemic. Indeed, with 21- and 28 days intervals for the BNT162b2 and mRNA-1273 vaccines respectively, there appeared to be good protection in the initial one to four months, but this was followed by a decline in vaccine efficacy against infection with waning of IgG antibodies and measures of neutralization (6). Studies of other vaccines, albeit prior to mRNA vaccine development, such as those for hepatitis B suggested that longer delays between primary series doses conferred higher antibody responses than shorter intervals (7).

In fact, for many individuals, the real-world between-dose interval was longer than 28 days because of logistical bottlenecks. Reserving vaccine doses to complete the primary series threatened to substantially delay even the partial immunity conferred by the first dose of the two-dose series for the less vulnerable, potentially contributing to persistently high levels of virus propagation. Therefore, a longer between-dose interval was adopted by jurisdictions such as the UK, Germany and Canada (8), justified by immunological studies from traditional vaccines which suggested that an initial vaccine and booster spaced too closely together might result in a suboptimal immune response (9). There were no large epidemiological studies, however, justifying

or confirming this. Nonetheless, some provinces in Canada decided to rapidly vaccinate as many citizens as possible with a first dose of vaccine and to employ between-dose intervals longer than those evaluated in the original clinical trials (10).

The upper limit of this interval varied from jurisdiction to jurisdiction and was adjusted over time. In the Canadian province of Quebec, a 16-week interval between vaccines was mandated in the winter of 2021 (11). As supply improved by the summer of 2021, the interval between first and second vaccination doses was decreased to approximately eight weeks. The variations in the interval between first and second dose have allowed us to examine antibody responses over time and in response to subsequent boosters, through analysis of a cohort of health care workers and researchers in Quebec. We therefore investigated the levels of IgG antibodies to components of the mRNA vaccines administered to determine if delaying vaccines for up to 16 weeks would induce higher IgG responses compared to the shorter, 8-week interval that was ultimately recommended in Quebec when vaccine supplies improved. Due to the nature of our cohort, we were also able to include and evaluate the impact of various co-variables, including age, sex, and infection status.

Methods

Ethics

The Research Ethics Board of the McGill University Health Centre approved all study procedures (Protocol Numbers 2021-6747 and 2021-7534). We provided a protocol description online and invited candidates to contact study personnel through a designated email address for any questions. All participants signed an electronic (e-) informed consent form using the REDCap (Research Electronic Data Capture) secured web application.

Design and population

This study is a prospective cohort analysis. We launched our original cohort (*Living Lab Seroprevalence Study)* in July 2020 to evaluate prevalence of symptomatic and asymptomatic COVID infection in a volunteer group of employees at the Research Institute of the McGill University Health Centre (RI-MUHC: Research Ethics Board of the MUHC; Protocol Number

2021-6747). Leveraging this infrastructure, we continued follow-up of this cohort and initiated the *Health Professional Vaccination* cohort in March 2021 (MUHC REB Protocol Numbers 2021-7534), which recruited physicians, nurses, and other clinical and research staff of the institution, with the goal of assessing immune responses to vaccination and the impact of differing between-dose intervals.

Eligibility criteria and recruitment

Participants could enter the study prior to their first vaccine, as was the case for the original Living Lab Seroprevalence study cohort members; following their first vaccine; or no more than 7 days following their second vaccine. Those more than 7 days past their second vaccine were excluded. We promoted the study through posters, social media and word of mouth within the MUHC community.

Questionnaires

We provided interested candidates with access to online REDCap questionnaires covering general health, exposure to COVID 19, symptoms if exposed or infected, and vaccination history, including dates and type of COVID vaccine. At each subsequent blood sampling timepoint, we forwarded participants a link to a follow-up questionnaire to collect any new information on COVID infection and vaccination.

Blood sample collection timepoints

Blood sample collection started in December 2020 and continues at defined intervals. In the present analysis, we evaluated antibody responses at the following time points: pre-2nd vaccine dose; approximately 28 days, 3 months, and 6 months post-2nd vaccine dose; and approximately 28 days post-3rd vaccine dose (Figure 1). We analyzed data from all participants who provided at least one blood sample at any of these time points.

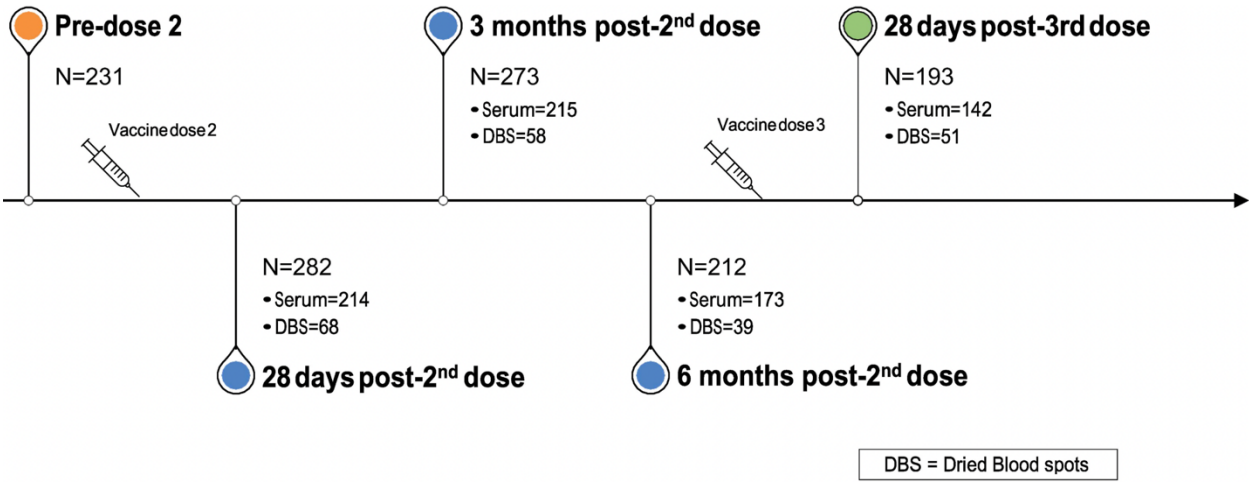


Figure 1 Blood (serum or DBS) samples procurement timepoints and participants' flowchart.

Sample procurement and processing

Participants had the option to provide their samples via either venipuncture or self-collection with cards for dried blood spots (DBS), which could be performed at home and mailed to the laboratory. For those opting for venipuncture, we collected 10 ml of venous blood in clot activator red-capped blood collection tubes (BD vacutainer, Cat. #367815). We centrifuged blood samples twice at 1200 rpm for 12 minutes, collected serum from these samples and stored them in aliquots at -80°C, until processing. We provided those opting for DBS with home kits that contained ethanol swabs, lancets (Microtainer Contact-Activated Lancet, Ref. 366594, BD) and filter paper (Whatman 903 Protein Saver Cards; GE Health Care, Boston MA). We included detailed instructions asking participants to fill 5 circles on the card and mail (stamped and addressed envelope) or deliver the sample to our study center. We stored cards in desiccation boxes at room temperature until processing, as we have previously reported (12).

Antibody measurement

We assessed IgG spike protein antibodies (S) as well as IgG antibodies specific for the receptor binding domain (RBD) and IgG nucleocapsid antibodies (N) as well as neutralizing antibodies, based upon and optimized from assays described by Colwill and colleagues (12). Automated chemiluminescent enzyme-linked immunosorbent assays (ELISA) were performed at the University of Ottawa, Faculty of Medicine, using Hamilton MicroLab Star Robotic Liquid Handlers and a 405 TS/LS LHC2 plate washer (Biotek Instruments). Incubations were performed at room temperature with shaking at 500–700 rpm. Antigens (S, RBD, aa 319–541, and N) diluted

in PBS were pipetted into 384-well high-binding polystyrene Nunc plates (Thermo-Fisher Scientific, #460372;50 ng/well). We then centrifuged the plates at 216 × g for 1 minute, incubated overnight at 4°C with rocking and the wells were blocked with 80 µL of 3% w/v skim milk powder dissolved in PBST for 1 hour, followed by washing. 10 µL of samples and controls (diluted to 1% w/v skim milk powder in PBS-T) were added to each well and the plates were washed after two hours of incubation. 10 µL of diluted secondary antibodies were then added to each well. After incubation for 1 hour, we washed the wells and added 10 µL of ELISA Pico Chemiluminescent Substrate (diluted 1:2 in MilliQ H20) to each well. After a 5-minute incubation with shaking, we read the plates on a Neo2 plate reader (BioTek Instruments) at 20 ms/well with a read height of 1.0 mm, which generated luminescence values. We converted these values to WHO Binding Antibody Units (BAU), as recently reported (12). We conducted separate analyses for participants with serum and DBS blood samples as these methodologies differ, as did the units of measure (i.e., per ml for blood samples through venipuncture and per mm^2 for DBS) (12). In addition, we employed a surrogate neutralization (sn)ELISA to measure inhibition of ACE2-spike or RBD interactions with subjects' antibodies, as described in our recent publication (12). Results of neutralization assays are reported in International Units (IU).

Between-dose intervals

To define long *vs*. short time intervals between the first and second vaccine doses, we examined the distribution of between-dose time intervals across the cohort. The distribution was bimodal with two clear peaks corresponding to Quebec's change in vaccine policy from a 16-week interval to an 8-week interval (Supplementary Figure 1). We stratified the cohort at the mean of this distribution, labelling below the mean as 'short interval' and above the mean as 'long interval,' thus creating two groups that mirrored the vaccine experience of Quebec's population.

Potential confounding variables and covariates

The potential confounding variables that we selected *a priori* included age, sex, time since 2^{nd} vaccine dose (corresponding to blood sample procurement; Figure 1), and infection status at baseline and at subsequent visits. We defined infection status at baseline as self-reported infection and/or IgG antibody to the nucleocapsid protein at any time prior to the second dose. At each subsequent blood draw, we defined infection status by the presence of IgG anti-N at that visit or

any previous visit. A further variable, sample batch, was identified in *post-hoc* analysis as a potential confounder due to considerable between-batch heterogeneity for antibody measures (Supplementary Figure 2). This variable represents the batching of serum samples for eventual analysis at the laboratory.

Statistical analyses

Descriptive statistics

We computed descriptive statistics for the long (>89 days) and short (≤89 days) interval groups (mean and standard deviation and/or median and interquartile range for continuous variables and percentages (%) for categorical variables) for age, sex, baseline infection status (defined as infection at any point before the 2nd vaccine dose), and infection status at each procurement time, separately for serum and DBS cohorts. We calculated these values with available data for each of the following timepoints: 28 days post-2nd dose; 3- and 6 months post-2nd dose; and 28 days post-3rd dose. Most participants contributed to more than one timepoint.

At the same time points, also stratified by long and short interval, we computed both means with 95% confidence intervals (CI) and medians with interquartile range (IQR) for IgG antibodies to S and RBD, and for neutralizing antibodies. We plotted mean and median values (Sina plots) to visualize trends in antibody levels over time.

Multivariable model

We constructed multivariable mixed-effects models to examine associations between short *vs.* long interval and antibody responses over time, adjusted for age, sex, time since second vaccine dose, presence of infection, and inter-batch variability (lme4 package within the R statistical software [version 4.0.3) (13, 14)]. The models included repeated measurements (i.e., antibody measures over time clustered by participant) and a random intercept to allow for baseline antibody measures to vary between participants. We log-transformed antibody values to correct for skewed distributions. This model considered blood sample as the unit of analysis and included blood samples from all four timepoints. In all models, infection status was treated as a time-dependent covariate and referred to current infection or infection at a prior time point. Separate models were

run for the serum and DBS cohorts, but we calculated the combined effect of the between-dose interval by taking a weighted average of the serum and DBS point estimates. Weights were inversely proportional to the variance of the point estimates.

Results

Participants' characteristics

Between January and March 2021, we recruited 328 participants, who provided either serum or DBS samples at one or more timepoints (Figure 1): 28 days post-2nd vaccine dose (n=282); 3 months post-2nd dose (n=273); 6 months post-2nd visit (n=212); and 28 days post-3rd dose (n=193). Over 73% of participants provided serum samples at each of the four time points. 226 unique participants provided a total of 743 serum samples and 75 unique participants provided 216 DBS samples across the four time points. Mean age (SD) across the four time points ranged from 43·5 (13·2) to 46·0 (13·2) years and approximately three quarters (72·3% to 75·5%) were female (Tables 1A-D).

Vaccination type and between-dose intervals

Over 80% of subjects received the Pfizer-BioNTech vaccine, with the remainder receiving either Moderna or AstraZeneca. The mean interval between the first and second vaccine doses was 89 days (SD: 21·2; range: 30 to 128 days) or 12·7 weeks. The distribution of the between-dose interval was bimodal, with peaks at 60 days (8·6 weeks) and 100 days (14·3 weeks). We opted to define short interval as at or below the 89 days average and long interval as above this value, such that the means of these intervals corresponded to the bimodal peaks (Tables 1A-D).

Table 1A Descriptive characteristics of participants who contributed blood at 28 days post-2nd dose, stratified by serum and DBS and long and short between-dose interval.

Baseline characteristics	Serum (n=214)		DBS (n=68)		All (n=282)
	Short interval (≤89 days); n=71	Long interval (>89 days); n=143	Short interval (≤89 days); n=30	Long interval (>89 days); n=38	
Age, mean (SD), yrs	38.8 (13.5)	45.3 (12.9)	38.5 (10.2)	49.3 (12.2)	43.5 (13.2)
Female, %	69.0%	74.8%	80.0%	78.9%	74.5%
Infection status at baseline*, %	7.0%	10.5%	23.3%	23.7%	12.8%
Infection status at time of visit, %	8.5%	11.2%	23.3%	26.3%	13.8%
Pfizer at 1st dose, %	87.3%	97.9%	80.0%	97.4%	93.3%
Pfizer at 2nd dose, %	90.1%	98.6%	76.7%	97.4%	94.0%
Interval between 1st and 2nd vaccine dose, mean (SD), days	63.5 (13.2)	102.4 (6.2)	58.4 (13.5)	103.3 (8.7)	88.0 (21.8)
Interval between 2nd vaccine dose and 28-day post-2nd dose blood draw, mean (SD), days	28.8 (4.4)	30.4 (3.6)	31.2 (8.0)	31.0 (6.6)	30.2 (4.9)

*Infection at any point before 2nd dose.

Table 1b Descriptive characteristics of participants who contributed blood at 3 months post-2nd dose, stratified by serum and DBS and long and short between-dose interval.

Baseline characteristics	Serum (n=214)		DBS (n=58)		All (n=272)
	Short interval (≤89 days); n=66	Long interval (>89 days); n=148	Short interval (≤89 days); n=26	Long interval (>89 days); n=32	
Age, mean (SD), yrs	38.7 (13.4)	45.7 (13.1)	38.4 (9.3)	52.2 (12.6)	44.1 (13.5)
Female, %	68.2%	75.0%	73.1%	75.0%	7329%
Infection status at baseline*, %	6.1%	11.5%	26.9%	25.0%	13.2%
Infection status at time of visit, %	7.6%	12.2%	30.8%	25.0%	14.3%
Pfizer at 1st dose, %	86.4%	97.3%	84.6%	96.9%	93.4%
Pfizer at 2nd dose, %	87.9%	98.6%	80.8%	87.5%	93.0%
Interval between 1st and 2nd vaccine dose, mean (SD), days	62.4 (13.7)	102.6 (7.1)	61.0 (14.1)	103.0 (7.2)	88.9 (21.6)
Interval between 2nd vaccine dose and 3-month post-2nd dose blood draw, mean (SD), days	92.5 (4.6)	90.5 (5.7)	96.0 (11.4)	94.2 (7.1)	91.9 (6.6)

*Infection at any point before 2nd dose.

Table 1C Descriptive characteristics of participants who contributed blood at 6 months post-2nd dose, stratified by serum and DBS and long and short between- dose interval.

Baseline characteristics	Serum (n=173)		DBS (n=39)		All (n=212)
	Short interval (≤89 days); n=33	Long interval (>89 days); n=140	Short interval (≤89 days); n=9	Long interval (>89 days); n=30	
Age, mean (SD), yrs	44.2 (14.0)	45.6 (13.3)	41.2 (10.4)	50.7 (11.6)	45.9 (13.2)
Female, %	66.7%	77.1%	77.8%	76.7%	75.5%
Infection status at baseline*, %	15.2%	12.9%	0.0%	26.7%	14.6%
Infection status at time of visit, %	24.2%	15.7%	22.2%	26.7%	18.9%
Pfizer at 1st dose, %	81.8%	97.9%	88.9%	100.0%	95.3%
Pfizer at 2nd dose, %	87.9%	98.6%	88.9%	100.0%	96.7%
Interval between 1st and 2nd vaccine dose, mean (SD), days	60.5 (16.5)	102.4 (7.1)	59.8 (11.0)	105.1 (8.2)	94.4 (19.4)
Interval between 2nd vaccine dose and 6-month post-2nd dose blood draw, mean (SD), days	187.6 (32.5)	181.8 (4.9)	182.4 (2.7)	185.2 (11.6)	183.3 (14.1)

*Infection at any point before 2nd dose.

Table 1D Descriptive characteristics of participants who contributed blood at 28 days post-3rd dose, stratified by serum and DBS and long and short between-dose interval.

Baseline characteristics	Serum (n=142)		DBS (n=51)		All (n=193)
	Short interval (≤89 days); n=48	Long interval (>89 days); n=94	Short interval (≤89 days); n=22	Long interval (>89 days); n=29	
Age, mean (SD), yrs	40.8 (14.6)	46.9 (12.3)	38.9 (10.7)	52.7 (12.8)	45.4 (13.5)
Female, %	64.6%	73.4%	72.7%	82.8%	72.5%
Infection status at baseline*, %	6.2%	12.8%	13.6%	27.6%	13.5%
Infection status at time of visit, %	31.2%	27.7%	45.5%	37.9%	32.1%
Pfizer at 1st dose, %	81.2%	96.8%	90.9%	96.6%	92.9%
Pfizer at 2nd dose, %	85.4%	97.9%	90.9%	96.6%	93.8%
Interval between 1st and 2nd vaccine dose, mean (SD), days	63.2 (12.5)	102.9 (7.2)	64.0 (6.8)	102.8 (8.1)	88.6 (21.0)
Interval between 3rd vaccine dose and 28-days post-3rd dose blood draw, mean (SD), days	29.8 (7.1)	–	–	–	–

*Infection at any point before 2nd dose.

COVID infection status at baseline and subsequent time points

Prior to their first vaccine dose, 27 participants (9·8%) were previously infected by SARS-CoV2 based on self-report and/or positive anti-N anti-body levels. The infection rate increased at each subsequent procurement time point, rising to 13·8% at 28 days after the second dose, 14·7% at 3

months post-2nd dose, 18·9% at 6 months post-2nd, and 31·9% 28 days post-3rd dose (Tables 1A-D). Thus, over the time course of the analysis, which spanned a period from January 2021 to May 2022, cumulative SARS-CoV2 infection rates rose from under 10% to over 30%. During the period of this analysis, infection status as measured by anti-N antibodies rose slowly in both groups (Figure 2C) and there was no statistically significant difference between the long and short vaccine dose interval groups (Table 2).

Table 2 Median antibody levels at 28 days post-2nd dose, 3 months post-2nd dose, 6 months post-2nd dose and 28-days post-3rd dose, Serum and DBS cohorts.

Median antibody levels (IQR)								
	28-day post 2nd dose visit		3 months post 2nd dose		6 months post 2nd dose		28-day post 3rd dose visit	
	Short interval (≤89 days)	Long interval (>89 days)	Short interval (≤89 days)	Long interval (>89 days)	Short interval (≤89 days)	Long interval (>89 days)	Short interval (≤89 days)	Long interval (>89 days)
SERUM	n=71	n=143	n=67	n=148	n=33	n=140	n=48	n=94
IgG RBD, BAU/ml	3458.2 (2582.4)	4733.4 (5164.5)	1607.6 (1638.8)	1419.8 (1545.4)	681.6 (1076.2)	1009.7 (805.3)	8494.7 (6650.4)	7208.5 (5768.0)
IgG Spike, BAU/ml	2470.9 (1933.2)	4116.2 (6060.5)	2020.2 (1599.4)	1432.2 (1265.8)	884.3 (1188.9)	1189.9 (746.6)	8870.2 (9882.5)	7746.6 (7985.1)
IgG N, BAU/ml	3.0 (6.9)	2.1 (6.0)	4.1 (7.0)	1.8 (4.6)	5.8 (9.1)	3.1 (7.2)	7.2 (21.7)	4.8 (13.2)
Neutralizing Ab, IU/ml	1713.7 (1418.5)	1718.7 (2118.5)	207.4 (541.5)	320.0 (651.7)	37.6 (167.2)	55.1 (106.3)	3694.0 (830.8)	3819.9 (996.9)
DBS	n=30	n=38	n=26	n=32	n=9	n=30	n=22	n=29
IgG RBD, BAU/ml	188.5 (48.6)	285.9 (139.1)	94.8 (75.2)	136.4 (70.1)	52.7 (29.2)	71.4 (45.0)	531.2 (506.4)	505.0 (655.7)
IgG Spike, BAU/ml	87.1 (41.1)	132.1 (50.9)	87.5 (64.4)	96.9 (25.6)	59.8 (20.1)	76.0 (54.0)	637.7 (1357.7)	685.3 (1619.7)
IgG N, BAU/ml	1.3 (1.2)	2.2 (1.0)	1.7 (0.7)	1.5 (1.1)	2.0 (0.9)	2.0 (0.9)	2.2 (2.0)	2.3 (3.4)

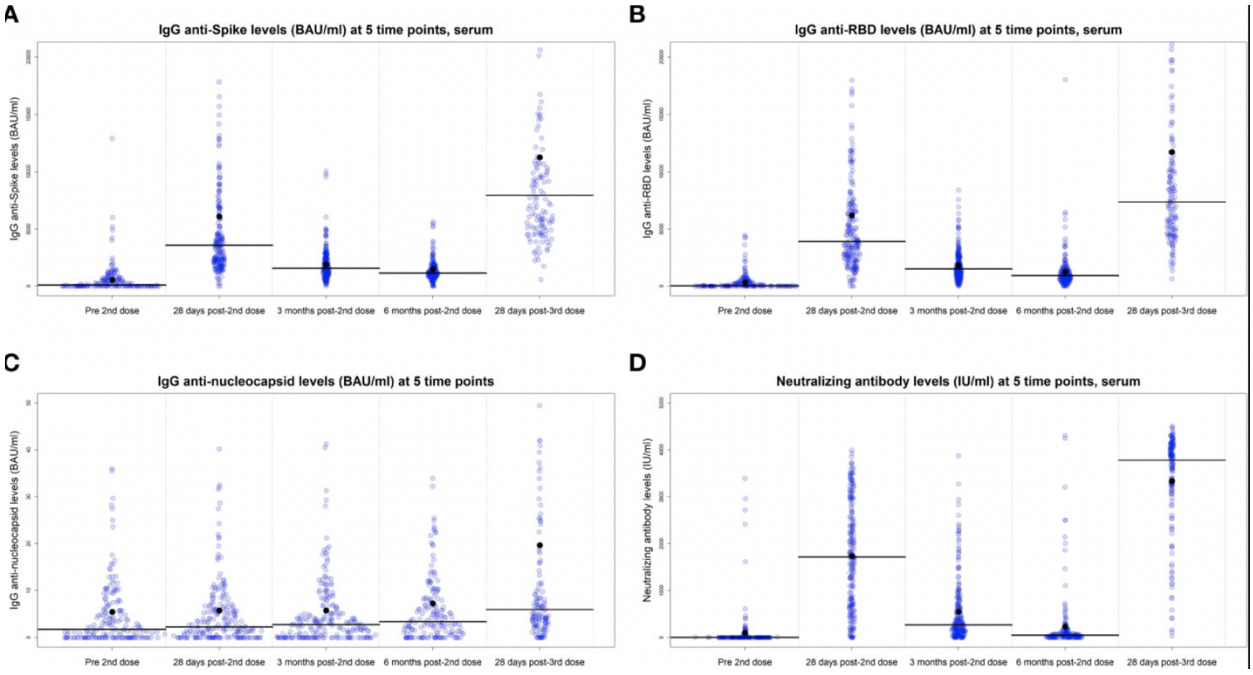


Figure 2 IgG antibodies levels of anti-Spike **(A)**, anti-RBD **(B)**, anti-N **(C)**, and neutralizing antibodies at 28 days post-2nd dose, 3- and 6 months post-2nd dose and 28 days post-3rd vaccine dose, serum cohort. Lines represent the median values and dots indicate the mean. Univariate analysis, the values are BAU/ml.

Antibody response over time for the cohort

Detection of IgG antibodies against the S and RBD proteins were negligible for the limited number of participants who provided a serum sample prior to any vaccination (n=50, data not shown). The majority of the cohort, who provided a sample within ±7 days of their second vaccine dose, exhibited relatively low levels of IgG anti-S and anti-RBD prior to the second dose (n=231). As expected, antibody levels increased at 28 days post-2nd dose and decreased significantly over the following 6 months (Figures 2A, B). For example, median IgG anti-RBD decreased from 3898 BAU/ml at 28 days post-2nd dose to 1565 BAU/ml and 929 BAU/ml at 3 months and 6 months post-2nd dose, respectively, and then increased to 7353 BAU/ml at 28 days post-3rd dose (Supplementary Table 1). Similar patterns were seen for IgG anti-Spike and neutralizing antibodies, for both serum (Figures 2B, D) and DBS cohorts (Supplementary Figures 3A, B). Anti-N antibodies (Figures 2C; Supplementary Figure 3C) slowly increased over time, with highest levels in the blood procurement after the third dose, as infections increased.

Delay of second dose influences antibody response

Serum cohort

There were 744 serum samples across the four time points (n= 214 at 28 days post-2nd vaccine dose; n=214 at three months post 2nd dose; n=173 at six months post-2nd dose; n=142 at 28 days post-3rd dose). Participants with the long interval between primary vaccine doses were slightly older compared to shorter interval participants (mean age 45.5 to 46.9 years *vs*. 38.6 to 44.4 years) and included a greater proportion of females (73.1% to 77.3% *vs*. 63.8% to 69.0% female) (Tables 1A-D).

Multivariable models indicated that participants with a long interval had IgG anti-S levels that were on average 24% higher (95% confidence interval (CI): 4% to 48%) [(1-antilog base 2(0.310))*100%] than those with the shorter between-dose intervals. They also had IgG anti-RBD levels that were 28% (95% CI: 3 to 58%) higher than those with a short interval. Although not statistically significant, serum neutralizing antibodies levels for participants with a long interval had a 35% higher point estimate (95% CI: -3 to 87%; Table 3).

Table 3 Multivariable regression analyses demonstrating the association of between-dose interval with antibody levels for participants with serum and DBS samples, separately.

	Serum (n=743)*			DBS (n=216)*		Combined effect†	
	IgG RBD	**IgG Spike**	**Neutralizing Ab**	**IgG RBD**	**IgG Spike**	**IgG RBD**	**IgG Spike**
	% change	% change	% change	% change	% change	% change	% change
	(95% CI)	(95% CI)	(95% CI)	(95% CI)	(95% CI)	(95% CI)	(95% CI)
IntervalLong	27.7 (3.2, 58.0)	24.0 (4.1, 47.6)	34.9 (-2.7, 87.0)	66.2 (16.8, 136.5)	64.6 (16.4, 132.6)	36.8 (13.7, 64.5)	31.1 (12.0, 53.5)
Short	Reference	Reference	Reference	Reference	Reference	Reference	Reference

*Separate regression models evaluating the impact of dose interval (long vs. short) on log antibody response were run for each of the three antibodies, expressed as BAU/ml for serum and BAU/mm2 for DBS. Models were adjusted for age as a continuous variable, sex, prior infection status, batch of analysis, and timepoint. Estimates (and 95% confidence intervals shown in parentheses) represent the percent change in backtransformed antibody levels [(2β -1)*100] comparing long vs. short interval groups.
† We calculated the combined effect of the between-dose interval by taking a weighted average of the serum and DBS point estimates. Weights were inversely proportional to the variance of the point estimates.

DBS cohort

There were 216 DBS samples (n= 68 at 28 days post-2nd vaccine dose; n= 58 at three months post 2nd dose; n=39 at six months post-2nd dose; n=51 at 28 days post-3rd dose). Participants with a long interval between the primary vaccine doses who provided DBS samples were slightly older than short interval DBS sample participants but were generally similar in the proportion of females (75.0% to 82.8% *vs*. 72.7% to 78.9%; Tables 1A-D).

Similar to the serum cohort, multivariable analyses demonstrated higher antibody levels in the long *vs*. short interval participants for both IgG anti-S (65% higher, 95% CI: 16% to 133%) and IgG anti-RBD levels (66% higher, 95% CI: 17% to 137%; Table 3).

Combined effect

The weighted average of the multivariable estimates from the combined DBS and serum cohorts showed that IgG anti-S was 31% higher (95% CI: 12% to 53%) and IgG anti-RBD was 37% higher (95% CI: 14% to 65%) in the long *vs*. short interval participants.

Association between other covariates and antibody response

Sex, infection status and age: Our fully adjusted models of participants who contributed serum samples indicate that mean IgG anti-Spike responses were 25% higher (95% CI: 6 to 48%); IgG anti-RBD were 37% higher (95% CI: 11 to 68%); and neutralizing antibody levels were 52% higher (95% CI: 11 to 108%) in females compared to males (Supplementary Table 2). In the smaller subset within the DBS cohort, no significant differences in antibody responses between males and females were detected.

As expected, having prior SARS-CoV2 infection resulted in higher antibody responses for IgG anti-S, IgG anti-RBD, and neutralizing antibodies, for both the serum and DBS cohorts. For those with prior SARS-CoV2 infection, serum IgG anti-S levels were 53% higher (95% CI: 29 to 82%), IgG anti-RBD were 66% higher (95% CI: 34 to 106%), and neutralizing antibodies were 87% higher; (95% CI: 35 to 159%), than those without prior infection.

IgG anti-S, IgG anti-RBD, and neutralizing antibody levels also were age dependent; the levels decreased with increasing age, for both the serum and DBS cohorts (Supplementary Table 2). Every 10-year increase in age was associated with a 16% (95% CI: 12 to 14%) decrease in serum IgG anti-RBD levels [(1-antilog base 2(-0.025*10))*100%], and a 10% (95% CI: 5 to 15%) decrease in serum IgG anti-S levels.

Inter-batch variability: The final adjusted model indicates that differences in antibody measures between batches was not fully explained by the other variables in the model. This heterogeneity occurred in measurement of serum but not DBS samples.

Discussion

Our large prospective cohort study demonstrates that subjects with 89 days or more between the two primary series doses of the SARS-CoV2 mRNA vaccine had higher levels of anti-S and anti-RBD IgG binding antibodies than those with less than 89 days between doses, after accounting for factors such as age, sex, and infection status. This difference was seen whether the subject provided a conventional serum sample, or a DBS sample. It was evident across time points that we evaluated post 2nd dose, including the response following the third booster dose. The long-interval group received their 2nd dose an average of approximately 100 days following the first dose, compared to 60 days between doses for the short-interval group.

Smaller studies evaluating vaccine delay have been carried out in the UK, Germany and in other Canadian provinces such as British Columbia and Ontario (8, 15–19). Delays in vaccine administration have ranged from over 28 days to up to 112 days. Studies indicate that intervals greater than 21-28 days lead to higher peak IgG anti-S and anti-RBD binding antibodies, in addition to other observations including improved neutralizing capacity and antibody dependent cellular cytotoxicity (20). However, in addition to being small and unadjusted for potential confounding factors, most studies only investigated the effects of vaccine administration interval on the primary series of vaccination; our study analyzed the impact up to and including 28-days following the third, booster dose.

Recently, data from a smaller cohort of just over 100 subjects (45 in the long interval group) suggested that while an interval of over 100 days elicits better humoral responses than 21 days, the effect of the longer interval was lost when evaluating the third booster dose of vaccine (21). This was not the case in our samples. Differences in sample size, as well as analysis parameters to address covariates may account for the difference in outcomes following the third vaccine dose compared to our cohort.

Due to limitations on travel and access for some members of the cohort, we gave subjects the opportunity to participate remotely by providing Whatman filter cards upon which they could prepare DBS. Canada has been a leader in advocating use of DBS for tracking COVID immunity. Protocols for collection, processing and optimal platforms for measurement were initiated early in the pandemic (22, 23) and several large surveys including those by Statistics Canada (24) and others (25, 26) were carried out with this flexible and user-friendly technique. DBS has significant advantages due to its low cost and wide range of potential analytes (27, 28). Our study provided a head-to-head comparison of these different procurement methods. Despite some modifications required for sample elution and measurement adjustment (12), both methods provided reliable measures and comparable results. This suggests that DBS may be an ideal method for monitoring of serologic responses in more remote geographic areas and other situations where venipuncture is not practical.

One other practical consideration underscored by this real-world study was the considerable between-batch heterogeneity in antibody measures. Sera and DBS were measured separately and temporally when the sampling was performed (Figure 1). We hypothesized that this heterogeneity was partly due to the design of our natural experiment, with participants who provided samples earlier in the study, and thus falling in earlier batches, were subject to Quebec's initial policy of a longer dose interval. Similarly, participants in later batches correlated with those who received third doses, and therefore higher antibody levels. Batch-to-batch and lot-to-lot variability is well recognized in laboratory medicine and calibration steps are conducted to be ensure that measurements are comparable. Our models accounted for this variability, which is an important consideration when dealing with large scale quantitative studies. For example, a recent meta-analysis of antibody levels following vaccination was unable to determine a correlation of protection due to the large amount of heterogeneity between studies (6). Other factors may contribute to batch-to-batch variability, such as sample dilution in the era post vaccine, when dilution of 1000-10,000 fold may be required; this can amplify small variations in measurement. Thus, consideration of batch effects in our model was important for ensuring harmonization of all results despite measurement taking place over almost a 12-month period. This finding also

highlights the need for studies to incorporate methods to decrease between-batch heterogeneity in the design phase of their study.

The immunologic basis for higher peak antibody levels with extended periods between doses is likely multifactorial. Following the initial dose of vaccine, antibody production generally peaks at 28 days. Reimmunizing at 21-28 days, as in the initial clinical trials (4, 5) risks having some of the antigen from the second vaccination dose neutralized by this pre-existing antibody, whereas re-vaccination when antibodies are waning diminishes this possibility (29). Secondly, the success of the second and subsequent doses likely depends on the presence of antigen in germinal centers. The interaction between B-cells and antigen presented by follicular dendritic cells continues long after the peak of antibody production (30). Re-exposure to the same antigen without sufficient time for previous antigen levels to diminish may also lead to suboptimal responses (30, 31). Responses to the third vaccine dose may be improved compared to the second of the primary series of vaccines due to higher baseline antibody levels. However, this may also be influenced by improved B-cell memory responses in those immunized with a longer interval (30) which is under investigation in our laboratory. The impact of longer intervals between vaccines on responses to the evolving variants of SARS-CoV2 also requires study. We have recently demonstrated using sera from our cohort that third and fourth doses of earlier COVID-19 vaccines (ancestral and/or BA4/BA5) can induce neutralizing antibodies to XBB1.5 (32). This may be a function of dose interval as well as multiple exposures to SARS-CoV2 spike proteins via repeat vaccinations.

The population we studied, health care workers and researchers, reflected a relatively healthy population. Our study does not directly provide evidence of the effectiveness of this approach in a pediatric population, in the frail elderly population or in immune compromised individuals; other cohorts have suggested similar results in the elderly (16). In addition to the immunologic outcomes that we followed, vaccine efficacy studies in Canada indicated that COVID outcomes such as hospitalization, severe diseases and mortality were comparable if not better with longer intervals between the primary two doses than similar jurisdictions which utilized standard vaccine protocols (33–35).

The recent CDC guidelines for future COVID-19 vaccination suggest a delay of 4-8 weeks between primary doses for mRNA vaccines depending on the subjects' ages. Longer intervals may decrease risk of myocarditis and pericarditis associated with vaccination (36). Our data not only supports this recommendation, but potentially supports longer intervals between the primary doses as we continue to shield the populations against future waves of COVID-19 infection. In addition, our study has important implications for future vaccination campaigns in low and middle- income countries, where vaccine supply issues are an important public health challenge. To date, only 30% of people in low-income countries have received even a single dose of COVID vaccination (37). Clearly, our data indicate that delays outside of FDA approved protocols can be utilized for catch up vaccination of these important jurisdictions. Indeed, our methodologically strong study strengthens the body of evidence underscoring the value of increasing the interval between vaccine doses, which would allow a larger number of people to receive at least one dose of the vaccine. This strategy, used in Quebec and British Columbia (34), would help to maximize the immediate impact of available vaccines while buying additional time to secure more vaccine doses, and should be applied to future vaccine campaigns in both high and low resource settings.

Limitations of the study

Our study cohort included health care workers and laboratory personnel and thus had a larger percentage of the females. The nature of the prospective-longitudinal study making the withdrawal rate and collection of samples unpredictable. We unfortunately did not have a 21- or 28-day vaccine control group readily available in Montreal, as only frail seniors in LTC were eligible for that. Despite extensive antibody studies we cannot predict any correlate of protection from this cohort.

Conclusion

Our study confirms that mRNA COVID-19 vaccines are highly effective in inducing strong antibody responses in real-world conditions among health care personnel, first responders, and other essential workers. The strategy of a 16 week delay in the primary series was associated with higher antibody responses affecting all subsequent time points including the 3rd vaccine/booster dose.

Data availability statement

The raw data supporting the conclusions of this article will be made available by the authors, without undue reservation.

Ethics statement

The studies involving humans were approved by The Research Ethics Board of the McGill University Health Centre (Protocol Numbers 2021-6747 and 2021-7534). The studies were conducted in accordance with the local legislation and institutional requirements. The participants provided their written informed consent to participate in this study.

Author contributions

NA: Conceptualization, Formal analysis, Investigation, Writing – original draft. IS: Formal analysis, Writing – review & editing, Data curation, Methodology, Validation. DK: Formal analysis, Project administration, Writing – review & editing. ES: Writing – original draft. MPl: Data curation, Investigation, Project administration, Supervision, Writing – review & editing. SV: Data curation, Project administration, Supervision, Writing – review & editing. AM: Investigation, Project administration, Writing – review & editing. MB: Data curation, Investigation, Project administration, Writing – review & editing. CL: Investigation, Writing – review & editing. NW: Data curation, Investigation, Writing – review & editing. JF: Conceptualization, Investigation, Validation, Writing – review & editing. CP: Conceptualization, Validation, Writing – review & editing. MPe: Formal analysis, Software, Writing – review & editing. CA: Formal analysis, Investigation, Methodology, Writing – review & editing. YG: Investigation, Methodology, Writing – review & editing. PM: Investigation, Methodology, Writing – review & editing. ML: Conceptualization, Formal analysis, Investigation, Methodology, Validation, Writing – original draft, Writing – review & editing. KD: Conceptualization, Formal analysis, Methodology, Writing – original draft, Writing – review & editing. BM: Conceptualization, Formal analysis, Funding acquisition, Project administration, Supervision, Writing – original draft, Writing – review & editing.

Funding

The author(s) declare financial support was received for the research, authorship, and/or publication of this article. Funding was provided by the McGill University Health Centre Foundation.

Acknowledgments

We would like to thank all the participants in the Living Lab Seroprevalence study as well as all technical personnel who helped in sample procurement, preparation and analysis.

Conflict of interest

The authors declare that the research was conducted in the absence of any commercial or financial relationships that could be construed as a potential conflict of interest.

The author(s) declared that they were an editorial board member of Frontiers, at the time of submission. This had no impact on the peer review process and the final decision.

Supplementary material

The Supplementary Material for this article can be found online at: https://www.frontiersin.org/articles/10.3389/fimmu.2024.1330549/full#supplementary-material

References

1. Wu F, Zhao S, Yu B, Chen YM, Wang W, Song ZG, et al. A new coronavirus associated with human respiratory disease in China. Nature (2020) 579(7798):265–9. doi: 10.1038/s41586-020-2008-3
2. Grunau B, Prusinkiewicz M, ASamoah-Boaheng M, Golding L, Lavoie PM, Petric M, et al. Correlation of SARS-coV-2 viral neutralizing antibody titers with anti-spike antibodies and ACE-2 inhibition among vaccinated individuals. Microbiol Spectr (2022) 10(5):e0131522. doi: 10.1128/spectrum.01315-22
3. Heinz FX, Stiasny K. Distinguishing features of current COVID-19 vaccines: knowns and unknowns of antigen presentation and modes of action. NPJ Vaccines (2021) 6(1):104. doi: 10.1038/s41541-021-00369-6
4. Baden LR, El Sahly HM, Essink B, Kotloff K, Frey S, Novak R, et al. Efficacy and safety of the mRNA-1273 SARS-coV-2 vaccine. N Engl J Med (2021) 384(5):403–16. doi: 10.1056/NEJMoa2035389
5. Polack FP, Thomas SJ, Kitchin N, Absalon J, Gurtman A, Lockhart S, et al. Safety and efficacy of the BNT162b2 mRNA covid-19 vaccine. N Engl J Med (2020) 383 (27):2603–15. doi: 10.1056/NEJMoa2034577
6. Menegale F, Manica M, Zardini A, Guzzetta G, Marziano V, d'Andrea V, et al. Evaluation of waning of SARS-coV-2 vaccine-induced immunity: A systematic review and meta-analysis. JAMA Netw Open (2023) 6(5):e2310650. doi: 10.1001/ jamanetworkopen.2023.10650
7. Di Lello FA, Martınez AP, Flichman DM. Insights into induction of the immune´ response by the hepatitis B vaccine. World J Gastroenterol (2022) 28(31):4249–62. doi: 10.3748/wjg.v28.i31.4249
8. Payne RP, Longet S, Austin JA, Skelly DT, Dejnirattisai W, Adele S, et al. Immunogenicity of standard and extended dosing intervals of BNT162b2 mRNA vaccine. Cell (2021) 184(23):5699–5714.e11. doi: 10.1016/j.cell.2021.10.011
9. Quach C, Deeks S. COVID-19 vaccination: Why extend the interval between doses? J Assoc Med Microbiol Infect Dis Can (2021) 6(2):73–8. doi: 10.3138/jammi-2021-0323
10. Miller A. A behind the scenes look at why Canada delayed 2nd doses of COVID-19 vaccines. Available at: https://www.cbc.ca/news/health/Canada-covid-19-vaccinedelay-risk-1.5939134.
11. Reuters. Quebec give Covid-19-vaccine doses as many as 90 days apart. Reuters Canada, Toronto, Canada. (2021). Available at: https://www.reuters.com/business/ healthcare-pharmaceuticals/ [updated 2021-01-14].
12. Colwill K, Galipeau Y, Stuible M, Gervais C, Arnold C, Rathod B, et al. A scalable serology solution for profiling humoral immune responses to SARS-CoV-2 infection and vaccination. Clin Transl Immunol (2022) 11(3):e1380. doi: 10.1002/cti2.1380
13. Team RC. R: A language and environment for statistical computing. Vienna, Austria: R Foundation for Statistical Computing (2020).
14. Bates D, Mächler M, Bolker B, Walker S. Fitting linear mixed-effects models using lme4. J Stat Software (2015) 67(1):1–48.
15. Parry H, Bruton R, Stephens C, Bentley C, Brown K, Amirthalingam G, et al. Extended interval BNT162b2 vaccination enhances peak antibody generation. NPJ Vaccines (2022) 7(1):14. doi: 10.1038/s41541-022-00432-w
16. Parry H, Bruton R, Ayodele R, Sylla P, McIlroy G, Logan N, et al. Vaccine subtype and dose interval determine immunogenicity of primary series COVID-19 vaccines in older people. Cell Rep Med (2022) 3(9):100739. doi: 10.1016/j.xcrm.2022.100739
17. Hall VG, Ferreira VH, Wood H, Ierullo M, Majchrzak-Kita B, Manguiat K, et al. Delayed-interval BNT162b2 mRNA COVID-19 vaccination enhances humoral immunity and induces robust T cell responses. Nat Immunol (2022) 23(3):380–5. doi: 10.1038/s41590-021-01126-6
18. Grunau B, ASamoah-Boaheng M, Lavoie PM, Karim ME, Kirkham TL, Demers PA, et al. A higher antibody response is generated with a 6- to 7-week (vs standard) severe acute respiratory syndrome

coronavirus 2 (SARS-coV-2) vaccine dosing interval. Clin Infect Dis (2022) 75(1):e888–91. doi: 10.1093/cid/ciab938
19. Grunau B, Goldfarb DM, ASamoah-Boaheng M, Golding L, Kirkham TL, Demers PA, et al. Immunogenicity of extended mRNA SARS-coV-2 vaccine dosing intervals. JAMA (2022) 327(3):279–81. doi: 10.1001/jama.2021.21921
20. Tauzin A, Gong SY, Beaudoin-Bussières G, Vézina D, Gasser R, Nault L, et al. Strong humoral immune responses against SARS-CoV-2 Spike after BNT162b2 mRNA vaccination with a 16-week interval between doses. Cell Host Microbe (2022) 30(1):97– 109.e5. doi: 10.1016/j.chom.2021.12.004
21. Tauzin A, Gong SY, Chatterjee D, Ding S, Painter MM, Goel RR, et al. A boost with SARS-CoV-2 BNT162b2 mRNA vaccine elicits strong humoral responses independently of the interval between the first two doses. Cell Rep (2022) 41 (4):111554. doi: 10.1016/j.celrep.2022.111554
22. Cholette F, Mesa C, Harris A, Ellis H, Cachero K, Lacap P, et al. Dried blood spot specimens for SARS-CoV-2 antibody testing: A multi-site, multi-assay comparison. PloS One (2021) 16(12):e0261003. doi: 10.1371/journal.pone.0261003
23. Cholette F, Fabia R, Harris A, Ellis H, Cachero K, Schroeder L, et al. Comparative performance data for multiplex SARS-CoV-2 serological assays from a large panel of dried blood spot specimens. Heliyon Sep (2022) 8(9):e10270. doi: 10.1016/ j.heliyon.2022.e10270
24. Statistics Canada. Canadian COVID 19 antibody and health survey. Government of Canada, Ottawa, ON, Canada (2022). Available at: https://www23.statcan.gc.ca/ imdb/p2sv.pl?Function=getSurvey&SDDS=5339. 25. Brown PE, Fu SH, Bansal A, Newcombe L, Colwill K, Mailhot G, et al. Omicron BA.1/1.1 SARS-coV-2 infection among vaccinated canadian adults. N Engl J Med (2022) 386(24):2337–9. doi: 10.1056/NEJMc2202879
26. Tang X, Sharma A, Pasic M, Brown P, Colwill K, Gelband H, et al. Assessment of SARS-coV-2 seropositivity during the first and second viral waves in 2020 and 2021 among canadian adults. JAMA Netw Open (2022) 5(2):e2146798. doi: 10.1001/ jamanetworkopen.2021.46798
27. Firkey MK, Tully LK, Bucci VM, Walsh ME, Maisto SA, Hahn JA, et al. Feasibility of remote self-collection of dried blood spots, hair, and nails among people with HIV with hazardous alcohol use. Alcohol Clin Exp Res (2023) 47:986–95. doi: 10.1111/acer.15063
28. Haberstroh H, Hirsch A, Goldacker S, Zessack N, Warnatz K, Grimbacher B, et al. A toolkit for monitoring immunoglobulin G levels from dried blood spots of patients with primary immunodeficiencies. J Clin Immunol (2023) 43(6):1185–92. doi: 10.1007/s10875-023-01464-0
29. Krammer F, Srivastava K, Alshammary H, Amoako AA, Awawda MH, Beach KF, et al. Antibody Responses in Seropositive Persons after a Single Dose of SARS-CoV-2 mRNA Vaccine. N Engl J Med (2021) 384(14):1372–4. doi: 10.1056/NEJMc2101667
30. Garg AK, Mittal S, Padmanabhan P, Desikan R, Dixit NM. Increased B cell selection stringency in germinal centers can explain improved COVID-19 vaccine efficacies with low dose prime or delayed boost. Front Immunol (2021) 12:776933. doi: 10.3389/fimmu.2021.776933
31. Berkane S, Harizi I, Tayebi A, Silverman MS, Stranges S. Should we delay the second COVID-19 vaccine dose in order to optimize rollout? A mathematical perspective. Int J Public Health (2021) 66:1604312. doi: 10.3389/ijph.2021.1604312
32. Sakr E, Almeida ND, Langlois MA, Dasgupta K, Mazer BD. Booster doses of COVID-19 vaccine enhance neutralization efficiency against XBB.1.5. J Allergy Clin Immunol (2023). doi: 10.1016/j.jaci.2023.11.912
33. Ionescu IG, Skowronski DM, Sauvageau C, Chuang E, Ouakki M, Kim S, et al. BNT162b2 effectiveness against delta and omicron variants of severe acute respiratory syndrome coronavirus 2 in adolescents aged 12-17 years, by dosing interval and duration. J Infect Dis (2023) 227(9):1073–10783. doi: 10.1093/infdis/jiad006
34. Skowronski DM, Febriani Y, Ouakki M, Setayeshgar S, El Adam S, Zou M, et al. Two-dose severe acute respiratory syndrome coronavirus 2 vaccine effectiveness with mixed schedules and extended dosing intervals: test-negative design studies from British Columbia and Quebec, Canada. Clin Infect Dis (2022) 75(11):1980–92. doi: 10.1093/cid/ciac290

35. Chung H, He S, Nasreen S, Sundaram ME, Buchan SA, Wilson SE, et al. Effectiveness of BNT162b2 and mRNA-1273 covid-19 vaccines against symptomatic SARS-CoV-2 infection and severe covid-19 outcomes in Ontario, Canada: test negative design study. BMJ (2021) 374:n1943. doi: 10.1136/bmj.n1943
36. Prevention CfDCa. Interim clinical considerations for use of COVID-19 vaccines in the United States. Available at: https://www.cdc.gov/vaccines/covid-19/clinicalconsiderations/interim-considerations-us.html.
37. Mathieu E, Ritchie H, Ortiz-Ospina E, Roser M, Hassel J, Appel C, et al. A global database of COVID-19 vaccinations. Oxford, England: Our World in Data. (2023). Available at: https://ourworldindata.org/covid-vaccinations.

A-1.9 Household transmission of SARS-CoV-2 from unvaccinated asymptomatic and symptomatic household members with confirmed SARS-CoV-2 infection: an antibody-surveillance study

Preface

(This work has been previously published as a research article)

Bhatt M, Plint AC, Tang K, Malley R, Huy AP, McGahern C, Dawson J, Pelchat M, Dawson L, Varshney T, Arnold C, **Galipeau Y**, Austin M, Thampi N, Alnaji F, Langlois MA, Zemek RL. **Household transmission of SARS-CoV-2 from unvaccinated asymptomatic and symptomatic household members with confirmed SARS-CoV-2 infection: an antibody-surveillance study**. CMAJ Open. 2022 Apr 12;10(2):E357-E366.

https://doi.org/10.9778/cmajo.20220026

© 2022 CMA Impact Inc. or its licensors
This is an Open Access article distributed in accordance with the terms of the Creative Commons Attribution (CC BY-NC-ND 4.0) licence, which permits use, distribution and reproduction in any medium, provided that the original publication is properly cited, the use is noncommercial (i.e., research or educational use), and no modifications or adaptations are made. See: https://creativecommons.org/licenses/by-nc-nd/4.0/

Abstract

Background
Household transmission contributes to SARS-CoV-2 spread, but the role of children in transmission is unclear. We conducted a study that included symptomatic and asymptomatic children and adults exposed to SARS-CoV-2 in their households with the objective of determining how SARS-CoV-2 is transmitted within households.

Methods
In this case-ascertained antibody-surveillance study, we enrolled households in Ottawa, Ontario, in which at least 1 household member had tested positive for SARS-CoV-2 on reverse transcription polymerase chain reaction testing. The enrolment period was September 2020 to March 2021. Potentially eligible participants were identified if they had tested positive for SARS-CoV-2 at an academic emergency department or affiliated testing centre; people who learned about the study through the media could also selfidentify for participation. At least 2 participants were required for a household to be eligible for study participation, and at least 1 enrolled participant per household had to be a child (age < 18 yr). Enzyme-linked immunosorbent assays were used to evaluate SARS-CoV-2-specific IgA, IgM and IgG against the spike-trimer and nucleocapsid protein. The primary outcome was household secondary attack rate, defined as the proportion of household contacts positive for SARS-CoV-2 antibody among the total number of household contacts participating in the study. We performed descriptive statistics at both the individual and household levels. To estimate and compare outcomes between patient subgroups, and to examine predictors of household transmission, we fitted a series of multivariable logistic regression with robust standard errors to account for clustering of individuals within households.

Results
We enrolled 695 participants from 180 households: 180 index participants (74 children, 106 adults) and 515 of their household contacts (266 children, 249 adults). A total of 487 household contacts (94.6%) (246 children, 241 adults) had SARS-CoV-2 antibody testing, of whom 239 had a positive result (secondary attack rate 49.1%, 95% confidence interval [CI] 42.9%–55.3%). Eighty-eight (36.8%, 95% CI 29.3%–43.2%) of the 239 were asymptomatic; asymptomatic rates were similar for children (51/130 [39.2%, 95% CI 30.7%48.5%]) and adults (37/115 [32.2%, 95% CI 24.2%–41.4%]) (odds ratio [OR] 1.3, 95% CI 0.8–2.1). Adults were more likely than children to transmit SARS-CoV-2 (OR 2.2, 95% CI 1.3–3.6). The odds of transmission from asymptomatic (OR 0.6, 95% CI 0.2–1.4) versus symptomatic (OR 0.9, 95% CI 0.6–1.4) index participants to household contacts was uncertain. Predictors of household transmission included household density (number of people per bedroom), relationship to index participant and number of cases in the household.

Interpretation
The rate of SARS-CoV-2 transmission within households was nearly 50% during the study period, and children were an important source of spread. The findings suggest that children are an important driver of the COVID-19 pandemic; this should inform public health policy.

Household transmission is an important contributor to the spread of SARS-CoV-2 infection.[1-5] Household exposure to an infected person is associated with a 10-fold higher risk of infection compared to exposure outside the home.[6] However, the reported rate of SARS-CoV-2 spread within households depends on the surveillance method.[6] Meta-analyses of household transmission studies in which viral swabs were primarily used for detection showed a secondary attack rate of 19%,[1,2] but reliance on viral swabs may underestimate transmission, and experts have advocated for the addition of serologic testing to enhance studies of household transmission.[7-9]

Evaluating SARS-CoV-2-specific antibodies provides additional information about recent and past infection, as antibodies are detected reliably within 1–2 weeks after symptom onset.[10-12] Previous studies using antibody detection suggested that the rate of household transmission may range from 20% to 80%.[13-18] These studies were limited: some tested small proportions of household members, and others excluded children or focused on transmission by adults.[9,13-15,17-21] Few investigated the proportion of household members who developed antibodies after exposure to an infected child.

The role of children in transmission warrants attention, since they are often asymptomatic or have mild symptoms. [16,22-28] Addressing this gap in the literature would allow a more evidence-based approach to public health initiatives, given that COVID-19 pandemic control strategies have often affected the lives of children and youth (e.g., school closures, suspension of recreational activities), as well as negatively affecting their overall well-being.[29,30]

Analysis of household transmission of SARS-CoV-2 is central to the development of health policies that protect vulnerable people while minimizing the impact on children. [29-31] We conducted an antibody surveillance study that included symptomatic and asymptomatic children and adults exposed to SARS-CoV-2 in their households with the objective of determining how SARS-CoV-2 infection is transmitted within households.

Methods

Study design and setting

We conducted a prospective, case-ascertained antibody-surveillance study of households in Ottawa, Ontario (population 1 million[32]) in which at least 1 member had SARS-CoV-2 infection from September 2020 to March 2021, when community cases ranged from 6 to 12 per 100 000 population.[33] The study was reported according to the STROBE guideline for cohort studies.[34]

Participants

Households were eligible if an adult or child tested positive for SARS-CoV-2 by reverse transcription polymerase chain reaction (RT-PCR) from a throat or nasopharyngeal swab. Polymerase chain reaction testing was voluntary and was performed in accordance with public health guidelines at the time (e.g., symptoms, history of travel, contact at high risk).[35] In addition to the SARS-CoV-2-positive person, enrolment of at least 1 additional household member was required; an attempt was made to enroll all household members. At least 1 member of the household had to be a child (age < 18 yr).

We defined household members as people residing in the same dwelling as the index participant. If more than 1 person in a household tested positive within 14 days, the index participant was the person who first developed symptoms or, in the absence of symptoms, the first to test positive. There was no maximum allowable time between index participant infection and study enrolment. Households were excluded if any member had received a COVID-19 vaccine before enrolment or was not comfortable communicating in English or French.

We informed the Ottawa population about the study through media and social media campaigns. Self-identified potentially eligible participants were invited to contact the study team via a dedicated study email address. Potentially eligible participants (those who tested positive for SARS-CoV-2 at any of the 3 academic emergency departments or the affiliated regional COVID-19 testing centre) were also identified by the study team.

Study protocol

In-person enrolment visits were booked within 14 days of patient screening or consent, but a minimum of 14 days was required between a positive RT-PCR test result and the study visit.

Enrolment visits were conducted by a trained study team at the Children's Hospital of Eastern Ontario; all household members attended the same appointment.

Data collection

A questionnaire informed by the World Health Organization household transmission investigation protocol[35] was administered by a trained research assistant to standardize and harmonize data collection in order to optimize accuracy; a questionnaire was completed for the index participant and each household member at the study visit. Data were collected on demographic characteristics, household composition and density (number of people per bedroom[36]), COVID-19 symptoms, distancing protocols in the home during the illness, medical and smoking histories, and all RT-PCR testing completed before enrolment. Blood samples for SARS-CoV-2 antibody testing were drawn from all participants at the study visit. Within 3 hours of phlebotomy, the serum was separated and stored at −80°C until ready for analysis at the Langlois Laboratory, University of Ottawa.

Automated chemiluminescent enzyme-linked immunosorbent assays (ELISAs), adapted and optimized from the assay described by Isho and colleagues,[37] were used to evaluate SARS-CoV-2-specific IgA, IgM and IgG against the spike-trimer and nucleocapsid protein. This serologic testing platform was validated and compared with 10 commercial platforms by the National Microbiology Laboratory of Canada and was found to perform as well as the most accurate commercial tests, with sensitivity and specificity greater than 98% (Appendix 1, Figure S1, available at www.cmajopen.ca/content/10/2/E357/suppl/DC1).[38]

For each sample of a specific plate, the average background luminescence value from up to 8 negative control samples was removed. The resulting values were rescaled based on the luminescence value corresponding to the half-maximal inhibitory concentration value of a 4-parameter log-logistic standard curve also included on the plate. Signal-to-cut-off values were calculated with cut-offs corresponding to a 2% false-discovery rate for each antigen–antibody pair, derived from the scaled luminescence of 580 prepandemic serum samples calculated by means of the same approach.

Samples were considered antibody positive for a particular isotype (IgG, IgA or IgM) when both antispike and anti-nucleocapsid antibodies were detected above the cut-off values (signal-to-cut-off value ≥ 1) for that isotype. Samples were considered positive for SARS-CoV-2 antibody if they were positive for IgG or for both IgA and IgM.

Outcomes

The primary outcome was the household secondary attack rate — the proportion of infected household contacts (positive for SARS-CoV-2 antibody) among the total number of household contacts participating in the study.[39] Household contacts were deemed infected if they met the criteria for SARS-CoV-2 antibody positivity. Secondary outcomes were the proportion of asymptomatic infections among household contacts, by age, and clinical risk factors for household transmission.

We defined asymptomatic infection as positivity for SARS-CoV-2 antibody in the absence of symptoms. We chose risk factors for transmission a priori, based on prior studies and clinical knowledge.[1,2,28] We defined distancing as isolating from the SARS-CoV-2-positive household member(s) or always masking indoors in the presence of the SARS-CoV-2-positive member(s), or both.[35]

Statistical analysis

We described patient and household characteristics using summary statistics. We described variables with patients stratified by participant type (index participants or household contact) or age (child or adult) subgroups, or both.

To estimate and compare the proportion of household contacts who developed SARS-CoV-2 antibodies among patient subgroups based on age of the index/household contact, we fitted logistic regression models specifying index participant's age alone; household contact's age alone; an interaction between index (child v. adult) and household contact's age (child v. adult); and an interaction between the index's age (6 categories) and household contact's age (child v. adult), with estimation of robust (Huber–White) standard errors to account for clustering of individuals within a household unit.[40,41] We derived estimates of proportions, odds ratios (ORs) and 95% confidence intervals (CIs) from these models.

To examine predictors of SARS-CoV-2 antibody development among household contacts, we applied a multivariable logistic regression with estimation of robust standard errors with household as the clustering unit. Predictors specified included age, sex, total number of SARS-CoV-2-positive household members (including the index participant), household density, mask-wearing frequency, whether completely isolated from index participant, presence of underlying comorbidity, whether present smoker or vaper, relationship to index participant, whether the index participant was admitted to hospital and whether the index participant was symptomatic. We expressed associations as adjusted OR and associated 95% CI. We assessed the discriminative ability of the model using the C-statistic. Observations were excluded if there were any missing data.

We performed statistical analyses using R software, version 4.0.5 (R Foundation for Statistical Computing).

Ethics approval

The study received approval from the Children's Hospital of Eastern Ontario Research Ethics Board (20/81X), the Ottawa Health Science Network Research Ethics Board (20200673-01K) and the University of Ottawa Health Sciences and Science Research Ethics Board (20200358). Informed written consent was obtained from all participants or their parent or guardian, and assent was obtained when appropriate.

Results

A total of 180 people (74 children, 106 adults) confirmed to be SARS-CoV-2-positive and 515 (266 children, 249 adults) of their household contacts were enrolled (Figure 1). Index participants and household contacts were enrolled a median of 46 days (interquartile range [IQR] 32–86 d) and 41 days (IQR 28–73 d), respectively, after infection was confirmed in the index participant. A median of 4 (IQR 3–4) members per household were enrolled; in 137 households (76.1%), all members were enrolled. In 156 households (87.2%), all children participated in the study, and in 147 households (82.1%), all adults participated. The median household density was 1.25 (IQR

1.0–1.3) people per bedroom. Of the 454 household contacts (88.1%) who reported being tested for SARS-CoV-2 before study enrolment, 158 (34.8%) had a positive result within 14 days of the index participant's positive test result.

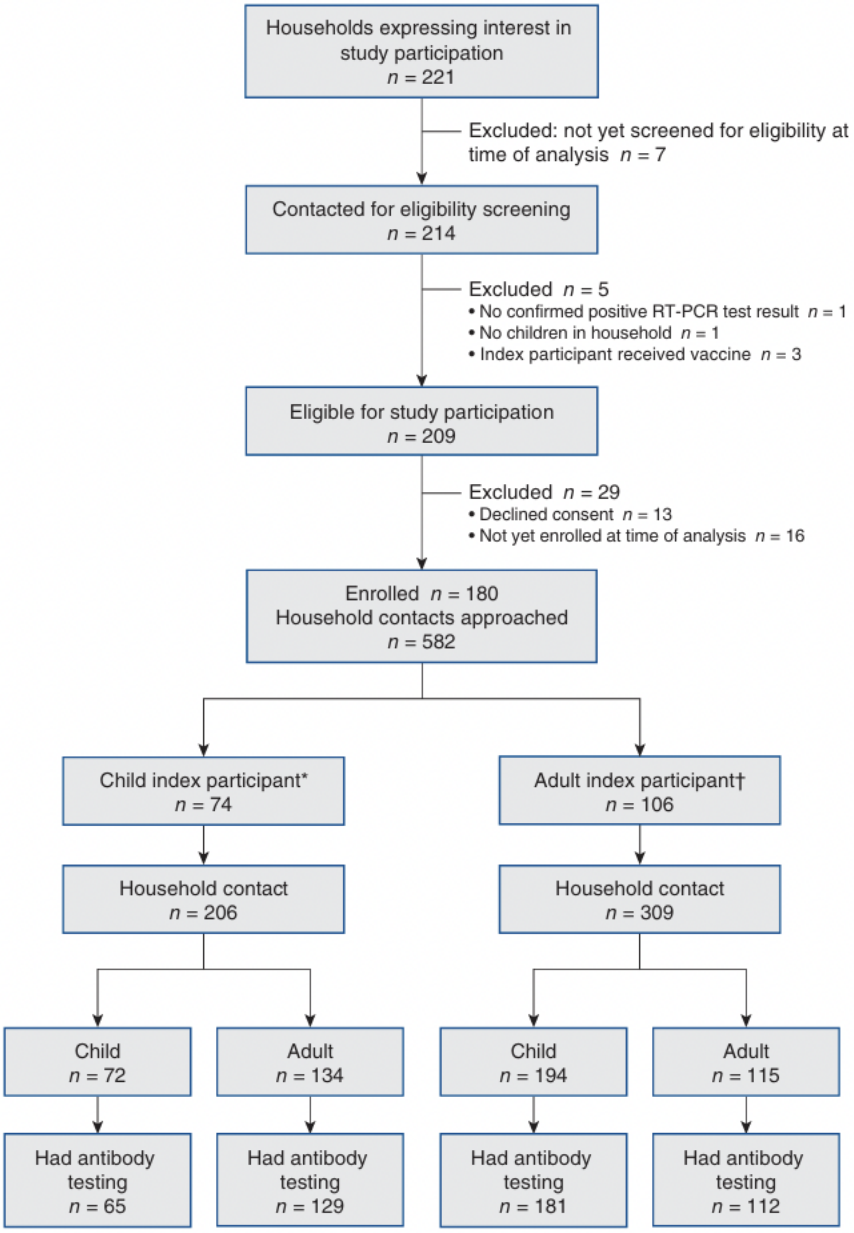


Figure 1: Flow diagram showing screening and enrolment of study population. *Age less than 18 years. †Age 18 years or more. Note: RTPCR = reverse transcription polymerase chain reaction.

Baseline characteristics of the index participants and household contacts are provided in (Table 1) and Appendix 1, Table S1. Of the 106 adult index participants, 57 (54.3%) were female, and the

median age was 40 (IQR 36–45) years. Of the 74 child index participants, 24 (32.4%) were female, and the median age was 8 (IQR 5–12) years. There were 19 asymptomatic infections among the index participants, 13 (68%) in children. Forty-five household contacts (8.7%) were completely isolated from the index participant, and 44 (8.5%) always wore a mask while indoors with the index participant.

Incidence of household infection and transmission

Testing for SARS-CoV-2 antibody was done in 487 household contacts (94.6%), of whom 239 had a positive result (secondary attack rate 49.1%, 95% CI 42.9%–55.3%) (Table 2). Of the 239, 88 (36.8%, 95% CI 29.3%–43.2%) were asymptomatic. Asymptomatic rates were similar among child household contacts (51/130 [39.2%, 95% CI 30.7%–48.5%) and adult household contacts (37/115 [32.2%, 95% CI 24.2%–41.4%]) (OR 1.3, 95% CI 0.8–2.1). Positivity rates among those tested less than 30 days, 30–90 days or more than 90 days after a positive SARS-CoV-2 test result were similar (Appendix 1, Table S2).

In 57/181 households (31.5%, 95% CI 25.2%–38.6%), all household members were positive for SARS-CoV-2 antibody; there was no secondary transmission in 27 households (14.9%, 95% CI 10.5%–20.8%).

Transmission by age

The proportion and associations of household contacts positive for SARS-CoV-2 antibody, by age of the index participant, are shown in (Table 2) and Appendix 1, Table S3. Adult index participants were more likely than child index participants to transmit infection (OR 2.2, 95% CI 1.3–3.6). In households in which the index participant was a child, 72/194 members (37.1%, 95% CI 27.7%–47.6%) had SARS-CoV-2 antibody; the odds of transmission to other children versus adults was 1.2 (95% CI 0.8–2.0).

Table 1: Baseline characteristics of people who tested positive for SARS-CoV-2 by reverse transcription polymerase chain reaction (index participants) and household contacts

	Index participants, no. (%)*			Household contacts, no. (%)*		
Characteristic	Overall *n* = 180	Children *n* = 74	Adults *n* = 106	Overall *n* = 515	Children *n* = 266	Adults *n* = 249
Age, median (IQR), yr	33.9 (9.6–41.5)	8.2 (5.4–12.5)	40.5 (36.3–45.3)	17.1 (8.7–41.4)	8.9 (5.2–12.9)	41.9 (36.6–47.0)
Age group, yr						
≤ 3	11 (6.1)	11 (14.9)	–	47 (9.1)	47 (17.7)	–
4–11	43 (23.9)	43 (58.1)	–	142 (27.6)	142 (53.4)	–
12–17	20 (11.1)	20 (27.0)	–	77 (15.0)	77 (28.9)	–
18–29	9 (5.0)	–	9 (8.5)	17 (3.3)	–	17 (6.8)
30–39	42 (23.3)	–	42 (39.6)	80 (15.5)	–	80 (32.1)
40–49	44 (24.4)	–	44 (41.5)	108 (21.0)	–	108 (43.4)
≥ 50	11 (6.1)	–	11 (10.4)	44 (8.5)	–	44 (17.7)
Sex						
Female	81 (45.0)	24 (32.4)	57 (53.8)	275 (53.4)	139 (52.3)	136 (54.6)
Male	98 (54.4)	50 (67.6)	48 (45.3)	238 (46.2)	126 (47.4)	112 (45.0)
Missing	1 (0.6)	0 (0.0)	1 (0.9)	2 (0.4)	1 (0.4)	1 (0.4)
Indigenous						
Yes	1 (0.6)	0 (0.0)	1 (0.9)	17 (3.3)	9 (3.4)	8 (3.2)
No	179 (99.4)	74 (100.0)	105 (99.0)	494 (95.9)	255 (95.9)	239 (96.0)
Missing	0 (0.0)	0 (0.0)	0 (0.0)	4 (0.8)	2 (0.8)	2 (0.8)
Race or ethnicity†						
Black	15 (8.3)	7 (9.5)	8 (7.5)	44 (8.6)	27 (10.2)	17 (6.9)
Asian	3 (1.7)	2 (2.7)	1 (0.9)	18 (3.5)	10 (3.8)	8 (3.2)
South Asian	0 (0.0)	0 (0.0)	0 (0.0)	4 (0.8)	3 (1.1)	1 (0.4)
West Asian/Arab	15 (8.3)	7 (9.5)	8 (7.5)	44 (8.6)	25 (9.5)	19 (7.7)
Latin American	5 (2.8)	5 (6.8)	0 (0.0)	8 (1.6)	4 (1.5)	4 (1.6)
White	149 (82.8)	62 (83.8)	87 (82.1)	415 (81.1)	216 (81.8)	199 (80.2)
Other‡	2 (1.1)	1 (1.4)	1 (0.9)	3 (0.6)	2 (0.8)	1 (0.4)
Missing	0 (0.0)	0 (0.0)	0 (0.0)	3 (0.6)	2 (0.8)	1 (0.4)
Underlying comorbidity						
Yes	46 (25.6)	7 (9.5)	39 (36.8)	93 (18.0)	42 (15.8)	51 (20.5)
No	134 (74.4)	67 (90.5)	67 (63.2)	419 (81.4)	222 (83.4)	197 (79.1)
Missing	0 (0.0)	0 (0.0)	0 (0.0)	3 (0.6)	2 (0.8)	1 (0.4)
Smoking or vaping	46 (25.6)	5 (6.8)	41 (38.7)	142 (27.6)	14 (5.3)	128 (51.4)
Daily/frequently	6 (13.0)	1 (20.0)	5 (12.2)	20 (14.1)	0 (0.0)	20 (15.6)
Sometimes/rarely	12 (26.1)	2 (40.0)	10 (24.4)	25 (17.6)	6 (42.8)	19 (14.8)
Past smoker/vaper	28 (60.9)	2 (40.0)	26 (63.4)	94 (66.2)	6 (42.8)	88 (68.8)
Missing	0 (0.0)	0 (0.0)	0 (0.0)	3 (2.1)	2 (14.3)	1 (0.8)
Working outside home§						
Yes	52 (28.9)	3 (4.1)	49 (46.2)	88 (17.1)	4 (1.5)	84 (33.7)
No	128 (71.1)	71 (95.9)	57 (53.8)	424 (82.3)	260 (97.7)	164 (65.9)
Missing	0 (0.0)	0 (0.0)	0 (0.0)	3 (0.6)	2 (0.8)	1 (0.4)
Student‡						
Yes	76 (42.2)	69 (93.2)	7 (6.6)	261 (50.7)	245 (92.1)	16 (6.4)
No	104 (57.8)	5 (6.8)	99 (93.4)	251 (48.7)	19 (7.1)	232 (93.2)
Missing	0 (0.0)	0 (0.0)	0 (0.0)	3 (0.6)	2 (0.8)	1 (0.4)
Symptom burden¶						
Asymptomatic	19 (10.6)	13 (17.6)	6 (5.7)	260 (50.5)	140 (52.6)	120 (48.2)
Mild	154 (85.6)	60 (81.1)	94 (88.7)	248 (48.2)	124 (46.6)	124 (49.8)
Moderate	5 (2.8)	1 (1.4)	4 (3.8)	3 (0.6)	0 (0.0)	3 (1.2)
Severe	2 (1.1)	0 (0.0)	2 (1.9)	1 (0.2)	0 (0.0)	1 (0.4)
Missing	0 (0.0)	0 (0.0)	0 (0.0)	3 (0.6)	2 (0.8)	1 (0.4)

Note: IQR = interquartile range. *Except where noted otherwise. †Self-reported. Participants could choose more than 1 category. ‡Unspecified selection of more than 1 category. §At the time the participant or a household member tested positive. ¶Mild = no hospital admission, moderate = hospital admission but not intensive care unit admission, severe = intensive care unit admission.

Table 2: Proportion of household contacts testing positive for SARS-CoV-2 antibodies by age of index participant

	Household contact, all ages		Child household contacts		Adult household contacts		
Group; age, yr	*n*/*N**	% (95% CI)	*n*/*N**	% (95% CI)	*n*/*N**	% (95% CI)	OR (95% CI)†
Index participants, all ages	239/487	49.1 (42.9–55.3)	130/246	52.8 (45.3–60.2)	109/241	45.2 (38.4–52.2)	0.8 (0.6–1.1)
Child index participants	72/194	37.1 (27.7–47.6)	23/65	35.4 (23.1–50.0)	49/129	38.0 (28.6–48.4)	1.2 (0.8–2.0)
≤ 3	6/32	18.8 (7.0–41.3)	1/11	9.1 (1.0–50.3)	5/21	23.8 (7.3–55.5)	3.2 (0.2–48.0)
4–11	47/113	41.6 (29.0–55.4)	17/40	42.5 (26.7–60.0)	30/73	41.1 (28.4–55.1)	1.0 (0.6–1.7)
12–17	19/49	38.8 (20.8–60.4)	5/14	35.7 (12.4–68.5)	14/35	40.0 (23.3–59.3)	1.6 (0.7–3.7)
Adult index participants	167/293	57.0 (49.5–64.2)	107/181	59.1 (50.3–67.4)	60/112	53.6 (44.8–62.1)	0.9 (0.6–1.3)
18–29	17/32	53.1 (32.3–72.9)	7/15	46.7 (26.0–68.6)	10/17	58.8 (34.0–79.9)	1.6 (0.8–3.3)
30–49	130/230	56.5 (47.7–64.9)	90/152	59.2 (49.4–68.3)	40/78	51.3 (40.7–61.8)	0.8 (0.6–1.2)
≥ 50	20/31	64.5 (43.9–80.9)	10/14	71.4 (34.9–92.1)	10/17	58.8 (39.0–76.1)	0.7 (0.2–2.8)

Note: CI = confidence interval, OR = odds ratio.
*n/N = number of household contacts with SARS-CoV-2 antibodies in households in which the index participant was in a specified age category/total number of household contacts in households in which the index participant was in specified age category.
†Odds that an adult versus a child in the household would become infected from index participant of a given age.

The youngest children (age ≤ 3 yr) transmitted to a lower proportion of household contacts (6/32 [18.8%, 95% CI 7.0%–41.3%]) than did those aged 4–11 (47/113 [41.6%, 95% CI 29.0%–55.4%]) and 12–17 (19/49 [38.8%, 95% CI 20.8%–60.4%]) (OR 3.0, 95% CI 0.9–10.0 and 2.7, 95% CI 0.7–10.5, respectively). In households in which the index participant was an adult, 167/293 members (57.0%, 95% CI 49.5%–64.2%) were positive for SARS-CoV-2 antibody; the odds of transmission to children versus adults was 0.9 (95% CI 0.6–1.3). For index participants of all ages, the secondary risk to child versus adult household contacts was similar (OR 0.8, 95% Cl 0.6–1.1).

Transmission by symptoms

The rate of transmission from asymptomatic index participants to household contacts was 35.3% (95% CI 18.5%–56.8%), and the rate of transmission from symptomatic index participants was 50.7% (95% CI 44.2%–57.1%) (OR 0.6, 95% CI 0.2–1.4) (Table 3).

Table 3: Proportion of household contacts who tested positive for SARS-CoV-2 antibodies by age group and symptom status of index participant

Age group; symptom status	Household contacts, all ages		Child household contacts		Adult household contacts		OR (95% CI)†
	n/*N**	% (95% CI)	*n*/*N**	% (95% CI)	*n*/*N**	% (95% CI)	
Index participants, all ages							
Asymptomatic	18/51	35.3 (18.5–56.8)	9/21	42.9 (20.4–68.7)	9/30	30.0 (14.3–52.4)	0.6 (0.3–1.4)
Symptomatic	221/436	50.7 (44.2–57.1)	121/225	53.8 (46.0–61.4)	100/211	47.4 (40.2–54.7)	0.9 (0.6–1.2)
OR (95% CI)‡	0.6 (0.2–1.4)		0.7 (0.3–1.9)		0.5 (0.2–1.3)		
Child index participants							
Asymptomatic	10/34	29.4 (12.3–55.3)	4/11	36.4 (15.7–63.7)	6/23	26.1 (9.7–53.6)	0.6 (0.3–1.3)
Symptomatic	62/160	38.8 (28.3–50.4)	19/54	35.2 (21.3–52.1)	43/106	40.6 (30.0–52.1)	1.4 (0.8–2.4)
OR (95% CI)§	0.7 (0.2–2.3)		1.3 (0.4–4.4)		0.6 (0.2–1.9)		
Adult index participants							
Asymptomatic	8/17	47.1 (13.1–84.0)	5/10	50.0 (10.9–89.1)	3/7	42.9 (11.0–82.0)	0.9 (0.2–4.1)
Symptomatic	159/276	57.6 (50.1–64.8)	102/171	59.6 (50.8–67.9)	57/105	54.3 (45.4–62.9)	0.9 (0.6–1.3)
OR (95% CI)¶	0.7 (0.1–3.0)		0.7 (0.1–3.6)		0.7 (0.1–3.6)		

Note: CI = confidence interval, OR = odds ratio.*n/N = number of household contacts with SARS-CoV-2 antibodies in households in which the index participant was in a specified age category/total number of household contacts in households in which the index participant was in specified age category. †Odds that a child versus an adult household contact would become infected from the index participant in the given category. ‡Odds that a given type of household contact would become infected from an asymptomatic versus a symptomatic index participant of any age. §Odds that a given type of household contact would become infected from an asymptomatic versus a symptomatic child index participant. ¶Odds that a given type of household contact would become infected from an asymptomatic versus a symptomatic adult index participant.

Risk factors for transmission

Results from the multivariable logistic regression analyses are summarized in (Figure 2) and Appendix 1, Table S4. Compared to households in which the index participant was the only infected person, the odds of transmission increased with every additional infected member (OR 3.0, 95% CI 2.1–4.2). Lower-density households were associated with lower transmission rates (OR 0.8, 95% CI 0.7–1.0). The odds of an adult's transmitting to a child were higher compared to the odds of a child's transmitting to another child (OR 2.0, 95% CI 1.0–4.2). The odds of transmission was 2.6 (95% CI 0.8–8.0) if the index participant was admitted to hospital. Isolation of the index participant and indoor masking were not associated with decreased transmission. The odds of transmission from symptomatic and from asymptomatic index participants was uncertain (OR 1.4, 95% CI 0.6–3.1).

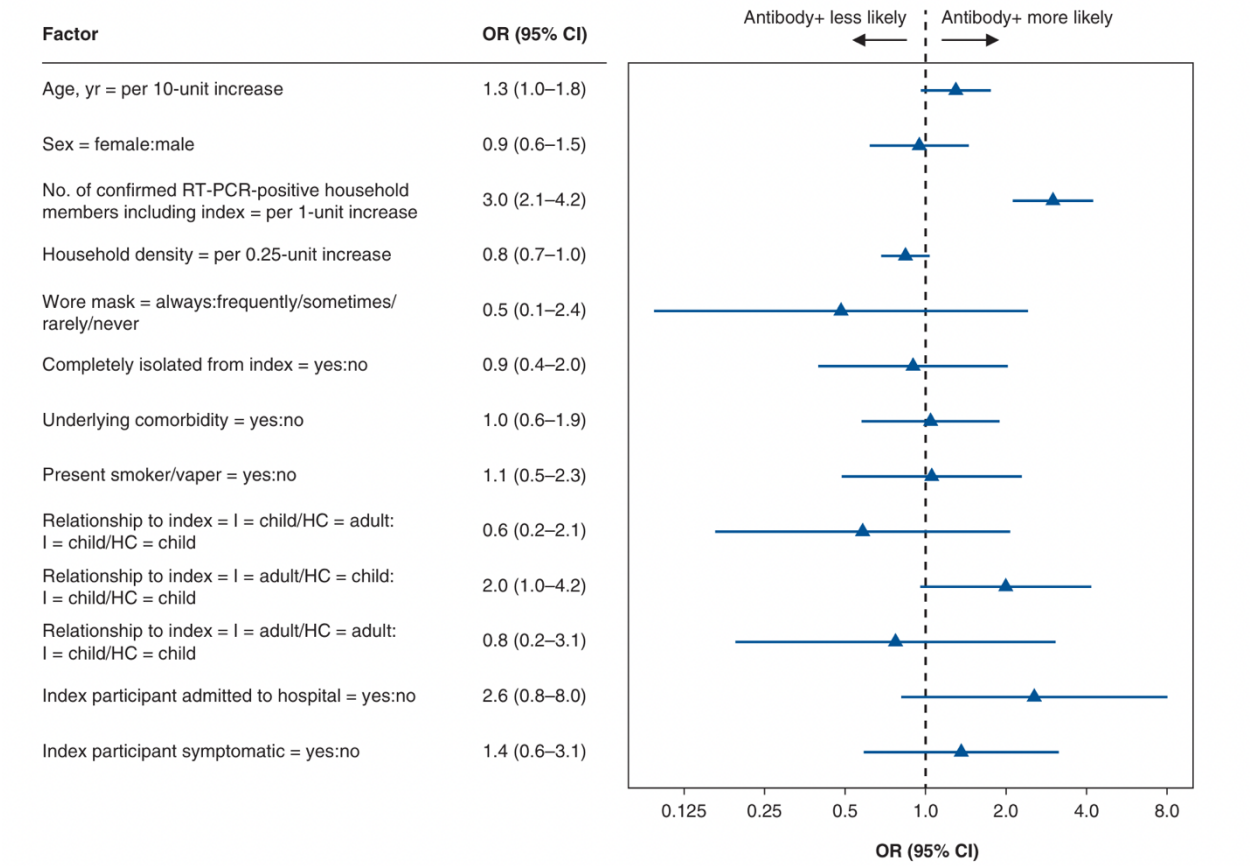


Figure 2: Risk factors for household transmission. Note: CI = confidence interval, HC = household contact, I = index participant, OR = odds ratio.

Interpretation

Our prospective study used a highly sensitive laboratory ELISA for SARS-CoV-2-specific antibodies to determine SARS-CoV-2 spread in households with children. We enrolled the majority of members from participating households and found high transmission by both children and adults, with a secondary attack rate of about 50%. Although adults were more likely to spread infection than children, children transmitted infection to roughly one-third of their household members. Children and adults were equally likely to be infected from the infected adult or child in their home.

A meta-analysis of household transmission of SARS-CoV-2 including 87 studies published between March 2020 and June 2021 from 30 countries showed an overall secondary attack rate of

19%.[1] The accuracy of this estimate may have been affected by a high degree of methodologic heterogeneity with respect to test type and frequency of testing for diagnosis of contacts, isolation practices of infected household members and duration of follow-up. Serologic testing to diagnose infection in household contacts was used in very few of the studies, and few looked at spread specifically from children. Serosurveillance can enhance the accuracy of household transmission estimates; however, most investigators using serosurveillance reported transmission from adult index cases only[13-15,17,19,21,42] or from specialized populations,[13–15,17,21] whereas others excluded child household contacts, which limits the generalizability of the results.[16,22,43]

Miller and colleagues[43] used a commercial ELISA assay on day 35 to test for IgG antibodies in household contacts of 92 child index cases in England. Children aged 10 years or less and those aged 11–18 transmitted to 25% (95% CI 12%–38%) and 30% (95% CI 19%–41%) of contacts, respectively. Although these results are similar to ours, the spread may not have been attributable exclusively to transmission within the home, as, unlike in our study setting, there was high community prevalence of SARS-CoV-2 during the study period.

Paul and colleagues[5] used a large provincial health administrative data set with viral swab results to examine household transmission among people with laboratory-confirmed SARS-CoV-2 infection in Ontario in 2020. They found that transmission occurred in only 27% of households; younger children (age ≤ 3 yr, 4–8 yr and 9–13 yr) were more likely to transmit SARS-CoV-2 within the home than those aged 14–17 (OR 1.4, 95% CI 1.2–1.7; OR 1.4, 95% CI 1.2–1.7; and OR 1.1, 95% CI 1.0–1.3, respectively). Although our results similarly show the important role of children as a source of viral spread, we found that the risk of transmission within households expanded as age increased within the pediatric age group (with the youngest children at lowest odds). Given that the omicron variant is more infectious than delta and that delta was at least twice as contagious as earlier SARS-CoV-2 strains,[44] we suspect that household transmission is, and will continue to be, even greater than observed in our study.

To provide evidence-based public health guidance to households with infected members, it is essential to understand risk factors for transmission. Factors found in the current study to be associated with increased transmission such as household density and relationship to the index

participant are not easily modifiable. We did not find reduced transmission when household members were isolated from those with confirmed infection within the home, although adherence to self-reported measures could not be verified. Consistent with the literature suggesting that household transmission is greater when illness is more severe in the index participant[1,45] we observed higher transmission rates when the index participant was admitted to hospital, although the width of the confidence interval made this association uncertain. We also found that both symptomatic and asymptomatic people were responsible for transmission within the home. With the increasing recognition of spread both by asymptomatic people[46] and from aerosolized droplets,[47,48] the benefits of advising people to isolate within a household may be minimal, particularly if isolation is delayed until a positive test result.

In many cases, children are exempt from COVID-19 safety measures. For example, in many jurisdictions, unvaccinated children are permitted to circulate in the community even if they are a close contact of a person with COVID-19; children are often not required to abide by quarantine rules if travelling with fully vaccinated adults; in certain provinces, length of isolation after confirmed SARS-CoV-2 infection is shorter for certain categories of children; and mask mandates for children are highly variable depending on location.[49–51] We found that children are sources of SARS-CoV-2 spread within the home, and we hypothesize that they will be an even greater source of spread with the emergence of more infectious variants. Children also have considerable potential to spread in settings such as school and daycare, where they congregate indoors for long periods and where mask wearing may not be consistent or continuous. More consistency in public health policies related to nonpharmacologic interventions such as mask wearing and ventilation is critically important to control spread.

Limitations

There was no maximum allowable time between confirmed infection and study enrolment, which led to highly varied times between infection and antibody testing. This may have affected our ability to detect infection; however, we measured 3 isotypes (IgM, IgA, IgG) to minimize the risk of missing very recent or remote infection. It may also have resulted in a falsely elevated estimation of transmission; however, COVID-19 case counts were very low (6–12 cases per 100 000) in

Ottawa during the study period (compared to 250 cases per 100 000 in February 2022[52]), which increases the certainty that transmission occurred in the home.

Our cohort was recruited before widespread vaccination and circulation of variants in our community. In the era before the omicron variant, decreased household transmission was observed when members had had at least 1 vaccine dose.[53,54] However, given the immunity-evading properties of the omicron variant,[55] our study population may mirror the current state of many Canadian households, with adults who have not received a booster vaccine, and unvaccinated or partially vaccinated children. The omicron variant, which is highly contagious, will likely further increase household transmission from all members.

We used a variety of strategies to identify eligible households, including self-identification. It is possible that characteristics of families who self-identified were different from those of families who were recruited through follow-up of a positive test result.

Finally, we defined the household member who first developed symptoms or, in the absence of symptoms, had the first positive RT-PCR test result for SARS-CoV-2 as the index participant. This assignment may have been erroneous if there was a co-primary infection or if the first-infected member was asymptomatic, as provincial guidelines at the time allowed PCR testing only for symptomatic people. Use of this definition may have underestimated the prevalence of asymptomatic spread and may have assigned directionality of transmission inaccurately.

Conclusion

People with SARS-CoV-2 infection transmitted extensively within their households, with a secondary attack rate of about 50%. Although children transmitted at a lower rate than adults, they still infected one-third of household members; this finding should inform public health policy. Asymptomatic spread occurred and should be accounted for in the formulation of public health and travel policies. Our findings have implications for in-person school or activities because the risk of transmission may be high when masks are not worn continuously or consistently in poorly ventilated settings. Nonpharmacologic interventions should continue to be considered for congregate settings.

Acknowledgements
The authors thank Ms. Dale Dalgleish, Mr. Tyrus Crawford and Ms. Taylor McNeely, as well as the research assistants and nurses, for their collaboration in patient recruitment and enrolment; Dr. Andrew Willmore for his important contributions to the system used to identify adult index participants; and Ms. Lynda Rocheleau for her assistance with data analysis in the Pelchat Laboratory, University of Ottawa.

Competing interests: None declared.

Contributors: Marc-André Langlois and Roger Zemek contributed equally as senior authors. Maala Bhatt, Roger Zemek, Marc-André Langlois, Amy Plint and Anne Pham Huy conceived and designed the study. Ken Tang, Martin Pelchat and Marc-André Langlois analyzed the data. Maala Bhatt, Jennifer Dawson, Ken Tang, Marc-André Langlois, Amy Plint and Roger Zemek drafted the manuscript. All of the authors acquired and interpreted the data, revised the manuscript critically for important intellectual content, approved the final version to be published and agreed to be accountable for all aspects of the work.

Funding: This study was supported by grants from the Children's Hospital Academic Medical Organization, the PSI Foundation (COV-6) and the Ontario COVID-19 Rapid Research Fund (C-741-1934-BHATT). The Langlois Laboratory was supported by a COVID-19 Rapid Response grant from the Canadian Institutes of Health Research (VR2-172722) and a grant supplement by the COVID-19 Immunity Task Force. Production of COVID-19 reagents was supported financially by the National Research Council Canada Pandemic Response Challenge program.

Data sharing: Aggregate data presented in this manuscript are accessible to interested parties by application to the corresponding author.

Supplemental information: For reviewer comments and the original submission of this manuscript, please see www.cmajopen.ca/content/10/2/E357/suppl/DC1.

References

1. Madewell ZJ, Yang Y, Longini IM Jr, et al. Factors associated with household transmission of SARS-CoV-2. JAMA Netw Open 2021;4:e2122240.
2. Koh WC, Naing L, Chaw L, et al. What do we know about SARS-CoV-2 transmission? A systematic review and meta-analysis of the secondary attack rate and associated risk factors. PLoS One 2020;15:e0240205.
3. Thompson HA, Mousa A, Dighe A, et al. Severe acute respiratory syndrome coronavirus 2 (SARS-CoV-2) setting-specific transmission rates: a systematic review and meta-analysis. Clin Infect Dis 2021;73:e754-64.
4. Chu VT, Yousaf AR, Chang K, et al.; Georgia Camp Investigation Team. Household transmission of SARS-CoV-2 from children and adolescents. N Engl J Med 2021;385:954-6.
5. Paul LA, Daneman N, Schwartz KL, et al. Association of age and pediatric household transmission of SARS-CoV-2 infection. JAMA Pediatr 2021;175:1151-8.
6. Lei H, Xu X, Xiao S, et al. Household transmission of COVID-19-a systematic review and meta-analysis. J Infect 2020;81:979-97.
7. Mallett S, Allen AJ, Graziadio S, et al. At what times during infection is SARS-CoV-2 detectable and no longer detectable using RT-PCR-based tests? A systematic review of individual participant data. BMC Med 2020;18:346.
8. Hippich M, Holthaus L, Assfalg R, et al. A public health antibody screening indicates a 6-fold higher SARS-CoV-2 exposure rate than reported cases in children. Med (N Y) 2021;2:149-63.e4.
9. Hyde Z. Difference in severe acute respiratory syndrome coronavirus 2 attack rate between children and adults may reflect bias. Clin Infect Dis 2022;74:152-5.
10. Arkhipova-Jenkins I, Helfand M, Armstrong C, et al. Antibody response after SARS-CoV-2 infection and implications for immunity. Ann Intern Med 2021; 174:811-21.
11. Post N, Eddy D, Huntley C, et al. Antibody response to SARS-CoV-2 infection in humans: a systematic review. PLoS One 2020;15:e0244126.
12. Metcalf CJE, Farrar J, Cutts FT, et al. Use of serological surveys to generate key insights into the changing global landscape of infectious disease. Lancet 2016; 388:728-30.
13. Ladhani SN, Andrews N, Aiano F, et al.; RAPID-19 Investigation Team. Secondary attack rate and family clustering of SARS-CoV-2 infection in children of healthcare workers with confirmed COVID-19. Clin Infect Dis 2021;73:e260-3.
14. Méndez-Echevarría A, Sainz T, de Felipe B, et al. High rates of SARS-CoV-2 family transmission in children of healthcare workers during the first pandemic wave in Madrid, Spain. Pediatr Infect Dis J 2021;40:e185-8.
15. Brotons P, Launes C, Buetas E, et al.; Kids Corona Study Group. Susceptibility to severe acute respiratory syndrome coronavirus 2 infection among children and adults: a seroprevalence study of family households in the Barcelona metropolitan region, Spain. Clin Infect Dis 2021;72:e970-7.
16. Kuwelker K, Zhou F, Blomberg B, et al. High attack rates of SARS-CoV-2 infection through household-transmission: a prospective study. medRxiv 2020 Nov. 4. doi: 10.1101/2020.11.02.20224485. 17. McDade TW, McNally EM, Zelikovich AS, et al. High seroprevalence for SARS-CoV-2 among household members of essential workers detected using a dried blood spot assay. PLoS One 2020;15:e0237833.
18. Ng OT, Marimuthu K, Koh V, et al. SARS-CoV-2 seroprevalence and transmission risk factors among high-risk close contacts: a retrospective cohort study. Lancet Infect Dis 2021;21:333-43.
19. Reukers DFM, van Boven M, Meijer A, et al. High infection secondary attack rates of SARS-CoV-2 in Dutch households revealed by dense sampling. Clin Infect Dis 2022;74:52-8.
20. Angulo-Bazán Y, Solis-Sánchez G, Cardenas F, et al. Household transmission of SARS-CoV-2 (COVID-19) in Lima, Peru. Cad Saude Publica 2021;37:e00238720.

21. Buonsenso D, Valentini P, De Rose C, et al.; Gemelli Against COVID-19 PostAcute Care Study Group. Seroprevalence of anti-SARS-CoV-2 IgG antibodies in children with household exposure to adults with COVID-19: preliminary f indings. Pediatr Pulmonol 2021;56:1374-7.
22. Galow L, Haag L, Kahre E, et al. Lower household transmission rates of SARS-CoV-2 from children compared to adults. J Infect 2021;83:e34-6.
23. Shah K, Kandre Y, Mavalankar D. Secondary attack rate in household contacts of COVID-19 Paediatric index cases: a study from Western India. J Public Health (Oxf) 2021;43:243-5.
24. Li F, Li YY, Liu MJ, et al. Household transmission of SARS-CoV-2 and risk factors for susceptibility and infectivity in Wuhan: a retrospective observational study. Lancet Infect Dis 2021;21:617-28.
25. Lugon P, Fuller T, Damasceno L, et al. SARS-CoV-2 infection dynamics in children and household contacts in a slum in Rio de Janeiro. Pediatrics 2021; 148:e2021050182.
26. Graff K, Smith C, Silveira L, et al. Risk factors for severe COVID-19 in children. Pediatr Infect Dis J 2021;40:e137-45.
27. Davies NG, Klepac P, Liu Y, et al.; CMMID COVID-19 working group. Agedependent effects in the transmission and control of COVID-19 epidemics. Nat Med 2020;26:1205-11.
28. Viner RM, Mytton OT, Bonell C, et al. Susceptibility to SARS-CoV-2 infection among children and adolescents compared with adults. JAMA Pediatr 2021; 175:143.
29. Gadermann AC, Thomson KC, Richardson CG, et al. Examining the impacts of the COVID-19 pandemic on family mental health in Canada: findings from a national cross-sectional study. BMJ Open 2021;11:e042871.
30. Li X, Vanderloo LM, Maguire JL, et al.; TARGet Kids! Collaboration. Public health preventive measures and child health behaviours during COVID-19: a cohort study. Can J Public Health 2021;112:831-42.
31. Ashikkali L, Carroll W, Johnson C. The indirect impact of COVID-19 on child health. Paediatr Child Health (Oxford) 2020;30:430-7.
32. Current population and household estimates. Ottawa: City of Ottawa. Available: https://ottawa.ca/en/living-ottawa/statistics-and-demographics/current -population-and-household-estimates (accessed 2022 Feb. 16).
33. Daily COVID-19 dashboard. Ottawa: Ottawa Public Health. Available: https:// www.ottawapublichealth.ca/en/reports-research-and-statistics/daily-covid19-dashboard.aspx (accessed 2021 Aug. 31).
34. von Elm E, Altman DG, Egger M, et al.; STROBE Initiative. Strengthening the Reporting of Observational Studies in Epidemiology (STROBE) statement: guidelines for reporting observational studies. BMJ 2007;335:806-8.
35. Epidemiological protocol: household transmission investigation protocol for 2019-novel coronavirus (COVID-19) infection. Geneva: World Health Organization; 2020. Available: https://www.who.int/publications/i/item/household -transmission-investigation-protocol-for-2019-novel-coronavirus-(2019-ncov) -infection (accessed 2021 May 3).
36. Chambers EC, Schechter C, Tow A, et al. Household density and obesity in young black and white adults. Ethn Dis 2010;20:366-9.
37. Isho B, Abe KT, Zuo M, et al. Persistence of serum and saliva antibody responses to SARS-CoV-2 spike antigens in patients with COVID-19. Sci Immunol 2020; 5:eabe5511.
38. Cholette F, Mesa C, Harris A, et al.; COVID-19 Immunity Task Force (CITF) Working Group. Dried blood spot specimens for SARS-CoV-2 antibody testing: a multi-site, multi-assay comparison. PLoS One 2021;16:e0261003.
39. Dicker R, Coronado F, Koo D, et al. Lesson 3: Measure of risk; Section 2: Morbidity frequency measures. In: Principles of epidemiology in public health practice, 3rd ed. Atlanta: Centers for Disease Control and Prevention; 2006. Available: https:// www.cdc.gov/csels/dsepd/ss1978/lesson3/section2.html (accessed 2022 Feb. 4).
40. Huber PJ. The behavior of maximum likelihood estimates under nonstandard conditions. Berkeley Symp Math Statist Prob 1967;1:221-33.

41. White H. A heteroskedasticity-consistent covariance matrix estimator and a direct test for heteroskedasticity. Econometrica 1980;48:817-30.
42. Cerami C, Popkin-Hall ZR, Rapp T, et al. Household transmission of SARSCoV-2 in the United States: living density, viral load, and disproportionate impact on communities of color. Clin Infect Dis 2021 Aug. 12 [Epub ahead of print]. doi: 10.1093/cid/ciab701.
43. Miller E, Waight PA, Andrews NJ, et al. Transmission of SARS-CoV-2 in the household setting: a prospective cohort study in children and adults in England. J Infect 2021;83:483-9.
44. What you need to know about variants. Atlanta: Centers for Disease Control and Prevention; updated 2022 Feb. 2. Available: https://www.cdc.gov/coronavirus/ 2019-ncov/variants/delta-variant.html (accessed 2022 Feb. 1).
45. Bi Q, Lessler J, Eckerle I, et al.; SEROCoV-POP Study Group. Insights into household transmission of SARS-CoV-2 from a population-based serological survey. Nat Commun 2021;12:3643.
46. Qiu X, Nergiz AI, Maraolo AE, et al. Defining the role of asymptomatic and pre-symptomatic SARS-CoV-2 transmission: a living systematic review. Clin Microbiol Infect 2021;27:511-9.
47. Scientific brief: SARS-CoV-2 transmission. Atlanta: Centers for Disease Control and Prevention; updated 2021 May 7. Available: https://www.cdc.gov/ coronavirus/2019-ncov/science/science-briefs/sars-cov-2-transmission.html (accessed 2022 Feb. 1).
48. Coronavirus disease (COVID-19): How is it transmitted? Geneva: World Health Organization; 2021. Available: https://www.who.int/news-room/ questions -and -answers/item/coronavirus-disease-covid-19-how-is-it-transmitted (accessed 2022 Jan. 27).
49. COVID-19 case and contact management in schools. Government of Saskatchewan. Available: https://www.saskatchewan.ca/government/health-care -administration-and-provider-resources/treatment-procedures-and-guidelines/ emerging-public-health-issues/2019-novel-coronavirus/about-covid-19/covid -19-case-and-contact-management-in-schools (accessed 2022 Feb. 16).
50. Staying safe and healthy this school year. Edmonton: Government of Alberta. Available: https://www.alberta.ca/k-12-learning-during-covid-19.aspx (accessed 2022 Feb. 16).
51. Wearing a mask or a face covering in public settings in the context of the COVID-19 pandemic. Gouvernement du Québec. Available: https://www. quebec.ca/en/health/health-issues/a-z/2019-coronavirus/mask-or-face-covering/ wearing-a-face-covering-in-public-settings-covid-19 (accessed 2022 Feb. 16).
52. Ontario COVID-19 Data Tool. Toronto: Ontario Agency For Health Protection and Promotion (Public Health Ontario). Available: https://www. publichealthontario.ca/en/data-and-analysis/infectious-disease/covid-19-data -surveillance/covid-19-data-tool?tab=maps (accessed 2022 Feb. 16).
53. Shah ASV, Gribben C, Bishop J, et al. Effect of vaccination on transmission of SARS-CoV-2. N Engl J Med 2021;385:1718-20.
54. Harris RJ, Hall JA, Zaidi A, et al. Effect of vaccination on household transmission of SARS-CoV-2 in England. N Engl J Med 2021;385:759-60.
55. Dejnirattisai W, Huo J, Zhou D, et al. SARS-CoV-2 Omicron-B.1.1.529 leads to widespread escape from neutralizing antibody responses. Cell 2022;185:467-84.e15.

A-1.10 Prevalence of SARS-CoV-2 infection among obstetric patients in Ottawa, Canada: a descriptive study

Preface

(This work has been previously published as a research article)

Fakhraei R, Erwin E, Alibhai KM, Murphy MSQ, Dingwall-Harvey ALJ, White RR, Dimanlig-Cruz S, LaRose R, Grattan K, Jia JJ, Liu G, Arnold C, **Galipeau Y**, Shir-Mohammadi K, Alton GD, Dy J, Walker MC, Fell DB, Langlois MA, El-Chaâr D. **Prevalence of SARS-CoV-2 infection among obstetric patients in Ottawa, Canada: a descriptive study**. CMAJ Open. 2022 Jul 12;10(3):E643-E651.

https://doi.org/10.9778/cmajo.20210228

© 2022 CMA Impact Inc. or its licensors
This is an Open Access article distributed in accordance with the terms of the Creative Commons Attribution (CC BY-NC-ND 4.0) licence, which permits use, distribution and reproduction in any medium, provided that the original publication is properly cited, the use is noncommercial (i.e., research or educational use), and no modifications or adaptations are made. See: https://creativecommons.org/licenses/by-nc-nd/4.0/

Abstract

Background
There is limited information on the prevalence of SARS-CoV-2 infection in obstetric settings in Canada, beyond the first wave of the COVID-19 pandemic (February to June 2020). We sought to describe the prevalence of SARS-CoV-2 infection in pregnant people admitted to triage units at a tertiary care hospital in Ottawa, Canada.

Methods
We conducted a descriptive study of pregnant people admitted to obstetric triage assessment units at The Ottawa Hospital between Oct. 19 and Nov. 27, 2020 (second local wave of the COVID-19 pandemic). Participants underwent SARS-CoV-2 polymerase chain reaction (PCR) (via naso- or oropharyngeal swabs) and serology testing upon admission. We excluded individuals younger than 18 years, those who did not speak English or French, those who enrolled in conflicting studies, those admitted for pregnancy termination and those triaged between 11:31 pm and 7:29 am. Swab and serology samples were analyzed using digital droplet PCR and enzyme-linked immunosorbent assays, respectively. We defined SARS-CoV-2 seropositivity as a positive result for immunoglobulin (Ig) G, either alone or in combination with IgM or IgA.

Results
Of the 632 eligible patients, 363 (57.4%) consented to participation and 362 collectively provided 284 swab and 352 blood samples eligible for analysis. Common reasons for declining participation included feeling overwhelmed or anxious, being worried about repercussions of testing, pain or discomfort with testing or disinterest in research. Participants were mostly multiparous (53.9%) and in their third trimester upon admission (88.4%). In all, 18 (4.9%) participants had evidence of SARS-CoV-2 exposure; 2 (0.7%) of 284 were positive for SARS-CoV-2 by PCR and 16 (4.5%) of 352 were positive for IgG antibodies to SARS-CoV-2.

Interpretation
During the second local wave of the COVID-19 pandemic, the prevalence of active SARS-CoV-2 infection among obstetric patients in Ottawa was 0.7% and seroprevalence was 4.5%. Our low participation rate highlights the need for improvements in patient education and public health messaging on the benefits of SARS-CoV-2 testing programs.

The onset of the COVID-19 pandemic saw the widespread implementation of policies in clinical care settings to protect vulnerable patient populations.[1] Among these populations are obstetric patients, who are at increased risk for severe complications related to COVID-19, including admission to hospital and to the intensive care unit.[2] Pregnant individuals require regular and frequent access to health care services and most are ultimately admitted to the hospital for delivery.[3]

Temporary adoption of universal COVID-19 screening and testing approaches in some obstetric departments provided important insight for local hospital administrators and public health authorities on the prevalence of SARS-CoV-2 infection in obstetric patients. Early estimates of SARS-CoV-2 prevalence among pregnant individuals are highly variable, ranging from 0.012% to 37%.[4,5] Variability in these estimates reflects differences in population density across settings, socioeconomic composition, available technology for laboratory testing, timing and duration of testing programs, and local community infection rates.[6] Furthermore, cautious and appropriate interpretation of serologic assays are necessary when estimating seroprevalence, given the emerging evidence on serologic cross-reactivity and antibody decay,[7,8] particularly in populations with low levels of exposure.[9]

There is limited information on the prevalence of SARS-CoV-2 infection from obstetric settings in Canada, and existing reports are limited to the first pandemic wave (about February to June 2020). In a single-centre investigation from Montréal, all obstetric patients (n = 803) admitted between March and July 2020 were tested for SARS-CoV-2; of these, 5% tested positive.[10] A subsequent study from Toronto reported 0.9% prevalence of SARS-CoV-2 infection among 446 pregnant individuals tested between April and May 2020.[11] Serologic analysis of more than 1000 antenatal maternal serum samples, collected from multiple provincial health units in British Columbia from March to June 2020, suggested that the seroprevalence of SARS-CoV-2 antibodies in this obstetric sample was less than 1%.[12]

Ongoing surveillance among obstetric patients is warranted to help characterize the burden of disease across different pandemic waves and inform local public health measures for future disease outbreaks. At the time of our study, Ontario was at the height of Canada's second pandemic wave (September 2020 to February 2021) and vaccinations were not yet available to the general public.[13] Our objective was to describe the prevalence of SARS-CoV-2 infection in pregnant individuals admitted to obstetric triage units at a tertiary care hospital in Ottawa, Ontario.

Methods

Study design and setting

We conducted a descriptive study of pregnant individuals admitted to obstetric triage units at The Ottawa Hospital. The Ottawa Hospital is a tertiary care centre with 2 obstetric triage units located at different campuses (General Campus and Civic Campus). Participant SARS-CoV-2 virus and serology testing was conducted over 5.5 weeks during the second local wave of the pandemic,[13] between Oct. 19 and Nov. 27, 2020. The COVID-19 restrictions that were in place during this time allowed only 1 support person to accompany the birthing mother and this was limited to admissions to the birthing unit (i.e., during active labour).[14]

Study population

Participants were pregnant individuals who were admitted to 1 of 2 obstetric triage units (generally ≥ 20 weeks' gestation, unless the circumstances are exceptional). Patients with or without symptoms of COVID-19 were eligible to participate. We excluded individuals who did not speak English or French, were younger than 18 years, were enrolled in conflicting research studies or were admitted for a pregnancy termination. Given the necessity of having research staff available to collect consent, individuals who presented to triage units overnight (i.e., between the hours of 11:31 pm and 7:29 am) were not eligible to participate.

Sample collection

We invited participants to provide both a blood sample and a naso- or oropharyngeal swab sample; however, provision of both sample types was not a requirement for participation. Thus, participants

in our study could provide both a swab sample and a blood sample, a swab sample alone or a blood sample alone.

Samples were collected at the participants' first presentation to the triage unit. If participants visited the triage unit more than once during the study period, subsequent samples were collected only if the participant was suspected to have COVID-19 based on the presence of symptoms, at-risk contact history or travel history, as determined from a Febrile Respiratory Illness Screening Tool used at hospital entry (Appendix 1, Section 1, available at www.cmajopen.ca/content/10/3/E643/suppl/DC1). For participants who provided samples across multiple study visits, we looked at all polymerase chain reaction (PCR) and serology results. We used results from the most recent triage visit in this analysis, unless positive PCR or serology findings were detected in the first round of samples but not the second round. In such scenarios, we used PCR and serology results from the first round of collected samples.

For participants who provided samples at multiple visits, we looked at all results. If there was a positive PCR or serology finding, we used this. If not, we used the results from the most recent visit.

Naso- and oropharyngeal samples were collected using sterile swabs (Norgen CM-96000 or Norgen CY-93050, respectively) and placed in viral transport media (Norgen Total Nucleic Acid Preservation Tubes Dx). Blood samples were collected as peripheral whole blood via venipuncture or as dried blood spots via finger prick.

SARS-CoV-2 virus and antibody testing

All viral and antibody testing occurred at a containment level 2 facility at the University of Ottawa. Swab samples were analyzed for SARS-CoV-2 RNA using digital droplet PCR assays (Bio-Rad QX200 Droplet Reader) targeting the *orf1ab* region (nsp14), the nucleocapsid gene and the envelope gene.[15] Participants who tested positive for SARS-CoV-2 infection through this research study were notified by their clinical care team and instructed to follow public health guidelines.[16]

Blood samples were evaluated for antibodies specific to SARS-CoV-2 (immunoglobulin [Ig] A, IgG, IgM) using enzyme-linked immunosorbent assays (ELISAs). Assays were run on automated high-throughput instruments (Hamilton Microlab STAR Liquid Handling System), to quantify antibody levels against the full-length viral spike protein and nucleoprotein. Assay signals were used as correlates of detected antibody levels in each patient sample.

A positive cut-off value was established for each assay plate as a value equal to the mean of negative control signal values (manual ELISA) or mean of negative samples (automated ELISA) plus 3 times the standard deviation (SD) of the optical density value distribution from plasma or serum negative for SARS-CoV-2. Antibody levels in positive samples were correlated to SARS-CoV-2 control antibodies for IgA, IgG and IgM (CR3022 antibody). We used a signal to cut-off ratio to classify serology results as positive or negative.

We required a positive result for antibody reactivity against both the full-length viral spike protein and the nucleoprotein for a sample to be classified as seropositive. A positive serologic result was determined to be a positive IgG antibody result alone, or a positive IgG result in combination with a positive IgM or IgA result. Full laboratory methodology is presented in the supplementary materials (Appendix 1, Section 2).

Data sources

To minimize the burden of this study on both participants and health care workers at The Ottawa Hospital, we linked individual laboratory results from SARS-CoV-2 virus and antibody testing to secondary data sources to ascertain participant sociodemographic, obstetric and medical information.

We used the Better Outcomes Registry & Network (BORN) Ontario,[17] Ontario's provincial birth registry, to ascertain data on participant demographics (i.e., maternal age, neighbourhood median family income quintile), medical history (i.e., parity, prepregnancy body mass index, preexisting conditions), lifestyle behaviours (i.e., substance use in pregnancy), pregnancy characteristics and complications (i.e., maternal anxiety or depression in pregnancy, gestational diabetes, hypertensive disorder in pregnancy, number of fetuses, antenatal health care provider type) and delivery and

newborn outcomes (i.e., mode of delivery, gestational age, preterm birth, live or stillbirth). Using this provincial birth registry, we had complete ascertainment of pregnancy and newborn outcomes. We also used BORN Ontario to obtain participant results from community SARS-CoV-2 testing during the study period. These data were derived from the Case and Contact Management System, which captures case-specific information on reportable diseases, including COVID-19, from public health units across Ontario. Case and Contact Management data on pregnant individuals are integrated into the BORN Ontario database on a monthly basis.

We used The Ottawa Hospital's electronic medical record system — Electronic Privacy Information Centre — to ascertain participant responses for the Febrile Respiratory Illness Screening Tool, administered at hospital entry (i.e., suspected COVID-19 symptoms, travel history, close contacts), and to verify results from in-hospital SARS-CoV-2 tests. We also used the Electronic Privacy Information Centre to verify information not yet posted or missing from BORN Ontario records (i.e., participant ethnicity, date of delivery).

We used The Ottawa Hospital Data Warehouse, a relational database that consolidates records from across the hospital's information systems, to determine the total number of pregnant people who presented to obstetric triage units during the study period and to estimate the study recruitment rate. More information on these data sources and how they were used are detailed in Appendix 1, Section 3.

Study outcomes

The primary outcome was the prevalence of SARS-CoV-2 infection. For the purpose of this study, SARS-CoV-2 infection was defined as either active, based on the presence of measurable SARS-CoV-2 virus in maternal samples at the time of presentation to the triage unit, or recovered, based on laboratory-confirmed history of infection earlier in pregnancy or positive serology results from maternal samples at the time of presentation to the triage unit.

Statistical analysis

We managed statistical analyses in the BORN Ontario environment. We linked results from SARS-CoV-2 PCR and serology testing, as well as medical records from the Electronic Privacy

Information Centre and The Ottawa Hospital Data Warehouse, to records in BORN Ontario using participant medical record numbers. In BORN Ontario, we mapped unique participant identifiers and medical record numbers to unique BORN Ontario identifiers to generate a single analytical file.

We calculated descriptive summary statistics for sociodemographic information, obstetric histories and delivery details for the overall study population. We summarized data using frequency distributions for categorical variables, and means and SDs or medians and interquartile ranges (IQRs) for continuous variables. We performed all analyses using SAS version 9.4 (SAS Institute).

Ethics approval

This study was approved by the Ottawa Health Science Network Research Ethics Board (20200640-01H). All participants provided informed consent at the time of enrolment.

Results

From Oct. 19 to Nov. 27, 2020, 888 pregnant people presented to an obstetric triage unit at The Ottawa Hospital. Of these, 650 arrived while research staff were on site and were screened for eligibility. A total of 18 people were ineligible (2.8%), 206 declined participation (31.7%) and 63 were discharged before consent could be obtained (9.7%). Thus, 363 (57.4%) of 632 eligible patients consented to sample collection, including 6 who provided 2 samples each. One participant was excluded after consent owing to sample contamination. Common reasons for declining participation included feeling too overwhelmed or anxious to participate, being unwilling to undergo the pain or discomfort of sample collection, being worried about the SARS-CoV-2 test results and generally not wanting to learn about the research study (Appendix 1, Section 4).

In total, the samples of 362 unique participants were included in the analysis (Figure 1), providing 284 swab samples and 352 blood samples. About three-quarters of participants (274/362) provided both sample types, and the remainder (88/362) provided only 1 type (either blood or swab).

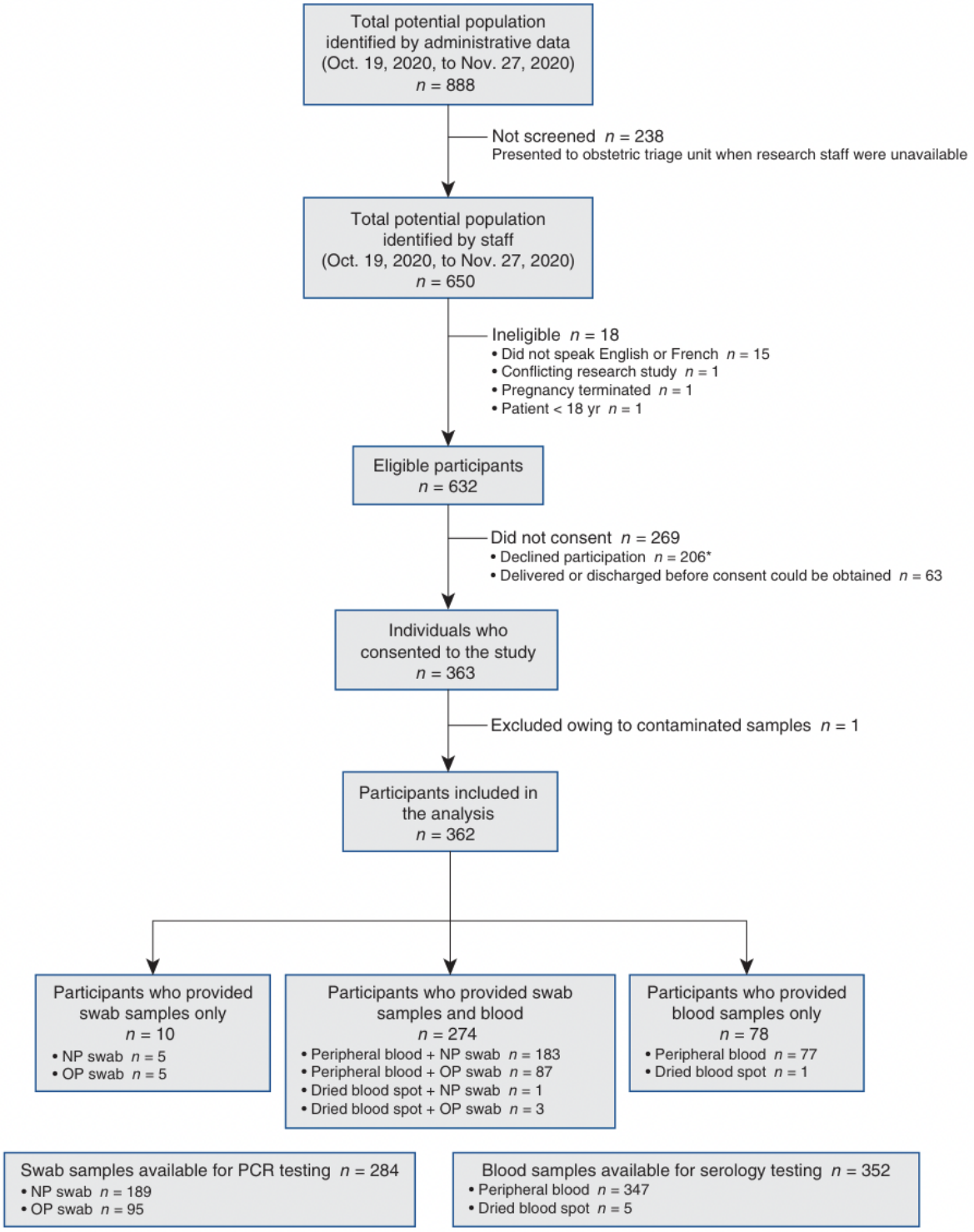


Figure 1: Flow chart of study enrolment and sample collection. Note: NP = nasopharyngeal, OP = oropharyngeal, PCR = polymerase chain reaction. *Common reasons for nonparticipation are summarized in Appendix 1, Section 4.

Participant characteristics

The sociodemographic, clinical and pregnancy characteristics of the study cohort are summarized in Table 1. Most participants (*n* = 320, 88.4%) were in their third trimester of pregnancy, multiparous (*n* = 195, 53.9%) and did not have preexisting health conditions (*n* = 306, 84.5%). The average maternal age was 32.4 (SD 4.9) years. Participants were evenly distributed across neighbourhood median family income quintiles. The median gestational age at delivery was 39.0 (IQR 38.0–40.0) weeks, and 141 (38.9%) participants gave birth by cesarean delivery. A total of 57 (15.7%) participants had symptoms consistent with COVID-19 upon presentation to triage.

Prevalence of SARS-CoV-2 infection

Among the 284 participants who provided a swab sample, 2 (0.7%) tested positive for SARS-CoV-2 by PCR.

Serology test results are summarized in Figure 2. Among the 352 participants who provided a blood sample, 45 (12.8%) had IgM antibodies against SARS-CoV-2 and 12 (3.4%) had IgA antibodies. However, based on the presence of IgG antibodies, 16 (4.5%) met the criteria for seropositivity for SARS-CoV-2. Of the 16 seropositive participants, 3 (18.8%) were also positive for IgA and 1 (6.2%) was also positive for IgM. Three of the seropositive participants had received a positive PCR result through community testing before the study; the remaining 13 had not previously tested positive for SARS-CoV-2. Neither of the 2 PCR-positive participants were seropositive.

Table 1 (part 1 of 2): Sociodemographic, clinical and pregnancy characteristics of study participants

Characteristic	No. (%) of participants* *n* = 362
Trimester at triage visit†	
1st (< 14 weeks' gestation)	< 6 (S)
2nd (14–28 weeks' gestation)	41 (11.3)
3rd (≥ 28 weeks' gestation)	320 (88.4)
Symptoms consistent with COVID-19 upon admission to triage‡	57 (15.7)
SARS-CoV-2 infection in pregnancy documented in medical chart§	5 (1.4)
Maternal age, yr, mean ± SD	32.4 ± 4.9
Parity	
0	166 (45.9)
≥ 1	195 (53.9)
Missing	< 6 (S)
Neighbourhood median family income quintile	
1 (lowest)	51 (14.1)
2	80 (22.1)
3	73 (20.2)
4	80 (22.1)
5 (highest)	76 (21.0)
Missing	< 6 (S)
Race and ethnicity¶	
White	203 (56.1)
Asian	28 (7.7)
Black	26 (7.2)
Other	45 (12.4)
Missing	60 (16.6)
Prepregnancy BMI, median (IQR)	25.6 (21.9–30.3)
Obese (BMI > 30.0)**	
No	228 (63.0)
Yes	86 (23.8)
Missing	48 (13.3)
Substance use during pregnancy††,‡‡	
No	323 (89.2)
Yes	35 (9.7)
Missing	< 6 (S)
Anxiety‡‡	
No	277 (76.5)
Yes	85 (23.5)
Depression‡‡	
No	311 (85.9)
Yes	51 (14.1)
Pre-existing maternal health conditions	
None	306 (84.5)
Asthma	44 (12.2)
Chronic hypertension	7 (1.9)
Diabetes	7 (1.9)

Table 1 (part 2 of 2): Sociodemographic, clinical and pregnancy characteristics of study participants

Characteristic	No. (%) of participants* n = 362
Gestational diabetes	
No	324 (89.5)
Yes	38 (10.5)
Hypertensive disorder in pregnancy§§	
No	314 (86.7)
Yes	48 (13.3)
Antenatal health care provider	
Family physician only	24 (6.6)
Obstetrician only	252 (69.6)
Family physician and obstetrician	44 (12.2)
Midwife	31 (8.6)
Other provider	8 (2.2)
No provider	< 6 (S)
Missing	< 6 (S)
Number of fetuses	
Singleton	345 (95.3)
Multiple	17 (4.7)
Gestational age at delivery, wk, median (IQR)	39.0 (38.0–40.0)
Preterm delivery (< 37 weeks' gestation)	
No	310 (85.6)
Yes	51 (14.1)
Missing	< 6 (S)
Mode of delivery	
Vaginal	221 (61.0)
Cesarean	141 (39.0)
Missing	< 6 (S)
Birth outcome	
Live birth	361 (99.7)
Intrapartum stillbirth	< 6 (S)

Note: BMI = body mass index, IQR = interquartile range, S = suppressed due to small cell size, SD = standard deviation.
*Unless indicated otherwise.
†Trimester of triage visit was calculated using the date that the patient was first enrolled in the study. ‡Participant reported symptoms consistent with COVID-19 on Febrile Respiratory Illness Screening Tool used at hospital entry. §Participant had documentation of a positive SARS-CoV-2 laboratory test result that was reported during pregnancy and within time period of study.
¶Information on race and ethnicity was obtained from the Ontario birth registry (Better Outcomes Registry & Network) and supplemented with medical chart review wherever possible. Racial and ethnic designations were assigned by the provider, sometimes through self-declaration by patients.
**BMI values below 10.3 and above 79.9 were excluded as outliers and set to missing for BMI grouping and obesity. ††Substance use during pregnancy is defined as alcohol, drug or smoking during pregnancy.
‡‡Self-reported variables obtained from the Ontario birth registry (Better Outcomes Registry & Network).
§§Conditions include eclampsia, gestational hypertension, HELLP (hemolysis, elevated liver enzymes and low platelets), preeclampsia and pre-existing hypertension with superimposed preeclampsia.

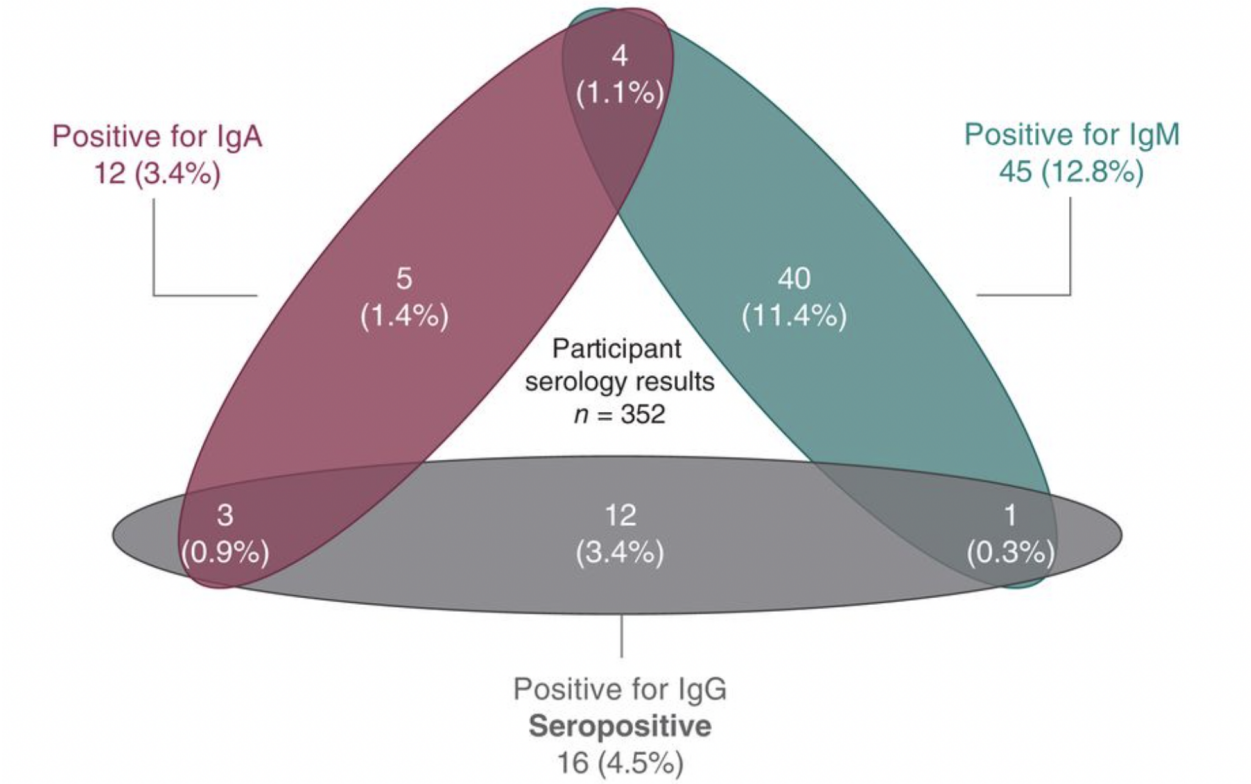


Figure 2: Serology results of participants (*n* = 352). Participants with immunoglobulin (Ig) G antibodies against SARS-CoV-2 were considered seropositive.

Overall, 4.9% (18/362) participants had evidence of current or previous SARS-CoV-2 infection, based on PCR or antibody testing. Five were symptomatic (2/2 PCR-positive participants and 3/16 seropositive participants) and 13 were asymptomatic at the time of testing. Participant-reported symptoms included dry cough, shortness of breath, congestion, nausea, vomiting, abdominal pain and unexplained fatigue.

Interpretation

In this descriptive study of patients admitted to obstetric triage units at The Ottawa Hospital during the second local wave of the COVID-19 pandemic, the prevalence of active SARS-CoV-2 infection was 0.7%. Seroprevalence based on the presence of IgG antibodies was 4.5%; 3.4% of

serology samples exhibited IgG alone, whereas 1.1% exhibited IgG in combination with either IgA or IgM.

Our findings are similar to those from a study conducted in Toronto during the first wave of the pandemic, where the prevalence of active SARS-CoV-2 infection in the obstetric population was estimated at 0.9%. However, seroprevalence in our sample was substantially higher than what was reported in BC during the first wave (< 1%).[12] This may, in part, reflect the later time period during which our study was conducted; the larger second wave of the pandemic in Canada began after a period of relaxation of public health measures during the late summer and early fall of 2020, and it follows that the number of individuals with a history of SARS-CoV-2 infection increased with time.

Antibodies to SARS-CoV-2 may develop days or weeks after onset of clinical illness.[18,19] Immunoglobulin G antibodies may persist for several months or more after infection,[20] whereas IgM and IgA antibodies decay more rapidly.[21] For this reason, we based our estimates of seroprevalence on the presence of IgG antibodies. The presence of IgM and IgA antibodies without IgG in 13.6% of our samples is likely the result of cross-reactivity in our assays with seasonal coronavirus strains.[22,23] Our finding that most seropositive participants exhibited IgG antibodies alone suggests that they had likely contracted SARS-CoV-2 weeks, if not months, before the study.

Interestingly, just 18.7% (3/16) of seropositive cases had documentation of a positive SARS-CoV-2 test in their medical records. At the time this study was conducted, PCR tests were available through local pharmacies and clinical assessment centres; however, access to PCR testing was limited in the early period of the pandemic, which may have contributed to the lack of testing among these cases. Alternatively, these individuals could have refrained from testing owing to asymptomatic presentation. Rapid tests were not widely available to the public.

Our study has several strengths. We determined active SARS-CoV-2 infection by digital droplet PCR, a more sensitive technique than traditional PCR methods (sensitivity 87.4%–97.6% v. 70%).[24,25] We employed serologic testing, a service that was not available through the Ontario

publicly funded health care system or private clinics at the time of the study. In secondary waves of disease outbreak and spread, serologic data provide essential complementary information to PCR data.[19] Indeed, this approach allowed us to identify participants with a history of SARS-CoV-2 infection, who otherwise would not have been identified through conventional PCR testing.

Although the prevalence data presented in this study alludes to the burden of COVID-19 in the local obstetric population, this study also provides insights on implementation of virus and serology testing of patients at our tertiary care centre. Testing was offered free of charge and provided participants with information as to whether they were currently infected or had recently been infected with SARS-CoV-2; however, about a third of eligible people declined participation. Leading reasons for not wanting to participate, as indicated during the consent process, included desire to avoid the physical discomfort caused by testing, and anxiety regarding possible care and lifestyle implications of testing positive.

Stigma and discrimination against individuals who have had COVID-19 are well documented[26,27] and are shown to influence individuals' decisions to get tested or seek treatment. [28,29] Where SARS-CoV-2 testing continues to be a predominantly elective process, more work is needed to examine and address individual-, community- and system-level barriers that inhibit SARS-CoV-2 test-seeking behaviours.[30] Implementation of universal testing protocols at our hospital centre may have improved our study's enrolment rate; however, the logistics of implementing such protocols are complex. Whether universal testing programs are a justifiable use of resources remains a subject of debate,[6,31] and such programs have only been adopted elsewhere as temporary measures early in the first wave of the pandemic.[4,6,32–34] For these programs to be effective, patients and visitors must be willing to submit to testing, testing methods need to be reliable, and staff and laboratory resources must be readily available to accommodate timely reporting of results. Finally, given the high financial costs, there must be substantive benefits to both patients and the health system.

Limitations

As our study was a single-centre initiative, our findings may not be generalizable to obstetric populations elsewhere. However, our sample was derived from a large patient population

accessing the largest hospital network in Ottawa–Gatineau and thus provides meaningful insight into the burden of COVID-19 in obstetric patients from Canada's National Capital Region. Further, our sample is well characterized, with detailed information on sociodemographic, clinical and pregnancy characteristics, facilitating comparison with other populations. As noted earlier, we did not test all patients who presented to the obstetric triage unit, and a large number of potential participants were missed or declined participation. It is therefore possible that our participants differ from the obstetric population of The Ottawa Hospital as a whole. The proportion of our study population that gave birth by cesarean delivery (39%) was slightly higher than what has been previously reported by The Ottawa Hospital (about 30%). It is possible that patients delivering via cesarean were more likely to participate in the study than those in active labour; however, it is unknown whether this selection bias would differ by SARS-CoV-2 infection status.[35] The presence or absence of COVID-19 symptoms was self-reported by participants at the time of consent, and we were unable to ascertain symptoms participants had outside of their triage visit. This limited our ability to capture information on symptoms that may have been experienced by recovered participants to determine if they were symptomatic or asymptomatic at the time of infection. It also limited our ability to capture symptom information from presymptomatic cases.

Conclusion

The prevalence of SARS-CoV-2 infection among obstetric patients who presented to obstetric triage units during Ottawa's second pandemic wave was 0.7% for active infection and 4.5% for recovered infection. Our low participation rate highlights opportunities to improve patient education and public health messaging about the benefits of testing programs.

Acknowledgements
The authors acknowledge the nurses, obstetricians, family physicians, midwives and clerks at the Birthing Unit and Mother Baby Unit, as well as the laboratory technicians, within The Ottawa Hospital for their support and assistance with this research study. They also gratefully acknowledge the patients who participated in the study. Lastly, they acknowledge several individuals for their assistance in study recruitment and coordination including Chantal Horth, Marisa Murray, Joseph Cyr and Kathryn Denize.

Competing interests: None declared.

Contributors: Romina Fakhraei, Malia Murphy, Alysha Dingwall-Harvey, Ruth Rennicks White, Deshayne Fell, Marc-André Langlois and Darine El-Chaâr contributed to the conception and design of the work. Romina Fakhraei, Erica Erwin, Kameela Alibhai, Sheryll Dimanlig-Cruz, Rosemary LaRose, Kimberly Grattan, Jian-Jun Jia, George Liu, Corey Arnold, Yannick Galipeau, Khatereh Shir-Mohammadi, Gillian Alton, Jessica Dy and Darine El-Chaâr contributed to the acquisition, analysis and interpretation of data. Romina Fakhraei, Erica Erwin, Kameela Alibhai and Malia Murphy drafted the manuscript. All of the authors revised it critically for important intellectual content, gave final approval of the version to be published and agreed to be accountable for all aspects of the work.

Supplemental information: For reviewer comments and the original submission of this manuscript, please see www.cmajopen.ca/content/10/3/E643/suppl/DC1.

Funding: This research was supported by the Canadian Institutes of Health Research (no. VR4-172760).

Data sharing: The data are not publicly available owing to their containing information that could compromise the privacy of research participants. The data that support the findings of this study are available on request from the corresponding author with the permission of the Better Outcomes Registry & Network Ontario.

References

1.de Oliveira Menezes M, Andreucci CB, Nakamura-Pereira M, et al. Universal COVID-19 testing in the obstetric population: impacts on public health [article in Portuguese]. Cad Saude Publica 2020;36:e00164820.

2. Wei SQ, Bilodeau-Bertrand M, Liu S, et al. The impact of COVID-19 on pregnancy outcomes: a systematic review and meta-analysis. CMAJ 2021;193:E540-8.

3. Gagliardi L, Danieli R, Suriano G, et al. Universal severe acute respiratory syndrome coronavirus 2 testing of pregnant women admitted for delivery in 2 Italian regions. Am J Obstet Gynecol 2020;223:291-2.

4. Naqvi M, Burwick RM, Ozimek JA, et al. Severe acute respiratory syndrome coronavirus 2 (SARS-CoV-2) universal testing experience on a Los Angeles labor and delivery unit. Obstet Gynecol 2020;136:235-6.

5. Maru S, Patil U, Carroll-Bennett R, et al. Universal screening for SARSCoV-2 infection among pregnant women at Elmhurst Hospital Center, Queens, New York. PLoS One 2020;15:e0238409.

6. LaCourse SM, Kachikis A, Blain M, et al. Low prevalence of severe acute respiratory syndrome coronavirus 2 among pregnant and postpartum patients with universal screening in Seattle, Washington. Clin Infect Dis 2021;72:869-72.

7. Yokoyama R, Kurano M, Morita Y, et al. Validation of a new automated chemiluminescent anti-SARS-CoV-2 IgM and IgG antibody assay system detecting both N and S proteins in Japan. PLoS One 2021;16:e0247711.

8. Ibarrondo FJ, Fulcher JA, Goodman-Meza D, et al. Rapid decay of anti-SARSCoV-2 antibodies in persons with mild Covid-19. N Engl J Med 2020; 383:1085-7.

9. Whitman JD, Hiatt J, Mowery CT, et al. Test performance evaluation of SARSCoV-2 serological assays. medRxiv 2020 May 17. doi: 10.1101/2020.04.25.20074856.

10. Trahan M-J, Mitric C, Malhamé I, et al. Screening and testing pregnant patients for SARS-CoV-2: first-wave experience of a designated COVID-19 hospitalization centre in Montréal. J Obstet Gynaecol Can 2021;43:571-5.

11. Mei-Dan E, Satkunaratnam A, Cahan T, et al. Questionnaire-based vs universal PCR testing for SARS-CoV-2 in women admitted for delivery. Birth 2021;48:96-103.

12. McClymont E, Elwood C, Sekirov I, et al. Population SARS-CoV-2 seroprevalence using antenatal serum samples in British Columbia, Canada. J Obstet Gynaecol Can 2021;43:1242-3.

13. COVID-19 cases and deaths in Ottawa [daily COVID-19 dashboard]. Ottawa: Ottawa Public Health; 2020. Available: https://www.arcgis.com/home/item. html?id=6bfe7832017546e5b30c5cc6a201091b (accessed 2021 Mar. 23). Login required to access content.

14. COVID-19 guidance: labour, delivery and newborn care - version 3. Ottawa: Ontario Ministry of Health; 2020 Nov. 10. Available: https://www.health.gov. on.ca/en/pro/programs/publichealth/coronavirus/docs/2019_labour_delivery_ newborn_guidance.pdf (accessed 2022 June 22).

15. Government of Canada invests in new research to address COVID-19 variants [news release]. Ottawa: Canadian Institutes of Health Research; 2021 Mar. 26. Available: https://www.canada.ca/en/institutes-health-research/news/2021/03/ government-of-canada-invests-in-new-research-to-address-covid-19-variants. html (accessed 2021 June 23).

16. Information for those who have symptoms, test positive for COVID-19 and high-risk contacts. Ottawa: Ottawa Public Health. Available: https://www. ottawapublichealth.ca/en/public-health-topics/self-isolation-instructions-for -novel-coronavirus-covid-19.aspx (accessed 2021 Aug. 24).

17. Murphy MSQ, Fell DB, Sprague AE, et al. Data resource profile: Better Outcomes Registry & Network (BORN) Ontario. Int J Epidemiol 2021; 50:1416-7h.

18. Molina LP, Chow S-K, Nickel A, et al. Prolonged detection of severe acute respiratory syndrome coronavirus 2 (SARS-CoV-2) RNA in an obstetric patient with antibody seroconversion. Obstet Gynecol

2020;136:838-41. 19. Galipeau Y, Greig M, Liu G, et al. Humoral responses and serological assays in SARS-CoV-2 infections. Front Immunol 2020;11:610688.
20. Dan JM, Mateus J, Kato Y, et al. Immunological memory to SARS-CoV-2 assessed for up to 8 months after infection. Science 2021;371:eabf4063.
21. Iyer AS, Jones FK, Nodoushani A, et al. Persistence and decay of human antibody responses to the receptor binding domain of SARS-CoV-2 spike protein in COVID-19 patients. Sci Immunol 2020;5:eabe0367. 22. Miyara M, Saichi M, Sterlin D, et al. Pre-COVID-19 immunity to common cold human coronaviruses induces a recall-type IgG response to SARSCoV-2 antigens without cross-neutralisation. Front Immunol 2022;13:790334.
23. Ivanov A, Semenova E. Long-term monitoring of the development and extinction of IgA and IgG responses to SARS-CoV-2 infection. J Med Virol 2021;93:5953-60.
24. Dong L, Zhou J, Niu C, et al. Highly accurate and sensitive diagnostic detection of SARS-CoV-2 by digital PCR. Talanta 2021;224:121726.
25. Suo T, Liu X, Feng J, et al. ddPCR: a more sensitive and accurate tool for SARS-CoV-2 detection in low viral load specimens. Emerg Microbes Infect 2020; 9:1259-68.
26. Taylor S, Landry CA, Rachor GS, et al. Fear and avoidance of healthcare workers: an important, under-recognized form of stigmatization during the COVID-19 pandemic. J Anxiety Disord 2020;75:102289.
27. Mukumbang FC. Pervasive systemic drivers underpin COVID-19 vulnerabilities in migrants. Int J Equity Health 2021;20:146.
28. COVID-19: reducing stigma. Gatineau (QC): Indigenous Services Canada; modified 2021 July 28. Available: https://www.sac-isc.gc.ca/ eng/1627070714082/1627070737178 (accessed 2022 Mar. 8).
29. Stigma and prejudice: How to combat the rise in discrimination that has been sparked by the COVID-19 pandemic. Toronto: Centre for Addiction and Mental Health. Available: https://www.camh.ca/en/health-info/mental -health-and-covid-19/stigma-and-prejudice (accessed 2022 Mar. 8).
30. Embrett M, Sim SM, Caldwell HAT, et al. Barriers to and strategies to address COVID-19 testing and testing hesitancy: a rapid scoping review. BMC Public Health 2022;22:750.
31. Metz TD. Is universal testing for severe acute respiratory syndrome coronavirus 2 (SARS-CoV-2) needed on all labor and delivery units? Obstet Gynecol 2020; 136:227-8.
32. Goldfarb IT, Diouf K, Barth WH, et al. Universal SARS-CoV-2 testing on admission to the labor and delivery unit: low prevalence among asymptomatic obstetric patients. Infect Control Hosp Epidemiol 2020;41:1095-6. 33. Ochiai D, Kasuga Y, Iida M, et al. Universal screening for SARS-CoV-2 in asymptomatic obstetric patients in Tokyo, Japan. Int J Gynaecol Obstet 2020; 150:268-9.
34. Breslin N, Baptiste C, Gyamfi-Bannerman C, et al. Coronavirus disease 2019 infection among asymptomatic and symptomatic pregnant women: two weeks of confirmed presentations to an affiliated pair of New York City hospitals. Am J Obstet Gynecol MFM 2020;2:100118.
35. Obstetric anesthesiology. Ottawa: The Ottawa Hospital; 2017 Jan. 6. Available: https://www.ottawahospital.on.ca/en/clinical-services/deptpgrmcs/departments/ anesthesiology/obstetric-anesthesiology/#:~:text=Our%20caesarean%20section %20rate%20is,9%20epidurals%20in%20a%20day (accessed 2022 June 22).

A-1.11 Antibody Seronegativity in COVID-19 RT-PCR–Positive Children

Preface

(This work has been previously published as a research article)

Bhatt M, Zemek RL, Tang K, Malley R, Plint AC, Pham-Huy A, Dawson J, McGahern C, Pelchat M, Arnold C, **Galipeau Y**, Langlois MA. **Antibody Seronegativity in COVID-19 RT-PCR-Positive Children**. Pediatr Infect Dis J. 2022 Aug 1;41(8):e318-e320.
doi: 10.1097/INF.0000000000003573. Epub 2022 Jul 13.

https://doi.org/10.1097/inf.0000000000003573

Copyright © 2022 Wolters Kluwer Health, Inc. All rights reserved.

Abstract

This substudy of a prospective case-ascertained household transmission study investigated severe acute respiratory syndrome coronavirus 2 reverse transcription polymerase chain reaction–positive individuals without antibody development and factors associated with nonseroconversion. Approximately 1 of 8 individuals with coronavirus disease 2019 did not seroconvert. Children, particularly the youngest, were approximately half as likely to seroconvert compared with adults. Apart from the absence of fever/chills, individual symptoms did not strongly predict nonseroconversion.

The standard for diagnosing acute symptomatic and asymptomatic coronavirus disease 2019 (COVID-19) infection is severe acute respiratory syndrome coronavirus (SARS-CoV-2) gene detection via nucleic acid amplification testing, such as reverse transcription polymerase chain reaction (RT-PCR). A humoral immune response consisting of SARS-CoV-2–specific antibodies (seroconversion) is often detectable 5 days postsymptom onset (IgM) and can remain detectable 12 months postinfection (IgG).[1] However, not all infected individuals seroconvert; disease severity, symptoms, and viral load may affect antibody response, and the response may differ between children and adults.[2–6] This study investigated SARS-CoV-2 RT-PCR–positive individuals without antibody development and factors associated with nonseroconversion.

Material and Methods

We conducted a secondary analysis of a prospective case-ascertained study of household COVID-19 transmission in Ottawa, Canada, from September 2020 to March 2021. All participating households had at least 1 member with RT-PCR–confirmed COVID-19 infection and where at least 1 participating member was a child (<18 years). Participants with a positive COVID-19 RT-PCR test were included in this substudy; vaccinated individuals were excluded. Participants underwent phlebotomy for SARS-CoV-2–specific antibody measurement at least 2 weeks after diagnosis (no maximum postinfection duration). Automated chemiluminescent enzyme-linked immunosorbent assay (ELISA) assays evaluated SARS-CoV-2–specific IgA, IgM and IgG against the spike-trimer and nucleocapsid protein (Langlois Laboratory, University of Ottawa). The validated serology platform used in the Langlois Laboratory has a sensitivity and specificity of >98%, and is comparable to 10 other commercial platforms.[7,8] Samples were considered isotype positive for an individual isotype (IgG, IgA or IgM) when both antispike and antinucleocapsid antibodies were detected above cutoff values (S/CO ≥ 1). Samples were considered SARS-CoV-2-antibody–positive (as a result of infection) when IgG was positive, or if both IgA and IgM were positive. The primary outcome was the proportion of participants who did not seroconvert (SARS-CoV-2-antibody–negative). Factors associated with nonseroconversion were examined. Univariable and multivariable logistic regressions were fitted with estimation of robust

(Huber-White) standard errors applying household as the clustering unit to examine factors related to nonseroconversion. The Research Ethics Boards of CHEO (20/81/X), The Ottawa Hospital (20200673-01K) and University of Ottawa (20200358) approved this study.

Results

Three hundred thirty RT-PCR–positive participants [162 children, median age 8.9 years (IQR 5.6–13.1) and 168 adults, median age 40.7 years (IQR 36.5–46.8)] completed blood sampling for SARS-CoV-2 antibodies. Forty-three [13%; 95% confidence interval (CI): 9.7–17.0] did not seroconvert, 63% (27/43) of whom were children (Table 1). All hospitalized participants (10/330, 3%) seroconverted. Individuals who were asymptomatic at time of RT-PCR testing were no more or less likely to seroconvert [odds ratio (OR) = 0.4; 95% CI: 0.1–1.2]. Seroconversion was not associated with time since infection (≤30 vs >30 days; OR = 0.9; 95% CI: 0.4–1.8).

Predictors of Nonseroconversion

Multivariable analysis revealed children 0–4 years of age had lower odds of seroconversion than older children (5–11 years: OR = 0.2; 95% CI: 0.1–0.7 and 12–17 years: OR = 0.1; 95% CI: 0.0–0.5) and adults (18–49 years: OR = 0.1; 95% CI: 0.1–0.4 and >50 years: OR = 0.1; 95% CI: 0.0–0.4). Odds of seroconversion decreased with decreasing age. Symptom count (1, 2 symptoms) was not associated with seroconversion (OR = 1.7; 95% CI: 0.2–14.3 and OR = 1.0; 95% CI: 0.1–8.2, respectively). The presence of fever/chills was associated with increased seroconversion (OR = 0.4; 95% CI: 0.2–0.9). There was no demonstrable association between nonseroconversion and the presence of cough/shortness-of-breath (OR = 2.1; 95% CI: 0.8–5.7), rhinorrhea when it was the only symptom (OR = 3.1; 95% CI: 0.6–15.2) and the presence of ≥3 symptoms (OR = 4.5; 95% CI: 0.9–23.9).

TABLE 1. - Clinical and Demographical Characteristics of COVID-19 Patients According to Seroconversion Status (Overall Call)

	Overall (n = 330) No. (%)	Seroconverters (n = 287) No. (%)	Nonseroconverters (n = 43) No. (%)
Age (yr), median (IQR)	19.3 (9.0–41.0)	30.3 (9.6–41.4)	12.0 (5.3–36.5)
Age group			
Preschool (0–4 yr)	34 (10.3)	24 (8.4)	10 (23.3)
School age (5–11 yr)	81 (24.5)	70 (24.4))	11 (25.6)
Adolescent (12–17 yr)	47 (14.2)	41 (14.3)	6 (14.0)
Adult (18–49 yr)	145 (43.9)	130 (45.3)	15 (34.9)
Older adult (>50 yr)	23 (7.0)	22 (7.7)	1 (2.3)
Female	169 (51.5)	149 (52.3)	20 (46.5)
Race			
Indigenous identity	4 (1.2)	4 (1.4)	0 (0.0)
Black	37 (11.2)	36 (12.5)	1 (2.3)
Asian	6 (1.8)	6 (2.1)	0 (0.0)
South Asian	2 (0.6)	2 (0.7)	0 (0.0)
West Asian	38 (11.5)	34 (11.8)	4 (9.3)
Latin American	8 (2.4)	7 (2.4)	1 (2.3)
White	256 (77.6)	218 (76.0)	38 (88.4)
Other*	2 (0.6)	2 (0.7)	0 (0.0)
1+ underlying comorbidities	69 (20.9)	60 (20.9)	9 (20.9)
Symptom burden			
Asymptomatic	61 (18.4)	57 (19.7)	4 (9.3)
Mild (no hospitalization)	261 (78.6)	222 (76.8)	39 (90.7)
Moderate (hospitalized, no ICU)	7 (2.1)	7 (2.4)	0 (0.0)
Severe/critical (ICU)	3 (0.9)	3 (1.0)	0 (0.0)
Symptoms			
Fever (≥38) or chills	145 (44.8)	131 (46.5)	14 (33.3)
Sore throat	132 (41.4)	110 (39.3)	22 (56.4)
Runny nose as the only symptom	20 (6.1)	15 (5.2)	5 (11.9)
Cough/SOB	169 (51.4)	142 (49.7)	27 (62.8)
Vomiting or diarrhea	73 (22.3)	65 (22.8)	8 (18.6)
Nausea	55 (16.9)	44 (15.4)	11 (26.8)
Headache	172 (53.6)	156 (55.1)	16 (42.1)
Rash	16 (4.9)	15 (5.3)	1 (2.3)
Conjunctivitis	13 (3.9)	12 (4.2)	1 (2.3)
Muscle aches	125 (38.6)	110 (38.7)	15 (37.5)
Joint aches	89 (27.5)	78 (27.5)	11 (27.5)
Loss of appetite	101 (30.8)	90 (31.6)	11 (25.6)
Loss of smell or taste	115 (35.7)	108 (38.3)	7 (17.5)

*Nonspecified selection of more than 1 category.
COVID indicates coronavirus disease; ICU, intensive care unit; IQR, interquartile range; SOB, shortness-of-breath.

Discussion

In this study, approximately 1 of 8 individuals with COVID-19 did not seroconvert. Children, particularly the youngest, were approximately half as likely to seroconvert compared with adults. Apart from the absence of fever/chills, individual symptoms did not strongly predict nonseroconversion. Although young children and adults have been found to have similar respiratory SARS-CoV-2 viral loads, children's failure to seroconvert could be due to robust mucosal immunity or lower expression of angiotensin converting enzyme-2-receptors in the nasal epithelium.[9,10] In a recent study by Toh et al,[6] 61% of children with RT-PCR–confirmed SARS-CoV-2 infection did not seroconvert. This proportion is significantly higher than we observed,

possibly due to their younger cohort [median age 4 years (IQR 2–10) vs. 9 years (IQR 6–13)], as we observed decreased odds of seroconversion with decreasing age. In this study, lower viral load was associated with nonseroconversion; it is possible that a greater proportion of children in this cohort had a low viral load leading to the high rate of nonseroconversion.

Our study has limitations. Because of noncentralized RT-PCR testing in our region, we could not obtain Ct values as a proxy for viral load. Highly sensitive RT-PCR testing has been associated with nonseroconversion.[4] We did not standardize time of antibody testing in relation to confirmed infection date. However, seroconversion did not differ between those tested ≤30 and >30 days from infection. Some symptoms (eg, loss of taste or smell) may be difficult to discern in infants and young children.

Our findings support emerging evidence of uneven antibody responses to SARS-CoV-2 infection, especially in children. Therefore, seroprevalence studies in children should be interpreted with caution, as they may underestimate prior infection. It is not known whether previously infected individuals who do not seroconvert are protected from subsequent infection; theoretically, memory B-cells and T-cells may be contributing to protection even in the absence of circulating antibodies. Nevertheless, natural infection should not diminish the recommendation for widespread vaccination as we continue to learn about the longevity of natural antibody protection, antibody neutralization and the interplay between natural and vaccine immunity. Public health messaging should inform populations that seroconversion, and possibly immunity, cannot be assumed after a symptomatic infection.

References

1. Post N, Eddy D, Huntley C, et al. Antibody response to SARS-CoV-2 infection in humans: a systematic review. PLoS One. 2020;15:e0244126.

2. Yang HS, Costa V, Racine-Brzostek SE, et al. Association of age with SARS-CoV-2 antibody response. JAMA Netw Open. 2021;4:e214302.

3. Majdoubi A, Michalski C, O'Connell SE, et al. A majority of uninfected adults show preexisting antibody reactivity against SARS-CoV-2. JCI Insight. 2021;6:146316.

4. Wei J, Matthews PC, Stoesser N, et al; COVID-19 Infection Survey team. Anti-spike antibody response to natural SARS-CoV-2 infection in the general population. Nat Commun. 2021;12:6250.

5. Alshami A, Al Attas R, Anan H, et al. Durability of antibody responses to SARS-CoV-2 infection and its relationship to disease severity assessed using a commercially available assay. Front Microbiol. 2021;12:770727.

6. Toh ZQ, Anderson J, Mazarakis N, et al. Comparison of seroconversion in children and adults with mild COVID-19. JAMA Netw Open. 2022;5:e221313.

7. Cholette F, Mesa C, Harris A, et al; COVID-19 Immunity Task Force (CITF) working group. Dried blood spot specimens for SARS-CoV-2 antibody testing: A multi-site, multi-assay comparison. PLoS One. 2021;16:e0261003.

8. Colwill K, Galipeau Y, Stuible M, et al. A "Made-in-Canada" serology solution for profiling humoral immune responses to SARS-CoV-2 infection and vaccination. medRxiv. 2021. doi: 10.1101/2021.10.25.21265476

9. Smith N, Goncalves P, Charbit B, et al. Distinct systemic and mucosal immune responses during acute SARS-CoV-2 infection. Nat Immunol. 2021;22:1428–1439.

10. Bunyavanich S, Do A, Vicencio A. Nasal gene expression of angiotensinconverting enzyme 2 in children and adults. JAMA. 2020;323:2427–2429.

A-1.12 LONGITUDINAL PROFILES OF PLASMA GELSOLIN, CYTOKINES AND ANTIBODY EXPRESSION PREDICT COVID-19 SEVERITY AND HOSPITALIZATION OUTCOMES

Preface

(This work has been previously published as a research article)

Asare-Werehene M, McGuinty M, Vranjkovic A, **Galipeau Y**, Cowan J, Cameron B, Cooper CL, Langlois MA, Crawley AM, Tsang BK. **Longitudinal profiles of plasma gelsolin, cytokines and antibody expression predict COVID-19 severity and hospitalization outcomes**. Front Immunol. 2022 Sep 6;13:1011084.

https://doi.org/10.3389/fimmu.2022.1011084

Copyright © 2022 Asare-Werehene, McGuinty, Vranjkovic, Galipeau, Cowan, Cameron, Cooper, Langlois, Crawley and Tsang

This is an open-access article distributed under the terms of the Creative Commons Attribution License (CC BY). The use, distribution or reproduction in other forums is permitted, provided the original author(s) and the copyright owner(s) are credited and that the original publication in this journal is cited, in accordance with accepted academic practice. No use, distribution or reproduction is permitted which does not comply with these terms.

Abstract

Background
Prognostic markers for COVID-19 disease outcome are currently lacking. Plasma gelsolin (pGSN) is an actin-binding protein and an innate immune marker involved in disease pathogenesis and viral infections. Here, we demonstrate the utility of pGSN as a prognostic marker for COVID-19 disease outcome; a test performance that is significantly improved when combined with cytokines and antibodies compared to other conventional markers such as CRP and ferritin.

Methods
Blood samples were longitudinally collected from hospitalized COVID-19 patients as well as COVID-19 negative controls and the levels of pGSN in μg/mL, cytokines and anti- SARS-CoV-2 spike protein antibodies assayed. Mean ± SEM values were correlated with clinical parameters to develop a prognostic platform.

Results
pGSN levels were significantly reduced in COVID-19 patients compared to healthy individuals. Additionally, pGSN levels combined with plasma IL-6, IP-10 and M-CSF significantly distinguished COVID-19 patients from healthy individuals. While pGSN and anti-spike IgG titers together strongly predict COVID-19 severity and death, the combination of pGSN and IL-6 was a significant predictor of milder disease and favorable outcomes.

Conclusion
Taken together, these findings suggest that multi-parameter analysis of pGSN, cytokines and antibodies could predict COVID-19 hospitalization outcomes with greater certainty compared with conventional clinical laboratory markers such as CRP and ferritin. This research will inform and improve clinical management and health system interventions in response to SARS-CoV-2 infection.

Introduction

COVID-19 is a respiratory infectious disease caused by SARS-CoV-2 (1–4). Currently, >599 million people are infected worldwide and >6.48 million SARS-CoV-2-related deaths have been recorded (World Health Organization) thus, requiring urgent health care interventions. SARS-CoV-2 suppresses the adaptive arm (B and T lymphocytes) of the immune system and overly activates the innate arm (macrophages, natural killer cells, dendritic cells), causing an inflammatory cytokine storm (TNF-α, IL-6, IL-8, IL-1β, MCP-1) (5). These immune reactions can result in lung damage, multiple organ dysfunctions and in severe cases, death (5, 6). To date, direct therapeutic options are limited to a modestly effective antiviral that remains inaccessible to most patients. Patients are managed using best supportive care including steroids, and in severe cases the use of mechanical ventilation and extracorporeal membrane oxygenation (ECMO) (7, 8). Identifying novel biomarkers will enable physicians to predict/assess the progress of COVID-19 patients and inform decision-making for available therapeutic intervention.

Lower viral titers contribute to false negative testing for SARS-CoV-2 (9, 10). Thus, an additional screening method that could detect possible infections despite lower viral titers will be highly beneficial. Antibodies directed to the nucleoprotein of SARS-COV-2 could be useful in identifying recent infections given most of the population will have detectable anti-spike antibody from prior infection and/or immunization (9, 10). As to whether their detection could be used to determine COVID-19 disease severity and clinical outcomes remain to be examined.

Laboratory markers including interleukin 6 (IL-6), C-reactive protein (CRP), ferritin, platelets, lactate dehydrogenase (LDH), erythrocyte sedimentation rate (ESR), D-dimer and lymphopenia are significantly implicated in COVID-19 complications (11, 12). Diseases like influenza, bacterial infection, and chronic inflammatory and neurodegenerative diseases trigger the elevation of these laboratory markers (13–15), hence casting doubts on their specificity and sensitivity as reliable prognostic markers for COVID-19 severity, hospitalization outcomes and ICU admissions.

Recently, proteomic screening of plasma samples from individuals with active COVID-19 disease has shown tha plasma gelsolin (pGSN) expression levels are downregulated compared to healthy controls (16–18). Gelsolin (GSN) is a 80-85kDa calcium-dependent multifunctional actin-binding protein which exists in three isoforms: cytoplasmic gelsolin (cGSN), pGSN, and gelsolin 3 (19, 20). pGSN has recently been shown to be a key player in the immune regulation of cancer (21). pGSN depletion significantly reduces its organ-protective function, leading to multi-organ dysfunction syndrome (MODS), increased mortality and long-term morbidity in survivors, complications that are commonly seen in COVID-19 patients (22–25).

Thus, it is conceivable that pGSN could be of clinical relevance in the pathogenesis of COVID-19. Its pathological significance and potential as a biomarker for COVID-19 severity and treatment response remains to be determined. In the present study, we have demonstrated a pGSN multi-analyte panel as a potential biomarker of poor COVID-19 outcomes and pGSN with cytokines and antibodies present as a significant predictor of COVID-19 hospitalization outcomes compared with conventional clinical laboratory markers.

Results

pGSN's combination with IL-6, IP-10 and M-CSF significantly distinguish hospitalized COVID-19 patients from healthy controls

COVID-19 negative and positive patients were recruited at TOH and their blood longitudinally collected. The subjects were stratified into COVID-19 negative and positive subjects and the levels of pGSN, cytokines and antibodies were quantified (Figure 1A). There were no significant differences in the levels of pGSN between males and females as well as age references (Supplementary Figure S1A, SB). pGSN levels were significantly lower ($p<0.0001$) in COVID-19 patients compared with the negative subjects (Figure 1B). On the contrary, IL-6 ($p=0.034$), M-CSF ($p=0.001$) and IP-10 ($p=0.023$) levels were significantly up-regulated in COVID-19 patients compared with the negative subjects whereas HGF and CTAK demonstrated a tendency to be significantly higher (Figure 1B). The ratio of pGSN and cytokines were calculated and used in several ratio analyses. The mean levels of pGSN/IL-6, pGSN/M-CSF, pGSN/HGF, pGSN/IP-10 and pGSN/CTAK were determined and compared between COVID-19 patients and

COVID-19 negative controls. All ratios tested were significantly decreased in COVID-19 patients compared with COVID-19 negative controls (Figure 1C; $p < 0.0001$). ROC curves were used to determine the diagnostic significance of these ratios in differentiating COVID-19+ patients from COVID-19- controls (Figure 1D). The combination of pGSN with IL-6, IP-10 and M-CSF but not HGF provided a significant 100% test accuracy with AUC of 1 (Figure 1D). Meanwhile, pGSN alone or cytokines alone provided a statistically significant AUC <1 (Figure 1D). To determine if these markers predicted disease progression in COVID-19 patients, pGSN levels measured over time were compared between days of sample collection. No significant differences were observed over time between the groups; however, a significant improvement ($p<0.002$) in the levels of pGSN were observed on day 30, potentially suggesting patients' conditions might be improving (Figure 1E and Supplementary Figures S1C-G).

The combination of pGSN and IL-6, IP-10, HGF, CTAK and M-CSF is associated with favorable COVID-19 outcomes

Having observed that pGSN significantly distinguishes COVID-19+ patients from COVID-19 negative controls, its prediction of disease severity, progression and hospitalization outcomes were subsequently investigated. Here, we correlated the levels of pGSN at day 1 of hospitalization with the clinical outcomes of the patients prior to being discharged alive or death (Figure 2). We observed that pGSN levels increased with increases in ICU admissions (Figure 2A). COVID-19 patients who were discharged had increased levels of pGSN suggesting their recovery (Figure 2A). Inflammatory cytokines (IL-6, IP-10, HGF, M-CSF and CTAK) as well as pGSN were elevated in severe COVID-19 patients reminiscent of reported cytokine storms (6, 26, 27) that are highly associated with increased organ damage (Figure 2B).

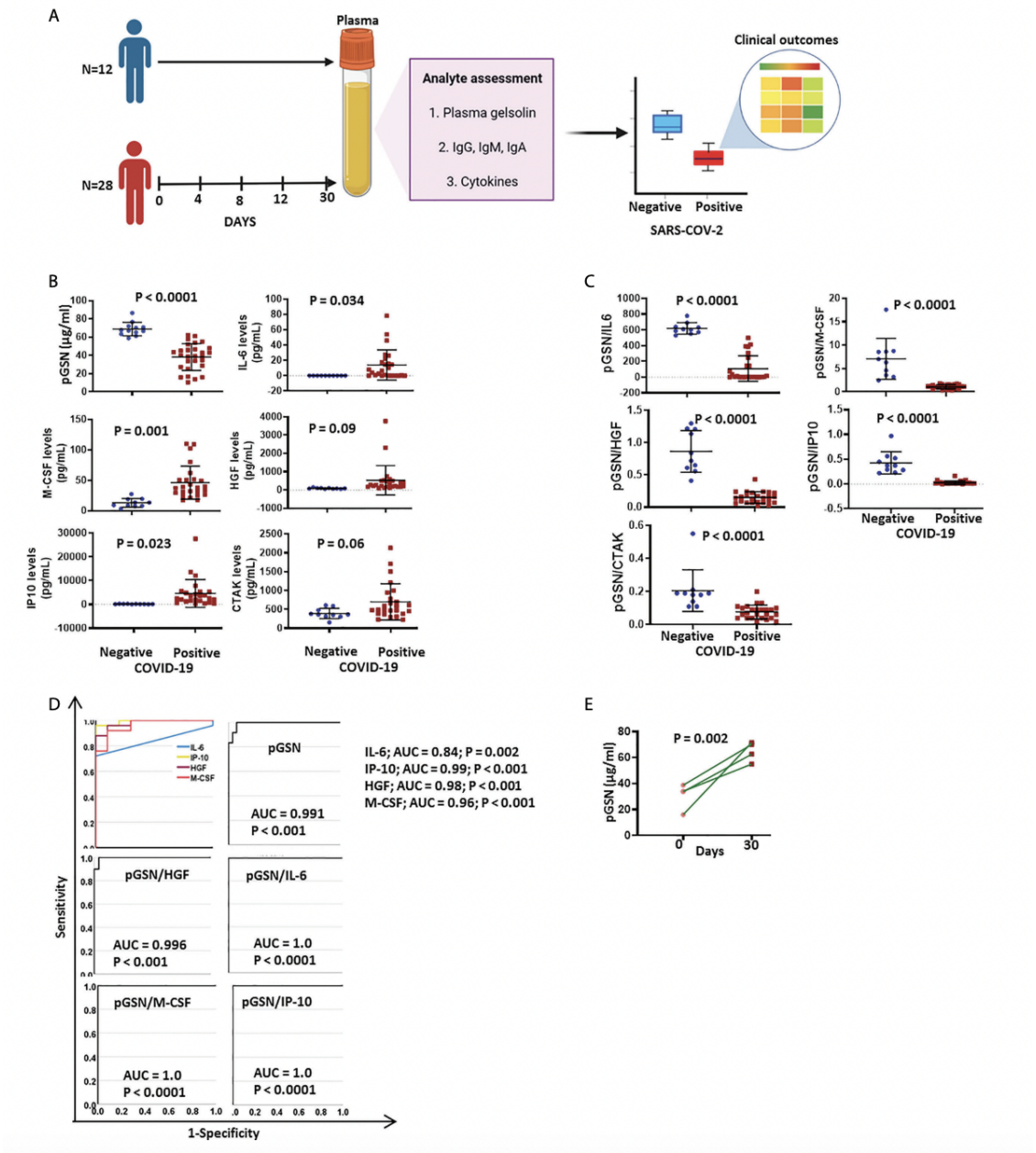


Figure 1 pGSN's combination with IL-6, IP-10 and M-CSF significantly discriminates COVID-19 positive patients from negative subjects. **(A)** 28 samples were serially collected from PCR-confirmed SARS-CoV-2-infected patients and 12 samples collected from non-COVID-19 controls. Samples were analyzed for the levels of pGSN, cytokines and anti-SARS-COV-2 antibodies. The mean levels of the analyte were compared between COVID-19 negative and positive subjects. The test performances of the biomarkers against clinical outcomes were analyzed. **(B)** The mean ± SEM levels of pGSN, IL-6, IP-10, M-CSF, HGF and CTAK were detected and compared between COVID-19 and non-COVID-19 patients. **(C)** The ratio of pGSN and cytokines were calculated and used as multi-analyte diagnostic panels. The mean ± SEM levels of pGSN/IL-6, pGSN/M-CSF, pGSN/HGF, pGSN/IP-10 and pGSN/CTAK were determined and compared between COVID-19 and non-COVID-19 subjects. **(D)** The test performances of pGSN, cytokines (IL-6, IP-10, HGF, M-CSF) and multi-analyte panels (pGSN/HGF, pGSN/IL-6, pGSN/M-CSF and pGSN/IP-10) in differentiating COVID-19 patients from non-COVID-19 subjects were determined using receiving operating characteristic (ROC) curves. **(E)** pGSN levels in blood collected on day 0 and 30 were compared. P-values were calculated by independent sample t-test.

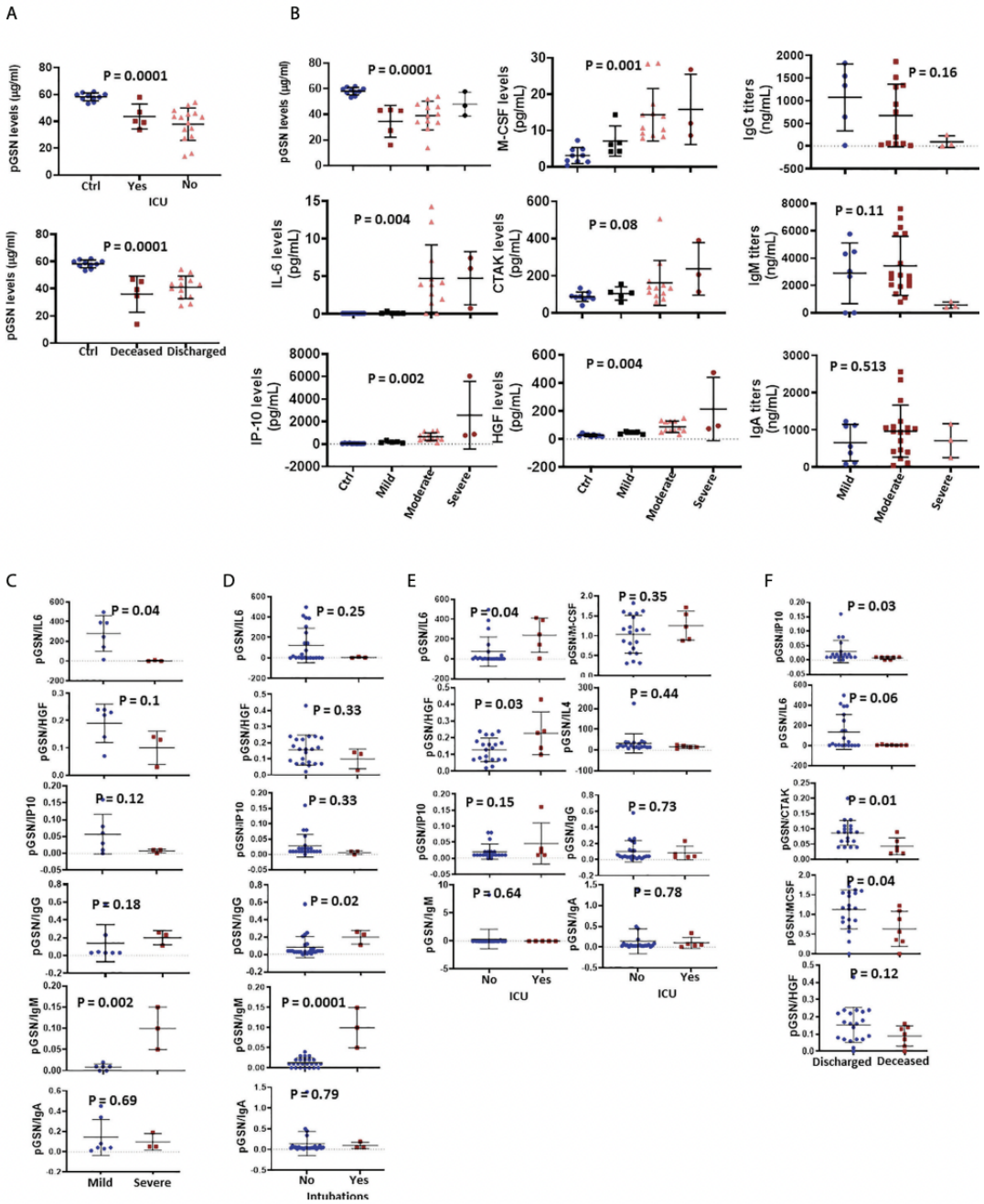


Figure 2 The combination of pGSN and IL-6, IP-10, HGF, CTAK and M-CSF is associated with favorable COVID-19 outcomes. **(A)** pGSN levels at day 0 were determined and the mean ± SEM compared between patients based on ICU admittance and hospitalization outcome. **(B)** The mean ± SEM levels of pGSN, IL-6, IP-10, M-CSF, HGF, CTAK, IgA, IgM and IgG were detected and compared between patients based on disease severity. The ratio of pGSN and cytokines were calculated and used as multi-analyte diagnostic panels. **(C)** The mean ± SEM levels of pGSN/IL-6, pGSN/HGF, pGSN/IP-10, pGSN/IgG, pGSN/IgM and pGSN/IgA were determined and compared between mild and severe COVID-19 patients as well as **(D)** intubation status and **(E)** ICU admittance with pGSN/IL-4 included. **(F)** The mean ± SEM levels of pGSN/IP-10, pGSN/IL-6, pGSN/CTAK, pGSN/M-CSF and pGSN/HGF were compared between deceased and discharged patients. P-values were calculated by one-way ANOVA and independent sample t-test.

Unlike cytokines, none of the antibody isotypes measured associated with disease severity (Figure 2B). In order to develop a stronger prognostic marker, pGSN was combined with selected cytokines in a ratio to be compared between mild and severe cases, ICU admission and hospitalization outcomes. pGSN/IL-6 was significantly higher in mild cases compared with severe cases; pGSN/HGF and pGSN/IP-10 showed a similar trend although not significant (Figure 2C). Meanwhile, pGSN/IgM was significantly higher in severe cases with pGSN/IgG (but not pGSN/IgA) showing a similar trend (Figure 2C). Although the ratio of pGSN and cytokines and IgA had no significant association with intubation, pGSN/IgM and pGSN/IgG at day 1 were significantly elevated in patients who were intubated during hospitalization (Figure 2D). In terms of ICU admissions, patients with significantly higher levels of pGSN/IL-6 and pGSN/HGF (but not pGSN/IP-10, pGSN/IL-4 and pGSN/M-CSF) were admitted to the ICU (Figure 2E) with the antibodies having no significant impact. The levels of pGSN/IP-10, pGSN/CTAK, pGSN/IL-6 and pGSN/M-CSF (but not pGSN/HGF) were elevated in patients that were discharged (Figure 2F), suggesting that pGSN levels in combination with inflammatory cytokines especially pGSN/IL-6, may predict mild and favorable outcomes for hospitalized COVID-19 patients.

The pGSN/IL-6 ratio is a strong predictor of disease progression and outcomes relative to symptoms onset

To further strengthen the potential of using pGSN and cytokines as a multi-analyte marker for COVID-19 outcomes, we investigated their utility in days from symptoms onset. Mild COVID-19 patients had significantly high pGSN/IL-6 amongst all the multi-analyte markers following day 4 of symptoms onset compared with moderate and severe COVID-19 patients, and pGSN/IP-10 and pGSN/HGF showed a trend toward this association (Figure 3A; Supplementary Figure S2A). Patients admitted into the ICU as well as those who died had lower pGSN/IL-6, with pGSN/HGF showing a similar trend (Figure 2A; Supplementary Figures S2B-C). Taken together, the pGSN/IL-6 ratio presents as a strong candidate which could be potentially used to monitor disease progression and hospitalization outcomes 4 days from symptom onset. Although pGSN levels correlated with SARS-COV-2 spike protein antibodies on day 8, their combination as a multi-analyte marker did not provide a significant output for monitoring patient outcomes days from symptom onset (Figure 3B; Supplementary Figures S2-S3).

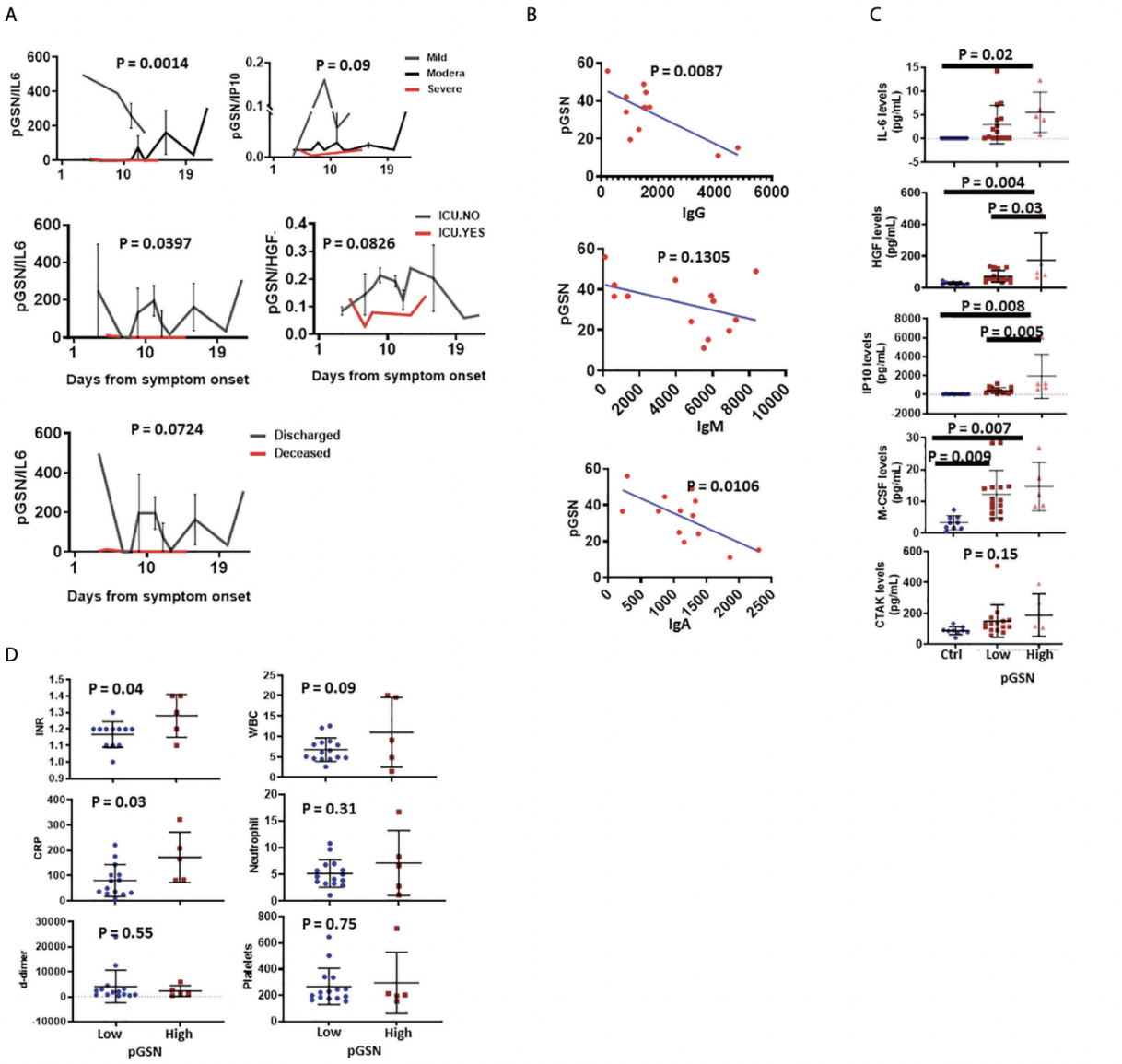


Figure 3 pGSN/IL-6 multi-analyte is a strong marker for monitoring disease severity and outcomes days from symptoms onset. **(A)** pGSN/IL-6, pGSN/IP-10 and pGSN/HGF levels were utilized to monitor disease severity, ICU admittance and discharge following day 1 from symptoms onset. **(B)** pGSN and SARS-COV-2 antibodies (IgG, IgM and IgA) were assessed on day 8 and correlated using Pearson's test. **(C)** Patients were stratified into low and high pGSN groups using an optimal cut-off point. The mean ± SEM levels of IL-6, HGF, IP-10, M-CSF and CTAK were compared between the groups using scatter plot. **(D)** The mean ± SEM levels of INR, CRP, d-dimer, WBC, neutrophils and platelets were compared between the pGSN groups using scatter plot. P-values were calculated by one-way ANOVA and independent sample t-test.

pGSN levels are elevated in response to cytokine storm

We have thus far demonstrated that pGSN and inflammatory cytokines are elevated in severe COVID-19 disease although we have yet to determine how they correlate with each other as well as that of the clinically used inflammatory markers. Here, we stratified patients into two groups based on their pGSN levels (low and high) using an optimal cut-off point determined by Fisher's Exact Test. The mean inflammatory cytokine levels (IL-6, IP-10, HGF, M-CSF and CTAK; Figure 3C) and clinically used laboratory markers (INR, d-dimer, CRP, WBC, platelets, neutrophils; Figure 3D) were determined and compared between the groups. The mean levels of the cytokines (except CTAK) were significantly higher in the high pGSN group compared with lower pGSN group (Figure 3C) whereas only INR and CRP were elevated in the high pGSN group. These findings suggest that pGSN could be upregulated as a feedback mechanism to fight the damage caused by the inflammatory state of the patient.

pGSN/IgG and pGSN/IgM are strong predictors of worse COVID-19 outcomes

We further tested how reliable pGSN would be to monitor disease severity and hospitalization outcomes either alone or in combination with SARS-COV-2 spike antibodies at the time of hospitalization (day 0). Using ROC curves, we derived AUC to assess the prognostic performances of these markers (Figure 4). Using pGSN, CRP, IgG, IgM or IgA alone were not significantly predictive, however the AUCs of pGSN/IgG and pGSN/IgM to predict severe COVID-19 were 0.893 (p=0.028) and 0.96 (p=0.01) respectively (Figure 4A; Supplementary S4A). Similar outcomes were observed for pGSN/IgG (AUC=0.776; p=0.032) and pGSN/IgM (AUC=0.735; p=0.067) when predicting COVID-19 death (Figure 4B; Supplementary S4B). These findings suggest that pGSN/IgG and pGSN/IgM could be potential markers for predicting disease severity and hospitalization outcomes for COVID-19.

pGSN/IL-6 is a strong predictor of mild COVID-19 and favorable outcomes

Unlike the antibodies, the inflammatory cytokines showed more promise when combined with pGSN for predicting mild and favorable COVID-19 outcomes (i.e. no-ICU admissions, and survival to hospital discharge). pGSN, CRP and individual cytokines alone provided an AUC < 0.6 in predicting mild COVID-19 disease **(**Figure 5A**;** Supplementary Figure S1C**)**. Meanwhile, combining pGSN with IL-6 (AUC=0.904; p=0.003) showed a more significant ability to predict mild COVID-19 and IP-10 (AUC=0.754; p=0.065), HGF (AUC=0.746; p=0.075) and TGF-β1

(AUC=0.765; p=0.078) demonstrated a trend toward significance **(**Figure 5A**;** Supplementary Figure S4C**)**.

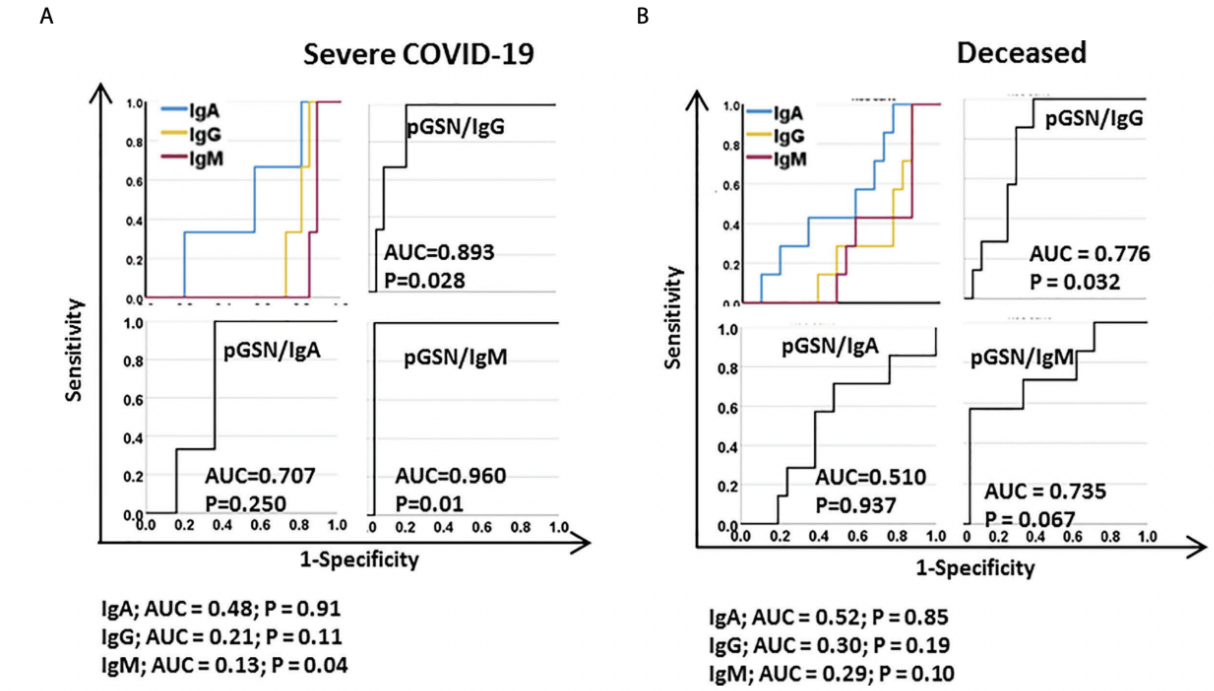


Figure 4 pGSN/IgG and pGSN/IgM are strong predictors of worst COVID-19 outcomes. ROC curves were used to assess the test performances of IgG, IgA, IgM, pGSN/IgG, pGSN/IgM and pGSN/IgA in predicting **(A)** disease severity and **(B)** death.

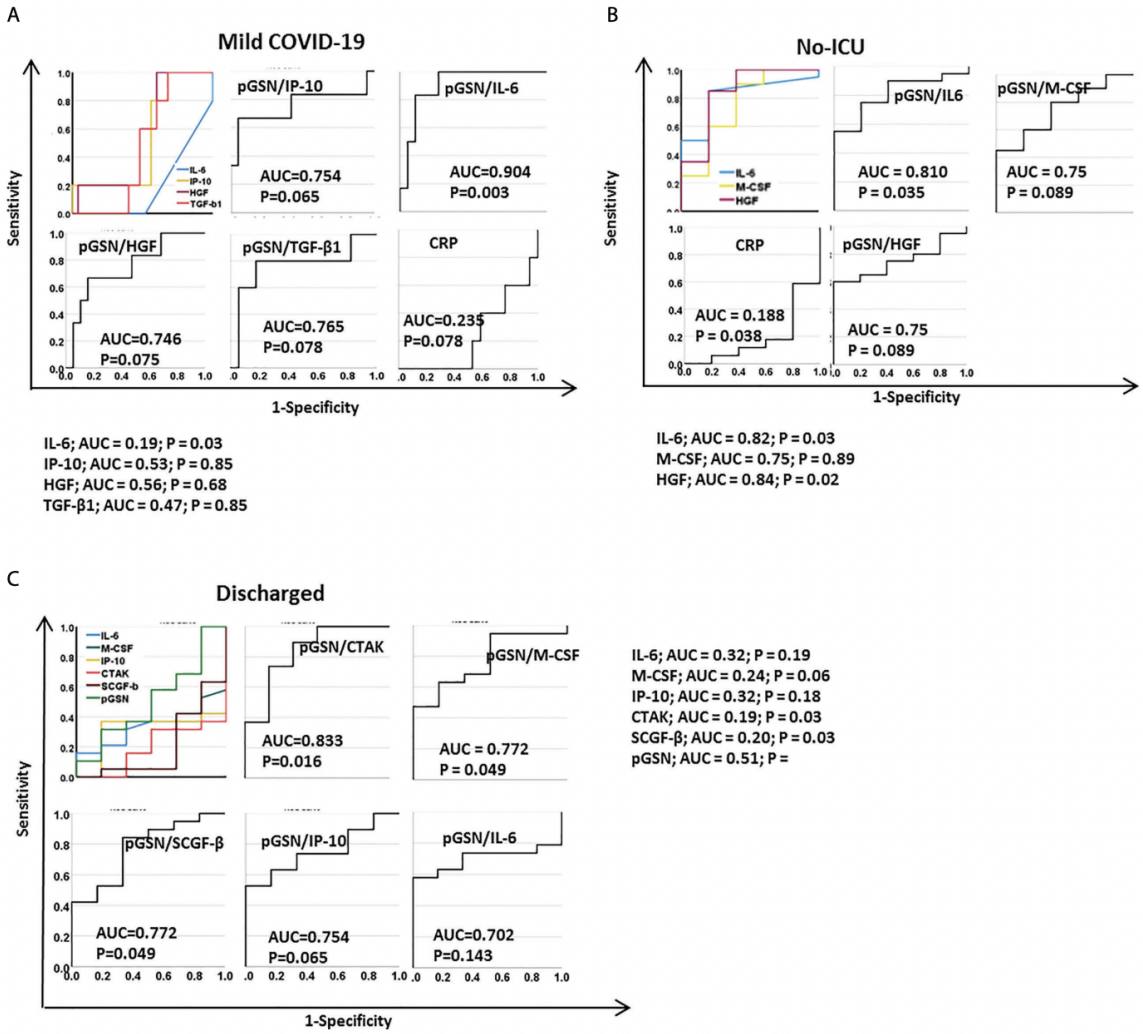


Figure 5 pGSN/IL-6 is a strong predictor of mild COVID-19 cases and favorable outcomes. ROC curves were used to assess the test performances of IL-6, IP-10, HGF, TGF-β1, M-CSF, CTAK, SCGF-β, CRP, pGSN, pGSN/IP-10, pGSN/IL-6, pGSN/HGF, pGSN/TGF-β, pGSN/M-CSF and pGSN/SCGF-β in predicting **(A)** mild COVID-19 cases, **(B)** no-ICU admissions and **(C)** discharged patients.

Unlike the mild cases, there were no significant differences between the pGSN/cytokine panels and pGSN alone when predicting non-ICU admissions **(**Figure 5B**;** Supplementary Figure S4D**)**. Interestingly, pGSN/CTAK (AUC=0.833; p=0.016), pGSN/M-CSF (AUC=0.772; p=0.049) and pGSN/SCGF-b (AUC=0.772; p=0.049) but not the other ratios, significantly predicted survival to hospital discharge of COVID-19 patients **(**Figure 5C**)**. As expected, a modest AUC (less than 6)

was observed with pGSN, cytokines or clinical inflammatory markers alone, suggesting the need for a multi-analyte marker for disease monitoring in COVID-19 **(**Figure 5C**;** Supplementary Figure S4E**)**.

Multi-analyte panel of pGSN with cytokines and antibodies predict more than one clinical outcome of COVID-19

Using heat maps, we demonstrated how our multi-analyte panels could enable us to predict two clinical outcomes at the same time; an approach that will be significantly useful in triaging patients. We observed that COVID-19 patients with increased levels of pGSN/IL-6, pGSN/HGF and pGSN/IgM compared with the other markers are more likely not to progress to severe disease and will eventually be discharged alive **(**Figure 6A**;** Supplementary Figure S5A**)**. The situation with pGSN/IgG was different since it is more predictive of severe disease and death in this study **(**Figure 6A**)**. Additionally, patients with increased levels of pGSN/IL-6, pGSN/IP-10 and pGSN/IgM compared with the other markers were more likely not to be admitted to the ICU and to survive to hospital discharge **(**Figure 6B**;** Supplementary Figure S5B**)**. When ICU and disease severity were used in the heat map analysis, we observed that patients with increased pGSN/IL-6, pGSN/IP-10 and pGSN/IgM are likely to present with mild cased and will eventually avoid ICU admission(Figure 6C). These findings suggest that by combining pGSN with cytokines more than one clinical outcome could be predicted in COVID-19 cases from the first day of hospital visit.

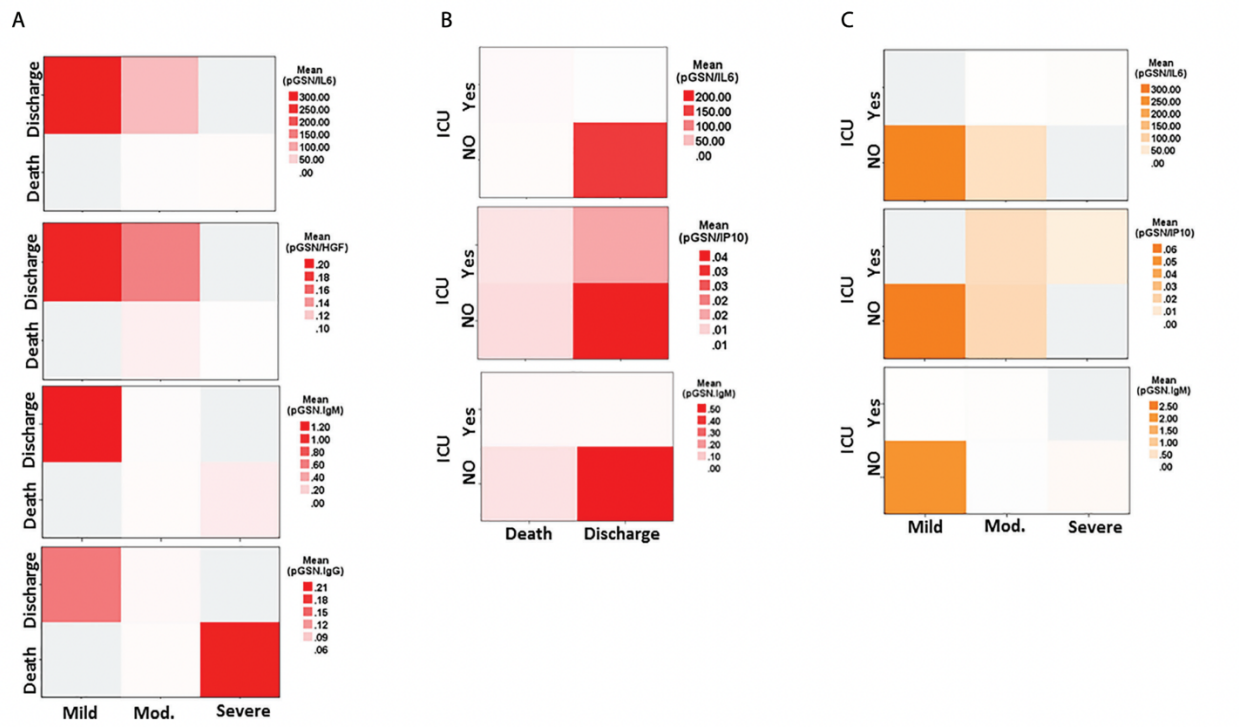


Figure 6 Multi-analyte panel of pGSN with cytokines and antibodies predict more than one clinical outcome of COVID-19. pGSN/IL-6, pGSN/HGF, pGSN/IP-10, pGSN/IgM and pGSN/IgG were used in a heat map analyses to predict **(A)** disease severity and hospitalization outcomes, **(B)** ICU admissions and hospitalization outcomes and **(C)** disease severity and ICU admissions.

Discussion

Our study reveals for the first time the prognostic significance of pGSN when combined with cytokines and anti-SARS-CoV-2 antibodies in COVID-19 infection. Specifically, we have demonstrated that pGSN is significantly downregulated in COVID-19 patients and in combination with cytokines and anti-SARS-COV-2 antibodies can predict COVID-19 severity and hospitalization outcomes.

Although pGSN levels were lower at the time of admission, a return to normal range in the levels were seen at day 30 which is associated with improved outcome (i.e. discharge) in patients with COVID-19 infection. pGSN alone outperformed cytokines (IL-6, IP-10, HGF and M-CSF) in discriminating COVID-19+ patients from non-COVID-19 suggesting that pGSN is a potential biomarker indicative of COVID-19 infection. As shown in previous studies (5, 6, 28, 29), COVID-19 is characterized by the upregulation of pro-inflammatory cytokines which was evident in our

study with the upregulation of IL-6, IP-10, M-CSF, HGF, CTAK and TGF-b1. It is interesting to note that the test accuracy of pGSN was enhanced when combined with IL-6, IP-10, HGF and C-MSF in a multi-analyte panel. During cytokine storm (5), multi-organ damage results in the release of actin filaments in the blood which are cleared, in part, by pGSN (30, 31), a process that may result in the decrease of pGSN in COVID-19 patients also. This might further explain why combining pGSN with the pro-inflammatory cytokines provided much greater accuracy since these markers are both systemically related to disease progression.

Prediction of hospitalization outcomes is key to the effective management of COVID-19 cases as well as allocation of hospital resources. However, there are currently no biomarkers which reliably predict COVID-19 severity, ICU admission and death. We have shown that a multi-analyte panel using pGSN and cytokines can predict favorable hospitalization outcomes. pGSN/IL-6 was the strongest predictive marker (amongst other cytokines) for mild COVID-19+ cases, ICU admissions and patient discharge. pGSN is a negative regulator of IL-6 and other pro-inflammatory cytokines secreted by monocytes and macrophages (32). Hence, pGSN could be secreted as a response to cytokine storm to prevent multiple organ damage as well as actin filament toxicity. This notion is consistent with the observation that pro-inflammatory cytokine levels were elevated in COVID-19+ patients with high pGSN. It is therefore note-worthy that combining pGSN and IL-6 provided robust test accuracy for favorable outcomes compared to individual markers alone, an indication of disease progression in the participants. Additionally, our findings are consistent with a previous study that has demonstrated the immunomodulatory effectiveness of human recombinant (rhu)-pGSN in the treatment of a single severe COVID-19 case (33). There is an ongoing double-blinded proof-of-concept trial (NCT04358406) to further assess the efficacy and safety of rhu-pGSN in severe COVID-19.

Another key observation in this study was the relationship between pGSN levels and antibodies (IgA, IgM and IgG) against SARS-CoV-2 spike protein. From day 1 of sample collection through day 30 we observed a pattern where the inverse relationship between pGSN and the antibodies increased. An indication that with improving clinical status, pGSN levels are restored while antibody levels, especially IgG, began to decline. This is consistent with the observation that antibody levels were lower in patients with severe COVID-19. Some patients were treated with

corticosteroids; which could impact antibody levels. Unlike the pro-inflammatory cytokines, combining pGSN with the anti-spike IgG and IgM were strong predictive markers for severe COVID-19 and COVID-19-related death. Actin remodeling is a crucial step in B-cell activation and B-cell receptor function (34, 35). Although pGSN is a key protein in actin binding and remodeling (20, 30), we have yet to investigate whether it is directly involved in COVID-19 humoral immunity. This could explain the relationship between pGSN and the antibodies as observed in these COVID-19 patients. As to whether pGSN has a direct function on the production of SARS-COV-2 antibodies is yet to be investigated.

An additional major finding was the ability to utilize pGSN/IL-6 as well as other markers (cytokines, antibodies and clinical laboratory inflammatory markers) to predict more than one clinical outcome. Of note, we observed that COVID-19 patients with high pGSN/IL-6 and pGSN/IgM presented with mild disease did not require ICU admission and were more likely to be discharged. The opposite was noted with pGSN/IgG. In situations where there are limited resources, this could potentially provide clinicians and hospital administrators' prior knowledge in prioritizing their resources such as ICU beds in terms of delivering care to COVID-19 patients.

In summary, a multi-analyte panel of pGSN, cytokines and SARS-COV-2 antibodies, present as potential biomarkers predicting disease severity, ICU admissions and COVID-19-related death. Despite these promising findings, there are limitations that need to be acknowledged. The sample size of this study is relatively small due to the difficulty in sampling patients longitudinally in a hospital setting. Antibody kinetics (levels and isotype) during the early infection could be influenced by time since infection. Also, the control samples consist of out-patient populations that had no recorded history of respiratory infection during sample collection. Having control samples from patients who are SARS-CoV-2 negative but positive for other respiratory diseases will further strengthen the reliability of pGSN multi-analyte panels. In future studies, patient sample size will be increased while we investigate the prognostic significance of pGSN multi-analyte panel in SARS-CoV-2 variant patients, vaccinated patients as well as convalescent plasma.

Materials and methods

Ethics statement

This study was approved by the Ottawa Health Science Network Research Ethics Board (OHSNREB; Protocol# 20200200-01H) and conducted in accordance with the appropriate guidelines. Written informed consent was obtained from all subjects.

Patient characteristics and plasma samples

Forty participants (unvaccinated) recruited at The Ottawa Hospital (TOH) from 2020 to 2021 were included in this study. Plasma samples were serially collected from 28 PCR-confirmed SARS-CoV-2-infected patients admitted to hospital at days 0, 4, 8, 12 and 30. Plasma samples had pre-determined laboratory markers such as C-reactive protein (CRP), ferritin, white blood cells (WBC), d-dimer, neutrophils, platelets and international normalized ratio (INR). Twelve samples collected from healthy controls were negative for SARS-COV-2. Non-COVID-19 subjects had no reported illnesses at the time of sample collection. COVID-19 severity was defined as mild (no supplemental oxygen), moderate [supplemental oxygen, not high flow or no flow listed, no intubation/mechanical ventilation – ex. No Bi-level Positive Airway Pressure (BiPap)/intubation)] and severe (high flow oxygen and non-invasive or invasive mechanical ventilation – ex. Yes BiPap/intubation). The range and median of follow-up period was 87 and 10 days respectively. Other details of patient demographics and baseline characteristics are described in Supplementary Table 1. Patients received interventional management including antiviral therapies (lopinavir/ritonavir, ribavirin, hydroxychloroquine and remdesivir) and non-antiviral adjunctive therapies (convalescent plasma, steroids, immune-modulators, anticoagulation, and antibiotics) in addition to appropriate supportive care.

pGSN ELISA

pGSN concentrations were assayed in the study participants by sandwich ELISA (Aviscera Bioscience, Inc. CA), according to manufacturer's instructions. The detection antibody was raised against human plasma (soluble) gelsolin. Plasma samples were diluted in a sample buffer (1/1500; Aviscera Bioscience, Inc. CA) and all analyses done in triplicate. Optical densities (OD) were determined using a microtiter plate reader at 450 nm. The blank was subtracted from the triplicate readings for each standard and sample and concentrations reported in µg/mL.

Cytokine assay

The concentrations of pro- and anti-inflammatory cytokines in plasma were quantified using multiplexing immunobead assays analyzed using the BioRad Luminex machine (Bio-Rad Laboratories, Hercules, CA, USA). Transforming growth factor β (TFG-β) -1, -2 and -3 were quantified using the TGF-Beta 1,2,3 Magnetic Bead Kit (Milliplex, Millipore SIGMA) while all remaining cytokines were assayed using the 48-plex Bio-Plex Pro™ Human Cytokine Screening Panel (BioRad, Mississauga, ON, CANADA). Cytokine concentrations were reported in pg/mL.

Anti-spike protein antibody assay

A manual colorimetric ELISA was used to measure antibodies targeting SARS-CoV-2 spike protein, a complete description of the methods can be found here (36). Briefly, high protein-binding Immulon 4 HBX clear 96-well plates (VWR International, Mississauga, ON, Canada, #62402-959) were coated with 50 µL of 2 µg/mL full length trimeric Spike protein (NRC) diluted in PBS and kept at 4°C on a shaker. After an overnight incubation, the plates were washed three times with 200uL of PBST and blocked with 200 µL of 3% w/v skim milk powder in PBST for 1 hour at room temperature on a shaker. During that time, plasma samples were diluted in 1% w/v skim milk powder. The plates were washed again and 100uL of diluted plasma samples was added to the plate. Additionally, positive and negative serum controls alongside an isotype-antigen specific calibration curve (CR3022 Human IgG1 (Absolute Antibody, Ab01680-10.0), anti-SARS-CoV-2 S CR3022 Human IgA (Absolute Antibody, Ab01680-16.0), or anti-SARS-CoV-2 S CR3022 Human IgM (Absolute Antibody, Ab01680-15.0)) was added to the plate and incubated for 2h with shaking. The plates were washed again and 50uL of isotype specific secondary antibodies (anti-human IgG#5-HRP (NRC), anti-human IgA-HRP (Jackson ImmunoResearch Labs, 109-035-011), and anti-human IgM-HRP (Jackson ImmunoResearch Labs, 109-035-129) added and incubated with shaking for 1 hour. The plates were then washed for one last time and developed using 100 µL of SIGMAFAST OPD Tablets (Sigma-Aldrich, P9187) dissolved in 20 mL of Water for Injection for Cell Culture (Thermo Fisher Scientific, A1287301). The reaction was stopped with the addition of 50uL of 3M HCl and the absorbance was measured at 490 nm using a PowerWave XS2 Plate Reader (BioTek Instruments). Absorbance reads were blank adjusted and correlated with the linear portion of the calibration curve, hereby taking into account plate-to-plate variability and dilution factor. Concentrations of antibodies were reported in ng/mL.

Biostatistical methods

The GraphPad Prism 8 (San Diego, CA, USA) and SPSS software version 28 (SPSS Inc., Chicago, IL, USA) were used to perform all statistical analyses and two-sided $P \leq 0.05$ considered to indicate statistical significance. Concentrations of pGSN in study groups were dichotomized by their median cut-offs into low or high concentrations and correlated to clinicopathological parameters (37) [age, sex, disease severity, inflammatory cytokines, IgG, IgA and IgM levels], using Pearson's correlation test (two-tailed), Fisher exact test, Students' *t* test and Kruskal Wallis test, as appropriate. Receiving operating characteristic (ROC) curves were used to assess the performance of pGSN, cytokines and multi-analyte panels over their entire range of values. The area under the curve (AUC) was used as an index of global test performance to predict disease severity. Heat maps were used to demonstrate the relationships between multi-analyte panels and clinical outcomes.

Data availability statement
The raw data supporting the conclusions of this article will be made available by the authors, without undue reservation.

Ethics statement
The studies involving human participants were reviewed and approved by Ottawa Health Science Network Research Ethics Board. The patients/participants provided their written informed consent to participate in this study.

Author contributions
MA-W and BT conceived and designed the study in partnership with AC Plasma samples were collected by BC, CC and MM and processed by AV, and AC Clinical information was collected and curated by BC, CC, and MM pGSN analyses were performed by MA-W and BT Cytokine assays were conducted by AV and AC while antibody measurements were completed by YG and M-AL MA-W analysed the data with scientific input from BT, BC, CC, M-AL, MM, JC and AC. MA-W wrote the paper with feedback from all authors. All authors contributed to the article and approved the submitted version.

Funding
This work was supported by a grant from The Ottawa Hospital Department of Medicine - Special Pandemic Agile Research Competition (MM, CC, JC, AC).

Conflict of interest
The authors declare that the research was conducted in the absence of any commercial or financial relationships that could be construed as a potential conflict of interest.

Supplementary material
The Supplementary Material for this article can be found online at: https://www.frontiersin.org/articles/10.3389/fimmu.2022.1011084/full#supplementary-material

References

1. Li T. Diagnosis and clinical management of severe acute respiratory syndrome coronavirus 2 (SARS-CoV-2) infection: An operational recommendation of Peking union medical college hospital (V2.0). Emerg Microbes Infect (2020) 9(1):582–5. doi: 10.1080/22221751.2020.1735265
2. Ng OT, Marimuthu K, Chia PY, Koh V, Chiew CJ, De Wang L, et al. SARSCoV-2 infection among travelers returning from wuhan, China. New Engl J Med (2020) 382(15):1476–8. doi: 10.1056/NEJMc2003100
3. Ozma MA, Maroufi P, Khodadadi E, Kose S, Esposito I, Ganbarov K, et al. Clinical manifestation, diagnosis, prevention and control of SARSCoV-2 (COVID-19) during the outbreak period. Infez Med (2020) 28 (2):153–65. 4. Corman VM, Landt O, Kaiser M, Molenkamp R, Meijer A, Chu DK, et al. Detection of 2019 novel coronavirus (2019-nCoV) by real-time RT-PCR. Euro Surveill (2020) 25(3):2000045. doi: 10.2807/1560-7917.ES.2020.25.3.2000045
5. Shi Y, Wang Y, Shao C, Huang J, Gan J, Huang X, et al. COVID-19 infection: The perspectives on immune responses. Cell Death Diff (2020) 27:1451–4. England. doi: 10.1038/s41418-020-0530-3
6. Conti P, Ronconi G, Caraffa A, Gallenga CE, Ross R, Frydas I, et al. Induction of pro-inflammatory cytokines (IL-1 and IL-6) and lung inflammation by coronavirus-19 (COVI-19 or SARS-CoV-2): Anti-inflammatory strategies. J Biol Regul Homeost Agents (2020) 34(2):327–31. doi: 10.23812/CONTI-E
7. Esposito S, Noviello S, Pagliano P. Update on treatment of COVID-19: Ongoing studies between promising and disappointing results. Infez Med (2020) 28 (2):198–211.
8. Tu YF, Chien CS, Yarmishyn AA, Lin YY, Luo YH, Lin YT, et al. A review of SARS-CoV-2 and the ongoing clinical trials. Int J Mol Sci (2020) 21(7):2657. doi: 10.3390/ijms21072657
9. Guo L, Ren L, Yang S, Xiao M, Chang D, Yang F, et al. Profiling early humoral response to diagnose novel coronavirus disease (COVID-19). Clin Infect Dis (2020) 71(15):778–85. doi: 10.1093/cid/ciaa310
10. Ni L, Ye F, Cheng ML, Feng Y, Deng YQ, Zhao H, et al. Detection of SARSCoV-2-Specific humoral and cellular immunity in COVID-19 convalescent individuals. Immunity (2020) 52(6):971–7.e3. doi: 10.1016/j.immuni.2020.04.023
11. Wang D, Hu B, Hu C, Zhu F, Liu X, Zhang J, et al. Clinical characteristics of 138 hospitalized patients with 2019 novel coronavirus-infected pneumonia in wuhan, China. JAMA (2020) 323(11):1061–9. doi: 10.1001/jama.2020.1585
12. Ponti G, Maccaferri M, Ruini C, Tomasi A, Ozben T. Biomarkers associated with COVID-19 disease progression. Crit Rev Clin Lab Sci (2020) 57(6):389–99. doi: 10.1080/10408363.2020.1770685
13. Goldberg I, Shalmon D, Shteinvil R, Berliner S, Paran Y, Zeltser D, et al. A second c-reactive protein (CRP) test to detect inflammatory burst in patients with acute bacterial infections presenting with a first relatively low CRP. Medicine (2020) 99(42):e22551. doi: 10.1097/MD.0000000000022551
14. Luan YY, Yao YM. The clinical significance and potential role of c-reactive protein in chronic inflammatory and neurodegenerative diseases. Front Immunol (2018) 9:1302. doi: 10.3389/fimmu.2018.01302
15. Woo PC, Tung ET, Chan KH, Lau CC, Lau SK, Yuen KY. Cytokine profiles induced by the novel swine-origin influenza A/H1N1 virus: Implications for treatment strategies. J Infect Dis (2010) 201(3):346–53. doi: 10.1086/649785
16. Messner CB, Demichev V, Wendisch D, Michalick L, White M, Freiwald A, et al. Ultra-High-Throughput clinical proteomics reveals classifiers of COVID-19 infection. Cell Syst (2020) 11(1):11–24.e4. doi: 10.1016/j.cels.2020.05.012
17. D'Alessandro A, Thomas T, Dzieciatkowska M, Hill RC, Francis RO, Hudson KE, et al. Serum proteomics in COVID-19 patients: Altered coagulation and complement status as a function of IL-6 level. J Proteome Res (2020) 19 (11):4417–27. doi: 10.1101/2020.05.29.20116889

18. Overmyer KA, Shishkova E, Miller IJ, Balnis J, Bernstein MN, Peters-Clarke TM, et al. Large-Scale multi-omic analysis of COVID-19 severity. medRxiv (2020):20156513. doi: 10.1101/2020.07.17.20156513
19. Kwiatkowski DJ, Stossel TP, Orkin SH, Mole JE, Colten HR, Yin HL. Plasma and cytoplasmic gelsolins are encoded by a single gene and contain a duplicated actin-binding domain. Nature (1986) 323(6087):455–8. doi: 10.1038/323455a0
20. Sun HQ, Yamamoto M, Mejillano M, Yin HL. Gelsolin, a multifunctional actin regulatory protein. J Biol Chem (1999) 274(47):33179–82. doi: 10.1074/ jbc.274.47.33179
21. Asare-Werehene M, Communal L, Carmona E, Han Y, Song YS, Burger D, et al. Plasma gelsolin inhibits CD8(+) T-cell function and regulates glutathione production to confer chemoresistance in ovarian cancer. Cancer Res (2020) 80 (18):3959–71. doi: 10.1158/0008-5472.CAN-20-0788
22. Rothenbach PA, Dahl B, Schwartz JJ, O'Keefe GE, Yamamoto M, Lee WM, et al. Recombinant plasma gelsolin infusion attenuates burn-induced pulmonary microvascular dysfunction. J Appl Physiol (1985) (2004) 96(1):25–31. doi: 10.1152/ japplphysiol.01074.2002
23. Yang Z, Chiou TT, Stossel TP, Kobzik L. Plasma gelsolin improves lung host defense against pneumonia by enhancing macrophage NOS3 function. Am J Physiol Lung Cell Mol Physiol (2015) 309(1):L11–6. doi: 10.1152/ajplung.00094.2015
24. Yang Z, Bedugnis A, Levinson S, DiNubile M, Stossel T, Lu Q, et al. Delayed administration of recombinant plasma gelsolin improves survival in a murine model of severe influenza. F1000Res (2019) 8:1860. doi: 10.12688/ f1000research.21082.1
25. Yang Z, Bedugnis A, Levinson S, Dinubile M, Stossel T, Lu Q, et al. Delayed administration of recombinant plasma gelsolin improves survival in a murine model of penicillin-susceptible and penicillin-resistant pneumococcal pneumonia. J Infect Dis (2019) 220(9):1498–502. doi: 10.1093/infdis/jiz353
26. Yang SS, Lipes J. Corticosteroids for critically ill COVID-19 patients with cytokine release syndrome: A limited case series. Can J Anaesthesia = J Canadien d'anesthesie (2020) 67(10):1462–4. doi: 10.1007/s12630-020-01700-w
27. Merad M, Martin JC. Pathological inflammation in patients with COVID19: A key role for monocytes and macrophages. Nat Rev Immunol (2020) 20 (6):355–62. doi: 10.1038/s41577-020-0331-4
28. Thevarajan I, Nguyen THO, Koutsakos M, Druce J, Caly L, van de Sandt CE, et al. Breadth of concomitant immune responses prior to patient recovery: A case report of non-severe COVID-19. Nat Med (2020) 26:453–5. United States. doi: 10.1038/s41591-020-0819-2
29. Liu J, Li S, Liu J, Liang B, Wang X, Wang H, et al. Longitudinal characteristics of lymphocyte responses and cytokine profiles in the peripheral blood of SARS-CoV-2 infected patients. EBioMedicine (2020) 55:102763. doi: 10.1016/j.ebiom.2020.102763
30. Lind SE, Smith DB, Janmey PA, Stossel TP. Role of plasma gelsolin and the vitamin d-binding protein in clearing actin from the circulation. J Clin Invest (1986) 78(3):736–42. doi: 10.1172/JCI112634
31. Feldt J, Schicht M, Garreis F, Welss J, Schneider UW, Paulsen F. Structure, regulation and related diseases of the actin-binding protein gelsolin. Expert Rev Mol Med (2019) 20:e7. doi: 10.1017/erm.2018.7
32. Cheng Y, Hu X, Liu C, Chen M, Wang J, Wang M, et al. Gelsolin inhibits the inflammatory process induced by LPS. Cell Physiol Biochem (2017) 41(1):205–12. doi: 10.1159/000456043
33. Catteeuw JV, DiNubile MJ. Recombinant human plasma gelsolin (rhupGSN) in a patient hospitalized with critical COVID-19 pneumonia. Clin Infect Pract (2021) 12:100088. doi: 10.1016/j.clinpr.2021.100088
34. Liu C, Miller H, Orlowski G, Hang H, Upadhyaya A, Song W. Actin reorganization is required for the formation of polarized b cell receptor signalosomes in response to both soluble and membrane-associated antigens. J Immunol (Baltimore Md: 1950) (2012) 188(7):3237–46. doi: 10.4049/ jimmunol.1103065
35. Song W, Liu C, Upadhyaya A. The pivotal position of the actin cytoskeleton in the initiation and regulation of b cell receptor activation. Biochim Biophys Acta (2014) 1838(2):569–78. doi: 10.1016/j.bbamem.2013.07.016 36. Colwill K, Galipeau Y, Stuible M, Gervais C, Arnold C, Rathod B, et

al. A scalable serology solution for profiling humoral immune responses to SARS-CoV-2 infection and vaccination. Clin Trans Immunol (2022) 11(3):e1380. doi: 10.1002/ cti2.1380
37. Huang C, Wang Y, Li X, Ren L, Zhao J, Hu Y, et al. Clinical features of patients infected with 2019 novel coronavirus in wuhan, China. Lancet (London England) (2020) 395(10223):497–506. doi: 10.1016/S0140-6736(20)30183-5

A-1.13 Multivariate analyses and machine learning link sex and age with antibody responses to SARS-CoV-2 and vaccination

Preface

(This work has been previously published as a research article)

Cuperlovic-Culf M, Bennett SAL, **Galipeau Y**, McCluskie PS, Arnold C, Bagheri S, Cooper CL, Langlois MA, Fritz JH, Piccirillo CA, Crawley AM. **Multivariate analyses and machine learning link sex and age with antibody responses to SARS-CoV-2 and vaccination**. iScience. 2024 Jul 10;27(8):110484.

https://doi.org/10.1016/j.isci.2024.110484

© 2024 The Authors

This is an open access article under the CC BY-NC license (http://creativecommons.org/licenses/by-nc/4.0/).

Highlights

- Network analysis of the interplay of complex antibody characteristics and sex and age
- Age and sex distinguish temporal dynamics of infection- and vaccine-induced immunity
- Less isotype switching and neutralization in older individuals with vaccination
- SARS-CoV-2 neutralization relation with antibodies is dependent on COVID-19 status

Abstract

Prevention of negative COVID-19 infection outcomes is associated with the quality of antibody responses, whose variance by age and sex is poorly understood. Network approaches identified sex and age effects in antibody responses and neutralization potential of *de novo* infection and vaccination throughout the COVID-19 pandemic. Neutralization values followed severe acute respiratory syndrome coronavirus 2 (SARS-CoV-2)-specific receptor binding immunoglobulin G (RIgG), spike immunoglobulin G (SIgG) and spike and receptor immunoglobulin G (S, and RIgA) levels based on COVID-19 status. Serum immunoglobulin A (IgA) antibody titers correlated with neutralization only in females 40–60 years old (y.o.). Network analysis found males could improve IgA responses after vaccination dose 2. Complex correlation analyses found vaccination induced less antibody isotype switching and neutralization in older persons, especially in females. Sex-dependent antibody and neutralization decayed the fastest in older males. Shown sex and age characterization can direct studies integrating cell-mediated responses to define yet elusive correlates of protection and inform age and sex precision-focused vaccine design.

Introduction

Sex and age differences in antiviral responses, vaccination, and long-term recovery are increasingly recognized in COVID-19[1,2,3,4] as key determinants to disease susceptibility and severity. During viral infections, females have greater inflammatory, antiviral, and humoral immune responses compared to males. Early in the COVID-19 pandemic, it was observed that infection prevalence is sex independent or possibly slightly higher in females. In contrast, males are more likely to experience severe disease, combined with increased hospitalization rates and higher mortality.[5,6] Increased disease severity was particularly significant in men over 60 years of age.2 In a large, hospitalized patient cohort study of 308,010 patients, the mortality rate was higher in males regardless of age, race, or comorbidities.[7] This is also observed with other coronaviruses including the Middle East respiratory syndrome epidemic, where mortality rate is also higher in males.[8] Differences in sex-related mortality risk have been observed in animal models of acute respiratory viral infections,[9] further suggesting significant sex effects influencing the outcomes. The molecular basis for these divergent immunological outcomes in males and females is thought to be related at least in part to differences in sex steroid synthesis, which can have a crucial role on the function and regulation of the immune response.[10,11] Indeed, sex steroids have been reported to exert a suppressive role in immune functions suppressing immune cell activity by promoting anti-inflammatory mediators. However, the nature and dynamics of antibody production throughout infection and vaccination in men and women are not well understood.[12]

Adaptive immunity to severe acute respiratory syndrome coronavirus 2 (SARS-CoV-2) infection depends on the concerted action of both humoral and cell-mediated immune components. Immunoglobulin (Ig)G, IgM, and IgA against spike and receptor-binding domain (RBD) are detected in plasma 7–8 days following the onset of symptoms in infection with IgA persisting for over 400 days after symptom onset.[13] Detectable IgM and IgG Abs occur concurrently with increased plasma B cells. While IgG levels reportedly decline modestly 8 weeks after symptom onset, recovered patients maintain high spike-specific IgG and IgA titers. Neutralizing antibodies (nAbs) as well as binding antibodies (bAbs) can control SARS-CoV-2 infection; convalescent plasma containing nAb and bAb administered as a therapeutic can improve clinical symptoms.[14] In SARS-CoV-2 convalescent subjects, IgG1, IgA1, and IgM antibodies against spike and RBD all

have capacity for virus neutralization.[13] Based on regression analysis, IgM and IgG1 show the strongest contribution to neutralization; however, direct analysis shows that IgA was also able to neutralize.[13]

Severe COVID-19 patients display an acute respiratory distress syndrome, which can be mediated directly by the virus and/or a hyper-active immune response. SARS-CoV-2 antigen-specific CD4+ and CD8+ T cells have been identified in recovered and active disease patients and contribute to protection from re-infection.[15,16,17,18] The immune profiles of COVID-19 patients with moderate disease indicate a protective T cell response, while patients with severe disease exhibit exaggerated systemic inflammation, signs of T cell exhaustion and lymphopenia, and decreased polyfunctionality or cytotoxicity, all features of dysregulated adaptive immunity. Different immunotypes predict the course of infection, whereby coordinated action between CD4+, CD8+ T cells, and antibodies contributes to optimal viral control, efficient immune protection, and better disease prognosis.

Viral-induced inflammation increases with age and is associated with a hyper-inflammatory responses leading to significant lung damage as well as increased morbidity and mortality rates in older adults. Elevated levels of inflammatory cytokines (e.g., interleukin [IL]-6), increased inflamm-aging, and T cell senescence, as well as higher titers of anti-S/-N IgG and IgM, correlate with worse clinical readouts with older age, suggesting adverse effects of the immune response on disease severity.[16,19,20]

Immune responses are known to differ in males and females leading to sex-specific responses to vaccination and infections.[21] Female mice have a more robust humoral and cellular immunity than their male counterparts following a primary challenge with influenza virus whereas vaccination yields equivalent protection in both sexes.[22] Transfer of immune sera from vaccinated females to naive mice provided better protection compared to transfer of sera from vaccinated males. This superior sex-associated protection is thought to be a consequence of an increase in antibody titers, IgG antibodies of greater neutralization capacity, and effective Ig isotype switching in females contributing to more effective antibody function and neutralization capacity. A meta-analysis of 117 peer-reviewed articles showing serum levels of IgA, IgG, or IgM in adult human beings[23] suggests that older age and male sex are associated with higher vaccine-specific IgA

levels and that lower IgM and IgG levels were not influenced by age and sex. A population-based study[24] supports these findings. Increased levels of serum IgA and decreased IgM with age and higher IgA titers in males than females were noted. Interestingly, IgG level decreases with age (up to 60).[24]

The use of computed network analyses can enable the extraction of important host response patterns from complex data and has been applied in the COVID-19 era.4 In an effort to better understand the observed sex and age differences in SARS-CoV-2 infection risk, disease outcome, and response to COVID-19 vaccination, we applied a novel network analysis strategy[25,26,27] to track the evolution of antibody generation and functionality following natural infection and/or vaccination in a large longitudinal cohort referred to as *Stop the Spread Ottawa* (SSO),[28] pinpointing changes in the response to infection and/or vaccination in immune-competent or immune-compromised individuals.

Results

Age and sex weakly affect overall response to vaccination and natural infection

In this analysis, serially collected serum samples from 970 participants (3,666 samples in total) were separated into groups by the vaccination period, age, and sex of the participant as well as by SARS-CoV-2 infection-acquired immunity status (Table 1). The primary goal of the study was to explore the relationship between serology measurements and viral neutralization in males and females separately in three age groups. Thus, we aimed to first ensure sufficient statistical power for each group and obtain correlative relationships (Figure S1). The specific SARS-CoV-2 strain that infected the study participants with known infection is not specified. All samples were collected between October 21, 2020, and August 20, 2021, before the emergence of Omicron COVID-19 variant. Nine different antibody responses were measured from each serum sample corresponding to IgG, IgA, and IgM titers specific for SARS-CoV-2 RBD (R), spike (S), and nucleoprotein (N) as well as neutralization measurements.

Table 1. Overview of study groups and time points assembled for this data analysis

	Unvaccinated (male/female)	Dose 1 (male/female)	Dose 2 (male/female)
Unique study participants (*n*=970)	198/394	122/244	140/290
Samples	393/643	205/422	440/1,012
Positive	177/163	84/90	119/168
Negative	216/480	121/332	321/844
<40 y.o.	99 (30.3 ± 4.5)/249 (30.6 ± 4.9)	44 (30.4 ± 5.2)/118 (31.2 ± 4.8)	111 (31.5 ± 4.6)/368 (31.4 ± 4.5)
Age (40–60) y.o.	173 (48.0 ± 6.3)/275 (49.1 ± 6.2)	53 (49.6 ± 5.7)/134 (50.6 ± 5.60)	172 (46.8 ± 5.4)/411 (50.3 ± 6.0)
≥60 y.o.	121 (66.6 ± 4.8)/119 (66.0 ± 4.3)	55 (68.0 ± 5.0)/67 (65.7 ± 4.7)	104 (65.7 ± 5.2)/135 (65.8 ± 4.7)

Dose #: 0 unvaccinated; dose 1 and 2: minimum day 14 post-vaccination and before next dose. Positive: seropositive for IgG-N (nucleoprotein); negative: seronegative for IgG-N; y.o.: years old.

An initial data overview was performed for the complete set using unsupervised visualization and clustering methods to determine dominant patterns in the data. Principal-component analysis (PCA) (Figure S2A) indicates a dominant effect of vaccination on serology profiles in all age groups with the most apparent separation between the unvaccinated and vaccination 1 groups. Change over time with vaccination is once again significantly different between COVID-19+ and COVID-19− groups, showing major value difference in SIgG between these two groups as well as lower level of neutralization in COVID-19− cohorts in all age groups and both sexes even after vaccination (Figure 1A). However, from observing individual serology factors, differences between age and sex groups is not apparent. However, effect of age and sex on the serology measure starts to be visible in the ANOVA analysis (Figure 1B) as well as guided PCA (gPCA) analysis, a semi-supervised method that shows group loadings in the PCA (Figure 1C) (Reese, Archer et al. 2013). Furthermore, t-distributed stochastic network embedding (t-SNE) analysis (Figure S2B), providing projection of sample points while preserving relationship between sample points, indicates some grouping of sample points based on sex as is shown with *p* values of the significance of the separation by sex in different subgroups (Figure S2C). The association of the effect of sex on antibody responses was particularly significant between male and female participants <40 years old (y.o.). who were either SARS-CoV-2 antibody negative or positive across all three first doses of vaccination. Meanwhile, the 40–60 y.o. group showed significance only in the SARS-CoV-2-positive subjects after vaccination 1 and 3, and there were limited/transient sex effects in the >60 y.o. group, reserved for SARS-CoV-2-seropositive individuals after the second vaccination dose. Thus, t-SNE suggests that age is a primary determinant of antibody response with complex dependence between the response and sex.

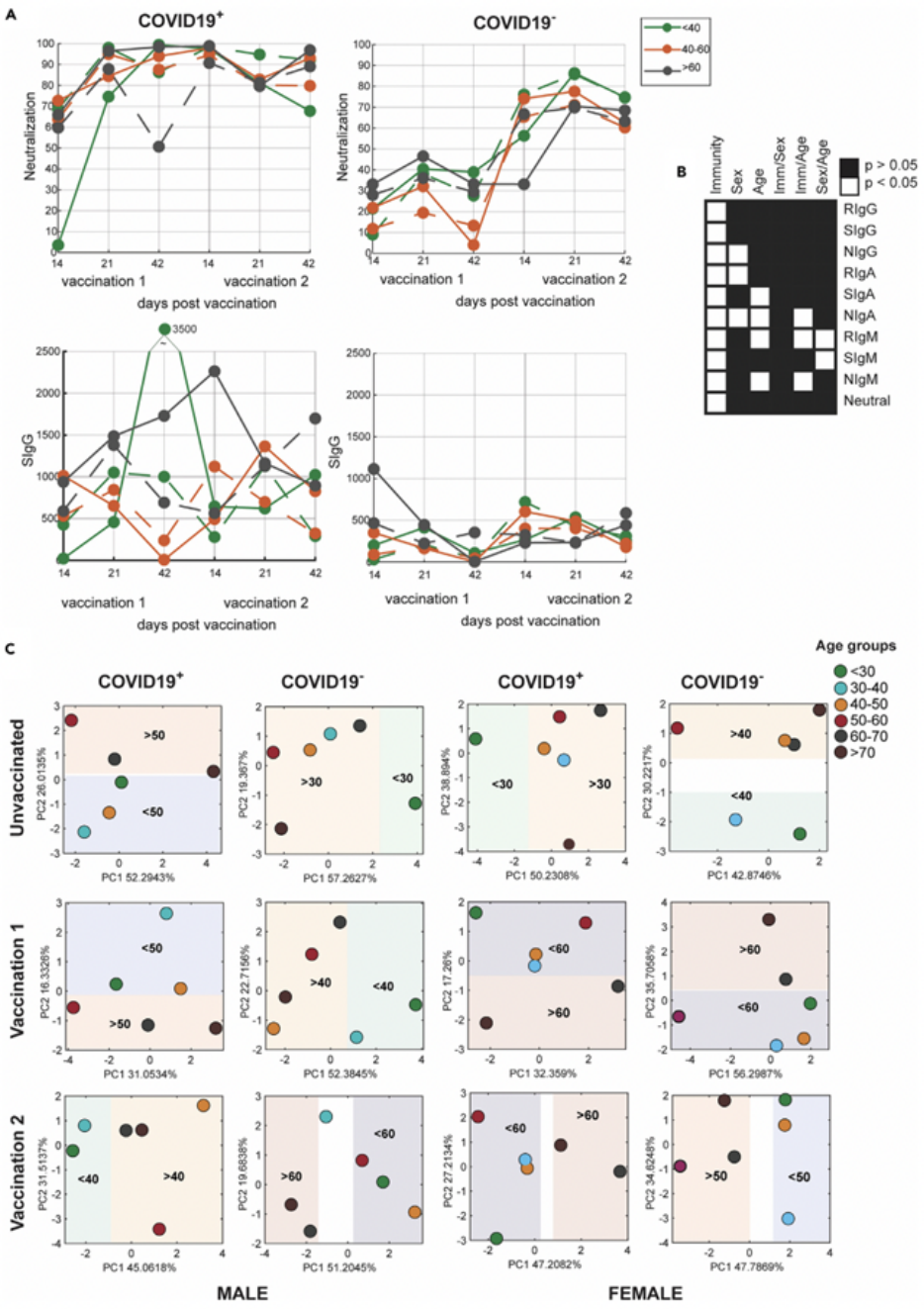


Figure 1. Small differences between sex and age groups in response to vaccination and infection are observed. Samples are divided byCOVID-19status (COVID-19 =noCOVID-19infectionhistory, confirmedby negative NIgGserology;COVID-19+= history ofCOVID-19 infection, confirmed by positive NIgG serology). (A and B) Graphical representation of the mean values for neutralization and SIgG at three time points after vaccination 1 and vaccination 2 (days 14, 21, and 42 post-vaccination) in cohorts grouped by sex and age (in three age groups <40, 40–60, and over 60 years of age). (B) Three-way ANOVA evaluation of the mean differences between measurements grouped by acquired immunity (COVID-19 or COVID-19+), sex (male/female), or age (under 40, 40–60, or over 60 years of age). Indicated as white boxes are statistically significant mean differences for direct and combined effect. (C) gPCA for log transformed and Z score scaled dataset of 9 different antibody responses and neutralization (10 features) with included PC1 for guided PCA (gPCA) for age groups for each subset divided by vaccination dose and sex; age groups are under 40, 40–60, and over 60 years of age. Shown are loadings for each group.

Further, hierarchical cluster analysis (HCL, Figure S3) indicates comparable separation between samples collected pre-and post-vaccination in all groups, independent of sex and infection status. Interestingly, vaccination-driven separation of samples is independent, in this type of analysis, of the time since vaccination. In all four groups of samples (including male and female groups distinguished by SARS-CoV-2 infection-acquired immunity status), HCL shows that neutralization values cluster most closely with receptor binding immunoglobulin G (RIgG), spike binding immunoglobulin G (SIgG), and spike binding immunoglobulin A (SIgA) levels. In COVID-19+ samples, neutralization is also clustered with receptor binding immunoglobulin A (RIgA). Uniquely in HCL of COVID-19- males, neutralizing immunoglobulin G (NIgG) clusters with neutralizing immunoglobulin M (NIgM), spike and receptor binding immunoglobulin M (SIgM and RIgM) while it is most strongly grouped with NIgA, RIgA, and SIgA in the other groups (Figure 1B). Additionally, Ig factors primarily cluster by size with exceptions of NIgG which in all four groups shows closer proximity to non-IgG features. Once again, these clustering results suggest a level of sex-dependent behavior in the relationships between measured antibody responses (Figure S3).

Co-behavior between antibody measures and neutralization is sex, age, and immunity dependent

Detailed analysis of feature co-clustering (i.e., similarities in behavior between neutralization and antibodies) was performed using the fuzzy C-means (FCM) clustering method. This approach provides information about the level of co-clustering for each feature to each group, allowing for possible multiple relationships. Data in Figure 2 show a weight for each antibody response feature for belonging to the cluster relative to their respective neutralization value. Cluster analysis is performed separately for subject groups divided by age, sex, and COVID-19 infection-acquired immunity status. Unlike HCL analyses of all age groups combined (Figure 1), this approach is applied to three age groups separately and shows differences between males and females, particularly in older and COVID-19-positive groups. Interestingly, in females >40 y.o., RIgA and SigA co-cluster with neutralization, and males co-cluster with RigM and SigM responses. In the <40y.o. groups, SigG and RigG levels correlate with neutralization in both males and females.

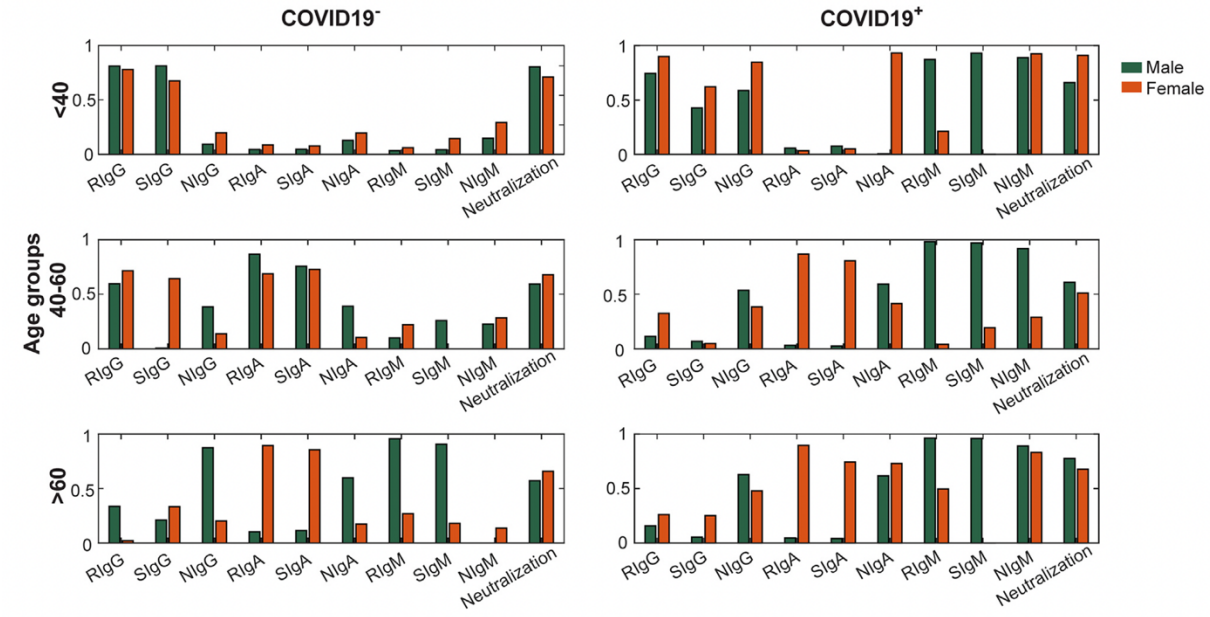


Figure 2. Cluster analysis of antibody responses relative to neutralization shows differences in co-behavior in males and females by age. Fuzzy C-means clustering of antibody response features across data in subgroups divided by age, sex (male in black, female in orange), and COVID-19 infection status (negative or positive SARS-CoV-2 history, confirmed by NIgG level). Shown are membership values, i.e., cluster association of features in different subject cohorts with clusters that have the strongestneutralization membership. Fuzzy C-means hereclusters featureseparately for eachof thegroups ofdata dividedby age, sex, and COVID-19 infection status. Shown are weights (0.0–1.0), i.e., cluster belongings for each antibody response feature relative to neutralization values (weights approaching 1.0 indicate strong clustering with neutralization).

Differences in antibody responses between males and females are dependent on age and infection-acquired immunity

We used three different feature selection methods (see STAR Methods) to determine the most significant feature differences (Figure 3). Features that are selected by all three methods are indicated. The data for all time points were combined in the analysis, but a separate analysis was performed for COVID-19-negative and COVID-19-positive samples across the age groups and is reported here (Figures S2 and S3 show feature selection in each vaccination group). Differences in IgG and IgA factors are identified in participants <40y.o. COVID-19-negative group. Differences in IgM levels are noted in individuals 40–60 y.o. and >60 y.o. The features selected as statistically different using these methods are largely in agreement with features showing major clustering differences in Figure 2.

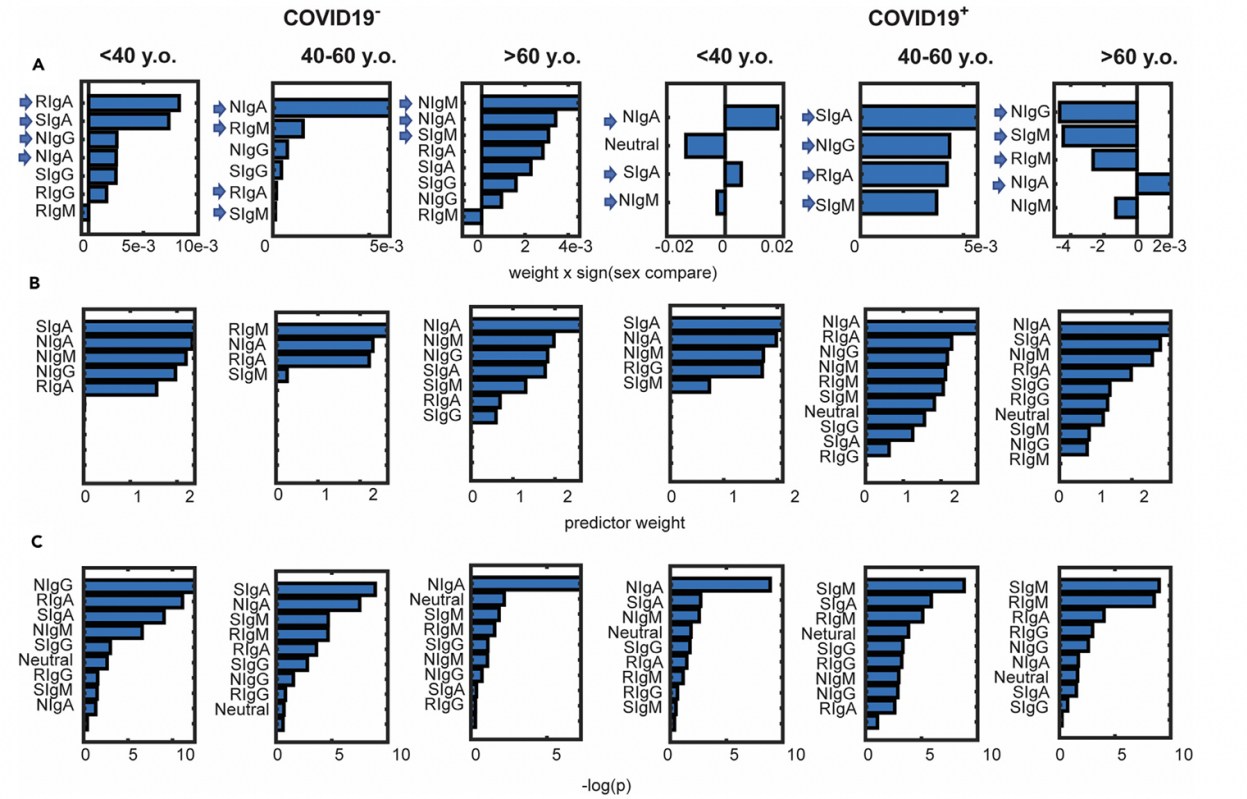


Figure 3. Selection of antibodies showing the largest difference between male and female cohorts in different age and acquired immunity subgroups. Three different feature selection methods were used to identify sex differences in antibody responses in each of the six sample subgroups separated based on the COVID-19 status and participants' age (<40, 40–60, and >60 y.o.). (A–C)Results from the(A)Relieff machine learning feature selection method,(B)feature selection method using neighborhood component analysis for regression (fsrnca), and (C) univariate feature ranking for regression using F-tests (fsrftest) method show major antibody measures that distinguish males from females within specified subgroups. Solid arrows indicate features selected by all three methods. Relieff plots show only antibody features with positive weight(i.e.,features that contribute to significant sex separation), and the sign (i.e., +/) in this representation is related to the male to female mean group ratios with positive sign indicating larger mean value in a male group.

It is important to observe that SIgM and NIgA come up as significant in 4 age and immunity subgroups and both antibodies show different clustering patterns in males and females (Figure 2). In addition to overall differences in these antibody features established by the three methods of feature selection analysis (Figure 3), there are significant changes in antibody responses over this period. In males, there is a rise in the RIgA, NIgA, and SIgA serum levels generally following dose 2 vaccination. In contrast, higher IgM serum levels are noted in females over 60 y.o. in both vaccination 1 and vaccination 2 periods.

Correlation analysis provides quantitative links between sex and antibody responses

Further investigation of the relationship between serological profile and sex was performed using point-biserial correlation specifically developed for analysis of correlations between binary and continuous variables. Figure 5 shows antibody responses correlate with subjects' sex. Once again, SIgM and RIgM are positively correlated with sex in individuals over 60 y.o. following both dose 1 and dose 2 vaccination. As is typical of antibody response evolution through Ig isotype switching with repeated vaccination (or even repeated infection), IgM levels show a negative correlation with sex in the younger age groups with values higher in males than in females.

In the point-biserial correlation analysis, antibody neutralization, an important indicator of protection against serious COVID-19 disease outcomes,[29,30] is only statistically significantly correlated with sex in the >60 group (Figure 4). However, time course analysis (Figure 5) as well as feature selection (Figure 3) indicate some differences in neutralization trends between males and females. To determine whether there are specificities in the contributions of antibodies to neutralization in age and sex groups, a distance correlation analysis was performed between antibody neutralization measurements and other antibody response features as a measure of co-behavior. In addition, relative square distance correlation was tested as a measure of contribution of each antibody response factor to the neutralization value. This analysis showed that, after vaccination 2, neutralization potential decays the fastest among older persons who are male than any other group. This co-behavior also suggests that females retain antibody-neutralization correlations longer than their male counterparts in all age groups.

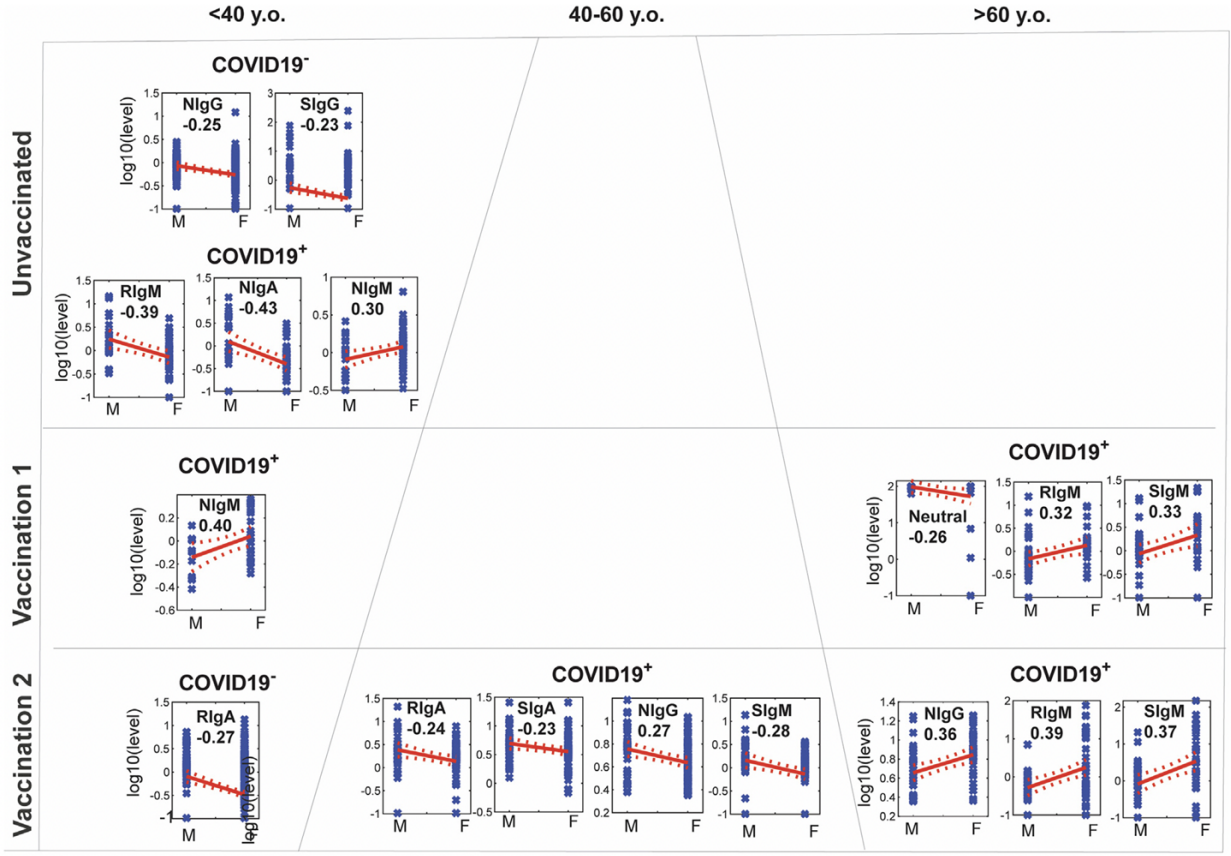


Figure 4. Direct correlation between antibody level and subjects' sex Point-biserial correlation between sex and serological factors. Shown are correlations with $p < 0.05$ and absolute correlation value >0.20 within subgroups. A correlation value between sexes and log10 transformed concentration levels is indicated.

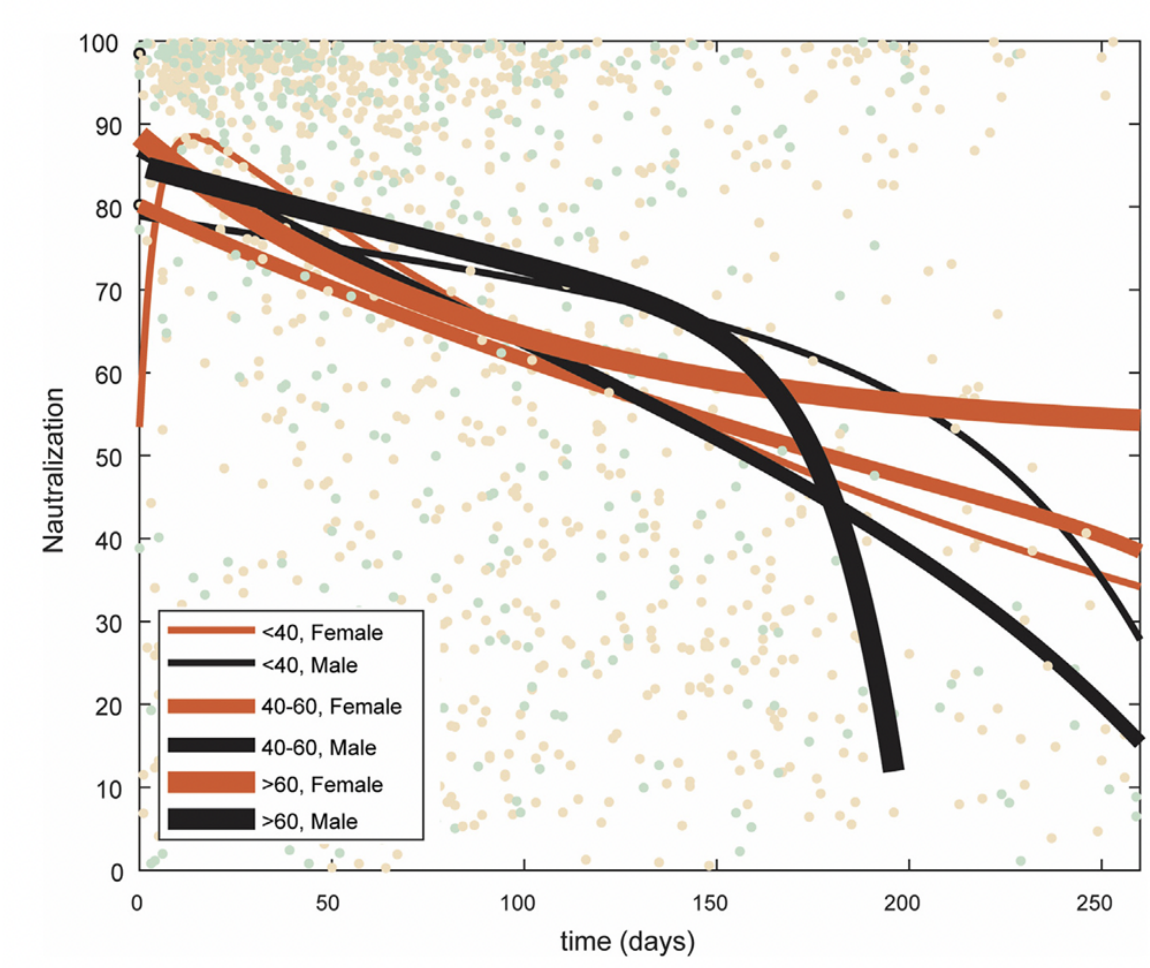


Figure 5 Antibody neutralization levels for over 60-year-old males decay faster than those for other sex and age groups. Values present neutralization measurements in males and females in 3 different age groups following the second dose of COVID-19 vaccination. Exponential fit is optimized separately for each represented group. Neutralization following vaccination 2 for males and females. Shown are exponential best fit lines (as a) exp(b) time)+c) exp(d) time)). Time is shown in days from vaccine 2. Y axis shows the original value. Lines represent dark green, male, and red, female. Also included are actual sample measures showing major individual differences.

Correlation between antibodies and neutralization varies over time differently in males and females

Square of the correlation between two features represents a measure of the contribution of one feature to the variance of the other. Analysis of distance correlation between neutralization and each antibody in male and female groups over time following vaccination dose 1 and dose 2 shows major differences in the pattern of antibody contribution to neutralization (Figure 6). As an example, the contribution of RIgG and NIgA to neutralization in males and females under 40 y.o. is positively correlated over time and highly comparable by sex. However, neutralization and SIgM and RIgM are negatively correlated over time in these same groups. In contrast, following dose 2 vaccination in those over 60 y.o., neutralization is similarly related to RIgG in males and females but inversely correlated with SIgG in the two groups. Thus, although the overall pattern in neutralization measurements is not correlated with sex, the observed levels of neutralization show different and complex relationships with antibody responses. Furthermore, the analysis shown in Figure 6 suggests changes in the correlation of individual antibody responses over time, differing between males and females and by age group. In the under 40-y.o. male group following vaccination 1, neutralization is initially strongly correlated to RIgG and NIgA concentrations and then more strongly to SIgG, NIgG, IgA, and IgM antibodies. In females of this age group assessed at earlier time points, the relationship with neutralization is the strongest with SIgG, NIgG, and SIgA and all three IgM specificities. Following administration of vaccination 2 in this group, the relative contribution of RIgG and SIgG to neutralization initially, at early time points post-vaccination, drops.

Changes in the contribution of antibody response features to neutralization over time in different groups can be further understood by exploring correlations in different time periods. For the ease of presentation and increased number of samples in this case, time was binned into 21-day periods. Distance correlation was calculated using samples for each period, and the square of individual values is divided with the sum of values for each time bin to provide a relative contribution. Thus, Figure 7 shows relative square distance correlation contributions to neutralization of each of the nine antibody response factors at 4 time points for each period. This representation is useful in

that it highlights sex and age differences that were otherwise less apparent in an unsupervised PCA (Figure 7).

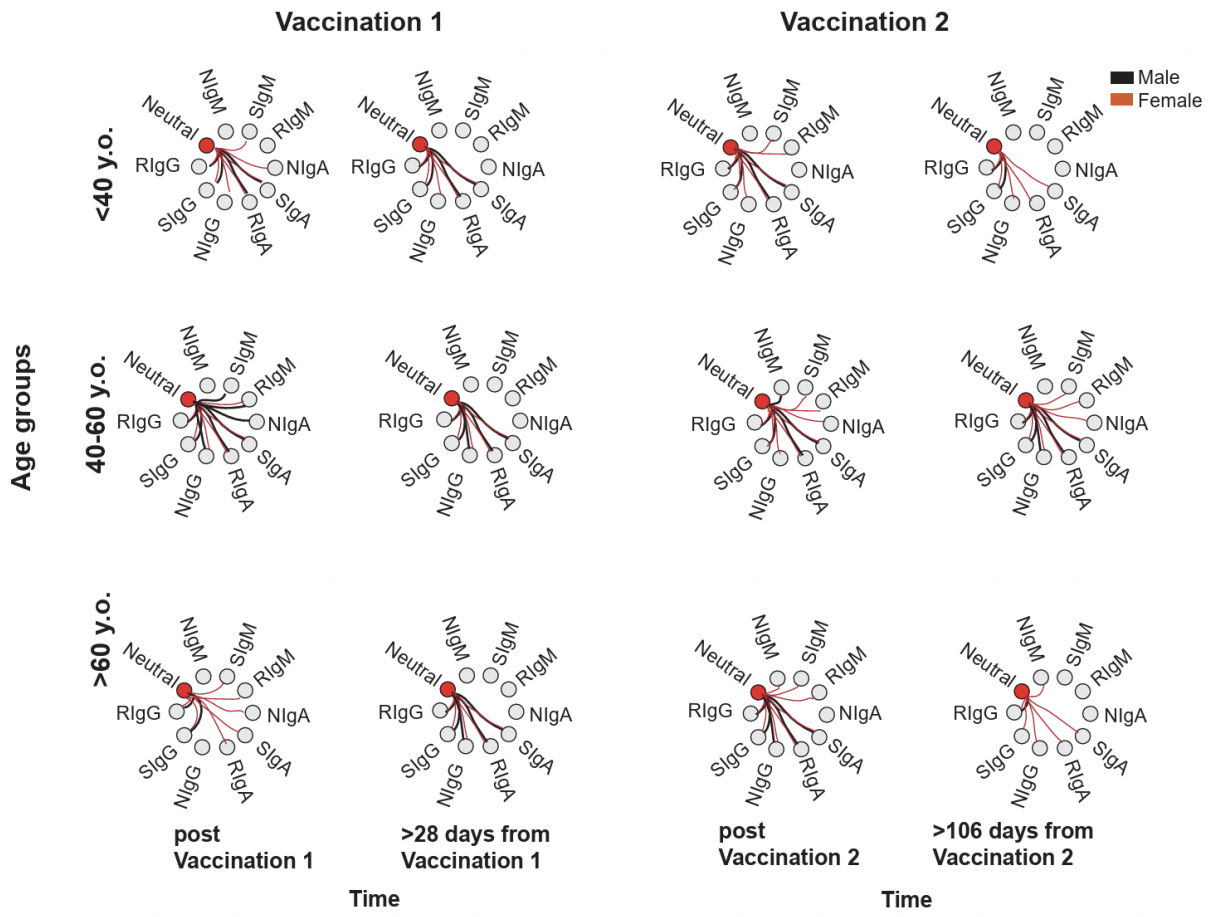


Figure 6 Correlation between neutralization and antibody isotypes is different in males and females in distinct age groups. Distance correlation between neutralization and all other features (pairwise) is calculated, and thresholds were set using sample size appropriate correlation thresholds and *p* values below 0.003 for measurements grouped by sex and age and time from vaccination. Vaccination groups include samples collected prior to half-time between dose 1 and 2 (vaccination 1) and dose 2 and 3 (vaccination 2) showing correlation for all time points following one dose and prior to the next and correlation after the half-time post-vaccination. Shown are correlation edges that pass the hard threshold separately for males (black line) and females (dark red line).

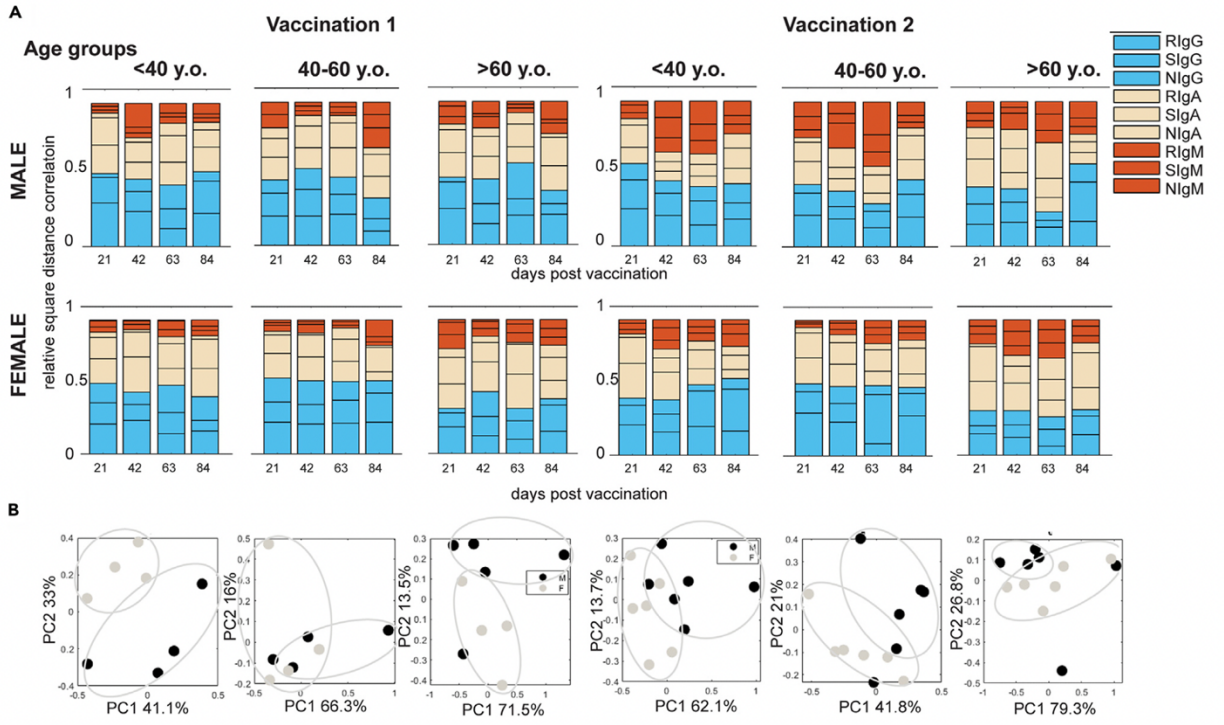


Figure 7 All measured antibody responses contribute to neutralization values at a level that is dependent on sex and age and changes over time. Relative square distance correlation (Y axis) between each antibody response was measured, and neutralization was calculated for 21-day periods post-vaccination 1 and post-vaccination 2 in each subgroup of patients. COVID-19+ and COVID-19- subjects are combined in this analysis. (A) Data are shown in bar graphs with relative contributions by immunoglobulin isotype responses (color-coded) over time (days 21, 42, 63, and 84 post-vaccination 2), and sex effects are depicted in plot groupings. (B) Unsupervised PCAs show separation of males and females square correlation profiles at 4 or 5, 21-day periods in vaccination 1 and 2 (as indicated) for different age groups. Ellipsoids indicate visual groupings of male and female data points.

This relative contribution of different antibody isotypes to neutralization over time depends on age and sex with differences observed in Ig isotype responses to all specific targeted proteins measured and is an important finding of this work. With this novel approach to data analysis, we show that the relationship between antibody responses with neutralization depends on the subject's age and

sex, even in cases where the actual value of neutralization is not significantly different between these subgroups. For example, following vaccination 2 in the oldest group, compared to all studied Ig, the relative contribution of IgG is smaller than that in younger groups particularly in females, while in under 40-y.o. males, the relative contribution of IgM is more significant than in females.

Discussion

We applied novel network analyses to a complex set of antibody response data collected longitudinally from a large cohort of individuals over an important period of the COVID-19 pandemic, bridging naive immunity, infection-acquired immunity, and immunity afforded across serial vaccination. The size and breadth of the cohort age range offered robust analytical outcomes by sex and age across multiple antibody parameters and repeated measures. Sex differences emerged with t-SNE analysis demonstrating that complex, non-linear analyses of these data would be required to understand factors driving antibody responses to COVID-19. Whether pre-immune status influences vaccine/infection/hybrid-mediated immunity remains to be determined, but sex effects identified by HCL analysis suggest that the SARS-CoV-2 serology patterns of unvaccinated COVID-19-negative males were categorically different than those of any other group pre- and post-vaccination (Figure S3). Correlations revealed important sex-associated co-behaviors of antibody responses with neutralization, some of which suggest the important finding that young females may have stronger linkages in mucosal immunity and protection as their serum IgA responses are associated well with neutralization levels. Feature selection methods continued to confirm clustering analysis findings by age, with particularly prominent sex effects in IgA and NIgG responses in individuals <60 y.o. The capacity for significant Ig isotype switching with repeated vaccination was found to be weaker in older females whereas IgA responses in males could improve after vaccination 2. This phenomenon was extended to yet-additional new observations of this study that highlighted an appreciation for the rate of antibody decay, which is quite rapid in males >60 y.o. and where females exhibited a superior retention of Ig isotype switching correlating with neutralization over time. These two latter results emerge as important findings of this study, alongside the expected observation that antibody response profiles are inherently complex patterns in relation to neutralization that differ by sex and age, as shown by distance correlations, and these changed over time. These analytical approaches afforded several

different angles by which to evaluate the complex relationships between antibody responses and neutralization showing that considerations for sex and age were highly important.

Demographic factors including age and sex are known to be associated with responses to both viral infection and immunization.[1,22,31] Our data show differences in antibody responses across vaccination periods, in convalescent individuals with SARS-CoV-2 acquired immunity compared to individuals that did not show naturally acquired SARS-CoV-2 immunity. Understanding the extent and type of this association and its change over time in relation to the resilience to an infection is crucial in attempts toward achieving more protective immunization and effective antiviral approaches. Extensive work on COVID-19 immune responses led to an appreciation that antigen specificity and Ig isotype can contribute to ACE2 neutralization.[13,32,33] While typical primary immune responses dominated by IgM evolve into recall immune responses composed of IgG, IgA, and IgE antibodies, there is variation in which factors contribute to protection against SARS-CoV-2, predictable in part based on antibody neutralization levels. Serum IgA is a dominant antibody soon after the onset of symptoms which peaks during the third week of the disease and provides the greatest contribution to neutralization. Assessment of bronchial alveolar fluid suggests this contributes predominantly to antibody-mediated virus neutralization activity in the lung compared to IgG.[34] Additionally, Ruggiero et al. showed that a coordinated response implicating both SIgM and SIgG is associated with protective immunity following vaccination.[33] While sex differences have been reported in disease outcomes, whether complex features of antibody responses to infection and vaccination play a role in determining immune protection to SARS-CoV-2 remains to be determined.

To identify potential differences in the coordination of the response over time in males and females of different ages, we have developed a novel methodology for analysis of correlation over time and applied it to a large longitudinal dataset spanning the COVID-19 pandemic period, prior to and through vaccination dose series, with robust representation of subjects across different age groups and in both sexes. Our regression analysis of the age dependence of the measured serology profile is consistent with earlier studies showing age of 40 and 60 as significant points in the relationship between serology and response to the virus. Analyses of major features separating measurements in males and females in different age groups (<40 y.o, 40–60 y.o., and >60 y.o.)

show changes at different points in the vaccination series, thus indicating differences in progression of antibody responses over time. In males, RIgA and SIgA show significantly faster increases following vaccination while the opposite is observed in SIgM and RIgM, particularly in the <40 y.o. and >60 y.o. groups. Although many selected antibodies have low weight in feature selection analysis, some are significantly correlated with subject's sex. This is demonstrated in point-biserial correlation for different age and vaccination dose groups. RIgM is significantly correlated with sex in both young adult and senior groups but with opposite ratios, where RIgM is higher in males <40 y.o. yet lower in females >60 y.o. Similarly, SIgM and NIgG are significantly correlated with sex in 40–60 y.o. and over 60 y.o. but are higher in males in the 40–60 y.o. and in females in the over >60 y.o. group. However, neutralization levels are not correlated with sex in any of the age or vaccination groups suggesting different contributors to neutralization. To determine the relationship between neutralization and antibody production in these groups, we first performed a cluster analysis which revealed sex differences in the grouping of antibodies and neutralization in different groups. Furthermore, distance correlation and squared distance correlation analyses across 21-day period bins were employed to determine the contribution of different antibody isotypes to neutralization. The level of correlation contribution differed for different antibody responses over time and by sex and age. Squared distance correlation, representing the relative contribution of a variable to the level of another variable, was also calculated for each antibody measurement pairwise to normalization. Representation of this analysis shows change of contributing factors levels over time. Importantly, contributions in males and females in different age groups are sufficiently distinct allowing PCA separation of male and female samples based on this information. Unlike in the direct analysis of antibody serum where the data based on sex were not clearly separated by PCA, analysis of contributions of these factors to neutralization is clearly very different between sexes.

In sum, our study exploits novel, multivariate, machine learning, and network analysis tools integrating complex immunological parameters over time and across a diverse population to delve into the temporal dynamics of antibody responses through the COVID-19 pandemic. Specifically, unsupervised and supervised machine learning strategies, coupled with square distance correlation, have enabled us to describe changes in the role of individual antibody responses in neutralization of ACE2. Contribution program changes over time, and vaccination dose clearly differs between

sex and age groups with major differences in infected vs. uninfected cohorts. In addition to the anticipated effects of age on the retention antibody responses, our analyses suggest that female antibody responses to SARS-CoV-2 vaccination may be of superior quality in their co-behavior with protection (i.e., neutralization). Our work demonstrates that understanding antibody response profiles and their role in predicting neutralization goes beyond merely measuring absolute titers. Thus, rather than aiming for antibody titer achievements and changing only individual factors therein, our analyses support the pursuit of optimized vaccination strategies that aim to alter the complete network of antibody responses. Furthermore, differences in antibody-mediated responses highlighted in this work suggest the possibility of underlying cell-mediated differences between groups. Immune response differences associated with aging are often associated with immunosenescence and inflamm-aging, which impact the T cell repertoire, innate cell populations, and more.[35] In addition, biological mechanisms underlying sexual dimorphism in immunity have been focused on sex hormone signaling, and variations in Toll-like receptor expression and downstream cytokine production have been[36] observed. It remains unclear how these directly impact SARS-CoV-2 antibody-mediated responses. This sophisticated analysis of antibody responses hereby provides guidance for the parallel study of cell-mediated immunity evaluating sex and age considerations. There is an urgent need for such highly integrated indices of antibody and cell-mediated immunity as the search for reliable correlates of protection against COVID-19 and other emerging pathogens continues, to best inform the design of highly effective vaccine approaches and aid in clinical care.

Limitations of the study

Although the presented study includes nearly 3,700 longitudinal samples from nearly 1,000 individuals, and permitted analysis by sex, age, infection status (i.e., NIgG+), statistical power decreased in subgroups based on vaccination dose and brand or comorbidities; hence these factors were not considered here.

Conclusion

Using a variety of novel tools for knowledge discovery in datasets, we show that age and sex are important variables which impact the nature and temporal dynamics of infection-induced, vaccination-induced, and hybrid immunity. Overall, this work describes a novel analytical pipeline

with the potential to pinpoint changes in the response to infection and/or vaccination in the general or immune-compromised individuals.

Resource availability

Lead contact

Further information and requests for resources and reagents should be directed to and will be fulfilled by the lead contact, Dr. Angela Crawley (acrawley@ohri.ca).

Materials availability

This study did not generate new unique reagents.

Data and code availability

-Data reported in this paper will be shared by the lead contact upon reasonable request.
-Original code is provided at: https://github.com/complimet/Analysis_SARS-CoV-2-infection-and-vaccination. Any additional information required to reanalyze the data reported in this paper is available from the lead contact upon request.
-The relevant data are available in the manuscript and the appendix. Data that are not presented in the Article or appendix are available upon reasonable request from the corresponding author.

Method details

Serology assay

Antibodies against SARS-CoV-2 were measured using a high-throughput direct chemiluminescent ELISA performed on MicroLab STAR robotic liquid handlers (Hamilton) fitted with a 405TS/LS LHC2 plate washer (Biotek/Agilent) (full methods described previously).37 Briefly, SARS-CoV-2 antigens (full trimeric Spike (Wuhan), receptor binding domain (RBD) (Wuhan) and the Nucleocapsid protein) were generously provided by Dr. Yves Durocher (National Research Council of Canada (NRC), Montréal) or purchased from the Metrology division of NRC and coated on assay plates. Human serum samples or controls were either diluted 1:100 for

measurement of all antibody-isotype combinations, or 1:10,000 to resolve saturating signals for Spike and RBD due to vaccination. Controls included an isotype-antigen specific calibration curve pooled human sera from SARS-CoV-2 naive, convalescent, vaccinated individuals as well as a general Ig control. Isotype-specific secondary antibodies detected bound Igs. Antibody titers were determined as lab-specific ug/mL concentrations in relation to the isotype-antigen specific calibration curve or, for IgG, converted to international units (binding antibody units (BAU)/mL) via modelized WHO Standard (NIBSC 20/136).

Antibody neutralization assay

A surrogate protein-based neutralization assay was used to determine the neutralization efficiency in sera. The detailed methods, validation and calibration of the assay is available here.[37] Briefly, SARS-CoV-2 full-trimeric Spike (Wuhan)-coated plates were blocked, and then human serum samples and controls were assayed. Controls included a calibration curve (NRCoV2-20-Fc, NRC) as well as pooled human sera from naive, convalescent, and vaccinated individuals. Subsequent incubation with biotinylated ACE2 (NRC) followed by streptavidin-HRP linkage and chemiluminescent substrate addition permitted the determination of a luminescent signal. Raw luminescence values were blank (serum-free, no ACE2) adjusted using ACE2-only wells (representing unimpeded ACE2-Spike interaction). Percentage inhibition was established by measuring the reduction in ACE2-Spike interaction (0% inhibition = maximal ACE2-Spike interaction).

Sample collection and processing

All biological specimens from SSO are stored in the Coronavirus Variants Rapid Response Network (CoVaRR-Net) Biobank, following the highest standards of biobanking practices in sample collection, processing, storage, access, and distribution (upon application). Sample collection followed approved ethics protocols (REB # H-09-20-6135).

Quantification and statistical analysis

Knowledge discovery in data

Data preprocessing

Data points generated from serology and neutralization assays that were below the level of detection were imputed using 1/5 of the lowest measurement for the given feature. Values above the upper level of quantification were imputed with the highest measured value for the assay. In some analyses, data for each feature across samples is normalized or log transformed, and this transformation is indicated. No other data manipulation was performed. Antibody and neutralization responses were evaluated in specimens collected at baseline and days 14, 21 and 42 post-vaccination (wherever possible).

Data Overview

General overview of the serology measurements was performed using Principal Component Analysis (PCA), guided PCA (gPCA), t-distributed stochastic network embedding (t-SNE) and hierarchical cluster (HCL) analysis. Cluster analysis was done using Fuzzy C-means clustering (function *fcm* in MATLAB). Briefly this approach determines the level of belonging of each feature to each cluster in this way allowing for possible multiple groupings. Fuzzy c-means (FCM) and related methods fuzzy j-means38 allows each feature to belong to more than one group by providing a degree of membership, "belonging", to each cluster by maximizing proximity between similar features and distance between dissimilar features. FCM is based on the minimization of the objective function: $J_m = \sum_{i=1}^{N}\sum_{j=1}^{C} u_{ij}^{m} \| x_i - c_j \|^2$ where $m \in (1, \infty)$ is the "fuzzyfication" factor, u_{ij}^{m} is the membership degree for feature x_i to the cluster j with $c_j$defining the cluster center. FCM clustering assigns objects to groups with features belonging to the same clusters showing more similarity to each other than to features in other clusters. Higher membership value indicates stronger belonging to the cluster with membership value of 1 ultimately indicating that feature is only associated with the single cluster. An optimal number of clusters in FCM analysis was determined using within-cluster sum of squares and silhouette methods applied to k-means clustering as a directly related crisp method. Clustering with this approach was performed to determine grouping of features in different subject cohorts. Function used to determine number of clusters in FCM is provided on GitHub.

Guided PCA (gPCA) was performed following method previously presented for identification and batch analysis.[39] MATLAB function for gPCA application presented here is provided on GitHub.

Briefly, this approach is focusing on the investigation of the importance of each group corresponding to the corresponding principal component (PC). In order to determine group loading contribution "batch" in our case group indicator matrix G, defined as *n* x *b* matrix where *n* is number of samples and *b* number of groups as assembled such as: $g_{ik} = \begin{cases} 1 \; if \; sampe \; i \; is \; in \; group \; k \\ 0 \; otherwise \end{cases}$. Then single value decomposition of the guided matrix calculated as $G'X$ gives group loadings in PCA and can be used to determine separation of groups in a guided sense.

Correlation analysis

Correlations were calculated using Pearson, distance and point bi-serial correlation. Pearson correlation is a standard method used for linear correlation assessment and was used for the determination of correlation between distance correlation level values for different subgroups of the cohort.

Distance correlation

Distance correlation was performed using previously published applications[27] and MATLAB function provided on GitHub. Briefly, distance correlation[40] was calculated using distance covariance, rather than direct covariance used in Pearson method. In this way, distance correlation provides information about both linear and non-linear correlations. Formally, distance correlation between features *X* and *Y* is calculated as:

$$dCor(X,Y) = \frac{dCov(X,Y)}{\sqrt{dVar(X)dVar(Y)}}$$

distance covariance is determined as:

$$dCov(X,Y)^2 = \frac{1}{n^2}\sum_{j=1}^{n}\sum_{k=1}^{n} A_{j,k}B_{j,k}$$

where *A* and *B* are calculated as simple linear functions of the pairwise distances between elements in samples *X* and *Y*. *A* and *B* are doubly centered distance matrices for variables *X* and *Y*, respectively, calculated from the pairwise distance between elements in each sample set calculated as:

$A_{j,k} = a_{j,k} - a_{j.} - a_{k.} + a_{..}$ where $a_{j,k} = \sqrt{\left(x_j - x_k\right)\left(x_j - x_k\right)'}$

and $a_{j.}$ and $a_{k.}$ are respectively the *j*-row and *k*-column mean values and $a_{..}$ is the overall mean of matrix *A*. The distance between x_j and x_k is calculated using Euclidian distance. Matrix *B* is populated using equivalent measures for variable *Y*.

Square distance correlation

Square distance correlation, i.e., the coefficient of determination, is used to represent the fraction of the variation in a variable that can be explained by the other variable. Relative square distance correlation is calculated as a square distance correlation divided by the sum of square distance correlation values for all features.

Correlation between binary values (e.g., sex) and continuous values (e.g., serological measurements) was determined using point-biserial correlation method as:

$$\rho_{pb} = \frac{M_1 - M_0}{s_n}\sqrt{\frac{n_1 n_o}{n^2}}$$

where correlation is calculated between binary and continuous variable by dividing continuous variable into two groups, 0 and 1, based on values of the binary feature and where *M0* and *M1* are mean values, *n0* and *n1* are numbers of samples of two subgroups and *sn* is the standard deviation for the complete continuous variable set.

Polynomial function regression analysis was performed using second order polynomial and exponential functions and bisquare robustness analysis. Briefly, the bisquare robustness method for polynomial fit determination minimizes a weight sum of squares with points near the line getting full weight and points further from the line getting a reduced weight. Points that are farther from the line are expected by random chance and hence are given a weight of zero. In this way, the bisquare method aims to find a function of best fit using a least squares approach while at the same time minimizing the effect of outliers.

Feature selection

Selection of the most significantly different features between different groups of samples was performed using three different methods to determine method-independent major features: 1) statistical feature selection using F-test (function *fsrftest* running under MATLAB); 2) machine learning methods Relieff (function relief in MATLAB); and 3) neighborhood component analysis

for regression (*fsrnca* function in MATLAB). Features were considered significantly different if selected by all three methods. Data was *Z* score normalized for each feature prior to analysis. In F-test features with $p < 0.05$, $-\log(p) > 3$ is selected as significant. In Relieff, all features with positive weight are determined as possibly contributing to group selection. Similarly, in fsrnca, all features with positive weights are kept as possibly significant. *Fsrnca* aims to find, i.e., learn, a distance metric to maximize leave-one-out classification performance. Thus, the feature selection analysis used here combines two different ML methods including filter (Relieff) and wrapper (fsrnca) with a statistical method (F-test) to determine consistently significant features. MATLAB Notebook for Relieff feature selection is provided on GitHub.

Acknowledgments
This study was supported by the Public Health Agency of Canada Immunity Task Force (grant #2122-HQ-000074) awarded to A.M.C., National Research Council of Canada Collaborative R&D Initiative Pandemic Response Challenge Program grant AI4D-102-3 to S.A.L.B. and M.C.-C., as well as a Canadian Institutes for Health Research (CIHR) Operating Grant (grant #175622) to the Coronavirus Variants Rapid Response Network (CoVaRR-Net) to M.-A.L. The funders had no role in the study design or in the decision to submit this manuscript.

Author contributions
M.C.-C. accessed and verified the data and contributed to the conceptualization, data curation, formal analysis, software, validation, visualization, writing – original draft, and writing – review and editing of the revised manuscript. S.B. accessed and verified the data and contributed to the data curation, formal analysis, software, visualization, and writing – original draft. Y.G., P.S.M., and C.A. contributed to the data curation, formal analysis, investigation, and writing – original draft. S.B. contributed to the conceptualization, methodology, validation, writing – review and editing, and editing of the revised manuscript. C.L.C. contributed to the conceptualization, methodology, resources, validation, and writing – original draft. M.-A.L. accessed and verified the data and contributed to the conceptualization, funding acquisition, methodology, project administration, resources, and supervision. J.F. and C.A.P. contributed to the conceptualization, methodology, validation, and writing – review and editing. A.M.C. accessed and verified the data and contributed to the conceptualization, funding acquisition, methodology, project administration, resources, supervision, and writing – review and editing. All authors have seen and approved of the final text.

Declaration of interests
The authors declare no competing interests.

Supplemental information: PDF (216.90 KB)

References

1. Scully, E.P., Haverfield, J., Ursin, R.L., Tannenbaum, C., and Klein, S.L. (2020). Considering how biological sex impacts immuneresponsesandCOVID-19outcomes. Nat. Rev. Immunol. 20, 442–447.
2. Arnold, C.G., Libby, A., Vest, A., Hopkinson, A., and Monte, A.A. (2022). Immune mechanisms associated with sex-based differences in severe COVID-19 clinical outcomes. Biol. Sex Differ. 13,7.
3. Chen, L., Liao, H., Huang, G., Ding, S., Guo, W., Huang, T., and Cai, Y. (2022). Identification of DNA Methylation Signature and Rules for SARS-CoV-2 Associated with Age. Front. Biosci. 27, 204–211.
4. Huang, F., Chen, L., Guo, W., Zhou, X., Feng, K., Huang, T., and Cai, Y. (2022). Identifying COVID-19 Severity-Related SARS-CoV-2 Mutation Using a Machine Learning Method. Life 12, 806.
5. Takahashi, T., Ellingson, M.K., Wong, P., Israelow, B., Lucas, C., Klein, J., Silva, J., Mao, T., Oh, J.E., Tokuyama, M., et al. (2020). Sex differences in immune responses that underlie COVID-19 disease outcomes. Nature 588, 315–320.
6. Dehingia, N., and Raj, A. (2021). Sex differences in COVID-19 case fatality: do we know enough? Lancet Global Health 9, e14–e15.
7. Nguyen, N.T., Chinn, J., de Ferrante, M., Kirby, K.A., Hohmann, S.F., and Amin, A. (2021). Male gender is a predictor of higher mortality in hospitalized adults with COVID19. PLoS One 16, e0254066.
8. Alghamdi, I.G., Hussain, I.I., Almalki, S.S., Alghamdi, M.S., Alghamdi, M.M., and ElSheemy, M.A. (2014). The pattern of Middle east respiratory syndrome coronavirus in Saudi Arabia: A descriptive epidemiological analysis of data from the Saudi Ministry of Health. Int. J. Gen. Med. 7, 417–423.
9. Channappanavar, R., Fett, C., Mack, M., Ten, E.P.P., Meyerholz, D.K., and Perlman, S. (2017). Sex-Based Differences in Susceptibility to Severe Acute Respiratory Syndrome Coronavirus Infection. J. Immunol. 198, 4046–4053.
10. Peckham, H., de Gruijter, N.M., Raine, C., Radziszewska, A., Ciurtin, C., Wedderburn, L.R., Rosser, E.C., Webb, K., and Deakin, C.T. (2020). Male sex identified by global COVID19 meta-analysis as a risk factor for death and ITU admission. Nat. Commun. 11, 6317.
11. Lott, N., Gebhard, C.E., Bengs, S., Haider, A., Kuster, G.M., Regitz-Zagrosek, V., and Gebhard, C. (2023). Sex hormones in SARSCoV-2 susceptibility: key players or confounders? Nat. Rev. Endocrinol. 19, 217–231.
12. Taneja, V. (2018). Sex hormones determine immune response. Front. Immunol. 9, 1931.
13. Klingler, J., Weiss, S., Itri, V., Liu, X., Oguntuyo, K.Y., Stevens, C., Ikegame, S., Hung,C.T., Enyindah-Asonye, G., Amanat, F., et al. (2021). Role of Immunoglobulin MandA Antibodies in the Neutralization of Severe Acute Respiratory Syndrome Coronavirus 2. J. Infect. Dis. 223, 957–970.
14. Meyer, E.G., Simmons, G., Grebe, E., Gannett, M., Franz, S., Darst, O., Di Germanio, C., Stone, M., Contestable, P., Prichard, A., et al. (2021). Selecting COVID-19 convalescent plasma for neutralizing antibody potency using a high-capacity SARS-CoV-2 antibody assay. Transfusion (Paris) 61, 1160–1170.
15. Diao, B., Wang, C., Tan, Y., Chen, X., Liu, Y., Ning, L., Chen, L., Li, M., Liu, Y., Wang, G., et al. (2020). Reduction and Functional Exhaustion of T Cells in Patients With Coronavirus Disease 2019 (COVID-19). Front. Immunol. 11, 827.
16. Giamarellos-Bourboulis, E.J., Netea, M.G., Rovina, N., Akinosoglou, K., Antoniadou, A., Antonakos, N., Damoraki, G., Gkavogianni, T., Adami, M.E., Katsaounou, P., et al. (2020). Complex Immune Dysregulation in COVID19 Patients with Severe Respiratory Failure. Cell Host Microbe 27, 992–1000.e3.
17. Grifoni, A., Weiskopf, D., Ramirez, S.I., Mateus, J., Dan, J.M., Moderbacher, C.R., Rawlings, S.A., Sutherland, A., Premkumar, L., Jadi, R.S., et al. (2020). Targets of T Cell Responses to SARS-CoV-2 Coronavirus in Humans with COVID-19 Disease and Unexposed Individuals. Cell 181, 14891501.e15.
18. Peng,Y.,Mentzer,A.J.,Liu,G., Yao,X.,Yin,Z., Dong, D., Dejnirattisai, W., Rostron, T., Supasa, P., Liu, C., et al. (2020). Broad and strong memory CD4+ and CD8+ T cells induced by SARS-CoV-2 in UK convalescent individuals following COVID-19. Nat. Immunol. 21, 1336–1345.

19. DelValle, D.M., Kim-Schulze, S., Huang, H.H., Beckmann, N.D., Nirenberg, S., Wang, B., Lavin, Y., Swartz, T.H., Madduri, D., Stock, A., et al. (2020). An inflammatory cytokine signature predicts COVID-19 severity and survival. Nat. Med. 26, 1636–1643. 20. Lucas, C., Wong, P., Klein, J., Castro, T.B.R., Silva, J., Sundaram, M., Ellingson, M.K., Mao, T., Oh, J.E., Israelow, B., et al. (2020). Longitudinal analyses reveal immunological misfiring in severe COVID-19. Nature 584, 463–469.
21. Leung,G.M.,Medley,A.J.,Ho, L.M.,Chau,P., Wong, I.O.L., Thach, T.Q., Ghani, A.C., Donnelly, C.A., Fraser, C., Riley, S., et al. (2004). The epidemiology of severe acute respiratory syndrome in the 2003 Hong Kong epidemic: An analysis of all 1755 patients. Ann. Intern. Med. 141, 662–673.
22. Fink, A.L., Engle, K., Ursin, R.L., Tang, W.Y., and Klein, S.L. (2018). Biological sex affects vaccine efficacy and protection against influenza in mice. Proc. Natl. Acad. Sci. USA 115, 12477–12482.
23. Khan, S.R., van der Burgh, A.C., Peeters, R.P., van Hagen,P.M., Dalm, V.A.S.H., andChaker, L. (2021). Determinants of Serum Immunoglobulin Levels: A Systematic Review and Meta-Analysis. Front. Immunol. 12, 664526.
24. Khan, S.R., Chaker, L., Ikram, M.A., Peeters, R.P., van Hagen, P.M., and Dalm, V.A.S.H. (2021). Determinants and Reference Ranges of Serum Immunoglobulins in Middle-Aged and Elderly Individuals: a Population-Based Study. J. Clin. Immunol. 41, 1902–1914.
25. Sha, C., Cuperlovic-Culf, M., and Hu, T. (2021). SMILE: systems metabolomics using interpretable learning and evolution. BMC Bioinf. 22, 284.
26. Cuperlovic-Culf, M., Nguyen-Tran, T., and Bennett, S.A.L. (2023). Machine Learning and Hybrid Methods for Metabolic Pathway Modeling. Methods Mol. Biol. 2553, 417–439.
27. Monti, F., Stewart, D., Surendra, A., Alecu, I., Nguyen-Tran, T., Bennett, S.A.L., and Cuperlovic-Culf, M. (2023). Signed Distance Correlation (SiDCo): an online implementation of distance correlation and partial distance correlation for data-driven network analysis. Bioinformatics 39, btad210.
28. Collins, E., Galipeau, Y., Arnold, C., Bosveld, C., Heiskanen, A., Keeshan, A., Nakka, K., Shir-Mohammadi, K., St-Denis-Bissonnette, F., Tamblyn, L., et al. (2022). Cohort profile: S top the Spread Ottawa (SSO)- a communitybased prospective cohort study on antibody responses, antibody neutralisation efficiency and cellular immunity to SARS-CoV-2 infection and vaccination. BMJ Open 12, e062187.
29. Ju,B.,Zhang,Q.,Ge,J.,Wang,R.,Sun,J.,Ge, X., Yu, J., Shan, S., Zhou, B., Song, S., et al. (2020). Human neutralizing antibodies elicited by SARS-CoV-2 infection. Nature 584, 115–119.
30. Piccoli, L., Park, Y.J., Tortorici, M.A., Czudnochowski, N., Walls, A.C., Beltramello, M., Silacci-Fregni, C., Pinto, D., Rosen, L.E.,Bowen, J.E., et al. (2020). Mapping Neutralizing and Immunodominant Sites on the SARS-CoV-2 Spike Receptor-Binding Domain by Structure-Guided HighResolution Serology. Cell 183, 10241042.e21.
31. Klein, S.L., and Flanagan, K.L. (2016). Sex differences in immune responses. Nat. Rev. Immunol. 16, 626–638.
32. Ma, H., Zeng, W., He, H., Zhao, D., Jiang, D., Zhou, P., Cheng, L., Li, Y., Ma, X., and Jin, T. (2020). Serum IgA, IgM, and IgG responses in COVID-19. Cell. Mol. Immunol. 17, 773–775.
33. Ruggiero, A., Piubelli, C., Calciano, L., Accordini, S., Valenti, M.T., Carbonare, L.D., Siracusano, G., Temperton, N., Tiberti, N., Longoni, S.S., et al. (2022). SARS-CoV-2 vaccination elicits unconventional IgM specific responses in naı ̈ve and previously COVID-19-infected individuals. EBioMedicine 77, 103888.
34. Sterlin, D., Mathian, A., Miyara, M., Mohr, A., Anna, F., Claë r, L., Quentric, P., Fadlallah, J., Devilliers, H., Ghillani, P., et al. (2021). IgA dominates the early neutralizing antibody response to SARS-CoV-2. Sci. Transl. Med. 13, eabd2223.
35. Fagnoni, F.F., Vescovini, R., Passeri, G., Bologna, G., Pedrazzoni, M., Franceschi, C., Passeri, M., Sansoni, P.G., Lavagetto, A., and Casti, C. (2000). Shortage of circulating naive CD8(+) T cells provides new insights on immunodeficiency in aging. Blood 95, 2860–2868.
36. Torcia, M.G., Nencioni, L., Clemente, A.M., Civitelli, L., Celestino, I., Limongi, D., Fadigati, G., Perissi, E., Cozzolino, F., Garaci, E., and Palamara, A.T.E. (2012). Sex differences in the response to viral

infections: TLR8 and TLR9 ligand stimulation induce higher IL10 production in males. PLoS One 7, e39853.
37. Colwill, K., Galipeau, Y., Stuible, M., Gervais, C., Arnold, C., Rathod, B., Abe, K.T., Wang, J.H., Pasculescu, A., Maltseva, M., et al. (2022). A scalable serology solution for profiling humoral immune responses to SARS-CoV-2 infection and vaccination. Clin. Transl. Immunol. 11, e1380.
38. Belacel, N., Cuperlovic-Culf, M., Laflamme, M., and Ouellette, R. (2004). Fuzzy J-Means and VNS methods for clustering genes from microarray data. Bioinformatics 20, 1690–1701.
39. Reese, S.E., Archer, K.J., Therneau, T.M., Atkinson, E.J., Vachon, C.M., De Andrade, M., Kocher, J.P.A., and Eckel-Passow, J.E. (2013). A new statistic for identifying batch effects in high-throughput genomic data that uses guided principal component analysis. Bioinformatics 29, 2877–2883.
40. Sze´kely, G.J., Rizzo, M.L., and Bakirov, N.K. (2007). Measuring and testing dependence by correlation of distances. Ann. Stat. 35,6

A-1.14 Seasonal human coronaviruses OC43, 229E, and NL63 induce cell surface modulation of entry receptors and display host cell-specific viral replication kinetics

Preface

(This work has been previously published as a research article)

Siragam V, Maltseva M, Castonguay N, **Galipeau Y**, Srinivasan MM, Soto JH, Dankar S, Langlois M-A. **Seasonal human coronaviruses OC43, 229E, and NL63 induce cell surface modulation of entry receptors and display host cell-specific viral replication kinetics**. Microbiol Spectr. 2024 Jul 2;12(7):e0422023. Epub 2024 Jun 12.

https://doi.org/10.1128/spectrum.04220-23

Copyright © 2024 Siragam et al.
This is an open-access article distributed under the terms of the Creative Commons Attribution 4.0 International license.

Abstract

The emergence of the COVID-19 pandemic prompted an increased interest in seasonal human coronaviruses. OC43, 229E, NL63, and HKU1 are endemic seasonal coronaviruses that cause the common cold and are associated with generally mild respiratory symptoms. In this study, we identified cell lines that exhibited cytopathic effects (CPE) upon infection by three of these coronaviruses and characterized their viral replication kinetics and the effect of infection on host surface receptor expression. We found that NL63 produced CPE in LLC-MK2 cells, while OC43 produced CPE in MRC-5, HCT-8, and WI-38 cell lines, while 229E produced CPE in MRC-5 and WI-38 by day 3 post-infection. We observed a sharp increase in nucleocapsid and spike viral RNA (vRNA) from day 3 to day 5 post-infection for all viruses; however, the abundance and the proportion of vRNA copies measured in the supernatants and cell lysates of infected cells varied considerably depending on the virus-host cell pair. Importantly, we observed modulation of coronavirus entry and attachment receptors upon infection. Infection with 229E and OC43 led to a downregulation of CD13 and GD3, respectively. In contrast, infection with NL63 and OC43 leads to an increase in ACE2 expression. Attempts to block entry of NL63 using either soluble ACE2 or anti-ACE2 monoclonal antibodies demonstrated the potential of these strategies to greatly reduce infection. Overall, our results enable a better understanding of seasonal coronaviruses infection kinetics in permissive cell lines and reveal entry receptor modulation that may have implications in facilitating co-infections with multiple coronaviruses in humans.

Importance

Seasonal human coronavirus is an important cause of the common cold associated with generally mild upper respiratory tract infections that can result in respiratory complications for some individuals. There are no vaccines available for these viruses, with only limited antiviral therapeutic options to treat the most severe cases. A better understanding of how these viruses interact with host cells is essential to identify new strategies to prevent infection-related complications. By analyzing viral replication kinetics in different permissive cell lines, we find that cell-dependent host factors influence how viral genes are expressed and virus particles released. We also analyzed entry receptor expression on infected cells and found that these can be up- or down-modulated depending on the infecting coronavirus. Our findings raise concerns over the possibility of infection enhancement upon co-infection by some coronaviruses, which may facilitate genetic recombination and the emergence of new variants and strains.

Introduction

Human coronaviruses (HCoVs) OC43, 229E, NL63, and HKU1 are seasonal endemic viruses circulating worldwide that cause mostly non-severe upper tract respiratory infections (1–5). It is estimated that they account for 15%–30% of all the common cold cases (6). Epidemiological studies on respiratory infections have reported that OC43 is the most prevalent strain in humans followed by NL63, 229E, and HKU1 (7–9). While HCoVs generally cause mild symptoms in healthy individuals, some reports have shown that NL63 and 229E can cause life-threating respiratory problems, such as pneumonia, leading to respiratory distress syndrome in immunocompromised individuals (10, 11).

Phylogenetically, OC43 and HKU1 belong to the betacoronavirus genus that includes highly pathogenic coronaviruses such as MERS-CoV, SARS-CoV, and SARS-CoV-2. Coronaviruses 229E and NL63, both belong to the alphacoronavirus genus (12). OC43, 229E, and NL63 use different viral attachment and entry receptors including peptidases, cell adhesion molecules, and sugars. In the case of 229E, the cellular receptor is CD13 (aminopeptidase N), while OC43 and HKU1 both bind sialic acid (9-O-acetylated ganglioside; GD3) for cell attachment, and HKU1 uses the protease TMPRSS2 as its protein receptor (12–15). NL63 makes use of heparin sulfate for

cell attachment and angiotensin-converting enzyme 2 (ACE2) for cell entry, while the protein receptor for OC43 has still not been identified (16, 17). Of interest, previous studies have reported the inhibitory role of soluble ACE2 (sACE2) to prevent SARS-CoV-2 infection, which also shares ACE2 as an entry receptor with NL63 (18). However, the blocking effect of sACE2 or monoclonal ACE2 antibody therapy for NL63 infections has not been reported. Alternatively, interferons as potential antiviral regulators against OC43 and 229E infections have been recently studied (19). Although some antiviral drugs such as the RNA-dependent RNA polymerase inhibitor remdesivir and the protease inhibitor nirmatrelvir can inhibit OC43, 229E, and NL63 in laboratory assays (20–22), these are not commonly prescribed to infected patients. In fact, there are very few antiviral drugs and no vaccines for common cold coronaviruses (23).

Although seasonal coronaviruses have been studied using animal models (24), most of our knowledge of these viruses has been acquired using cell line models (4, 25–27). Cell lines of various types and animal origins have been used to understand the mechanism of virus entry into cells (15, 17, 28), viral replication (4, 29), cytopathic effects (CPE) (26, 30), and to test the neutralizing ability of antibodies (31). While viral replication and pathogenesis have been extensively characterized for highly pathogenic coronaviruses like SARS-CoV-2, there is a gap in knowledge of HCoV viral replication kinetics in permissive cell lines and their effects on the host cells. In this study, we identified permissive cell lines susceptible to cytopathic effects upon OC43, 229E, and NL63 infection and then characterized replication kinetics in these cells by tracking vRNA transcripts coding for the nucleocapsid (N) and spike (S) proteins. We also investigated the modulation of key cell receptors and attachment markers following infection. Finally, we tested the effects of soluble ACE2 and anti-ACE2 monoclonal antibodies at blocking NL63 infection. This detailed study of HCoV infection provides a better understanding of the replication and infection of these viruses in cell culture models which can help prompt the development of treatments, antivirals, and cures for the common cold.

Material and methods

Cell culture

HCT-8 cells (human ileocecal adenocarcinoma; ATCC/CCL-244), HEK 293T cells (human embryonic kidney; CRL-3216/ATCC), HEK293/ACE2-stable cell line (HEK293 cells stably expressing angiotensin-converting enzyme 2; BEI Resources/NR-52511) were grown in RPMI-1640 medium supplemented with 100 units/mL penicillin (P), 100 µg/mL streptomycin, and 10% FBS. MRC-5 cells (human lung fibroblasts; CCL-17/ATCC), WI-38 cells (human fetal lung; CCL-75/ATCC), Vero E6 cells (African green monkey kidney cells; CRL-1586/ATCC), and Calu-3 cells (human non-small-cell lung adenocarcinoma; HTB-55/ATCC) were grown in DMEM (MUTICELL#319-005-CL) medium supplemented with 100 units/mL penicillin, 100 µg/mL streptomycin, and 10% FBS. BEAS-2B cells (human bronchial epithelial; CRL-9609ATCC) were grown in bronchial epithelial cell growth basal media (Lonza/CC-3170). LLC-MK-2 cells (rhesus monkey kidney; CCL-7/ATCC) were cultured in MEM (GIBCO #11095-080) supplemented with 100 units/mL penicillin and 100 µg/mL streptomycin (P/S), 2 mM L-glutamine, 1× non-essential amino acids (NEAA), and 3% FBS. All cell lines were cultured in a ventilate T-75 flask at 37°C in a 5% CO2 humidified incubator. All cell lines were tested for mycoplasma contamination and remained negative.

Seasonal virus strains and stock propagation

Virus strains were obtained from ATCC and were used to infect their recommended permissive cell line. 229E (stock, VR-740/ATCC) was propagated on MRC-5 cells, OC43 (CR-1558/ATCC) on HCT-8 cells, and NL63 (BEI Resources/NR-470) on LLC-MK2 cells. The permissive host cells (MRC-5, or HCT and LLC MK2) were maintained at a confluency of 80%–90% 24–48 hours prior to infection. The cells were infected with a multiplicity of infection (MOI) of 0.1 or 0.01 at 35°C for 229E, 33°C for OC43, and 34°C for NL63 for 1 hour for virus adsorption with rocking every 10–20 minutes. The virus culture media for 229E (DMEM + 3% FBS + 1% P/S), OC43 (RPMI + 3% FBS + 1% P/S), and NL63 (MEM + 3% FBS + 1% P/S) were added to the dish (e.g., 1 mL per 25 cm2) to stop the virus adsorption. Viruses were harvested by scrapping the infected cells with a cell scrapper followed by centrifugation at 500 × *g* for 10 minutes. The supernatant was collected in aliquots and quickly frozen at −80°C.

TCID50 and CPE assays

Virus titers of 229E, or OC43 and NL63 were determined by tissue culture infection dose 50 (TCID50) assay on their ATCC-recommended cell lines. MRC-5 (20,000 cells), HCT-8 cells (100,000 cells), and LLC-MK2 cells (300,000 cells) were seeded at their respective densities in 48-well plate (Fig. 1). The cells were checked for confluency (70%–80%), and the virus dilutions (10-fold serial dilution) were performed. Cell culture media (360 µL) were added to each well, and 40 µL of the virus dilution (10-fold) was added to each well. Mock represents the negative control having media only. The plates were incubated at their respective temperatures (229E at 35°C; OC43 at 33°C; NL63 at 34°C/5% CO2). The plates were shaken every 20 minutes. After 1–2 hours of incubation, media were removed, and 400 µL of the culture media supplemented with 1× DMEM-high glucose + 10% BSA + 100× NEAA + 100× (100 mM) sodium pyruvate + 100× (200 mM) L-glutamine, 100× penicillin (10,000 units/mL)-streptomycin (10,000 µg/mL), and TPCK-treated trypsin (0.5 µg/mL) was added. TCID50 of the viruses was calculated according to Reed-Muench method (32). Based on virus titers (TCID50) and cell number, multiplicities of infection were determined for the infection experiments.

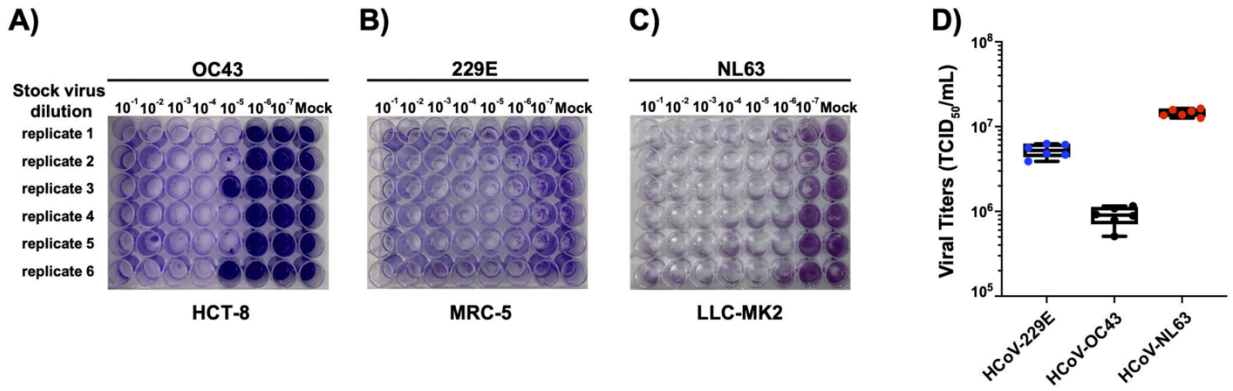


Fig 1 OC43, 229E, and NL63 titration by TCID50. (**A**) HCT-8 cells, (**B**) MRC-5 cells, and (**C**) LLC-MK2 were grown in 48-well tissue culture plates under standard conditions. When the cells (**A–C**) were confluent (75%), the media were removed, and the cells were infected with seven different 10-fold dilutions (10−1–10−7) of OC43 virus (HCT-8), 229E virus (MRC-5), or NL63 virus (LLC-MK2). The cytopathic effect in the wells was monitored for 7 days under a ZOE Cell Imager. A significant CPE is noted as cell death and disturbed cell morphology. The number of wells with CPE (empty wells) and without CPE (filled with crystal violet stain) was counted according to Reed and Muench method (31). (**D**) Shows the calculation of viral TCID50 titers. Each individual data point in D represents a viral TCID50 titer calculation from one of six biological replicates for each virus (229E, OC43, and NL63). The TCID50 titer is the average of the six biological replicates.

All cell lines detailed in Table 1 were tested for cytopathic effects following infection at an MOI of 0.1 by all three HCoVs studied here. The cells were observed daily for CPE following infection under a ZOE Cell Imager (BIO-RAD/1450031) using its phase-contrast setting to monitor cell

rounding, clumping, and detachment 3 days post-infection (dpi). CPE was rated empirically by operator-perceived intensity of cellular deformation and detachment: +, less than 20% cell detachment and mild morphological changes start to appear; ++, 20%–60% cell detachment and clear morphological changes in most cells; +++, 60%–100% cell detachment and severe morphological changes.

Table 1 Susceptibility of various cell lines to CPE following infection by HCoVs

Cell line tested	Cell type	Human coronavirus tested	Intensity of CPE at day 3 pi[a]
BEAS-2B	Human bronchial	OC43	–
		229E	–
		NL63	–
Calu-3	Human lung cancer	OC43	–
		229E	–
		NL63	–
HCT-8	Human colon cancer	OC43	+
		229E	–
		NL63	–
LLC-MK2	Rhesus monkey kidney cells	OC43	–
		229E	–
		NL63	++
MRC-5	Human fetal lung	OC43	+++
		229E	+
		NL63	–
Vero E6	African green monkey kidney	OC43	±**
		229E	–
		NL63	–
WI-38	Human fetal lung	OC43	+++
		229E	++
		NL63	–
293T and 293T ACE2	Human embryonic kidney	OC43	–
		229E	–
		NL63	–

[a] Infection was confirmed by detection of both S and N by droplet digital PCR. Infection was performed at an MOI of 0.01. CPE was assessed by phase-contrast light microscopy. +, less than 20% cell detachment and mild morphological changes start to appear; ++, 20%–60% cell detachment and clear morphological changes in most cells; +++, 60%–100% cell detachment and severe morphological changes; **, very mild CPE at 3 dpi was inconsistent across biological replicates (n = 3).

HCoV infection and RNA extraction

MRC-5, HCT-8, and LLC-MK2 cell lines were cultured to reach 60%–80% confluence in 6-well plates. The following day, cell lines were inoculated with their respective virus strains at MOI 0.01 and 0.1. Virus adsorption was done for 1 hour at 35°C (229E virus), 33°C (OC43 virus), or 34°C (NL63) followed by the addition of the respective virus culture media. Cells were infected with their respective virus strains and further incubated for the following days to monitor the infection and CPE (Table 1): 7 days for OC43, 5–7 days for 229E, and 7–10 days for NL63. HCoV-infected cells were examined under ZOE Cell Imager for the CPE formation followed by total vRNA extraction (QIAamp vRNA Mini Kit [Qiagen # 52904]) from culture supernatants and cell lysates along with uninfected cells (control mock) on different dpi (1–5). Absolute quantification of vRNA copies of N and S for OC43, 229E, or NL63 viruses was determined by Bio-Rad one-step reverse transcription droplet digital PCR (RT-ddPCR).

RT-ddPCR on vRNA

Duplex, probe-based, one-step RT-ddPCR (1-Step RT-ddPCR Advanced Kit for Probes, Bio-Rad, Hercules, CA) was used to determine the absolute quantification of N and S vRNA copy numbers in culture supernatants and cell lysates using the OC43, 229E, or NL63 primer-probe sets, and 18S was used as reference gene control to normalize the levels of intracellular vRNA. Primers and probes used in this study were synthesized by Integrated DNA Technologies, Inc (IDT, Kanata, Canada) (Table 2). For all the experimental samples, a master mix for each virus (e.g., OC43, or 229E, or NL63) was prepared having 5.5 µL One-Step RT-ddPCR advanced supermix, 2.2 µL RT, 1.1 µL DTT, 1.1 µL (250 nM) 20× primer/probe, 5.5 µL RNA template, and 6.6 µL RNase-free water to make a total reaction volume of 22 µL. The blank for the RNA extraction control is nuclease-free water. Mock-uninfected and -infected samples were included with three biological replicates. The reactions were then emulsified by using a QX200 droplet generator (Bio-Rad, Hercules, CA). Droplets that are generated were transferred to a new microplate, and PCR was performed in a thermocycler C1000 (Bio-Rad, Hercules, CA). The reaction conditions for target gene N and S were as follows: reverse transcription step was performed at 50°C, for 60 minutes, followed by polymerase activation at 95°C/10 minutes, and 39 cycles of denaturation at 95°C/30 s, annealing/extension at 55°C/60 s (target gene N), or 60°C/60 s (target gene S), respectively. Deactivation of polymerase was done at 98°C for 10 minutes, and droplets were stabilized at 4°C for 30 minutes. Droplets were then read by a Bio-Rad two-channel automated QX200 droplet

reader. The results were then analyzed by QuantaSoft Analysis Pro v.1.0 (Bio-Rad, Hercules, CA). VRNA levels of target genes N or S were normalized to 18S. In this article, the data from the ddPCR experiments are presented as vRNA genome copies per microliter (VRG) of reaction mix calculated from the number of positive and negative droplets in the samples based on the following equation (33). VRG = ($C \cdot V1$) ($5 \cdot V2$) × D; C = number of copies per 20 µL of reaction mix; $V1$ = elution volume of extracted RNA in microliter (e.g., 60 µL); $V2$ = sample volume used for RNA extraction in microliter (e.g., 140 µL); and D = dilution factor (df) for vRNA. The following dilutions were applied to the above equation for RNA viruses—NL63 (df: 10,000), OC43 (df: 5,000), and 229E (df: 50,000).

Table 2 Primers and probes used for ddPCR

Target gene	Forward primer	Reverse primer	Probe
N OC43	5′-*GGCGCAATTAGGTTTGACAG*-3′	5′-*TCCTCTGCAGTCAACTCTCT*-3′	5′–6 FAM/TG CCC AAA A/ZEN/G CCG CGT GCA G/3′IABkFQ
N 229E	5′-*ACTTTGGAAGTGCAGGTGTT*-3′	5′-*AAGGTGATGGTCTTTGGG*-3′	5′–6 FAM/TG AGC TTG T/ZEN/G CCG TCA ACA GCT GC/3′IABkFQ
N NL63	5′-*ATAAGCCTCTTTCTCAACCCAG*-3′	5′-*ATCACGAGGACCAAAGCAC*-3′	5′–6 FAM/AA ACC TCG T/ZEN/T GGA AGC GTG TTC CT/3′IABkFQ
RBD OC43	5′-*TCTTTAGTTGGCATAGGTGAGC*-3′	5′-*GGTCGGCAAGTACAAGAATTG*-3′	5′–6 FAM/AC TGT TCG G/ZEN/G TCT TGC TGT TAA AAG TGA/3′IABkFQ
RBD 229E	5′-*CCTGTTGAGGGTGTTAGTTCC*-3′	5′-*GTTACCTGAAGTTGATGTGTACG*-3′	5′–6 FAM-TC TGG TGT G/ZEN/G GTG TTA TTC GCG T/3′IABkFQ
RBD NL63	5′-*CTTGGTTTTAAAAATGTTTCCACTGG*-3′	5′-*TGTAGTAAGTTTTGCAAGCCATATC*-3′	5′–6 FAM/TG GTG CCA T/ZEN/G ACC GCT GTT AAT GA/3′IABkFQ
18S	5′-*CGCCGCTAGAGGTGAAATTCT*-3′	5′-*CATTCTTGGCAAATGCTTTCG*-3′	5′-HEX/AA GTG GAC T/ZEN/C ATT CCA ATT ACA GGG CCT/3′IABkFQ

Detection of surface markers and receptors by flow cytometry following coronavirus infection

Permissive cells (MRC-5, HCT-8, and NL63) were cultured in 6-well plate to attain 75% confluency. Cells were infected at an MOI of 0.1. Five days post-infection, cells were harvested to prepare single-cell suspension by lifting the cells with 5 mM EDTA followed by centrifugation at 500 × *g* for 5 minutes, and 0.5 × 106 cells were aliquoted per FACS tube. The following antibodies and isotypes were used to quantify the surface marker expression and receptor modulation in the uninfected (control) and infected cells: PE anti-human CD13, anti-human CD147 (isotype-control antibody mouse IgG1 κ, BioLegend); and anti-human CD326 (isotype-control antibody mouse IgG2a κ; BioLegend); human anti-ACE2 antibody (isotype-control antibody Goat IgG; R&D Systems) and anti-GD3, 9-O-acetyl (clone UM4D4; isotype-control antibody mouse IgM κ; Millipore Sigma). Cells were stained with CD13, CD147, CD326, ACE2, and GD3 antibodies, and their corresponding isotypes were incubated for 30 minutes on ice followed by washing with 0.2% BSA-PBS two times. Cells stained with anti-ACE2 and anti-GD3 were further incubated with secondary antibodies Alexa Fluor 488-labeled sheep anti-goat and goat anti-mouse (Invitrogen) for 30 minutes. After incubation, cells were washed twice with 0.2% BSA-PBS, resuspended in 2% BSB-PFA, and analyzed by Flow Cytometry on BD Celesta instrument (Beckman Coulter) using FlowJo software. Flow cytometry data were further analyzed using FlowJo Software v.10.7.1 (FlowJo, Ashland, OR). For cell analysis, SSC-area vs FSC-area followed by FSC-height vs FSC-area and SSC-area vs FSC-area were used to exclude cell aggregates and debris. Live/dead stain BV421 dye was used to exclude dead cells from analysis.

Blocking of NL63 infection by soluble ACE2 and monoclonal anti-ACE2 antibody

LLC MK2 cells were seeded in 48-well plates (5 × 105 cells per well) in MEM medium containing 3% FBS. Prior to incubation of soluble ACE2 (National Research Council Canada) with NL63 virus on LLC MK2 cells, the following dilution of sACE2 and NL63 virus was prepared. sACE2 (5 or 15 mg) or control protein OVA albumin (Sigma/A5503) was mixed with NL63 virus at MOI 0.1 (1:1) in a final volume of 100 µL in a separate 48-well plate in MEM medium (3% FBS) at 37°C for 30 minutes. After incubation, the sACE2 + NL63 virus mixture was added to the host cells LLC MK2 (24 hours post-seeding) and incubated at 34°C for a second incubation for 24 hours. The following day, the treated LLC MK2 cells were washed with PBS and replaced with infection media (MEM 3% FBS), and cells were monitored to check the blocking effect on NL63 infection until 7 dpi. At the end point day 7, the culture supernatants and cell lysates are harvested

to measure the vRNA copies of N and S by ddPCR following vRNA extraction. In a similar approach to monitor the blocking effect on NL63 infection using anti-ACE2 (human), monoclonal blocking antibody that recognizes ACE2 (AdipoGen Life Sciences#AC384), host LLC MK2 cells (48-well plate, 5 × 105 cells/well) were incubated with human ACE2 monoclonal blocking antibody (10, 40, and 120 µg/mL) or unrelated control antibody (40 µg/mL; anti-DC-SIGN) for 1–2 hours with intermittent shaking followed by the addition of NL63 virus (MOI #0.1) in a final volume of 100 µL per well at 34°C. After 24 hours post-infection, cells were washed with PBS and replaced with infection media (3%).

Statistical analysis

Statistical analyses were performed with multiple unpaired *t*-test with Welch's correction, and unpaired Mann-Whitney test was performed using GraphPad Prism (GraphPad Software, San Diego, CA version 9.5.1).

Result

Characterization of cell lines and evaluation of cytopathic effects

We selected a number of cell lines that were previously reported in the literature to be permissive to infection and viral replication of HCoVs (Table 1) (4, 25, 27, 29, 34). Our first objective was to identify the cell lines most susceptible to infection by HCoV and that also display cytopathic effects within a short 3-day time frame. We infected these cells with the three most prevalent HCoVs, OC43, 229E, and NL63, and assessed which ones displayed CPE that resulted in morphological changes and dysmorphic appearances in the cell monolayer with disturbed cell-to-cell aggregates or clumps after 3 days. The intensity of CPE, ranging from − to +++, was determined empirically by phase-contrast microscopy. Cells exhibiting CPE were tested by ddPCR to confirm the expression of S and N vRNAs. We used a TCID50 assay (Fig. 1) to determine the viral titers for the infections by taking into consideration the number of wells with and without CPE based on the methodology of Reed and Muench (32). Permissive cell lines identified in this study are HCT-8 (human colon cancer), MRC-5 (human fetal lung), LLC-MK2 (Rhesus monkey kidney), and WI-38 (human fetal lung). Infection of HCT-8, WI-38, and MRC-5 with OC43 virus

showed apparent CPE at day 3 pi with complete disturbance (+++) of the cell monolayer at day 5 pi (Fig. 2A, D, and G). MRC-5 and WI-38 cells infected with 229E showed increasing CPE from day 3 pi (Fig. 3A and D). Similarly, LLC-MK2 cells also started to display CPE upon NL63 infection from day 3 pi (Fig. 4A). At day 5 pi, the infected LLC-MK2 cells showed aggregation. We also assessed infection of MRC-5, WI-38, and HCT-8 cells infected with NL63; however, no CPE or viral replication was measured in these cells, in agreement with the previous reports (25).

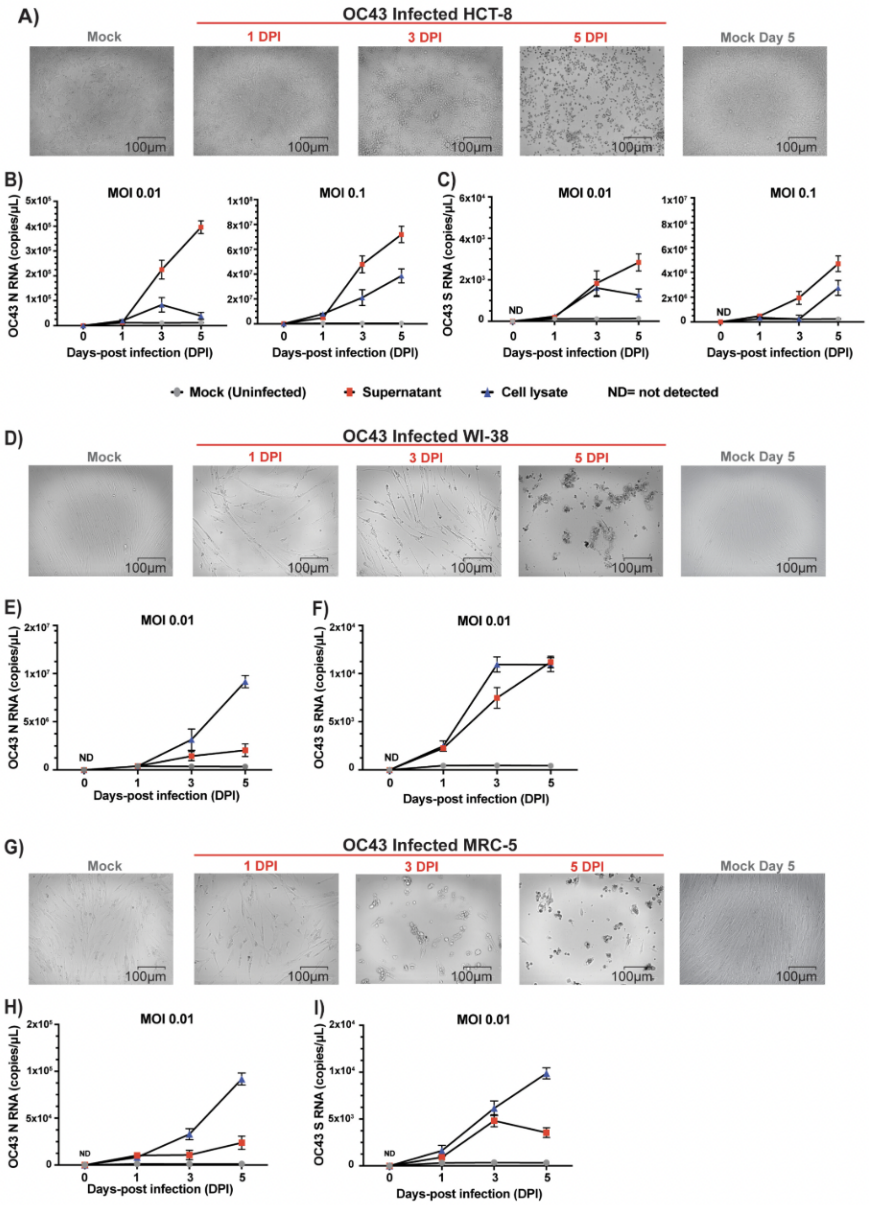


Fig 2 CPE evaluation and replication kinetics of OC43 infection. (**A**) HCT-8, (**D**) WI-38, or (**G**) MRC-5 cells were infected with OC43 (virus titer: 8.89 × 105 TCID50/mL) at an MOI of 0.01. CPE of the infected cells along with mock (uninfected cells) were monitored for morphological changes in the cell monolayer. Images of the cells were captured

at different days post-infection (day 0 to day 5 dpi) along with uninfected mock by ZOE Cell Imager. The reference bar is 100 microns. HCT-8 cells (**B and C**), WI-38 cells (**E and F**), or MRC-5 cells (**H and I**) infected with OC43 virus (MOI = 0.01 and/or 0.1) and cell lysates and supernatants were harvested at 0, 1, 3, and 5 days post-infection. Viral RNA copies of nucleocapsid (N), panels B, E, and H, and spike (S), panels C, F, and I, were then quantified by ddPCR. ND, not detected. Data represent the average MOI and standard deviation of three biological replicates with each three technical replicates per time point (n = 9).

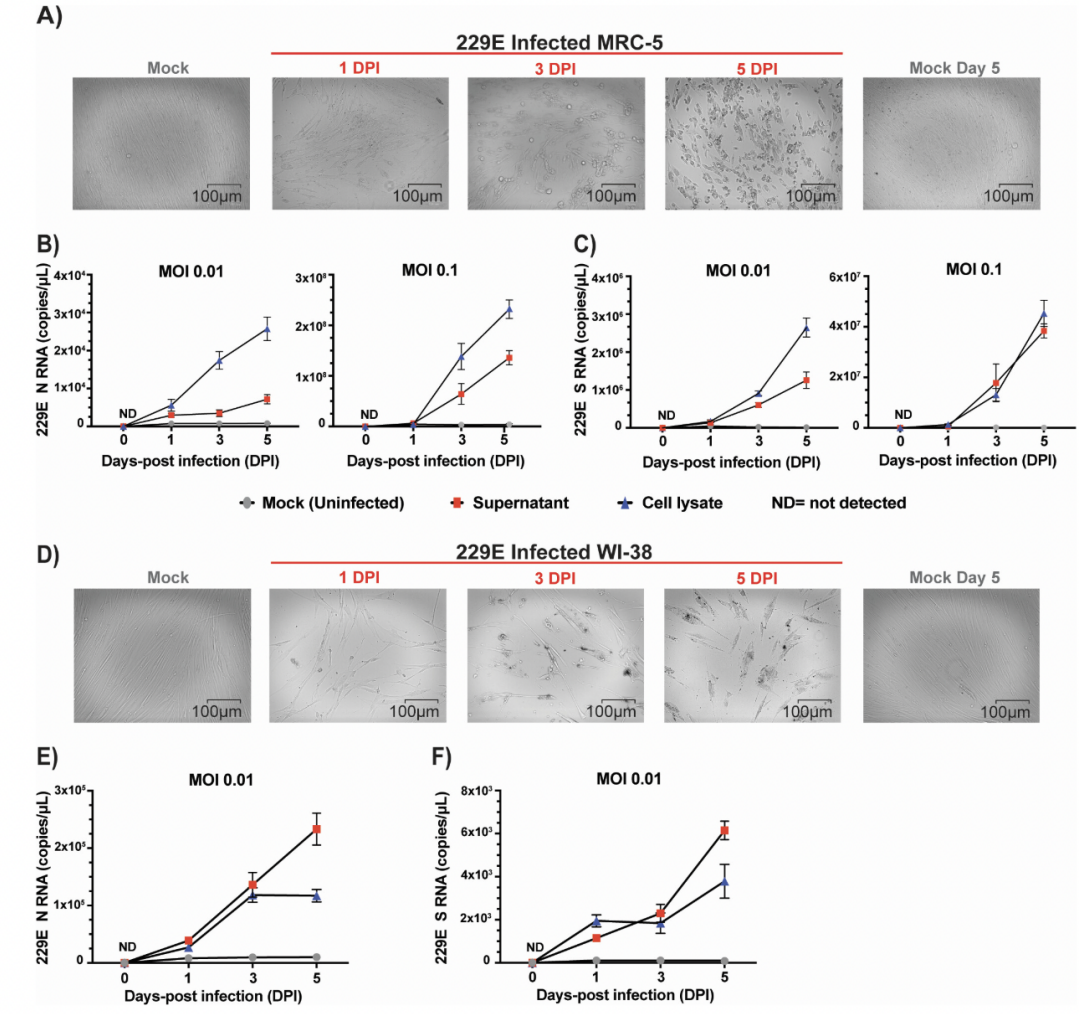


Fig 3 CPE evaluation and replication kinetics of 229E infection. (**A**) MRC-5 cells or WI-38 cells (**D**) were infected with HCoV-229E (virus titer: 5.64 × 106 TCID50/mL) at an MOI of 0.01. CPE of the infected cells along with mock (uninfected cells) were monitored for morphological changes in the cell monolayer. Images of the cells were captured at different days post-infection (day 0 to day 5 dpi) along with uninfected mock by ZOE Cell Imager. The reference bar is 100 microns. MRC-5 cells (**B and C**) or WI-38 cells (**E and F**) were infected with 229E virus (MOI = 0.01 and/or 0.1), and cell lysates and supernatants were harvested at 0, 1, 3, and 5 days post-infection. Viral RNA copies of nucleocapsid (N), panels B and E, and spike (S), panels C and F, were then quantified by ddPCR. ND, not detected. Data represent the average MOI and standard deviation of three biological replicates with each three technical replicates per time point (n = 9).

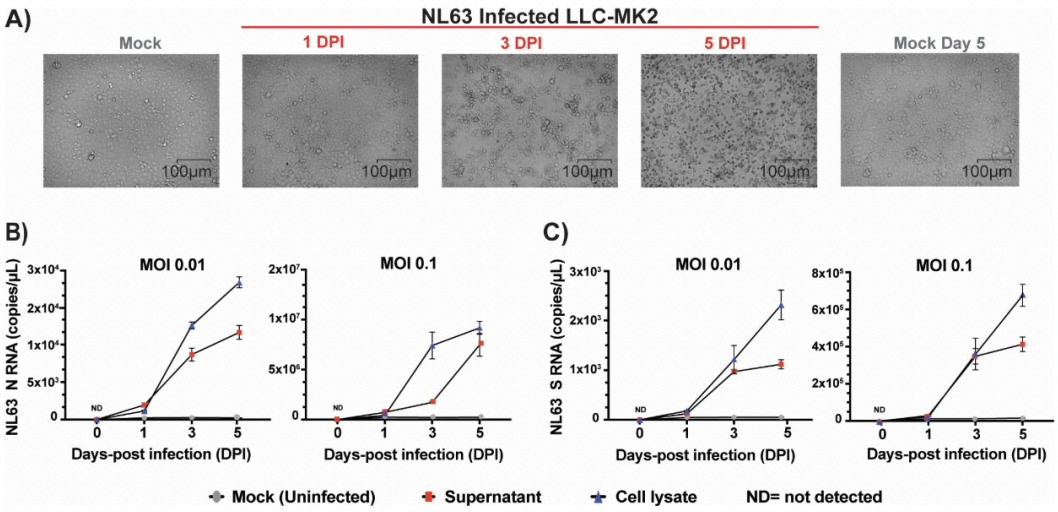


Fig 4 CPE evaluation and replication kinetics of NL63 infection. (**A**) LLC-MK2 cells infected with NL63 (virus titer: 1.58 × 106 TCID50/mL) at an MOI of 0.01. CPE of the infected cells along with mock (uninfected cells) were monitored for morphological changes in the cell monolayer. Images of the cells were captured at different days post-infection (day 0 to day 5 dpi) along with uninfected mock by ZOE Cell Imager. The reference bar is 100 microns. LLC-MK2 cells were infected with NL63 virus (MOI = 0.01 and/or 0.1), and cell lysates and supernatants were harvested at 0, 1, 3, and 5 days post-infection. Viral RNA copies of nucleocapsid (N), panel B, and spike (S), panel C, were then quantified by ddPCR. ND, not detected. Data represent the average MOI and standard deviation of three biological replicates with each three technical replicates per time point (n = 9).

Characterization of OC43, 229E, and NL63 viral replication kinetics

The culture supernatants and the cell lysates of permissive cells were infected with OC43, 229E, and NL63 at an MOI of 0.01 and were harvested at days 1, 3, and 5 post-infection. For OC43 with MRC-5 and WI-38 (Fig. 2B, C, E, F, H, and I), 229E (Fig. 3B, C, E, and F), and NL63 (Fig. 4B and C), cell lysates show similar or higher vRNA copies of N and S in comparison to supernatants. However, for OC43 propagation in HCT-8 cells, we observe higher vRNA copies of N and S in the culture supernatant than in the cell lysate (Fig. 2B and C). We also see in these cells an increase in OC43 N and S vRNA copies starting from day 3 to day 5 post-infection and a drop in S vRNA levels in the lysates for HCT-8 at day 5 pi (Fig. 2B and C), possibly due to advanced cell death. Considering data from previous reports of NL63 infection in LLC-MK2 cells, the lower NL63 N and S vRNA levels detected in the supernatants compared to the lysates may be due to inefficient

release of virions in the supernatants (17, 29, 35). Also, total vRNA copies detected varied depending on the cell types tested. For OC43 and 229E, WI-38 appeared the most favorable cell line for vRNA N expression, with ranges above 106 copies/mL for OC43 and above 105 copies/mL for 229E in the lysates at day 7 (Fig. 2E and 3E). Additionally, for all conditions tested, except infection of MRC-5 by 229E (Fig. 3B and C) and LLC-MK2 infection by NL63 (Fig. 4B and C), N vRNA levels are consistently several logs higher than S levels. For these combinations of virus and cells, it was the opposite where S transcripts were more abundant than N. Overall, the results show that HCoV displays variable replication kinetics depending on the specific virus and permissive host cell combination.

Cell surface marker expression on HCT-8 cells following OC43 infection

Here, we characterized surface expression of GD3, CD13, CD147, CD326, and ACE2 protein on HCT-8 prior and after infection with OC43. We measured receptor expression as the percentage of total cells expressing a given receptor, and we also measured the mean fluorescence intensity (MFI) emitted from all positive cells. CD13 (aminopeptidase N; APN) is the main surface protein receptor for 229E infection and is highly expressed on respiratory epithelial cells (12, 36). ACE2 is the primary receptor for NL63, and SARS-CoV and SARS-CoV-2 (16, 37, 38). CD147 is a transmembrane glycoprotein expressed on epithelial and immune cells that is proposed to be an alternative receptor for SARS-CoV and SARS-CoV-2 infection (39, 40). It is unknown if CD147 plays a role in NL63 entry. CD326 is a marker of colon carcinoma cells; it is known to be highly expressed on HCT-8 cells and is used in our study as a control that is unlikely to be affected by infection. OC43 binds to 9-*O*-acetylated sialic acid attached to oligosaccharide molecules located on glycoproteins on the surface of cells (14, 41). As such, this virus does not have a known specific protein surface receptor. However, ganglioside GD3 (9-*O*-acetyl-GD3) can be used by OC43 as a cellular entry receptor and is highly expressed in human leukemia cells (42).

Our assays detected low expression (8%) of GD3 in uninfected HCT-8 cells (Fig. 5A and D). We present the data as a scatter plot of a single representative assay (Fig. 5A and B) and the compiled data summary of two-three biological repeats (Fig. 5D and E). Histogram plots of stained uninfected and infected cells relative to the corresponding isotype controls: IgG1 (CD13 and CD147) and IgG2b (CD326) and goat IgG (ACE2) are presented in Fig. 5C. After infection of

HCT-8, significantly fewer cells expressed the OC43 attachment receptor GD3 (2% of total), and those that did expressed less of it as shown by a reduction of about twofold in MFI (Fig. 5D and E). We also detected expression of CD147 (100%) and CD326 (100%) surface antigens in all cells, and lower levels of CD13 (12%) and ACE-2 (17%) expression (Fig. 5A and D). Expression profiles detected for these antigens are in-line with previous observations made on colon tissues (43–47). Interestingly, infection with OC43 leads to a significant upregulation of ACE2 expression (30%) when compared to uninfected cells (Fig. 5D and E). In contrast, we observed significant downregulation of CD326 MFI following infection (Fig. 5E), while there were no differences in overall cell expression for CD326, CD13, and CD147 (Fig. 5D). We did not present surface marker expression on WI-38 cells infected with 229E or OC43, or MRC-5 infected with OC43, given the intense and rapid CPE and cell death that compromised flow cytometry analysis.

Cell surface marker expression on MRC-5 cells following 229E infection

Next, we characterized surface expression of CD13, CD147, CD326, and ACE2 proteins in uninfected and infected MRC-5 cells with 229E. No detectable expression of GD3 was measured on MRC-5 or LLC-MK2 cells (data not shown). Nearly all MRC-5 cells expressed high levels of CD13 (91%) and CD147 (100%) surface antigens and much lower levels of CD326 (0.8%) and ACE2 (13%) markers (Fig. 6A and C). High expression of CD147 was in-line with previously reported studies characterizing lung epithelial cells (46, 48). Infection of MRC-5 cells with 229E virus leads to an important decrease in cells expressing 229E cellular receptor CD13, from 99% to 55% (Fig. 6A and B). MFI and the percentage of cells expressing each marker prior and following infection with OC43 are summarized in Fig. 6D and E. Although CD326 and ACE2 expression were slightly reduced following 229E infection, these did not attain statistical significance.

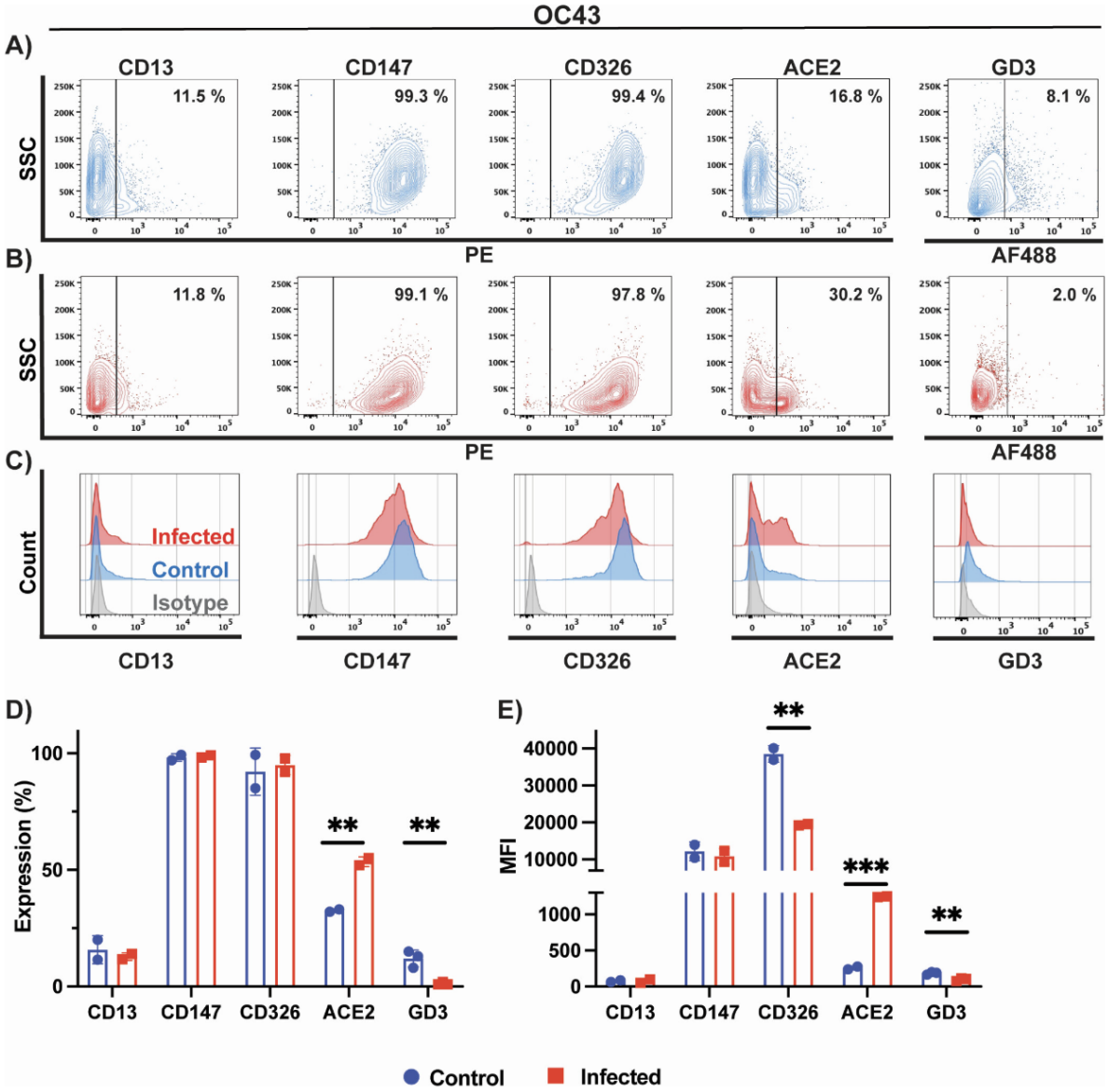


Fig 5 Phenotypic characterization of cell surface markers of OC43-infected cells. Phenotypic characterization of (**A**) uninfected (blue) and (**B**) OC43-infected HCT-8 cells (red). CD13, CD147, CD326, ACE2, and GD3 expression were probed by flow cytometry. (**C**) Histogram plots of control and infected HCT-8 cells relative to isotype control (gray). Histograms plots showing (**D**) percentage of cells expressing a given marker and (**E**) mean fluorescence intensity. Data in panels **D** and **E** represent the mean of two biological replicates for all antigens except GD3, where three biological replicates were carried out. Statistical analysis was performed with the multiple unpaired *t*-test with Welch's correction. Only results that reached statistical significance were identified: * $P \leq 0.033$, ** $P \leq 0.002$, *** $P \leq 0.0001$, **** $P \leq 0.0001$.

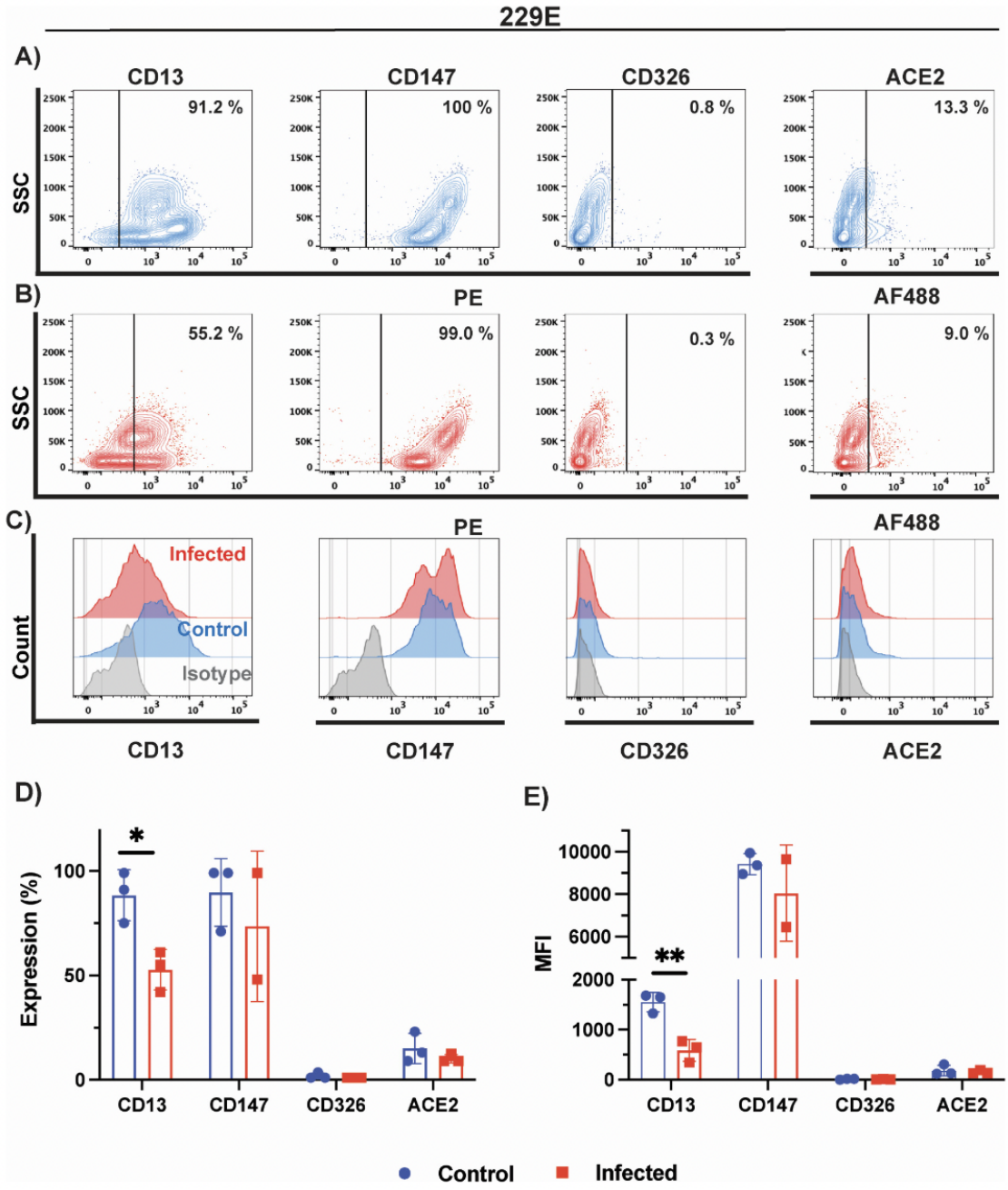


Fig 6 Phenotypic characterization of cell surface markers of 229E-infected cells. Phenotypic characterization of (**A**) uninfected (blue) and (**B**) 229E-infected MRC-5 cells (red). CD13, CD147, CD326, and ACE2 expression were probed by flow cytometry. (**C**) Histogram plots of control and infected MRC-5 cells relative to isotype control (gray). Histograms plots showing (**D**) percentage of cells expressing a given marker and (**E**) mean fluorescence intensity. Data in panels **D** and **E** represent the mean of three biological replicates, except for CD147 where two biological replicates were carried out. Statistical analysis was performed with the multiple unpaired *t*-test with Welch's correction. Only results that reached statistical significance were identified: * $P \leq 0.033$, ** $P \leq 0.002$, *** $P \leq 0.0001$, **** $P \leq 0.0001$.

Cell surface marker expression on LLC-MK2 cells following NL63 infection

Lastly, we characterized surface expression of CD13, CD147, CD326, and ACE2 proteins in uninfected and infected LLC-MK2 cells with NL63 virus. We detected high expression of CD13 (81%), as previously reported (47, 49), and CD147 (99%), and lower expression of ACE2 (27%) surface receptor in uninfected LLC-MK2 cells (Fig. 7A). Infection with NL63 leads to a 2.3-fold increase in cells expressing NL63 cellular receptor ACE2 (Fig. 7B through D). Although we did observe a small upregulation of CD13 and CD326 expression in infected cells, these did not reach statistical significance (Fig. 7D). Previous studies have shown the involvement of CD147 in SARS-CoV-2 infections (40, 50). However, CD147 expression remained unaffected by NL63 infection as shown here (Fig. 7D and E).

Soluble ACE2 protein and anti-ACE2 antibody effectively inhibit NL63 infection

Given that ACE2 is the major receptor for NL63 infection and having now established viral infection assays to measure vRNA expression, we wanted to investigate the efficiency of blocking antibodies and soluble ACE2 as infection prevention strategies. While therapeutic approaches that target ACE2 have been developed for SARS-CoV-2, it is not known if these can also inhibit NL63 infection (51–56).

LLC-MK2 cells were infected with NL63 (MOI of 0.1), and supernatants were harvested 5 days later. Supernatants (MOI equivalent of 0.1) were pre-treated with sACE2 or control protein (soluble ovalbumin) for 30 minutes prior to infection of LLC-MK2 cells (Fig. 8A and C). Similarly, LLC-MK2 cells were pre-treated with a blocking anti-ACE2 mAb or an unrelated control antibody (anti-DC-SIGN) for 30 minutes prior to infection (Fig. 8B and D). Five days after infection, we measured S and N vRNAs in the supernatants and lysates of infected cells. Both the culture supernatants and cell lysates of virus-infected LLC-MK2 cells with prior treatment of the virus with sACE2 led to a significantly attenuated production of N and S vRNA copies, of about 83% and 89% in supernatants and 96% and 88 % in lysates at the highest dose of 10 μg/mL, respectively (Fig. 8C). Similarly, treatment of LLC-MK2 cells with the human monoclonal ACE2 (anti-ACE2 mAb) blocking antibody shown to be capable of SARS-CoV-2 inhibition (56) also inhibited NL63 infection in a dose-dependent manner (Fig. 8B and D). Both the NL63 N and S vRNA levels were significantly reduced by 76% and 68% in supernatants and 89% and 86% in

lysates at the highest dose of 120 mg/mL, respectively (Fig. 8D). However, neither soluble ACE2 nor anti-ACE2 was capable of completely blocking the infection in these conditions.

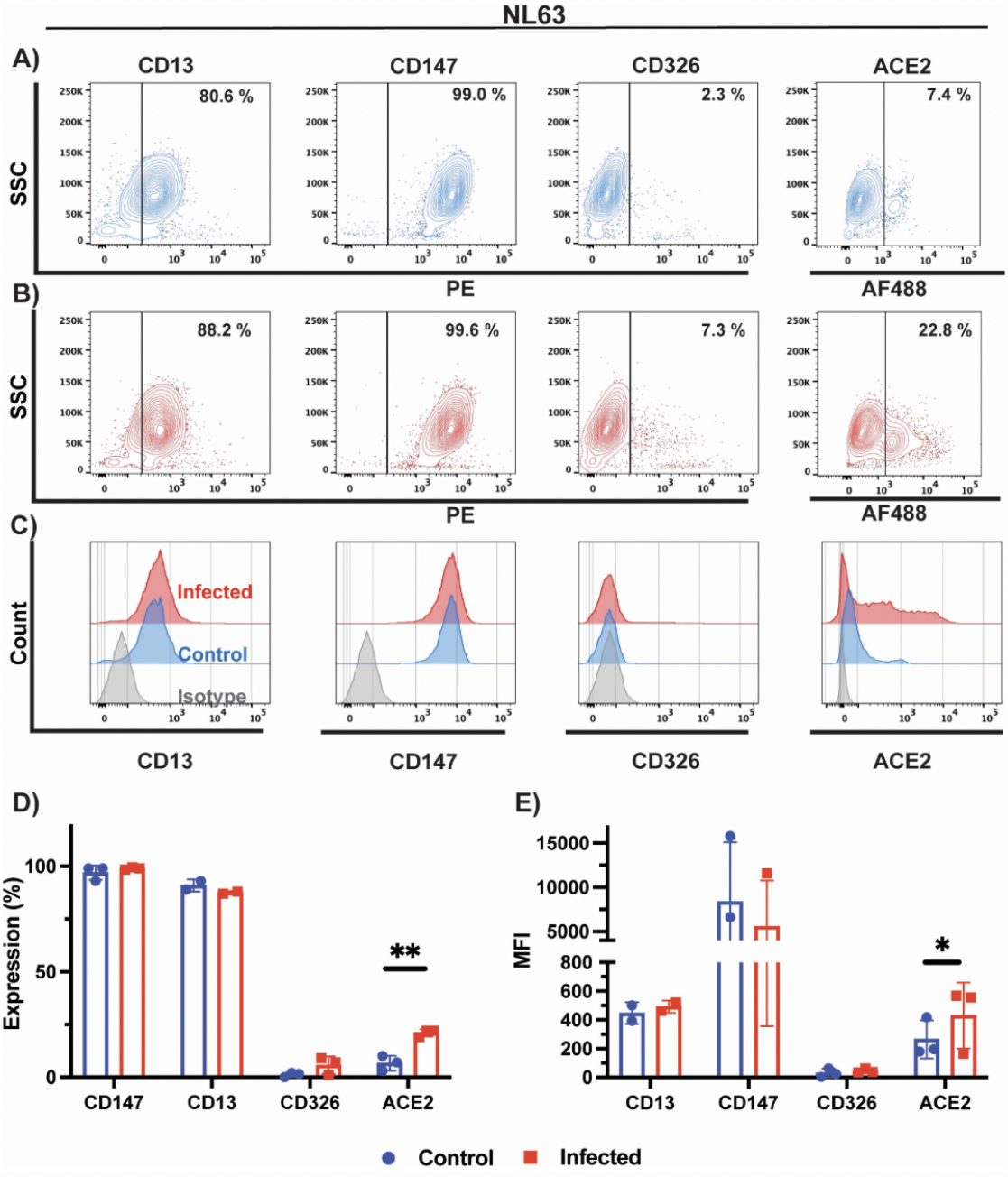


Fig 7 Phenotypic characterization of cell surface markers of NL63-infected cells. Phenotypic characterization of (**A**) uninfected (blue) and (**B**) NL63-infected LLC-MK2 cells (red). CD13, CD147, CD326, and ACE2 expression were probed by flow cytometry. (**C**) Histogram plots of control and infected LLC-MK2 cells relative to isotype control (gray). Histograms plots showing (**D**) percentage of cells expressing a given marker and (**E**) mean fluorescence intensity. Data in panels **D** and **E** represent the mean of three biological replicates, except for CD13 where two biological replicates were carried out. Statistical analysis was performed with the multiple unpaired *t*-test with Welch's correction. Only results that reached statistical significance were identified: * $P \leq 0.033$, ** $P \leq 0.002$, *** $P \leq 0.0001$, **** $P \leq 0.0001$.

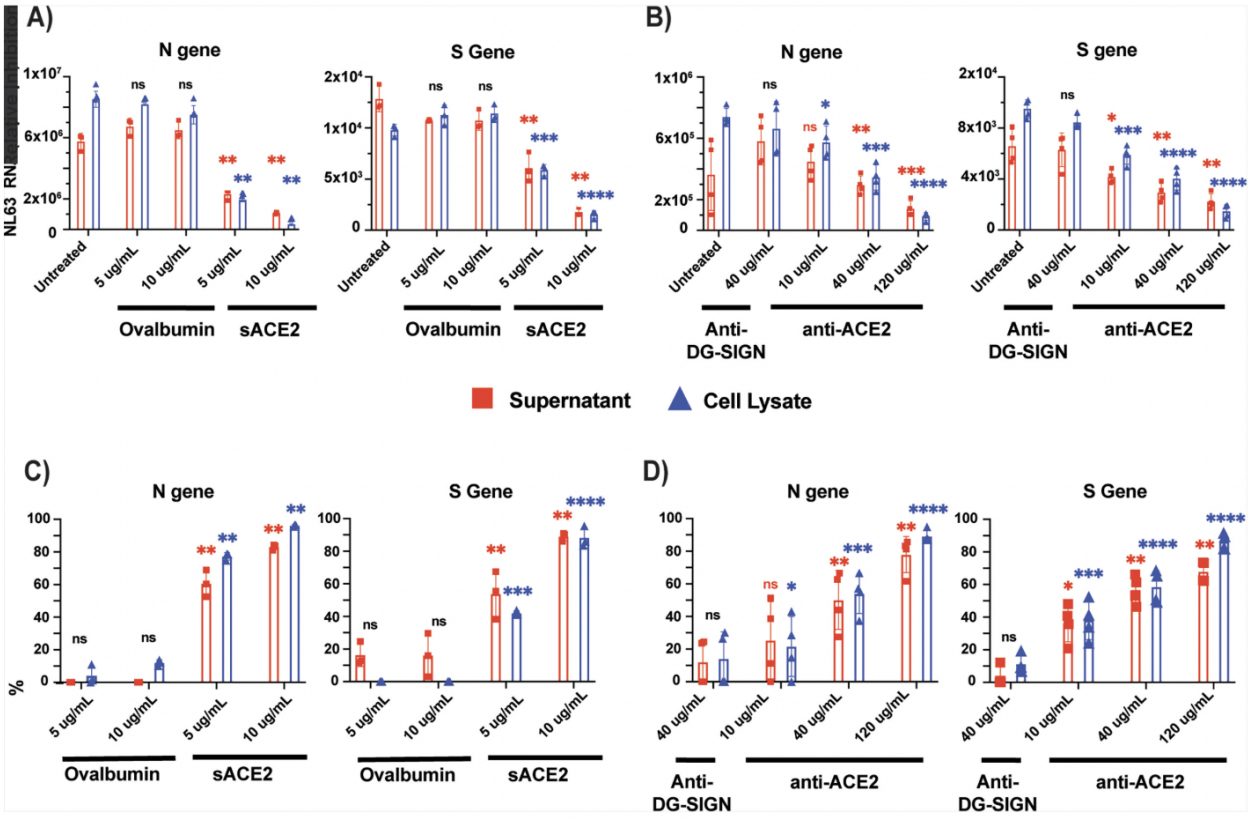


Fig 8 Soluble ACE2 protein and anti-ACE2 monoclonal blocking antibody inhibit NL63 infection in LLC-MK2 cells. (**A**) Treatment with soluble ACE2 or control protein ovalbumin at 5 and 10 mg/mL was pre-incubated with NL63 virus at MOI 0.1 (virus titer: 8.89 × 105 TCID50/mL) for 1 hour, and the protein and virus mixture complex was added to the LLC-MK2 cells. (**B**) Similarly, cells were incubated for 1 hour with human anti-ACE2 monoclonal blocking antibody (10, 40, and 120 µg/mL) or unrelated control antibody (anti-DC-SIGN; 40 µg/mL) followed by addition of NL63 virus (MOI 0.1). Five days post-infection, both culture supernatants and cell lysates were harvested for quantification of nucleocapsid (N) and spike (S) vRNA copies by ddPCR. Percent relative viral inhibition following treatment with (C) sACE2 or (D) anti-ACE2 monoclonal antibody compared to their respective untreated control. Data represent three biological replicates for sACE2 or four (anti-ACE2) with three technical replicates per experiment. Statistical analysis was performed using an unpaired *t*-test with Welch's correction ($P < 0.05$) relative to untreated control. n.s. denoted as no statistical difference; * $P \leq 0.033$, ** $P \leq 0.002$, *** $P \leq 0.0001$, **** $P \leq 0.0001$.

Discussion

An in-depth understanding of common cold seasonal coronavirus transmission, infection, pathogenicity, and the impact of reoccurring infections on human health is incomplete (2, 57, 58). In fact, only very recently was the functional receptor for HKU1 identified (15). Moreover, given that these viruses have zoonotic and co-infection potential to create new recombinant strains, they are of particular interest in light of the current SARS-CoV-2 pandemic (59, 60). This work studied

the characteristics of HCoVs-host cell interactions, CPE, and replication kinetics in commonly used human and animal cell lines. We used cell culture models of human lung, colon cancer, and rhesus monkey kidney cell lines that are fibroblastic and epithelial in origin as platforms to study the impact of infection on the host cell and attachment receptors.

Viral replication and CPE analysis demonstrated that of all the cell lines tested (Table 1), MRC-5, HCT-8, and LLC MK2 are the most suitable in our conditions to study OC43, 229E, and NL63 *in vitro*. While WI-38 did get infected by OC43 and 229E, the cells exhibited severe CPE that compromised our ability to perform flow cytometry analysis. We also considered to perform plaque assays for our study; however, we were unsuccessful to obtain sufficiently defined plaques that were amenable to quantification following OC43, 229E, and NL63 infection (data not shown). Cells that are permissive to infection do not necessarily demonstrate CPE or support plaque formation using standard methods (26, 30). However, some other groups have reported, albeit with varying success, plaques following HCoV infection using specialized protocols (4, 61). Viral RNA analyses revealed that OC43, 229E, and NL63 replication in host cells steadily increased by day 3 pi, followed by CPE and dysmorphic cell appearances (Fig. 1 to 4). This is supported by previous reports of HCT-8 and MRC-5 infections with OC43, where the cells displayed obvious CPE at day 2 or 3 pi (26). However, the expression profiles and abundance of vRNAs in both supernatants and cell lysates for each virus-host cell pair varied significantly over the 5-day analysis period. Accumulation of vRNA was consistently higher in cell lysates than in supernatants, except for OC43 infecting HCT-8 cells where it was the opposite (Fig. 2B and C). Also, there was a general trend whereby more N than S vRNA was measured in both lysates and supernatants for all virus-host cell pairs, except for MRC-5 cells infected by 229E that displayed 100-fold higher levels of S than N (104 vs 106 copies per mL) (Fig. 3B and C). The overall canvas that emerges is one where cell-intrinsic factors influence the outcome of viral replication and release. These can include restriction factors that inhibit viral, for instance, budding and egress, or hinder viral genome replication and stability such as RNA-editing enzymes (62–65). Interferon and antiviral responses may also play an important role in viral spread and CPE in cell cultures (19).

Some viruses modulate surface receptors and co-receptors on the surface of the cell. For example, in the case of HIV, the virus downregulates CD4 expression on lymphocytes via the viral nef

protein to avoid co-infections and superinfections that could lead to host cell genome instability (66). In this study, we analyzed the surface expression of CD13, CD147, CD326, GD3, and ACE2 on infected and uninfected MRC-5, HCT-8, and LLC-MK2 cells by flow cytometry. We tracked both the proportion of cells expressing the receptor and the receptor expression intensity, MFI. While we observed a fourfold decrease in GD3 on HCT-8 cells following OC43 infection, as well as a 1.7-fold decrease in CD13 expression following 229E infection, we were surprised to observe a significant increase in ACE2 receptor expression and MFI following NL63 infection of LLC-MK2 cells (2.3-fold) but also following OC43 infection (1.8-fold). Induction of ACE2 expression following infection with NL63 and the highly prevalent OC43 may be a source of concern for coronavirus co-infections. Although cytokine and interferon responses induced during the primary infection by OC43 and NL63 will likely have an inhibitory effect on co-infection by another coronavirus utilizing ACE2 for entry (67), a strong induction in receptor expression could tilt the balance in favor of the incoming virus. There is currently very little information in the published literature about the frequency of such co-infections and their possible role in creating recombination events with SARS-CoV-2 (68).

Currently, there are no approved or licensed antiviral compounds for the treatment of the common cold caused by seasonal HCoV infections. Previous studies have shown that sACE2 or engineered variants of sACE2 may be beneficial for the treatment of COVID-19 infection (18, 69). LLC-MK2 cells treated with the highest dose of sACE2 (120 µg/mL) reduced the expression of N and S vRNA of NL63 by 90% in viral lysates (Fig. 8B and D). Similarly, human anti-ACE2 monoclonal blocking antibody inhibited in a dose-dependent manner (10, 40, and 120 µg) NL63 infection (Fig. 8B and D). These data indicate that targeting the entry receptor appears to be very effective at inhibiting this virus. However, we also attempted to use a polyclonal anti-ACE2 antibody to block NL63 without success (data not shown), suggesting that there may be few critical neutralizing epitopes in the spike-ACE2 interface for NL63 entry and that these should be prioritized to develop a therapy. Soluble ACE2 also proved to a capable inhibitor of NL63 but to somewhat a lesser degree.

In summary, our study showed that HCoVs OC43, 229E, and NL63 display differential replication kinetics and CPE in permissive host cells, highlighting the underlying involvement of cell-intrinsic

factors that influence the expression of viral genes and virus egress. We also demonstrate that HCoV OC43 and NL63 infection upregulate the expression of the entry receptor ACE2 on host cells, raising opportunities for possible co-infection and recombination with other HCoVs (68, 70, 71). How HCoVs recombine and evolve in a given host remains an important topic to better understand the emergence of new viral strains of coronaviruses.

Acknowledgment

This study was supported by a COVID-19 Rapid Response grant by the Canadian Institutes of Health Research (CIHR; #VR2-172722) to M.-A.L. M.M. holds an Ontario Graduate Scholarship. Y.G. holds a Canadian Institute of Health Research (CIHR) Frederick Banting and Charles Best graduate scholarship (CGS-Doctoral, 476885). N.C. holds a CIHR Frederick Banting and Charles Best graduate scholarship (CGS-M). M.-A.L. holds a Faculty of Medicine Chair of Excellence in Pandemic Viruses and Preparedness Research.

V.S., M.M., and M.-A.L. designed the study. V.S., M.M., N.C., M.M.S., J.H.S., and S.D. performed the experiments. V.S., M.M., Y.G., and M.-A.L. analyzed the data. V.S., M.M., Y.G., and M.A.L. wrote the manuscript. All authors edited the final version of the manuscript.

References

1. Channappanavar R, Perlman S. 2020. Age-related susceptibility to coronavirus infections: role of impaired and dysregulated host immunity. J Clin Invest 130:6204–6213. https://doi.org/10.1172/ JCI144115
2. Pyrc K, Berkhout B, van der Hoek L. 2007. Antiviral strategies against human coronaviruses. Infect Disord Drug Targets 7:59–66. https://doi. org/10.2174/187152607780090757
3. Gorse GJ, Patel GB, Vitale JN, O'Connor TZ. 2010. Prevalence of antibodies to four human coronaviruses is lower in nasal secretions than in serum. Clin Vaccine Immunol 17:1875–1880. https://doi.org/10.1128/ CVI.00278-10
4. Bracci N, Pan HC, Lehman C, Kehn-Hall K, Lin SC. 2020. Improved plaque assay for human coronaviruses 229E and OC43. PeerJ 8:e10639. https:// doi.org/10.7717/peerj.10639
5. Jin M, Shi N, Wang M, Shi C, Lu S, Chang Q, Sha S, Lin Y, Chen Y, Zhou H, Liang K, Huang X, Shi Y, Huang G. 2020. CD45: a critical regulator in immune cells to predict severe and non-severe COVID-19 patients. Aging12:19867–19879. https://doi.org/10.18632/aging.103941
6. Corman VM, Muth D, Niemeyer D, Drosten C. 2018. Hosts and sources of endemic human coronaviruses. Adv Virus Res 100:163–188. https://doi. org/10.1016/bs.aivir.2018.01.001
7. Masse S, Capai L, Villechenaud N, Blanchon T, Charrel R, Falchi A. 2020. Epidemiology and clinical symptoms related to seasonal coronavirus identified in patients with acute respiratory infections consulting in primary care over six influenza seasons (2014-2020) in France. Viruses 12:630. https://doi.org/10.3390/v12060630
8. Nickbakhsh S, Ho A, Marques DFP, McMenamin J, Gunson RN, Murcia PR. 2020. Epidemiology of seasonal coronaviruses: establishing the context for the emergence of coronavirus disease 2019. J Infect Dis 222:17–25. https://doi.org/10.1093/infdis/jiaa185
9. Jean A, Quach C, Yung A, Semret M. 2013. Severity and outcome associated with human coronavirus OC43 infections among children. Pediatr Infect Dis J 32:325–329. https://doi.org/10.1097/INF.- 0b013e3182812787
10. Vassilara F, Spyridaki A, Pothitos G, Deliveliotou A, Papadopoulos A. 2018. A rare case of human coronavirus 229E associated with acute respiratory distress syndrome in a healthy adult. Case Rep Infect Dis 2018:6796839. https://doi.org/10.1155/2018/6796839
11. Wang Y, Li X, Liu W, Gan M, Zhang L, Wang J, Zhang Z, Zhu A, Li F, Sun J, Zhang G, Zhuang Z, Luo J, Chen D, Qiu S, Zhang L, Xu D, Mok CKP, Zhang F, Zhao J, Zhou R, Zhao J. 2020. Discovery of a subgenotype of human coronavirus Nl63 associated with severe lower respiratory tract infection in China, 2018. Emerg Microbes Infect 9:246–255. https://doi.org/10. 1080/22221751.2020.1717999
12. Lachance C, Arbour N, Cashman NR, Talbot PJ. 1998. Involvement of aminopeptidase N (CD13) in infection of human neural cells by human coronavirus 229E. J Virol 72:6511–6519. https://doi.org/10.1128/JVI.72.8. 6511-6519.1998
13. Szczepanski A, Owczarek K, Bzowska M, Gula K, Drebot I, Ochman M, Maksym B, Rajfur Z, Mitchell JA, Pyrc K. 2019. Canine respiratory coronavirus, bovine coronavirus, and human coronavirus OC43: receptors and attachment factors. Viruses 11:328. https://doi.org/10. 3390/v11040328
14. Hulswit RJG, Lang Y, Bakkers MJG, Li W, Li Z, Schouten A, Ophorst B, van Kuppeveld FJM, Boons G-J, Bosch B-J, Huizinga EG, de Groot RJ. 2019. Human coronaviruses OC43 and HKU1 bind to 9-O-acetylated sialic acids via a conserved receptor-binding site in spike protein domain A. Proc Natl Acad Sci U S A 116:2681–2690. https://doi.org/10.1073/pnas. 1809667116
15. Saunders N, Fernandez I, Planchais C, Michel V, Rajah MM, Baquero Salazar E, Postal J, Porrot F, Guivel-Benhassine F, Blanc C, et al. 2023. TMPRSS2 is a functional receptor for human coronavirus HKU1. Nature 624:207–214. https://doi.org/10.1038/s41586-023-06761-7
16. Hofmann H, Pyrc K, van der Hoek L, Geier M, Berkhout B, Pöhlmann S. 2005. Human coronavirus Nl63 employs the severe acute respiratory syndrome coronavirus receptor for cellular entry. Proc Natl Acad Sci U S A 102:7988–7993. https://doi.org/10.1073/pnas.0409465102

17. Milewska A, Nowak P, Owczarek K, Szczepanski A, Zarebski M, Hoang A, Berniak K, Wojarski J, Zeglen S, Baster Z, Rajfur Z, Pyrc K. 2018. Entry of human coronavirus NL63 into the cell. J Virol 92:e01933-17. https://doi. org/10.1128/JVI.01933-17
18. Monteil V, Kwon H, Prado P, Hagelkrüys A, Wimmer RA, Stahl M, Leopoldi A, Garreta E, Hurtado Del Pozo C, Prosper F, Romero JP, Wirnsberger G, Zhang H, Slutsky AS, Conder R, Montserrat N, Mirazimi A, Penninger JM. 2020. Inhibition of SARS-CoV-2 infections in engineered human tissues using clinical-grade soluble human ACE2. Cell 181:905–913. https://doi. org/10.1016/j.cell.2020.04.004
19. Duncan JKS, Xu D, Licursi M, Joyce MA, Saffran HA, Liu K, Gohda J, Tyrrell DL, Kawaguchi Y, Hirasawa K. 2023. Interferon regulatory factor 3 mediates effective antiviral responses to human coronavirus 229E and OC43 infection. Front Immunol 14:930086. https://doi.org/10.3389/ fimmu.2023.930086
20. Brown AJ, Won JJ, Graham RL, Dinnon KH, Sims AC, Feng JY, Cihlar T, Denison MR, Baric RS, Sheahan TP. 2019. Broad spectrum antiviral remdesivir inhibits human endemic and zoonotic deltacoronaviruses with a highly divergent RNA dependent RNA polymerase. Antiviral Res 169:104541. https://doi.org/10.1016/j.antiviral.2019.104541
21. Wang Y, Li P, Rajpoot S, Saqib U, Yu P, Li Y, Li Y, Ma Z, Baig MS, Pan Q. 2021. Comparative assessment of favipiravir and remdesivir against human coronavirus Nl63 in molecular docking and cell culture models. Sci Rep 11:23465. https://doi.org/10.1038/s41598-021-02972-y
22. Li J, Wang Y, Solanki K, Atre R, Lavrijsen M, Pan Q, Baig MS, Li P. 2023. Nirmatrelvir exerts distinct antiviral potency against different human coronaviruses. Antiviral Res 211:105555. https://doi.org/10.1016/j. antiviral.2023.105555
23. Zumla A, Chan JFW, Azhar EI, Hui DSC, Yuen K-Y. 2016. Coronaviruses - drug discovery and therapeutic options. Nat Rev Drug Discov 15:327– 347. https://doi.org/10.1038/nrd.2015.37
24. Liu D, Chen C, Chen D, Zhu A, Li F, Zhuang Z, Mok CKP, Dai J, Li X, Jin Y, et al. 2023. Mouse models susceptible to HCoV-229E and HCoV-NL63 and cross protection from challenge with SARS-CoV-2. Proc Natl Acad Sci U S A 120:e2202820120. https://doi.org/10.1073/pnas.2202820120
25. Schildgen O, Jebbink MF, de Vries M, Pyrc K, Dijkman R, Simon A, Müller A, Kupfer B, van der Hoek L. 2006. Identification of cell lines permissive for human coronavirus Nl63. J Virol Methods 138:207–210. https://doi. org/10.1016/j.jviromet.2006.07.023
26. Schirtzinger EE, Kim Y, Davis AS. 2022. Improving human coronavirus OC43 (HCoV-OC43) research comparability in studies using HCoV-OC43 as a surrogate for SARS-CoV-2. J Virol Methods 299:114317. https://doi. org/10.1016/j.jviromet.2021.114317
27. Weil T, Lawrenz J, Seidel A, Münch J, Müller JA. 2022. Immunodetection assays for the quantification of seasonal common cold coronaviruses OC43, Nl63, or 229E infection confirm nirmatrelvir as broad coronavirus inhibitor. Antiviral Res 203:105343. https://doi.org/10.1016/j.antiviral. 2022.105343 140
28. Owczarek K, Szczepanski A, Milewska A, Baster Z, Rajfur Z, Sarna M, Pyrc K. 2018. Early events during human coronavirus OC43 entry to the cell. Sci Rep 8:7124. https://doi.org/10.1038/s41598-018-25640-0
29. Dijkman R, Jebbink MF, Deijs M, Milewska A, Pyrc K, Buelow E, van der Bijl A, van der Hoek L. 2012. Replication-dependent downregulation of cellular angiotensin-converting enzyme 2 protein expression by human coronavirus Nl63. J Gen Virol 93:1924–1929. https://doi.org/10.1099/vir. 0.043919-0
30. Hirose R, Watanabe N, Bandou R, Yoshida T, Daidoji T, Naito Y, Itoh Y, Nakaya T. 2021. A cytopathic effectbased tissue culture method for HCoV-OC43 titration using TMPRSS2-expressing VeroE6 cells. mSphere 6:e00159-21 https://doi.org/10.1128/mSphere.00159-21
31. Mukherjee S, Dowd KA, Manhart CJ, Ledgerwood JE, Durbin AP, Whitehead SS, Pierson TC. 2014. Mechanism and significance of cell type-dependent neutralization of flaviviruses. J Virol 88:7210–7220. https://doi.org/10.1128/JVI.03690-13
32. Reed LJ, Muench H. 1938. A simple method of estimating fifty per cent endpoints12. Am J Epidemiol. 27:493–497. https://doi.org/10.1093/ oxfordjournals.aje.a118408

33. Enlow W, Piret J, Boivin G. 2020. Droplet digital PCR and immunohistochemistry techniques to detect Zika virus in the central nervous system of mice, p 41–57. In Kobinger GRacine T (ed), Zika virus: methods and protocols. Springer US, New York.
34. Friedman HM, Koropchak C. 1978. Comparison of WI-38, MRC-5, and IMR-90 cell strains for isolation of viruses from clinical specimens. J Clin Microbiol 7:368–371. https://doi.org/10.1128/jcm.7.4.368-371.1978 35. Milewska A, Zarebski M, Nowak P, Stozek K, Potempa J, Pyrc K. 2014. Human coronavirus Nl63 utilizes heparan sulfate proteoglycans for attachment to target cells. J Virol 88:13221–13230. https://doi.org/10. 1128/JVI.02078-14
36. Wang G, Deering C, Macke M, Shao J, Burns R, Blau DM, Holmes KV, Davidson BL, Perlman S, McCray PB. 2000. Human coronavirus 229E infects polarized airway epithelia from the apical surface. J Virol 74:9234–9239. https://doi.org10.1128jvi.74.19.9234-9239.2000
37. Walls AC, Park YJ, Tortorici MA, Wall A, McGuire AT, Veesler D. 2020. Structure, function, and antigenicity of the SARS-CoV-2 spike glycoprotein. Cell 181:281–292. https://doi.org/10.1016j.cell.2020.02.058
38. Shang J, Ye G, Shi K, Wan Y, Luo C, Aihara H, Geng Q, Auerbach A, Li F. 2020. Structural basis of receptor recognition by SARS-CoV-2. Nature 581:221–224. https://doi.org/10.1038/s41586-020-2179-y
39. Chen Z, Mi L, Xu J, Yu J, Wang X, Jiang J, Xing J, Shang P, Qian A, Li Y, Shaw PX, Wang J, Duan S, Ding J, Fan C, Zhang Y, Yang Y, Yu X, Feng Q, Li B, Yao X, Zhang Z, Li L, Xue X, Zhu P. 2005. Function of HAb18G/CD147 in invasion of host cells by severe acute respiratory syndrome coronavirus. J Infect Dis 191:755–760. https://doi.org/10.1086/427811
40. Wang K, Chen W, Zhang Z, Deng Y, Lian J-Q, Du P, Wei D, Zhang Y, Sun XX, Gong L, et al. 2020. CD147-spike protein is a novel route for SARSCoV-2 infection to host cells. Sig Transduct Target Ther 5:283. https://doi. org/10.1038/s41392-020-00426-x
41. Tortorici MA, Walls AC, Lang Y, Wang C, Li Z, Koerhuis D, Boons G-J, Bosch B-J, Rey FA, de Groot RJ, Veesler D. 2019. Structural basis for human coronavirus attachment to sialic acid receptors. Nat Struct Mol Biol 26:481–489. https://doi.org/10.1038/s41594-019-0233-y
42. Li Z, Lang Y, Liu L, Bunyatov MI, Sarmiento AI, de Groot RJ, Boons G-J. 2021. Synthetic O-acetylated sialosides facilitate functional receptor identification for human respiratory viruses. Nat Chem 13:496–503. https://doi.org/10.1038/s41557-021-00655-9
43. Jahangiri L, Ishola T, Pucci P, Trigg RM, Pereira J, Williams JA, Cavanagh ML, Gkoutos GV, Tsaprouni L, Turner SD. 2021. The role of autophagy and lncRNAs in the maintenance of cancer stem cells. Cancers (Basel) 13:1239. https://doi.org/10.3390/cancers13061239
44. Vázquez-Iglesias L, Barcia-Castro L, Rodríguez-Quiroga M, Páez de la Cadena M, Rodríguez-Berrocal J, Cordero OJ. 2019. Surface expression marker profile in colon cancer cell lines and sphere-derived cells suggests complexity in CD26(+) cancer stem cells subsets. Biol Open 8:bio041673. https://doi.org/10.1242/bio.041673
45. Belov L, Zhou J, Christopherson RI. 2010. Cell surface markers in colorectal cancer prognosis. Int J Mol Sci 12:78–113. https://doi.org/10. 3390/ijms12010078
46. Iacono KT, Brown AL, Greene MI, Saouaf SJ. 2007. CD147 immunoglobulin superfamily receptor function and role in pathology. Exp Mol Pathol 83:283–295. https://doi.org/10.1016/j.yexmp.2007.08.014
47. Dixon J, Kaklamanis L, Turley H, Hickson ID, Leek RD, Harris AL, Gatter KC. 1994. Expression of aminopeptidase-N (CD 13) in normal tissues and malignant neoplasms of epithelial and lymphoid origin. J Clin Pathol 47:43–47. https://doi.org/10.1136/jcp.47.1.43
48. Landras A, Reger de Moura C, Jouenne F, Lebbe C, Menashi S, Mourah S. 2019. CD147 is a promising target of tumor progression and a prognostic biomarker. Cancers (Basel) 11:1803. https://doi.org/10.3390/ cancers11111803
49. Van der Hauwaert C, Savary G, Gnemmi V, Glowacki F, Pottier N, Bouillez A, Maboudou P, Zini L, Leroy X, Cauffiez C, Perrais M, Aubert S. 2013. Isolation and characterization of a primary

proximal tubular epithelial cell model from human kidney by CD10/CD13 double labeling. PLoS One 8:e66750. https://doi.org/10.1371/journal.pone.0066750
50. Fenizia C, Galbiati S, Vanetti C, Vago R, Clerici M, Tacchetti C, Daniele T. 2021. SARS-CoV-2 entry: at the crossroads of CD147 and ACE2. Cells 10:1434. https://doi.org/10.3390/cells10061434
51. Du W, Hurdiss DL, Drabek D, Mykytyn AZ, Kaiser FK, GonzálezHernández M, Muñoz-Santos D, Lamers MM, van Haperen R, Li W, et al. 2022. An ACE2-blocking antibody confers broad neutralization and protection against omicron and other SARS-CoV-2 variants of concern. Sci Immunol 7:eabp9312. https://doi.org/10.1126/sciimmunol.abp9312
52. 52. Zhang H, Lv P, Jiang J, Liu Y, Yan R, Shu S, Hu B, Xiao H, Cai K, Yuan S, Li Y. 2023. Advances in developing ACE2 derivatives against SARS-CoV-2. Lancet Microbe 4:e369–e378. https://doi.org/10.1016/S2666- 5247(23)00011-3
53. Krishnamurthy S, Lockey RF, Kolliputi N. 2021. Soluble ACE2 as a potential therapy for COVID-19. Am J Physiol Cell Physiol 320:C279– C281. https://doi.org/10.1152/ajpcell.00478.2020
54. Abd El-Aziz TM, Al-Sabi A, Stockand JD. 2020. Human recombinant soluble ACE2 (hrsACE2) shows promise for treating severe COVID-19. Signal Transduct Target Ther 5:258. https://doi.org/10.1038/s41392-020- 00374-6
55. Monteil V, Dyczynski M, Lauschke VM, Kwon H, Wirnsberger G, Youhanna S, Zhang H, Slutsky AS, Hurtado Del Pozo C, Horn M, Montserrat N, Penninger JM, Mirazimi A. 2021. Human soluble ACE2 improves the effect of remdesivir in SARS-CoV-2 infection. EMBO Mol Med 13:e13426. https://doi.org/10.15252/emmm.202013426
56. Wang C, Li W, Drabek D, Okba NMA, van Haperen R, Osterhaus ADME, van Kuppeveld FJM, Haagmans BL, Grosveld F, Bosch B-J. 2020. A human monoclonal antibody blocking SARS-CoV-2 infection. Nat Commun 11:2251. https://doi.org/10.1038/s41467-020-16256-y
57. Fischer N, Dauby N, Bossuyt N, Reynders M, Gérard M, Lacor P, Daelemans S, Lissoir B, Holemans X, Magerman K, Jouck D, Bourgeois M, Delaere B, Quoilin S, Van Gucht S, Thomas I, Barbezange C, Subissi L. 2021. Monitoring of human coronaviruses in Belgian primary care and hospitals, 2015-20: a surveillance study. Lancet Microbe 2:e105–e114. https://doi.org/10.1016/S2666-5247(20)30221-4
58. Edridge AWD, Kaczorowska J, Hoste ACR, Bakker M, Klein M, Loens K, Jebbink MF, Matser A, Kinsella CM, Rueda P, Ieven M, Goossens H, Prins M, Sastre P, Deijs M, van der Hoek L. 2020. Seasonal coronavirus protective immunity is short-lasting. Nat Med 26:1691–1693. https://doi.org/10.1038/s41591-020-1083-1
59. Li Q, Shah T, Wang B, Qu L, Wang R, Hou Y, Baloch Z, Xia X. 2022. Crossspecies transmission, evolution and zoonotic potential of coronaviruses. Front Cell Infect Microbiol 12:1081370.
60. Kane Y, Wong G, Gao GF. 2023. Animal models, zoonotic reservoirs, and cross-species transmission of emerging human-infecting coronaviruses. Annu Rev Anim Biosci 11:1–31. https://doi.org/10.1146/annurev-animal- 020420-025011
61. Fausto A, Otter CJ, Bracci N, Weiss SR. 2023. Improved culture methods for human coronaviruses HCoV-OC43, HCoV-229E, and HCoV-NL63. Curr Protoc 3:e914. https://doi.org/10.1002/cpz1.914
62. Dudley JP. 2023. APOBECs: our fickle friends? PLoS Pathog 19:e1011364. https://doi.org/10.1371/journal.ppat.1011364
63. Chemudupati M, Kenney AD, Bonifati S, Zani A, McMichael TM, Wu L, Yount JS. 2019. From APOBEC to ZAP: diverse mechanisms used by cellular restriction factors to inhibit virus infections. Biochim Biophys Acta Mol Cell Res 1866:382–394. https://doi.org/10.1016/j.bbamcr.2018. 09.012
64. Song Y, He X, Yang W, Wu Y, Cui J, Tang T, Zhang R. 2022. Virusspecific editing identification approach reveals the landscape of A-to-I editing and its impacts on SARS-CoV-2 characteristics and evolution. Nucleic Acids Res 50:2509–2521. https://doi.org/10.1093/nar/gkac120
65. Ringlander J, Fingal J, Kann H, Prakash K, Rydell G, Andersson M, Martner A, Lindh M, Horal P, Hellstrand K, Kann M. 2022. Impact of ADAR-induced editing of minor viral RNA populations on

replication and transmission of SARS-CoV-2. Proc Natl Acad Sci U S A 119:e2112663119. https://doi. org/10.1073/pnas.2112663119
66. Lama J. 2003. The physiological relevance of CD4 receptor downmodulation during HIV infection. Curr HIV Res 1:167–184. https://doi. org/10.2174/1570162033485276
67. Karki R, Kanneganti TD. 2022. Innate immunity, cytokine storm, and inflammatory cell death in COVID-19. J Transl Med 20:542. https://doi. org/10.1186/s12967-022-03767-z
68. Pollett S, Conte MA, Sanborn M, Jarman RG, Lidl GM, Modjarrad K, Maljkovic Berry I. 2021. A comparative recombination analysis of human coronaviruses and implications for the SARS-CoV-2 pandemic. Sci Rep 11:17365. https://doi.org/10.1038/s41598-021-96626-8
69. Chan KK, Dorosky D, Sharma P, Abbasi SA, Dye JM, Kranz DM, Herbert AS, Procko E. 2020. Engineering human ACE2 to optimize binding to the spike protein of SARS coronavirus 2. Science 369:1261–1265. https://doi. org/10.1126/science.abc0870
70. Shao N, Zhang C, Dong J, Sun L, Chen X, Xie Z, Xu B, An S, Zhang T, Yang F. 2022. Molecular evolution of human coronavirus-NL63, -229E, -HKU1 and -OC43 in hospitalized children in China. Front Microbiol 13:1023847. https://doi.org/10.3389/fmicb.2022.1023847
71. Müller NF, Kistler KE, Bedford T. 2022. A bayesian approach to infer recombination patterns in coronaviruses. Nat Commun 13:4186. https:// doi.org/10.1038/s41467-022-31749-8

A-1.15 PLATELET ACTIVATION BY SARS-COV-2 IMPLICATES THE RELEASE OF ACTIVE TISSUE FACTOR BY INFECTED CELLS

Preface

(This work has been previously published as a research article)

Puhm F, Allaeys I, Lacasse E, Dubuc I, **Galipeau Y**, Zaid Y, Khalki L, Belleannée C, Durocher Y, Brisson AR, Wolberg AS, Langlois MA, Flamand L, Boilard E. **Platelet activation by SARS-CoV-2 implicates the release of active tissue factor by infected cells**. Blood Adv. 2022 Jun 28;6(12):3593-3605.

https://doi.org/10.1182/bloodadvances.2022007444

© 2022 by The American Society of Hematology.
Licensed under Creative Commons Attribution-NonCommercial-NoDerivatives 4.0 International (CC BY-NC-ND 4.0), permitting only noncommercial, nonderivative use with attribution. All other rights reserved.

Abstract

Platelets are hyperactivated in coronavirus disease 2019 (COVID-19). However, the mechanisms promoting platelet activation by severe acute respiratory syndrome coronavirus 2 (SARS-CoV-2) are not well understood. This may be due to inherent challenges in discriminating the contribution of viral vs host components produced by infected cells. This is particularly true for enveloped viruses and extracellular vesicles (EVs), as they are concomitantly released during infection and share biophysical properties. To study this, we evaluated whether SARS-CoV-2 itself or components derived from SARS-CoV-2-infected human lung epithelial cells could activate isolated platelets from healthy donors. Activation was measured by the surface expression of P-selectin and the activated conformation of integrin αIIbβ3, degranulation, aggregation under flow conditions, and the release of EVs. We find that neither SARS-CoV-2 nor purified spike activates platelets. In contrast, tissue factor (TF) produced by infected cells was highly potent at activating platelets. This required trace amounts of plasma containing the coagulation factors FX, FII, and FVII. Robust platelet activation involved thrombin and the activation of protease-activated receptor (PAR)-1 and -4 expressed by platelets. Virions and EVs were identified by electron microscopy. Through size-exclusion chromatography, TF activity was found to be associated with a virus or EVs, which were indistinguishable. Increased TF messenger RNA (mRNA) expression and activity were also found in lungs in a murine model of COVID-19 and plasma of severe COVID-19 patients, respectively. In summary, TF activity from SARS-CoV-2–infected cells activates thrombin, which signals to PARs on platelets. Blockade of molecules in this pathway may interfere with platelet activation and the coagulation characteristic of COVID-19.

Introduction

Coronavirus disease 2019 (COVID-19) is a respiratory tract infection caused by severe acute respiratory syndrome coronavirus 2 (SARS-CoV-2).[1] Since the onset of this pandemic, millions of people have died.[2] Acute respiratory distress syndrome is one of the main characteristics of severe COVID-19, and its manifestation influences the outcome of infection.[3] A high degree of generalized inflammation and thrombosis is also reported.[1,4-6] Autopsies show that the formation of microthrombi is common in the lung vasculature and other organs distant from the lungs, suggesting a role for dysregulated coagulation.[7-10] Furthermore, age, hypertension, diabetes, and coronary heart disease, well-known risk factors for thrombosis and associated with chronic inflammation, are the main determinants of COVID-19 severity and mortality.[3,4,11,12]

Platelets are anucleated cells at the interface of thrombosis and inflammation.[13-15] They are critical in hemostasis, interact with pathogens, and can alert other immune cells.[14,15] It is notable that hyperactivated platelets are present in COVID-19.[16-22] Hyperactivation is characterized by high expression of P-selectin (CD62P), degranulation (release of platelet factor 4 [PF4] and serotonin [5-HT]), and release of platelet extracellular vesicles (EVs), as well as increased aggregation and adhesion of platelets to other cells, particularly monocytes, and changes in platelet gene expression.[16-22]

Different laboratories have detected SARS-CoV-2 RNA in association with platelets in patients.[16,17,23] While compelling studies confirmed that SARS-CoV-2 could be taken up by platelets, leading to programmed cell death, platelets failed to activate in these conditions.[23] Angiotensin-converting enzyme-2 (ACE2), abundantly expressed by epithelial cells in the lungs, is the cognate cell receptor for the SARS-CoV-2 spike protein.[24,25] An ACE2-dependent SARS-CoV-2 and platelet interaction has been suggested as a potential mechanism for platelet hyperactivation.[26] However, platelet expression of ACE2 could not be conclusively demonstrated,[27] and some studies indicated SARS-CoV-2 interacts with platelets through ACE2-dependent and independent mechanisms.[23,28] Another putative receptor for a SARS-CoV-2 platelet interaction is CD147.[29-31] While evidence of interaction between SARS-CoV-2 and

CD147 has been challenged,[32] one study suggests that SARS-CoV-2 pseudovirus and recombinant spike proteins activate platelets, characterized by the release of $HMGB1^+$ EVs and soluble P-selectin, in a CD147-dependent manner.[33] Another study suggests that spike may engage platelet CD42b, thereby promoting interactions with monocytes and cytokine production by monocytes.[34] However, overexpression of spike protein (resulting from vaccination) did not result in platelet activation.[35] Thus, there exists conflicting data as to whether and how SARS-CoV-2 activates platelets.

Initiation of the coagulation cascade may also underlie platelet activation. Coagulation abnormalities have been reported in COVID-19,[36] which may be the consequence of extensive tissue damage associated with SARS-CoV-2 infection and subsequent engagement of the coagulation cascade. Tissue factor (TF) is the main cellular initiator of coagulation and a highly potent stimulus that is absent in blood under physiological conditions.[37-39] Active TF in blood activates the extrinsic (TF) pathway of coagulation, leading to the conversion of prothrombin to thrombin and subsequent fibrin clot formation. Thrombin is a highly potent stimulus of platelet activation and has been previously found to contribute to the H1N1-mediated activation of platelets.[40] Several studies detected TF activity in the blood of COVID-19 patients.[41-43] Moreover, SARS-CoV-2 spike protein pseudotyped viral infection of human monocyte-derived macrophages induces the expression of active TF in vitro.[44] Furthermore, SARS-CoV-2 infection of endothelial cells or endothelial dysfunction have been suggested as a potential source of TF.[45]

SARS-CoV-2 is an enveloped virus that may acquire host molecules during the budding process.[46-51] The propagation of viruses in cell lines is essential, as viral replication requires a cellular host.[52] Infected cell supernatants are thus used as a source of the virus, but the potential role of concomitantly released host molecules and EVs must be considered when examining the effects of cell supernatants on target cells. Supernatants containing viruses may be pelleted by centrifugation to reduce the presence of soluble molecules.[53,54] Moreover, polyethylene glycol (PEG) precipitation can be used to concentrate viruses from supernatants. However, both centrifugation and PEG precipitation can also enrich EVs.[54,55] Given that viruses, protein aggregates, and EVs share biophysical properties,[53,54] they cannot be efficiently separated from

each other using any of these approaches.[53,54] Whether SARS-CoV-2 or host-derived molecules activate platelets has not been studied.

In this study, we examined whether SARS-CoV-2 or components from infected cells could activate platelets.

Methods

A detailed description is provided in the supplemental Material.

Platelet isolation from human donors

Venous blood from healthy donors was collected into citrate anticoagulant solution and centrifuged for 10 minutes at 231*g*. One mL of platelet-rich plasma (PRP) was transferred to fresh microcentrifuge tubes, and 250 µL of acid-citrate-dextrose (ACD) and ethylene diamine tetraacetic acid (10 mM) were added. PRP was centrifuged (2 minutes at 300*g*). One mL of the supernatant was transferred to fresh tubes and centrifuged (5 minutes at 1100*g*). The supernatant was aspirated, and the platelet pellet was resuspended in 100 µL of Tyrode's buffer (pH, 6.5). Another 900 µL of Tyrode's buffer (pH, 7.4), 250 µL ACD, and ethylene diamine tetraacetic acid (10 mM) were added. Platelets were then centrifuged for 5 minutes at 1300*g*. The supernatant was aspirated, and platelets were recovered (200×10^6/mL) in Tyrode's buffer (pH, 7.4). All steps were performed at room temperature.

Propagation of SARS-CoV-2

SARS-CoV-2 (strain LSPQ, B1 lineage) was obtained from the Laboratoire de Santé Publique du Québec. A549-hACE2 cells were infected at a multiplicity of infection (MOI) of 1 for 1 hour, then washed twice with phosphate-buffered saline (PBS) before the addition of new culture media. The virus was harvested from cell-free media after 4 days and inactivated by the addition of β-propiolactone as described.[56]

Platelet activation assay

Blood, collected in a 3.2% citrate anticoagulant solution, was centrifuged (2 × 2500*g* at 15 minutes) to obtain platelet-free plasma (PFP). PFP was incubated in Tyrode's buffer (pH, 7.4; 10 mM $CaCl_2$) in the presence of stimuli (thrombin, SARS-CoV-2, or controls; 2× concentrated) for 60 minutes. Then, platelets (100 × 10^6/mL final concentration) were added. All incubations were performed at room temperature. Unless indicated otherwise, platelet activation was assessed after 60 minutes by staining (20 minutes) with antibodies for CD41, activated integrin αIIbβ3*, and CD62P, and platelets were fixed with paraformaldehyde (1%) thereafter.

Results

SARS-CoV-2 activates platelets in a plasma-dependent manner

SARS-CoV-2 was propagated in ACE2-overexpressing human lung epithelial A549 cells. Culture supernatant (C.Med) from noninfected cells used at the same volume as CoV2 was used as a negative control. For safety reasons and convenience, unless specified otherwise, we used β-propiolactone–inactivated SARS-CoV-2 or β-propiolactone–treated C.Med.[56] We evaluated the ability of SARS-CoV-2 to induce platelet activation, as assessed by the frequency of platelets expressing the active conformation of αIIbβ3 integrin (αIIbβ3*) and CD62P (αIIbβ3*CD62P), the expression density of αIIbβ3*, and the liberation of EVs ($CD41^+$ EVs). To account for a potential plasma–SARS-CoV-2 interaction independent of a direct virus–platelet interaction, we preincubated virus or C.Med in the presence or absence of recalcified PFP before the addition to washed platelets. The plasma preparations were obtained from nonimmune donors, as determined by the absence of SARS-CoV-2 antibodies (supplemental Figure 1).

Flow cytometric analyses revealed that the presence of SARS-CoV-2 (1:25 vol/vol; 1.9E+05 virus per mL) induced a rapid and significant increase in the percentage of αIIbβ3*$CD62P^+$ platelets (7.5 minutes) and an increase in expression intensity of αIIbβ3* (15 minutes) (Figure 1A). Following a 60-minute stimulation with SARS-CoV-2, the vast majority of platelets expressed αIIbβ3*CD62P, and the levels of $CD41^+$ EVs were increased (Figure 1A). Platelet activation required the presence of plasma (0.5%) (Figure 1A). Platelets failed to activate in response to SARS-CoV-2 (1:25 vol/vol; 1.9E+05 virus per mL) in the absence of plasma or in the presence of C.Med (1:25 vol/vol) in the presence or absence of plasma (Figure 1A). In contrast, platelets

efficiently responded to thrombin (1 U/mL) in the presence or absence of plasma (0/0.25/0.5/1%) (supplemental Figure 2).

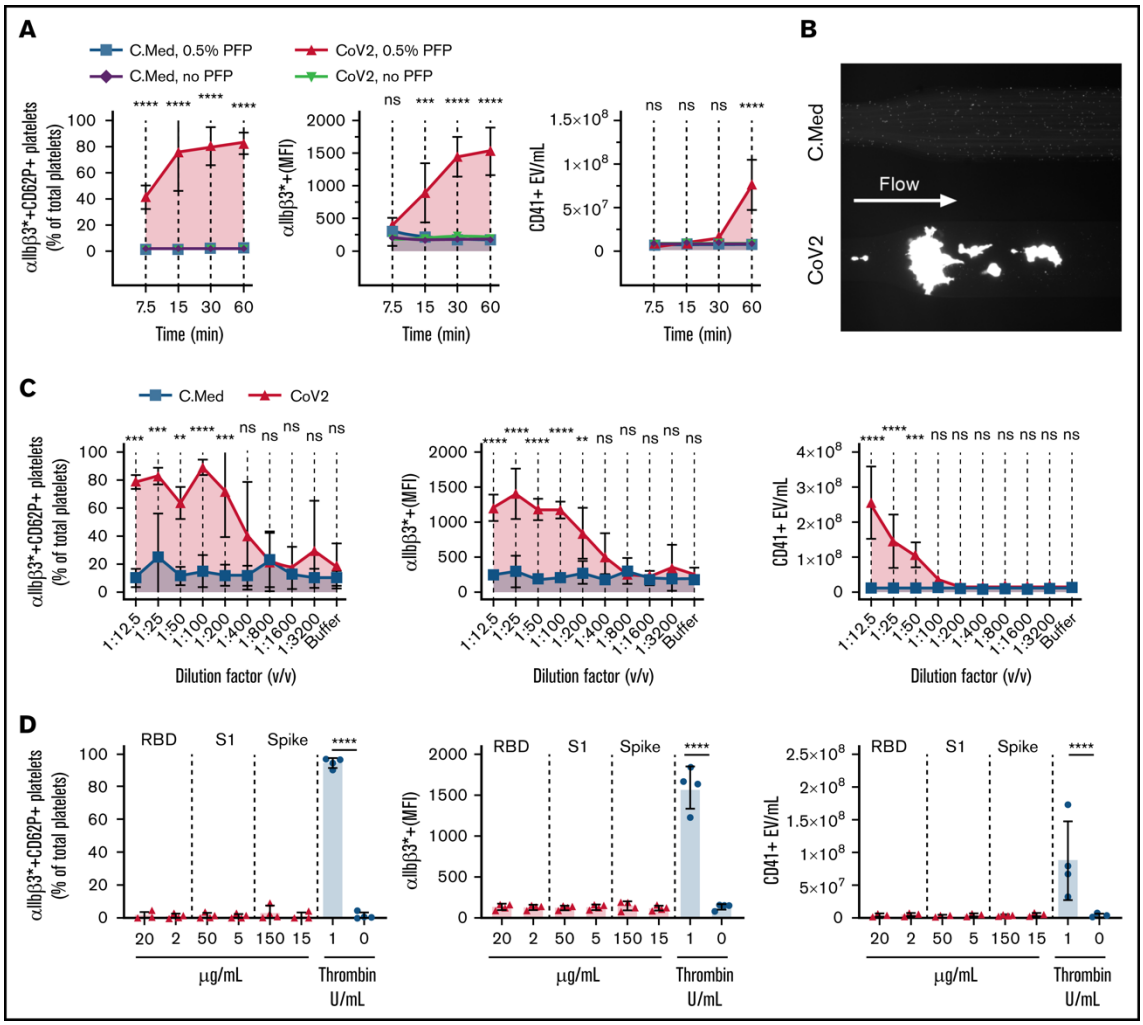


Figure 1. SARS-CoV-2 activates platelets in a plasma-dependent manner. Platelet responses to β-propiolactone–inactivated SARS-CoV-2 (CoV2, red) obtained from human A549 (ACE2) cell infection or conditioned media (C.Med, blue) solution (A549 [ACE2] cell culture supernatant obtained after 4 days of culture and treatment with β-propiolactone [1:1000 vol/vol]). (A) Platelets were stimulated with C.Med or CoV2 in the presence or absence of PFP (0.5%). Platelets were labeled and fixed after stimulation for 7.5, 15, 30, or 60 minutes, and platelet activation was determined by flow cytometry. N = 3. (B) Platelets were stimulated with C.Med or CoV2 (1:25 vol/vol) in the presence of PFP (0.5%) and injected into a microfluidics system. The images were taken after 15 minutes and show fluorescently-labeled platelets in the fibrinogen-coated channel. Representative images. N = 4. (C) Platelets were stimulated with C.Med or CoV2 in the presence of PFP (0.5%). N = 4. (D) Platelets were stimulated for 60 minutes with receptor-binding domain (RBD) peptide, S1 subunit of spike, full trimeric spike protein, or thrombin in the presence of platelet-free plasma (0.5%). N = 4. Data are represented as mean ± SD. Statistical analysis: (A, C, D) Ordinary two-way ANOVA followed by Sidak's multiple comparison test. ***P* < .01, ****P* < .001, and *****P* < .0001. ns, not significant.

As αIIbβ3* expressed on platelets is a major receptor for platelet adhesion to fibrinogen, we tested the ability of platelets to adhere under physiological flow in a fibrinogen-coated microfluidics chamber. Visualization of fluorescently-labeled platelets revealed the formation of large clots induced by SARS-CoV-2 (1:25 vol/vol; 1.9E+05 virus per mL), but only when plasma was present. Clots did not form when platelets were in the presence of C.Med (1:25 vol/vol) and plasma (Figure 1B; supplemental Figure 3).

The response to increasing concentrations of SARS-CoV-2 (1:12.5 to 1:3200 vol/vol; 3.8E+05 to 1.5E+03 virus per mL) was determined in the presence of plasma to assess SARS-CoV-2 platelet activation. Strong platelet activation, based on all measured parameters, was observable with SARS-CoV-2 at 1:12.5 to 1:50 vol/vol (1.5E+03 to 9.5E+04 virus per mL) (Figure 1C). With the exception of $CD41^+$ EVs, which were not significantly increased by SARS-CoV-2 at 1:200 vol/vol dilution (2.4E+04 virus per mL), this lower concentration sufficed to induce the surface expression of αIIbβ3* and CD62P (Figure 1C). In contrast, C.Med did not induce platelet activation within the tested concentration range (1:12.5 to 1:3200 vol/vol) (Figure 1C).

The possibility that the prominently expressed spike protein of SARS-CoV-2 may be able to induce plasma-dependent activation of platelets was examined next. Recombinant full-trimeric SARS-CoV-2 spike protein, the S1 subunit containing the receptor-binding domain (RBD), or a recombinant SARS-CoV-2 RBD peptide, were preincubated in plasma and then added to platelets to assess activation. No platelet activation was observed in response to any of the tested proteins (Figure 1D), which contrasted with the profound platelet activation induced by thrombin (1 U/mL) under the same conditions (Figure 1D). Thus, the combination of SARS-CoV-2 and plasma components activated platelets. This is likely independent of the spike as recombinant SARS-CoV-2 spike proteins failed to activate platelets.

SARS-CoV-2 activates platelets in a TF- and thrombin-dependent manner

We hypothesized that an active component associated with SARS-CoV-2 might be triggering the coagulation cascade. Thus, we incubated plasma deficient in individual coagulation factors (FXIII, FXII, FXI, FX, FIX, FVIII, FVII, FV, FII, FI, Protein C, Protein S, and von Willebrand factor [VWF])[57] with SARS-CoV-2 or C.Med, and thereafter added platelets to assess activation (Figure 2A; supplemental Figure 4). Strong activation occurred despite the absence of FXIII, FXII, FXI, FIX, FVIII, FV, FI, Protein C, Protein S, or VWF in plasma (Figure 2A; supplemental Figure 4). However, in the absence of FX, FII, and FVII, SARS-CoV-2 failed to activate platelets, as activation remained at the background level and was not statistically different from that of the negative control (C.Med) (Figure 2A; supplemental Figure 4). These observations point to an involvement of the TF pathway of coagulation.

Coagulation factors in plasma are present as inactive zymogens, which may become catalytic enzymes when the coagulation cascade is initiated.[38,57] The active form of FX is FXa, which is responsible for the conversion of prothrombin (FII) to thrombin. Thrombin mediates the formation of a fibrin clot and is a potent physiological stimulus of platelet activation.[57] We hypothesized that thrombin is responsible for the plasma-dependent SARS-CoV-2–mediated platelet activation. To test this, we incubated plasma with SARS-CoV-2 in the presence or absence of the selective and irreversible thrombin inhibitor d-phenylalanyl-prolyl-arginyl chloromethyl ketone before the addition of platelets. The activation was completely blocked by thrombin inhibition (Figure 2B). We further confirmed that SARS-CoV-2 activation of naïve wild-type mouse platelets critically required plasma and thrombin activation (supplemental Figure 5). Murine ACE2 is not recognized by SARS-CoV-2 spike protein,[58] and wild-type mouse platelets do not express FcyRIIA, thereby ruling out that platelet activation was ACE2- or Fc-receptor dependent.

Similar to the replication-incompetent fixed virus, infectious SARS-CoV-2 (1:4 or 1:25 vol/vol; 1.2E+06 or 1.9E+05 virus per mL) promptly activated platelets, but only in the presence of plasma (supplemental Figure 6). The activation was blocked by the thrombin inhibitor, demonstrating that the initiation of coagulation and generation of thrombin were not due to the virus fixation (supplemental Figure 6). Moreover, concentrations as high as 1:4/1:25 vol/vol of C.Med, β-propiolactone–treated or untreated, failed to activate platelets even after a 60-minute incubation

(supplemental Figure 6). Thus, infectious and fixed SARS-CoV-2 activate platelets in a plasma- and thrombin-dependent manner.

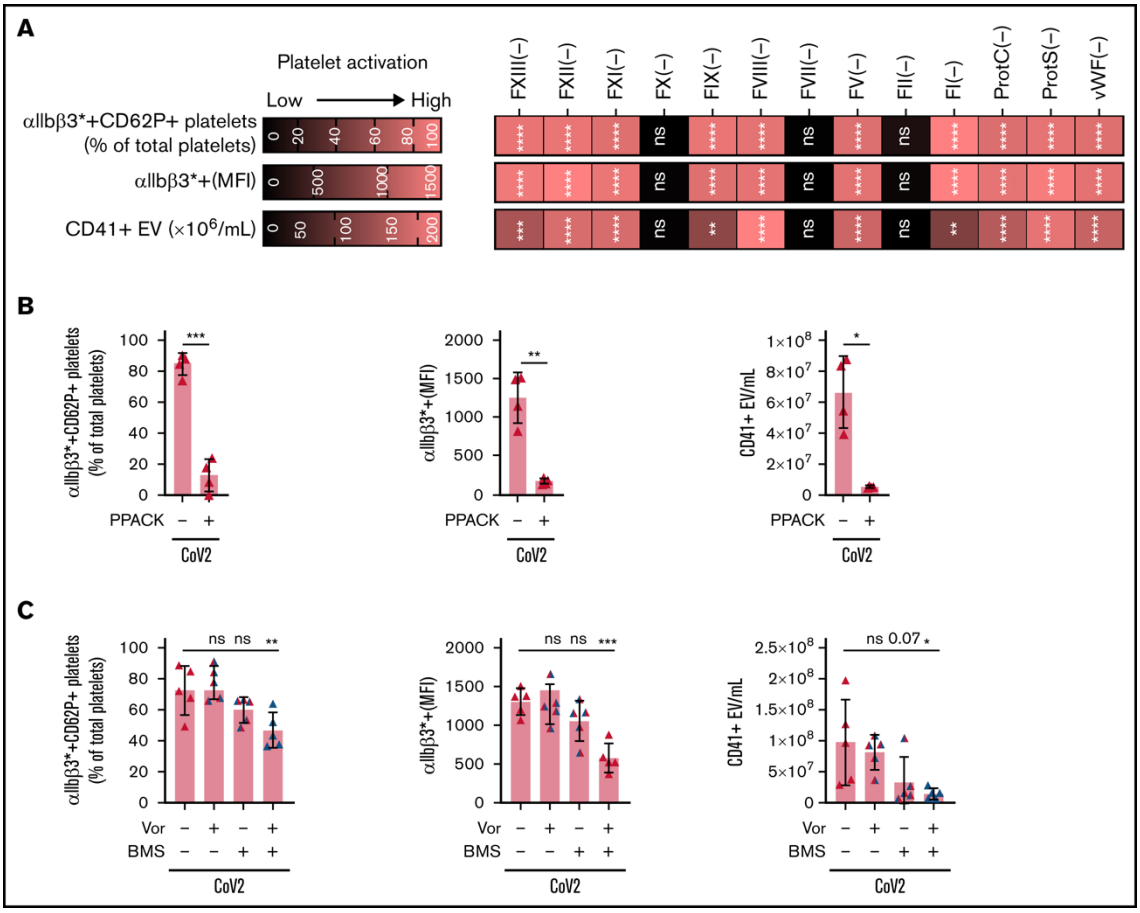


Figure 2. SARS-CoV-2 activates platelets in a TF pathway and thrombin-dependent manner. Platelet responses to β-propiolactone–inactivated SARS-CoV-2 (CoV2) obtained from human A549 (ACE2) cell infection or conditioned media (C.Med) solution (A549 [ACE2] cell culture supernatant obtained after 4 days of culture and treatment with β-propiolactone [1:1000 vol/vol]). (A) Platelets were stimulated with C.Med or CoV2 (1:25 vol/vol) in the presence of platelet-free plasma (0.5%) deficient in individual coagulation factors. The heatmap indicates the mean platelet activation by CoV2 stimulation. The statistical significance symbols indicate comparisons of CoV2 with C.Med-stimulated platelets. N = 5. (B) Platelet stimulation with CoV2 (1:25 vol/vol) in the presence of PFP (0.5%) and in the presence of d-phenylalanyl-prolyl-arginyl chloromethyl ketone (PPACK) (0/10 μM). CoV2 was preincubated for 15 minutes with PPACK before incubation with PFP. N = 4. (C) Platelets were preincubated for 15 minutes with vorapaxar (20 μM) and BMS-9861200 (20 μM), a PAR-1 and PAR-4 inhibitor, respectively, or DMSO (0.45%). Thereafter, platelets were stimulated with CoV2 (1:25 vol/vol) in the presence of PFP (0.5%). N = 5. Data are represented as mean ± SD. Statistical analysis: (A) Ordinary two-way ANOVA followed by Sidak's multiple

comparison test. (B) Paired *t*-test. (C) Ordinary one-way ANOVA followed by Dunnett's multiple comparison test. **P* < .05, ***P* < .01, ****P* < .001, and *****P* < .0001. ns, not significant.

The main cellular receptors for thrombin are PAR-1 and PAR-4, which are expressed by human platelets.[59] Hence, we tested if the PAR blockers vorapaxar (PAR-1 blocker) and BMS-9861200 (PAR-4 blocker) could interfere with the activation. Individual receptor blockade by vorapaxar or BMS-9861200 failed to reduce platelet activation (Figure 2C). Treating platelets with both vorapaxar and BMS-9861200 before their addition to plasma-containing SARS-CoV-2 significantly reduced, but did not fully block, platelet activation, as seen by a lower frequency of αIIbβ3*CD62P-expressing platelets (46% [standard deviation (SD), 11.42] compared with 72.7% [SD, 15.73]), 2.3× lower expression of αIIbβ3* and 6.5× lower $CD41^+$ EV release (Figure 2C). The data suggest both PAR receptors are involved. The incomplete blockade indicates that the used inhibitors failed at completely blocking PAR-1 and PAR-4 signaling or that other receptors on platelets, such as GP1bα (CD42b), may respond to thrombin in addition to PAR-1 and PAR-4.[60,61]

TF is implicated in SARS-CoV-2–mediated platelet activation

The role of factors FX, FII, and FVII pointed to the involvement of the upstream cofactor TF, the primary cellular initiator of coagulation.[57,38] While CoV-2 might bear an intrinsic TF-like activity, the most probable explanation was the presence of actual TF associated with virus production. To assess the contribution of TF, the specific levels of TF activity in SARS-CoV-2 and C.Med were determined. To account for potential nonspecific detection of TF activity, a known confounder in these activity assays,[62-64] a specific TF-blocking antibody (clone HTF-1) was included in the assay (supplemental Figure 7). While significant TF activity (8.62 pM [SD, 2.8]) was found in SARS-CoV-2 preparations, TF activity was undetectable in C.Med (Figure 3A; supplemental Figure 7), suggesting that (1) CoV-2 infection of cells induced active TF, and (2) SARS-CoV-2 is associated with active TF.

Blockade of TF using an anti-TF antibody completely prevented platelet activation (Figure 3B) and platelet degranulation measured by PF4 and serotonin release (Figure 3C-D). These findings were replicated with a major SARS-CoV-2 variant of concern, as SARS-CoV-2-Δ (1:8/1:25 vol/vol; 1.8E+04/0.57E+04 virus per mL) also induced platelet activation in the presence of plasma (0.5%) and was prevented by TF blockade (Figure 3E). These data indicate that the platelet activation by SARS-CoV-2 was mediated by TF-induced coagulation.

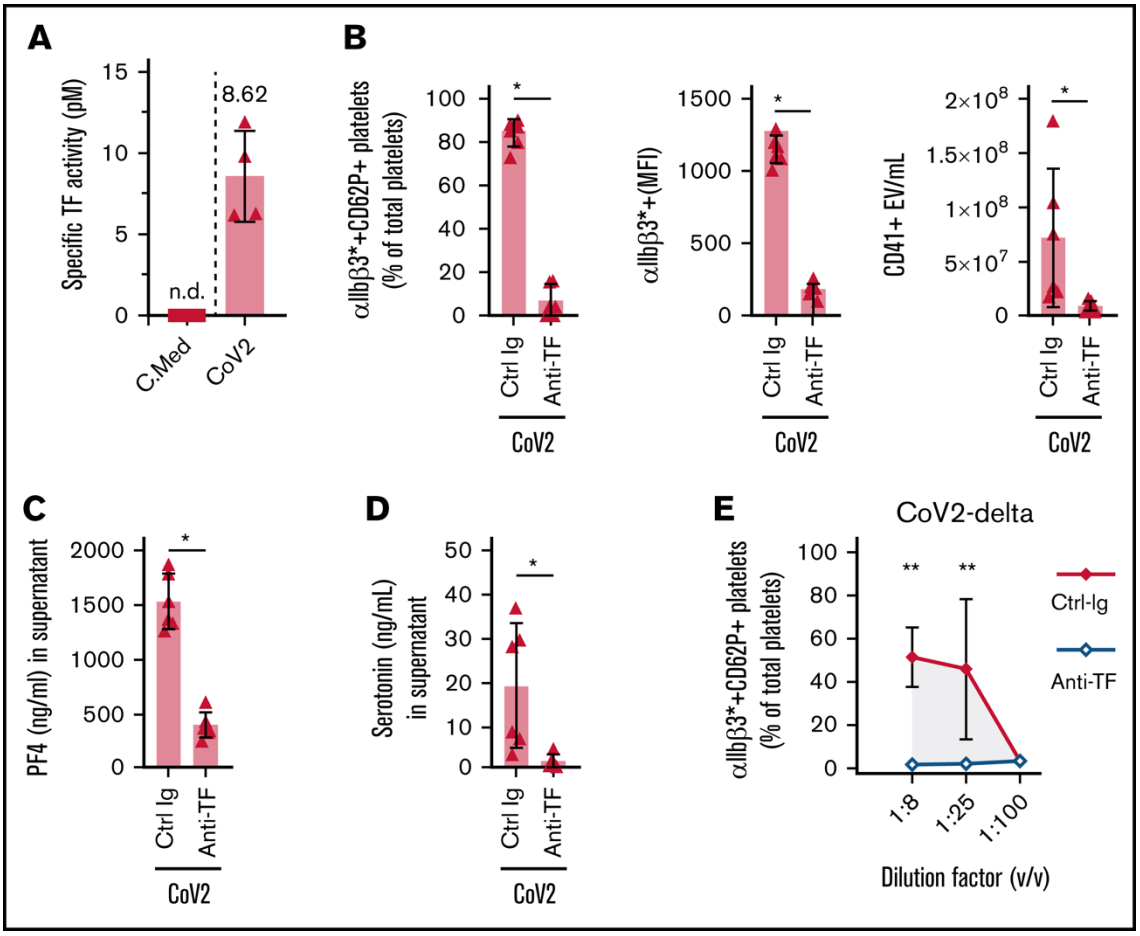


Figure 3. SARS-CoV-2 activates platelets in a TF-dependent manner. Platelet responses to β-propiolactone–inactivated SARS-CoV-2 (CoV2) obtained from human A549 (ACE2) cell infection or conditioned media (C.Med) solution (A549 [ACE2] cell culture supernatant obtained after 4 days of culture and treatment with β-propiolactone [1:1000 vol/vol]). (A) TF activity was assessed by TF/FVII-mediated conversion of FX to FXa and subsequent conversion of FXa substrate. TF activity was measured in an undiluted sample. The specific TF activity indicated is calculated as total TF activity measured in the presence of control Ig minus the total TF activity measured in the presence of anti-TF antibody HTF-1. Samples were preincubated for 15 minutes with control Ig or HTF-1. The numbers above bars indicate the estimated TF activity in pM. N = 4 (replicates measured in 4 separate assays). n.d. = not detected. (B) Platelet stimulation with CoV2 (1:25 vol/vol) in the presence of control Ig (control Ig, 10 μg/mL) or anti-TF antibody HTF-1 (10 μg/mL) and in the presence of PFP (0.5%). CoV2 was preincubated for 15 minutes with control Ig or HTF-1 before incubation with PFP. N = 6. (C) PF4 measurement by ELISA in platelet supernatant. N = 6. (D) 5-HT (serotonin) measurement by ELISA in platelet supernatant. N = 6. (E) Platelet stimulation with CoV2-Δ in the presence of control Ig (control Ig, 10 μg/mL) or anti-TF antibody HTF-1 (10 μg/mL) and in the presence of PFP (0.5%). CoV2-Δ was preincubated for 15 minutes with control Ig or HTF-1 before incubation with PFP. N = 3. Data

are represented as mean ± SD. Statistical analysis: (B-D) Wilcoxon test. (E) Ordinary two-way ANOVA followed by Sidak's multiple comparison test. *P < .05 and **P < .01.

TF is usually indirectly detected by the assessment of its cofactor activity and ability to stimulate coagulation. Femtomolar amounts of TF activity suffice to accelerate blood coagulation[37] and, therefore, promote platelet activation. Indeed, we found that stimulating platelets with plasma incubated with TF (lipoprotein) at concentrations as low as 18.8 fM led to increased expression of αIIbβ3* and CD62P (93.03% [SD, 1.7]), while 75 fM sufficed to induce the release of $CD41^+$ EVs (90.7E+06 mL [SD, 29]) (supplemental Figure 8). This suggests that even extremely low concentrations of active TF in plasma are sufficient to trigger full activation of platelets.

SARS-CoV-2 and EVs, but not soluble proteins, are coisolated with TF activity

While electron microscopy (EM) has been successfully used to characterize SARS-CoV-2 viral architecture,[65,66] the presence of EVs in virus preparations has been overlooked so far. Using cryo-EM, we confirm the presence of heterogeneous populations of EVs in releasates of SARS-CoV2–infected cells (Figure 4). Most EVs ranged in size from 80 nm to 500 nm and were either isolated or associated in small clusters. The presence of a population of EVs exposing the procoagulant lipid phosphatidylserine was demonstrated by specific binding of annexin-V conjugated with gold particles[67] (Figure 4B). Phosphatidylserine-positive EVs constitute more than half of isolated EVs. In addition, a homogenous population of spherical particles was observed, characterized by their narrow size range (80-130 nm), their typical granular density, likely corresponding to the protein and genome package of SARS-CoV-2, and the presence of extended proteins protruding from the particle surface, most likely representing spike projections (Figure 4C). Thus, virus preparations contained both SARS-CoV-2 and EVs.

EVs and viruses share many biophysical features, and enveloped viruses may acquire host proteins during the budding process.[46] ,, -[51,53,54] TF is primarily expressed as a membrane-bound protein that may be associated with EVs, although a soluble isoform exists.[38,39] As direct detection of TF

at these concentrations is not technically achievable,[62,68] whether TF activity specifically associated with EVs, viruses, or soluble proteins was investigated through fractionation by size-exclusion chromatography (SEC).

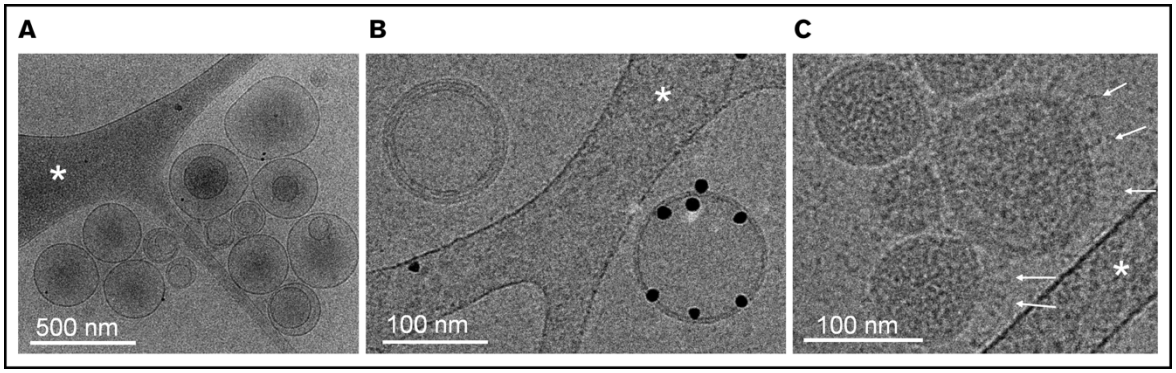


Figure 4. Cryo-electron microscopy of releasate from SARS-CoV-2–infected cells. (A) A set of EVs, ranging in size from 100 to 500 nm. Some EVs contain smaller EVs, as frequently observed in EV samples from various origins. (B) Two EVs side-by-side. One EV is specifically labeled with Anx5 gold particles, thus exposing the procoagulant lipid phosphatidylserine; the other one is unlabeled, thus does not expose phosphatidylserine. (C) A group of virus particles, characterized by their homogenous granularity and the presence of long protein protrusions (white arrows) corresponding most likely to spike proteins. (A-C) The white stars indicate thin threads of the carbon support film.

Concentrated SARS-CoV-2 in A549-hACE2 cell culture supernatant was subjected to SEC, and elution fractions were collected (Figure 5A). The majority of EVs (71.23%) were found in fractions 3 to 5, with fraction 4 (41.70%) containing most EVs, whereas soluble proteins (91.25%) were found in fractions 9 to 20 (Figure 5B). Consistent with quantifications of EVs, the highest levels of 18S rRNA (as a marker for host-derived EV content[69]) were found in fractions 3 to 5 (supplemental Figure 9). The highest concentration of particles expressing SARS-CoV-2 spike protein and SARS-CoV-2 RNA was found in fraction 4 (Figure 5C; supplemental Figure 10). SARS-CoV-2 RNA was particularly enriched compared with 18S rRNA in fraction 4 (threefold, ±SD 0.12), indicating a higher quantity of particles carrying viral content compared with host cell EVs. Thus, EVs and SARS-CoV-2 are indistinguishable using SEC.

Next, specific TF activity was uniquely detected in fractions 3 through 5 (Figure 5D; supplemental Figure 11), demonstrating that TF activity is coisolated with EVs and SARS-CoV-2. Accordingly, strong and significant platelet activation (αIIbβ3*CD62P expression) was induced by fraction 4 (1:25 vol/vol) (Figure 5D), thereby coinciding with the fraction containing the highest level of TF activity and both EVs and virus. In sum, EV fractions are enriched in SARS-CoV-2, and these fractions (and not soluble proteins) contain the TF activity responsible for platelet activation.

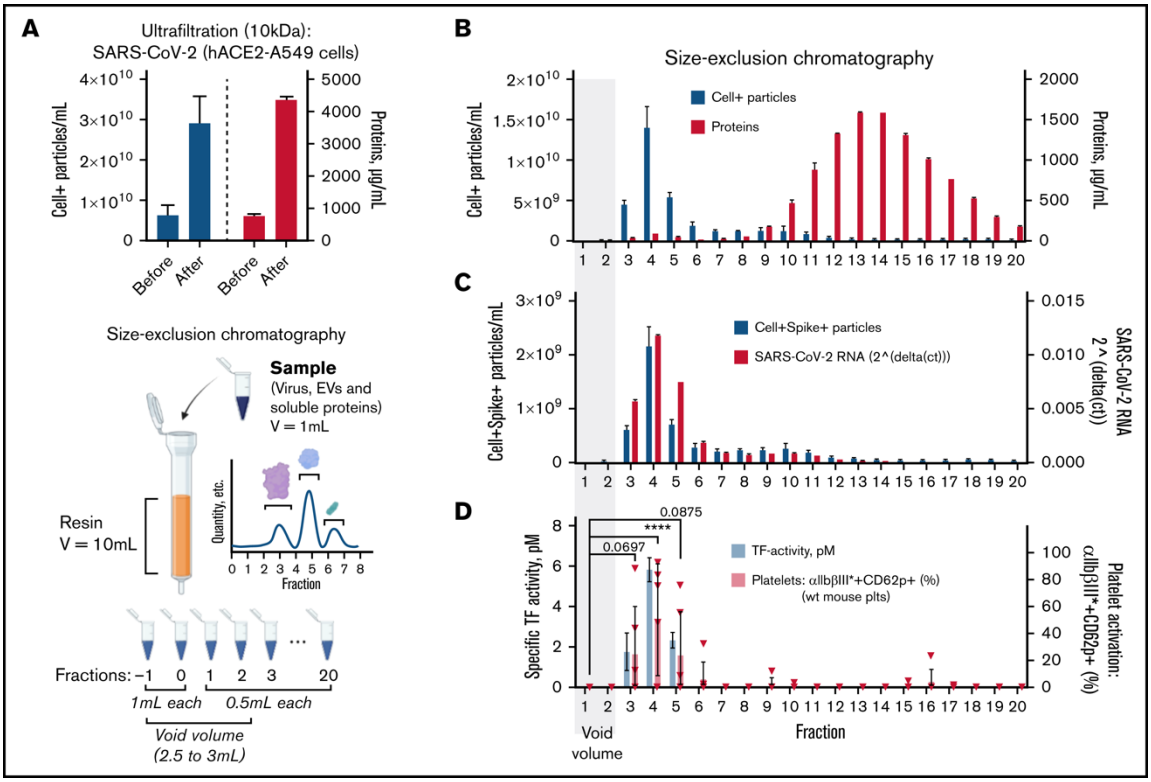


Figure 5. TF activity is exclusively found in SARS-CoV-2 and EV-containing chromatography fractions. (A) β-propiolactone–inactivated SARS-CoV-2 obtained from human A549 (ACE2) cell infection was concentrated by Ultrafiltration (10 kDa filter columns) as size-exclusion chromatography dilutes samples up to 10 times. Celltracker-DR–positive (Cell+) particles (EVs/virus) and protein content before and after sample ultrafiltration were quantified by flow cytometry (left y-axis, 3 technical replicates) and BCA assay (right y-axis, 2 technical replicates), respectively. The concentrated sample was then loaded on an SEC column, and fractions of 0.5 mL after the void volume were collected (see cartoon created with Biorender). (B) Celltracker-DR–positive particles (EVs/virus) and protein content of each SEC fraction were quantified by FACS (left y-axis, 3 technical replicates) and BCA assay (right y-axis, 2 technical replicates), respectively. (C) Celltracker-DR–positive and spike-positive (samples labeled by mouse IgG1 anti-spike SARS-CoV-2, fluorescein-conjugated) particles (EV/virus) and SARS-CoV-2 RNA content (left or right y-axis, respectively) were quantified in each SEC fraction. (D) Left y-axis. TF activity was assessed by TF/FVII-mediated conversion of FX to FXa and subsequent conversion of FXa substrate. The specific TF activity indicated is calculated as total TF activity measured in the presence of control Ig minus the total TF activity measured in the presence of anti-TF antibody HTF-1. Samples were preincubated for 15 minutes with control Ig or HTF-1. The numbers above the bars indicate the estimated TF activity in pM. Measured in 3 technical replicates. (D) Right y-axis, wt C57BL/6J mouse platelet stimulation (n = 6) with SEC fractions (1:25 vol/vol) in the presence of pooled, recalcified

(10 mM CaCl2) mouse PFP (0.5%). The amount of $CaCl_2$ was twofold higher than in previous platelet stimulations as phosphate contained in SEC buffer (PBS) may chelate free calcium. Data are represented as mean ± SD. Statistical analysis: (D) one-way ANOVA followed by Dunnett's multiple comparison test. ****P < .0001.

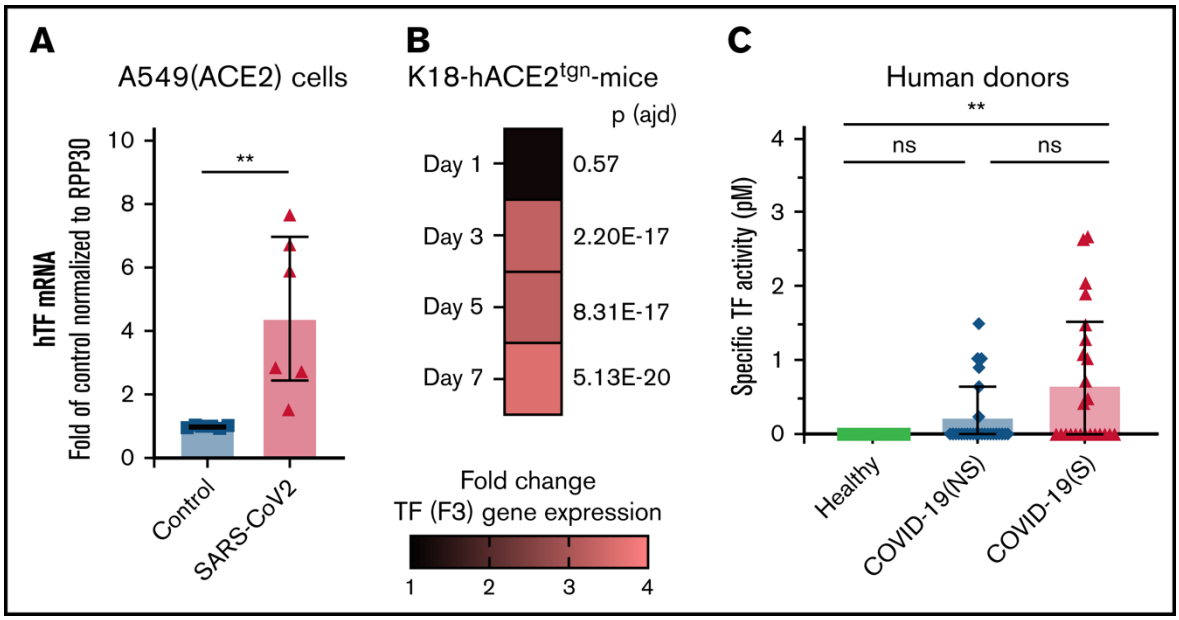


Figure 6. TF expression is associated with SARS-CoV-2 infection in vitro, in a murine infection model, and COVID-19 patients. TF expression (mRNA) or TF activity was assessed in vitro, in mice, and in plasma from human donors. (A) human TF (F3) mRNA expression quantified in SARS-CoV-2–infected A549 (ACE2) cells compared with uninfected (control) A549 (ACE2) cells. mRNA expression levels were normalized to RPP30. (B) Mouse TF (F3) gene expression determined by RNAseq in K18-$ACE2^{tgn}$ mouse lungs infected with SARS-CoV-2 on days 1, 3, 5, and 7 postinfection compared with uninfected K18-$ACE2^{tgn}$ mouse. To consider a differential gene expression statistically significant, thresholds of 0.01 and |log2(3)| were applied for the adjusted P value (P adj) and the minimum fold-change, respectively. N = 4 per group. (C) Human TF activity assessed in plasma from healthy donors (n = 15), COVID-19 patients with nonsevere (n = 25) or severe (n = 25) disease. TF activity was assessed by TF/FVII-mediated conversion of FX to FXa and subsequent conversion of FXa substrate. The specific TF activity indicated is calculated as total TF activity measured in the presence of control Ig minus the total TF activity measured in the presence of anti-TF antibody HTF-1. The numbers above the bars indicate the estimated TF activity in pM. Data are represented as mean ± SD. Statistical analysis: (A) Mann-Whitney test. (C) Kruskal-Wallis test followed by Dunn's multiple comparison test. **P < .01. ns, not significant.

TF expression is induced during SARS-CoV-2 infection

As TF is the trigger for coagulation and platelet activation, we determined whether TF is associated with SARS-CoV-2 infection. The presence of RNA coding for TF (F3) was investigated in naïve and infected A549-hACE2 cells. Quantitative transcriptomic analyses revealed a 4.57-fold (SD, 2.5) increase in TF mRNA 36 hours postinfection, at a time of robust infection in the absence of apparent cell death and destruction, in comparison with uninfected cells (Figure 6A).

The kinetics of infection of K18-hACE2^{tgn} mice by CoV-2 are well described.[70-72] We thus infected these mice with SARS-CoV-2. Transcriptomic analysis of RNA isolated from lung tissues revealed that TF gene expression was upregulated starting on day 3 (3.27-fold; *P* adj = 2.20E-17) postinfection and remained elevated on day 5 (3.24-fold; *P* adj = 8.31E-17) and Day 7 (3.59-fold; *P* adj = 5.13E-20) postinfection relative to uninfected mice (Figure 6B).

The presence of specific TF activity was investigated in the blood of COVID-19 individuals with nonsevere disease (n = 25), severe disease (n = 25), and healthy donors (n = 15) (supplemental Table 2). TF activity was assessed by TF/FVII-mediated conversion of FX to FXa and subsequent conversion of FXa substrate. To specifically attribute activity to TF,[62-64] plasma samples were preincubated with a TF-blocking antibody or a control antibody (supplemental Figure 12). Compared with healthy donors, TF activity was increased in both patient groups, although activity was only significantly higher in patients with severe disease (Figure 6C). These data indicate that SARS-CoV-2 infection induces TF expression and activity, which may be a mechanism for platelet activation by SARS-CoV-2.

Discussion

We found that supernatants from SARS-CoV-2−infected cells induced platelet activation, as seen by the expression of classical activation markers, degranulation, the release of EVs, and aggregation under flow conditions. This activation was not mediated by SARS-CoV-2 spike proteins and was critically dependent on coagulation factors provided by plasma. We identified thrombin as the ligand for platelet activation and TF activity associated with SARS-CoV-2 as the trigger. This suggests that platelet hyperactivation observed in COVID-19 may be mediated by TF activity induced by SARS-CoV-2 infection rather than direct SARS-CoV-2 platelet interaction.

This finding may explain some of the reported coagulation abnormalities in COVID-19 and provide a rationale to specifically target TF, thrombin, and/or PARs when developing treatments for COVID-19. These findings are recapitulated in Figure 7.

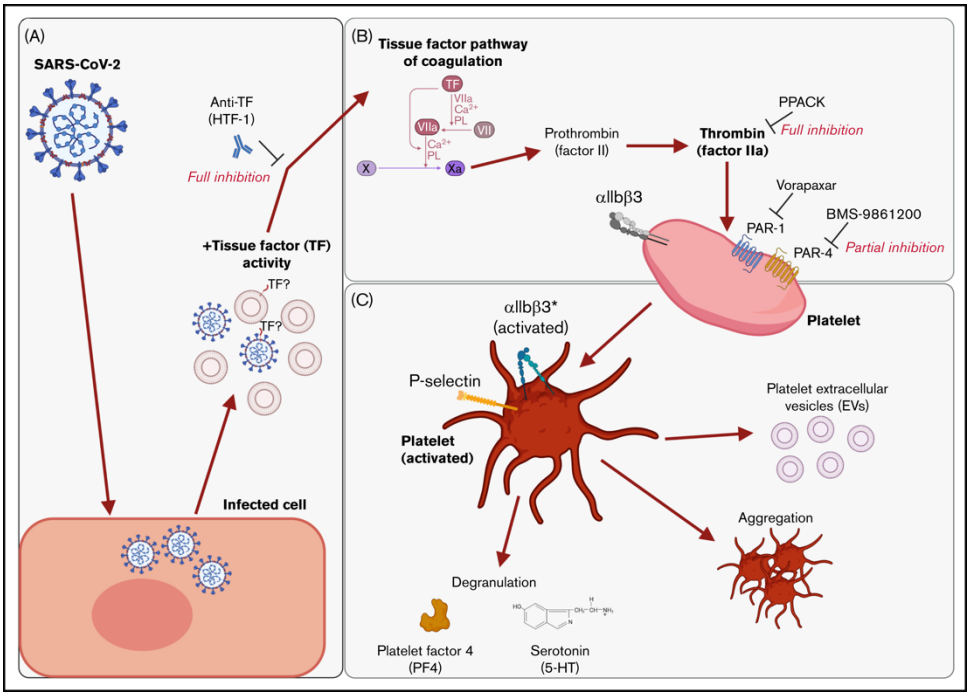


Figure 7. Graphical summary of the described mechanism. (A) SARS-CoV-2–infected cells release virus and EVs with associated TF activity. (B) This initiates the TF pathway of coagulation in plasma, thereby converting prothrombin into thrombin. Thrombin signals to platelets via PAR-1 and PAR-4. (C) Platelet activation is characterized by the expression of activated integrin αIIbβ3 and P-selectin, degranulation, aggregation, and the release of EVs. The graphical summary was created with BioRender.com.

SARS-CoV-2 RNA in association with platelets was reported in patients,[16,17,23] and viremia in plasma has been detected in 27% of patients hospitalized with COVID-19.[73] Increased viral load may be associated with disease severity.[73] However, the SARS-CoV-2 viral RNA copy number in blood was in the range of 63 to 6310 copies per mL of blood.[73] In contrast, the concentration of platelets is 1.50E+08 to 4.50E+08 per mL of blood in healthy adults. Therefore, the estimated virus-to-platelets ratio ranges from 1 virus per 23 800 (MOI, 4.2E-5) to 7.14E+06 (MOI, 1.4E-7) platelets per mL of blood in individuals with detectable viremia.[73] We found that platelets were activated in the presence of SARS-CoV-2 in the range of up to 1 virus per 4200 platelets (23 805

PFU per 100E+06 platelets; MOI, 2.38E-4) and only in the presence of plasma. In contrast, lower concentrations of SARS-CoV-2 (similar to those reported in vivo[73]) were insufficient. Moreover, while other viruses, such as dengue virus[74] and human immunodeficiency virus,[75] infect,[74,75] and replicate[74] in platelets, only uptake and degradation by platelets have been demonstrated by electron microscopy for SARS-CoV-2.[23] Even at high viral concentrations (1 virus per 10 platelets; MOI, 0.1), no platelet activation was observed in the absence of plasma.[23] We cannot exclude that lung megakaryocytes, rather than platelets, may directly interact with SARS-CoV-2,[22,76,77] but overall, these observations suggest that direct platelet–SARS-CoV-2 interactions in the blood may be rare and may not explain platelet hyperactivation in COVID-19.

Although more work is needed to address whether and how the mechanism revealed herein is clinically relevant in patients, we found TF activity associated with SARS-CoV-2 infection and that a TF-blocking antibody completely prevented plasma-dependent activation of platelets by SARS-CoV-2 in vitro. Active TF is absent from blood under normal conditions, and even small increases in TF activity have a marked effect.[37,39] Several studies reported increased TF expression in COVID-19.[41,43,78-81] We estimated that the level of TF activity associated with SARS-CoV-2 that was required to induce platelet activation was as low as 43 fM (based on Figure 1C and Figure 3A), which was comparable to the activity of recombinant TF required for platelet stimulation (supplemental Figure 8). Guervilly and colleagues[41] report that TF activity levels of 78.3 fM and higher in the circulation correlate with disease severity and mortality in COVID-19,[41] indicating that such low levels of TF activity in the circulation may be clinically relevant. We also observed that TF expression can be induced in vitro and in vivo in a K18-ACE2^{tgn} murine model of infection. In accordance with other reports, we observed that TF activity in plasma was increased in COVID-19, particularly in individuals with severe disease. TF-activity associated with SARS-CoV-2 infection may thereby present a mode of platelet activation even though the low concentrations of SARS-CoV-2 in the circulation make direct virus–platelet interactions unlikely.

TF is primarily expressed as a membrane-bound protein, although a soluble isoform exists.[38,39] However, the soluble form of TF is less procoagulant,[38] and efficient propagation of coagulation requires the presence of lipid membranes,[38] particularly those exposing phosphatidylserine.[38,39] Thus, high levels of TF activity may be associated with

phosphatidylserine-exposing cells or EVs.[38,39] Intriguingly, SARS-CoV-2 spike protein pseudotyped viral infection of human monocyte-derived macrophage cells can induce the release of EVs with associated TF activity that critically required the decryption (activation) of TF by sphingomyelinase.[44,82] It is currently not known whether this novel mechanism of TF decryption is responsible for increased TF activity observed in the plasma of patients with COVID-19.[82] While the mechanism of TF upregulation is unknown, it is interesting to consider that TF is structurally related to interferon receptors[83] and increases in TF activity, or expression seems to be common in viral infections.[84] Furthermore, through the budding process of enveloped viruses, host-derived membrane proteins may be acquired.[46-51] Thus, other than in association with EVs, TF might be acquired during the maturation process of SARS-CoV-2. We characterized supernatants of infected cells by electron microscopy and found that these contained both SARS-CoV-2 virions and EVs, which could not be separated from each other by SEC. SEC, however, enabled us to establish the particulate nature of the TF activity. As direct detection of TF protein and separation of virions from EVs are not possible,[53,54,62,68] it remains unknown whether TF protein was inherited by virions and/or EVs. However, as both enveloped viruses and EVs comprise host cell membranes, there is currently no rationale for excluding the possibility that TF may be expressed by both EVs and SARS-CoV-2.

In conclusion, we describe a potential mechanism for SARS-CoV-2–mediated platelet hyperactivation and highlight the importance of distinguishing host-derived from viral components when studying the biological activity of viruses. The study suggests further directions for the development of new therapeutic approaches for the treatment of COVID-19.

Acknowledgments

The authors are grateful to the blood donors who participated in this study. The authors thank the next-generation sequencing core facility of the Centre Hospitalier Universitaire de Quebec Research for its excellent service and expertise, the Laboratoire de Santé Publique du Québec, and the Public Health Agency of Canada's National Microbiology Laboratory for providing the SARS-CoV-2 isolates used in this study. The authors also thank members of the Mammalian Cell Expression Section (NRC-HHT) for their precious help in producing and purifying the S proteins and the financial support from the NRC's Pandemic Response Challenge Program, and Yannick Doyon (CHUL) for providing reagents and advice.

F.P. is the recipient of a postdoctoral fellowship from Fonds de Recherche du Québec en Santé (FRQS). E.B. is the recipient of the senior award from the FRQS. This work was supported by grants from the Canadian Institutes of Health Research (L.F. and E.B.). This study was supported in part by a COVID-19 Rapid Response grant by the Canadian Institutes of Health Research (CIHR; #OV1-170355) to M.-A.L. Y.Z. was supported by the Cheikh Zaid Foundation.

Authorship

Contribution: F.P., L.F., and E.B. conceived the concept and designed the study; F.P. designed experiments and assays; F.P., I.A., I.D., and E.L. participated in the study design, performed experiments, and were involved in the data extraction; A.R.B. performed electron microscopy analyses and interpretation of the data and contributed to redaction; I.D., E.L., Y.G., Y.Z., L.K., C.B., Y.D., M.-A.L., and L.F. contributed critical reagents, biospecimens, and instruments; A.S.W. and L.F. gave critical advice on experiments; F.P. and E.B. wrote the article; and all authors read and approved the final article.

Conflict-of-interest disclosure: The authors declare no competing financial interests.

Correspondance: Eric Boilard, Centre de Recherche du Centre Hospitalier Universitaire de Québec, Faculté de Médecine de l'Université Laval and Centre de Recherche ARThrite, 2705 Laurier Blvd, Room T1-49, Quebec, QC G1V 4G2, Canada; e-mail: eric.boilard@crchudequebec.ulaval.ca; and Louis Flamand, Centre de Recherche du Centre Hospitalier Universitaire de Québec-Université Laval, 2705 Laurier Blvd, Room T1-49, Quebec, QC G1V 4G2, Canada; e-mail: louis.flamand@crchudequebec.ulaval.ca.

Supplemental data

Supplement File 1- pdf file

References

1. Tay MZ, Poh CM, Re,nia L, MacAry PA, Ng LFP. The trinity of COVID-19: immunity, inflammation and intervention. *Nat Rev Immunol.* 2020;20(6): 363-374.
2. World Health Organization. WHO Coronavirus Disease (COVID-19) Dashboard. 2020. Available at: covid19.who.int. Accessed 1 March 2021.
3. Zhou F, Yu T, Du R, et al. Clinical course and risk factors for mortality of adult inpatients with COVID-19 in Wuhan, China: a retrospective cohort study. *Lancet.* 2020;395(10229):1054-1062.
4. Bilaloglu S, Aphinyanaphongs Y, Jones S, Iturrate E, Hochman J, Berger JS. Thrombosis in hospitalized patients with COVID-19 in a New York City health system. *JAMA.* 2020;324(8):799-801.
5. Middleton EA, He X-Y, Denorme F, et al. Neutrophil extracellular traps contribute to immunothrombosis in COVID-19 acute respiratory distress syndrome. *Blood.* 2020;136(10):1169-1179.
6. Bonaventura A, Vecchie, A, Dagna L, et al. Endothelial dysfunction and immunothrombosis as key pathogenic mechanisms in COVID-19. *Nat Rev Immunol.* 2021;21(5):319-329.
7. Rapkiewicz AV, Mai X, Carsons SE, et al. Megakaryocytes and platelet-fibrin thrombi characterize multi-organ thrombosis at autopsy in COVID-19: a case series. *EClinicalMedicine.* 2020;24:100434.
8. Iba T, Levy JH, Connors JM, Warkentin TE, Thachil J, Levi M. The unique characteristics of COVID-19 coagulopathy. *Crit Care.* 2020;24(1):360.
9. Becker RC. COVID-19 update: Covid-19-associated coagulopathy. *J Thromb Thrombolysis.* 2020;50(1):54-67.
10. Fox SE, Akmatbekov A, Harbert JL, Li G, Quincy Brown J, Vander Heide RS. Pulmonary and cardiac pathology in African American patients with COVID-19: an autopsy series from New Orleans. *Lancet Respir Med.* 2020;8(7):681-686.
11. Liberale L, Montecucco F, Tardif JC, Libby P, Camici GG. Inflamm-ageing: the role of inflammation in age-dependent cardiovascular disease. *Eur Heart J.* 2020;41(31):2974-2982.
12. Libby P. Inflammation in atherosclerosis-no longer a theory. *Clin Chem.* 2021;67(1):131-142.
13. Jenne CN, Urrutia R, Kubes P. Platelets: bridging hemostasis, inflammation, and immunity. *Int J Lab Hematol.* 2013;35(3):254-261.
14. Machlus KR, Italiano JE Jr. The incredible journey: from megakaryocyte development to platelet formation. *J Cell Biol.* 2013;201(6):785-796.
15. Marcoux G, Laroche A, Espinoza Romero J, Boilard E. Role of platelets and megakaryocytes in adaptive immunity. *Platelets.* 2021;32(3):340-351.
16. Zaid Y, Puhm F, Allaeys I, et al. Platelets can associate with SARS-Cov-2 RNA and are hyperactivated in COVID-19. *Circ Res.* 2020;127(11): 1404-1418.
17. Manne BK, Denorme F, Middleton EA, et al. Platelet gene expression and function in patients with COVID-19. *Blood.* 2020;136(11):1317-1329.
18. Hottz ED, Azevedo-Quintanilha IG, Palhinha L, et al. Platelet activation and platelet-monocyte aggregate formation trigger tissue factor expression in patients with severe COVID-19. *Blood.* 2020;136(11):1330-1341.
19. Zaid Y, Guessous F, Puhm F, et al. Platelet reactivity to thrombin differs between patients with COVID-19 and those with ARDS unrelated to COVID-19. *Blood Adv.* 2021;5(3):635-639.
20. Barrett TJ, Lee AH, Xia Y, et al. Platelet and vascular biomarkers associate with thrombosis and death in coronavirus disease. *Circ Res.* 2020;127 (7):945-947.
21. Barrett TJ, Cornwell M, Myndzar K, et al. Platelets amplify endotheliopathy in COVID-19. *Sci Adv.* 2021;7(37):eabh2434.
22. Barrett TJ, Bilaloglu S, Cornwell M, et al. Platelets contribute to disease severity in COVID-19. *J Thromb Haemost.* 2021;19(12):3139-3153.
23. Koupenova M, Corkrey HA, Vitseva O, et al. SARS-CoV-2 initiates programmed cell death in platelets. *Circ Res.* 2021;129(6):631-646.

24. Xu H, Zhong L, Deng J, et al. High expression of ACE2 receptor of 2019-nCoV on the epithelial cells of oral mucosa. *Int J Oral Sci.* 2020;12(1):8.
25. Kuba K, Imai Y, Rao S, et al. A crucial role of angiotensin converting enzyme 2 (ACE2) in SARS coronavirus-induced lung injury. *Nat Med.* 2005; 11(8):875-879.
26. Zhang S, Liu Y, Wang X, et al. SARS-CoV-2 binds platelet ACE2 to enhance thrombosis in COVID-19. *J Hematol Oncol.* 2020;13(1):120.
27. Campbell RA, Boilard E, Rondina MT. Is there a role for the ACE2 receptor in SARS-CoV-2 interactions with platelets? *J Thromb Haemost.* 2021; 19(1):46-50.
28. Shen S, Zhang J, Fang Y, et al. SARS-CoV-2 interacts with platelets and megakaryocytes via ACE2-independent mechanism. *J Hematol Oncol.*
2021;14(1):72.
29. Wang K, Chen W, Zhou Y-S, et al. SARS-CoV-2 invades host cells via a novel route: CD147-spike protein. *bioRxiv.* 2020;2020.03.14.988345.
30. Seizer P, Borst O, Langer HF, et al. EMMPRIN (CD147) is a novel receptor for platelet GPVI and mediates platelet rolling via GPVI-EMMPRIN interaction. *Thromb Haemost.* 2009;101(4):682-686.
31. Schmidt R, Bu€ltmann A, Fischel S, et al. Extracellular matrix metalloproteinase inducer (CD147) is a novel receptor on platelets, activates platelets, and augments nuclear factor kappaB-dependent inflammation in monocytes. *Circ Res.* 2008;102(3):302-309.
32. Shilts J, Crozier TWM, Greenwood EJD, Lehner PJ, Wright GJ. No evidence for basigin/CD147 as a direct SARS-CoV-2 spike binding receptor.
Sci Rep. 2021;11(1):413.
33. Maugeri N, De Lorenzo R, Clementi N, et al. Unconventional CD147-dependent platelet activation elicited by SARS-CoV-2 in COVID-19. *J Thromb Haemost.* 2021;20(2):434-448.
34. Li T, Yang Y, Li Y, et al. Platelets mediate inflammatory monocyte activation by SARS-CoV-2 spike protein. *J Clin Invest.* 2022;132(4):e150101.
35. Klug M, Lazareva O, Kirmes K, et al. Platelet surface protein expression and reactivity upon TRAP stimulation after BNT162b2 vaccination [published online ahead of print 13 August 2021]. *Thromb Haemost.* doi:10.1055/s-0041-1733934.
36. Levi M, Thachil J, Iba T, Levy JH. Coagulation abnormalities and thrombosis in patients with COVID-19. *Lancet Haematol.* 2020;7(6):e438-e440.
37. Butenas S, Bouchard BA, Brummel-Ziedins KE, Parhami-Seren B, Mann KG. Tissue factor activity in whole blood. *Blood.* 2005;105(7):2764-2770.
38. Gajsiewicz JM, Morrissey JH. Structure-function relationship of the interaction between tissue factor and factor VIIa. *Semin Thromb Hemost.* 2015; 41(7):682-690.
39. Grover SP, Mackman N. Tissue factor: an essential mediator of hemostasis and trigger of thrombosis. *Arterioscler Thromb Vasc Biol.* 2018;38(4): 709-725.
40. Boilard E, Pare, G, Rousseau M, et al. Influenza virus H1N1 activates platelets through FcgRIIA signaling and thrombin generation. *Blood.* 2014; 123(18):2854-2863.
41. Guervilly C, Bonifay A, Burtey S, et al. Dissemination of extreme levels of extracellular vesicles: tissue factor activity in patients with severe COVID-19. *Blood Adv.* 2021;5(3):628-634.
42. Rosell A, Havervall S, von Meijenfeldt F, et al. Patients With COVID-19 have elevated levels of circulating extracellular vesicle tissue factor activity that is associated with severity and mortality-brief report. *Arterioscler Thromb Vasc Biol.* 2021;41(2):878-882.
43. Campbell RA, Hisada Y, Denorme F, et al. Comparison of the coagulopathies associated with COVID-19 and sepsis. *Res Pract Thromb Haemost.*
2021;5(4):e12525.
44. Wang J, Pendurthi UR, Yi G, Rao LVM. SARS-CoV-2 infection induces the activation of tissue factor-mediated coagulation via activation of acid sphingomyelinase [published online ahead fo print 29 July 2021]. *Blood*. doi:10.1182/blood.2021010685.

45. Huertas A, Montani D, Savale L, et al. Endothelial cell dysfunction: a major player in SARS-CoV-2 infection (COVID-19)? [published online ahead of print 30 July 2020]. *Eur Respir J*. doi:10.1183/13993003.01634-2020.
46. Jalaguier P, Cantin R, Maaroufi H, Tremblay MJ. Selective acquisition of host-derived ICAM-1 by HIV-1 is a matrix-dependent process. *J Virol.* 2015;89(1):323-336.
47. Imbeault M, Ouellet M, Gigue're K, et al. Acquisition of host-derived CD40L by HIV-1 in vivo and its functional consequences in the B-cell compart- ment. *J Virol.* 2011;85(5):2189-2200.
48. Thibault S, Tardif MR, Gilbert C, Tremblay MJ. Virus-associated host CD62L increases attachment of human immunodeficiency virus type 1 to endothelial cells and enhances trans infection of $CD4^1$ T lymphocytes. *J Gen Virol.* 2007;88(Pt 9):2568-2573.
49. Barat C, Martin G, Beaudoin AR, Se,vigny J, Tremblay MJ. The nucleoside triphosphate diphosphohydrolase-1/CD39 is incorporated into human immunodeficiency type 1 particles, where it remains biologically active. *J Mol Biol.* 2007;371(1):269-282.
50. Giguere J-F, Diou J, Madrenas J, Tremblay MJ. Virus attachment and replication are promoted after acquisition of host CD28 and CD152 by HIV-1. *J Infect Dis.* 2005;192(7):1265-1268.
51. Martin G, Tremblay MJ. HLA-DR, ICAM-1, CD40, CD40L, and CD86 are incorporated to a similar degree into clinical human immunodeficiency virus type 1 variants expanded in natural reservoirs such as peripheral blood mononuclear cells and human lymphoid tissue cultured ex vivo. *Clin Immunol.* 2004;111(3):275-285.
52. Takayama K. In vitro and animal models for SARS-CoV-2 research. *Trends Pharmacol Sci.* 2020;41(8):513-517.
53. Nolte-'t Hoen E, Cremer T, Gallo RC, Margolis LB. Extracellular vesicles and viruses: are they close relatives? *Proc Natl Acad Sci USA.* 2016;113 (33):9155-9161.
54. Zhou Y, McNamara RP, Dittmer DP. Purification methods and the presence of RNA in virus particles and extracellular vesicles [published online ahead of print 21 August 2020]. *Viruses*. doi:10.3390/v12090917.
55. Rider MA, Hurwitz SN, Meckes DG Jr. ExtraPEG: a polyethylene glycol-based method for enrichment of extracellular vesicles. *Sci Rep.* 2016;6: 23978.
56. Roberts A, Lamirande EW, Vogel L, et al. Immunogenicity and protective efficacy in mice and hamsters of a b-propiolactone inactivated whole virus SARS-CoV vaccine. *Viral Immunol.* 2010;23(5):509-519.
57. Palta S, Saroa R, Palta A. Overview of the coagulation system. *Indian J Anaesth.* 2014;58(5):515-523.
58. Sun SH, Chen Q, Gu HJ, et al. A mouse model of SARS-CoV-2 infection and pathogenesis. *Cell Host Microbe.* 2020;28(1):124-133.e4.
59. De Candia E. Mechanisms of platelet activation by thrombin: a short history. *Thromb Res.* 2012;129(3):250-256.
60. Celikel R, McClintock RA, Roberts JR, et al. Modulation of a-thrombin function by distinct interactions with platelet glycoprotein Ibalpha. *Science*. 2003;301(5630):218-221.
61. Brass LF. Thrombin and platelet activation. *Chest.* 2003;124(suppl 3):18S-25S.
62. Mackman N, Hisada Y, Grover SP, et al. Response by Mackman et al to letter regarding article, "patients with COVID-19 have elevated levels of circulating extracellular vesicle tissue factor activity that is associated with severity and mortality-brief report." *Arterioscler Thromb Vasc Biol.* 2021; 41(6):e381-e382.
63. Rosell A, Moser B, Hisada Y, et al. Evaluation of different commercial antibodies for their ability to detect human and mouse tissue factor by western blotting. *Res Pract Thromb Haemost.* 2020;4(6):1013-1023.

64. Hisada Y, Mackman N. Measurement of tissue factor activity in extracellular vesicles from human plasma samples. *Res Pract Thromb Haemost.* 2018;3(1):44-48.
65. Ke Z, Oton J, Qu K, et al. Structures and distributions of SARS-CoV-2 spike proteins on intact virions. *Nature.* 2020;588(7838):498-502.
66. Liu C, Yang Y, Gao Y, et al. Viral architecture of SARS-CoV-2 with post-fusion spike revealed by cryo-em. *bioRxiv.* Preprint posted online 5 March 2020. doi:10.1101/2020.03.02.972927.
67. Arraud N, Linares R, Tan S, et al. Extracellular vesicles from blood plasma: determination of their morphology, size, phenotype and concentration. *J Thromb Haemost.* 2014;12(5):614-627.
68. Østerud B, Bouchard BA. Detection of tissue factor in platelets: why is it so troublesome? *Platelets.* 2019;30(8):957-961.
69. Puhm F, Afonyushkin T, Resch U, et al. Mitochondria are a subset of extracellular vesicles released by activated monocytes and induce type I IFN and TNF responses in endothelial cells. *Circ Res.* 2019;125(1):43-52.
70. Winkler ES, Bailey AL, Kafai NM, et al. SARS-CoV-2 infection of human ACE2-transgenic mice causes severe lung inflammation and impaired function. *Nat Immunol.* 2020;21(11):1327-1335.
71. Yinda CK, Port JR, Bushmaker T, et al. K18-hACE2 mice develop respiratory disease resembling severe COVID-19. *PLoS Pathog.* 2021;17(1): e1009195.
72. Oladunni FS, Park J-G, Pino PA, et al. Lethality of SARS-CoV-2 infection in K18 human angiotensin-converting enzyme 2 transgenic mice. *Nat Commun.* 2020;11(1):6122.
73. Fajnzylber J, Regan J, Coxen K, et al; Massachusetts Consortium for Pathogen Readiness. SARS-CoV-2 viral load is associated with increased disease severity and mortality. *Nat Commun.* 2020;11(1):5493.
74. Simon AY, Sutherland MR, Pryzdial ELG. Dengue virus binding and replication by platelets. *Blood.* 2015;126(3):378-385.
75. Chaipan C, Soilleux EJ, Simpson P, et al. DC-SIGN and CLEC-2 mediate human immunodeficiency virus type 1 capture by platelets. *J Virol.* 2006; 80(18):8951-8960.
76. Lefranc¸ais E, Ortiz-Mun~oz G, Caudrillier A, et al. The lung is a site of platelet biogenesis and a reservoir for haematopoietic progenitors. *Nature.* 2017;544(7648):105-109.
77. Pariser DN, Hilt ZT, Ture SK, et al. Lung megakaryocytes are immune modulatory cells. *J Clin Invest.* 2021;131(1):e137377.
78. Subrahmanian S, Borczuk A, Salvatore S, et al. Tissue factor upregulation is associated with SARS-CoV-2 in the lungs of COVID-19 patients. *J Thromb Haemost.* 2021;19(9):2268-2274.
79. Francischetti IMB, Toomer K, Zhang Y, et al. Upregulation of pulmonary tissue factor, loss of thrombomodulin and immunothrombosis in SARS- CoV-2 infection. *EClinicalMedicine.* 2021;39:101069.
80. Eslamifar Z, Behzadifard M, Soleimani M, Behzadifard S. Coagulation abnormalities in SARS-CoV-2 infection: overexpression tissue factor. *Thromb J.* 2020;18(1):38.
81. Krishnamachary B, Cook C, Spikes L, et al. The potential role of extracellular vesicles in COVID-19 associated endothelial injury and pro-inflamma- tion. *medRxiv.* Preprint posted online 1 September 2020. doi:10.1101/2020.08.27.20182808.
82. Nieuwland R. Novel mechanism regulating tissue factor activity. *Blood.* 2021;138(4):289-291.
83. de Weerd NA, Samarajiwa SA, Hertzog PJ. Type I interferon receptors: biochemistry and biological functions. *J Biol Chem.* 2007;282(28): 20053-20057.
84. Mackman N, Grover SP, Antoniak S. Tissue factor expression, extracellular vesicles, and thrombosis after infection with the respiratory viruses influenza A virus and coronavirus. *J Thromb Haemost.* 2021;19(11):2652-2658.

A-1.16 SARS-CoV-2 Seroprevalence in Those Utilizing Public Transportation or Working in the Transportation Industry: A Rapid Review

Preface

(This work has been previously published as a review article)

Heiskanen A, **Galipeau Y**, Langlois MA, Little J, Cooper CL. **SARS-CoV-2 Seroprevalence in Those Utilizing Public Transportation or Working in the Transportation Industry: A Rapid Review**. Int J Environ Res Public Health. 2022 Sep 15;19(18):11629.

https://doi.org/10.3390/ijerph191811629

© 2022 by the authors.

Licensee MDPI, Basel, Switzerland. This article is an open access article distributed under the terms and conditions of the Creative Commons Attribution (CC BY) license (https://creativecommons.org/licenses/by/4.0/).

Abstract
Proximity and duration of social contact while working or using public transportation may increase users' risk of SARS-CoV-2 exposure. This review aims to assess evidence of an association between use of public transportation or work in the transportation industry and prevalence of SARS-CoV-2 antibodies as well as to identify factors associated with seropositivity in transit users. A literature search of major databases was conducted from December 2019 to January 2022 using key worlds including "seroprevalence", "SARS-CoV-2", and "public transit". A narrative review of included studies was completed for the following categories: those working in the transportation industry, healthcare workers relying on public transit, and population-based studies. The association between work in the transit industry and seroprevalence varied based on location, demographic characteristics, and test sensitivities. No association was found in healthcare workers. Several population-based studies indicated higher seroprevalence in those using public transit. Overall seroprevalence estimates varied based on geographic location, population demographics, study methodologies, and calendar date of assessment. However, seropositivity was consistently higher in racial minorities and low-income communities.

1. Introduction

The coronavirus disease (COVID-19) caused by severe acute respiratory syndrome coronavirus 2 (SARS-CoV-2) remains an international threat with over 550 million confirmed cases and 6 million deaths worldwide [1]. The virus has had a major impact on the transportation industry, shutting down international borders and influencing travel within municipalities. The drastic reduction in public transit ridership is a result of the introduction of remote work, switch to active transportation (i.e., walking or cycling), increased perception of risk associated with public transit use, and government and/or public health recommendations. However, public transit is an essential service with economic benefit that has been continuously relied on by many throughout the pandemic. The increased proximity and duration of social contact accompanying transit use may increase users' risk of SARS-CoV-2 infection. Racial minorities and those with lower education and income are at particular risk as they are over-represented in those continuing to use public transit during the pandemic and are already at increased risk for SARS-CoV-2 occupational exposure [2,3,4].

Serological testing provides a robust estimate of prior infection by capturing both symptomatic and asymptomatic individuals. This can provide information on virus transmission patterns, measure herd immunity, and predict the number of people susceptible to the virus. With the introduction of vaccinations and evolving variants, serosurveys can help identify gaps in immunity associated with demographic characteristics or risk factors and can focus vaccination programs on susceptible communities. Several systematic reviews have attempted to consolidate and analyze results from hundreds of serosurveys world-wide to determine overall SARS-CoV-2 seroprevalence [5,6,7]. Many serosurveys report the prevalence of SARS-CoV-2 antibodies stratified by sex, gender, health status, and employment history with substantial heterogeneity of results. A systematic review and meta-analysis of 60 countries estimated that the pooled seroprevalence of SARS-CoV-2 was 9.47% as of 30 March 2021 [8]. Several seroprevalence studies have reported similar levels of exposure [9,10,11]; however, results varied by population. This indicates that at the time of study, most of the population had not been exposed to SARS-CoV-2. Seroprevalence is generally found to be similar among men and women [11,12]; however, some studies have found differences between the sexes [8,10]. A literature review of

seroprevalence studies found that HCW are often considered a high-risk group; however, those that use adequate PPE are at no higher risk of infection than other groups [12]. Public transportation has been recognized as a high-risk environment for COVID-19 infection prompting the introduction of safety measures such as mask wearing, enhanced cleaning, and reduced capacity to promote physical distancing. Despite this, the risk of infection while using public transport is largely unknown with few studies focusing on this topic and even fewer that evaluate the risk of infection considering social determinants of health such as income and ethnicity. Our literature review aims to assess the prevalence of SARS-CoV-2 seropositivity associated with (1) employment in the transportation industry (e.g., pilots, bus drivers, or taxi drivers) and (2) use of public transportation. Secondary outcomes included identifying demographic characteristics and risk factors associated with seropositivity in these populations.

2. Materials and Methods

A literature search of major databases including MEDLINE, Embase, PubMed, and Google Scholar, as well as the MEDRXIV and BIORXIV pre-print servers was performed. Databases were searched from December 2019 to January 2022. Studies were excluded if they were conducted when Omicron became the dominant variant in the Fall of 2021. Only studies that were written in English and incorporated demographic information were included. Populations of interest included those using public transportation and those working in occupations with high risk of exposure to SARS-CoV-2 (i.e., healthcare workers, taxi drivers, or bus operators). The search strategy included a combination of key words such as: “COVID-19” or “SARS-CoV-2”, “respiratory virus”, “seroprevalence”, “public transit”, “public transportation”, “transportation”, “demographic”, “COVID-19 antibodies”, and “socio-demographic”. Citation and reference tracking was performed and relevant materials manually searched. Databases were systematically reviewed. A risk of bias or quality assessment tool was not used; however, studies were informally assessed for limitations or aspects of the study that may have influenced results which were included in the narrative review. Data was extracted using Excel. Studies were organized in accordance with the Human Development Index (HDI) developed by United Nations [**13**]. This measure is a summary of average achievement in key dimensions such as length and quality of life, knowledge, and standard of living. On this scale, any country scoring higher than 0.8 in 2019 was considered to

have very high human development, between 0.7 and 0.799 high human development, 0.55–0.699 medium human development, and less than 0.55 low human development. Outcomes of interest included the effect measure (relative risk and mean difference) of the association between seroprevalence of antibodies to SARS-CoV-2 and any form of transit use and variables that were predictive of seropositivity.

3. Results

Twenty-two relevant studies were identified and narratively reviewed. Publications were identified from African, European, North American, South American, and Asian countries. A list of included studies and their characteristics can be found in Table 1. A summary of findings from studies addressing the association between SARS-CoV-2 seropositivity and work in the transportation industry is presented in Table 2. Studies evaluating the association between SARS-CoV-2 seropositivity and use of public transportation were divided by population. Studies concentrating on healthcare workers and the risk associated with their commute to work are presented in Table 3. Those that focus on the risk associated with transit use in the general population are presented in Table 4.

Table 1. Characteristics of included studies from highest to lowest HDI.

Author	Location	HDI	Date	Type of Study	Study Population	# Participants	Serology			
							Assay	Target	Sensitivity (%) *	Specificity (%) *
Meylan	Lausanne, Switzerland	0.955	18 May–12 June 2020	Cross-sectional	Centre Hospitalier Universitaire Vaudois and Centre for Primary Care and Public Health staff	1874	Luminex-based assay (IgG)	S-protein	97	98
Pathela	New York City, USA	0.926	13 May–21 July 2020	Cross-sectional	NYC adult resident; occupation subgroups	45,367	Liaison SARS-CoV-2 S1/S2	S1/S2 subunits of S protein	97.6	99.3
Soffin	New York City, USA	0.926	6 May–5 June 2020	Cross-sectional	Surgeons and Anaesthesiologists at Hospital for Special Surgery	143	Abbott Architect SARS-CoV-2 IgG	Nucleocapsid	94–100 [a]	99.4–100 [a]
Venugopal	New York City, USA	0.926	May 2020	Cross sectional	Frontline HCWs of NYC hospitals	500	Abbott Architect IgG Assay	Nucleocapsid	100 (95% CI 95.8–100%)	99.6 (95% CI: 99–99.99%)
Feehan	Baton Rouge, USA	0.926	15–31 July 2020	Cross sectional	Representative sample of residents	2138	Abbott Architect i2000SR IgG Assay	Not specified	Not specified	Not specified
Chan	Rhode Island, USA	0.926	5–22 May 2020	Cross-sectional	Households, oversampled African Americans/Blacks and Hispanics/Latinos	1043	Not specified	Not specified	Not specified	Not specified
Mahajan	Connecticut, USA	0.926	4 June–29 July 2020		Adults living in non- congregate settings (exclude those living in LTC homes, nursing homes, prisons); also oversampled non-Hispanic black and Hispanic individuals	567	Ortho-Clinical Diagnostics Vitros anti-SARS-CoV-2 IgG (some negative samples retested with Abbott Architect IgG—targeting nucleocapsid protein)	S-protein	90	100
Yamamoto	Toyama and Kohnoda, Japan	0.919	October–December 2020	Repeated cross-sectional	National Center for Global Health and Medicine employees	2563	Abbott Architect (IgG); Roche Elecsys (total antibodies), confirmatory analysis of positive results using EUROIMMUN anti-S IgG immunoassay	Nucleocapsid protein	Not specified	Not specified
Nishida	Osaka Prefecture, Japan	0.919	12–19 June 2020	Cross-sectional	Toyonaka Municipal Hospital employees	925	Abbott Architect SARS-CoV-2 IgG Assay	Nucleocapsid	100	99.6
Pollan	Spain	0.904	27 April–11 May 2020	Population-based cohort study	Spanish population	66,805	Orient Gene Biotech COVID-19 IgG/IgM Rapid Test Cassette (Point-of-Care Test);	RBD of S protein	IgG: 97.2; IgM: 87.9	100
							Abbott Architect IgG assay	Nucleoprotein	100 [a]	99.6
Airoldi	Piedmont region, Northwest Italy	0.892	28 April–7 August 2020	Cross-sectional	Company workers through screening program	23,568	ZEUS ELISA SARS-CoV-2 IgG Test system	Not specified	93.3 (95% CI: 78.7–98.2)	100 (95% CI: 94.8–100)
Berselli	Emilia Romagna region, Northern Italy	0.892	1 June–25 September 2020	Cross-sectional	Company workers, self-referred individuals	7561	EUROIMMUNE ELISA anti-SARS-CoV-2 test for IgA and IgG	Not specified	100 [c]	92.5
							Roche Elecsys	Not specified	100 [a]	99.8

Table 1. Cont.

Author	Location	HDI	Date	Type of Study	Study Population	# Participants	Serology			
							Assay	Target	Sensitivity (%) *	Specificity (%) *
Berselli	Emilia Romagna region, Northern Italy	0.892	1 June–25 September 2020	Cross-sectional	Company workers, self-referred individuals	7561	KHB SARS-CoV-2 IgM/IgG antibody Colloidal Gold	Not specified	98.81 [c]	98.02
Alsuwaldi	Abu, Dhabi, United Arab Emirates	0.890	July 19–August 14 2020	Cross-sectional	Households in region; labour camps	8831 (households); 4855 (labour camp worker)	Roche Elecsys Anti-SARS-CoV-2	Nucleocapsid	100 (95% CI: 88.1–100) [a]	99.8 (95% CI: 99.6–99.1)
							LIAISON SARS-CoV-2 S1/S2 IgG Assay	S1 and S2 subunits of S protein	97.4 (95% CI: 86.6–99.5) [a]	98·5 (95% CI: 97·6–99·1)
Poustchi	18 Iranian Cities	0.783	17 April –2 June 2020	Cross sectional	General population; high-risk occupations	8902	Pishtaz Teb SARS-CoV-2 ELISA IgG and IGM	Not specified	IgG: 94.1; IgM: 79.4	IgG: 98.3; IgM: 97.3
Cruz-Arenas	Mexico City, Mexico	0.779	10 August–9 September 2020	Cross-sectional	Instituto Nacional de Rehabilitación employees	300	LFA: IgG/IgM Rapid Test Cassette;	Not specified	79.5	100
							ELISA: Euroimmun Anti-SARS-CoV-2 NCP IgG Assay	Nucleocapsid protein	Not specified	Not specified
Colmenares-Mejía	Bucaramanga, Colombia	0.767	28 September–24 December 2020	Cross-sectional	Workers from health, construction, public transportation, public force (army, police, transit officers), bike delivery messengers, independent or informal commercial (shopkeepers)	7045	Abbot ARC COV2 (IgG and IgM)	Not specified	85.2	97.3
De Oliveira	São Paulo, Brazil	0.765	March–July 2020	Cross-sectional	Sírio-Libanês Hospital employees	1996	ELISA (IgG), unspecified	Nucleocapsid	86–95 [a]	100 [a]
Acurio-Paez	Cuenca, Ecuador	0.759	11 August–1 November 2020	Cross sectional	Randomly selected inhabitants of Cuenca, Ecuador	2457	SD BIOSNSOR Standard Q COVID-19 IgG/IgM Plus	Not specified	94.3 [b]	87.9 [b]
Babu	Karnataka, India	0.645	3–16 September 2020	Cross-sectional	Statewide population; risk subgroups	16,416	COVID Kavach Anti SARS-CoV-2 IgG antibody detection ELISA	Not specified	92.1	97.7
Gupta	New Delhi, India	0.645	22 June–24 July 2020	Cross-sectional	HCW—All India Institute of Medical Sciences Staff	3739	ADVIA Centaur COV2T chemiluminescence IgG and IgM immunoassay	S-protein RBD	100 [a]	99.8 [a]
Naushin	India	0.645	August–September 2020	Longitudinal, Cohort	Phenome-India Cohort	10,427	Roche Elecsys Anti-SARS-CoV-2; positive samples tested using GENScript cPass SARS-CoV-2 Neutralization Antibody Detection Kit	Nucleocapsid; S-protein	Undefined	Undefined
Halatoko	Lome, Togo	0.515	23 April 2020–8 May 2020	Cross sectional	Occupational sectors: health care, air transport, police, road transport, informal (market sellers, craftsmen)	955	Lungene Rapid Test (IgG and IgM)	Not specified	72.9	85.0

S-protein: spike protein; RBD: receptor binding domain; ELISA: enzyme-linked immunosorbent assay; LFA: lateral flow assay. * Does not include sensitivities and specificities from validation tests performed by authors. [a] at least 14 days after symptom onset or positive RT-PCR test. [b] at least 15 days post infection. [c] at least 10 days after symptom onset.

Table 2. Summary of findings from studies that assessed the association between seropositivity and work in the transportation industry from highest to lowest HDI.

Author	HDI Category	Outcome	Overall Seroprevalence (%)	Transit Outcomes		Variables Associated with Seropositivity	Conclusion
				Seroprevalence (%)	Regression Analysis (i.e., OR, RR)		
Pathela	Very high	Seroprevalence (%), Poisson regression (RR; 95% CI)	23.6% (95% CI: 23.2–24)	Air transport (n = 137): 25%; Public transit, taxis and private drivers (n = 479): 35%; Other transportation and warehousing (n = 440) 27%	Essential worker (food services, construction, retail trade, transportation) compared to other industries RR: 1.63 (95% CI: 1.5–1.7); Adjusted for sex at birth, age, borough, poverty level, working outside the home RR: 1.33 (95% CI: 1.3–1.4)	Male sex, age 44–64, non-White race/ethnicity, living in a borough other than Manhattan or Staten Island, living in neighborhoods with high or very high poverty levels, employment in health care or essential worker category, not being unemployed at the time of serosurvey, working outside the home, having contact with someone with COVID-19, COVID-19 symptoms, being overweight or obese, increasing number of household members	Those working in the transportation industry more likely to have SARS-CoV-2 antibodies
Feehan	Very high	Seroprevalence (%), census weighted bivariate analysis (OR)	3.6% (95% CI: 2.8–4.4)	N/A	Working in the transportation industry (n = 11) compared to an office OR: 6 (95% CI: 0.1–100)	Single marital status, public-facing job compared to office, healthcare career, black non-Hispanic race/ethnicity, younger than 29 years old	Work in the transportation industry comparable to risk associated with work in an office
Pollan	Very high	Seroprevalence (%) using two assays	POC test: 5% (95% CI: 4.7–5.4); Immunoassay: 4.6% (95% CI: 4.3–5.0)	POC test: (n = 800); 5.9% (95% CI: 3.9–8.7); Immunoassay (n = 731): 5.8% (3.6–9.2)	N/A	Province, working in healthcare, confirmed COVID-19 case in household or among non-cohabitating family members and friends or among caregivers and cleaning staff or clients, COVID-19 symptoms	Seroprevalence of those working in the transport industry comparable to overall seroprevalence; comparable between tests
Airoldi	Very high	Seroprevalence (%)	4.97% (95% CI: 4.69–5.25)	4.36% (95% CI: 1.95–6.78)	N/A	Geographical location, those working in logistics or weaving factories	Seroprevalence in transportation industry workers comparable to general population
Berselli	Very high	Seroprevalence (%)	4.7% (95% CI: 4.2–5.2)	1%	N/A	Seroprevalence higher in women, older age groups, HCW, dealers and vehicle repair workers, sport sector employees	No evidence of increased seroprevalence
Alsuwaldi -Household population *	Very high	Seroprevalence (%), bivariate model, multiple logistic regression model (OR)	10.4% (95% CI: 9.5–11.4)	20.8% (95% CI: 15.9–26.7)	OR: 1.5 (95% CI: 0.7–3.2) adjusted for age, sex, region, education, nationality, ethnicity, occupation, contact with someone diagnosed with COVID-19	Households: Region, education level, Asian ethnicity, not from UAE, contact with someone with COVID-19, COVID-19 symptoms	No association with transit use in multivariable analysis
Alsuwaldi -Labour camp population *	Very high	Seroprevalence (%), bivariate model, multiple logistic regression model (OR)	68.6% (95% CI: 61.7–74.7)	72.1% (95% CI: 60.4–81.5)	OR: 2.7 (1.8–4.0) adjusted for age, sex, region, education, nationality, ethnicity, occupation, contact with someone diagnosed with COVID-19	Education, non-Arabic ethnicity, occupation, contact with someone with COVID-19, COVID-19 symptoms	Transit use and high-risk occupations associate with seropositivity
Poustchi	High	Seroprevalence (%) adjusted for population weighting and test performance	General population: 17.1% (95% CI: 14.6–19.5); High-risk population: 20% (95% CI: 18.5–21.7)	Taxi drivers (n = 718): 18.8% (95% CI: 14.7–23.2)	N/A	60 years or older, those in contact with someone with COVID-19, region, COVID-19 symptoms	Seroprevalence similar between high-risk occupations

Table 2.1 Cont.

Author	HDI Category	Outcome	Overall Seroprevalence (%)	Transit Outcomes		Variables Associated with Seropositivity	Conclusion
				Seroprevalence (%)	Regression Analysis (i.e., OR, RR)		
Colmenares-Mejía	High	Seroprevalence (%) corrected for test performance and study design	19.5% (95% CI: 18.6–20.4)	Commute to work: bike: 25.7% (95% CI: 16.6–34.8); public transportation: 23.9% (95% CI: 21.8–26); taxi 15.5% (95% CI: 12.3–18.7) Those working in the public transport industry: 16% (95% CI: 11.7–20.3)	N/A	Occupational groups with multiple contacts with others during work hours, delivery drivers, grocery store tenants, informal commerce workers, those that used a bike, motorcycle, public transit than own car, COVID-19 symptoms	Similar seroprevalence in those working in the transportation industry and other high-risk occupations. Higher seroprevalence in those that use public transit to commute to work compared to those that use their own vehicle
Babu	Medium	Seroprevalence (%), generalized linear model-based multinomial regression (OR)	16.8% (95% CI: 15.5–18.1)	Bus conductors/auto drivers (n = 1008): 16.1% (95% CI: 11.7–20.6);	Bus conductors/auto drivers compared to low-risk occupations: OR: 2.12 (95% CI: 1.3–3.5)	Diarrhoea, chest-pain, rhinorrhea, fatigue, fever, professions who had more contact with the public, residence in containment zones, urbanisation level of the district	Those working in the transportation industry twice as likely to have SARS-CoV-2 antibodies
Halatoko	Low	Seroprevalence (%)	IgM or IgG: 0.9% (95% CI: 0.4–1.8)	Air transport (n = 212); IgM positive: 0.5% (95% CI: 0.01–2.6); IgG positive: 0.9% 95% CI: 0.1–3.4) Road Transport (n = 122) IgM positive: 0% (95% CI: 0–2.9); IgG 0.8% 95% CI: 0–4.5)	N/A	N/A	Low seroprevalence in general, similar among high-risk populations

RR: relative risk; OR: odds ratio; POC: point of care. * Alsuwaldi reported separate results for two different populations. Results varied by population so were presented as two separate studies.

Table 3. Summary of findings from studies that assessed the association between seropositivity and use of public transportation in healthcare workers from highest to lowest HDI.

Author	HDI Category	Outcome	Overall Seroprevalence (%)	Transit Outcomes		Variables Associated with Seropositivity	Conclusions
				Seroprevalence (%)	Regression Analysis (i.e., OR, RR)		
Meylan	Very high	Seropositivity (%), multivariable logistic regression (OR)	10% (95% CI: 8.7–11.5)	Frequency of transit use (# per week) 1 (n = 104): 7.7% (95% CI: 3.4–14.6); 2 (n = 135): 9.6% (95% CI: 5.2–15.9); 3 (n = 148): 10.1% (95% CI: 5.8–16.2); 4 (n = 199): 12.1 (95% CI: 7.9–17.4); 5 (n = 275): 14.2% (95% CI: 10.3–18.9); >5 (n = 220): 5.9% (95% CI: 3.2–9.9); Use of face mask on public transport (n = 151): 5.3% (95% CI: 2.3–10.2) Does not use face mask on public transport (n = 930): 11.2% (95% CI: 9.2–13.4)	Use of mask at public transport compared to those that do not: OR = 0.42 (95% CI: 0.198–0.896) adjusted for daily contact w patients, work in ICU, COVID-19 case at home, and COVID-19 symptoms	Household contact with confirmed COVID-19, use of mask while using public transport, COVID-19 symptoms	Seropositivity increased with transit usage; face mask while using public transit reduced odds of seropositivity

Table 3. Summary of findings from studies that assessed the association between seropositivity and use of public transportation in healthcare workers from highest to lowest HDI.

Author	HDI Category	Outcome	Overall Seroprevalence (%)	Transit Outcomes		Variables Associated with Seropositivity	Conclusions
				Seroprevalence (%)	Regression Analysis (i.e., OR, RR)		
Soffin	Very high	Seroprevalence (%), bivariate logistic regression (OR)	9.8%	N/A	OR: 1.48 (95% CI: 0.2–6.3)	Fatigue, myalgia, fever, headache, spouse diagnosed with COVID-19	No association with mode of commute (public transport, walking/cycling, private)
Venugopal	Very high	Seroprevalence (%), bivariable, multivariable linear regression (OR)	27%	29%	Public transit compared to private OR: 1.3 (95% CI: 0.9–2.0) Adjusted for ethnicity, symptoms, duration of symptoms: OR: 0.84 (95% CI: 0.47–1.52)	Ethnicity other than Caucasian, living in an apartment/condo, walking to work, symptoms of COVID-19, community exposure	Type of transport to hospital not associated with seropositivity
Yamamoto	Very high	Seropositivity (%), Poisson regression (PR)	0.7% (95% CI: 0.4–1.1)	N/A	Compared to those that used transit <1 time/week, those that used it 1 or more times/week prevalence ratio was 0.57 (95% CI: 0.2–1.4)	Close contact with patients with COVID-19 at home and in the community	No association with transit
Nishida	Very high	Seropositivity (%)	IgG: 0.43% (95% CI: 0.2–1.1)	0.76% (n = 396) (95% CI: 0.3–2.2)	N/A	No significant factors	No association with transit
Cruz-Arenas	High	Seropositivity (%), multiple logistic regression (OR)	LFA: 11% ELISA: (IgG only) 13%	N/A	Use of public transport for work commute OR: 1.62 95% CI: 0.82–3.21)	Olfactory alterations, security or janitorial occupations, education below a university degree increasing number of people in household	Type of transport to hospital not associated with seropositivity
De Oliveira	High	Prevalence (%), bivariate analysis, multivariate logistic regression (OR)	5.5%	N/A	Public transport (bus, metro): OR 1.17 (95% CI: 0.79–1.75) Adjusted for gender, cleaning, working at COVID-19 units, type of transport OR: 1.103 (95% CI: 0.731–1.665)	Professional category of cleaning and male gender	Type of transport to hospital not associated with seropositivity
Gupta	Medium	Seroprevalence (%)	13%	Public transit (n = 235): 20%; Hospital transport (n = 676): 16.9%; Own vehicle (n = 1986): 12.4%; on foot (n = 544): 11.2%; did not declare (n = 298): 6%	N/A	Contact with COVID positive individuals, COVID-19 symptoms, region of residence	Seroprevalence significantly higher in HCW that used public, or hospital transit compared to those that used other modes of commute ($p < 0.05$)

OR: odds ratio; PR: prevalence ratio.

Table 4. Summary of findings from studies that assessed the association between seropositivity and use of public transportation in population-based studies from highest to lowest HDI.

Author	HDI Category	Outcome	Overall Seroprevalence (%)	Transit Outcomes		Variables Associated with Seropositivity	Conclusions
				Seroprevalence (%)	Regression Analysis (i.e., OR, RR)		
Chan	Very high	Seroprevalence (%), age weighted	2.9% (95% CI: 1–6.2)	Public transportation/carpool (n = 52): 6% (95% CI: 0.1–20.5); own vehicle (n = 920): 1.9% (95% CI: 0.4–4.1); walking/biking (n = 34): 2.8% (95% CI: 0–16.7)	N/A	Those living in a condo or apartment, those that rely on public transportation or carpool, race/ethnicity other than Caucasian, primary mode of transportation	Higher seroprevalence in transit users
Mahajan	Very high	Seroprevalence (%), weighted for non-response and population characteristics of Connecticut	General population: 4% (90% CI: 2–6); non-Hispanic black subpopulation: 6.4% (90% CI: 0.9–11.9); Hispanic subpopulation: 19.9% (90% CI: 13.2–26.6)	General population: 0% or too small to calculate Non-Hispanic Black subpopulation Airplane: 4% (±4.8); public transportation: 23.7% (±7.5) Hispanic subpopulation Airplane: 4.8% (±3.3); public transportation: 13.1% (±5.5) *	N/A	Race and ethnicity	No association with transit use in general population, seroprevalence significantly higher in transit users of ethnic minorities
Acurio-Paez	High	Seroprevalence (%), bivariate regression, multivariate regression (OR)	Maximum: 13.2% (95% CI: 12–14.6) (IgG or IgM); Minimum: 4% (95% CI: 3.2–4.8) (IgG and IgM positive)	Foot (n = 529): 12.5% (9.6–15.5); Bicycle/moto/trolley car (n = 106): 11.3% (6.2–19.3); Private car (n = 912): 11% (9.0–13.1); Public (bus/taxi) (n = 742): 18.2% (15.5–21.2)	Public (bus/taxi) compared to private (own car, foot, bicycle) OR: 1.73 (95% CI: 1.4–2.2) Adjusted for age, resources, COVID-19 in household, contact with flu-like symptoms, number of people in household, physical contact with someone outside the household: 1.65 (95% CI: 1.28–2.14)	Age 35–49 years old, COVID-19 positive person in the home, using public transit, at least 6 people in a household, physical contact with a person outside the household, contact with someone with flu-like symptoms, not having enough resources for living	Those using public transit at increased risk of seropositivity
Nausin	Medium	Seropositivity (%), bivariate logistic regression (OR)	10.14% (95% CI: 9.6–10.7)	N/A	OR: 1.79 (95% CI: 1.4–2.2) OR males: 1.91 (95% CI: 1.44–2.55); OR females: 1.83 (95% CI: 1.26–2.69)	Higher population density, high exposure work, those using public transit, non-smokers	Those using public transit at increased risk of seropositivity

* ± margin of error at 90% CI.

4. Review

4.1. Transportation Industry

Essential workers in the transportation industry typically have a high number of social and professional contacts over a comparably large geographic distance which may increase their risk of SARS-CoV-2 exposure. Several serosurveys have purposely targeted industry workers thought to be at high risk of infection during the first wave of the COVID-19 pandemic [14,15,16,17,18,19,20,21,22,23]. The association between work in the transit industry and seroprevalence is far from clear with conflicting results found across numerous studies.

4.1.1. Very High HDI Countries

A population-based study in New York City during the first wave of the pandemic in Spring 2020 found that seroprevalence of SARS-CoV-2 antibodies was significantly higher in those working in the air (25.0%) and ground transportation (35.0%) industries compared to those who did not work outside the home during a government mandated stay at home order (22.2%) [14]. Of note, test validation was not reported. In contrast, another smaller American population-based study by Feehan et al. found no association [14]. This study population was 63.3% female and 66.9% white, with a small number or participants working in the transportation industry (n = 11) leading to broad confidence intervals and uncertainty in results [15]. A multivariate analysis was not included, so the effect of demographic and socioeconomic factors was unknown. In a nation-wide longitudinal seroepidemiological study conducted during the first wave of the COVID-19 pandemic in Spain, Pollan et al. found no difference in seroprevalence between those working in the transportation industry and those working from home [16]. This analysis used sampling weights and post-stratification to adjust for selection probabilities and considered clustering by household and census tract when determining seroprevalence. A large representative sample including children, adolescents, and elderly largely of Spanish nationality were recruited. These subpopulations are unlikely to be employed in the transportation industry and could potentially introduce bias if included in the overall estimate of seroprevalence in transit workers. Both Feehan and Pollan found that the only occupation associated with higher seroprevalence was within healthcare. Two Italian studies targeted workers from a variety of occupational sectors to identify high-risk jobs during the first wave of the pandemic. Both studies had comparable overall seroprevalence at

approximately 5% and found that work in the transportation industry was not associated with increased prevalence of antibodies to SARS-CoV-2. However, Airoldi et al. identified clusters of cases that were independent of a single industrial sector indicating that the safety measures initiated by corporations could affect the epidemic situation in each company [17]. PPE use and company policy was not measured in this study so authors were unable to explore this hypothesis. Although the overall sample size was large, the number of participants in each occupation group varied greatly. The sample size was small in several industry sectors resulting in broad confidence intervals which may impact the validity of results. Berselli et al.'s study focused on occupational risks and included mostly participants nominated by their employer, however also included self-referred individuals from whom occupational information was not collected [18]. Reason for self-referral and information on symptoms was not collected. Seroprevalence may have been overestimated if those with symptoms were more likely to participate. This study allowed participants to choose from qualitative tests, quantitative tests, or both. Summary results of each test were available, but results would have been strengthened if participants were randomly assigned a test group or if results were stratified by test. They also switched from testing for IgA and IgG using the EUROIMMUN anti-SARS-CoV-2 test to testing for IgG and IgM using the Roch Elecsys Anti-SARS-CoV-2 test kit for IgG and IgM halfway through the study. The reason for the switch was not indicated and could impact results, especially for IgM which was measured using two separate tests and presented as a single result. The United Arab Emirates has a large community of expatriates living and working in unregulated and often precarious conditions (e.g., construction). Alsuwaldi et al. sampled labor camp workers living in these congregate settings and random households after the first wave in Abu Dhabi, United Arab Emirates [19]. Labour camp workers have different socio-demographic characteristics and were analyzed separately from randomly sampled households representing the general population. They found work in the transportation industry was associated with seropositivity in labor camp workers (OR: 2.7; 95% CI: 1.8–4.0), but not in the general population (OR: 1.5; 95% CI: 0.7–3.2) compared to healthcare workers adjusted for age, sex, region, education, nationality, ethnicity, occupation, and contact with a person diagnosed with COVID-19. This may indicate that seropositivity was associated with labour camp conditions such as congregate living and eating in densely populated areas, and not work in the transportation industry itself.

4.1.2. High HDI Countries

Poustchi et al. and Colmenares-Mejiad et al. both performed studies in countries with high HDI (Iran and Colombia, respectively) and found similar seroprevalences between transportation workers and other high-risk occupations (pharmacy workers, retail, health care workers, and other customer-facing staff) [20,21] indicating no increased risk of infection. Poustchi et al.'s study population was approximately 50% male, mostly between the ages of 30–49 and with no contact with confirmed COVID-19 patients. Serology results from a wide range of assays with differing sensitivities and specificities were reported across studies. Poustchi et al. used Pishtaz Teb SARS-CoV-2 ELISA kits which had not been fully assessed before this study and had the lowest sensitivity (66.9% in their validation study) compared to tests used in other included studies where the sensitivity was in the 90% range. Although they accounted for test performance in a sensitivity analysis, a low sensitivity could increase the number of false negatives and underestimate seroprevalence in this population. Tests with high sensitivity and specificity are required to ensure accurate estimation of seropositivity, especially when COVID-19 prevalence in the population is low. The median age of the study population used by Colmenares et al. was 37.4, 59.9% were female, and most were classified as having a socioeconomic status between 2–4 on a six-point scale. Almost all the studies focusing on the transportation industry were conducted in the first wave of the pandemic. However, Colemenares et al. performed their study during the transition period between the first and second waves in Colombia. They recruited participants over four months, a broad time frame during which transmission patterns and public health recommendations frequently changed. It is possible that the staggered resumption of economic sectors and the effect of time could confound the effect of transportation use on seropositivity in this cross-sectional study.

4.1.3. Medium HDI Countries

In a state-wide survey of over 16,000 individuals in Karnataka, India, the population was divided into groups based on occupation risk [22]. Those that worked as bus conductors and auto drivers had twice the odds of seropositivity compared to low-risk individuals (e.g., those attending outpatient departments for minor ailments) (OR: 2.12; 95% CI: 1.28–3.51). The risk groups in this study were poorly defined and recruited from different populations. The low-risk group included only HCW and patients coming in for periodic care or visits to outpatient departments while the

moderate and high-risk groups were chosen from the general population. This makes comparisons between groups challenging and reduces study generalizability.

4.1.4. Low HDI Countries

A Togolese study where almost 50% of the study participants worked in air or road transport found that there was no association between work in the transportation industry and seropositivity [23]. Most participants were male (71.6%), had a post-secondary education (51%), and were of Togolese nationality (98%). The overall seroprevalence in the study of 955 individuals was 0.9% (95% CI: 0.4–1.8). This sample size and low seroprevalence prohibited evaluation of the association with key variables.

4.1.5. Transportation Industry Trends

The majority of studies found that there was no association between work in the transportation industry and SARS-CoV-2 seroprevalence or that the risk of working in this industry was comparable to other occupations considered high risk. Of the studies conducted in countries with very high HDI, seroprevalence was only found to be associated with work in the transportation industry by one study [14] and those working in labour camps [19]. The economic inequality seen by those working in labour camps compared to the general population of Abu Dhabi may make this population more comparable with studies in the medium or low HDI category. Both studies conducted in countries with high HDI found seroprevalence was similar among high-risk occupations, while in countries with medium and low HDI results were inconsistent. The study population and restrictions imposed on economic sectors during the pandemic are key factors that should be considered when evaluating the transportation industry. Historically, the transportation industry has been male dominated which was reflected in several studies [19,23] and may limit generalizability of results. Public safety measures such as lockdowns and travel restrictions varied broadly between regions as the pandemic progressed and likely contributed to the heterogeneity of results. This also related to corporate policies as was noted by Airoldi where clusters of cases were found independent of a single industrial sector. Although some general trends were established, results broadly varied between studies and no overall consensus was reached. This was likely implicated by the various study populations, sample methods, test specifications and timing of included studies.

4.2. Healthcare Workers

Healthcare worker (HCW) populations have been a focus of serosurveys due to their high rates of exposure to COVID-19 and the potential threat to patients and other healthcare workers if infected. Several studies have examined the occupational and environmental risks faced by HCW during the first wave of the COVID-19 pandemic, including commute via public transport with mixed results.

4.2.1. Very High HDI Countries

A cross-sectional study in a large group of HCW in Switzerland found a gradient of effect, where the proportion of individuals that tested positive for SARS-CoV-2 antibodies increased with the number of times they used public transit in a week. This study also found that wearing a mask while using public transit reduced the odds of seropositivity by 58.0% (OR: 0.42; 95% CI: 0.2–0.9) [24]. Soffin et al. found no association in one hundred forty-three surgeons and anesthesiologists in a specialty hospital in New York City [25]. The small sample included mostly young, white, educated males with few comorbidities which reflected a lower overall seroprevalence (9.8%) compared to other studies conducted in New York during this period (27% and 23.6%; Venugopal and Pathela [14,26]). These results should be interpreted with caution as they may not be representative of the general population. A study evaluating a more representative population of HCW in New York during the same period identified a higher seroprevalence in those that walked to work compared to those that used private transportation. The study population included those over the age of 20, and had significant representation of Hispanic, Black, Asian, and Caucasian ethnicities. No association with mode of travel to work was identified when controlled for ethnicity, close contact with someone diagnosed or with symptoms of COVID-19, not wearing a face mask in healthcare or community setting, unprotected direct contact with infection secretions or excretions, and symptoms associated with COVID-19 infection (fever, cough, myalgia, ageusia, anosmia, nausea, diarrhea) [26]. This study also thoroughly described risk of exposure in concordance with CDC regulations [27], ensuring precise evaluation of risk. Two similar studies conducted in Japan following the first wave of the pandemic reported overall seroprevalence of less than 1% within their respective hospitals (0.7% Yamamoto; 0.43% Nishida) [28,29]. Although a large proportion of workers relied on public transit to travel to work, no association was found

with mode of travel. Of note, seropositivity was lower in HCW compared to overall seropositivity measured in the public.

4.2.2. High HDI Countries

Two studies from high HDI countries were identified; both of which found no significant association between seropositivity and transit use in HCWs. The study populations were similar where at least 60% were female and the majority were between 30–50 years of age. Cruz Arenas et al. performed their study in a private hospital not accepting COVID-19 patients, so it seems likely that the risk of exposure for HCW in this hospital would be lower than other locations accepting COVID-19 patients [30].This evaluation had a relatively small sample size (n = 300) that was stratified into ten groups according to occupation thereby reducing statistical power compared to the other studies. De Olivieria et al. sampled primarily HCW working in COVID-19 units in São Paulo, Brazil [31]. However, did not clearly define risk of exposure according to frequency of contact with COVID-19 patients, instead classifying risk as high, medium, or low.

4.2.3. Medium HDI Countries

In contrast to the majority of studies focusing on HCWs, one prospective study conducted in India found seroprevalence was significantly higher in those that relied on public transportation (20.0%) or transportation provided by the hospital (16.9%) compared to private modes of transportation (12.0%). However, multivariate analysis was not conducted [32]. The authors speculated that seropositivity was highest in administrative staff and lowest in physicians due to better adherence to control practices. However, PPE use was measured by voluntary disclosure and not controlled for in a multivariate analysis.

4.2.4. Healthcare Worker Trends

All studies conducted in very high and high HDI countries found there was no association between mode of transport and seroprevalence in HCW, indicating that it is not a risk factor in these populations. It is possible that these regions have implemented effective emergency management procedures and PPE use that has protected employees from exposure. The single study that found an association with mode of transport in HCWs was conducted in India, a medium HDI country. This could be implicated with inefficient public transportation systems and mobility problems that

are a product of India's increasing population density. This may lead to longer or more crowded commutes via public transit with increased risk of infection compared to studies conducted in other countries. There was consensus that seropositivity was higher in those with a household or community contact diagnosed with COVID-19 compared to those that encountered COVID-19 patients in the workplace, suggesting personal protective equipment (PPE) use and hospital policies have been effective in reducing the risk of infection in the workplace [25,27,28,31,32]. These combined findings could indicate HCW are diligently following mask wearing and physical distancing procedures while using public transit. However, this was not documented in most studies. All studies relied on retrospective self-reporting of symptoms associated with COVID-19 and PPE use which could introduce recall or reporting bias if participants do not report or are or unwilling to disclose any breach in protocol associated with PPE use. Similarly, the hospital disposition and number of COVID-19 patients accepted may impact risk of exposure and affect reported seroprevalence between studies. Reliance on voluntary participation within hospitals could introduce response bias if those with higher risk of exposure are the ones volunteering to participate.

4.3. Population-Based Studies

Well-designed population-based serosurveys can offer more representative findings and more accurate estimate of overall and subgroup infection risk. Several national or state-wide serosurveys have been conducted at different stages of the pandemic to estimate the extent of infection and identify risk factors among the population, including use of public transit.

4.3.1. Very High HDI Countries

Two population-based studies of representative samples were conducted in the United States between May and July 2020, one in Rhode Island [33], and another in Connecticut [34]. Chan et al. found higher seroprevalence in those that relied on public transit (6.0%) compared to those that used a private vehicle (1.9%) and those that walked/biked (2.8%) [33]. Mahajan found no association between transit use and seropositivity in the general population. Of note, public transit use was low (3.4%). However, a greater proportion used public transit in a subgroup of non-Hispanic black and Hispanic participants and the seroprevalence was considerably higher (23.7%) in black transit users [34]. Non-response bias may threaten the validity of results given response

rates as low as 11% and 7% in each study, respectively. Chan found response rates lower in men, those under the age of 35, and non-whites. Mahajan did not perform an analysis on those that did not respond but did consider the nonresponse rate when weighting the sample. The potential to introduce bias is high if those that are more likely to test seropositive such as racial minorities have higher non-response rates.

4.3.2. High HDI Countries

A provincial-wide serosurvey in Ecuador during the same period determined that the odds of seropositivity associated with transportation use in a bivariate analysis was 1.73 (95% CI: 1.4–2.2) [35]. This study did not consider assay sensitivity/specificity but did adjust for key covariates (age, gender, having enough resources for living, household COVID-19 contact, contact with the flu, number of occupants in house, physical contact with someone with COVID-19), which did not change the results. In this study the seroprevalence was highest in those using public transit (bus/taxi) (18.2% (95% CI: 15.5–21.2)) compared to those who walked (12.5% (95% CI: 9.6–15.5)), used a bicycle/moto/trolley car (11.3% (95% CI: 6.2–19.3)), or private car (11.0% (95% CI: 9.0–13.1)).

4.3.3. Medium HDI Countries

A national scale study of over 10,000 participants assessed the spread of infection in India from August to September 2020 [36]. Results revealed that those using public transport were almost twice as likely to have antibodies to SARS-CoV-2 compared to those using private transport (OR 1.79; 95% CI: 1.4–2.2). However, the authors did not consider the sensitivity/specificity of the antibody assays utilized or adjust for demographic characteristics which could affect validity of results.

4.3.4. Population-Based Study Trends

The two studies conducted in very high HDI countries had opposing results, likely a result of differing population demographics and test methods. Mahajan was the only study that found transit use was not associated with seropositivity in the general population, but did find SARS-CoV-2 seroprevalence considerably higher in black and Hispanic transit users [28]. Although conducted in two very different locations, the studies conducted in high and medium HDI countries both

found that public transit users were almost twice as likely to have antibodies for SARS-CoV-2. This indicates that transit use is likely a risk factor for SARS-CoV-2 infection for the general population regardless of region. Most studies relied on random sampling weighted by census data to obtain a representative sample. It can be difficult to obtain a representative population sample of elderly and young adults using household surveys and census information. Young adults have higher mobility and may be officially registered to live in their parents' home but have relocated elsewhere. Public health measures and timing of lockdowns within communities may alter the estimated seroprevalence between studies. Acurio-Páez et al. performed their study while restrictions were relaxed and almost all activities were operating normally [35]. They reported over 90% adherence to physical distancing and mask wearing preventative measures, although reporting bias may be prevalent as adherence was measured by voluntary disclosure. In contrast, Chan et al. performed their study during a time of strict lockdown with mandated mask use, where adherence to COVID-19 preventative measures was unknown or not reported [33]. Observing preventative safety measures and adhering to lockdown protocol has been proven to reduce SARS-CoV-2 transmission, and likely the risk of exposure to the public. This could explain why overall seropositivity measured by Acurio-Páez et al. was more than 10% higher than what was found by Chan.

4.4. Race and Ethnicity

Race and ethnicity are potential confounding variables when analyzing the relationship between transit use and seropositivity as there are complex interactions between occupational, social, and structural inequalities that increase the risk of COVID-19 in minority communities. Several studies examining socioeconomic factors and spatiotemporal transit use across neighborhoods have shown that decline in magnitude of ridership seen throughout the COVID-19 pandemic is much lower in people of color, those with less education, and lower income [2,3,4]. Black and Hispanic Americans make up a large proportion of the essential workforce, in jobs that require travel and public interaction (i.e., service industry, transportation, health care, cleaners, or seasonal workers) [37]. They are also less likely to own personal cars and require access to public transportation to get to school, work and access essential services such as childcare throughout the COVID-19 pandemic [38]. Several of the studies were conducted in a local population with low diversity [23,35] or did not report information on race or ethnicity [20,21,22,30,31,32,36]. Pollan et al. and

Alsuwaldi et al. found that seroprevalence was lower in those of native nationality compared to other nationalities [16,19]. Five of the six studies conducted in the United States sampled a diverse population and found that non-Hispanic black and Hispanic individuals had higher seroprevalence for SARS-CoV-2 antibodies compared to white individuals [14,15,26,33,34]. Venugopal et al. and Pathela et al. both conducted studies during the first wave of the pandemic in New York City and concluded that black and Hispanic individuals were almost twice as likely to have evidence of infection compared to white participants [14,26]. Pathela et al. estimated that the seropositivity in Hispanics was 35.3% (95% CI: 34.4–36.2) and 33.5% (95% CI: 32.0–35.1) in non-Hispanic black compared to non-Hispanic white 16.0% (95% CI: 15.5–16.6). In a regression analysis adjusted for sex, age, area of residence and level of poverty, the risk of seropositivity was almost twice as high in black and Hispanic individuals compared to non-Hispanic white individuals (RR: 1.83; 95% CI: 1.7–1.9 and RR: 1.84; 95% CI: 1.8–1.9), respectively [14]. Very similar results were found by Venugopal et al., where Hispanic and black individuals were more than twice as likely to test positive for SARS-CoV-2 antibodies compared to white participants in unadjusted OR of 2.42 (95% CI: 1.3–4.5) for Hispanics and 2.55 (95% CI: 1.3–5.0) for black participants [26]. These disparities disappear when added to a multivariate analysis that adjusts for ethnicity, mode of travel, moderate or high risk of community or occupational exposure, and symptoms attributable to COVID-19 infection.

4.5. Factors Associated with Seropositivity

Overall seroprevalence for SARS-CoV-2 antibodies varied geographically within single studies, where sampling techniques and testing procedures remained consistent. This indicates that regardless of methodology, risk of exposure, demographic variables, and population density likely contribute to risk of SARS-CoV-2 infection. The effect of population density was measured in several studies and revealed a clear relationship between increasing number of people in a region or household and seropositivity for SARS-CoV-2 antibodies. Similarly, higher seroprevalence was found in urban settings where quarantine and separation from household members may not be realistic. An association between flu-like symptoms and SARS-CoV-2 antibody prevalence was consistent across studies. Common symptoms included ageusia, anosmia, fever, diarrhea and olfactory alterations. Comparable to results found in more extensive systematic reviews [7,39], most studies found no association between sex and seropositivity for SARS-CoV-2 antibodies.

Inherent differences between countries with high and low HDI relate to how citizens are impacted by COVID-19 and contribute to the heterologous results of this evaluation. In countries with lower HDI, inadequate housing may make physical distancing and quarantine impractical. There is a large amount of informal economic activity where workers are paid on a daily wage, are self-employed or are involved in informal organizations [40]. A greater proportion of these workers have no choice but to work outside the home during the pandemic, often in hazardous conditions which could lead to greater seroprevalence for SARS-CoV-2. Not all reviewed studies conducted in lower HDI countries reported higher seroprevalence. This could indicate lack of testing capacity or insufficient sampling techniques caused by lack of organization in informal industries. Countries with higher HDI generally experienced higher burdens of COVID-19 earlier in the pandemic [41]. These countries have greater contributions to the global economy encouraging business and tourism travellers that potentiate the spread of infectious disease. This was especially true early in the pandemic prior to the introduction of travel restrictions. Similarly, developed urban areas have widespread and efficient domestic transport systems that support connectivity but also facilitate COVID-19 transmission. Compared to lower HDI countries, higher HDI countries have a higher proportion of elderly people, putting them at greater risk of severe outcomes and mortality [42]. In Asian countries, masks are often worn during influenza season. This may have translated to greater adherence to COVID-19 public safety measures such as mask wearing during public transit use compared to other countries where mask wearing is a novelty. This might explain why COVID-19 seroprevalence was lower in Japanese studies.

5. Study Limitations

Several common limitations were observed across included studies. Most were observational cross-sectional studies. As such, they cannot be used to establish temporal association or causality. Cohort or longitudinal studies would be beneficial to analyze the change in seroprevalence and detect seroconversion that could be missed due to early testing or delayed antibody response. Longitudinal studies in particular are required to measure the effect of vaccination rates and introduction of new variants that were not captured in any of the included studies. Many of the

studies relied on voluntary participation for recruitment. This method has the potential to introduce bias if those with COVID-19 symptoms are more likely to participate. This concern was evaluated by Pathela et al. who determined that 60% of participants had previous symptoms of COVID-19. Almost all studies relied on self-reported questionnaires to determine transit use and demographic characteristics. This method is prone to self-report bias as participants may provide inaccurate responses to preserve social desirability or control perception of themselves. Alternatively, if questions are ambiguous or wording is not inclusive to all reading levels, participants may interpret questions differently leading to inconsistencies in results. The validity of serosurveys has been questioned due to inconsistent sampling techniques and assay accuracy. High-quality serosurveys use validated tests, standardized lab methods and correct for demographic characteristics and test performance in seroprevalence estimates [43]. Several of the studies included in this analysis did not define the cut-off value used to estimate positivity, which could impact the calculated specificity and result in inaccurate seroprevalence estimates [44]. Similarly, an assortment of serological tests with their own sensitivities and specificities were used to estimate seroprevalence making comparison between studies difficult. Furthermore, the lack of reference samples in the early days of the pandemic complicated assay calibration and standardization. Serosurveys may not capture all past infections due to variations in antibody kinetics such as time to seroconversion, duration of antibody response and rate of antibody waning. Cross-reactivity with common human coronavirus strains and other respiratory viruses is also a concern based on the assay and protein used and could impact seroprevalence results [45,46,47].

This rapid review has several limitations. Most included studies were conducted during the first wave of the pandemic. There are several reasons for this. Many seroprevalence studies were conducted at the beginning of the pandemic to better understand risk factors for this novel disease. Studies were also limited to only include those conducted before the emergence of the Omicron variant. Omicron has vastly different epidemiological characteristics and COVID-19 restrictions have changed with time, so these studies were excluded to improve comparability of results. Another limitation was the presence of several confounding factors that influenced the evaluation of the effect of public transportation use and seroprevalence of SARS-CoV-2. Results of seroprevalence studies are time-dependent and vary based on the location and type of test method. Therefore, conclusions from individual studies reflect the context of each region and may not be

applicable to predict seroprevalence in neighboring regions. This limitation reflects the heterogeneity of findings found in this review and other seroprevalence studies worldwide and should be expected as a natural circumstance of the pandemic. Although there are limitations, results from seroprevalence studies do show general trends in levels of population exposure and can help disentangle confounding factors to help identify risk factors as the pandemic evolves.

6. Conclusions

Most studies focusing on industry risk factors found no association between SARS-CoV-2 seroprevalence and work in the transportation industry, or that the risk of infection was no higher than other high-risk occupations. However, findings were not universal with conflicting results found in several studies. In HCWs, there was a consensus that mode of transport was not associated with SARS-CoV-2 seroprevalence. In population-based studies, use of public transit was generally associated with higher seropositivity and was implicated by race and ethnicity. A major limitation of these findings was that results could not be generalized due to the involvement of several confounding factors. Of the few studies that considered this topic, results varied based on study population, sociodemographic characteristics, type of assay used, sampling strategies, statistical analysis techniques, occupational hazards and timing of economic closures. However, several studies did report that SARS-CoV-2 seroprevalence was higher in transit users and results from these individual studies should be deliberated. Policy makers should consider transit use a risk factor when planning, implementing, monitoring, and improving strategies for reducing SARS-CoV-2 transmission. In regions where seroprevalence was associated with transit use in transportation workers, employers and policy makers may consider enforcing stricter adherence to public safety measures or implementing additional measures to protect employees. Similarly, across all studies seroprevalence was found to be higher in ethnic minorities and areas with lower socioeconomic status. Policy makers and practitioners should be aware that these populations may have higher rates of exposure and may be more severely impacted by SARS-CoV-2. Further high-quality studies focused solely on this topic are required, as are longitudinal studies as the COVID-19 pandemic progresses.

Author Contributions
Conceptualization, A.H. and C.L.C.; writing—original draft preparation, A.H.; writing—review and editing, C.L.C., Y.G., M.-A.L. and J.L.; supervision, C.L.C. All authors have read and agreed to the published version of the manuscript.

Funding
This research received no external funding.

Institutional Review Board Statement
Not applicable because this study is based exclusively on published literature.

Informed Consent Statement
Patient consent not applicable as this was an observational review of published literature.

Conflicts of Interest
The authors declare no conflict of interest.

References

1. WHO Coronavirus (COVID-19) Dashboard. Available online: https://covid19.who.int/ (accessed on 7 July 2022).
2. Turcotte, M.; Savage, K. Commuting to Work during COVID-19. Available online: https://www150.statcan.gc.ca/n1/pub/45-28- 0001/2020001/article/00069-eng.htm (accessed on 9 February 2021).
3. Sy, K.T.L.; Martinez, M.E.; Rader, B.; White, L.F. Socioeconomic Disparities in Subway Use and COVID-19 Outcomes in New York City. Am. J. Epidemiol. 2021, 190, 1234–1242. [CrossRef] [PubMed]
4. Brough, R.; Freedman, M.; Phillips, D.C. Understanding Socioeconomic Disparities in Travel Behavior during the COVID-19 Pandemic. J. Reg. Sci. 2021, 61, 753–774. [CrossRef] [PubMed]
5. Rostami, A.; Sepidarkish, M.; Leeflang, M.M.; Riahi, S.M.; Shiadeh, M.N.; Esfandyari, S.; Mokdad, A.H.; Hotez, P.J.; Gasser, R.B. SARS-CoV-2 Seroprevalence Worldwide: A Systematic Review and Meta-Analysis. Clin. Microbiol. Infect. 2021, 27, 331–340. [CrossRef] [PubMed]
6. Galanis, P.; Vraka, I.; Fragkou, D.; Bilali, A.; Kaitelidou, D. Seroprevalence of SARS-CoV-2 Antibodies and Associated Factors in Healthcare Workers: A Systematic Review and Meta-Analysis. J. Hosp. Infect. 2021, 108, 120–134. [CrossRef] [PubMed]
7. Chen, X.; Chen, Z.; Azman, A.S.; Deng, X.; Sun, R.; Zhao, Z.; Zheng, N.; Chen, X.; Lu, W.; Zhuang, T. Serological Evidence of Human Infection with SARS-CoV-2: A Systematic Review and Meta-Analysis. Lancet Glob. Health 2021, 9, e598–e609. [CrossRef]
8. Rostami, A.; Sepidarkish, M.; Fazlzadeh, A.; Mokdad, A.H.; Sattarnezhad, A.; Esfandyari, S.; Riahi, S.M.; Mollalo, A.; Dooki, M.E.; Bayani, M.; et al. Update on SARS-CoV-2 Seroprevalence: Regional and Worldwide. Clin. Microbiol. Infect. Off. Publ. Eur. Soc. Clin. Microbiol. Infect. Dis. 2021, 27, 1762–1771. [CrossRef]
9. Palmateer, N.E.; Dickson, E.; Furrie, E.; Godber, I.; Goldberg, D.J.; Gousias, P.; Jarvis, L.; Mathie, L.; Mavin, S.; McMenamin, J. National Population Prevalence of Antibodies to SARS-CoV-2 in Scotland during the First and Second Waves of the COVID-19 Pandemic. Public Health 2021, 198, 102–105. [CrossRef]
10. Paduano, S.; Galante, P.; Berselli, N.; Ugolotti, L.; Modenese, A.; Poggi, A.; Malavolti, M.; Turchi, S.; Marchesi, I.; Vivoli, R. Seroprevalence Survey of Anti-SARS-CoV-2 Antibodies in a Population of Emilia-Romagna Region, Northern Italy. Int. J. Environ. Res. Public. Health 2022, 19, 7882. [CrossRef]
11. Kislaya, I.; Gonçalves, P.; Gómez, V.; Gaio, V.; Roquette, R.; Barreto, M.; Sousa-Uva, M.; Torres, A.R.; Santos, J.; Matos, R. SARS-CoV-2 Seroprevalence in Portugal Following the Third Epidemic Wave: Results of the Second National Serological Survey (ISN2COVID-19). Infect. Dis. 2022, 54, 418–424. [CrossRef]
12. Lai, C.-C.; Wang, J.-H.; Hsueh, P.-R. Population-Based Seroprevalence Surveys of Anti-SARS-CoV-2 Antibody: An up-to-Date Review. Int. J. Infect. Dis. 2020, 101, 314–322. [CrossRef]
13. Human Development Reports. Human Development Index (HDI). Available online: https://hdr.undp.org/data-center/human -development-index?utm_source=EN&utm_medium=GSR&utm_content=US_UNDP_PaidSearch_Brand_English&utm_cam paign=CENTRAL&c_src=CENTRAL&c_src2=GSR&gclid=CjwKCAjw6MKXBhA5EiwANWLODGdWKBmqNIDKXTIr8ZN82 ThQa5vaG_eYYrE5-UIEmgsSO9r1Go8yjhoCWrkQAvD_BwE#/indicies/HDI (accessed on 2 August 2022).
14. Pathela, P.; Crawley, A.; Weiss, D.; Maldin, B.; Cornell, J.; Purdin, J.; Schumacher, P.K.; Marovich, S.; Li, J.; Daskalakis, D. Seroprevalence of SARS-CoV-2 Following the Largest Initial Epidemic Wave in the United States: Findings from New York City, 13 May–21 July 2020. J. Infect. Dis. 2021, jiab200.
15. Feehan, A.K.; Velasco, C.; Fort, D.; Burton, J.H.; Price-Haywood, E.G.; Katzmarzyk, P.T.; Garcia-Diaz, J.; Seoane, L. Racial and Workplace Disparities in Seroprevalence of SARS-CoV-2, Baton Rouge, Louisiana, USA. Emerg. Infect. Dis. 2021, 27, 314. [CrossRef] [PubMed]
16. Pollán, M.; Pérez-Gómez, B.; Pastor-Barriuso, R.; Oteo, J.; Hernán, M.A.; Pérez-Olmeda, M.; Sanmartín, J.L.; Fernández-García, A.; Cruz, I.; de Larrea, N.F. Prevalence of SARS-CoV-2 in Spain

(ENE-COVID): A Nationwide, Population-Based Seroepidemiological Study. Lancet 2020, 396, 535–544. [CrossRef]
17. Airoldi, C.; Calcagno, A.; Di Perri, G.; Valinotto, R.; Gallo, L.; Locana, E.; Trunfio, M.; Patrucco, F.; Vineis, P.; Faggiano, F. Seroprevalence of SARS-CoV-2 among Workers in Northern Italy. Ann. Work Expo. Health 2022, 66, 224–232. [CrossRef] [PubMed]
18. Berselli, N.; Filippini, T.; Paduano, S.; Malavolti, M.; Modenese, A.; Gobba, F.; Borella, P.; Marchesi, I.; Vivoli, R.; Perlini, P. Seroprevalence of Anti-SARS-CoV-2 Antibodies in the Northern Italy Population before the COVID-19 Second Wave. Int. J. Occup. Med. Environ. Health 2022, 35, 63–74. [CrossRef] [PubMed]
19. Alsuwaidi, A.R.; Al Hosani, F.I.; Al Memari, S.; Narchi, H.; Abdel Wareth, L.; Kamal, H.; Al Ketbi, M.; Al Baloushi, D.; Elfateh, A.; Khudair, A. Seroprevalence of COVID-19 Infection in the Emirate of Abu Dhabi, United Arab Emirates: A Population-Based Cross-Sectional Study. Int. J. Epidemiol. 2021, 50, 1077–1090. [CrossRef]
20. Poustchi, H.; Darvishian, M.; Mohammadi, Z.; Shayanrad, A.; Delavari, A.; Bahadorimonfared, A.; Eslami, S.; Javanmard, S.H.; Shakiba, E.; Somi, M.H. SARS-CoV-2 Antibody Seroprevalence in the General Population and High-Risk Occupational Groups across 18 Cities in Iran: A Population-Based Cross-Sectional Study. Lancet Infect. Dis. 2021, 21, 473–481. [CrossRef] 21. Colmenares-Mejía, C.C.; Serrano-Díaz, N.; Quintero-Lesmes, D.C.; Meneses, L.; Salazar Acosta, I.; Idrovo, Á.J.; SanabriaEcheverry, D.Y.; Cordero-Rebolledo, H.; Castillo, V. Seroprevalence of SARS-CoV-2 Infection among Occupational Groups from the Bucaramanga Metropolitan Area, Colombia. Int. J. Environ. Res. Public. Health 2021, 18, 4172. [CrossRef]
22. Babu, G.R.; Sundaresan, R.; Athreya, S.; Akhtar, J.; Pandey, P.K.; Maroor, P.S.; Padma, M.R.; Lalitha, R.; Shariff, M.; Krishnappa, L. The Burden of Active Infection and Anti-SARS-CoV-2 IgG Antibodies in the General Population: Results from a Statewide Sentinel-Based Population Survey in Karnataka, India. Int. J. Infect. Dis. 2021, 108, 27–36. [CrossRef]
23. Halatoko, W.A.; Konu, Y.R.; Gbeasor-Komlanvi, F.A.; Sadio, A.J.; Tchankoni, M.K.; Komlanvi, K.S.; Salou, M.; Dorkenoo, A.M.; Maman, I.; Agbobli, A. Prevalence of SARS-CoV-2 among High-Risk Populations in Lomé (Togo) in 2020. PLoS ONE 2020, 15, e0242124. [CrossRef]
24. Meylan, S.; Dafni, U.; Lamoth, F.; Tsourti, Z.; Lobritz, M.A.; Regina, J.; Bressin, P.; Senn, L.; Grandbastien, B.; Andre, C. SARS-CoV-2 Seroprevalence in Healthcare Workers of a Swiss Tertiary Care Centre at the End of the First Wave: A Cross-Sectional Study. BMJ Open 2021, 11, e049232. [CrossRef] [PubMed]
25. Soffin, E.M.; Reisener, M.-J.; Padgett, D.E.; Kelly, B.T.; Sama, A.A.; Zhu, J.; Salzmann, S.N.; Chiapparelli, E.; Okano, I.; Oezel, L. Coronavirus Disease 2019 Exposure in Surgeons and Anesthesiologists at a New York City Specialty Hospital: A Cross-Sectional Study of Symptoms and SARS-CoV-2 Antibody Status. J. Occup. Environ. Med. 2021, 63, 521. [CrossRef] [PubMed] 26. Venugopal, U.; Jilani, N.; Rabah, S.; Shariff, M.A.; Jawed, M.; Batres, A.M.; Abubacker, M.; Menon, S.; Pillai, A.; Shabarek, N. SARS-CoV-2 Seroprevalence among Health Care Workers in a New York City Hospital: A Cross-Sectional Analysis during the COVID-19 Pandemic. Int. J. Infect. Dis. 2021, 102, 63–69. [CrossRef] [PubMed]
27. Public Health Guidance for Community-Related Exposure. Available online: https://www.cdc.gov/coronavirus/2019ncov/php /public-health-recommendations (accessed on 22 December 2020).
28. Yamamoto, S.; Tanaka, A.; Oshiro, Y.; Ishii, M.; Ishiwari, H.; Konishi, M.; Matsuda, K.; Ozeki, M.; Miyo, K.; Maeda, K. Seroprevalence of SARS-CoV-2 Antibodies in a National Hospital and Affiliated Facility after the Second Epidemic Wave of Japan. J. Infect. 2021, 83, 237–279. [CrossRef] [PubMed]
29. Nishida, T.; Iwahashi, H.; Yamauchi, K.; Kinoshita, N.; Okauchi, Y.; Suzuki, N.; Inada, M.; Abe, K. Seroprevalence of SARSCoV-2 Antibodies among 925 Staff Members in an Urban Hospital Accepting COVID-19 Patients in Osaka Prefecture, Japan: A Cross-Sectional Study. Medicine 2021, 100, e26433. [CrossRef] [PubMed]

30. Cruz-Arenas, E.; Cabrera-Ruiz, E.; Laguna-Barcenas, S.; Colin-Castro, C.A.; Chavez, T.; Franco-Cendejas, R.; Ibarra, C.; PerezOrive, J. Serological Prevalence of SARS-CoV-2 Infection and Associated Factors in Healthcare Workers in a “Non-COVID” Hospital in Mexico City. PLoS ONE 2021, 16, e0255916. [CrossRef]
31. de Oliveira, M.S.; Lobo, R.D.; Detta, F.P.; Vieira-Junior, J.M.; de Souza Castro, T.L.; Zambelli, D.B.; Cardoso, L.F.; Borges, I.C.; Tozetto-Mendoza, T.R.; Costa, S.F. SARS-CoV-2 Seroprevalence and Risk Factors among Health Care Workers: Estimating the Risk of COVID-19 Dedicated Units. Am. J. Infect. Control 2021, 49, 1197–1199. [CrossRef]
32. Gupta, R.; Dwivedi, T.; Gajendra, S.; Sahoo, B.; Gupta, S.K.; Vikas, H.; Singh, A.R.; Mohan, A.; Bhatnagar, S.; Singh, S. Seroprevalence of Antibodies to SARS-CoV-2 in Healthcare Workers & Implications of Infection Control Practice in India. Indian J. Med. Res. 2021, 153, 207.
33. Chan, P.A.; King, E.; Xu, Y.; Goedel, W.; Lasher, L.; Vargas, M.; Brindamour, K.; Huard, R.; Clyne, A.; McDonald, J. Seroprevalence of SARS-CoV-2 Antibodies in Rhode Island from a Statewide Random Sample. Am. J. Public Health 2021, 111, 700–703. [CrossRef]
34. Mahajan, S.; Srinivasan, R.; Redlich, C.A.; Huston, S.K.; Anastasio, K.M.; Cashman, L.; Massey, D.S.; Dugan, A.; Witters, D.; Marlar, J.; et al. Seroprevalence of SARS-CoV-2-Specific IgG Antibodies Among Adults Living in Connecticut: Post-Infection Prevalence (PIP) Study. Am. J. Med. 2021, 134, 526–534.e11. [CrossRef]
35. Acurio-Páez, D.; Vega, B.; Orellana, D.; Charry, R.; Gómez, A.; Obimpeh, M.; Verhoeven, V.; Colebunders, R. Seroprevalence of SARS-CoV-2 Infection and Adherence to Preventive Measures in Cuenca, Ecuador, October 2020, a Cross-Sectional Study. Int. J. Environ. Res. Public. Health 2021, 18, 4657. [CrossRef] [PubMed]
36. Naushin, S.; Sardana, V.; Ujjainiya, R.; Bhatheja, N.; Kutum, R.; Bhaskar, A.K.; Pradhan, S.; Prakash, S.; Khan, R.; Rawat, B.S.; et al. Insights from a Pan India Sero-Epidemiological Survey (Phenome-India Cohort) for SARS-CoV-2. eLife 2021, 10, e66537. [CrossRef] [PubMed]
37. Millett, G.A.; Jones, A.T.; Benkeser, D.; Baral, S.; Mercer, L.; Beyrer, C.; Honermann, B.; Lankiewicz, E.; Mena, L.; Crowley, J.S.; et al. Assessing Differential Impacts of COVID-19 on Black Communities. Ann. Epidemiol. 2020, 47, 37–44. [CrossRef]
38. Wilbur, M.; Ayman, A.; Ouyang, A.; Poon, V.; Kabir, R.; Vadali, A.; Pugliese, P.; Freudberg, D.; Laszka, A.; Dubey, A. Impact of COVID-19 on Public Transit Accessibility and Ridership. arXiv 2020, arXiv:200802413.
39. Bobrovitz, N.; Arora, R.K.; Cao, C.; Boucher, E.; Liu, M.; Donnici, C.; Cheng, M.P. Global seroprevalence of SARS-CoV-2 antibodies: A systematic review and meta-analysis. PLoS ONE 2021, 16, e0252617. [CrossRef] [PubMed]
40. Narula, R. Policy Opportunities and Challenges from the COVID-19 Pandemic for Economies with Large Informal Sectors. J. Int. Bus. Policy 2020, 3, 302–310. [CrossRef]
41. Assefa, Y.; Gilks, C.F.; Reid, S.; van de Pas, R.; Gete, D.G.; Van Damme, W. Analysis of the COVID-19 pandemic: Lessons towards a more effective response to public health emergencies. Glob. Health 2022, 18, 10. [CrossRef]
42. Verity, R.; Okell, L.C.; Dorigatti, I.; Winskill, P.; Whittaker, C.; Imai, N.; Cuomo-Dannenburg, G.; Thompson, H.; Walker, P.G.; Fu, H.; et al. Estimates of the severity of coronavirus disease 2019: A model-based analysis. Lancet Infect. Dis. 2020, 20, 669–677. [CrossRef]
43. den Hartog, G.; Schepp, R.M.; Kuijer, M.; GeurtsvanKessel, C.; van Beek, J.; Rots, N.; Koopmans, M.P.; van der Klis, F.R.; van Binnendijk, R.S. SARS-CoV-2–Specific Antibody Detection for Seroepidemiology: A Multiplex Analysis Approach Accounting for Accurate Seroprevalence. J. Infect. Dis. 2020, 222, 1452–1461. [CrossRef]
44. Scozzari, G.; Costa, C.; Migliore, E.; Coggiola, M.; Ciccone, G.; Savio, L.; Scarmozzino, A.; Pira, E.; Cassoni, P.; Galassi, C. Prevalence, Persistence, and Factors Associated with SARS-CoV-2 IgG Seropositivity in a Large Cohort of Healthcare Workers in a Tertiary Care University Hospital in Northern Italy. Viruses 2021, 13, 1064. [CrossRef]

45. Khan, S.; Nakajima, R.; Jain, A.; De Assis, R.R.; Jasinskas, A.; Obiero, J.M.; Adenaiye, O.; Tai, S.; Hong, F.; Milton, D.K. Analysis of Serologic Cross-Reactivity between Common Human Coronaviruses and SARS-CoV-2 Using Coronavirus Antigen Microarray. BioRxiv 2020. [CrossRef]
46. Li, Q.; Deng, H.-J.; Yuan, J.; Hu, J.-L.; Xu, W.; Zhang, Y.; Lv, F.-J. Clinical and Immunological Assessment of Asymptomatic SARS-CoV-2 Infections. Nat. Med. 2020, 26, 1200–1204.
47. Galipeau, Y.; Siragam, V.; Laroche, G.; Marion, E.; Greig, M.; McGuinty, M.; Booth, R.A.; Durocher, Y.; Cuperlovic-Culf, M.; Bennett, S.A. Relative Ratios of Human Seasonal Coronavirus Antibodies Predict the Efficiency of Cross-Neutralization of SARS-CoV-2 Spike Binding to ACE2. EBioMedicine 2021, 74, 103700. [CrossRef] [PubMed]

A-1.17 REDUCED SEASONAL CORONAVIRUS INCIDENCE IN HIGH RISK POPULATION GROUPS DURING THE COVID 19 PANDEMIC

Preface

(This work has been previously published as a research article)

Heiskanen A, **Galipeau Y**, Little J, Langlois MA, Cooper CL**. Reduced seasonal coronavirus incidence in high-risk population groups during the COVID-19 pandemic.**
Immun Inflamm Dis. 2024 Jul;12(7):e1342.. PMID: 39023424; PMCID: PMC11256882.

https://doi.org/10.1002/iid3.1342

© 2024 The Author(s). *Immunity, Inflammation and Disease* published by John Wiley & Sons Ltd. This is an open access article under the terms of the http://creativecommons.org/licenses/by/4.0/ License, which permits use, distribution and reproduction in any medium, provided the original work is properly cited.

Abstract

Background
Epidemiological data on seasonal coronaviruses (sCoVs) may provide insight on transmission patterns and demographic factors that favor coronaviruses (CoVs) with greater disease severity. This study describes the incidence of CoVs in several high-risk groups in Ottawa, Canada, from October 2020 to March 2022.

Methods
Serological assays quantified IgG and IgM antibodies to SARS-CoV-2, HCoV-OC43, HCoV-NL63, HCoV-HKU1, and HCoV-229E. Incident infections were compared between four population groups: individuals exposed to children, transit users, immunocompromised, and controls. Associations between antibody prevalence indicative of natural infection and demographic variables were assessed using regression analyses.

Results
Transit users and those exposed to children were at no greater risk of infection compared to the control group. Fewer infections were detected in the immunocompromised group ($p = .03$). SARS-CoV-2 seroprevalence was greater in individuals with low income and within ethnic minorities.

Conclusions
Our findings suggest that nonpharmaceutical interventions intended to reduce SAR-CoV-2 transmission protected populations at high risk of exposure. The re-emergence of sCoVs and other common respiratory viruses alongside SARS-CoV-2 may alter infection patterns and increase the risk in vulnerable populations.

Introduction

The impact of SARS-CoV-2 has been experienced worldwide, resulting in over 6.9 million deaths.[1] The pandemic has focused attention on the antigenically diverse coronavirus family. Seasonal coronaviruses (sCoVs) typically circulate at high levels in the community and are associated with 15%–30% of common cold cases.[2] Understanding the epidemiological data related to sCoVs may help identify factors that favor infection and inform surveillance and control strategies.[3]

The relatively high recombination and mutation rate of human coronaviruses (HCoVs) has resulted in great genetic diversity and unpredictable changes in virulence.[4] The emergence of cross-species transmission events observed with SARS-CoV-1, MERS-CoV, and SARS-CoV-2 has shown that CoVs represent an ongoing threat of emergence from multiple existing animal reservoirs. Humans are routinely infected by two genera of coronaviruses: alphacoronaviruses (HCoV-229E and HCoV-NL63) and betacoronaviruses (HCoV-OC43, HCoV-HKU1, SARS-CoV-1, MERS-CoV, and SARS-CoV-2). Seasonal coronaviruses (HCoV-OC43, HCoV-NL63, HCoV-229E, and HCoV-HKU1) are omnipresent and typically circulate in the winter months. Reinfections are a common characteristic of seasonal coronaviruses, where adults are typically infected every 2–3 years, and reinfection can occur within months of initial infection.[5, 6] Typical symptoms of sCoVs include rhinitis, headache, fever, and cough. Severe diseases and lower respiratory tract illness, such as pneumonia and bronchitis, are rare but more likely to occur in children, elderly, and immunocompromised individuals.[4]

Pre-existing immunity to SARS-CoV-2 from previous seasonal coronavirus infection has been reported.[7-9] However, the translation of neutralizing capabilities and durable cross-immunity between sCoVs and pandemic coronaviruses is not fully understood. Pre-existing immunity from sCoVs in the form of antibodies or B and T cell memory may enhance immune response to SARS-CoV-2 and reduce COVID-19 severity.[7, 10] Correlates of immunity are further complicated by cross-reactivity among coronaviruses with antigenically related epitopes. Prior sCoV exposures may negatively impact the immune response to SARS-CoV-2 infection. Boosted antibodies may

not be associated with protection or neutralization and have reduced affinity towards the novel SARS-CoV-2 virus. This suggests immune imprinting or original antigenic sin (OAS) and has been associated with negative clinical outcomes.[11-13] The relationship between SARS-CoV-2 and sCoV antibodies and immunity is unclear but does impact vaccination strategies and disease outcomes.

SARS-CoV-2 seroprevalence is highly variable among studies and is dependent on demographic characteristics, variant of concern, assay type, and public health measures in place at the time of evaluation. Ottawa, Canada, is an economically affluent city and the headquarters of multiple federal government departments and home of multiple technology companies. Almost 20% of citizens used public transit before the COVID-19 pandemic, placing it fourth among Canadian cities for proportion of usage.[14] The culturally and linguistically diverse population, with high reliance on public transit, makes Ottawa an ideal location to assess respiratory virus infection and immunity. As in most other settings, the SARS-CoV-2 wild-type was the primary local variant until March 2021. Thereafter, the alpha variant, and to a lesser extent, the delta variant became prominent in Ontario.[15] Key public health measures in place during the study period included closure or reduced capacity in public areas, limits on close contacts, stay-at-home orders, masking, utilization of remote school modalities and reduced class sizes, vaccination requirements, and travel restrictions, which all impacted population exposure risk.

Understanding sCoV epidemiology can serve as an informative model for what may be expected of SARS-CoV-2 or other emerging CoVs in a post-pandemic setting. Identifying demographic groups and factors associated with infection can be used to inform intervention methods and protect vulnerable populations. This study aimed to describe the incidence of SARS-CoV-2 and seasonal coronavirus infection in several high-risk groups in Ottawa, Ontario, from October 2020 to March 2022. We also aimed to identify demographic factors associated with coronavirus antibody prevalence acquired from natural infection.

2 Methods

Study participants were enrolled in the Stop the Spread Ottawa Study (SSO) described elsewhere.[16, 17] SSO is approved by the Ottawa Health Science Network Research Ethics Board (#2020-0481-01H). Of the 1112 participants enrolled in the initial SSO study, 245 were selected for this cross-sectional nested cohort analysis (Figure 1). Participants were prioritized for inclusion if they had plasma samples available from three separate time points: baseline, Month 3, and Month 10. If samples were unavailable from these time points, the sample collected closest to the time point of interest was selected. All visits occurred between October 22, 2020 and February 28, 2022. Covariates suspected to influence SARS-CoV-2 seroprevalence were determined a priori. Missing demographic variables from participant questionnaires were verified using medical records where available and by participant call-back. The main outcome of interest was incident HCoV-OC43, HCoV-NL63, HCoV-229E, HCoV-HKU1, and SARS-CoV-2 infections (Supporting Information S1: Appendix Table 1). Incident infections were compared between population groups of interest. We also assessed associations between demographic characteristics and antibody prevalence. Seasonal coronavirus IgG titers were used to assess associations with demographic variables because all participants were seropositive at baseline. Serology methodology, infection definitions, and cutoff points can be found in Section 2.2.

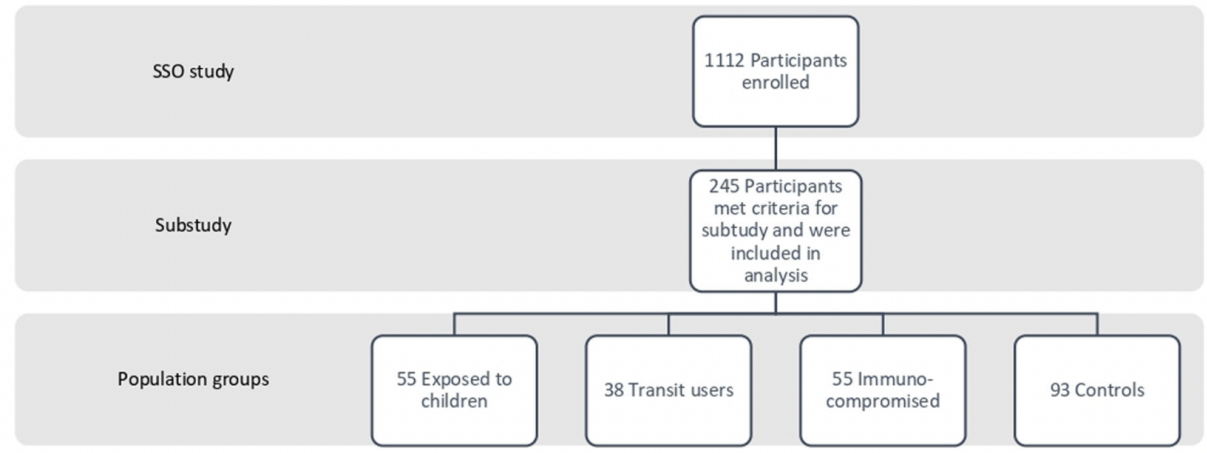


Figure 1. Flow diagram of participants selected from Stop the Spread Ottawa study for the subgroup analysis presented in this article.

2.1 Population groups

Participants were selected for this study if they met the criteria for one of three population groups of interest: high level of exposure to children at home or in the workplace, transit users or those that work in the public transportation industry, or immunocompromised individuals. Participants were categorized into the group exposed to children if they worked in a school or daycare or lived with one or more children in their household. Participants were classified in the transit user group they used public transportation at least once a week on average across follow-up or worked in the public transportation industry (i.e., city bus operator, lightrail operator, and taxi driver). Participants were classified as immunocompromised if they had a primary or secondary immunodeficiency or required immunomodulatory treatment incorporating a range of conditions such as multiple sclerosis, rheumatoid arthritis, cancer, diabetes, HIV, asthma or COPD requiring medication, and organ/bone marrow transplant recipients. A control group of healthy individuals with minimal to no exposure to transit or children was included. Participants who met inclusion criteria for more than one group were categorized into the group with greater hypothesized exposure. Those exposed to children and transit users were hypothesized to be at greater risk of exposure compared to the control group. Children are frequently identified as the index case of respiratory disease in households and are known to be the primary drivers of viral transmission in the community, increasing exposure in this group.[18, 19] Use of or work in the public transportation industry involves prolonged social contact in an enclosed space which has historically been assumed to increase the risk of respiratory virus transmission.[20] If a participant was both exposed to children and a transit user, they were categorized as a transit user. Immunocompromised individuals were hypothesized to be at reduced risk as we assumed they would take more precautions to avoid exposure. Sensitivity analyses were conducted removing participants that met criteria for more than one group.

2.2 Laboratory methods

Immunoglobulin G (IgG) titers (BAU/mL) against SARS-CoV-2 spike (S), receptor binding domain (RBD), and nucleocapsid (N) proteins in participant serum were quantified using a high throughput chemiluminescent direct ELISA as described before.[21] Incident COVID-19 infections were identified through serology and self-report of positive PCR and rapid antigen test (RAT). Self-reported positive results were validated using medical records where possible. Natural immunity was defined if a participant was positive (signal-to-cut-off [SCO] > 1) for anti-N IgG

and either anti-S or anti-RBD IgG. Thresholds were established at a rate of 3% false discover rate (FDR) from the density distribution of pre-pandemic sera. In the event of indiscriminate positive serum samples for those with no self-reported test results, natural immunity was determined by examining the signal strength (magnitude of SCO) and the preceding and subsequent serum results.17 Participants with an infection confirmed by PCR or positive serology before baseline visit were considered SARS-CoV-2 seropositive at baseline.

Plasma IgG and IgM titers (relative luminescent units [RLUs]) against HCoV-OC43, HCoV-HKU1, HCoV-229E, and HCoV-NL63 spike proteins were quantified using a chemiluminescent ELISA modified from previously described assays.[21, 22] Both IgG and IgM were measured at a single dilution and data was scaled to account for inter-plate variability. The distribution of fold changes for each sCoV was evaluated separately. It was assumed that in most cases, there would be limited CoV infection during the period of evaluation, so any changes in antibody titer caused by infection would appear as an outlier.[6] A twofold increase in titer between paired samples was used to define IgG seroconversion. Acute infection was defined if the IgM titer was greater than the mean +(3SD/2SD). Examination of IgG and IgM titers over time was used to verify infection in all instances where either IgG or IgM seroconversion was observed. Serology results where a participant tested positive for more than one seasonal coronavirus at a single time point were assumed to indicate cross-reactivity rather than a co-infection. It was assumed the infection was caused by the most prevalent seasonal coronavirus in the Ottawa region. Infections were classified using the following hierarchal ranking system from highest to lowest expected prevalence: OC43 > NL63 > HKU1 > 229E.[23-26]

2.3 Statistical analysis

Categorical or dichotomous variables were presented as proportions. Continuous variables with a normal distribution were presented as means with standard deviation. Normality of data was assessed using Q-Q plots and histograms. Linearity was assessed through visual inspection of scatter plots. Differences between categorical or dichotomous variables were assessed using chi-square tests. Differences between continuous variables were assessed using Student's *t* test. The number of incident infections was compared between groups using the chi-square test and Fisher's exact test for small cell sizes. The groups exposed to children and public transit were combined

and classified as a high-risk group where sample size was a concern. SARS-CoV-2 seropositivity resulting from natural infection was used as the dependent variable in logistic regression. HCoV-NL63, HCoV-OC43, HCoV-HKU1, and HCoV-229E IgG antibody titers were used as dependent variables in generalized linear models. A univariate regression analysis was performed as part of an exploratory analysis for all variables to determine associations between SARS-CoV-2 seroprevalence and sCoV antibody titers and demographic variables. Variables that were significant using a cutoff of 0.2 or were determined clinically important a priori were added to a multivariable model. Likelihood ratio tests were used to assess the fit of nested models. Logistic regression model fit was evaluated using the Hosmer–Lemeshow test and ROC statistics. Results were presented as odds ratios (ORs) and 95% confidence intervals (CIs). Residual plots were used to assess the model fit of linear models. Variable estimates and *p* values were presented. Sensitivity analyses were conducted removing participants that fit the criteria for more than one population group. The significance level was defined at $p < .05$. All analyses were conducted using SAS Analytics Software.

3 Results

3.1 Participant characteristics

Two-hundred forty-five participants were included in the analysis. Fifty-five were identified as exposed to children, 38 were classified as transit users, 59 were immunocompromised, and 93 served as controls. The demographic characteristics of all participants are reported in Table 1. Across all participants, the average age was 50 years, 54.7% were women, 91.0% were white, and 63.6% had at least a university degree. A comparison of demographic characteristics between each population group of interest and the control group revealed transit users and those exposed to children to be younger ($p < .01$, $p < .01$), and that those exposed to children have a higher household income ($p < .01$). The immunocompromised group was older ($p = .02$) and more likely to be male compared to the control group ($p = .02$).

Table 1. Characteristics of 245 participants stratified into population groups of interest.

Characteristic	All participants ($n = 245$)	Population group				p Value
		Exposed to children ($n = 55$)	Transit user ($n = 38$)	Immuno-compromised ($n = 59$)	Control ($n = 93$)	
Sex (n, %)						
Female	134 (54.69)	34 (61.82)	23 (60.53)	23 (38.98)	54 (58.06)	.047
Male	111 (45.31)	21 (38.18)	15 (39.47)	36 (61.02)	39 (41.94)	
Age (mean, SD)	50 (14.21)	46 (9.15)	42 (14.06)	57 (12.18)	51 (15.71)	<.001
Income (n, %)						
<$59,999	40 (16.33)	3 (5.45)	8 (21.05)	16 (27.12)	13 (13.98)	<.001
$60,000–89,999	44 (17.96)	3 (5.45)	9 (23.68)	14 (23.73)	18 (19.35)	
$90,000–119,999	43 (17.55)	14 (25.45)	5 (13.16)	11 (20)	13 (13.98)	
>$120,000	93 (37.96)	34 (61.82)	13 (34.21)	18 (19.35)	34 (36.56)	
No response	25 (10.20)	1 (1.82)	3 (7.89)	6 (10.17)	15 (16.13)	
Ethnicity (n, %)						
White	223 (91.02)	50 (90.91)	34 (89.47)	51 (86.44)	88 (94.62)	.214[b]
Other[a]	22 (8.98)	5 (9.10)	4 (10.53)	8 (13.56)	5 (5.38)	
Education (n, %)						
Highschool or less	20 (8.16)	3 (5.45)	6 (15.79)	4 (6.78)	7 (7.53)	.557[b]
Trade/college	62 (25.31)	10 (18.18)	9 (23.68)	20 (33.90)	23 (24.73)	
Bachelor's degree	100 (40.82)	26 (47.27)	12 (31.58)	22 (37.29)	40 (43.01)	
Graduate or higher	56 (22.86)	16 (29.09)	10 (26.32)	10 (16.95)	20 (21.51)	
No response	7 (2.86)	0	1 (2.7)	3 (5.45)	3 (2.94)	
Smoking status (n, %)						
Current smokers	14 (5.71)	2 (3.64)	3 (7.89)	6 (10.17)	3 (3.23)	.216[b]
Non-smokers	231 (94.29)	53 (96.36)	35 (92.11)	53 (89.83)	90 (96.77)	

Note: Continuous variables are presented as mean (SD) and categorical variables presented as N (%). Differences between groups were assessed using Student's t tests for continuous variables and chi-square tests for categorical variables.

[a]Ethnicity was classified as either white or other due to small number of nonwhite participants. The "other" category included the following ethnicities: South Asian ($n = 5$), West Asian ($n = 4$), Filipino ($n = 2$), Latin American ($n = 2$), Indigenous ($n = 2$), Black ($n = 1$), Chinese ($n = 1$), and Other ($n = 5$).

[b]Groups exposed to children and transit users combined to account for small cell sizes.

3.2 Incident infections

Among the 245 participants, 34 (13.9%) had antibody titers to SARS-COV-2, HCoV-OC43, HCoV-NL63, HCoV-E229, or HCoV-HKU1 over the 16-month follow-up period suggestive of recent infection. Incident SARS-CoV-2 infections were identified in 12 (4.9%) participants, and 23 (9.4%) participants were recently infected by at least one sCoV (Table 2). HCoV-HKU1 was

the most common sCoV identified (proportion with an infection: 5.3% [$n = 13$]), followed by HCoV-OC43 (3.3% [n = 8]), HCoV-NL63 (0.8% [n = 2]), and HCoV-229E (no infections detected). Among the population groups of interest, the proportion with sCoV infection was greatest among the control group (14.0% [$n = 13$]), followed by those exposed to children (9.1% [$n = 5$]), transit users (7.9% [$n = 3$]), and immunocompromised participants (3.4% [$n = 2$]) (Table 2). The proportion of participants with sCoV infection(s) did not differ between those exposed to children, transit users, and our control group. Considerably fewer infections were observed in those with an immune compromising condition compared to the control group ($p = .03$). At baseline, all 245 participants had elevated plasma IgG for HCoV-229E, HCoV-NL63, HCoV-HKU1, and HCoV-OC43 and 70 (28.6%) of participants were seropositive for SARS-CoV-2, denoting a prior infection. The control group had the greatest number of SARS-CoV-2 anti-N seropositive participants (44.0% [$n = 41$]), followed by those exposed to children (30.9% [$n = 17$]), transit users (18.4% [n = 7]) and immunocompromised individuals (8.5% [$n = 5$]) (Table 3).

Table 2. Number of coronavirus infections detected among 245 participants from October 22, 2020, to February 28, 2022 stratified by population group.

		Participant group			
Virus	Total participants ($n = 245$)	Control ($n = 93$)	Exposed to children ($n = 55$)	Transit ($n = 38$)	Immuno-compromised ($n = 59$)
SARS-CoV-2	12 (4.9)	5 (5.38)	4 (7.27)	1 (2.63)	2 (3.39)
HCoV-HKU1	13 (5.31)	9 (9.68)	2 (3.64)	1 (2.63)	1 (1.69)
HCoV-OC43	8 (3.27)	3 (3.23)	3 (5.45)	2 (5.26)	0 (0)
HCoV-NL63	2 (0.82)	1 (1.08)	0 (0)	0	1 (1.08)
HCoV-229E	0 (0)	0 (0)	0 (0)	0	0 (0)
Total sCoV[b]	23 (9.39)	13 (13.98)	5 (9.09)[a]	3 (7.89)	2 (3.39)*
Total CoV[c]	34 (13.88)	18 (19.35)	8 (14.55)[a]	4 (10.53)	4 (6.78)*

Note: Comparisons between those exposed to children, transit users, and immunocompromised groups and the control group were conducted using Fisher's exact test. Results are presented as the number of participants infected by each virus (*N*) and the proportion of the group infected (%).

*Significant at $p < .05$.

[a]Chi-square test used.

[b]Number (%) of participants that tested positive for HCoV-NL63, HCoV-OC43, HCoV-HKU1, or HCoV-229E.

[c]Number (%) of participants that tested positive for HCoV-NL63, HCoV-OC43, HCoV-HKU1, HCoV-OC43, and SARS-CoV-2. A participant in the group with exposure to children tested positive for SARS-CoV-2 and HCoV-OC43, so sCoV and SARS-CoV-2 infections do not sum to the total in the "Total Participants" and "Exposed to children" columns.

Table 3. Demographic variables of 245 participants stratified by SARS-CoV-2 seropositivity status indicative of prior natural infection.

Variable	SARS-CoV-2 Seropositive ($n = 70$)	SARS-CoV-2 Seronegative ($n = 175$)	OR	95% CI
Population group				
Exposed to children	17/55 (30.90)	38/55 (69.09)	0.81	0.35–1.86
Transit user	7/38 (18.42)	31/38 (81.58)	**0.35**	**0.13–0.96**
Immunocompromised	5/59 (8.47)	54/59 (91.53)	**0.05**	**0.02–0.17**
Control	41/93 (44.09)	52/93 (55.91)	Ref	Ref
Sex				
Male	34/111 (30.63)	77/111 (69.37)	Ref	Ref
Female	36/134 (26.87)	98/134 (73.13)	0.58	0.29–1.16
Ethnicity				
White	59/223 (26.46)	164/223 (73.54)	Ref	Ref
Other	11/22 (50.0)	11/22 (50.0)	**6.73**	**2.06–21.94**
Age	53.04 (SD: 15.29)	48.77 (13.60)	**1.04**	**1.02–1.07**
Smoking status				
Smoker	1/14 (7.14)	13/14 (92.86)	0.25	0.03–2.38
Nonsmoker	69/231 (29.87)	162/231 (70.13)	Ref	Ref
Education				
Highschool or less	7/27 (25.93)	20/27 (74.07)	0.77	0.21–2.78
Trade/college	13/62 (20.97)	49/62 (79.03)	0.59	0.22–1.58
Bachelor's degree	34/100 (34.0)	66/100 (66.0)	1.24	0.53–2.89
Masters' or higher	16/56 (28.57)	40/56 (71.43)	Ref	Ref
Income				
<$59,999	13/20 (65.0)	7/20 (35.0)	**3.14**	**1.06–9.27**
$60,000–$89,999	10/44 (22.72)	34/44 (77.27)	0.96	0.35–2.64
$90,000–$120,000	8/43 (18.60)	35/43 (81.40)	0.76	0.27–2.10
+$120,000	28/93 (30.11)	65/93 (69.89)	Ref	Ref

Note: Continuous variables are presented as mean (SD), and categorical variables are presented as the number of seropositive participants divided by the number of participants in that group (%). Multivariate logistic regression was used to assess associations between SARS-CoV-2 seroprevalence and demographic variables at baseline, presented as odds ratios (ORs) and 95% confidence intervals (CIs). Significant associations are highlighted.

3.3 Factors associated with natural infection

SARS-CoV-2 seropositivity suggestive of natural infection was greater in older participants, those with a household income less than $59,999 and those of ethnic minority in a multivariable logistic regression analysis (Table 3). The odds of seropositivity was no greater in those exposed to children compared to our control group. Immunocompromised individuals were less likely to have anti-N SARS-CoV-2 antibodies at baseline (OR: 0.05; 95% CI: 0.02–0.17) compared to our control group. Increasing age had a small positive association with SARS-CoV-2 antibody prevalence (OR: 1.04; 95% CI: 1.02–1.07). The odds of seropositivity was more than six times greater in those of ethnic minority compared to white participants (OR: 6.73, 95% CI: 2.06–21.94). The odds of seropositivity increased threefold in those with a household income less than $59,999 compared to those reporting a household income greater than $120,000 (OR: 3.14; 95% CI: 1.06–9.27). Increasing number of children in the household and level of public transportation use were not associated with SARS-CoV-2 seroprevalence (Supporting Information S1: Appendix Table 2).

Few associations were found between anti-sCoV IgG antibody titers and demographic characteristics in multivariate linear regression models adjusted for age, sex, smoking status, income, education, and ethnicity (Table 4). Of consequence, smokers were found to have higher anti-HCoV-HKU1 antibody titers compared to non-smokers ($p = .03$). Those that used public transportation daily or worked in the transportation industry were found to have higher anti-HCoV-HKU1 antibody titers compared to those that did not use public transit but this result was not consistent across the four sCoVs. Sensitivity analyses excluding participants that may have been categorized in more than one population group ($n = 28$) showed no appreciable change in results, with limited changes in p values and magnitude of effect (Supporting Information S1: Appendix Table 3).

Table 4. Demographic characteristics associated with coronavirus antibody titers for 245 participants at baseline.

	HKU1		OC43		NL63		229E	
Variable	**Estimate**	***p* Value**	**Estimate**	***p* Value**	**Estimate**	***p* Value**	**Estimate**	***p* Value**
Population group								
Control	Ref	Ref	Ref	Ref	Ref	Ref	Ref	Ref
Exposed to children	0.06	.38	0.01	.89	−0.01	.99	0.03	.77
Transit Users	0.10	.17	0.02	.85	−0.08	.35	−0.06	.48
Immunocompromised	−0.08	.20	−0.13	.13	−0.06	.42	−0.08	.34
Male	Ref	Ref	Ref	Ref	Ref	Ref	Ref	Ref
Female	0.05	.80	<0.01	.95	0.02	.72	−0.07	.25
Age	0.001	.53	<0.01	.80	<−0.01	.88	<−0.01	.28
Nonsmoker	Ref	Ref	Ref	Ref	Ref	Ref	Ref	Ref
Current smoker	0.11	**.03**	0.05	.71	−0.20	.12	−0.15	.26
Household income								
+$120,000	Ref	Ref	Ref	Ref	Ref	Ref	Ref	Ref
<$59,999	−0.14	.06	−0.05	.65	−0.03	.72	0.01	.91
$60,000–$89,999	−0.03	.69	−0.08	.42	−0.07	.40	−0.11	.20
$90,000–$120,000	−0.02	.76	−0.10	.30	−0.09	.31	−0.03	.74
Education								
Masters or higher	Ref	Ref	Ref	Ref	Ref	Ref	Ref	Ref
Highschool or less	−0.04	.66	−0.06	.64	−0.16	.19	−0.18	.14
Trade/college	−0.06	.39	−0.10	.31	−0.06	.50	0.04	.67
Bachelor's degree	<−0.01	.99	0.03	.73	−0.07	.38	−0.11	.15
White ethnicity	Ref	Ref	Ref	Ref	Ref	Ref	Ref	Ref
Nonwhite ethnicity	0.08	.34	0.18	.12	0.08	.45	0.03	.72

Note: Multivariate linear regression analysis was used to assess associations. Separate models were used for each virus. Results significant at the $p < .05$ level are highlighted.

4 Discussion

The proportion of the study population with incident sCoV infections was 9.4%. Similar values were reported in the Ottawa region by the Eastern Ontario Regional Laboratory Association regional reference laboratory lab, where sCoV percent positivity ranged from 0% to 10% from October 2020 to December 2021.[27] Given the ubiquitous nature of seasonal coronaviruses and high frequency of reinfections,[5] under normal circumstances it is expected that

most participants would experience a sCoV infection within the follow-up period. A dramatic decline in common respiratory viruses, including influenza, RSV, parainfluenza viruses, rhinovirus, and sCoVs, was observed worldwide following the introduction of SARS-COV-2.[28-30] This phenomenon has been partially attributed to public health-mandated nonpharmaceutical COVID-19 interventions initiated to slow SARS-CoV-2 transmission. These measures appear to have been effective in reducing sCoV transmission as well, contributing to the low number of incident infections observed in this observation period.

While children have been documented to have lower prevalence and severity of COVID-19,[31, 32] they still play an important role in SARS-CoV-2 transmission. Hundreds of students mix in an often crowded and poorly ventilated indoor school environment facilitating transmission.[33] Additionally, children are more likely to have mild or asymptomatic infections and unknowingly propagate outbreaks among households and communities.[32] In contrast to our analysis, a higher risk of SARS-CoV-2 infection has been reported in adults living with children in the United States34 and the United Kingdom.[35] Other studies in North America have found that SARS-CoV-2 infection was no greater among school staff than in the community and that most COVID-19 cases among students and teachers were acquired outside the school environment.[36-38] One of these studies was conducted in Ontario during the first wave of the pandemic.[37] As with our cohort, participants in this study were subject to similar community-based nonpharmaceutical public health interventions so we believe it is appropriate to compare results between studies. A possible explanation for the discrepancy between the above-mentioned studies is that Ontario schools were closed for a total of 20 weeks (March 14 to May 15, 2021), substantially longer than in any other Canadian province or territory.[39] Intermittent school closures and shifts to online learning likely reduced exposure in this group and contributed to the reduced number of infections detected in SSO. Pre-existing immunity caused by frequent respiratory infections has been proposed as a mechanism to explain lower susceptibility to SARS-CoV-2 infection in children.[35, 40] A similar mechanism may explain why adults exposed to children experienced fewer SARS-CoV-2 infections. Adults living with children have been shown to experience more frequent respiratory infections than those who do not live with children, which may provide a greater degree of immune-mediated protection against SARS-CoV-2.[41]

The proportion of transit users with CoV infections was comparable to our control group despite the hypothesized increased risk of exposure. The small number of CoV infections detected in transit users may be a consequence of effective public health measures implemented at the start of the pandemic to protect both transit users and operators. This included frequent cleaning and disinfection of facilities and high-touch surfaces, limited capacity, and installation of physical barriers.[42, 43] The considerable decline in transit ridership observed in Canada and worldwide throughout the pandemic[20, 44] may also explain why fewer infections were observed in transit users. The reduction in transit usership was partially attributed to reduced travel demand in response to stay-at home orders[44] and the greater perception of SARS-CoV-2 transmission risk associated with public transit use.[20] The restrictions on capacity and reduced ridership limited crowding and allowed those who continued to use public transit during the pandemic adequate space to maintain physical distancing recommendations. Similarly, the perception of increased risk may have encouraged adherence to recommended public health protocols. The light rail transit system in Ottawa was also shut down for several months during the study period for mechanical issues which may have altered transit usage. SARS-CoV-2 transmission risk while using public transit has been correlated with exposure time.[45] While this occurrence was not consistently observed in this study, those who used public transit at least several times a week had higher anti-HKU1 IgG antibody titers compared to those who did not use public transit at all (Supporting Information S1: Appendix Table 2). We were unable to assess for similar trends with HCoV-OC43, HCoV-NL63, and HCoV-229E due to low incidence.

Immunocompromised individuals had reduced odds of SARS-CoV-2 seropositivity from natural infection at baseline and fewer CoV infections over the period of observation compared to our controls. Insufficient serological response to COVID-19 vaccination has also been observed in solid organ transplant recipients receiving immunosuppressive agents.[46] Disparities in antibody kinetics may explain why fewer infections were observed in the immunocompromised individuals. These individuals may develop fewer antibodies in response to natural infection or vaccination or experience rapid antibody waning. Alternatively, immunocompromised individuals and those with a higher burden of comorbidities are at greater risk of severe disease if infected by SARS-CoV-2 or other common respiratory viruses. These individuals may have taken more precautions during the COVID-19 pandemic to avoid exposure such as limiting close contacts, avoiding crowds, and

adhering more strictly to public health measures. As public health restrictions are removed, policymakers and healthcare professionals should be aware that this population remains at risk and may require continued special measures.

Few demographic variables were correlated with baseline IgG titers against HCoV-HKU1, HCoV-NL63, HCoV-229E, and HCoV-OC43. The high prevalence of these viruses resulted in antibody titers being consistently high among all individuals, leading to difficulties in detecting any titer differences between groups. By contrast, most of the population was naïve to SARS-CoV-2, enabling detection of differences in levels of exposure between demographic groups. The odds of seroprevalence were greater in those with a low household income and of ethnic minority. Our findings add to extensive evidence showing the burden of SARS-CoV-2 is greater among minority groups and those of low socioeconomic status.[47, 48] Many factors may contribute to demonstrated inequities, such as living in more crowded households, education and finances, language or cultural barriers, and increased work in an environment that required in-person presence during the pandemic.

The strengths of this study include well-characterized reports of clinical and self-reported data. We were able to analyze multiple serial blood samples for each participant with a low attrition rate over time. The combined use of serology, self-reported PCR and RAT tests, and clinical symptoms reduce misclassification of COVID-19 infections. Finally, the shifting landscape of public health measures and emerging variants of concern complicates the interpretation of SARS-CoV-2 seroprevalence in other studies. This issue was less impactful with SSO as almost all samples were collected before the arrival of the Omicron variant.

This study is subject to several limitations. The study cohort consisted of highly educated, high-income individuals with limited ethnic diversity, which limited our ability to infer associations within lower socioeconomic groups and reduced the generalizability of results. Several factors complicate the interpretation of sCoV serology results. First, the World Health Organization does not have standardized guidelines for units, controls, or recommended thresholds when reporting sCoV serology results, so determining a threshold of infection can be challenging. Similarly, almost all individuals have detectable antibodies indicating a prior infection, so obtaining a true

negative control is difficult. Evaluation of IgG and IgM titers over time were used to verify infection. However, in some cases, samples were not available from all desired time points, and the interval between available samples was too broad to detect a rise in antibody titers. For this reason, sCoV infection incidence is likely underreported and we were not always able to determine when a seasonal coronavirus infection occurred with precision. Longitudinal antibody kinetics and serologic response to infection vary by individual and are dependent on many factors including demographics, comorbidities, and disease severity.[49] The heterogeneity in antibody response may underestimate the number of detected infections. Several participants tested positive for more than one coronavirus and one participant tested positive for all four sCoVs (Supporting Information S1: Appendix Table 4). Cross-reactivity among CoVs is a well-documented concern with CoV serology[10, 50] and simultaneous infection for all viruses is highly improbable. Unfortunately, only one antigen was used in the serological assay and acute infection were not diagnosed by PCR, so we are unable to corroborate assay results. Future studies may consider the use of multiple antigens to improve the reliability of sCoV results. Analysis of other common respiratory viruses, including influenza and RSV in at-risk populations, would enhance our coronavirus-specific observations.

5 Conclusion

This analysis demonstrates that CoV incidence was reduced in immunocompromised individuals and similar between those exposed to children, transit users, and controls. This is likely a consequence of effective nonpharmaceutical public health interventions which limit viral transmission. Relaxation of these measures has resulted in a return of sCoV and other common respiratory viruses including influenza and RSV. The reappearance of seasonal respiratory viruses may have a greater impact on individuals of nonwhite ethnicity, those of low socioeconomic status, and those with an immunocompromising condition. The lasting presence of SARS-CoV-2 in a post-pandemic era may continue to alter seasonal respiratory virus circulation and have consequences for population susceptibility to disease.

Author Contributions
Aliisa Heiskanen: Conceptualization; data curation; formal analysis; methodology; writing—original draft; writing—review and editing. Yannick Galipeau: Data curation; methodology; writing—review and editing. Julian Little: Writing—review and editing. Marc-André Langlois: Writing—review and editing. Curtis L. Cooper: Conceptualization; formal analysis; methodology; supervision; writing—original draft; writing—review and editing.

Acknowledgments
This research was supported by a Canadian Institute of Health Research (CIHR) grant (VR2-172722) and from a supplement by the COVID-19 Immunity Task Force (CITF) to M.-A.L. Additionally, Y.G. is supported by a Charles Best and Frederick Banting CGS-D from CIHR (476885). M.-A.L. holds a Faculty of Medicine Chair of Excellence in Pandemic Viruses and Preparedness Research.

Conflict of interest statement
The authors declare no conflict of interest.

Ethics statement
All participants provided informed consent. Stop the Spread Ottawa study is approved by the Ottawa Health Science Network Research Ethics Board (#2020-0481-01H).

Supplementary material
iid31342-sup-0001-CoV_Manuscript_Appendix.docx

References

1. World Health Organization. WHO Coronavirus (COVID 19)Dashboard. World Health Organization. n.d. https://covid19.who.int/
2. Harrison CJ, Weldon WC, Pahud BA, Jackson MA, Oberste MS,Selvarangan R. Neutralizing antibody against enterovirus d68 inchildren and adults before 2014 outbreak, Kansas City, Missouri,USA1. Emerging Infect Dis. 2019;25(3):585 588. doi:10.3201/eid2503.180960
3. Nickbakhsh S, Ho A, Marques DFP, McMenamin J,Gunson RN, Murcia PR. Epidemiology of seasonal corona-viruses: establishing the context for the emergence ofcoronavirus disease 2019. J Infect Dis. 2020;222(1):17 25.doi:10.1093/infdis/jiaa185
4. Su S, Wong G, Shi W, et al. Epidemiology, geneticrecombination, and pathogenesis of coronaviruses. TIM.2016;24(6):490 502.
5. Callow KA, Parry HF, Sergeant M, Tyrrell DA. The timecourse of the immune response to experimental coronavirusinfection of man. Epidemiol Infect. 1990;105(2):435 446.
6. Edridge AWD, Kaczorowska J, Hoste ACR, et al. Seasonalcoronavirus protective immunity is short lasting. Nature Med.2020;26(11):1691 1693. doi:10.1038/s41591-020-1083-1
7. Wang Y, Zhang L, Sang L, et al. Kinetics of viral load andantibody response in relation to COVID 19 severity. J ClinInvest. 2020;130(10):5235 5244.
8. de Vries RD. SARS CoV 2 specific T cells in unexposedhumans: presence of cross reactive memory cells does notequal protective immunity. Signal Transduct Target Ther.2020;5(1):224.
9. Kaplonek P, Wang C, Bartsch Y, et al. Early cross coronavirusreactive signatures of humoral immunity against COVID 19.Sci Immunol. 2021;6(64):eabj2901.
10. Lineburg KE, Grant EJ, Swaminathan S, et al. CD8+ T cellsspecific for an immunodominant SARS CoV 2 nucleocapsidepitope cross react with selective seasonal coronaviruses.Immunity. 2021;54(5):1055 1065.e5.
11. Aguilar Bretones M, Fouchier RA, Koopmans MP, vanNierop GP. Impact of antigenic evolution and originalantigenic sin on SARS CoV 2 immunity. J Clin Invest.2023;133(1):e162192.
12. Aguilar Bretones M, Westerhuis BM, Raadsen MP, et al.Seasonal coronavirus specific B cells with limited SARS CoV 2cross reactivity dominate the IgG response in severe COVID 19.J Clin Invest. 2021;131(21):e150613.
13. Focosi D, Genoni A, Lucenteforte E, et al. Previous humoralimmunity to the endemic seasonal alphacoronaviruses NL63 and229E is associated with worse clinical outcome in COVID 19 andsuggests original antigenic sin. Life. 2021;11(4):298.
14. Layton AT, Sadria M. Understanding the dynamics of SARS CoV 2 variants of concern in Ontario, Canada: a modelingstudy. Sci Rep. 2022;12(1):2114.
15. Government of Canada, Statistics Canada. Census inBrief: Commuters Using Sustainable Transportation InCensus Metropolitan Areas. Statistics Canada; 2017.10 of 12 | HEISKANEN ET AL .https://www12.statcan.gc.ca/census-recensement/2016/as-sa/98-200-x/2016029/98-200-x2016029-eng.cfm?wbdisable=true
16. Collins E, Galipeau Y, Arnold C, et al. Cohort profile: stop thespread Ottawa (SSO)—a community based prospective cohortstudy on antibody responses, antibody neutralisation effi-ciency and cellular immunity to SARS CoV 2 infection andvaccination. BMJ Open. 2022;12(9):e062187.
17. Keeshan A, Galipeau Y, Heiskanen A, et al. Results of the stopthe spread Ottawa (SSO) cohort study: a Canadian urban based prospective evaluation of antibody responses andneutralisation efficiency to SARS CoV 2 infection and vacci-nation. BMJ Open. 2023;13(10):e077714. doi:10.1136/bmjopen-2023-077714
18. Viboud C, Boëlle PY, Cauchemez S, et al. Risk factors ofinfluenza transmission in households. Br J Gen Pract.2004;54(506):684 689.

19. Monto AS, Malosh RE, Petrie JG, Thompson MG, Ohmit SE.Frequency of acute respiratory illnesses and circulation ofrespiratory viruses in households with children over 3surveillance seasons. J Infect Dis. 2014;210(11):1792 1799.
20. Zafri NM, Khan A, Jamal S, Alam BM. Risk perceptions ofCOVID 19 transmission in different travel modes. Transp ResInterdiscip Perspect. 2022;13:100548.
21. Colwill K, Galipeau Y, Stuible M, et al. A scalable serologysolution for profiling humoral immune responses to SARS CoV 2 infection and vaccination. Clin Transl Immunol.2022;11(3):1380.
22. Galipeau Y, Siragam V, Laroche G, et al. Relative ratios ofhuman seasonal coronavirus antibodies predict the efficiencyof cross neutralization of SARS CoV 2 spike binding to ACE2.EBioMedicine. 2021;74:103700.
23. Killerby ME, Biggs HM, Haynes A, et al. Human coronaviruscirculation in the United States 2014–2017. J Clin Virol.2018;101:52 56.
24. Zimmermann P, Curtis N. Coronavirus infections in childrenincluding COVID 19: an overview of the epidemiology,clinical features, diagnosis, treatment and prevention optionsin children. Pediatr Infect Dis J. 2020;39(5):355 368.
25. Gaunt ER, Hardie A, Claas ECJ, Simmonds P, Templeton KE.Epidemiology and clinical presentations of the four humancoronaviruses 229E, HKU1, NL63, and OC43 detected over3 years using a novel multiplex real time PCR method. J ClinMicrobiol. 2010;48(8):2940 2947.
26. Cabeça TK, Granato C, Bellei N. Epidemiological and clinicalfeatures of human coronavirus infections among differentsubsets of patients. Influenza Other Respir Viruses. 2013;7(6):1040 1047.
27. Heiskanen A, Galipeau Y, Little J, et al. Seasonal respiratoryvirus circulation was diminished during the COVID 19pandemic. Influenza Other Respir Viruses. 2023;17(1):e13065.
28. Groves HE, Piché Renaud PP, Peci A, et al. The impact of theCOVID 19 pandemic on influenza, respiratory syncytial virus,and other seasonal respiratory virus circulation in Canada:a population based study. Lancet Reg Health Am. 2021;1:100015.
29. Yeoh DK, Foley DA, Minney Smith CA, et al. Impact ofcoronavirus disease 2019 public health measures on detectionsof influenza and respiratory syncytial virus in children duringthe 2020 Australian winter. Clin Infect Dis. 2021;72(12):2199 2202.
30. Olsen SJ, Winn AK, Budd AP, et al. Changes in influenzaand other respiratory virus activity during the COVID 19pandemic—United States, 2020–2021. Morb Mortal Wkly Rep.2021;70(29):1013.
31. Brodin P. SARS CoV 2 infections in children: understandingdiverse outcomes. Immunity. 2022;55:201 209.
32. Poletti P, Tirani M, Cereda D, et al. Association of age withlikelihood of developing symptoms and critical disease amongclose contacts exposed to patients with confirmed SARS CoV 2 infection in Italy. JAMA Netw Open. 2021;4(3):e211085.
33. Pierce CA, Herold KC, Herold BC, et al. COVID 19 andchildren. Science. 2022;377(6611):1144 1149.
34. Lessler J, Grabowski MK, Grantz KH, et al. HouseholdCOVID 19 risk and in person schooling. Science. 2021;372(6546):1092 1097.
35. Forbes H, Morton CE, Bacon S, et al. Association between livingwith children and outcomes from covid 19: OpenSAFELY cohortstudy of 12 million adults in England. BMJ. 2021;372:n628.
36. Watts AW, Mâsse LC, Goldfarb DM, et al. SARS CoV 2 cross sectional seroprevalence study among public school staff inMetro Vancouver after the first Omicron wave in BritishColumbia, Canada. BMJ Open. 2023;13(6):e071228.
37. Naimark D, Mishra S, Barrett K, et al. Simulation basedestimation of SARS CoV 2 infections associated withschool closures and community based nonpharmaceuticalinterventions in Ontario, Canada. JAMA Netw Open.2021;4(3):e213793. doi:10.1001/jamanetworkopen.2021.3793
38. Varma JK, Thamkittikasem J, Whittemore K, et al. COVID 19infections among students and staff in New York City publicschools. Pediatrics. 2021;147(5):e2021050605.
39. Gallagher Mackay K, Srivastava P, Underwood K, et al.COVID 19 and Education Disruption in Ontario: EmergingEvidence on Impacts; 2021.

40. Zimmermann P, Curtis N. Why is COVID 19 less severe inchildren? A review of the proposed mechanisms underlyingthe age related difference in severity of SARS CoV 2 infec-tions. Arch Dis Child. 2021;106(5):429 439.
41. Viner RM, Mytton OT, Bonell C, et al. Susceptibility to SARS CoV 2 infection among children and adolescents comparedwith adults: a systematic review and meta analysis. JAMAPediatr. 2021;175(2):143 156.
42. Pringle J. Ottawa's transit service making face masks manda-tory for staff and passengers. CTV News; 2020. https://ottawa.ctvnews.ca/ottawa-s-transit-service-making-face-masks-mandatory-for-staff-and-passengers-1.4958933
43. Charron J. OC Transpo implements additional measures tomake work environment safe after spike in covid cases. CTVNews; 2020. https://ottawa.ctvnews.ca/oc-transpo-implements-additional-measures-to-make-work-environment-safe-after-spike-in-covid-cases-1.5075899
44. Diaz F, Abbasi SJ, Fuller D, Diab E. Canadian transit agenciesresponse to COVID 19: understanding strategies, informationaccessibility and the use of social media. Transp Res InterdiscipPerspect. 2021;12:100465.
45. Zhao Q, Qi Y, Wali MM. A method for assessing the COVID 19infection risk of riding public transit. Int J Transp Sci Technol.2023;12(1):301 314.
46. Sakuraba A, Luna A, Micic D. A systematic review and meta analysis of serologic response following coronavirus disease 2019 (COVID 19) vaccination in solid organ transplantrecipients. Viruses. 2022;14(8):1822. doi:10.3390/v14081822
47. Seroprevalence in Canada—Covid 19 Immunity Task Force.COVID; 2023. https://www.covid19immunitytaskforce.ca/seroprevalence-in-canada/
48. Rostami A, Sepidarkish M, Leeflang MMG, et al. SARS CoV 2seroprevalence worldwide: a systematic review and meta analysis. Clin Microbiol Infect. 2021;27(3):331 340.
49. Gong F, Wei H, Li Q, Liu L, Li B. Evaluation and comparisonof serological methods for COVID 19 diagnosis. Front MolBiosci. 2021;8:682405.
50. Huang AT, Garcia Carreras B, Hitchings MDT, et al. Asystematic review of antibody mediated immunity to corona-viruses: kinetics, correlates of protection, and association with severity. Nat Commun. 2020;11(1):4704.

A-1.18 Alcohol consumption does not influence SARS-CoV-2 vaccine immunogenicity: A stop the spread Ottawa cohort analysis

Preface

(This work has been previously published as a research article)

Vachon A, Keeshan A, **Galipeau Y**, Crawley AM, Langlois M-A, Cooper CL. **Alcohol consumption does not influence SARS-CoV-2 vaccine immunogenicity: A stop the spread Ottawa cohort analysis**. Vaccine. 2025;55:127034.

https://doi.org/10.1016/j.vaccine.2025.127034

© 2025 The Authors. Published by Elsevier Ltd. This is an open access article under the CC BY-NC-ND license (http://creativecommons.org/licenses/bync-nd/4.0/).

Abstract
The effect of alcohol consumption on COVID-19 vaccine immunogenicity was evaluated. Participants from the Stop the Spread Ottawa cohort were categorized by alcohol consumption categorized as excessive or non-excessive based on the Canadian Centre on Substance Abuse and Addiction's (CCSA) 2023 guidelines on alcohol use. Our analyses showed that alcohol consumption did not influence SARS-CoV-2 antibody baseline levels, post vaccine increase or decay over time.

Introduction

COVID-19 vaccination induces spike (S) protein-specific antibody and SARS-CoV-2-specific T cell immune response [[1], [2], [3]]. While absolute antibody titres and neutralizing capacity decline over time, cellular immunity persists following vaccination and infection [4]. Evaluation of modifiable risk factors affecting the extent and durability of vaccine-mediated immunity and risk for breakthrough infections remain necessary to inform vaccine policy [5].

Chronic alcohol consumption has been shown to negatively affect both humoral and cellular immunity by decreasing lymphocyte and T cell proliferation and function, decreasing dendritic cell and monocyte migration and function, inducing the release of pro-inflammatory cytokines, and altering IgA and IgM production [[6], [7], [8], [9]]. While chronic high level alcohol use dampens immune responses to vaccines and infection in both animal models and human studies [[10], [11], [12], [13]], the effect, if any, of moderate alcohol use on vaccine immunogenicity remains unresolved [6,10,[14], [15], [16]].

Factors established to decrease COVID-19 vaccine immunogenicity and increase the risk of severe SARS-CoV-2 infection include older age, obesity, tobacco smoking, and various co-morbidities including diabetes and autoimmune disorders [[16], [17], [18]]. Access alcohol consumption has been identified as a predictor of COVID-19 infection and reinfection, hospitalization, intensive care admission and 30-day morality. [13,19]Alcohol consumption could also impact COVID-19 vaccine immunogenicity. However, despite several efforts to provide clarity the effect of alcohol on COVID-19 vaccine immunogenicity remains uncertain [4,12,16,[20], [21], [22]]. Although valuable in increasing understanding, many of these studies are limited by small sample size, evaluation of relatively uniform populations, use of a single vaccine type, short duration of follow-up, restricted focus on the initial vaccine dose(s) and limited array of immune measures assessed. We addressed these limitations utilizing a diverse, urban-based population participating in the Stop the Spread Ottawa Cohort. Our evaluation is longitudinal over a multi-year period and evaluates anti-S and anti-R IgG, IgM, and IgA as well as neutralizing antibody responses over four COVID-19 vaccine doses.

2. Methods

All data used for this study was collected as part of the Stop the Spread Ottawa (SSO) Cohort study [23]. Initiated in September 2020, SSO is a prospective, longitudinal cohort study investigating immune response to SARS-CoV-2 natural infection and vaccination. Conduct of this study was approved by the Ottawa Health Science Network Research Ethics Board (#2020–0481-01H).

Eligible participants were 18 years or older, residing in the Ottawa, Canada-region, and at-risk for SARS-CoV-2 exposure/infection due to occupation or health condition or having a documented history of COVID-19 natural infection confirmed by PCR and/or serology testing. COVID-19 vaccination and positive SARS-CoV-2 diagnostic results were self-reported by participants and/or reported with serology results and confirmed through vaccination histories and medical records where available. Information on demographics and medical history was collected from serial participant surveys. Participants provided serial blood samples for serum and peripheral blood mononuclear cell (PBMC) isolation. Antibody titers from participants lacking recorded vaccination dates from samples obtained prior to vaccine rollout were incorporated in baseline data.

Alcohol consumption was documented by participants in baseline and follow-up surveys as standard drinks (SD), defined as 13.5 g of alcohol [24], or more precisely as 341 mL (12 oz.) bottle of 5 % beer, cider, or cooler; 142 mL (5 oz.) glass of 12 % wine; 43 mL (1.5 oz.) serving of 40 % distilled alcohol; (e.g., rye, gin, rum, vodka). Reported alcohol consumption was stratified based on the Canadian Centre on Substance Abuse and Addiction's (CCSA) 2023 guidelines on alcohol use [25]. High level alcohol use was defined as 3 or more SD/week and non-high level alcohol use was defined as 0–2.9 SD/week. Binary stratification was also used in which high level alcohol use was defined as 7 or more SD/week and non-high level alcohol use was defined as 0–6.9 SD/week to analyse the impact of higher alcohol consumption on vaccine immunogenicity.

Humoral immunity to natural SARS-CoV-2 infection and/or COVID-19 vaccination was measured by immunoglobulins G (IgG), M (IgM), A (IgA), and neutralizing antibody activity (%) from serum as previously described [23,26]. Briefly, IgG (BAU/mL and μg/mL), IgM (μg/mL) and IgA (μg/mL) titres against SARS-CoV-2 spike (S) and receptor-binding domain (R) proteins in participant serum samples were quantified using a high-throughput chemiluminescent direct

ELISA. Neutralizing percentage of serum anti-S IgG was determined using a surrogate neutralization ELISA assay utilizing the full-trimeric S protein from the Wuhan Hu-1 strain. The presence of anti-N IgG titres was utilized to distinguish natural immunity resulting from SARS-CoV-2 infection from vaccine-acquired immunity. Vaccine-elicited immune responses take approximately 14 days to manifest [27]. To account for this delay, participants with a COVID-19 infection up to 14 days after their vaccination date, were considered as having an infection prior to vaccination.

Participants lacking recorded alcohol consumption and individuals who were pregnant during the study period were excluded from this specific analysis. Participant characteristics and antibody titres and neutralization activity were compared according to reported alcohol (SD/week) consumption at baseline. The Shapiro-Wilk test, comparison of means and medians and examination of histograms was employed to determine normality of data. The chi-square statistical test was employed for categorical variables when assumptions were met; otherwise, the Fisher's exact test was employed. The Student's *t*-test or the non-parametric Mann-Whitney *U* test was used depending on normality. Monte Carlo simulation (n = 1,000,000 samples) was employed to estimate *p*-values for large contingency tables with high computational loads.

Univariable and multivariable multilevel linear regression analyses were conducted to model log-adjusted anti-S and anti-R levels and neutralization activity over time to assess, where sufficient data was available, whether alcohol use (high level alcohol defined as 3 or more standard drinks/week and non-high level alcohol defined as 0 to 2.9 standard drinks/week) was a predictor of peak antibody titre and whether the slopes of antibody titre increase and decay varied according to alcohol consumption with time as an interaction term. Other higher cut-points of alcohol use were assessed for exploratory purposes as well. Antibody titres were shifted up by 1 unit to account for zero values that would have resulted in undefined values following log-transformation. Models were generated at each vaccination time point separately for surveillance and convalescent participants. Convalescent models included samples from participants who had a prior infection at the time of vaccination. Any samples collected following an additional infection during follow-up relative to the dose were excluded. Time points were restricted to isolate the region of linear increase at time of vaccination and to exclude regions of sparse data at longer follow-up times or

samples after subsequent vaccine doses. Random effects were included to allow the slopes and intercepts to vary for individuals to account for autocorrelation between serial observations. Linear splines were incorporated with knots located at the antibody peak to separate regions of antibody increase and antibody decay. Interaction terms between time and alcohol consumption were included to assess if the rate of antibody increase and decay varied according to alcohol consumption.

Statistical analyses were conducted using Statistical Analysis System (SAS) version 9.4. Plots were constructed using RStudio version 2023.06.1 (ggplot2 package).

3. Results

3.1. Participant characteristics

Baseline demographics are described in Table 1. The majority of cohort participants were female (65.3 %), white (89.2 %) and Canadian-born (87.0 %). The median (IQR) age was 45.0 (34, 56) years. The most prevalent baseline co-morbidities in the SSO Cohort included allergies (43.1 %), chronic lung conditions (13.4 %), hypertension (10.8 %), and dyslipidemia (10.1 %). Twenty-eight percent of the cohort were classified as immune compromised due to immunocompromising medication use and/or condition(s). Most of the cohort never smoked (72.4 %) and 4.0 % were current smokers.

Of 909 participants included in this analysis, 387 participants were identified as high level alcohol consumers at baseline (i.e. 3 or more standard drinks per week). Median alcohol consumption was 2.0 (IQR 0.0, 4.0) SD/week. The median (IQR) alcohol consumption was 5.0 (4.0, 7.0) SD/week and 1.0 (0.0, 1.0) SD/week in the group with excessive alcohol use and the group with no excessive alcohol use. Those consuming high level alcohol were more likely to be male, white and Canadian-born. They were less likely to be immune compromised.

There were several imbalances in the baseline characteristic of high level alcohol consumers compared to those without excessive alcohol. We attempted to account for this in our regression analyses (see below).

Table 1
Characteristics of participants at baseline according to alcohol consumption (n = 909).

Variable	Study cohort (n = 909)	High Level Alcohol Use* ǂ (n = 387)	Non-High Level Alcohol Use (n = 522)	P-value
Age (years)				
Median (IQR)	45.0 (34.0, 56.0)	46.0 (34.0, 58.0)	45.0 (34.0, 55.0)	$p = 0.17$ (W = 95,632.50)
Range	18.0, 79.0	20.0, 79.9	18.0, 79.0	
Sex				
Male, n (%)	315 (34.7 %)	154 (39.8 %)	161 (30.8 %)	$p = 0.0050$** ($X^2 = 7.86$)
Female, n (%)	594 (65.3 %)	233 (60.2 %)	361 (69.2 %)	
Ethnicity (self-declared)				
Arab/West Asian, n (%)	19 (2.1 %)	5 (1.3 %)	14 (2.7 %)	
Black, n (%)	5 (0.6 %)	0 (0.0 %)	5 (1.0 %)	
East Asian, n (%)	9 (1.0 %)	3 (0.8 %)	6 (1.1 %)	
Southeast Asian, n (%)	6 (0.7 %)	0 (0.0 %)	6 (1.1 %)	$p = 0.019$** ($X^2 = 19.84$)
Indigenous, n (%)	14 (1.5 %)	3 (0.8 %)	11 (2.1 %)	
Latin American, n (%)	8 (0.9 %)	2 (0.5 %)	6 (1.1 %)	
South Asian, n (%)	13 (1.4 %)	3 (0.8 %)	10 (1.9 %)	
White, n (%)	810 (89.2 %)	363 (94.0 %)	447 (85.6 %)	
Other, n (%)	25 (2.6 %)	8 (1.8 %)	17 (3.3 %)	
Immigration Status				
Immigrated to Canada, n (%)	116 (13.0 %)	33 (8.7 %)	83 (16.2 %)	$p = 0.00099$** ($X^2 = 10.85$)
Unknown	16	7	9	
Smoking history				
Current Smoker, n (%)	36 (4.0 %)	19 (4.9 %)	17 (3.3 %)	
Former Smoker, n (%)	214 (23.6 %)	100 (25.9 %)	114 (22.0 %)	$p = 0.14$ ($X^2 = 3.92$)
Never Smoker, n (%)	655 (72.4 %)	267 (69.2 %)	388 (74.8 %)	
Missing	4	1	3	
Alcohol consumption (standard units/week)				$p < 2.2e\text{-}16$** (W = 0.00)
Median (IQR)	2.0 (0.0, 4.0)	5.0 (4.0, 7.0)	1.0 (0.0, 1.0)	
Range	0.0, 30.0	2.5, 30.0	0.0, 2.0	
Body mass index (kg/m^2)				
Median (IQR)	26.5 (23.2, 30.4)	26.1 (23.1, 29.5)	26.7 (23.2, 31.1)	$p = 0.60$ (W = 101,440.50)
Range	15.7, 55.1	16.3, 49.1	15.7, 55.1	
Missing	329	136	193	
Immune deficiency				
Yes, n (%)	207 (22.8 %)	75 (19.4 %)	132 (25.3 %)	$p = 0.036$** ($X^2 = 4.41$)
No, n (%)	702 (77.2 %)	312 (80.6 %)	390 (74.7 %)	
Degree of immunosuppression †				
High immunosuppression, n (%)	104 (11.4 %)	31 (8.0 %)	73 (14.0 %)	$p = 0.011$** ($X^2 = 9.11$)
Low immunosuppression, n (%)	152 (16.7 %)	61 (15.8 %)	91 (17.4 %)	
No immunosuppression, n (%)	653 (71.8 %)	295 (76.2 %)	358 (68.6 %)	
Number of total self-reported & serology-based COVID-19 infections during follow-up				
1 infection, n (%)	228 (25.1 %)	93 (24.0 %)	135 (25.9 %)	$p = 0.068$ ($X^2 = 7.11$)
2 infections, n (%)	17 (1.9 %)	12 (3.1 %)	5 (1.0 %)	
3 infections, n (%)	1 (0.1 %)	1 (0.3 %)	0 (0.0 %)	
No infections, n (%)	663 (72.9 %)	281 (72.6 %)	382 (73.2 %)	
COVID-19 infection prior to dose 1, n (%)	215 (23.7 %)	103 (26.6 %)	112 (21.5 %)	
COVID-19 infection after dose 1, n (%)	3 (0.3 %)	1 (0.3 %)	2 (0.4 %)	
COVID-19 infection after dose 2, n (%)	40 (4.4 %)	24 (6.2 %)	16 (3.1 %)	
COVID-19 infection after dose 3, n (%)	133 (14.6 %)	52 (13.4 %)	81 (15.5 %)	
COVID-19 infection after dose 4, n (%)	48 (5.3 %)	23 (5.9 %)	25 (4.8 %)	
COVID-19 infection after dose 5, n (%)	7 (0.8 %)	4 (1.0 %)	3 (0.6 %)	
Baseline COVID-19 infection (self-reported)				
Yes, n (%)	204 (22.4 %)	101 (26.1 %)	103 (19.7 %)	$p = 0.023$** ($X^2 = 5.18$)
No, n (%)	705 (77.6 %)	286 (73.9 %)	419 (80.3 %)	
COVID-19 infection prior to/during study period (self-reported/ serology)				$p = 0.13$ ($X^2 = 2.26$)
Yes, n (%)	413 (45.4 %)	187 (48.3 %)	226 (43.3 %)	
No, n (%)	496 (54.6 %)	200 (51.7 %)	296 (56.7 %)	

† Participants were classified as immune compromised if they had a primary immunodeficiency, rheumatological condition, organ-specific autoimmune disease or immune dysfunction, neuromuscular autoimmune disease, inflammatory condition, cancer, HIV, diabetes, asthma requiring medication, were receiving immunosuppressive treatment, or were an organ/bone marrow recipient. Alcohol consumption was not considered for immune status classification.

* High level alcohol use was characterized as 3 or more standard drinks per week. Missing values excluded from percentage calculation and statistical tests.

** Indicates statistical significance.

3.2. COVID infection and vaccination summary

Among all participants, 22.4 % had at least one incident COVID-19 infection before enrolment, identified through self-report of a positive test result (Table 1). This was higher in those consuming high level alcohol. Forty-five percent of participants had at least one infection prior to and during the study period identified through self-report and serology. Rates of baseline infection and infection confirmed during the course of the study were similar between alcohol use groups (Table 1).

Among all participants, 34.9 % were COVID-19 vaccinated at the time of SSO enrolment (Table 2). At the time of data analysis, 97.8 % and 97.2 % of the entire cohort received at least one or two COVID-19 vaccine doses, respectively. Additionally, 72.4 % of participants received at least one additional vaccine dose. These proportions and for subsequence booster doses did not differ by alcohol consumption level. The median (IQR) days between the first and second COVID-19 vaccine doses was 58 (35, 76) days and ranged from 19 to 344 days. The median (IQR) length of time in days between second and third vaccine doses was 185 (174, 211) days and ranged from 22 and 546 days. There was no clinically relevant difference in time between vaccine doses as a function of alcohol use at these time points.

Humoral Immune Response following Vaccine Doses according to Alcohol Consumption.

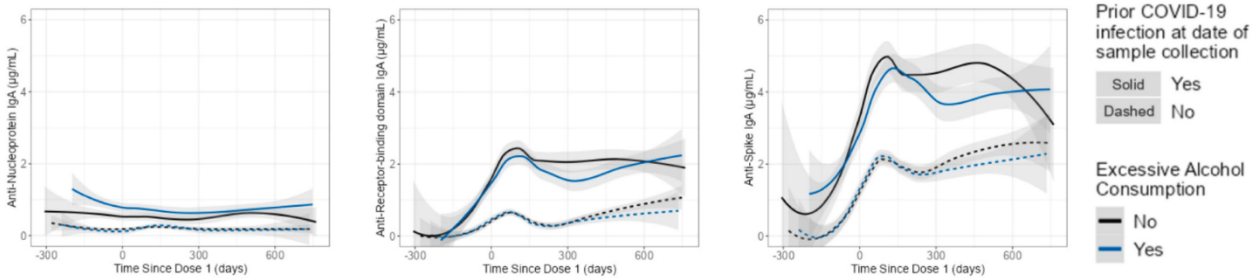
Loess smooth plots of log-adjusted anti-N, anti-R, and anti-S IgA, IgG, and IgM levels are represented in Fig. 1. IgG titres in BAU/mL are described in Supplemental Fig. S1. Higher titres were achieved following vaccination in those with prior SARS-CoV-2 infection. While anti-N antibody levels were relatively stable over time, more distinct peaks were observed in anti-R and anti-S titres, suggesting differences in the immunogenicity imparted by natural infection (anti-N IgG) compared to vaccination. Consistent with prior serum Ig concentrations as a rule, IgG signals were stronger than IgA and IgM signals.

Table 2
Participant COVID-19 vaccination information as of analysis cut-off data according to cohort allocation at baseline.

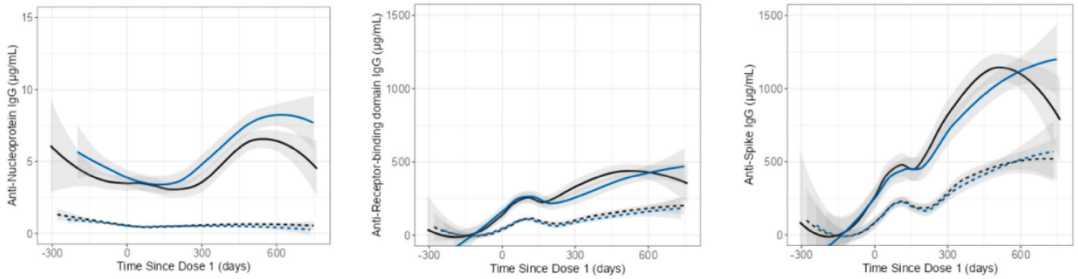
Variable	Study cohort (n = 909)	High Level Alcohol Use* (n = 387)	Non-High Level Alcohol Use (n = 522)	P-value (0.05 cut-off)
Vaccinated at baseline (first blood draw, self-reported)				
Yes, n (%)	311 (34.9 %)	123 (32.2 %)	188 (37.0 %)	$p = 0.12$ ($X^2 = 4.32$)
No, n (%)	579 (65.1 %)	259 (67.8 %)	320 (63.0 %)	
Missing	19	5	14	
Received dose 1				
Yes, n (%)	889 (97.8 %)	380 (98.2 %)	509 (97.5 %)	$p = 0.49$ ($X^2 = 0.48$)
No, n (%)	20 (2.2 %)	7 (1.8 %)	13 (2.5 %)	
Received dose 2				
Yes, n (%)	884 (97.2 %)	377 (97.4 %)	507 (97.1 %)	$p = 0.79$ ($X^2 = 0.070$)
No, n (%)	25 (2.8 %)	10 (2.6 %)	15 (2.9 %)	
Received dose 4				
Yes, n (%)	658 (72.4 %)	277 (71.6 %)	381 (73.0 %)	$p = 0.64$ ($X^2 = 0.22$)
No, n (%)	251 (27.6 %)	110 (28.4 %)	141 (27.0 %)	
Received dose 3				
Yes, n (%)	207 (22.8 %)	87 (22.5 %)	120 (23.0 %)	$p = 0.86$ ($X^2 = 0.033$)
No, n (%)	702 (77.2 %)	300 (77.5 %)	402 (77.0 %)	
Received dose 5				
Yes, n (%)	80 (8.8 %)	32 (8.3 %)	48 (9.2 %)	$p = 0.63$ ($X^2 = 0.24$)
No, n (%)	829 (91.2 %)	355 (91.7 %)	474 (90.8 %)	
Time between first and second doses in days				
Median (IQR)	58.0 (35.0, 76.0)	61 (35.8, 77.0)	57 (25.0, 75.0)	$p = 0.046$** (W = 87,668)
Range	19.0, 344.0	19.0, 147.0	20.0, 344.0	
Missing data/ Missing dose	27	11	16	
Time between first and second doses in days, n (%)				
<35	249 (28.2 %)	94 (25.0 %)	155 (30.6 %)	$p = 0.18$ ($X^2 = 3.39$)
35–75	410 (46.5 %)	182 (48.4 %)	228 (45.1 %)	
>75	223 (25.3 %)	100 (26.6 %)	123 (24.3 %)	
Missing data/ Missing dose	27	11	16	
Time between second and third doses in days				
Median (IQR)	185.0 (174.0, 211.0)	187.0 (176.0, 228.0)	184 (172.0, 206.0)	$p = 0.034$** (W = 47,194)
Range	22.0, 546.0	65.0, 541.0	22.0, 546.0	
Missing data/ Missing dose	254	112	142	
Time between second and third doses in days, n (%)				$p = 0.090$ ($X^2 = 4.81$)
<175	187 (28.5 %)	66 (24.0 %)	121 (31.8 %)	
175–210	303 (46.3 %)	135 (49.1 %)	168 (44.2 %)	
>210	165 (25.2 %)	74 (26.9 %)	91 (23.9 %)	
Missing data/ Missing dose	254	112	142	

* High level alcohol use was characterized as 3 or more standard drinks per week. Missing values excluded from percentage calculation and statistical tests.
** Indicates statistical significance.

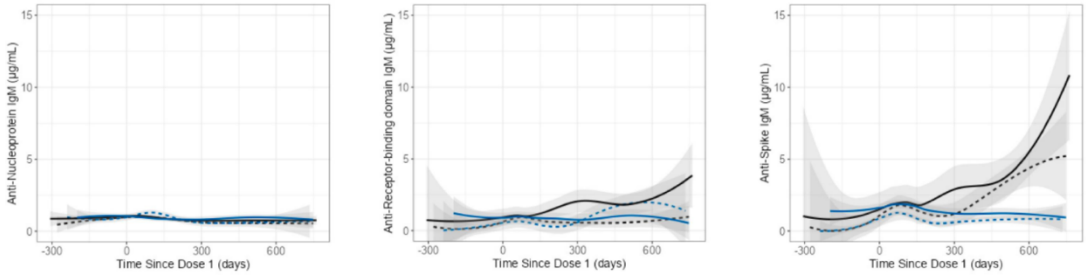
(A)



(B)



(C)



(D)

Median (IQR) Time Since Dose 1 in Days					
Dose 2 (n=882)	Dose 3 (n=658)	Dose 4 (n=207)	Dose 5 (n=80)	Dose 6 (n=15)	Dose 7 (n=4)
58.0 (35.0, 76.0)	255.0 (235.0, 286.0)	463.0 (380.0, 560.0)	582.5 (536.5, 644.0)	713.0 (580.0, 734.0)	727.5 (679.5, 737.5)

Fig. 1. Loess smooth plots of (A) IgA titres (µg/mL), (B) IgG titres (µg/mL), and (C) IgM titres (µg/mL) against the SARS-CoV-2 nucleocapsid (N), receptor-binding domain (R), and spike (S) proteins over time according to COVID-19 infection history at the date of sample collection and baseline alcohol consumption. Separate lines are presented according to COVID-19 infection history and excessive alcohol consumption groupings. Solid lines are used for those with a prior infection at sample collection and dashed lines indicate no prior infection. Blue lines represent data for participants with excessive alcohol consumption at baseline and black lines represent no excessive alcohol consumption. Excessive alcohol consumption was defined as 3 or more standard drinks/week. Panel (D) shows median time between dose 1 and subsequent doses. These results are descriptive in nature due to variability in the number and timing of vaccination doses and SARS-CoV-2 infections during follow-up and show the crude antibody titres over time in the cohort.

3.3. Alcohol as a predictor of humoral immune responses

UVA models with interaction terms to account for time were developed (Appendix Tables). These models focused on those with and without a history of SARS-CoV-2 infection prior to vaccination as well as intervals before and after the first, second, third and fourth dose of vaccination. IgG, IgA and IgM antibodies were considered. Overall, these results did not reveal a consistent difference in anti-S and anti-R antibody titres or neutralization antibody function between alcohol use groups over time. In general, the slopes of antibody decay following vaccination were not influenced by alcohol consumption grouping.

To further explore the influence of alcohol consumption of vaccine immunogenicity, MVA with time interaction terms and controlling for age, sex, ethnicity, obesity status, immune compromise status, vaccine type, interval between vaccine doses, and time since last COVID-19 infection where applicable, were constructed (data not shown). No effect of alcohol use on SARS-CoV-2 IgG, IgA and IgM antibody titres or neutralization was identified. The slope of antibody decay following vaccination was not consistently influenced by amount of alcohol use.

Several sensitivity models were developed. Comparable results were obtained when alcohol use of 7 or more SD/week was compared with 0–6.9 SD/week and when alcohol use of 3 or more SD/week and 7 or more SD/week were compared with 0 SD/week (data not shown). A sensitivity analysis was performed to evaluate the potential bias introduced by participants who altered their alcohol consumption during the evaluation period. Participants reporting a change in alcohol consumption that would have resulted in a change in their alcohol consumption classification were removed from analysis of anti-S and anti-R IgG and neutralization models. The results were overall similar (data not shown).

4. Discussion

Chronic excessive alcohol causes immune impairment and consequently decreases vaccine efficacy [[9], [10], [11],17,28]. In contrast, low to moderate alcohol use has a neutral effect or may, according to some reports, even potentiate immune function in animal models thereby hypothetically improving vaccine immunogenicity [10,29]. The mechanism behind this is unclear. Existing cohort studies evaluating the effect of alcohol use on COVID-19 vaccine efficacy have generated conflicting results [21,22]. In our analysis, we studied the effect of high level and

non-high level alcohol use on the immunogenicity of COVID-19 vaccines in a North American cohort, specifically focusing on humoral immunity, measured as SARS-CoV-2-targetting antibody titers. We identified no consistent effect of alcohol, using multiple cut-points of use, on COVID-19 vaccine immunogenicity.

It is well understood that multiple factors influence immune response after COVID-19 vaccination including age, immunocompromised status, and tobacco smoking [16,20]. While some studies have found that alcohol consumption is a negative predictor of the titre of certain antibodies [4,18], [30] the generalizability of results to the general population and how these results directly translate to immune protection from SARS-CoV-2 remain unclear. Additionally, comparisons made between non-alcohol consumers and active users fail to consider the effect of moderate consumption on vaccine efficacy.

Many studies evaluating the effect of alcohol on COVID-19 vaccine immunogenicity are limited by small sample size, narrow focus of immune measures evaluated, short time periods of evaluation, focus on only the first dose of vaccine, use of a single vaccine types and evaluation of a uniform population types. It is therefore predictable that results from these analyses are discordant. Given the large size and heterogeneous characteristics of our cohort, we were able to address many of these limitations. In our study, we found that alcohol use did not have a consistent effect on humoral immune response over time. This is consistent with at least one other population-based study addressing the influence of alcohol use on COVID-19 vaccine immunogenicity [21]. We assessed multiple antibody subtypes (IgG, IgA, IgM) and neutralizing antibodies; a decidedly robust analytical approach to evaluate potential effects of alcohol consumption on vaccine-induced immunity to SARS-CoV-2.

Our study has many strengths. Notably, alcohol stratification is based on current CCSA guidelines, which highlight the health risks associated with different levels of weekly standard drink consumption. Some studies only make binary comparisons between non-consumers and participants with alcohol use [4,12], resulting in a lack of granularity when evaluating the effect of alcohol consumption on the immune system. Our analysis stratified alcohol use in multiple different ways to address this issue. Additional strengths of this analysis include a large sample size enabling evaluation up to the fourth vaccine dose and extensive information on those with

immunocompromising conditions in out cohort. We employed multiple methods for capturing and validating COVID-19 infections in the participant population. We utilized robust biostatistics approaches including use of random effects for slopes and intercepts thereby accounting for autocorrelation between repeated measures that occurs with the use of longitudinal data.

We acknowledge several limitations. Firstly, while cellular immunity is considered to be an important part of the immune response to COVID-19 vaccination [31], it was not evaluated in this analysis. We expect that further study of B-cell and T-cell responses of this cohort will offer knowledge that will compliment our analyses reported here. This study was conducted in a developed nation and consists primarily of white participants. This may impact generalizability. The use of self reported participant questionnaires to quantitate alcohol use could introduce biases which would impact the quality of our analysis. Prospective longitudinal studies have potential selection bias arising from volunteer bias and loss of follow-up. Further evaluation is needed to evaluate alcohol consumption as a risk factor for severe COVID-19 and its effect on long-term COVID-19 vaccine effectiveness [13]. [32] There were differences in some key baseline characteristics of high level alcohol consumers compared to those without excessive alcohol use (Table 1, Table 2). We attempted to account for this in our regression analyses but acknowledge that we may have fallen short of completely accounting for these imbalances. Assay limitations and sparse data samples at longer follow-up periods (fifth and subsequent vaccine doses) and for some subgroups (non-white individuals, non-mRNA vaccine recipients) also represent study limitations. The abundance of modeling results in this study for different titres and time points increase the risk of type I error.

In conclusion, our analysis of a large urban-based North American population cohort showed that high level alcohol use (three or more and 7 or more standard drinks/week) did not have a consistent effect on SARS-CoV-2 anti-S and anti-R IgG, IgM, and IgA at baseline or following vaccination. Similarly, alcohol use did not have a consistent effect on increase, decay, or baseline levels of SARS-CoV-2 neutralizing antibodies over time.

CRediT authorship contribution statement
Alicia Vachon: Writing – review & editing, Writing – original draft, Conceptualization. Alexa Keeshan: Methodology, Formal analysis. Yannick Galipeau: Writing – review & editing, Investigation. Angela M. Crawley: Resources. Marc-André Langlois: Writing – review & editing, Supervision, Investigation. Curtis L. Cooper: Writing – review & editing, Supervision, Methodology, Investigation, Conceptualization.

Declaration of competing interest
The authors declare the following financial interests/personal relationships which may be considered as potential competing interests: Curtis Cooper reports financial support was provided by Canadian Institutes of Health Research. Curtis Cooper reports a relationship with Gilead Sciences Inc. that includes: speaking and lecture fees and travel reimbursement. If there are other authors, they declare that they have no known competing financial interests or personal relationships that could have appeared to influence the work reported in this paper.

Acknowledgments
This study is funded by the Canadian Institutes of Health Research - Instituts de recherche en santé du Canada (CIHR) (424425), the COVID-19 Immunity Task Force (CITF), and the University of Ottawa. The study extension is funded by the Coronavirus Variants Rapid Response Network (CoVaRR-Net) (156941) (https://covarrnet.ca/investigating-long-term-variables-to-sars-cov-2-infection-and-vaccine-immunity/). CoVaRR-Net is funded by an operating grant from CIHR (FRN# 175622). YG is supported by a Charles Best and Frederick Banting CGS-D from CIHR (476885).

Supplementary material
Supplementary data to this article can be found online at https://doi.org/10.1016/j.vaccine.2025.127034.

References

[1] Castro Dopico X, Ols S, Lore K, Karlsson Hedestam GB. Immunity to SARS-CoV-2 induced by infection or vaccination. J Intern Med 2022;291(1):32–50. https://doi. org/10.1111/joim.13372.

[2] Gobbi F, Buonfrate D, Moro L, et al. Antibody Response to the BNT162b2 mRNA COVID-19 Vaccine in Subjects with Prior SARS-CoV-2 Infection. Viruses 2021;13 (3). https://doi.org/10.3390/v13030422.

[3] Teijaro JR, Farber DL. COVID-19 vaccines: modes of immune activation and future challenges. Nat Rev Immunol 2021;21(4):195–7. https://doi.org/10.1038/s41577- 021-00526-x.

[4] Kato H, Miyakawa K, Ohtake N, et al. Vaccine-induced humoral response against SARS-CoV-2 dramatically declined but cellular immunity possibly remained at 6 months post BNT162b2 vaccination. Vaccine 2022;40(19):2652–5. https://doi. org/10.1016/j.vaccine.2022.03.057.

[5] Talaei M, Faustini S, Holt H, et al. Determinants of pre-vaccination antibody responses to SARS-CoV-2: a population-based longitudinal study (COVIDENCE UK). BMC Med 2022;20(1):87. https://doi.org/10.1186/s12916-022-02286-4.

[6] Barr T, Helms C, Grant K, Messaoudi I. Opposing effects of alcohol on the immune system. Prog Neuro-Psychopharmacol Biol Psychiatry 2016;65:242–51. https:// doi.org/10.1016/j.pnpbp.2015.09.001.

[7] Bautista AP. Free radicals, chemokines, and cell injury in HIV-1 and SIV infections and alcoholic hepatitis. Free Radic Biol Med 2001;31(12):1527–32. https://doi. org/10.1016/s0891-5849(01)00745-6.

[8] Gonzalez-Quintela A, Alende R, Gude F, et al. Serum levels of immunoglobulins (IgG, IgA, IgM) in a general adult population and their relationship with alcohol consumption, smoking and common metabolic abnormalities. Clin Exp Immunol 2008;151(1):42–50. https://doi.org/10.1111/j.1365-2249.2007.03545.x.

[9] Solopov PA, Colunga Biancatelli RML, Catravas JD. Alcohol increases lung angiotensin-converting enzyme 2 expression and exacerbates severe acute respiratory syndrome coronavirus 2 spike protein subunit 1-induced acute lung injury in K18-hACE2 transgenic mice. Am J Pathol 2022;192(7):990–1000. https://doi.org/10.1016/j.ajpath.2022.03.012.

[10] Messaoudi I, Asquith M, Engelmann F, et al. Moderate alcohol consumption enhances vaccine-induced responses in rhesus macaques. Vaccine 2013;32(1): 54–61. https://doi.org/10.1016/j.vaccine.2013.10.076.

[11] Nalpas B, Thepot V, Driss F, et al. Secondary immune response to hepatitis B virus vaccine in alcoholics. Alcohol Clin Exp Res 1993;17(2):295–8. https://doi.org/ 10.1111/j.1530-0277.1993.tb00766.x.

[12] Tamura M, Fujita R, Sato T, et al. Immunological responses following the third dose of the BNT162b2 SARS-CoV-2 vaccine among Japanese healthcare workers. J Infect Chemother 2022;28(11):1478–82. https://doi.org/10.1016/j. jiac.2022.07.006.

[13] Wang L, Wang Q, Davis PB, Volkow ND, Xu R. Increased risk for COVID-19 breakthrough infection in fully vaccinated patients with substance use disorders in the United States between December 2020 and august 2021. World Psychiatry 2022;21(1):124–32. https://doi.org/10.1002/wps.20921.

[14] Cohen S, Tyrrell DA, Russell MA, Jarvis MJ, Smith AP. Smoking, alcohol consumption, and susceptibility to the common cold. Am J Public Health 1993;83 (9):1277–83. https://doi.org/10.2105/ajph.83.9.1277.

[15] Solopov PA. COVID-19 vaccination and alcohol consumption: justification of risks. Pathogens 2023;12(2). https://doi.org/10.3390/pathogens12020163.
[16] Yamamoto S, Oshiro Y, Inamura N, et al. Durability and determinants of anti-SARS- CoV-2 spike antibodies following the second and third doses of mRNA COVID-19 vaccine. Clin Microbiol Infect 2023;29(9):1201. e1-1201 e5, https://doi. org/10.1016/j.cmi.2023.05.020.
[17] Friske MM, Spanagel R. Chronic alcohol consumption and COVID-19 infection risk: a narrative review. Alcohol Clin Exp Res (Hoboken) 2023;47(4):629–39. https:// doi.org/10.1111/acer.15041.
[18] Kageyama T, Ikeda K, Tanaka S, et al. Antibody responses to BNT162b2 mRNA COVID-19 vaccine and their predictors among healthcare workers in a tertiary referral hospital in Japan. Clin Microbiol Infect 2021;27(12):1861. e1-1861 e5, htt ps://doi.org/10.1016/j.cmi.2021.07.042.
[19] Tuan WJ, Kindt HM, Lennon RP. Assessing the risk of COVID-19 reinfection and severe outcomes among individuals with substance use disorders: a retrospective study using real-world electronic health records. BMJ Open 2023;13(12):e074993. https://doi.org/10.1136/bmjopen-2023-074993.
[20] Ikezaki H, Nomura H, Shimono N. Dynamics of anti-spike IgG antibody level after the second BNT162b2 COVID-19 vaccination in health care workers. J Infect Chemother 2022;28(6):802–5. https://doi.org/10.1016/j.jiac.2022.02.024.
[21] Jolliffe DA, Faustini SE, Holt H, et al. Determinants of antibody responses to SARS- CoV-2 vaccines: population-based longitudinal study (COVIDENCE UK). Vaccines (Basel) 2022;10(10). https://doi.org/10.3390/vaccines10101601.
[22] Yamamoto S, Tanaka A, Ohmagari N, et al. Use of heated tobacco products, moderate alcohol drinking, and anti-SARS-CoV-2 IgG antibody titers after BNT162b2 vaccination among Japanese healthcare workers. Prev Med 2022;161: 107123. https://doi.org/10.1016/j.ypmed.2022.107123.
[23] Collins E, Galipeau Y, Arnold C, et al. Cohort profile: stop the spread Ottawa (SSO)- a community-based prospective cohort study on antibody responses, antibody neutralisation efficiency and cellular immunity to SARS-CoV-2 infection and vaccination. BMJ Open 2022;12(9):e062187. https://doi.org/10.1136/bmjopen- 2022-062187.
[24] Health Canada. Low-risk alcohol drinking guidelines. Web Page. Government of Canada. February 7. Updated July 5. Accessed February 7, 2024, https://www. canada.ca/en/health-canada/services/substance-use/alcohol/low-risk-alcohol-dr inking-guidelines.html; 2024.
[25] Paradis C, Butt P, Shield K, et al. Canada's guidance on alcohol and health: final report. PDF Canadian Centre on Substance Use and Addiction February 2024;7. Accessed February 7, 2024, https://www.ccsa.ca/sites/default/files/2023-0
1/CCSA_Canadas_Guidance_on_Alcohol_and_Health_Final_Report_en.pdf.
[26] Colwill K, Galipeau Y, Stuible M, et al. A scalable serology solution for profiling humoral immune responses to SARS-CoV-2 infection and vaccination. Clin Transl Immunology 2022;11(3):e1380. https://doi.org/10.1002/cti2.1380.
[27] Wei J, Stoesser N, Matthews PC, et al. Antibody responses to SARS-CoV-2 vaccines in 45,965 adults from the general population of the United Kingdom. Nat Microbiol 2021;6(9):1140–9. https://doi.org/10.1038/s41564-021-00947-3.
[28] McMahon BJ, Parkinson AJ, Bulkow L, et al. Immunogenicity of the 23-valent pneumococcal polysaccharide vaccine in Alaska native chronic alcoholics compared with nonalcoholic native and non-native controls. Am J Med 1993;95 (6):589–94. https://doi.org/10.1016/0002-9343(93)90354-r.

[29] Messaoudi I, Pasala S, Grant K. Could moderate alcohol intake be recommended to improve vaccine responses? Expert Rev Vaccines 2014;13(7):817–9. https://doi. org/10.1586/14760584.2014.924405.
[30] Azizov V, Dietel K, Steffen F, et al. Ethanol consumption inhibits T(FH) cell responses and the development of autoimmune arthritis. Nat. Commun. 2020;11 (1):1998. https://doi.org/10.1038/s41467-020-15855-z.
[31] Paramithiotis E, Sugden S, Papp E, et al. Cellular immunity is critical for assessing COVID-19 vaccine effectiveness in immunocompromised individuals. Front Immunol 2022;13:880784. https://doi.org/10.3389/fimmu.2022.880784.
[32] Anderson BO, Berdzuli N, Ilbawi A, et al. Health and cancer risks associated with low levels of alcohol consumption. Lancet Public Health 2023;8(1):e6–7. https:// doi.org/10.1016/S2468-2667(22)00317-6.

A-1.19 Systemic and Mucosal Antibody Responses to SARS-CoV-2 Variant-Specific Prime-and-Boost and Prime-and-Spike Vaccination: A Comparison of Intramuscular and Intranasal Bivalent Vaccine Administration in a Murine Model

Preface

(This work has been previously published as a research article)

Maltseva M, **Galipeau Y**, McCluskie P, Castonguay N, Cooper CL, Langlois M-A. **Systemic and Mucosal Antibody Responses to SARS-CoV-2 Variant-Specific Prime-and-Boost and Prime-and-Spike Vaccination: A Comparison of Intramuscular and Intranasal Bivalent Vaccine Administration in a Murine Model**. *Vaccines*. 2025; 13(4):351.

https://doi.org/10.3390/vaccines13040351

© 2025 by the authors. Licensee MDPI, Basel, Switzerland. This article is an open access article distributed under the terms and conditions of the Creative Commons Attribution (CC BY) license (https://creativecommons.org/ licenses/by/4.0/).

Abstract

Background
The rapid genetic evolution of SARS-CoV-2 has led to the emergence of immune-evading, highly transmissible variants of concern (VOCs). This prompts the need for next-generation vaccines that elicit robust mucosal immunity in the airways to directly curb viral infection.

Objective
Here, we investigate the impact of heterologous variant prime–boost regimens on humoral responses, focusing on intramuscular (IM) and intranasal (IN) routes of administration. Using a murine model, we assessed the immunogenicity of unadjuvanted protein boosts with Wu-1, Omicron BA.4/5, or Wu-1 + BA.4/5 spike antigens following monovalent or bivalent IM priming with mRNA-LNP vaccines.

Results
IM priming induced strong systemic total and neutralizing antibody responses that were further enhanced by IN boosts with BA.4/5. IN boosting achieved the broadest serum neutralization across all VOCs tested. Notably, bivalent mRNA-LNP IM priming induced robust, cross-variant serum neutralizing antibody production, independent of subsequent IN boost combinations.

Conclusions
Our findings highlight the benefit of including distinct antigenic variants in the prime vaccination followed by a variant-tailored IN boost to elicit both systemic and mucosal variant-specific responses that are potentially capable of reducing SARS-CoV-2 transmission.

Introduction

The ongoing genetic evolution of severe acute respiratory syndrome coronavirus2 (SARS-CoV-2) and the emergence of highly transmissible variants of concern (VOCs) have significantly hampered vaccine effectiveness against transmission and symptomatic infection [1–17]. Although booster doses offer protection against severe disease and hospitalization, challenges such as waning immunity, continuous exposure to immune-evasive VOCs, and insufficient induction of mucosal immunity have notably decreased vaccine effectiveness, contributing to the sustained circulation of SARS-CoV-2 [5–11,17–23]. The spike protein of SARS-CoV-2 serves as the primary antigenic target of currently approved vaccines, owing to its high immunogenicity, which elicits robust cellular and humoral responses [24–30]. The substantial antigenic distance between the recently emerged VOCs and the ancestral (Wu-1) SARS-CoV-2 strain, on which the initial COVID-19 vaccines were based, prompts the need to update and tailor vaccines to match the spike proteins of predicted circulating variants, akin to the strategy used in seasonal influenza vaccination.

Following the emergence of Omicron and its sub-variants, vaccine effectiveness and the induction of de novo variant-specific responses has varied after boosting with updated, variant-tailored vaccines [31–40]. While boosting with these updated vaccines led to a marked increase in neutralizing antibody titers, the highest responses were directed against the ancestral strain, with varying levels of neutralization of recently emerged VOCs, such as Omicron sub-variants XBB.1.5, EG.5.1, and JN.1 [4,20,32,38,41–46]. These sub-variants possess mutations in key antigenic sites, enabling them to still evade neutralizing antibodies boosted by updated, variant-tailored vaccines [44,45,47]. This diminished neutralization of current VOCs emphasizes the immune system’s propensity to favor cross-reactive recall responses with greater affinity to the original strain over the generation of de novo antibodies specific to latest exposure, an immunological phenomenon known as immune imprinting [4,20,38,41,42,48–54]. Thus, boosting strategies that address immune evasion and enhance cross-protection at the site of viral entry are crucial to counter the challenges posed by the continuous emergence of antigenically mismatched variants.

Although intramuscular (IM) vaccination elicits potent systemic cellular and humoral immune responses against respiratory viruses, it leaves vaccine recipients susceptible to infection and viral replication at the primary entry point for SARS-CoV-2, the upper respiratory tract (URT). Mucosal humoral and cellular responses have been shown to correlate with protection against breakthrough infections caused by recently emerged VOCs [22,23,43,55–59]. Several studies have demonstrated superior protection in vivo with oral and intranasal (IN) vaccinations compared to IM vaccination, due to the induction of local immunity in the URT, which limits viral replication and significantly reduces onward transmission of SARS-CoV-2 [22,60–79]. Recent studies have explored several prime–boost approaches, including different vaccine platforms and IN boosting strategies, in the context of pre-existing systemic immunity [22,70,72–75,79,80]. Notably, Mao et al. showed that an IM prime with an mRNA-LNP vaccine followed by an IN boost with an unadjuvanted SARS-CoV-2 spike protein—a strategy referred to as "Prime and Spike"—leverages preexisting systemic immunity to induce robust mucosal immune responses without the need for an adjuvant [73]. Collectively, these studies indicate that IN boosting, rather than relying on repeated IM vaccinations, may be a more effective strategy for achieving sustained and potent protection against SARS-CoV-2 reinfection. Despite extensive studies on serum responses to variant-specific boosting, a critical gap remains in understanding how intranasal boosting strategies tailored to circulating variants influence humoral immunity in individuals with pre-existing immunity to an antigenically distant strain. In particular, the effects of heterologous boosting on mucosal variant-specific immunity remain poorly characterized.

In this study, we adapted the "Prime and Spike" approach by Mao et al. to examine the effects of heterologous prime–boost regimens on humoral responses, focusing on different administration routes and variant-tailored vaccine formulations [73]. Understanding the impact of different vaccination strategies on immune responses across different anatomical compartments may aid in inducing protective mucosal responses against SARS-CoV-2 variants. Our findings indicate that the IM prime predominantly shapes the systemic humoral responses, driven primarily by neutralizing antibodies, while the IN boost further amplifies and focuses them. In contrast, only IN vaccination, rather than IM, induced mucosal responses, with variant-specific IN boosts eliciting distinct antigen-specific IgA responses in nasal wash and BALF. Notably, we highlight that bivalent priming with two distinct variants significantly broadened the repertoire of overall

neutralizing antibody responses against circulating VOCs at the start, which was further enhanced and focused by variant-specific IN boosting.

2. Materials and Methods

2.1. Mice Immunization and Sample Collection

All animal experiments were conducted in accordance with the Ontario Animals for Research Act and approved by the University of Ottawa Animal Ethics Committee (protocol BMI-3649). Female, 8-week-old BALB/c mice were obtained from Charles River Laboratories (Saint-Constant, QC, Canada). Prior to each immunization, mice were anesthetized by inhalation of isoflurane in an induction chamber, with the vaporizer set to a 3–5% concentration and an oxygen flow rate of 0.8–1.5 L/min, and vaccinated either intramuscularly or intranasally. Intramuscular vaccinations were administered in the left quadriceps muscle using a 31-gauge syringe, delivering a final dose of 1 µg of Pfizer-Comirnaty monovalent Wuhan (Wu-1) or bivalent (Wu-1 + BA.4/5) vaccine in 20 µL of solution. As described previously in Maltseva et al., intranasal vaccinations involved administering 25 µL per nare, with a total dose of either 1 µg or 10 µg of spike protein formulations consisting of Wu-1, BA.4/5, or Wu-1 + BA.4/5 variants, resuspended in endotoxin-free PBS (Sigma-Aldrich, St. Louis, MO, USA) [66]. SARS-CoV-2 antigens, including full trimeric spike proteins for Wuhan (Wu-1) and Omicron (BA.4/5), were obtained from the Metrology Division of the National Research Council Canada (Montreal, QC, Canada). Briefly, SARS-CoV-2 antigens in prefusion formats were produced in stably transfected CHO (CHOBRI/2353™) cells and purified as described [81]. Control groups included mice vaccinated with phosphatebuffered saline (PBS), either a single- or two-dose regimen of monovalent (Wu-1) or bivalent (Wu-1 + BA.4/5) mRNA vaccine administered IM. Additional groups included mice receiving two IN doses of Wu-1 protein, or a prime–boost regimen consisting of a monovalent (Wu-1) mRNA IM prime followed by a boost with NL63 seasonal human coronavirus spike protein (Creative Diagnostics, Shirley, NY, USA, DAGC133), as summarized in Table 1.

Table 1. Vaccination regimens administered to mice.

Mode of Administration (Prime–Boost) *	Type of Vaccine Antigenic Formulation	Prime (Day 1)	Boost (Day 21)
IM–IN	-	PBS	PBS
IM–IN	-	Monovalent mRNA-LNP	PBS
IM–IN	-	Bivalent mRNA-LNP	PBS
IN–IN	Homologous	Wu-1 protein	Wu-1 protein
IM–IM	Homologous	Monovalent mRNA-LNP	Monovalent mRNA-LNP
IM–IN	Homologous	Monovalent mRNA-LNP	Wu-1 protein
IM–IN	Heterologous	Monovalent mRNA-LNP	BA4/5 protein
IM–IN	Heterologous	Monovalent mRNA-LNP	Wu-1 + BA4/5 protein
IM–IM	Homologous	Bivalent mRNA-LNP	Bivalent mRNA-LNP
IM–IN	Homologous	Bivalent mRNA-LNP	Wu-1 protein
IM–IN	Homologous	Bivalent mRNA-LNP	BA4/5 protein
IM–IN	Homologous	Bivalent mRNA-LNP	Wu-1 + BA4/5 protein
IM–IN	Heterologous	Bivalent mRNA-LNP	NL63 protein

* IM: intramuscular LNP-mRNA Monovalent: Pfizer-Comirnaty monovalent Wuhan (Wu-1) or bivalent (Wu-1 + BA.4/5) (1 µg dose of total vaccine); IN: intranasal unadjuvanted spike protein as indicated (1 µg or 10 µg doses of total antigen).

Plasma samples were collected periodically throughout the study via the submandibular vein, with terminal samples obtained by cardiac puncture. Two weeks after the booster dose, plasma, bronchoalveolar lavage fluid (BALF), nasal washes, and intestinal lumen contents were collected to assess mucosal humoral responses, following the method described in Maltseva et al. [66]. At the endpoint of the study, mice were anesthetized via inhalation of isoflurane using an induction chamber, with the vaporizer set to a 3–5% concentration and an oxygen flow rate of 0.8–1.5 L/min. Anesthesia was maintained with a nose cone at the same concentration for euthanasia by cardiac puncture, followed by cervical dislocation. Mucosal samples were collected using PBS supplemented with protease inhibitors (Complete Mini Protease Inhibitor Cocktail tablets, Cat. No.: 11836153001, Basel, Switzerland). A 10 cm section of the small intestine, free of fecal matter, was cut into 1–2 mm pieces and placed in an Eppendorf tube containing 200 µL PBS with protease inhibitors. The sample was incubated on a rocker at 4 ◦C overnight and centrifuged at 8000× g for 10 min at 4 ◦C, and the supernatants were stored at −80 ◦C for downstream ELISA analysis. Nasal wash and BALF samples were further concentrated using 50 kDa Pierce Protein Concentrator columns (Thermo Fisher Scientific, Waltham, MA, USA) following the manufacturer's instructions. Sample volumes were normalized before concentration, and the concentrates were stored at −80 ◦C until the ELISA assay was performed.

2.2. SARS-CoV-2-Specific Antibody Measurements

SARS-CoV-2-specific antibody responses were evaluated as previously described in Maltseva et al. [66]. Briefly, using trimeric spike proteins corresponding to the same variants used for immunizations, spike proteins were diluted to 4 µg/mL in sterile 1X PBS (Multicell Wisent, Saint-Jean-Baptise, QC, Canada, #311-010-CL) and coated onto 384-well immunoplates (ThermoFisher, Waltham, MA, USA, #460372) at 10 µL per well, followed by overnight incubation at 4 ◦C. Plates were washed three times with 100 µL of PBS-T (PBS + 0.05% Tween-20) to remove unbound antigen and blocked for 1 h at room temperature with shaking using blocking buffer (PBS-T + 3% w/v non-fat milk powder). Following blocking, serum, BALF, nasal wash, and intestinal supernatant samples were prepared and diluted in dilution buffer (PBS-T + 1% w/v non-fat milk powder). Serum was diluted 1:300 after the first immunization and 1:500 after the second immunization. BALF samples were diluted between 4- to 30-fold, while nasal wash and intestinal supernatant samples were diluted 4-fold and 2-fold, respectively. After washing the plates three times with PBS-T, 10 µL of the diluted samples was added to the respective wells. The plates were incubated for 2 h at room temperature with shaking and washed three times with PBS-T. Next, 10 µL of the respective secondary-HRP antibody at specified dilutions 1:4000 secondary IgG Anti-Mouse, Human ads-HRP (Southern Biotech, Homewood, AL, USA, #1030-05) and 1:1000 secondary anti-mouse IgA-HRP (Southern Biotech, #1040-05) was added. Plates were incubated for one hour on a shaker, washed thrice with PBS-T, followed by the addition of 10 µL of the SuperSignal ELISA Pico Chemiluminescent Substrate (Thermo Scientific, #37069). Luminescence intensity was measured with BIO-TEK Synergy Neo2 (Agilent, Mississauga, ON, Canada) plate reader for 20 ms/well at a read height of 1.0 mm. Wells containing dilution buffer in place of sample served as negative controls to determine background luminescence. We expressed the SARS-CoV-2-specific antibody levels as relative luminescence values compared to a pooled sample from the Wu-1 + BA.4/5-boosted group, with a pooled sample for each biofluid included as a standard control on every plate. This approach ensured plate-to-plate consistency aligned with results from normalization to the standard IgG and IgA controls (9A9C9 clone) (Genscript, Piscataway, NJ, USA).

2.3. Surrogate Neutralization ELISA (snELISA) Assay to Evaluate Neutralization Activity in Serum and BALF Samples

Surrogate neutralization ELISA was performed as previously described in Colwill et al. and Maltseva et al. for the evaluation of the relative inhibition of neutralizing antibodies to spike protein from binding to soluble ACE2 [30,48,81]. Briefly, SARS-CoV-2 proteins, including Wuhan (NRC Metrology), BA4/5 (NRC Metrology), and XBB1.5 (Abwiz Bio, San Diego, CA, USA, 2712), were diluted in sterile 1X PBS to 8 µg/mL and coated onto 384-well Immuno plates (12.5 µL/well) overnight at 4 ◦C. Plates were washed three times with PBS-T (PBS containing 0.05% Tween-20) and blocked for one hour while shaking. Plasma samples were 1:5 serially diluted in dilution buffer, while BALF samples were diluted 1:3. Diluted samples (20 µL/well) were applied to coated plates and incubated at room temperature for 2 h while shaking. After incubation, plates were washed three times and biotinylated ACE2 (NRC Metrology), diluted to 0.35 ng/µL in a dilution buffer, was added to the wells (20 µL/well). Plates were washed again three times with PBS-T and 20 µL per well of Streptavidin-Peroxidase polymer (Sigma, #S2438) diluted in dilution buffer to 1.25 ng/µL was added. Following one hour incubation at room temperature while shaking, plates were washed thrice with PBS-T and 20 µL per well of freshly prepared SuperSignal ELISA Pico Chemiluminescent Substrate (prepared by mixing a 1:1 ratio of components and further diluted with equal volume dH2O) was applied. After 5 min of incubation with shaking, luminescence intensity was measured with a BIO-TEK Synergy Neo2 plate reader for 20 ms/well at a read height of 1.0 mm. To determine the maximum binding signal, control wells were filled with dilution buffer in place of serum, followed by the addition of ACE2 under the same conditions. The relative percentage of inhibition was calculated using the following formula:

$$\%\ Inhibition = \left(1 - \frac{average\ mean\ of\ serum\ sample}{average\ mean\ of\ maxium\ signal}\right) \times 100$$

The serum and BALF dilutions required to achieve 50% inhibition of spike or RBD protein binding to the ACE2 receptor (half-maximal inhibitory dilution, ID50) were determined using a 4-parameter logistic (4PL) curve fitting analysis in GraphPad Prism (9.1.2 software, San Diego, CA, USA). For samples where no neutralization activity was detected, the ID50 value was arbitrarily assigned as half of the lowest dilution tested.

2.4. Principal Component Analysis of Neutralization and Serology Data

Principal component analysis (PCA) was performed on normalized serology and neutralization efficiency data from various prime and boost mouse groups. The analysis was conducted using the prcomp function in R 4.2.3, with scaling applied to ensure comparability across variables. Data visualization, including PCA plots and eigenvectors, was carried out using the ggplot2 package. During visualization, samples were annotated based on their prime and boost classifications. Animals with missing values in any measured parameter were excluded from the PCA analysis.

3. Results

We set out to assess the effect of heterologous prime and boost vaccine regimens based on different administration routes (IM prime—IM boost vs. IM prime—IN boost) and vaccine formulations (homologous or heterologous prime—boost) on humoral responses in bulb/c mice (Table 1). Mice were initially IM primed with either 1 µg of monovalent mRNA-LNP encoding for SARS-CoV-2 Wu-1 antigen (n = 5 per group) or a bivalent mRNA-LNP encoding for SARS-CoV-2 Wu-1 and BA4/5 antigens (n = 7 per group). After 21 days, mice were boosted with either a second dose of a matching IM mRNA-LNP vaccine or an IN administration of an unadjuvanted Wu-1, BA.4/5, or admixed Wu-1 + BA4/5 formulation of stabilized SARS-CoV-2 spike protein at 1 or 10 µg doses (Figure 1A and Supplementary Figure S3). Control groups received PBS, one dose of IM mRNA-LNP, two doses of unadjuvanted protein via IN only, or 1 dose of IM mRNA followed by IN boost with unadjuvanted NL63 seasonal coronavirus spike protein (Table 1). To evaluate the immunogenicity of the different immunization routes and heterologous prime–boost vaccine formulations, we focused on characterizing IgG and IgA antibody responses in distinct immunological and anatomical compartments. Thus, two weeks post-boost, we collected plasma, bronchoalveolar lavage (BAL), and nasal and intestinal biofluids for a direct comparison of induced antibody profiles following different vaccine regimens (Figure 1A).

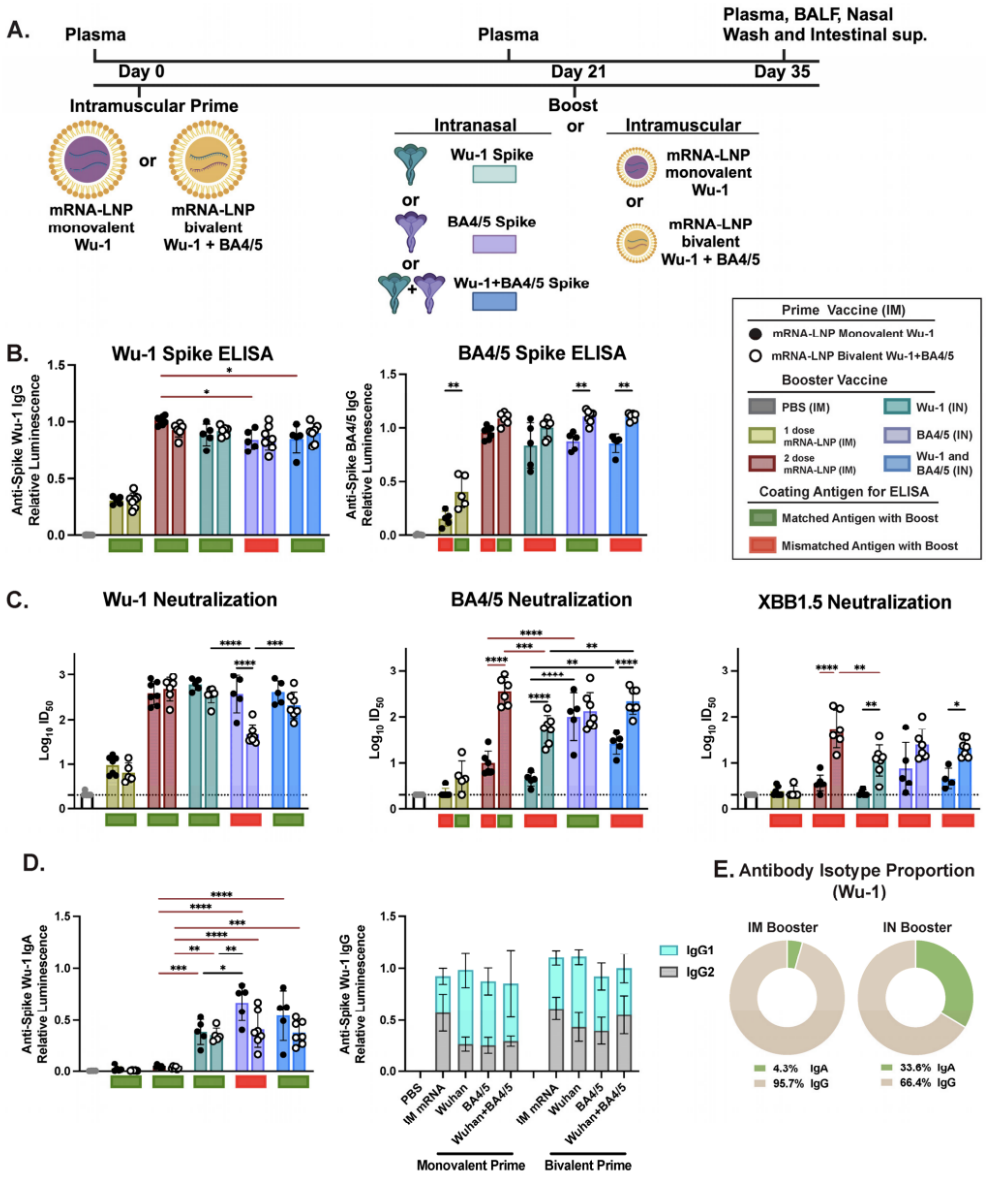


Figure 1. Characterization of systemic immune responses following a heterologous systemic prime and mucosal IN boost vaccination. (A) Schematic of the experimental design and vaccine formulations. BALB/c mice were intramuscularly (IM) primed with either a monovalent (Wu-1) or bivalent (Wu-1 + BA.4/5) mRNA vaccine, followed by an intranasal (IN) boost with unadjuvanted Wu-1 spike, BA.4/5 spike, or Wu-1 + BA.4/5 spike on days 0 and 21, respectively. Control groups received PBS, one or two IM mRNA doses, or two IN protein-only doses. Two weeks post-boost, plasma, bronchoalveolar lavage fluid (BALF), nasal wash, and intestines were collected for humoral response analysis. (B) Measurement of serum Wu-1 and BA4/5 spike IgG relative titers at endpoint (day 35). (C) Reciprocal ID50 neutralization titers based on inhibition of soluble ACE2 binding to immobilized Wu-1, BA.4/5, and XBB.1.5 spike proteins. (D) Measurement of Wu-1-spike-specific IgA titers and superimposed IgG1 and IgG2 titers in serum. (E) Relative proportion of Wu-1-specific IgG and IgA isotypes in serum. Serum was diluted 1:500 for the measure of IgG-specific titers. Data reflect results from one biological replicate, with values shown as the average of three technical replicates. Antibody titers were log-transformed and analyzed using one-way ANOVA with Tukey's multiple comparisons test. Unless otherwise stated, all vaccine groups showed significantly higher responses than PBS and one-dose controls and dotted line represents neutralization assay cutoff. Pairwise comparisons were conducted between different booster formulations within monovalent or bivalent prime cohorts, as well as between counterparts with different priming regimens. **** $p \leq 0.0001$, *** $p \leq 0.001$, ** $p \leq 0.01$, * $p \leq 0.05$.

Following a single dose of either the monovalent or bivalent mRNA-LNP IM vaccination, all mice exhibited detectable levels of IgG antibodies in serum (Supplementary Figure S1A). IN administration of a 1 µg or 10 µg dose of unadjuvanted protein boosted both IgG and IgA levels in serum, whereas IM administration of the mRNA-LNP vaccine only boosted IgG responses (Figure 1 and Supplementary Figure S3). An IM prime followed by IN boost induced systemic Wu-1-specific IgG levels comparable to those observed after two IM mRNA-LNP doses. However, significantly higher IgA levels were detected in intranasally boosted mice (Figure 1B,D,E), indicating that IN boosting with an unadjuvanted protein can effectively enhance humoral immunity by building upon pre-existing systemic immunity, consistent with previous findings by Mao et al. [73]. Indeed, Wu-1-specific IgG levels were comparable among mice receiving either a homologous or heterologous IN boost (Figure 1B). Notably, we detected significantly higher BA4/5-specific IgG titers in mice primed bivalently and boosted IN with BA4.5 or BA4.5 + Wu-1 antigens compared to their monovalently primed counterparts. A strong correlation ($r = 0.84$, $p \leq 0.001$) was observed between BA4/5- and Wu-1-specific IgG antibodies in monovalently primed mice, indicating high antibody cross-reactivity between these antigens. In contrast, no correlation ($r = 0.39$) was detected in bivalently primed mice, potentially suggesting presence of BA4/5-specific antibody responses (Supplementary Figure S1D). Additionally, although T follicular helper cells were not evaluated in this study, we detected lower ratios of IgG1 over IgG2 in bivalent-primed mice (Figure 1D), suggesting a potential skewing towards a Th1 response [82].

Mao et al. previously reported that unadjuvanted IN boosting with SARS-CoV-1 spike protein, which shares 76% amino acid identity with Wu-1 SARS-CoV-2 spike, leveraged systemic immunity induced by prior vaccination with monovalent Wu-1 mRNA-LNP, and elicited cross-reactive humoral responses [73]. We next sought to determine whether IN boosting with an unadjuvanted NL63 spike, a divergent seasonal coronavirus that also utilizes the ACE2 receptor for cell entry and shares 26% amino acid identity with Wu-1 SARS-CoV-2 spike, could boost and induce cross-reactive humoral responses. However, we found that IgG levels were comparable to those observed in mice after a single dose of IM mRNA-LNP, with no detectable NL63-specific IgG responses (Supplementary Figure S1B). This finding highlights the specificity of memory responses and the importance of using a more closely matched boosting antigen to leverage

systemic immunity induced by prior vaccination. This experiment clearly shows that the IM mRNA-LNP prime response did not produce antibodies, or cross-reactive antibodies that could be boosted by an unadjuvanted divergent protein boost.

3.1. IM Prime Shapes Systemic Humoral Responses, Primarily Driven by Variant-Specific Neutralizing Responses

Although some statistically significant differences were observed, overall, total antibody responses showed minimal variation among the different vaccination groups (Figure 1B). We next assessed neutralizing activity using a surrogate neutralization ELISA assay (snELISA) to evaluate the breadth of antibody responses from heterologous prime– boost formulations and administration routes (Figure 1C; Supplementary Figure S3B), as systemic neutralizing responses are a well-established correlate of vaccine efficacy [83,84]. The snELISA assay we used measures the relative inhibition of spike to ACE2 receptor binding, as previously described by our group and shown to quantitatively correlate with pseudotyped or infectious virus neutralization assays [85].

Spike binding inhibition for a specific variant was generally superior in mice boosted with the corresponding matched antigen, regardless of whether the boost was administered IN or IM (Figure 1C; Supplementary Figure S3B). In line with the serological data, we observed comparable Wu-1 spike inhibition in mice that were boosted via IM or IN, except those primed with the bivalent mRNA-LNP vaccine and boosted with BA4/5 antigen (mismatched), likely due to significantly lower levels of Wu-1 RBD-specific IgG antibody (Supplementary Figure S1A). In contrast, a significant reduction in BA4/5 spike neutralization was observed in monovalently primed and Wu-1 (mismatched)-boosted mice compared to those boosted with BA4/5 antigen (matched) or their bivalently primed counterparts (Figure 1C; Supplementary Figure S3B). Furthermore, boosting with Wu-1 antigen failed to elicit any neutralizing activity against XBB1.5 spike, while boosting with the more closely related BA4/5 antigen enhanced neutralization.

Notably, IN boost with BA4/5 antigen (matched) induced significantly superior BA4/5 spike neutralization and, although not statistically significant, enhanced neutralization against XBB1.5 compared to mice receiving monovalent mRNA-LNP vaccine IM boost. However, boosting with either Wu-1 or BA4/5 antigens resulted in skewed neutralizing response specific to the boosting

antigen (Figures 1C and 2A). Indeed, Wu-1 homologous prime–boost vaccination resulted in significant decrease in neutralization activity against antigenically distant SARS-CoV-2 variants (Figures 1C and 2A,B). This effect was mitigated by heterologous boosting with the BA4/5 antigen, which likely elicited cross-reactive or de novo BA4/5-specific responses given the maintained inhibition of Wu-1 spike but markedly improved neutralization against BA4/5 spike (Figures 1C and 2A,B). Interestingly, we found that BA4/5 + Wuhan boost elicited comparable or superior spike neutralization across all three variants evaluated in bivalent-primed mice, relative to matched or mismatched variant-specific boosts (Figures 1C and 2A,B). In contrast, mice that were primed with the monovalent Wu-1 mRNA-LNP vaccine and boosted with the BA4/5 + Wuhan vaccine exhibited diminished neutralization of BA4/5 and XBB1.5. This suggests that the BA4/5 + Wuhan boost led to the induction of cross-reactive recall responses to epitopes shared between the primary (Wu-1) and secondary (Wu-1 and BA4/5) exposures, rather than generating BA4/5-specific de novo antibodies, indicating an immune imprinting response.

3.2. Bivalent mRNA-LNP IM Prime Broadens Neutralizing Responses in Serum

Overall, we found a positive correlation between spike neutralization activity and Wu1- or BA4/5-specific IgG antibody titers when the boosting antigen matched with the variant used in the snELISA (Supplementary Figure S1C). Importantly, significantly superior BA4/5 and XBB1.5 spike neutralization was noted in bivalent-primed mice. Indeed, we observed a strong positive correlation (Spearman $r = 0.877$, $p \leq 0.0001$) between BA4/5 and XBB1.5 spike neutralization in bivalently primed mice compared to monovalently primed groups (Spearman $r = 0.380$, $p = 0.081$) (Figure 2B). Next, we performed a principal components analysis (PCA) which included paired total and neutralizing responses across the various prime and boost groups (Figure 2C,D). The first two principal components explained 77% of the variation in the data. By coloring the data points according to the type of prime or boost vaccine formulation, we were able to visualize the relative influence of each vaccine formulation on the overall humoral response outcome. Notably, we observed differential clustering based on the type of prime rather than the boost, which was primarily driven by variant-specific neutralizing responses (Figure 2C,D).

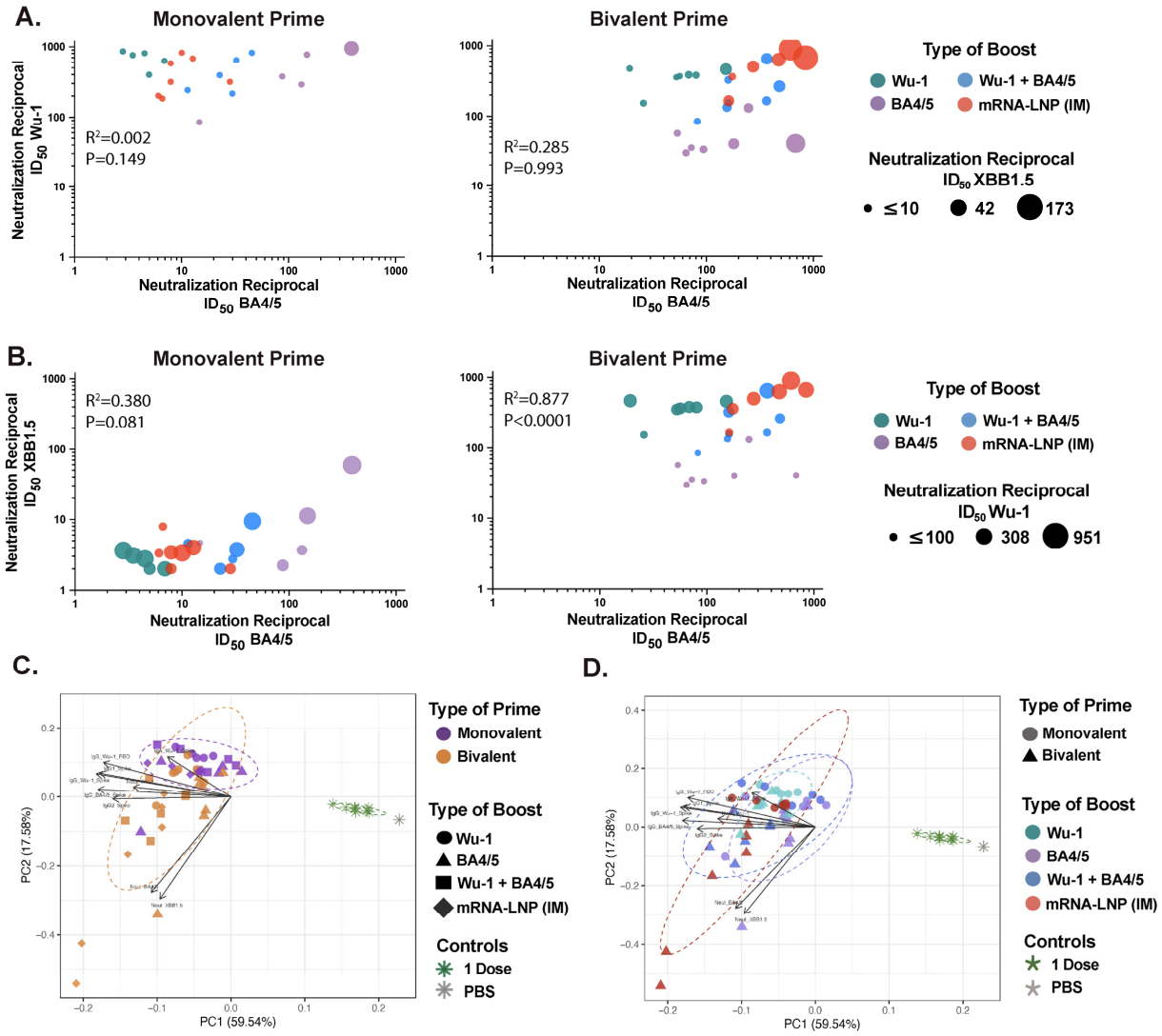


Figure 2. Prime vaccination drives distinct humoral (total and neutralizing) responses in serum, while booster vaccination further refines these responses. (A) Correlation between BA4/5 and Wu1 neutralization (ID50) reciprocal titers, with data points colored by booster type. Point size reflects neutralization potency against the XBB.1.5 variant. (B) Correlation between BA.4/5 and XBB.1.5 ID50 titers, with data points colored by booster type. Point size reflects neutralization potency against the Wu-1 variant. (C,D) Principal component analysis (PCA) of serum antibody responses. Each point represents an individual mouse, incorporating all antibody response measurements from Figure 1 and dotted ellipses represent confidence interval for each group. PCA plots are colored by (i) prime vaccine type and (ii) booster type to illustrate distinct clustering patterns elicited by different vaccination regimens.

Following an IN boost with a 1 µg dose of unadjuvanted protein, similar patterns in variant-specific systemic responses emerged where groups boosted with the corresponding (matched) antigen generally developed the greatest reactivity and variant-specific neutralizing responses (Supplementary Figure S3A,B). Notably, the Wu-1 homologous prime–boost regimen led to Wu-1-skewed total and neutralizing responses while bivalently primed mice exhibited significantly

greater total and neutralizing responses (Supplementary Figure S3E). Indeed, although 1 μg IN-boosted mice grouped separately in the PCA, the bivalently primed mice clustered more closely with the 10 μg-boosted groups (Supplementary Figure S4A,B). Taken together, these results suggest that bivalent priming expands the breadth of neutralizing responses beyond what can be elicited with variant-specific boosting. Therefore, our data suggest that the prime vaccine shapes the outcome of total and neutralizing responses in serum, while the booster further refines these responses.

3.3. Variant-Specific IN Vaccines Induce Distinct Antigen-Specific IgA Responses in Nasal and BAL Biofluids

IM administration typically favors Ig class switching to IgG over IgA. However, stimulating the respiratory mucosa through vaccination or infection has been shown to induce robust production of IgA locally or in other distinct mucosal compartments. Indeed, the IN boost, but not the IM boost, induced robust mucosal Ig responses as detected in BAL and nasal biofluids, which predominantly favored IgA. We observed that the antigen dose administered via the IN route was important, as total Ig and neutralizing responses were significantly lower following a 1 μg dose of unadjuvanted protein IN boost relative to the 10 μg dose, which effectively boosted both IgG and IgA levels (Figure 3 and Supplementary Figure S5). We found that an IN boost induced comparable Wu-1-specific IgA levels across the differentially (matched or mismatched) boosted mice, which was significantly higher than those observed after two doses of mRNA-LNP administered IM (Figure 3A). However, we detected significantly greater BA4/5-specific IgA levels in mice IN-boosted with the BA4/5 (matched) and, although not statistically significant, with Wu-1 + BA4/5 antigen (matched), than with the Wu-1 antigen (mismatched) boost. While we observed an overall positive correlation between BA.4/5- and Wu-1-specific IgA antibodies when all IN-boosted mice were analyzed together ($r = 0.837$, $p \leq 0.0001$) (Supplementary Figure S2A), this correlation was only positive in groups boosted with BA.4/5 ($r = 0.87$, $p = 0.001$) and Wu-1 + BA.4/5 ($r = 0.87$, $p = 0.003$) antigens. No correlation was observed in the Wu-1-boosted group ($r = 0.20$, $p = 0.543$). In general, in contrast to differences in BA4/5-specific IgG levels between monovalently and bivalently primed mice observed in serum, differences in BA4/5-specific IgA levels were influenced by the vaccine formulation of the boost rather than the prime.

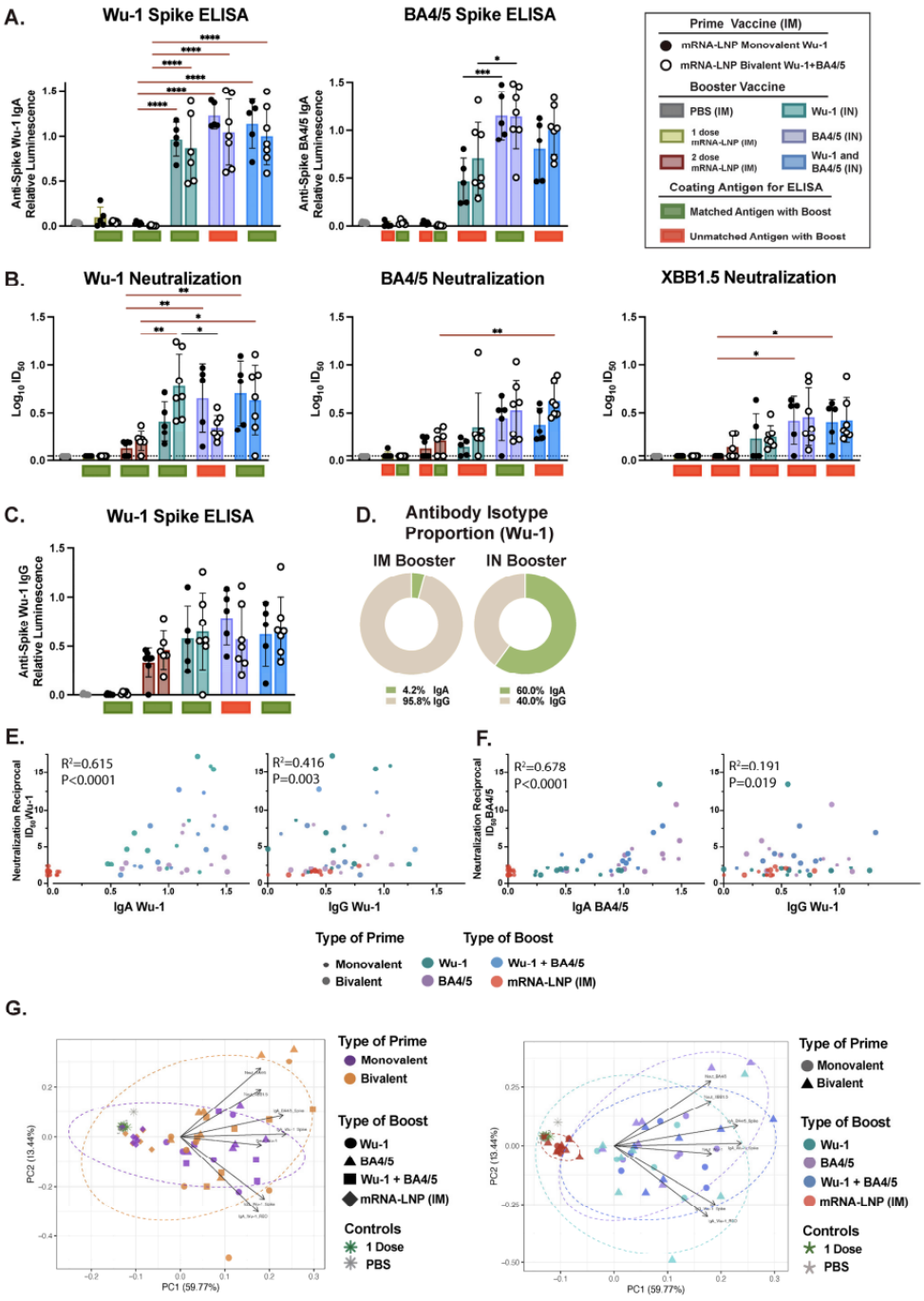


Figure 3. Characterization of mucosal immune responses in bronchoalveolar lavage fluid (BALF) following a heterologous systemic prime and mucosal boost vaccination. (A) Measurement of Wu-1 and BA4/5-spike-specific IgA in BALF at endpoint (day 35). (B) Reciprocal ID50 neutralization titers based on inhibition of soluble ACE2 binding to immobilized Wu-1, BA.4/5, and XBB.1.5 spike proteins. (C) Measurement of Wu-1-spike-specific IgG titers. (D) Relative proportion of Wu-1-specific IgG and IgA isotypes in BALF. (E,F) Correlations between (E) Wu-1 and (F) BA.4/5 neutralization (ID50) titers and IgG/IgA isotypes, with data points colored by booster type. (G) Principal component analysis (PCA) of antibody responses in BALF. Each point represents an individual mouse, incorporating all measured antibody responses and dotted ellipses represent confidence interval for each group. PCA plots are colored by (i) prime vaccine type and (ii) booster type to illustrate distinct clustering patterns driven by different vaccination regimens. Data are from one biological replicate and represent the average of three technical

replicates and dotted line represents neutralization assay cutoff. BALF was diluted 1:30 for IgA titer measurements. Antibody titers were log-transformed and analyzed using one-way ANOVA with Tukey's multiple comparisons test. **** $p \leq 0.0001$, *** $p \leq 0.0001$, ** $p \leq 0.01$, * $p \leq 0.05$.

Next, we evaluated spike neutralizing activity in BALF and found detectable but weak neutralization activity in mice that were IN-boosted with the 10 µg dose of unadjuvanted protein (Figure 3B). Consistent with systemic neutralizing responses, spike–ACE2 binding inhibition for specific variants was superior in mice boosted with the corresponding (matched) or closely related antigen. In line with the serological data, we observed comparable Wu-1 inhibition in mice across differentially IN-boosted mice and was notably higher than that observed following two doses of mRNA-LNP via IM vaccination. However, similar to the findings in serum, mice primed with the bivalent mRNA-LNP vaccine and boosted with BA4/5 antigen (mismatched) exhibited significantly lower Wu-1 spike inhibition. Generally, an IN boost with BA4/5 + Wu-1 antigen (matched) elicited enhanced BA4/5 and XBB1.5 spike neutralization, which was significantly higher than that observed in mice IM-boosted with the monovalent mRNA-LNP. Given that mucosal IgA has been shown to effectively inhibit viral infection in vitro across both animal models and human studies [23,66,73,76,80,86], we sought to determine the contribution of IgA relative to IgG in mucosal neutralization activity in vitro. We found that IgA antibody titers positively correlated with spike neutralizing activity against Wu-1 ($r = 0.615$, $p \leq 0.0001$) and BA4/5 ($r = 0.678$, $p \leq 0.0001$) compared to IgG (Figure 3E,F). Furthermore, no correlation was observed between Wu-1 and BA4/5 or BA4/5 and XBB1.5 neutralization (Supplementary Figure S2B,C). Indeed, we observed distinct clustering based on the route of administration in the PCA and dose of the IN booster, where the 1 µg IN- and IM-boosted mice grouped independently from the 10 µg-boosted mice (Figure 3G and Supplementary Figure S5E). Taken together, these findings suggest that in contrast to serum, where the prime vaccination overwhelmingly dictated the humoral response outcome, humoral responses in the BALF were predominantly influenced by the booster formulation, with antigen-specific IgA response as the primary driver.

Next, we assessed mucosal IgG and IgA levels in the nasal biofluid (Figure 4A and Supplementary Figure S6). Only mice that received the 10 µg IN boost developed high levels of IgA, which were significantly greater than in those that received two doses of mRNA-LNP via IM. Notably, as in BALF, a similar pattern emerged in variant-specific IgA responses, with groups boosted with the

BA4/5 or BA4.5 + Wu-1 exhibiting significantly higher BA4/5-specific IgA titers. We found a strong correlation ($r = 0.81$, $p \leq 0.001$) between BA4/5- and Wu-1-specific IgA antibodies, but only in the Wu-1 + BA4/5-boosted mice (Supplementary Figure S2F). Both IM mRNA-LNP and IN protein vaccinations elicited comparable IgG responses, which were detectable but not significantly higher than the PBS control group (Figure 5B). Furthermore, while the 1 µg dose IN boost elicited detectable IgA levels in the nasal biofluid, these levels were not significantly higher in all IN-boosted groups compared to the PBS control (Supplementary Figure S6A,B). Interestingly, we observed differential clustering in nasal biofluid compared to both serum and BALF, with the IM-boosted group clustering independently from both the 1 µg dose and the 10 µg dose the 10 µg dose IN boost in the PCA (Figure 4D and Supplementary Figure S6E). Furthermore, distinct clustering was observed based on the type of booster, which was primarily driven by antigen-specific IgA response. Given the Th2-skewed immune response in BALB/c mice, vaccine formulations should also be evaluated in Th1-prone strains, such as C57BL/6, to ensure a comprehensive assessment of immune responses [87,88].

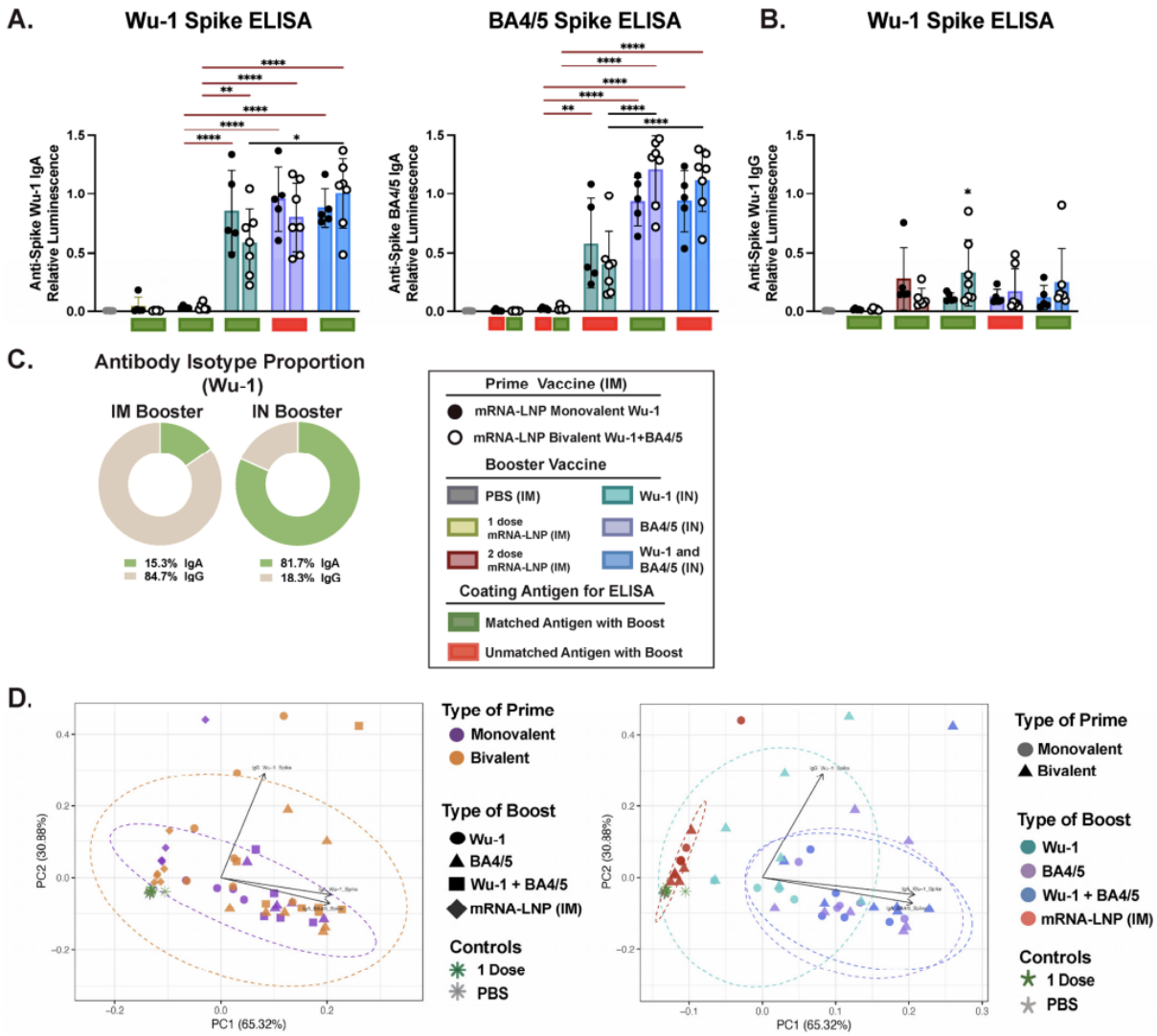


Figure 4. Characterization of mucosal immune responses in nasal wash following a heterologous systemic prime and mucosal boost vaccination. (A) Measurement of Wu-1- and BA4/5-spike-specific IgA in nasal wash at endpoint (day 35). (B) Measurement of Wu-1-spike-specific IgG titers and (C) relative proportion of Wu-1-specific IgG and IgA isotypes in nasal wash. (D) Principal component analysis (PCA) of antibody responses in nasal wash and dotted ellipses represent confidence interval for each group. Each point represents an individual mouse, incorporating all measured antibody responses. PCA plots are colored by (i) prime vaccine type and (ii) booster type to illustrate distinct clustering patterns driven by different vaccination regimens. Data reflect results obtained from one biological replicate and are representative as average of 2–3 technical replicates. Nasal wash was diluted 1:5 for the measure of IgA-specific titers. For statistical analysis, antibody titers were log-transformed and then analyzed by a one-way ANOVA with Tukey's multiple comparisons. **** $p \leq 0.0001$, ** $p \leq 0.01$, * $p \leq 0.05$.

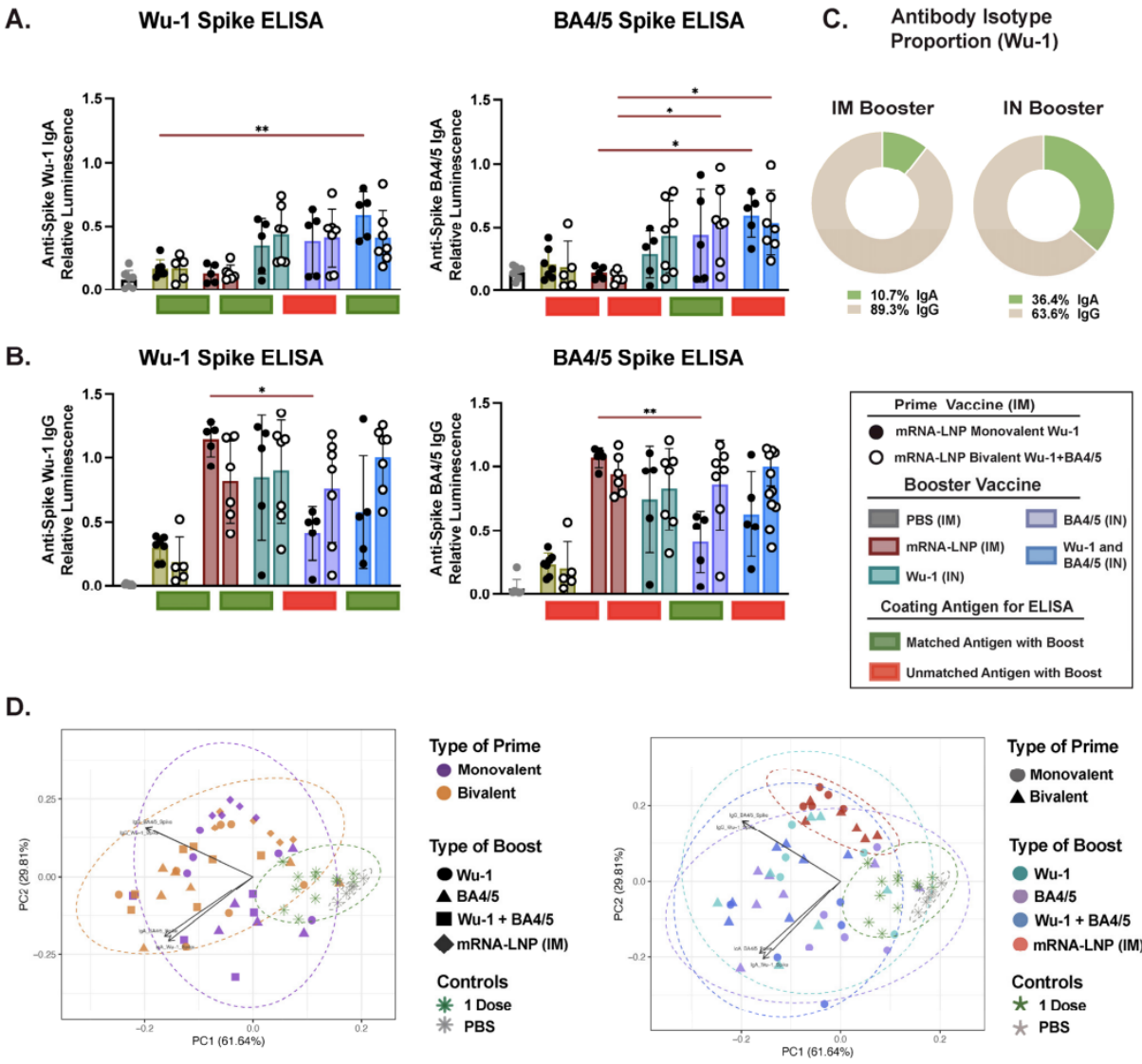


Figure 5. Characterization of mucosal immune responses in intestines following a heterologous systemic prime and mucosal boost vaccination. (A) Measurement of Wu-1- and BA4/5-spike-specific IgA titers in intestinal fluid at endpoint (day 35). (B) Measurement of Wu-1- and BA4/5-spike-specific IgG titers. (C) Relative proportion of Wu-1-specific IgG and IgA isotypes in intestinal fluid. (D) Principal component analysis (PCA) of antibody responses in nasal wash. Each point represents an individual mouse, incorporating all measured antibody responses and dotted ellipses represent confidence interval for each group. PCA plots are colored by (i) prime vaccine type and (ii) booster type to illustrate distinct clustering patterns driven by different vaccination regimens. Data reflect results obtained from one biological replicate and are representative as average of 2–3 technical replicates. Intestinal supernatant was diluted 1:2 for the measure of IgA-specific titers. For statistical analysis, antibody titers were log-transformed and then analyzed by a one-way ANOVA with Tukey's multiple comparisons. ** $p \leq 0.01$, * $p \leq 0.05$.

3.4. IM and IN Vaccination Induce Potent IgG Responses in the Intestinal Lumen

A single dose of mRNA-LNP administered IM induced detectable levels of IgG antibodies in the intestinal fluid (Figure 6 and Supplementary Figure S7). While IN administration of a 10 µg dose of unadjuvanted protein boosted both IgG and IgA levels, the 1 µg dose or IM administration of the mRNA-LNP vaccine only boosted IgG responses (Figure 5A,B; Supplementary Figure S7A,B). Notably, IM administration induced IgG levels that were either superior to or comparable with those elicited by the 10 µg IN boost. However, unlike in other mucosal compartments, both routes of administration elicited an IgG-predominant response in the intestinal fluid (Figure 5C and Supplementary Figure S7C). Furthermore, no variant-specific IgG- or IgA-skewed response corresponding to the type of prime or boost vaccine formulation was observed, which contrasts to findings in other compartments (Supplementary Figure S2G). We observed differential clustering based on the administration route and number of vaccine doses received, which were primarily driven by both IgG and IgA responses (Figure 5D and Supplementary Figure S7D).

3.5. Effect of Administration Route on Humoral Response Profiles and Antibody Correlations Across Compartments

Next, we sought to further dissect the relative influence of each administration route and vaccine formulation on the overall humoral response outcome. For this analysis, we included paired serological data from each distinct compartment across the various prime and boost groups. Notably, we observed five separate clusters primarily driving IgG and IgA responses (Figure 6A). The mRNA-LNP IM-boosted group clustered independently from the 10 µg and 1 µg protein IN-boosted groups, and was driving predominantly IgG responses, while the 1 µg dose groups clustered more closely to the 10 µg-boosted groups, with the IgA response as the primary driver. Furthermore, we additionally noted differential clustering based on the type of prime, similar to our observation in the serum. Several groups have previously reported strong to moderate IgG correlation between paired serum and saliva in convalescent COVID-19 patients, while IgA responses exhibited weaker correlation, highlighting possible compartmentalization of the IgA response [23,89–91].

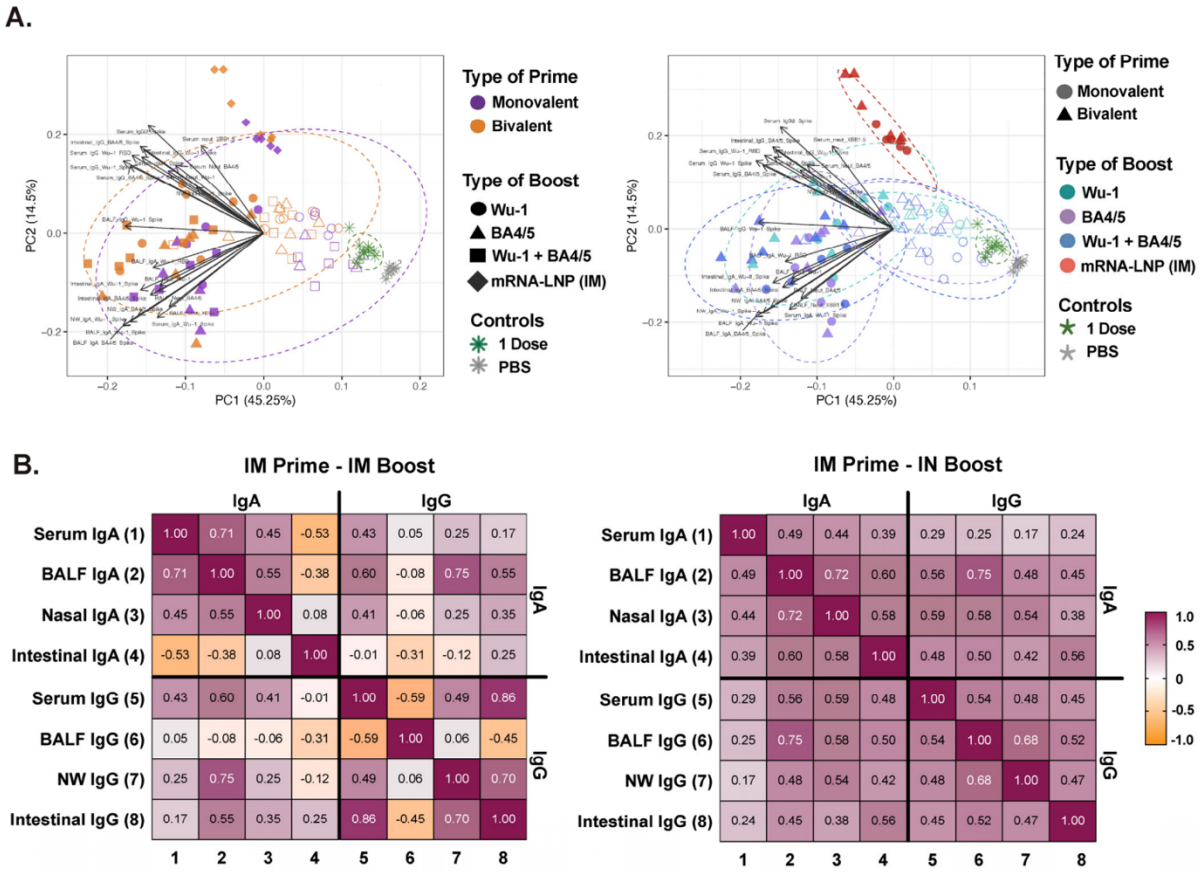


Figure 6. Humoral response kinetics and analysis of IgA and IgG antibodies from different compartments. (A) Principal component analysis (PCA) of antibody responses across serum, BALF, nasal wash, and intestinal fluid. Each point represents an individual mouse, incorporating all antibody measurements across compartments and dotted ellipses represent confidence interval for each group. PCA plots are colored by prime and boost type to illustrate differential clustering patterns based on vaccination regimens. (B) Correlation between IgG and IgA antibody levels in serum, BALF, nasal wash, and intestinal fluid. Each square represents total antibody responses from all mice combined, categorized by intranasal (IN) boost formulation (1 µg or 10 µg dose) or IM mRNA-LNP boost.

Next, we analyzed the correlation between IgG and IgA responses across three anatomical compartments to better understand the distribution and coordination of the induced immune responses, determining whether they are compartmentalized or consistently aligned across the mucosal compartments (Figure 6B). Paired serological data from each mouse were analyzed, with antibody profiles stratified by administration route to reflect the distinct clustering observed between IN- and IM-boosted groups in Figure 6A. Of the three mucosal compartments, we observed high IgA ($r = 0.72$, $p \leq 0.0001$) and IgG ($r = 0.68$, $p \leq 0.0001$) correlation between BALF and nasal wash in IN-boosted mice only. While a positive correlation ($r = 0.75$, $p \leq 0.0001$)

between IgG and IgA responses was observed in BALF in IN-boosted mice, no correlation between these antibody isotypes in other biofluids was observed. While a positive IgA correlation ($r = 71$, $p = 0.008$) was observed between serum and BALF in IM-boosted mice, it was likely confounded given the very low IgA titers detected in BALF following IM vaccination. Interestingly, we found a strong positive correlation ($r = 0.86$, $p = 0.001$) between serum and intestinal IgG antibody titers in IM-boosted mice levels, which was not observed in IN-boosted mice.

4. Discussion

In this study, we aimed to examine the effects of heterologous prime–boost regimens on humoral responses, focusing on IM and IN administration routes and variant-tailored vaccine formulations. Our findings indicate that the IM prime predominantly shapes systemic humoral responses, primarily driven by variant-specific neutralizing responses, while the IN boost further amplifies and refines them. Indeed, homologous prime and boost antigen vaccination resulted in Wu-1-skewed humoral responses. This effect was mitigated by heterologous IN boosting with the Omicron BA4/5 antigen, which significantly improved neutralization against antigenically distant VOCs compared to mice that received two doses of the monovalent mRNA-LNP IM vaccine, while retaining neutralization activity against the ancestral Wu-1 strain. Importantly, our results highlight the value of incorporating distinct antigenic variants in the prime vaccine, as the bivalent prime significantly enhanced the breadth of total and neutralizing responses against circulating VOCs in serum. The IN boost, rather than the IM prime, had a greater impact on mucosal responses, primarily driven by antigen-specific IgA responses in nasal wash and BALF. Higher IgA titers correlated more strongly with neutralizing activity than IgG, with the BA4/5- and BA4/5 + Wu-1-boosted groups showing the highest neutralizing titers against BA4/5. Furthermore, we show differential induction of IgG and IgA antibody isotypes across distinct immune compartments following IM relative to IN boosting. Indeed, a strong IgA antibody correlation between mucosal compartments was observed only in IN-vaccinated mice. Taken together, our findings highlight the merit of including distinct antigenic variants, if possible, in the prime vaccine to enhance VOC neutralization and support the use of variant-tailored IN boosters, which simultaneously boost systemic responses and elicit mucosal responses at the viral point of entry.

Additionally, we demonstrate that IN was significantly superior to IM vaccination at driving a predominantly IgA-favored response in nasal, BAL, and intestinal biofluids. This observation aligns with recent studies evaluating heterologous prime–boost regimens in vivo, which highlight the potent induction of cellular and humoral responses in BALF following IN or oral vaccination in mice with pre-existing immunity [22,70,72–75,79,80]. However, while variant-specific total and neutralizing responses after variant-tailored boosting are well documented in serum, the effects of heterologous boosting strategies on the induction of variant-specific responses in saliva, nasal, and BAL biofluids remain poorly characterized. Here, we demonstrate that variant-specific IgA responses in BALF and nasal wash were predominantly shaped by the vaccine antigens delivered via IN rather than IM immunization, highlighting the compartmentalization of mucosal responses as recently suggested [23,89–91]. Given that transmission of SARS-CoV-2 primarily occurs via inhalation of aerosolized virus, local immune responses are uniquely positioned to act as a rapid, first line of defense against infection. Initial mRNA-LNP IM vaccines were up to 90% effective against symptomatic infection following exposure to antigenically matched VOCs [15–17,29], likely due to potent induction of systemic IgG response, which could diffuse into the URT [56,92]. Our findings of robust IgG titers in BALF and nasal wash following the mRNA-LNP boost support this. However, Omicron and its sub-variants evolved to preferentially replicate in the URT and have shorter incubation times and thereby reduce the immune recall response window [93–95]. This leads to increased viral transmissibility and emphasizes the need for a persistent virus-neutralizing capacity at the initial replication site

A growing body of literature highlights the importance of stimulating the respiratory mucosa and the role of sIgA in respiratory mucosa to protect against breakthrough infections [22,23,43,55–59,96]. Despite similar systemic IgG levels, individuals with hybrid immunity (vaccination plus infection) exhibit higher mucosal IgA levels, which were associated with a lower incidence of subsequent breakthrough infections compared to vaccinated-only individuals [22,43,55–58]. We found that IgA responses in BALF correlated more strongly with neutralizing activity than the IgG isotype, consistent with studies showing sIgA’s potent neutralization capacity against SARS-CoV-2 in vitro [23,66,73,76,80,86]. Notably, we observed comparable BA4/5- and XBB1.5-neutralizing activity in BALF, suggesting that IgA, abundant in dimeric or pentameric

forms at the mucosal surface, may be more effective than monomeric IgG at neutralizing variants with escape [86,97]. While systemic neutralizing antibodies are an established correlate of vaccine protection [83], analogous correlates of mucosal immunity against viral infection and transmission have yet to be established. Identifying these will be key to assessing the efficacy of intranasal vaccines. Indeed, antibody kinetics at distinct mucosal sites in response to different vaccination regimens remain poorly characterized. In this study, we found a strong correlation between IgA in BAL and nasal compartments only in IN-vaccinated mice, suggesting IgA compartmentalization, as observed in studies assessing IgA correlations in serum and saliva [23,89–91].

Recent evidence shows that SARS-CoV-2 breakthrough infections induce durable tissue-resident memory T and B cells, including plasma and germinal center B cells, persisting for up to a year in humans, with IgA+ memory B cells significantly enriched in the upper airways compared to blood [98]. IgA is the predominant immunoglobulin at mucosal surfaces, while IgG, though less abundant, can constitute 15–20% of total immunoglobulins at certain sites [99,100] and plays a protective role in the lower respiratory tract through complement activation and antibody-dependent cellular cytotoxicity (ADCC) [92,101]. In serum, IgA exists primarily in monomeric form, accounting for approximately 15% of total immunoglobulins [102,103], contributing to immune defense via phagocytosis, ADCC, and, under specific conditions, complement activation. Building on these observations, our study offers a comprehensive comparison of relative IgA and IgG levels in serum and across distinct anatomical compartments following IN or IM SARS-CoV-2 vaccination. This comparison is crucial for understanding how different vaccination routes shape antibody distribution across compartments and contribute to mucosal and systemic immunity, informing strategies for optimizing vaccine efficacy.

Interestingly, we observed IgG responses in the intestinal mucosa following both IM and IN immunization. While plasma cells can disseminate between distinct mucosal compartments after mucosal immunization [96,104,105], it remains unclear how IgG responses were generated after IM vaccination. Spike protein has been detected in plasma for up to five days following mRNA-LNP IM vaccination [106], suggesting that these antibody responses might be induced directly in Peyer’s patches, which are present in the intestinal tissue we analyzed. Notably, residual SARS-CoV-2 antigens have also been detected in intestinal mucosa and stool samples, even after viral

clearance from the URT [107–109]. Thus, this potent induction of humoral responses in the intestinal lumen following IM vaccination with mRNA-LNP should be studied and potentially leveraged to reduce viral replication and transmission of gastrointestinal viruses.

We observed reduced BA4/5 and XBB.1.5 neutralization in mice primed with the monovalent Wu-1 vaccine and boosted with the BA4/5 + Wu-1 combination, compared to those boosted with BA.4/5 antigen alone. In contrast, mice bivalently primed and boosted with either BA.4/5 alone or the BA.4/5 + Wu-1 combination showed comparable neutralization activity across both formulations. These findings suggest that the BA4/5 + Wu-1 boost in monovalent-primed mice primarily triggered cross-reactive recall responses to shared epitopes, rather than inducing BA.4/5-specific antibodies, indicating the presence of immune imprinting. This aligns with recent studies showing that variant-specific boosting primarily promoted recall responses, with the highest neutralizing titers against the ancestral strain [4,20,38,41,42,50–53]. This immune imprinting effect was further exacerbated by retaining the ancestral antigen in the bivalent vaccines. The generation of variant-specific de novo antibodies has been observed, although at low levels, with monovalent Omicronand XBB1.5-specific mRNA-LNP boosters, highlighting the benefits of updating vaccines to match circulating variants [41,42,110,111]. However, these findings highlight the influence of immune imprinting, which can be overcome by boosting with antigens that are sufficiently distinct from the priming antigen [110], through repeated boosting [112], or by incorporating adjuvants [113], as we have previously reviewed [48].

Early after SARS-CoV-2 infection, cellular immune responses are crucial in controlling infection severity and providing long-term protection, while vaccine-elicited total and neutralizing antibody responses are more closely associated with protection against infection and symptomatic disease [83,84]. Given that most T cell epitopes remain relatively unchanged in VOCs [114], and that cellular responses were characterized in detail in the “Prime and Spike” vaccination approach by Mao et al., this study focused exclusively on examining only the humoral antibody profiles across different anatomical compartments using monovalent and bivalent vaccines.

Our findings demonstrate that bivalent priming with two distinct variants significantly broadened the neutralization responses, which can be further enhanced by IN boosting. The inclusion of

multivalent viral strains or a highly conserved antigen in vaccine formulations, as proposed for some universal vaccine strategies, can leverage immune imprinting to shape a broadly reactive B cell repertoire. This approach may be particularly beneficial for immunologically naïve populations, such as young children, by providing broad protection against circulating SARS-CoV-2 variants. Additionally, it could be an effective strategy for combating future emerging respiratory viruses before widespread exposure occurs. Understanding the impact of different vaccination strategies on immune responses across different anatomical compartments may aid in inducing protective mucosal responses against SARS-CoV-2 variants.

5. Conclusions

Our study showcases the benefits of heterologous prime–boost vaccination strategies, particularly the role of IN boosting in enhancing both systemic and mucosal immunity against SARS-CoV-2 variants. We demonstrate that an IM prime predominantly drives systemic IgG responses, while an IN boost significantly amplifies variant-specific neutralization and elicits robust mucosal IgA responses, which correlate strongly with neutralization activity in the respiratory tract. Importantly, incorporating antigenically distinct variants in the prime vaccine broadens humoral responses and mitigates immune imprinting. Our findings support the inclusion of variant-adapted IN boosters to enhance protection at the viral entry site, highlighting their potential in mitigating breakthrough infections and transmission. Understanding the differential impact of IM and IN vaccination across immune compartments will be crucial for optimizing next-generation vaccine strategies against SARS-CoV-2 and other respiratory pathogens.

Supplementary Materials: The following supporting information can be downloaded at: https://www.mdpi.com/article/10.3390/vaccines13040351/s1,

Author Contributions: M.M. and M.-A.L. designed the study. M.M. developed the assays and conducted the in vitro experiments. Animal sample processing was carried out by M.M., P.M., Y.G. and N.C. C.L.C. provided the LNP-mRNA vaccines. Data analysis and curation were performed by M.M., Y.G., C.L.C., and M.-A.L. M.M. prepared and wrote the original draft. M.M., C.L.C. and M.-A.L. reviewed and edited the manuscript. M.-A.L. supervised the project, managed funding, and oversaw project administration. All authors have read and agreed to the published version of the manuscript.

Funding: This work was supported by a Canadian Institute of Health Research (CIHR) grant (VR2- 172722) and from a supplement by the COVID-19 Immunity Task Force (CITF) to M-A.L. M.M. holds the Queen Elizabeth II scholarship in Science and Technology. YG is supported by a Charles Best and Frederick Banting CGS-D from CIHR (476885). M.-A.L. holds a Faculty of Medicine Chair of Excellence in Pandemic Viruses and Preparedness Research.

Institutional Review Board Statement: All animal experiments were conducted in accordance with the Ontario Animals for Research Act and approved by the University of Ottawa Animal Ethics Committee (protocol BMI-3649, 07/04/2022).

Acknowledgments: We sincerely thank Anthony Carter and the uOttawa surgical ACVS core for their technical support with sample set up and acquisition. Schematics were created in Biorender.com.

Conflicts of Interest: The authors declare no conflicts of interest.

References

1. Cele, S.; Jackson, L.; Khoury, D.S.; Khan, K.; Moyo-Gwete, T.; Tegally, H.; San, J.E.; Cromer, D.; Scheepers, C.; Amoako, D.; et al. SARS-CoV-2 Omicron has extensive but incomplete escape of Pfizer BNT162b2 elicited neutralization and requires ACE2 for infection. medRxiv 2021. [CrossRef]
2. Chemaitelly, H.; Tang, P.; Hasan, M.R.; AlMukdad, S.; Yassine, H.M.; Benslimane, F.M.; Al Khatib, H.A.; Coyle, P.; Ayoub, H.H.; Al Kanaani, Z.; et al. Waning of BNT162b2 Vaccine Protection against SARS-CoV-2 Infection in Qatar. N. Engl. J. Med. 2021, 385, e83. [CrossRef] [PubMed]
3. Greaney, A.J.; Starr, T.N.; Gilchuk, P.; Zost, S.J.; Binshtein, E.; Loes, A.N.; Hilton, S.K.; Huddleston, J.; Eguia, R.; Crawford, K.H.D.; et al. Complete Mapping of Mutations to the SARS-CoV-2 Spike Receptor-Binding Domain that Escape Antibody Recognition. Cell Host Microbe 2021, 29, 44–57.e49. [CrossRef] [PubMed]
4. Tortorici, M.A.; Addetia, A.; Seo, A.J.; Brown, J.; Sprouse, K.; Logue, J.; Clark, E.; Franko, N.; Chu, H.; Veesler, D. Persistent immune imprinting occurs after vaccination with the COVID-19 XBB.1.5 mRNA booster in humans. Immunity 2024, 57, 904–911.e4. [CrossRef]
5. Tan, S.T.; Kwan, A.T.; Rodriguez-Barraquer, I.; Singer, B.J.; Park, H.J.; Lewnard, J.A.; Sears, D.; Lo, N.C. Infectiousness of SARS-CoV-2 breakthrough infections and reinfections during the Omicron wave. Nat. Med. 2023, 29, 358–365. [CrossRef]
6. Regenhardt, E.; Kirsten, H.; Weiss, M.; Lubbert, C.; Stehr, S.N.; Remane, Y.; Pietsch, C.; Honemann, M.; von Braun, A. SARS-CoV-2 Vaccine Breakthrough Infections of Omicron and Delta Variants in Healthcare Workers. Vaccines 2023, 11, 958. [CrossRef]
7. Singanayagam, A.; Hakki, S.; Dunning, J.; Madon, K.J.; Crone, M.A.; Koycheva, A.; Derqui-Fernandez, N.; Barnett, J.L.; Whitfield, M.G.; Varro, R.; et al. Community transmission and viral load kinetics of the SARS-CoV-2 delta (B.1.617.2) variant in vaccinated and unvaccinated individuals in the UK: A prospective, longitudinal, cohort study. Lancet Infect. Dis. 2022, 22, 183–195. [CrossRef]
8. Chu, L.; Vrbicky, K.; Montefiori, D.; Huang, W.; Nestorova, B.; Chang, Y.; Carfi, A.; Edwards, D.K.; Oestreicher, J.; Legault, H.; et al. Immune response to SARS-CoV-2 after a booster of mRNA-1273: An open-label phase 2 trial. Nat. Med. 2022, 28, 1042–1049. [CrossRef]
9. Kaku, C.I.; Bergeron, A.J.; Ahlm, C.; Normark, J.; Sakharkar, M.; Forsell, M.N.E.; Walker, L.M. Recall of preexisting cross-reactive B cell memory after Omicron BA.1 breakthrough infection. Sci. Immunol. 2022, 7, eabq3511. [CrossRef]
10. Kuhlmann, C.; Mayer, C.K.; Claassen, M.; Maponga, T.; Burgers, W.A.; Keeton, R.; Riou, C.; Sutherland, A.D.; Suliman, T.; Shaw, M.L.; et al. Breakthrough infections with SARS-CoV-2 omicron despite mRNA vaccine booster dose. Lancet 2022, 399, 625–626. [CrossRef]
11. Lange, B.; Gerigk, M.; Tenenbaum, T. Breakthrough Infections in BNT162b2-Vaccinated Health Care Workers. N. Engl. J. Med. 2021, 385, 1145–1146. [CrossRef] [PubMed]
12. Kustin, T.; Harel, N.; Finkel, U.; Perchik, S.; Harari, S.; Tahor, M.; Caspi, I.; Levy, R.; Leshchinsky, M.; Ken Dror, S.; et al. Evidence for increased breakthrough rates of SARS-CoV-2 variants of concern in BNT162b2-mRNA-vaccinated individuals. Nat. Med. 2021, 27, 1379–1384. [CrossRef]
13. Bergwerk, M.; Gonen, T.; Lustig, Y.; Amit, S.; Lipsitch, M.; Cohen, C.; Mandelboim, M.; Levin, E.G.; Rubin, C.; Indenbaum, V.; et al. COVID-19 Breakthrough Infections in Vaccinated Health Care Workers. N. Engl. J. Med. 2021, 385, 1474–1484. [CrossRef] [PubMed]
14. Hager, K.J.; Perez Marc, G.; Gobeil, P.; Diaz, R.S.; Heizer, G.; Llapur, C.; Makarkov, A.I.; Vasconcellos, E.; Pillet, S.; Riera, F.; et al. Efficacy and Safety of a Recombinant Plant-Based Adjuvanted COVID-19 Vaccine. N. Engl. J. Med. 2022, 386, 2084–2096. [CrossRef] [PubMed]
15. Thomas, S.J.; Moreira, E.D., Jr.; Kitchin, N.; Absalon, J.; Gurtman, A.; Lockhart, S.; Perez, J.L.; Perez Marc, G.; Polack, F.P.; Zerbini, C.; et al. Safety and Efficacy of the BNT162b2 mRNA COVID-19 Vaccine through 6 Months. N. Engl. J. Med. 2021, 385, 1761–1773. [CrossRef]

16. Polack, F.P.; Thomas, S.J.; Kitchin, N.; Absalon, J.; Gurtman, A.; Lockhart, S.; Perez, J.L.; Perez Marc, G.; Moreira, E.D.; Zerbini, C.; et al. Safety and Efficacy of the BNT162b2 mRNA COVID-19 Vaccine. N. Engl. J. Med. 2020, 383, 2603–2615. [CrossRef]
17. Tenforde, M.W.; Self, W.H.; Adams, K.; Gaglani, M.; Ginde, A.A.; McNeal, T.; Ghamande, S.; Douin, D.J.; Talbot, H.K.; Casey, J.D.; et al. Association Between mRNA Vaccination and COVID-19 Hospitalization and Disease Severity. JAMA 2021, 326, 2043–2054. [CrossRef]
18. Menni, C.; May, A.; Polidori, L.; Louca, P.; Wolf, J.; Capdevila, J.; Hu, C.; Ourselin, S.; Steves, C.J.; Valdes, A.M.; et al. COVID-19 vaccine waning and effectiveness and side-effects of boosters: A prospective community study from the ZOE COVID Study. Lancet Infect. Dis. 2022, 22, 1002–1010. [CrossRef]
19. Lucas, C.; Vogels, C.B.F.; Yildirim, I.; Rothman, J.E.; Lu, P.; Monteiro, V.; Gehlhausen, J.R.; Campbell, M.; Silva, J.; Tabachnikova, A.; et al. Impact of circulating SARS-CoV-2 variants on mRNA vaccine-induced immunity. Nature 2021, 600, 523–529. [CrossRef]
20. Weber, T.; Dahling, S.; Rose, S.; Affeldt, P.; Vanshylla, K.; Ullrich, L.; Gieselmann, L.; Teipel, F.; Gruell, H.; Di Cristanziano, V.; et al. Enhanced SARS-CoV-2 humoral immunity following breakthrough infection builds upon the preexisting memory B cell pool. Sci. Immunol. 2023, 8, eadk5845. [CrossRef]
21. Kemp, S.A.; Cheng, M.T.K.; Hamilton, W.L.; Kamelian, K.; Indian, S.-C.-G.C.; Singh, S.; Rakshit, P.; Agrawal, A.; Illingworth, C.J.R.; Gupta, R.K. Transmission of B.1.617.2 Delta variant between vaccinated healthcare workers. Sci. Rep. 2022, 12, 10492. [CrossRef]
22. Tang, J.; Zeng, C.; Cox, T.M.; Li, C.; Son, Y.M.; Cheon, I.S.; Wu, Y.; Behl, S.; Taylor, J.J.; Chakraborty, R.; et al. Respiratory mucosal immunity against SARS-CoV-2 following mRNA vaccination. Sci. Immunol. 2022, 7, eadd4853. [CrossRef] [PubMed] 23. Sheikh-Mohamed, S.; Isho, B.; Chao, G.Y.C.; Zuo, M.; Cohen, C.; Lustig, Y.; Nahass, G.R.; Salomon-Shulman, R.E.; Blacker, G.; Fazel-Zarandi, M.; et al. Systemic and mucosal IgA responses are variably induced in response to SARS-CoV-2 mRNA vaccination and are associated with protection against subsequent infection. Mucosal Immunol. 2022, 15, 799–808. [CrossRef] 24. Krammer, F. SARS-CoV-2 vaccines in development. Nature 2020, 586, 516–527. [CrossRef] [PubMed]
25. Brouwer, P.J.M.; Caniels, T.G.; van der Straten, K.; Snitselaar, J.L.; Aldon, Y.; Bangaru, S.; Torres, J.L.; Okba, N.M.A.; Claireaux, M.; Kerster, G.; et al. Potent neutralizing antibodies from COVID-19 patients define multiple targets of vulnerability. Science 2020, 369, 643–650. [CrossRef]
26. Liu, L.; Wang, P.; Nair, M.S.; Yu, J.; Rapp, M.; Wang, Q.; Luo, Y.; Chan, J.F.; Sahi, V.; Figueroa, A.; et al. Potent neutralizing antibodies against multiple epitopes on SARS-CoV-2 spike. Nature 2020, 584, 450–456. [CrossRef]
27. Rogers, T.F.; Zhao, F.; Huang, D.; Beutler, N.; Burns, A.; He, W.T.; Limbo, O.; Smith, C.; Song, G.; Woehl, J.; et al. Isolation of potent SARS-CoV-2 neutralizing antibodies and protection from disease in a small animal model. Science 2020, 369, 956–963. [CrossRef]
28. Bartsch, Y.C.; Wang, C.; Zohar, T.; Fischinger, S.; Atyeo, C.; Burke, J.S.; Kang, J.; Edlow, A.G.; Fasano, A.; Baden, L.R.; et al. Humoral signatures of protective and pathological SARS-CoV-2 infection in children. Nat. Med. 2021, 27, 454–462. [CrossRef] 29. Baden, L.R.; El Sahly, H.M.; Essink, B.; Kotloff, K.; Frey, S.; Novak, R.; Diemert, D.; Spector, S.A.; Rouphael, N.; Creech, C.B.; et al. Efficacy and Safety of the mRNA-1273 SARS-CoV-2 Vaccine. N. Engl. J. Med. 2021, 384, 403–416. [CrossRef]
30. Demone, J.; Maltseva, M.; Nourimand, M.; Nasr-Sharif, M.; Galipeau, Y.; Alarcon, E.I.; Langlois, M.A.; MacLean, A.M. Scalable agroinfiltration-based production of SARS-CoV-2 antigens for use in diagnostic assays and subunit vaccines. PLoS ONE 2022, 17, e0277668. [CrossRef]
31. Chalkias, S.; Whatley, J.L.; Eder, F.; Essink, B.; Khetan, S.; Bradley, P.; Brosz, A.; McGhee, N.; Tomassini, J.E.; Chen, X.; et al. Original SARS-CoV-2 monovalent and Omicron BA.4/BA.5 bivalent COVID-19 mRNA vaccines: Phase 2/3 trial interim results. Nat. Med. 2023, 29, 2325–2333. [CrossRef]
32. Kurhade, C.; Zou, J.; Xia, H.; Liu, M.; Chang, H.C.; Ren, P.; Xie, X.; Shi, P.Y. Low neutralization of SARS-CoV-2 Omicron BA.2.75.2, BQ.1.1 and XBB.1 by parental mRNA vaccine or a BA.5 bivalent booster. Nat. Med. 2023, 29, 344–347. [CrossRef] [PubMed]

33. Chalkias, S.; Harper, C.; Vrbicky, K.; Walsh, S.R.; Essink, B.; Brosz, A.; McGhee, N.; Tomassini, J.E.; Chen, X.; Chang, Y.; et al. A Bivalent Omicron-Containing Booster Vaccine against COVID-19. N. Engl. J. Med. 2022, 387, 1279–1291. [CrossRef] [PubMed] 34. Davis-Gardner, M.E.; Lai, L.; Wali, B.; Samaha, H.; Solis, D.; Lee, M.; Porter-Morrison, A.; Hentenaar, I.T.; Yamamoto, F.; Godbole, S.; et al. Neutralization against BA.2.75.2, BQ.1.1, and XBB from mRNA Bivalent Booster. N. Engl. J. Med. 2023, 388, 183–185. [CrossRef] [PubMed]
35. Zou, J.; Kurhade, C.; Patel, S.; Kitchin, N.; Tompkins, K.; Cutler, M.; Cooper, D.; Yang, Q.; Cai, H.; Muik, A.; et al. Neutralization of BA.4-BA.5, BA.4.6, BA.2.75.2, BQ.1.1, and XBB.1 with Bivalent Vaccine. N. Engl. J. Med. 2023, 388, 854–857. [CrossRef]
36. Collier, A.Y.; Miller, J.; Hachmann, N.P.; McMahan, K.; Liu, J.; Bondzie, E.A.; Gallup, L.; Rowe, M.; Schonberg, E.; Thai, S.; et al. Immunogenicity of BA.5 Bivalent mRNA Vaccine Boosters. N. Engl. J. Med. 2023, 388, 565–567. [CrossRef]
37. Wang, Q.; Bowen, A.; Valdez, R.; Gherasim, C.; Gordon, A.; Liu, L.; Ho, D.D. Antibody Response to Omicron BA.4-BA.5 Bivalent Booster. N. Engl. J. Med. 2023, 388, 567–569. [CrossRef]
38. Wang, Q.; Guo, Y.; Tam, A.R.; Valdez, R.; Gordon, A.; Liu, L.; Ho, D.D. Deep immunological imprinting due to the ancestral spike in the current bivalent COVID-19 vaccine. Cell Rep. Med. 2023, 4, 101258. [CrossRef]
39. Wang, Q.; Bowen, A.; Tam, A.R.; Valdez, R.; Stoneman, E.; Mellis, I.A.; Gordon, A.; Liu, L.; Ho, D.D. SARS-CoV-2 neutralising antibodies after bivalent versus monovalent booster. Lancet Infect. Dis. 2023, 23, 527–528. [CrossRef]
40. Wang, Q.; Bowen, A.; Ho, J.; Zhang, R.M.; Valdez, R.; Stoneman, E.; Gordon, A.; Liu, L.; Ho, D.D. SARS-CoV-2 neutralising antibodies after a second BA.5 bivalent booster. Lancet 2023, 402, 1827–1828. [CrossRef]
41. Johnston, T.S.; Li, S.H.; Painter, M.M.; Atkinson, R.K.; Douek, N.R.; Reeg, D.B.; Douek, D.C.; Wherry, E.J.; Hensley, S.E. Immunological imprinting shapes the specificity of human antibody responses against SARS-CoV-2 variants. Immunity 2024, 57, 912–925.e914. [CrossRef] [PubMed]
42. Wang, Q.; Guo, Y.; Bowen, A.; Mellis, I.A.; Valdez, R.; Gherasim, C.; Gordon, A.; Liu, L.; Ho, D.D. XBB.1.5 monovalent mRNA vaccine booster elicits robust neutralizing antibodies against XBB subvariants and JN.1. Cell Host Microbe 2024, 32, 315–321.e313. [CrossRef]
43. Altarawneh, H.N.; Chemaitelly, H.; Ayoub, H.H.; Tang, P.; Hasan, M.R.; Yassine, H.M.; Al-Khatib, H.A.; Al Thani, A.A.; Coyle, P.; Al-Kanaani, Z.; et al. Effects of previous infection, vaccination, and hybrid immunity against symptomatic Alpha, Beta, and Delta SARS-CoV-2 infections: An observational study. EBioMedicine 2023, 95, 104734. [CrossRef]
44. Carabelli, A.M.; Peacock, T.P.; Thorne, L.G.; Harvey, W.T.; Hughes, J.; Consortium, C.-G.U.; Peacock, S.J.; Barclay, W.S.; de Silva, T.I.; Towers, G.J.; et al. SARS-CoV-2 variant biology: Immune escape, transmission and fitness. Nat. Rev. Microbiol. 2023, 21, 162–177. [CrossRef] [PubMed]
45. Aguilar-Bretones, M.; Fouchier, R.A.; Koopmans, M.P.; van Nierop, G.P. Impact of antigenic evolution and original antigenic sin on SARS-CoV-2 immunity. J. Clin. Investig. 2023, 133, e162192. [CrossRef]
46. Lin, D.Y.; Xu, Y.; Gu, Y.; Zeng, D.; Sunny, S.K.; Moore, Z. Durability of Bivalent Boosters against Omicron Subvariants. N. Engl. J. Med. 2023, 388, 1818–1820. [CrossRef]
47. Han, A.X.; de Jong, S.P.J.; Russell, C.A. Co-evolution of immunity and seasonal influenza viruses. Nat. Rev. Microbiol. 2023, 21, 805–817. [CrossRef] [PubMed]
48. Maltseva, M.; Keeshan, A.; Cooper, C.; Langlois, M.A. Immune imprinting: The persisting influence of the first antigenic encounter with rapidly evolving viruses. Hum. Vaccin. Immunother. 2024, 20, 2384192. [CrossRef]
49. Koutsakos, M.; Ellebedy, A.H. Immunological imprinting: Understanding COVID-19. Immunity 2023, 56, 909–913. [CrossRef] 50. Huang, C.Q.; Vishwanath, S.; Carnell, G.W.; Chan, A.C.Y.; Heeney, J.L. Immune imprinting and next-generation coronavirus vaccines. Nat. Microbiol. 2023, 8, 1971–1985. [CrossRef]

51. Carreno, J.M.; Singh, G.; Simon, V.; Krammer, F.; PVI Study Group. Bivalent COVID-19 booster vaccines and the absence of BA.5-specific antibodies. Lancet Microbe 2023, 4, e569. [CrossRef] [PubMed]
52. Park, Y.J.; Pinto, D.; Walls, A.C.; Liu, Z.; De Marco, A.; Benigni, F.; Zatta, F.; Silacci-Fregni, C.; Bassi, J.; Sprouse, K.R.; et al. Imprinted antibody responses against SARS-CoV-2 Omicron sublineages. Science 2022, 378, 619–627. [CrossRef]
53. Roltgen, K.; Nielsen, S.C.A.; Silva, O.; Younes, S.F.; Zaslavsky, M.; Costales, C.; Yang, F.; Wirz, O.F.; Solis, D.; Hoh, R.A.; et al. Immune imprinting, breadth of variant recognition, and germinal center response in human SARS-CoV-2 infection and vaccination. Cell 2022, 185, 1025–1040.e1014. [CrossRef] [PubMed]
54. Aydillo, T.; Rombauts, A.; Stadlbauer, D.; Aslam, S.; Abelenda-Alonso, G.; Escalera, A.; Amanat, F.; Jiang, K.; Krammer, F.; Carratala, J.; et al. Immunological imprinting of the antibody response in COVID-19 patients. Nat. Commun. 2021, 12, 3781. [CrossRef]
55. Marking, U.; Bladh, O.; Havervall, S.; Svensson, J.; Greilert-Norin, N.; Aguilera, K.; Kihlgren, M.; Salomonsson, A.C.; Mansson, M.; Gallini, R.; et al. 7-month duration of SARS-CoV-2 mucosal immunoglobulin-A responses and protection. Lancet Infect. Dis. 2023, 23, 150–152. [CrossRef]
56. Sheikh-Mohamed, S.; Sanders, E.C.; Gommerman, J.L.; Tal, M.C. Guardians of the oral and nasopharyngeal galaxy: IgA and protection against SARS-CoV-2 infection. Immunol. Rev. 2022, 309, 75–85. [CrossRef]
57. Havervall, S.; Marking, U.; Svensson, J.; Greilert-Norin, N.; Bacchus, P.; Nilsson, P.; Hober, S.; Gordon, M.; Blom, K.; Klingstrom, J.; et al. Anti-Spike Mucosal IgA Protection against SARS-CoV-2 Omicron Infection. N. Engl. J. Med. 2022, 387, 1333–1336. [CrossRef] [PubMed]
58. Sano, K.; Bhavsar, D.; Singh, G.; Floda, D.; Srivastava, K.; Gleason, C.; Group, P.S.; Carreno, J.M.; Simon, V.; Krammer, F. SARS-CoV-2 vaccination induces mucosal antibody responses in previously infected individuals. Nat. Commun. 2022, 13, 5135. [CrossRef]
59. Bhavsar, D.; Singh, G.; Sano, K.; Gleason, C.; Srivastava, K.; Group, P.S.; Carreno, J.M.; Simon, V.; Krammer, F. Mucosal antibody responses to SARS-CoV-2 booster vaccination and breakthrough infection. mBio 2023, 14, e0228023. [CrossRef]
60. Stark, F.C.; Akache, B.; Deschatelets, L.; Tran, A.; Stuible, M.; Durocher, Y.; McCluskie, M.J.; Agbayani, G.; Dudani, R.; Harrison, B.A.; et al. Intranasal immunization with a proteosome-adjuvanted SARS-CoV-2 spike protein-based vaccine is immunogenic and efficacious in mice and hamsters. Sci. Rep. 2022, 12, 9772. [CrossRef]
61. Hassan, A.O.; Feldmann, F.; Zhao, H.; Curiel, D.T.; Okumura, A.; Tang-Huau, T.L.; Case, J.B.; Meade-White, K.; Callison, J.; Lovaglio, J.; et al. A single intranasal dose of chimpanzee adenovirus-vectored vaccine protects against SARS-CoV-2 infection in rhesus macaques. bioRxiv 2021. [CrossRef] [PubMed]
62. Bricker, T.L.; Darling, T.L.; Hassan, A.O.; Harastani, H.H.; Soung, A.; Jiang, X.; Dai, Y.N.; Zhao, H.; Adams, L.J.; Holtzman, M.J.; et al. A single intranasal or intramuscular immunization with chimpanzee adenovirus-vectored SARS-CoV-2 vaccine protects against pneumonia in hamsters. Cell Rep. 2021, 36, 109400. [CrossRef]
63. Langel, S.N.; Johnson, S.; Martinez, C.I.; Tedjakusuma, S.N.; Peinovich, N.; Dora, E.G.; Kuehl, P.J.; Irshad, H.; Barrett, E.G.; Werts, A.; et al. Adenovirus type 5 SARS-CoV-2 vaccines delivered orally or intranasally reduced disease severity and transmission in a hamster model. Sci. Transl. Med. 2022, 14, eabn6868. [CrossRef]
64. Afkhami, S.; D'Agostino, M.R.; Zhang, A.; Stacey, H.D.; Marzok, A.; Kang, A.; Singh, R.; Bavananthasivam, J.; Ye, G.; Luo, X.; et al. Respiratory mucosal delivery of next-generation COVID-19 vaccine provides robust protection against both ancestral and variant strains of SARS-CoV-2. Cell 2022, 185, 896–915.e819. [CrossRef]
65. Du, Y.; Xu, Y.; Feng, J.; Hu, L.; Zhang, Y.; Zhang, B.; Guo, W.; Mai, R.; Chen, L.; Fang, J.; et al. Intranasal administration of a recombinant RBD vaccine induced protective immunity against SARS-CoV-2 in mouse. Vaccine 2021, 39, 2280–2287. [CrossRef]

66. Maltseva, M.; Galipeau, Y.; Renner, T.M.; Deschatelets, L.; Durocher, Y.; Akache, B.; Langlois, M.A. Characterization of Systemic and Mucosal Humoral Immune Responses to an Adjuvanted Intranasal SARS-CoV-2 Protein Subunit Vaccine Candidate in Mice. Vaccines 2022, 11, 30. [CrossRef] [PubMed]
67. Diaz, M.F.; Calderon, K.; Rojas-Neyra, A.; Vakharia, V.N.; Choque-Guevara, R.; Montalvan-Avalos, A.; Poma-Acevedo, A.; Rios-Matos, D.; Agurto-Arteaga, A.; Cauti-Mendoza, M.G.; et al. Intranasal vaccination of hamsters with a Newcastle disease virus vector expressing the S1 subunit protects animals against SARS-CoV-2 disease. Sci. Rep. 2022, 12, 10359. [CrossRef]
68. van Doremalen, N.; Purushotham, J.N.; Schulz, J.E.; Holbrook, M.G.; Bushmaker, T.; Carmody, A.; Port, J.R.; Yinda, C.K.; Okumura, A.; Saturday, G.; et al. Intranasal ChAdOx1 nCoV-19/AZD1222 vaccination reduces viral shedding after SARS-CoV-2 D614G challenge in preclinical models. Sci. Transl. Med. 2021, 13, eabh0755. [CrossRef] [PubMed]
69. King, R.G.; Silva-Sanchez, A.; Peel, J.N.; Botta, D.; Dickson, A.M.; Pinto, A.K.; Meza-Perez, S.; Allie, S.R.; Schultz, M.D.; Liu, M.; et al. Single-Dose Intranasal Administration of AdCOVID Elicits Systemic and Mucosal Immunity against SARS-CoV-2 and Fully Protects Mice from Lethal Challenge. Vaccines 2021, 9, 881. [CrossRef]
70. Lapuente, D.; Fuchs, J.; Willar, J.; Vieira Antao, A.; Eberlein, V.; Uhlig, N.; Issmail, L.; Schmidt, A.; Oltmanns, F.; Peter, A.S.; et al. Protective mucosal immunity against SARS-CoV-2 after heterologous systemic prime-mucosal boost immunization. Nat. Commun. 2021, 12, 6871. [CrossRef]
71. Hassan, A.O.; Kafai, N.M.; Dmitriev, I.P.; Fox, J.M.; Smith, B.K.; Harvey, I.B.; Chen, R.E.; Winkler, E.S.; Wessel, A.W.; Case, J.B.; et al. A Single-Dose Intranasal ChAd Vaccine Protects Upper and Lower Respiratory Tracts against SARS-CoV2. Cell 2020, 183, 169–184.e113. [CrossRef] [PubMed]
72. Agbayani, G.; Akache, B.; Renner, T.M.; Tran, A.; Stuible, M.; Dudani, R.; Harrison, B.A.; Duque, D.; Bavananthasivam, J.; Deschatelets, L.; et al. Intranasal administration of unadjuvanted SARS-CoV-2 spike antigen boosts antigen-specific immune responses induced by parenteral protein subunit vaccine prime in mice and hamsters. Eur. J. Immunol. 2024, 54, e2350620. [CrossRef]
73. Mao, T.; Israelow, B.; Suberi, A.; Zhou, L.; Reschke, M.; Pena-Hernandez, M.A.; Dong, H.; Homer, R.J.; Saltzman, W.M.; Iwasaki, A. Unadjuvanted intranasal spike vaccine booster elicits robust protective mucosal immunity against sarbecoviruses. Science 2022, 378, eabo2523. [CrossRef]
74. Christensen, D.; Polacek, C.; Sheward, D.J.; Hanke, L.; Moliner-Morro, A.; McInerney, G.; Murrell, B.; Hartmann, K.T.; Jensen, H.E.; Jungersen, G.; et al. Protection against SARS-CoV-2 transmission by a parenteral prime-Intranasal boost vaccine strategy. EBioMedicine 2022, 84, 104248. [CrossRef] [PubMed]
75. Beitari, S.; Agbayani, G.; Hewitt, M.; Duque, D.; Bavananthasivam, J.; Sandhu, J.K.; Akache, B.; Hadzisejdic, I.; Tran, A. Effectiveness of VSV vectored SARS-CoV-2 spike when administered through intranasal, intramuscular or a combination of both. Sci. Rep. 2023, 13, 21390. [CrossRef] [PubMed]
76. Gagne, M.; Flynn, B.J.; Andrew, S.F.; Flebbe, D.R.; Mychalowych, A.; Lamb, E.; Davis-Gardner, M.E.; Burnett, M.R.; Serebryannyy, L.A.; Lin, B.C.; et al. Mucosal Adenoviral-vectored Vaccine Boosting Durably Prevents XBB.1.16 Infection in Nonhuman Primates. bioRxiv 2023. [CrossRef]
77. Darling, T.L.; Harastani, H.H.; Joshi, A.; Bricker, T.L.; Soudani, N.; Seehra, K.; Hassan, A.O.; Diamond, M.S.; Boon, A.C.M. Mucosal immunization with ChAd-SARS-CoV-2-S prevents sequential transmission of SARS-CoV-2 to unvaccinated hamsters. Sci. Adv. 2024, 10, eadp1290. [CrossRef]
78. Braun, M.R.; Martinez, C.I.; Dora, E.G.; Showalter, L.J.; Mercedes, A.R.; Tucker, S.N. Mucosal immunization with Ad5-based vaccines protects Syrian hamsters from challenge with omicron and delta variants of SARS-CoV-2. Front. Immunol. 2023, 14, 1086035. [CrossRef]
79. Laghlali, G.; Wiest, M.J.; Karadag, D.; Warang, P.; O'Konek, J.J.; Chang, L.A.; Park, S.; Farazuddin, M.; Landers, J.J.; Janczak, K.W.; et al. Enhanced mucosal B- and T-cell responses against SARS-CoV-2 after heterologous intramuscular mRNA prime/intranasal protein boost vaccination with a combination adjuvant. bioRxiv 2024. [CrossRef]
80. Wang, Q.; Yang, C.; Yin, L.; Sun, J.; Wang, W.; Li, H.; Zhang, Z.; Chen, S.; Liu, B.; Liu, Z.; et al. Intranasal booster using an Omicron vaccine confers broad mucosal and systemic immunity against SARS-CoV-2 variants. Signal Transduct. Target. Ther. 2023, 8, 167. [CrossRef]

81. Colwill, K.; Galipeau, Y.; Stuible, M.; Gervais, C.; Arnold, C.; Rathod, B.; Abe, K.T.; Wang, J.H.; Pasculescu, A.; Maltseva, M.; et al. A scalable serology solution for profiling humoral immune responses to SARS-CoV-2 infection and vaccination. Clin. Transl. Immunol. 2022, 11, e1380. [CrossRef]
82. Lederer, K.; Castano, D.; Gomez Atria, D.; Oguin, T.H., 3rd; Wang, S.; Manzoni, T.B.; Muramatsu, H.; Hogan, M.J.; Amanat, F.; Cherubin, P.; et al. SARS-CoV-2 mRNA Vaccines Foster Potent Antigen-Specific Germinal Center Responses Associated with Neutralizing Antibody Generation. Immunity 2020, 53, 1281–1295.e1285. [CrossRef]
83. Khoury, D.S.; Schlub, T.E.; Cromer, D.; Steain, M.; Fong, Y.; Gilbert, P.B.; Subbarao, K.; Triccas, J.A.; Kent, S.J.; Davenport, M.P. Correlates of Protection, Thresholds of Protection, and Immunobridging among Persons with SARS-CoV-2 Infection. Emerg. Infect. Dis. 2023, 29, 381–388. [CrossRef] [PubMed]
84. Khoury, D.S.; Cromer, D.; Reynaldi, A.; Schlub, T.E.; Wheatley, A.K.; Juno, J.A.; Subbarao, K.; Kent, S.J.; Triccas, J.A.; Davenport, M.P. Neutralizing antibody levels are highly predictive of immune protection from symptomatic SARS-CoV-2 infection. Nat. Med. 2021, 27, 1205–1211. [CrossRef]
85. Walls, A.C.; Miranda, M.C.; Schafer, A.; Pham, M.N.; Greaney, A.; Arunachalam, P.S.; Navarro, M.J.; Tortorici, M.A.; Rogers, K.; O'Connor, M.A.; et al. Elicitation of broadly protective sarbecovirus immunity by receptor-binding domain nanoparticle vaccines. Cell 2021, 184, 5432–5447.e5416. [CrossRef]
86. Wang, Z.; Lorenzi, J.C.C.; Muecksch, F.; Finkin, S.; Viant, C.; Gaebler, C.; Cipolla, M.; Hoffmann, H.H.; Oliveira, T.Y.; Oren, D.A.; et al. Enhanced SARS-CoV-2 neutralization by dimeric IgA. Sci. Transl. Med. 2021, 13, eabf1555. [CrossRef]
87. Neurath, M.F.; Finotto, S.; Glimcher, L.H. The role of Th1/Th2 polarization in mucosal immunity. Nat. Med. 2002, 8, 567–573. [CrossRef] 88. Mosmann, T.R.; Coffman, R.L. TH1 and TH2 cells: Different patterns of lymphokine secretion lead to different functional properties. Annu. Rev. Immunol. 1989, 7, 145–173. [CrossRef] [PubMed]
89. Faustini, S.E.; Jossi, S.E.; Perez-Toledo, M.; Shields, A.M.; Allen, J.D.; Watanabe, Y.; Newby, M.L.; Cook, A.; Willcox, C.R.; Salim, M.; et al. Development of a high-sensitivity ELISA detecting IgG, IgA and IgM antibodies to the SARS-CoV-2 spike glycoprotein in serum and saliva. Immunology 2021, 164, 135–147. [CrossRef]
90. Isho, B.; Abe, K.T.; Zuo, M.; Jamal, A.J.; Rathod, B.; Wang, J.H.; Li, Z.; Chao, G.; Rojas, O.L.; Bang, Y.M.; et al. Persistence of serum and saliva antibody responses to SARS-CoV-2 spike antigens in COVID-19 patients. Sci. Immunol. 2020, 5, eabe5511. [CrossRef]
91. Pisanic, N.; Randad, P.R.; Kruczynski, K.; Manabe, Y.C.; Thomas, D.L.; Pekosz, A.; Klein, S.L.; Betenbaugh, M.J.; Clarke, W.A.; Laeyendecker, O.; et al. COVID-19 Serology at Population Scale: SARS-CoV-2-Specific Antibody Responses in Saliva. J. Clin. Microbiol. 2020, 59, 1–13. [CrossRef]
92. Reynolds, H.Y. Immunoglobulin G and its function in the human respiratory tract. Mayo Clin. Proc. 1988, 63, 161–174. [CrossRef]
93. Wu, Y.; Kang, L.; Guo, Z.; Liu, J.; Liu, M.; Liang, W. Incubation Period of COVID-19 Caused by Unique SARS-CoV-2 Strains: A Systematic Review and Meta-analysis. JAMA Netw. Open 2022, 5, e2228008. [CrossRef]
94. Hui, K.P.Y.; Ho, J.C.W.; Cheung, M.C.; Ng, K.C.; Ching, R.H.H.; Lai, K.L.; Kam, T.T.; Gu, H.; Sit, K.Y.; Hsin, M.K.Y.; et al. SARS-CoV-2 Omicron variant replication in human bronchus and lung ex vivo. Nature 2022, 603, 715–720. [CrossRef] [PubMed]
95. Huang, N.; Perez, P.; Kato, T.; Mikami, Y.; Okuda, K.; Gilmore, R.C.; Conde, C.D.; Gasmi, B.; Stein, S.; Beach, M.; et al. SARS-CoV-2 infection of the oral cavity and saliva. Nat. Med. 2021, 27, 892–903. [CrossRef] [PubMed]
96. Iwasaki, A. Exploiting Mucosal Immunity for Antiviral Vaccines. Annu. Rev. Immunol. 2016, 34, 575–608. [CrossRef]
97. Suzuki, T.; Kawaguchi, A.; Ainai, A.; Tamura, S.; Ito, R.; Multihartina, P.; Setiawaty, V.; Pangesti, K.N.; Odagiri, T.; Tashiro, M.; et al. Relationship of the quaternary structure of human secretory IgA to neutralization of influenza virus. Proc. Natl. Acad. Sci. USA 2015, 112, 7809–7814. [CrossRef]

98. Ramirez, S.I.; Faraji, F.; Hills, L.B.; Lopez, P.G.; Goodwin, B.; Stacey, H.D.; Sutton, H.J.; Hastie, K.M.; Saphire, E.O.; Kim, H.J.; et al. Immunological memory diversity in the human upper airway. Nature 2024, 632, 630–636. [CrossRef]
99. Schroeder, H.W., Jr.; Cavacini, L. Structure and function of immunoglobulins. J. Allergy Clin. Immunol. 2010, 125, S41–S52. [CrossRef]
100. Corthesy, B. Multi-faceted functions of secretory IgA at mucosal surfaces. Front. Immunol. 2013, 4, 185. [CrossRef]
101. Renegar, K.B.; Small, P.A., Jr.; Boykins, L.G.; Wright, P.F. Role of IgA versus IgG in the control of influenza viral infection in the murine respiratory tract. J. Immunol. 2004, 173, 1978–1986. [CrossRef]
102. Woof, J.M.; Kerr, M.A. The function of immunoglobulin A in immunity. J. Pathol. 2006, 208, 270–282. [CrossRef] [PubMed] 103. Kerr, M.A. The structure and function of human IgA. Biochem. J. 1990, 271, 285–296. [CrossRef]
104. Isho, B.; Florescu, A.; Wang, A.A.; Gommerman, J.L. Fantastic IgA plasma cells and where to find them. Immunol. Rev. 2021, 303, 119–137. [CrossRef] [PubMed]
105. Rojas, O.L.; Probstel, A.K.; Porfilio, E.A.; Wang, A.A.; Charabati, M.; Sun, T.; Lee, D.S.W.; Galicia, G.; Ramaglia, V.; Ward, L.A.; et al. Recirculating Intestinal IgA-Producing Cells Regulate Neuroinflammation via IL-10. Cell 2019, 177, 492–493. [CrossRef]
106. Nahass, G.R.; Salomon-Shulman, R.E.; Blacker, G.; Haider, K.; Brotherton, R.; Teague, K.; Yiu, Y.Y.; Brewer, R.E.; Galloway, S.D.; Hansen, P. Intramuscular SARS-CoV-2 vaccines elicit varying degrees of plasma and salivary antibody responses as compared to natural infection. Medrxiv 2021. [CrossRef]
107. Park, S.K.; Lee, C.W.; Park, D.I.; Woo, H.Y.; Cheong, H.S.; Shin, H.C.; Ahn, K.; Kwon, M.J.; Joo, E.J. Detection of SARSCoV-2 in Fecal Samples from Patients with Asymptomatic and Mild COVID-19 in Korea. Clin. Gastroenterol. Hepatol. 2021, 19, 1387–1394.e1382. [CrossRef]
108. Gaebler, C.; Wang, Z.; Lorenzi, J.C.C.; Muecksch, F.; Finkin, S.; Tokuyama, M.; Cho, A.; Jankovic, M.; Schaefer-Babajew, D.; Oliveira, T.Y.; et al. Evolution of antibody immunity to SARS-CoV-2. Nature 2021, 591, 639–644. [CrossRef]
109. Morone, G.; Palomba, A.; Iosa, M.; Caporaso, T.; De Angelis, D.; Venturiero, V.; Savo, A.; Coiro, P.; Carbone, D.; Gimigliano, F.; et al. Incidence and Persistence of Viral Shedding in COVID-19 Post-acute Patients with Negativized Pharyngeal Swab: A Systematic Review. Front. Med. 2020, 7, 562. [CrossRef]
110. Schiepers, A.; van't Wout, M.F.L.; Greaney, A.J.; Zang, T.; Muramatsu, H.; Lin, P.J.C.; Tam, Y.K.; Mesin, L.; Starr, T.N.; Bieniasz, P.D.; et al. Molecular fate-mapping of serum antibody responses to repeat immunization. Nature 2023, 615, 482–489. [CrossRef]
111. Alsoussi, W.B.; Malladi, S.K.; Zhou, J.Q.; Liu, Z.; Ying, B.; Kim, W.; Schmitz, A.J.; Lei, T.; Horvath, S.C.; Sturtz, A.J.; et al. SARS-CoV-2 Omicron boosting induces de novo B cell response in humans. Nature 2023, 617, 592–598. [CrossRef] [PubMed] 112. Yisimayi, A.; Song, W.; Wang, J.; Jian, F.; Yu, Y.; Chen, X.; Xu, Y.; Yang, S.; Niu, X.; Xiao, T.; et al. Repeated Omicron exposures override ancestral SARS-CoV-2 immune imprinting. Nature 2024, 625, 148–156. [CrossRef] [PubMed]
113. Kim, J.H.; Davis, W.G.; Sambhara, S.; Jacob, J. Strategies to alleviate original antigenic sin responses to influenza viruses. Proc. Natl. Acad. Sci. USA 2012, 109, 13751–13756. [CrossRef] [PubMed]
114. Grifoni, A.; Sidney, J.; Vita, R.; Peters, B.; Crotty, S.; Weiskopf, D.; Sette, A. SARS-CoV-2 human T cell epitopes: Adaptive immune response against COVID-19. Cell Host Microbe 2022, 30, 1788. [CrossRef]

A-1.20 Characterization of Systemic and Mucosal Humoral Immune Responses to an Adjuvanted Intranasal SARS-CoV-2 Protein Subunit Vaccine Candidate in Mice

Preface

(This work has been previously published as a research article)

Maltseva M, **Galipeau Y**, Renner TM, Deschatelets L, Durocher Y, Akache B, Langlois MA. **Characterization of Systemic and Mucosal Humoral Immune Responses to an Adjuvanted Intranasal SARS-CoV-2 Protein Subunit Vaccine Candidate in Mice**. Vaccines (Basel). 2022 Dec 23;11(1):30.

https://doi.org/10.3390/vaccines11010030

© 2022 by the authors. Licensee MDPI, Basel, Switzerland. This article is an open access article distributed under the terms and conditions of the Creative Commons Attribution (CC BY) license (https:// creativecommons.org/licenses/by/ 4.0/).

Abstract

Continuous viral evolution of SARS-CoV-2 has resulted in variants capable of immune evasion, vaccine breakthrough infections and increased transmissibility. New vaccines that invoke mucosal immunity may provide a solution to reducing virus transmission. Here, we evaluated the immunogenicity of intranasally administered subunit protein vaccines composed of a stabilized SARS-CoV-2 spike trimer or the receptor binding domain (RBD) adjuvanted with either cholera toxin (CT) or an archaeal lipid mucosal adjuvant (AMVAD). We show robust induction of immunoglobulin (Ig) G and IgA responses in plasma, nasal wash and bronchoalveolar lavage in mice only when adjuvant is used in the vaccine formulation. While the AMVAD adjuvant was more effective at inducing systemic antibodies against the RBD antigen than CT, CT was generally more effective at inducing overall higher IgA and IgG titers against the spike antigen in both systemic and mucosal compartments. Furthermore, vaccination with adjuvanted spike led to superior mucosal IgA responses than with the RBD antigen and produced broadly targeting neutralizing plasma antibodies against ancestral, Delta and Omicron variants in vitro; whereas adjuvanted RBD elicited a narrower antibody response with neutralizing activity only against ancestral and Delta variants. Our study demonstrates that intranasal administration of an adjuvanted protein subunit vaccine in immunologically naïve mice induced both systemic and mucosal neutralizing antibody responses that were most effective at neutralizing SARS-CoV-2 variants when the trimeric spike was used as an antigen compared to RBD.

1. Introduction

The ongoing emergence of highly transmissible SARS-CoV-2 variants of concern (VOCs) have significantly hampered vaccine effectiveness against infection, COVID-19 disease and transmission [1,2,3]. Reduced vaccine effectiveness can also be attributed to immune evasion by VOCs, waning immunity following prolonged periods post vaccination or natural infection and poor induction of mucosal immunity [4,5]. Currently, approved intramuscular (IM) vaccines induce robust systemic immunity which protects against severe disease yet leaves the individual vulnerable to infection and reinfection at the primary point of viral entry at the upper respiratory tract (URT) [6,7]. Indeed, breakthrough infections with viral shedding, with both Delta and Omicron variants, have been reported in fully vaccinated individuals, highlighting the possibility of onward viral transmission despite vaccination [8,9,10]. While vaccine boosting has significantly increased vaccine effectiveness against severe disease and hospitalization, continued viral evolution and emergence of highly transmissible VOCs highlight the need for revaluating our vaccine strategy, due to the shortcomings of currently available vaccines in reducing transmission [4]. In the effort to curtail the COVID-19 pandemic, next generation vaccines must address immune evasion and provide improved cross-protection against rapidly emerging SARS-CoV-2 variants at the point of entry in order to reduce viral transmission.

Several groups have been evaluating transmission blocking strategies that target SARS-CoV-2 entry. The spike protein of SARS-CoV-2 is the primary antigenic target of currently approved vaccines due to its high immunogenicity, abundant viral surface expression and ability to elicit both humoral and cell-mediated responses [11,12,13,14,15,16,17,18]. The spike protein also demonstrates effective mucosal and systemic induction of humoral and cell-mediated immunity through oral and intranasal vaccination in various animal models [19,20,21,22,23,24,25,26,27,28,29,30]. Notably, a majority of these vaccine candidates are based on an adenoviral platform which expresses the spike trimer protein of the parental strain of SARS-CoV-2. Indeed, these groups demonstrated superior protection with intranasal vaccination relative to intramuscular immunization upon subsequent viral challenge, in both the upper and lower respiratory tract, against the ancestral strain and VOCs [19,21,23,24,28]. These strategies targeting

the respiratory mucosa reveal effective protection against disease and reduced viral shedding in mice, hamsters and non-human primates [19,20,21,23,24,25,30,31]. While spike trimer formulations are more commonplace, vaccines targeting the receptor binding domain (RBD) of the spike have been proposed, given its direct interaction with the cognate entry receptor, angiotensin-converting enzyme 2 (ACE2) [32]. Additionally, many potent RBD-specific neutralizing antibodies have been characterized from convalescent and vaccinated individuals [13,16,17,33,34,35,36]. While the immunogenicity of these antigens has been extensively characterized following intramuscular immunization in pre-clinical animal models, their relative immunogenicity as intranasal vaccine targets against emerging VOC remain unclear. To our knowledge, this is the first study directly comparing the systemic and mucosal humoral responses following the intranasal administration of SARS-CoV-2 spike and RBD antigens in mice.

Adjuvants are often essential for directing antigen-specific immune responses and overcoming weak immunogenicity of protein subunit vaccines. Due to adjuvants' intrinsic immunomodulatory properties, their combined administration with an antigen elicits superior and long-lasting immune responses while overcoming natural tolerances of mucosal compartments to antigens administered alone [7,37,38]. Indeed, mucosal adjuvants need to overcome the harsh conditions of mucosal tissues (e.g., low pH, continuous mucociliary clearance and local enzymes) and rapidly permeate mucus layers in order to induce efficacious responses and establish immune memory [39,40]. Cholera toxin (CT) is produced by *Vibrio cholerae* and its combined intranasal administration with an antigen has been shown to elicit potent antigen-specific IgA responses in the URT and T cell-mediated responses in animal models [41,42,43,44,45]. Although CT is among the most effective mucosal adjuvants in animal models, due to safety concerns linked to toxin-mediated neuroinflammation that correlate with Bell's palsy, its use as an adjuvant has been precluded from the clinic [43,46,47]. In contrast, the archaeal polar lipid mucosal vaccine adjuvant and delivery (AMVAD) system used in this study is a self-adjuvating mucosal vaccine delivery system with an established preclinical safety profile that does not require any additional immunostimulants and can withstand a broad range of pH [48,49,50,51]. AMVAD is characterized by its polar lipid and large spherical structure which aggregates in a grape-like formation, thereby encapsulating the antigen [48,52]. Various antigens and formulations of lipid archaeosome-based adjuvants administered intramuscularly have been evaluated in vivo and were shown to elicit robust

cell-mediated and humoral responses through recruitment and activation of macrophages and dendritic cells [53,54,55,56]. In turn, while intranasal immunization using these specific adjuvants is less explored, Patel et al. demonstrate that intranasally administered ovalbumin adjuvanted with AMVAD induced robust mucosal and systemic ovalbumin IgA responses in mice [48].

In this study, we investigated the immunogenicity of an intranasally administered protein subunit vaccine expressing the stabilized SARS-CoV-2 full spike trimer ectodomain or RBD adjuvanted with either CT or AMVAD. We show robust induction of IgG and IgA responses in plasma, nasal wash and bronchoalveolar lavage fluid (BALF) in mice. We observed induction of mucosal and systemic neutralizing IgA and IgG responses. The observed systemic responses were of superior or similar neutralization capacity compared to serum antibodies elicited in humans by SARS-CoV-2 infection or two doses of mRNA vaccine, respectively. Mucosal IgA and systemic IgG antibody titers correlated with neutralizing antibody levels in BALF and plasma, respectively. Given the need for the development of next generation vaccines that target SARS-CoV-2 at the primary site of infection, our findings highlight the immunogenicity of an adjuvanted subunit vaccine platform in stimulating both mucosal and systemic humoral responses in mice and eliciting neutralizing antibodies against emerging SARS-CoV-2 variants.

2. Materials and Methods

2.1. Protein Production

RBD protein was produced in HEK 293F cells and purified. Briefly, a plasmid generously provided by Florian Krammer (Mount Sinai, New York, NY, USA) encoding the Wuhan-Hu-1 RBD (MN908947) sequence coding for the amino acid 319–541 and fused with the N-terminal SARS-CoV-2 spike secretory signal and a C-terminal hexa-histidine tag was transfected into 293F cells cultivated in Freestyle 293 expression media (Thermo Fisher, #12338018) at 37 °C, 7% CO2, while shaking (125 rpm). A total of 600 million cells resuspended in 200 mL were transfected with 200 µg of plasmid using ExpiFectamine (Thermo Fisher, 14525, Waltham, MA, USA). Three days post-transfection, cell supernatant was harvested by centrifugation (4000× *g* for 20 min at 4 °C) and filtered through a low binding 0.22 µm Stericup vacuum filter (Millipore Sigma, S2GPU10RE, Burlington, MA, USA). The filtered supernatant was incubated for 2 h at room temperature with 6

mL of Ni-NTA resin (Qiagen, 30210, Hilden, Germany). The column containing the mix of supernatant and resin was washed four times with a washing buffer containing 20 mM imidazole, 300 mM NaCl and 57.5 mM of NaH2PO4·H2O. The RBD protein was then eluted with three column volumes of the elution buffer containing 234 mM of imidazole, 300 mM NaCl and 57.5 mM of NaH2PO4·H2O. The eluted solution was concentrated, and the buffer was replaced with PBS using a 10 kDa Amicon filter (Millipore Sigma, UFC901008). RBD protein integrity was verified by SDS-PAGE, aliquoted to minimize freeze–thaw cycles and stored at −80 °C. Prefusion trimer spike production details are published elsewhere [57].

2.2. Mice Immunization and Sample Collection

All experiments performed on mice were conducted in accordance with Ontario Animals for Research Act and were approved by the University of Ottawa Animal Ethics Committee (protocol BMI-3649). Female BALB/C mice (6–12 weeks) were obtained from Charles River Laboratories (Saint-Constant, Canada). Prior to each immunization, mice were anesthetized with isoflurane and vaccinated intranasally (25 µL per nare) with 20 µg RBD or spike protein admixed with cholera toxin (CT) (1 µg per dose) used here as a positive control (Sigma, Oakville, ON, Canada) or AMVAD mucosal adjuvant (400 µg per dose) on days 0 and 21. The AMVAD formulation was prepared with total polar lipids from *Methanobrevibacter smithii* and combined with antigen in a saline-based solution containing a final concentration of 15 mM CaCl2, as previously described [48,51]. Control groups include mice vaccinated with phosphate-buffered saline (PBS), protein alone (spike) and adjuvant alone (CT or AMVAD). Plasma was collected periodically throughout the study via submandibular vein and heart puncture at end point. Seven days post boost, bronchoalveolar lavage fluids (BALF) and nasal wash were collected to assess for mucosal humoral responses. Nasal wash and BALF samples were concentrated through 50 kDa Pierce Protein Concentrators column (Thermo Fisher Scientific, Waltham, MA, USA) according to the manufacturer's instructions, with volumes normalized prior to concentration.

2.3. Indirect ELISA to Evaluate Anti-SARS-CoV-2 Immunoreactivity in Serum Samples (Serology)

The same SARS-CoV-2 trimer spike or RBD antigens that were administered for immunizations for used as coating antigens for serological assays. SARS-CoV-2 trimer spike or RBD were diluted in sterile 1X PBS (Wisent Bioproducts, 311-010-CL, St-Bruno, QC, Canada) to 4 µg/mL and

coated onto 384-well Immuno plates (Thermo Fisher, #60372, Waltham, MA, USA) (10 µL/well) overnight at 4 °C. Plates were washed three times with 100 µL of PBS-T and blocked for 1 h with a blocking buffer (PBS-T + 3% non-fat milk powder, *w*/*v*) on a shaker at room temperature. Serum samples were diluted 1:100 (following first immunization) and (1:2000 following second immunization), BALF was diluted 4- to 30-fold and nasal wash was diluted 4-fold in dilution buffer (PBS-T + 1% non-fat milk powder, *w*/*v*). After blocking, plates were washed thrice with PBS-T, and followed by addition of 10 µL of the respective diluted samples. The plates were incubated for 2 h on a shaker at room temperature, washed thrice with PBS-T followed by the addition of 10 µL of the respective secondary-HRP antibody at specified dilutions: 1:4000 secondary IgG Anti-Mouse, Human ads-HRP (Southern Biotech, 1030-05, Birmingham, AL, USA) and 1:1000 secondary Anti-Mouse IgA-HRP (Southern Biotech, 1040-05, Birmingham, AL, USA). Plates were incubated for 1 h on a shaker, washed thrice with PBS-T followed by the addition with 10 µL of the SuperSignal ELISA Pico Chemiluminescent Substrate (Thermo Scientific, 37069, Waltham, MA, USA). Luminescence intensity was measured with BIO-TEK Synergy Neo2 plate reader for 20 ms/well at a read height of 1.0 mm. Wells filled with dilution buffer in place of sample accounted for background luminescence and were subtracted from the sample values.

2.4. Surrogate Neutralization ELISA (snELISA) Assay to Evaluate Neutralization Activity in Serum Samples

The described methodology was adapted from the surrogate neutralization ELISA assay, as shown in Colwill et al. and Demone et al., for the evaluation of the relative inhibition of neutralizing antibodies to spike or RBD protein from binding to soluble ACE2 [57,58]. Briefly, SARS-CoV-2 spike or RBD protein were diluted in sterile 1X PBS to 8 µg/mL and coated onto 384-well Immuno plates (12.5 µL/well) overnight at 4 °C. Plates were washed 3 times with PBS-T and blocked for 1 h while shaking. Plasma samples were 1:6 serially diluted in a dilution buffer while BALF was left undiluted, applied to wells (20 µL/well) and incubated for 2 h while shaking at room temperature. Plates were washed thrice, followed by the addition of biotinylated ACE2, as shown in Abe et al. [59], diluted to 0.35 ng/µL in a dilution buffer (20 µL/well). Plates were washed thrice with PBS-T followed by the addition of 20 µL per well of Streptavidin–Peroxidase polymer (Sigma, S2438, Oakville, ON, Canada) diluted in dilution buffer to 1.25 ng/µL. Following 1 h incubation, plates

were washed thrice with PBS-T and freshly diluted SuperSignal ELISA Pico Chemiluminescent Substrate (mixed 1:1 ratio and diluted in equal volume with dH2O, (*V*:*V*)) was applied (20 µL/well). Following 5 min of incubation while shaking, luminescence intensity was measured with BIO-TEK Synergy Neo2 plate reader for 20 ms/well at a read height of 1.0 mm. To assess the maximum binding signal, control wells were filled with a dilution buffer in place of serum followed by the addition of ACE2, as previously. Relative percent inhibition was calculated as follows:

% Inhibiton = (1- (Average mean of serum sample / Average mean of maximum signal)) X100

Serum dilution resulting in a 50% inhibition (half-maximal inhibitory dilution (ID50)) of spike or RBD protein from binding ACE2 receptor was determined using 4-parameter fitting with GraphPad Prism 9.1.2 software. When no neutralization activity was observed, the ID50 of the sample was arbitrarily set as half of the lowest dilution.

2.5. Patient Samples, Collection and Ethics Approval

Use of human samples for this study was approved by the University of Ottawa Ethics Review Board: Certificates H-04-20-5727, H-04-21-6643 and H-07-20-6009. The negative sample was taken from an individual with no history of SARS-CoV-2 infection and tested with PCR. Pooled negative samples were obtained from individuals negative for SARS-CoV-2 as tested by PCR and serology assay. Pooled serum samples were obtained from convalescent (2–16 weeks post-infection) or vaccinated patients (2–4 weeks post-vaccination) enrolled in surveillance studies from different research studies post-2019. Samples were collected using standard phlebotomy procedures. Samples were de-identified and held at 4 °C for short-term handling and testing at University of Ottawa CL2+ biocontainment facility. All research was performed in accordance with current guidelines and regulations.

3. Results

3.1. Intranasal Administration of Adjuvanted RBD and Spike Antigens Induces Robust Humoral Systemic Responses in Mice

To assess immunogenicity of the intranasal subunit protein vaccine platform, we compared the ability of a stabilized prefusion trimeric spike or the RBD in eliciting mucosal and systemic antibody responses. Given that intranasally administered protein subunit vaccines have been shown to be poorly immunogenic on their own, we additionally assessed two different adjuvants: AMVAD and CT. Balb/c mice (n = 3/group) were immunized with controls (phosphate-buffered saline (PBS), soluble full spike trimer ectodomain, RBD, AMVAD or CT alone) or protein adjuvanted vaccine combinations (AMVAD + RBD, CT + RBD, AMVAD + spike, CT + spike) on day 0 and 21 (Figure 1A). Due to the limited amount of sample volumes obtained during the study and the numerous analyses we wanted to conduct, samples from immunized mice in each group were pooled together after confirming that the antibody responses in individual mice were similar. Figure 1B shows RBD or spike-specific IgG titers at various dilutions of three individual mice relative to pooled plasma samples, highlighting highly consistent seroconversion and antibody levels between mice within each group. Systemic antigen-specific IgG and IgA responses in plasma were measured after prime (day 20) (Figure 1C) or boost (day 35) (Figure 1D) immunization by enzyme-linked immunosorbent assay (ELISA) against RBD or spike. Following a single immunization, we show that there was poor induction of IgA antibodies with controls, including unadjuvanted antigens, as expected. In contrast, adjuvanted spike protein with AMVAD or CT elicited robust IgG titers in plasma (Figure 1C) that were significantly greater than with the adjuvanted RBD vaccine formulation after a single dose. As expected, we observed similar levels of RBD- and spike-directed IgG antibodies in mice immunized with the AMVAD + RBD vaccine formulation, highlighting that antibodies generated against RBD can access their epitopes on the trimeric spike. Following boosting, we observed a significant increase in both IgA and IgG antibody titers in plasma of mice immunized with either RBD- or spike-adjuvanted formulations, while controls showed no responses (Figure 1D). Consistent with previous results, we observed comparable levels of RBD- and spike-directed IgG titers in mice immunized with adjuvanted RBD. While there was a greater titer of spike- compared to RBD-directed IgG responses in the AMVAD + spike formulation; boosting induced a greater proportion of RBD-specific antibodies in this group. In contrast, vaccination with CT + spike induced the greatest humoral responses of all vaccine combinations tested, consistent with previously reported results [41,43,48,60], with endpoint IgG titers near assay saturation (~5 × 106) (Figure 1D).

Induction of robust systemic humoral immunity, in particular neutralizing responses, has been shown to be a strong correlate of protection against severe disease [11,33,61,62]. Next, we functionally assessed the neutralizing responses of antibodies in plasma following the second immunization using a surrogate ELISA neutralization (snELISA) assay shown to quantitatively correlate with pseudotyped or infectious virus neutralization assay [57]. We evaluated the relative inhibition of ACE2–spike and ACE2–RBD ligand interactions and showed that neutralization responses followed the trends of systemic IgG titers (Figure 2A). Consistent with previous observations with antibody responses, we saw similar ID50 values of ACE2–RBD and ACE2–spike interactions with plasma of mice immunized with AMVAD + RBD (Figure 2B). In alignment with the ELISA results (Figure 1D), mice immunized with AMVAD + RBD showed significantly greater inhibition of ACE2–RBD than that observed with AMVAD + spike, thus suggesting that RBD immunogen focused antibody responses upon protective neutralizing epitopes localized within the RBD, preventing ACE2–RBD ligand interaction. In contrast, the ID50 of ACE2–spike interactions was comparable following immunizations with either AMVAD + RBD or AMVAD + spike, highlighting that neutralizing activity is not exclusively RBD directed. This is in line with other studies that suggest the influence of alternative neutralizing epitopes on the spike protein beyond the RBD, such as those in the N-terminal domain (Figure 2B) [18,33,63,64,65].

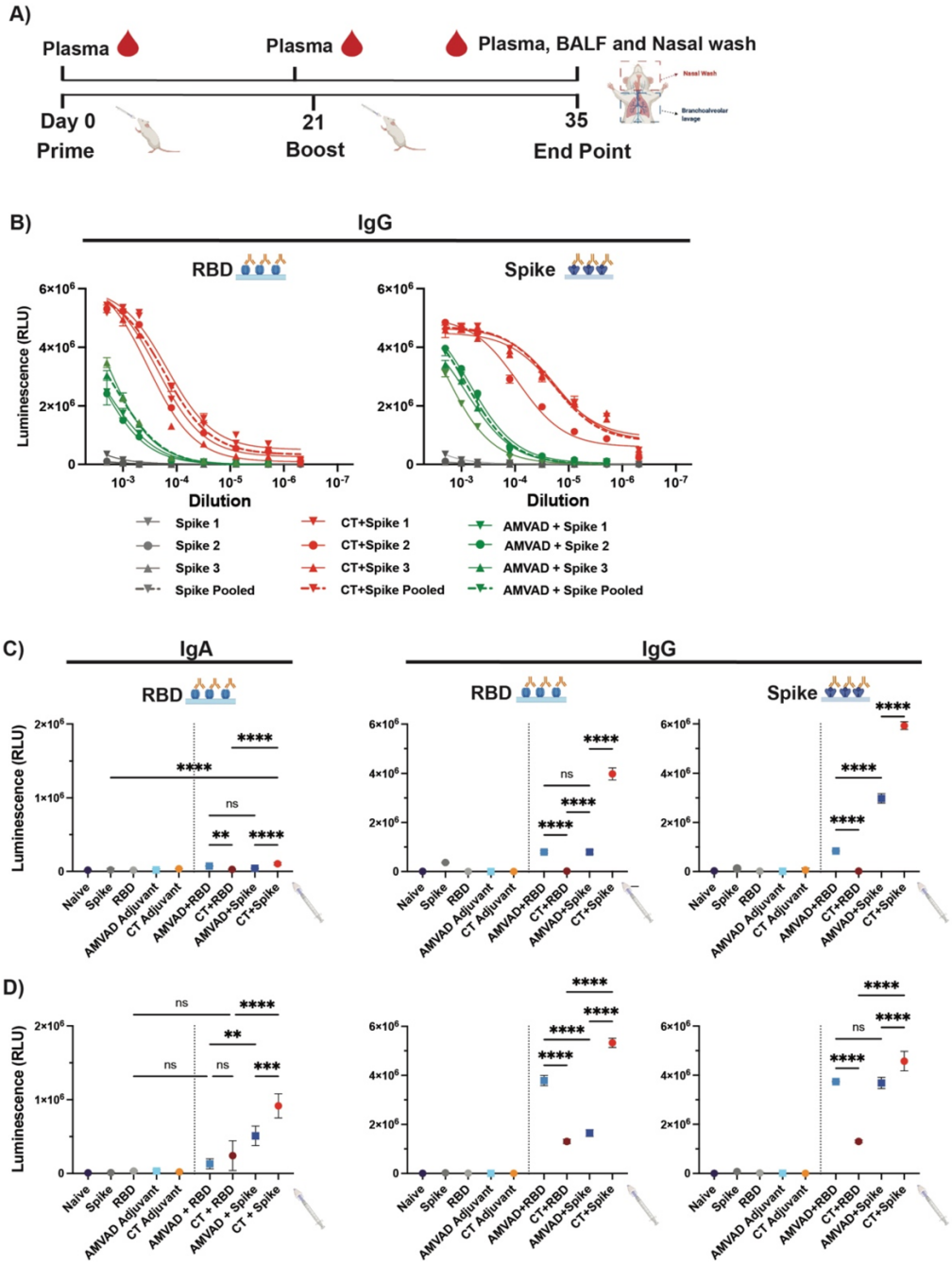


Figure 1. Humoral systemic responses from intranasal administration with adjuvanted RBD or spike antigens. (**A**) Experimental design: Balb/c mice were intranasally immunized with RBD or spike protein adjuvanted with CT or AMVAD mucosal adjuvant on days 0 and 21. Control groups include mice vaccinated with phosphate-buffered saline (PBS), protein alone (RBD or spike) and adjuvant alone (CT or AMVAD). Seven days post-boost, plasma, bronchoalveolar lavage fluids (BALF) and nasal wash were collected to assess humoral responses. (**B**) Evaluation of RBD- and spike-specific IgG titers in plasma of individual mice vs. pooled plasma collected at end point. (**C**) Measurement of RBD- and spike-specific IgA and IgG responses in plasma collected after first dose (day 20) (1/100 dilution) and (**D**) after second dose (day 35) (1/2000 dilution), analyzed by an indirect ELISA. Statistical significance was calculated by one-way ANOVA followed by Tukey correction; n.s.: no statistical difference; ** $p \leq 0.01$, *** $p \leq 0.001$, **** $p \leq 0.0001$. Individual mice samples were pooled and analyzed in triplicate.

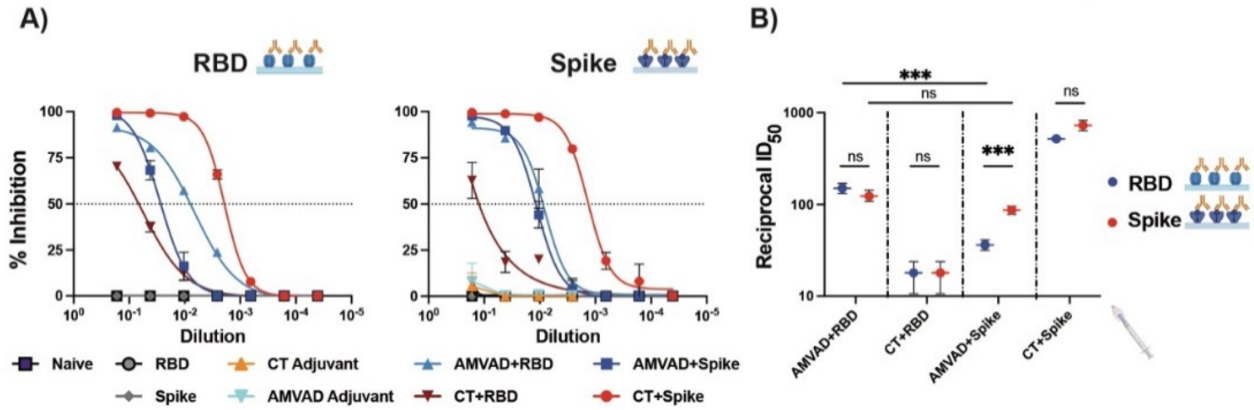


Figure 2. Systemic neutralizing antibodies induced by the intranasal administration with adjuvanted RBD or spike antigens. (**A**) Measurement of relative inhibition of soluble ACE2 and immobilized RBD or spike interaction by neutralizing antibodies in plasma collected at endpoint by surrogate neutralization ELISA (snELISA). (**B**) Reciprocal ID50 neutralizing titer of adjuvanted vaccine formulations in blocking RBD (blue) or spike (red) and ACE2 ligand interaction. This assay is representative of technical triplicates and presented as mean ± standard deviation. Statistical significance was calculated by one-way ANOVA followed by Tukey correction; n.s.: no statistical difference; *** $p \leq 0.001$. Individual mice samples were pooled and analyzed in triplicate.

3.2. Adjuvanted Spike Antigen Immunization Induces Robust and Neutralizing Mucosal Responses in Mice

Given the limited ability of currently available vaccines in inducing mucosal immunity, we set out to investigate mucosal humoral responses at the point of viral entry, the respiratory mucosa. To this end, we characterized IgA and IgG responses in BALF and nasal wash collected at the end point. We show that adjuvants are required for the induction of robust IgG and IgA responses (Figure 3). In particular, we observed significantly greater IgA and IgG titers in mice immunized with spike-adjuvanted formulations. Consistent with systemic antibody levels, AMVAD + spike-immunized mice showed robust spike- and RBD-specific IgA titers in BALF; however, AMVAD + RBD antibody levels were very low against both antigens at the experimental endpoint and did not reach statistical significance relative to RBD control (Figure 3A). While both of the RBD-adjuvanted formulations induced IgG responses against spike and RBD in BALF, only CT + RBD-vaccinated mice showed measurable IgA titers. Interestingly, the AMVAD + RBD formulation induced measurable IgA titers in the nasal wash that are comparable to AMVAD + spike (Figure 3B), and these are overall higher than IgG levels. This highlights the ability of intranasal adjuvated-antigen administration to more specifically induce IgA responses depending on the anatomical location within the mucosal compartment. Of note, the relative mucosal antibody titers measured

in our study could be skewed given the high collection volume of buffer used during BALF and nasal wash sample acquisition relative to plasma collection.

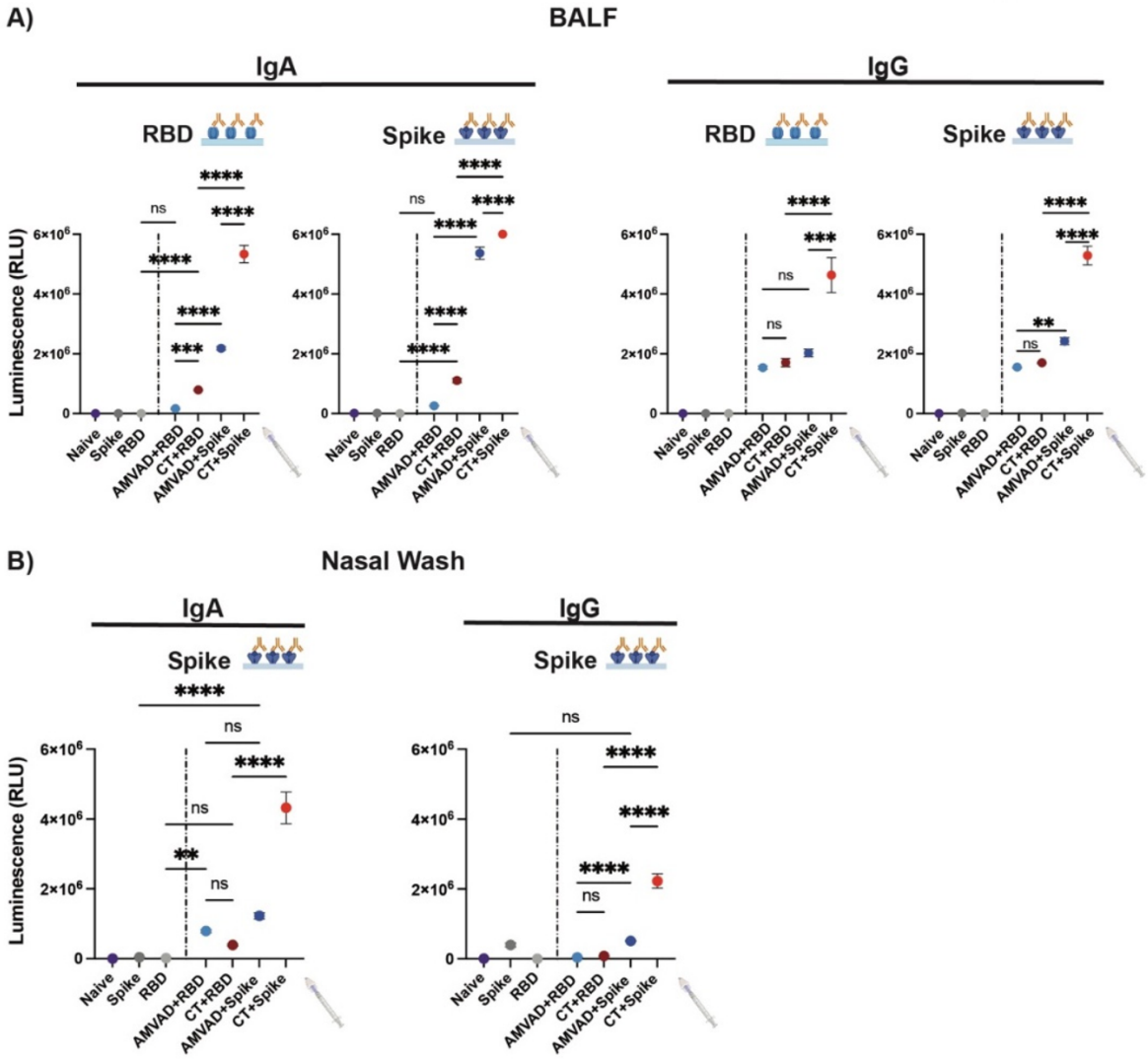


Figure 3. Antibody responses in BALF and the nasal cavity from intranasal administration with adjuvanted RBD or spike antigens. Measurement of RBD- and spike-specific IgA and IgG responses in (**A**) BALF and (**B**) nasal wash collected at end point. BALF was diluted 4- and 30-fold for measurement of IgA and IgG specific titers, respectively. Nasal wash was diluted four-fold. Statistical significance was calculated by one-way ANOVA followed by Tukey correction; n.s.: no statistical difference; ** $p \leq 0.01$, *** $p \leq 0.001$, **** $p \leq 0.0001$. Individual mice samples were pooled and analyzed in triplicate.

3.3. Production of Neutralization Responses in Plasma of Immunized Mice against Ancestral and Variants of SARS-CoV-2

Next, we compared the relative inhibition of ACE2–spike interactions by neutralizing antibodies in plasma and BALF for the ancestral, Delta and Omicron variants (Figure 4). We show that both adjuvanted RBD and spike formulations induced neutralizing antibodies in plasma against the spike proteins of Delta, but only CT–spike and, to a lesser extent, AMVAD + spike, induced the production of neutralizing antibodies against the spike of the Omicron variant (B.1.1.529) (Figure 4A,B). In particular, vaccination of mice with AMVAD-adjuvanted RBD or spike elicited superior inhibition of ACE2–spike interactions for Wuhan and Delta variants compared to natural SARS-CoV-2 infection in humans (i.e., pooled convalescent (pooled conv.); Alpha variant) and similar inhibition as pooled plasma from individuals vaccinated with two doses of the Pfizer mRNA vaccine (Figure 4A,B). Despite overall lower neutralization titers in BALF relative to levels observed in plasma, we showed that neutralization responses significantly correlated to IgA titers. Indeed, only spike-adjuvanted immunized mice showed weak but detectable neutralizing titers against SARS-CoV-2, with only CT + spike showing neutralizing activity against all the variants tested, while there was poor induction of mucosal neutralization with the adjuvanted RBD formulations (Figure 4C).

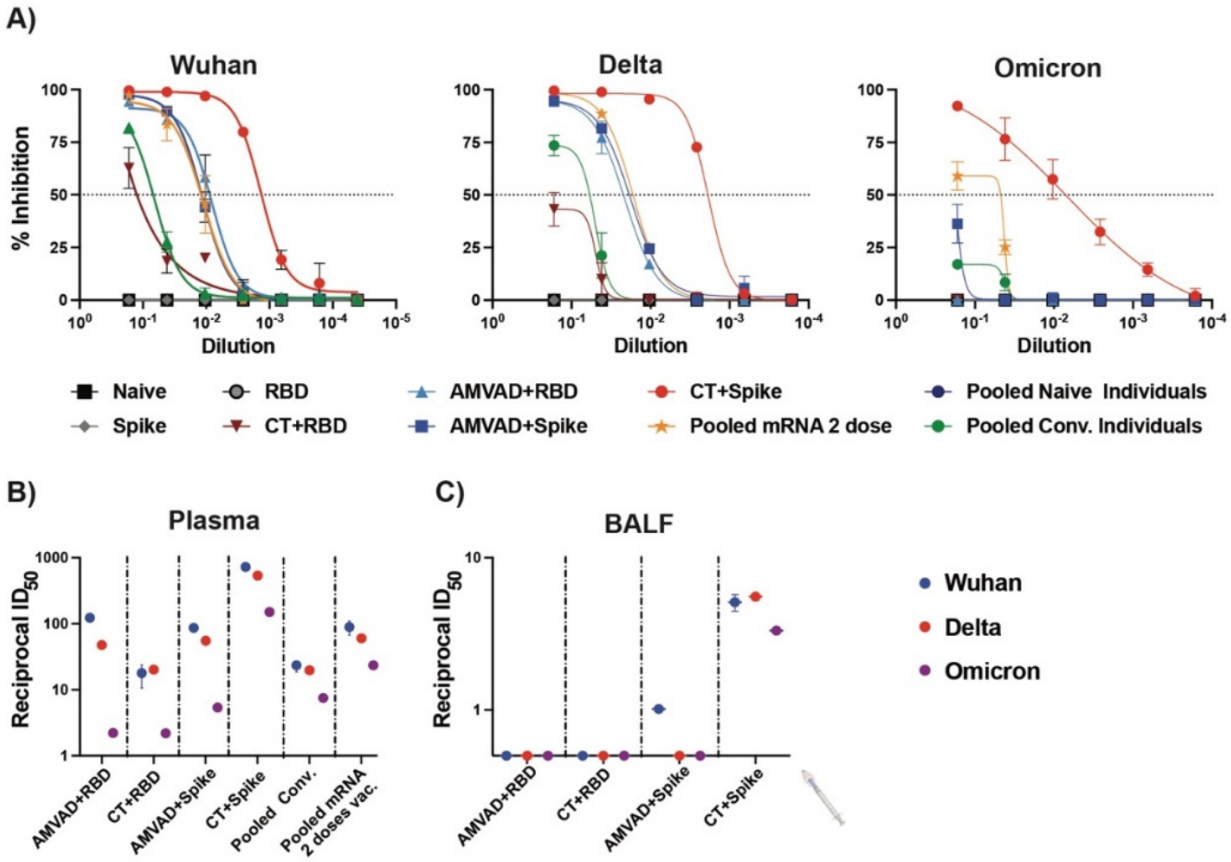


Figure 4. Neutralizing antibodies produced in plasma and BALF against SARS-CoV-2 variants. (**A**) Measurement of relative inhibition of ligand interaction between soluble ACE2 and Wuhan ancestral reference strain, Delta variant and Omicron variant spike protein by neutralizing antibodies in plasma at endpoint analyzed by snELISA. Reciprocal ID50 neutralizing titer of adjuvanted vaccine formulations in (**B**) plasma and (**C**) BALF blocking Wuhan reference strain (blue), Delta variant (red) and Omicron variant (purple) spike and ACE2 ligand interaction. This assay is representative of technical triplicates and presented as mean ± standard deviation.

4. Discussion

Currently approved vaccines for SARS-CoV-2 induce robust humoral and cell-mediated immunity, which protect against severe disease, yet leave individuals vulnerable to infection at the URT where entry and replication first arise. Continued persistence of SARS-CoV-2, emergence of VOCs and poor induction of mucosal immunity contribute to decreased vaccine effectiveness against COVID-19 infection and onward transmission. Mucosal immunity is a critical component in the prevention and reduction of respiratory pathogen transmission [6,7]. Indeed, humoral responses in the mucosal compartment eliminate pathogens through various mechanisms, including blocking viral attachment to the cognate receptor via neutralizing antibodies, complement fixation and antibody-dependent cellular cytotoxicity [66,67]. As such, a growing

body of work in the literature highlights the important role of mucosal secretory IgA in protecting against respiratory bacterial and viral pathogens that infect through the oral or nasal routes [7,19,20,21,23,26,27,28,29,30,66,67,68,69,70,71,72,73,74,75]. Stimulation of these humoral- and tissue-specific cell-mediated responses could be indispensable to blunt viral infection at the site of SARS-CoV-2 replication and limit viral transmission.

Since potent humoral responses have been shown to be a strong correlate of vaccine effectiveness and protection against COVID-19, we first analyzed mucosal and systemic IgG and IgA responses in mice vaccinated with spike and RBD adjuvanted with either CT or AMVAD. We show robust induction of IgG and IgA in plasma, nasal wash and BALF in mice vaccinated with two doses of adjuvanted protein vaccines, but not with protein or adjuvant alone. In line with previous reports, our data suggests that the combined administration of antigen with AMVAD likely led to its direct delivery to antigen-presenting cells for effective protein processing and presentation. Although the mechanism of action of AMVAD remains to be elucidated, its grape-like structure encompasses the antigen and acts as a delivery vehicle to elicit both humoral and cellular response [48,52]. Of note, we observed that vaccination with the RBD-adjuvanted vaccine favored RBD directed antibodies in both systemic and mucosal compartments, while immunization with adjuvanted spike induced broadly targeting antibodies that encompassed epitopes within and beyond the RBD domain. These findings were recapitulated when we evaluated relative inhibition of ACE2–spike and ACE2–RBD ligand interaction, where there was significantly lower inhibition of ACE2–RBD interaction in mice immunized with AMVAD + spike relative to AMVAD + RBD, yet comparable inhibition of ACE2–spike interaction between these two groups. Although immunization with RBD led to robust induction of systemic neutralizing antibodies blocking ACE2–RBD interactions for both ancestral and Delta variants, these neutralizing antibodies were poorly cross-reactive against the Omicron variant, which harbors more than 15 mutations within the RBD alone, suggesting that these antibodies likely targeted epitopes on the RBD prone to antigenic drift and escape by emerging VOCs [29,76,77,78,79]. In line with other comparative protein subunit antigen immunogenicity studies via intramuscular vaccination [1,53,80,81], our findings suggest that intranasal immunization with adjuvanted spike formulation induced greater breadth of neutralizing antibodies that target both conserved and variable epitopes of the spike. In addition, trimeric spike has been shown to be more immunogenic given the larger T cell epitope repertoire leading to a greater recruitment of T helper follicular cells and, thereby, an enhanced humoral response relative

to the RBD antigen, as shown by Tan et al. [80]. Indeed, non-RBD directed antibodies have been shown to be important for both mucosal and systemic humoral immunity in preventing severe disease from both SARS-CoV-1 and SARS-CoV-2 infection [64,82,83].

In plasma, we observed that high levels of IgG correlated with increased neutralization titers, while in BALF, potent IgA levels correlated with neutralizing responses as observed in previous influenza and SARS-CoV-2 vaccination studies [29,66,75,84]. Notably, AMVAD + spike formulation induced significantly greater IgA levels in both plasma and BALF relative to AMVAD + RBD immunization. Given that RBD + AMVAD-immunized mice showed low levels of IgA and undetectable neutralizing activity in BALF, we speculate that mucosal IgA antibodies largely contributed to ACE2–spike inhibition observed in spike-adjuvanted groups. Thus, the spike's superior immunogenicity could also be attributed to its larger and stabilized trimeric structure compared to RBD's monomer, where the spike protein's repetitive trimeric antigen presentation could increase cross-linking to B cell receptors, inducing greater B cell activation and IgA response [85,86].

Induction of protective humoral immunity has been a major focus in COVID-19 vaccine development. Nevertheless, robust induction of secretory IgA antibodies is crucial given their potent and broadly neutralizing capabilities [20,29,66,67,68,69,71,87,88]. Studies of intranasal vaccines against influenza have highlighted that mucosal vaccination, compared to the intramuscular route, elicited potent cross-protection against heterosubtypic challenge of influenza and showed long-term immunity [66,89]. Additionally, in a proof-of-concept study, Xiao et al. demonstrated that intranasal immunization with defective viral particles provides powerful prophylactic, broad-spectrum protection from infection by SARS-CoV-2 and influenza virus by blocking viral replication and preventing reinfection [90]. This is further reiterated by several groups that showed superior protection with intranasal relative to intramuscular immunization in mice against challenge with ancestral SARS-CoV-2 strain and VOCs [19,20,21,23,24,30]. Indeed, Langel et al., demonstrated reduced SARS-CoV-2 airborne transmission in intranasally immunized hamsters [21]. In addition, Tang et al. demonstrated that convalescent individuals show increased levels of broadly neutralizing antibodies in BALF relative to vaccinated individuals, despite similar systemic IgG titers [29]. Epidemiological surveillance studies highlight the

important role that mucosal IgA may have in preventing SARS-CoV-2 infection. In fact, Sheikh et al. and Havervall et al. demonstrated that vaccinated participants who experienced breakthrough infections with divergent VOCs had lower titers of serum and mucosal IgA relative to those who did not experience an infection despite having comparable serum IgG titers [72,73]. Here, we showed an adjuvanted subunit vaccine platform that induced robust mucosal and systemic total and neutralizing antibody responses against rapidly emerging SARS-CoV-2 variants. In our direct comparison of the immunogenic profiles of SARS-CoV-2 spike and RBD antigens, we highlight the relative merit of additional epitopes of the larger spike protein that improve protein immunogenicity at the respiratory mucosa and neutralizing activity against VOCs. Continued SARS-CoV-2 transmission and replication, and selection pressure induced by vaccination or prior infection has led to the emergence of highly transmissible VOCs. Given the persistence of the SARS-CoV-2 pandemic and the shortcomings of currently available vaccines in effectively blocking transmission, our study may offer insights for selecting immunogenic targets for intranasal vaccine design against current and future VOCs. Thus, new modalities of vaccination that invoke mucosal immunity are crucial to neutralize the virus, limit the initial infection at the point of entry, prevent onward transmission and curtail the COVID-19 pandemic.

Author Contributions
Conceptualization, M.-A.L., B.A. and M.M.; methodology, M.-A.L., B.A., Y.G. and M.M.; formal analysis, M.-A.L., T.M.R., B.A. and M.M.; investigation, M.-A.L., T.M.R., L.D., Y.D., B.A. and M.M.; data curation, M.-A.L., T.M.R., B.A. and M.M.; writing—original draft preparation, M.-A.L., and M.M.; writing—review and editing, M.-A.L., T.M.R., L.D., Y.D., B.A., Y.G. and M.M.; supervision, M.-A.L.; project administration, M.-A.L.; funding acquisition, M.-A.L. All authors have read and agreed to the published version of the manuscript.

Funding
This study was supported in part by a COVID-19 Rapid Response grant by the Canadian Institutes of Health Research (CIHR; #VR2-172722) and by a grant supplement by the COVID-19 Immunity Task Force (CITF) to M-A Langlois. Production of COVID-19 reagents was financially supported by the NRC's Pandemic Response Challenge Program. M.M. holds an Ontario Graduate Scholarship. Y.G. holds a CIHR Frederick Banting and Charles Best graduate scholarship (CGS-Doctoral).

Institutional Review Board Statement
Use of human samples for this study was approved by the University of Ottawa Ethics Review Board: Certificates H-04-20-5727, H-04-21-6643 and H-07-20-6009. All experiments performed on mice were conducted in accordance with Ontario Animals for Research Act and were approved by the University of Ottawa Animal Ethics Committee (protocol BMI-3649).

Informed Consent Statement
Informed consent was obtained from all subjects involved in the study.

Data Availability Statement
The data presented in this study are available on request from the corresponding author. The data are not publicly available due to confidentiality issues with interviewees.

Acknowledgments
We sincerely thank Anthony Carter and the uOttawa surgical ACVS core for their technical support with sample set up and acquisition.

Conflicts of Interest
The authors declare no conflict of interest.

References

1. Cele, S.; Jackson, L.; Khoury, D.S.; Khan, K.; Moyo-Gwete, T.; Tegally, H.; San, J.E.; Cromer, D.; Scheepers, C.; Amoako, D.; et al. SARS-CoV-2 Omicron has extensive but incomplete escape of Pfizer BNT162b2 elicited neutralization and requires ACE2 for infection. medRxiv 2021. [CrossRef]
2. Chemaitelly, H.; Tang, P.; Hasan, M.R.; AlMukdad, S.; Yassine, H.M.; Benslimane, F.M.; Al Khatib, H.A.; Coyle, P.; Ayoub, H.H.; Al Kanaani, Z.; et al. Waning of BNT162b2 Vaccine Protection against SARS-CoV-2 Infection in Qatar. N. Engl. J. Med. 2021, 385, e83. [CrossRef] [PubMed]
3. Greaney, A.J.; Starr, T.N.; Gilchuk, P.; Zost, S.J.; Binshtein, E.; Loes, A.N.; Hilton, S.K.; Huddleston, J.; Eguia, R.; Crawford, K.H.D.; et al. Complete Mapping of Mutations to the SARS-CoV-2 Spike Receptor-Binding Domain that Escape Antibody Recognition. Cell Host Microbe 2021, 29, 44–57.e9. [CrossRef] [PubMed]
4. Menni, C.; May, A.; Polidori, L.; Louca, P.; Wolf, J.; Capdevila, J.; Hu, C.; Ourselin, S.; Steves, C.J.; Valdes, A.M.; et al. COVID-19 vaccine waning and effectiveness and side-effects of boosters: A prospective community study from the ZOE COVID Study. Lancet Infect. Dis. 2022, 22, 1002–1010. [CrossRef] [PubMed]
5. Singanayagam, A.; Hakki, S.; Dunning, J.; Madon, K.J.; Crone, M.A.; Koycheva, A.; Derqui-Fernandez, N.; Barnett, J.L.; Whitfield, M.G.; Varro, R.; et al. Community transmission and viral load kinetics of the SARS-CoV-2 delta (B.1.617.2) variant in vaccinated and unvaccinated individuals in the UK: A prospective, longitudinal, cohort study. Lancet Infect. Dis. 2022, 22, 183–195. [CrossRef]
6. Krammer, F. SARS-CoV-2 vaccines in development. Nature 2020, 586, 516–527. [CrossRef] [PubMed]
7. Lavelle, E.C.; Ward, R.W. Mucosal vaccines—Fortifying the frontiers. Nat. Rev. Immunol. 2022, 22, 236–250. [CrossRef]
8. Kemp, S.A.; Cheng, M.T.K.; Hamilton, W.L.; Kamelian, K.; Indian, S.-C.-G.C.; Singh, S.; Rakshit, P.; Agrawal, A.; Illingworth, C.J.R.; Gupta, R.K. Transmission of B.1.617.2 Delta variant between vaccinated healthcare workers. Sci. Rep. 2022, 12, 10492. [CrossRef]
9. Chia, P.Y.; Ong, S.W.X.; Chiew, C.J.; Ang, L.W.; Chavatte, J.M.; Mak, T.M.; Cui, L.; Kalimuddin, S.; Chia, W.N.; Tan, C.W.; et al. Virological and serological kinetics of SARS-CoV-2 Delta variant vaccine breakthrough infections: A multicentre cohort study. Clin. Microbiol. Infect. 2022, 28, 612.e1–612.e7. [CrossRef]
10. Lange, B.; Gerigk, M.; Tenenbaum, T. Breakthrough Infections in BNT162b2-Vaccinated Health Care Workers. N. Engl. J. Med. 2021, 385, 1145–1146. [CrossRef]
11. Bartsch, Y.C.; Fischinger, S.; Siddiqui, S.M.; Chen, Z.; Yu, J.; Gebre, M.; Atyeo, C.; Gorman, M.J.; Zhu, A.L.; Kang, J.; et al. Discrete SARS-CoV-2 antibody titers track with functional humoral stability. Nat. Commun. 2021, 12, 1018. [CrossRef] [PubMed]
12. Bartsch, Y.C.; Wang, C.; Zohar, T.; Fischinger, S.; Atyeo, C.; Burke, J.S.; Kang, J.; Edlow, A.G.; Fasano, A.; Baden, L.R.; et al. Humoral signatures of protective and pathological SARS-CoV-2 infection in children. Nat. Med. 2021, 27, 454–462. [CrossRef] [PubMed]
13. Brouwer, P.J.M.; Caniels, T.G.; van der Straten, K.; Snitselaar, J.L.; Aldon, Y.; Bangaru, S.; Torres, J.L.; Okba, N.M.A.; Claireaux, M.; Kerster, G.; et al. Potent neutralizing antibodies from COVID-19 patients define multiple targets of vulnerability. Science 2020, 369, 643–650. [CrossRef]
14. Cao, Y.; Su, B.; Guo, X.; Sun, W.; Deng, Y.; Bao, L.; Zhu, Q.; Zhang, X.; Zheng, Y.; Geng, C.; et al. Potent Neutralizing Antibodies against SARS-CoV-2 Identified by High-Throughput Single-Cell Sequencing of Convalescent Patients' B Cells. Cell 2020, 182, 73–84.e16. [CrossRef] [PubMed]
15. Kreer, C.; Zehner, M.; Weber, T.; Ercanoglu, M.S.; Gieselmann, L.; Rohde, C.; Halwe, S.; Korenkov, M.; Schommers, P.; Vanshylla, K.; et al. Longitudinal Isolation of Potent Near-Germline SARS-CoV-2-Neutralizing Antibodies from COVID-19 Patients. Cell 2020, 182, 843–854.e12. [CrossRef] [PubMed]

16. Rogers, T.F.; Zhao, F.; Huang, D.; Beutler, N.; Burns, A.; He, W.T.; Limbo, O.; Smith, C.; Song, G.; Woehl, J.; et al. Isolation of potent SARS-CoV-2 neutralizing antibodies and protection from disease in a small animal model. Science 2020, 369, 956–963. [CrossRef]
17. Zost, S.J.; Gilchuk, P.; Case, J.B.; Binshtein, E.; Chen, R.E.; Nkolola, J.P.; Schafer, A.; Reidy, J.X.; Trivette, A.; Nargi, R.S.; et al. Potently neutralizing and protective human antibodies against SARS-CoV-2. Nature 2020, 584, 443–449. [CrossRef]
18. Liu, L.; Wang, P.; Nair, M.S.; Yu, J.; Rapp, M.; Wang, Q.; Luo, Y.; Chan, J.F.; Sahi, V.; Figueroa, A.; et al. Potent neutralizing antibodies against multiple epitopes on SARS-CoV-2 spike. Nature 2020, 584, 450–456. [CrossRef]
19. Afkhami, S.; D'Agostino, M.R.; Zhang, A.; Stacey, H.D.; Marzok, A.; Kang, A.; Singh, R.; Bavananthasivam, J.; Ye, G.; Luo, X.; et al. Respiratory mucosal delivery of next-generation COVID-19 vaccine provides robust protection against both ancestral and variant strains of SARS-CoV-2. Cell 2022, 185, 896–915.e19. [CrossRef]
20. Mao, T.; Israelow, B.; Suberi, A.; Zhou, L.; Reschke, M.; Pena-Hernandez, M.A.; Dong, H.; Homer, R.J.; Saltzman, W.M.; Iwasaki, A. Unadjuvanted intranasal spike vaccine booster elicits robust protective mucosal immunity against sarbecoviruses. Science 2022, 378, eabo2523. [CrossRef]
21. Langel, S.N.; Johnson, S.; Martinez, C.I.; Tedjakusuma, S.N.; Peinovich, N.; Dora, E.G.; Kuehl, P.J.; Irshad, H.; Barrett, E.G.; Werts, A.; et al. Adenovirus type 5 SARS-CoV-2 vaccines delivered orally or intranasally reduced disease severity and transmission in a hamster model. Sci. Transl. Med. 2022, 14, eabn6868. [CrossRef] [PubMed]
22. Diaz, M.F.; Calderon, K.; Rojas-Neyra, A.; Vakharia, V.N.; Choque-Guevara, R.; Montalvan-Avalos, A.; Poma-Acevedo, A.; Rios-Matos, D.; Agurto-Arteaga, A.; Cauti-Mendoza, M.G.; et al. Intranasal vaccination of hamsters with a Newcastle disease virus vector expressing the S1 subunit protects animals against SARS-CoV-2 disease. Sci. Rep. 2022, 12, 10359. [CrossRef] [PubMed]
23. Hassan, A.O.; Feldmann, F.; Zhao, H.; Curiel, D.T.; Okumura, A.; Tang-Huau, T.L.; Case, J.B.; Meade-White, K.; Callison, J.; Lovaglio, J.; et al. A single intranasal dose of chimpanzee adenovirus-vectored vaccine protects against SARS-CoV-2 infection in rhesus macaques. bioRxiv 2021. [CrossRef] [PubMed]
24. Bricker, T.L.; Darling, T.L.; Hassan, A.O.; Harastani, H.H.; Soung, A.; Jiang, X.; Dai, Y.N.; Zhao, H.; Adams, L.J.; Holtzman, M.J.; et al. A single intranasal or intramuscular immunization with chimpanzee adenovirus-vectored SARS-CoV-2 vaccine protects against pneumonia in hamsters. Cell Rep. 2021, 36, 109400. [CrossRef] [PubMed]
25. van Doremalen, N.; Purushotham, J.N.; Schulz, J.E.; Holbrook, M.G.; Bushmaker, T.; Carmody, A.; Port, J.R.; Yinda, C.K.; Okumura, A.; Saturday, G.; et al. Intranasal ChAdOx1 nCoV-19/AZD1222 vaccination reduces viral shedding after SARS-CoV-2 D614G challenge in preclinical models. Sci. Transl. Med. 2021, 13, eabh0755. [CrossRef] [PubMed]
26. King, R.G.; Silva-Sanchez, A.; Peel, J.N.; Botta, D.; Dickson, A.M.; Pinto, A.K.; Meza-Perez, S.; Allie, S.R.; Schultz, M.D.; Liu, M.; et al. Single-Dose Intranasal Administration of AdCOVID Elicits Systemic and Mucosal Immunity against SARS-CoV-2 and Fully Protects Mice from Lethal Challenge. Vaccines 2021, 9, 881. [CrossRef]
27. An, X.; Martinez-Paniagua, M.; Rezvan, A.; Sefat, S.R.; Fathi, M.; Singh, S.; Biswas, S.; Pourpak, M.; Yee, C.; Liu, X.; et al. Singledose intranasal vaccination elicits systemic and mucosal immunity against SARS-CoV-2. iScience 2021, 24, 103037. [CrossRef]
28. Du, Y.; Xu, Y.; Feng, J.; Hu, L.; Zhang, Y.; Zhang, B.; Guo, W.; Mai, R.; Chen, L.; Fang, J.; et al. Intranasal administration of a recombinant RBD vaccine induced protective immunity against SARS-CoV-2 in mouse. Vaccine 2021, 39, 2280–2287. [CrossRef]
29. Tang, J.; Zeng, C.; Cox, T.M.; Li, C.; Son, Y.M.; Cheon, I.S.; Wu, Y.; Behl, S.; Taylor, J.J.; Chakraborty, R.; et al. Respiratory mucosal immunity against SARS-CoV-2 following mRNA vaccination. Sci. Immunol. 2022, 7, eadd4853. [CrossRef]
30. Stark, F.C.; Akache, B.; Deschatelets, L.; Tran, A.; Stuible, M.; Durocher, Y.; McCluskie, M.J.; Agbayani, G.; Dudani, R.; Harrison, B.A.; et al. Intranasal immunization with a proteosome-adjuvanted

SARS-CoV-2 spike protein-based vaccine is immunogenic and efficacious in mice and hamsters. Sci. Rep. 2022, 12, 9772. [CrossRef]
31. Hassan, A.O.; Kafai, N.M.; Dmitriev, I.P.; Fox, J.M.; Smith, B.K.; Harvey, I.B.; Chen, R.E.; Winkler, E.S.; Wessel, A.W.; Case, J.B.; et al. A Single-Dose Intranasal ChAd Vaccine Protects Upper and Lower Respiratory Tracts against SARS-CoV-2. Cell 2020, 183, 169–184.e13. [CrossRef] [PubMed]
32. Kleanthous, H.; Silverman, J.M.; Makar, K.W.; Yoon, I.K.; Jackson, N.; Vaughn, D.W. Scientific rationale for developing potent RBD-based vaccines targeting COVID-19. npj Vaccines 2021, 6, 128. [CrossRef] [PubMed] 33. Garcia-Beltran, W.F.; Lam, E.C.; Astudillo, M.G.; Yang, D.; Miller, T.E.; Feldman, J.; Hauser, B.M.; Caradonna, T.M.; Clayton, K.L.; Nitido, A.D.; et al. COVID-19-neutralizing antibodies predict disease severity and survival. Cell 2021, 184, 476–488 e411. [CrossRef] [PubMed]
34. Pinto, D.; Park, Y.J.; Beltramello, M.; Walls, A.C.; Tortorici, M.A.; Bianchi, S.; Jaconi, S.; Culap, K.; Zatta, F.; De Marco, A.; et al. Cross-neutralization of SARS-CoV-2 by a human monoclonal SARS-CoV antibody. Nature 2020, 583, 290–295. [CrossRef]
35. Barnes, C.O.; Jette, C.A.; Abernathy, M.E.; Dam, K.A.; Esswein, S.R.; Gristick, H.B.; Malyutin, A.G.; Sharaf, N.G.; Huey-Tubman, K.E.; Lee, Y.E.; et al. SARS-CoV-2 neutralizing antibody structures inform therapeutic strategies. Nature 2020, 588, 682–687. [CrossRef]
36. Piccoli, L.; Park, Y.J.; Tortorici, M.A.; Czudnochowski, N.; Walls, A.C.; Beltramello, M.; Silacci-Fregni, C.; Pinto, D.; Rosen, L.E.; Bowen, J.E.; et al. Mapping Neutralizing and Immunodominant Sites on the SARS-CoV-2 Spike Receptor-Binding Domain by Structure-Guided High-Resolution Serology. Cell 2020, 183, 1024–1042. [CrossRef]
37. Liang, Z.; Zhu, H.; Wang, X.; Jing, B.; Li, Z.; Xia, X.; Sun, H.; Yang, Y.; Zhang, W.; Shi, L.; et al. Adjuvants for Coronavirus Vaccines. Front. Immunol. 2020, 11, 589833. [CrossRef]
38. Fujkuyama, Y.; Tokuhara, D.; Kataoka, K.; Gilbert, R.S.; McGhee, J.R.; Yuki, Y.; Kiyono, H.; Fujihashi, K. Novel vaccine development strategies for inducing mucosal immunity. Expert Rev. Vaccines 2012, 11, 367–379. [CrossRef]
39. Chugh, Y.; Kapoor, P.; Kapoor, A.K. Intranasal drug delivery: A novel approach. Indian J. Otolaryngol. Head Neck Surg. 2009, 61, 90–94. [CrossRef]
40. Wang, Y.Y.; Lai, S.K.; So, C.; Schneider, C.; Cone, R.; Hanes, J. Mucoadhesive nanoparticles may disrupt the protective human mucus barrier by altering its microstructure. PLoS ONE 2011, 6, e21547. [CrossRef]
41. McGee, D.W.; Elson, C.O.; McGhee, J.R. Enhancing effect of cholera toxin on interleukin-6 secretion by IEC-6 intestinal epithelial cells: Mode of action and augmenting effect of inflammatory cytokines. Infect. Immun. 1993, 61, 4637–4644. [CrossRef] [PubMed]
42. Lucas, C.; Vogels, C.B.F.; Yildirim, I.; Rothman, J.E.; Lu, P.; Monteiro, V.; Gehlhausen, J.R.; Campbell, M.; Silva, J.; Tabachnikova, A.; et al. Impact of circulating SARS-CoV-2 variants on mRNA vaccine-induced immunity. Nature 2021, 600, 523–529. [CrossRef] [PubMed]
43. Lycke, N.; Bemark, M. Mucosal adjuvants and long-term memory development with special focus on CTA1-DD and other ADP-ribosylating toxins. Mucosal Immunol. 2010, 3, 556–566. [CrossRef] [PubMed]
44. Kim, Y.G. Microbiota Influences Vaccine and Mucosal Adjuvant Efficacy. Immune Netw. 2017, 17, 20–24. [CrossRef]
45. Clements, J.D.; Norton, E.B. The Mucosal Vaccine Adjuvant LT(R192G/L211A) or dmLT. mSphere 2018, 3, e00215-18. [CrossRef]
46. Lewis, D.J.; Huo, Z.; Barnett, S.; Kromann, I.; Giemza, R.; Galiza, E.; Woodrow, M.; Thierry-Carstensen, B.; Andersen, P.; Novicki, D.; et al. Transient facial nerve paralysis (Bell's palsy) following intranasal delivery of a genetically detoxified mutant of Escherichia coli heat labile toxin. PLoS ONE 2009, 4, e6999. [CrossRef]
47. Mutsch, M.; Zhou, W.; Rhodes, P.; Bopp, M.; Chen, R.T.; Linder, T.; Spyr, C.; Steffen, R. Use of the inactivated intranasal influenza vaccine and the risk of Bell's palsy in Switzerland. N. Engl. J. Med. 2004, 350, 896–903. [CrossRef]

48. Patel, G.B.; Zhou, H.; Ponce, A.; Chen, W. Mucosal and systemic immune responses by intranasal immunization using archaeal lipid-adjuvanted vaccines. Vaccine 2007, 25, 8622–8636. [CrossRef]
49. Patel, G.B.; Zhou, H.; Ponce, A.; Harris, G.; Chen, W. Intranasal immunization with an archaeal lipid mucosal vaccine adjuvant and delivery formulation protects against a respiratory pathogen challenge. PLoS ONE 2010, 5, e15574. [CrossRef]
50. Patel, G.B.; Chen, W. Archaeal lipid mucosal vaccine adjuvant and delivery system. Expert Rev. Vaccines 2010, 9, 431–440. [CrossRef]
51. Patel, G.B.; Ponce, A.; Zhou, H.; Chen, W. Safety of intranasally administered archaeal lipid mucosal vaccine adjuvant and delivery (AMVAD) vaccine in mice. Int. J. Toxicol. 2008, 27, 329–339. [CrossRef]
52. Patel, G.B.; Ponce, A.; Zhou, H.; Chen, W. Structural characterization of archaeal lipid mucosal vaccine adjuvant and delivery (AMVAD) formulations prepared by different protocols and their efficacy upon intranasal immunization of mice. J. Liposome Res. 2008, 18, 127–143. [CrossRef] [PubMed]
53. Akache, B.; Renner, T.M.; Tran, A.; Deschatelets, L.; Dudani, R.; Harrison, B.A.; Duque, D.; Haukenfrers, J.; Rossotti, M.A.; Gaudreault, F.; et al. Immunogenic and efficacious SARS-CoV-2 vaccine based on resistin-trimerized spike antigen SmT1 and SLA archaeosome adjuvant. Sci. Rep. 2021, 11, 21849. [CrossRef] [PubMed] 54. Akache, B.; Deschatelets, L.; Harrison, B.A.; Dudani, R.; Stark, F.C.; Jia, Y.; Landi, A.; Law, J.L.M.; Logan, M.; Hockman, D.; et al. Effect of Different Adjuvants on the Longevity and Strength of Humoral and Cellular Immune Responses to the HCV Envelope Glycoproteins. Vaccines 2019, 7, 204. [CrossRef] [PubMed]
55. Krishnan, L.; Sad, S.; Patel, G.B.; Sprott, G.D. The potent adjuvant activity of archaeosomes correlates to the recruitment and activation of macrophages and dendritic cells In Vivo. J. Immunol. 2001, 166, 1885–1893. [CrossRef] [PubMed]
56. Krishnan, L.; Dicaire, C.J.; Patel, G.B.; Sprott, G.D. Archaeosome vaccine adjuvants induce strong humoral, cell-mediated, and memory responses: Comparison to conventional liposomes and alum. Infect. Immun. 2000, 68, 54–63. [CrossRef]
57. Colwill, K.; Galipeau, Y.; Stuible, M.; Gervais, C.; Arnold, C.; Rathod, B.; Abe, K.T.; Wang, J.H.; Pasculescu, A.; Maltseva, M.; et al. A scalable serology solution for profiling humoral immune responses to SARS-CoV-2 infection and vaccination. Clin. Transl. Immunol. 2022, 11, e1380. [CrossRef]
58. Demone, J.; Maltseva, M.; Nourimand, M.; Nasr-Sharif, M.; Galipeau, Y.; Alarcon, E.I.; Langlois, M.A.; MacLean, A.M. Scalable agroinfiltration-based production of SARS-CoV-2 antigens for use in diagnostic assays and subunit vaccines. PLoS ONE 2022, 17, e0277668. [CrossRef]
59. Abe, K.T.; Li, Z.; Samson, R.; Samavarchi-Tehrani, P.; Valcourt, E.J.; Wood, H.; Budylowski, P.; Dupuis, A.P., II; Girardin, R.C.; Rathod, B.; et al. A simple protein-based surrogate neutralization assay for SARS-CoV-2. JCI Insight 2020, 5, e142362. [CrossRef]
60. Mattsson, J.; Schon, K.; Ekman, L.; Fahlen-Yrlid, L.; Yrlid, U.; Lycke, N.Y. Cholera toxin adjuvant promotes a balanced Th1/Th2/Th17 response independently of IL-12 and IL-17 by acting on Gsalpha in CD11b+ DCs. Mucosal Immunol. 2015, 8, 815–827. [CrossRef]
61. Cromer, D.; Steain, M.; Reynaldi, A.; Schlub, T.E.; Wheatley, A.K.; Juno, J.A.; Kent, S.J.; Triccas, J.A.; Khoury, D.S.; Davenport, M.P. Neutralising antibody titres as predictors of protection against SARS-CoV-2 variants and the impact of boosting: A meta-analysis. Lancet Microbe 2022, 3, e52–e61. [CrossRef] [PubMed]
62. Khoury, D.S.; Cromer, D.; Reynaldi, A.; Schlub, T.E.; Wheatley, A.K.; Juno, J.A.; Subbarao, K.; Kent, S.J.; Triccas, J.A.; Davenport, M.P. Neutralizing antibody levels are highly predictive of immune protection from symptomatic SARS-CoV-2 infection. Nat. Med. 2021, 27, 1205–1211. [CrossRef] [PubMed]
63. Li, T.; Han, X.; Gu, C.; Guo, H.; Zhang, H.; Wang, Y.; Hu, C.; Wang, K.; Liu, F.; Luo, F.; et al. Potent SARS-CoV-2 neutralizing antibodies with protective efficacy against newly emerged mutational variants. Nat. Commun. 2021, 12, 6304. [CrossRef] [PubMed]
64. Ng, K.W.; Faulkner, N.; Finsterbusch, K.; Wu, M.; Harvey, R.; Hussain, S.; Greco, M.; Liu, Y.; Kjaer, S.; Swanton, C.; et al. SARS-CoV-2 S2-targeted vaccination elicits broadly neutralizing antibodies. Sci. Transl. Med. 2022, 14, eabn3715. [CrossRef] [PubMed]

65. Chi, X.; Yan, R.; Zhang, J.; Zhang, G.; Zhang, Y.; Hao, M.; Zhang, Z.; Fan, P.; Dong, Y.; Yang, Y.; et al. A neutralizing human antibody binds to the N-terminal domain of the Spike protein of SARS-CoV-2. Science 2020, 369, 650–655. [CrossRef] [PubMed]
66. Oh, J.E.; Song, E.; Moriyama, M.; Wong, P.; Zhang, S.; Jiang, R.; Strohmeier, S.; Kleinstein, S.H.; Krammer, F.; Iwasaki, A. Intranasal priming induces local lung-resident B cell populations that secrete protective mucosal antiviral IgA. Sci. Immunol. 2021, 6, eabj5129. [CrossRef] [PubMed]
67. Iwasaki, A. Exploiting Mucosal Immunity for Antiviral Vaccines. Annu. Rev. Immunol. 2016, 34, 575–608. [CrossRef] [PubMed]
68. Lindley, R.A.; Steele, E.J. Analysis of SARS-CoV-2 haplotypes and genomic sequences during 2020 in Victoria, Australia, in the context of putative deficits in innate immune deaminase anti-viral responses. Scand. J. Immunol. 2021, 94, e13100. [CrossRef]
69. Gorczynski, R.M.; Lindley, R.A.; Steele, E.J.; Wickramasinghe, N.C. Nature of Acquired Immune Responses, Epitope Specificity and Resultant Protection from SARS-CoV-2. J. Pers. Med. 2021, 11, 1253. [CrossRef]
70. Wilkie, B.N. Respiratory tract immune response to microbial pathogens. J. Am. Vet. Med. Assoc. 1982, 181, 1074–1079.
71. Sheikh-Mohamed, S.; Sanders, E.C.; Gommerman, J.L.; Tal, M.C. Guardians of the oral and nasopharyngeal galaxy: IgA and protection against SARS-CoV-2 infection. Immunol. Rev. 2022, 309, 75–85. [CrossRef] [PubMed]
72. Sheikh-Mohamed, S.; Isho, B.; Chao, G.Y.C.; Zuo, M.; Cohen, C.; Lustig, Y.; Nahass, G.R.; Salomon-Shulman, R.E.; Blacker, G.; Fazel-Zarandi, M.; et al. Systemic and mucosal IgA responses are variably induced in response to SARS-CoV-2 mRNA vaccination and are associated with protection against subsequent infection. Mucosal Immunol. 2022, 15, 799–808. [CrossRef] [PubMed]
73. Havervall, S.; Marking, U.; Svensson, J.; Greilert-Norin, N.; Bacchus, P.; Nilsson, P.; Hober, S.; Gordon, M.; Blom, K.; Klingstrom, J.; et al. Anti-Spike Mucosal IgA Protection against SARS-CoV-2 Omicron Infection. N. Engl. J. Med. 2022, 387, 1333–1336. [CrossRef] [PubMed]
74. Cervia, C.; Nilsson, J.; Zurbuchen, Y.; Valaperti, A.; Schreiner, J.; Wolfensberger, A.; Raeber, M.E.; Adamo, S.; Weigang, S.; Emmenegger, M.; et al. Systemic and mucosal antibody responses specific to SARS-CoV-2 during mild versus severe COVID-19. J. Allergy Clin. Immunol. 2021, 147, 545–557.e9. [CrossRef]
75. Sterlin, D.; Mathian, A.; Miyara, M.; Mohr, A.; Anna, F.; Claer, L.; Quentric, P.; Fadlallah, J.; Devilliers, H.; Ghillani, P.; et al. IgA dominates the early neutralizing antibody response to SARS-CoV-2. Sci. Transl. Med. 2021, 13, eabd2223. [CrossRef]
76. Schmidt, F.; Muecksch, F.; Weisblum, Y.; Da Silva, J.; Bednarski, E.; Cho, A.; Wang, Z.; Gaebler, C.; Caskey, M.; Nussenzweig, M.C.; et al. Plasma Neutralization of the SARS-CoV-2 Omicron Variant. N. Engl. J. Med. 2022, 386, 599–601. [CrossRef]
77. Burki, T.K. Omicron variant and booster COVID-19 vaccines. Lancet Respir. Med. 2022, 10, e17. [CrossRef] 78. Liu, L.; Iketani, S.; Guo, Y.; Chan, J.F.; Wang, M.; Liu, L.; Luo, Y.; Chu, H.; Huang, Y.; Nair, M.S.; et al. Striking antibody evasion manifested by the Omicron variant of SARS-CoV-2. Nature 2022, 602, 676–681. [CrossRef] 79. Yamasoba, D.; Kimura, I.; Nasser, H.; Morioka, Y.; Nao, N.; Ito, J.; Uriu, K.; Tsuda, M.; Zahradnik, J.; Shirakawa, K.; et al. Virological characteristics of the SARS-CoV-2 Omicron BA.2 spike. Cell 2022, 185, 2103–2115.e19. [CrossRef]
80. Tan, H.X.; Juno, J.A.; Lee, W.S.; Barber-Axthelm, I.; Kelly, H.G.; Wragg, K.M.; Esterbauer, R.; Amarasena, T.; Mordant, F.L.; Subbarao, K.; et al. Immunogenicity of prime-boost protein subunit vaccine strategies against SARS-CoV-2 in mice and macaques. Nat. Commun. 2021, 12, 1403. [CrossRef]
81. Mandolesi, M.; Sheward, D.J.; Hanke, L.; Ma, J.; Pushparaj, P.; Perez Vidakovics, L.; Kim, C.; Adori, M.; Lenart, K.; Lore, K.; et al. SARS-CoV-2 protein subunit vaccination of mice and rhesus macaques elicits potent and durable neutralizing antibody responses. Cell Rep. Med. 2021, 2, 100252. [CrossRef] [PubMed]

82. Zhong, X.; Yang, H.; Guo, Z.F.; Sin, W.Y.; Chen, W.; Xu, J.; Fu, L.; Wu, J.; Mak, C.K.; Cheng, C.S.; et al. B-cell responses in patients who have recovered from severe acute respiratory syndrome target a dominant site in the S2 domain of the surface spike glycoprotein. J. Virol. 2005, 79, 3401–3408. [CrossRef] [PubMed]
83. Zohar, T.; Loos, C.; Fischinger, S.; Atyeo, C.; Wang, C.; Slein, M.D.; Burke, J.; Yu, J.; Feldman, J.; Hauser, B.M.; et al. Compromised Humoral Functional Evolution Tracks with SARS-CoV-2 Mortality. Cell 2020, 183, 1508–1519.e12. [CrossRef] [PubMed]
84. Butler, S.E.; Crowley, A.R.; Natarajan, H.; Xu, S.; Weiner, J.A.; Bobak, C.A.; Mattox, D.E.; Lee, J.; Wieland-Alter, W.; Connor, R.I.; et al. Distinct Features and Functions of Systemic and Mucosal Humoral Immunity Among SARS-CoV-2 Convalescent Individuals. Front. Immunol. 2020, 11, 618685. [CrossRef] [PubMed]
85. Bachmann, M.F.; Zinkernagel, R.M. Neutralizing antiviral B cell responses. Annu. Rev. Immunol. 1997, 15, 235–270. [CrossRef]
86. Bachmann, M.F.; Jennings, G.T. Vaccine delivery: A matter of size, geometry, kinetics and molecular patterns. Nat. Rev. Immunol. 2010, 10, 787–796. [CrossRef]
87. Suzuki, T.; Kawaguchi, A.; Ainai, A.; Tamura, S.; Ito, R.; Multihartina, P.; Setiawaty, V.; Pangesti, K.N.; Odagiri, T.; Tashiro, M.; et al. Relationship of the quaternary structure of human secretory IgA to neutralization of influenza virus. Proc. Natl. Acad. Sci. USA 2015, 112, 7809–7814. [CrossRef]
88. Zeng, W.; Ma, H.; Ding, C.; Yang, Y.; Sun, Y.; Huang, X.; He, W.; Xiang, Y.; Gao, Y.; Jin, T. Characterization of SARS-CoV-2-specific antibodies in COVID-19 patients reveals highly potent neutralizing IgA. Signal Transduct. Target. Ther. 2021, 6, 35. [CrossRef]
89. Zens, K.D.; Chen, J.K.; Farber, D.L. Vaccine-generated lung tissue-resident memory T cells provide heterosubtypic protection to influenza infection. JCI Insight 2016, 1, e85832. [CrossRef]
90. Xiao, Y.; Lidsky, P.V.; Shirogane, Y.; Aviner, R.; Wu, C.T.; Li, W.; Zheng, W.; Talbot, D.; Catching, A.; Doitsh, G.; et al. A defective viral genome strategy elicits broad protective immunity against respiratory viruses. Cell 2021, 184, 6037–6051.e14. [CrossRef]

A-1.21 Differential Adaptive Immune Responses Following SARS-CoV-2 Infection in Children Compared to Adults

Preface

(This work is available as a pre-print research article)

Sabryna Nantel, Corey Arnold, Maala Bhatt, **Yannick Galipeau**, Benoîte Bourdin, Jennifer Bowes, Roger L. Zemek, Marc-André Langlois, Caroline Quach, Hélène Decaluwe, Anne Pham-Huy. **Differential Adaptive Immune Responses Following SARS-CoV-2 Infection in Children Compared to Adults**. 2025.

https://doi.org/10.1101/2024.04.05.24305283

© The copyright holder for this preprint is the author/funder, who has granted medRxiv a license to display the preprint in perpetuity. It is made available under a CC-BY-NC-ND 4.0 International license.

Abstract

Background : SARS-CoV-2 infection elicits distinct clinical features in children and adults. Profiling the adaptive immune response following infection in children is essential to better understand and characterize these differences.

Methods : Humoral and cell-mediated immune responses from unvaccinated pediatric and adult participants were analyzed following asymptomatic or mild non-Omicron SARS-CoV-2 infection. Levels of IgG and IgA targeting spike (S), receptor-binding domain (RBD), and nucleocapsid (N) proteins of SARS-CoV-2 were measured, while neutralizing antibody (nAb) titers were assessed against three viral strains (Wuhan, Omicron BA.1 and BA.4/BA.5). Specific T-cell memory responses were investigated by quantifying interferon-gamma (IFN-γ) secreting cells after stimulation with ancestral and variant strains of SARS-CoV-2, and seasonal human βcoronaviruses (HCoV)-OC43 and -HKU1.

Results : The study comprised 28 children (3 to 17 [median=10] years old) and 28 adults (19 to 62 [median=42]). At a mean time of seven months (+/- 2.8 months) after SARS-CoV-2 infection, children and adults mounted comparable antibody levels against S and RBD, as well as similar neutralization capacity. However, children displayed a weaker cellular memory response to SARSCoV-2 than adults, with a median of 88 [28-184] spot forming units per million of PBMCs in children compared to 208 [141-340] in adults (***, $P < .001$). In children, the level of IFN-γ secreting cells in response to SARS-CoV-2 corresponds to that of seasonal coronaviruses.

Conclusion : Long-term memory T-cell responses to SARS-CoV-2 are enhanced in adults compared to children who demonstrate equivalent responses to SARS-CoV-2 and other HCoV.

Highlights

• Children infected with SARS-CoV-2 show comparable binding and neutralizing antibody levels as adults seven months after infection.

• There are notable differences in the intensity of the T-cell response following SARS-CoV2 infection between children and adults.

• Children have more pronounced T-cell immunodominance towards the spike versus nonspike proteins compared to adults at seven months post-infection

• In contrast, T-cell responses to SARS-CoV-2 are globally reduced in children compared to adults but are alike to other seasonal β-coronaviruses.

Introduction

Since the beginning of the COVID-19 pandemic, there has been age-related differences in clinical presentations and outcomes of SARS-CoV-2 infection. Severe disease disproportionately impacts older adults, in contrast to children, who generally have mild or asymptomatic disease.[1-3] Several factors could account for these differences, such as fewer co-morbidities in children, frequency of exposure to SARS-CoV-2 and seasonal coronaviruses, differential expression of angiotensin-converting enzyme 2 (ACE2), which is required for viral entry, and host immune responses.[4-8] Compared to adults, immunological studies following SARS-CoV-2 infection in children remain limited.[9,10] Many studies have focused on humoral immunity following SARSCoV-2 infection.[10,11] Distinct antibody immune response dynamics are suggested in children compared to adults, but some results are conflicting between studies and many questions remain.[10,12,13] Cell-mediated immunity is more complex to study and less has been published on the role of T cells in the acute and convalescent phases of infection in children, despite its importance in antiviral immunity and vaccine development.[14-17]

The goal of this study was to describe and compare the long-term adaptive immunity following SARS-CoV-2 infection in children and adults. To better understand the differences in memory immune responses following infection, humoral immunity was assessed through direct ELISA to measure binding antibody levels and surrogate neutralization ELISA to establish neutralizing antibody (nAb) titers. Cell-mediated immune responses were measured through ELISpot assay for the detection of functional antigen-specific T cells.

Methods

Study Design and Data Collection

This study was a multicenter, longitudinal study, combining two existing prospective cohorts. Pediatric participants were recruited from the Persistence of Antibody Titers to COVID-19 in Households (PATCH Study), a case-ascertained antibody-surveillance initiative based in Ottawa,

Ontario.[18] Children or adolescents with confirmed SARS-CoV-2 infection defined by either positive testing through PCR or positive anti-nucleocapsid (anti-N) SARS-CoV-2 IgG from the PATCH cohort were eligible to participate (n=38). Adult participants were selected from the REInfection in COVID-19 Estimation of Risk Cohort (RECOVER Study), which consisted of health care workers who were recruited following PCR-confirmed SARS-CoV-2 infection (n=569).[19,20] Adult samples were matched to the pediatric samples based on sex, ethnicity, and time since infection. All selected samples were from unvaccinated participants. Our study included one-time point per participant, which was around seven months post-infection. Questionnaires documented demographics, medical history, COVID-19 symptoms, and potential recent or recurrent SARSCoV-2 infection.[18-20]

Sample Collection and Processing

Blood samples from the pediatric cohort were collected at the Children's Hospital of Eastern Ontario (CHEO) and cryopreserved at the Coronavirus Variants Rapid Response Network (CoVaRR-Net) Biobank within four hours (and up to 24 hours) of procurement, while those from the adult cohort were processed and cryopreserved at the Mother Child Biobank at the Sainte Justine University Hospital and Research Center (CR-CHUSJ). Serum and peripheral blood mononuclear cells (PBMCs) were isolated for the assessment of antibody levels and T-cell studies, respectively. This was done according to standard operating procedures (SOPs) using SepMateTM tubes (Stemcell Technologies, Canada). PBMCs were resuspended in complete Roswell Park Memorial Institute (RPMI) media (Gibco) with 10% dimethyl sulfoxide (DMSO) and cryopreserved in liquid nitrogen, while serum aliquots were cryopreserved at -80°C. Frozen samples from both cohorts were sent and analyzed using the same ELISpot assays (Dr. Decaluwe's laboratory) and antibody and neutralization assays (University of Ottawa's Serology and Diagnostics High-Throughput Facility, Dr. Langlois' laboratory).

Date of Infection

The date of infection was determined by the earliest of either 1) the onset of symptoms, or 2) the confirmed testing date. For asymptomatic individuals who were never tested but had confirmed

infection through the presence of anti-N IgG, the infection date was estimated based on symptom onset or testing date of the first-infected member of the household.

Study Period and SARS-CoV-2 Variant Circulation

Blood samples were collected from May to December 2021. The initial SARS-CoV-2 infections occurred between December 2020 and April 2021, before the emergence of the Omicron (BA.1) variant. Specific testing to identify SARS-CoV-2 variants was not conducted. Instead, the likely strain of SARS-CoV-2 was determined based on prevalent local epidemiology. Infections from March 2020 to March 2021 were most likely caused by the ancestral (Wuhan-like) strain, while those from March 2021 to April 2021 were predominantly attributed to the Alpha (B.1.1.7) variant.[21]

Ethic Approvals

The study was approved by the Research Ethics Boards at the CHEO (CHEOREB#21/08X) and the CR-CHUSJ (MP-21-2021-3035 and MP-21-2021-3046). Consent, and assent when indicated, were obtained from all participants and/or their guardian.

Humoral Immunity

Chemiluminescent direct enzyme-linked immunosorbent assay (ELISA) for antibody detection Serum samples were analyzed using automated chemiluminescent ELISAs for SARS-CoV-2 specific IgA and IgG targeting the whole spike (S) protein, the receptor binding domain of S (RBD), and the nucleocapsid (N) protein. This analysis was conducted with the Hamilton MicroLab STAR robotic liquid handlers at the University of Ottawa's Serology and Diagnostics High-Throughput Facility (Faculty of Medicine), as previously described.[22] Briefly, diluted serum samples were incubated in 384-well assay plates (Thermo Fisher Scientific, Waltham, MA, USA) coated with 50 ng/well of S, RBD or N (S and N from NRC Metrology Division, RBD from the laboratory of Dr. Yves Durocher). Secondary HRP-conjugated antibodies against IgG and IgA were added to the wells, and detected following incubation using SuperSignal Pico chemiluminescent substrate (Thermo Fisher Scientific, Waltham, MA, USA). Plate reader raw

luminescence values were measured, blank-subtracted and scaled to an on-plate standard curve. Scaled values were then converted to international binding antibody units (BAU/mL) based on the WHO international standard (NIBSC code 20/136) and to lab-specific units (µg/mL) using established four-parameters logarithmic conversion models.[22] For each antigen (S, RBD, and N), a cut-off was established based on false discovery rates in a pre-pandemic cohort (3%, 2%, and 5% respectively).[22,23]

Chemiluminescent surrogate neutralization ELISA for nAb detection

Surrogate neutralization ELISA (snELISA) assesses the capacity of serum samples to inhibit the interaction between the S protein of SARS-CoV-2 and the ACE2 cell receptor.22 384-wells assay plates were coated with 100 ng/well of trimeric S protein for ancestral SARS-CoV-2 (Wuhan, NRC Metrology Division) or the Omicron variant strains BA.1 and BA.4/5 (from the laboratory of Dr. Yves Durocher). Samples were serially diluted to generate five data points and incubated on the assay plates. Following incubation, 6.5 ng of biotinylated ACE2 (NRC Metrology Division, Nova Scotia, Canada) was incubated in each well, and subsequently detected using a streptavidinperoxidase polymer (Thermo Fisher Scientific, Waltham, MA, USA) and SuperSignal Pico chemiluminescent substrate (Thermo Fisher Scientific, Waltham, MA, USA). Luminescence readings were background-subtracted, and each dilution point was expressed as a percentage of the average signal from wells with uninhibited antigen-ACE2 interaction (maximum signal). Three-parameter logarithmic regression was applied to model the % of inhibition as a function of the dilution factor, with fixed upper and lower points at 100% and 0%, respectively. The inhibitory dilution at 50% inhibition (ID50) for each sample was determined from its regression and presented as the reciprocal dilution factor (an ID50 of 100 indicates a sample diluted 1:100 has the capacity to inhibit 50% of ACE2-antigen binding).

Cell-Mediated Immunity

Enzyme-linked immunospot (ELISpot) for the quantification of functional cellular immunity

Interferon-gamma (IFN-γ) secreting cells were detected through ELISpot assay. After rapid thawing and overnight resting, PBMCs were stimulated with one µg/mL of spike (S), nucleocapsid (N) or membrane (VME1) mega pools of SARS-CoV-2 peptides from the ancestral strain, as well as the spike from variants B.1.1.7 (Alpha), B.1.351 (Beta), P.1 (Gamma), B.1.617.2 (Delta), and

B.1.1.529 (Omicron) and from two other beta−coronaviruses (HCoV-OC43 and HCoV-HKU1) (JPT Peptide Technologies, JPT, Berlin, Germany) as described elsewhere.[24] Culture media without peptide (AIM-V® Medium (1X), Thermo Fisher Scientific, Waltham, MA, USA) and CytoStimTM (Miltenyi Biotec, MA, USA) were used as negative and positive controls respectively. Spots were quantified using CTL ImmunoSpot® SS UV Analyzer (Cellular Technology Ltd., OH, USA). The positive threshold response was defined as 25 spot-forming units (SFU) per million of PBMCs, as previously published by our team.[19,25]

Statistics

Mann-Whitney or Kruskal-Wallis unpaired nonparametric tests were performed using Prism 9, version 9.2.0 (2021 GraphPad Software, LLC) to assess statistical significance. Significance was set as *P <.05, **P <.01, ***P <.001 and ****P <.0001. Time since infection is presented as mean +/- SD, while experimental data are displayed as median [interquartile range, 25th – 75th percentile].

Results

Participant Characteristics

There were 28 children (median age = 10 years old [Min-Max, 3-17], 50 % female) and 28 adults (42 years old [19-62], 50 % female) included in this study for which samples were suitable for analysis (Table 1). One time point was analyzed per study participant, with a mean time since infection of 7.4 +/- 2.8 months for children and 7.0 +/- 2.5 months for adults. Most children reported mild COVID-19 symptoms, categorized as WHO scale 2-3, similar to the adult group, with the exception of four children who were asymptomatic and identified through household exposure history (Table 1). All children and 46.4% (n=13) of the adult cohort were presumed to be infected with the ancestral (Wuhan-like) strain as it was the predominant circulating strain at the time of infection. The remaining adults (n=15) were likely infected by the B.1.1.7 Alpha variant.

Table 1. Characteristics of participants included in the analysis.

Characteristics	Number (%) of children (n=28)	Number (%) of adults (n=28)
Age (years)		
Median [Min, Max]	10 [3, 17]	42 [19, 62]
Sex		
Male	14 (50)	14 (50)
Female	14 (50)	14 (50)
Race or Ethnicity		
White	15 (54)	17 (61)
Middle Eastern	3 (11)	3 (11)
Asian	8 (29)	8 (29)
Unknown	2 (7)	0 (0)
Primary SARS-CoV-2 infection		
Asymptomatic - WHO Score 1	4 (14)	0 (0)
Symptomatic (Mild) - WHO Score 2-3	24 (86)	28 (100)
Severe/Hospitalized - WHO Score 4-5	0 (0)	0 (0)
Presumed strain based on infection period		
Ancestral (Wuhan-1 like)	28 (100)	13 (46)
Alpha variant	0 (0)	15 (54)
Time since infection at analysis (months)		
Mean (SD)	7.4 (2.8)	7.0 (2.5)
Median [Min, Max]	7.3 [2.7, 15.4]	7.2 [2.7, 15.4]
Serology status at analysis		
Seronegative	2 (7)	2 (7)
Asymptomatic	1 (4)	0 (0)
Symptomatic	1 (4)	2 (7)
Seropositive	26 (93)	26 (93)
Asymptomatic	3 (11)	0 (0)
Symptomatic	23 (82)	26 (93)
Recurrence of SARS-CoV-2 infection (confirmed by testing)		
Yes	0 (0)	3 (11)
No	28 (100)	25 (89)

Children show comparable levels of anti-spike antibodies but reduced anti-nucleocapsid antibodies when compared to adults

Seropositivity to the virus long after infection was assessed using SARS-CoV-2-specific IgG ELISA in both children and adult serum (Table 1). Most subjects were seropositive (93% in each cohort) at the time of immune response analysis. Children and adults had comparable levels of anti-S and anti-RBD antibodies, but children had lower antibody levels against non-spike components of SARS-CoV-2 (Fig. 1). Notably, both IgG (Fig. 1A) and IgA (Fig. 1B) binding to the N protein were significantly lower in children than in adults with a median of 31.0 [20.2-53.8] BAU/mL in children compared to 56.1 [32.6-113.8] BAU/mL in adults (*P < .05) for IgG and 0.02 [0.00-0.31] µg/mL in children compared to 0.29 [0.11-0.92] µg/mL in adults (**P < .01) for IgA. Because we previously reported that symptomatology and serology status affected the strength of the immune response in infected adults, we questioned if it may influence results in the pediatric population as well.19 When asymptomatic (n=4) and seronegative (n=1) children were excluded from the analysis, the difference in IgA levels against the nucleocapsid remained, while it was less evident for anti-N IgG levels (Fig. S1).

Children and adults exhibit comparable neutralizing capacity

Blockade of SARS-CoV-2 viral entry through the ACE2 receptor is largely mediated by immunoglobulins targeting the spike protein and its RBD component.[26-28] Here, we assessed neutralizing capacity more than six months post-infection through surrogate neutralization ELISA against the ancestral SARS-CoV-2 as well as Omicron variants BA.1 and BA.4/BA.5. Children and adults had similar neutralizing capacity against all three strains assessed. As demonstrated in other studies, neutralizing capacity decreased against newer variants (Omicron BA.1 and BA.4/BA.5) compared to the ancestral strain, a finding equivalent in children and adults (Fig. 2).[29] When analyzing only participants with symptomatic SARS-CoV-2 infection, we noted comparable neutralizing antibody levels for ancestral and Omicron BA.1, but slightly increased nAb titers against Omicron BA.4/BA.5 in children, with a median nAb titer of 2.58 [1.08-8.25] compared to 0.52 [0.07-3.72] in adults (*P < .05) (Fig. S2).

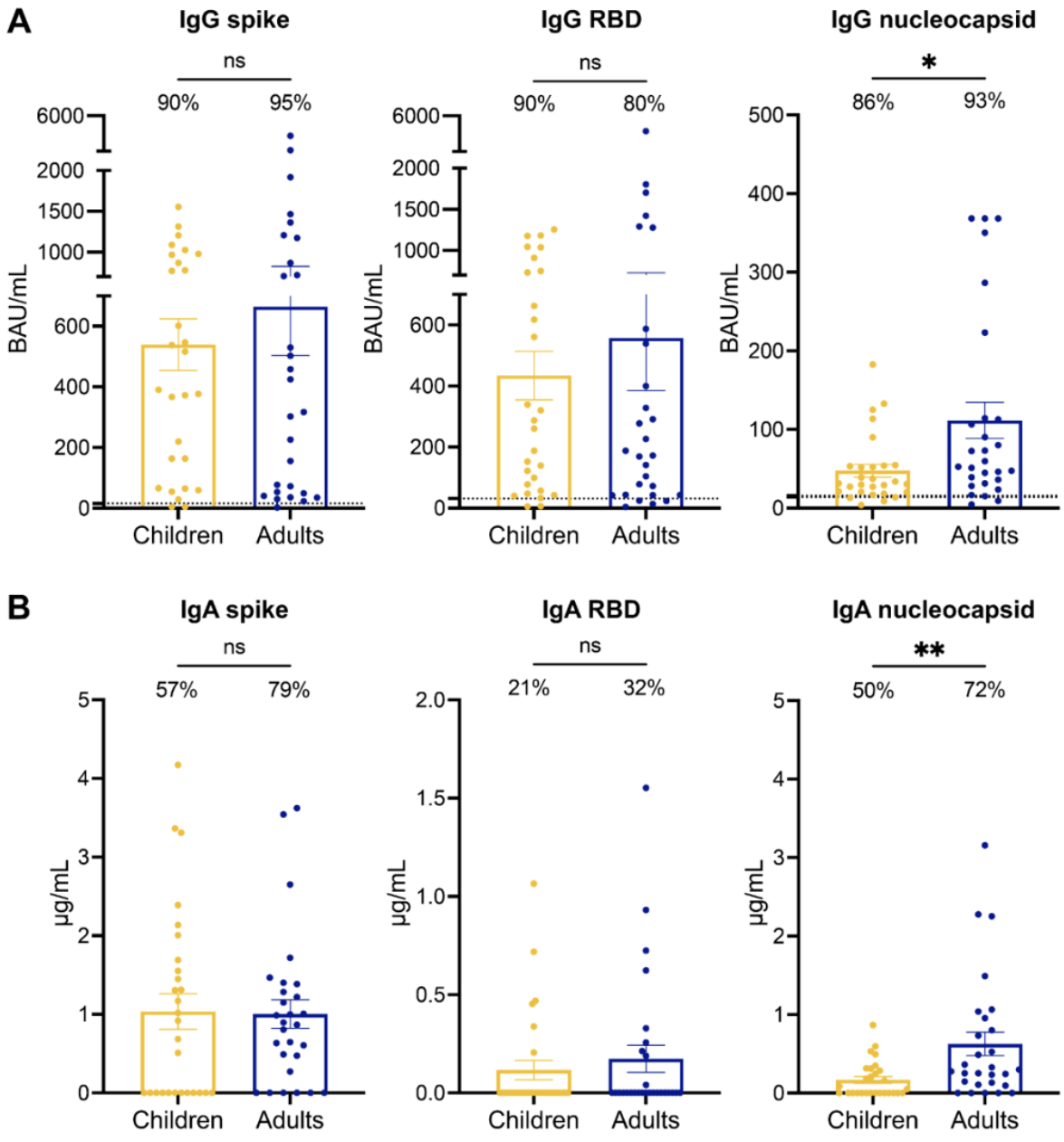


Figure 1. Children develop lower antibody levels against non-spike components of SARS-CoV-2 compared to adults. ELISA were conducted to measure the anti-spike (left panels), anti-RBD (middle panels) and anti-nucleocapsid (right panels) IgG (A) and IgA (B) levels in the serum of children (n = 28, yellow) and adults (n = 28, blue) infected with SARS-CoV-2. (A) The percentage of participants with IgG responses above the positive cut-off value (15.53216 for spike, 31.34807 for RBD and 13.83556 for nucleocapsid) are indicated for each group. (B) The percentage of participants with detectable IgA are

indicated for each group. Error bars indicate mean ± SEM. Statistical significance was established as : ns (not significant) P >.05, *P <.05, **P <.01.

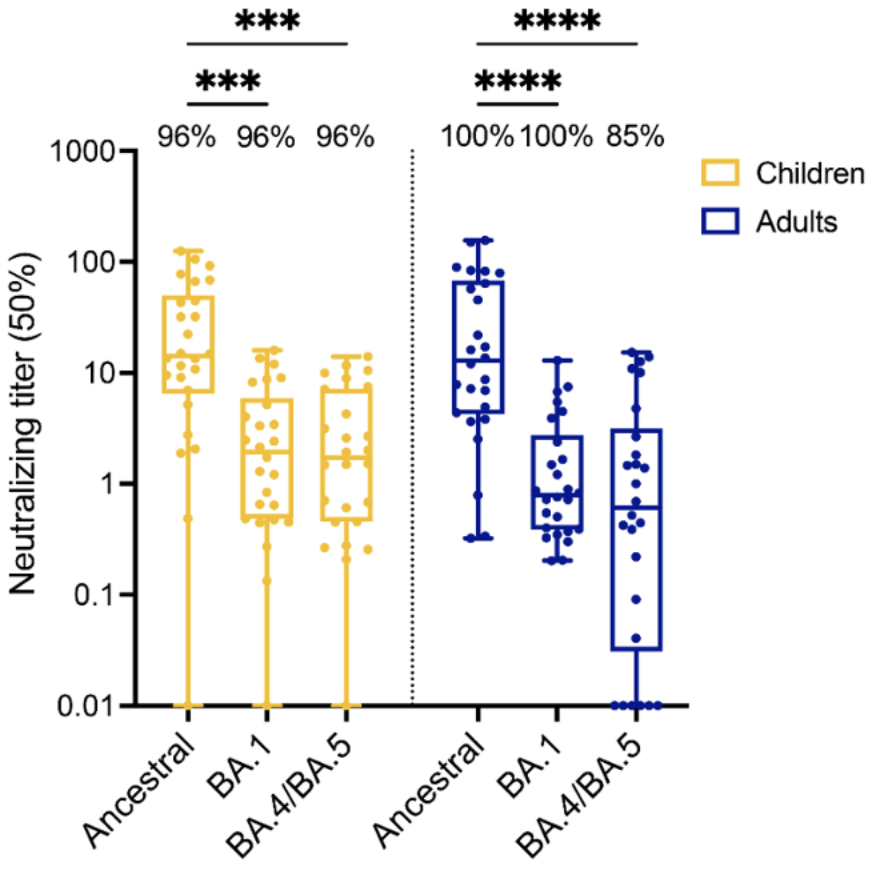


Figure 2. Children develop similar neutralizing capacity to adults after infection with SARS-CoV-2. Surrogate neutralization ELISA were conducted to establish the serum dilution level (ID50) required to inhibit 50% of the binding between the trimeric spike protein and the ACE2 receptor, thus neutralizing the virus attachment capability to cells. Neutralizing antibody titers were measured for the ancestral SARS-CoV-2 spike, as well as Omicron BA.1 and BA.4/BA.5 variants. Serums were analyzed after SARS-CoV-2 infection in children (n = 26, yellow) and adults (n = 26, blue). The percentage of participants with detectable neutralizing antibodies against specific variants are indicated for each group. Statistical significance was established as : ns (not significant, not shown) P >.05, ***P<.001, ****P<.0001.

The strength of T-cell response to SARS-CoV-2 is reduced in children compared to adults and is analogous to responses to other seasonal beta−coronaviruses

Cell-mediated immune responses are critical mediators of reduced disease severity and long-term protection.[26,30,31] Memory T-cell responses were assessed through ELISpot for the detection of IFN- secreting cells in response to different stimulations. For all SARS-CoV-2 strains tested, children displayed less IFN- secreting cells compared to adults seven months after SARS-CoV2 infection (Fig. 3A). The number of antigen-responding T cells per million PBMCs was two-fold lower in children compared to adults, with a median of 88 [28-184] spot forming units (SFU) per million of PBMCs in children compared to 208 [141-340] in adults (***, P < .001). There was strong immunodominance of the T-cell response towards the spike protein in children. The frequency of children displaying IFN- secreting cells against non-Spike components (nucleocapsid and membrane protein) of SARS-CoV-2 was much lower than in adults, ****P <.0001 for both (Fig. 3B). The reduced magnitude of the T-cell response in children compared to adults was also observed when children who had an asymptomatic infection were excluded from the analysis (Fig. S3). Unexpectedly, children displayed response to SARS-CoV-2 of similar strength as they did to other seasonal beta-coronaviruses, including HCoV-OC43 and HCoV-HKU1 (median of 88 [28-184] for SARS-CoV-2 compared to 58 [29-163] and 60 [33-168] SFU per million PBMCs for HCoV-OC43 and HCoV-HKU1 respectively, P >.05, not significant). In contrast, adults exhibited robust IFN-y secretion to SARS-CoV-2 (median of 208 [141-340]) and significantly lower responses to common beta-coronaviruses (median of 80 [45-135], ****P <.0001 for HCoV-OC43 compared to SARS-CoV-2 and 98 [59-151], **P <.01 for HCoV-HKU1 compared to SARS-CoV-2) (Fig. 3C).

For all three assays used to evaluate the memory humoral and cellular responses to SARS-CoV-2 infection, no sex-based difference was observed (Fig. S4).

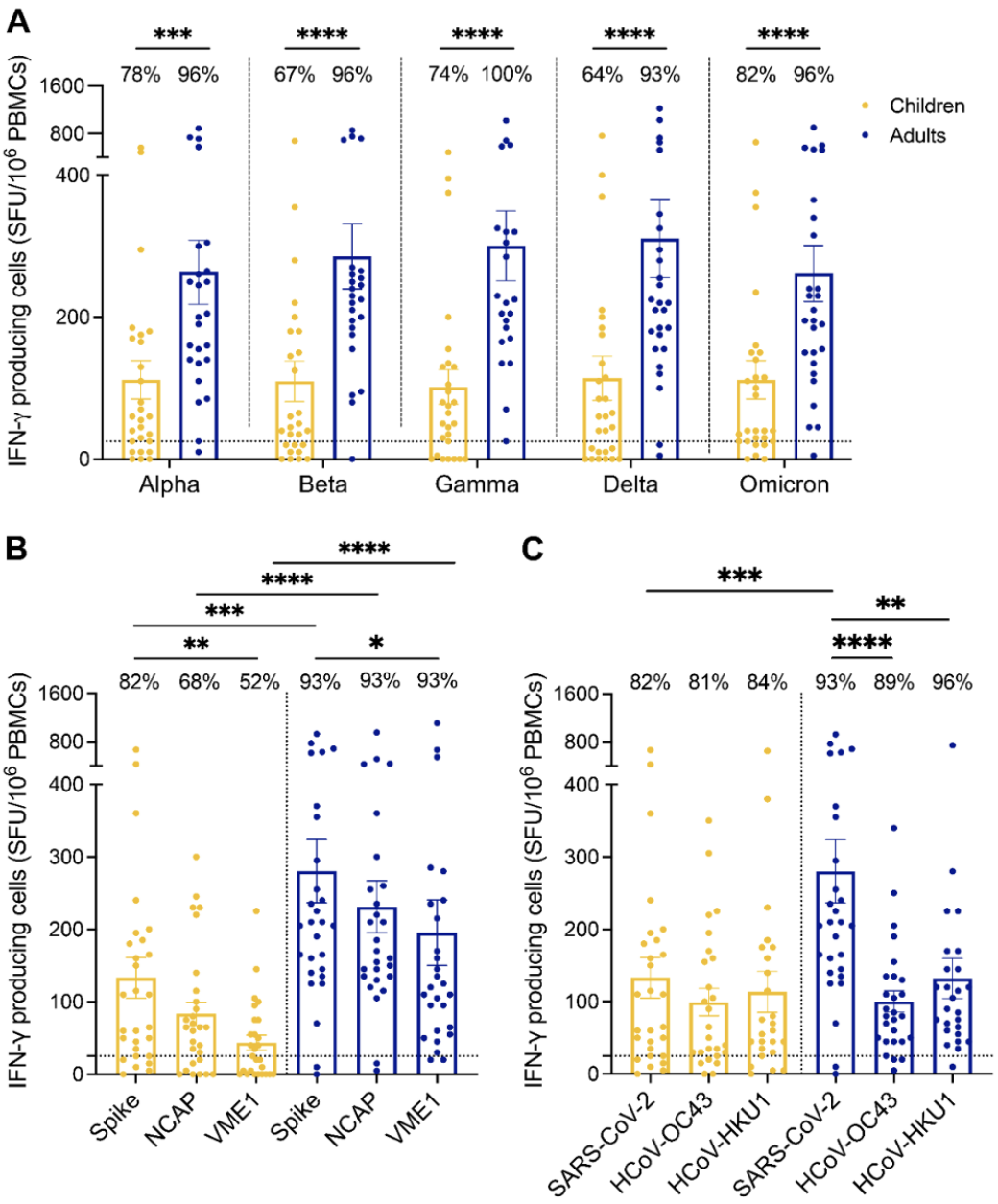


Figure 3. Cellular immune responses to SARS-CoV-2 are enhanced compared to other ß-coronaviruses in adults, but not in children. T-cell responses were assessed by ELISpot assay after peptide stimulation. Samples were collected from SARS-CoV-2 infected children (n = 28, yellow) and adults (n = 28, blue). (A) PBMCs were stimulated with SARS-CoV-2 spike peptide from five different variant strains (Alpha, Beta, Gamma, Delta, Omicron BA.1). (B) PBMCs were stimulated with peptide pools from the ancestral SARS-CoV-2 spike, nucleocapsid (NCAP) and membrane (VME1) protein. (C) PBMCs were stimulated with spike peptides from SARS-CoV-2 and common cold ß-coronaviruses HCoVOC43 and HCoV-HKU1. Results are expressed in number of IFN-γ producing cells per million PBMCs. Dotted line indicates the positive threshold value of 25 IFN-γ secreting cells. The number of participants with responses above the positive cut-off value are indicated for each group and condition.

Error bars indicate mean ± SEM. Statistical significance was established as : ns (not significant, not shown) P >.05, *P <.05, **P <.01, ***P<.001, ****P<.0001.

Discussion

Our study aimed to further contribute to better understanding the dynamics of the immune responses following SARS CoV 2 infection in children. We describe the production and persistence of adaptive humoral and cellular immune responses following mild SARS-CoV-2 infection in both children and adults, with differences noted between the two groups. In the convalescence phase following acute SARS-CoV-2 infection, adults retained enhanced T-cell immune responses compared to children. In contrast, pediatric participant's T-cell responses were lower and indistinguishable from other seasonal ß-coronaviruses. While serum immunoglobulin levels and neutralizing capacity were comparable in both children and adults, we observed more pronounced immunodominance towards the spike versus non-spike proteins in children compared to adults at seven months post-infection. This observation is supported by other studies, who consistently report that children mount an early and effective anti-nucleocapsid response that wanes and declines more rapidly compared to adults.[10,32-34]

More importantly, we described notable differences in the intensity of the T-cell response following SARS-CoV-2 infection with lower responses in children compared to adults, when measured over six months post-infection. This observation is similar to increasing number of reports.[32,35-37] T cells have an important role in limiting disease severity, leading to recovery but also to immune memory and protection against reinfection by future variants.[38] Reports have shown that the severity of initial SARS-CoV-2 infection impacts the amplitude of the T-cell response, with stronger but often impaired and pathogenic responses in individuals with severe disease.[14,15,19] Our study shows that mild disease led to higher T-cell responses to SARS-CoV-2 in adults than in children. This is consistent with the study by Khoo et al. who described multimodal immune responses, including cellular responses, in a cohort of five children and seven adults in the acute and convalescent phases of infection.[37] Their results showed that adults generated stronger T-cell immune memory responses and that children showed less activation of the T-cell compartment.[37] Our data also concurs with Cohen et al. who also showed that CD4+ memory Tcell responses to structural SARS-CoV-2 proteins increased with age.[35] This phenomenon was suggested to be correlated to prior exposure to beta-coronaviruses, with adults being exposed more

frequently than children to HCoV.[35,39] However, our data contrasts with those of Dowell et al., who reported that children mount more robust adaptive humoral and cell-mediated immune responses than adults.[34] However, their pediatric participants were younger than our cohort, which may influence the strength of the adaptive immune response.[11] Further, recent exposure to beta-coronaviruses and elevated level of HCoV cross-reactivity observed in their cohort could contribute to the differences observed between our studies. Importantly, here we show that T-cell responses to SARS-CoV-2 are strikingly elevated in adults compared to responses to OC43 and HKU1, an analysis that was not performed in the study by Dowell et al. Collectively, this may also highlight distinct dynamics of the immune response over time in young children compared to adults.

As mentioned above, memory T cells generated following HCoV infections are able to cross-react with SARS-CoV-2 antigens, as demonstrated using pre-pandemic samples, in both adults and children.[39-41] This cross-reactivity is established very early in life.[39] However, despite numerous HCoV exposures, Humbert et al. showed the capacity of T cells to cross-react declines with age, as does the capacity of CD4+ T cells to respond to HCoV.[39,41] In line with this, we report that the increased level of T-cell memory observed in adults is unique to SARS-CoV-2 and is not seen when evaluating responses to other seasonal HCoV, as demonstrated by their lower level of response to HCoV-HKU1 and HCoV-OC43. In our study, children exhibited cellular responses to SARS-CoV-2 comparable to that elicited in response to other seasonal ß-coronaviruses. This is interesting as the clinical picture of SARS-CoV-2 for the majority of children is also very similar to other HCoV. It may suggest that SARS-CoV-2 leads to inherently distinct immune responses in adults and children, with SARS-CoV-2 being recognized as would other seasonal coronaviruses in children.

The differences between adults and children in the strength of the T-cell responses to SARS-CoV2 could be explained by a rapid and extremely efficient innate response in children. Indeed, it is thought that children have pre-activated and robust innate immune responses that are very effective at controlling and clearing SARS-CoV-2 infection.[17,42] This would greatly impact the secondary T-cell response as early viral clearance by the innate immune response would restrict antigen availability and the amplitude of long-lived T-cell responses.[17,43] Further, an accelerated innate

immune response may lead to a more coordinated and balanced adaptive immune response in children, which could contribute to their milder symptoms and reduced inflammatory complications.

Although there is general homogeneity in the clinical presentation of the cases, there are limitations to our study, mostly related to sampling. The time from infection to blood sampling was variable between study participants, ranging from two to fifteen months post-infection (median of seven months). Blood sampling was also limited due to pediatric volume restrictions. Lastly, due to the limited cell numbers, peptide or protein-specific mapping was not possible. The main strength of our study is the direct comparison of both humoral and cell-mediated immunity following mild SARS-CoV-2 infection in adults and children, also interrogating responses to seasonal coronaviruses. Collectively, our results suggest that in the long-term convalescent phase, T-cell responses to SARS-CoV-2 are attenuated in children compared to adults and are similar to that of other common seasonal coronaviruses.

Conclusion

Previous studies suggest that robust innate immune responses help to clear SARS-CoV-2 infection rapidly in children, similar to other seasonal coronaviruses. This highly effective clearance of viral antigens may lead to less T-cell activation, therefore inducing a distinct T-cell differentiation program and dampened IFN-y+ T-cell responses in children compared to adults. Further longitudinal studies are needed to establish the diversity and duration of protection mediated by T cells in children and whether vaccination is useful in broadening and increasing the durability of protection against SARS-CoV-2 infection and severe disease in children.

Awknowlegments

We first want to recognize and warmly thank all of the participants and their parents/guardians who agreed to participate in these studies, as well as the nurses and research coordinators from each participating centers. We are also very grateful for the Children's Hospital of Eastern Ontario, the Coronavirus Variants Rapid Response Network (CoVaRR-Net) Biobank and the Sainte-Justine University Hospital Mother Child Biobank personnel for processing and storing the samples from the studies. Special thanks to Candice McGahern, Fazia Tadount, Kelsey Adams, Louise Wang and Sylvie Nicholson for their role in participant recruitment and sampling as well as Angela Crawley, Laura Tamblyn, Jocelyne Ayotte, Jessie Beauchemin, Vanessa Truong, Annie Bilodeau and Amal Abdi for their role in sample preparation. ELISA assays were performed by the University of Ottawa Serology and Diagnostics High Throughput Facility. Special thanks to Danielle Dewar-Darch, Justino Hernandez-Soto, Abishek Xavier, Kiran Nakka, Smita Upamaka and Yuchu Dou. COVID-19 antigens (variant S trimer and RBD proteins), as well as the antihIgG#5-HRP fusion antibody were generously provided by Dr. Yves Durocher, National Research Council of Canada (NRC), Montréal.

Author contributions

Conceptualization: RLZ, MB, HD, APH Methodology: SN, CA, YG, BB, RLZ, MAL, MB, HD, APH Investigation: HD, APH Visualization: SN, BB, HD Funding acquisition: RLZ, CQ, MB, HD, APH Project administration: BB, JB Subject recruitment: JB, CQ, APH Supervision: HD, APH Writing – original draft: SN, BB, HD, APH . Writing – review & editing: SN, CA, BB, JB, RLZ, CQ, MB, HD, APH

Funding/Support:

This study was funded by the CHAMO Innovation Fund (FPOC# CHA-21010) and PSI Foundation (Grant # 21-22). The RECOVER study was supported by grants from the Canadian Institutes of Health Research VR2172712 (CQ, HD) and the Public Health Agency of Canada 2122-HQ-000225 (CQ, HD). CQ is supported through a Tier 1 Canada Research Chair in Infection Prevention (CRC-2019-00055). HD and SN are supported by the Fonds de Recherche du Québec – Santé through a Senior Clinical Research Scholar award (HD) and a doctoral research scholarship (SN). HD is also supported by the Coalition for Epidemic Preparedness Innovations and Canadian Institutes of Health Research (CVL - 179495). The funders had no role in the study design, data collection or analysis, manuscript preparation or the decision to submit for publication.

Conflicts of Interest and Financial Disclosure

No conflict of interest or other financial disclosure.

Supplementary Material:

https://www.medrxiv.org/content/10.1101/2024.04.05.24305283v1.supplementary-material

References

1 Camporesi, A., Soares Lanziotti, V., Bulut, Y., Behrens, D. & Buonsenso, D. Editorial: Covid, Long Covid, Mental Health, Schools and Masks: how and why we failed child health communication during a pandemic. Front Pediatr 11, 1104518, doi:10.3389/fped.2023.1104518 (2023).
2 Castagnoli, R. et al. Severe Acute Respiratory Syndrome Coronavirus 2 (SARS-CoV-2) Infection in Children and Adolescents: A Systematic Review. JAMA Pediatr 174, 882- 889, doi:10.1001/jamapediatrics.2020.1467 (2020).
3 Mehta, N. S. et al. SARS-CoV-2 (COVID-19): What Do We Know About Children? A Systematic Review. Clinical infectious diseases : an official publication of the Infectious Diseases Society of America 71, 2469-2479, doi:10.1093/cid/ciaa556 (2020). 4 Brodin, P. Immune determinants of COVID-19 disease presentation and severity. Nat Med 27, 28-33, doi:10.1038/s41591-020-01202-8 (2021).
5 Buonsenso, D. et al. Duration of immunity to SARS-CoV-2 in children after natural infection or vaccination in the omicron and pre-omicron era: A systematic review of clinical and immunological studies. Frontiers in immunology 13, 1024924, doi:10.3389/fimmu.2022.1024924 (2022).
6 Williamson, E. J. et al. Factors associated with COVID-19-related death using OpenSAFELY. Nature 584, 430-436, doi:10.1038/s41586-020-2521-4 (2020).
7 Chou, J., Thomas, P. G. & Randolph, A. G. Immunology of SARS-CoV-2 infection in children. Nat Immunol 23, 177-185, doi:10.1038/s41590-021-01123-9 (2022).
8 Zhang, J. J., Dong, X., Liu, G. H. & Gao, Y. D. Risk and Protective Factors for COVID19 Morbidity, Severity, and Mortality. Clin Rev Allergy Immunol 64, 90-107, doi:10.1007/s12016-022-08921-5 (2023).
9 Dunay, G. A. et al. Long-Term Antibody Response to SARS-CoV-2 in Children. Journal of Clinical Immunology 43, 46-56, doi:10.1007/s10875-022-01355-w (2023).
10 Weisberg, S. P. et al. Distinct antibody responses to SARS-CoV-2 in children and adults across the COVID-19 clinical spectrum. Nat Immunol 22, 25-31, doi:10.1038/s41590- 020-00826-9 (2021).
11 Toh, Z. Q. et al. Comparison of Seroconversion in Children and Adults with Mild COVID-19. JAMA Network Open 5, 1-14, doi:10.1001/jamanetworkopen.2022.1313 (2022).
12 Tomasi, L. et al. Younger Children Develop Higher Effector Antibody Responses to SARS-CoV-2 Infection. Open Forum Infectious Diseases 9, 1-10, doi:10.1093/ofid/ofac554 (2022).
13 Yang, H. S. et al. Association of Age with SARS-CoV-2 Antibody Response. JAMA Network Open 4, 1-12, doi:10.1001/jamanetworkopen.2021.4302 (2021).
14 Rumke, L. W. et al. Impaired SARS-CoV-2 specific T-cell response in patients with severe COVID-19. Frontiers in immunology 14, 1046639, doi:10.3389/fimmu.2023.1046639 (2023).
15 Moss, P. The T cell immune response against SARS-CoV-2. Nature Immunology 23, 186-193, doi:10.1038/s41590-021-01122-w (2022)
16 Moga, E., Lynton-Pons, E. & Domingo, P. The Robustness of Cellular Immunity Determines the Fate of SARS-CoV-2 Infection. Frontiers in immunology 13, 904686, doi:10.3389/fimmu.2022.904686 (2022).
17 Yoshida, M. et al. Local and systemic responses to SARS-CoV-2 infection in children and adults. Nature 602, 321-327, doi:10.1038/s41586-021-04345-x (2022).
18 Bhatt, M. et al. Household transmission of SARS-CoV-2 from unvaccinated asymptomatic and symptomatic household members with confirmed SARS-CoV-2 infection: an antibody-surveillance study. CMAJ open 10, E357-E366, doi:10.9778/cmajo.20220026 (2022).
19 Nantel, S. et al. Symptomatology during previous SARS-CoV-2 infection and serostatus before vaccination influence the immunogenicity of BNT162b2 COVID-19 mRNA vaccine. Frontiers in immunology 13, 1-13, doi:10.3389/fimmu.2022.930252 (2022).
20 Racine, É. et al. The REinfection in COVID-19 Estimation of Risk (RECOVER) study: Reinfection and serology dynamics in a cohort of Canadian healthcare workers. Influenza and other Respiratory Viruses 16, 916-925, doi:10.1111/irv.12997 (2022).
21 Ontario, O. A. f. H. P. a. P. P. H. COVID-19 Infection in Children : January 15, 2020 to June 30, 2021. Enhanced Epidemiologicla summary (2021).

22 Colwill, K. et al. A scalable serology solution for profiling humoral immune responses to SARS-CoV-2 infection and vaccination. Clin Transl Immunology 11, e1380, doi:10.1002/cti2.1380 (2022).
23 Cholette, F. et al. Comparative performance data for multiplex SARS-CoV-2 serological assays from a large panel of dried blood spot specimens. Heliyon 8, e10270, doi:10.1016/j.heliyon.2022.e10270 (2022).
24 Salem Fourati, I. et al. Development of an IFN-γ ELISpot assay to assess varicella-zoster virus-specific cell-mediated immunity following umbilical cord blood transplantation. Journal of visualized experiments : JoVE, doi:10.3791/51643 (2014).
25 Nantel, S. et al. Comparison of Omicron Breakthrough Infection Versus Monovalent SARS-CoV-2 Intramuscular Booster Reveals Differences in Mucosal and Systemic Humoral Immunity. Mucosal Immunol, doi:10.1016/j.mucimm.2024.01.004 (2024). 26 Dan, J. M. et al. Immunological memory to SARS-CoV-2 assessed for up to 8 months after infection. Science (New York, N.Y.) 371, doi:10.1126/science.abf4063 (2021).
27 Barnes, C. O. et al. Structures of Human Antibodies Bound to SARS-CoV-2 Spike Reveal Common Epitopes and Recurrent Features of Antibodies. Cell 182, 828-842 e816, doi:10.1016/j.cell.2020.06.025 (2020).
28 Noval, M. G. et al. Antibody isotype diversity against SARS-CoV-2 is associated with differential serum neutralization capacities. Sci Rep 11, 5538, doi:10.1038/s41598-021- 84913-3 (2021).
29 Cao, Y. et al. Omicron escapes the majority of existing SARS-CoV-2 neutralizing antibodies. Nature 602, 657-663, doi:10.1038/s41586-021-04385-3 (2022).
30 Tan, A. T. et al. Early induction of functional SARS-CoV-2-specific T cells associates with rapid viral clearance and mild disease in COVID-19 patients. Cell reports 34, 108728, doi:10.1016/j.celrep.2021.108728 (2021).
31 Guo, L. et al. Durability and cross-reactive immune memory to SARS-CoV-2 in individuals 2 years after recovery from COVID-19: a longitudinal cohort study. Lancet Microbe 5, e24-e33, doi:10.1016/S2666-5247(23)00255-0 (2024).
32 Jacobsen, E.-M. et al. High antibody and reduced cellular response in children up to one year after SARS-CoV-2 infection. Nature communications 28, 7315.-7315., doi:10.1038/s41467-022-35055-1 (2022).
33 Gentles, L. E. et al. Dynamics of infection-elicited SARS-CoV-2 antibodies in children over time. medRxiv, doi:10.1101/2022.01.14.22269235 (2022).
34 Dowell, A. C. et al. Children develop robust and sustained cross-reactive spike-specific immune responses to SARS-CoV-2 infection. Nature Immunology 23, 40-49, doi:10.1038/s41590-021-01089-8 (2022).
35 Cohen, C. A. et al. SARS-CoV-2 specific T cell responses are lower in children and increase with age and time after infection. Nature communications 12, 1-14, doi:10.1038/s41467-021-24938-4 (2021).
36 Kaaijk, P. et al. Children and Adults With Mild COVID-19: Dynamics of the Memory T Cell Response up to 10 Months. Frontiers in immunology 13, 1-15, doi:10.3389/fimmu.2022.817876 (2022).
37 Khoo, W. H. et al. Tracking the clonal dynamics of SARS-CoV-2-specific T cells in children and adults with mild/asymptomatic COVID-19. Clinical Immunology 246, doi:10.1016/j.clim.2022.109209 (2023).
38 Kedzierska, K. & Thomas, P. G. Count on us: T cells in SARS-CoV-2 infection and vaccination. Cell Rep Med 3, 100562, doi:10.1016/j.xcrm.2022.100562 (2022).
39 Humbert, M. et al. Functional SARS-CoV-2 cross-reactive CD4(+) T cells established in early childhood decline with age. Proceedings of the National Academy of Sciences of the United States of America 120, e2220320120, doi:10.1073/pnas.2220320120 (2023).
40 Grifoni, A. et al. Targets of T Cell Responses to SARS-CoV-2 Coronavirus in Humans with COVID-19 Disease and Unexposed Individuals. Cell 181, 1489-1501.e1415, doi:10.1016/j.cell.2020.05.015 (2020).
41 Richards, K. A. et al. Circulating CD4 T Cells Elicited by Endemic Coronaviruses Display Vast Disparities in Abundance and Functional Potential Linked to Antigen Specificity and Age. J Infect Dis 223, 1555-1563, doi:10.1093/infdis/jiab076 (2021).

42 Vono, M. et al. Robust innate responses to SARS-CoV-2 in children resolve faster than in adults without compromising adaptive immunity. Cell reports 37, 109773, doi:10.1016/j.celrep.2021.109773 (2021).
43 Loske, J. et al. Pre-activated antiviral innate immunity in the upper airways controls early SARS-CoV-2 infection in children. Nature Biotechnology 40, 319-324, doi:10.1038/s41587-021-01037-9 (2022).

A-1.22 HUMORAL RESPONSES AND SEROLOGICAL ASSAYS IN SARS-COV-2 INFECTIONS

Preface

(This work has been previously published as a review article)

Galipeau Y., Greig M., Liu G., Driedger M., Langlois MA. **Humoral Responses and Serological Assays in SARS-CoV-2 Infections.** Front Immunol. 2020 Dec 18;11:610688.

https://doi.org/10.3389/fimmu.2020.610688

Copyright © 2020 Galipeau, Greig, Liu, Driedger and Langlois.

This is an open-access article distributed under the terms of the Creative Commons Attribution License (CC BY). The use, distribution or reproduction in other forums is permitted, provided the original author(s) and the copyright owner(s) are credited and that the original publication in this journal is cited, in accordance with accepted academic practice. No use, distribution or reproduction is permitted which does not comply with these terms.

Abstract

In December 2019, the novel betacoronavirus Severe Acute Respiratory Disease Coronavirus 2 (SARS-CoV-2) was first detected in Wuhan, China. SARS-CoV-2 has since become a pandemic virus resulting in hundreds of thousands of deaths and deep socioeconomic implications worldwide. In recent months, efforts have been directed towards detecting, tracking, and better understanding human humoral responses to SARS-CoV-2 infection. It has become critical to develop robust and reliable serological assays to characterize the abundance, neutralization efficiency, and duration of antibodies in virus-exposed individuals. Here we review the latest knowledge on humoral immune responses to SARS-CoV-2 infection, along with the benefits and limitations of currently available commercial and laboratory-based serological assays. We also highlight important serological considerations, such as antibody expression levels, stability and neutralization dynamics, as well as cross-reactivity and possible immunological back-boosting by seasonal coronaviruses. The ability to accurately detect, measure and characterize the various antibodies specific to SARS-CoV-2 is necessary for vaccine development, manage risk and exposure for healthcare and at-risk workers, and for monitoring reinfections with genetic variants and new strains of the virus. Having a thorough understanding of the benefits and cautions of standardized serological testing at a community level remains critically important in the design and implementation of future vaccination campaigns, epidemiological models of immunity, and public health measures that rely heavily on up-to-date knowledge of transmission dynamics.

Introduction

In late 2019, a novel betacoronavirus with sustained human-to-human transmission emerged from China's Hubei Province (1, 2). This new coronavirus was identified as Severe Acute Respiratory Syndrome Coronavirus 2 (SARS-CoV-2) and is currently responsible for the worldwide Coronavirus Disease 2019 (COVID-19) pandemic (3, 4). Currently, a large proportion of the global population remains in various forms of temporary confinement to limit the spread of this virus, leading to significant disruptions in international travel and local socioeconomic activities. Thus, there is a pressing need to better understand the nature and duration of immunity against SARS-CoV-2 infection since nearly all epidemiological models, future vaccination campaigns, and public health measures assume that SARS-CoV-2 convalescence imparts some degree of immunity (5–7). Based on previous serological studies of SARS-CoV (the agent responsible for the 2003 epidemic) and of the Middle East Respiratory Syndrome coronavirus (MERS), neutralizing antibodies are relatively short lived, detectable for approximately three years following infection (8–11). However, the duration of immunity to these specific CoVs is not known. But according to reinfections frequencies by seasonal coronaviruses (sCoVs), this immunity may only last a year (12). Given the global spread and prevalence of SARS-CoV-2, this lethal virus is expected to become endemic (13).

As the pandemic continues its course and convalescent individuals recover, there is an increasing demand to develop validated serological assays that assess the antibody-mediated immunity conferred by a SARS-CoV-2 infection. The utility of serological assays in COVID-19 is manifold. From an epidemiological perspective, a validated serological assay could be used to identify the proportion of individuals exposed to the virus in various populations, such that the evolving disease incidence can be closely monitored. Measuring population seroprevalence can also be used to evaluate the prevalence of asymptomatic transmission and risk factors for acquiring the disease, which remain key research priorities. Furthermore, reliable serological assays are required to determine whether antibody titers, and more importantly neutralizing antibody titers, correlate with sterilizing immunity to SARS-CoV-2. These immunological features could prove to be robust

predictors of the efficacy of future vaccines candidates. At the patient level, serological testing can be used as an adjunct to the current PCR-based assays to improve diagnostic sensitivity. Lastly, serological testing will have profound clinical and epidemiological implications by determining the duration and magnitude of immunity conferred by SARS-CoV-2 infection, characterizing the risk of reinfection, and predicting whether a given vaccine will require further boosters (14, 15). Ultimately, accurate serological data will be crucial for understanding the epidemiological and clinical characteristics of COVID-19 that must be established to inform effective and ethical response strategies to the COVID-19 pandemic, especially as policymakers discuss future approaches to resume economic activities and re-open borders.

Serological tests commonly use blood, serum, plasma, or saliva to detect multiple isotypes of circulating antibodies generated by B lymphocytes. Various private, academic, and public health labs are currently developing platforms for SARS-CoV-2 serological testing, utilizing technologies such as classical immunoassays (mostly Enzyme-Linked Immunosorbent Assays; ELISA), chemiluminescent immunoassays (CLIA), flow cytometry-based methods, and various other approaches, all with varying degrees of automation ranging from manual to high-throughput systems (16–20). Furthermore, point-of-care (POC) lateral flow immunochromatographic assays (LFAs) are becoming increasingly popular for their ease of use and rapid detection capabilities (21, 22). Although all serological testing methods share a common function in detecting antibodies against SARS-CoV-2, major differences exist among tests depending on the viral antigens being targeted, the subclass of antibody being detected, and the overall accuracy and reliability.

The urgency to produce serological assays has led to a recent surge In protocols, testing devices, and literature, each with varying degrees of quality and reliability. Here we review current advances in knowledge regarding the antibody response towards SARS-CoV-2 infection. We then look at current commercial and laboratory-based serological assays for SARS-CoV-2 and discuss their strengths and limitations as they relate to cross-reactivity, sensitivity, and specificity. Lastly, we investigate which epidemiological characteristics of COVID-19 may be gleaned from existing serological data, and how these can be applied to public health policy domains such as vaccination, herd immunity modeling, and other public health interventions.

Down to the Basics: Antibody Classes and Class Switching

Multiple classes of antibodies (i.e., IgM, IgA, IgG, and IgE) are involved in antibody-mediated immune responses to viral infections (Figure 1). These classes are characterized by their intrinsic biophysical properties, functions, tissue distributions, and half-lives. Together with IgD, IgM immunoglobulins are normally the first to be expressed during naïve B cell development, comprising the majority of antibodies produced between B cell activation and class switching. IgM represents approximately 10% of all antibodies in the serum (24, 25). IgM antibodies demonstrate a relatively low affinity compared to IgG due to limited affinity maturation through somatic mutations. However, IgM antibodies demonstrate high avidity for the target antigen because they form pentamers that utilize multimeric interactions with the target antigen to facilitate neutralization (25). IgM antibodies are found mostly in circulation where they can facilitate antigen opsonization (26). Recent studies have also revealed diverse roles for secretory IgM in the mucosa of the gastrointestinal and respiratory tracts (27). Human IgA immunoglobulins, which can be further subdivided into the IgA1 and IgA2 subclasses (28), generally exceed levels of IgM in serum and are significantly more present in mucosal surfaces and secretions (i.e., saliva, breast milk, etc.) where they are central to mucosal immunity. IgA immunoglobulins form dimers upon secretion, which contributes to their increased avidity. Although IgA antibodies do not fix complement effectively like IgM, IgA antibodies secreted by plasma cells into the respiratory tract play a key role in mucosal immunity *via* pathogen neutralization, a process that facilitates aggregation and prevents the initial infection of host cells, thereby conferring sterilizing immunity to a pathogen (29, 30).

IgG antibodies start appearing later in the immune response because they undergo affinity maturation through somatic mutations, resulting in high affinity for the target antigen and a heightened capacity to neutralize pathogens (31). In addition to their role in neutralizing antigen, IgG antibodies also have other critically important roles, most notably Fc-mediated effector functions such as cell activations and antibody-dependent cellular cytotoxicity (ADCC) (32–34). IgG immunoglobulins are monomeric and represent about 75% of all antibodies in serum. They are associated with lasting Immunity given their long half-life in blood and association with

differentiated memory B cells (25). IgG can also bind C1q, activating the classical complement pathway of the innate immune system (35).

IgG antibodies can be subdivided into multiple subtypes (i.e., IgG1, IgG2, IgG3, and IgG4), each with slightly different roles in humoral immunity (32). For example, IgG1, IgG3, and occasionally IgG4 (upon repeated exposure) are secreted in response to protein antigens, while IgG2 almost solely responds to polysaccharide antigens (32). Given that different pathogens elicit different ratios of IgG subtypes, these can be used as characteristic profiles for monitoring the efficacy of vaccine designs with regards to correlates of protection (36, 37). Finally, IgE antibodies predominately mediate allergic reactions and immune responses against parasitic infections and comprise less than 0.01% of all total antibodies. IgE antibodies are monomeric and demonstrate a strong affinity for FcεRI receptors expressed on numerous innate immune cells (e.g., mast cells, basophils, eosinophils), allowing for the generation of a generalized inflammatory response through innate immune system activation (38).

Current published data support that SARS-CoV-2 induces a classic viral response pattern, where IgM is the first isotype to appear, followed closely by IgA which peaks at 2-3 weeks post-symptom onset (PSO) before declining, and finally with IgG antibodies that remain detectable for several months PSO (39, 40). However, some studies have also reported the detection of virus-specific IgA responses preceding that of IgM, although the implications of this new pattern are not entirely understood (39, 41). Of particular interest, detectable levels of neutralizing antibodies against SARS-CoV-2 have been shown to start declining within three months of infection, especially among mild and asymptomatic cases (42–45). This, however, is not uncommon and resembles findings from patients infected with sCoVs (12, 46). Given the frequency of reinfections with sCoVs, this observation is likely a predictor of impermanent immunity and of heightened risk of reinfection in the short term.

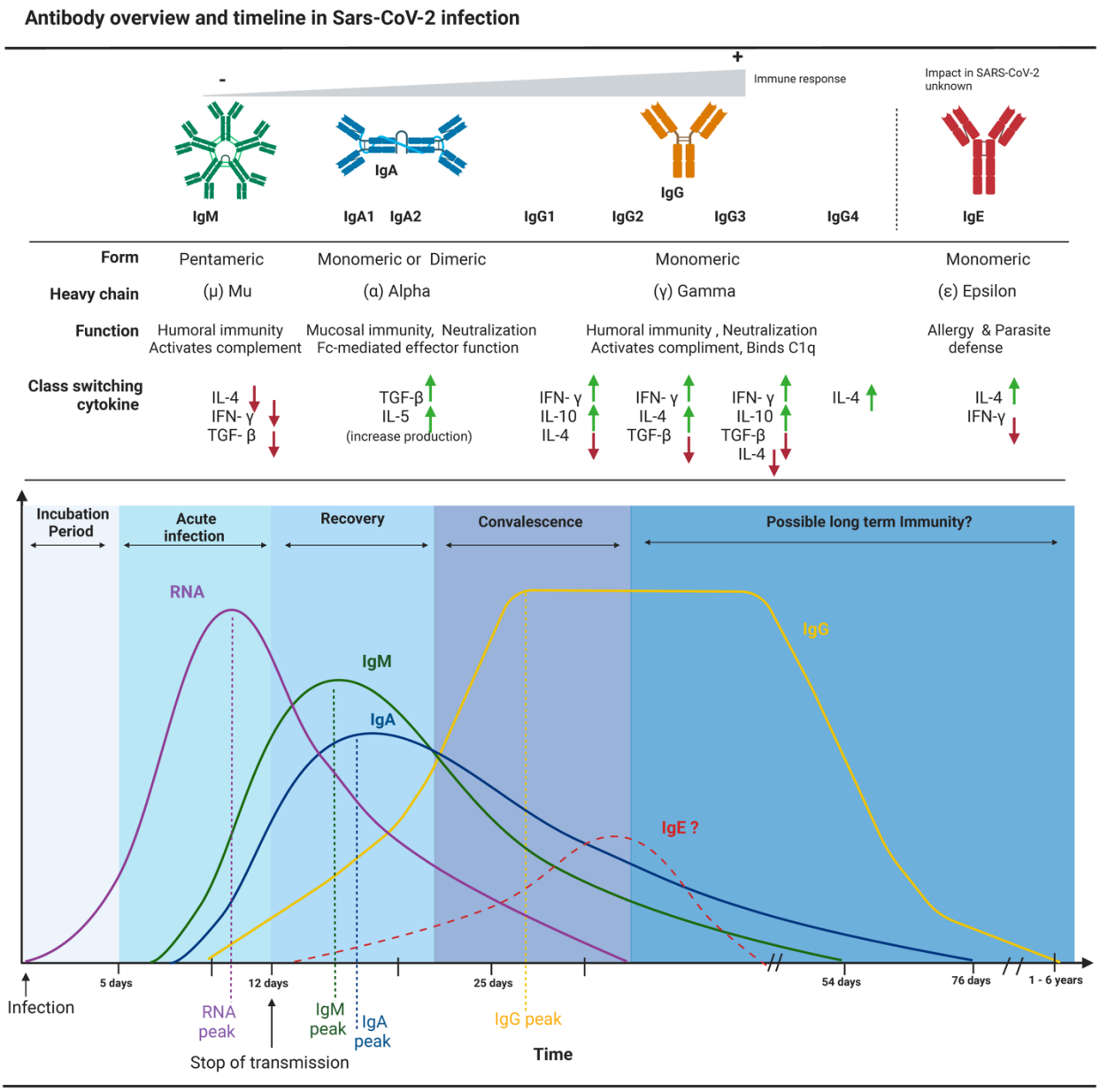


Figure 1 Overview of antibody isotype characteristics and an approximate timeline from SARS-CoV-2 infection to possible immunity. Each antibody isotype is represented with their typical form and associated heavy chain. A brief description of their main function as well as a representation of upregulated and downregulated cytokine necessary for each class switching is also included. The approximate timeline of appearance and subsequent decrease of each isotype in relation to the viral RNA is shown. The curves and values are based on recent serological studies discussed in this review. Since limited literature is available on the implication of IgE in the pathogenesis and antibody mediated immunity to SARS-CoV-2, as such the representation of the IgE timeline is purely hypothetical. Figures were generated using (23).

SARS-CoV-2 Viral Antigens

The effectiveness of an antibody response is largely dependent on the capacity of antibodies raised against native viral antigens during a natural infection, or against antigens in a vaccine, to act when exposed to the virus. These antibodies can either be present in blood, or produced *de novo* by memory B cells and plasma cells upon re-exposure to the viral antigens (47). Antibodies play a direct role in neutralizing incoming virus to prevent reinfections (i.e., sterilizing immunity), or by tagging viral antigens expressed on the surface of infected cells thereby triggering downstream Fc effector functions. In the case of CoVs, the viral antigens to which most antibodies are directed against are the viral spike (S) and nucleocapsid (N) proteins (48, 49).

The SARS-CoV-2 S protein is a trimeric transmembrane glycoprotein that is exposed on the surface of virions and mediates viral entry into host cells (Figure 2A) (50). This S protein constitutes the primary target of all current leading vaccine candidates (51). This large, exposed protein is readily targeted by neutralizing antibodies, which indirectly creates selective pressure for the emergence of evasion mutations. The propensity for S to mutate may limit its future use in serological assays and vaccines, as antibodies directed against the current variant may not bind emerging mutated epitopes, resulting in reduced vaccine efficacy while producing more false negatives in serological assays.

The S protein Is further divided Into two functional subunits, S1 and S2. S1 Is responsible for binding to the host cell surface receptor ACE2 through its receptor-binding domain (RBD) found within subunit S1-, while S2 is involved in the fusion between the viral envelope and cellular membranes upon attachment (52) (Figure 2B). Along with orchestrating viral entry into host cells, the RBD region of S1 is of specific importance as many antibodies raised against RBD have neutralizing potential. Indeed, numerous viral epitopes that that are targeted by neutralizing antibodies are located within this region (53–57).

The viral N protein Is an abundant nucleoprotein that binds the viral RNA genome and Is contained within the virion. Each N protein contains three highly conserved and distinct regions: an

N-terminal RNA-binding domain, a central Serine/Arginine-rich linker, and a C-terminal dimerization domain (58). The N protein has many functions associated with viral RNA packaging, RNA transcription, and viral replication. Since the N protein is abundantly expressed during infection, it is capable of inducing high levels of antibody production, making it a suitable target for serological assays (59–62). However, given that the N protein is not involved in viral entry and is shielded from antibodies by the viral envelope, most N protein antibodies are not likely to be neutralizing (63, 64). This was demonstrated by one study which showed that immunization with the SARS-CoV N protein induced antibodies with undetectable neutralizing activity (65).

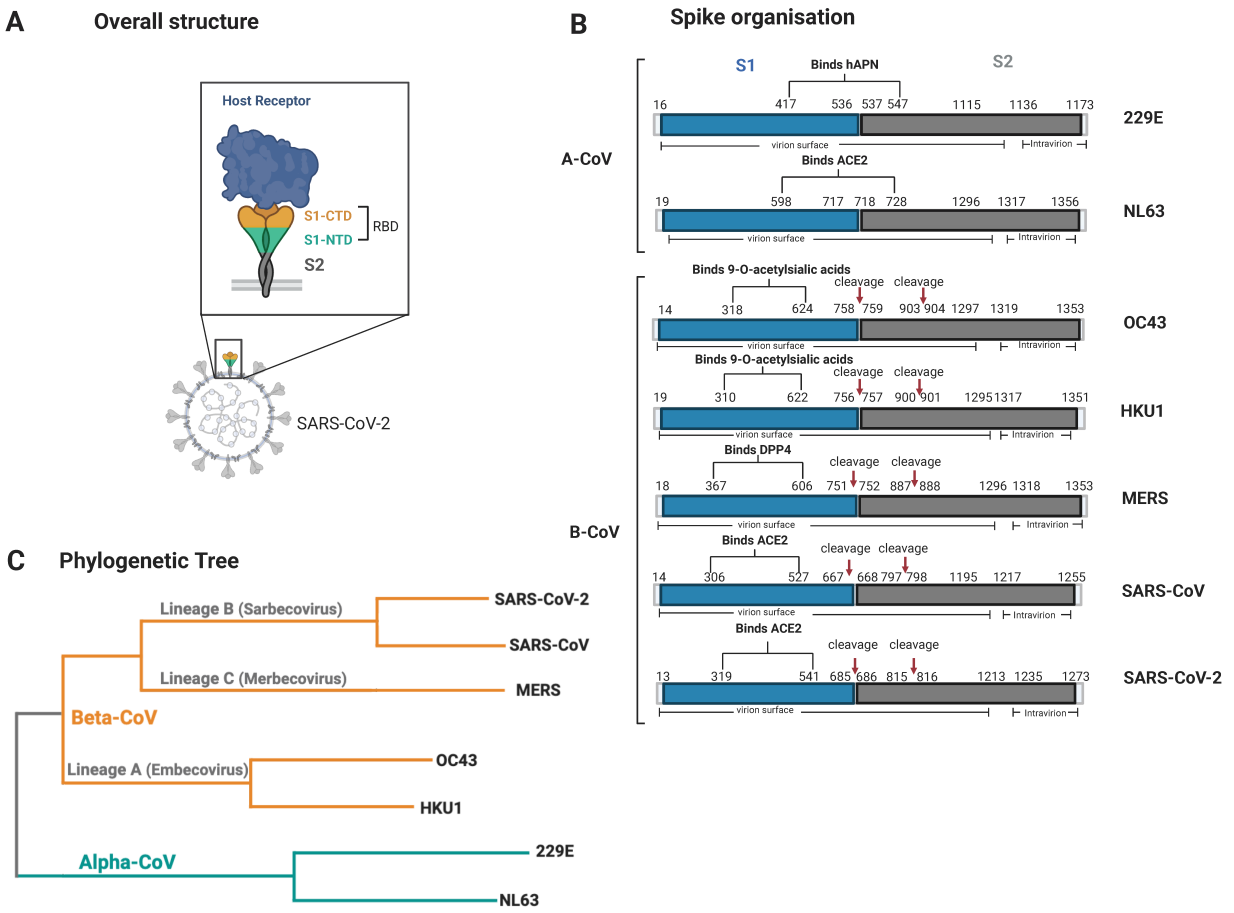


Figure 2 Structure and organization of the spike glycoprotein and phylogenetic tree of all seven human CoVs. **(A)** A cartoon structure of the Spike protein and its receptor (i.e., ACE2) is shown in relation to its localization on the virion surface. The S1 domain interacts directly with the receptor through its RBD *via* it's C-terminal domain (CTD). **(B)** Graphical representation of the various spike human CoV proteins. The RBD, S1 (blue), and S2 (gray) domain locations and all other relevant sites (cleavage sites), and other topological features are shown with their respective amino acid sequence number. The information for each spike was obtained using Uniprot with the following

accession numbers: 229E P15423, NL63 Q6Q1S2, HKU1 Q0ZME7, OC43 P36334, MERS K9N5Q8, SARS-CoV P59594, SARS-CoV-2 P0DTC2. **(C)** A phylogenetic tree based on the complete genome of all seven human CoVs was made using Clustal Omega multiple alignment tool using the reference genome sequenced from NCBI with the following accession numbers: 229E NC002645.1, NL63 NC005831.2, HKU1 NC006577.2, OC43 NC006213.1, MERS NC019843.3, SARS-CoV NC_004718.3, SARS-CoV-2 NC_045512.2. Figures were generated using (23).

Testing for SARS-CoV-2 Antibodies

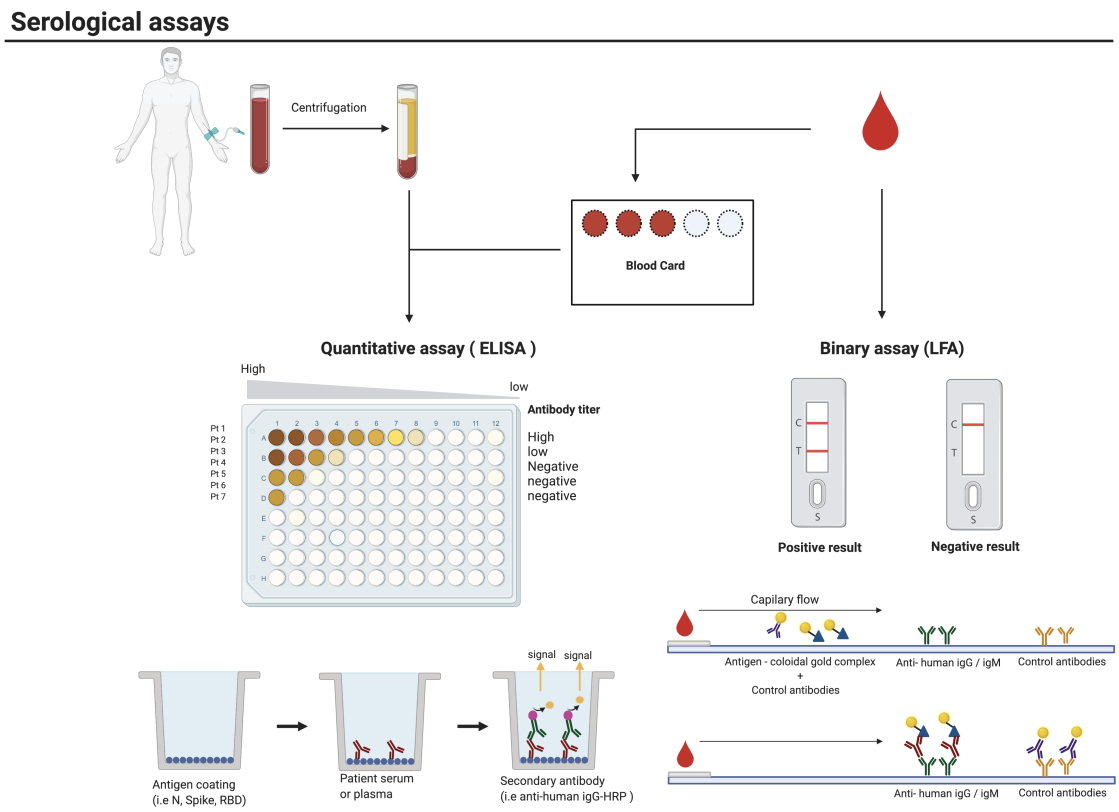
Serological tests are designed to detect the presence of antibodies against a given pathogen, in this case, SARS-CoV-2. A positive serological test result is indicative of a past exposure to one or several of the pathogen's antigenic epitopes and therefore is not an indicator of an active infection. Furthermore, if the pathogen of interest shares antigenic epitope sequences with the proteins of other microbes or even that of vaccine antigens, a test can be reported as falsely positive. During a natural Infection by SARS-CoV-2, the levels of viral RNA rapidly decrease during the second week and may become undetectable (66–68). Antibodies therefore become the primary and most accurate modality to detect a recently resolved or past infection (Figure 1). Serological tests are also critical for the detection of asymptomatic and previously undiagnosed infections in the population. This information is essential to guide public health interventions during an epidemic to mitigate the spread of a pathogen to the most vulnerable members of the population.

Serological tests can be broadly divided into two categories: Rapid Diagnostic Tests (RDTs) and non-rapid tests (Figure 3) (49). A list of clinical serological tests currently approved are presented in Table S1. RDTs are most commonly LFAs which detect the presence of antibodies against multiple SARS-CoV-2 antigens within a 30-min time window. LFAs for SARS-CoV-2 detection work through the addition of a liquid sample (e.g., blood or saliva) – potentially containing the target antibodies – to one side of the testing device. The sample then diffuses by capillary action to a conjugation pad, where viral antigens conjugated to a colorimetric detection molecule (e.g., colloidal gold) are deposited. If SARS-CoV-2 antibodies are present, they will capture and dislodge these antigens and then migrate by continued capillary flow to a nitrocellulose membrane where anti-human capture antibodies are immobilized, usually anti-IgG and anti-IgM. If anti-SARS-CoV-2 antibodies are present, the colloidal gold (or another detection agent) will accumulate on a thin strip of anti-IgG and anti-IgM to create a colored line (Figure 3) (69). LFAs

do not require multiple steps, nor the addition of any solution other than the patient sample. LFAs provide fast, qualitative, and easy-to-understand readouts that are designed for usage at home or in a POC setting without the need for equipment (70). Drawbacks of LFAs include their higher cost-per-test rate, their inability to analyze multiple samples simultaneously, their general lack of quantitative data, and importantly, a several-fold reduced sensitivity when compared to non-rapid testing methods (71, 72). Although RDTs are theoretically ideal for POC usage, recent studies have demonstrated that many newly developed RDTs for SARS-CoV-2 have failed to meet the necessary standards for sensitivity and specificity when compared to non-rapid testing (71–76). Therefore, for research purposes, LFAs are not the ideal choice.

Non-rapid serological testing methods include solid-phase immunoassays, microarrays, viral neutralizing tests, bead-based flow cytometry-based methods, and immunofluorescent microscopy, among others. These are all primarily laboratory tests that are carried out by trained personnel. Solid-phase immunoassays including ELISA, CLIA, Electrochemiluminescence Immunoassay (ECLIA), Enzyme-linked Fluorescent Assay (ELFA), and Dried Blood Spot ELISA (DBS-ELISA) are currently the most commonly used non-rapid, high-throughput methods for the detection of SARS-CoV-2 antibodies within a population (49).

Non-rapid tests generally involve the capture of primary SARS-CoV-2 antibodies within a saliva or blood sample to a solid support, like a dish or plate, coated with a SARS-CoV-2 antigen. This is followed by an initial wash step and the addition of a detection antibody, which is usually conjugated to a fluorophore or an enzyme like the horse radish peroxidase (HRP). Excess antibody is washed off and detection is performed. Colorimetric, fluorescent, and/or luminescent methods can be used as the final detection method depending on the detection antibody conjugate. Throughput can be easily scaled up using robotic liquid handlers.



	Quantitative assay (ELISA)	Binary assay (LFA)
Readout	Quantitative titer	Positive or negative
Usage	Laborotary assay	At home, clinic testing , POC
High throughput	Yes	No
Reliability	High / Moderate	Low
Cost	Moderate	Low

Figure 3 Comparison of various serological assays. **(A)** The sampling method and subsequent treatment of the blood before performing the serological assay is shown. Either a tube of blood is collected to isolate serum/plasma, or blood from a finger prick is used to fill a dried blood spot card or used directly in a LFA. Here we show the 2 main types of serological assays: on the left, a quantitative ELISA, or on the right, a binary result LFA. **(B)** The experimental procedure of each test is shown in their most simple form. Many variations are now available and are being used (see Table S1). **(C)** Comparison of the strengths and weaknesses of each method. POC, point of care; LFA, lateral flow assay. Figures were generated using (23).

Unlike LFAs, non-rapid tests can also provide valuable information on the quantity of each antibody within the samples (77). Non-rapid methods are generally much more sensitive than RDTs. Low-level antibody detection is especially important in the first 7 to 21 days of SARS-CoV-2 infection, when IgG levels are still rising, as well as >2 weeks post-infection when IgM

antibodies begin to diminish (Figure 1) (67). Although most non-rapid tests currently use venous serum or plasma, or saliva samples in a liquid phase, DBS-ELISAs provide a practical alternative to venous samples by using only a few microliters of blood taken by pinprick and deposited onto an absorbent paper (Figure 3). Antibodies can then be eluted from a circular punch taken from the paper using a small amount of buffer. The ELISA is then performed in a standard fashion. This simple and convenient approach to collecting blood eliminates the need for a healthcare provider to perform venipuncture and provides an opportunity to conduct large-scale population-level seroprevalence studies using high throughput liquid handlers to perform DBS-ELISAs (78).

Neutralization Assays and Their Importance

Although serological tests can determine prior immune exposure to SARS-CoV-2, neutralization assays provide critical knowledge on whether the detected antibodies are capable of neutralizing the virus and providing likely protection upon subsequent exposure. Currently, the most reliable neutralization assays involve live authentic SARS-CoV-2 viruses produced in cell culture and therefore require all procedures to be carried out in a Biosafety Level 3 (BSL3) facility (79). A current challenge is to develop a reliable neutralization assay that can be carried out in a standard BSL2 laboratory, at home, or in the clinic. To circumvent biosafety containment requirements, researchers are currently developing lab-based assays using viruses that consist of a less-harmful or non-infectious virus, such as murine leukemia virus (MLV) or vesicular stomatitis virus (VSV), pseudotyped with the SARS-CoV-2 S glycoprotein (80, 81). Other options include assays that utilize purified ACE2 to determine the effect of neutralizing antibodies on the ACE2-Spike interaction without the requirement of live cells or viruses. One example of a neutralization assay is the cPass SARS-CoV-2 Neutralization Antibody Detection Kit from GenScript Biotech. This test kit is advertised to test for pan-Ig neutralizing antibodies using the SARS-CoV-2 RBD as the viral antigen for antibody capture (82). Other promising surrogate neutralization assays have been proposed which utilize an ELISA-based competition binding assay against ACE2 (83, 84). Antibodies against RBD have been shown to be the primary source of neutralizing antibodies against the virus (53, 85–88). However, it should be noted that not all antibodies that bind RBD demonstrate neutralization potential, and that anti-RBD antibodies capable of neutralization may

only be present at very low concentrations in some individuals post-infection (89, 90). Furthermore, RBD is not the only viral antigen that is a target for antibody-mediated neutralization; additional non-RBD epitopes elsewhere on the S protein have also been shown to neutralize the virus when targeted by antibodies (57, 91, 92). One caveat of the aforementioned neutralization assays is that they provide limited information on possible Fc-dependent effector functions, which likely also play an important role in protecting against SARS-CoV-2 (93). Therefore, current single-antigen neutralization assays only detect a subset of the total pool of neutralizing antibodies.

Of note, several commercial serology tests use the N antigen for antibody capture (Table S1). Given the high abundance of anti-N antibodies, targeting this viral antigen has the potential to increase test sensitivity (94). However, N proteins are located on the interior surface of intact viruses, and thus remain inaccessible to circulating antibodies. Therefore, tests that use N are unlikely to identify neutralizing antibodies that provide sterilizing immunity upon infection. Nevertheless, effector functions of anti-N antibodies could still provide protection (64). Currently, the RBD and S proteins are the most reliable antigens for measuring the abundance of neutralizing antibodies.

Sensitivity and Specificity of Serological Assays for SARS-CoV-2

The quality and usefulness of a serological test is primarily evaluated by its degree of sensitivity and specificity (95). Sensitivity describes the ability of a serological test to provide a positive result from samples that contain antibodies against SARS-CoV-2 (“true positives”). Thus, a highly sensitive test would have a very low frequency of false negatives. Meanwhile, specificity describes the ability of a test to provide a negative result when a sample does not contain SARS-CoV-2 antibodies. Thus, a high specificity SARS-CoV-2 serological assay would have no or few false positives, including those resulting from cross-reactivity to any of the other six human CoVs (96, 97). The sensitivity and specificity of an assay are influenced by the cut-off point at which a test result is deemed positive. A receiver operating characteristic (ROC) curve is a useful graphical tool to visualize the relationship and trade-off between the sensitivity and specificity of an assay (98), but its details are beyond the scope of this review.

Serological tests that target IgM, which naturally has a lower affinity for the viral antigen than IgG, will be at a higher risk of producing false positives, and therefore should require a higher specificity threshold. Testing thresholds for specificity and sensitivity are arbitrary values established experimentally and differ between serological tests and methods. SARS-CoV-2 thresholds are primarily determined based on test results of negative control samples collected prior to the pandemic, as well as on positive control samples that have been confirmed by a certified clinical RT-PCR diagnostic test (99). Currently, there are no international reference standards for reporting test sensitivity and specificity, making it very challenging to compare the different serological tests and assays without carrying out a direct experimental comparison. Recent studies have sought to compare multiple testing kits with a small group of common samples (100–102). While this represents progress, what is ultimately required is a well-characterized set of standard sera that could be tested against any approved serology testing kit, allowing for the sensitivity and specificity of these kits to be compared (103). Other variables that require standardization for serological testing and kit comparisons include the length of time PSO for samples to be collected from patients, since the sensitivity and specificity of commercial tests can differ depending on the time at which the sample is collected (104), as well as the method by which samples are sometimes inactivated for lab safety (97, 105).

Sensitivity and specificity thresholds are also important for epidemiological considerations unique to certain situations and environments. These thresholds can be altered to allow for greater sensitivity of testing at the expense of specificity, or the opposite, whereby specificity is favored at the expense of sensitivity. For example, in a region with high SARS-CoV-2 seroprevalence, sensitivity may be prioritized over specificity to ensure the majority of positive cases are identified. The opposite is also true in low-prevalence regions (16). If the prevalence in a given region is very rare, then higher specificity and relatively lower sensitivity would be favored so that fewer patients would have false-positive results while still detecting the majority of true positives. It is essential to have the correct balance between sensitivity and specificity, as the epidemiological implications of disproportionate false negatives or false positives can be profound. A test with too many false positives will keep people isolated for longer than necessary, creating otherwise avoidable social and economic strains. A test with too many false negatives will result in the underestimation of disease prevalence, which may lead to a premature easing of disease containment policies and

resurgent waves of infection as misidentified patients unknowingly continue to transmit the disease (16).

Dynamics of the Antibody-Mediated Immune Response to SARS-CoV-2

Understanding the temporal profile by which circulating antibody classes are produced following SARS-CoV-2 infection is essential for the interpretation and clinical application of serological test results. During a viral infection, plasma B lymphocytes of the adaptive immune system produce different classes of antibodies in response to temporally regulated cytokine expression in a process called class switching or class switch recombination (CSR) (106). A given infecting pathogen type normally induces a characteristic cytokine profile that is responsible for triggering CSR for the production of the various isotypes and subtypes that are optimally suited to neutralize that type of microbe. Individuals suffering from severe COVID-19 are known to exhibit a dysregulation of pro-inflammatory cytokine release, also known as a cytokine storm (107–110). How this large release in cytokines alters the humoral response compared to asymptomatic, mild or moderate COVID-19 cases that do not exhibit this same cytokine storm is not yet clear.

While it is expected that IgM immunoglobulins are the first class detected following infection by SARS-CoV-2, as supported by a number of studies (37, 39, 40, 111), others have paradoxically demonstrated IgG responses that precede the IgM response (38, 112–115). This surprising discrepancy is likely related to cross-reactivity with pre-existing immunity to sCoVs (40, 111, 116–118). Nevertheless, the largest body of evidence suggests that nearly all SARS-CoV-2 infected individuals begin to produce IgM, IgA, and then IgG by 1 to 2 weeks PSO (Figure 1) (39, 90, 114, 119, 120). In fact, IgM antibodies against the viral N protein have been detected as early as 1 to 7 days PSO in 85% of individuals (39). However, these figures vary considerably depending on the type of serological assay and target antigen used. For example, *Long et al.* detected IgM antibodies against N protein in only 12% to 40% of cases during this same time period (i.e., 1–7 days) (121). The majority of patients appeared to have seroconverted by day 14 PSO, with approximately 94% of infected individuals having detectable levels of IgM against the RBD of the SARS-CoV-2 S protein, and 88% against the N protein (114, 122). IgM antibodies decline rapidly at approximately 20 days PSO, becoming undetectable at 60 days PSO on average

(Figure 1) (123, 124). The impermanence of the IgM response suggests that the diagnostic role for IgM serology is most relevant in the detection of current and recent infections, within the first 1 to 2 weeks PSO, at which point its sensitivity for the diagnostic of an active infection may actually exceed that of PCR (39, 125, 126).

IgG immunoglobulins broadly have the most significant implications with respect to serological testing and antibody responses, given its high affinity for the antigen, capacity for viral neutralization, ability to activate complement, and predominant role in long-term immunity following infection or vaccination. Indeed, serological studies on other human CoVs including SARS-CoV and MERS have found the IgG antibody class to yield assays with greater specificity compared to IgM, to be significantly longer-lasting in comparison to IgM and IgA (127, 128), and to have strong links to neutralization and patient outcomes (114, 122). During acute SARS-CoV-2 infection, class switching from IgM to IgG occurs relatively quickly, with a median time to IgG detection ranging from as early as 7 days (120, 121) to approximately 14 days (39, 125, 129). IgG production also peaks later and is much slower to decrease than IgM (124, 130). The duration and intensity of the reported IgG antibody response for SARS-CoV-2 varies according to several study parameters that include disease severity and outcome, and antigens used in the serology assays. One study demonstrated an important reduction in IgG over 8 weeks in both symptomatic and asymptomatic cases, with many patients becoming seronegative during the study period (40% asymptomatic, 12.9% symptomatic) (121). Such observations are also supported by a number of additional studies that also measured a decline of IgG antibodies after several weeks PSO (44, 131). However, most groups have demonstrated that IgG levels against SARS-CoV-2 remained relatively stable within a 3 to 5 month observation period PSO (43, 124, 130–135).

Interestingly, among individuals infected by SARS-CoV-2, detectable antibody subtypes included RBD-specific IgG1 & IgG3, but rarely IgG2 or IgG4 (136). If a consistent subtype ratio is reliably established, this could help in identifying true seropositive individuals (convalescent from SARS-CoV-2) as opposed to false-positives with cross-reactive antibodies (convalescent from other sCoVs). Similar to IgM, IgA antibodies are produced shortly after PSO, with a median time to detection of 1 to 2 weeks PSO (39, 40, 67, 128). However, while IgM peaks at approximately 10 to 12 days, IgA levels appear to be relatively more persistent, peaking at approximately 20 to 30

days PSO (39, 123, 124, 133). To date, there is no serological evidence for the induction of IgE production in patients with COVID-19.

Duration of SARS-CoV-2 Neutralizing Antibodies

Nearly all individuals who become infected with SARS-CoV-2 develop antibodies and neutralizing antibodies following infection, demonstrating a successful adaptive antibody-mediated immune response (43, 45, 87, 88, 110, 121, 123, 124, 130, 134, 137). This is consistent with non-human primate (NHP) studies where exposure to the live virus provided protection against reinfection without clinical illness, with corresponding neutralizing antibody responses (138, 139). Therefore, regardless of the discrepancies between studies regarding persistence or decline of total antibodies, it is imperative to note that persistence of IgG antibodies does not necessarily imply persistence of neutralizing antibodies during this same period. In fact, most studies report various intensities of decline in neutralizing antibodies after three months PSO, with disease severity being a factor strongly correlating with the decay rate of neutralization (42–44, 90, 121, 124, 140).

In contrast, data from some studies have indicated that neutralizing antibody titers remain stable ranging from 75 days to 6 months PSO in COVID-19 convalescent individuals with a broad spectrum of disease severity (130, 134, 141, 142). In particular, a large cohort study by Wajnberg et al. analyzed humoral responses in 30,032 antibody-positive individuals in New York City, and demonstrated relatively stable anti-S IgG antibody titers over five months, with these titers correlating with virus neutralization (130). Similar findings were demonstrated in a convalescent cohort study in China over a six month follow-up period with anti-S and anti-N IgG antibodies detectable in 70% of patients, with associated stability in neutralization titers, although these results are yet to be peer-reviewed (141).

One factor that could influence the persistence of neutralizing antibodies within specific cohorts is a high prevalence of the virus in a defined geographical region or in a specific subpopulation of individuals such as frontline healthcare workers. Regular re-exposure to the virus may help sustain higher antibody and neutralizing antibody levels. A second factor may be the persistence of

antigens in tissues or as immune complexes on follicular dendritic cells. In fact, new evidence suggests that memory B cell responses continue to evolve in recovered individuals for at least six months after infection (143). During this time, somatic mutations accumulate to produce neutralizing antibodies with increased potency. This suggests that regardless of whether neutralizing antibodies wane over time, re-exposure to the virus is likely to stimulate memory B cells to mount a rapid and effective humoral response.

Taken together, while the specific conditions that influence the total duration of SARS-CoV-2 humoral immunity remain to be more precisely defined, decreasing antibody titers do not necessarily imply waning or defective immunity. In fact, antibody titers are expected to decrease following the resolution of an acute infection as a natural consequence of the depletion of short-lived plasma cells when immediate and sustained immune responses are no longer necessary (144, 145). Furthermore, the half-life of IgG in serum is about 26 days (146). Without continuous antibody output from plasma cells, antigen-specific antibodies will naturally decline. As such, while more severe COVID-19 symptoms may elicit longer protection for convalescent individuals, it Is plausible that milder symptoms may provide much shorter windows of sterilizing Immunity. However, it is established knowledge that adaptive immune responses rely on immunological memory from both B cells and T cells to not only prevent reinfections but also diminish disease severity; this is also the basis of vaccination.

Antibody-Dependent Enhancement (ADE)

Evidence demonstrating a positive association between high antibody titers and increased clinical severity of COVID-19 has raised the possibility that antibody-dependent enhancement (ADE) could, in some instances, contribute to an excessive immune response that exacerbates SARS-CoV-2 pathogenesis (123, 125, 147–149). ADE is a process in which antibodies bind to viruses to form virus-antibody complexes which potentiates and facilitates host cell entry *via* cell surface Fc receptors, causing infection of Fc-expressing cells such as B cells, dendritic cells, macrophages, and monocytes. Cellular Fc receptors bind to the constant region of antibodies that define the isotype (e.g., Fcγ receptors bind IgG). ADE has been shown to cause increased pathogenicity of some viruses such as Dengue virus, Ebola virus, and Zika virus (150–152). ADE has also been

observed in certain human CoV challenges in immunized animals. These include MERS as well as SARS-CoV, where anti-S protein antibodies have potentiated viral entry *via* an ACE2 receptor-dependent mechanism, or independently of ACE2 by facilitating virus uptake *via* FcγRII (153–157). ADE has been observed to induce pro-inflammatory cytokine release from Fc-expressing immune cells in mice and NHPs (157–159). While there is no direct evidence yet to support this hypothesis in the context of COVID-19, the biphasic course of infection that has been described, in which severe hypoxia and respiratory distress typically manifest 7 to 14 days after onset of fever and viremia, coincides with the chronology of seroconversion and IgG class switching (160). Fortunately, animal studies thus far in immunized NHPs re-challenged with SARS-CoV-2 have not shown signs of ADE (149). However, these studies were limited to small numbers of animals and more studies are needed to understand if these animal models can successfully be used to understand ADE in humans. Furthermore, there have been two large-cohort studies published to date on the use of convalescent plasma in human patients, both deeming the incidence of serious adverse events to be low (161, 162). Cumulatively, this would suggest that ADE is unlikely to be a major cause of pathogenesis in SARS-CoV-2 infection in humans. Nevertheless, ADE should be investigated further as it could impact the efficacy and safety of serum therapy, as well as vaccination programs. In particular, if future vaccine candidates are to require booster shots because of impermanent immunity, ADE must be considered as repeated doses generate an increase in antibodies that could potentially contribute to ADE upon virus exposure.

Cross-Reactivity of SARS-CoV-2 Antibodies to Seasonal CoVs

A significant challenge in developing a specific SARS-CoV-2 serological assay is the potential for cross-reactivity of SARS-CoV-2 capture antigens with antibodies against other human CoVs (163). SARS-CoV-2 shares amino acid sequences and antigenic T and B cell epitopes with the highly prevalent sCoVs that cause the common cold including 229E, OC43, NL63, and HKU1, and also with the now rare MERS and extinct SARS-CoV that both cause severe and fatal respiratory disease (Figure 2) (62, 164–168). A recent prevalence survey of the sCoVs using RT-PCR revealed that OC43 is the most prevalent sCoV followed by NL63, HKU1, and finally 229E

(169). While infection with the sCoVs induce antibody responses as would be expected, these wane over time and render the hosts susceptible to reinfection. An impressive study of the occurrence of reinfection for all four sCoVs over more than a 35 year span revealed that reinfections with the same sCoV occurred most frequently after 12 months (12). While sterilizing immunity to sCoVs is relatively short-lived, here we will review current knowledge about cross-reactivity of these antibodies to SARS-CoV-2 antigens.

Given that the prevalence of antibodies against all four sCoVs may be as high as 90%, as demonstrated in one sample of American adults (170), antigens used in SARS-CoV-2 serological assays may in some instances be detected by these naturally circulating and highly prevalent antibodies, thereby limiting test specificity and creating the potential for false-positive results. While the greatest probability for cross-reactivity exists between antibodies directed against SARS-CoV-2, SARS-CoV, and MERS, the latter two are exceedingly rare given the low case numbers of these infections (171, 172). Therefore, issues related to cross-reactivity between SARS-CoV-2 and the circulating sCoVs are of foremost concern.

Several serological studies have demonstrated cross-reactivity of SARS-CoV-2 S protein with SARS-CoV, MERS, and sCoVs (43, 53, 116, 118, 165, 173–175). The spike S2 domain is believed to be primarily responsible for this cross-recognition given its slightly higher level of sequence similarity than the other S domains (118). When comparing the amino acid sequence by both percent identity and percent similarity of all human CoVs, the S2 domain has the highest identity and similarity compared to full S, S1, RBD, or N domains (Tables 1 and 2) (173). Cross-reactivity between SARS-CoV-2 antibodies and the S2 domain of the SARS-CoV S protein has also been shown (176). Some studies examined the specificity of ELISAs and demonstrated cross-reactivity of sCoVs, MERS, and SARS-CoV sera only with the full SARS-CoV-2 S protein, and not with the S1 antigen (53, 173), which is in agreement with several other groups that failed to measure cross-reactivity of sCoV antibodies with SARS-CoV-2 RBD (62, 134, 176). Importantly, the lack of cross-reactivity demonstrated between the S1 subdomain of SARS-CoV-2 and sCoVs antibodies may point to its potential application as a target antigen for highly specific serological assays.

Table 1 Percent identity of amino acid sequences between human CoVs and SARS-CoV-2.

	Alphacoronavirus		Betacoronavirus			
	229E	NL63	OC43	HKU1	MERS	SARS
Full spike	31.4	29.8	30.2	29.5	34.8	76.0
S1 Domain	31.2	25.0	23.8	23.7	28.3	60.3
S2 Domain	35.0	33.1	42.3	41.2	43.6	90.0
RBD	24.1	27.8	23.8	29.4	21.7	73.1
Nucleoprotein	28.4	32.6	34.6	33.9	49.7	90.5

Alignments between amino acid sequences of all 7 human coronavirus were done for the Full spike, spike domains S1, S2, and RBD and the nucleoprotein (N).

Table 2 Percent similarity of amino acid sequences between human CoVs and SARS-CoV-2.

	Alphacoronavirus		Betacoronavirus			
	229E	NL63	OC43	HKU1	MERS	SARS
Full spike	61.8	60.0	57.9	58.0	65.7	91.5
S1 Domain	62.5	51.4	51.7	55.6	61.9	84.2
S2 Domain	66.5	66.3	72.7	72.7	73.9	98.1
RBD	59.3	59.3	54.7	67.6	56.0	88.9
Nucleoprotein	57.9	65.1	62.1	65.1	75.4	97.2

Alignments between amino acid sequences of all 7 human coronavirus were done for the Full spike, spike domains S1, S2, and RBD and the nucleoprotein (N).

There may also be cross-reactivity issues that affect the specificity of tests that use the N protein. The N protein of SARS-CoV-2 shows 97% similarity to that of SARS-CoV, 75% to MERS, and 58% to 65% similarity to the sCoVs (Table 2). One previous study analyzed the cross-reactivity of the N protein between the various CoV groups (177). They found that antibodies against the seasonal alphacoronaviruses 229E and NL63 demonstrated cross-reactivity towards each other but did not cross-react with betacoronavirus antigens, which would include SARS-CoV-2. Meanwhile, betacoronavirus (NL63 and OC43) sera primarily cross-reacted with N proteins from other betacoronaviruses, with the exception of SARS-CoV (177). While the SARS-CoV-2 N antigen was not included in the study, this suggests that it is likely that other betacoronaviruses would similarly cross-react with SARS-CoV-2. Indeed, *Ng et al.* also showed that sCoV-reactive serum could bind to the SARS-CoV-2 N protein in their flow cytometry-based detection assay (20). Therefore, there is also the potential for cross-reactivity between pre-existing antibodies towards sCoVs and the N antigen of SARS-CoV-2. While the high abundance of the N protein otherwise makes it a promising candidate for diagnostic serological assays, the potential for poor specificity due to cross-reactivity with prevalent sCoVs may be a critical limitation to its use. Indeed, in a

pre-print manuscript, Anderson *et al.* demonstrated in a cohort of 207 pre-pandemic samples that 5% reacted to the SARS-CoV-2 S proteins, 2% against the RBD, and 19% against N (116). A closer analysis of these samples revealed that most had antibodies against OC43, 229E, and NL63 but these were non-neutralizing.

Protection From SARS-CoV-2 Infections by sCoVs Antibodies

While there is strong evidence that antibodies raised against sCoVs antigens can bind to SARS-CoV-2 proteins and interfere with serological assays, there is conflicting information concerning the protective role of these sCoV antibodies. While most neutralizing antibodies target the RBD to disrupt binding to the host-expressed ACE2 receptor (61, 178, 179), cross-reactive sCoVs primarily target the S2 domain of the SARS-CoV-2 spike protein (118, 167). Furthermore, non-RBD S1 as well as S2-binding neutralizing antibodies have been identified for both SARS-CoV and SARS-CoV-2 (92, 165, 180–182). As of this moment, two studies have shown evidence that the presence of sCoV antibodies is associated with less severe COVID-19 symptoms (183, 184), while two more have shown some neutralizing activity in pre-pandemic samples (118, 165).

More specifically, Ng *et al.* showed that healthy individuals with recent sCoV exposure had antibodies capable of limiting SARS-CoV-2 entry into host cells in an experimental system (118). It has been proposed that the protection conferred by sCoV antibodies may also contribute to the age disparity in COVID-19 susceptibility (118, 185). Seroprevalence of sCoVs varies considerably between age groups, with especially high prevalence in very young children (<1 year of age), an observation that aligns well with the fewer number of severe cases of COVID-19 in children (186, 187). The high prevalence of protective sCoV antibodies in younger individuals provides a plausible explanation for why young adults under the age of 20 are estimated to be half as susceptible to COVID-19 as those above the age of 20, and why children comprise only 21% of symptomatic cases, compared to upwards of 69% for those above 70 years of age (188). This hypothesis, however, remains to be tested in a well-designed randomized clinical trial.

However, mounting evidence support that few to no cross-neutralizing sCoV antibodies do in fact exist (116, 117). Nevertheless, one must be cognizant that most neutralizing assays utilize spike-pseudotyped viruses or surrogate (virus-free) assays with purified antigen. It is possible that such experimental systems fail to measure the overall protection of sCoV pre-exposure as seen in a living person. Indeed, sCoV-induced cross-reactive T cell responses and Fc effector functions of antibodies may also play a role in COVID-19 severity and outcomes (62, 164, 166, 168).

Immunological Back-Boosting by sCoV Antibodies and the Original Antigenic Sin

As described above, cross-reactivity of sCoVs antibodies to SARS-CoV-2 antigens has now been well characterized. It is also well established that most people have had prior exposure and produce antibodies to several sCoVs. While there is some evidence that sCoV antibodies can neutralize SARS-CoV-2, so far neutralization appears to be weak if at all detectable. Given that most cross-reactive antibodies bind the S2 region of the SARS-CoV-2 spike and are non-neutralizing, a very interesting an important question arises: can this cross-recognition of antigens give rise to immunological imprinting?

Immunological imprinting, also called original antigenic sin, relates to the concept of mounting an antibody response to a new pathogen using memory cells recognizing past antigens over stimulating a *de novo* antibody response (189). Such responses have been shown for influenza and dengue virus and are associated with poor virus neutralization and can have profound consequences on vaccine efficacy (190–193). For SARS-CoV-2 infections, a number of studies have now reported back-boosting of non-neutralizing sCoV antibody production (116, 118, 167, 194, 195). These antibodies appear to be most prominently targeted against conserved epitopes in OC43 and HKU1, both betacoronaviruses (194, 195). Interestingly, none of these studies presented evidence that a sCoV antibody boost was associated with either protection against SARS-CoV-2 infection or COVID-19 severity. In fact, a negative correlation was observed in some studies, providing additional support to a disfavorable consequence of immunological imprinting (194, 195). Given that most of the leading SARS-CoV-2 vaccine candidates being currently developed use the full (S1-S2) spike protein as the primary viral antigen, special

consideration needs to be given as to whether inclusion of the S2 domain will be a factor that that impedes vaccine efficacy.

Epidemiological Implications of Serology Testing for SARS-CoV-2

As the COVID-19 pandemic continues around the world, with second and third waves of infections already taking form, it is becoming increasingly important to monitor serological data at the population level. Effective and ethical response strategies to the COVID-19 pandemic can only be formulated once it is accurately determined if neutralizing antibodies are present, how effective those antibodies are at preventing disease and viral spread, and how long that immunity will last. Ongoing epidemiological considerations include the concepts of herd immunity, shield immunity, and immunity passports. However, these ideas remain largely based on the assumption that a humoral response implies lasting immunity, making their implementation for SARS-CoV-2 premature on an ethical basis. It must be reiterated that further functional serological studies must be performed to measure long-term effectiveness of humoral responses.

One of the most widely discussed epidemiological concepts surrounding COVID-19 is the possibility of achieving herd immunity. Herd immunity is a population-level phenomenon where the risk of infection for susceptible and disproportionately vulnerable individuals is mitigated by the presence and proximity of immune individuals. As more people develop immunity, the risk to susceptible population decreases, resulting in fewer opportunities for pathogen transmission (196). Herd immunity is particularly important for protecting those who cannot be effectively vaccinated, such as the very young and the immunocompromised (197). For COVID-19, where the majority of deaths and severe symptoms are observed in patients 60 and older (198), herd immunity will also play an important role in protecting the vulnerable elderly population.

In order to achieve protection, a minimum percentage of the population, known as the herd immunity threshold (HIT), must develop immunity. In its most basic form, the HIT is estimated with the formula $(R_0 – 1)/R_0$, where R_0 (the basic reproduction number for an infectious disease) represents the number of secondary cases generated by each infected individual in a fully

susceptible population (199). Early models investigating the localized outbreaks in China estimated R_0 for COVID-19 to range from 1.4 to 6.49, with a mean value of 3.28 (threshold = 69.5%) (200). While estimates continue to vary, there is a general consensus that the average value of R_0 for COVID-19 is approximately between 2 and 3, implying that a minimum of 50% to 67% of a population must achieve immune resistance before herd immunity can take effect (201).

Herd immunity can either be achieved through natural acquisition (i.e., natural herd immunity) or by controlled vaccination programs (202). Natural herd immunity assumes that convalescence imparts sterilizing immunity, and therefore widespread infection is necessary for widespread immunity. In the context of COVID-19, while natural herd immunity is theoretically possible, its pursuit is difficult to ethically justify given the high mortality and lasting morbidity caused by the virus, and it is also difficult to implement practically. Recent seroprevalence data shows that no country is even close to achieving herd immunity through natural acquisition (Table 3). In Sweden, where no official lockdown measures were enforced throughout the pandemic, as of May 2020, there was only a seroprevalence of 15% in Stockholm (compared to their predicted seroprevalence of 40%) (214). Furthermore, in several COVID-19 “hotspots” like Iran and New York City, where large numbers of cases were observed in short timespans, seroprevalence still never exceeded 25%. In the vast majority of other cities and countries, seroprevalence is usually much lower than 10% (Table 3). Most importantly, given the high risk of long-term morbidity due to tissue damage caused by COVID-19, naturally acquired herd immunity cannot be ethically pursued or encouraged (215–218). Therefore, the pursuit of natural herd immunity against SARS-CoV-2 is not justifiable in any form or manner and will be associated with very high immediate and long-term healthcare costs due to chronic disease.

Table 3 Seroprevalence of antibodies against SARS-CoV-2 in various countries and cities.

Location	Seroprevalence (%)[1]	N[2]	Reference
Iran	22.89	5877	(203)
Switzerland	7.58	16758	(203)
Geneva	10.8	775	(204)
United Kingdom	6.94	182072	(203)
London	13	9547	(205)
Sweden	5.6	1200	(206)
Stockholm	11.5	>100[3]	
USA	4.89	4.89	(203)
New York City	19.5	1581	(207)
Spain	4.66	1018251	(203)
Madrid	11.3	3186	(208)
France	2.78	5534	(203)
Netherlands	2.77	36791	(203)
Brazil	1.29	157360	(203)
Canada	1.06	50269	(203)
Montreal	3.05	7691	(209)
Toronto	1.5	1837	(210)
Vancouver	0.55	885	(211)
Italy	1.04	904	(203)
Milan	5.2	789	(212)
China	0.8	10449	(203)
Wuhan	2.29	17794	(213)
Iceland	0.3	18609	(135)
Reykjavik	0.4	4843	

A sampling of published SARS-CoV-2 seroprevalence studies are listed below to demonstrate the wide range of values observed around the world and relatively low worldwide seropositivity.[1]Reported seroprevalences reflect the most recent data available, although some values are from as early as April 2020.[2]Sample sizes for data from SeroTracker (203) are summations of the "N" column values for all relevant studies included at the time of publication;[3]The exact sample size was not reported, simply that it was greater than 100.

A safer, more effective, and ethically sound alternative to acquiring natural herd Immunity Is to deploy controlled vaccination programs. Rigorously tested and formally approved vaccines offer a safe and effective method to quickly increase a population's immunity to a harmful pathogen (219). Furthermore, vaccines are designed to elicit a neutralizing antibody response without the severe pathogenesis associated with the corresponding disease, in this case, COVID-19. Therefore, while it may take several more months for a safe and effective SARS-CoV-2 vaccine to be developed, tested and deployed, it is widely agreed upon that vaccine-acquired herd immunity is faster, safer, cheaper, and more effective than natural herd immunity. However, cautious optimism is warranted over vaccines. Based on knowledge acquired from SARS-CoV convalescent individuals, long-term protective immunity may last for only a few months (6, 9). With waning humoral immunity over time against a highly prevalent and infectious virus, maintaining herd immunity at the population level will almost certainly require booster shots and updated vaccines to maintain immunity against reinfections by SARS-CoV-2 and its inevitable genetic variants that are poised to emerge.

Conclusions

Significant progress has been made with respect to understanding the antibody-mediated immune response to SARS-CoV-2 infections. The applications and utility of serological assays are manifold, spanning from the development of screening modalities for epidemiological monitoring and drafting effective public health policy, to the creation of vaccines, and finally to the diagnosis of past infections.

However, the appropriate utilization of serological data requires an understanding of its limitations and ensuring these limitations are accounted for in the current and future pandemic response. For example, it remains unclear whether differences exist between the effectiveness and duration of immunity procured by a natural SARS-CoV-2 infection or vaccine-mediated immunity. Furthermore, existing serological testing approaches are widely varied in their sensitivity, specificity, and practicality, and require an adept understanding of the characteristics of each test in order to determine which should be suitably used in which context. Finally, studying the characteristics of the main SARS-CoV-2 antigens has revealed how some may be better suited for either vaccine development versus serological testing. However, cross-reactivity to sCoVs, the risk of ADE, and emergence of mutations will have profound implications on how these antigens should be employed in vaccination or screening technologies.

As the COVID-19 pandemic continues to impart substantial human suffering and economic losses throughout the world, various governments and stakeholders are experiencing increasing urgency and pressure to re-open commercial and social activities. Nevertheless, folding under this pressure has the risk of driving pre-emptive action based on inconclusive evidence, as large-scale policy mistakes such as encouraging natural herd immunity, the implementation of unstandardized serological assays, or the distribution of unproven immunity passports may reverse progress and incur unacceptable human and financial costs. Instead, this motivation to resolve the pandemic should prompt the thoughtful application of existing research, as well as support initiatives that seek to address the remaining evidence gaps within epidemiology and questions of long-term immunity to COVID-19. Such a grounded approach will be required if we are to create safe and

effective solutions for the rapid diagnosis and prevention of COVID-19 and, ultimately, return to our daily activities without having to wear a mask.

Author Contributions

YG and MG equally carried out the literature review, prepared the figures and tables, and the drafting of the manuscript. GL and MD contributed to the drafting of the manuscript. M-AL contributed to the literature review and drafting of the manuscript. All authors contributed to the article and approved the submitted version.

Conflict of Interest

The authors declare that the research was conducted in the absence of any commercial or financial relationships that could be construed as a potential conflict of interest.

Acknowledgments

M-AL holds a Canada Research Chair in Molecular Virology and Intrinsic Immunity. This work was supported by a grant from the Canadian Institutes for Health Research (CIHR) to M-AL.

Supplementary Material

The Supplementary Material for this article can be found online at:
https://www.frontiersin.org/articles/10.3389/fimmu.2020.610688/full#supplementary-material

References

1. Zhu N, Zhang D, Wang W, Li X, Yang B, Song J, et al. A Novel Coronavirus from Patients with Pneumonia in China, 2019. N Engl J Med (2020) 382 (8):727–33. Doi: 10.1056/NEJMoa2001017
2. Wu F, Zhao S, Yu B, Chen YM, Wang W, Song ZG, et al. A new coronavirus associated with human respiratory disease in China. Nature (2020) 579 (7798):265–9. Doi: 10.1038/s41586-020-2008-3
3. Sohrabi C, Alsafi Z, O'Neill N, Khan M, Kerwan A, Al-Jabir A, et al. World Health Organization declares global emergency: A review of the 2019 novel coronavirus (COVID-19). Int J Surg (2020) 76:71–6. Doi: 10.1016/ j.ijsu.2020.02.034
4. Hamid S, Mir MY, Rohela GK. Novel coronavirus disease (COVID-19): a pandemic (epidemiology, pathogenesis and potential therapeutics). New Microbes New Infect (2020) 35:100679. Doi: 10.1016/j.nmni.2020.100679
5. Read JM, Bridgen JR, Cummings DA, Ho A, Jewell CP. Novel coronavirus 2019-nCoV: early estimation of epidemiological parameters and epidemic predictions. medRxiv (2020) 2020.01.23.20018549. doi: 10.1101/ 2020.01.23.20018549
6. Kissler SM, Tedijanto C, Goldstein E, Grad YH, Lipsitch M. Projecting the transmission dynamics of SARS-CoV-2 through the postpandemic period. Science (2020) 368(6493):860–8. Doi: 10.1126/science.abb5793
7. Kucharski AJ, Russell TW, Diamond C, Liu Y, Edmunds J, Funk S, et al. Early dynamics of transmission and control of COVID-19: a mathematical modelling study. Lancet Infect Dis (2020) 20(5) :553–8. Doi : 10.1101/ 2020.01.31.20019901
8. Liu W, Fontanet A, Zhang PH, Zhan L, Xin ZT, Baril L, et al. Two-year prospective study of the humoral immune response of patients with severeacute respiratory syndrome. J Infect Dis (2006) 193(6):792–5. Doi: 10.1086/ 500469
9. Wu LP, Wang NC, Chang YH, Tian XY, Na DY, Zhang LY, et al. Duration of antibody responses after severe acute respiratory syndrome. Emerg Infect Dis (2007) 13(10) :1562–4. Doi : 10.3201/eid1310.070576
10. Tang F, Quan Y, Xin ZT, Wrammert J, Ma MJ, Lv H, et al. Lack of peripheral memory B cell responses in recovered patients with severe acute respiratory syndrome: a six-year follow-up study. J Immunol (2011) 186(12):7264–8. Doi: 10.4049/jimmunol.0903490
11. Payne DC, Iblan I, Rha B, Alqasrawi S, Haddadin A, Al Nsour M, et al. Persistence of Antibodies against Middle East Respiratory Syndrome Coronavirus. Emerg Infect Dis (2016) 22(10):1824–6. Doi: 10.3201/ eid2210.160706
12. Edridge AWD, Kaczorowska J, Hoste ACR, Bakker M, Klein M, Loens K, et al. Seasonal coronavirus protective immunity is short-lasting. Nat Med (2020) 26:1691–3. Doi: 10.1101/2020.05.11.20086439
13. Shaman J, Galanti M. Will SARS-CoV-2 become endemic? Science (2020) 370(6516):527–9. Doi: 10.1126/science.abe5960
14. Ohst C, Saschenbrecker S, Stiba K, Steinhagen K, Probst C, Radzimski C, et al. Reliable Serological Testing for the Diagnosis of Emerging Infectious Diseases. Adv Exp Med Biol (2018) 1062:19–43. Doi: 10.1007/978-981-10- 8727-1_3
15. Gaebler C, Nussenzweig MC. All eyes on a hurdle race for a SARS-CoV-2 vaccine. Nature (2020) 586(7830) :501–2. Doi : 10.1038/d41586-020-02926-w
16. Bryant JE, Azman AS, Ferrari MJ, Arnold BF, Boni MF, Boum Y, et al. Serology for SARS-CoV-2: Apprehensions, opportunities, and the path forward. Sci Immunol (2020) 5(47). Doi : 10.1126/sciimmunol.abc6347
17. Grzelak L, Temmam S, Planchais C, Demeret C, Tondeur L, Huon C, et al. A comparison of four serological assays for detecting anti-SARS-CoV-2 antibodies in human serum samples from different populations. Sci Transl Med (2020) 12(559). Doi: 10.1126/scitranslmed.abc3103

18. Amanat F, Stadlbauer D, Strohmeier S, Nguyen THO, Chromikova V, McMahon M, et al. A serological assay to detect SARS-CoV-2 seroconversion in humans. Nat Med (2020) 26:1033–6. Doi: 10.1038/s41591-020-0913-5
19. Okba NMA, Muller MA, Li W, Wang C, GeurtsvanKessel CH, Corman VM, et al. Severe Acute Respiratory Syndrome Coronavirus 2-Specific Antibody Responses in Coronavirus Disease Patients. Emerg Infect Dis (2020) 26 (7):1478–88. Doi: 10.3201/eid2607.200841
20. Ng K, Faulkner N, Cornish G, Rosa A, Earl C, Wrobel A, et al. Pre-existing and de novo humoral immunity to SARS-CoV-2 in humans. bioRxiv (2020). 2020.05.14.095414. doi: 10.1101/2020.05.14.095414
21. Whitman JD, Hiatt J, Mowery CT, Shy BR, Yu R, Yamamoto TN, et al. Test performance evaluation of SARS-CoV-2 serological assays. medRxiv (2020). Doi: 10.1101/2020.04.25.20074856
22. Koczula KM, Gallotta A. Lateral flow assays. Essays Biochem (2016) 60 (1):111–20. Doi: 10.1042/EBC20150012 23. Image created with BioRender (2020). Available at: https://biorender.com/.
24. Janeway CA Jr, Travers P, Walport M, Shlomchik MJ. Immunobiology: The Immune system in health and Disease. 5th ed. New York: Garland Science (2001).
25. Schroeder HW Jr., Cavacini L. Structure and function of immunoglobulins. J Allergy Clin Immunol (2010) 125(2 Suppl 2):S41–52. Doi: 10.1016/ j.jaci.2009.09.046
26. Boes M. Role of natural and immune IgM antibodies in immune responses. Mol Immunol (2000) 37(18):1141–9. Doi: 10.1016/S0161-5890(01)00025-6
27. Planchais C, Mouquet H. Easy pan-detection of human IgA immunoglobulins. J Immunol Methods (2020) 484–5:112833. Doi: 10.1016/j.jim.2020.112833
28. Breedveld A, van Egmond M. IgA and FcaRI: Pathological Roles and Therapeutic Opportunities. Front Immunol (2019) 10:553. Doi: 10.3389/ fimmu.2019.00553
29. Woof JM, Mestecky J. Mucosal immunoglobulins. Immunol Rev (2005) 206:64–82. Doi: 10.1111/j.0105-2896.2005.00290.x
30. Freihorst J, Ogra PL. Mucosal immunity and viral infections. Ann Med (2001) 33(3):172–7. Doi: 10.3109/07853890109002074
31. Zan H, Casali P. Immunoglobulin Somatic Hypermutation and Class-Switch DNA Recombination. In: IR Mackay, NR Rose, B Diamond and A Davidson, editors. Encyclopedia of Medical Immunology: Autoimmune Diseases. New York, NY: Springer New York (2014). Doi: 10.1007/978-0-387-84828-0_556 32. Vidarsson G, Dekkers G, Rispens T. IgG subclasses and allotypes: from structure to effector functions. Front Immunol (2014) 5:520. Doi: 10.3389/ fimmu.2014.00520
33. Lu LL, Suscovich TJ, Fortune SM, Alter G. Beyond binding: antibody effector functions in infectious diseases. Nat Rev Immunol (2018) 18(1):46–61. Doi: 10.1038/nri.2017.106
34. van Erp EA, Luytjes W, Ferwerda G, van Kasteren PB. Fc-Mediated Antibody Effector Functions During Respiratory Syncytial Virus Infection and Disease. Front Immunol (2019) 10(548). Doi: 10.3389/fimmu.2019. 00548
35. Holers VM. Complement and its receptors: new insights into human disease. Annu Rev Immunol (2014) 32:433–59. Doi: 10.1146/annurev-immunol032713-120154
36. Soininen A, Seppälä I, Nieminen T, Eskola J, Käyhty H. IgG subclass distribution of antibodies after vaccination of adults with pneumococcal conjugate vaccines. Vaccine (1999) 17(15-16):1889–97. Doi: 10.1016/S0264- 410X(98)00475-7
37. Isa MB, Martınez L, Giordano M, Passeggi C, de Wolff MC, Nates S.´ Comparison of immunoglobulin G subclass profiles induced by measles virus in vaccinated and naturally infected individuals. Clin Diagn Lab Immunol (2002) 9(3):693–7. Doi: 10.1128/CDLI.9.3.693-697.2002
38. Amarasekera M. Immunoglobulin E in health and disease. Asia Pac Allergy (2011) 1(1):12–5. Doi: 10.5415/apallergy.2011.1.1.12
39. Guo L, Ren L, Yang S, Xiao M, Chang D, Yang F, et al. Profiling Early Humoral Response to Diagnose Novel Coronavirus Disease (COVID-19). Clin Infect Dis (2020) 71(15):778–85. Doi: 10.1093/cid/ciaa310 40. Padoan A, Sciacovelli L, Basso D, Negrini D, Zuin S, Cosma C, et al. IgA-Ab

response to spike glycoprotein of SARS-CoV-2 in patients with COVID-19: A longitudinal study. Clin Chim Acta (2020) 507:164–6. Doi: 10.1016/ j.cca.2020.04.026
41. Jaaskelainen AJ, Kekalainen E, Kallio-Kokko H, Mannonen L, Kortela E, Vapalahti O, et al. Evaluation of commercial and automated SARS-CoV-2 IgG and IgA ELISAs using coronavirus disease (COVID-19) patient samples. Euro Surveill (2020) 25(18). Doi : 10.2807/1560-7917.ES.2020.25.18.2000603
42. Long QX, Tang XJ, Shi QL, Li Q, Deng HJ, Yuan J, et al. Clinical and immunological assessment of asymptomatic SARS-CoV-2 infections. Nat Med (2020) 26:1200–4. Doi: 10.1038/s41591-020-0965-6 43. Prevost J, Gasser R, Beaudoin-Bussieres G, Richard J, Duerr R, Laumaea A, et al. Cross-Sectional Evaluation of Humoral Responses against SARS-CoV2 Spike. Cell Rep Med (2020) 1(7):100126. Doi: 10.1016/j.xcrm.2020.100126
44. Seow J, Graham C, Merrick B, Acors S, Pickering S, Steel KJA, et al. Longitudinal observation and decline of neutralizing antibody responses in the three months following SARS-CoV-2 infection in humans. Nat Microbiol (2020) 5:1598–607. Doi: 10.1038/s41564-020-00813-8
45. Beaudoin-Bussieres G, Laumaea A, Anand SP, Prevost J, Gasser R, Goyette G, et al. Decline of Humoral Responses against SARS-CoV-2 Spike in Convalescent Individuals. mBio (2020) 11(5). Doi: 10.1128/mBio.02590-20
46. Galanti M, Shaman J. Direct Observation of Repeated Infections With Endemic Coronaviruses. J Infect Dis (2020). Doi: 10.1101/2020.04.27. 20082032
47. Palm A-KE, Henry C. Remembrance of Things Past: Long-Term B Cell Memory After Infection and Vaccination. Front Immunol (2019) 10(1787). Doi: 10.3389/fimmu.2019.01787
48. Huang AT, Garcia-Carreras B, Hitchings MDT, Yang B, Katzelnick LC, Rattigan SM, et al. A systematic review of antibody mediated immunity to coronaviruses: kinetics, correlates of protection, and association with severity. Nat Commun (2020) 11(1):4704. Doi: 10.1038/s41467-020- 18450-4
49. Weissleder R, Lee H, Ko J, Pittet MJ. COVID-19 diagnostics in context. Sci Transl Med (2020) 12(546):eabc1931. Doi: 10.1126/scitranslmed.abc1931
50. Tortorici MA, Veesler D. Structural insights into coronavirus entry. Adv Virus Res (2019) 105:93–116. Doi: 10.1016/bs.aivir.2019.08.002
51. Krammer F. SARS-CoV-2 vaccines in development. Nature (2020) 586 (7830):516–27. Doi: 10.1038/s41586-020-2798-3
52. Walls AC, Park YJ, Tortorici MA, Wall A, McGuire AT, Veesler D. Structure, Function, and Antigenicity of the SARS-CoV-2 Spike Glycoprotein. Cell (2020) 181(2):281–92.e6. doi: 10.1016/j.cell.2020.02.058 53. Ju B, Zhang Q, Ge X, Wang R, Yu J, Shan S, et al. Potent human neutralizing antibodies elicited by SARS-CoV-2 infection. bioRxiv (2020) 2020. 03.21.990770. doi: 10.1101/2020.03.21.990770
54. Yi C, Sun X, Ye J, Ding L, Liu M, Yang Z, et al. Key residues of the receptor binding motif in the spike protein of SARS-CoV-2 that interact with ACE2 and neutralizing antibodies. Cell Mol Immunol (2020) 17(6):621–30. Doi: 10.1038/s41423-020-0458-z
55. Yuan M, Wu NC, Zhu X, Lee CD, So RTY, Lv H, et al. A highly conserved cryptic epitope in the receptor binding domains of SARS-CoV-2 and SARSCoV. Science (2020) 368(6491):630–3. Doi: 10.1126/science.abb7269
56. Lan J, Ge J, Yu J, Shan S, Zhou H, Fan S, et al. Structure of the SARS-CoV-2 spike receptor-binding domain bound to the ACE2 receptor. Nature (2020) 581(7807) :215–20. Doi : 10.1038/s41586-020-2180-5
57. Liu L, Wang P, Nair MS, Yu J, Rapp M, Wang Q, et al. Potent neutralizing antibodies against multiple epitopes on SARS-CoV-2 spike. Nature (2020) 584(7821):450–6. Doi: 10.1038/s41586-020-2571-7
58. Kang S, Yang M, Hong Z, Zhang L, Huang Z, Chen X, et al. Crystal structure of SARS-CoV-2 nucleocapsid protein RNA binding domain reveals potential unique drug targeting sites. Acta Pharm Sin B (2020) 10(7):1228–38. Doi: 10.1101/2020.03.06.977876

59. Ahmed SF, Quadeer AA, McKay MR. Preliminary Identification of Potential Vaccine Targets for the COVID-19 Coronavirus (SARS-CoV-2) Based on SARS-CoV Immunological Studies. Viruses (2020) 12(3). Doi: 10.3390/ v12030254
60. Liu SJ, Leng CH, Lien SP, Chi HY, Huang CY, Lin CL, et al. Immunological characterizations of the nucleocapsid protein based SARS vaccine candidates. Vaccine (2006) 24(16) :3100–8. Doi : 10.1016/j.vaccine.2006.01.058
61. Piccoli L, Park YJ, Tortorici MA, Czudnochowski N, Walls AC, Beltramello M, et al. Mapping Neutralizing and Immunodominant Sites on the SARS-CoV-2 Spike Receptor-Binding Domain by Structure-Guided HighResolution Serology. Cell (2020) 183(4) :1024–42.e21. doi : 10.1016/ j.cell.2020.09.037
62. Shrock E, Fujimura E, Kula T, Timms RT, Lee IH, Leng Y, et al. Viral epitope profiling of COVID-19 patients reveals cross-reactivity and correlates of severity. Science (2020) 370(6520). Doi: 10.1126/science.abd4250
63. Wajnberg A, Amanat F, Firpo A, Altman D, Bailey M, Mansour M, et al. SARS-CoV-2 infection induces robust, neutralizing antibody responses that are stable for at least three months. medRxiv (2020) 2020.07.14.20151126. doi: 10.1101/2020.07.14.20151126
64. McAndrews KM, Dowlatshahi DP, Dai J, Becker LM, Hensel J, Snowden LM, et al. Heterogeneous antibodies against SARS-CoV-2 spike receptor binding domain and nucleocapsid with implications for COVID-19 immunity. JCI Insight (2020) 5(18). Doi: 10.1172/jci.insight.142386
65. Deming D, Sheahan T, Heise M, Yount B, Davis N, Sims A, et al. Vaccine efficacy in senescent mice challenged with recombinant SARS-CoV bearing epidemic and zoonotic spike variants. PloS Med (2006) 3(12):e525. Doi: 10.1371/journal.pmed.0030525
66. Wolfel R, Corman VM, Guggemos W, Seilmaier M, Zange S, Muller MA, et al. Virological assessment of hospitalized patients with COVID-2019. Nature (2020) 581(7809):465–9. Doi: 10.1038/s41586-020-2196-x
67. Wang Y, Zhang L, Sang L, Ye F, Ruan S, Zhong B, et al. Kinetics of viral load and antibody response in relation to COVID-19 severity. J Clin Invest (2020) 130(10):5235–44. Doi: 10.1172/JCI138759
68. Borremans B, Gamble A, Prager KC, Helman SK, McClain AM, Cox C, et al. Quantifying antibody kinetics and RNA detection during early-phase SARS-CoV2 infection by time since symptom onset. Elife (2020) 9. Doi: 10.7554/eLife.60122
69. Biosciences I. Guide to Lateral Flow Immunoassays. (2020). Available at: https://fnkprddata.blob.core.windows.net/domestic/download/pdf/IBS_A_ guide_to_lateral_flow_immunoassays.pdf.
70. Bissonnette L, Bergeron MG. Diagnosing infections–current and anticipated technologies for point-of-care diagnostics and home-based testing. Clin Microbiol Infect (2010) 16(8):1044–53. Doi: 10.1111/j.1469-0691.2010. 03282.x
71. Lisboa Bastos M, Tavaziva G, Abidi SK, Campbell JR, Haraoui L-P, Johnston JC, et al. Diagnostic accuracy of serological tests for covid-19: systematic review and meta-analysis. BMJ (2020) 370:m2516. Doi: 10.1136/bmj.m2516
72. Pallett SJC, Rayment M, Patel A, Fitzgerald-Smith SAM, Denny SJ, Charani E, et al. Point-of-care serological assays for delayed SARS-CoV-2 case identification among health-care workers in the UK: a prospective multicentre cohort study. Lancet Respir Med (2020) 8(9):885–94. Doi: 10.1016/S2213-2600(20)30315-5
73. Pickering S, Betancor G, Galao RP, Merrick B, Signell AW, Wilson HD, et al. Comparative assessment of multiple COVID-19 serological technologies supports continued evaluation of point-of-care lateral flow assays in hospital and community healthcare settings. PloS Pathog (2020) 16(9) :e1008817. Doi : 10.1101/2020.06.02.20120345
74. Patel EU, Bloch EM, Clarke W, Hsieh YH, Boon D, Eby Y, et al. Comparative performance of five commercially available serologic assays to detect antibodies to SARS-CoV-2 and identify individuals with high neutralizing titers. medRxiv (2020). Doi: 10.1101/2020.08.31.20184788

75. Conklin SE, Martin K, Manabe YC, Schmidt HA, Keruly M, Klock E, et al. Evaluation of Serological SARS-CoV-2 Lateral Flow Assays for Rapid Point of Care Testing. medRxiv (2020) 2020.07.31.20166041. doi: 10.1101/2020. 07.31.20166041
76. National SARS-CoV-2 Serology Assay Evaluation Group. Performance characteristics of five immunoassays for SARS-CoV-2: a head-to-head benchmark comparison. Lancet Infect Dis (2020) 20(12):1390–400. Doi: 10.1016/S1473-3099(20)30634-4
77. Morrison A, Li Y, Loshak H. Serological Test for COVID-19. Ottawa: CADTH horizon Scan (2020). May 2020. Contract No.: 188.
78. McDade TW, McNally E, D'Aquila RT, Mustanski B, Miller A, Vaught L, et al. Enzyme immunoassay for SARS-CoV-2 antibodies in dried blood spot samples: A minimally-invasive approach to facilitate community- and population-based screening. medRxiv (2020) 2020.04.28.20081844. doi: 10.1101/2020.04.28.20081844
79. Center for Disease Control. Interim Laboratory Biosafety Guidelines for Handling and Processing Specimens Associated with Coronavirus Disease 2019 (COVID-19). CDC. (2020). Available at: https://www.cdc.gov/ coronavirus/2019-ncov/lab/lab-biosafety-guidelines.html.
80. Nie J, Li Q, Wu J, Zhao C, Hao H, Liu H, et al. Establishment and validation of a pseudovirus neutralization assay for SARS-CoV-2. Emerg Microbes Infect (2020) 9(1):680–6. Doi: 10.1080/22221751.2020.1743767
81. Schmidt F, Weisblum Y, Muecksch F, Hoffmann H-H, Michailidis E, Lorenzi JCC, et al. Measuring SARS-CoV-2 neutralizing antibody activity using pseudotyped and chimeric viruses. J Exp Med (2020) 217(11). Doi: 10.1084/jem.20201181
82. GenScript. GenScript cPass™ SARS-CoV-2 Neutralization Antibody Detection Kit (2020). Available at: https://www.genscript.com/cpass-sarscov-2-neutralization-antibody-detection-Kit.html.
83. Abe KT, Li Z, Samson R, Samavarchi-Tehrani P, Valcourt EJ, Wood H, et al. A simple protein-based surrogate neutralization assay for SARS-CoV-2. JCI Insight (2020) 5(19). Doi: 10.1172/jci.insight.142362 84. Tan CW, Chia WN, Qin X, Liu P, Chen MI, Tiu C, et al. A SARS-CoV-2 surrogate virus neutralization test based on antibody-mediated blockage of ACE2-spike protein-protein interaction. Nat Biotechnol (2020) 38 :1073–8. Doi : 10.21203/rs.3.rs-24574/v1
85. Wang Q, Zhang Y, Wu L, Niu S, Song C, Zhang Z, et al. Structural and Functional Basis of SARS-CoV-2 Entry by Using Human ACE2. Cell (2020) 181(4):894–904.e9. doi: 10.1016/j.cell.2020.03.045
86. Seydoux E, Homad LJ, MacCamy AJ, Parks KR, Hurlburt NK, Jennewein MF, et al. Analysis of a SARS-CoV-2 infected individual reveals development of potent neutralizing antibodies to distinct epitopes with limited somatic mutation. Immunity (2020) 53(1):98–105.e5. doi: 10.1016/j.immuni. 2020.06.001
87. Suthar MS, Zimmerman M, Kauffman R, Mantus G, Linderman S, Vanderheiden A, et al. Rapid generation of neutralizing antibody responses in COVID-19 patients. medRxiv (2020) 2020.05.03.20084442. doi: 10.1101/2020.05.03.20084442
88. Premkumar L, Segovia-Chumbez B, Jadi R, Martinez DR, Raut R, Markmann A, et al. The receptor binding domain of the viral spike protein is an immunodominant and highly specific target of antibodies in SARS-CoV-2 patients. Sci Immunol (2020) 5(48). Doi: 10.1126/sciimmunol.abc8413
89. Shen C, Wang Z, Zhao F, Yang Y, Li J, Yuan J, et al. Treatment of 5 Critically Ill Patients With COVID-19 With Convalescent Plasma. Jama (2020) 323 (16) :1582–9. Doi : 10.1001/jama.2020.4783
90. Robbiani DF, Gaebler C, Muecksch F, Lorenzi JCC, Wang Z, Cho A, et al. Convergent antibody responses to SARS-CoV-2 in convalescent individuals. Nature (2020) 584(7821) :437–42. Doi : 10.1038/s41586-020-2456-9
91. Brouwer PJM, Caniels TG, van der Straten K, Snitselaar JL, Aldon Y, Bangaru S, et al. Potent neutralizing antibodies from COVID-19 patients define multiple targets of vulnerability. Science (2020) 369(6504) :643–50. Doi : 10.1101/2020.05.12.088716
92. Chi X, Yan R, Zhang J, Zhang G, Zhang Y, Hao M, et al. A neutralizing human antibody binds to the N-terminal domain of the Spike protein of SARS-CoV-2. Science (2020) 369(6504) :650–5. Doi : 10.1126/science.abc6952

93. Schäfer A, Muecksch F, Lorenzi JCC, Leist SR, Cipolla M, Bournazos S, et al. Antibody potency, effector function and combinations in protection from SARS-CoV-2 infection in vivo. bioRxiv (2020) 2020.09.15.298067. doi: 10.1101/2020.09.15.298067
94. Burbelo PD, Riedo FX, Morishima C, Rawlings S, Smith D, Das S, et al. Detection of Nucleocapsid Antibody to SARS-CoV-2 is More Sensitive than Antibody to Spike Protein in COVID-19 Patients. medRxiv (2020) 2020.04.20.20071423. doi: 10.1101/2020.04.20.20071423
95. Trevethan R. Sensitivity, Specificity, and Predictive Values: Foundations, Pliabilities, and Pitfalls in Research and Practice. Front Public Health (2017) 5(307). Doi: 10.3389/fpubh.2017.00307
96. FDA. EUA Authorized Serology Test Performance. FDA (2020). Available at: https://www.fda.gov/medical-devices/emergency-situations-medicaldevices/eua-authorized-serology-test-performance. 97. Serodiagnostics for Severe Acute Respiratory Syndrome–Related Coronavirus-2: A Narrative Review. Ann Internal Med (2020) 173(6):450– 60. Doi: 10.7326/M20-2854
98. Zou KH, O'Malley AJ, Mauri L. Receiver-operating characteristic analysis for evaluating diagnostic tests and predictive models. Circulation (2007) 115 (5):654–7. Doi: 10.1161/CIRCULATIONAHA.105.594929
99. GISAID. Genomic epidemiology of novel coronavirus – Global subsampling. (GISAID (2020)). Available at: https://nextstrain.org/ncov/global?animate= 2019-12-09,2020-04-10,1,1,15000&f_country=USA.
100. Haselmann V, Kittel M, Gerhards C, Thiaucourt M, Eichner R, Costina V, et al. Comparison of test performance of commercial anti-SARS-CoV-2 immunoassays in serum and plasma samples. Clin Chim Acta (2020) 510:73– 8. Doi: 10.1016/j.cca.2020.07.007
101. Traugott M, Aberle SW, Aberle JH, Griebler H, Karolyi M, Pawelka E, et al. Performance of Severe Acute Respiratory Syndrome Coronavirus 2 Antibody Assays in Different Stages of Infection: Comparison of Commercial EnzymeLinked Immunosorbent Assays and Rapid Tests. J Infect Dis (2020) 222 (3):362–6. Doi: 10.1093/infdis/jiaa305
102. Jaaskelainen AJ, Kuivanen S, Kekalainen E, Ahava MJ, Loginov R, KallioKokko H, et al. Performance of six SARS-CoV-2 immunoassays in comparison with 865uebec865er865865ion865tion. J Clin Virol (2020) 129:104512. Doi: 10.1016/j.jcv.2020.104512
103. Adams E, Ainsworth M, Anand R, Andersson M, Auckland K, Baillie J, et al. Antibody testing for COVID-19: A report from the†National COVID Scientific Advisory Panel [version 1; peer review: 1 approved]. Wellcome Open Res (2020) 5(139). Doi: 10.12688/wellcomeopenres.15927.1
104. Muecksch F, Wise H, Batchelor B, Squires M, Semple E, Richardson C, et al. Longitudinal analysis of clinical serology assay performance and 865uebec865er865865i antibody levels in COVID19 convalescents. medRxiv (2020) 2020.08.05.20169128. doi: 10.1101/2020.08.05.20169128
105. Hu X, An T, Situ B, Hu Y, Ou Z, Li Q, et al. Heat inactivation of serum interferes with the immunoanalysis of antibodies to SARS-CoV-2. J Clin Lab Anal (2020) 34(9):e23411. Doi: 10.1002/jcla.23411
106. Xu Z, Zan H, Pone EJ, Mai T, Casali P. Immunoglobulin class-switch DNA recombination: induction, targeting and beyond. Nat Rev Immunol (2012) 12 (7):517–31. Doi: 10.1038/nri3216
107. YeQ,Wang B,Mao J. The pathogenesis and treatment of the `Cytokine Storm'in COVID-19. J Infect (2020) 80(6):607–13. Doi: 10.1016/j.jinf.2020.03.037
108. Coperchini F, Chiovato L, Croce L, Magri F, Rotondi M. The cytokine storm in COVID-19: An overview of the involvement of the chemokine/ chemokine-receptor system. Cytokine Growth Factor Rev (2020) 53:25–32. Doi: 10.1016/j.cytogfr.2020.05.003
109. Pedersen SF, Ho YC. SARS-CoV-2: a storm is raging. J Clin Invest (2020) 130 (5):2202–5. Doi: 10.1172/JCI137647
110. Woodruff MC, Ramonell RP, Nguyen DC, Cashman KS, Saini AS, Haddad NS, et al. Extrafollicular B cell responses correlate with neutralizing antibodies and morbidity in COVID-19. Nat Immunol (2020) 21 :1506– 1516. Doi : 10.1038/s41590-020-00814-z

111. Azkur AK, Akdis M, Azkur D, Sokolowska M, van de Veen W, Bruggen MC, et al. Immune response to SARS-CoV-2 and mechanisms of immunopathological changes in COVID-19. Allergy (2020) 75(7):1564–81. Doi: 10.1111/all.14364
112. Long Q-x, Deng H-j, Chen J, Hu J, Liu B-z, Liao P, et al. Antibody responses to SARS-CoV-2 in COVID-19 patients: the perspective application of serological tests in clinical practice. medRxiv (2020). Doi: 10.1101/ 2020.03.18.20038018.
113. Lee YL, Liao CH, Liu PY, Cheng CY, Chung MY, Liu CE, et al. Dynamics of anti-SARS-Cov-2 IgM and IgG antibodies among COVID-19 patients. J Infect (2020) 81(2):e55–e8. Doi: 10.1016/j.jinf.2020.04.019 114. To KK, Tsang OT, Leung WS, Tam AR, Wu TC, Lung DC, et al. Temporal profiles of viral load in posterior oropharyngeal saliva samples and serum antibody responses during infection by SARS-CoV-2: an observational cohort study. Lancet Infect Dis (2020) 20(5) :565–74. Doi : 10.1016/S1473- 3099(20)30196-1
115. Zhang W, Du RH, Li B, Zheng XS, Yang XL, Hu B, et al. Molecular and serological investigation of 2019-nCoV infected patients: implication of multiple shedding routes. Emerg Microbes Infect (2020) 9(1):386–9. Doi: 10.1080/22221751.2020.1729071
116. Anderson EM, Goodwin EC, Verma A, Arevalo CP, Bolton MJ, Weirick ME, et al. Seasonal human coronavirus antibodies are boosted upon SARS-CoV-2 infection but not associated with protection. medRxiv (2020). Doi: 10.1101/ 2020.11.06.20227215.
117. Poston D, Weisblum Y, Wise H, Templeton K, Jenks S, Hatziioannou T, et al. Absence of SARS-CoV-2 neutralizing activity in pre-pandemic sera from individuals with recent seasonal coronavirus infection. medRxiv (2020) 2020.10.08.20209650. doi: 10.1101/2020.10.08.20209650
118. Ng KW, Faulkner N, Cornish GH, Rosa A, Harvey R, Hussain S, et al. Preexisting and de novo humoral immunity to SARS-CoV-2 in humans. Science (2020) eabe1107. Doi : 10.1126/science.abe1107
119. Jin Y, Wang M, Zuo Z, Fan C, Ye F, Cai Z, et al. Diagnostic value and dynamic variance of serum antibody in coronavirus disease 2019. Int J Infect Dis (2020) 94 :49–52. Doi : 10.1016/j.ijid.2020.03.065
120. Sun B, Feng Y, Mo X, Zheng P, Wang Q, Li P, et al. Kinetics of SARS-CoV-2 specific IgM and IgG responses in COVID-19 patients. Emerg Microbes Infect (2020) 9(1) :940–8. Doi : 10.1080/22221751.2020.1762515
121. Long QX, Liu BZ, Deng HJ, Wu GC, Deng K, Chen YK, et al. Antibody responses to SARS-CoV-2 in patients with COVID-19. Nat Med (2020) 26 (6):845–8. Doi: 10.1038/s41591-020-0897-1
122. Robbiani DF, Gaebler C, Muecksch F, Lorenzi JCC, Wang Z, Cho A, et al. Convergent Antibody Responses to SARS-CoV-2 Infection in Convalescent Individuals. bioRxiv (2020). Doi: 10.1101/2020.05.13.092619
123. Seow J, Graham C, Merrick B, Acors S, Steel KJA, Hemmings O, et al. Longitudinal evaluation and decline of antibody responses in SARS-CoV-2 infection. medRxiv (2020) 2020.07.09.20148429. doi: 10.1101/2020.07. 09.20148429
124. Isho B, Abe KT, Zuo M, Jamal AJ, Rathod B, Wang JH, et al. Persistence of serum and saliva antibody responses to SARS-CoV-2 spike antigens in COVID-19 patients. Sci Immunol (2020) 5(52). Doi : 10.1101/2020.08.01. 20166553
125. Zhao J, Yuan Q, Wang H, Liu W, Liao X, Su Y, et al. Antibody responses to SARS-CoV-2 in patients of novel coronavirus disease 2019. Clin Infect Dis (2020) 71(16) :2027–34. Doi : 10.1101/2020.03.02.20030189
126. Stavnezer J, Guikema JE, Schrader CE. Mechanism and regulation of class switch recombination. Annu Rev Immunol (2008) 26 :261–92. Doi : 10.1146/ annurev.immunol.26.021607.090248
127. Meyer B, Drosten C, Müller MA. Serological assays for emerging coronaviruses: challenges and pitfalls. Virus Res (2014) 194:175–83. Doi: 10.1016/j.virusres.2014.03.018
128. Hsueh PR, Huang LM, Chen PJ, Kao CL, Yang PC. Chronological evolution of IgM, IgA, IgG and 866uebec866er866866ion antibodies after infection with SARSassociated coronavirus. Clin Microbiol Infect (2004) 10(12):1062–6. Doi: 10.1111/j.1469-0691.2004.01009.x

129. Xiang F, Wang X, He X, Peng Z, Yang B, Zhang J, et al. Antibody Detection and Dynamic Characteristics in Patients with COVID-19. Clin Infect Dis (2020) 71(8):1930–4. Doi: 10.1093/cid/ciaa461
130. Wajnberg A, Amanat F, Firpo A, Altman DR, Bailey MJ, Mansour M, et al. Robust neutralizing antibodies to SARS-CoV-2 infection persist for months. Science (2020). Doi : 10.1126/science.abd7728
131. Chen Y, Zuiani A, Fischinger S, Mullur J, Atyeo C, Travers M, et al. Quick COVID-19 Healers Sustain Anti-SARS-CoV-2 Antibody Production. Cell (2020) 183:1–12. Doi: 10.1016/j.cell.2020.10.051
132. Ripperger TJ, Uhrlaub JL, Watanabe M, Wong R, Castaneda Y, Pizzato HA, et al. Detection, prevalence, and duration of humoral responses to SARSCoV-2 under conditions of limited population exposure. medRxiv (2020) 2020.08.14.20174490. doi: 10.1101/2020.08.14.20174490
133. Isho B, Abe KT, Zuo M, Jamal AJ, Rathod B, Wang JH, et al. Mucosal versus systemic antibody responses to SARS-CoV-2 antigens in COVID-19 patients. medRxiv (2020) 2020.08.01.20166553. doi: 10.1101/2020.08.01. 20166553
134. Iyer AS, Jones FK, Nodoushani A, Kelly M, Becker M, Slater D, et al. Persistence and decay of human antibody responses to the receptor binding domain of SARS-CoV-2 spike protein in COVID-19 patients. Sci Immunol (2020) 5(52). Doi: 10.1126/sciimmunol.abe0367
135. Gudbjartsson DF, Norddahl GL, Melsted P, Gunnarsdottir K, Holm H, Eythorsson E, et al. Humoral Immune Response to SARS-CoV-2 in Iceland. N Engl J Med (2020) 383(18):1724–34. Doi: 10.1056/NEJMoa2026116
136. Suthar MS, Zimmerman MG, Kauffman RC, Mantus G, Linderman SL, Hudson WH, et al. Rapid Generation of Neutralizing Antibody Responses in COVID-19 Patients. Cell Rep Med (2020) 1(3):100040. Doi: 10.1101/ 2020.05.03.20084442
137. Kreer C, Zehner M, Weber T, Ercanoglu MS, Gieselmann L, Rohde C, et al. Longitudinal Isolation of Potent Near-Germline SARS-CoV-2-Neutralizing Antibodies from COVID-19 Patients. Cell (2020) 182(4):843–54.e12. doi: 10.1016/j.cell.2020.06.044
138. Deng W, Bao L, Liu J, Xiao C, Liu J, Xue J, et al. Primary exposure to SARSCoV-2 protects against reinfection in rhesus macaques. Science (2020) 369 (6505):818–23. Doi: 10.1126/science.abc5343
139. Chandrashekar A, Liu J, Martinot AJ, McMahan K, Mercado NB, Peter L, et al. SARS-CoV-2 infection protects against rechallenge in rhesus macaques. Science (2020) 369(6505) :812–7. Doi : 10.1126/science.abc4776
140. Chen Y, Tong X, Li Y, Gu B, Yan J, Liu Y, et al. A comprehensive, longitudinal analysis of humoral responses specific to four recombinant antigens of SARS-CoV-2 in severe and non-severe COVID-19 patients. PloS Pathog (2020) 16(9):e1008796. Doi: 10.1371/journal.ppat.1008796
141. Wu J, Liang B, Chen C, Wang H, Fang Y, Shen S, et al. SARS-CoV-2 infection induces sustained humoral immune responses in convalescent patients following symptomatic COVID-19. medRxiv (2020) 2020.07.21.20159178. doi: 10.1101/2020.07.21.20159178
142. Ripperger TJ, Uhrlaub JL, Watanabe M, Wong R, Castaneda Y, Pizzato HA, et al. Orthogonal SARS-CoV-2 Serological Assays Enable Surveillance of Low-Prevalence Communities and Reveal Durable Humoral Immunity. Immunity (2020) 53(5):925–33. Doi: 10.1016/j.immuni.2020.10.004
143. Gaebler C, Wang Z, Lorenzi JCC, Muecksch F, Finkin S, Tokuyama M, et al. Evolution of Antibody Immunity to SARS-CoV-2. bioRxiv (2020). Doi: 10.1101/2020.11.03.367391
144. Slifka MK, Ahmed R. Long-lived plasma cells: a mechanism for maintaining persistent antibody production. Curr Opin Immunol (1998) 10(3):252–8. Doi: 10.1016/S0952-7915(98)80162-3
145. Nutt SL, Hodgkin PD, Tarlinton DM, Corcoran LM. The generation of antibody-secreting plasma cells. Nat Rev Immunol (2015) 15(3):160–71. Doi: 10.1038/nri3795
146. Mankarious S, Lee M, Fischer S, Pyun KH, Ochs HD, Oxelius VA, et al. The half-lives of IgG subclasses and specific antibodies in patients with primary immunodeficiency who are receiving intravenously administered immunoglobulin. J Lab Clin Med (1988) 112(5) :634–40.
147. Zhang B, Zhou X, Zhu C, Song Y, Feng F, Qiu Y, et al. Immune Phenotyping Based on the Neutrophil-to-Lymphocyte Ratio and IgG Level Predicts Disease Severity and Outcome for Patients With COVID-19. Front Mol Biosci (2020) 7:157. Doi: 10.3389/fmolb.2020.00157

148. Lee WS, Wheatley AK, Kent SJ, DeKosky BJ. Antibody-dependent enhancement and SARS-CoV-2 vaccines and therapies. Nat Microbiol (2020) 5(10):1185–91. Doi: 10.1038/s41564-020-00789-5
149. Arvin AM, Fink K, Schmid MA, Cathcart A, Spreafico R, Havenar-Daughton C, et al. A perspective on potential antibody-dependent enhancement of SARS-CoV-2. Nature (2020) 584:353–63. Doi: 10.1038/s41586-020-2538-8
150. Negro F. Is antibody-dependent enhancement playing a role in COVID-19 pathogenesis? Swiss Med Wkly (2020) 150:w20249. Doi: 10.4414/smw.2020.20249
151. Bardina SV, Bunduc P, Tripathi S, Duehr J, Frere JJ, Brown JA, et al. Enhancement of Zika virus pathogenesis by preexisting antiflavivirus immunity. Science (2017) 356(6334):175–80. Doi: 10.1126/science.aal4365
152. Kuzmina NA, Younan P, Gilchuk P, Santos RI, Flyak AI, Ilinykh PA, et al. Antibody-Dependent Enhancement of Ebola Virus Infection by Human Antibodies Isolated from Survivors. Cell Rep (2018) 24(7):1802–15.e5. doi: 10.1016/j.celrep.2018.07.035
153. Wang SF, Tseng SP, Yen CH, Yang JY, Tsao CH, Shen CW, et al. Antibodydependent SARS coronavirus infection is mediated by antibodies against spike proteins. Biochem Biophys Res Commun (2014) 451(2):208–14. Doi: 10.1016/j.bbrc.2014.07.090
154. Wan Y, Shang J, Sun S, Tai W, Chen J, Geng Q, et al. Molecular Mechanism for Antibody-Dependent Enhancement of Coronavirus Entry. J Virol (2020) 94(5). Doi: 10.1128/JVI.02015-19
155. Jaume M, Yip MS, Cheung CY, Leung HL, Li PH, Kien F, et al. Anti-severe acute respiratory syndrome coronavirus spike antibodies trigger infection of human immune cells via a pH- and cysteine protease-independent FcgR pathway. J Virol (2011) 85(20):10582–97. Doi: 10.1128/JVI.00671-11
156. Zohar T, Alter G. Dissecting antibody-mediated protection against SARSCoV-2. Nat Rev Immunol (2020) 1–3. Doi: 10.1038/s41577-020-0359-5
157. Iwasaki A, Yang Y. The potential danger of suboptimal antibody responses in COVID-19. Nat Rev Immunol (2020) 20(6):339–41. Doi: 10.1038/s41577- 020-0321-6
158. Yasui F, Kai C, Kitabatake M, Inoue S, Yoneda M, Yokochi S, et al. Prior immunization with severe acute respiratory syndrome (SARS)-associated coronavirus (SARS-CoV) nucleocapsid protein causes severe pneumonia in mice infected with SARS-CoV. J Immunol (2008) 181(9):6337–48. Doi: 10.4049/jimmunol.181.9.6337
159. Liu L, Wei Q, Lin Q, Fang J, Wang H, Kwok H, et al. Anti-spike IgG causes severe acute lung injury by skewing macrophage responses during acute SARS-CoV infection. JCI Insight (2019) 4(4). Doi: 10.1172/ jci.insight.123158
160. Siddiqi HK, Mehra MR. COVID-19 illness in native and immunosuppressed states: A clinical-therapeutic staging proposal. J Heart Lung Transplant (2020) 39(5):405–7. Doi: 10.1016/j.healun.2020.03.012
161. Agarwal A, Mukherjee A, Kumar G, Chatterjee P, Bhatnagar T, Malhotra P. Convalescent plasma in the management of moderate covid-19 in adults in India: open label phase II multicentre 868uebec868 er868 controlled trial (PLACID Trial). Bmj (2020) 371 :m3939. Doi : 10.1136/bmj.m3939
162. Joyner MJ, Bruno KA, Klassen SA, Kunze KL, Johnson PW, Lesser ER, et al. Safety Update: COVID-19 Convalescent Plasma in 20,000 Hospitalized Patients. Mayo Clin Proc (2020) 95(9):1888–97. Doi: 10.1016/j.mayocp. 2020.09.032
163. Su S, Wong G, Shi W, Liu J, Lai ACK, Zhou J, et al. Epidemiology, Genetic Recombination, and Pathogenesis of Coronaviruses. Trends Microbiol (2016) 24(6):490–502. Doi: 10.1016/j.tim.2016.03.003
164. Braun J, Loyal L, Frentsch M, Wendisch D, Georg P, Kurth F, et al. SARSCoV-2-reactive T cells in healthy donors and patients with COVID-19. Nature (2020) 587(7833):270–4. Doi: 10.1038/s41586-020-2598-9
165. Song G, He WT, Callaghan S, Anzanello F, Huang D, Ricketts J, et al. Crossreactive serum and memory B cell responses to spike protein in SARS-CoV-2 and endemic coronavirus infection. bioRxiv (2020). Doi: 10.1101/ 2020.09.22.308965

166. Woldemeskel BA, Kwaa AK, Garliss CC, Laeyendecker O, Ray SC, Blankson JN. Healthy donor T-cell responses to common cold coronaviruses and SARS-CoV-2. J Clin Invest (2020) 130(12) :6631–8. Doi : 10.1172/JCI143120
167. Nguyen-Contant P, Embong AK, Kanagaiah P, Chaves FA, Yang H, Branche AR, et al. S Protein-Reactive IgG and Memory B Cell Production after Human SARS-CoV-2 Infection Includes Broad Reactivity to the S2 Subunit. mBio (2020) 11(5). Doi: 10.1128/mBio.01991-20
168. Mateus J, Grifoni A, Tarke A, Sidney J, Ramirez SI, Dan JM, et al. Selective and cross-reactive SARS-CoV-2 T cell epitopes in unexposed humans. Science (2020) 370(6512):89–94. Doi: 10.1126/science.abd3871
169. Masse S, Capai L, Villechenaud N, Blanchon T, Charrel R, Falchi A. Epidemiology and Clinical Symptoms Related to Seasonal Coronavirus Identified in Patients with Acute Respiratory Infections Consulting in Primary Care over Six Influenza Seasons (2014-2020) in France. Viruses (2020) 12(6). Doi: 10.3390/v12060630
170. Gorse GJ, Patel GB, Vitale JN, O'Connor TZ. Prevalence of antibodies to four human coronaviruses is lower in nasal secretions than in serum. Clin Vaccine Immunol (2010) 17(12):1875–80. Doi: 10.1128/CVI.00278-10
171. WHO. Middle East respiratory syndrome coronavirus (MERS-CoV). (2019). (WHO). Available at: https://www.who.int/emergencies/mers-cov/en/.
172. WHO. Summary of probable SARS cases with onset of illness from 1 November 2002 to 31 July 2003. WHO (2004). Available at: https://www. Who.int/csr/sars/country/table2004_04_21/en/.
173. Okba NMA, Muller MA, Li W, Wang C, GeurtsvanKessel CH, Corman VM, et al. SARS-CoV-2 specific antibody responses in COVID-19 patients. medRxiv (2020) 2020.03.18.20038059. doi: 10.1101/2020.03.18.20038059
174. Hicks J, Klumpp-Thomas C, Kalish H, Shunmugavel A, Mehalko J, Denson JP, et al. Serologic cross-reactivity of SARS-CoV-2 with endemic and seasonal Betacoronaviruses. medRxiv (2020). Doi: 10.1101/2020.06.22. 20137695
175. Ladner JT, Henson SN, Boyle AS, Engelbrektson AL, Fink ZW, Rahee F, et al. Epitope-resolved profiling of the SARS-CoV-2 antibody response identifies cross-reactivity with an endemic human CoV. bioRxiv (2020) 2020.07.27.222943. doi: 10.1101/2020.07.27.222943
176. Lv H, Wu NC, Tsang OT, Yuan M, Perera R, Leung WS, et al. Cross-reactive Antibody Response between SARS-CoV-2 and SARS-CoV Infections. Cell Rep (2020) 31(9) :107725. Doi : 10.1016/j.celrep.2020.107725
177. Trivedi SU, Miao C, Sanchez JE, Caidi H, Tamin A, Haynes L, et al. Development and Evaluation of a Multiplexed Immunoassay for Simultaneous Detection of Serum IgG Antibodies to Six Human Coronaviruses. Sci Rep (2019) 9(1):1390. Doi: 10.1038/s41598-018-37747-5
178. Zost SJ, Gilchuk P, Chen RE, Case JB, Reidy JX, Trivette A, et al. Rapid isolation and profiling of a diverse panel of human monoclonal antibodies targeting the SARS-CoV-2 spike protein. Nat Med (2020) 26(9) :1422–7. Doi : 10.1101/2020.05.12.091462
179. Ju B, Zhang Q, Ge J, Wang R, Sun J, Ge X, et al. Human neutralizing antibodies elicited by SARS-CoV-2 infection. Nature (2020) 584(7819):115– 9. Doi: 10.1038/s41586-020-2380-z
180. Duan J, Yan X, Guo X, Cao W, Han W, Qi C, et al. A human SARS-CoV neutralizing antibody against epitope on S2 protein. Biochem Biophys Res Commun (2005) 333(1):186–93. Doi: 10.1016/j.bbrc.2005.05.089
181. Elshabrawy HA, Coughlin MM, Baker SC, Prabhakar BS. Human monoclonal antibodies against highly conserved HR1 and HR2 domains of the SARS-CoV spike protein are more broadly neutralizing. PloS One (2012) 7(11):e50366. Doi: 10.1371/journal.pone.0050366
182. Wang C, Li W, Drabek D, Okba NMA, van Haperen R, Osterhaus A, et al. A human monoclonal antibody blocking SARS-CoV-2 infection. Nat Commun (2020) 11(1):2251. Doi: 10.1038/s41467-020-16452-w
183. Sagar M, Reifler K, Rossi M, Miller NS, Sinha P, White L, et al. Recent endemic coronavirus infection is associated with less severe COVID-19. J Clin Invest (2020). Doi : 10.1172/JCI143380

184. Dugas M, Grote-Westrick T, Vollenberg R, Lorentzen E, Brix T, Schmidt H, et al. Less severe course of COVID-19 is associated with elevated levels of antibodies against seasonal human coronaviruses OC43 and HKU1 (HcoV OC43, HcoV HKU1). medRxiv (2020) 2020.10.12.20211599. doi: 10.1101/ 2020.10.12.20211599
185. Sun K, Chen J, Viboud C. Early epidemiological analysis of the coronavirus disease 2019 outbreak based on crowdsourced data: a population-level observational study. Lancet Digital Health (2020) 2(4):e201–e8. Doi: 10.1016/S2589-7500(20)30026-1
186. Shao X, Guo X, Esper F, Weibel C, Kahn JS. Seroepidemiology of group I human coronaviruses in children. J Clin Virol (2007) 40(3) :207–13. Doi : 10.1016/j.jcv.2007.08.007
187. Nickbakhsh S, Ho A, Marques DFP, McMenamin J, Gunson RN, Murcia PR. Epidemiology of Seasonal Coronaviruses: Establishing the Context for the Emergence of Coronavirus Disease 2019. J Infect Diseases (2020) 222(1):17– 25. Doi: 10.1093/infdis/jiaa185
188. Davies NG, Klepac P, Liu Y, Prem K, Jit M, Eggo RM. Age-dependent effects in the transmission and control of COVID-19 epidemics. Nat Med (2020) 26:1205–11. Doi: 10.1101/2020.03.24.20043018
189. Vatti A, Monsalve DM, Pacheco Y, Chang C, Anaya JM, Gershwin ME. Original antigenic sin: A comprehensive review. J Autoimmun (2017) 83:12– 21. Doi: 10.1016/j.jaut.2017.04.008
190. Zompi S, Harris E. Original antigenic sin in dengue revisited. Proc Natl Acad Sci U S A (2013) 110(22):8761–2. Doi: 10.1073/pnas.1306333110
191. Rothman AL. Immunity to dengue virus: a tale of original antigenic sin and tropical cytokine storms. Nat Rev Immunol (2011) 11(8):532–43. Doi: 10.1038/nri3014
192. Meade P, Kuan G, Strohmeier S, Maier HE, Amanat F, Balmaseda A, et al. Influenza Virus Infection Induces a Narrow Antibody Response in Children but a Broad Recall Response in Adults. mBio (2020) 11(1). Doi: 10.1128/ mBio.03243-19
193. Devarajan P, Swain SL. Original Antigenic Sin: Friend or Foe in Developing a Broadly Cross-Reactive Vaccine to Influenza? Cell Host Microbe (2019) 25 (3) :354–5. Doi : 10.1016/j.chom.2019.02.009 194. Aydillo T, Rombauts A, Stadlbauer D, Aslam S, Abelenda-Alonso G, Escalera A, et al. Antibody Immunological Imprinting on COVID-19 Patients. medRxiv (2020) 2020.10.14.20212662. doi : 10.1101/2020.10.14. 20212662
195. Westerhuis BM, Aguilar-Bretones M, Raadsen MP, de Bruin E, Okba NMA, Haagmans BL, et al. Severe COVID-19 patients display a back boost of seasonal coronavirus-specific antibodies. medRxiv (2020) 2020.10.10. 20210070. Doi: 10.1101/2020.10.10.20210070
196. Randolph HE, Barreiro LB. Herd Immunity: Understanding COVID-19. Immunity (2020) 52(5):737–41. Doi: 10.1016/j.immuni.2020.04.012
197. Fine P, Eames K, Heymann DL. “Herd immunity”: a rough guide. Clin Infect Dis (2011) 52(7):911–6. Doi: 10.1093/cid/cir007
198. Severe Outcomes Among Patients with Coronavirus Disease 2019 (COVID19) – United States, February 12-March 16, 2020. MMWR Morb Mortal Wkly Rep (2020) 69(12):343–6. Doi: 10.15585/mmwr.mm6912e2
199. Anderson RM, May RM. Vaccination and herd immunity to infectious diseases. Nature (1985) 318(6044):323–9. Doi: 10.1038/318323a0
200. Liu Y, Gayle AA, Wilder-Smith A, Rocklov J. The reproductive number of COVID-19 is higher compared to SARS coronavirus. J Travel Med (2020) 27 (2). Doi: 10.1093/jtm/taaa021
201. WHO. Report of the WHO-China Joint Mission on Coronavirus Disease 2019 (COVID-19) 2020 (2020). Available at: https://www.who.int/docs/defaultsource/coronaviruse/who-china-joint-mission-on-covid-19-final-report.pdf. 24 February 2020.
202. Brett T, Rohani P. COVID-19 herd immunity strategies: walking an elusive and dangerous tightrope. medRxiv (2020). Doi: 10.1101/2020.04.29. 20082065
203. Arora RK, Joseph A, Van Wyk J, Rocco S, Atmaja A, May E, et al. SeroTracker: a global SARS-CoV-2 seroprevalence dashboard. Lancet Infect Dis (2020). Doi: 10.1016/S1473-3099(20)30631-9

204. Stringhini S, Wisniak A, Piumatti G, Azman AS, Lauer SA, Baysson H, et al. Seroprevalence of anti-SARS-CoV-2 IgG antibodies in Geneva, Switzerland (SEROCoV-POP): a population-based study. Lancet (2020) 396(10247):313– 9. Doi: 10.1016/S0140-6736(20)31304-0
205. Ward H, Atchison CJ, Whitaker M, Ainslie KEC, Elliott J, Okell LC, et al. Antibody prevalence for SARS-CoV-2 in England following first peak of the pandemic: REACT2 study in 100,000 adults. medRxiv (2020) 2020.08.12.20173690. doi: 10.1101/2020.08.12.20173690
206. Folkhälsomyndigheten. Nya resultat om antikroppar mot covid-19 I olika grupper I befolkningen. Folkhälsomyndigheten (2020). Available at: https:// www.folkhalsomyndigheten.se/871uebec871-och-press/nyhetsarkiv/2020/ 871uebec871er/nya-resultat-om-antikroppar-mot-covid-19-i-olika-grupper-ibefolkningen/.
207. Centers for Disease Control and Prevention. Commercial laboratory Seroprevalence Survey Data. CDC (2020). Available at: https://www.cdc. gov/coronavirus/2019-ncov/cases-updates/commercial-lab-surveys. Html#interpreting-serology-results.
208. Pollán M, Pérez-Gómez B, Pastor-Barriuso R, Oteo J, Hernán MA, PérezOlmeda M, et al. Prevalence of SARS-CoV-2 in Spain (ENE-COVID): a nationwide, population-based seroepidemiological study. Lancet (2020) 396 (10250):535–44. Doi: 10.1016/S0140-6736(20)32266-2
209. Héma-Quebec. Blood donor seroprevalence study : 2.23 % of 871uebec adults contracted covid-19. Héma-Québec (2020). Available at : https://www.hemaquebec.qc.ca/publications/communiques/archives/2020/communiques2020/etude-seroprevalence-resultats.en.html.
210. Ontario). OafHPaPPH. Weekly epidemiologic summary: COVID-19 Seroprevalence in Ontario : March 27, 2020 to June 30, 2020. Toronto, ON: Queen's printer for Ontario (2020). P. 10.
211. Skowronski DM, Sekirov I, Sabaiduc S, Zou M, Morshed M, Lawrence D, et al. Low SARS-CoV-2 sero-prevalence based on anonymized residual serosurvey before and after first wave measures in British Columbia, Canada, March-May 2020. medRxiv (2020) 2020.07.13.20153148. doi: 10.1101/2020. 07.13.20153148
212. Valenti L, Bergna A, Pelusi S, Facciotti F, Lai A, Tarkowski M, et al. SARSCoV-2 seroprevalence trends in healthy blood donors during the COVID-19 Milan outbreak. medRxiv (2020) 2020.05.11.20098442. doi: 10.1101/ 2020.05.11.20098442
213. Chang L, Hou W, Zhao L, Zhang Y, Wang Y, Wu L, et al. The prevalence of antibodies to SARS-CoV-2 among blood donors in China. medRxiv (2020) 2020.07.13.20153106. doi: 10.2139/ssrn.3633170
214. Orlowski EJW, Goldsmith DJA. Four months into the COVID-19 pandemic, Sweden's prized herd immunity is nowhere in sight. J R Soc Med (2020) 113 (8):292–8. Doi: 10.1177/0141076820945282
215. Carfì A, Bernabei R, Landi F. Persistent Symptoms in Patients After Acute COVID-19. Jama (2020) 324(6):603–5. Doi: 10.1001/jama.2020.12603
216. Yelin D, Wirtheim E, Vetter P, Kalil AC, Bruchfeld J, Runold M, et al. Longterm consequences of COVID-19: research needs. Lancet Infect Dis (2020) 20 (10):1115–7. Doi: 10.1016/S1473-3099(20)30701-5
217. Rimmer A. Covid-19: Impact of long term symptoms will be profound, warns BMA. BMJ (2020) 370 :m3218. Doi : 10.1136/bmj.m3218
218. Rapkiewicz AV, Mai X, Carsons SE, Pittaluga S, Kleiner DE, Berger JS, et al. Megakaryocytes and platelet-fibrin thrombi characterize multi-organ thrombosis at autopsy in COVID-19: A case series. EclinicalMedicine (2020) 24:100434. Doi: 10.1016/j.eclinm.2020.100434
219. Papachristodoulou E, Kakoullis L, Parperis K, Panos G. Long-term and herd immunity against SARS-CoV-2: implications from current and past knowledge. Pathog Dis (2020) 78(3). Doi: 10.1093/femspd/ftaa025
220. Johns Hopkins Center for Health Security. Serology-based tests for COVID19. (2020). Available at: https://www.centerforhealthsecurity.org/ resources/COVID-19/serology/Serology-based-tests-for-COVID-19. Html#sec4.

221. US Food and Drug Administration. EUA Authorized Serology Test Performance. (2020). Available at: https://www.fda.gov/medical-devices/ coronavirus-disease-2019-covid-19-emergency-use-authorizations-medicaldevices/eua-authorized-serology-test-performance.
222. Hayes Emily L. FDA pulls plug on wayward coronavirus antibody tests. (2020). Available at: https://www.labpulse.com/index.aspx?sec=sup&sub= mic&pag=dis&ItemID=801254.
223. GenomeWeb. Coronavirus Test Tracker: Commercially Available COVID-19 Diagnostic Tests. (2020). Available at: https://www.360dx.com/coronavirustest-tracker-launched-covid-19-tests.

A-1.23 Autoantibodies in COVID-19: implications for disease severity and clinical outcomes

Preface

(This work has been previously published as a review article)

Galipeau Y, Cooper C, Langlois MA. **Autoantibodies in COVID-19: implications for disease severity and clinical outcomes**. Front Immunol. 2025 Jan 6;15:1509289

https://doi.org/10.3389/fimmu.2024.1509289

© 2025 Galipeau, Cooper and Langlois. This is an open-access article distributed under the terms of the Creative Commons Attribution License (CC BY). The use, distribution or reproduction in other forums is permitted, provided the original author(s) and the copyright owner(s) are credited and that the original publication in this journal is cited, in accordance with accepted academic practice. No use, distribution or reproduction is permitted which does not comply with these terms.

Abstract

Few pathogens have historically been subjected to as intense scientific and clinical scrutiny as SARS-CoV-2. The genetic, immunological, and environmental factors influencing disease severity and post-infection clinical outcomes, known as correlates of immunity, remain largely undefined. Clinical outcomes of SARS-CoV-2 infection vary widely, ranging from asymptomatic cases to those with life-threatening COVID-19 symptoms. While most infected individuals return to their former health and fitness within a few weeks, some develop debilitating chronic symptoms, referred to as long-COVID. Autoimmune responses have been proposed as one of the factors influencing long-COVID and the severity of SARS-CoV-2 infection. The association between viral infections and autoimmune pathologies is not new. Viruses such as Epstein-Barr virus and cytomegalovirus, among others, have been shown to induce the production of autoantibodies and the onset of autoimmune conditions. Given the extensive literature on SARS-CoV-2, here we review current evidence on SARS-CoV-2-induced autoimmune pathologies, with a focus on autoantibodies. We closely examine mechanisms driving autoantibody production, particularly their connection with disease severity and long-COVID.

Introduction

SARS-CoV-2 has profoundly impacted the lives of the global community since its emergence from Hubei province, China, in late 2019 (1, 2). This novel beta-coronavirus rapidly spread among humans and animals causing the COVID-19 pandemic. Fortunately, the prompt development of vaccines and extensive immunization efforts significantly reduced the mortality rate following infection. Nonetheless, over seven million deaths have so far been attributed to SARS-CoV-2 (3). Despite these medical advances, the incidence of breakthrough infections and vaccine hesitancy among some individuals means that SARS-CoV-2 continues to impose a significant burden on healthcare systems worldwide (4–7).

While most infected individuals return to their pre-infection health levels, some do not. These individuals continue to experience ongoing and/or new chronic symptoms for months after the initial infection (8–10). Although diagnostic guidelines remain unclear, these individuals are generally referred to as having post-acute sequelae of SARS-CoV-2, also known as long-COVID patients or long-haulers (11–13).

Another question that has stymied the scientific community is the highly heterogeneous nature of COVID-19 disease severity (14, 15). While many individuals experience mild or even asymptomatic infections (16, 17), others suffer severe infections requiring hospitalization, which can sometimes result in death (18, 19). Multiple studies have identified independent factors and co-morbidities that increase the likelihood of poor outcomes following infection, such as older age, respiratory illnesses, cardiovascular conditions, obesity, and weak antibody immunity (20, 21). However, these factors do not account for all severe clinical outcomes following infection. Given this conundrum, some have suggested that SARS-CoV-2-induced autoimmune pathologies may be a contributing factor (22–24). It has also been hypothesized that autoantibodies are a contributing factor to long-COVID (25).

The underlying factors governing the etiology and development of autoimmune responses and disease are not well understood and are believed to have roots in genetics, demographic characteristics (e.g., age and sex), and environmental factors (26–28). Viruses are considered one

of several central exogenous factors able to trigger autoimmunity (26). Correlational studies have highlighted close links between certain viruses and the subsequent development of autoimmune pathologies. For example, Bjornevik et al. showed that individuals who seroconverted to Epstein-Barr virus (EBV) had a 32-fold increased risk of being diagnosed with multiple sclerosis (MS) (29). Other studies have also linked EBV infections to systemic lupus erythematosus (SLE), rheumatoid arthritis (RA), and other autoimmune pathologies (30–33). Type 1 diabetes mellitus is another example of a disease with possible linkages to viral infections and autoimmunity. Enteroviruses such as coxsackievirus and rotavirus have been linked with beta-cell autoimmunity (26, 34–36). Although multiple mechanisms have been proposed to explain viral-induced autoimmunity, the etiological link remains unclear due to the scarcity of underlying mechanistic evidence.

Here, we review the association between SARS-CoV-2 infection and autoimmune pathologies, emphasizing the production of various autoantibody classes. We present current experimental evidence on the presence and induction of these autoantibodies in the context of SARS-CoV-2 infection, and explore potential mechanisms underlying their emergence. Additionally, we address the complexities of establishing causal relationships between autoimmunity and disease processes, situating these findings within the broader context of SARS-CoV-2 disease severity and the evolving clinical picture of long-COVID.

2 Types of autoantibodies detected in SARS-CoV-2 infections

Autoantibodies are immunoglobulins that recognize and bind to self-antigens (e.g., serum proteins, cellular proteins, phospholipids, nucleic acids) (37–39). These antibodies, which seem to defy tolerance mechanisms, have been detected in many vertebrates including sharks, fish, turtles, mice, and humans (40–43). Their ubiquitous prevalence suggests a broader role in homeostasis (44). Some propose that autoantibodies are important for immune regulation and function, clearance of apoptotic cells, transport and modulation of biologically active molecules, and other physiological processes (45). Autoantibodies can differ in isotype and binding properties. Some can bind multiple self-antigens with varying affinities and can be constituted of minimally mutated recombined V(D)J gene sequences, while others have undergone more intense somatic hypermutation resulting in higher affinity autoantibodies (46). While these antibodies can occur in

healthy individuals without any obvious impact on health, environmental exposures such as viral infections can sometimes trigger the generation of pathogenic autoantibodies or increase existing autoantibodies to pathogenic levels. This section summarizes experimental evidence and describes various potentially pathogenic autoantibodies linked with SARS-CoV-2 infections (Figure 1).

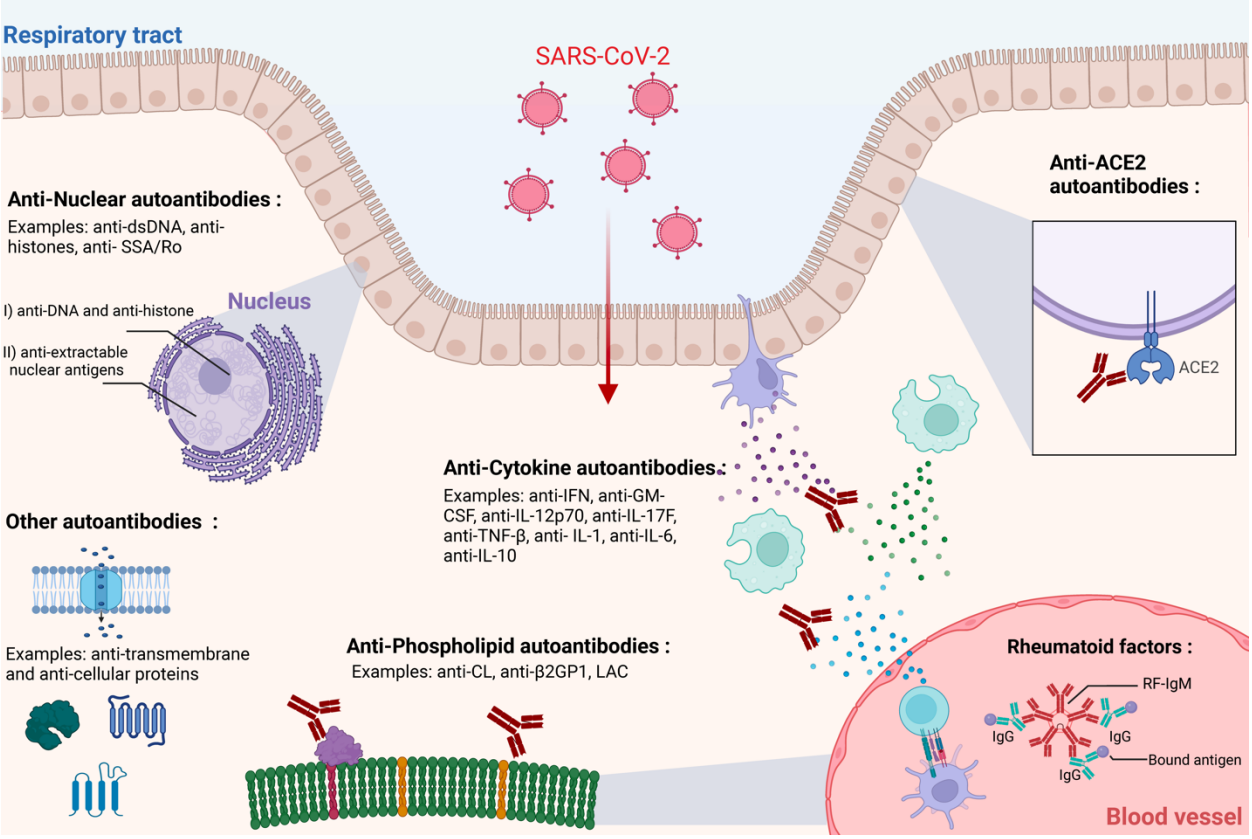


Figure 1. Types of autoantibodies associated with SARS-CoV-2 infection. Multiple studies have highlighted the association, induction, and possible roles of various types of autoantibodies in SARS-CoV-2 infection. This figure illustrates the primary categories of autoantibodies: Anti-ACE2, Anti-Cytokine Antibodies (ACAs), Antinuclear Antibodies (ANAs), and Anti-Phospholipid Antibodies (APLAs), Rheumatoid factors (RFs). Autoantibodies can generally be detected in circulation but may act in specific physiological locations (e.g., blood, respiratory tract epithelium). For simplicity, IgG antibodies are mostly depicted here, although IgM and IgA antibodies may also be present. The respiratory epithelium layer is shown as a representative site for SARS-CoV-2 infection, although the virus can infect multiple other tissues. The figure was created in https://BioRender.com.

2.1 Anti-nuclear antibodies

Antinuclear antibodies (ANA) are a well-known group of autoantibodies that recognize and bind to antigens within the nuclear compartment (47–49). These autoantibodies are generally classified into two large groups: (I) antibodies targeting DNA and histones, and (II) antibodies targeting

extractable nuclear antigens, including RNA-binding proteins complexed to RNA (50, 51). Examples of ANA antibodies include anti-dsDNA, anti-histones, anti-Smith antigen, anti-SSA/Ro, anti-SSB/La, anti-Scl70, and anti-Jo-1 (51). Their combinatorial presence has been used as laboratory biomarkers for several autoimmune diseases such as rheumatoid arthritis (RA), systemic lupus erythematosus (SLE), Sjögren's disease, and systemic sclerosis (50, 52–54).

The prevalence of ANA autoantibodies in SARS-CoV-2 infections has been explored by multiple groups. Early in 2020, studies reported ANA seroprevalence in small cohorts of SARS-CoV-2-infected individuals that ranged from 34.5% to 54.5% (55–57). Larger cohorts estimated ANA prevalence at around 35.6% by Gazzaruso et al., around 25% by Lerma et al., and around 57.5% by Sacchi et al. (58–60). Interestingly, ANA autoantibodies cannot simply be explained by hyperglobulinemia, as they are produced in different proportions to total immunoglobulin levels in plasma (61). The notable heterogeneity in seroprevalence of ANA antibodies across studies could be explained by SARS-CoV-2 severity and cohort characteristics. For example, Taeschler et al. observed a higher trend of ANA antibodies in individuals with severe COVID-19 compared to those with milder infections (62). Despite numerous seroprevalence studies on ANA, mechanistic studies are limited. Recently, a longitudinal cohort study of 106 convalescent individuals identified ANA antibodies as a predictor of long-COVID (63). Interestingly, in another large recent study, the authors found an increased risk of an autoimmune pathology diagnosis after COVID-19 in those with detectable ANA antibodies (64). Nonetheless, it is important to note that ANA antibodies are also found in 14-27% of healthy individuals without symptomatic presentations (65–68). The low predictive value of positive antinuclear antibodies (ANA) requires careful correlation with clinical findings to support an autoimmune diagnosis. Consequently, studies linking SARS-CoV-2 infection with ANA positivity must be interpreted within the context of the study's healthy control cohorts, the specific assays used, and the established positivity thresholds.

2.2 Anti-cytokine antibodies

Antibodies recognizing various cytokines have been described in the context of viral infections prior to the COVID-19 pandemic (69, 70). Anti-cytokine antibodies (ACA) have been shown to bind a vast array of common cytokines such as IL-1, IL-6, IL-8, IL-12, GM-CSF, IFN-α, IFN-γ, and TNF-α (71–80). Interestingly, certain categories of anti-cytokine antibodies have been linked

with disease. For example, anti-GM-CSF autoantibodies are believed to be responsible for idiopathic pulmonary alveolar proteinosis (PAP). While primary PAP is caused by a mutation in the GM-CSF receptor, idiopathic PAP is caused by the neutralization of GM-CSF itself (81–83). Anti-cytokine autoantibodies, particularly anti-IFN-γ, have been linked with poor clinical outcomes and increased disease severity in individuals infected with nontuberculous mycobacteria and other opportunistic infections (84–87). These antibodies can effectively neutralize interferon-gamma, leading to poor immune engagement and an overall compromised immune response (84, 88). Immune suppression by ACA has led to their inclusion in the IUIS classification of primary immunodeficiency diseases, commonly referred to as adult-onset immunodeficiency syndrome (AOID) (89, 90). Bastard et al. first reported that in a cohort of 987 individuals with severe COVID-19, 10.2% had detectable levels of autoantibodies against type I IFN. These autoantibodies were not found in individuals with mild or asymptomatic SARS-CoV-2 infections. The overall seroprevalence of these autoantibodies in healthy individuals was approximately 0.33%, underscoring a significant association with severe COVID-19 (91). These observations have been confirmed by other groups across various demographics (92–96). Anti-IFN antibodies are thought to pre-exist in certain individuals rather than being induced by infection. This highlights their potential to exacerbate common infection severity through IFN neutralization, thereby inhibiting downstream antiviral signaling pathways (91). Other types of ACA have also been identified in severe cases of SARS-CoV-2. For example, Chang et al. used a multiplex protein array to identify antibodies targeting IL-1, -6, -10, -15, -17A, -22, -21, MIP-α, and VEGF-B (61). Another group reported similar findings, including IFN-γ, GM-CSF, IL-12p70, IL-17F, and TNF-β, but only found anti-IL-12p70, anti-IL-22, and anti-IL-6 to be neutralizing. Non-neutralizing anti-cytokine antibodies can still have clinical relevance; however, their role in SARS-CoV-2 infection is not well defined. Key questions remain regarding the triggers for their induction and the persistence of ACA levels over time. Additionally, the clinical impact of most ACAs is poorly understood. In the context of long-COVID, there is currently no evidence to suggest that ACAs contribute to the condition.

2.3 Anti-ACE2 antibodies

Intensive research has centered on the angiotensin-converting enzyme 2 (ACE2) protein, recognized as the entry receptor for both SARS-CoV-1 and SARS-CoV-2. Additionally, ACE2

serves as the entry receptor for NL63, a common human alphacoronavirus (97). Given the key role of this protein in viral entry, some hypothesized that auto-reactivity to ACE2 could contribute to severe COVID-19 symptoms (22, 98). Building on these questions, several studies examined anti-ACE2 autoantibodies in SARS-CoV-2-infected individuals. Arthur et al. found that antibodies recognizing ACE2 were detected in 93% of inpatients, and 81% of convalescent controls, but in none of the healthy controls (99). Another study found IgM antibodies to ACE2 in 27.2% of individuals with severe infections but only 3.8% of those with mild disease, similar to the control cohort (4%) (100). Additional studies have documented the presence of anti-ACE2 antibodies (101, 102). However, anti-ACE2 antibodies have not shown significant capacity to inhibit ACE2 enzymatic activity (99, 100). Interestingly, a study demonstrated the induction of anti-ACE2 antibodies following immunization with recombinant RBD in mice (101). While there is evidence that SARS-CoV-2 infection can induce anti-ACE2 autoantibodies, the topic remains controversial. For example, Chang et al. did not find elevated anti-ACE2 autoantibodies in hospitalized SARS-CoV-2 patients compared to other autoantibodies (61). In a cohort study of 464 individuals, anti-ACE2 IgG autoantibodies were detected in 10.3% of participants, IgA in 6.3%, and IgM in 18.8%, with no association found with SARS-CoV-2 vaccination or infection (103). ACE2 autoantibodies are not exclusive to SARS-CoV-2 infection, having been detected in conditions such as Parkinson’s disease, vasculopathy, and rheumatoid arthritis (104–108). The presence and function of anti-ACE2 antibodies in serum remain unclear, with mixed evidence of their association with SARS-CoV-2 infections.

2.4 Anti-phospholipid antibodies

Anti-phospholipid antibodies (APLAs) target phospholipids and phospholipid-binding proteins such as cardiolipin (CL), β2-glycoprotein-1 (β2GP1), and non-classical antigens like prothrombin (PT) and annexin-V (109–113). These autoantibodies are primarily associated with antiphospholipid syndrome (APS), a condition characterized by thrombotic events and pregnancy complications (113, 114). While murine models have demonstrated APLA pathogenicity in APS, the underlying etiology remains unclear (115, 116).

Historically, APLAs were first identified in fetuses with congenital syphilis in 1906 and have since been linked to infections such as HIV and HCV (117, 118). COVID-19 coagulopathy shares

similarities with thrombotic events observed in both standard and catastrophic APS (119, 120). In early 2020, a case report suggested a potential role for APLAs in severe COVID-19 (121). Subsequent studies have further explored this association. For example, critically ill COVID-19 patients were reported to exhibit elevated levels of APLAs, such as IgA against CL and IgG/IgA against β2GP1 (122).

While several other studies have also highlighted the prevalence of elevated APLAs in COVID-19 patients (59, 123–125), Trahtemberg et al., however, found that APLAs associated with increased disease severity of patients with respiratory failure regardless if they were infected by SARS-CoV-2 or not (126). Reports have also correlated APLAs with thrombosis. Helms et al., for instance, identified APLAs in 87.7% of 57 SARS-CoV-2 patients with coagulation abnormalities (127). Supporting evidence from other studies has confirmed similar findings (122, 128).

Mechanistically, Zuo et al. demonstrated that IgG fractions from COVID-19 patients with APLAs induced neutrophil extracellular trap (NET) release in healthy neutrophils and promoted venous thrombosis in mice (129). However, Serrano et al. observed elevated anti-β2GP1 levels in COVID-19 patients but found no association with thrombosis (130). Additionally, some studies reported no link between APLAs and thrombosis (123, 124, 131).The relationship between COVID-19-associated coagulopathy and APLAs remains ambiguous. It is unclear whether these coagulopathies are independent of APLAs, whether APLA prevalence is specific to COVID-19, or if it is simply a feature of severe illness and hospitalization. Uncharacterized APLAs may play a role in these coagulopathies. Notably, baseline APLA levels vary with age and may be influenced by other infections or autoimmune disorders (118, 132, 133).

2.5 Rheumatoid factors

Rheumatoid factors (RFs) are a common class of autoantibodies that recognize and bind the Fc region of IgG immunoglobulins (Figure 1) (134, 135). RFs can be of any isotype and have been described extensively in the context of rheumatoid arthritis but have also been associated with other autoimmune conditions (e.g., SLE, Sjögren’s disease) (136–138). Notably, RFs have also been described in the context of viral infections, such as hepatitis C virus (HCV) (139, 140). Recently, RFs have been linked to COVID-19. In a cohort of 129 individuals, Xu et al. detected

RFs in 20% of individuals infected with COVID-19 (141). Other studies have reported a variable RF seroprevalence among COVID-19 patients, ranging from 20% to 50% (141–144). One study found higher rates of death, ICU admission, and mechanical ventilation in COVID-19 patients that were RF-positive, suggesting a link with disease severity (142). Interestingly, another study identified novel polyreactive RFs in COVID-19, with one RF able to bind epitopes on IgG and the spike protein (145). The role of RFs in SARS-CoV-2 infection and recovery remains unclear. Previous research has suggested that RFs may neutralize virus-antibody complexes (146) and enhance viral clearance (147). Additionally, RF-positive B cells have been shown to present antigens to T cells, potentially augmenting cellular immune responses during viral infections (148).These findings raise the possibility that RFs may play a protective role during SARS-CoV-2 infection; however, further mechanistic studies are required to elucidate their exact function.

2.6 Other types of autoantibodies

Anti-citrullinated protein antibodies (ACPAs) are a notable class of autoantibodies that recognize peptides containing citrulline, a post-translational modification of arginine (149). ACPAs are strongly associated with autoimmunity and serve as a hallmark marker of rheumatoid arthritis (150–152). Early in the COVID-19 pandemic, a case study reported a potential association between ACPAs and SARS-CoV-2 infection (153). However, subsequent studies have produced mixed results, with some supporting a connection between ACPAs and COVID-19, while others have not found a significant link (154–156).

Another group of autoantibodies relevant to SARS-CoV-2 infections are anti-neutrophil cytoplasmic antibodies (ANCAs). These autoantibodies are primarily associated with ANCA-associated vasculitis (AAV) (157). Case reports have documented instances of AAV occurring in the context of SARS-CoV-2 infection (158, 159). However, the association of both ACPAs and ANCAs with COVID-19 requires validation through studies involving larger cohorts.

Recent advancements in high-throughput multiplexed approaches have significantly enhanced our understanding of autoantibody prevalence. For instance, human exoproteome display analysis using a yeast library has facilitated the profiling of several hundred potential autoantigens. These techniques have been applied to studies of SARS-CoV-2 infection and long-COVID. Interestingly,

Klein et al. utilized these methods to evaluate autoantibodies against thousands of putative self-antigens. They observed no significant differences in autoantibody levels or specific enrichment in individuals with long COVID (160). However, in severe COVID-19 cases, the same approach revealed a broad range of autoantibodies targeting lymphocyte function, cytokines, complement factors, growth factors, cell surface proteins, and more (95). Other high-throughput approaches confirmed that severe SARS-CoV-2 infections induce autoantibodies against a broad array of secreted and non-secreted proteins (61, 161, 162). These unbiased assays provide a comprehensive assessment of circulating autoantibody distributions.

3 Mechanisms for autoantibody induction during viral infection

Studies on the prevalence of autoantibodies across various health conditions, including viral infections such as SARS-CoV-2, are relatively common; however, the mechanisms leading to increased self-tolerance breakdown during viral infections remain unclear. In this review, we describe, explain, and discuss the most relevant mechanisms thought to drive autoantibody production and potential pathogenesis in the context of viral infections (Figure 2). These mechanisms are not mutually exclusive, and multiple pathways may contribute to the pool of circulating autoantibodies. While T cells are also crucial in the generation and maintenance of autoantibodies, their role is beyond the scope of this review.

3.1 Natural autoantibodies

Natural autoantibodies are commonly occurring, low-specificity, and polyreactive antibodies found in all vertebrates (44, 163–165). These antibodies can occur independently of antigenic encounters and are able to recognize both endogenous and exogenous antigens (43, 166, 167). Networks of natural antibodies have been proposed to be remnants of evolution prior to the appearance of specific adaptive immune responses (163, 168). The presence of natural autoantibodies raises critical questions about our understanding of self-tolerance mechanisms. Central and peripheral tolerance mechanisms during B cell development are designed to eliminate autoreactive clones. For instance, in the bone marrow, negative selection of immature B cells upon recognition of self-antigens can lead to B cell receptor (BCR) editing (169). In addition, auto-reactive immature B cells that are unable to rescue a self-reactive BCR may undergo apoptosis by a mechanism known as clonal deletion (170). Despite this, a large number of self-reactive clones

persist in the periphery where other tolerance checkpoints are in place such as B cell anergy (171). Nevertheless, the immune system appears capable of maintaining a repertoire of B cell receptors that are polyreactive and can secrete polyreactive immunoglobulins. These are believed to be secreted primarily by B1-cells co-expressing CD5, although other subsets have been reported (172–175). Given this, it is crucial to consider that some of the autoantibodies detected during and after SARS-CoV-2 infection may be natural autoantibodies or could result from the expansion or upregulation of polyreactive B cells already present in circulation due to inflammation or immune system activation during infection. A better characterization of the affinities and rate of somatic hypermutation, as well as identifying B-cell subsets able to generate such autoantibodies is critical to understand if natural antibodies play a key role in SARS-CoV-2 related autoantibodies.

3.2 Molecular mimicry

Molecular mimicry is one of the most widely recognized mechanisms associated with autoimmunity. In its simplest form, it refers to the phenomenon where certain exogenous antigens, such as viral proteins, including those from SARS-CoV-2, share common epitopes with endogenous antigens (26, 176–178). Antibodies raised against these regions of high homology can in some cases lead to cross-reactive antibodies that can be pathogenic to the host (179–181). In 1962, the work and observations of Kaplan et al. showed that antibodies against group A streptococci can cross-react with cardiac tissues, leading to the death of an individual due to rheumatic pancarditis caused by a streptococcal infection (182). In the following years, multiple lines of evidence led to the acceptance of molecular mimicry as a mechanism explaining cross-reactive antibodies following infection. In fact, molecular mimicry has been observed with various viruses such as Influenza, Zika, Epstein-Barr virus (EBV), and others (183–189). For instance, mimicry between EBV nuclear antigen 1 (EBNA1) and the central nervous system protein glial cell adhesion molecule (GlialCAM) has been shown to generate cross-reactive antibodies, which are detected in approximately 25% of multiple sclerosis (MS) patients (190).

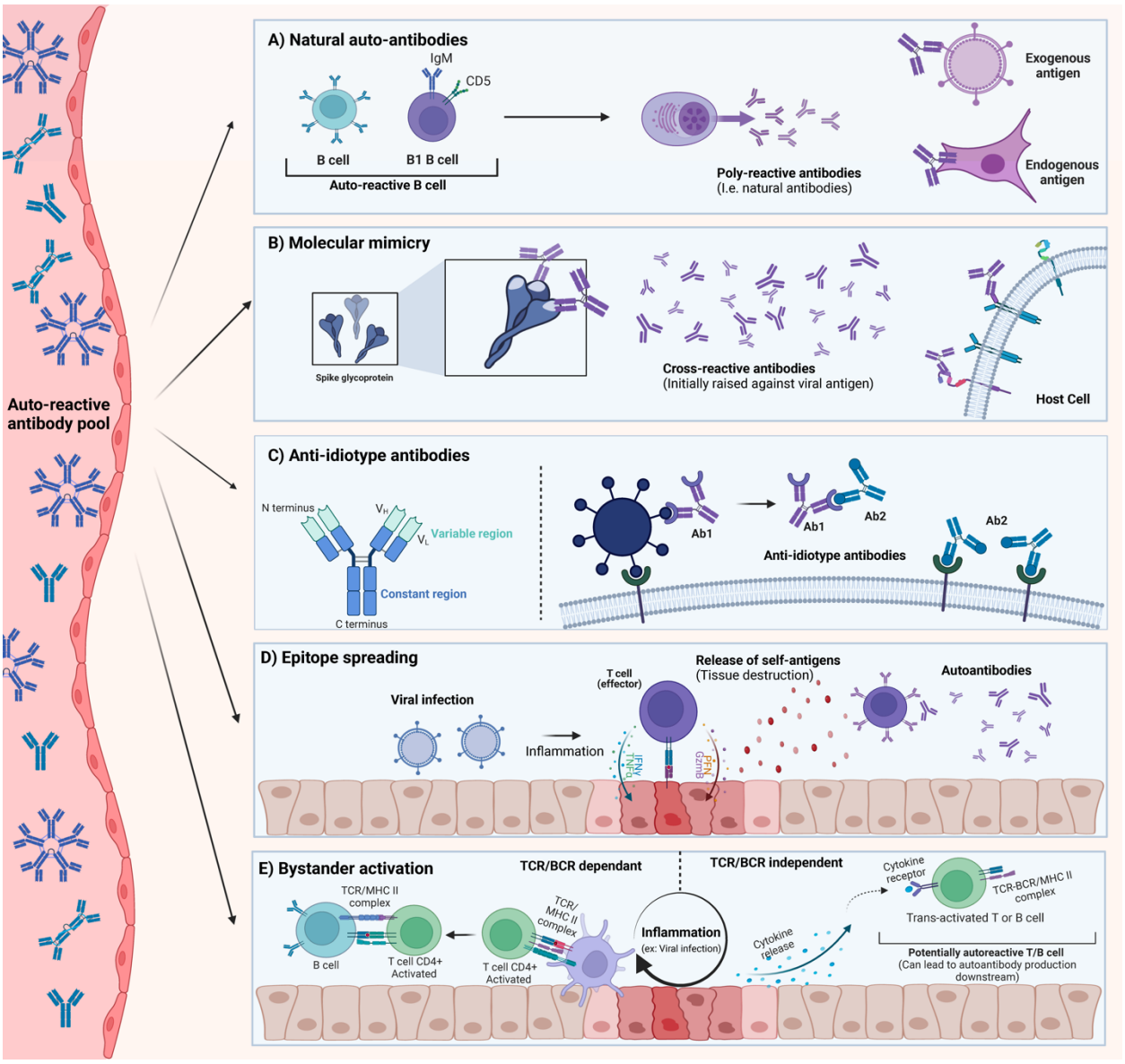


Figure 2. Description of possible mechanisms for autoantibody generation. These mechanisms should be considered as non-exclusive, as more than one mechanism can explain the pool of autoantibodies detected in SARS-CoV-2. **(A)** Natural Autoantibodies can be found in most vertebrates and seem to be important in normal physiological processes. They are believed to arise mainly from the B1 cell subset. These autoantibodies usually exhibit poly-reactivity to endogenous and exogenous proteins. **(B)** Molecular Mimicry occurs when an epitope is shared between an exogenous antigen and an endogenous protein. This can result in cross-reactive autoantibodies that bind to host-derived proteins. **(C)** Anti-Idiotype Autoantibodies (Ab2) are generated against the variable region of another antibody (Ab1). This antibody (Ab2) can potentially retain structural determinants of the original antigen, and in some cases, could bind its target. **(D)** Epitope Spreading (Intermolecular) can occur when an ongoing inflammatory process (initiated by a viral infection) results in the release of normally sequestered self-antigens. T and B cell specificity can then extend to self-antigens that would not normally be presented. **(E)** Bystander Activation refers to the loss of TCR/BCR engagement requirement for activation that can happen to immune cells in proximity to a highly inflammatory milieu.

Other signals (such as cytokine release) decouple the need for proper engagement with innate cells and BCR/TCR-MHC interaction. This can result in the activation of auto-reactive clones. The figure was created in https://BioRender.com.

Recent computational analyses of structural homology between SARS-CoV-2 antigens and the human proteome have identified several shared epitopes. For example, Kanduc et al. identified several linear hexapeptide epitopes that displayed conserved homology between SARS-CoV-2 proteins and 460 human proteins (191). Other groups, using slightly different approaches, have also reported several SARS-CoV-2 proteins containing regions that can be referred to as "molecular mimicry hot-spots" (192–194). Interestingly, immunization of mice with the receptor-binding domain (RBD) protein, as demonstrated by Lai et al. generated antibodies capable of binding to ACE2, suggesting the presence of cross-reactive epitopes (101). Validation of these findings from animal models in larger cohorts of vaccinated individuals remains to be conducted. Importantly, molecular mimicry is not a binary "all-or-nothing" model; genetic factors, such as HLA haplotypes, and environmental factors, such as infections, can influence antigen processing and peptide presentation (195).

3.3 Anti-idiotype antibodies

Anti-idiotype antibodies are not often discussed in the context of autoimmunity. However, these types of antibodies remain interesting as they could explain, at least partially, some of the autoantibodies detected during SARS-CoV-2 infections. The concept of anti-idiotype antibodies, first introduced by Niels Jerne in 1974, suggests that antibodies generated in response to infection (Ab1) possess an immunogenic component within their variable regions that constitutes the idiotype. This region could then be recognized as an antigen, and as such, new antibodies (Ab2) generated against this region would structurally mimic the original antigen (196). This can hypothetically have ramifications whereby anti-idiotype Ab2 antibodies could bind membrane-bound proteins of the host, form immune complexes, and potentially drive pathogenic effects (197, 198). In the context of the SARS-CoV-2 spike protein, one can hypothesize that antibodies against the spike protein could represent the Ab1, and newly generated Ab2 antibodies would be able to bind Ab1 antibodies, but also potentially the ACE2 protein. Interestingly, anti-idiotype antibodies have been explored as possible vaccine candidates for infectious diseases and cancer therapies (199–203). Despite this intriguing hypothesis, at the time of writing this review, no

experimental evidence has been reported to support this mechanism in the context of SARS-CoV-2.

3.4 Epitope spreading

Epitope spreading (ES) can be described as the broadening of reactive lymphocytes to other antigen/epitopes (204, 205). Epitope spreading can be subdivided into intramolecular ES when reactive lymphocytes are able to react with cryptic, non-presented, non-available, or sub-dominant epitopes (206, 207). In contrast, ES can also occur through the diversification of reactive T and B lymphocytes toward antigens distinct from the initially presented antigen that triggered their expansion, a phenomenon commonly referred to as intermolecular ES. Intermolecular ES is frequently discussed in contexts of tissue damage, whether caused by direct trauma or by tissue destruction through phagocytic and inflammatory mechanisms (208, 209). Several factors influence the magnitude of ES, some of which include the type and intensity of the primary inflammatory process and the magnitude of the tissue damage (210). It is also important to consider that ES can be a normal feature of immunity, allowing for more efficient and diverse adaptive responses (208). While ES has been associated with multiple viruses, whether ES contributes to SARS-CoV-2-related autoantibodies remains inconclusive (26, 211). However, tissue damage has been extensively described in severe COVID-19 (212, 213). As such, it is reasonable to suggest that ES is a valid possibility that could explain the generation of some of the autoantibodies identified following SARS-CoV-2 infections.

3.5 Bystander activation

Bystander activation has been proposed as a mechanism that may explain the activation of auto-reactive lymphocytes independently of their BCR/TCR specificity (214, 215). This antigen-independent activation relies on several co-stimulatory signals that decouple the requirement of BCR/TCR signaling with their specific antigen (214, 216). Some of these signaling mediators include ligands (co-signaling receptors, pathogen-associated molecular patterns), cytokines, and chemokines (214, 217–221). These signaling mediators can all occur during infection, resulting in a localized pro-inflammatory environment that can trigger bystander activation of nearby lymphocytes. For example, during primary HIV infection, CD8+ T cells against influenza, EBV,

and CMV show markers of activation and expansion in some individuals, despite the absence of cognate antigens (219). Several autoimmune disorders have been associated with bystander activation such as rheumatoid arthritis (RA), systemic lupus erythematosus (SLE), Grave's disease, and Hashimoto's thyroiditis (222–225). While direct evidence of bystander activation in SARS-CoV-2 infections is limited, it is well known that severe infections have been correlated with an overall release of pro-inflammatory cytokines (226, 227), which have the potential to initiate bystander activation in some individuals.

3.6 Other proposed mechanisms

In addition to the mechanisms discussed in this review, several other processes may contribute to the generation of autoantibodies. These include direct infection of lymphocytes, the activity of superantigens, and the breakdown of immune tolerance mechanisms (228, 229). It is also important to recognize that polyreactive antibody-secreting cells can positively contribute to antibody-mediated immune responses during infection. For instance, in the context of influenza infections, polyreactive monoclonal antibodies (mAbs) have demonstrated increased binding breadth to antigenically drifted and shifted influenza A virus (IAV) antigens (230). Similarly, in HIV infections, two well-characterized broadly neutralizing mAbs were found to be polyreactive and cross-reactive to cardiolipin (231).

4 Possible regulatory roles of autoantibodies

Autoantibodies have also been linked to the relief of inflammatory pathologies, suggesting possible regulatory functions. It is important to consider that autoantibodies may not all be pathogenic, and some may possibly be important features of normal physiology. For example, Sjöwall et al. showed that in patients with systemic lupus erythematosus (SLE) a reduction of TNFα autoantibodies was linked with disease exacerbation (78). Similarly, another group showed that autoantibodies against type 1 IFN in SLE correlated with lower levels of IFN bioactivity and reduced downstream IFN pathways, which correlated with a lower disease score (77). It is also important to consider the regulatory role of antibodies in the treatment of numerous autoimmune or inflammatory conditions. For example, Guillain-Barré syndrome, chronic inflammatory demyelinating polyneuropathy, vasculitis, immune thrombocytopenic purpura, and several others

are often treated with intravenous immunoglobulins (IVIG) (232–234). Anti-idiotype interactions, inhibition of complement deposition, saturation of the neonatal Fc receptor (FcRn) involved in antibody recycling, and competitive blockade of activating Fc gamma receptors are all non-exclusive mechanisms proposed to explain the effects of intravenous immunoglobulin (IVIG) (233, 235). These examples highlight that antibodies, including autoantibodies, can be important in controlling aberrant or excessive inflammatory processes. Whether autoantibodies associated with SARS-CoV-2 are of regulatory importance in viral infections or post-infection physiological processes remains unclear but represents an interesting proposition.

5 Link with disease severity

Research on autoantibodies in individuals infected with or recovering from SARS-CoV-2 has primarily focused on those with severe COVID-19, aiming to elucidate their role in adverse outcomes. As a result, most studies have reported autoantibody presence in hospitalized patients with severe disease, leaving limited data on those with mild or asymptomatic infections. The definitive relationship between autoantibody production and disease severity remains under investigation.

A recent study stratified participants by disease severity, including healthy controls, and found an increased prevalence of autoantibodies—particularly those targeting cardiolipin, claudin, and platelet glycoproteins—with escalating disease severity and advancing age (236). Mechanistically, severe SARS-CoV-2 infections may result in a temporary loss of T cell tolerance. Woodruff et al. demonstrated that severe COVID-19 is associated with the expansion of antibody-secreting B cell populations with low somatic hypermutation, which contract upon recovery, indicating a transient period of reduced selection pressure (229). Similar findings have been observed in acute respiratory distress syndrome caused by bacterial pneumonia, suggesting this phenomenon may represent a physiological response to severe pulmonary infections (229). Recent data from Jaycox et al. suggest that the increase in autoantibodies seen in SARS-CoV-2 infections is not a feature of mRNA vaccinations, suggesting that severe infection may well be the cause (237). While anecdotal reports and small cohort studies have identified autoantibodies after vaccination (238, 239), vaccination remains protective against the development of autoimmune diseases (240, 241).

The underlying mechanisms driving autoantibody production during SARS-CoV-2 infection remain unclear. It is hypothesized that factors such as the intensity of the immune response, inflammation (e.g., cytokine storm), or viral proteins may contribute to their development. Variability in symptom profiles and infection characteristics, such as viral variants, may also influence autoantibody production.

Interestingly, one study highlighted that autoantibodies are not unique to SARS-CoV-2 but are a common feature in critically ill patients with non-SARS-CoV-2 respiratory infections (242).Anti-cytokine autoantibodies were more prevalent in critically ill patients with non-SARS-CoV-2 infections compared to non-infected critically ill individuals (242). Although baseline levels of anti-cytokine autoantibodies (ACAs) in SARS-CoV-2 patients remain understudied, ACAs are recognized as potential risk factors for severe disease. Future longitudinal studies are needed to quantify the risk of severe COVID-19 associated with pre-existing ACAs and to monitor whether specific ACAs are induced during infection.

6 Interpretation and considerations related to SARS-CoV-2-induced autoantibodies

The COVID-19 pandemic has highlighted the established link between viral infections and autoantibodies with a remarkable volume of literature emerging on this topic. Reaching robust conclusions about the causative factors behind autoantibody production and their physiological roles is challenging due to the wide diversity of study designs (e.g., cross-sectional, longitudinal, retrospective, case reports), laboratory assay methodologies, and the varying characteristics of SARS-CoV-2 infections and clinical outcomes (e.g., disease severity, hospitalization, viral variants, therapeutic interventions, vaccination status, and co-morbidities) (Figure 3).

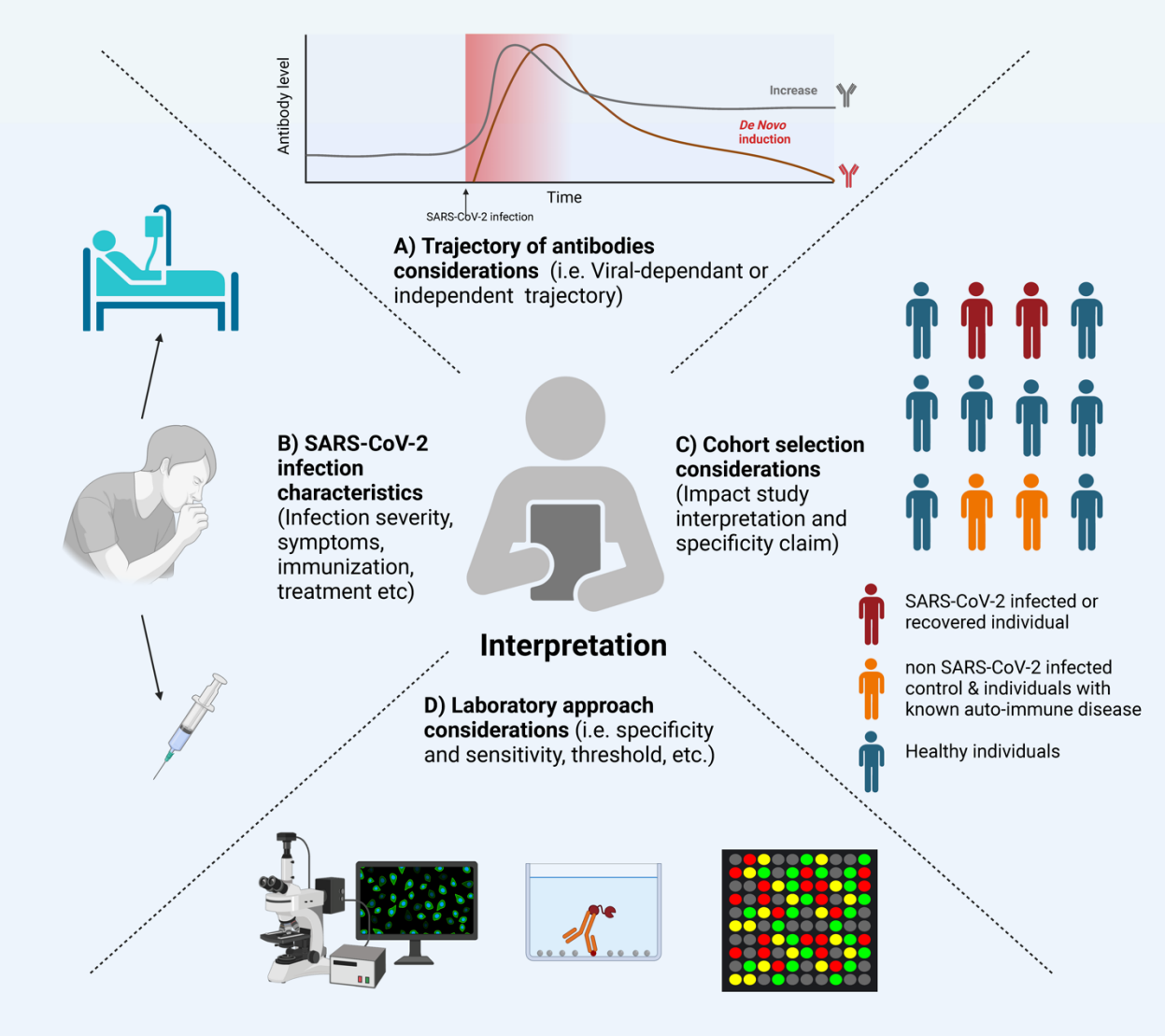


Figure 3. Considerations for Interpreting Experimental Evidence of Autoantibodies Following SARS-CoV-2 Infection. Several factors can influence the interpretation of SARS-CoV-2 induced autoantibodies. Here is a visual representation of a non-exclusive list of factors: **(A)** The Trajectory of Autoantibodies: Understanding whether autoantibodies are present chronically, induced independently of SARS-CoV-2, or induced by SARS-CoV-2 infection. **(B)** SARS-CoV-2 Infection Characteristics: Factors such as infection severity, treatment, and immunization status can significantly influence the presence and levels of autoantibodies. **(C)** Cohort Selection: The selection of cohorts, including characteristics like age, sex, underlying health conditions, and control groups, can have a substantial impact on the interpretation of results. **(D)** Laboratory Considerations: The experimental methods employed can significantly influence the sensitivity and specificity of autoantibody detection. The figure was created in https://BioRender.com.

6.1 Interpretation of laboratory assay data

The wide range of validated and in-house assays used to measure autoantibodies results in variability in reporting and interpretation, which often depends on the specific method employed. Taking ANA detection as an example, it has traditionally been performed using indirect immunofluorescence (IIF), which is considered the gold standard method (243). However, the development of alternative methods, such as solid-phase assays and bead-based multiplex platforms, has introduced challenges in standardizing results across different techniques (244). Beyond the challenges of standardization, each experimental system has distinct sensitivity and specificity profiles. While most assays used in clinical settings have been validated, in-house assays are inherently more flexible but their performance more heterogeneous. Therefore, it is essential to carefully select the assay type based on the specific research questions being asked. Furthermore, the choice of thresholds for seroprevalence measurements should be considered when comparing findings across different studies.

6.2 Pathogenicity potential of autoantibodies

The presence of autoreactive antibodies during and after SARS-CoV-2 infection is of significant clinical interest, but whether these antibodies are directly induced by the virus remains unclear. For example, Lebedin et al. demonstrated that some autoantibodies associated with COVID-19 are non-specific, polyreactive IgG. These polyreactive antibodies can interfere with the accurate quantification of target-specific and functionally relevant autoantibodies, which may have greater clinical importance (245). Additionally, the profiles of these autoantibodies before, during, and after infection are becoming increasingly well-characterized, enabling the proposal of distinct autoantibody trajectories (Figure 4).

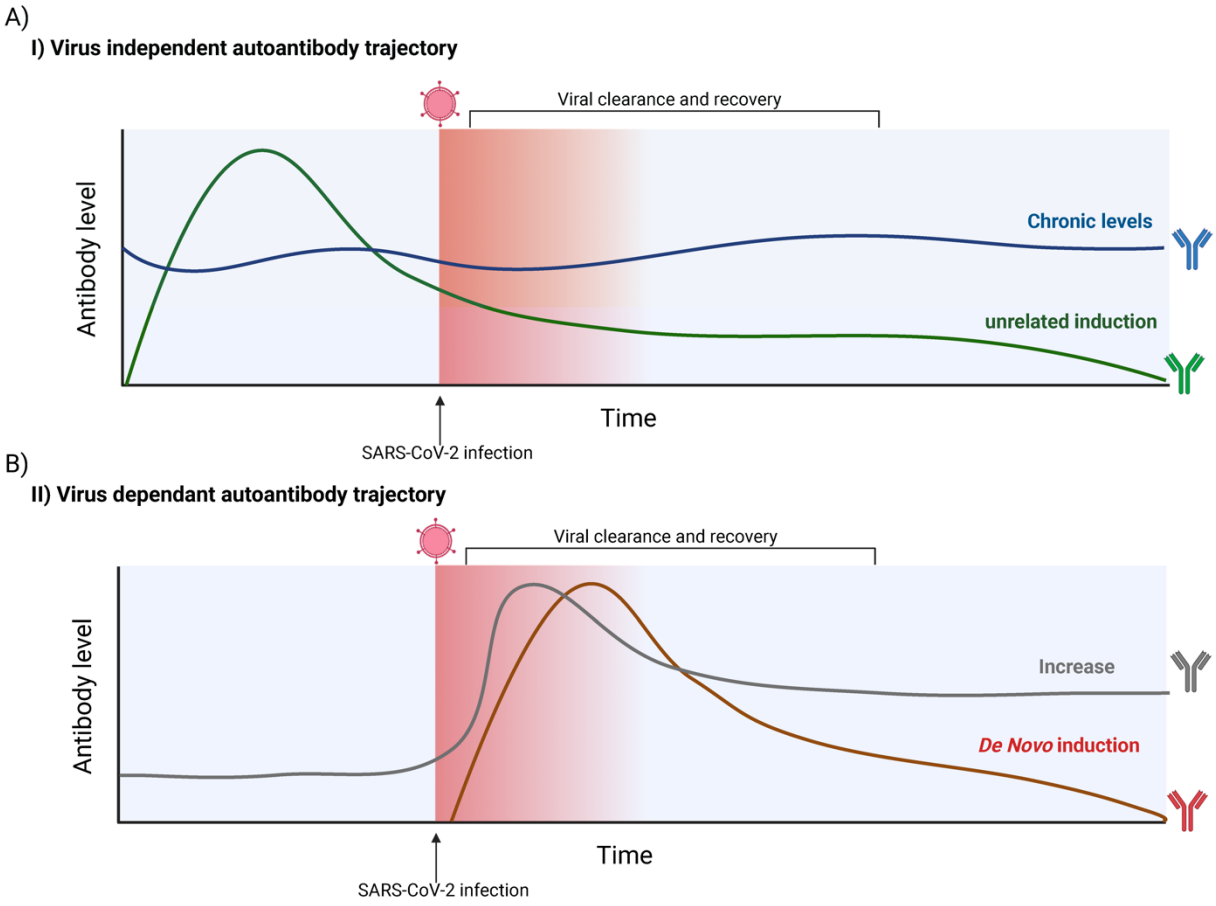


Figure 4. Possible SARS-CoV-2-dependant and -independent trajectories of autoantibody production. **(A)** Hypothetical trajectories of virus-independent autoantibodies. Autoantibody levels are not influenced by SARS-CoV-2 infection. Such antibodies are generally already present but can vary in level. A chronically present autoantibody (Blue) can remain relatively stable over time, with slight biological fluctuations. A SARS-CoV-2-independent induction can also occur (Green), in which antibody levels can rapidly increase and possibly decay over time. **(B)** Hypothetical trajectories virus-dependent autoantibodies detected in individuals. The presence and/or quantity of an autoantibody is influenced by SARS-CoV-2 infection. It is possible to see an increase in the titer of an autoantibody already detected in the infected host (Grey). This trajectory contrasts with a *de novo* induction, where SARS-CoV-2 infection leads to the induction of an autoantibody that was not in circulation prior to the infection (Red). These features of possible trajectories need to be considered when interpreting experimental evidence. The figure was created in https://BioRender.com.

Observational studies and those with limited control cohorts often cannot establish whether SARS-CoV-2 infection directly triggers autoantibody production. Given the heterogeneity of autoantibodies observed across various diseases, it is plausible that some findings may be unrelated to SARS-CoV-2 infection (246). For cases where a link between SARS-CoV-2 and autoantibodies has been demonstrated, a key question remains: are these autoantibodies induced *de novo*, or are pre-existing antibodies elevated to higher titers? For instance, Bastard et al. showed that autoantibodies targeting interferons (IFNs), associated with severe COVID-19, were present prior to infection but did not cause symptoms (91). This indicates that such autoantibodies may preexist in predisposed individuals. Further longitudinal studies that assess baseline autoantibody levels are needed to clarify their trajectories over time and elucidate their origins.

It is important to understand that the presence of autoreactive antibodies does not automatically indicate a causal relationship with the onset of autoimmune diseases. Notably, conditions associated with autoimmunity, such as myocarditis, arthritis, vasculitis, and encephalitis, have been reported following SARS-CoV-2 infection (247, 248). Retrospective studies in unvaccinated individuals have confirmed that SARS-CoV-2 infection significantly increases the risk of developing autoimmune disorders (240, 247). One study reported a 42.6% higher likelihood of autoimmune disease in individuals previously infected with SARS-CoV-2 (249). However, no definitive mechanistic studies have linked these conditions to autoantibodies, making it difficult to establish causality.

Despite this, the detection of autoantibodies raises important questions about their clinical significance and their potential utility as biomarkers for disease. Future research should focus on disentangling the pathogenic and non-pathogenic roles of these autoantibodies to better understand their implications in post-infection outcomes.

Conclusion

Autoantibodies have been extensively reported in association with SARS-CoV-2 infections, reinforcing the notion that viral infections, are important environmental factors that can induce *de novo* autoantibody production or amplify existing autoantibody levels. However, there remains a significant gap in our understanding of the precise mechanisms by which these autoantibodies are generated following infection and, more specifically, whether and how they contribute to

pathology in the host. It is also plausible that some autoantibodies contribute to regulatory physiological processes during infection or recovery, highlighting their multiple complex roles beyond their known pathogenic effects. Moreover, there is a scarcity of studies exploring therapeutic interventions, such as plasmapheresis or immunosuppressants, specifically targeting these autoantibodies. These gaps in our knowledge represent both challenges and valuable research opportunities. The findings related to SARS-CoV-2 and its association to autoantibodies underscore the complex and intertwined relationship between viral infections and autoimmunity, inviting further exploration into their clinical significance and therapeutic potential.

Author contributions

YG: Conceptualization, Investigation, Visualization, Writing – original draft, Writing – review & editing. CC: Writing – original draft, Writing – review & editing. M-AL: Conceptualization, Investigation, Supervision, Writing – original draft, Writing – review & editing, Funding acquisition.

Funding

The author(s) declare financial support was received for the research, authorship, and/or publication of this article. This study was supported in part by a COVID-19 Rapid Response grant by the Canadian Institute of Health Research (CIHR) (VR2-172722) and by a grant supplement by the Canadian Immunity Task Force (CITF) to M-AL. YG holds a Canadian Institute of Health Research (CIHR) Frederick Banting and Charles Best graduate scholarship (CGS-Doctoral) (476885). M-AL holds the Faculty of Medicine Chair of Excellence in Pandemic Viruses and Preparedness Research.

Conflict of interest

The authors declare that the research was conducted in the absence of any commercial or financial relationships that could be construed as a potential conflict of interest.

References

1. Wu F, Zhao S, Yu B, Chen YM, Wang W, Song ZG, et al. A new coronavirus associated with human respiratory disease in China. Nature. 2020;579(7798):265-9.
2. Zhu N, Zhang D, Wang W, Li X, Yang B, Song J, et al. A Novel Coronavirus from Patients with Pneumonia in China, 2019. N Engl J Med. 2020;382(8):727-33.
3. WHO. COVID-19 Dashboard Geneva2023 [Available from: https://covid19.who.int/.
4. Myers LC, Liu VX. The COVID-19 Pandemic Strikes Again and Again and Again. JAMA Network Open. 2022;5(3):e221760-e.
5. Blumenthal D, Fowler EJ, Abrams M, Collins SR. Covid-19 — Implications for the Health Care System. New England Journal of Medicine. 2020;383(15):1483-8.
6. Farrenkopf PM. The Cost of Ignoring Vaccines. Yale J Biol Med. 2022;95(2):265-9.
7. Duong D, Vogel L. Canada's public health system is stretched "dangerously thin". Canadian Medical Association Journal. 2022;194(2):E57-E.
8. Peghin M, Palese A, Venturini M, De Martino M, Gerussi V, Graziano E, et al. Post-COVID-19 symptoms 6 months after acute infection among hospitalized and non-hospitalized patients. Clinical Microbiology and Infection. 2021;27(10):1507-13.
9. Augustin M, Schommers P, Stecher M, Dewald F, Gieselmann L, Gruell H, et al. Post-COVID syndrome in non-hospitalised patients with COVID-19: a longitudinal prospective cohort study. The Lancet Regional Health - Europe. 2021;6:100122.
10. Fernández-de-las-Peñas C, Palacios-Ceña D, Gómez-Mayordomo V, Florencio LL, Cuadrado ML, Plaza-Manzano G, et al. Prevalence of post-COVID-19 symptoms in hospitalized and non-hospitalized COVID-19 survivors: A systematic review and meta-analysis. European Journal of Internal Medicine. 2021;92:55-70.
11. Crook H, Raza S, Nowell J, Young M, Edison P. Long covid—mechanisms, risk factors, and management. BMJ. 2021;374:n1648.
12. Davis HE, McCorkell L, Vogel JM, Topol EJ. Long COVID: major findings, mechanisms and recommendations. Nature Reviews Microbiology. 2023.
13. Proal AD, VanElzakker MB. Long COVID or Post-acute Sequelae of COVID-19 (PASC): An Overview of Biological Factors That May Contribute to Persistent Symptoms. Frontiers in Microbiology. 2021;12.
14. Wiersinga WJ, Rhodes A, Cheng AC, Peacock SJ, Prescott HC. Pathophysiology, Transmission, Diagnosis, and Treatment of Coronavirus Disease 2019 (COVID-19): A Review. Jama. 2020;324(8):782-93.
15. Lamers MM, Haagmans BL. SARS-CoV-2 pathogenesis. Nature Reviews Microbiology. 2022;20(5):270-84.
16. Oran DP, Topol EJ. The Proportion of SARS-CoV-2 Infections That Are Asymptomatic. Annals of Internal Medicine. 2021;174(5):655-62.
17. Sah P, Fitzpatrick MC, Zimmer CF, Abdollahi E, Juden-Kelly L, Moghadas SM, et al. Asymptomatic SARS-CoV-2 infection: A systematic review and meta-analysis. Proceedings of the National Academy of Sciences. 2021;118(34):e2109229118.
18. Zhou F, Yu T, Du R, Fan G, Liu Y, Liu Z, et al. Clinical course and risk factors for mortality of adult inpatients with COVID-19 in Wuhan, China: a retrospective cohort study. The Lancet. 2020;395(10229):1054-62.
19. Goh KJ, Choong MC, Cheong EH, Kalimuddin S, Duu Wen S, Phua GC, et al. Rapid Progression to Acute Respiratory Distress Syndrome: Review of Current Understanding of Critical Illness from Coronavirus Disease 2019 (COVID-19) Infection. Ann Acad Med Singap. 2020;49(3):108-18.
20. Ng WH, Tipih T, Makoah NA, Vermeulen JG, Goedhals D, Sempa JB, et al. Comorbidities in SARS-CoV-2 Patients: a Systematic Review and Meta-Analysis. mBio. 2021;12(1).

21. Mason KE, Maudsley G, McHale P, Pennington A, Day J, Barr B. Age-Adjusted Associations Between Comorbidity and Outcomes of COVID-19: A Review of the Evidence From the Early Stages of the Pandemic. Frontiers in Public Health. 2021;9.
22. McMillan P, Dexhiemer T, Neubig RR, Uhal BD. COVID-19—A Theory of Autoimmunity Against ACE-2 Explained. Frontiers in Immunology. 2021;12.
23. Mobasheri L, Nasirpour MH, Masoumi E, Azarnaminy AF, Jafari M, Esmaeili S-A. SARS-CoV-2 triggering autoimmune diseases. Cytokine. 2022;154:155873.
24. Kocivnik N, Velnar T. A Review Pertaining to SARS-CoV-2 and Autoimmune Diseases: What Is the Connection? Life. 2022;12(11):1918.
25. Anaya J-M, Herrán M, Beltrán S, Rojas M. Is post-COVID syndrome an autoimmune disease? Expert Review of Clinical Immunology. 2022;18(7):653-66.
26. Smatti MK, Cyprian FS, Nasrallah GK, Al Thani AA, Almishal RO, Yassine HM. Viruses and Autoimmunity: A Review on the Potential Interaction and Molecular Mechanisms. Viruses. 2019;11(8).
27. Arleevskaya MI, Manukyan G, Inoue R, Aminov R. Editorial: Microbial and Environmental Factors in Autoimmune and Inflammatory Diseases. Front Immunol. 2017;8:243.
28. Rosenblum MD, Remedios KA, Abbas AK. Mechanisms of human autoimmunity. J Clin Invest. 2015;125(6):2228-33.
29. Bjornevik K, Cortese M, Healy BC, Kuhle J, Mina MJ, Leng Y, et al. Longitudinal analysis reveals high prevalence of Epstein-Barr virus associated with multiple sclerosis. Science. 2022;375(6578):296-301.
30. Moon UY, Park SJ, Oh ST, Kim WU, Park SH, Lee SH, et al. Patients with systemic lupus erythematosus have abnormally elevated Epstein-Barr virus load in blood. Arthritis Res Ther. 2004;6(4):R295-302.
31. Draborg AH, Jørgensen JM, Müller H, Nielsen CT, Jacobsen S, Iversen LV, et al. Epstein-Barr virus early antigen diffuse (EBV-EA/D)-directed immunoglobulin A antibodies in systemic lupus erythematosus patients. Scand J Rheumatol. 2012;41(4):280-9.
32. Draborg AH, Duus K, Houen G. Epstein-Barr virus and systemic lupus erythematosus. Clin Dev Immunol. 2012;2012:370516.
33. Dostál C, Newkirk MM, Duffy KN, Palecková A, Bosák V, Cerná M, et al. Herpes viruses in multicase families with rheumatoid arthritis and systemic lupus erythematosus. Ann N Y Acad Sci. 1997;815:334-7.
34. Laitinen OH, Honkanen H, Pakkanen O, Oikarinen S, Hankaniemi MM, Huhtala H, et al. Coxsackievirus B1 Is Associated With Induction of β-Cell Autoimmunity That Portends Type 1 Diabetes. Diabetes. 2014;63(2):446-55.
35. Yeung WC, Rawlinson WD, Craig ME. Enterovirus infection and type 1 diabetes mellitus: systematic review and meta-analysis of observational molecular studies. Bmj. 2011;342:d35.
36. Honeyman MC, Coulson BS, Stone NL, Gellert SA, Goldwater PN, Steele CE, et al. Association between rotavirus infection and pancreatic islet autoimmunity in children at risk of developing type 1 diabetes. Diabetes. 2000;49(8):1319-24.
37. Elkon K, Casali P. Nature and functions of autoantibodies. Nat Clin Pract Rheumatol. 2008;4(9):491-8.
38. Lutz HU, Binder CJ, Kaveri S. Naturally occurring auto-antibodies in homeostasis and disease. Trends in Immunology. 2009;30(1):43-51.
39. Casali P, Schettino EW, editors. Structure and Function of Natural Antibodies. Immunology of Silicones; 1996 1996//; Berlin, Heidelberg: Springer Berlin Heidelberg.
40. Adelman MK, Schluter SF, Marchalonis JJ. The natural antibody repertoire of sharks and humans recognizes the potential universe of antigens. Protein J. 2004;23(2):103-18.
41. Gonzalez R, Charlemagne J, Mahana W, Avrameas S. Specificity of natural serum antibodies present in phylogenetically distinct fish species. Immunology. 1988;63(1):31-6.
42. Hunter KW, duPré SA, Sharp T, Sandmeier FC, Tracy CR. Western blot can distinguish natural and acquired antibodies to Mycoplasma agassizii in the desert tortoise (Gopherus agassizii). Journal of Microbiological Methods. 2008;75(3):464-71.

43. Haury M, Sundblad A, Grandien A, Barreau C, Coutinho A, Nobrega A. The repertoire of serum IgM in normal mice is largely independent of external antigenic contact. European Journal of Immunology. 1997;27(6):1557-63.
44. Avrameas S. Natural autoantibodies: from 'horror autotoxicus' to 'gnothi seauton'. Immunology Today. 1991;12(5):154-9.
45. Siloşi I, Siloşi CA, Boldeanu MV, Cojocaru M, Biciuşcă V, Avrămescu CS, et al. The role of autoantibodies in health and disease. Rom J Morphol Embryol. 2016;57(2 Suppl):633-8.
46. Detanico T, St Clair JB, Aviszus K, Kirchenbaum G, Guo W, Wysocki LJ. Somatic mutagenesis in autoimmunity. Autoimmunity. 2013;46(2):102-14.
47. Li H, Zheng Y, Chen L, Lin S. High titers of antinuclear antibody and the presence of multiple autoantibodies are highly suggestive of systemic lupus erythematosus. Scientific Reports. 2022;12(1):1687.
48. Holborow EJ, Weir DM, Johnson GD. A serum factor in lupus erythematosus with affinity for tissue nuclei. Br Med J. 1957;2(5047):732-4.
49. Irure-Ventura J, López-Hoyos M. The Past, Present, and Future in Antinuclear Antibodies (ANA). Diagnostics (Basel). 2022;12(3).
50. Pisetsky DS. Antinuclear antibody testing — misunderstood or misbegotten? Nature Reviews Rheumatology. 2017;13(8):495-502.
51. Kumar Y, Bhatia A, Minz RW. Antinuclear antibodies and their detection methods in diagnosis of connective tissue diseases: a journey revisited. Diagn Pathol. 2009;4:1.
52. Schulte-Pelkum J, Fritzler M, Mahler M. Latest update on the Ro/SS-A autoantibody system. Autoimmun Rev. 2009;8(7):632-7.
53. Hoffman IE, Peene I, Meheus L, Huizinga TW, Cebecauer L, Isenberg D, et al. Specific antinuclear antibodies are associated with clinical features in systemic lupus erythematosus. Ann Rheum Dis. 2004;63(9):1155-8.
54. Gunawardena H. The Clinical Features of Myositis-Associated Autoantibodies: a Review. Clin Rev Allergy Immunol. 2017;52(1):45-57.
55. Gagiannis D, Steinestel J, Hackenbroch C, Schreiner B, Hannemann M, Bloch W, et al. Clinical, Serological, and Histopathological Similarities Between Severe COVID-19 and Acute Exacerbation of Connective Tissue Disease-Associated Interstitial Lung Disease (CTD-ILD). Frontiers in Immunology. 2020;11.
56. Zhou Y, Han T, Chen J, Hou C, Hua L, He S, et al. Clinical and Autoimmune Characteristics of Severe and Critical Cases of COVID-19. Clin Transl Sci. 2020;13(6):1077-86.
57. Vlachoyiannopoulos PG, Magira E, Alexopoulos H, Jahaj E, Theophilopoulou K, Kotanidou A, et al. Autoantibodies related to systemic autoimmune rheumatic diseases in severely ill patients with COVID-19. Annals of the Rheumatic Diseases. 2020;79(12):1661-3.
58. Lerma LA, Chaudhary A, Bryan A, Morishima C, Wener MH, Fink SL. Prevalence of autoantibody responses in acute coronavirus disease 2019 (COVID-19). J Transl Autoimmun. 2020;3:100073.
59. Gazzaruso C, Carlo Stella N, Mariani G, Nai C, Coppola A, Naldani D, et al. High prevalence of antinuclear antibodies and lupus anticoagulant in patients hospitalized for SARS-CoV2 pneumonia. Clin Rheumatol. 2020;39(7):2095-7.
60. Sacchi MC, Tamiazzo S, Stobbione P, Agatea L, De Gaspari P, Stecca A, et al. SARS-CoV-2 infection as a trigger of autoimmune response. Clin Transl Sci. 2021;14(3):898-907.
61. Chang SE, Feng A, Meng W, Apostolidis SA, Mack E, Artandi M, et al. New-onset IgG autoantibodies in hospitalized patients with COVID-19. Nature Communications. 2021;12(1):5417.
62. Taeschler P, Cervia C, Zurbuchen Y, Hasler S, Pou C, Tan Z, et al. Autoantibodies in COVID-19 correlate with antiviral humoral responses and distinct immune signatures. Allergy. 2022;77(8):2415-30.
63. Son K, Jamil R, Chowdhury A, Mukherjee M, Venegas C, Miyasaki K, et al. Circulating anti-nuclear autoantibodies in COVID-19 survivors predict long COVID symptoms. Eur Respir J. 2023;61(1).
64. Hileman CO, Malakooti SK, Patil N, Singer NG, McComsey GA. New-onset autoimmune disease after COVID-19. Frontiers in Immunology. 2024;15.

65. Watanabe A, Kodera M, Sugiura K, Usuda T, Tan EM, Takasaki Y, et al. Anti-DFS70 antibodies in 597 healthy hospital workers. Arthritis & Rheumatism. 2004;50(3):892-900.
66. Wandstrat AE, Carr-Johnson F, Branch V, Gray H, Fairhurst A-M, Reimold A, et al. Autoantibody profiling to identify individuals at risk for systemic lupus erythematosus. Journal of Autoimmunity. 2006;27(3):153-60.
67. Li X, Liu X, Cui J, Song W, Liang Y, Hu Y, et al. Epidemiological survey of antinuclear antibodies in healthy population and analysis of clinical characteristics of positive population. Journal of Clinical Laboratory Analysis. 2019;33(8):e22965.
68. Grygiel-Górniak B, Rogacka N, Puszczewicz M. Antinuclear antibodies in healthy people and non-rheumatic diseases - diagnostic and clinical implications. Reumatologia. 2018;56(4):243-8.
69. Knight V, Merkel PA, O'Sullivan MD. Anticytokine Autoantibodies: Association with Infection and Immune Dysregulation. Antibodies (Basel). 2016;5(1).
70. Browne SK, Holland SM. Anticytokine autoantibodies in infectious diseases: pathogenesis and mechanisms. Lancet Infect Dis. 2010;10(12):875-85.
71. Mizutani H, Ohmoto Y, Kupper TS, Shimizu M. Endogenous neutralizing anti-IL-1 alpha autoantibodies in inflammatory skin diseases: possible natural inhibitor for over expressed epidermal IL-1. J Dermatol Sci. 1998;20(1):63-71.
72. Takemura H, Suzuki H, Yoshizaki K, Ogata A, Yuhara T, Akama T, et al. Anti-interleukin-6 autoantibodies in rheumatic diseases. Increased frequency in the sera of patients with systemic sclerosis. Arthritis Rheum. 1992;35(8):940-3.
73. Fudala R, Krupa A, Stankowska D, Allen TC, Kurdowska AK. Anti-interleukin-8 autoantibody:interleukin-8 immune complexes in acute lung injury/acute respiratory distress syndrome. Clin Sci (Lond). 2008;114(6):403-12.
74. Meager A, Vincent A, Newsom-Davis J, Willcox N. Spontaneous neutralising antibodies to interferon--alpha and interleukin-12 in thymoma-associated autoimmune disease. Lancet. 1997;350(9091):1596-7.
75. Uchida K, Beck DC, Yamamoto T, Berclaz PY, Abe S, Staudt MK, et al. GM-CSF autoantibodies and neutrophil dysfunction in pulmonary alveolar proteinosis. N Engl J Med. 2007;356(6):567-79.
76. Czaja CA, Merkel PA, Chan ED, Lenz LL, Wolf ML, Alam R, et al. Rituximab as successful adjunct treatment in a patient with disseminated nontuberculous mycobacterial infection due to acquired anti-interferon-γ autoantibody. Clin Infect Dis. 2014;58(6):e115-8.
77. Morimoto AM, Flesher DT, Yang J, Wolslegel K, Wang X, Brady A, et al. Association of endogenous anti-interferon-α autoantibodies with decreased interferon-pathway and disease activity in patients with systemic lupus erythematosus. Arthritis Rheum. 2011;63(8):2407-15.
78. Sjöwall C, Ernerudh J, Bengtsson AA, Sturfelt G, Skogh T. Reduced anti-TNFalpha autoantibody levels coincide with flare in systemic lupus erythematosus. J Autoimmun. 2004;22(4):315-23.
79. Strunz B, Maucourant C, Mehta A, Wan H, Du L, Sun D, et al. Type I Interferon Autoantibodies Correlate With Cellular Immune Alterations in Severe COVID-19. The Journal of Infectious Diseases. 2024;230(2):e318-e26.
80. Saheb Sharif-Askari N, Saheb Sharif-Askari F, Bayram OS, Hafezi S, Alsayed HAH, Kasim F, et al. Salivary autoantibodies to type I IFNs: Mirror plasma levels, predispose to severe COVID-19, and enhance feasibility for clinical screening. Heart Lung. 2024;66:31-6.
81. Rosen SH, Castleman B, Liebow AA. Pulmonary alveolar proteinosis. N Engl J Med. 1958;258(23):1123-42.
82. Uchida K, Nakata K, Trapnell BC, Terakawa T, Hamano E, Mikami A, et al. High-affinity autoantibodies specifically eliminate granulocyte-macrophage colony-stimulating factor activity in the lungs of patients with idiopathic pulmonary alveolar proteinosis. Blood. 2004;103(3):1089-98.
83. Kitamura T, Tanaka N, Watanabe J, Uchida, Kanegasaki S, Yamada Y, et al. Idiopathic pulmonary alveolar proteinosis as an autoimmune disease with neutralizing antibody against granulocyte/macrophage colony-stimulating factor. J Exp Med. 1999;190(6):875-80.

84. Höflich C, Sabat R, Rosseau S, Temmesfeld B, Slevogt H, Döcke WD, et al. Naturally occurring anti-IFN-gamma autoantibody and severe infections with Mycobacterium cheloneae and Burkholderia cocovenenans. Blood. 2004;103(2):673-5.
85. Döffinger R, Helbert MR, Barcenas-Morales G, Yang K, Dupuis S, Ceron-Gutierrez L, et al. Autoantibodies to interferon-gamma in a patient with selective susceptibility to mycobacterial infection and organ-specific autoimmunity. Clin Infect Dis. 2004;38(1):e10-4.
86. Patel SY, Ding L, Brown MR, Lantz L, Gay T, Cohen S, et al. Anti-IFN-gamma autoantibodies in disseminated nontuberculous mycobacterial infections. J Immunol. 2005;175(7):4769-76.
87. Ishii T, Tamura A, Matsui H, Nagai H, Akagawa S, Hebisawa A, et al. Disseminated Mycobacterium avium complex infection in a patient carrying autoantibody to interferon-γ. J Infect Chemother. 2013;19(6):1152-7.
88. Kampmann B, Hemingway C, Stephens A, Davidson R, Goodsall A, Anderson S, et al. Acquired predisposition to mycobacterial disease due to autoantibodies to IFN-gamma. J Clin Invest. 2005;115(9):2480-8.
89. Al-Herz W, Bousfiha A, Casanova JL, Chatila T, Conley ME, Cunningham-Rundles C, et al. Primary immunodeficiency diseases: an update on the classification from the international union of immunological societies expert committee for primary immunodeficiency. Front Immunol. 2014;5:162.
90. Bousfiha A, Jeddane L, Picard C, Ailal F, Bobby Gaspar H, Al-Herz W, et al. The 2017 IUIS Phenotypic Classification for Primary Immunodeficiencies. J Clin Immunol. 2018;38(1):129-43.
91. Bastard P, Rosen LB, Zhang Q, Michailidis E, Hoffmann H-H, Zhang Y, et al. Autoantibodies against type I IFNs in patients with life-threatening COVID-19. Science. 2020;370(6515):eabd4585.
92. Goncalves D, Mezidi M, Bastard P, Perret M, Saker K, Fabien N, et al. Antibodies against type I interferon: detection and association with severe clinical outcome in COVID-19 patients. Clinical & Translational Immunology. 2021;10(8):e1327.
93. Troya J, Bastard P, Planas-Serra L, Ryan P, Ruiz M, de Carranza M, et al. Neutralizing Autoantibodies to Type I IFNs in >10% of Patients with Severe COVID-19 Pneumonia Hospitalized in Madrid, Spain. Journal of Clinical Immunology. 2021;41(5):914-22.
94. Koning R, Bastard P, Casanova J-L, Brouwer MC, van de Beek D, van Agtmael M, et al. Autoantibodies against type I interferons are associated with multi-organ failure in COVID-19 patients. Intensive Care Medicine. 2021;47(6):704-6.
95. Wang EY, Mao T, Klein J, Dai Y, Huck JD, Jaycox JR, et al. Diverse functional autoantibodies in patients with COVID-19. Nature. 2021;595(7866):283-8.
96. Solanich X, Rigo-Bonnin R, Gumucio V-D, Bastard P, Rosain J, Philippot Q, et al. Pre-existing Autoantibodies Neutralizing High Concentrations of Type I Interferons in Almost 10% of COVID-19 Patients Admitted to Intensive Care in Barcelona. Journal of Clinical Immunology. 2021;41(8):1733-44.
97. Hofmann H, Pyrc K, van der Hoek L, Geier M, Berkhout B, Pöhlmann S. Human coronavirus NL63 employs the severe acute respiratory syndrome coronavirus receptor for cellular entry. Proc Natl Acad Sci U S A. 2005;102(22):7988-93.
98. Townsend A. Autoimmunity to ACE2 as a possible cause of tissue inflammation in Covid-19. Med Hypotheses. 2020;144:110043.
99. Arthur JM, Forrest JC, Boehme KW, Kennedy JL, Owens S, Herzog C, et al. Development of ACE2 autoantibodies after SARS-CoV-2 infection. PLOS ONE. 2021;16(9):e0257016.
100. Casciola-Rosen L, Thiemann DR, Andrade F, Trejo-Zambrano MI, Leonard EK, Spangler JB, et al. IgM anti-ACE2 autoantibodies in severe COVID-19 activate complement and perturb vascular endothelial function. JCI Insight. 2022;7(9).
101. Lai Y-C, Cheng Y-W, Chao C-H, Chang Y-Y, Chen C-D, Tsai W-J, et al. Antigenic Cross-Reactivity Between SARS-CoV-2 S1-RBD and Its Receptor ACE2. Frontiers in Immunology. 2022;13.
102. Rodriguez-Perez AI, Labandeira CM, Pedrosa MA, Valenzuela R, Suarez-Quintanilla JA, Cortes-Ayaso M, et al. Autoantibodies against ACE2 and angiotensin type-1 receptors increase severity of COVID-19. J Autoimmun. 2021;122:102683.

103. Galipeau Y, Castonguay N, McCluskie PS, Sonoda MT, Keeshan A, Collins E, et al. Autoantibodies Targeting Angiotensin Converting Enzyme 2 Are Prevalent and Not Induced by SARS-CoV-2 Infection. medRxiv. 2024:2024.11.18.24317488.
104. Khajeh Pour S, Scoville C, Tavernier SS, Aghazadeh-Habashi A. Plasma angiotensin peptides as biomarkers of rheumatoid arthritis are correlated with anti-ACE2 auto-antibodies level and disease intensity. Inflammopharmacology. 2022;30(4):1295-302.
105. Labandeira CM, Pedrosa MA, Quijano A, Valenzuela R, Garrido-Gil P, Sanchez-Andrade M, et al. Angiotensin type-1 receptor and ACE2 autoantibodies in Parkinson´s disease. npj Parkinson's Disease. 2022;8(1):76.
106. Takahashi Y, Haga S, Ishizaka Y, Mimori A. Autoantibodies to angiotensin-converting enzyme 2 in patients with connective tissue diseases. Arthritis Research & Therapy. 2010;12(3):R85.
107. Miziołek B, Sieńczyk M, Grzywa R, Łupicka-Słowik A, Kucharz E, Kotyla P, et al. The prevalence and role of functional autoantibodies to angiotensin-converting-enzyme-2 in patients with systemic sclerosis. Autoimmunity. 2021;54(4):181-6.
108. Mecoli CA, Yoshida A, Paik JJ, Lin CT, Danoff S, Hanaoka H, et al. Presence and Implications of Anti-Angiotensin Converting Enzyme-2 Immunoglobulin M Antibodies in Anti-Melanoma-Differentiation-Associated 5 Dermatomyositis. ACR Open Rheumatol. 2022;4(5):457-63.
109. Cristiano A, Fortunati V, Cherubini F, Bernardini S, Nuccetelli M. Anti-phospholipids antibodies and immune complexes in COVID-19 patients: a putative role in disease course for anti-annexin-V antibodies. Clinical Rheumatology. 2021;40(7):2939-45.
110. Deegan MJ. Anti-Phospholipid Antibodies. American Journal of Clinical Pathology. 1992;98(4):390-1.
111. Shoenfeld Y, Twig G, Katz U, Sherer Y. Autoantibody explosion in antiphospholipid syndrome. Journal of Autoimmunity. 2008;30(1):74-83.
112. Rauch J, D'Agnillo P, Subang R, Levine JS. Anti-phospholipid antibodies (aPL) and apoptosis: prothrombin-dependent aPL as a paradigm for phospholipid-dependent interactions with apoptotic cells. Thromb Res. 2004;114(5-6):371-82.
113. Mackworth-Young CG. Antiphospholipid syndrome: multiple mechanisms. Clin Exp Immunol. 2004;136(3):393-401.
114. Levine JS, Branch DW, Rauch J. The Antiphospholipid Syndrome. New England Journal of Medicine. 2002;346(10):752-63.
115. Branch DW, Dudley DJ, Mitchell MD, Creighton KA, Abbott TM, Hammond EH, et al. Immunoglobulin G fractions from patients with antiphospholipid antibodies cause fetal death in BALB/c mice: A model for autoimmune fetal loss. American Journal of Obstetrics and Gynecology. 1990;163(1, Part 1):210-6.
116. Mason AN, Mageed RA, Mackworth-Young CG. The effects of a human IgM monoclonal anticardiolipin antibody on pregnancy in a transgenic mouse model. Lupus. 2001;10(4):289-94.
117. Wassermann A, Neisser A, Bruck C. Eine serodiagnostische Reaktion bei Syphilis. Dtsch Med Wochenschr. 1906;32(19):745-6.
118. Uthman IW, Gharavi AE. Viral infections and antiphospholipid antibodies. Seminars in Arthritis and Rheumatism. 2002;31(4):256-63.
119. Cervera R, Rodríguez-Pintó I, Espinosa G. The diagnosis and clinical management of the catastrophic antiphospholipid syndrome: A comprehensive review. J Autoimmun. 2018;92:1-11.
120. Serrano M, Espinosa G, Serrano A, Cervera R. Antigens and Antibodies of the Antiphospholipid Syndrome as New Allies in the Pathogenesis of COVID-19 Coagulopathy. Int J Mol Sci. 2022;23(9).
121. Zhang Y, Xiao M, Zhang S, Xia P, Cao W, Jiang W, et al. Coagulopathy and Antiphospholipid Antibodies in Patients with Covid-19. N Engl J Med. 2020;382(17):e38.
122. Xiao M, Zhang Y, Zhang S, Qin X, Xia P, Cao W, et al. Antiphospholipid Antibodies in Critically Ill Patients With COVID-19. Arthritis Rheumatol. 2020;72(12):1998-2004.
123. Bowles L, Platton S, Yartey N, Dave M, Lee K, Hart DP, et al. Lupus Anticoagulant and Abnormal Coagulation Tests in Patients with Covid-19. N Engl J Med. 2020;383(3):288-90.

124. Siguret V, Voicu S, Neuwirth M, Delrue M, Gayat E, Stépanian A, et al. Are antiphospholipid antibodies associated with thrombotic complications in critically ill COVID-19 patients? Thromb Res. 2020;195:74-6.
125. Devreese KMJ, Linskens EA, Benoit D, Peperstraete H. Antiphospholipid antibodies in patients with COVID‐19: A relevant observation? Journal of Thrombosis and Haemostasis. 2020;18(9):2191-201.
126. Trahtemberg U, Rottapel R, Dos Santos CC, Slutsky AS, Baker A, Fritzler MJ. Anticardiolipin and other antiphospholipid antibodies in critically ill COVID-19 positive and negative patients. Ann Rheum Dis. 2021;80(9):1236-40.
127. Helms J, Tacquard C, Severac F, Leonard-Lorant I, Ohana M, Delabranche X, et al. High risk of thrombosis in patients with severe SARS-CoV-2 infection: a multicenter prospective cohort study. Intensive Care Med. 2020;46(6):1089-98.
128. Gil-Etayo FJ, Garcinuño S, Lalueza A, Díaz-Simón R, García-Reyne A, Pleguezuelo DE, et al. Anti-Phospholipid Antibodies and COVID-19 Thrombosis: A Co-Star, Not a Supporting Actor. Biomedicines. 2021;9(8).
129. Zuo Y, Estes SK, Ali RA, Gandhi AA, Yalavarthi S, Shi H, et al. Prothrombotic autoantibodies in serum from patients hospitalized with COVID-19. Sci Transl Med. 2020;12(570).
130. Serrano M, Espinosa G, Lalueza A, Bravo-Gallego LY, Diaz-Simón R, Garcinuño S, et al. Beta-2-Glycoprotein-I Deficiency Could Precipitate an Antiphospholipid Syndrome-like Prothrombotic Situation in Patients With Coronavirus Disease 2019. ACR Open Rheumatol. 2021;3(4):267-76.
131. Previtali G, Seghezzi M, Moioli V, Sonzogni A, Cerutti L, Marozzi R, et al. The pathogenesis of thromboembolic disease in covid-19 patients: Could be a catastrophic antiphospholipid syndrome? Thromb Res. 2020;194:192-4.
132. Meroni PL, Borghi MO. Antiphospholipid antibodies and COVID-19 thrombotic vasculopathy: one swallow does not make a summer. Annals of the Rheumatic Diseases. 2021;80(9):1105-7.
133. Manukyan D, Rossmann H, Schulz A, Zeller T, Pfeiffer N, Binder H, et al. Distribution of antiphospholipid antibodies in a large population-based German cohort. Clinical Chemistry and Laboratory Medicine (CCLM). 2016;54(10):1663-70.
134. Pike RM, Sulkin SE, Coggeshall HC. Serological Reactions in Rheumatoid Arthritis: I. Factors Affecting the Agglutination of Sensitized Sheep Erythrocytes in Rheumatoid-Arthritis Serum1. The Journal of Immunology. 1949;63(4):441-6.
135. Ingegnoli F, Castelli R, Gualtierotti R. Rheumatoid Factors: Clinical Applications. Disease Markers. 2013;35(6):726598.
136. Witte T, Hartung K, Sachse C, Matthias T, Fricke M, Kalden JR, et al. Rheumatoid factors in systemic lupus erythematosus: association with clinical and laboratory parameters. SLE study group. Rheumatol Int. 2000;19(3):107-11.
137. Maślińska M, Mańczak M, Kwiatkowska B, Ramsperger V, Shen L, Suresh L. IgA immunoglobulin isotype of rheumatoid factor in primary Sjögren's syndrome. Rheumatol Int. 2021;41(3):643-9.
138. Moore S, Ruska K, Peters L, Olsen NJ. Associations of IgA and IgA-rheumatoid factor with disease features in patients with rheumatoid arthritis. Immunol Invest. 1994;23(6-7):355-65.
139. Banks SE, Riley TR, 3rd, Naides SJ. Musculoskeletal complaints and serum autoantibodies associated with chronic hepatitis C and nonalcoholic fatty liver disease. Dig Dis Sci. 2007;52(5):1177-82.
140. Charles ED, Orloff MI, Nishiuchi E, Marukian S, Rice CM, Dustin LB. Somatic hypermutations confer rheumatoid factor activity in hepatitis C virus-associated mixed cryoglobulinemia. Arthritis Rheum. 2013;65(9):2430-40.
141. Xu C, Fan J, Luo Y, Zhao Z, Tang P, Yang G, et al. Prevalence and Characteristics of Rheumatoid-Associated Autoantibodies in Patients with COVID-19. J Inflamm Res. 2021;14:3123-8.
142. Jeong H, Baek AR, Park SW, Kim T, Choo EJ, Jeon CH. Rheumatoid factor is associated with severe COVID-19. International Journal of Rheumatic Diseases. 2023;26(5):850-61.
143. Elghali M, Bannour I, Touil I, Changuel M, Brahem Y, Jaoued O, et al. Increased Rheumatoid Factor production in patients with severe COVID-19. Diagn Microbiol Infect Dis. 2024;109(3):116284.

144. Anaya JM, Monsalve DM, Rojas M, Rodríguez Y, Montoya-García N, Mancera-Navarro LM, et al. Latent rheumatic, thyroid and phospholipid autoimmunity in hospitalized patients with COVID-19. J Transl Autoimmun. 2021;4:100091.
145. Amjadi MF, Parker MH, Adyniec RR, Zheng Z, Robbins AM, Bashar SJ, et al. Novel and unique rheumatoid factors cross-react with viral epitopes in COVID-19. J Autoimmun. 2024;142:103132.
146. Ashe WK, Daniels CA, Scott GS, Notkins AL. Interaction of Rheumatoid Factor with Infectious Herpes Simplex Virus-Antibody Complexes. Science. 1971;172(3979):176-7.
147. Van Snick JL, Van Roost E, Markowetz B, Cambiaso CL, Masson PL. Enhancement by IgM rheumatoid factor of in vitro ingestion by macrophages and in vivo clearance of aggregated IgG or antigen-antibody complexes. European Journal of Immunology. 1978;8(4):279-85.
148. Roosnek E, Lanzavecchia A. Efficient and selective presentation of antigen-antibody complexes by rheumatoid factor B cells. J Exp Med. 1991;173(2):487-9.
149. Alghamdi M, Alasmari D, Assiri A, Mattar E, Aljaddawi AA, Alattas SG, et al. An Overview of the Intrinsic Role of Citrullination in Autoimmune Disorders. J Immunol Res. 2019;2019:7592851.
150. Girbal-Neuhauser E, Durieux JJ, Arnaud M, Dalbon P, Sebbag M, Vincent C, et al. The epitopes targeted by the rheumatoid arthritis-associated antifilaggrin autoantibodies are posttranslationally generated on various sites of (pro)filaggrin by deimination of arginine residues. J Immunol. 1999;162(1):585-94.
151. Rantapää-Dahlqvist S, de Jong BA, Berglin E, Hallmans G, Wadell G, Stenlund H, et al. Antibodies against cyclic citrullinated peptide and IgA rheumatoid factor predict the development of rheumatoid arthritis. Arthritis Rheum. 2003;48(10):2741-9.
152. Willemze A, Trouw LA, Toes REM, Huizinga TWJ. The influence of ACPA status and characteristics on the course of RA. Nature Reviews Rheumatology. 2012;8(3):144-52.
153. Perrot L, Hemon M, Busnel JM, Muis-Pistor O, Picard C, Zandotti C, et al. First flare of ACPA-positive rheumatoid arthritis after SARS-CoV-2 infection. Lancet Rheumatol. 2021;3(1):e6-e8.
154. Derksen VFAM, Kissel T, Lamers-Karnebeek FBG, van der Bijl AE, Venhuizen AC, Huizinga TWJ, et al. Onset of rheumatoid arthritis after COVID-19: coincidence or connected? Annals of the Rheumatic Diseases. 2021;80(8):1096-8.
155. Ursini F, Ruscitti P, D'Angelo S, Cacciapaglia F, De Angelis R, Campochiaro C, et al. Broad clinical spectrum of SARS-CoV-2-associated inflammatory joint disease in adults: a report of 35 cases from the COVID-19 & Autoimmune Systemic Disease Italian study group. Annals of the Rheumatic Diseases. 2021;80(11):1498-501.
156. Lingel H, Meltendorf S, Billing U, Thurm C, Vogel K, Majer C, et al. Unique autoantibody prevalence in long-term recovered SARS-CoV-2-infected individuals. J Autoimmun. 2021;122:102682.
157. Kitching AR, Anders H-J, Basu N, Brouwer E, Gordon J, Jayne DR, et al. ANCA-associated vasculitis. Nature Reviews Disease Primers. 2020;6(1):71.
158. Selvaraj V, Moustafa A, Dapaah-Afriyie K, Birkenbach MP. COVID-19-induced granulomatosis with polyangiitis. BMJ Case Reports. 2021;14(3):e242142.
159. Uppal NN, Kello N, Shah HH, Khanin Y, De Oleo IR, Epstein E, et al. De Novo ANCA-Associated Vasculitis With Glomerulonephritis in COVID-19. Kidney Int Rep. 2020;5(11):2079-83.
160. Klein J, Wood J, Jaycox JR, Dhodapkar RM, Lu P, Gehlhausen JR, et al. Distinguishing features of long COVID identified through immune profiling. Nature. 2023;623(7985):139-48.
161. Credle JJ, Gunn J, Sangkhapreecha P, Monaco DR, Zheng XA, Tsai H-J, et al. Unbiased discovery of autoantibodies associated with severe COVID-19 via genome-scale self-assembled DNA-barcoded protein libraries. Nature Biomedical Engineering. 2022;6(8):992-1003.
162. Matsuda KM, Kawase Y, Iwadoh K, Kurano M, Yatomi Y, Okamoto K, et al. Proteome-wide autoantibody screening and holistic autoantigenomic analysis unveil COVID-19 signature of autoantibody landscape. medRxiv. 2024:2024.06.07.24308592.
163. Avrameas S, Alexopoulos H, Moutsopoulos HM. Natural Autoantibodies: An Undersugn Hero of the Immune System and Autoimmune Disorders—A Point of View. Frontiers in Immunology. 2018;9.
164. Boes M. Role of natural and immune IgM antibodies in immune responses. Mol Immunol. 2000;37(18):1141-9.

165. Lee W, Gaca JG, Edwards LA, Braedehoeft SJ, Parker W, Davis RD. Binding of polyreactive antibodies to self versus foreign antigens. Immunobiology. 2002;205(1):95-107.
166. Coutinho A, Kazatchkine MD, Avrameas S. Natural autoantibodies. Current Opinion in Immunology. 1995;7(6):812-8.
167. Maddur MS, Lacroix-Desmazes S, Dimitrov JD, Kazatchkine MD, Bayry J, Kaveri SV. Natural Antibodies: from First-Line Defense Against Pathogens to Perpetual Immune Homeostasis. Clinical Reviews in Allergy & Immunology. 2020;58(2):213-28.
168. Stewart J. Immunoglobulins did not arise in evolution to fight infection. Immunology Today. 1992;13(10):396-9.
169. Duong BH, Ota T, Aoki-Ota M, Cooper AB, Ait-Azzouzene D, Vela JL, et al. Negative Selection by IgM Superantigen Defines a B Cell Central Tolerance Compartment and Reveals Mutations Allowing Escape. The Journal of Immunology. 2011;187(11):5596-605.
170. Nemazee D. Mechanisms of central tolerance for B cells. Nature Reviews Immunology. 2017;17(5):281-94.
171. Cambier JC, Gauld SB, Merrell KT, Vilen BJ. B-cell anergy: from transgenic models to naturally occurring anergic B cells? Nature Reviews Immunology. 2007;7(8):633-43.
172. Baumgarth N. B-1 Cell Heterogeneity and the Regulation of Natural and Antigen-Induced IgM Production. Frontiers in Immunology. 2016;7.
173. Lalor PA. An Evolutionarily-Conserved Role for Murine Ly-1 B Cells in Protection Against Bacterial Infections. Autoimmunity. 1991;10(1):71-6.
174. Baumgarth N. The double life of a B-1 cell: self-reactivity selects for protective effector functions. Nature Reviews Immunology. 2011;11(1):34-46.
175. Zhou ZH, Notkins AL. Polyreactive antigen-binding B (PAB-) cells are widely distributed and the PAB population consists of both B-1+ and B-1- phenotypes. Clin Exp Immunol. 2004;137(1):88-100.
176. Rojas M, Restrepo-Jiménez P, Monsalve DM, Pacheco Y, Acosta-Ampudia Y, Ramírez-Santana C, et al. Molecular mimicry and autoimmunity. Journal of Autoimmunity. 2018;95:100-23.
177. Kohm AP, Fuller KG, Miller SD. Mimicking the way to autoimmunity: an evolving theory of sequence and structural homology. Trends in Microbiology. 2003;11(3):101-5.
178. Kanduc D, Stufano A, Lucchese G, Kusalik A. Massive peptide sharing between viral and human proteomes. Peptides. 2008;29(10):1755-66.
179. Agmon-Levin N, Blank M, Paz Z, Shoenfeld Y. Molecular mimicry in systemic lupus erythematosus. Lupus. 2009;18(13):1181-5.
180. Oldstone MB. Molecular mimicry and immune-mediated diseases. Faseb j. 1998;12(13):1255-65.
181. Wildner G, Diedrichs-Möhring M. Molecular Mimicry and Uveitis. Frontiers in Immunology. 2020;11.
182. Kaplan M, Meyeserian M. AN IMMUNOLOGICAL CROSS-REACTION BETWEEN GROUP-A STREPTOCOCCAL CELLS AND HUMAN HEART TISSUE. The Lancet. 1962;279(7232):706-10.
183. He D, Zhang H, Xiao J, Zhang X, Xie M, Pan D, et al. Molecular and clinical relationship between live-attenuated Japanese encephalitis vaccination and childhood onset myasthenia gravis. Ann Neurol. 2018;84(3):386-400.
184. Lucchese G, Kanduc D. Zika virus and autoimmunity: From microcephaly to Guillain-Barré syndrome, and beyond. Autoimmun Rev. 2016;15(8):801-8.
185. Lindsey JW. Antibodies to the Epstein-Barr virus proteins BFRF3 and BRRF2 cross-react with human proteins. J Neuroimmunol. 2017;310:131-4.
186. Robinson WH, Steinman L. Epstein-Barr virus and multiple sclerosis. Science. 2022;375(6578):264-5.
187. Anaya J-M, Ramirez-Santana C, Salgado-Castaneda I, Chang C, Ansari A, Gershwin ME. Zika virus and neurologic autoimmunity: the putative role of gangliosides. BMC Medicine. 2016;14(1):49.
188. Luo G, Ambati A, Lin L, Bonvalet M, Partinen M, Ji X, et al. Autoimmunity to hypocretin and molecular mimicry to flu in type 1 narcolepsy. Proceedings of the National Academy of Sciences. 2018;115(52):E12323-E32.

189. Zhao Z-S, Granucci F, Yeh L, Schaffer PA, Cantor H. Molecular Mimicry by Herpes Simplex Virus-Type 1: Autoimmune Disease After Viral Infection. Science. 1998;279(5355):1344-7.
190. Lanz TV, Brewer RC, Ho PP, Moon JS, Jude KM, Fernandez D, et al. Clonally expanded B cells in multiple sclerosis bind EBV EBNA1 and GlialCAM. Nature. 2022;603(7900):321-7.
191. Kanduc D. From Anti-SARS-CoV-2 Immune Responses to COVID-19 via Molecular Mimicry. Antibodies (Basel). 2020;9(3).
192. Khavinson V, Terekhov A, Kormilets D, Maryanovich A. Homology between SARS CoV-2 and human proteins. Sci Rep. 2021;11(1):17199.
193. O'Donoghue SI, Schafferhans A, Sikta N, Stolte C, Kaur S, Ho BK, et al. SARS-CoV-2 structural coverage map reveals viral protein assembly, mimicry, and hijacking mechanisms. Mol Syst Biol. 2021;17(9):e10079.
194. Nunez-Castilla J, Stebliankin V, Baral P, Balbin CA, Sobhan M, Cickovski T, et al. Potential Autoimmunity Resulting from Molecular Mimicry between SARS-CoV-2 Spike and Human Proteins. Viruses. 2022;14(7).
195. Liblau R, Gautam AM. HLA, molecular mimicry and multiple sclerosis. Rev Immunogenet. 2000;2(1):95-104.
196. Jerne NK. Towards a network theory of the immune system. Ann Immunol (Paris). 1974;125c(1-2):373-89.
197. Murphy WJ, Longo DL. A Possible Role for Anti-idiotype Antibodies in SARS-CoV-2 Infection and Vaccination. New England Journal of Medicine. 2021;386(4):394-6.
198. Shukla AK, Misra S. Clinical implications of anti-idiotype antibodies in COVID-19. Journal of Basic and Clinical Physiology and Pharmacology. 2022;33(6):727-33.
199. Burdette S, Schwartz RS. Idiotypes and Idiotypic Networks. New England Journal of Medicine. 1987;317(4):219-24.
200. Lanier LL, Babcock GF, Raybourne RB, Arnold LW, Warner NL, Haughton G. Mechanism of B cell lymphoma immunotherapy with passive xenogeneic anti-idiotype serum. The Journal of Immunology. 1980;125(4):1730-6.
201. Hamblin T, Cattan A, Glennie M, MacKenzie M, Stevenson F, Watts H, et al. Initial experience in treating human lymphoma with a chimeric univalent derivative of monoclonal anti-idiotype antibody. Blood. 1987;69(3):790-7.
202. Bona C, Moran T. Idiotype vaccines. Annales de l'Institut Pasteur / Immunologie. 1985;136(3, Part 3):299-312.
203. Sharpe AH, Gaulton GN, McDade KK, Fields BN, Greene MI. Syngeneic monoclonal antiidiotype can induce cellular immunity to reovirus. Journal of Experimental Medicine. 1984;160(4):1195-205.
204. Powell AM, Black MM. Epitope spreading: protection from pathogens, but propagation of autoimmunity? Clin Exp Dermatol. 2001;26(5):427-33.
205. Lehmann PV, Forsthuber T, Miller A, Sercarz EE. Spreading of T-cell autoimmunity to cryptic determinants of an autoantigen. Nature. 1992;358(6382):155-7.
206. Li N, Aoki V, Hans-Filho G, Rivitti EA, Diaz LA. The role of intramolecular epitope spreading in the pathogenesis of endemic pemphigus foliaceus (fogo selvagem). J Exp Med. 2003;197(11):1501-10.
207. Didona D, Di Zenzo G. Humoral Epitope Spreading in Autoimmune Bullous Diseases. Frontiers in Immunology. 2018;9.
208. Vanderlugt CL, Miller SD. Epitope spreading in immune-mediated diseases: implications for immunotherapy. Nature Reviews Immunology. 2002;2(2):85-95.
209. Chan LS, Vanderlugt CJ, Hashimoto T, Nishikawa T, Zone JJ, Black MM, et al. Epitope Spreading: Lessons From Autoimmune Skin Diseases. Journal of Investigative Dermatology. 1998;110(2):103-9.
210. Cornaby C, Gibbons L, Mayhew V, Sloan CS, Welling A, Poole BD. B cell epitope spreading: Mechanisms and contribution to autoimmune diseases. Immunology Letters. 2015;163(1):56-68.
211. Miller SD, Katz-Levy Y, Neville KL, Vanderlugt CL. Virus-induced autoimmunity: Epitope spreading to myelin autoepitopes in theiler's virus infection of the central nervous system. Advances in Virus Research. 56: Academic Press; 2001. p. 199-217.

212. D'Agnillo F, Walters K-A, Xiao Y, Sheng Z-M, Scherler K, Park J, et al. Lung epithelial and endothelial damage, loss of tissue repair, inhibition of fibrinolysis, and cellular senescence in fatal COVID-19. Science Translational Medicine. 2021;13(620):eabj7790.
213. Sauter JL, Baine MK, Butnor KJ, Buonocore DJ, Chang JC, Jungbluth AA, et al. Insights into pathogenesis of fatal COVID-19 pneumonia from histopathology with immunohistochemical and viral RNA studies. Histopathology. 2020;77(6):915-25.
214. Pacheco Y, Acosta-Ampudia Y, Monsalve DM, Chang C, Gershwin ME, Anaya J-M. Bystander activation and autoimmunity. Journal of Autoimmunity. 2019;103:102301.
215. Tough DF, Borrow P, Sprent J. Induction of Bystander T Cell Proliferation by Viruses and Type I Interferon in Vivo. Science. 1996;272(5270):1947-50.
216. Lee H, Jeong S, Shin E-C. Significance of bystander T cell activation in microbial infection. Nature Immunology. 2022;23(1):13-22.
217. Di Genova G, Savelyeva N, Suchacki A, Thirdborough SM, Stevenson FK. Bystander stimulation of activated CD4+ T cells of unrelated specificity following a booster vaccination with tetanus toxoid. European Journal of Immunology. 2010;40(4):976-85.
218. Eberl Gr, Brawand P, MacDonald HR. Selective Bystander Proliferation of Memory CD4+ and CD8+ T Cells Upon NK T or T Cell Activation. The Journal of Immunology. 2000;165(8):4305-11.
219. Doisne J-M, Urrutia A, Lacabaratz-Porret C, Goujard Cc, Meyer L, Chaix M-L, et al. CD8+ T Cells Specific for EBV, Cytomegalovirus, and Influenza Virus Are Activated during Primary HIV Infection1. The Journal of Immunology. 2004;173(4):2410-8.
220. Chu T, Tyznik AJ, Roepke S, Berkley AM, Woodward-Davis A, Pattacini L, et al. Bystander-activated memory CD8 T cells control early pathogen load in an innate-like, NKG2D-dependent manner. Cell Rep. 2013;3(3):701-8.
221. Kim T-S, Shin E-C. The activation of bystander CD8+ T cells and their roles in viral infection. Experimental & Molecular Medicine. 2019;51(12):1-9.
222. Pan Q, Liu Z, Liao S, Ye L, Lu X, Chen X, et al. Current mechanistic insights into the role of infection in systemic lupus erythematosus. Biomedicine & Pharmacotherapy. 2019;117:109122.
223. Quaglia M, Merlotti G, De Andrea M, Borgogna C, Cantaluppi V. Viral Infections and Systemic Lupus Erythematosus: New Players in an Old Story. Viruses. 2021;13(2).
224. Kobayashi M, Yasui N, Ishimaru N, Arakaki R, Hayashi Y. Development of autoimmune arthritis with aging via bystander T cell activation in the mouse model of Sjögren's syndrome. Arthritis Rheum. 2004;50(12):3974-84.
225. McLachlan SM, Rapoport B. Breaking Tolerance to Thyroid Antigens: Changing Concepts in Thyroid Autoimmunity. Endocrine Reviews. 2014;35(1):59-105.
226. Montazersaheb S, Hosseiniyan Khatibi SM, Hejazi MS, Tarhriz V, Farjami A, Ghasemian Sorbeni F, et al. COVID-19 infection: an overview on cytokine storm and related interventions. Virology Journal. 2022;19(1):92.
227. Neufeldt CJ, Cerikan B, Cortese M, Frankish J, Lee J-Y, Plociennikowska A, et al. SARS-CoV-2 infection induces a pro-inflammatory cytokine response through cGAS-STING and NF-κB. Communications Biology. 2022;5(1):45.
228. Wucherpfennig KW. Mechanisms for the induction of autoimmunity by infectious agents. The Journal of Clinical Investigation. 2001;108(8):1097-104.
229. Woodruff MC, Ramonell RP, Haddad NS, Anam FA, Rudolph ME, Walker TA, et al. Dysregulated naive B cells and de novo autoreactivity in severe COVID-19. Nature. 2022;611(7934):139-47.
230. Guthmiller JJ, Lan LY, Fernández-Quintero ML, Han J, Utset HA, Bitar DJ, et al. Polyreactive Broadly Neutralizing B cells Are Selected to Provide Defense against Pandemic Threat Influenza Viruses. Immunity. 2020;53(6):1230-44.e5.
231. Haynes BF, Fleming J, St. Clair EW, Katinger H, Stiegler G, Kunert R, et al. Cardiolipin Polyspecific Autoreactivity in Two Broadly Neutralizing HIV-1 Antibodies. Science. 2005;308(5730):1906-8.
232. Jolles S, Sewell WA, Misbah SA. Clinical uses of intravenous immunoglobulin. Clin Exp Immunol. 2005;142(1):1-11.

233. Berger M, McCallus DE, Lin CS. Rapid and reversible responses to IVIG in autoimmune neuromuscular diseases suggest mechanisms of action involving competition with functionally important autoantibodies. J Peripher Nerv Syst. 2013;18(4):275-96.
234. Siragam V, Crow AR, Brinc D, Song S, Freedman J, Lazarus AH. Intravenous immunoglobulin ameliorates ITP via activating Fcγ receptors on dendritic cells. Nature Medicine. 2006;12(6):688-92.
235. Ben Mkaddem S, Benhamou M, Monteiro RC. Understanding Fc Receptor Involvement in Inflammatory Diseases: From Mechanisms to New Therapeutic Tools. Frontiers in Immunology. 2019;10.
236. Fonseca DLM, Filgueiras IS, Marques AHC, Vojdani E, Halpert G, Ostrinski Y, et al. Severe COVID-19 patients exhibit elevated levels of autoantibodies targeting cardiolipin and platelet glycoprotein with age: a systems biology approach. NPJ Aging. 2023;9(1):21.
237. Jaycox JR, Lucas C, Yildirim I, Dai Y, Wang EY, Monteiro V, et al. SARS-CoV-2 mRNA vaccines decouple anti-viral immunity from humoral autoimmunity. Nature Communications. 2023;14(1):1299.
238. Sacchi MC, Pelazza C, Bertolotti M, Agatea L, De Gaspari P, Tamiazzo S, et al. The onset of de novo autoantibodies in healthcare workers after mRNA based anti-SARS-CoV-2 vaccines: a single centre prospective follow-up study. Autoimmunity. 2023;56(1):2229072.
239. Ning W, Xu W, Cong X, Fan H, Gilkeson G, Wu X, et al. COVID-19 mRNA vaccine BNT162b2 induces autoantibodies against type I interferons in a healthy woman. J Autoimmun. 2022;132:102896.
240. Peng K, Li X, Yang D, Chan SCW, Zhou J, Wan EYF, et al. Risk of autoimmune diseases following COVID-19 and the potential protective effect from vaccination: a population-based cohort study. EClinicalMedicine. 2023;63:102154.
241. Olivieri B, Betterle C, Zanoni G. Vaccinations and Autoimmune Diseases. Vaccines (Basel). 2021;9(8).
242. Feng A, Yang EY, Moore AR, Dhingra S, Chang SE, Yin X, et al. Autoantibodies are highly prevalent in non–SARS-CoV-2 respiratory infections and critical illness. JCI Insight. 2023;8(3).
243. Meroni PL, Schur PH. ANA screening: an old test with new recommendations. Annals of the Rheumatic Diseases. 2010;69(8):1420-2.
244. Mahler M. Lack of standardisation of ANA and implications for drug development and precision medicine. Annals of the Rheumatic Diseases. 2019;78(5):e33-e.
245. Lebedin M, García CV, Spatt L, Ratswohl C, Thibeault C, Ostendorf L, et al. Discriminating promiscuous from target-specific autoantibodies in COVID-19. Eur J Immunol. 2023;53(5):e2250210.
246. Shome M, Chung Y, Chavan R, Park JG, Qiu J, LaBaer J. Serum autoantibodyome reveals that healthy individuals share common autoantibodies. Cell Reports. 2022;39(9):110873.
247. Chang R, Yen-Ting Chen T, Wang S-I, Hung Y-M, Chen H-Y, Wei C-CJ. Risk of autoimmune diseases in patients with COVID-19: a retrospective cohort study. eClinicalMedicine. 2023;56.
248. Machhi J, Herskovitz J, Senan AM, Dutta D, Nath B, Oleynikov MD, et al. The Natural History, Pathobiology, and Clinical Manifestations of SARS-CoV-2 Infections. Journal of Neuroimmune Pharmacology. 2020;15(3):359-86.
249. Tesch F, Ehm F, Vivirito A, Wende D, Batram M, Loser F, et al. Incident autoimmune diseases in association with SARS-CoV-2 infection: a matched cohort study. Clin Rheumatol. 2023;42(10):2905-14.

A-1.24 Dried blood spot specimens for SARS-CoV-2 antibody testing: a multi-site multi-assay comparison

Preface

(This work has been previously published as a research article)

Cholette F., Mesa C., Harris A., Ellis H., Cachero K., Lacap P., **Galipeau Y.**, Langlois MA., Gingras AC., Yansouni CP., Papenburg J., Cheng MP., Chakraborty P., Stein DR., Van Caeseele P., Bartlett S., Krajden M., Goldfarb D., McGeer A., Osiowy C., Hankins C., Mazer B., Drebot M., Kim J.; COVID-19 Immunity Task Force (CITF) working group. **Dried blood spot specimens for SARS-CoV-2 antibody testing: A multi-site, multi-assay comparison.** PLoS One. 2021 Dec 7;16(12):e0261003.

https://doi.org/10.1371/journal.pone.0261003

© 2021 Cholette et al. This is an open access article distributed under the terms of the Creative Commons Attribution License, which permits unrestricted use, distribution, and reproduction in any medium, provided the original author and source are credited.

Abstract

The true severity of infection due to COVID-19 is under-represented because it is based on only those who are tested. Although nucleic acid amplifications tests (NAAT) are the gold standard for COVID-19 diagnostic testing, serological assays provide better population-level SARS-CoV-2 prevalence estimates. Implementing large sero-surveys present several logistical challenges within Canada due its unique geography including rural and remote communities. Dried blood spot (DBS) sampling is a practical solution but comparative performance data on SARS-CoV-2 serological tests using DBS is currently lacking. Here we present test performance data from a well-characterized SARS-CoV-2 DBS panel sent to laboratories across Canada representing 10 commercial and 2 in-house developed tests for SARS-CoV-2 antibodies. Three commercial assays identified all positive and negative DBS correctly corresponding to a sensitivity, specificity, positive predictive value, and negative predictive value of 100% (95% CI = 72.2, 100). Two in-house assays also performed equally well. In contrast, several commercial assays could not achieve a sensitivity greater than 40% or a negative predictive value greater than 60%. Our findings represent the foundation for future validation studies on DBS specimens that will play a central role in strengthening Canada's public health policy in response to COVID-19.

Introduction

According to the latest estimates from John Hopkins University (last accessed on 9 September 2021), severe acute respiratory syndrome coronavirus (SARS-CoV2), the etiological agent of coronavirus disease 2019 (COVID-19) [1], is responsible for over 220 million confirmed cases, including over 4.5 million deaths globally [2]. While nucleic acid amplification tests (NAAT) on respiratory samples remain the gold standard for COVID-19 diagnostic testing [3], they cannot provide reliable prevalence and incidence estimates at the population level given the narrow window for reliable results (<14 days post-symptom onset) [4], global supply shortages [5], and limited access due to symptom-based testing prioritization [6]. On the other hand, serological assays may provide more reliable population-level SARS-CoV-2 prevalence estimates to better inform ongoing public health responses [7]. Serological testing is also vitally important for monitoring both individual and population-level humoral immune responses to COVID-19 vaccination [8].

Several commercial serological assays rapidly became available through measures such as the US Food and Drug Administration's (FDA) Emergency Use Authorization programme [9]. These assays have been primarily designed for the detection of SARS-CoV-2 antibodies in serum, plasma, or whole blood [10–13]. Implementing large-scale integrated biological-behavioural surveys poses a significant challenge since phlebotomy requires highly trained personnel when most health care professionals have been re-deployed to assist in the COVID-19 response [14]. Furthermore, reaching rural and remote communities adds to the complexity of providing reliable and timely testing for several reasons including lack of trained personnel to collect biological specimens, limited access to laboratory facilities, difficulties in maintaining the cold chain, and unreliable specimen transportation even within the Canadian context. The implementation of SARS-CoV-2 point-of-care (POC) testing [15–18] could alleviate some of these challenges but may not be appropriate in all settings. Rural and remote communities tend to be small and have close-knit social networks thereby making confidential or anonymous SARS-CoV-2 POC testing difficult. Thus, a practical solution is required to be able to achieve large scale sampling and

circumvent these problematic issues. Dried blood spot (DBS) collection may be a practical solution owing to this method's simplicity.

DBS are prepared by placing a few drops of blood on a card made of filter paper. A finger prick is performed using standard spring-loaded lancets that do not require specialised training to utilize. Home-self collection is also a viable option that is already playing a significant role in SARS-CoV-2 sero-surveillance [19,20]. Once the DBS cards are dry, they can be stored and transported at ambient temperature to centralized laboratories through regular mail services without any adverse effect on downstream testing [21]. However, comparative performance data on SARS-CoV-2 serological assays using DBS specimens are limited. Here we present test performance data from a SARS-CoV-2 DBS panel sent to various public health and academic laboratories across Canada representing 10 commercial and 2 in-house developed assays for SARS-CoV-2 antibodies. As part of the COVID-19 Immunity Task Force (CITF, www.covid19immunitytaskforce.ca/), our goal was to provide preliminary performance data on each test to guide future large-scale validations.

Results

Assay performance

Sensitivity, specificity, positive predictive values (PPV), and negative predictive values (NPV) were assessed for 10 commercial and 2 in-house assays on 10 known negative plasma samples and 10 plasma samples from COVID-19 patients (Table 1) contrived as DBS. Nearly one third of all commercial assays (EUROIMMUN, Elecsys spike, and GSP/DELFIA) identified all positive and negative DBS correctly corresponding to a sensitivity, specificity, PPV, and NPV of 100% (95% CI = 72.2, 100) even when using a wide range of prevalence estimates (Figs 1 and S1). The Elecsys spike and GSP/DELFIA showed almost perfect agreement with EUROIMMUN as well as with one another (Tables 1 and S1, Fig 2).

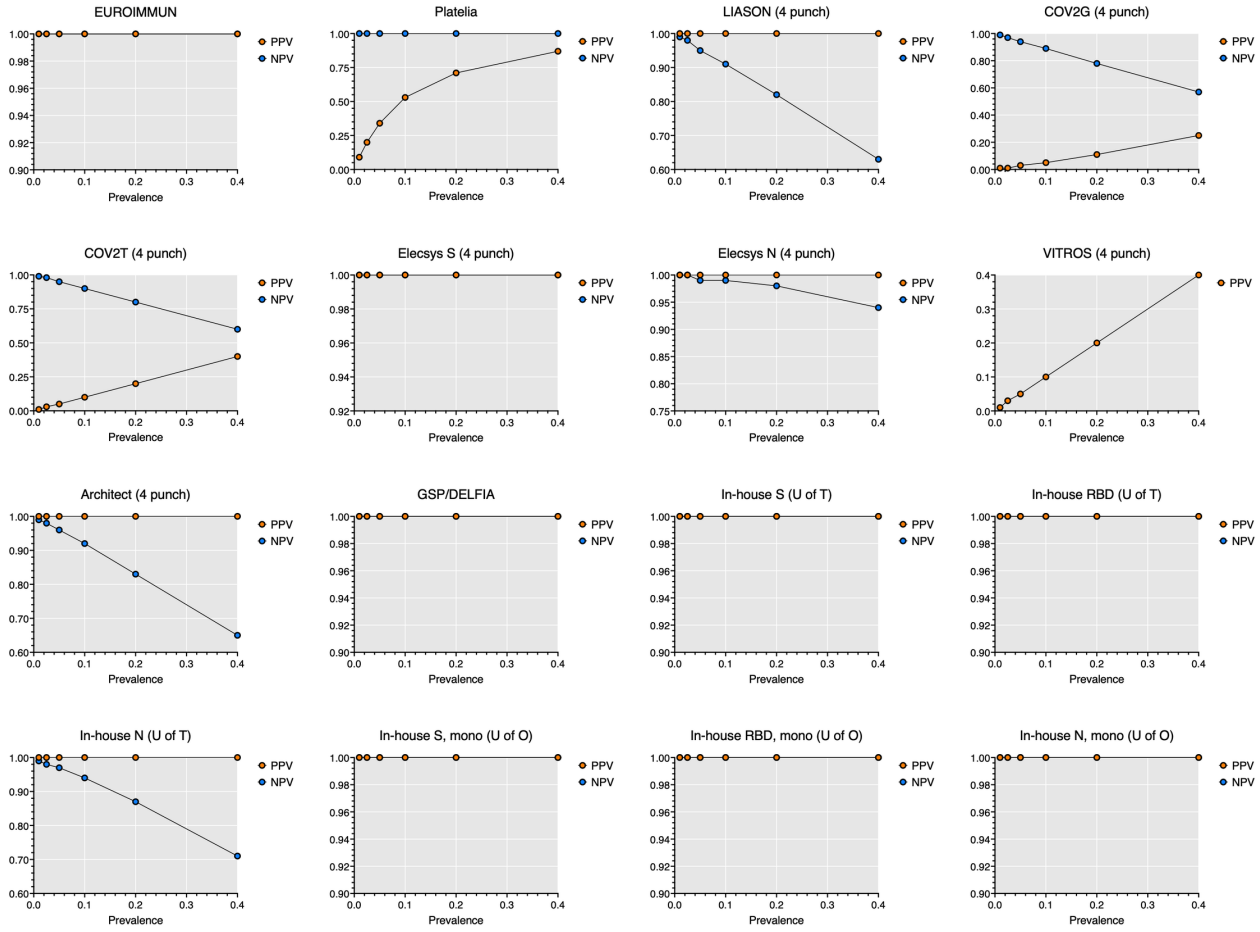


Fig 1. Positive predictive values (PPV) and negative predictive values (NPV) by prevalence for each commercial and in-house assay on dried blood spot specimens. PPV and NPV is presented for *n* = 10 SARS-CoV-2 antibody negative DBS specimens and *n* = 10 SARS-CoV-2 antibody positive DBS specimens. One 6 mm (1/4 inch) punch was used for the EUROIMMUN assay and two 6 mm (1/4 inch) punches were used for the Platelia and in-house assays. Data from four 6 mm (1/4 inch) punches is presented for all other assays. EUROIMMUN = Anti-SARS-CoV-2 ELISA assay (EUROIMMUN, Lübeck, Germany). Platelia = SARS-CoV-2 assay (Bio-Rad, Hercules, California). LIASON = SARS-CoV-2 assay (DiaSorin, Saluggia, Italy). COV2G = SARS-CoV-2 COV2G assay (Siemens, Erlangen, Germany). COV2T = SARS-CoV-2 COV2T assay (Siemens). Elecsys S = Quantitative Anti-SARS-CoV-2 assay (Elecsys spike; Roche, Basel, Switzerland). Elecsys N = Anti-SARS-CoV-2 assay (Elecsys nucleocapsid; Roche). VITROS = Anti-SARS-CoV-2 assay (Ortho Clinical Diagnostics, Raritan, New Jersey). Architect = SARS-CoV-2 assay (Abbott, Mississauga, Canada). GSP/DELFIA = Anti-SARS-CoV-2 assay (PerkinElmer, Waltham, Massachusetts). In-house S (U of T) = In-house spike assay (University of Toronto). In-house RBD (U of T) = In-house RBD assay (University of Toronto). In-house N (U of T) = In-house nucleocapsid assay (University of Toronto). In-house S, mono (U of O) = In-house monoclonal spike assay (University of Ottawa). In-house RBD, mono (U of O) = In-house monoclonal RBD assay (University of Ottawa). In-house N, mono (U of O) = In-house monoclonal nucleocapsid assay (University of Ottawa). The VITROS assay could not achieve a specificity greater than 0% therefore, only PPV is shown.

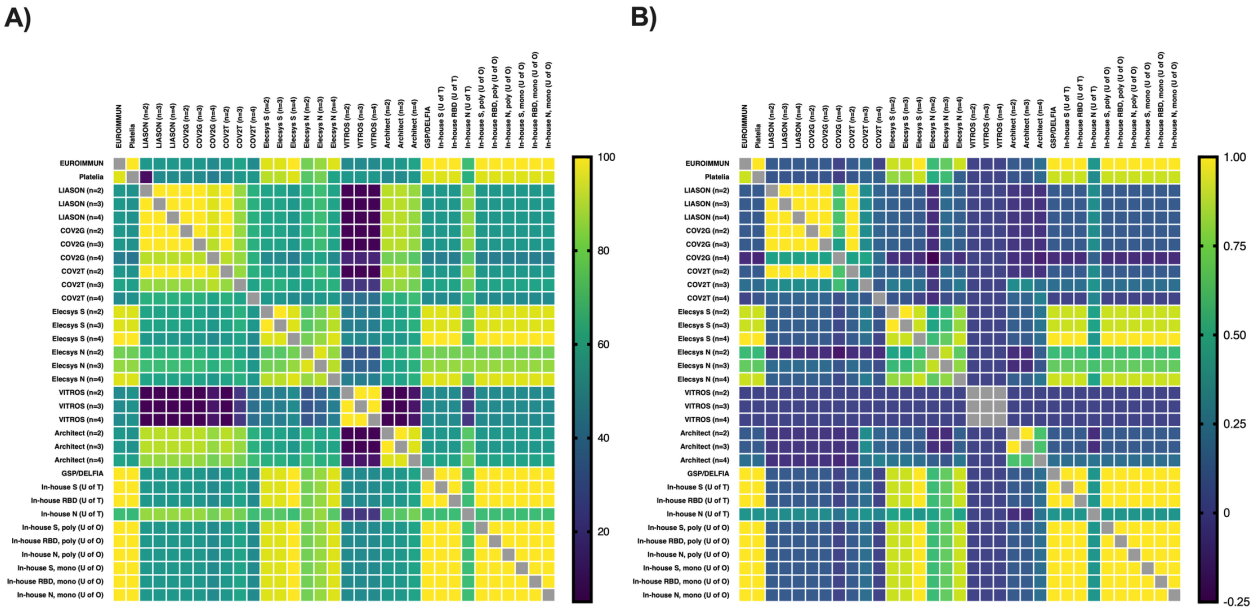


Fig 2. Inter-assay concordance (A) and Cohen's kappa coefficient (B) for SARS-CoV-2 antibody testing on dried blood spot specimens. Concordance (%) and Cohen's kappa coefficient are presented for n = 10 SARS-CoV-2 antibody negative DBS specimens and n = 10 SARS-CoV-2 antibody positive DBS specimens. One 6 mm (1/4 inch) punch was used for the EUROIMMUN assay and two 6 mm (1/4 inch) punches were used for the Platelia and in-house assays. EUROIMMUN = Anti-SARS-CoV-2 ELISA assay (EUROIMMUN, Lübeck, Germany). Platelia = SARS-CoV-2 assay (Bio-Rad, Hercules, California). LIASON = SARS-CoV-2 assay (DiaSorin, Saluggia, Italy). COV2G = SARS-CoV-2 COV2G assay (Siemens, Erlangen, Germany). COV2T = SARS-CoV-2 COV2T assay (Siemens). Elecsys S = Quantitative Anti-SARS-CoV-2 assay (Elecsys spike; Roche, Basel, Switzerland). Elecsys N = Anti-SARS-CoV-2 assay (Elecsys nucleocapsid; Roche). VITROS = Anti-SARS-CoV-2 assay (Ortho Clinical Diagnostics, Raritan, New Jersey). Architect = SARS-CoV-2 assay (Abbott, Mississauga, Canada). GSP/DELFIA = Anti-SARS-CoV-2 assay (PerkinElmer, Waltham, Massachusetts). In-house S (U of T) = In-house spike assay (University of Toronto). In-house RBD (U of T) = In-house RBD assay (University of Toronto). In-house N (U of T) = In-house nucleocapsid assay (University of Toronto). In-house S, mono (U of O) = In- house monoclonal spike assay (University of Ottawa). In-house RBD, mono (U of O) = In-house monoclonal RBD assay (University of Ottawa). In-house N, mono (U of O) = In-house monoclonal nucleocapsid assay (University of Ottawa).

Table 1. Assay performance for SARS-CoV-2 antibody testing on dried blood spot specimens (DBS).

Assay	DBS punches (*n* =)	TP (*n* =)	FN (*n* =)	TN(*n* =)	FP (*n* =)	Eq (*n* =)	Se (95% CI [LL, UL])	Sp (95% CI [LL, UL])	PPV (95% CI [LL, UL])	NPV (95% CI [LL, UL])	Kappa[a] (95% CI [LL, UL])
EUROIMMUN	2	10	0	10	0	0	100% (72.2, 100)	100% (72.2, 100)	100% (72.2, 100)	100% (72.2, 100)	Reference
Platelia	2	10	0	9	0	1	100% (72.2, 100)	90% (59.6, 99.5)	90.9% (62.3, 99.5)	100% (70.1, 100)	0.95 (0.86, 1.00)
LIASON	2	1	9	10	0	0	10% (0.5, 40.4)	100% (72.2, 100)	100% (5.1, 100)	52.6% (31.7, 72.7)	0.45 (0.20, 0.70)
LIASON	3	1	9	10	0	0	10% (0.5, 40.4)	100% (72.2, 100)	100% (5.1, 100)	52.6% (31.7, 72.7)	0.45 (0.20, 0.70)
LIASON	4	1	9	10	0	0	10% (0.5, 40.4)	100% (72.2, 100)	100% (5.1, 100)	52.6% (31.7, 72.7)	0.45 (0.20, 0.70)
COV2G	2	1	9	10	0	0	10% (0.5, 40.4)	100% (72.2, 100)	100% (5.1, 100)	53% (32, 73)	0.05 (-0.26, 0.36)
COV2G	3	1	9	10	0	0	10% (0.5, 40.4)	100% (72.2, 100)	100% (5.1, 100)	53% (32, 73)	0.05 (-0.26, 0.36)
COV2G	4	1	9	8	2	0	10% (0.5, 40.4)	80% (49, 96.4)	33.3% (1.7, 88.2)	47.1% (26.2, 69)	0.15 (-0.16, 0.46)
COV2T	2	1	9	10	0	0	10% (0.5, 40.4)	100% (72.2, 100)	100% (5.1, 100)	52.6% (31.7, 72.7)	0.55 (0.32, 0.78)
COV2T	3	3	7	9	1	0	30% (10.8, 60.3)	90% (59.6, 99.5)	75% (30.1, 98.7)	56.3% (33.2, 76.9)	0.60 (0.36, 0.84)
COV2T	4	4	6	6	4	0	40% (16.8, 68.7)	60% (31.3, 83.2)	50% (21.5, 78.5)	50% (25.4, 74.6)	0.50 (0.23, 0.77)
Elecsys S	2	9	1	0	10	0	90% (59.6, 99.5)	100% (72.2, 100)	100% (70.1, 100)	90.9% (62.3, 99.5)	0.45 (0.203, 0.70)
Elecsys S	3	9	1	0	10	0	90% (59.6, 99.5)	100% (72.2, 100)	100% (70.1, 100)	90.9% (62.3, 99.5)	0.45 (0.203, 0.70)
Elecsys S	4	10	0	10	0	0	100% (72.2, 100)	100% (72.2, 100)	100% (72.2, 100)	100% (72.2, 100)	1.00 (1.00, 1.00)
Elecsys N	2	6	4	10	0	0	60% (31.3, 83.2)	100% (72.2, 100)	100% (72.2, 100)	71.4% (45.4, 88.3)	0.80 (0.62, 0.98)
Elecsys N	3	7	3	10	0	0	70% (39.7, 89.2)	100% (72.2, 100)	100% (39.7, 89.2)	76.9% (49.7, 91.8)	0.85 (0.69, 1.00)
Elecsys N	4	9	1	10	0	0	90% (59.6, 99.5)	100% (72.2, 100)	100% (70.1, 100)	90.9% (62.3, 99.5)	0.95 (0.85, 1.00)
VITROS	2	10	0	0	10	0	100%(72.2–100)	0% (0, 27.8)	50% (29.9, 70.1)	N/A	0.50 (0.27, 0.73)
VITROS	3	10	0	0	10	0	100% (72.2, 100)	0% (0, 27.8)	50% (29.9, 70.1)	N/A	0.50 (0.27, 0.73)
VITROS	4	10	0	0	10	0	100% (72.2, 100)	0% (0, 27.8)	50% (29.9, 70.1)	N/A	0.50 (0.27, 0.73)
Architect	2	1	9	0	10	0	10% (0.5, 40.4)	100% (72.2, 100)	100% (5.1, 100)	52.6%(31.7, 72.7)	0.05 (-0.26, 0.36)
Architect	3	2	8	0	10	0	20% (3.6, 51)	100% (72.2, 100)	100% (17.8, 100)	55.6% (33.7, 75.4)	0.10 (-0.21, 0.41)
Architect	4	2	8	0	10	0	20% (3.6, 51)	100% (72.2, 100)	100% (17.8, 100)	55.6% (33.7, 75.4)	0.10 (-0.21, 0.41)
GSP/DELFIA	2	10	0	10	0	0	100% (72.2, 100)	100% (72.2, 100)	100% (72.2, 100)	100% (72.2, 100)	1.00 (1.00, 1.00)
In-house S (U of T)	2	10	0	10	0	0	100% (72.2, 100)	100% (72.2, 100)	100% (72.2, 100)	100% (72.2, 100)	1.00 (1.00, 1.00)
In-house RBD (U of T)	2	10	0	10	0	0	100% (72.2, 100)	100% (72.2, 100)	100% (72.2, 100)	100% (72.2, 100)	1.00 (1.00, 1.00)
In-house N (U of T)	2	4	6	10	0	0	40% (16.8, 68.7)	100% (72.2, 100)	100% (51.0, 100)	62.5% (38.6, 81.5)	0.70 (0.49, 0.91)
In-house S, polyclonal (U of O)	2	10	0	10	0	0	100% (72.2, 100)	100% (72.2, 100)	100% (72.2, 100)	100% (72.2, 100)	1.00 (1.00, 1.00)
In-house RBD, polyclonal (U of O)	2	10	0	10	0	0	100% (72.2, 100)	100% (72.2, 100)	100% (72.2, 100)	100% (72.2, 100)	1.00 (1.00, 1.00)
In-house N, polyclonal (U of O)	2	10	0	10	0	0	100% (72.2, 100)	100% (72.2, 100)	100% (72.2, 100)	100% (72.2, 100)	1.00 (1.00, 1.00)
In-house S, monoclonal (U of O)	2	10	0	10	0	0	100% (72.2, 100)	100% (72.2, 100)	100% (72.2, 100)	100% (72.2, 100)	1.00 (1.00, 1.00)
In-house RBD, monoclonal (U of O)	2	10	0	10	0	0	100% (72.2, 100)	100% (72.2, 100)	100% (72.2, 100)	100% (72.2, 100)	1.00 (1.00, 1.00)
In-house N, monoclonal (U of O)	2	10	0	10	0	0	100% (72.2, 100)	100% (72.2, 100)	100% (72.2, 100)	100% (72.2, 100)	1.00 (1.00, 1.00)

DBS punches: 6 mm (1/4 inch) dried blood spot punch; TP: True positive; FN: False negative; TN: True negative; FP: False positive; Eq: Equivocal; Se: Sensitivity; Sp: Specificity; PPV: Positive predictive value; NPV: Negative predictive value; 95% CI (LL, UL): 95% confidence intervals (lower limit, upper limit); S: Spike; RBD: Receptor binding domain; N: Nucleocapsid; U of T: University of Toronto; U of O: University of Ottawa.

[a]Kappa statistics interpreted as follows: <0 = no agreement, 0–0.20 = slight agreement, 0.21–0.40 = fair agreement, 0.41–0.60 = moderate agreement, 0.61–0.80 = substantial agreement, and 0.81–1.00 = almost perfect agreement.

The panel consisted of 10 unique SARS-CoV-2 antibody positive DBS cards contrived from patient samples and 10 unique SARS-CoV-2 negative DBS cards spotted directly from EDTA whole blood.

https://doi.org/10.1371/journal.pone.0261003.t001

The Platelia assay achieved a sensitivity, specificity, PPV, and NPV of 100% (95% CI = 72.2, 100), 90% (95% CI = 59.6, 99.5), 90.9% (95% CI = 62.3, 99.5), and 100% (95% CI = 70.1, 100)

respectively due to one equivocal result from a negative DBS sample. As a result, it appears that the Platelia assay can only achieve a PPV ≥90% in high prevalence settings (Fig 1). The Platelia assay showed almost perfect agreement with EUROIMMUN (Table 1) and other high performing commercial assays (S1 Table, Fig 2). The Elecsys nucleocapsid assay achieved a sensitivity, specificity, PPV, and NPV of 90% (95% CI = 59.6, 99.5), 100% (95% CI = 72.2, 100), 100% (95% CI = 70.1, 100), and 90.9% (95% CI = 62.3, 99.5) respectively after increasing the sample input from 2 to 4 DBS punches. Increasing the sample input also significantly reduces the number of false negatives in high prevalence settings (S1 Fig) and improves agreement with other commercial assays such as EUROIMMUN, Platelia, GSP/DELFIA, and Elecsys spike (Tables 1 and S1, Fig 2).

Performance varied for the remaining commercial assays. The LIASON, Architect, and COV2G assays achieved a specificity and PPV of 100% (95% CI = 72.2, 100) and 100% (95% CI = 5.1, 100) respectively but could not achieve a sensitivity greater than 20% (95% CI = 3.6, 51) or an NPV greater than 55.6% (95% CI = 33.7, 75.4) despite increasing the sample input from 2 to 4 DBS punches. The COV2T assay achieved a sensitivity, specificity, PPV, and NPV of 40% (95% CI = 16.8, 68.7), 60% (95% CI = 31.3, 83.2), 50% (95% CI = 21.5, 78.5), and 50% (95% CI = 25.4, 74.6) respectively after increasing the sample input from 2 to 4 DBS punches. Similarly, the VITROS assay achieved a sensitivity and PPV of 100% (95% CI = 72.2, 100) and 50% (95% CI = 29.9, 70.1) respectively but could not achieve a specificity greater than 0% despite increasing sample input. This would suggest that the LIASON and Architect assays would yield a high number of false negative results in high prevalence settings (≥5.0%) while the COV2G and COV2T assays would yield a high number of false negative and false positive results in low to high prevalence settings (Figs 1 and S1). The VITROS assay is likely not to be useful under any prevalence setting since all DBS samples produced positive results (Table 1). As expected, these commercial assays had no agreement to moderate agreement with EUROIMMUN (Table 1) and the higher performing assays Platelia, Elecsys spike, Elecsys nucleocapsid, and GSP/DELFIA (S1 Table, Fig 2).

The in-house assays from the University of Ottawa and University of Toronto performed well and successfully identified all positive and negative DBS correctly corresponding to a sensitivity,

specificity, PPV, and NPV of 100% (95% CI = 72.2, 100) even when using a wide range of prevalence estimates. However, the in-house nucleocapsid (U of T) assay only achieved a sensitivity, specificity, PPV, and NPV of 40% (95% CI = 16.8, 68.7), 100% (95% CI = 72.2, 100), 100% (95% CI = 51, 100), and 62.5% (95% CI = 38.6, 81.5) respectively suggesting that this assay would yield a high number of false negatives in high prevalence settings (Fig 1). All the in-house assays, apart from the in-house nucleocapsid (U of T) had almost perfect agreement with EUROIMMUN (Table 1) and other high performing commercial assays (S1 Table, Fig 2).

Separation between positive and negative samples

Raw data values were plotted, and receiver operating characteristic (ROC) curves were computed (Figs 3 and 4, Table 2, S2 and S3 Figs) to evaluate each assay's ability to separate the 10 known negative plasma samples and 10 plasma samples from COVID-19 patients contrived as DBS. Among the commercial assays, the EUROIMMUN, Platelia, Elecsys spike, Elecsys nucleocapsid, and Architect showed the clearest separation of positive and negative samples by DBS testing and their overall performance was rated as excellent (Table 2). On the other hand, the LIASON, COV2G, and COV2T could not clearly distinguish between positive and negative DBS specimens and showed an overall performance ranging from bad to sufficient (Table 2). The VITROS assay showed good separation of positive and negative DBS and excellent performance according to the area under the ROC curve (AUC) suggesting that increasing the signal to cut-off (S/Co) ratio from 1.0 to 3.4 could potentially increase this assay's sensitivity and specificity to 90% (95% CI = 60, 99) and 100% (95% CI = 72.2, 100) respectively.

The in-house assays from the University of Ottawa and University of Toronto (spike, RBD, and nucleocapsid) showed a clear separation between positive and negative DBS (Figs 3 and 4, Table 2, S2 and S3 Figs). However, the in-house nucleocapsid (University of Toronto) assay was unable to differentiate all positive and negative DBS successfully.

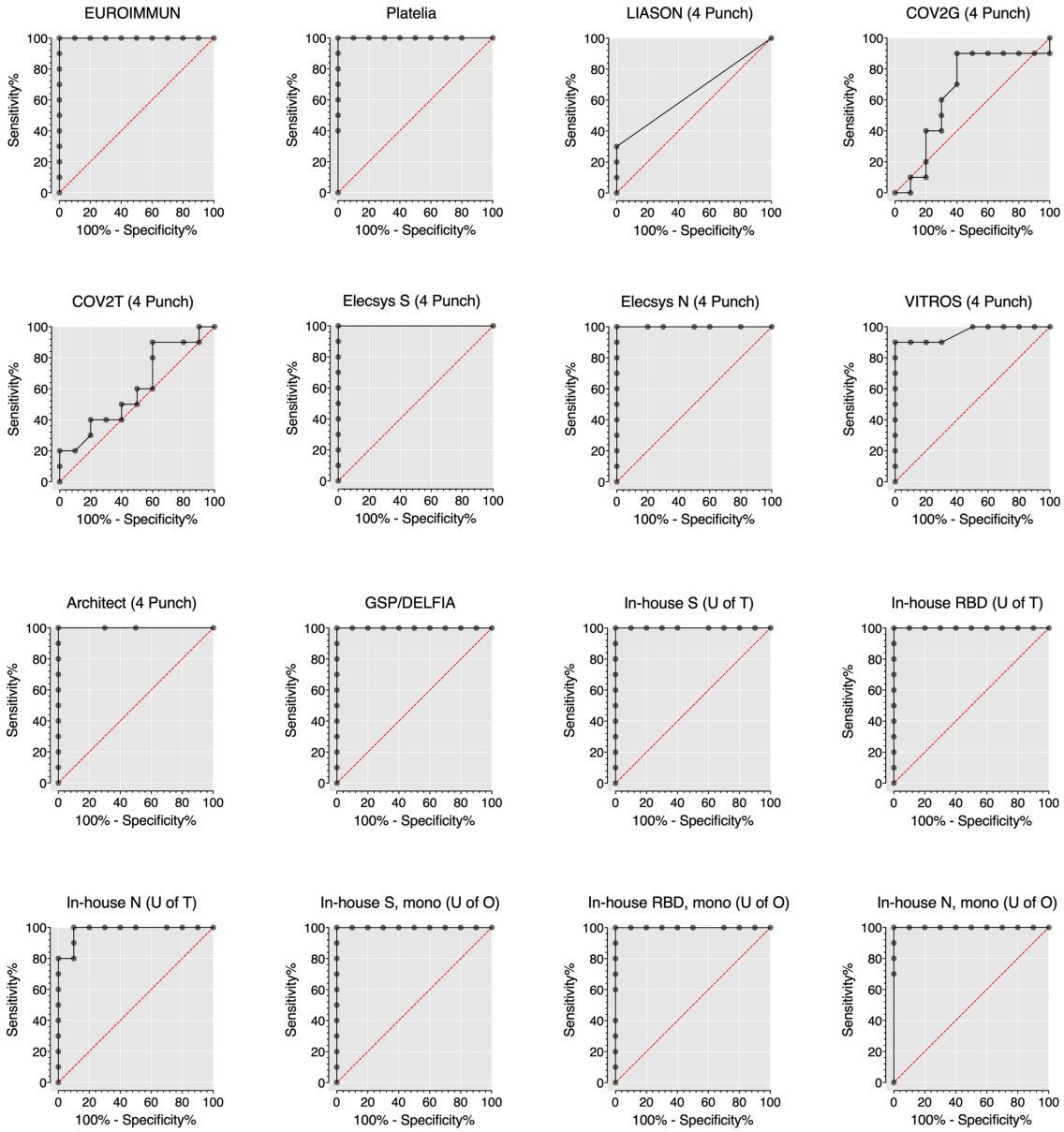


Fig 3. Receiver operating characteristic (ROC) curve for each commercial and in-house assay on dried blood spot specimens. ROC curves are presented for n = 10 SARS-CoV-2 antibody negative DBS specimens and n = 10 SARS-CoV-2 antibody positive DBS specimens. One 6 mm (1/4 inch) punch was used for the EUROIMMUN assay and two 6 mm (1/4 inch) punches were used for the Platelia and in-house assays. Data from four 6 mm (1/4 inch) punches is presented for all other assays. EUROIMMUN = Anti-SARS-CoV-2 ELISA assay (EUROIMMUN, Lübeck, Germany). Platelia = SARS-CoV-2 assay (Bio-Rad, Hercules, California). LIASON = SARS-CoV-2 assay (DiaSorin, Saluggia, Italy). COV2G = SARS-CoV-2 COV2G assay (Siemens, Erlangen, Germany). COV2T = SARS-CoV-2 COV2T assay (Siemens). Elecsys S = Quantitative Anti-SARS-CoV-2 assay (Elecsys spike; Roche, Basel, Switzerland). Elecsys N = Anti-SARS-CoV-2 assay (Elecsys nucleocapsid; Roche). VITROS = Anti-SARS-CoV-2 assay (Ortho Clinical Diagnostics, Raritan, New Jersey). Architect = SARS-CoV-2 assay (Abbott, Mississauga, Canada). GSP/DELFIA = Anti-SARS-CoV-2 assay (PerkinElmer, Waltham, Massachusetts). In-house S (U of T) = In-house spike assay (University of Toronto). In-house RBD (U of T) = In-house RBD assay (University of Toronto). In-house N (U of T) = In-house nucleocapsid assay (University of Toronto). In-house S, mono (U of O) = In-house monoclonal spike assay (University of Ottawa). In-house RBD, mono (U of O) = In-house monoclonal RBD assay (University of Ottawa). In-house N, mono (U of O) = In-house monoclonal nucleocapsid assay (University of Ottawa).

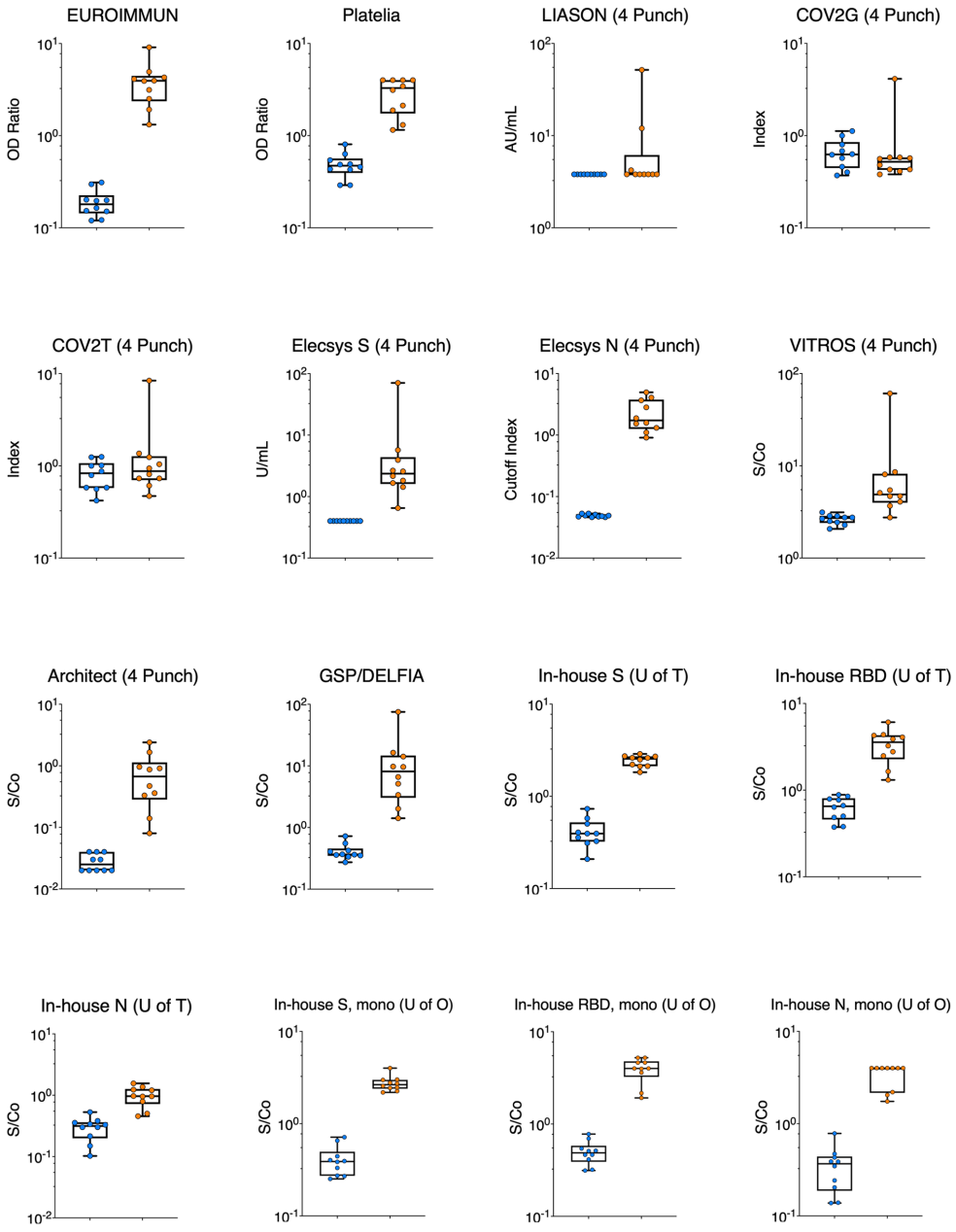


Fig 4. Distribution of values obtained for each commercial and in-house assay on dried blood spot (DBS) specimens. Each panel shows the optical density ratio (OD Ratio), arbitrary units per mL (AU/mL), index, units per mL (U/mL), cut-off index, or signal to cut-off ratio (S/Co) for SARS-CoV-2 antibody negative DBS specimens (n = 10) represented in blue and SARS-CoV-2 antibody positive DBS specimens (n = 10) represented in orange. All values are $\log_{10}$ transformed to aid with visualisation. One 6 mm (1/4 inch) punch was used for the EUROIMMUN assay and two 6 mm (1/4 inch) punches were used for the Platelia and in-house assays. Data from four 6 mm (1/4 inch) punches is presented for all other assays. EUROIMMUN = Anti-SARS-CoV-2 ELISA assay (EUROIMMUN, Lübeck, Germany). Platelia = SARS-CoV-2 assay (Bio-Rad, Hercules, California). LIASON = SARS-CoV-2 assay (DiaSorin, Saluggia, Italy). COV2G = SARS-CoV-2 COV2G assay (Siemens, Erlangen, Germany). COV2T = SARS-CoV-2 COV2T assay (Siemens). Elecsys S = Quantitative Anti-SARS-CoV-2 assay (Elecsys spike; Roche, Basel, Switzerland). Elecsys N = Anti-SARS-CoV-2 assay (Elecsys nucleocapsid; Roche). VITROS = Anti-SARS-CoV-2 assay (Ortho Clinical Diagnostics, Raritan, New Jersey). Architect = SARS-CoV-2 assay (Abbott, Mississauga, Canada). GSP/DELFIA = Anti-SARS-CoV-2 assay (PerkinElmer, Waltham, Massachusetts). In-house S (U of T) =

In-house spike assay (University of Toronto). In-house RBD (U of T) = In-house RBD assay (University of Toronto). In-house N (U of T) = In-house nucleocapsid assay (University of Toronto). In-house S, mono (U of O) = In-house monoclonal spike assay (University of Ottawa). In-house RBD, mono (U of O) = In-house monoclonal RBD assay (University of Ottawa). In-house N, mono (U of O) = In-house monoclonal nucleocapsid assay (University of Ottawa).

Table 2. Area under the receiver operating characteristic curve (AUC) for each commercial and in-house assay on dried blood spot specimens (DBS).

Assay	DBS punches (*n* =)	AUC[a] (95% CI [LL, UL])	P value	Performance
EUROIMMUN	2	1.0 (1.0, 1.0)	<0.05	Excellent
Platelia	2	1.0 (1.0, 1.0)	<0.05	Excellent
LIASON	2	0.60 (0.35, 0.85)	0.45	Bad
LIASON	3	0.60 (0.35, 0.85)	0.45	Bad
LIASON	4	0.65 (0.40, 0.90)	0.26	Sufficient
COV2G	2	0.59 (0.33, 0.85)	0.50	Bad
COV2G	3	0.66 (0.40, 0.91)	0.24	Sufficient
COV2G	4	0.66 (0.39, 0.92)	0.24	Sufficient
COV2T	2	0.59 (0.33, 0.85)	0.50	Bad
COV2T	3	0.55 (0.29, 0.81)	0.71	Bad
COV2T	4	0.61 (0.35, 0.86)	0.43	Sufficient
Elecsys S	2	0.95 (0.84, 1.0)	<0.05	Excellent
Elecsys S	3	1.0 (1.0, 1.0)	<0.05	Excellent
Elecsys S	4	1.0 (1.0, 1.0)	<0.05	Excellent
Elecsys N	2	1.0 (1.0, 1.0)	<0.05	Excellent
Elecsys N	3	1.0 (1.0, 1.0)	<0.05	Excellent
Elecsys N	4	1.0 (1.0, 1.0)	<0.05	Excellent
VITROS	2	0.93 (0.78, 1.0)	<0.05	Excellent
VITROS	3	0.93 (0.81, 1.0)	<0.05	Excellent
VITROS	4	0.96 (0.87, 1.0)	<0.05	Excellent
Architect	2	1.0 (1.0, 1.0)	<0.05	Excellent
Architect	3	1.0 (1.0, 1.0)	<0.05	Excellent
Architect	4	1.0 (1.0, 1.0)	<0.05	Excellent
GSP/DELFIA	2	1.0 (1.0, 1.0)	<0.05	Excellent
In-house S (U of T)	2	1.0 (1.0, 1.0)	<0.05	Excellent
In-house RBD (U of T)	2	1.0 (1.0, 1.0)	<0.05	Excellent
In-house N (U of T)	2	0.98 (0.93, 1.0)	<0.05	Excellent
In-house S, polyclonal (U of O)	2	1.0 (1.0, 1.0)	<0.05	Excellent
In-house RBD, polyclonal (U of O)	2	1.0 (1.0, 1.0)	<0.05	Excellent
In-house N, polyclonal (U of O)	2	1.0 (1.0, 1.0)	<0.05	Excellent
In-house S, monoclonal (U of O)	2	1.0 (1.0, 1.0)	<0.05	Excellent
In-house RBD, monoclonal (U of O)	2	1.0 (1.0, 1.0)	<0.05	Excellent
In-house N, monoclonal (U of O)	2	1.0 (1.0, 1.0)	<0.05	Excellent

DBS punches: 6 mm (1/4 inch) dried blood spot punch; 95% CI (LL, UL): 95% confidence intervals (lower limit, upper limit); S: Spike; RBD: Receptor binding domain; N: Nucleocapsid; U of T: University of Toronto; U of O: University of Ottawa.

[a]Test performance classified according to AUC as follows: <0.5 = not useful, 0.5–0.6 = bad, 0.6–0.7 = sufficient, 0.7–0.8 = good, 0.8–0.9 = very good, and 0.9–1.0 = excellent.

The panel consisted of 10 unique SARS-CoV-2 antibody positive DBS cards and 10 unique SARS-CoV-2 negative DBS cards contrived from patient samples.

https://doi.org/10.1371/journal.pone.0261003.t002

Discussion

On a small panel of DBS, this study has shown that the EUROIMMUN, Elecsys spike, and GSP/DELFIA commercial assays as well in-house assays are capable of achieving a sensitivity,

specificity, PPV, and NPV of 100% (95% CI = 72.2, 100) under a broad range of prevalence scenarios following testing of DBS eluate samples collected ≥36 days post symptom onset without optimization. We interpret these findings cautiously since a recent systematic review by Lisboa Bastos *et al*. [22] assessing 40 serological studies reported that the maximum pooled sensitivities for enzyme linked immunosorbent assays measuring IgG or IgM (ELISAs) and chemiluminescent immunoassays (CLIAs) was 84.3% (95% CI = 75.6, 90.9) and 97.8% (95% CI = 46.2, 100) respectively. The accuracy of serological assays also varies according to sampling time frames and sensitivity typically exceeds 90% between 15–35 days post symptom onset [22]. We were unable to stratify our analysis according to days post symptom onset due to our sample size and narrow range of collection dates. Furthermore, our samples consisted of COVID-19 convalescent plasma donors who are likely to have significant antibody titers [23]. Nonetheless, we clearly show that certain assays like the LIASON, COV2G, and COV2T could not reliably identify positive and negative specimens by DBS testing and are unlikely to be useful in various prevalence settings.

Based on our ROC curve analysis, assays like the Platelia, Elecsys nucleocapsid, VITROS, and Architect, which did not reach 100% for all performance characteristics, could clearly distinguish between positive and negative samples therefore could also potentially achieve a sensitivity, specificity, PPV, and NPV near 100% via threshold adjustments [24–26]. However, establishing appropriate thresholds will require a study using a large number of well characterised clinical samples representing a broad range of factors associated with developing robust immune responses to SARS-CoV-2 such as sex, age, immunodeficiencies, and disease severity [27].

This validation study has several limitations that must be considered. First, our panel was small, albeit well characterized. Current efforts are underway to validate in-house and commercial multiplex assays using a larger DBS panel that covers a broader range of days between infection and sample collection. Second, we did not take into consideration other capillary blood collection methods such as capillary tubes. While capillary tubes have been shown to be a practical alternative to venepuncture for SARS-CoV-2 antibody testing [28,29], they cannot be transported as easily or safely as DBS therefore their applicability are somewhat limited for large sero-surveys within the Canadian context. Last, DBS eluates, prepared using a well-characterized buffer used specifically

by the National Laboratory for HIV Reference Services (NLHRS), were sent to the participants (with the exception of the GSP/DELFIA). The assessment of different buffers or the further optimization of DBS elution conditions was beyond the scope of this study. Additional refinement of these procedures may have yielded more optimistic results on the assays that were not reported to fare well in this evaluation. However, the purpose of this evaluation was to develop a simplified procedure based on simple well-characterized practices previously developed within the NLHRS. Implementing this standardized approach allowed for an effective and timely identification of promising platforms that could be used for DBS testing for anti-SARS-CoV-2 antibodies without extensive modification. We believe that this was accomplished despite these limitations.

In conclusion, we assessed the performance of 10 commercial and 2 in-house serological assays for DBS eluate testing. Several of these assays achieved a specificity, sensitivity, PPV, and NPV adequate for sero-surveys even in low-prevalence settings. These findings suggest that the high demand for SARS-CoV-2 serology testing, mainly driven by sero-surveys within the Canadian context, could be met by the collection and testing of DBS by several different assays, thereby minimizing the risk of shortages. Furthermore, DBS collection has the potential to expand testing use and access while limiting the requirements for specimen collection on healthcare professionals already overtaxed with the COVID-19 response. While our sample size was small, this validation study, undertaken initially to determine the feasibility of a nationally representative household-based sero-survey that would be based on DBS, resulted in the selection of the in-house assays. They were chosen not only because of their test performance, but also because they are capable of distinguishing between infection- and vaccine-induced antibody responses which will be important in informing public health strategies in diverse jurisdictions across Canada. Our study represents the foundation for future validation studies on DBS specimens, that will undoubtedly play a central role in shaping Canada’s public health policy in response to COVID-19. However, larger DBS panels representing a broader range of days between symptom onset and sample collection as well as socio-demographic and clinical characteristics of COVID-19 patients will be required to substantiate our findings.

Methods

Ethics statement

All experiments were carried out in accordance with relevant guidelines and regulations. Written informed consent was obtained from all participants who provided blood samples from which we contrived SARS-CoV-2 antibody positive and negative DBS cards. All participants were 18 years of age or older. Ethical approval was obtained from the Health Canada and Public Health Agency of Canada Research Ethics Board (REB no. 2020-022P).

Patient specimens

SARS-CoV-2 antibody positive and negative plasma used to contrive DBS specimens are described in Table 3. SARS-CoV-2 antibody positive plasma was collected from COVID-19 convalescent donors at Mount Sinai Hospital (Toronto, Canada). Plasma was tested for SARS-CoV-2 antibodies using the Platelia SARS-CoV-2 Total Ab (Bio-Rad, Hercules, California) or Anti-SARS-CoV-2 ELISA IgG (EUROIMMUN, Lübeck, Germany) kits. SARS-CoV-2 negative plasma was collected from healthy donors within the National Microbiology Laboratory (Winnipeg, Canada). To prepare plasma, blood was collected in EDTA Vacutainer tubes (Beckton Dickinson, Franklin Lates, NJ) and centrifuged at 1,500 RPM for 7 minutes. Plasma was tested using the Platelia SARS-CoV-2 Total Ab (Bio-Rad) or Anti-SARS-CoV-2 ELISA IgG (EUROIMMUN, Lübeck, Germany) kits to verify donors were negative for SARS-CoV-2 antibodies. All assays were performed according to the manufacturer's instructions.

Contrived dried blood spot specimens

A panel consisting of 10 unique SARS-CoV-2 antibody positive DBS cards were contrived and 10 unique SARS-CoV-2 negative DBS cards were directly spotted from EDTA whole blood to assess the performance of commercial and in-house serological tests (S4 Fig). Each testing site was blinded to the status of the DBS cards. SARS-CoV-2 antibody positive plasma samples were contrived into DBS specimens by using blood collected from healthy donors within the National Microbiology Laboratory. SARS-CoV-2 antibody negative blood was centrifuged at 1,500 RPM for 7 minutes and the plasma was removed. The remaining red blood cells were re-suspended with SARS-CoV-2 antibody positive plasma using a 1:1 ratio and 75 µL was spotted onto each circle of a Whatman 903 Protein Saver card (GE Healthcare, Boston, MA). Spotted cards were allowed

to air-dry for at least 2 hours in a biosafety cabinet and then packaged in a gas impermeable bag with a desiccant pack and a humidity indicator card. Packaged cards (maximum 10 per bag) were stored at -80°C until further testing. SARS-CoV-2 antibody negative blood was spotted directly from the EDTA Vacutainer tubes onto Whatman 903 Proteinsaver cards as described above.

Table 3. SARS-CoV-2 antibody positive and negative plasma used to contrive dried blood spot specimens.

Sample ID	Description	Sample collection, days post infection	EUROIMMUN Anti-SARS-CoV-2		Bio-Rad Platelia SARS-CoV-2	
			OD ratio	Interpretation[a]	OD_MR4 ratio	Interpretation[b]
J12	Healthy donor	Pre-COVID-19	0.20	Negative	0.08	Negative
D17	Healthy donor	Pre-COVID-19	0.12	Negative	0.11	Negative
J11	Healthy donor	Pre-COVID-19	0.16	Negative	0.08	Negative
J1	Healthy donor	Pre-COVID-19	0.15	Negative	0.08	Negative
D142	Healthy donor	Pre-COVID-19	0.13	Negative	0.09	Negative
J19	Healthy donor	Pre-COVID-19	0.49	Negative	0.08	Negative
D9	Healthy donor	Pre-COVID-19	0.18	Negative	0.09	Negative
J30	Healthy donor	Pre-COVID-19	0.17	Negative	0.10	Negative
J15	Healthy donor	Pre-COVID-19	0.18	Negative	0.07	Negative
J7	Healthy donor	Pre-COVID-19	0.41	Negative	0.10	Negative
20–1887	COVID-19 convalescent donor	44	2.45	Positive	≥4.00	Positive
20–1954	COVID-19 convalescent donor	57	2.32	Positive	3.14	Positive
20–1955	COVID-19 convalescent donor	42	1.36	Positive	2.12	Positive
20–1877	COVID-19 convalescent donor	41	4.10	Positive	≥4.00	Positive
20–1878	COVID-19 convalescent donor	51	4.01	Positive	≥4.00	Positive
20–1882	COVID-19 convalescent donor	66	2.90	Positive	≥4.00	Positive
20–1886	COVID-19 convalescent donor	52	4.62	Positive	≥4.00	Positive
20–1879	COVID-19 convalescent donor	36	11.04	Positive	≥4.00	Positive
20–1885	COVID-19 convalescent donor	38	5.78	Positive	≥4.00	Positive
20–1952	COVID-19 convalescent donor	42	4.39	Positive	≥4.00	Positive

OD: Optical density; OD_MR4: Optical density for cut-off control R4.

[a]Results were evaluated by calculating the ratio of the OD of the plasma specimen over the OD of the assay calibrator. Results were interpreted as follows: OD ratio <0.8 reported as positive; OD ratio ≧0.8 to <1.1 reported as borderline; OD ratio ≧1.1 reported as positive.

[b]Results were evaluated by calculating the ratio of the OD of the plasma specimen over the OD of the kit cut-off control R4. Results were interpreted as follows: OD_MR4 ratio <0.8 reported as negative; OD_MR4 ratio o ≧0.8 to <1.0 reported as equivocal; OD_MR4 ratio ≧1.0 reported as positive.

https://doi.org/10.1371/journal.pone.0261003.t003

Dried blood spot elution

DBS samples were punched using a 6 mm hole punch into a 96 deep well plate. One to four 6 mm (1/4 inch) punches were added to each well and eluted in DPBS buffer (pH 7.4) containing 0.5% BSA and 0.05% Tween-20 overnight at 4°C with agitation (400 RPM). For the Anti-SARS-CoV-2 ELISA IgG (EUROIMMUN) a single punch was eluted in 500 ul of Sample Buffer overnight without agitation and 100 μL of eluate was transferred to the assay plate. For Platelia SARS-CoV-2 Total Ab (Bio-Rad) assay, two punches were eluted in 130 μL of Sample Diluent overnight with

gentle agitation (400 RPM), 75 μL of eluate was mixed with conjugate, and 100 μL of the eluate-conjugate mixture was transferred to the assay plate. Elution volumes were adjusted for all other assays according to manufacturer's specifications or in-house developed protocols (Table 4). Afterwards, plates were incubated at room temperature for 30 minutes with agitation (400 RPM) and each DBS eluate was transferred to an individual 2.0 mL screw cap tube. Eluates were stored at -80°C until shipment on dry ice to each testing site.

Table 4. Commercial and in-house serological tests assessed for SARS-CoV-2 antibody testing on dried blood spot specimens.

Assay	Manufacturer	Site	Antibody class	Target	Elution volume (μL)[a]	Interpretation		
						Negative	Equivocal	Positive
Anti-SARS-CoV-2 ELISA	EUROIMMUN	J.C. Wilt	IgG	S1	500	OD ratio <0.8	OD ratio ≥0.8 <1.1	OD ratio ≥1.1
LIASON SARS-CoV-2	DiaSorin	Cadham	IgG	S1, S2	200	<15.0 AU/mL	N/A	≥15.0 AU/mL
SARS-CoV-2 COV2G	Siemens	U of T (DID)	IgG	S1	300	Index <1.0	N/A	Index ≥1.0
SARS-CoV-2 COV2T	Siemens	U of T (DID)	Total	S1	300	Index <1.0	N/A	Index ≥1.0
Architect SARS-CoV-2	Abbott	McGill	IgG	N	180	S/Co <1.40	N/A	S/Co ≥1.40
GSP/DELFIA Anti-SARS-CoV-2	Perkin Elmer	CHEO	IgG	S1	N/A[b]	S/Co <1.4	N/A	S/Co ≥1.4
Platelia SARS-CoV-2	Bio-Rad	J.C. Wilt	Total	N	130	OD ratio <0.8	OD ratio ≥0.8 <1.0	OD ratio ≥1.1
Elecsys Anti-SARS-CoV-2	Roche	NML	Total	S	250	<0.8 U/mL	N/A	≥0.8 U/mL
Elecsys Anti-SARS-CoV-2	Roche	NML	Total	N	250	Cutoff index <1.0	N/A	Cutoff index ≥1.0
VITROS Anti-SARS-CoV-2	Ortho Clinical Diagnostics	BCCDC	Total	S1	300	S/Co <1.0	N/A	S/Co ≥1.0
Abe KT, *et al.* 2020[30]	In-house	U of T	IgG	S	100	S/Co <1.0	N/A	S/Co ≥1.0
Abe KT, *et al.* 2020[30]	In-house	U of T	IgG	RBD	100	S/Co <1.0	N/A	S/Co ≥1.0
Abe KT, *et al.* 2020[30]	In-house	U of T	IgG	N	100	S/Co <1.0	N/A	S/Co ≥1.0
Adapted from Amanat F, *et al.* 2020[31]	In-house	U of O	IgG (polyclonal)	S	100	S/Co <1.0	N/A	S/Co ≥1.0
Adapted from Amanat F, *et al.* 2020[31]	In-house	U of O	IgG (monoclonal)	S	100	S/Co <1.0	N/A	S/Co ≥1.0
Adapted from Amanat F, *et al.* 2020[31]	In-house	U of O	IgG (polyclonal)	RBD	100	S/Co <1.0	N/A	S/Co ≥1.0
Adapted from Amanat F, *et al.* 2020[31]	In-house	U of O	IgG (monoclonal)	RBD	100	S/Co <1.0	N/A	S/Co ≥1.0
Adapted from Amanat F, *et al.* 2020[31]	In-house	U of O	IgG (polyclonal)	N	100	S/Co <1.0	N/A	S/Co ≥1.0
Adapted from Amanat F, *et al.* 2020[31]	In-house	U of O	IgG (monoclonal)	N	100	S/Co <1.0	N/A	S/Co ≥1.0

J.C. Wilt: National Microbiology Laboratory at the J.C. Wilt Infectious Diseases Research Centre, Winnipeg, Canada; U of T (DID): Division of Infectious Diseases, University of Toronto; McGill: McGill University Health Centre, McGill University; CHEO: Children's Hospital of Eastern Ontario, Ottawa, Canada; NML: National Microbiology Laboratory at the Canadian Science Centre for Human and Animal Health, Winnipeg, Canada; BCCDC: British Columbia Centre for Disease Control, Vancouver, Canada; U of T: University of Toronto, Toronto, Canada; U of O: University of Ottawa, Ottawa, Canada; S1: Spike S1; S2: Spike S2; S: Total spike; N: Nucleocapsid; RBD: Receptor binding domain; OD: Optical density; S/Co: Signal cut-off; AU/mL: Arbitrary units/mL; N/A: Not applicable.

[a] The elution volume was based on the minimum volume required to perform the assay, the assay's dead volume, and an additional 30 μL of buffer for each 6 mm (1/4 inch) DBS punch to account for liquid absorbed by the filter paper.

[b]DBS cards shipped directly to testing site. The GSP/DELFIA performs automated, onboard DBS punching (1 x 3.2 mm) and elution.

https://doi.org/10.1371/journal.pone.0261003.t004

SARS-CoV-2 antibody testing

DBS eluates were tested for SARS-CoV-2 antibodies with 10 commercial assays and 2 in-house assays (Table 4) according to the manufacturer's instructions or laboratory developed protocols respectively. No attempts were made at this point to optimize protocols for DBS specimens. The commercial tests consisted of 6 IgG based assays: Anti-SARS-CoV-2 ELISA (EUROIMMUN), LIASON SARS-CoV-2 (DiaSorin, Saluggia, Italy), SARS-CoV-2 COV2G (Siemens, Erlangen, Germany), Architect SARS-CoV-2 (Abbott, Mississauga, Canada), and GSP/DELFIA Anti-SARS-CoV-2 (PerkinElmer, Waltham, Massachusetts); and 5 total antibody assays: Platelia SARS-CoV-2 (Bio-Rad), SARS-CoV-2 COV2T (Siemens), Elecsys quantitative Anti-SARS-CoV-2 (Elecsys spike; Roche, Basel, Switzerland), Elecsys Anti-SARS-CoV-2 (Elecsys nucleocapsid; Roche), and VITROS Anti-SARS-CoV-2 (Ortho Clinical Diagnostics, Raritan, New Jersey). EUROIMMUN was included since it is the only assay currently approved by Health Canada for use with serum which also has a manufacturer developed protocol for use with DBS (CE marked). Both in-house tests, described in greater detail elsewhere [30] and Table 2, consist of IgG assays targeting SARS-CoV-2 spike, receptor binding domain (RBD), and nucleocapsid proteins. Each testing site was responsible for interpreting and reporting their own data.

Statistical analysis

Statistical analysis was conducted using Prism version 9.0.0 (GraphPad Software, San Diego, CA). Test performance on DBS expressed in terms of sensitivity, specificity, positive predictive values (PPV), and negative predictive values (NPV), was computed in comparison with the serum-based Anti-SARS-CoV-2 ELISA (EUROIMMUN) assay results as the reference because it is the only assay currently approved by Health Canada for use with serum which also has a manufacturer developed protocol for use with DBS (CE marked). PPV (sensitivity x prevalence/sensitivity x prevalence + [1 –specificity] x [1 –prevalence]) and NPV (specificity x [1 –prevalence]/specificity x [1 –prevalence] + [1 –sensitivity) x prevalence) was also re-calculated using a prevalence of 1.0%, 2.5%, 5.0%, 10.0%, 20.0%, and 40.0%. Equivocal results were considered positive.

Agreement with the reference test was quantified using Cohen's kappa coefficient (https://www.graphpad.com/quickcalcs/kappa1/?K=2) and interpreted as follows: <0 = no agreement, 0–0.20 = slight agreement, 0.21–0.40 = fair agreement, 0.41–0.60 = moderate

agreement, 0.61–0.80 = substantial agreement, and 0.81–1.00 = almost perfect agreement [32]. Confidence intervals were computed using the hybrid Wilson/Brown method [33].

Receiver operating characteristics (ROC) curves were also computed using the Wilson/Brown method. A P-value ≤0.05 was considered statistically significant. Test performance classified according to the area under the ROC curve (AUC) was interpreted as follows: <0.5 = not useful, 0.5–0.6 = bad, 0.6–0.7 = sufficient, 0.7–0.8 = good, 0.8–0.9 = very good, and 0.9–1.0 = excellent [34,35].

Overall positive and negative percent concordance and Cohen's kappa coefficient were used to quantify inter-assay agreement between the 10 commercial assays and 2 in-house assays. Confidence intervals were computed using the hybrid Wilson/Brown method. Cohen's kappa coefficient was interpreted as described above.

Acknowledgments

We thank Elizabeth Giles and Jacqueline Day of the Viral Hepatitis and Blood Borne Pathogens unit (National Microbiology Laboratory) for their assistance with serological testing on the Roche platform. We also like to acknowledge the vital support from David Taylor, Timothy Evans, Carrie Bourassa, Vivek Goel, Philippe Gros, Scott Halperin, Charu Kauschic, James D. Kellner, Susan Kirkland, Gary Kobinger, Christie Lutsiak, Richard Massé, Deborah Money, Gina Ogilvie, Jutta Preiksaitis, Caroline Quach-Thanh, Rosann Seviour, and Gail Tomblin Murphy of the CITF working group.

References

1. Wu F, Zhao S, Yu B, Chen Y-M, Wang W, Song Z-G, et al. A new coronavirus associated with human respiratory disease in China. Nature. 2020; 579(7798):265–9. https://doi.org/10.1038/s41586-020- 2008-3 PMID: 32015508

2. Centre for Systems and Science Engineering at John Hopkins University. COVID-19 dashboard [cited 2021 January 19]. Available from: https://coronavirus.jhu.edu/map.html.

3. Corman VM, Landt O, Kaiser M, Molenkamp R, Meijer A, Chu DK, et al. Detection of 2019 novel coronavirus (2019-nCoV) by real-time RT-PCR. Euro Surveillance. 2020; 25(3):23–30. https://doi.org/10. 2807/1560-7917.ES.2020.25.3.2000045 PMID: 31992387

4. Mallett S, Allen AJ, Graziadio S, Taylor SA, Sakai NS, Green K, et al. At what times during infection is SARS-CoV-2 detectable and no longer detectable using RT-PCR-based tests? A systematic review of PLOS ONE Dried blood spot specimens for SARS-CoV-2 antibody testing PLOS ONE | https://doi.org/10.1371/journal.pone.0261003 December 7, 2021 17 / 19 individual participant data. BMC Medicine. 2020; 18(1):346. https://doi.org/10.1186/s12916-020-01810- 8 PMID: 33143712

5.Becker MG, Taylor T, Kiazyk S, Cabiles DR, Meyers AFA, Sandstrom PA. Recommendations for sample pooling on the Cepheid GeneXpertI system using the Cepheid XpertI Xpress SARS-CoV-2 assay. PloS ONE. 2020; 15(11):e0241959. https://doi.org/10.1371/journal.pone.0241959 PMID: 33166373

6. Callahan A, Steinberg E, Fries JA, Gombar S, Patel B, Corbin CK, et al. Estimating the efficacy of symptom-based screening for COVID-19. NPJ Digital Medicine. 2020; 3:95. https://doi.org/10.1038/s41746- 020-0300-0 PMID: 32695885

7. Van Caeseele P, Canadian Public Health Laboratory N, Bailey D, Canadian Society of Clinical C, Forgie SE, Association of Medical M, et al. SARS-CoV-2 (COVID-19) serology: implications for clinical practice, laboratory medicine and public health. CMAJ. 2020; 192(34):E973–E9. https://doi.org/10.1503/ cmaj.201588 PMID: 32753391

8. Abe KT, Li Z, Samson R, Samavarchi-Tehrani P, Valcourt EJ, Wood H, et al. A simple protein-based surrogate neutralization assay for SARS-CoV-2. JCI Insight. 2020; 5(19):e142362. https://doi.org/10. 1172/jci.insight.142362 PMID: 32870820

9. Petherick A. Developing antibody tests for SARS-CoV-2. The Lancet. 2020; 395(10230):1101–2. https://doi.org/10.1016/S0140-6736(20)30788-1 PMID: 32247384

10. Tan SS, Saw S, Chew KL, Wang C, Pajarillaga A, Khoo C, et al. Comparative clinical evaluation of the Roche Elecsys and Abbott severe acute respiratory syndrome coronavirus 2 (SARS-CoV-2) serology assays for coronavirus disease 2019 (COVID-19). Archives of Pathology & Laboratory Medicine. 2021; 145(1):32–8. https://doi.org/10.5858/arpa.2020-0499-SA PMID: 33367664

11. Whitman JD, Hiatt J, Mowery CT, Shy BR, Yu R, Yamamoto TN, et al. Evaluation of SARS-CoV-2 serology assays reveals a range of test performance. Nat Biotechnol. 2020; 38(10):1174–83. https://doi.org/ 10.1038/s41587-020-0659-0 PMID: 32855547

12. Herroelen PH, Martens GA, De Smet D, Swaerts K, Decavele AS. Humoral Immune Response to SARS-CoV-2. Am J Clin Pathol. 2020; 154(5):610–9. https://doi.org/10.1093/ajcp/aqaa140 PMID: 32808976

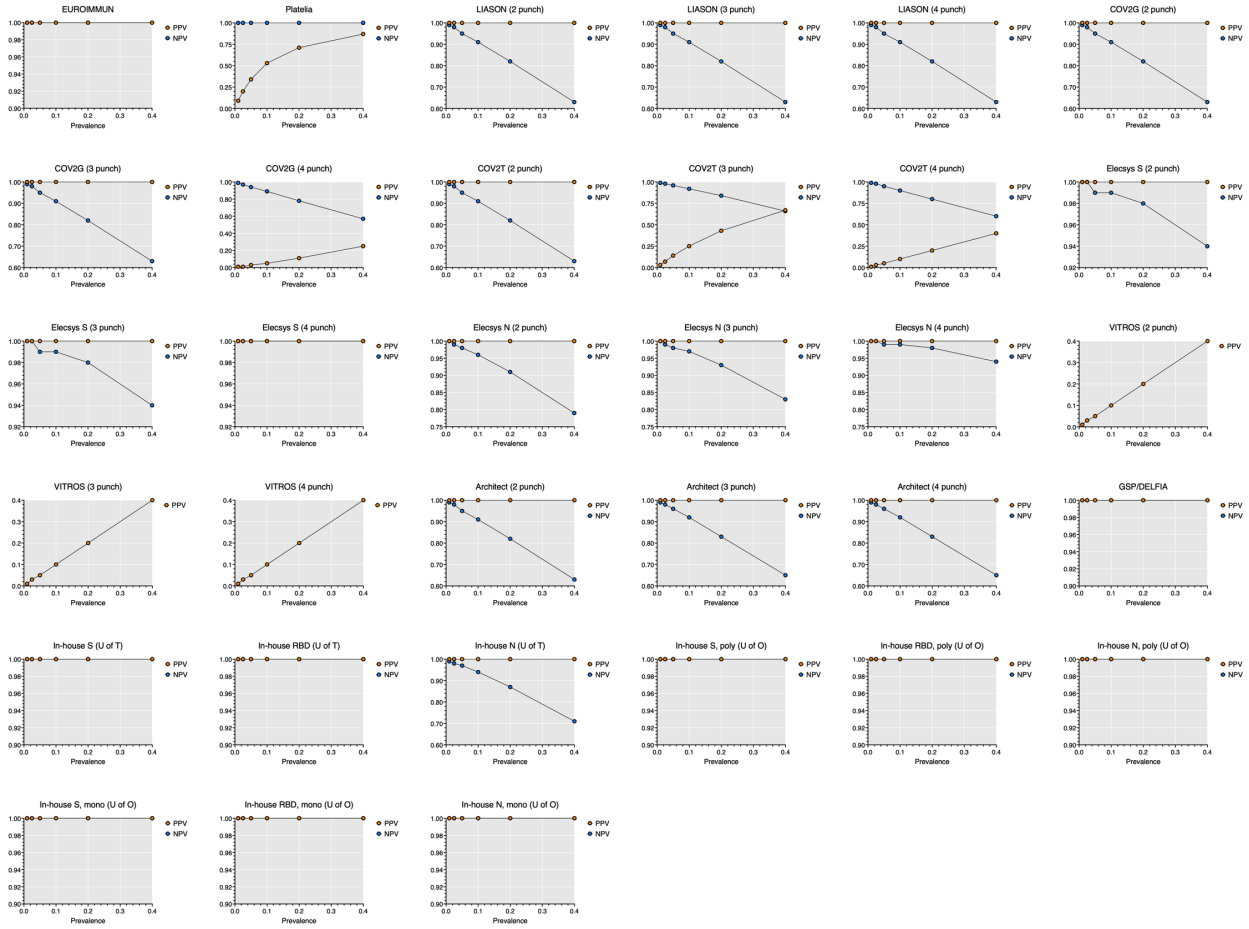
13. Ainsworth M, Andersson M, Auckland K, Baillie JK, Barnes E, Beer S, et al. Performance characteristics of five immunoassays for SARS-CoV-2: a head-to-head benchmark comparison. The Lancet Infectious Diseases. 2020; 20(12):1390–400. https://doi.org/10.1016/S1473-3099(20)30634-4 PMID: 32979318

14. Rasmussen S, Sperling P, Poulsen MS, Emmersen J, Andersen S. Medical students for health-care staff shortages during the COVID-19 pandemic. The Lancet. 2020; 395(10234) :e79–e80. https://doi. Org/10.1016/S0140-6736(20)30923-5 PMID : 32334649

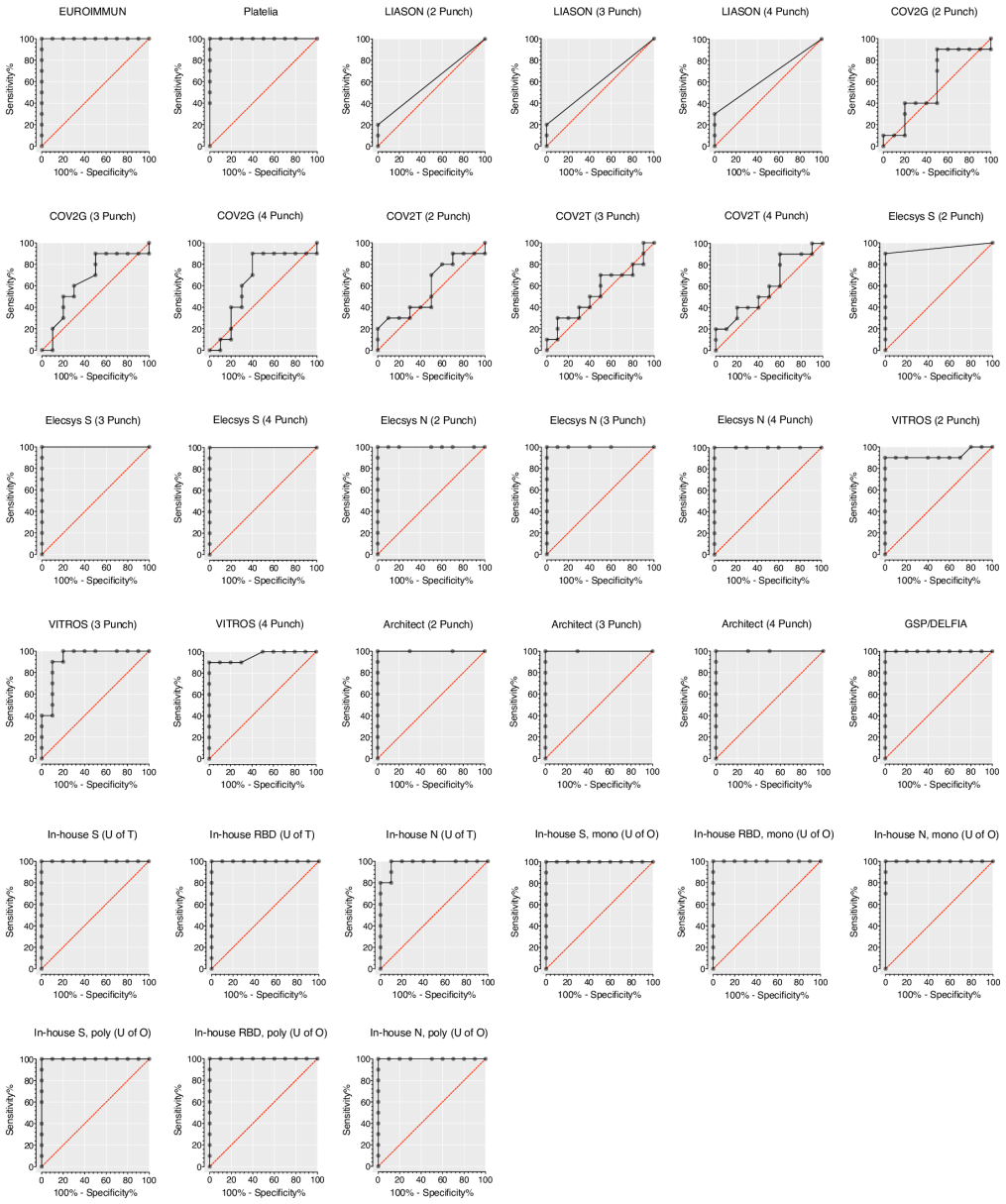
15. Visseaux B, Le Hingrat Q, Collin G, Bouzid D, Lebourgeois S, Le Pluart D, et al. Evaluation of the QIAstat-Dx Respiratory SARS-CoV-2 Panel, the first rapid multiplex PCR commercial assay for SARSCoV-2 detection. J Clin Microbiol. 2020; 58(8). https://doi.org/10.1128/JCM.00630-20 PMID: 32341142
16.Collier DA, Assennato SM, Warne B, Sithole N, Sharrocks K, Ritchie A, et al. Point of care nucleic acid testing for SARS-CoV-2 in hospitalized patients: a clinical validation trial and implementation study. Cell Rep Med. 2020; 1(5):100062. https://doi.org/10.1016/j.xcrm.2020.100062 PMID: 32838340
17. Wolters F, van de Bovenkamp J, van den Bosch B, van den Brink S, Broeders M, Chung NH, et al. Multi-center evaluation of cepheid XpertI Xpress SARS-CoV-2 point-of-care test during the SARSCoV-2 pandemic. J Clin Virol. 2020; 128:104426. https://doi.org/10.1016/j.jcv.2020.104426 PMID: 32417674
18. Young S, Taylor SN, Cammarata CL, Varnado KG, Roger-Dalbert C, Montano A, et al. Clinical evaluation of BD Veritor SARS-CoV-2 point-of-care test performance compared to PCR-based testing and versus the Sofia 2 SARS antigen point-of-care test. J Clin Microbiol. 2020; 59(1). https://doi.org/10.1128/JCM.02338-20 PMID: 33023911
19. Karp DG, Danh K, Espinoza NF, Seftel D, Robinson PV, Tsai CT. A serological assay to detect SARSCoV-2 antibodies in at-home collected finger-prick dried blood spots. Sci Rep. 2020; 10(1):20188. https://doi.org/10.1038/s41598-020-76913-6 PMID: 33214612
20. COVID-19 Immunity Task Force. New study to determine how many Canadians have been infected with SARS-CoV-2 2020 [cited 2021 14 March 2021]. Available from: https://www.Covid19immunitytaskforce.ca/new-study-to-determine-how-many-canadians-have-been-infected-withsars-cov-2/.
21. Morley GL, Taylor S, Jossi S, Perez-Toledo M, Faustini SE, Marcial-Juarez E, et al. Sensitive detection of SARS-CoV-2-specific antibodies in dried blood spot samples. Emerg Infect Dis. 2020; 26(12):2970– 3. https://doi.org/10.3201/eid2612.203309 PMID: 32969788
22.Deeks JJ, Dinnes J, Takwoingi Y, Davenport C, Spijker R, Taylor-Phillips S, et al. Antibody tests for identification of current and past infection with SARS-CoV-2. Cochrane Database of Systematic Reviews. 2020; 6:CD013652. https://doi.org/10.1002/14651858.CD013652 PMID: 32584464
23. Wu J, Liang B, Chen C, Wang H, Fang Y, Shen S, et al. SARS-CoV-2 infection induces sustained humoral immune responses in convalescent patients following symptomatic COVID-19. medRxiv. 2020. https://doi.org/10.1101/2020.07.21.20159178
24. Adams ER, Ainsworth M, Anand R, Andersson MI, Auckland K, Baillie JK, et al. Evaluation of antibody testing for SARS-CoV-2 using ELISA and lateral flow immunoassays. medRxiv. 2020. https://doi.org/ 10.1101/2020.04.15.20066407
25. Plebani M, Padoan A, Negrini D, Carpinteri B, Sciacovelli L. Diagnostic performances and thresholds: The key to harmonization in serological SARS-CoV-2 assays? Clin Chim Acta. 2020; 509:1–7. https://doi.org/10.1016/j.cca.2020.05.050 PMID: 32485157
26. Bowsher RR, Devanarayan V. Are lessons learned in setting cut points for detection of anti-drug antibodies also useful in serology assays for robust detection of SARS-CoV-2 reactive antibodies? AAPS J. 2020; 22(6):127. https://doi.org/10.1208/s12248-020-00510-8 PMID: 33025311
27. Brodin P. Immune determinants of COVID-19 disease presentation and severity. Nat Med. 2021; 27 (1):28–33. https://doi.org/10.1038/s41591-020-01202-8 PMID: 33442016
28. Brown L, Byrne RL, Fraser A, Owen SI, Cubas-Atienzar AI, Williams CT, et al. Self-sampling of capillary blood for SARS-CoV-2 serology. Sci Rep. 2021; 11(1):7754. https://doi.org/10.1038/s41598-021-86008-5 PMID: 33833246
29. Matthews MM, Kim TG, Shibata S, Shibata N, Butcher C, Hyun J, et al. COVID-19 serological survey using micro blood sampling. Sci Rep. 2021; 11(1):9475. https://doi.org/10.1038/s41598-021-88850-z PMID: 33947894
30. Abe KT, Li Z, Samson R, Samavarchi-Tehrani P, Valcourt EJ, Wood H, et al. A simple protein-based surrogate neutralization assay for SARS-CoV-2. JCI Insight. 2020; 5(19). https://doi.org/10.1172/jci.Insight.142362 PMID: 32870820

31. Amanat F, Stadlbauer D, Strohmeier S, Nguyen THO, Chromikova V, McMahon M, et al. A serological assay to detect SARS-CoV-2 seroconversion in humans. Nat Med. 2020; 26(7):1033–6. https://doi.org/10.1038/s41591-020-0913-5 PMID: 32398876
32. Landis JR, Koch GG. The measurement of observer agreement for categorical data. Biometrics. 1977; 33(1):159–74. https://doi.org/10.2307/2529310 PMID: 843571
33. Brown LD, Cai TT, DasGupta A. Interval estimation for a binomial proportion. Statistical Science. 2001; 16(2):101–33. https://doi.org/10.1214/ss/1009213286
34. Simundic A-M. Measures of diagnostic accuracy: basic definitions. EJIFCC. 2009; 19(4):203–11. PMID: 27683318
35. Younes S, Al-Jighefee H, Shurrab F, Al-Sadeq DW, Younes N, Dargham SR, et al. Diagnostic efficiency of three fully automated serology assays and their correlation with a novel surrogate virus neutralization test in symptomatic and asymptomatic SARS-CoV-2 individuals. Microorganisms. 2021; 9(2). https:// doi.org/10.3390/microorganisms9020245 PMID: 33504067

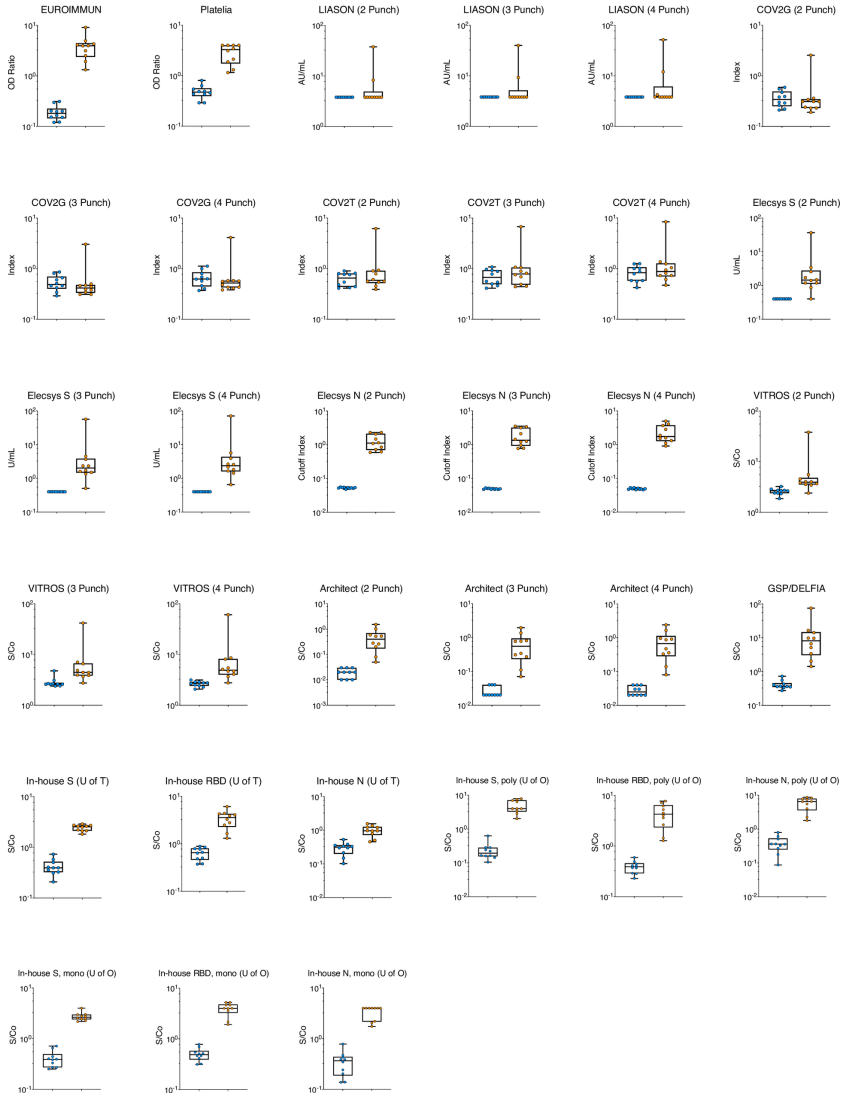
Supplementary Files



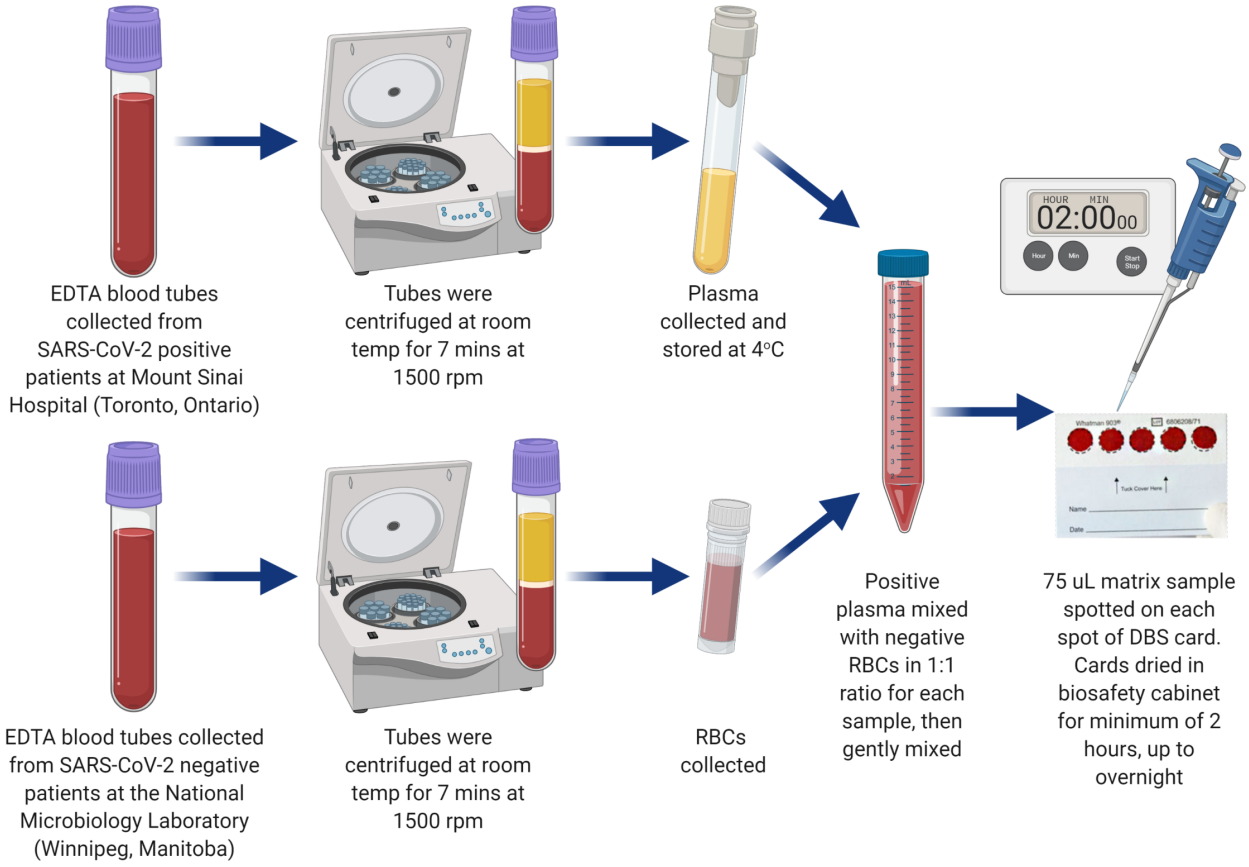
S1 Fig. Positive predictive values (PPV) and negative predictive values (NPV) by prevalence for each commercial and in-house assay on dried blood spot specimens. ROC curves are presented for n = 10 SARS-CoV-2 antibody negative DBS specimens and n = 10 SARS-CoV-2 antibody positive DBS specimens. One 6 mm (1/4 inch) punch was used for the EUROIMMUN assay and two 6 mm (1/4 inch) punches were used for the Platelia and in-house assays. EUROIMMUN = Anti-SARS-CoV-2 ELISA assay (EUROIMMUN, Lübeck, Germany). Platelia = SARS-CoV-2 assay (Bio-Rad, Hercules, California). LIASON = SARS-CoV-2 assay (DiaSorin, Saluggia, Italy). COV2G = SARS-CoV-2 COV2G assay (Siemens, Erlangen, Germany). COV2T = SARS-CoV-2 COV2T assay (Siemens). Elecsys S = Quantitative Anti-SARS-CoV-2 assay (Elecsys spike; Roche, Basel, Switzerland). Elecsys N = Anti-SARS-CoV-2 assay (Elecsys nucleocapsid; Roche). VITROS = Anti-SARS-CoV-2 assay (Ortho Clinical Diagnostics, Raritan, New Jersey). Architect = SARS-CoV-2 assay (Abbott, Mississauga, Canada). GSP/DELFIA = Anti-SARS-CoV-2 assay (PerkinElmer, Waltham, Massachusetts). In-house S (U of T) = In-house spike assay (University of Toronto). In-house RBD (U of T) = In-house RBD assay (University of Toronto). In-house N (U of T) = In-house nucleocapsid assay (University of Toronto). In-house S, mono (U of O) = In- house monoclonal spike assay (University of Ottawa). In-house RBD, mono (U of O) = In-house monoclonal RBD assay (University of Ottawa). In-house N, mono (U of O) = In-house monoclonal nucleocapsid assay (University of Ottawa). The VITROS assay could not achieve a specificity greater than 0% therefore, only PPV is shown.



S2 Fig. Receiver operating characteristic curve for each commercial and in-house assay on dried blood spot specimens. ROC curves are presented for n = 10 SARS-CoV-2 antibody negative DBS specimens and n = 10 SARS-CoV-2 antibody positive DBS specimens. One 6 mm (1/4 inch) punch was used for the EUROIMMUN assay and two 6 mm (1/4 inch) punches were used for the Platelia and in-house assays. EUROIMMUN = Anti-SARS-CoV-2 ELISA assay (EUROIMMUN, Lübeck, Germany). Platelia = SARS-CoV-2 assay (Bio-Rad, Hercules, California). LIASON = SARS-CoV-2 assay (DiaSorin, Saluggia, Italy). COV2G = SARS-CoV-2 COV2G assay (Siemens, Erlangen, Germany). COV2T = SARS-CoV-2 COV2T assay (Siemens). Elecsys S = Quantitative Anti-SARS-CoV-2 assay (Elecsys spike; Roche, Basel, Switzerland). Elecsys N = Anti-SARS-CoV-2 assay (Elecsys nucleocapsid; Roche). VITROS = Anti-SARS-CoV-2 assay (Ortho Clinical Diagnostics, Raritan, New Jersey). Architect = SARS-CoV-2 assay (Abbott, Mississauga, Canada). GSP/DELFIA = Anti-SARS-CoV-2 assay (PerkinElmer, Waltham, Massachusetts). In-house S (U of T) = In-house spike assay (University of Toronto). In-house RBD (U of T) = In-house RBD assay (University of Toronto). In-house N (U of T) = In-house nucleocapsid assay (University of Toronto). In-house S, mono (U of O) = In- house monoclonal spike assay (University of Ottawa). In-house RBD, mono (U of O) = In-house monoclonal RBD assay (University of Ottawa). In-house N, mono (U of O) = In-house monoclonal nucleocapsid assay (University of Ottawa).



S3 Fig. Distribution of values obtained for each commercial and in-house assay on dried blood spot (DBS) specimens. Distribution of values obtained for each commercial and in-house assay on dried blood spot (DBS) specimens. Each panel shows the optical density ratio (OD Ratio), arbitrary units per mL (AU/mL), index, units per mL (U/mL), cut-off index, or signal to cut-off ratio (S/Co) for SARS-CoV-2 antibody negative DBS specimens (n = 10) represented in blue and SARS-CoV-2 antibody positive DBS specimens (n = 10) represented in orange. All values are $\log_{10}$ transformed to aid with 932uebec932er932932io. One 6 mm (1/4 inch) punch was used for the EUROIMMUN assay, and two 6 mm (1/4 inch) punches were used for the Platelia and in-house assays. EUROIMMUN = Anti-SARS-CoV-2 ELISA assay (EUROIMMUN, Lübeck, Germany). Platelia = SARS-CoV-2 assay (Bio-Rad, Hercules, California). LIASON = SARS-CoV-2 assay (DiaSorin, Saluggia, Italy). COV2G = SARS-CoV-2 COV2G assay (Siemens, Erlangen, Germany). COV2T = SARS-CoV-2 COV2T assay (Siemens). Elecsys S = Quantitative Anti-SARS-CoV-2 assay (Elecsys spike; Roche, Basel, Switzerland). Elecsys N = Anti-SARS-CoV-2 assay (Elecsys nucleocapsid; Roche). VITROS = Anti-SARS-CoV-2 assay (Ortho Clinical Diagnostics, Raritan, New Jersey). Architect = SARS-CoV-2 assay (Abbott, Mississauga, Canada). GSP/DELFIA = Anti-SARS-CoV-2 assay (PerkinElmer, Waltham, Massachusetts). In-house S (U of T) = In-house spike assay (University of Toronto). In-house RBD (U of T) = In-house RBD assay (University of Toronto). In-house N (U of T) = In-house nucleocapsid assay (University of Toronto). In-house S, mono (U of O) = In-house monoclonal spike assay (University of Ottawa). In-house RBD, mono (U of O) = In-house monoclonal RBD assay (University of Ottawa). In-house N, mono (U of O) = In-house monoclonal nucleocapsid assay (University of Ottawa). In-house S, poly (U of O) = In-house polyclonal spike assay (University of Ottawa). In-house RBD, poly (U of O) = In-house polyclonal RBD assay (University of Ottawa). In-house N, poly (U of O) = In-house polyclonal nucleocapsid assay (University of Ottawa).



S4 Fig. Procedure for contriving dried blood spot specimens.

S1 Table. Inter-assay concordance and Cohen's kappa coefficient for SARS-CoV-2 antibody testing on dried blood spot specimens.
https://doi.org/10.1371/journal.pone.0261003.s005

S2 Table. Raw data generated during this study for each commercial and in-house assay on dried blood spot specimens.
https://doi.org/10.1371/journal.pone.0261003.s006

A-1.25 Comparative performance data for multiplex SARS-CoV-2 serological assays from a large panel of dried blood spot specimens

Preface

(This work has been previously published as a research article)

Cholette F., Fabia R., Harris A., Ellis H., Cachero K., Schroeder L., Mesa C., Lacap P., Arnold C., **Galipeau Y**., Langlois MA., Colwill K., Gingras AC., McGeer A., Giles E., Day J., Osiowy C., Durocher Y., Hankins C., Mazer B., Drebot M., Kim J.; COVID-19 Immunity Task Force (CITF) working group. **Comparative performance data for multiplex SARS-CoV-2 serological assays from a large panel of dried blood spot specimens**. Heliyon. 2022 Sep;8(9):e10270. Epub 2022 Aug 28.

https://doi.org/10.1016/j.heliyon.2022.e10270

© 2022 Published by Elsevier Ltd. This is an open access article under the CC BY-NC-ND license (http://creativecommons.org/licenses/by-nc-nd/4.0/).

Abstract

The extent of the COVID-19 pandemic will be better understood through serosurveys and SARS-CoV-2 antibody testing. Dried blood spot (DBS) samples will play a central role in large scale serosurveillance by simplifying biological specimen collection and transportation, especially in Canada. Direct comparative performance data on multiplex SARS-CoV-2 assays resulting from identical DBS samples are currently lacking. In our study, we aimed to provide performance data for the BioPlex 2200 SARS-CoV-2 IgG (Bio-Rad), V-PLEX SARS-CoV-2 Panel 2 IgG (MSD), and Elecsys Anti-SARS-CoV-2 (Roche) commercial assays, as well as for two highly scalable in-house assays (University of Ottawa and Mount Sinai Hospital protocols) to assess their suitability for DBS-based SARS-CoV-2 DBS serosurveillance. These assays were evaluated against identical panels of DBS samples collected from convalescent COVID-19 patients (n = 97) and individuals undergoing routine sexually transmitted and bloodborne infection (STBBI) testing prior to the COVID-19 pandemic (n = 90). Our findings suggest that several assays are suitable for serosurveillance (sensitivity >97% and specificity >98%). In contrast to other reports, we did not observe an improvement in performance using multiple antigen consensus-based rules to establish overall seropositivity. This may be due to our DBS panel which consisted of samples collected from convalescent COVID-19 patients with significant anti-spike, -receptor binding domain (RBD), and -nucleocapsid antibody titers. This study demonstrates that biological specimens collected as DBS coupled with one of several readily available assays are useful for large-scale COVID-19 serosurveillance.

Introduction

While molecular and antigen tests remain the standard for diagnosing active coronavirus disease 2019 (COVID-19) [1,2], the breadth and depth of the pandemic will be better understood with the help of serological testing for the presence of antibodies against the severe acute respiratory syndrome coronavirus 2 (SARS-CoV-2) [3]. Serological assays currently authorized or under review by Health Canada require serum or plasma to be collected using standard phlebotomy (https://www.canada.ca/en/health-canada/services/drugs-health-products/covid19-industry/medical-devices/testing/serological.html). This requirement poses significant challenges in implementing population-based serosurveillance due to cost [4], increased risk of exposures during in-person biological specimen collection [5], shortages of healthcare resources [6], as well as geographical and structural barriers especially in northern, remote or isolated settings [7, 8, 9]. Serological tests based on point-of-care (POC) lateral flow immunoassays (LFIAs) would circumvent the need for phlebotomy, but their performance is currently sub-optimal [10]. In contrast, dried blood spot (DBS) specimens are an attractive choice for utilization in serological procedures considering their simplicity [11], acceptability for self-sampling [10, 11, 12, 13, 14], stability at room temperature [15, 16], and proven clinical utility for other viral infections including HIV, hepatitis C, and hepatitis B [17, 18].

Although not used as frequently for SARS-CoV-2, earlier DBS validation studies have reported encouraging performance [4, 14, 15, 19, 20, 21, 22, 23]. DBS were found to be comparable to serum specimens with most studies reporting a sensitivity and specificity of ≥90% and 100% respectively [4, 15, 19, 22, 23]. The serological tests under investigation were largely based on single antigens for the S1 subunit of the spike glycoprotein [4, 5, 24, 25], receptor binding domain (RBD) [22, 24], or nucleocapsid phosphoprotein [15, 21, 26, 27], but these tests may be of limited use in the context of population-based serosurveillance [28]. Antibody responses following a SARS-CoV-2 infection are dynamic in nature and vary according to the antigen of interest. Studies conducted in healthcare workers estimate that the half-life for anti-spike antibodies was more than double the half-life of anti-nucleocapsid antibodies [29, 30], findings that suggest trends in antibody decline have possible impacts on seroprevalence estimates and for follow-up testing in

suspected cases of multisystem inflammatory syndrome [28, 31, 32]. Furthermore, it is difficult to resolve infection-acquired immunity from vaccine-induced immunity without the nucleocapsid antigen or other non-spike antigens [33, 34]. Orthogonal testing could be considered but is likely impractical for DBS given the limited amount of blood that is collected on a standard DBS card (400 µL) compared to phlebotomy (10 mL/tube). DBS sampling in combination with multi-antigen (multiplex) serological testing may be the most appropriate option for serosurveillance since it addresses all concerns related to biological specimen collection and single antigen-based testing [28]. To date, all reports of DBS validation studies with multiplex serological tests have been limited to in-house developed tests [23, 35] and MESO electrochemiluminescence immunoassays (MSD, Rockville, MD) [36]. Direct comparative performance data on multiplex SARS-CoV-2 serological tests derived from identical DBS specimens are significantly lacking.

Here, our objective Is to provide performance data for the BioPlex 2200 SARS-CoV-2 IgG (Bio-Rad, Hercules, CA), V-PLEX SARS-CoV-2 Panel 2 IgG (MSD), and Elecsys Anti-SARS-CoV-2 (Roche, Basel, Switzerland) commercial multiplex assays, as well as for two in-house multiplex assays (University of Ottawa and Mount Sinai Hospital protocols) to evaluate their ability to detect SARS-CoV-2 antibodies in DBS for the purpose of serosurveillance. All the assays are evaluated against identical panels of DBS collected from convalescent COVID-19 patients (n = 97) and individuals undergoing routine sexually transmitted and bloodborne infection (STBBI) testing prior to the COVID-19 pandemic (n = 90). Performance is quantified using sensitivity, specificity, positive predictive values (PPV), and negative predictive values (NPV).

Materials and methods

Ethics statement

All experiments were carried out in accordance with relevant guidelines and regulations. Written informed consent was obtained from all participants who provided blood samples. All participants were 18 years of age or older. Ethical approval was obtained from the Health Canada and Public Health Agency of Canada Research Ethics Board (no. 2020–022P).

Dried blood spot panel

A DBS panel consisting of 97 unique SARS-CoV-2 antibody positive and 90 unique SARS-CoV-2 negative DBS specimens was used to assess performance defined in terms of sensitivity, specificity, negative predictive values (NPV), and positive predictive values (PPV) [37]. The assays are described in greater detail in Table 1. All testing sites were blinded to the status of the DBS specimens and they were asked to perform testing as per standard operating procedures. SARS-CoV-2 antibody positive blood was collected from convalescent COVID-19 patients (positive diagnostic nucleic acid test) at Mount Sinai Hospital (Toronto, Canada) using standard phlebotomy. DBS specimens were collected during the first wave of the pandemic before the availability of vaccines. Therefore, these patients were likely infected by wild type SARS-CoV-2. Several variants of concern (VOCs) have been detected in Canada since our study, but they have not impacted assay performance (personal communications). Blood from BD Vacutainer EDTA tubes (BD, Mississauga, Canada) was directly spotted onto each circle of a Whatman 903 Proteinsaver cards (5 × 75 µL; GE Healthcare, Boston, MA) using pipettes, air-dried at room temperature for a minimum of 3 h (maximum 24 h), and stored at -80 °C in Bitran SARANEX bags (Fisher Scientific, Ottawa, Canada) with desiccant. The commercial assays under investigation require 1 or 4 × 6 mm punches corresponding to approximately 14 µL and 56 µL of whole blood respectively. The in-house assays only required 1 × 3.2 mm punches or approximately 7.5 µL of whole blood. DBS were prepared by applying multiple drops to fill each circle instead of overlaying drops to facilitate uniform blood distribution and drying. Each DBS panel was visually inspected prior to shipment to ensure sample quality was satisfactory to minimize punch-to-punch variability. DBS specimens were prepared from venous blood to minimize patient discomfort i.e., prevent concurrent finger and venous punctures.

Table 1. Overview of the SARS-CoV-2 multiplex serological assays evaluated in this study.

	In-house	In-house	Bioplex 2200 SARS-CoV-2 IgG	V-PLEX SARS-CoV-2 Panel 2 (IgG)	Elecsys Anti-SARS-CoV-2	Elecsys Anti-SARS-CoV-2
Manufacturer	University of Ottawa	Mount Sinai Hospital	Bio-Rad Laboratories	Meso Scale Diagnostics	Roche	Roche
Testing site	CI3	Mount Sinai Hospital	NML at JC Wilt	NML at JC Wilt	NML at CSCHAH	NMAL at CSCHAH
Assay principal	CLIA	CLIA	MFI	ECLIA	ECLIA	ECLIA
Format	384-well plates	384-well plates	Individual tubes	96-well plates	Individual tubes	Individual tubes
Antigen(s)	S, RBD, N	S, RBD, N	S1, RBD, N	S, RBD, N	RBD	N
Antibody class	IgG	IgG	IgG	IgG	Total antibody	Total antibody
Output	S/CO	RR	U/mL	AU/mL	U/mL	COI
Thresholds						
Non-reactive (S)	S/CO < 1.0	<3SD mean of control	<10 U/mL	<1,960 AU/mL	<0.8 U/mL	COI <1.0
Reactive (S)	S/CO ≥ 1.0	≥3SD mean of control	>10 U/mL to ≤100 U/mL[a]	≥1,960 AU/mL	≥0.8 U/mL	COI ≥1.0
Non-reactive (RBD)	S/CO < 1.0	<3SD mean of control	<10 U/mL	<538 AU/mL	<0.8 U/mL	COI <1.0
Reactive (RBD)	S/CO ≥ 1.0	≥3SD mean of control	>10 U/mL to ≤100 U/mL[a]	≥538 AU/mL	≥0.8 U/mL	COI ≥1.0
Non-reactive (N)	S/CO < 1.0	<3SD mean of control	<10 U/mL	<5,000 AU/mL	<0.8 U/mL	COI <1.0
Reactive (N)	S/CO ≥ 1.0	≥3SD mean of control	>10 U/mL to ≤100 U/mL[a]	≥5,000 AU/mL	≥0.8 U/mL	COI ≥1.0
Reported sensitivity %[b,c] 95% CI (LL, UL)			0–7 days: 81.3 (64.7, 91.1) 8–14 days: 96.3 (81.7, 99.3) ≥15 days: 93.9 (90.1, 96.2)	-	0–6 days: 88.6 7–13 days: 85.5 14–20 days: 89.2 21–27 days: 98.3 28–34 days: 100 >35 days: 100 0–13 days: 86.1 (80.3, 90.7) Overall: 98.8 (98.1, 99.3)	0–6 days: 60.2 (52.3, 67.8) 7–13 days: 85.3 (78.6, 90.6) ≥14 days: 99.5 (97.0, 100)
S	94.4	100.0	-	0–14 days: 84.2 (68.7, 94.0) ≥15 days:98.3 (95.1, 99.6)	-	-
RBD	89.0	100.0	-	0–14 days: 71.1 (54.1, 84.6) ≥15 days: 98.3 (95.1, 99.6)	-	-
N	78.6	100.0	-	0–14 days: 71.1 (54.1, 84.6) ≥15 days: 93.8 (89.1, 96.8)	-	-
Reported specificity %[b] 95% CI (LL, UL)			99.9 (99.64, 99.99)	-	99.97 (99.9, 100)	99.8 (99.7, 99.8)
S	98.9	98.0	-	99.5 (97.2, 100)	-	-
RBD	100.0	99.0	-	98.5 (95.7, 99.7)	-	-
N	99.3	94.0	-	100 (98.2, 100)	-	-
Instrument time	10.5 hours/5,760 samples	5–6 hours/384 samples	4 hours/96 samples	6 hours/96 samples	5 hours/96 samples	5 hours/96 samples

CI3: The Centre for Infection, Immunity, and Inflammation in Ottawa, Canada; Mount Sinai Hospital in Toronto, Canada; NML at JC Wilt: National Microbiology Laboratory at the JC Wilt Infectious Diseases Research Centre in Winnipeg, Canada; NML at CSCHAH: National Microbiology Laboratory at the Canadian Science Centre for Human and Animal Health in Winnipeg, Canada; CLIA: Chemiluminescence immunoassay; MFI: Multiplex flow immunoassay; ECLIA: Electrochemiluminescence immunoassay; S: Spike; S1: Spike S1 subunit; RBD: Receptor binding domain; N: Nucleocapsid; RR: Relative ratio; S/CO: Signal to cutoff ratio: COI: Cutoff index; SD: Standard deviation; 95% CI (LL, UL): 95% confidence interval (lower limit, upper limit). A Values >100 U/mL also considered reactive, but above the upper limit of the measuring interval. B Clinical performance reported in serum/plasma. C Clinical performance reported for days between symptom onset and sample collection (Bio-Rad Laboratories SARS-CoV-2 IgG) or days after diagnosis with positive PCR test (both Elecsys and V-PLEX SARS-CoV-2 assays).

EUROIMMUN anti-SARS-CoV-2 ELISA IgG

All DBS specimens were tested using the EUROIMMUN anti-SARS-CoV-2 ELISA IgG assay (EUROIMMUN, Lübeck, Germany) according to the manufacturer's instructions for DBS prior to distribution to each testing site. DBS specimens were punched (1 × 6 mm) using a semi-automated BSD600 Ascent puncher (BSD Robotics, Brisbane, Australia) into 2 mL 96-well polypropylene plates (ThermoFisher Scientific, Waltham, MA). DBS punches were eluted in 500 µL of Sample Buffer (EUROIMMUN) overnight at 4 °C without agitation. Afterwards, plates were incubated at room temperature for 30 min with agitation (400 RPM) and 100 µL of DBS eluate was transferred directly into microplate wells coated with SARS-CoV-2 recombinant structural protein (S1 domain; EUROIMMUN). This plate was shaken at 400 rpm for 1 h at 37 °C during the first incubation step. Results were evaluated by calculating the ratio of the extinction of the patient sample over the extinction of the calibrator. A ratio of <0.8, ≥0.8 to ≤1.1, and ≥1.1 was interpreted as negative, grey zone, and positive respectively. The anti-SARS-CoV-2 ELISA IgG assay from EUROIMMUN was considered as the reference test since it is the only assay approved by Health Canada for use with serum which also has a manufacturer developed protocol for use with DBS (CE marked).

In-house University of Ottawa protocol

DBS specimens were tested using an in-house chemiluminescent direct enzyme-linked immunosorbent assay (CLIA) within the bio-containment CL2+ facility at the Department of Biochemistry, Microbiology, and Immunology (University of Ottawa, Ottawa, Canada) according to laboratory developed protocols validated during earlier work [23]. DBS specimens were punched (1 × 3.2 mm) manually or with semi-automated punchers (PerkinElmer DBS puncher, PerkinElmer, Woodbridge, Canada; BSD6000 Ascent puncher, BSD Robotics) into 2 mL 96-well propylene plates (ThermoFisher Scientific). DBS punches were eluted in 100 µL of PBS containing 1% Triton X-100 (PBST) for a minimum of 4 h up to a maximum of 16 h with agitation 400 RPM at room temperature. Afterwards, DBS eluates were centrifuged at 216 x g for 2 min and diluted with PBST containing 2% milk using a 1:2 ratio. A signal-to-cutoff ratio (S/CO) < 1 and ≥1 was interpreted as negative and positive respectively.

In-house Mount Sinai Hospital protocol

DBS specimens were tested using an in-house CLIA at the Lunenfeld-Tanenbaum Research Institute (Mount Sinai Hospital, Sinai Health, Toronto, Canada) according to laboratory developed protocols validated during earlier work [23]. DBS specimens were punched (1 × 6 mm) manually or with a semi-automated BSD6000 Ascent puncher (BSD Robotics) into 2 mL 96-well polypropylene plates (ThermoFisher Scientific). DBS punches were eluted in 160 µL of PBS containing 0.1% Tween 20 and 1% Triton X-100 for a minimum of 4 h with agitation (150 rpm). Afterwards, DBS eluates were centrifuged at 1,000 x g for 30 s, transferred to new 2 mL 96-well plates, and diluted in 1.3% Blocker BLOTTO buffer (ThermoFisher Scientific) using a 1:4 ratio. Results were interpreted as follows. Spike: a relative ratio (RR) < 0.46 and ≥0.46 was interpreted as negative and positive respectively; RBD: a RR < 0.27 and ≥0.27 was interpreted as negative and positive respectively; nucleocapsid: a RR < 0.74 and ≥0.74 was interpreted as negative and positive respectively. Cutoffs represent three standard deviations from the mean of the log10 distribution of the RR from the negative controls for each antigen [23].

Bio-Rad BioPlex 2200 SARS-CoV-2 IgG

DBS specimens were tested using the BioPlex 2200 SARS-CoV-2 IgG assay (Bio-Rad Laboratories, Hercules, CA) at the NLHRS (Public Health Agency of Canada, Winnipeg, Canada) according to the manufacturer's instructions coupled with BioPlex 2200 SARS-CoV-2 IgG Calibrators diluted in BioPlex 2200 Wash Buffer (Bio-Rad) using a 1:8 ratio. DBS specimens were punched (1 × 6 mm) using a semi-automated BSD600 Ascent puncher (BSD Robotics) into 400 µL 96-well polypropylene plates (ThermoFisher Scientific). DBS punches were eluted in 130 µL of DPBS containing 0.5% BSA and 0.05% Tween 20 overnight at 4 °C without agitation. Afterwards, plates were incubated at room temperature for 30 min with agitation (400 RPM) and 100 µL of DBS eluate was transferred into 2 mL microtubes for direct loading onto the BioPlex 2200 system (Bio-Rad). A result of <10 U/mL and ≥10 U/mL was interpreted as negative and positive respectively. DBS punching and elution protocols were validated using an earlier DBS panel [9] and took into consideration minimal input volumes for the BioPlex 2200 system.

MSD V-PLEX SARS-CoV-2 panel 2 IgG

DBS specimens were tested using the V-PLEX SARS-CoV-2 Panel 2 IgG assay (MSD, Rockville, MD) at the NLHRS (Public Health Agency of Canada, Winnipeg, Canada) according to the manufacturer's instructions. DBS specimens were punched (1 × 6 mm) using a semi-automated BSD600 Ascent puncher (BSD Robotics) into 400 µL 96-well polypropylene plates (ThermoFisher Scientific). DBS punches were eluted in 100 µL of DPBS containing 0.5% BSA and Tween 20 overnight at 4 °C without agitation. Afterwards, plates were incubated at room temperature for 30 min with agitation (400 RPM) and 25 µL of DBS eluate was transferred directly into MULTI-SPOT 96-well plates spotted with SARS-CoV-2 antigens (MSD). Results were interpreted as follows unless stated otherwise. Spike: a result of <4.6 AU/mL and ≥4.6 AU/mL was interpreted as negative and positive respectively; RBD: <2.1 AU/mL and ≥2.1 AU/mL was interpreted as negative and positive respectively; Nucleocapsid: <9.7 AU/mL and ≥9.7 AU/mL was interpreted as negative and positive respectively. Cutoffs as well as DBS punching and elution protocols were established using an earlier DBS panel [9].

Roche Elecsys Anti-SARS-CoV-2

DBS specimens were tested using the Elecsys Anti-SARS-CoV-2 (nucleocapsid) and Elecsys Anti-SARS-CoV-2 S (RBD) assays (Roche Diagnostics, Basel, Switzerland) at the National Microbiology Laboratory (NML; Public Health Agency of Canada, Winnipeg, Canada) according to the manufacturer's instructions. DBS samples were punched (4 × 6 mm) using a semi-automated BSD600 Ascent puncher (BSD Robotics) into 2 mL 96-well polypropylene plates (ThermoFisher Scientific). DBS punches were eluted in 370 µL of DPBS containing 0.5% BSA and 0.05% Tween 20 overnight at 4 °C with agitation (400 RPM). Afterwards, plates were incubated at room temperature for 30 min with agitation (400 RPM) and 250 µL of DBS eluate was transferred into 2 mL microtubes for direct loading onto a cobas e 411 analyser (Roche Diagnostics). A result of <0.8 U/mL and ≥0.8 U/mL was interpreted as negative and positive respectively with the Elecsys Anti-SARS-CoV-2 S. A cutoff index <1.0 and ≥1.0 was interpreted as negative and positive respectively with the Elecsys Anti-SARS-CoV-2 assay. DBS punching and elution protocols were validated using an earlier DBS panel [9].

Statistical analysis

Continuous data were summarized using the median and interquartile range (IQR), while categorical data were presented using exact numbers and proportions. Performance expressed in terms of sensitivity, specificity, NPV, and PPV was computed using the anti-SARS-CoV-2 ELISA IgG assay (EUROIMMUN) as the reference test. PPV and NPV were also computed using a prevalence ranging from 0.5% to 50% as follows: PPV = (sensitivity x prevalence)/[(sensitivity x prevalence) + ((1 – specificity) x (1 – prevalence))]; NPV = (specificity x (1 – prevalence))/[(specificity x (1 – prevalence)) + ((1 – sensitivity) x prevalence)] [38].

The strength of agreement between the Index test and the reference test was quantified with kappa coefficients (https://www.graphpad.com/quickcalcs/kappa1/?K=2) and interpreted as follows: <0 = no agreement, 0–0.20 = slight agreement, 0.21–0.40 = fair agreement, 0.41–0.60 = moderate agreement, 0.61–0.80 = substantial agreement, and 0.81–1.00 = almost perfect agreement [39]. Confidence intervals for kappa coefficients were computed according to Fleiss [40].

Receiver operating characteristic (ROC) curves were computed using the Wilson/Brown method [41]. Test performance was quantified according to the area under the ROC curve (AUC) and interpreted as follows: <0.5 = not useful, 0.5–0.6 = bad, 0.6–0.7 = sufficient, 0.7–0.8 = good, 0.8–0.9 = very good, and 0.9–1.0 = excellent [41, 42]. Youden's J statistic was computed as follows: J = sensitivity + specificity – 1. Prism version 9.0.0 (GraphPad Software, San Diego, CA) was used for all data analysis and 943uebec943er943943io.

Data availability

All data generated or analysed during this study are included in this published article (and its Supplementary Information files).

Results

COVID-19 patient population

Demographic and clinical characteristics of the COVID-19 patient population are provided in Table 2. The patient population included 21 outpatients (21.6%), 51 inpatients (52.6%), and 25 patients admitted to the intensive care unit (ICU; 25.8%). Patient age ranged from 24 to 97 years (median = 62) and 48 (49.5%) were female. Days between symptom onset and sample collection ranged from 1 to 188 days (median = 21). According to the EUROIMMUN anti-SARS-CoV-2 IgG assay (Figure 1), antibody readings were higher in the ICU patient group (median S/CO = 6.1; IQR = 4.8, 7.5) compared to the outpatient group (median S/CO = 4.6; IQR = 2.5, 5.6) and inpatient group (median S/CO = 4.8; IQR = 4.8, 7.5). Antibody readings were trending higher in DBS collected 15–28 days between symptom onset and sample collection (median S/CO = 5.6; IQR = 3.9, 6.7) and lower in DBS collected ≤14 days (median S/CO = 4.7; IQR = 2.8, 6.0) or >28 days (median S/CO = 5.1; IQR = 2.6, 6.5) between symptom onset and sample collection however, these observations were not statistically significant (Figure 1). Furthermore, antibody readings did not vary significantly according to sex or age (Figure 1).

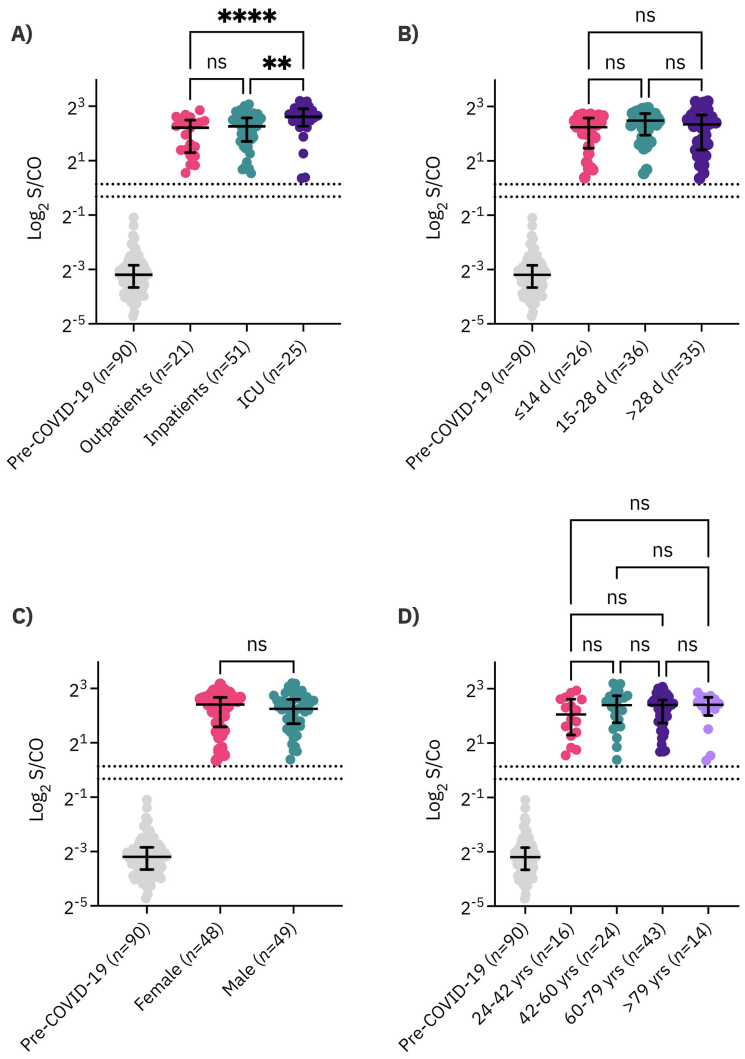


Figure 1 EUROIMMUN anti-SARS-CoV-2 ELISA IgG signal to cutoff ratios (S/CO) from DBS collected from COVID-19 patients. A) Highest level of care; B) Days between symptom onset and sample collection; C) Sex; D) Age categories. Bars represent the median and interquartile range (IQR). Test cutoffs are represented by dashed lines. Significant differences between S/CO means are represented by)) ($p < 0.002$) and)))) ($p < 0.0001$) while non-significant differences are represented by ns. S/CO values are $\log_2$ transformed to aid with visualisation.

COVID-19 patient DBS versus pre-COVID-19 DBS

SARS-CoV-2 antibody readings from the two in-house and three commercial multiplex assays are summarized in Figures 2 and S1 Table. Both in-house assays could clearly distinguish DBS from COVID-19 patients and those collected pre-COVID-19 regardless of antigen, days between symptom onset and sample collection, or level of care (Figure 2). Antibody readings were generally highest in the ICU patient group and DBS collected 15–28 days between symptom onset and sample collection (S1 Table). Among the commercial assays, the BioPlex and V-PLEX assays

clearly differentiated DBS from COVID-19 patients and those collected pre-COVID-19, while the separation was not as clear with the Elecsys assay (Figure 2).

Table 2. Demographic and clinical characteristics of COVID-19 patients.

Variable	≤14 days[a] (*n* = 26)	15–28 days (*n* = 36)	>28 days (*n* = 35)	All patients (*n* = 97)
Median age (IQR)	62.0 (57.0, 70.5)	70.0 (58.0, 77.8)	55.0 (39.0, 67.0)	62.0 (50.0, 75.0)
Female sex (%)	9 (34.6)	22 (61.1%)	18 (51.4)	48 (49.5)
Outpatient (%)	-	-	21 (60.0)	21 (21.6)
Inpatient (%)	9 (34.6)	26 (72.2)	6 (17.1)	51 (52.6)
ICU (%)	17 (65.4)	10 (27.8)	8 (22.9)	25 (25.8)
Median S/CO (IQR)[b]	4.7 (2.8, 6.0)	5.6 (3.9, 6.7)	5.1 (2.6, 6.5)	5.1 (3.3, 6.3)

ICU: Intensive care unit; IQR: Interquartile range; S/CO: Signal to cutoff ratio. A Days between symptom onset and sample collection. B EUROIMMUN anti-SARS-CoV-2 IgG assay.

Sensitivity and specificity

Sensitivity and specificity were computed using cutoffs established elsewhere or those recommended by the manufacturers (Tables 3, S2 Table). Overall sensitivity of the assays ranged from 96.9 to 99.0%, 82.5–97.9%, and 55.7–97.9% for the spike, RBD, and nucleocapsid antigens respectively. The highest sensitivities were achieved in DBS samples taken from severely ill patients (outpatients or ICU patients) and samples taken 15–28 or >28 days between symptom onset and sample collection (S2 Table). Most false negative results were reported in DBS collected ≤14 days post symptom onset. Overall specificity of the assays ranged from 92.2 to 100.0%, 93.0–100.0%, and 92.2–100.0% for the spike, RBD, and nucleocapsid antigens respectively (Table 3). All assays were in "almost perfect" agreement with the reference test based on kappa coefficients except the Elecsys assay which only had "moderate" agreement (nucleocapsid, kappa = 0.547; 95% CI = 0.441, 0.653).

Similar observations were made using multiple antigen consensus-based rules to establish overall positivity. Overall sensitivity of the assays ranged from 96.9 to 99.0% if using spike or RBD. Most false negative results were reported in DBS collected ≤14 days post symptom onset. Therefore, sensitivity was typically higher in DBS collected ≥15 days post symptom onset. Overall specificity of the assays ranged from 90.0 to 98.9% if using spike or RBD All assays were in “almost perfect” agreement with the reference test based on kappa coefficients (Table 3).

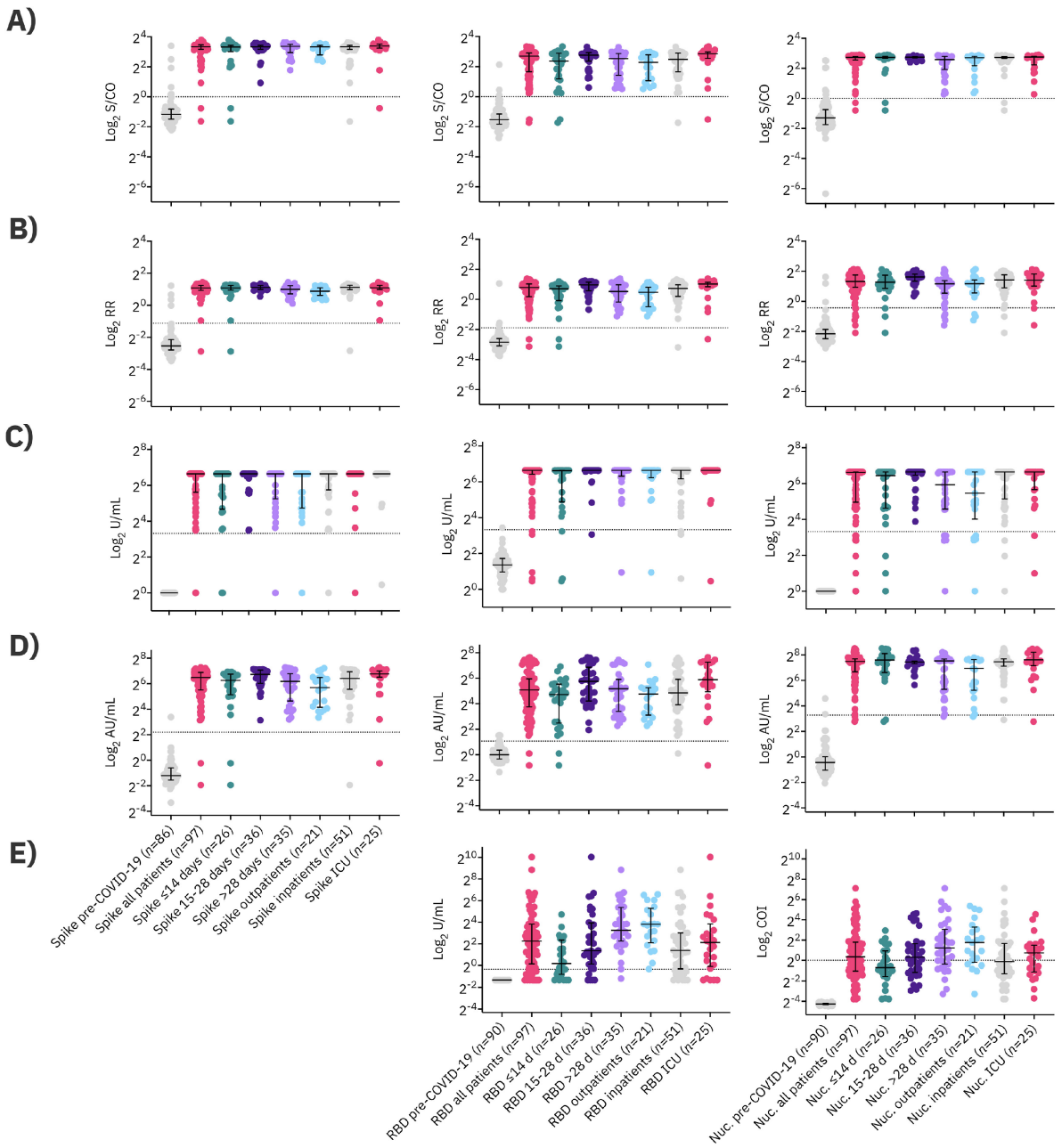


Figure 2 SARS-CoV-2 antibody readings in DBS from convalescent COVID-19 patients and DBS collected pre-COVID-19. A) University of Ottawa protocol; B) Mount Sinai Hospital protocol; C) Bio-Rad BioPlex 2200 SARS-CoV-2 IgG; D) MSD V-PLEX SARS-CoV-2 Panel IgG; E) Roche Elecsys Anti-SARS-CoV-2. Bars represent the median and interquartile range. Test cutoffs are represented by dashed lines. Antibody readings are $\log_2$ transformed to aid with visualisation.

Table 3 Summary performance statistics in dried blood specimens.

Spike	University of Ottawa protocol	Mount Sinai Hospital protocol	Bio-Rad BioPlex 2200 SARS-CoV-2 IgG	MSD V-Plex SARS-CoV-2 Panel 2 IgG[a]	Roche Elecsys Anti-SARS-CoV-2
Sensitivity (*n*/N) % (95% CI)	95/97 97.9 (92.8, 99.6)	96/97 99.0 (94.4, 99.9)	94/97 96.9 (91.3, 99.2)	95/97 97.9 (92.8, 99.6)	
Specificity (*n*/N) % (95% CI)	83/90 92.2 (84.8, 96.2)	86/90 95.6 (89.1, 98.3)	90/90 100.0 (95.9, 100.0)	85/86 98.8 (93.7, 99.9)	
PPV (*n*/N) % (95% CI)	7/90 93.1 (86.5, 96.6)	4/90 96.0 (90.2, 98.4)	0/90 100.0 (96.1, 100.0)	1/86 99.0 (94.3, 99.9)	
NPV (*n*/N) % (95% CI)	2/97 97.6 (91.8, 99.6)	1/97 98.9 (93.8, 99.9)	3/97 96.8 (90.9, 99.1)	2/97 97.7 (92.0, 99.6)	
Kappa (95% CI)	0.903 (0.841, 0.965)	0.946 (0.900, 0.993)	0.968 (0.932, 1.000)	0.967 (0.930, 1.000)	
RBD	**University of Ottawa protocol**	**Mount Sinai Hospital protocol**	**Bio-Rad BioPlex 2200 SARS-CoV-2 IgG**	**MSD V-Plex SARS-CoV-2 Panel 2 IgG[a]**	**Roche Elecsys Anti-SARS-CoV-2**
Sensitivity (*n*/N) % (95% CI)	95/97 97.9 (92.8, 99.6)	95/97 97.9 (92.8, 99.6)	92/97 94.8 (88.5, 97.8)	95/97 97.9 (92.8, 99.6)	80/97 82.5 (73.7, 88.8)
Specificity (*n*/N) % (95% CI)	87/90 96.7 (90.7, 99.1)	87/90 96.7 (90.7, 99.1)	89/90 98.9 (94.0, 99.9)	80/86 93.0 (85.6, 96.8)	90/90 100.0 (95.9, 100.0)
PPV (*n*/N) % (95% CI)	3/90 96.9 (91.4, 99.2)	3/90 96.9 (91.4, 99.2)	1/90 98.9 (94.2, 99.9)	6/86 94.1 (87.6, 97.2)	0/90 100.0 (95.4, 100.0)
NPV (*n*/N) % (95% CI)	2/97 97.8 (92.2, 99.6)	2/97 97.8 (92.2, 99.6)	5/97 94.7 (88.1, 97.7)	2/97 97.6 (91.5, 99.6)	17/97 84.1 (76.0, 89.8)
Kappa (95% CI)	0.946 (0.900, 0.993)	0.946 (0.900, 0.993)	0.936 (0.885, 0.986)	0.912 (0.852, 0.972)	0.819 (0.739, 0.900)
Nucleocapsid	**University of Ottawa protocol**	**Mount Sinai Hospital protocol**	**Bio-Rad BioPlex 2200 SARS-CoV-2 IgG**	**MSD V-Plex SARS-CoV-2 Panel 2 IgG[a]**	**Roche Elecsys Anti-SARS-CoV-2**
Sensitivity (*n*/N) % (95% CI)	95/97 97.9 (92.8, 99.6)	89/97 91.8 (84.6, 95.8)	87/97 89.7 (82.1, 94.3)	94/97 96.9 (91.3, 99.2)	54/97 55.7 (45.8, 65.2)
Specificity (*n*/N) % (95% CI)	83/90 92.2 (84.8, 96.2)	87/90 96.7 (90.7, 99.1)	90/90 100.0 (95.9, 100.0)	84/86 97.7 (91.9, 99.6)	90/90 100.0 (95.9, 100.0)
PPV (*n*/N) % (95% CI)	7/90 93.1 (86.5, 96.6)	3/90 96.7 (90.8, 99.1)	0/90 100.0 (95.8, 100.0)	2/86 97.9 (92.7, 99.6)	0/90 100.0 (93.4, 100.0)
NPV (*n*/N) % (95% CI)	2/97 97.6 (91.8, 99.6)	8/97 91.6 (84.3, 95.7)	10/97 90.0 (82.6, 94.5)	3/97 96.6 (90.3, 99.1)	43/97 67.7 (59.3, 75.0)
Kappa (95% CI)	0.903 (0.842, 0.965)	0.882 (0.815, 0.950)	0.893 (0.829, 0.957)	0.945 (0.898, 0.993)	0.547 (0.441, 0.653)
Spike or RBD	**University of Ottawa protocol**	**Mount Sinai Hospital protocol**	**Bio-Rad BioPlex 2200 SARS-CoV-2 IgG**	**MSD V-Plex SARS-CoV-2 Panel 2 IgG[a]**	**Roche Elecsys Anti-SARS-CoV-2**
Sensitivity (*n*/N) % (95% CI)	95/97 97.9 (92.8, 99.6)	96/97 99.0 (94.4, 99.9)	94/97 96.9 (91.3, 99.2)	95/97 97.9 (92.8, 99.6)	
Specificity (*n*/N) % (95% CI)	81/90 90.0 (82.1, 94.6)	84/90 93.3 (86.2, 96.9)	89/90 98.9 (94.0, 99.9)	79/86 91.9 (84.1, 96.0)	
PPV (*n*/N) % (95% CI)	9/90 91.3 (84.4, 95.4)	6/90 94.1 (87.8, 97.3)	1/90 98.9 (94.3, 99.9)	7/86 93.1 (86.5, 96.6)	
NPV (*n*/N) % (95% CI)	2/97 97.6 (91.6, 99.6)	1/97 98.8 (93.6, 99.9)	3/97 96.7 (90.8, 99.1)	2/97 97.5 (91.4, 99.6)	
Kappa (95% CI)	0.882 (0.814, 0.949)	0.925 (0.870, 0.979)	0.957 (0.916, 0.999)	0.901 (0.838, 0.964)	

[a] Four pre-COVID-19 DBS omitted from analysis due to insufficient quantity for testing.

Predictive values

Predictive values for the two in-house and three commercial multiplex assays with DBS are summarized in Tables 3 and S2 Table. All assays achieved overall positive predictive values (PPV) of >93%, >94%, and >93% with the spike, RBD, and nucleocapsid antigen respectively (Table 3). All assays achieved overall negative predictive values (NPV) of >97%, >84%, and >67% with the spike, RBD, and nucleocapsid antigen respectively (Table 3). PPV and NPV improved for all assays in DBS collected ≥15 days post symptom onset (S2 Table). Similar PPV were observed using multiple antigen consensus-based rules. More specifically, all assays achieved an overall PPV of >91% with spike or RBD antigens above the cutoff (Table 3). All assays achieved an overall NPV of >96% with spike or RBD antigens above the cutoff (Table 3).

Granted prevalence has a significant impact on PPV and NPV, predictive values were re-computed using a wide range of prevalence estimates (Figure 3). As expected, all assays achieved a wide range of PPV and NPV depending on prevalence and antigen. In general terms, the spike and RBD antigens would result in the lowest proportion of false negatives and false positives in low and high prevalence settings respectively. Likewise, commercial assays would offer better PPV and NPV in low prevalence settings compared to the in-house assays. Using multiple antigen consensus-based rules would perform similarly to using spike or RBD alone (Figure 3).

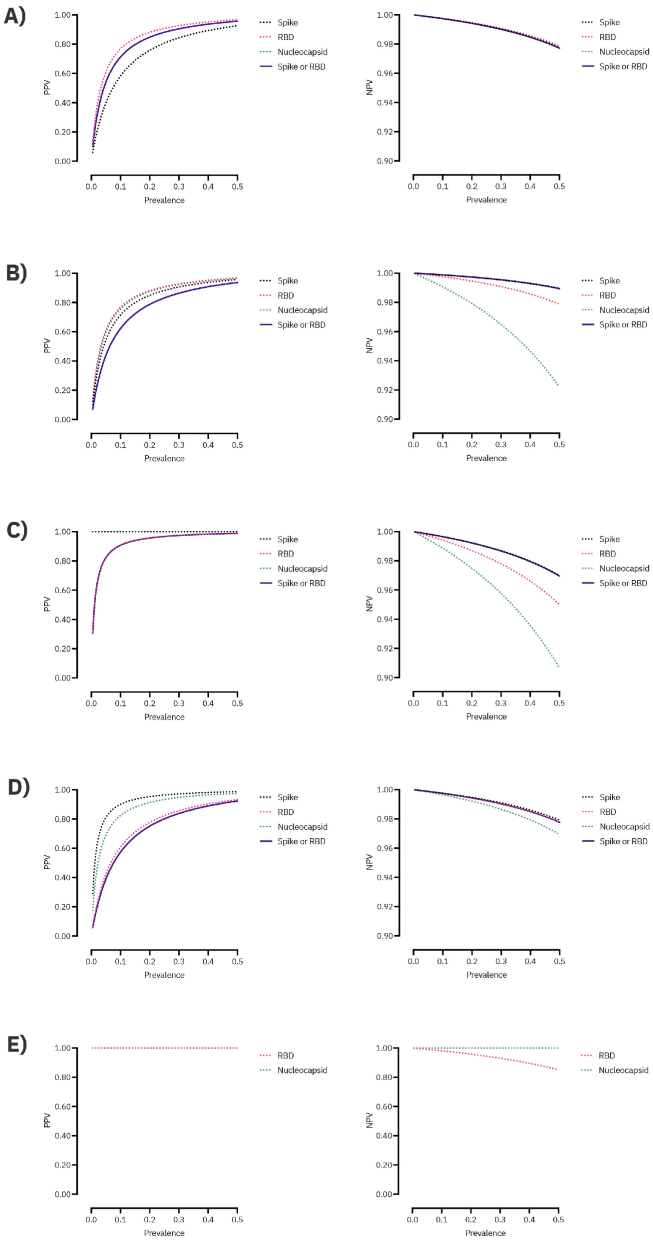


Figure 3 Positive and negative predictive values according to prevalence. A) University of Ottawa protocol; B) Mount Sinai Hospital protocol; C) BioPlex 2200 SARS-CoV-2 IgG (Bio-Rad); D) V-PLEX SARS-CoV-2 Panel 2 IgG (MSD); E) Elecsys Anti-SARS-CoV-2 (Roche).

ROC curve analysis

According to receiver operating characteristic (ROC) curves (Figure 4), all assays demonstrated excellent performance (area under the curve >95%) regardless of antigen, days post symptom onset, and highest level of care suggesting that performance could be improved by adjusting cutoffs (Figure 4).

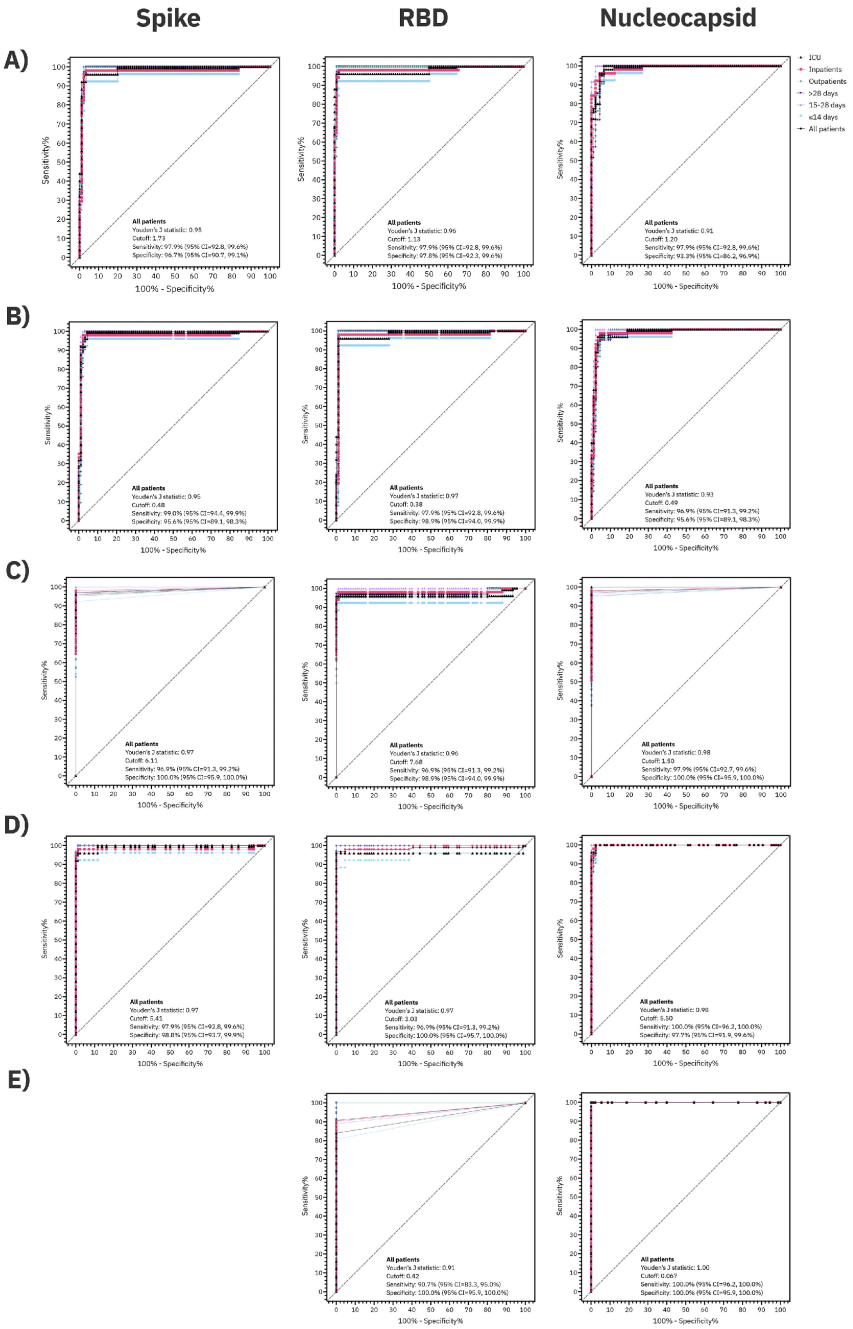


Figure 4 Receiver operating characteristic (ROC) curves. ROC curves are presented for *n* = 90 SARS-CoV-2 antibody negative DBS specimens and *n* = 97 SARS-CoV-2 antibody positive DBS specimens. Four SARS-CoV-2 antibody negative DBS specimens were removed from the V-PLEX SARS-CoV-2 Panel 2 IgG (MSD) analysis due to insufficient quantity for testing. A) University of Ottawa protocol; B) Mount Sinai Hospital protocol; C) BioPlex 2200 SARS-CoV-2 IgG (Bio-Rad); D) V-PLEX SARS-CoV-2 Panel 2 IgG (MSD); E) Elecsys Anti-SARS-CoV-2 (Roche).

Discussion

Our study describes the performance of three commercial and two in-house multiplex assays for the qualitative analysis of SARS-CoV-2 antibodies in a well pedigreed panel of DBS specimens.

These assays were evaluated using a panel of 187 unique DBS specimens collected from 97 convalescent COVID-19 patients and 90 individuals undergoing routine STBBI testing pre-COVID-19. Overall, higher antibody responses were observed in ICU patients and in DBS collected >14 days between symptom onset and sample collection which is consistent with the current literature. Higher antibody titers are typically reported in severely ill patients compared to patients exhibiting milder forms of COVID-19 [43, 44, 45, 46]. Seroconversion typically occurs within 2 weeks post-infection [46]. Taken altogether, we expected some heterogeneity in performance according to disease severity and the number of days between symptom onset and sample collection. Future assessments should incorporate DBS specimens collected during multiple waves of the pandemic since VOCs may elicit varying levels of immune responses compared to wild-type SARS-CoV-2 [47,48], especially the omicron variant which has been associated with milder disease severity [49].

Overall sensitivities ranged from 96.9% to 99.0%, 82.5%–97.9%, and 55.7%–97.9% for the spike, RBD, and nucleocapsid antigens respectively. A similar observation was made using a consensus-based rule (spike or RBD) to establish overall seropositivity. While varying levels of performance are expected based on the antigen of interest [28, 29, 30], our ROC curve analysis suggests that better performance could be achieved by adjusting laboratory-developed or manufacturer recommended cutoffs for DBS specimens [5, 21, 50, 51]. These observations are comparable to performance estimates reported by others with commercial assays like the Roche Elecsys [15, 21]. However, we are the first group to report performance data on the BioPlex 2200 SARS-CoV-2 IgG with DBS specimens to the best of our knowledge. We also clearly demonstrate that laboratory developed assays have the potential to perform as well as or better than commercial assays [23, 52]. Future inter-laboratory comparisons will be conducted with DBS collected from the latest iteration of the Canadian COVID-19 antibody and Health Survey (April 1 2022 to August 31 2022; https://www.statcan.gc.ca/en/survey/household/5339).

Although adjusting cutoffs might be helpful in improving performance, this approach may be inadequate in population-wide serosurveys where SARS-CoV-2 infected individuals may be mostly asymptomatic. Multi-antigen approaches have been proposed as a better alternative especially since they allow to distinguish between vaccine-induced immunity and infection

acquired immunity [28]. We did not observe marked improvements in assay performance using a two-antigen strategy (spike or RBD) compared to using the spike or RBD antigen alone, contrary to other studies that have shown improvements in performance using a multiplex approach to establish seropositivity [28, 53, 54]. This could be due to our choice of patient population which consisted of convalescent COVID-19 patients with elevated antibody titers for spike, RBD, and nucleocapsid.

In low prevalence settings, a high PPV is critical and tests with high specificity (≥99%) should be chosen to limit the number of false positives. This may no longer be a significant issue for the spike and RBD antigens due to high vaccine uptake [55], but it is still an important consideration for the nucleocapsid antigen to allow the distinction between infection- and vaccine-induced antibody responses [34]. In this study, overall specificity ranged from 92.2% to 100% for the nucleocapsid antigen. The highest specificities (100%) were observed with the BioPlex and Elecsys assays while the lowest specificities (<97%) were observed with the in-house assays resulting in lower PPV in low prevalence settings (<5%). However, this could be improved by adjusting cutoffs as mentioned above.

At the time of this writing, information regarding SARS-CoV-2 antibody seroprevalence in Canadians was lacking but, overall seroprevalence was estimated at 3.6% (95% CI = 2.6,4.2) during the first wave of the pandemic [56, 57]. The BioPlex 2200 SARS-CoV-2 IgG, MSD V-PLEX SARS-CoV-2 Panel 2 IgG, or Roche Elecsys are therefore mostly like better suited for epidemiological studies in low prevalence settings compared to the in-house assays. However, further validation in asymptomatic populations and longer delays between symptom onset and DBS collection (>6 months) will be required to substantiate our findings especially if SARS-CoV-2 becomes endemic [58]. Other laboratories seeking to implement their own serosurveillance may benefit from adopting commercial assays versus in-house assays due to their performance and lower technical barriers to implementation. For example, the BioPlex 2200 system is a fully automated system capable of delivering results for all three antigens simultaneously while the in-house assays require customized liquid handling platforms where three singleton assays are necessary to deliver results for all three antigens.

Our study revealed acceptable performance of three multiplex SARS-CoV-2 antibody assays: BioPlex 2200 SARS-CoV-2 IgG, MSD V-PLEX SARS-CoV-2 Panel 2 IgG, or Roche Elecsys. Several false positives were observed with the in-house assays resulting in low PPV in low prevalence settings, but it would be important to note that the University of Ottawa and Mount Sinai Hospital enforce a requirement that two or more of the individual assays pass their cutoffs for a sample to be considered seropositive overall [23]. In this study, our findings suggest that performance could improve by simply adjusting cutoffs for DBS specimens. Adjusting manufacturer's cutoff values will have to be undertaken independently by laboratories and is likely not generalizable. While others have reported greater performance using a multiplexed approach versus single-antigens, we did not make this observation. This is likely due to the patient population that was chosen to make up the DBS panel. Our findings will have to be substantiated with further validation in asymptomatic populations and DBS specimens collected during the latest wave of the pandemic to confirm assay performance. Nonetheless, our study demonstrates that DBS specimens coupled with several different assays are useful tools for large-scale application of epidemiological COVID-19 studies.

Author contribution statement
François Cholette: Conceived and designed the experiments; Analyzed and interpreted the data; Wrote the paper. Christine Mesa, Philip Lacap, Marc-André Langlois, Karen Colwill, Anne-Claude Gingras, Carla Osiowy and John Kim: Conceived and designed the experiments; Analyzed and interpreted the data. Michael Drebot: Conceived and designed the experiments. Rissa Fabia, Angela Harris, Hannah Ellis, Karla Cachero, Lukas Schroeder, Elizabeth Giles and Jacqueline Day: Performed the experiments. Corey Arnold, Yannick Galipeau: Performed the experiments; Analyzed and interpreted the data. Allison McGeer, Yves Durocher, Catherine Hankins, Bruce Mazer: Contributed reagents, materials, analysis tools or data.

Funding statement
This research did not receive any specific grant from funding agencies in the public, commercial, or not-for-profit sectors.

Data availability statement
Data included in article/supplementary material/referenced in article.

Declaration of interests statement
The authors declare no conflict of interest.

Additional information
No additional information is available for this paper.

Acknowledgements
We thank David Taylor, Timothy Evans, Heather Hannah, Mona Nemer, Howard Njoo, Gina Olgilvie, Jutta Preiksaitis, Gail Tomblin Murphy, Paul Van Caeseele, Theresa Tam, Stephen Lucas, Vivek Goel, Philippe Gros, Scott Halperin, Charu Kauschic, James D. Kellner, Susan Kirkland, Gary Kobinger, Mel Krajden, Christie Lutsiak, Richard Massé, Deborah Money, Caroline Quach-Thanh, and Rosann Seviour of the CITF Leadership Group for their support. We also thank Bhavisha Rathod and members of the Network Biology Collaborative Centre (nbcc.lunenfeld.ca; a facility supported by the Canada Foundation for Innovation, the Ontario Government, and Genome Canada and Ontario Genomics [OGI-139]) for the assays using the Mount Sinai Hospital protocol.

References

[1] Vandenberg, O., Martiny, D., Rochas, O., van Belkum, A. & Kozlakidis, Z. Considerations for diagnostic COVID-19 tests. Nat. Rev. Microbiol. 19, 171-183,
[2] Y. Mardian, H. Kosasih, M. Karyana, A. Neal, C.Y. Lau, Review of current COVID-19 diagnostics and opportunities for further development, Front. Med. 8 (2021), 615099.
[3] N. Bobrovitz, et al., Global seroprevalence of SARS-CoV-2 antibodies: a systematic review and meta-analysis, PloS One 16 (2021), e0252617.
[4] G.L. Morley, et al., Sensitive detection of SARS-CoV-2-specific antibodies in dried blood spot samples, Emerg. Infect. Dis. 26 (2020) 2970–2973.
[5] C.T. Turgeon, et al., Detection of SARS-CoV-2 IgG antibodies in dried blood spots, Diagn. Microbiol. Infect. Dis. 101 (2021), 115425.
[6] H. Wu, et al., Hospital Capacities and Shortages of Healthcare Resources Among US Hospitals during the Coronavirus Disease 2019 (COVID-19) Pandemic, National Healthcare Safety Network (NHSN), March 27-July 14, 2020, Infection Control & Hospital Epidemiology, 2021, pp. 1–4.
[7] G. Johnson, et al., Clinical evaluation of the GeneXpert® Xpert® xpress SARS-CoV2/flu/RSV combination test, J. Clin. Virol. 1 (2021).
[8] P. Sandstrom, A. Meyers, Interim guidance on the use of the Abbott ID NOW™ instrument and COVID-19 assay, Can. Comm. Dis. Rep. 46 (2020) 422–426.
[9] F. Cholette, et al., Dried blood spot specimens for SARS-CoV-2 antibody testing: a multi-site, multi-assay comparison, PloS One 16 (2021).
[10] M. Lisboa Bastos, et al., Diagnostic accuracy of serological tests for covid-19: systematic review and meta-analysis, BMJ 370 (2020) m2516.
[11] A.K. Sakhi, et al., Feasibility of self-sampled dried blood spot and saliva samples sent by mail in a population-based study, BMC Cancer 15 (2015) 265.
[12] T. Prinsenberg, et al., Dried blood spot self-sampling at home is a feasible technique for hepatitis C RNA detection, PloS One 15 (2020), e0231385.
[13] J. Beyerl, et al., A dried blood spot protocol for high throughput analysis of SARSCoV-2 serology based on the Roche Elecsys anti-N assay, EbioMedicine 70 (2021), 103502.
[14] Brown, L. et al. Self-sampling of capillary blood for SARS-CoV-2 serology. Sci. Rep. 11, 7754,.
[15] E. Fontaine, C. Saez, Analysis of SARS-CoV-2 antibodies from dried blood spot samples with the Roche Elecsys Immunochemistry method, Practical Laboratory Medicine 25 (2021), e00234.
[16] Bjorkesten, J. € et al. Stability of proteins in dried blood spot biobanks. Mol. Cell. Proteomics 16, 1286-1296,
[17] E. Tuaillon, et al., Dried blood spot tests for the diagnosis and therapeutic monitoring of HIV and viral hepatitis B and C, Front. Microbiol. 11 (2020) 373.
[18] F. Amini, et al., Reliability of dried blood spot (DBS) cards in antibody measurement: a systematic review, PloS One 16 (2021), e0248218.
[19] F. Cholette, et al., Dried blood spot specimens for SARS-CoV-2 antibody testing: a multi-site, multi-assay comparison, PloS One 16 (2021).
[20] Weisser, H. et al. Evaluation of dried blood spots as alternative sampling material for serological detection of anti-SARS-CoV-2 antibodies using established ELISAs. Clin. Chem.

Lab. Med. 59, 979-985 [21] R. Mulchandani, et al., Use of dried blood spot samples for SARS-CoV-2 antibody detection using the Roche Elecsys I high throughput immunoassay, J. Clin. Virol. 136 (2021), 104739
[22] D. Brinc, et al., Evaluation of dried blood spot testing for SARS-CoV-2 serology using a quantitative commercial assay, Viruses 13 (2021) 962.
[23] K. Colwill, et al., A scalable serology solution for profiling humoral immune responses to SARS-CoV-2 infection and vaccination, Clinical & Translational Immunology 11 (2021), e1380.
[24] S.J. Moat, et al., Development of a high-throughput SARS-CoV-2 antibody testing pathway using dried blood spot specimens, Ann. Clin. Biochem. 58 (2021) 123–131.
[25] D.G. Karp, et al., A serological assay to detect SARS-CoV-2 antibodies in at-home collected finger-prick dried blood spots, Sci. Rep. 10 (2020), 20188.
[26] S. Gaugler, P.E. Sottas, K. Blum, M. Luginbuhl, Fully automated dried blood spot sample handling and extraction for serological testing of SARS-CoV-2 antibodies, Drug Test. Anal. 13 (2021) 223–226. [27] W.F. Garcia-Beltran, et al., Remote Fingerstick Blood Collection for Severe Acute Respiratory Syndrome Coronavirus 2 (SARS-CoV-2) Antibody Testing, 145, Archives of Pathology & Laboratory Medicine, 2021, pp. 415–418.
[28] Fotis, C. et al. Accurate SARS-CoV-2 seroprevalence surveys require robust multiantigen assays. Sci. Rep. 11, 6614,.
[29] S.F. Lumley, et al., The duration, dynamics, and determinants of severe acute respiratory syndrome coronavirus 2 (SARS-CoV-2) antibody responses in individual healthcare workers, Clin. Infect. Dis. 73 (2021) e699–e709.
[30] J. Van Elslande, L. Gruwier, L. Godderis, P. Vermeersch, Estimated half-life of SARSCoV-2 anti-spike antibodies more than double the half-life of anti-nucleocapsid antibodies in healthcare workers, Clin. Infect. Dis. 73 (2021) 2366–2368.
[31] E.R. Adams, et al., Evaluation of antibody testing for SARS-CoV-2 using ELISA and lateral flow immunoassays, medRxiv (2020).
[32] Prevention, C. f. D. C. a., Information for Healthcare Providers about Multisystem Inflammatory Syndrome in Children (MIS-C), 2021. https://www.cdc.gov/mis/mis - c/hcp/index.html%3e%20.
[33] N. Post, et al., Antibody response to SARS-CoV-2 infection in humans: a systematic review, PloS One 15 (2020), e0244126.
[34] N. Duarte, et al., Adapting serosurveys for the SARS-CoV-2 vaccine era, Open Forum Infect. Dis. 9 (2022) ofab632.
[35] J.S. Schultz, et al., Development and validation of a multiplex microsphere immunoassay using dried blood spots for SARS-CoV-2 seroprevalence: application in first responders in Colorado, USA, J. Clin. Microbiol. 59 (2021).
[36] A.M. Nikiforuk, et al., Performance of immunoglobulin G serology on finger prick capillary dried blood spot samples to measure SARS-CoV-2 humoral immunogenicity, medRxiv (2021).
[37] R. Trevethan, Sensitivity, specificity, and predictive values: foundations, pliabilities, and pitfalls in research and practice, Front. Public Health 5 (2017) 307.
[38] E. Huyghe, et al., Performance of three automated SARS-CoV-2 antibody assays and relevance of orthogonal testing algorithms, Clin. Chem. Lab. Med. 59 (2020) 411–419.
[39] J.R. Landis, G.G. Koch, The measurement of observer agreement for categorical data, Biometrics 33 (1977) 159–174.
[40] J.L. Fleiss, B. Levin, M.C. Paik, Statistical Methods for Rates and Proportions, 800, third ed., John Wiley & Sons, 2003.

[41] A.-M. Simundic, Measures of diagnostic accuracy: basic definitions, EJIFCC 19 (2009) 203–211. [42] S. Younes, et al., Diagnostic efficiency of three fully automated serology assays and their correlation with a novel surrogate virus neutralization test in symptomatic and asymptomatic SARS-CoV-2 individuals, Microorganisms 9 (2021).
[43] N. Wellinghausen, M. Voss, R. Ivanova, S. Deininger, Evaluation of the SARS-CoV-2- IgG response in outpatients by fiver commercial immunoassays, GMS Infectious Diseases 8 (2020).
[44] E. Tuaillon, et al., Detection of SARS-CoV-2 antibodies using commercial assays and seroconversion patterns in hospitalized patients, J. Infect. 81 (2020) e39–e45.
[45] E. Catry, et al., Analytical and clinical evaluation of four commercial SARS-CoV-2 serological immunoassays in hospitalized patients and ambulatory individuals, J. Virol Methods 289 (2021), 114060.
[46] J. Zhao, et al., Antibody responses to SARS-CoV-2 in patients with novel coronavirus disease 2019, Clin. Infect. Dis. 71 (2020) 2027–2034.
[47] A.J. Greaney, et al., A SARS-CoV-2 variant elicits an antibody response with a shifted immunodominance hierarchy, PloS Pathog. 18 (2022), e1010248.
[48] S.M. Hirabara, et al., SARS-CoV-2 variants: differences and potential of immune evasion, Front. Cell. Infect. Microbiol. 11 (2021), 781429.
[49] N. Wolter, et al., Early assessment of the clinical severity of the SARS-CoV-2 omicron variant in South Africa: a data linkage study, Lancet 399 (2022) 437–446.
[50] M. Egger, et al., Comparison of the ElecsysI Anti-SARS-CoV-2 immunoassay with the EDI enzyme linked immunosorbent assays for the detection of SARS-CoV-2 antibodies in human plasma, Clin. Chim. Acta 509 (2020) 18–21.
[51] M. Tre-Hardy, et al., Validation of a chemiluminescent assay for specific SARS-CoV2 antibody, Clin. Chem. Lab. Med. 58 (2020) 1357–1364.
[52] Itell, H. L. et al. SARS-CoV-2 antibody binding and neutralization in dried blood spot eluates and paired plasma. Microbiol. Spectr. 9, e0129821,.
[53] N. Cook, et al., Multiplex assessment of SARS-CoV-2 antibodies improves assay sensitivity and correlation with neutralizing antibodies, Clin. Biochem. 97 (2021) 54–61.
[54] C. Gillot, et al., An original ELISA-based multiplex method for the simultaneous detection of 5 SARS-CoV-2 IgG antibodies directed against different antigens, J. Clin. Med. 9 (2020).
[55] D.J. Hunter, et al., Addressing vaccine inequity – covid-19 vaccines as a global public good, N. Engl. J. Med. 386 (2022) 1176–1179.
[56] P. Jha, COVID Seroprevalence, Symptoms and Mortality during the First Wave of SARS-CoV-2 in Canada. medRxiv, 2021.
[57] S. Canada, SARS-CoV-2 Antibody Seroprevalence in Canadians, by Age Group and Sex, 2021. November 2020 to April 2021, https://www150.statcan.gc.ca/t1/tbl1/en/tv.action?pid¼1310081801.
[58] Phillips, N. The coronavirus will become endemic. Nature 590, 382-384.

Supplementary Files

S1 Table

	Spike	RBD	Nucleocapsid
University of Ottawa protocol	**Median S/CO (IQR)**	**Median S/CO (IQR)**	**Median S/CO (IQR)**
≤14 days (*n*=26)	9.9 (8.1, 10.8)	5.2 (2.3, 7.4)	6.6 (6.4, 7.0)
15-28 days (*n*=36)	10.0 (8.9, 10.8)	6.8 (5.1, 7.7)	6.7 (6.4, 6.9)
>28 days[a] (*n*=35)	10.3 (7.7, 11.3)	5.8 (2.7, 7.3)	6.0 (3.8, 7.0)
Outpatient (*n*=21)	10.0 (6.9, 10.8)	4.9 (2.1, 6.9)	6.5 (4.5, 7.0)
Inpatient (*n*=51)	10.1 (8.9, 10.8)	5.6 (3.2, 7.5)	6.6 (6.3, 6.9)
ICU (*n*=25)	10.4 (9.5, 11.4)	7.3 (5.9, 7.8)	6.8 (4.7, 7.0)
All COVID-19 patients (*n*=97)	10.1 (8.9, 11.0)	6.5 (3.2, 7.5)	7.0 (5.9, 7.0)
Pre-COVID-19 (*n*=90)	0.4 (0.4, 0.6)	0.3 (0.3, 0.5)	0.4 (0.3, 0.6)
Mount Sinai Hospital protocol	**Median RR (IQR)**	**Median RR (IQR)**	**Median RR (IQR)**
≤14 days (*n*=26)	2.1 (1.9, 2.4)	1.6 (1.0, 1.9)	2.4 (1.8, 3.3)
15-28 days (*n*=36)	2.2 (2.0, 2.4)	2.0 (1.5, 2.2)	3.1 (2.5, 3.5)
>28 days (*n*=35)	2.0 (1.6, 2.3)	1.4 (0.9, 2.0)	2.2 (1.5, 2.6)
Outpatient (*n*=21)	1.8 (1.5, 2.1)	1.4 (0.7, 1.8)	2.2 (1.5, 2.7)
Inpatient (*n*=51)	2.2 (2.0, 2.4)	1.7 (1.2, 2.0)	2.7 (1.9, 3.4)
ICU (*n*=25)	2.1 (2.0, 2.4)	2.0 (1.8, 2.2)	2.6 (2.0, 3.5)
All COVID-19 patients (*n*=97)	2.1 (1.9, 2.4)	1.7 (1.1, 2.0)	2.5 (1.9, 3.4)
Pre-COVID-19 (*n*=90)	0.2 (0.1, 0.2)	0.1 (0.1, 0.2)	0.2 (0.2, 0.3)
Bio-Rad BioPlex 2200 SARS-CoV-2 IgG	**Median U/mL (IQR)**	**Median U/mL (IQR)**	**Median U/mL (IQR)**
≤14 days (*n*=26)	100.0 (25.5, 100.0)	98.4 (29.4, 100.0)	87.0 (24.7, 100.0)
15-28 days (*n*=36)	100.0 (100.0, 100.0)	100.0 (100.0, 100.0)	100.0 (88.7, 100.0)
>28 days (*n*=35)	100.0 (38.2, 100.0)	100.0 (80.0, 100.0)	61.1 (23.9, 100.0)
Outpatient (*n*=21)	100.0 (26.7, 100.0)	100.0 (75.3, 100.0)	44.1 (16.2, 100.0)
Inpatient (*n*=51)	100.0 (53.7, 100.0)	100.0 (71.7, 100.0)	100.0 (35.5, 100.0)
ICU (*n*=25)	100.0 (100.0, 100.0)	100.0 (100.0, 100.0)	100.0 (50.7, 100.0)
All COVID-19 patients (*n*=97)	100.0 (49.1, 100.0)	100.0 (85.8, 100.0)	98.8 (31.2, 100.0)
Pre-COVID-19 (*n*=90)	1.0 (1.0, 1.0)	2.6 (2.0, 3.3)	1.0 (1.0, 1.0)
MSD V-PLEX SARS-CoV-2 Panel 2 IgG	**Median AU/mL**	**Median AU/mL**	**Median AU/mL**
≤14 days (*n*=26)	76.7 (35.1, 107.4)	26.3 (5.6, 46.4)	193.4 (98.3, 276.2)
15-28 days (*n*=36)	105.8 (65.4, 134.8)	53.7 (18.6, 116.2)	175.1 (159.9, 182.2)
>28 days (*n*=35)	72.3 (25.1, 110.4)	36.1 (10.6, 60.1)	185.5 (39.4, 204.8)
Outpatient (*n*=21)	51.8 (17.7, 89.5)	27.1 (8.6, 38.3)	122.9 (37.4, 198.8)
Inpatient (*n*=51)	85.2 (47.4, 122.5)	28.8 (15.1, 60.3)	176.6 (138.5, 205.8)
ICU (*n*=25)	109.3 (91.3, 128.0)	59.1 (30.8, 153.4)	195.9 (142.6, 296.8)
All COVID-19 patients (*n*=97)	89.7 (45.5, 118.4)	33.8 (13.5, 61.6)	179.3 (102.0, 206.0)
Pre-COVID-19 (*n*=86)[b]	0.4 (0.3, 0.7)	1.0 (0.8, 1.3)	0.7 (0.5, 1.0)
Roche Elecsys Anti-SARS-CoV-2		**Median AU/mL (IQR)**	**Median COI (IQR)**
≤14 days (*n*=26)	-	1.1 (0.6, 5.1)	0.6 (0.3, 1.9)
15-28 days (*n*=36)	-	2.6 (1.1, 15.2)	1.2 (0.4, 3.1)
>28 days (*n*=35)	-	9.5 (4.8, 41.2)	2.3 (0.8, 8.3)
Outpatient (*n*=21)	-	14.0 (4.3, 39.1)	3.4 (0.9, 9.7)
Inpatient (*n*=51)	-	2.6 (0.8, 8.1)	0.9 (0.4, 3.2)
ICU (*n*=25)	-	4.4 (0.9, 14.2)	1.7 (0.5, 2.8)

All COVID-19 patients (*n*=97)	-	4.8 (1.1, 14.1)	1.3 (0.5, 3.5)
Pre-COVID-19 (*n*=90)	-	0.4 (0.4, 0.4)	0.05 (0.05, 0.05)

[a]Days between symptom onset and sample collection.
[b]Four DBS omitted from analysis due to insufficient quantity for testing.
CLIA: chemiluminescent direct enzyme-linked immunosorbent assay COI: Cutoff index; ICU: Intensive care unit; IQR: Interquartile range; RBD: Receptor binding domain; RR: Relative ratio; S/CO: Signal to cutoff ratio.

S2 Table

Spike (≤14 days)	**University of Ottawa protocol**	**Mount Sinai Hospital protocol**	**Bio-Rad BioPlex 2200 SARS-CoV-2 IgG**	**MSD V-Plex SARS-CoV-2 Panel 2 IgG[a]**	**Roche Elecsys Anti-SARS-CoV-2**
Sensitivity (*n*/N) % (95% CI)	24/26 92.3 (75.9, 98.6)	25/26 96.2 (81.1, 99.8)	24/26 92.3 (75.9, 98.6)	24/26 92.3 (75.9, 98.6)	
Specificity (*n*/N) % (95% CI)	83/90 92.2 (84.8, 96.2)	86/90 95.6 (89.1, 98.3)	90/90 100.0 (95.9, 100.0)	85/86 98.8 (93.7, 99.9)	
PPV (*n*/N) % (95% CI)	7/90 77.4 (60.2, 88.6)	4/90 86.2 (69.4, 94.5)	0/90 100.0 (86.2, 100.0)	1/86 96.0 (80.5, 99.8)	
NPV (*n*/N) % (95% CI)	2/26 97.6 (91.8, 99.6)	1/26 98.9 (93.8, 99.9)	2/26 97.8 (92.4, 99.6)	2/26 97.8 (92.4, 99.6)	
Kappa (95% CI)	0.791 (0.662, 0.921)	0.881 (0.779, 0.983)	0.949 (0.879, 1.000)	0.924 (0.839, 1.000)	
Spike (15-28 days)	**University of Ottawa protocol**	**Mount Sinai Hospital protocol**	**Bio-Rad BioPlex 2200 SARS-CoV-2 IgG**	**MSD V-Plex SARS-CoV-2 Panel 2 IgG[a]**	**Roche Elecsys Anti-SARS-CoV-2**
Sensitivity (*n*/N) % (95% CI)	36/36 100.0 (90.4, 100.0)	36/36 100.0 (90.4, 100.0)	36/36 100.0 (90.4, 100.0)	36/36 100.0 (90.4, 100.0)	
Specificity (*n*/N) % (95% CI)	83/90 92.2 (84.8, 96.2)	86/90 95.6 (89.1, 98.3)	90/90 100.0 (95.9, 100.0)	85/86 98.8 (93.7, 99.9)	
PPV (*n*/N) % (95% CI)	7/90 83.7 (70.0, 91.9)	4/90 90.0 (76.9, 96.0)	0/90 100.0 (90.4, 100.0)	1/86 97.3 (86.2, 99.9)	
NPV (*n*/N) % (95% CI)	0/36 100.0 (95.6, 100.0)	0/36 100.0 (95.7, 100.0)	0/36 100.0 (95.9, 100.0)	0/36 100.0 (95.7, 100.0)	
Kappa (95% CI)	0.871 (0.780, 0.963)	0.925 (0.852, 0.997)	1.000 (1.000, 1.000)	0.980 (0.942, 1.000)	
Spike (>28 days)	**University of Ottawa protocol**	**Mount Sinai Hospital protocol**	**Bio-Rad BioPlex 2200 SARS-CoV-2 IgG**	**MSD V-Plex SARS-CoV-2 Panel 2 IgG[a]**	**Roche Elecsys Anti-SARS-CoV-2**
Sensitivity (*n*/N) % (95% CI)	35/35 100.0 (90.1, 100.0)	35/35 100.0 (90.1, 100.0)	34/35 97.1 (85.5, 99.9)	35/35 100.0 (90.1, 100.0)	
Specificity (*n*/N)	83/90	86/90	90/90	85/86	

% (95% CI)	92.2 (84.8, 96.2)	95.6 (89.1, 98.3)	100.0 (95.9, 100.0)	98.8 (93.7, 99.9)	
PPV (*n*/N) **% (95% CI)**	7/90 83.3 (69.4, 91.7)	4/90 89.7 (76.4, 95.9)	0/90 100.0 (89.8, 100.0)	1/86 97.2 (85.8, 99.9)	
NPV (*n*/N) **% (95% CI)**	0/35 100.0 (95.6, 100.0)	0/35 100.0 (95.7, 100.0)	1/35 98.9 (94.0, 99.9)	0/35 100.0 (95.7, 100.0)	
Kappa **(95% CI)**	0.869 (0.776, 0.963)	0.923 (0.850, 0.997)	0.980 (0.941, 1.000)	0.980 (0.941, 1.000)	
RBD (≤14 days)	**University of Ottawa protocol**	**Mount Sinai Hospital protocol**	**Bio-Rad BioPlex 2200 SARS-CoV-2 IgG**	**MSD V-Plex SARS-CoV-2 Panel 2 IgG**[a]	**Roche Elecsys Anti-SARS-CoV-2**
Sensitivity (*n*/N) **% (95% CI)**	24/26 92.3 (75.9, 98.6)	24/26 92.3 (75.9, 98.6)	23/26 88.5 (71.0, 96.0)	24/26 92.3 (75.9, 98.6)	15/26 57.7 (38.9. 74.5)
Specificity (*n*/N) **% (95% CI)**	87/90 96.7 (90.7, 99.1)	87/90 96.7 (90.7, 99.1)	89/90 98.9 (94.0, 99.9)	80/86 93.0 (85.6, 96.8)	90/90 100.0 (95.9, 100.0)
PPV (*n*/N) **% (95% CI)**	3/90 88.9 (71.9, 96.1)	3/90 88.9 (71.9, 96.1)	1/90 95.8 (79.8, 99.8)	6/86 80.0 (62.7, 90.5)	0/90 100.0 (79.6, 100.0)
NPV (*n*/N) **% (95% CI)**	2/26 97.8 (92.2, 99.6)	2/26 97.8 (92.2, 99.6)	3/26 96.7 (90.8, 99.1)	2/26 97.6 (91.5, 99.6)	11/26 89.1 (81.5, 93.8)
Kappa **(95% CI)**	0.878 (0.773, 98.2)	0.878 (0.773, 0.982)	0.898 (0.800, 0.996)	0.810 (0.684, 0.936)	0.679 (0.508, 0.850)
RBD (15-28 days)	**University of Ottawa protocol**	**Mount Sinai Hospital protocol**	**Bio-Rad BioPlex 2200 SARS-CoV-2 IgG**	**MSD V-Plex SARS-CoV-2 Panel 2 IgG**[a]	**Roche Elecsys Anti-SARS-CoV-2**
Sensitivity (*n*/N) **% (95% CI)**	36/36 100.0 (90.4, 100.0)	36/36 100.0 (90.4, 100.0)	35/36 97.2 (85.8, 99.9)	36/36 100.0 (90.4, 100.0)	31/36 86.1 (71.3, 93.9)
Specificity (*n*/N) **% (95% CI)**	87/90 96.7 (90.7, 99.1)	87/90 96.7 (90.7, 99.1)	89/90 98.9 (94.0, 99.9)	80/86 93.0 (85.6, 96.8)	90/90 100.0 (95.9, 100.0)
PPV (*n*/N) **% (95% CI)**	3/90 92.3 (79.7, 97.3)	3/90 92.3 (79.7, 97.3)	1/90 97.2 (85.8, 99.9)	6/86 85.7 (72.2, 93.3)	0/90 100.0 (89.0, 100.0)
NPV (*n*/N) **% (95% CI)**	0/36 100.0 (95.8, 100.0)	0/36 100.0 (95.8, 100.0)	1/36 98.9 (94.0, 99.9)	0/36 100.0 (95.4, 100.0)	5/36 94.7 (88.3, 97.7)
Kappa **(95% CI)**	0.943 (0.880, 1.000)	0.943 (0.880, 1.000)	0.961 (0.908, 1.000)	0.887 (0.800, 0.975)	0.899 (0.812, 0.985)
RBD (>28 days)	**University of Ottawa protocol**	**Mount Sinai Hospital protocol**	**Bio-Rad BioPlex 2200 SARS-CoV-2 IgG**	**MSD V-Plex SARS-CoV-2 Panel 2 IgG**[a]	**Roche Elecsys Anti-SARS-CoV-2**
Sensitivity (*n*/N) **% (95% CI)**	35/35 100.0 (90.1, 100.0)	35/35 100.0 (90.1, 100.0)	34/35 97.1 (85.5, 99.9)	35/35 100.0 (90.1, 100.0)	34/35 97.1 (85.5, 99.9)
Specificity (*n*/N)	87/90	87/90	89/90	80/86	90/90

% (95% CI)	96.7 (90.7, 99.1)	96.7 (90.7, 99.1)	98.9 (94.0, 99.9)	93.0 (85.6, 96.8)	100.0 (95.9, 100.0)
PPV (*n*/N) **% (95% CI)**	3/90 92.1 (79.2, 97.3)	3/90 92.1 (79.2, 97.3)	1/90 97.1 (85.5, 99.9)	6/86 85.4 (71.6, 93.1)	0/90 100.0 (89.8, 100.0)
NPV (*n*/N) **% (95% CI)**	0/35 100.0 (95.8, 100.0)	0/35 100.0 (95.8, 100.0)	1/35 98.9 (94.0, 99.9)	0/35 100.0 (95.4, 100.0)	1/35 98.9 (94.0, 99.9)
Kappa **(95% CI)**	0.942 (0.877, 1.000)	0.942 (0.877, 1.000)	0.960 (0.906, 1.000)	0.885 (0.796, 0.974)	0.980 (0.941, 1.000)
Nucleocapsid (≤14 days)	**University of Ottawa protocol**	**Mount Sinai Hospital protocol**	**Bio-Rad BioPlex 2200 SARS-CoV-2 IgG**	**MSD V-Plex SARS-CoV-2 Panel 2 IgG**[a]	**Roche Elecsys Anti-SARS-CoV-2**
Sensitivity (*n*/N) **% (95% CI)**	24/26 92.3 (75.9, 98.6)	23/26 88.5 (71.0, 96.0)	23/26 88.5 (71.0, 96.0)	24/26 92.3 (75.9, 98.6)	9/26 34.6 (19.4, 53.8)
Specificity (*n*/N) **% (95% CI)**	83/90 92.2 (84.8, 96.2)	87/90 96.7 (90.7, 99.1)	90/90 100.0 (95.9, 100.0)	84/86 97.7 (91.9, 99.6)	90/90 100.0 (95.9, 100.0)
PPV (*n*/N) **% (95% CI)**	7/90 77.4 (60.2, 88.6)	3/90 88.5 (71.0, 96.0)	0/90 100.0 (85.7, 100.0)	2/86 92.3 (75.9, 98.6)	0/90 100.0 (70.1, 100.0)
NPV (*n*/N) **% (95% CI)**	2/26 97.6 (91.8, 99.6)	3/26 96.7 (90.7, 99.1)	3/26 96.8 (90.9, 99.1)	2/26 97.7 (91.9, 99.6)	17/26 84.1 (76.0, 89.8)
Kappa **(95% CI)**					
Nucleocapsid (15-28 days)	**University of Ottawa protocol**	**Mount Sinai Hospital protocol**	**Bio-Rad BioPlex 2200 SARS-CoV-2 IgG**	**MSD V-Plex SARS-CoV-2 Panel 2 IgG**[a]	**Roche Elecsys Anti-SARS-CoV-2**
Sensitivity (*n*/N) **% (95% CI)**	36/36 100.0 (90.4, 100.0)	36/36 100.0 (90.4, 100.0)	36/36 100.0 (90.4, 100.0)	36/36 100.0 (90.4, 100.0)	21/36 58.3 (42.2, 72.9)
Specificity (*n*/N) **% (95% CI)**	83/90 92.2 (84.8, 96.2)	87/90 96.7 (90.7, 99.1)	90/90 100.0 (95.9, 100.0)	84/86 97.7 (91.9, 99.6)	90/90 100.0 (95.9, 100.0)
PPV (*n*/N) **% (95% CI)**	7/90 83.7 (70.0, 91.9)	3/90 92.3 (79.7, 97.3)	0/90 100.0 (90.4, 100.0)	2/86 94.7 (82.7, 99.1)	0/90 100.0 (84.5, 100.0)
NPV (*n*/N) **% (95% CI)**	0/36 100.0 (95.6, 100.0)	0/36 100.0 (95.8, 100.0)	0/36 100.0 (95.9, 100.0)	0/36 100.0 (95.6, 100.0)	15/36 85.7 (77.8, 91.1)
Kappa **(95% CI)**	0.871 (0.780, 0.963)	0.943 (0.880, 1.000)	1.000 (1.000, 1.000)	0.961 (0.908, 1.000)	0.667 (0.517, 0.816)
Nucleocapsid (>28 days)	**University of Ottawa protocol**	**Mount Sinai Hospital protocol**	**Bio-Rad BioPlex 2200 SARS-CoV-2 IgG**	**MSD V-Plex SARS-CoV-2 Panel 2 IgG**[a]	**Roche Elecsys Anti-SARS-CoV-2**
Sensitivity (*n*/N) **% (95% CI)**	35/35 100.0 (90.1, 100.0)	30/35 85.7 (70.6, 93.7)	28/35 80.0 (64.1, 90.0)	34/35 97.1 (85.5, 99.9)	24/35 68.6 (52.0, 81.4)
Specificity (*n*/N) **% (95% CI)**	83/90 92.2 (84.8, 96.2)	87/90	90/90	84/86	90/90

		96.7 (90.7, 99.1)	100.0 (95.9, 100.0)	97.7 (91.9, 99.6)	100.0 (95.9, 100.0)
PPV (*n*/N) % (95% CI)	7/90 83.3 (69.4, 91.7)	3/90 90.9 (76.4, 96.9)	0/90 100.0 (87.9, 100.0)	2/86 94.4 (81.9, 99.0)	0/90 100.0 (86.2, 100.0)
NPV (*n*/N) % (95% CI)	0/35 100.0 (95.6, 100.0)	5/35 94.6 (87.9, 97.7)	7/35 92.8 (85.8, 96.5)	1/35 98.8 (93.6, 99.9)	11/35 89.1 (81.5, 93.8)
Kappa (95% CI)					
Spike or RBD (≤14 days)	**University of Ottawa protocol**	**Mount Sinai Hospital protocol**	**Bio-Rad BioPlex 2200 SARS-CoV-2 IgG**	**MSD V-Plex SARS-CoV-2 Panel 2 IgG[a]**	**Roche Elecsys Anti-SARS-CoV-2**
Sensitivity (*n*/N) % (95% CI)	24/26 92.3 (75.9, 98.6)	25/26 96.2 (81.1, 99.8)	24/26 92.3 (75.9, 98.6)	24/26 92.3 (75.9, 98.6)	
Specificity (*n*/N) % (95% CI)	81/90 90.0 (82.1, 94.6)	84/90 93.3 (86.2, 96.9)	89/90 98.9 (94.0, 99.9)	79/86 91.9 (84.1, 96.0)	
PPV (*n*/N) % (95% CI)	9/90 72.7 (55.8, 84.9)	6/90 80.6 (63.7, 90.8)	1/90 96.0 (80.5, 99.8)	7/86 77.4 (60.2, 88.6)	
NPV (*n*/N) % (95% CI)	2/26 97.6 (91.6, 99.6)	1/26 98.8 (93.6, 99.9)	2/26 97.8 (92.3, 99.6)	2/26 97.5 (91.4, 99.6)	
Kappa (95% CI)	0.751 (0.614, 0.889)	0.838 (0.722, 0.953)	0.925 (0.841, 1.000)	0.789 (0.658, 0.920)	
Spike or RBD (15-28 days)	**University of Ottawa protocol**	**Mount Sinai Hospital protocol**	**Bio-Rad BioPlex 2200 SARS-CoV-2 IgG**	**MSD V-Plex SARS-CoV-2 Panel 2 IgG[a]**	**Roche Elecsys Anti-SARS-CoV-2**
Sensitivity (*n*/N) % (95% CI)	36/36 100.0 (90.4, 100.0)	36/36 100.0 (90.4, 100.0)	36/36 100.0 (90.4, 100.0)	36/36 100.0 (90.4, 100.0)	
Specificity (*n*/N) % (95% CI)	81/90 90.0 (82.1, 94.6)	84/90 93.3 (86.2, 96.9)	89/90 98.9 (94.0, 99.9)	79/86 91.9 (84.1, 96.0)	
PPV (*n*/N) % (95% CI)	9/90 80.0 (66.2, 89.1)	6/90 85.7 (72.2, 93.3)	1/90 97.3 (86.2, 99.9)	7/86 83.7 (70.0, 91.9)	
NPV (*n*/N) % (95% CI)	0/36 100.0 (95.5, 100.0)	0/36 100.0 (95.6, 100.0)	0/36 100.0 (95.9, 100.0)	0/36 100.0 (95.4, 100.0)	
Kappa (95% CI)	0.837 (0.736, 0.938)	0.889 (0.803, 0.975)	0.981 (0.943, 1.000)	0.869 (0.776, 0.963)	
Spike or RBD (>28 days)	**University of Ottawa protocol**	**Mount Sinai Hospital protocol**	**Bio-Rad BioPlex 2200 SARS-CoV-2 IgG**	**MSD V-Plex SARS-CoV-2 Panel 2 IgG[a]**	**Roche Elecsys Anti-SARS-CoV-2**
Sensitivity (*n*/N) % (95% CI)	35/35 100.0 (90.1, 100.0)	35/35 100.0 (90.1, 100.0)	34/35 97.1 (85.5, 99.9)	35/35 100.0 (90.1, 100.0)	
Specificity (*n*/N) % (95% CI)	81/90 90.0 (82.1, 94.6)	84/90	89/90	79/86	

		93.3 (86.2, 96.9)	98.9 (94.0, 99.9)	91.9 (84.1, 96.0)	
PPV (*n*/N) % (95% CI)	9/90 79.5 (65.5, 88.8)	6/90 85.4 (71.6, 93.1)	1/90 97.1 (85.5, 99.9)	7/86 83.3 (69.4, 91.7)	
NPV (*n*/N) % (95% CI)	0/35 100.0 (95.5, 100.0)	0/35 100.0 (95.6, 100.0)	1/35 98.9 (94.0, 99.9)	0/35 100.0 (95.4, 100.0)	
Kappa (95% CI)	0.834 (0.732, 0.937)	0.887 (0.799, 0.975)	0.960 (0.906, 1.000)	0.867 (0.773, 0.962)	

[a]Four pre-COVID-19 DBS omitted from analysis due to insufficient quantity for testing.

S3 Table is available here:
https://www.cell.com/cms/10.1016/j.heliyon.2022.e10270/attachment/3ed1f676-db1a-437d-bf7f-f0040e0e29eb/mmc3.docx

A-1.26 Cohort profile: Stop the Spread Ottawa (SSO)—a community-based prospective cohort study on antibody responses, antibody neutralization efficiency and cellular immunity to SARS-CoV-2 infection and vaccination

Preface

(This work has been previously published as a research article)

Collins E., **Galipeau Y.**, Arnold C., Bosveld C., Heiskanen A., Keeshan A., Nakka K., Shir-Mohammadi K., St-Denis-Bissonnette F., Tamblyn L., Vranjkovic A., Wood LC., Booth R., Buchan CA., Crawley AM., Little J., McGuinty M., Saginur R., Langlois MA., Cooper CL. **Cohort profile: Stop the Spread Ottawa (SSO)-a community-based prospective cohort study on antibody responses, antibody neutralisation efficiency and cellular immunity to SARS-CoV-2 infection and vaccination.** BMJ Open. 2022 Sep 8;12(9):e062187.

https://doi.org/10.1136/bmjopen-2022-062187

© Author(s) (or their employer(s)) 2022. Re-use permitted under CC BY-NC. No commercial re-use. See rights and permissions. Published by BMJ.

This is an open access article distributed in accordance with the Creative Commons Attribution Non Commercial (CC BY-NC 4.0) license, which permits others to distribute, remix, adapt, build upon this work non-commercially, and license their derivative works on different terms, provided the original work is properly cited, appropriate credit is given, any changes made indicated, and the use is non-commercial.

Abstract

Purpose
To investigate the robustness and longevity of SARS-CoV-2 immune responses conferred by natural infection and vaccination among priority populations such as immunocompromised individuals and people with post-acute sequelae of COVID-19 in a prospective cohort study (Stop the Spread Ottawa—SSO) in adults living in the Ottawa region. In this paper, we describe the study design, ongoing data collection and baseline characteristics of participants.

Participants
Since October 2020, participants who tested positive for COVID-19 (convalescents) or at high risk of exposure to the virus (under surveillance) have provided monthly blood and saliva samples over a 10-month period. As of 2 November 2021, 1026 adults had completed the baseline survey and 976 had attended baseline bloodwork. 300 participants will continue to provide bimonthly blood samples for 24 additional months (ie, total follow-up of 34 months).

Findings to date
The median age of the baseline sample was 44 (IQR 23, range: 18–79) and just over two-thirds (n=688; 67.1%) were female. 255 participants (24.9%) had a history of COVID-19 infection confirmed by PCR and/or serology. Over 600 participants (60.0%) work in high-risk occupations (eg, healthcare, teaching and transportation). 108 participants (10.5%) reported immunocompromising conditions or treatments at baseline (eg, cancer, HIV, other immune deficiency, and/or use of immunosuppressants).

Future plans
SSO continues to yield rich research potential, given the collection of pre-vaccine baseline data and samples from the majority of participants, recruitment of diverse subgroups of interest, and a high level of participant retention and compliance with monthly sampling. The 24-month study extension will maximise opportunities to track SARS-CoV-2 immunity and vaccine efficacy, detect and characterise emerging variants, and compare subgroup humoral and cellular response robustness and persistence.

Strengths and limitations of this study

-Stop the Spread Ottawa (SSO) is a large-scale longitudinal cohort study with frequent and comprehensive monitoring of SARS-CoV-2 immune response among diverse subgroups, including priority populations such as immunocompromised people and people with post-acute sequelae of COVID-19 (PASC).

-Pre-vaccine baseline data and samples were collected from the majority of participants, made possible through a successful recruitment plan and rapid launch early on in the pandemic.

-Study extension allows for up to 34 months of follow-up of SARS-CoV-2 immunity elicited from natural infection and/or vaccination; severity, duration and changes in PASC; and breakthrough infections by emerging variants.

-The study population was not intended to be, and is not, representative of the general population of the Ottawa region in terms of age, sex, ethnicity and total household income, and there is poor representation of ethnic minorities and no adults ≥80 years of age.

-There is a risk of misclassification of some variables as participants self-reported data through online questionnaires, including dates of positive PCR test, vaccination history and health conditions.

Introduction

A beta-coronavirus, severe acute respiratory syndrome coronavirus 2 (SARS-CoV-2), continues to drive the COVID-19 pandemic.[1] Since December 2019, the virus has infected over 300 million people and caused more than 5.4 million deaths worldwide.[2] Efforts have been made by the international research community to describe the robustness and longevity of SARS-CoV-2 immune response conferred by natural infection and/or vaccination among different groups of people,[3–9] including immunocompromised individuals[10–15] and people with PASC (post-acute sequelae of COVID-19).[16–19] People with an immunocompromised state may not elicit sufficient humoral and cellular response to vaccination.[20–26] PASC continues to be a major public health concern, causing severe and pervasive impacts on physical and mental health four or more weeks post-infection.[27–29] Given ongoing COVID-19 vaccinations and emerging variants of concern (VOC), there is still a need for longitudinal analyses of SARS-CoV-2 immune response and COVID-19 impacts among diverse groups at risk of infection/reinfection, severe disease and/or persistent symptoms.[30–39]

Most persons recovering from SARS-CoV-2 develop IgM, IgG and IgA antibodies targeting the SARS-CoV-2 nucleocapsid (N) or spike (S) proteins between 7 and 14 days post-onset of symptoms.[40 41] Seroconversion is dependent on the virological and clinical profile over time.[42] The receptor binding domain (RBD) of the S protein is the primary target of neutralising antibodies.[43] During the pandemic, several SARS-CoV-2 variants have become dominant in many countries in different periods.[34 35 44] These variants harbour mutations of the spike protein that can restrict antibody neutralisation capacity and hinder vaccine efficacy.[45–47] Neutralising antibodies comprise a core function of adaptive humoral immune response, predictive of COVID-19 severity and survival.[48 49] Substantial correlations have been found between neutralising antibody profile and disease severity,[50] anti-S IgG and neutralising titres,[51 52] anti-S/-N levels and PASC,[53 54] and immunosuppression and anti-S IgG non-response.[26 55–58]

Research to date has focused on hospitalised patients, more likely to have severe COVID-19 disease than people in community settings, and on small cohorts of people with specific conditions.

Reports on serology continue to dominate analyses of SARS-CoV-2 immune responses. Other human coronaviruses, which do not confer strong protection against SARS-CoV-2,[59] [60] may confound interpretation of serological analyses. Factors that influence the detection of cross-reactive antibodies include choice of antigen, the antibody isotype being detected and the relative sensitivity of various detection methods.[61–64] In addition to serology, immunoassays of complementary T-cell responses are required to assess impacts of exposure to SARS-CoV-2 and endemic human coronaviruses on coordinated antibody-mediated and cell-mediated responses to vaccination.[65–67] As an example, B.1.1.7 and B.1.351 variants were found to partially escape SARS-CoV-2-induced humoral immunity, but there were no observed changes in CD4+ T-cell activation.[68] Investigation as to protection conferred by heterologous or homologous vaccination, and by different time intervals between vaccine doses is ongoing.[69–71] Impacts of infection and vaccination on emerging viral variants continue to be of major public health concern.[32] [34] [35] Priority topics given emerging variants include the transmissibility, pathogenicity and vaccine resistance of VOC,[3] [34] [44] and the impacts of vaccination and VOC on post-infection symptoms.[71–74]

To characterise the nature, intensity and longevity of immune response to the SARS-CoV-2 virus, we established a large longitudinal prospective cohort study, Stop the Spread Ottawa, with the objectives of:

- Assessing COVID-19 humoral immune response over time;
- Increasing knowledge of protective SARS-CoV2-specific immune responses through virus neutralisation and T-cell activation studies on a surveillance cohort and COVID-19 convalescent patients;
- Comparing the use of dried blood spot cards and serum for monitoring antibody responses;
- Tracking participant protocol adherence and drop-out;
- Understanding the psychological and socioeconomic impacts of testing positive for COVID-19;
- Assessing the seroprevalence of other common community-acquired viral respiratory illnesses by risk group; and
- Comparing COVID-19 specific immunity derived from natural infection and from immunisation.

- All participants provide monthly collection of blood and saliva samples and complete extensive serial questionnaires, used to track health history (eg, vaccinations), COVID-19 disease severity, persistent SARS-CoV-2 symptoms, risk factors of exposure, and socioeconomic and psychosocial impacts of the pandemic. This article describes our study protocol and cohort composition.

Cohort description

Study setting and participants

The Stop the Spread Ottawa (SSO) prospective cohort study on SARS-CoV-2 immune response recruited over 1000 adults in the Ottawa region from 14 September 2020 to 28 September 2021. Since 19 October 2020, participants testing positive for COVID-19 or at high risk of exposure have provided monthly blood and saliva samples over a 10-month period. Three hundred participants will continue to provide bimonthly blood samples for 24 months (ie, for up to 34 months overall). Individuals ≥18 years of age in the Ottawa region (1) at risk of SARS-CoV-2 exposure/infection due to occupation or health condition, or (2) with any history of COVID-19 natural infection, confirmed by positive PCR test and/or serology, were eligible to participate. Participants at risk of exposure, but without a history of SARS-CoV-2 infection, were enrolled into the Surveillance cohort (n=750). Individuals known to have current or past COVID-19 infection confirmed by positive SARS-CoV-2 quantitative reverse transcription PCR (RT-PCR) or serology test were recruited into the Convalescent cohort (n=250). Beginning January 2021, vaccinated participants in the Surveillance cohort were given the option of transferring to the Convalescent protocol, to facilitate the collection of monthly post-vaccine whole blood samples (figure 1). To date, over 200 Surveillance participants have transferred. Approximately 500 adults will be participating in each cohort by end of study.

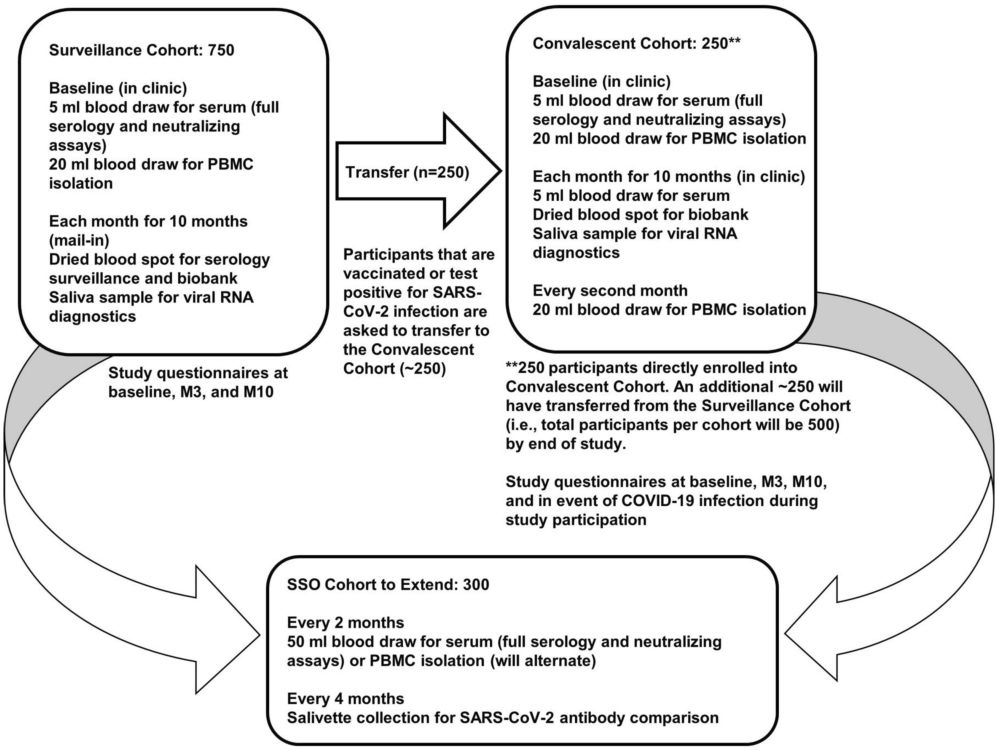


Figure 1 Procedures for Stop the Spread Ottawa (SSO) study participants, baseline to month 10 and extension to month 34. PBMC, peripheral blood mononuclear cell.

Multiple strategies were used to facilitate rapid recruitment early on in the pandemic, including a study website (https://omc.ohri.ca/SSO/) and SARS-CoV-2 antibody results portal; distribution of promotional materials to healthcare and dental staff, teachers and transportation workers; collaboration with organisations representing key target populations; and use of Eastern Ontario Regional Laboratory Association (EORLA) reports and The Ottawa Hospital COVID-19 Registry to identify SARS-CoV-2 positive cases for follow-up. Target populations for the Surveillance cohort included healthcare workers, long-term care facility staff, transportation workers and patients with HIV, chronic viral hepatitis and haematological malignancy. Other populations of interest include homeless shelter staff, dentists/allied dental care workers, elementary and secondary school teachers, elderly individuals living in high-density, long-term retirement homes, and daycare workers.

Enrolment closed 28 September 2021. Data collection is ongoing. The expected duration of the study with extension is 60 months. Primary results should be known approximately 6 months after the last participant has been recruited and completed testing procedures.

Data collection

All individuals who enrolled on the Stop the Spread Ottawa website (https://omc.ohri.ca/SSO) were sent a link to access an informed consent form. As of 2 November 2021, 1108 consented participants had been screened by the research coordinator (figure 2). One participant was ineligible as underaged (<18 years old) and approximately 30 participants resided outside of the Ottawa region. All eligible participants were sent a unique study identifier and links to book baseline bloodwork and complete a study questionnaire by secure email. By 2 November, 1026 participants had completed the baseline questionnaire and 976 had attended baseline visits. During the initial 10 months of this study, participants have a 7-day window to schedule bloodwork visits and send in saliva and/or sputum and dried blood spot samples. Thereafter (11–34 months post-baseline), a 21-day window to attend study visits is allotted.

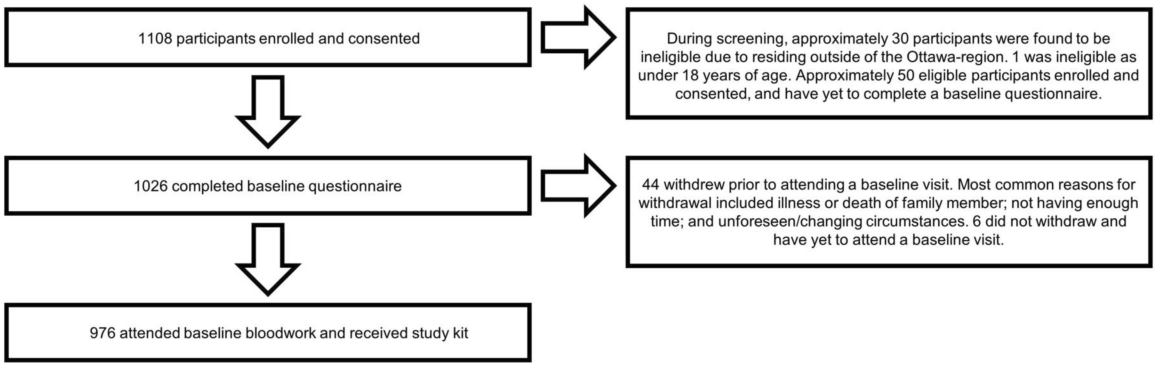


Figure 2 Flow diagram of enrolled participants, as of 2 November 2021.

Bloodwork

At baseline, for all participants, one (5 mL) tube with a separator gel with clot activator for serum and two (10 mL × 2) tubes with EDTA for lymphocyte isolation were drawn. During the first 10 months of the study, up to 500 participants with history of SARS-CoV-2 infection and/or

vaccination in the Convalescent cohort attend monthly blood draws for serum and bimonthly plasma and peripheral mononuclear cells (PBMCs). After 10 months, participants who consent to study extension provide blood draws every 2 months over the next 24 months (figure 1). During this time, 10 (5 mL × 10) tubes with separator gel with clot activator will be collected every 4 months. Five (10 mL × 5) tubes with EDTA will be drawn every 4 months alternating.

Saliva/sputum and dried blood spot collection

Over the initial 10 study months, participants used home collection kits to submit monthly dried blood spots (DBS) for serology surveillance and saliva/sputum samples[75–77] (DNA Genotek: OMNIgene·ORAL OM-505) for viral RNA testing by mail to EORLA or drop-off at The Ottawa Hospital. Participants in the Convalescent cohort self-collect monthly DBS in addition to attending monthly blood draws for serum. We note that the sensitivity and specificity of DBS for detecting SARS-CoV-2 spike glycoprotein antibodies relative to serum have been documented previously.[78 79] However, as well as for quality control purposes, we compared serology results from DBS and serum to be able to report DBS results in international units, thus facilitating inter-study comparisons.[80 81]

Participants were provided with access to video demonstrations through the study website to aid self-collection. As per manufacturer instructions,[82] participants were asked to spit into the OM-505 kit first thing in the morning, prior to food or drink. While we acknowledge passive drool as the gold standard for saliva collection,[83] we opted to use the OM-505 kits given they are easy to use without professional assistance, thus encouraging monthly compliance, and contain a preservative and viricidal fluid, allowing for safe and stable storage and transport of samples.[82 84] Participants who were identified as SARS-CoV-2 PCR positive were contacted by the research coordinator, promptly linked to Public Health as needed, and advised to seek emergency medical care in the event of life-threatening symptoms. Disease transmission mitigation and self-isolation measures were explained over the phone. After 10 months, participants in the extension will collect and submit one salivette (Sarstedt, Numbrecht, Germany: 51.1534) for SARS-CoV-2 antibody testing every 4 months, starting month 16. Salivettes have been successfully used in other Canadian studies to detect IgM, IgG and IgA response to SARS-CoV-2 spike and RBD proteins.[85]

Questionnaires

Electronic study questionnaires are completed at baseline, and at 3 and 10 months post-baseline. Three hundred participants in extended follow-up complete questionnaires every 6 months (months 16, 22, 28 and 34). Participants who are infected or reinfected during the study are asked to complete an immediate follow-up questionnaire.

Study questionnaire categories include:

35. Demographics (eg, age, ethnic group, gender)
36. Health history (eg, vaccinations, medications)
37. Severity of COVID-19 signs and symptoms
38. Risks of SARS-CoV-2 exposure
39. Socioeconomic impacts of the pandemic
40. Psychosocial impacts of the pandemic

All participants are asked to notify the research coordinator if and when they test positive or receive a COVID-19 vaccine. The research coordinator collects and logs dates of infection/vaccination and vaccine type in a shared tracking file. All participants who report new infections/reinfections complete an immediate follow-up questionnaire, documenting positive test date and symptom type, severity, and duration.

Laboratory investigations

Full serology includes detection of the main antibody isotypes IgA, IgM, IgG and subtypes IgG1, IgG2, IgG3, IgG4 against the N, RBD and the full-length trimeric spike of SARS-CoV-2. Neutralisation efficiency against SARS-CoV-2 spike protein and antibodies against the full trimeric spike of all four seasonal human coronaviruses (229E, OC43, NL63, HKU-1) are also assessed. T-Cell characterisation studies include SARS-CoV-2-specific T-cell responses, cytokine production profiles and determination of immunodominant sequence domains on the S protein, the membrane glycoprotein (M) and N protein. Bimonthly sampling for plasma and PBMCs during the initial 10-month study will enable correlation of seroprevalence (anti-SARS-CoV-2 antibody titres and neutralising antibody profile) with CD4+ and CD8+ T-cell responses at five time points.

Serological testing of monthly blood samples submitted by Surveillance cohort participants will be performed using an automated high-throughput chemiluminescent direct ELISA[80] located

within the University of Ottawa. This assay has been used in several studies across Canada[86–91] and has a reported sensitivity of 100% for the spike, RBD and N protein (IgG) and false-positive rates of 2% for spike, 1% for RBD and 6% for N.[80] All viral antigens required for serological assessment and anti-human IgG-HRP (horseradish peroxidase) fusion secondary antibody are provided by Yves Durocher at the National Research Council of Canada. Proteins are expressed in a CHO-DXB11-derived clone (CHOBRI/55E1) with yields estimated at 70–100 mg/L.[92 93] Briefly, 384-well plates are coated with the antigen of choice overnight at 4°C. Diluted patient sample is applied following a blocking step and incubated. Bound SARS-CoV-2 antibodies are then detected using an isotype-specific HRP-conjugated antibody. The plate is developed using a chemiluminescent substrate, which is compatible with automated instruments. Each assay plate contains commercially purified humanised antibodies (clones CR3022, CR3018 and HC2003), pooled positive and negative serum, and non-specific Ig control and blanks. A consistent layout and set of robust controls allow for quality control assessments and are key to raw data processing and subsequent analysis. To enable interplate comparison, background-corrected luminescence values are scaled in relation to the calibration curve. We used 123 serum samples and 320 DBS samples representative of pre-pandemic adults to generate thresholds to determine signal to cut-off ratios.[80] Samples with signal to cut-off values greater than 1.0 are considered positive. While positive and negative calls are interesting in the optics of seroprevalence surveys, quantification of antibody titres enables more robust analyses. As such, we have established a data analysis pipeline to report international antibody binding units (BAU) by correlating scaled luminescence values in linear range to the WHO-generated international standard (NIBSC 20/136).

We will investigate variabilities over time in the virus-neutralising properties and abundance of anti-SARS-CoV-2 antibodies and correlate these with individual case severity in the Convalescent cohort. In addition, we will analyse T cells to determine the proportion that are reactive to SARS-CoV-2 peptide antigens. Given the large number of samples from SSO and class three biocontainment restrictions on replicative SARS-CoV-2, we have implemented a high-throughput protein-based surrogate neutralisation assay, adapted from Abe *et al*.[94] The protein-based surrogate neutralisation was shown to correlate with lentiviral pseudotype-based neutralisation assay and with PRNT50.[94] In this assay, trimeric spike or RBD is coated in a 384-well plate and

blocked. Diluted serum samples are applied and incubated to allow binding of antibodies to antigen. Unbound antibodies are washed off, and recombinant biotin-conjugated ACE2 is applied to compete with antibodies for binding to antigen. The presence of strongly neutralising antibodies will inhibit spike–ACE2 or RBD–ACE2 interaction. A streptavidin-HRP polymer is then applied to detect bound ACE2 and the plate developed using a chemiluminescent substrate. In this competitive binding assay[94], the signal is inversely correlated to the neutralisation efficiency. Results of this assay can be reported in titres using international units (IU/mL) as per WHO standards (NIBSC 20/136) or, alternatively, by reporting half maximal inhibitory dilution (ID50) or per cent inhibition as compared with maximum ACE2 binding.

To maximise the efficiency of high-quality sample analysis and data acquisition, we developed a Core Facility that has enabled massive upscaling of the output of the assays we have developed for (1) SARS-CoV-2 antibody measurements and neutralisation efficiency in blood and (2) viral diagnostics using reverse transcription droplet digital PCR technology (RT-ddPCR). Core architecture includes the following: (1) a robotic liquid handler (Hamilton MicroLab Star) dedicated to isolating serum or plasma from clinical bar-coded collection tubes and performing ELISAs using an integrated plate washer (Biotek 405 TS/LS LHC2) and plate reader (Biotek Synergy NEO2); (2) an instrument dedicated to isolating viral RNA from nasopharyngeal swabs (NPS) in viral transport media (VTM) or from human sputum in VTM and dispensing the purified RNA in a storage plate with barcode tracking (Hamilton MicroLab Star); (3) an automated ddPCR platform from Bio-Rad (AutoDG) for detecting and quantifying viral RNA. RT-ddPCR is a biotechnological refinement of RT-qPCR that provides absolute quantification of viral genomes in a sample and has demonstrated improved sensitivity and accuracy for SARS-CoV-2 detection, especially for tests involving samples with low viral load. Given this automation, the system can process >3200 blood samples and >2000 NPS/sputum samples per 5-day work week.

Power calculations and analyses

We have recruited over 1000 participants, of which more than 250 have current or past COVID-19 infection. Given limited knowledge of SARS-CoV-2 at the time of study conception (spring 2020) and the urgency to launch this study early on in the pandemic, no formal sample size

calculations were performed to determine the number of required participants with history of COVID-19 infection (n=250) and the number of participants required overall (n=1000). These decisions were largely based on the funding and resources available to our team; we aimed to recruit the highest numbers feasible, to permit flexibility for a wide range of planned projects.

Primary and secondary outcomes were determined in advance of mass SARS-CoV-2 vaccination. At time of study conception, we had planned to (1) compare the proportion of IgG antibody in convalescent participants with and without comorbidities at month 6 post–COVID-19 infection, and (2) consider the influence of biological sex on the proportion of those with COVID-19 infection possessing IgG seropositivity at month 6 post–COVID-19 infection. Over the course of the pandemic, we have had to continuously adapt our plans for analyses, especially to account for SARS-CoV-2 vaccination history and circulating VOC at different sampling timepoints. Following March 2022, our team used the WHO International Standard[81] for anti-SARS-CoV-2 immunoglobulins to determine binding antigen units (BAU/mL) and neutralising antibodies (IU/mL) for collected serum. Plans to analyse these results are in progress and will be reported in future publications. As well as enabling the quantification of post-vaccine levels, as opposed to simply reporting a binary cut-off, the International Standard reduces inter-laboratory variation, thereby supporting combined analyses of results through ongoing collaborations with multiple teams.

Finally, the research team will undertake robust multivariate logistic regression analyses of predictors of PASC determined a priori based on clinical expertise and reviews selected using AMSTAR 2 guidelines. Purposeful selection of serological and non-serological predictors will be used to fit a multivariable logistic regression model. We will include a number of predictors to target a mean absolute prediction error <0.05 (Lasso).[95] As prevalence estimates of PASC continue to vacillate,[96 97] we will use Bayesian updating to estimate the prevalence of PASC using the most current data available.[98] Multiple imputation will be used to handle missing data, assumed to be MCAR or MAR. Potential overfitting of the final model will be determined through internal validation using bootstrap methods. Opportunities to collaborate with similar studies will allow for external validation of the model, as well as combined analyses with higher power. SAS V.9.4, GraphPad Prism V.9.3.1 and R V.3.6.1 will be used for all analyses.

Patient and public involvement

Our team is committed to engaging actively and meaningfully with key stakeholders and partners, especially people who have endured COVID-19 infection and post-COVID symptoms. We continue to embrace community input and work to ensure that our research plan addresses the needs and concerns of affected Canadians. A virtual presentation and discussion forum were hosted by SSO Principal Investigators on 18 October 2021, to address participant questions about the study and related research in depth. All participants are sent a letter from the research team thanking them for their commitment to COVID-19 research. Finally, due to multiple requests for access to SARS-CoV-2 antibody results, we created a secure antibody results portal, which participants can access throughout the study.

Findings to date

Of participants to complete a baseline questionnaire by 2 November 2021 (n=1026), 67.1% (n=688) are female, and the median age is 44 years (IQR 23, range 18–79, table 1).

Table 1. Baseline demographics of Stop the Spread Ottawa participants, recruited 14 September 2020 to 28 September 2021

	Stop the Spread Ottawa cohort (n=1026)[a]
Age, median (IQR)	44 (23)
Sex, female (%) [b]	688 (67.1)
Ethnicity (%)	
Aboriginal (Inuit, Métis, North American Indian)	10 (1.0)
Arab/West Asian (e.g., Armenian, Egyptian, Iranian)	20 (1.9)9 (0.9)
Black (e.g., African, Haitian, Jamaican, Somali)	7 (0.7)
Chinese	7 (0.7)
Filipino	3 (0.3)
Korean	9 (0.9)
Latin American	15 (1.5)
South Asian	9 (0.9)
White South East Asian	909 (88.6)
South East Asian	26 (2.5)
Other	

Born in Canada (%) [b]	875 (85.3)
Smoking (%)	
Never	744 (72.5)
Former	231 (22.5)
Current	46 (4.5)
Currently employed (%) [b]	837 (81.6)
Annual household income (%)	
<$60,000	139 (13.5)
$60,000 - $89,999	179 (17.4)
$90,000 - $119,999	197 (19.2)
$120,000 to $149,999	110 (10.7)
$150,000 or more	282 (27.5)
Prefer not to answer	81 (7.9)
Do not know	11 (1.1)
Education level (%)	
Less than high school	2 (0.2)
High school	70 (6.8)
College/some university	281 (27.4)
Undergraduate degree	405 (39.5)
Graduate degree	227 (22.1)
Prefer not to answer	18 (1.8)
SARS-CoV-2 vaccination status (%)	
Number of participants who received ≥ 1 SARS-CoV-2 vaccine prior to baseline visit	316 (30.8)
1 dose received prior to baseline	74 (7.2)
2 doses received prior to baseline	242 (23.6)
SARS-CoV-2 vaccine types received prior to baseline visit (%)[c]	
≥ 1 dose BNT162b2 (Pfizer–BioNTech)	204 (19.9)
≥ 1 dose mRNA-1273 (Moderna)	57 (5.6)
≥ 1 dose AZD1222 (Oxford–AstraZeneca)	34 (3.3)

[a]Number to complete baseline questionnaire as of November 2, 2021. Number missing for each variable: Ethnicity 2, Born in Canada 21, Smoking 5, Employed 23, Income 27 Education 23 Number of participants to receive ≥ 1 SARS-

CoV-2 vaccine before baseline 51 Vaccine types received before baseline 49. Missing data for any single variable is <5%.

[b]Binary response

[c]Participants to receive 2 doses of SARS-CoV-2 vaccine prior to baseline may have received different vaccine types.

In addition, 88.6% (n=909) are white and 85.3% (n=875) are born in Canada; 27% (n=277) are current or former smokers, 14% (n=144) are obese and 4.2% (n=43) have diabetes; 81.6% (n=837) are employed, and 38.2% (n=392) report an annual household income ≥$C120 000; 61.6% (n=632) have an undergraduate or graduate degree.

Furthermore, 24.9% (n=255) have COVID-19 infection history, by positive PCR test (n=231) or by positive serology result during the study without previous positive PCR test (n=24). Table 2 displays demographics by infection status. Members of the Convalescent cohort with history of laboratory-confirmed SARS-CoV-2 infection (n=255) had an older median age (47, IQR 26) than members without infection history (n=771, median age: 43, IQR 22). There were less females in the Convalescent cohort (61.2%) than in the Surveillance cohort (69.3%).

Table 2. Baseline demographics of Surveillance and Convalescent cohorts in the Stop the Spread Ottawa study, recruited 14 September 2020 to 28 September 2021

	Convalescent Cohort (n=255)[a]	**Surveillance Cohort (n=771)[b]**
Age, median (IQR)	47 (26)*	43 (22)
Sex, female (%) [d]	156 (61.2)*	534 (69.3)
Ethnicity, white (%)	222 (87.1)	687 (89.1)
Smoking (%)		
Never	189 (74.1)	555 (72.0)
Former	56 (22.0)	175 (22.7)
Current	9 (3.5)	37 (4.8)

Currently employed (%) [d]	201 (78.8)	636 (82.5)

*P< 0.05 compared to Surveillance Cohort by chi-square/Fisher's test (categorical variables), or t-test (continuous variables)

[a]Number missing for each variable, Convalescent Cohort: Employed 5 Smoking 1

[b]Number missing for each variable, Surveillance Cohort: Ethnicity 2 , Smoking 5 , Employed 18

[c]Convalescent: history of SARS-CoV-2 infection by positive PCR test and/or serology

[d]Binary response

We enrolled priority populations with conditions of clinical significance, including members with self-report of immunocompromising conditions/treatments (eg, cancer, HIV, other immune deficiency and/or use of immunosuppressants, n=108). Table 3 lists baseline health conditions, 2.4% (n=25) report cancer, 3% (n=31) HIV, 7.5% (n=77) other immune deficiency and 6.5% (n=67) use of treatment that weakens the immune system. Over 600 at-risk workers (60.0%), including healthcare workers, teachers and transportation workers, were recruited.

Table 3: Baseline health conditions of Stop the Spread Ottawa participants

Health conditions, frequency (%) [b]	**Participants (n=1026)[a]**
Pregnancy	
Yes	12 (1.2)
No	762 (74.3)
Unknown	237 (23.1)
Not applicable	8 (0.8)
Cancer	25 (2.4)
Diabetes	43 (4.2)
HIV	31 (3.0)
Other immune deficiency	77 (7.5)
Obesity	144 (14.0)
Heart disease	42 (4.1)
Asthma	112 (10.9)
Chronic lung disease	23 (2.2)

Chronic liver disease	14 (1.4)
Chronic kidney disease	12 (1.2)
Chronic hematological disorder	18 (1.8)
Chronic neurological impairment/disease	27 (2.6)
Organ or bone recipient	21 (2.0)
Other health condition(s)	292 (28.5)
Treatment that weakens immune system	67 (6.5)

[a]Number missing for each variable: Pregnancy 7, Cancer 14, Diabetes 10, HIV 10, Other immune deficiency 11, Obesity 11, Heart disease 11, Asthma 17, Chronic lung disease 10, Chronic liver disease 5, Chronic kidney disease 14, Chronic hematological disorder 16, Chronic neurological impairment/disease 26, Organ or bone recipient 20, Other health condition(s) 24, Treatment that weakens immune system 9. Missing data for any single variable is <5%
[b]Binary response, unless stated otherwise

Also, 21.1% (n=216) of all study participants report having sought medical attention for SARS-CoV-2 symptoms at baseline. Of these, 29.2% were diagnosed with COVID-19 and 6.9% (n=15) were hospitalised for SARS-CoV-2 symptoms. In addition, 77.2% of all study participants report no impact of the pandemic on ability to meet essential/financial needs and a majority (69.9%) report no change in employment status in relation to the pandemic.

Strengths and limitations

SSO continues to generate rich research potential, given a majority of participants with pre-vaccine baselines, recruitment of priority populations, and a high level of participant retention and compliance with monthly sampling, driven by active research team communications, automated e-reminders, an interactive study website and an innovative antibody results portal. Frequent and comprehensive sampling since October 2020 has yielded tens of thousands of blood and saliva specimens for use in SARS-CoV-2 immune analyses. The extension of follow-up for a subgroup of participants will maximise opportunities to track SARS-CoV-2 immune and vaccine efficacy, detect and characterise emerging variants, and compare subgroup humoral response robustness and persistence.

Demographics of the cohort have limitations in regards to diversity in age, race and income status. The sampling strategy of SSO involved the enrolment of multiple at-risk groups for SARS-CoV-2 exposure (eg, healthcare workers, transportation workers, teachers, immunocompromised patients, residents in retirement homes, elderly). Recruiting a high number of healthcare workers contributed to a larger proportion of females in the study than observed in the total Ottawa population. Participants also tend to be well educated with high total household income which will limit any inferences made in relation to pandemic economic impacts. The study population was not intended to be, and is not, representative of the general population of the Ottawa region in terms of age, sex, and total household income.

Another limitation is vulnerability of clinical data to response bias as self-reported through online study questionnaires. However, participants have frequent opportunities to add free text and explain responses throughout study questionnaires. In this way, study team members can more accurately assess answers to questions which may be broad or subjective. For example, participants are asked to report any history of immune deficiency or use of immunosuppressants. Participants may perceive themselves to have a deficiency which has minimal impact on their immune response. Ongoing data curation procedures include comparisons of selected health conditions with free-text entries on health history and documentation of rationale for any revisions based on the same. We anticipate that all data curation for the 10-month study will be completed 6 months after the last participants have attended the tenth study visit.

We have recruited over 100 participants with immunocompromising health conditions. This group is highly diverse; we acknowledge small numbers ($n<50$) of participants with specific conditions relative to other international cohorts.[14 15 22 25 26] We will compare serology trends among all participants to report immunocompromising conditions or treatments at baseline and healthy controls without these conditions. To investigate immune response for people with specific immunocompromising health conditions, we will pursue combined analyses with other studies.

Finally, lags in laboratory results are ongoing given the immensity of this project, staffing shortages and a high number of ongoing COVID-19 studies

Future plans

Extended follow-up of a subset of participants for SSO launched 30 September 2021. The primary aims of study extension are to (1) evaluate and compare subgroup durability of SARS-CoV-2 immune responses over a lengthened time period, (2) advance ongoing investigations of VOC immunity and vaccine effectiveness, (3) maximise serial blood specimens for biobanking from participants with pre-immune baselines and (4) supply controls for multiple ongoing studies on SARS-CoV-2 vaccine immunogenicity in special populations, including 'PLAN-V: Pregnant and Lactating Individuals & Newborn COVID-19 Vaccination Study' (CIHR), 'Immunogenicity outcomes in people living with HIV following vaccination for COVID-19' (CITF)[99] and 'A prospective multi-site observational study of SARS-CoV-2 vaccination immunogenicity in patients with hematologic malignancies' (CITF, https://omc.ohri.ca/vip), all with planned 6-month and 12-month post-vaccine blood collections. Finally, the extension will augment ongoing efforts to identify correlates of protection through 'Fine analysis of longitudinal immune responses to SARS-CoV-2 in vaccination: Harnessing the power of 'Stop the Spread Ottawa' to understand immune protection in COVID-19' (CITF).

Collaboration

Initial data analyses and publications will be generated by study investigators. The research team is open to potential research collaborations. Researchers interested in collaboration should contact the corresponding author. Access to data and analytical files can only be granted with permission from the approving research ethics committees and data custodians. Analysis of linked data is currently authorised to occur at one location, given ethical considerations. The Ottawa Methods Centre, the University of Ottawa, and the Coronavirus Variants Rapid Response Network (CoVaRR-Net) Biobank are the custodians of SSO biological materials and data.

Data availability statement
Data may be obtained from a third party and are not publicly available. Direct access to the data and analytical files is not permitted without the expressed permission of the approving human research ethics committees and data custodians. Researchers interested in collaboration should contact the corresponding author.

Ethics statements
Patient consent for publication
Not applicable.

Ethics approval
This study involves human participants and the conduct of this study was reviewed and approved by the Ottawa Health Science Network Research Ethics Board (2020-0481). No authors were involved in the REB approval process. Participants gave informed consent to participate in the study before taking part.

Acknowledgments
The authors acknowledge all investigators and partner organisations contributing to the project: CIs: Steffany Bennett, Pranesh Chakraborty, Miroslava Culf-Cuperlovic, Yves Durocher, Jennifer Quaid, Mary Simmerling. Partner organisations: National Research Council (NRC) of Canada, the Ottawa Hospital Research Institute, the University of Ottawa, and CoVaRR-Net (Coronavirus Variants Rapid Response Network). COVID-19 reagents (viral antigens, ACE2-biotin and anti-human IgG-HRP fusion) were generously provided by Dr Yves Durocher at the NRC Montreal. The authors thank all involved with PBMC and plasma isolation, including Yuchu Dou, Matthew Greig, Katrina Jorritsma, David A Lawton, Kiera Levesque, Jiafeng Li, Jood Madani, Janna Mohamed, Justino Hernandez Soto, Abishek Xavier and Danielle Dewar-Darch. UOttawa Serology and Diagnostics High Throughput Facility is supported by Danielle Dewar-Darch, Justino Hernandez Soto, Yuchu Dou, Abishek Xavier, Erika Marion (past), Jian-Jun Jia (past) and Smita Upamaka (past). We also acknowledge in-kind support from the NRC's Pandemic Response Challenge Program.

References

1. Hu B, Guo H, Zhou P, Shi ZL. Characteristics of SARS-CoV-2 and COVID-19. Nat Rev Microbiol. 2021;19(3):141-154. doi:10.1038/s41579-020-00459-7
2. WHO Coronavirus (COVID-19) Dashboard. Accessed January 10, 2022.
3. Khan NA, Al-Thani H, El-Menyar A. The emergence of new SARS-CoV-2 variant (Omicron) and increasing calls for COVID-19 vaccine boosters-The debate continues. *Travel Med Infect Dis*. 2022;45:102246. doi:10.1016/j.tmaid.2021.102246
4. Boyton RJ, Altmann DM. The immunology of asymptomatic SARS-CoV-2 infection: what are the key questions? Nat Rev Immunol. 2021;21(12):762-768. doi:10.1038/s41577-021-00631-x
5. Mangge H, Kneihsl M, Schnedl W, Sendlhofer G, Curcio F, Domenis R. Immune Responses against SARS-CoV-2—Questions and Experiences. Biomedicines. 2021;9(10):1342. doi:10.3390/biomedicines9101342
6. The durability of immunity against reinfection by SARS-CoV-2: a comparative evolutionary study. The Lancet Microbe. 2021;2(12):e666-e675. doi:10.1016/S2666-5247(21)00219-6
7. Shrotri M, Schalkwyk MCI van, Post N, et al. T cell response to SARS-CoV-2 infection in humans: A systematic review. PLOS ONE. 2021;16(1):e0245532. doi:10.1371/journal.pone.0245532
8. Bajaj V, Gadi N, Spihlman AP, Wu SC, Choi CH, Moulton VR. Aging, Immunity, and COVID-19: How Age Influences the Host Immune Response to Coronavirus Infections? Front Physiol. 2021;0. doi:10.3389/fphys.2020.571416
9. Prabhu Das M, Fuldner R, Farber D, et al. Research and resource needs for understanding host immune responses to SARS-CoV-2 and COVID-19 vaccines during aging. Nat Aging. 2021;1(12):1073-1077. doi:10.1038/s43587-021-00156-x
10. Serologic Response to Coronavirus Disease 2019 (COVID-19) Vaccination in Patients With Immune-Mediated Inflammatory Diseases: A Systematic Review and Meta-analysis. Gastroenterology. 2022;162(1):88-108.e9. doi:10.1053/j.gastro.2021.09.055
11. Kinoshita H, Durkee-Shock J, Jensen-Wachspress M, et al. Robust Antibody and T Cell Responses to SARS-CoV-2 in Patients with Antibody Deficiency. J Clin Immunol. 2021;41(6):1146-1153. doi:10.1007/s10875-021-01046-y
12. The effect of methotrexate and targeted immunosuppression on humoral and cellular immune responses to the COVID-19 vaccine BNT162b2: a cohort study. The Lancet Rheumatology. 2021;3(9):e627-e637. doi:10.1016/S2665-9913(21)00212-5
13. Galmiche S, Luong Nguyen LB, Tartour E, et al. Immunological and clinical efficacy of COVID-19 vaccines in immunocompromised populations: a systematic review. *Clinical Microbiology and Infection*. Published online November 17, 2021. doi:10.1016/j.cmi.2021.09.036
14. Banham GD, Godlee A, Faustini SE, et al. Hemodialysis Patients Make Long-Lived Antibodies against SARS-CoV-2 that May Be Associated with Reduced Reinfection. JASN. 2021;32(9):2140-2142. doi:10.1681/ASN.2021020188
15. Shields AM, Faustini SE, Hill HJ, et al. Increased Seroprevalence and Improved Antibody Responses Following Third Primary SARS-CoV-2 Immunization: An Update From the COV-AD Study. Front Immunol. 2022;0. doi:10.3389/fimmu.2022.912571
16. Yelin D, Wirtheim E, Vetter P, et al. Long-term consequences of COVID-19: research needs. The Lancet Infectious Diseases. 2020;20(10):1115-1117. doi:10.1016/S1473-3099(20)30701-5
17. Long-term Health Consequences of COVID-19 | Cardiology | JAMA | JAMA Network. Accessed March 9, 2021. https://jamanetwork.com/journals/jama/fullarticle/2771581
18. Carvalho T, Krammer F, Iwasaki A. The first 12 months of COVID-19: a timeline of immunological insights. Nat Rev Immunol. 2021;21(4):245-256. doi:10.1038/s41577-021-00522-1

19. Sivan M, Rayner C, Delaney B. Fresh evidence of the scale and scope of long covid. BMJ. Published online April 1, 2021:n853. doi:10.1136/bmj.n853
20. Response to SARS-CoV-2 vaccination in immune mediated inflammatory diseases: Systematic review and meta-analysis. Autoimmunity Reviews. 2022;21(1):102927. doi:10.1016/j.autrev.2021.102927
21. Nejad MMM, Shobeiri P, Dehghanbanadaki H, et al. Seroconversion Following the First, Second, and Third Dose of SARS-CoV-2 Vaccines in Immunocompromised Population; A Systematic Review and Meta-Analysis. In Review; 2021. doi:10.21203/rs.3.rs-1125353/v1
22. Linardou H, Spanakis N, Koliou GA, et al. Responses to SARS-CoV-2 Vaccination in Patients with Cancer (ReCOVer Study): A Prospective Cohort Study of the Hellenic Cooperative Oncology Group. Cancers. 2021;13(18):4621. doi:10.3390/cancers13184621
23. Giannella M, Pierrotti LC, Helanterä I, Manuel O. SARS-CoV-2 vaccination in solid-organ transplant recipients: What the clinician needs to know. Transplant International. 2021;34(10):1776-1788. doi:10.1111/tri.14029
24. Rincon-Arevalo H, Choi M, Stefanski AL, et al. Impaired humoral immunity to SARS-CoV-2 BNT162b2 vaccine in kidney transplant recipients and dialysis patients. Science Immunology. Published online June 15, 2021. Accessed January 19, 2022. https://www.science.org/doi/abs/10.1126/sciimmunol.abj1031
25. Parry H, McIlroy G, Bruton R, et al. Impaired neutralisation of SARS-CoV-2 delta variant in vaccinated patients with B cell chronic lymphocytic leukaemia. J Hematol Oncol. 2022;15(1):1-12. doi:10.1186/s13045-021-01219-7
26. Am S, S V, S S, et al. SARS-CoV-2 vaccine responses following CD20-depletion treatment in patients with haematological and rheumatological disease: a West Midlands Research Consortium study. Clinical and experimental immunology. 2022;207(1). doi:10.1093/cei/uxab018
27. Greenhalgh T, Knight M, A'Court C, Buxton M, Husain L. Management of post-acute covid-19 in primary care. BMJ. 2020;370:m3026. doi:10.1136/bmj.m3026
28. Skyrud K, Telle K, Magnusson K. Impacts of COVID-19 on Long-Term Health and Health Care Use. Public and Global Health; 2021. doi:10.1101/2021.02.16.21251807
29. Nalbandian A, Sehgal K, Gupta A, et al. Post-acute COVID-19 syndrome. Nature Medicine. 2021;27(4):601-615. doi:10.1038/s41591-021-01283-z
30. Antibody response induced by the BNT162b2 mRNA COVID-19 vaccine in a cohort of health-care workers, with or without prior SARS-CoV-2 infection: a prospective study. Clinical Microbiology and Infection. 2021;27(12):1845-1850. doi:10.1016/j.cmi.2021.07.024
31. Government of Canada. Emerging COVID-19 Research Gaps and Priorities. Published March 4, 2022. https://www.canada.ca/en/institutes-health-research/news/2022/03/emerging-covid-19-research-gaps-and-priorities.html
32. Dupont L, Snell LB, Graham C, et al. Neutralizing antibody activity in convalescent sera from infection in humans with SARS-CoV-2 and variants of concern. Nat Microbiol. 2021;6(11):1433-1442. doi:10.1038/s41564-021-00974-0
33. Reinfection with new variants of SARS-CoV-2 after natural infection: a prospective observational cohort in 13 care homes in England. The Lancet Healthy Longevity. 2021;2(12):e811-e819. doi:10.1016/S2666-7568(21)00253-1
34. Tao K, Tzou PL, Nouhin J, et al. The biological and clinical significance of emerging SARS-CoV-2 variants. Nat Rev Genet. 2021;22(12):757-773. doi:10.1038/s41576-021-00408-x
35. Karim SSA, Karim QA. Omicron SARS-CoV-2 variant: a new chapter in the COVID-19 pandemic. The Lancet. 2021;398(10317):2126-2128. doi:10.1016/S0140-6736(21)02758-6
36. Ghorbani SS, Taherpour N, Bayat S, Ghajari H, Mohseni P, Nazari SSH. Epidemiologic characteristics of cases with reinfection, recurrence, and hospital readmission due to COVID-19: A systematic review and meta-analysis. Journal of Medical Virology. 2022;94(1):44-53. doi:10.1002/jmv.27281

37. SARS CoV2 infection _The longevity study perspectives. Ageing Research Reviews. 2021;67:101299. doi:10.1016/j.arr.2021.101299
38. Grzelak L, Velay A, Madec Y, et al. Sex Differences in the Evolution of Neutralizing Antibodies to Severe Acute Respiratory Syndrome Coronavirus 2. *J Infect Dis*. 2021;224(6):983-988. doi:10.1093/infdis/jiab127
39. Antequera A, Lawson DO, Noorduyn SG, et al. Improving Social Justice in COVID-19 Health Research: Interim Guidelines for Reporting Health Equity in Observational Studies. Int J Environ Res Public Health. 2021;18(17):9357. doi:10.3390/ijerph18179357
40. Wu L xiang, Wang H, Gou D, Fu G, Wang J, Guo B qin. Clinical significance of the serum IgM and IgG to SARS-CoV-2 in coronavirus disease-2019. *Journal of Clinical Laboratory Analysis*. 2021;35(1):e23649. doi:10.1002/jcla.23649
41. Ma H, Zeng W, He H, et al. Serum IgA, IgM, and IgG responses in COVID-19. Cell Mol Immunol. 2020;17(7):773-775. doi:10.1038/s41423-020-0474-z
42. Masiá M, Telenti G, Fernández M, et al. SARS-CoV-2 Seroconversion and Viral Clearance in Patients Hospitalized With COVID-19: Viral Load Predicts Antibody Response. Open Forum Infectious Diseases. 2021;8(2):ofab005. doi:10.1093/ofid/ofab005
43. Jackson CB, Farzan M, Chen B, Choe H. Mechanisms of SARS-CoV-2 entry into cells. Nat Rev Mol Cell Biol. 2022;23(1):3-20. doi:10.1038/s41580-021-00418-x
44. Dubey A, Choudhary S, Kumar P, Tomar S. Emerging SARS-CoV-2 Variants: Genetic Variability and Clinical Implications. Curr Microbiol. 2022;79(1):1-18. doi:10.1007/s00284-021-02724-1
45. Complete Mapping of Mutations to the SARS-CoV-2 Spike Receptor-Binding Domain that Escape Antibody Recognition. Cell Host & Microbe. 2021;29(1):44-57.e9. doi:10.1016/j.chom.2020.11.007
46. Wang P, Nair MS, Liu L, et al. Antibody resistance of SARS-CoV-2 variants B.1.351 and B.1.1.7. Nature. 2021;593(7857):130-135. doi:10.1038/s41586-021-03398-2
47. Lipsitch M, Krammer F, Regev-Yochay G, Lustig Y, Balicer RD. SARS-CoV-2 breakthrough infections in vaccinated individuals: measurement, causes and impact. Nat Rev Immunol. 2022;22(1):57-65. doi:10.1038/s41577-021-00662-4
48. Vanshylla K, Di Cristanziano V, Kleipass F, et al. Kinetics and correlates of the neutralizing antibody response to SARS-CoV-2 infection in humans. Cell Host & Microbe. Published online May 2021:S1931312821001918. doi:10.1016/j.chom.2021.04.015
49. COVID-19-neutralizing antibodies predict disease severity and survival. Cell. 2021;184(2):476-488.e11. doi:10.1016/j.cell.2020.12.015
50. Chen W, Zhang J, Qin X, et al. SARS-CoV-2 neutralizing antibody levels are correlated with severity of COVID-19 pneumonia. Biomedicine & Pharmacotherapy. 2020;130:110629. doi:10.1016/j.biopha.2020.110629
51. Salazar E, Kuchipudi SV, Christensen PA, et al. Convalescent plasma anti–SARS-CoV-2 spike protein ectodomain and receptor-binding domain IgG correlate with virus neutralization. J Clin Invest. 2020;130(12):6728-6738. doi:10.1172/JCI141206
52. Dolscheid-Pommerich R, Bartok E, Renn M, et al. Correlation between a quantitative anti-SARS-CoV-2 IgG ELISA and neutralization activity. Journal of Medical Virology. 2022;94(1):388-392. doi:10.1002/jmv.27287
53. Peghin M, Palese A, Venturini M, et al. Post-COVID-19 symptoms 6 months after acute infection among hospitalized and non-hospitalized patients. Clinical Microbiology and Infection. 2021;27(10):1507-1513. doi:10.1016/j.cmi.2021.05.033
54. Seeßle J, Waterboer T, Hippchen T, et al. Persistent Symptoms in Adult Patients 1 Year After Coronavirus Disease 2019 (COVID-19): A Prospective Cohort Study. Clin Infect Dis. Published online July 5, 2021:ciab611. doi:10.1093/cid/ciab611
55. Lindemann M, Klisanin V, Thümmler L, et al. Humoral and Cellular Vaccination Responses against SARS-CoV-2 in Hematopoietic Stem Cell Transplant Recipients. Vaccines. 2021;9(10):1075. doi:10.3390/vaccines9101075

56. Munro C. Covid-19: 40% of patients with weakened immune system mount lower response to vaccines. BMJ. 2021;374. doi:10.1136/bmj.n2098
57. Grinshpun A, Rottenberg Y, Ben-Dov IZ, Djian E, Wolf DG, Kadouri L. Serologic response to COVID-19 infection and/or vaccine in cancer patients on active treatment. ESMO Open. 2021;6(6):100283. doi:10.1016/j.esmoop.2021.100283
58. Liu, W. et al. Two-year prospective study of the humoral immune response of patients with severe acute respiratory syndrome. J Infect Dis 193, 792-795, doi:10.1086/500469 (2006).
59. Seasonal human coronavirus antibodies are boosted upon SARS-CoV-2 infection but not associated with protection. *Cell*. 2021;184(7):1858-1864.e10. doi:10.1016/j.cell.2021.02.010
60. Cross-reactive humoral immune responses against seasonal human coronaviruses in COVID-19 patients with different disease severities. International Journal of Infectious Diseases. 2021;111:68-75. doi:10.1016/j.ijid.2021.08.026
61. Lv H, Wu NC, Tsang OTY, et al. Cross-reactive Antibody Response between SARS-CoV-2 and SARS-CoV Infections. Cell Reports. 2020;31(9). doi:10.1016/j.celrep.2020.107725
62. Ladner JT, Henson SN, Boyle AS, et al. Epitope-resolved profiling of the SARS-CoV-2 antibody response identifies cross-reactivity with endemic human coronaviruses. CR Med. 2021;2(1). doi:10.1016/j.xcrm.2020.100189
63. Okba NMA, Müller MA, Li W, et al. Severe Acute Respiratory Syndrome Coronavirus 2−Specific Antibody Responses in Coronavirus Disease Patients - Volume 26, Number 7—July 2020 - Emerging Infectious Diseases journal - CDC. doi:10.3201/eid2607.200841
64. Galipeau Y, Siragam V, Laroche G, et al. Relative Ratios of Human Seasonal Coronavirus Antibodies Predict the Efficiency of Cross-Neutralization of SARS-CoV-2 Spike Binding to ACE2. eBioMedicine. 2021;74. doi:10.1016/j.ebiom.2021.103700
65. Lustig Y, Sapir E, Regev-Yochay G, et al. BNT162b2 COVID-19 vaccine and correlates of humoral immune responses and dynamics: a prospective, single-centre, longitudinal cohort study in health-care workers. The Lancet Respiratory Medicine. 2021;9(9):999-1009. doi:10.1016/S2213-2600(21)00220-4
66. Cox RJ, Brokstad KA. Not just antibodies: B cells and T cells mediate immunity to COVID-19. Nat Rev Immunol. 2020;20(10):581-582. doi:10.1038/s41577-020-00436-4
67. Bertoletti A, Le Bert N, Qui M, Tan AT. SARS-CoV-2-specific T cells in infection and vaccination. Cell Mol Immunol. 2021;18(10):2307-2312. doi:10.1038/s41423-021-00743-3
68. D G, Mc S, S B, et al. SARS-CoV-2 variants of concern partially escape humoral but not T-cell responses in COVID-19 convalescent donors and vaccinees. Science immunology. 2021;6(59). doi:10.1126/sciimmunol.abj1750
69. B G, M AB, Pm L, et al. A Higher Antibody Response Is Generated With a 6- to 7-Week (vs Standard) Severe Acute Respiratory Syndrome Coronavirus 2 (SARS-CoV-2) Vaccine Dosing Interval. Clinical infectious diseases : an official publication of the Infectious Diseases Society of America. Published online November 30, 2021. doi:10.1093/cid/ciab938
70. Richardson CD. Heterologous ChAdOx1-nCoV19–BNT162b2 vaccination provides superior immunogenicity against COVID-19. The Lancet Respiratory Medicine. 2021;9(11):1207-1209. doi:10.1016/S2213-2600(21)00366-0
71. Powell AA, Power L, Westrop S, et al. Real-world data shows increased reactogenicity in adults after heterologous compared to homologous prime-boost COVID-19 vaccination, March−June 2021, England. Eurosurveillance. 2021;26(28):2100634. doi:10.2807/1560-7917.ES.2021.26.28.2100634
72. Tregoning JS, Flight KE, Higham SL, Wang Z, Pierce BF. Progress of the COVID-19 vaccine effort: viruses, vaccines and variants versus efficacy, effectiveness and escape. *Nat Rev Immunol*. 2021;21(10):626-636. doi:10.1038/s41577-021-00592-1
73. Scherlinger M, Pijnenburg L, Chatelus E, et al. Effect of SARS-CoV-2 Vaccination on Symptoms from Post-Acute Sequelae of COVID-19: Results from the Nationwide VAXILONG Study. Vaccines. 2022;10(1):46. doi:10.3390/vaccines10010046

74. Desimmie BA, Raru YY, Awadh HM, He P, Teka S, Willenburg KS. Insights into SARS-CoV-2 Persistence and Its Relevance. Viruses. 2021;13(6):1025. doi:10.3390/v13061025
75. Ibrahimi N, Delaunay-Moisan A, Hill C, et al. Screening for SARS-CoV-2 by RT-PCR: Saliva or nasopharyngeal swab? Rapid review and meta-analysis. *PLOS ONE*. 2021;16(6):e0253007. doi:10.1371/journal.pone.0253007
76. Moreira VM, Mascarenhas P, Machado V, et al. Diagnosis of SARS-Cov-2 Infection by RT-PCR Using Specimens Other Than Naso- and Oropharyngeal Swabs: A Systematic Review and Meta-Analysis. Diagnostics. 2021;11(2):363. doi:10.3390/diagnostics11020363
77. Warsi I, Khurshid Z, Shazam H, et al. Saliva Exhibits High Sensitivity and Specificity for the Detection of SARS-COV-2. Diseases. 2021;9(2). doi:10.3390/diseases9020038
78. Morley GL, Taylor S, Jossi S, et al. Sensitive Detection of SARS-CoV-2–Specific Antibodies in Dried Blood Spot Samples - Volume 26, Number 12—December 2020 - Emerging Infectious Diseases journal - CDC. doi:10.3201/eid2612.203309
79. Cholette F, Mesa C, Harris A, et al. Dried blood spot specimens for SARS-CoV-2 antibody testing: A multi-site, multi-assay comparison. PLOS ONE. 2021;16(12):e0261003. doi:10.1371/journal.pone.0261003
80. Colwill K, Galipeau Y, Stuible M, et al. A scalable serology solution for profiling humoral immune responses to SARS-CoV-2 infection and vaccination. Clinical & Translational Immunology. 2022;11(3):e1380. doi:10.1002/cti2.1380
81. Kristiansen PA, Page M, Bernasconi V, et al. WHO International Standard for anti-SARS-CoV-2 immunoglobulin. Lancet (London, England). 2021;397(10282):1347. doi:10.1016/S0140-6736(21)00527-4
82. DNA Genotek - Saliva Microbiome DNA and RNA Collection Kit. Accessed June 26, 2022. https://www.dnagenotek.com/ROW/products/collection-infectious-disease/omnigene-oral/OM-505.html
83. Saliva Collection Handbook. Salimetrics. Published June 27, 2017. Accessed June 26, 2022. https://salimetrics.com/saliva-collection-handbook/
84. Salivary Detection of COVID-19 | Annals of Internal Medicine. Accessed June 26, 2022. https://www.acpjournals.org/doi/full/10.7326/M20-4738
85. Poulain, A. *et al.* Rapid protein production from stable CHO cell pools using plasmid vector and the cumate gene-switch. *Journal of biotechnology* 255, 16-27 (2017).
86. Poulain, A., Mullick, A., Massie, B. & Durocher, Y. Reducing recombinant protein expression during CHO pool selection enhances frequency of high-producing cells. *J Biotechnol* 296, 32-41, doi:10.1016/j.jbiotec.2019.03.009 (2019)
87. Abe KT, Li Z, Samson R, et al. A simple protein-based surrogate neutralization assay for SARS-CoV-2.. for SARS-CoV-2. JCI Insight. 2020;5(19). doi:10.1172/jci.insight.142362
88. JCI Insight - A simple protein-based surrogate neutralization assay for SARS-CoV-2. Accessed February 16, 2022. https://insight.jci.org/articles/view/142362
89. Riley RD, Ensor J, Snell KIE, et al. Calculating the sample size required for developing a clinical prediction model. BMJ. 2020;368. doi:10.1136/bmj.m441
90. Domingo FR, Waddell LA, Cheung AM, et al. Prevalence of long-term effects in individuals diagnosed with COVID-19: An updated living systematic review. Epidemiology; November 2021. doi:10.1101/2021.06.03.21258317
91. Chen C, Haupert SR, Zimmermann L, Shi X, Fritsche LG, Mukherjee B. Global prevalence of post COVID-19 condition or long COVID: A meta-analysis and systematic review. J Infect Dis; April 2022. doi:10.1093/infdis/jiac136
92. Gao X, Dong Q. A primer on Bayesian estimation of prevalence of COVID-19 patient outcomes. Jamia Open. 2021;3(4):628-631. doi:10.1093/jamiaopen/ooaa062

93. Costiniuk CT, Singer J, Langlois MA, et al. CTN 328: immunogenicity outcomes in people living with HIV in Canada following vaccination for COVID-19 (HIV-COV): protocol for an observational cohort study. *BMJ Open*. 2021;11(12):e054208. doi:10.1136/bmjopen-2021-054208

A-1.27 Results of the Stop the Spread Ottawa (SSO) cohort study: a Canadian urban-based prospective evaluation of antibody responses and neutralization efficiency to SARS-CoV-2 infection and vaccination

Preface

(This work has been previously published as a research article)

Keeshan A, **Galipeau Y**, Heiskanen A, Collins E, McCluskie PS, Arnold C, Saginur R, Booth R, Little J, McGuinty M, Buchan CA, Crawley A, Langlois MA, Cooper C. **Results of the Stop the Spread Ottawa (SSO) cohort study: a Canadian urban-based prospective evaluation of antibody responses and neutralisation efficiency to SARS-CoV-2 infection and vaccination.** BMJ Open. 2023 Oct 31;13(10):e077714.

https://doi.org/10.1136/bmjopen-2023-077714

© Author(s) (or their employer(s)) 2023. This is an open access article distributed in accordance with the Creative Commons Attribution Non Commercial (CC BY-NC 4.0) license, which permits others to distribute, remix, adapt, build upon this work non-commercially, and license their derivative works on different terms, provided the original work is properly cited, appropriate credit is given, any changes made indicated, and the use is non-commercial.

Abstract

Background
Predictors of COVID-19 vaccine immunogenicity and the influence of prior severe acute respiratory syndrome coronavirus 2 (SARS-CoV-2) infection require elucidation.

Methods
Stop the Spread Ottawa is a prospective cohort of individuals at-risk for or who have been infected with SARS-CoV-2, initially enrolled for 10 months beginning October 2020. This cohort was enriched for public-facing workers. This analysis focuses on safety and immunogenicity of the initial two doses of COVID-19 vaccine.

Results
Post-vaccination data with blood specimens were available for 930 participants. 22.8% were SARS-CoV2 infected prior to the first vaccine dose. Cohort characteristics include: median age 44 (IQR: 22–56), 66.6% women, 89.0% white, 83.2% employed. 38.1% reported two or more comorbidities and 30.8% reported immune compromising condition(s). Over 95% had detectable IgG levels against the spike and receptor binding domain (RBD) 3 months post second vaccine dose. By multivariable analysis, increasing age and high-level immune compromise predicted diminishing IgG spike and RBD titres at month 3 post second dose. IgG spike and RBD titres were higher immediately post vaccination in those with SARS-CoV-2 infection prior to first vaccination and spike titres were higher at 6 months in those with wider time intervals between dose 1 and 2. IgG spike and RBD titres and neutralisation were generally similar by sex, weight and whether receiving homogeneous or heterogeneous combinations of vaccines. Common symptoms post dose 1 vaccine included fatigue (64.7%), injection site pain (47.5%), headache (27.2%), fever/chills (26.2%) and body aches (25.3%). These symptoms were similar with subsequent doses.

Conclusion
The initial two COVID-19 vaccine doses are safe, well-tolerated and highly immunogenic across a broad spectrum of vaccine recipients including those working in public facing environments.

Strengths and limitations of this study

- The Stop the Spread Ottawa (SSO) cohorts is representative of males and female adults as well as a broad range of ages.
- A large proportion of SSO participants is employed in public facing occupations or is subject to frequent exposures to other individuals.
- A large proportion of SSO participants is immune compromised.
- A small proportion of the SSO cohort is non-white, limiting our ability for evaluation of racialised populations.

Introduction

COVID-19 vaccines have proven to be a key tool for combating the pandemic and have lowered infection rates and risk of severe disease.[1] [2] Pragmatic vaccine roll-out in Canada resulted in extended dosing schedules beyond the time periods used in clinical trials, the mixing of vaccine types and the widespread administration of vaccines primarily based on messenger RNA (mRNA) technology.[3] [4] As new viral variants have evolved over time, additional booster doses have been employed and bivalent vaccines have been introduced.

Clinical trials and observational population studies indicate that multiple vaccine technologies induce robust IgG levels against SARS-CoV-2.[5] An analysis involving 30 individuals from two randomised controlled trials (RCTs) for the ChAdOx1 vaccine in the UK (COV001 and COV002) found that longer intervals between the first and second doses (up to 44–45 weeks) resulted in higher antibody titres 28 days after the second dose. Heightened humoral response and slower antibody decay up to 6 months were observed in the Com-COV2 RCT following mixed vaccination with ChAdOx1 and then Pfizer-BioNTech or Moderna vaccines compared with homologous vaccination. However, immunogenicity varies in different populations[6] and the generalisability of the phase I–III randomised clinical trials for COVID-19 vaccines was limited due to restricted eligibility criteria that excluded older, younger and at-risk populations.[2] [7] Therefore, prospective observational evaluation of COVID-19 vaccine immunogenicity in diverse populations and in real-world settings is needed to fully elucidate the role of vaccine type, time between doses, number of doses and patient characteristics (such as sex, race, age and comorbidities). The long-term durability of vaccine-mediated immunity and risk for breakthrough infections are not fully characterised. Longitudinal research is required to determine how long vaccine response persists, the level of protection provided against emerging variants of concern, and the immunogenicity of bivalent COVID-19 vaccines.

The Stop the Spread Ottawa (SSO) cohort was established in September of 2020 to address these knowledge gaps. SSO employed less restrictive eligibility criteria than clinical trials and multiple subgroups are represented in the cohort such as those working in public-facing occupations such

as healthcare, childcare and the transportation sector. Additionally, older age groups, immune compromised individuals, those with multimorbidities and people with post-COVID condition (PCC) were also specifically sought.[8] In this paper we report on a multiparameter humoral response to COVID-19 vaccination and identify factors that influence vaccine immunogenicity in a complex, real-world population.

Methods

SSO is a prospective, longitudinal, cohort study investigating immune response to SARS-CoV-2 natural infection and vaccination.[8] Recruitment began 14 September 2020 and was completed 28 September 2021. Enrolled participants were followed for 10 months with the option to extend for an additional 24 months. Those with a documented history of SARS-CoV-2 infection at baseline based on quantitative reverse transcription PCR (RT-PCR) or serology testing were allocated to the *convalescent cohort* for longitudinal sampling and participants without prior SARS-CoV-2 infection were included in the *surveillance cohort*. During follow-up, participants who tested positive for SARS-CoV-2 by RT-PCR or rapid antigen test (RAT) or received SARS-CoV-2 vaccine(s) were asked to cross-over from the surveillance cohort to follow the study protocol for the convalescent cohort.

Individuals 18 years or older, residing in the Ottawa-region and at-risk for SARS-CoV-2 exposure/infection due to occupation or health condition or having a documented history of COVID-19 natural infection confirmed by PCR and/or serology testing were eligible.[8] Recruitment efforts prioritised inclusion of individuals at-risk of SARS-CoV-2 infection based on occupation (healthcare, long-term care facilities, air travel cabin crew, dental care, teachers, daycare) or a pre-existing health condition. Participants were classified as having a compromised immune system if they had a primary or secondary immunodeficiency, rheumatological condition, autoimmune disease, inflammatory condition, cancer, diabetes, asthma or chronic obstructive pulmonary disease requiring medication, organ/bone marrow transplant and/or received immunosuppressive treatment. Those reporting excessive alcohol consumption (men: 15 or more standard drinks a week; women: 8 or more standard drinks) were also considered immune compromised.[9]

Participants completed electronic questionnaires at baseline; at months 3, 10, 16, 22, 28 and 34; and following documented SARS-CoV-2 infection(s).[8] Information on demographics, medical history, socioeconomic and psychosocial status, exposure risk factors, acute and persistent COVID-19 symptoms and vaccine reactogenicity was collected. Self-reported COVID-19 vaccinations and positive SARS-CoV-2 diagnostic results were tracked by the study coordinator and COVID-19 infection and vaccination histories were confirmed through medical records, where available. At baseline, participants provided blood samples for serum and peripheral blood mononuclear cell (PBMC) isolation.[8] Convalescent participants completed monthly serum and bimonthly PBMC draws for 10 months. During months 11–34, extension participants provided blood specimens every other month. All biological specimens are stored in the Coronavirus Variants Rapid Response Network biobank, following the highest standards of biobanking practices in sample collection, processing, storage, access and distribution (on application).

IgG titres (BAU/mL) against SARS-CoV-2 spike (S), receptor-binding domain (RBD) and nucleocapsid (N) proteins in participant serum samples were quantified using a high-throughput chemiluminescent direct ELISA as previously described.[8 10 11] A surrogate neutralisation ELISA assay using the full-trimeric S protein from the Wuhan Hu-1 strain was performed to determine neutralisation efficiency in sera. This surrogate protein-based assay enables the quantification of spike-ACE2 interaction in a high-throughput fashion. This approach has been validated with WHO reference serum and internal control.[10] Incident COVID-19 infections were identified through self-report of positive PCR and RAT results to the study coordinator and through serology testing. Anti-N IgG titres were used to distinguish between vaccine-acquired immunity and infection-acquired immunity from a prior SARS-CoV-2 infection. Participants were classified as having vaccine-based immunity if they were positive (signal-to-cut-off (SCO)>1) for anti-S and anti-RBD IgG and infection-acquired immunity if they were positive for anti-N IgG and either anti-S or anti-RBD IgG. In the case of one-off or intermittent positive serum sample results for infection-acquired immunity for individuals with no self-reported positive test results, natural immunity was determined by examining the signal strength (the magnitude of SCO) and the preceding and subsequent serum results. The date of the first positive serum sample was taken as the best

available estimate of date of infection for participants with COVID-19 infections identified through serum testing.

Participant characteristics and titres were compared according to study cohort at baseline, vaccine type and immune status. Student's t-test and $\chi 2$ statistical tests were employed for continuous and categorical variables when assumptions were met. Fisher's exact test as well as non-parametric Mann-Whitney U and Kruskal-Wallis tests were used in the case of low cell values or non-normal distribution. Monte Carlo simulation (n=1 000 000 samples) was employed to estimate p values for large contingency tables with high computational loads. Univariate and multivariable quantile regression analyses were conducted to compare log-adjusted anti-S and anti-RBD levels due to non-normal distribution of the log transformed data. Time points included week 6 post first vaccine dose (data from specimens collected from 4 to 8 weeks post first dose included in analysis), 3 months post second dose (2−4 months data included) and 6 months post second dose (4−6 months data included). Statistical tests and regression analyses were conducted using Statistical Analysis System (SAS) V.9.4 (copyright 2016 by SAS Institute, Cary, North Carolina, USA). Nested models which included or excluded the main term and interaction term were compared through a joint Wald test of the overall models using the R package 'quantreg' to obtain joint p values. Plots were constructed using RStudio (ggplot2 package).

Patient and public involvement

Consultation with members of the public at risk for exposure to SARS-CoV-2 was conducted during the design and implementation of this cohort study. This resulted in the creation of several 'participant friendly' pathways for providing serial blood specimens. A web-based, user-friendly study portal was designed which enabled participation and direct access to personal study data was created based on patient and public input. Feedback was sought and implemented throughout the conduct of this study to facilitate patient participation and retention. Consented participants assisted in recruitment as they were provided the opportunity to direct interested individuals to our study team and/or study website to explore enrolling in the SSO cohort study. Patient-focused webinars led by Dr Cooper and his study team were held during the course of the study conduct to provide SSO updates and the opportunity to ask questions related to the study and COVID-19 in general. Study updates were also provided on the SSO website. Our study coordinators and Dr

Cooper also provided individualise SSO updates to participants on request. We remain deeply grateful for the considerable time, commitment, data and biological specimens provided by our SSO participants.

Results

Participant characteristics

A total of 1112 participants were consented and enrolled in SSO (supplemental figure 1). Participant retention was high with 67% of participants completing the initial 10 months of follow-up despite the challenges of public health measures and an arduous study protocol. Participant protocol compliance was high and the number of missing samples was low. Baseline questionnaire and serum draws were completed by 730 surveillance and 257 convalescent participants. Of participants in the surveillance cohort, 20.9% had at least one incident COVID-19 infection after enrolment, identified through self-report of a positive test result and/or serum IgG antibodies. At least one COVID-19 infection was identified in 10% of all convalescent SSO participants during the study period. Of note, assay failure rates were low (0.6%, 0.6% and 0.1% for anti-N, anti-RBD and anti-S IgG).

During the initial 10-month follow-up period, 195 individuals transitioned from the surveillance cohort into the convalescent cohort following COVID-19 infection (n=22) or vaccination (n=173). Thirty-three per cent of participants were lost to follow-up (13%) or withdrew (20%).

A high proportion of participants were women (67.1%), white (89.0%) and Canada-born (87.1%) (table 1). A high proportion of participants (63.0%) were engaged in public facing occupations. Nearly two-thirds (64.2%) had obtained an undergraduate or advanced degree, 83.3% were employed at baseline and 65% earned at least $C90 000 annually. Those with a history of a prior COVID-19 infection at baseline were older (mean age 46.8 vs 44.4 years) and more likely to be obese (19.1% obese vs 12.6%) than those without prior infection. The most prevalent comorbidities at baseline included allergy (42.7%), obesity (14.1%), hypertension (10.4%), dyslipidaemia (9.0%), endocrine disorder (10.1%), heart disease (4.0%) and chronic neurological

condition (3.0%). Current or past smoking was reported in 27.3% of participants. Just over 30% of participants were classified as immune compromised.

Table 1 Characteristics of study participants (n=1034) at baseline in the surveillance cohort (no history of COVID-19 infection at baseline) and convalescent cohort (history of a COVID-19 infection at baseline)

Variable	All participants (n=1,034)	Surveillance Cohort (n=803)	Convalescent Cohort (n=231)	P value
Age				
Mean (SD)	45.0 (13.9)	44.4 (13.7)	46.8 (14.6)	0.02
Range (min, max)	61 (18, 79)	61 (18, 79)	54 (22, 76)	
Sex, n (%)				
Male	340 (32.9)	254 (31.6)	86 (37.2)	0.11
Female	694 (67.1)	549 (68.4)	145 (62.8)	
Missing	7	7	0	
Race, n (%)				
Arab/West Asian	20 (1.9)	15 (1.9)	5 (2.2)	0.49
Black	9 (0.9)	5 (0.6)	4 (1.7)	
Indigenous	19 (1.9)	15 (1.9)	4 (1.7)	
Latin American	9 (0.9)	5 (0.6)	4 (1.7)	
South Asian	15 (1.5)	12 (1.5)	3 (1.3)	
Southeast Asian	17 (1.7)	14 (1.8)	3 (1.3)	
White	916 (89.0)	715 (89.6)	201 (87.0)	
Other	24 (2.33)	17 (2.1)	7 (3.0)	
Missing	5	5	0	
Immigration status, n (%)				
Born in Canada	879 (87.1)	682 (87.2)	197 (86.8)	0.87
Immigrated to Canada	130 (12.9)	100 (12.8)	30 (13.2)	
Missing	25	21	4	
Education level, n (%)				
Elementary school	1 (0.1)	0 (0)	1 (0.5)	0.13
High school	70 (7.1)	56 (7.3)	14 (6.5)	
Trade / Technical Degree / Apprenticeship	35 (3.6)	25 (3.3)	10 (4.6)	
Community College	219 (22.2)	160 (20.8)	59 (27.2)	
University Certificate	28 (2.8)	23 (3.0)	5 (2.3)	
Bachelor's Degree	407 (41.2)	330 (42.9)	77 (34.5)	
Graduate Degree (MSc, MBA, MD, PhD)	227 (23.0)	176 (22.9)	51 (23.5)	
Prefer not to answer	18	11	7	
Missing	29	22	7	
Annual income before taxes in the past 12 months, n (%)				
$0-$29,999	42 (4.6)	30 (4.2)	12 (6.1)	0.07

Variable	All participants (n=1,034)	Surveillance Cohort (n=803)	Convalescent Cohort (n=231)	P value
$30,000-$59,999	98 (10.8)	68 (9.5)	30 (15.3)	
$60,000-$89,999	179 (19.7)	147 (20.6)	32 (16.3)	
$90,000-$119,999	197 (21.7)	163 (22.8)	34 (17.4)	
$120,000-$149,999	111 (12.2)	89 (12.5)	22 (11.2)	
$150,000+	283 (31.1)	217 (30.4)	66 (33.7)	
Prefer not to answer/ Unknown	92	65	27	
Missing	32	24	8	
Employed, n (%)				
Yes	837 (83.3)	657 (83.8)	180 (81.5)	0.41
No	168 (16.7)	127 (16.2)	41 (18.6)	
Missing	29	19	10	
Smoking history[†], n (%)				
Current Smoker	45 (4.4)	37 (4.7)	8 (3.5)	0.70
Former Smoker	234 (22.9)	179 (22.6)	55 (23.8)	
Never Smoker	745 (72.8)	577 (72.8)	168 (72.7)	
Missing	10	10	0	
Average number of standard drinks of alcohol consumed per week[‡]				
Median (IQR)	2.0 (0, 4)	2.0 (0, 4)	2.0 (0.5, 5.0)	0.08
Range (min, max)	30 (0, 30)	25 (0, 25)	30 (0, 30)	
Missing	11	8	3	
Allergies, n (%)				
Yes	437 (42.7)	333 (42.0)	104 (45.2)	0.38
No	586 (57.3)	460 (58.0)	126 (54.8)	
Missing	11	10	1	
Obesity (self-reported), n (%)				
Yes	143 (14.1)	99 (12.6)	44 (19.1)	0.01
No	874 (85.9)	688 (87.4)	186 (80.9)	
Missing	17	16	1	
Body Mass Index (BMI) [§]				
Median (IQR)	26.6 (23.4, 30.4)	26.1 (23.0, 30.1)	28.2 (25.1, 32.8)	<0.0001
Range (min, max)	38.7 (16.3, 55.1)	38.7 (16.4, 55.1)	33.6 (19.4, 53.0)	
Missing	528	404	124	
Immune Compromised [¶], n (%)				
Yes	316 (30.6)	247 (30.8)	69 (29.9)	0.80
No	718 (69.4)	556 (69.2)	162 (70.1)	
Number of Co-Morbidities				
Median (IQR)	1 (0, 2)	1 (0, 2)	1 (0, 2)	0.35
Range (min, max)	8 (0, 8)	7 (0, 8)	8 (0, 9)	

Variable	All participants (n=1,034)	Surveillance Cohort (n=803)	Convalescent Cohort (n=231)	P value
Two or more Co-Morbidities, n (%)				
Yes	388 (37.5)	292 (36.4)	96 (41.6)	0.15
No	646 (62.5)	511 (63.6)	135 (58.4)	

† Number of packs are reported for current and former smokers. Six smokers reported zero packs due to smoking a product other than cigarettes (e.g., cigars).

‡ One standard drink equals: 341 mL (12 oz.) bottle of 5% beer, cider, or cooler; 142 mL (5 oz.) glass of 12% wine; 43 mL (1.5 oz.) serving of 40% distilled alcohol; (e.g., rye, gin, rum, vodka).

§ BMI is categorized as per Centers for Disease Control and Prevention: BMI<18.5, underweight; 18.5≤BMI<25 healthy weight; 25≤BMI<30, overweight; BMI≥30.0 obese.

¶ Participants were classified as immune compromised if they had a primary immunodeficiency, rheumatological condition, organ-specific autoimmune disease or immune dysfunction, neuromuscular autoimmune disease, inflammatory condition, cancer, HIV, diabetes, asthma requiring medication, or were receiving immunosuppressive treatment, were an organ/bone marrow recipient, or reported excessive alcohol consumption (15+ standard drinks a week for males, 8+ standard drinks a week for females).

Vaccination and infection summary

At the time of data analysis, 98.5% and 97.7% of participants had received at least one or two vaccine doses, respectively, and 70.9% had received one or more booster shot(s) (table 2). The majority of participants (87.4%) were vaccinated with mRNA vaccines (Pfizer-BioNTech (Pfizer) (77.6% first dose and 73.7%second dose); Moderna (10.1% for dose 1 and 25.0% dose 2). Adenovirus-based ChAdOx1 vaccine (AstraZeneca) was administered to 12.3% of dose 1 and 1.2% of dose 2 recipients. The median days between the first and second COVID-19 vaccine doses was 58 (IQR: 35–76) and ranged from 11 to 344 days. The length of time in days between second and third vaccine doses was 185 IQR (IQR: 174–212). Post COVID-19 condition symptoms were reported in 224 (21.7%) participants.

Table 2 Participant COVID-19 vaccination information as of analysis cut-off date (September 2022) according to cohort allocation at the time of initial cohort entry

Variable	All participants (n=1034)	Surveillance cohort (n=803)	Convalescent cohort* (n=231)
Vaccinated for COVID-19, n (%)			
Yes	952 (98.7)	739 (99.2)	213 (96.8)
No	13 (1.4)	6 (0.8)	7 (3.2)
Missing	69	58	11
Number of COVID-19 vaccine dose received, n (%)			
None	13 (1.4)	6 (0.8)	7 (3.2)
1	8 (0.8)	6 (0.8)	2 (0.9)
2	259 (26.8)	215 (28.9)	44 (20.0)
3	562 (58.2)	416 (55.8)	146 (66.4)
4	119 (12.3)	98 (13.2)	21 (9.6)
5	4 (0.4)	4 (0.5)	0 (0)
Missing	69	58	11
Types of COVID-19 vaccines received, dose 1, n (%)			
ChAdOx1	117 (12.3)	93 (12.6)	24 (11.3)
Moderna	96 (10.1)	62 (8.4)	34 (16.0)
Pfizer	737 (77.6)	582 (79.0)	155 (72.8)
Missing	84	66	18
Types of COVID-19 vaccines received, dose 2, n (%)			
ChAdOx1	11 (1.2)	8 (1.1)	3 (1.4)
Pfizer	696 (73.7)	552 (75.3)	144 (68.3)
Moderna	236 (25.0)	172 (23.5)	64 (30.3)
Sinovac	1 (0.1)	1 (0.1)	0 (0)
Missing	90	70	20
Types of COVID-19 vaccine received, dose 1 and dose 2, n (%)			
ChAdOx1–ChAdOx1	10 (1.1)	7 (1.0)	3 (1.4)
Pfizer–Pfizer	629 (67.8)	501 (69.6)	128 (61.5)
Moderna–Moderna	90 (9.7)	59 (8.2)	31 (14.9)
ChAdOx1-Pfizer	52 (5.6)	42 (5.8)	10 (4.8)
ChAdOx1-Moderna	54 (5.8)	44 (6.1)	10 (4.8)
Pfizer-Moderna	92 (9.9)	66 (9.2)	26 (12.5)
Moderna-Sinovac	1 (0.1)	1 (0.1)	0 (0)
Missing	106	83	23
Time between first and second COVID-19 vaccine doses, in days			
Median (IQR)	58 (35−76)	58 (35−75)	60 (37−77)
Range (min, max)	333 (11−344)	114 (11−276)	323 (21−344)
Missing	106	86	20

[†] Infection history was determined by self-reported positive COVID-19 PCR or RAT test results and serology testing. Participants tested positive for prior natural COVID-19 infection by serology if they were positive (SCO>1) for anti-N IgG antibodies and anti-S or anti-RBD IgG antibodies.

Humoral immune response following first and second vaccine doses

After excluding those with history of COVID-19 infection, 95.9% tested positive for humoral antibody evidence of vaccine-based immunity 6 weeks after dose 1. This proportion increased after full vaccination (97.7% 3 months after dose 2 and 100% 6 months after dose 2). These proportions were similar by vaccine type. Participants who tested negative for vaccine-based immunity 6 weeks after dose 1 were older (median age 59.0 (IQR: 44.0–72.5) vs 54.0 (41.0–60.0), p=0.03) and were more likely to be immune compromised (87.5% vs 29.1%, p<0.01) to a severe degree (85.7% vs 38.2%, p=0.04) than those who tested positive.

An increase in log-adjusted anti-S and anti-RBD IgG titres were observed following vaccination across the cohort (table 3, supplemental figure 2). Median anti-S and anti-RBD IgG titres (log10 BAU/mL) 6 weeks post dose 1 were higher with mRNA vaccination (Moderna (S: 3.348 (IQR: 3.189–3.776), RBD: 2.950 (2.645–3.461))) and Pfizer doses (S: 3.101 (IQR: 2.564–3.634), RBD: 2.643 (2.252–3.767)) compared with adenovirus vector vaccine (AstraZeneca (S: 1.893 (1.737–2.582), RBD: 1.939 (1.751–2.550))) (S: p<0.0001, RBD: p<0.001). Median anti-S and anti-RBD IgG titres were comparable regardless of vaccine type 3 months following dose 1.

Maximum median log-adjusted anti-S and anti-RBD titres were observed following completion of the second dose schedule after which median titres declined over time until the next vaccination or natural infection (table 3, supplemental figure 2). Median anti-S and anti-RBD IgG titres were comparable regardless of vaccine type 6 months following dose 2. Receiving two mRNA vaccines resulted in a higher humoral response compared with receiving first adenovirus vector vaccine and then an mRNA vaccine 6 weeks post dose 1 (anti-S: 3.118 (IQR: 2.573–3.637) vs 1.893 (IQR: 1.737–2.582); p<0.0001) but not 6 weeks post dose 2 (anti-S: 3.539 (IQR: 3.286–3.706) vs 3.680 (IQR: 3.512–4.053); p<0.01). The humoral response was comparable by vaccine type 3 months following dose 2 as well.

At all time points, those with a history of COVID-19 infection prior to first vaccination had higher median log-adjusted anti-S and anti-RBD IgG titres (table 3).

Table 3 Median log-adjusted IgG titres (log10 BAU/mL) against the SARS-CoV-2 spike (S) and receptor-binding domain (RBD) proteins at time points prior to and following COVID-19 vaccination, according to COVID-19 infection history*

IgG titre (log10 BAU/mL)	All participants (n=981)	Prior infection (n=399)	No prior infection (n=582)	P value
Anti-S, 6 weeks pre-dose 1	n=224	n=116	n=108	
Median (IQR)	1.20 (0.44 to 2.08)	2.02 (1.69 to 2.79)	0.45 (−3.00 to 0.78)	<0.0001
Range (min, max)	6.52 (–3.00 to 3.52)	6.52 (–3.00 to 3.52)	6.48 (–3.00 to 3.48)	
Anti-RBD, 6 weeks pre-dose 1	n=216	n=116	n=100	
Median (IQR)	1.44 (0.81 to 2.03)	1.90 (1.53 to 2.23)	0.83 (0.65 to 1.15)	<0.0001
Range (min, max)	3.54 (–0.09 to 3.45)	3.43 (–0.02 to 3.41)	3.54 (–0.09 to 3.45)	
Anti-S, 6 weeks post dose 1	n=353	n=148	n=205	
Median (IQR)	3.42 (2.65 to 3.97)	3.91 (3.24 to 4.28)	3.08 (2.12 to 3.61)	<0.0001
Range (min, max)	7.45 (–3.00 to 4.45)	3.41 (1.04 to 4.45)	7.45 (–3.00 to 4.45)	
Anti-RBD, 6 weeks post dose 1	n=353	n=148	n=205	
Median (IQR)	3.34 (2.42 to 3.93)	3.87 (3.37 to 4.11)	2.60 (2.21 to 3.63)	<0.0001
Range (min, max)	4.83 (0.25 to 5.09)	3.93 (1.16 to 5.09)	4.17 (0.25 to 4.42)	
Anti-S, 6 weeks post dose 2	n=325	n=129	n=196	
Median (IQR)	3.59 (3.28 to 3.82)	3.73 (2.12 to 4.04)	3.55 (3.30 to 3.73)	<0.01
Range (min, max)	7.45 (–3.00 to 4.45)	2.74 (1.71 to 4.45)	7.45 (–3.00 to 4.45)	
Anti-RBD, 6 weeks post dose 2	n=326	n=129	n=197	
Median (IQR)	3.63 (3.18 to 3.86)	3.78 (3.41 to 4.02)	3.51 (3.04 to 3.76)	<0.0001
Range (min, max)	4.69 (0.40 to 5.09)	2.84 (2.24 to 5.09)	4.02 (0.40 to 4.41)	
Anti-S, 3 months post dose 2	n=576	n=209	n=367	
Median (IQR)	3.43 (3.19 to 3.65)	3.65 (3.43 to 3.93)	3.35 (3.12 to 3.50)	<0.0001
Range (min, max)	7.45 (–3.00 to 4.45)	2.65 (1.80 to 4.45)	7.45 (–3.00 to 4.45)	
Anti-RBD, 3 months post dose 2	n=571	n=209	n=362	
Median (IQR)	3.44 (2.98 to 3.68)	3.65 (3.41 to 3.98)	3.32 (2.64 to 3.53)	<0.0001
Range (min, max)	4.48 (0.60 to 5.09)	2.75 (2.34 to 5.09)	3.89 (0.60 to 4.49)	
Anti-S, 6 months post dose 2	n=214	n=67	n=147	
Median (IQR)	3.16 (2.94 to 3.34)	3.40 (3.21 to 3.66)	3.06 (2.77 to 3.22)	<0.0001
Range (min, max)	3.17 (1.28 to 4.45)	2.41 (2.04 to 4.45)	2.46 (1.28 to 3.74)	
Anti-RBD, 6 months post dose 2	n=212	n=65	n=147	
Median (IQR)	3.03 (2.48 to 3.28)	3.34 (3.17 to 3.59)	2.64 (2.41 to 3.15)	<0.0001
Range (min, max)	3.04 (1.17 to 4.21)	2.01 (2.20 to 4.21)	2.59 (1.17 to 3.69)	

* 399 participants had a positive COVID-19 RAT or PCR test prior to baseline or during follow-up or were positive for natural immunity by serum testing during follow-up (SCO>1 for anti-N IgG titres and eitherr anti-S or anti-RBD titres). Samples obtained after the administration of a third vaccine dose were excluded.

Predictors of humoral immune responses by regression analysis

Univariate analysis was used to identify variables potentially influencing vaccine immunogenicity following the initial two doses in those without a history of SARS-CoV2 infection (data not shown). After adjusting for immune compromised status, sex, obesity, vaccine type(s) administered for dose 1 and 2, and days between first and second doses by multivariable quantile regression, older age was identified as a predictor of lower median anti-S and anti-RBD IgG titres 3 months after dose 2 for participants with no history of infection (table 4). By 6 months following vaccine dose 2, age no longer was associated with anti-S and anti-RBD IgG titres. Immune compromised status also predicted lower median log-adjusted anti-S IgG and anti-RBD titres 3 months post dose 2. Increased time between first and second doses predicted higher anti-RBD IgG titres at month 3 and anti-S IgG titres at 6 months after dose 2.

Shorter duration of time from SARS-CoV-2 infection to dose 1 of vaccine predicted higher IgG S and RBD titre at month 6 post second dose of vaccine. No other covariates consistently predicted higher or lower anti-S or anti-RBD IgG titres for participants with COVID-19 infection history prior to vaccination (table 4).

Consistent with IgG antibody titre findings, older age and longer time between first and second vaccine dose predicted higher neutralisation at 3 months after vaccine dose 2 in those without SARS-CoV-2 infection prior to vaccination (table 5, supplemental figure 3). Immune compromised state also predicted diminished vaccine neutralisation at months 3 and 6 post second vaccine dose. Similar to IgG antibody titre findings, duration of time from SARS-CoV-2 infection to dose 1 of vaccine predicted higher IgG neutralisation at month 6 post second dose of vaccine.

Vaccine tolerability and reactogenicity

Results are reported for the initial two doses plus the first booster dose. No serious adverse events (SAEs) related to vaccination were reported by SSO participants. One participant died due to malignancy deemed unrelated to vaccination. Commonly reported vaccination symptoms following dose 1 included fatigue (64.7%), pain at the injection site or arm soreness (47.5%), headache (27.2%), fever or chills (26.2%) and body aches (25.3%) (supplemental table 1). The type and proportion of symptoms was similar with subsequent vaccinations. Symptoms lasted the longest after dose 1 (median of 2.0 days (IQR: 1.0–3.0)) compared with subsequent vaccinations.

Table 4: Difference in median log-adjusted IgG titres (log10 BAU/mL) against the SARS-CoV-2 spike and receptor-binding domain proteins following the initial two COVID-19 vaccine doses by multivariable quantile regression, stratified by SARS-CoV-2 infection history: A) Participants without history of SARS-CoV-2 infection [†]; B) Participants with a history of one SARS-CoV-2 infection prior to vaccination. [‡, §†]Samples obtained after the administration of a third vaccine dose, a self-reported positive COVID-19 RAT or PCR test, or natural immunity identified by serum testing (SCO>1 for anti-N IgG titres and either anti-S or anti-RBD titres) were excluded.

Participants without a history of SARS-CoV-2 infection				
IgG spike (log10 BAU/mL)				
Variable	3 months post dose 2 (±1 month)		6 months post dose 2 (±2 months)	
	Difference (95% CI)	P value	Difference (95% CI)	P value
Age (per 1 year increase)	0.01 (−0.01 to −0.001)	0.03	0.0006 (−0.01 to 0.004)	0.82
Sex				
Male	0.06 (−0.05 to 0.16)	0.29	0.03 (−0.16 to 0.21)	0.79
Female	Referent		Referent	
Obese				
Yes	0.02 (−0.14 to 0.17)	0.82	0.02 (−0.23 to 0.19)	0.85
No	Referent		Referent	
Immune compromised				
Yes - high	0.19 (−0.35 to −0.02)	0.03	0.10 (−0.57 to 0.36)	0.66
Yes - low	0.10 (−0.22 to 0.02)	0.09	0.07 (−0.20 to 0.06)	0.28
No	Referent		Referent	
Time between first and second doses, in days	0.0002 (−0.002 to 0.002)	0.85	0.002 (0.0007 to 0.007)	0.02

IgG RBD (log10 BAU/mL)				
Variable	3 months post dose 2 (±1 month)		6 months post dose 2 (±2 months)	
	Difference (95% CI)	P value	Difference (95% CI)	P value
Age (per 1 year increase)	0.02 (−0.02 to −0.01)	<0.0001	0.0003 (−0.006 to 0.006)	0.91
Sex				
Male	0.15 (−0.01 to 0.30)	0.07	0.57 (0.40 to 0.74)	<0.0001
Female	Referent		Referent	
Obesity				
Yes	0.01 (−0.26 to 0.24)	0.95	0.07 (−0.43 to 0.29)	0.71
No	Referent		Referent	
Immune compromised				
Yes - high	0.39 (−0.73 to −0.05)	0.03	0.15 (−0.50 to 0.21)	0.41
Yes - low	0.01 (−0.19 to 0.21)	0.90	0.09 (−0.25 to 0.08)	0.29
No	Referent		Referent	
Time between first and second doses, in days	0.003 (0.0008 to 0.006)	0.01	0.005 (−0.005 to 0.01)	0.33

Participants with a history of SARS-CoV-2 infection				
IgG spike (log10 BAU/mL)				
Variable	3 months post dose 2 (±1 month)		6 months post dose 2 (±2 months)	
	Difference (95% CI)	P value	Difference (95% CI)	P value
Age (per 1 year increase)	0.01 (−0.0004 to 0.01)	0.07	0.004 (−0.003 to 0.01)	0.23
Sex				
Male	0.02 (−0.14 to 0.18)	0.84	0.09 (−0.05 to 0.23)	0.22
Female	Referent		Referent	
Obesity				
Yes	0.17 (−0.12 to 0.45)	0.25	–	
No	Referent		–	
Immune compromised				
Yes - high	0.06 (−0.31 to 0.44)	0.74	0.11 (−0.44 to 0.23)	0.53
Yes - low	0.08 (−0.10 to 0.26)	0.36	0.24 (−0.04 to 0.52)	0.09
No	Referent		Referent	
Time between first and second doses, in days	0.001 (−0.005 to 0.003)	0.52	0.0008 (−0.003 to 0.004)	0.64
Time from SARS-CoV-2 infection to dose 1	0.003 (−0.01 to 0.001)	0.11	0.002 (−0.01 to 0.0006)	0.12
Quadratic term	8.0E-6 (6.0E-7 to 2.0E-5)	0.07	7.1E-6 (−3.5E-7 to 1.5E5)	0.06
		0.18 (joint)†		0.03 (joint)†

IgG RBD (log10 BAU/mL)				
Variable	3 months post dose 2 (±1 month)		6 months post dose 2 (±2 months)	
	Difference (95% CI)	P value	Difference (95% CI)	P value
Age (per 1 year increase)	0.007 (−0.0003 to 0.02)	0.06	0.004 (−0.002 to 0.01)	0.23
Sex				
Male	0.10 (−0.07 to 0.28)	0.25	0.01 (−0.19 to 0.17)	0.95
Female	Referent		Referent	
Obesity				
Yes	0.12 (−0.25 to 0.50)	0.52	–	
No	Referent		–	
Immune compromised				
Yes - high	0.10 (−0.20 to 0.40)	0.50	0.02 (−0.39 to 0.35)	0.91
Yes - low	0.05 (−0.21 to 0.31)	0.72	0.28 (0.08 to 0.47)	<0.01
No	Referent		Referent	
Time between first and second doses, in days	0.001 (−0.01 to 0.003)	0.53	0.0008 (−0.004 to 0.003)	0.68
Time from SARS-CoV-2 infection to dose 1	0.004 (−0.01 to −0.0001)	0.04	0.002 (−0.004 to 0.001)	0.22
Quadratic term	4.6E-6 (1.0E-6 to 1.9E-5)	0.03	7.0E-6 (2.5E-8 to 1.4E5)	0.05
		0.11 (joint)†		0.02 (joint)†

‡, §†Samples obtained after the administration of a third vaccine dose, a self-reported positive COVID-19 RAT or PCR test, or natural immunity identified by serum testing (SCO>1 for anti-N IgG titres and either anti-S or anti-RBD titres) were excluded. ‡Samples obtained after the administration of a third vaccine dose, prior to a self-reported positive COVID-19 RAT or PCR test, natural immunity identified by serum testing (SCO>1 for anti-N IgG titres and either anti-S or anti-RBD titres) or following a second positive COVID-19 test were excluded.
§Participants were classified as obese if they had a BMI of 35 or greater. IC severity was classified high if participants were receiving immunosuppressive treatment, had active HIV, cancer, had received an organ/bone marrow transplant, had a primary immunodeficiency, a neuromuscular autoimmune diseases. IC was low is the participant had localized autoimmune disease, excessive alcohol consumption, fully supressed HIV, or diabetes.

¶Participant who received AstraZeneca vaccines for dose 1 and 2 was excluded due to small sample size.

[5]Nested models which included or excluded the main term and interaction term were compared through a joint Wald test of the overall models using the R package ‘quantreg’ to obtain joint p values.

Table 5: Difference in median IgG neutralization percentage (%) against the Wuhan-Hu-1 SARS-CoV-2 spike protein following two COVID-19 vaccine doses in those without a history of SARS-CoV-2 infection † (A) and those with a history of one SARS-CoV-2 infection prior to vaccination ‡ (B) by multivariable quantile regression.

Participants without a history of SARS-CoV-2 infection				
Neutralisation percentage against spike protein (%)				
Variable	3 months post dose 2 (±1 month)		6 months post dose 2 (±2 months)	
	Difference (95% CI)	P value	Difference (95% CI)	P value
Age (per 1 year increase)	1.17 (−1.72 to –0.61)	<0.01	0.07 (−0.51 to 0.37)	0.77
Sex				
Male	18.20 (5.10 to 31.31)	<0.01	9.59 (−10.26 to 29.43)	0.34
Female	Referent		Referent	
Obese		0.17		0.70
Yes	19.00 (−45.91 to 7.92)		4.05 (−25.06 to 16.96)	
No	Referent		Referent	
Immune compromised				
Yes - high	0.75 (−22.75 to 24.24)	0.95	7.87 (−32.83 to 17.10)	0.54
Yes - low	25.36 (−42.76 to –7.96)	<0.01	20.89 (−34.23 to −7.54)	<0.01
No	Referent		Referent	
Types of COVID-19 vaccines received, dose 1 and 2§				
ChAdOx1-mRNA	19.96 (1.09 to 41.00)	0.06	–	
mRNA–mRNA	Referent		–	
Time between first and second doses, in days	0.47 (0.24 to 0.71)	<0.01	0.06 (−0.42 to 0.54)	0.81

Participants with a history of SARS-CoV-2 infection				
Neutralisation percentage against spike protein (%)				
Variable	3 months post dose 2 (±1 month)		6 months post dose 2 (±2 months)	
	Difference (95% CI)	P value	Difference (95% CI)	P value
Age (per 1 year increase)	0.10 (−0.16 to 0.36)	0.44	0.10 (−0.35 to 0.54)	0.67
Sex				
Male	1.03 (−4.82 to 6.88)	0.73	0.98 (−11.63 to 9.66)	0.86
Female	Referent		Referent	
Obese		0.60		
Yes	2.79 (−13.21 to 7.64)		–	
No	Referent		–	
Immune compromised				
Yes – high	2.73 (−11.56 to 6.10)	0.54	33.41 (−67.58 to 0.76)	0.06
Yes – low	3.43 (−3.53 to 10.38)	0.33	7.36 (−6.16 to 20.89)	0.28
No	Referent		Referent	
Types of COVID-19 vaccines received, dose 1 and 2§				
ChAdOx1-mRNA	7.68 (−31.42 to 16.06)	0.52	–	
mRNA–mRNA	Referent		–	
Time between first and second doses, in days	0.02 (−0.18 to 0.15)	0.85	0.17 (−0.51 to 0.17)	0.33
Time from prior SARS-CoV-2 infection to dose 1	0.04 (−0.15 to 0.07)	0.47	0.08 (−0.12 to 0.29)	0.41
Quadratic term	0.0001 (−0.0001 to 0.0004)	0.28	0.0001 (−0.0004 to 0.0006)	0.83
		0.23 (joint)¶		<0.01 (joint)¶

§ † Samples obtained after the administration of a third vaccine dose, a self-reported positive COVID-19 RAT or PCR test, or natural immunity identified by serum testing (SCO>1 for anti-N IgG titres and either anti-S or anti-RBD titres) were excluded.
‡ Samples obtained after the administration of a third vaccine dose, prior to a self-reported positive COVID-19 RAT or PCR test, or natural immunity identified by serum testing (SCO>1 for anti-N IgG titres and either anti-S or anti-RBD titres) or following a second positive COVID-19 test were excluded.
§ Participants were classified as obese if they had a BMI of 35 or greater. IC severity was classified high if participants were receiving immunosuppressive treatment, had active HIV, cancer, had received an organ/bone marrow transplant, had a primary immunodeficiency, or a neuromuscular autoimmune diseases. IC was low is the participant had localized disease, excessive alcohol consumption, fully supressed HIV, or diabetes.
¶ Participants who received Sinovac for dose 2 and 3 and participants who received AstraZeneca for dose 1 and dose 2 were excluded due to small sample size.
5 Nested models which included or excluded the main term and interaction term were compared through a joint Wald test of the overall models using the R package 'quantreg' to obtain joint p values.

Discussion

Large scale administration of novel COVID-19 vaccines was deployed to combat the SARS-CoV-2 pandemic. In Canada, supply constraints during initial roll-out lead to staged administration in which high-risk groups were prioritised (eg, healthcare workers, older adults, adults in Indigenous communities), an increase in the length of time between priming and boosting doses beyond the recommended 21 days (for Pfizer) or 28 days (for Moderna) up to 4 months, and the mixing of different vaccine types.[3 4 12] Our analysis suggest that these strategies all ultimately achieved a potent induction of humoral immunity. In fact, a longer interval than recommended by the manufacturer between dose 1 and 2 increased durability of humoral responses.

Most SSO participants had received two mRNA vaccines at the time of analysis. mRNA and adenovirus vector COVID-19 vaccines elicited robust humoral responses that were sustained 3 months after dose 2. Crude median anti-S and anti-RBD titres (log10 BAU/mL) peaked 6 weeks after the second dose and then generally decreased over time. All vaccine types demonstrated acceptable safety and tolerability profiles with no reported vaccine-specific SAEs. Mild

reactogenicity symptoms were commonly reported but generally lasted a few days. Our results are consistent with prior studies which have found the mRNA COVID-19 vaccine to be overall safe and effective.[13]

In our analysis, vaccine-elicited antibody responses persisted 6 months post vaccination. Of note, all participants without a history of infection at baseline were found to possess evidence of humoral immunity at 6 months following the second vaccine dose. However, to date the correlates of protection for COVID-19 infection remains poorly defined and it is unclear if the titres reported in this study 6 months post vaccination are sufficient to protect individuals from infection, especially variants of concern, or how long this protection will last beyond 6 months.[14 15] Other studies have observed a gradual decline in titres following initial two dose vaccination which is consistent with our findings.[6 14] There is evidence that humoral responses decline at the 4–6 months point after vaccination, especially in immune compromised individuals.[16 17] Podrazil *et al* observed a sharp decline in humoral and cellular immune responses 6 months after vaccination with the mRNA Pfizer vaccine in asthma patients receiving biological therapy.[16] Breakthrough COVID-19 infections further raise concerns regarding the durability of protection following two doses.[18]

Vaccine immunogenicity was robust in young and middle age participants; many of which worked in public-facing occupations including as healthcare providers, teachers, daycare and in the transport sector. Achieving protective immunity with these occupation groups is a critical public health piece in minimising community transmission of SARS-CoV-2. Older age predicted lower anti-S and anti-RBD IgG titres and neutralisation at 3 months following vaccination in those without prior SARS-CoV-2 infection. Immune senescence is a phenomenon that leads to chronic inflammation as well as suboptimal T cell, B cell, neutrophil and dendritic cell activity and counts.[19] These changes increase the risk of acquiring infections and reduce vaccine immunogenicity (eg, as shown for influenza and herpes zoster vaccines) in the elderly.[19 20] Immune senescence is likely a contributing factor to the decrease in SARS-CoV-2 immunogenicity with older age, although the specific mechanism as it relates to COVID-19 remain to be characterised. The elderly are at higher risk of severe outcomes from COVID-19.[21] These findings, in combination with the observed accelerated decline in anti-S and anti-RBD IgG titres over time, support current recommendations to receive a booster dose 4–6 months after full vaccination.[15]

High level immune compromised status was associated with diminished COVID-19 vaccine humoral responses in those without prior SARS-CoV-2 infection. Adjusted median anti-S and anti-RBD titres 3 months after the second vaccine dose as well as anti-RBD and neutralisation at month 6 were lower for immune compromised participants. Our cohort includes a heterogeneous collection of immune compromising conditions including cancer, chronic inflammatory, autoimmune or rheumatological disease, HIV and those receiving immune suppressants medications (eg, transplant recipients). Our results are consistent with other COVID-19 vaccination studies focused on immune compromised populations.[6 16 22 23]

There is emerging evidence that extending the time interval between the first and second COVID-19 vaccine doses improves immune responses.[15 24] Due to the variation in the number of days between vaccine doses received by SSO participants, we were able to prospectively investigate the impact of the time interval on vaccine immunogenicity. In those without pre-vaccine SARS-CoV-2 infection, increasing the number of days between vaccine doses was associated with higher anti-S and RBD IgG titres in the 6-month period vaccination and higher anti-S IgG neutralisation at month 3 following vaccine dosing. These results show that concerns regarding decreased efficacy from extending the interval between doses are unwarranted and suggest a potential benefit.[25] Extending the vaccine schedule may improve long-term durability of COVID-19 vaccine immunogenicity and prolong protection from SARS-CoV-2 infection and severe symptoms.

SARS-CoV-2 infection prior to initial vaccination was a consistent predictor of anti-S and anti-RBD IgG antibody titres and neutralisation identified in this study. At all time points, having a history of infection increased humoral response to the vaccine. The time interval between SARS-CoV-2 infection and first vaccine predicted anti-S and anti-RBD titres as well as neutralisation in the 6-month period following the second vaccine dose. The crude difference in IgG titres compared with those with no prior infection gradually increased over time following the initial two doses of vaccine suggesting that the slope of antibody decay may be less marked in those with hybrid immunity. Recent research has found that breakthrough infections increase humoral response and neutralisation of SARS-CoV-2 variants.[26 27] Our results warrant further investigation into the joint effect of vaccine-mediated and infection-acquired immunity compared with either independently.

The findings in this study are subject to several strengths and limitations. The SSO cohort has a large sample size of over 1000 participants at baseline with high retention. Prospective, longitudinal data collection commenced prior to widespread vaccine roll-out enabling the collection of pre-vaccination baseline data.[8] Information on many different variables was collected allowing for many key covariates to be included in multivariable analyses. Self-reported infection and vaccination histories were validated using medical records. Multiple testing methods (rapid antigen tests, PCR and serology testing) were used to confirm present and past COVID-19 infections.

SSO participants are primarily white, characterised by a high level of employment and many reported high-income status. The study was conducted in a developed nation with a robust public health infrastructure. With this in mind, our results may not be fully generalisable to all settings. Adults over 80 years of age are not well represented.[8] Because non-white individuals comprised only 11% of our cohort, we could not explore this important variable in our evaluation of vaccine safety and immunogenicity. Blood draws occurred based on time of enrolment and were not fixed to vaccination dates. Therefore, blood samples for humoral immune assessment were not always available for each post-vaccination time point evaluated. The high-throughput chemiluminescent direct ELISA antibody assay used is subject to a range of uncertainty in the quantification method (3% false discovery rate). Natural infection histories of participants with intermittent or one-off positive results for infection-acquired immunity were manually adjusted but misclassification is possible. There is also a risk of misclassification when relying on self-reported data. Selection bias may have been introduced by the 33% of participants who were lost to follow-up or withdrew. However, we believe that the potential for selection bias is minimal as those who provided serum data and those who were lost to follow-up were similar in terms of baseline data. Our sample size was not of sufficient size to identify rare side effects of vaccination.

Despite these limitations, our analysis of a large, heterogeneous cohort followed for a prolonged duration during the SARs-CoV-2 pandemic demonstrates that the initially administered COVID-19 vaccinations were safe, well-tolerated and highly immunogenic across a broad spectrum of recipients including those employed in public-facing occupations. Our analysis continues to assess

durability of vaccine immunogenicity as well as the influence of additional vaccine boosters and natural infection.

Data availability statement
Data are available upon reasonable request.

Ethics statements

Patient consent for publication
Consent obtained directly from patient(s).

Ethics approval
All participants provided informed consent. Stop the Spread Ottawa is approved by the Ottawa Health Science Network Research Ethics Board (#2020-0481-01H).

Contributors
AK: data analysis, manuscript preparation. YG: laboratory analysis, data analysis, manuscript preparation. AH: data analysis, manuscript preparation. EC: study design, study recruitment, manuscript preparation. PSM: laboratory analysis, data analysis. CA: laboratory analysis, data analysis. RS: study design, manuscript preparation. RB: laboratory analysis, manuscript preparation. JL: study design, data analysis, manuscript preparation. MM: study design, manuscript preparation. CAB: study design, manuscript preparation. AC: study design, laboratory analysis, data analysis, manuscript preparation. M-AL: study design, laboratory analysis, data analysis, manuscript preparation. CLC: study design, study recruitment, data analysis, manuscript preparation. CC: guarantor.

Funding
This study is funded by the Canadian Institutes of Health Research - Instituts de recherche en santé du Canada (CIHR) (424425), the COVID-19 Immunity Task Force (CITF) and the University of Ottawa. The study extension is funded by the Coronavirus Variants Rapid Response Network (CoVaRR-Net) (156941) (https://covarrnet.ca/investigating-long-term-variables-to-sars-cov-2-infection-and-vaccine-immunity/). CoVaRR-Net is funded by an operating grant from CIHR (FRN# 175622). Production of COVID-19 reagents was financially supported by the National Research Council of Canada's Pandemic Response Challenge Program. YG is supported by a Charles Best and Frederick Banting (CGS-Doctoral award) from CIHR (476885). M-AL holds a Faculty of Medicine Chair of Excellence in Pandemic Viruses and Preparedness Research. The authors thank the uOttawa High Throughput Serology and Diagnostics facility staff: Danielle Dewar-Darch, Gwendoline Ward, Justino Hernandez Soto, Klaudia Baumann, Nicholas Bradette, Yuchu Dou, Abishek Xavier and Lynda Rocheleau

Competing interests None declared.

Patient and public involvement

Patients and/or the public were not involved in the design, or conduct, or reporting, or dissemination plans of this research.

References

1 Kreuzberger N, Hirsch C, Andreas M, et al. Immunity after COVID-19 vaccination in people with higher risk of compromised immune status: a Scoping review. Cochrane Database Syst Rev 2022;8:CD015021.
2 Li Z, Liu S, Li F, et al. Efficacy, Immunogenicity and safety of COVID-19 vaccines in older adults: a systematic review and metaanalysis. Front Immunol 2022;13:965971.
3 National Advisory Committee on Immunization (NACI). Archived: guidance on the Prioritization of initial doses of COVID-19 Vaccine(S). 2020. Available: https://www.canada.ca/en/public-health/services/immunization/national-advisory-committee-on-immunization-naci/ guidance-prioritization-initial-doses-covid-19-vaccines.html#shr-pg0
4 National Advisory Committee on Immunization (NACI. Archived 5: NACI rapid response: Extended dose intervals for COVID-19 vaccines to optimize early vaccine rollout and population protection in Canada, . 2021Available: https://www.canada.ca/en/publichealth/services/immunization/national-advisory-committee-onimmunization-naci/rapid-response-extended-dose-intervals-covid19-vaccines-early-rollout-population-protection.html
5 Polack FP, Thomas SJ, Kitchin N, et al. Safety and efficacy of the BNT162b2 mRNA Covid-19 vaccine. N Engl J Med 2020;383:2603–15.
6 Addo IY, Dadzie FA, Okeke SR, et al. Duration of immunity following full vaccination against SARS-Cov-2: a systematic review. Arch Public Health 2022;80:200.
7 Badell ML, Dude CM, Rasmussen SA, et al. Covid-19 vaccination in pregnancy. BMJ 2022;378:e069741.
8 Collins E, Galipeau Y, Arnold C, et al. Cohort profile: stop the spread Ottawa (SSO)-A community-based prospective cohort study on antibody responses, antibody Neutralisation efficiency and cellular immunity to SARS-Cov-2 infection and vaccination. BMJ Open 2022;12:e062187.
9 Division of Population Health - National Center for Chronic Disease Prevention and Health Promotion - Centers for Disease Control and Prevention. Alcohol use and your health: U.S Department of health & human services. 2022. Available: https://www.cdc.gov/alcohol/factsheets/alcohol-use.htm
10 Colwill K, Galipeau Y, Stuible M, et al. A Scalable Serology solution for profiling humoral immune responses to SARS-Cov-2 infection and vaccination. Clin Transl Immunology 2022;11:e1380.
11 Rocheleau L, Laroche G, Fu K, et al. Identification of a highfrequency Intrahost SARS-Cov-2 spike variant with enhanced cytopathic and Fusogenic effects. mBio 2021;12:e00788-21.
12 Kriss JL, Reynolds LE, Wang A, et al. COVID-19 vaccine seconddose completion and interval between first and second doses among vaccinated persons — united states, december 14, 2020−february 14, 2021. MMWR Morb Mortal Wkly Rep 2020;70:389–95.
13 Centers for Disease Control and Prevention (CDC). Safety of COVID-19 vaccines. 2023. Available: https://www.cdc.gov/ coronavirus/2019-ncov/vaccines/safety/safety-of-vaccines.html
14 Brockman MA, Mwimanzi F, Lapointe HR, et al. Reduced magnitude and durability of humoral immune responses to COVID-19 mRNA vaccines among older adults. J Infect Dis 2022;225:1129–40.
15 Government of Canada. COVID-19 vaccine: Canadian immunization guide (for health professionals). 2022. Available: https://www.canada. ca/en/public-health/services/publications/healthy-living/canadianimmunization-guide-part-4-active-vaccines/page-26-covid-19-vaccine.html#a6.4.considerations
16 Podrazil M, Taborska P, Stakheev D, et al. Effectiveness and durability of mRNA vaccine-induced SARS-Cov-2-specific humoral and cellular immunity in severe asthma patients on biological therapy. Front Immunol 2022;13:892277.

17 Suthar MS, Arunachalam PS, Hu M, et al. Durability of immune responses to the BNT162b2 mRNA vaccine. Med 2022;3:25–7.
18 Ben Fredj S, Ghammem R, Zammit N, et al. Risk factors for severe COVID-19 breakthrough infections: an observational longitudinal study. BMC Infect Dis 2022;22:894.
19 Oh SJ, Lee JK, Shin OS. Aging and the immune system: the impact of Immunosenescence on viral infection. Immunity and Vaccine Immunogenicity Immune Netw 2019;19:e37.
20 Quach HQ, Kennedy RB. Enhancing Immunogenicity of influenza vaccine in the elderly through intradermal vaccination: A literature analysis. Viruses 2022;14:2438.
21 Booth A, Reed AB, Ponzo S, et al. Population risk factors for severe disease and mortality in COVID-19: A global systematic review and meta-analysis. PLoS One 2021;16:e0247461.
22 Mehrabi Nejad M-M, Moosaie F, Dehghanbanadaki H, et al. Immunogenicity of COVID-19 mRNA vaccines in immunocompromised patients: a systematic review and metaanalysis. Eur J Med Res 2022;27:23.
23 Napuri NI, Curcio D, Swerdlow DL, et al. Immune response to COVID-19 and mRNA vaccination in immunocompromised individuals: A narrative review. Infect Dis Ther 2022;11:1391–414.
24 National Advisory Committee on Immunization (NACI). Interim guidance on planning considerations for a fall 2022 COVID-19 vaccine booster program in Canada. Ottawa: Government of Canada, 2022.
25 Mahase E. Covid-19: assess the effects of extending Pfizer vaccine dosing interval, expert URGES. BMJ 2021;372:162.
26 Bates TA, McBride SK, Winders B, et al. Antibody response and variant cross-neutralization after SARS-Cov-2 breakthrough infection. JAMA 2022;327:179–81.
27 Public Health Agency of Canada. Evidence Brief on Protective Immunity Post Infection with Omicron: Government of Canada, . 2022Available: https://www.canada.ca/en/public-health/services/diseases/2019-novel-coronavirus-infection/canadas-reponse/ summaries-recent-evidence/protective-immunity-post-infectionomicron.html